Evaporation, Evapotranspiration and Irrigation Water Requirements

Second Edition

Prepared by the Task Committee on
Revision of Manual 70
of the Committee on
Evapotranspiration in Irrigation and Hydrology
of the Environmental and Water Resources Institute
of the American Society of Civil Engineers

This is a restructured
and updated version of
Manual 70 published in 1990

Editors
Marvin E. Jensen
Richard G. Allen

Task Committee Members
Richard G. Allen
Marvin E. Jensen
Derrel L. Martin
Terry A. Howell
Richard L. Snyder
Ivan A. Walter

Peer Review Committee Members
Paul W. Brown
Ronald L. Elliott
Thomas W. Ley
Thomas Trout

Published by the
American Society of Civil Engineers
1801 Alexander Bell Drive
Reston, VA 20191-4400

ABSTRACT
This manual, Evaporation and Evapotranspiration (Manual 70-Revised), replaces the Manual 70 published in 1990. It has been restructured and incorporates user experience and recent advances in the understanding of evaporation and transpiration processes. The first chapter describes the development of the revised Manual 70, the contents of the 14 chapters, the evolution of consumptive use studies in the USA, and the global understanding of the evaporation processes. Chapters 2 and 3 describe the evaporation and evapotranspiration processes and the soil-plant atmosphere system. Chapters 4 and 5 describe the energy balance at the water and soil surfaces and surface energy-air mass interactions. Chapter 6 describes evaporation from water surfaces and methods for estimating evaporation. Chapter 7 describes general methods for estimating evaporation from land surfaces. Chapters 8 through 11 describe various approaches to estimating evapotranspiration from land surfaces including the reference evapotranspiration- crop coefficient method, and direct application of the Penman-Monteith equation. Chapter 12 provides guidelines for estimating regional evapotranspiration, Chapter 13 provides guidelines for selecting the appropriate estimating methodology and Chapter 14 describes methodology for estimating irrigation requirements. Appendices provide conversion factors, a table of saturation vapor pressure over water, basic thermodynamic constants for air and water vapor, several sets of crop coefficients for use with estimated reference evapotranspiration, a glossary of terms, some estimating methods not commonly used in the USA that were included in the first edition, and selected results comparing estimating methods that were in the first edition.

Library of Congress Cataloging-in-Publication Data (to be updated by ASCE)

Evaporation and Evapotranspiration: a manual/prepared by the Task Committee on Revision of Manual 70 Evapotranspiration and Irrigation Water Requirements, a task committee of the Environmental and Water Resources Institute of the American Society of Civil Engineers; edited by Marvin E. Jensen and Richard G. Allen; task committee members T.A. Howell, D.L. Martin, R. Snyder, and I.A. Walter.
p. cm—(ASCE manuals and reports on engineering practice; no. 70)
Includes bibliographical references (p.) and index.
ISBN _____

Evaporation, evapotranspiration and irrigation water requirements: a manual/prepared by the Task Committee on Revision of Manual 70 Evapotranspiration and Irrigation Water Requirements, a task committee of the Environmental and Water Resources Institute of the American Society of Civil Engineers; edited by Marvin E. Jensen and Richard G. Allen; task committee members T.A. Howell, D.L. Martin, R. Snyder, and I.A. Walter.
p. cm—(ASCE manuals and reports on engineering practice; no. 70)
Includes bibliographical references (p.) and index.
ISBN _____
1. Evapotranspiration—Handbooks, manuals, etc. 2. Energy balance—Handbooks, manuals, etc. Estimating methods—Handbooks, manuals, etc. 4. Crop coefficients—Handbooks, manuals, etc. I. Jensen, Marvin Eli, 1926- II. Allen, Richard Glen, 1952- III. American Society of Civil Engineers, Evapotranspiration in Irrigation and Hydrology Technical Committee. IV. Series.
S_____

The material presented in this publication has been prepared in accordance with generally recognized engineering principles and practices, and is for general information only. This information should not be used without securing competent advice with respect to its suitability for any general or specific application.

The contents of this publication are not intended to be and should not be construed to be a standard of the American Society of Civil Engineers (ASCE) and are not intended for use as a reference in purchase specifications, contracts, regulations, statutes, or any legal document.

No reference made in this publication to any specific method, product, process, or service constitutes or implies an endorsement, recommendation, or warranty thereof by ASCE.

ASCE makes no representation or warranty of any kind, whether express or implied, concerning the accuracy, completeness, suitability or utility of any information, apparatus, product, or process discussed in this publication, and assumes no liability therefor.

Anyone utilizing this information assumes all liability arising from such use, including but not limited to infringement of any patent or patents.

(To be updated by ASCE) Authorization to photocopy material for internal or personal use under circumstances not falling within the fair use provisions of the Copyright Act is granted by ASCE to libraries and other users registered with the Copyright Clearance Center (CCC) Transactional Reporting Service, provided that the base fee of $____ per article plus $____ per page is paid directly to CCC, 27 Congress Street, Salem, MA 01970. The identification for ASCE Books is _____/__. $___ + $___. Requests for special permission or bulk copying should be addressed to /Permisions Department.

Copyright © 20__ by the American Society of Civil Engineers, All Rights Reserved.

Library of Congress Catalog Card No. _____
ISBN _____
Manufactured in the United States of America

MANUALS AND REPORTS ON ENGINEERING PRACTICE

(From ASCE Hydrology Handbook, 1996)
(As developed by the ASCE Technical Procedures Committee,
July 1930, and revised March 1935, February 1962, April 1982)

A manual or report in this series consists of an orderly presentation of facts on a particular subject, supplemented by an analysis of limitations. and applications of those facts. It contains information useful to the average engineer in his everyday work, rather than the findings that may be useful only occasionally or rarely. It is not in any sense a "standard," however; nor is it so elementary or so conclusive as to provide a "rule of thumb" for nonengineers.

Furthermore, material in this series, in distinction from a paper (which expresses only one person's observations or opinions), is the work of a committee or group selected to assemble and express information on a specific topic. As often as practicable the committee is under the direction of one or more of the Technical Divisions and Councils, and the product evolved has been subjected to review by the Executive Committee of the Division or Council. As a step in the process of this review, proposed manuscripts are often brought before the members of the Technical Divisions and Councils for comment, which may serve as the basis for improvement. When published, each work shows the names of the committees by which it was compiled and indicates clearly the several processes through which it has passed in review, in order that its merits may be definitely understood.

In February 1962 (and revised in April, 1982) the Board of Direction voted to establish:

> A series entitled 'Manuals and Reports on Engineering Practice,' to include the Manuals published and authorized to date, future Manuals of Professional Practice, and reports on Engineering Practice. All such Manual or Report Material of the Society would have been refereed in a manner approved by the Board Committee on Publications and would be bound, with applicable discussion, in books similar to past Manuals. Numbering would be consecutive and would be a continuation of present Manual numbers. In some cases of reports of joint committees, bypassing of Journal publication may be authorized.

AVAILABLE MANUALS AND REPORTS OF ENGINEERING PRACTICE

Number

List to be provided by ASCE.

EDITORS, TASK COMMITTEE AND REVIEW COMMITTE

Task Committee

Marvin E. Jensen, Co-Editor	Consultant, Fort Collins, Colorado (Formerly Director, Colorado Institute for Irrigation Management, and National Program Leader for Water Management, Agricultural Research Service, USDA).
Richard G. Allen, Co-Editor	Water Resources Engineering Professor, Kimberly Research and Extension Center, University of Idaho, Kimberly
Terry A. Howell	Laboratory Director, Conservation and Research Leader, Conservation and Production Laboratory, Agricultural Research Service, USDA, Bushland, Texas.
Derrel L. Martin	Professor, Department of Biological Systems, Engineering, University of Nebraska, Lincoln
Richard Snyder	Biometeorologist Specialist, Department of Land, Air and Water Resources, University of California, Davis
Ivan A. Walter	Principle, Ivan's Engineering, Centennial, CO.

Review Committee

Paul W. Brown	University of Arizona, Tucson
Ronald L. Elliott	University of Oklahoma (retired) Stillwater
Thomas W. Ley	Colorado Division of Water Resources, Pueblo
Thomas Trout	ARS, USDA , Fort Collins, CO

EVAPORATION AND EVAPOTRANSPIRATION (Manual 70 revised)
CONTENTS

Foreword xii

List of Frequently Used Symbols xiv

1. Introduction 1
- 1.1 Introduction to Second Edition 1
- 1.2. Development of ET and CU Studies in the USA 4
- 1.3 Second Edition 11

2. Evaporation and Evapotranspiration Processes 13
- 2.1 Introduction 13
- 2.2 The Water Budget 13
- 2.3 The Energy Budget 14
- 2.4 Controlling Factors 15
- 2.5 Estimating Concepts 19
- 2.6 Measurement Methods 20

3. Soil-Water-Plant-System 25
- 3.1 Introduction 25
- 3.2 Physical Properties of Water, Water Vapor and Air 25
- 3.3 Soil Properties 32
- 3.4 Soil-Water System 34
- 3.5 Vegetative (Crop) Properties 42

4. Energy Balance 47
- 4.1 Introduction 47
- 4.2 Energy Balance 47
- 4.3 Net Radiation 48
- 4.4 Soil Heat Flux Density. 67
- 4.6 Radiation Absorption and Energy Storage in Water 73

5. Surface Energy-Air Mass Interactions and the Concept of Reference ET 75
- 5.1. Introduction 75
- 5.2 Energy Balance-Air Mass Interactions. 78
- 5.3 Standardizing the Vegetative Cover 79

6. Evaporation from Water Surfaces 85
- 6.1 Introduction 85
- 6.2 Methods of Estimating Water Surface Evaporation 85
- 6.3 Example Applications of the Combination Method 107
- 6.4 Summary, Methods of Estimating Evaporation 116

7. Evapotranspiration from Land Surfaces: Water and Energy Balance Components for Measurement and Estimation 119
7.1 Introduction to Chapters 7-11 119
7.2 Volumetric Measurements for Estimating Land Surface ET 119
7.3 Mass Balance Methods 125
7.4 Energy Balance Methods 129
7.5 Mass Transfer Methods 135
7.6 Combined Energy Balance and Mass Transfer Methods 144
7.7 ET Estimates by Analogy or Association 155

8. Evapotranspiration from Land Surfaces: Reference Crop ET 161
8.1 Introduction 161
8.2 The Penman-Monteith Equation 161
8.3 Aerodynamic and Surface Parameters for the PM Equation 164
8.4 Reference ET_o K_c Approach 166
8.5 Bad or Missing Data 173

9. Evapotranspiration from Land Surfaces: Evaporation from Soil 185
9.1 Introduction 185
9.2 Evaporation from Soil 185
9.3 Diurnal Effects and Redistribution of Soil Water 186
9.4 Stage 1 Evaporation 187
9.5 Stage 2 Evaporation 188
9.6 Evaporation Models 190
9.7 Relations between Evaporation and Transpiration 203
9.8 Water Balance of the Evaporation Layer 204
9.8 Example Estimates of Evaporation 206

10. Evapotranspiration from Land Surfaces: Crop Coefficient Method 221
10.1 Introduction 221
10.2 The Crop Coefficient 221
10.3 Crop (Vegetation Cover) Coefficients 224
10.4 FAO Grass-Based Crop Coefficients 231
10.5 Alfalfa-Based Crop Coefficients. 242
10.6 Estimating K_c Curve for Natural and Agricultural Vegetation 245
10.7 Landscape Coefficients 251
10.8 Estimating K_c During Wintertime and Nongrowing Season 265
10.9 Summary 276

11. Evapotranspiration from Land Surfaces: Direct Penman-Monteith and Energy-Balance Equations 277
11.1 Introduction 277
11.2 Common Forms of Resistance-based Models 278
11.3 Challenges with Types of Resistance-based Models 291
11.4 Parameterizing the Penman-Monteith for Equivalency with Other Models . . 293

11.5 Comparative Model Performance 294
11.6 Roughness Length and Zero Plane Displacement 295
11.7 Bulk Surface (Stomatal) Resistance. 303

11.8 Evaporation from Soil and Surface Resistance 323
11.9 Direct Measurements for Direct Application of the PM and AFIB Methods . 331
11.10 Example Applications of the Single Layer Penman-Montheith 339
11.11 Applications of Evapotranspiration Models using Remote Sensing Inputs . . 350

11.12 Measurement and Estimation of ET on Sloping Lands. 351
11.13 Evaporation of Intercepted Rainfall 352

12. Evapotranspiration from Land Surfaces: Regional Estimates 355
12.1 Introduction 355
12.2 Theory 355
12.3 Applications 357

13. Selecting the Appropriate ET Estimating Technology 363
13.1 Introduction 363
13.2 Timeframe and Required Accuracy 363
13.3 Input Data Collection, Screening and Processing 363
13.4 Crop Coefficient Method vs. Direct Methods 364
13.4 Evaporation and Evapotranspiration Calculations 366
13.5 Summary. 367

14. Estimating Irrigation Water Requirements and Streamflow Depletions 369
14.1 Introduction 369
14.2 Evaporation and Evapotranspiration 369
14.3 Net Irrigation Requirements and Effective Precipitations 370
14.4 Leaching Requirement 372
14.5 Miscellaneous Water Requirements 376
14.6 System Losses 377
14.7 Improvements in Estimating Water Requirements 381

Appendices 385
A. Conversion and Meteorological Tables 385
B. Mean Crop Coefficients, K_c, for Well-managed Crops in Sub-Humid Climates for use with clipped grass reference ET_o, Range of Maximum Effective Rooting Depth, and Soil Water Depletion Fraction for No Stress, p, based on FAO-56. 395
C. Lengths of Crop Development Stages for Various Planting Periods and Climatic Regions 397
D. Basal Crop Coefficients, K_{cb}, for Well-managed Crops in Sub-Humid Climates for use with clipped grass reference ET_o, based on FAO-56 399
E. Mean and Basal Crop Coefficients, K_c and K_{cb}, for Crops Common to Temperate and Continental Climates for use with Alfalfa Reference ETr as Computed by the ASCE Standardized Penman-Monteith Reference Method 409

F. Basal Crop Coefficients, K_{cb}, for Crops Common to Temperate and Continental Climates for use with Alfalfa Reference ET_r as Computed by the ASCE Standardized Penman-Monteith Reference Method using a Growing-Degree-Day Basis 411
G. Documentation for Crop Coefficient and ET Data Reporting and Determination of ET from Remote Sensing and Sap Flow Measurement 413
H. Weather Data Integrity 419
I. Contributions of Capillary Flow From a Shallow Water Table to E & T. 457
J. Derivation of the Penman-Monteith Equation 465
K. Regional Estimating Methods and Methods not Commonly Used in the USA 471
L. Comparison and Ranking of Methods for Estimating ET 481
M. Glossary 503

References 509

Index 553

COMMITTEE ON
EVAPOTRANSPIRATION IN IRRIGATION AND HYDROLOGY

The purpose of this committee is to advance the science and practice of measuring and estimating evapotranspiration by irrigated and rain-fed agriculture and of naturally occurring vegetation. Emphasis will be placed on the development and evaluation of procedures and tools for the advancement of integrated water management and determination of water requirements and water balances in relation to planning, design, and management of irrigation projects, hydrologic units and water resources systems.

This committee was originally the Committee on Consumptive Use of Water for Irrigated Crops and Native Vegetation. It began planning a manual in 1965. The Committee was restructured in 1968 and renamed Committee on Irrigation Requirements. The new Committee held its first meeting December 6, 1968 to plan a consumptive use report. The camera-ready copy of the Consumptive Use Report was completed in 1973 and the Report was published in 1974.

During the 1974-1989 period, numerous revisions and reviews of the CU Report were made by members of this Committee. A concentrated effort by the editors working with the Review Committee during the period 1985-87 resulted in a complete revision of the CU Report and publication of Manual 70 in 1990.

M. E. Jensen served as Chairman of this committee from October 1, 1968 to September 30, 1973. R. D. Burman served as Chairman from October 1, 1973 to September 30, 1983. R. W. Hill served as Chairman from October 1, 1983 to September 30, 1985. R. H. Cuenca served as Chairman from October 1, 1985 to September 30, 1987. E. L. Johns served as Chairman from October 1, 1987 to September 30, 1989.

R. G. Allen served as Chairman from October 1, 1989 to September 30, 1992; T. A. Howell from October 1, 1992 to September 30, 1993; I. A. Walter from October 1, 1993 to September 30, 1995.

The Committee was renamed the “Evapotranspiration in Irrigation and Hydrology” Technical Committee in 1995 so as to include evapotranspiration for non-irrigated lands. B. J. Bowman served as Chairman from October 1, 1995 to September 30, 1997; D. L. Martin from October 1, 1997 to September 30, 1999; R. L. Elliott from October 1, 1999 to November 30, 2000; and R. G. Allen from October 1, 2000 to September 30, 2003; Daniel Itenfisu from October 1, 2003 to September 30, 2005, Douglas Hunsaker from October 1, 2005 to September 30, 2007, Michael Dukes from October 1, 2007 to September 30, 2009, Suat Irmak from October 1, 2009 to September 30, 2011, Thomas Ley from October 1, 2011 to September 30, 2013, Prasanna Gowda from October 1, 2013 to the present.

In June 2000, the 1700 copies of Manual 70 had been sold. The Task Committee to revise Manual 70 under the co-leadership of Marvin Jensen and Richard Allen was established.

Foreword

This manual revises ASCE Manual "Evapotranspiration and Irrigation Water Requirements" published in 1990. It incorporates many years of user experience with the previous Manual and recent advances in the physics of evaporation from plant and soil surfaces. It incorporates extensive material from the ASCE Hydrology Handbook. The first edition of the Manual required many years of planning and its organization evolved through a series of revisions starting with the report "Consumptive Use and Irrigation Water Requirements" published in 1974. Manual 70 has been used widely by researchers, practicing engineers, and students in their basic training and in graduate work. Manual 70 followed the same organization as the CU Report with several new sections added. This revised edition has been restructured based on the experience gained by users of Manual 70. A chapter on procedures for estimating evaporation from shallow and deep water bodies has been added to assist the estimation of water losses associated with irrigation regulating reservoirs and other small storage reservoirs.

Data sets used for the evaluations have been revised based on new data and information from the test sites. In this edition, evaluations have focused on accuracy of estimates rather than on comparing various estimating methods as was done in the first edition. Some comparative statistics among ET methods as was done in the first edition is repeated in Appendix L of this edition.

SI units are used throughout the manual as was done in the first edition. The SI unit used for daily total energy, megajoules per square meter, was retained even though some users may prefer to work with average daily or hourly energy units of watts per square meter.

This manual provides information on evaporation and evapotranspiration that are needed by practicing engineers, hydrologists and others in evaluating data received from various sources. It also provides background information to enable practicing engineers, educators and researchers to improve procedures for estimating evapotranspiration to achieve the accuracy needed for specific purposes.

Background information on consumptive use in Chapter 1 of the first edition was originally prepared by early experts such as H. F. Blaney, Sr. Part of this information was retained in the second edition for historical purposes.

Co-Editors: Marvin E. Jensen, and Richard G. Allen

ACKNOWLEDGEMENTS

The following organizations contributed valuable assistance in the research and preparation of the 2nd edition of this manual.

- University of Idaho Research and Extension Center, Kimberly, ID
- Agricultural Research Service, U.S. Department of Agriculture, Bushland, TX
- Agricultural Research Service, U.S. Department of Agriculture, Kimberly, ID
- Department of Land, Air and Water Resources, University of California, Davis, CA
- Department of Biological Systems, Engineering, University of Nebraska, Lincoln, NE
- Ivan's Engineering, Inc., Centennial, CO
- Dr. Frank H. Quinn, Great Lakes Environmental Research Laboratory, NOAA, Ann Arbor, MI and Prof. Emeritus William O. Pruitt, University of California, Davis, CA were primary contributors to Chapter 4 - Evaporation and Evapotranspiration of the ASCE Hydrology Handbook (2nd ed.) which served as a major source of material for this revised version of Manual 70.
- The meticulous and long-term collection of accurate and representative agricultural ET data from weighing lysimeter systems by W.O. Pruitt of the University of California, Davis, and Dr. James L. Wright of the USDA-ARS, Kimberly, ID, (ret.) contributed substantially to the foundation of crop coefficient tables summarized in this 2nd edition. Lysimeter measurement of grass reference ET by Pruitt and alfalfa reference ET by Wright provided much of the basis for the form and calibration of the ASCE Standardized Penman-Monteith equation recommended in this revised edition.
- The ASCE-EWRI Task Committee (ASCE-EWRI, 2005) on Standardized Calculation of Reference Evapotranspiration Calculation recommended definitions and calculation procedures for reference ET and supporting equations.
- United Nations Food and Agriculture Organization and International Commission on Irrigation, Drainage and Flood Control (ICID) supported development of international standardization of ET and associated crop coefficients and helped organize data and methods for ET estimation in FAO-24 (Doorenbos and Pruitt 1977) and FAO-56 (Allen et al. 1998). Crop coefficient material from these publications is included in Appendices B-F.
- Blue Ribbon Panel Reviewers Thomas W. Ley, Colorado Division of Water Resources, Pueblo; Ronald L. Elliott, University of Oklahoma (retired) Stillwater; Thomas Trout, ARS, USDA, Fort Collins, CO; Paul W. Brown, University of Arizona, Tucson contributed substantially to the completeness and accuracy of the manuscript.
- Professor Luis Santos-Pereira and students of the University of Lisbon, Portugal provided long-term review, testing and validation of many concepts and methodologies described in this Manual.
- Thanks are due to the Northern Colorado Water Conservancy District for hosting the Task Committee and providing facilities for the task committee to meet in November 2004.
- Co-editor Marvin Jensen, who has retired and donated his books, greatly appreciates the tremendous input to the revised manual provided by Rick Allen. Rick has kept abreast of recent developments on measurement and methods for measuring and estimating ET.

FREQUENTLY USED ACRONYMS AND SYMBOLS[1]

In a few cases, the same symbol is used for different variables. Not all symbols are listed, only those most frequently used.

Acronym	Explanation	Common Units[2]
AW	Available soil water	general use
BREB	Bowen Ratio Energy Balance	general use
E	Evaporation	general use
ET	Evapotranspiration	general use
LAI	Leaf area index	general use
PM	Penman-Monteith	general use
VPD	Vapor pressure deficit	general use

Symbol	Explanation	Common Units[3]
A	Area	m^2
C_n	Numerator coefficient for the ASCE Standardized PM Equation	- - -
C_d	Denominator coefficient for the ASCE Standardized PM Equation	- - -
λE	Latent heat flux density	MJ m^{-2} d^{-1}, MJ m^{-2} h^{-1}, W m^{-2}
E	Evaporation, depth rate	mm d^{-1}, mm h^{-1}
	E_o = rate from free water	mm d^{-1}, mm h^{-1}
	as latent heat flux density, λE	MJ m^{-2} d^{-1}, MJ m^{-2} h^{-1}, W m^{-2}
EC_e	Electrical conductivity of the saturated soil extract (1 mmho cm^{-1} = 1 dS m^{-1})	dS m^{-1}
E_{eq}	Equilibrium evaporation	mm d^{-1}, mm h^{-1}
E_{pan}	Evaporation rate from Class A pan	mm d^{-1}
ET	Evapotranspiration rate	mm d^{-1}, mm h^{-1}
ET_c	ET from a particular crop	mm d^{-1}, mm h^{-1}
ET_o	ET from a well-watered grass reference crop	mm d^{-1}, mm h^{-1}
	as latent heat flux density, λET_o	MJ m^{-2} d^{-1}, MJ m^{-2} h^{-1}, W m^{-2}
ET_r	ET from a well-watered alfalfa reference crop	mm d^{-1}, mm h^{-1}
	as latent heat flux density, λET_r	MJ m^{-2} d^{-1}, MJ m^{-2} h^{-1}, W m^{-2}
ET_{ref}	Reference evapotranspiration, general	mm d^{-1}, mm h^{-1}
G	Heat flux density to the ground	MJ m^{-2} d^{-1}, MJ m^{-2} h^{-1}, W m^{-2}
G_{sc}	Solar constant	MJ m^{-2} h^{-1}, W m^{-2}
H	Heat flux density to the air	MJ m^{-2} d^{-1}, MJ m^{-2} h^{-1}, W m^{-2}
J	Day of the year	- - -
K_s	Adjustment coefficient for water stress	- - -
K_A	Clearness index for solar radiation	
K_B	Clearness index for direct beam solar radiation	- - -
K_c	Crop coefficient general (not the same as the Blaney-Criddle K)	- - -
K_{cb}	Crop coefficient (basal), soil water not limiting transpiration, but the soil surface is visually dry	- - -
K_{cm}	Mean, or single, crop coefficient	- - -

[1] Less frequently used symbols and empirical expressions are as defined in the text.
[2] Other dimensions as specified in the text.
[3] Other dimensions as specified in the text.

Symbol	Explanation	Common Units[4]
K_e	Coefficient to adjust for increased evaporation from the soil	- - -
K_t	Turbidity coefficient	- - -
LAI	Leaf area index	- - -
LF	Leaching fraction	- - -
LR	Leaching requirement	- - -
P	Atmospheric pressure	kPa
P	Precipitation	mm
Q_i	Inflow rate	$m^3\ d^{-1}$
Q_o	Outflow rate	$m^3\ d^{-1}$
R	Gas constant	kJ kg^{-1} K^{-1}
R	Universal gas constant	kJ kg^{-1} K^{-1}
R	Radiation, general	MJ m^{-2} d^{-1}, MJ m^{-2} h^{-1}, W m^{-2}
R_a	Extraterrestrial solar radiation on a horizontal surface	MJ m^{-2} d^{-1}, MJ m^{-2} h^{-1}, W m^{-2}
R_b	Net outgoing long-wave radiation	MJ m^{-2} d^{-1}, MJ m^{-2} h^{-1}, W m^{-2}
R_{bo}	Net outgoing longwave radiation on a cloudless day	MJ m^{-2} d^{-1}, MJ m^{-2} h^{-1}, W m^{-2}
R_n	Net incoming radiation	MJ m^{-2} d^{-1}, MJ m^{-2} h^{-1}, W m^{-2}
R_{nl}	Net outgoing long-wave radiation	MJ m^{-2} d^{-1}, MJ m^{-2} h^{-1}, W m^{-2}
R_{ns}	Net solar radiation	MJ m^{-2} d^{-1}, MJ m^{-2} h^{-1}, W m^{-2}
R_s	Solar radiation at the surface on a horizontal plane	MJ m^{-2} d^{-1}, MJ m^{-2} h^{-1}, W m^{-2}
R_{so}	Solar radiation on a cloudless day	MJ m^{-2} d^{-1}, MJ m^{-2} h^{-1}, W m^{-2}
RH	Relative humidity	%
RH_{max}	Daily maximum relative humidity	%
RH_{min}	Daily minimum relative humidity	%
T	Temperature	°C, K, °F
T_o	Surface temperature	°C, K
T_{max}	Maximum daily air temperature	°C, K
T_{min}	Minimum daily temperature	°C, K
T_d	Dewpoint temperature of the air	EC
T_w	Wetbulb temperature of the air	EC
VPD	Vapor pressure deficit	kPa
W_f	Wind function, linear $W_f = a_w + b_w u_2$	- - -
a, b	Constants	See usage
c_p	Specific heat at constant pressure	kJ kg^{-1} EC^{-1}
d	Zero plane displacement of wind profile	cm, m
e	Water vapor pressure in air	kPa
e_a	Actual vapor pressure	kPa
e_s	Saturation vapor pressure	kPa
e^o_d	Saturation vapor pressure at dew point temperature of air	kPa
e^o_z	Saturation vapor pressure of air at height z	kPa
e^o_w	Saturation vapor pressure at wet bulb temperature	kPa
g	Acceleration of gravity	m s^{-2}

[4] Other dimensions as specified in the text.

Symbol	Explanation	Common Units[2]
g_s	Surface conductance	m s^{-1}
h	Height of vegetation	cm, m
k	von Karman's constant	- - -
k_p	Evaporation pan coefficient	- - -
m	Mass, m_v for water vapor, m_a for dry air, m_s for soil	kg m^{-3}
q	Specific humidity = $m_v (m_v + m_a)^{-1}$	- - -
r_a	Diffusion resistance of air layer (aerodynamic resistance)	s m^{-1}
	r_{ah} for sensible heat flux	s m^{-1}
	r_{av} for vapor flux	s m^{-1}
r_i	Internal leaf diffusion resistance	s m^{-1}
r_l	Single leaf stomatal resistance	s m^{-1}
r_s	Surface resistance (generally a bulk canopy resistance)	s m^{-1}
t	Time	s, h, d
u_z	Horizontal wind speed at height z	m s^{-1}, km d^{-1}
z	Elevation	cm, m
z_{ov}	Roughness length, heat and water vapor	cm, m
z_{om}	Roughness length, momentum	cm, m
α	Shortwave reflectance coefficient or albedo	- - -
β	Bowen ratio, = $H/\lambda E$	- - -
γ	Psychrometric constant, $\gamma = c_p P/(0.622\lambda)$	kPa EC^{-1}
γ^*	Psychrometric constant modified by the ratio of surface resistance to atmospheric resistance, $\gamma^* = \gamma(1 + r_s/r_a)$	kPa EC^{-1}
Γ	Adiabatic lapse rate	^oC m^{-1} and K m^{-1}
Δ	Slope of the saturation vapor pressure-temperature curve, de/dT	kPa $^oC^{-1}$
Δ	Difference	See usage
ε	Emissivity, ε' = net emissivity, ε_a = atmospheric emissivity and ε_{vs} = vegetative and soil emissivity	- - -
θ	Volumetric soil water content	- - -
λ	Latent heat of vaporization	MJ kg^{-1}
π	Pi, $\pi = 3.14159$	- - -
ρ_a	Air density, ρ_w for water vapor, ρ_b for bulk soil, and ρ_y for absolute humidity	kg m^{-3}
σ	Stefan-Boltzmann constant	kJ m^{-2} s^{-1} K^{-4}, MJ m^{-2} d^{-1} K^{-4}, W m^{-2} K^{-4}
ω_s	Sunset hour angle	radians

MAIN SUBSCRIPTS

a	Property of air
o	Property at the atmosphere-surface interface, or reference value
s	Property of soil or the surface
v	Property of vegetation or vapor
w	Property of water
z	Property at height z
$1, 2$	Reference times

MAIN SUPERSCRIPT

o	Saturation

[1] Symbols for empirical equations are as defined in the text.
[2] Other dimensions are as specified in the text.

INTERNATIONAL SYSTEM OF UNITS (SI)

Frequently used SI units and symbols (ASTM, 1976; Wandmacher and Johnson, 1995):

Quantity	*Unit*	*Symbol*	*Formula*
	Base Units		
length	meter	m	
mass	kilogram	kg	
time	second	s	
electric current	ampere	A	
thermodynamic temperature	kelvin	K	
amount of substance	mole	mol	
	Derived Units		
force	newton	N	$kg\ m\ s^{-2}$
pressure	pascal	Pa	$N\ m^{-2}$
energy, work, quantity of heat	joule	J	N m
radiant flux	watt	W	$J\ s^{-1}$
electric potential	volt	V	$W\ A^{-1}$
conductance	siemens	S	$A\ V^{-1}$

Prefixes		
Multiplication factor	*Prefix*	*Symbol*
$1000\ 000\ 000 = 10^9$	giga	G
$1\ 000\ 000 = 10^6$	mega	M
$1\ 000 = 10^3$	kilo	k
$0.1 = 10^{-1}$	deci	d
$0.01 = 10^{-2}$	centi	c
$0.001 = 10^{-3}$	milli	m
$0.000\ 001 = 10^{-6}$	micro	:
$0.000\ 000\ 001 = 10^{-9}$	nano	η

Units in Use with SI

Quantity	*Unit*	*Symbol*	*Definition*
time	minute	min	1 min = 60 s
	hour	h	1 h = 60 min = 3600 s
	day	d	1 d = 24 h = 86 400 s
temperature	degree Celsius	EC	EC = K - 273.15
volume	liter	L	$1\ L = 1\ dm^3 = 10^{-3}\ m^3$
mass	metric ton	t	$1\ t = 10^3\ kg$

In Memory

In loving memory of Doris Jensen, 1929 – 2009, life-long spouse, supporter, encourager and traveling companion of Marvin Jensen.

In fond memory of William Oregon Pruitt, 1922 – 2009, Irrigation Engineer at the University of California-Davis, who was a primary leader in developing and advancing the concept of reference crop evapotranspiration and transferrable crop coefficients, in trusting the use of energy balance equations to estimate ET, in advocating data and research quality and integrity, and promoting education in experimental methods.

In fond memory of John Lennox Monteith, 1929 – 2012, who influenced many Americans in the application of physical principles to describe how plants interact with their immediate environment and microclimate, with his own work leading to the evolution of the Penman combination equation into the Penman-Monteith equation that has become a primary basis for estimating irrigation water requirements.

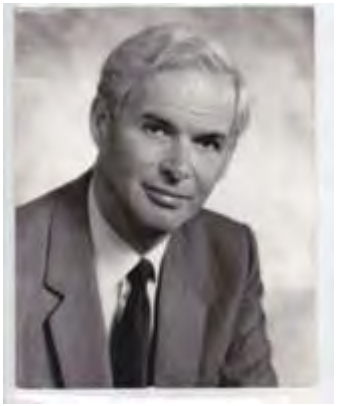

1

Introduction and History

1.1. Introduction to Second Edition

In 1990, the American Society of Civil Engineers (ASCE) published the first edition of *Manuals and Reports on Engineering Practice—No. 70*, which was prepared by the Irrigation Water Requirements Committee of the Irrigation and Drainage Division. In 1995, the Committee was renamed the "Evapotranspiration in Irrigation and Hydrology Technical Committee" so as to include evapotranspiration on non-irrigated lands. The mission of the committee is to advance the science and practice of measuring and estimating evapotranspiration with emphasis on developing and evaluating procedures and tools for integrated water management needed in planning, design, and management of irrigation projects, hydrologic units and water resources systems. In 2000, when the stock of printed copies had been sold, the Committee appointed a Task Committee to prepare an updated revised edition of the *Manual*.

Since its publication, *Manual 70* has served as a valuable reference for specialists working in agro-meteorology, hydrology and irrigation planning and management. The first edition contained a broad range of equations for estimating evapotranspiration, both theoretical and empirical, and a broad range of equations to calculate parameters in the ET equations and for various components of the energy balance. Since the general knowledge base of users has improved greatly over the past two decades, the manual has been restructured for greater ease in applying new technology and standardized calculations, and new information has been included. The manual's current focus is on state-of-the-art technology with less emphasis on older empirical equations and comparisons among various methods of estimating evapotranspiration (ET).

This revised edition includes extensive material from the ASCE Hydrology Handbook, chapter 4 (Allen et al. 1996) that was a product of the same ET technical committee noted above. In addition, additional material on the standardization of reference ET calculation and clarification of its application developed by a task committee of the ET committee from 1999 through 2004 (ASCE-EWRI 2005) has been brought into this edition. Since integrated water management often involves estimating evaporation from water bodies such as storage and regulating reservoirs, new material on estimating evaporation (E) from water surfaces has been added.

The revised edition presents a variety of methods for estimating ET as well as example calculations as a guide to users in applying the new technology. Graduate students preparing to enter one of these fields should find this manual to be useful as a source of basic information. Tables of basic air and water properties, conversion factors, and meteorological tables are retained for reference purposes.

Objectives

Objectives of the first edition of Evapotranspiration and Irrigation Water Requirements were:

1. To define and interpret ET, or consumptive use, terminology.
2. To provide practicing engineers, hydrologists, educators and researchers with a concise summary of factors controlling ET.

3. To describe modern methods for measuring and estimating ET.
4. To describe the major factors that must be considered in determining irrigation water requirements for fields, farms, projects and river basins.
5. To summarize representative measured ET from irrigated crops.
6. To evaluate the accuracy of various estimating procedures under various climatic regimes.
7. To present improvements in methods for estimating ET.
8. To present a selected bibliography for additional information.

The large volume of recent literature on ET makes it impractical for the engineer who does not specialize in this field to review and evaluate available ET data and methodology best suited for solving a particular hydrology, irrigation or water supply problem. The first edition of this manual was intended to meet this continuing need. Many of these same objectives are still current, however, recent improvements and acceptance of standardized methods for estimating ET make review of historic, or empirical, methods less relevant. The new objectives include more focus on the latest technology for estimating ET and E during both the growing and the non-growing season and E from water bodies that may be associated with irrigation projects. These include numerical models and the use of remotely sensed variables for estimating ET over large areas.

Chapter Content

This chapter presents a brief summary of the history of activities leading to the development of the first edition and preparation of the revised edition. As competition for available water resources continues to increase, transfers of water rights and associated litigation require background on historical water use measurements and the methods that were used previously to estimate crop water requirements. Summaries of older ET estimating procedures have been retained in the appendices for reference purposes along with a summary of comparisons of estimating methods that were presented in the first edition.

Chapter 2 presents a brief summary of evaporation (E) and evapotranspiration (ET) processes. Factors controlling the E and ET processes are briefly described. These include water and energy budgets, and vegetation, soil, and management factors. Concepts for estimating evaporation from soils and water surfaces and estimating ET are summarized in chapter 2 and presented in detail in chapters 4 to 6. Brief descriptions of E and ET measurement methods from land surfaces including measuring changes in soil water content over time, lysimetry, Bowen ratio energy balance, eddy covariance and water balance are introduced in chapter 2 and are discussed in detail in chapters 7-11.

Chapter 3 describes the soil-water-plant system beginning with a summary of the physical properties of water, water vapor and air. Equations relating the various variables are presented. Soil properties are summarized along with equations relating the energy state of soil water. Equations describing the soil water characteristics along with basic equations of water flow through soil are presented. A summary of soil water properties as influenced by soil texture is presented followed by a summary of soil-plant characteristics. Vegetative, or crop, properties and plant root characteristics are described.

Chapter 4 presents a detailed summary of the surface energy balance with descriptions of the components of net radiation. Surface properties affecting the absorption and reflection of solar

radiation are summarized. Equations are presented for calculating components of net radiation. The surface energy balance is emphasized throughout the revised edition because of its importance in establishing upper limits on the transformation of liquid water to vapor and consequently ET. The surface energy balance forms the basis of the most complete and accurate ET equations, including the Penman and Penman-Monteith methods.

Chapter 5 describes surface-atmosphere interactions that affect net radiation and the ET process. Emphasis is placed on the use of a standardized surface so as to isolate the evaporative demand due to weather effects. Two surfaces are described. These are a short crop such as clipped grass and a tall crop such as alfalfa having about 0.5-m plant height.

Chapter 6 describes typical methods of estimating evaporation from water surfaces. These include use of an evaporation pan with appropriate coefficients, water balance, aerodynamic and energy balance procedures along with the use of combination methods. Several examples of estimating evaporation using a combination method are presented as well as important precautions.

Chapter 7 describes methods of estimating ET from land surfaces using various methods. These methods include a detailed discussion of volumetric measurement of soil water depletion, and the use of lysimeters and evaporimeters. Procedures based on energy balance and aerodynamic methods are described. These include the Bowen ratio energy balance and eddy covariance methods along with fetch requirements for these methods. Detailed descriptions of the methods are presented along with example calculations and recommendations for collection of accurate data.

Chapter 8 describes the procedures for estimating ET from land surfaces using the Penman-Monteith (PM) equation. Detailed description of the PM equation is presented with guidelines for characterizing the surface parameters that determine the bulk aerodynamic resistance. Special emphasis is placed on the development of the standardized equation for estimating ET from a reference crop surface and the use of vegetative coefficients to estimate ET.

Chapter 9 describes the development of typical soil water profiles during evaporation from soils, stage 1 and stage 2 evaporation, evaporation models for estimating evaporation and evaporation-transpiration relations, and example estimates of evaporation compared with measured evaporation.

Chapter 10 describes the crop coefficient (and landscape coefficient) method for estimating evaporation from land surfaces. It summarizes the development of coefficients to characterize ET as a function of the amount of natural or landscape vegetation or the development of annual or perennial crops. These coefficients are used in conjunction with an estimate of evaporative demand or reference ET such as short clipped grass or 0.5-m tall alfalfa. An example of generalized mean crop coefficient illustrates the effects of increasing leaf area, surface wetness, and decreasing available soil water. Basal crop coefficients, representing conditions when the soil surface is visually dry are also described. With basal coefficients, adjustments are made when the surface is wetted by rainfall or irrigation. Characteristics of evaporation from bare soils are described along with typical soil water profiles in the upper layers of soil. The effects of leaf area on the rate of evaporation are described along with several methods for estimating the amount of evaporation. The typical linear FAO-style crop coefficient curve is described along with procedures for estimating the magnitude of the various growth stages and durations including several example calculations.

Chapter 11 describes procedures for estimating evaporation from land surfaces using the direct Penman-Monteith (PM) equation and full energy balance equations. Procedures include

estimating surface roughness, zero-plane displacement, relationships between surface roughness and plant height, example roughness length scalars, determining roughness and zero plane displacement from wind profile measurements, estimating leaf areas and leaf resistances, bulk surface resistance for various types of green vegetation cover and stomatal conductance. Procedures for estimating evaporation from soil using the direct PM method and evaporation from intercepted rainfall are also described. Required weather measurements for using the direct PM are described along with procedures for adjusting non-characteristic data. Several calculation examples are presented, including estimates for sloping lands.

Chapter 12 describes several methods for regional estimates of evaporation from land surfaces. These include the complementary approach and the use of energy balance models for forests and grasslands and for cultivated lands. Approximating monthly streamflow for ungaged watersheds is briefly described along with data sources for cultivated areas and natural vegetation.

Chapter 13 briefly summarizes the factors to consider in selecting a method for estimating ET. These include the available timeframe, required accuracy, and the screening of input climate data. A brief summary of the various methods available for ET calculations is presented.

Chapter 14 summarizes methodology for estimating irrigation water requirements and refers to various chapters and sections in the manual for specific details. It includes procedures for estimating soil leaching requirements, miscellaneous water requirements, and effective precipitation. Brief descriptions of storage and distribution system losses and methods to account for non-uniform water applications are provided.

The appendices include several appendices from the first edition such as a saturation vapor pressure-temperature table, conversion factors, thermodynamic constants, air density equations, and an updated glossary. New appendices include several sets of crop coefficients, a listing of recent publications that include crop coefficients, weather data assessment, contribution of capillary flow to E and ET, a summary of estimating methods no longer commonly used in the USA, a derivation of the Penman-Monteith equation, and a summary of comparisons of estimating methods that were presented in the first edition.

1.2. Development of ET and CU Studies in the USA

Consumptive Use and Evapotranspiration

Consumptive use (CU) of water, or *evapotranspiration*, is one of the most basic components of the hydrologic cycle. It affects the water balance from the time water falls upon the land as precipitation until the residual reaches the ocean. Consumptive use, which includes evaporation of water from land and water surfaces, transpiration by vegetation, and the generally small volume of water contained in the harvested vegetation, continues to be of foremost importance in water resources planning and management and in irrigation management. Consumptive use has been particularly important in arid and semiarid irrigated areas of the world. It will become more important as available water resources are reallocated to meet various needs of growing populations. Its importance in humid areas has been increasing with the expansion of supplemental irrigation and inadequate water storage.

The term *evapotranspiration* (ET) has become more common than the term consumptive use. ET is the same as consumptive use except the latter includes water that is retained in the plant tissue that is minor relative to the total ET. The term ET is used throughout this edition.

Knowledge of ET is necessary in planning and operating water resource projects. ET is involved in problems of water supply, both surface and underground, water management, and in the economics of multiple-purpose water projects for irrigation, power, water transportation, flood control, municipal and industrial water uses, and in waste water reuse systems.

ET is important in negotiating water compacts and treaties and in the litigation and adjudication of water rights in major river systems in which the welfare of people in urban centers, states and even nations is involved. ET data are essential for estimating irrigation water requirements. They also are useful for estimating municipal and industrial water needs, in sizing wastewater reuse systems, in estimating water yield from watersheds, estimates of recharge to and safe yields from ground water basins, and stream-flow depletions in river basins.

Numerous formulae have been developed that relate ET and climatological data based on physical theory and experimental data collected by engineers and scientists. These formulae are used to transpose observed ET data from one area to other areas where few or no data, except climatological records, are available.

The standardization of methodology and availability of data for estimating ET have been improved greatly since the 1950s, and they are still evolving. Engineers, agronomists, soil scientists, and water planners need to adapt relationships that are based on sound physical laws and principles. Future estimates of ET will need to be more accurate than in the past as competition for water increases and its value increases. The legal system involved in water rights transfer can no longer justify "simple" estimating procedures if more accurate methods are available.

Historical Background (USA)

The first edition contained a brief summary of developments of methodology for estimating consumptive use, or ET. Evaporation and transpiration have been studied for centuries (Brutsaert 1982), but the term "consumptive use" probably was not applied to water consumption prior to 1900 in the USA. The first edition also briefly summarized extensive early plot and field studies of ET using soil-sampling techniques.

In 1938, the National Resources Committee (Blaney et al. 1938) published definitions of consumptive use (ET). The ASCE Hydrology Handbook (Anonymous 1949), stated: "...the terms 'evapotranspiration' and 'consumptive use' have received general acceptance, these terms denote the quantity of water transpired by plants during their growth or retained in the plant tissue, plus the moisture evaporated from the surface of the soil and the vegetation, expressed in feet or inches depth of water lost or used in a specified time."

Definitions of some other terms such as *duty of water* sometimes have been confused with consumptive use. In this manual, the terms "consumptive use" and "evapotranspiration" are considered synonymous because the amount of water contained within plant tissue is very small compared with that evaporated from soil and plant surfaces.

An excellent summary of seasonal consumptive use of water was prepared by the Duty of Water Committee of the Irrigation Division, ASCE, and presented in 1927 and later published (Anonymous 1930). Major changes made by engineers and scientists during the second half of the last century are summarized in a number of publications such as the proceedings of a meeting of physicists in 1955 (Penman 1956a), various conferences on ET (Jensen 1966; ASAE 1985, and Camp et al. 1996), and recent publications such as FAO-56 (Allen et al. 1998). Jensen and Allen (2000) summarized historic events and methods for estimating ET at the ASAE 2000

National Irrigation Symposium. An early, major compilation of energy balance theory, current methods and comparisons was made by the ASCE Consumptive Use committee and compiled by Jensen (1974). That publication served as the basis for the first edition of the committee's Manual 70.

Studies of irrigation water requirements can be traced back many centuries to when irrigation was first practiced as civilization began to rely on agriculture as a way of life. In the first edition, a brief summary of irrigation water requirement studies was presented to show that many recent investigations have only refined general concepts that have been known for decades. Other studies have advanced the science of ET, and have formed the foundation of current and future, modern irrigation management technology.

Problems of non-representative environmental conditions plaguing studies that measured ET using pots and containers and biases caused by unsaturated drainage between sampling dates were recognized in the 1920s. The energy balance concept, which was applied to evaporation from water surfaces in the twenties and thirties, was applied to cropped surfaces by Penman (1948) and Budyko (1948). Penman combined energy balance and aerodynamic equations into what is commonly known as the "combination equation." The Penman equation is well known and improved versions of the combination equation have been and are used extensively throughout the world. Monteith (1987) presented background and history of Penman's career and equation developments.

With modern and continuously evolving electronic instrumentation, investigations of evaporation and transpiration literally mushroomed during the 1960s, 1970s, and 1980s. Special studies have now been conducted in many countries. Unfortunately, increased sophistication of, or reduced costs of measurement methods have not necessarily improved the accuracy of data collection and, in fact, have frequently facilitated measurement by individuals having too little experience, care or understanding of the physics and methodology, resulting in data having relatively poor accuracy. Allen et al. (2011a) summarized errors common to modern ET measurement methods. Much of that material is repeated in Chapter 2. Since water resources management has played an increasingly more dominant role in regional, national, and international affairs, crop water requirements and irrigation water management have received more attention at all levels of planning.

The Food and Agricultural Organization (FAO) of the United Nations produced and landmark publication on crop water requirements in 1975 (Doorenbos and Pruitt 1975) that was revised in 1977 (Doorenbos and Pruitt 1977). This publication, referred to as FAO-24, almost singly converted ET estimation practices worldwide to the use of reference ET and reference ET-based crop coefficients. The International Commission on Irrigation and Drainage (ICID) Work Group on Crop Water Requirements sponsored a round table conference on evapotranspiration in Budapest, Hungary, in May 1977 (Perrier and Jensen 1979). Definitions originating with the 1977 conference were published in 1985 (Perrier 1985). The Work Group organized an international conference on Crop Water Requirements in Paris in September 1984 (Perrier 1985).

A workshop on Evapotranspiration from Plant Communities was held in Bunbury, West Australia in May 1982. A selection of papers presented at that workshop was later published (Sharma 1984). The American Society of Agricultural Engineers sponsored a symposium on Advances in Evapotranspiration in December 1985 that involved several international speakers (ASAE 1985). This symposium summarized advancements in evapotranspiration theory, measurement and application methods. In 1990, the FAO organized an expert's conference to discuss updating FAO-24 (Smith et al. 1991). The results of that conference were incorporated

into an expanded and refined version of FAO-24 that was published as FAO-56 (Allen et al. 1998) where a single equation for reference ET in the form of the standardized Penman-Monteith equation was recommended. This ASCE Committee organized an international symposium on Lysimetry for Evapotranspiration and Environmental Measurements in 1991 (Allen et al. 1991b). In 1993, a second workshop on Crop-Water Models was organized by the Working Group on Crops and Water Use of the International Commission on Irrigation and Drainage (Pereira 1995). In 1996, the American Society of Agricultural Engineers sponsored an international conference on Evapotranspiration and Irrigation Scheduling (Camp et al. 1996)

The references cited above, along with many other references cited in the first edition of this manual, provide detailed coverage of extensive studies of evapotranspiration and crop water requirements. Readers interested in more detailed aspects of evapotranspiration will find these references to be useful starting points. In addition, many books on hydrology and climatology include sections on evapotranspiration. Some books focus on the principles of the evaporation process such as those of Monteith (1973), Brutsaert (1982), Rosenberg et al. (1983), Monteith and Unsworth (1990) and Campbell and Norman (1998). Other books summarize the results of recent conferences. For example, the publication by The Netherlands Committee on Hydrologic Research contains a series of papers that were presented at Technical Meeting 44 at Ede, The Netherlands on 25 March 1987. These papers summarized progress that had been made on this subject in Europe (Hooghart 1987).

Evolution of ET Estimating Methods

Development of new technology is motivated by the need to improve accuracy or efficiency of application. Current methodology based on energy balance and mass transfer evolved rapidly during the second half of the 20th century as competition for available water resources increased and development of new electronics and instrumentation technology enabled measuring variables controlling the ET process.

Jensen and Allen (2000) traced the evolution of practical ET estimating methods over the past century. In the U.S., engineers, the main users of ET estimating methods, did not begin with rigorous theories in developing new ET estimating methods, but generally sought empirically-based relationships that reproduced measurements. Also, agro-meteorological theory and methodology were not well developed until after the 1960's. Most early estimating methods were based on mean air temperature as an index of evaporative demand, or as an indicator of solar radiation. Few early estimating methods involved air humidity and none involved wind speed directly.

During the 1896-1939 period, many irrigation investigations involving plot and field studies were conducted to determine the relation between quantity of water used by crops and crop yields. Similar studies were conducted to determine the loss of water by evaporation from soils. For example, Sleight (1917) studied evaporation near Denver, CO in 1916. He reviewed early work starting with Dalton in 1802 and cited Livingston's bibliography on evaporation (Livingston 1908). The need for estimating evaporation from reservoirs was the driving force for many evaporation studies. Houk (1926), in a detailed paper, summarized investigations of evaporation by the Reclamation Bureau (USBR). This paper included discussions by 13 other engineers and specialists. Rohwer (1931) conducted a comprehensive study of evaporation from pans of various sizes and exposures at Fort Collins, CO in cooperation with the Colorado Agricultural Experiment Station. The work of Rohwer was cited as classic by Penman (1948)

who compared his own empirically derived aerodynamic equation with that obtained by Rohwer. Later studies and reports on evaporation included measurements made on Lake Hefner (USGS 1954), on pans and lakes (Kohler et al. 1955), and on Lake Mead (Harbeck et al. 1958).

Many measurements of annual or seasonal ET (or consumptive use, CU) were made from 1890 through 1925. The Duty of Water Committee of the Irrigation Division, ASCE summarized seasonal CU data in a progress report presented by O.W. Israelsen in 1927 and later published (Duty of Water Committee 1930).

Interest in understanding the daily rate of transpiration (T) produced studies of the impact of climate on transpiration by plants in containers began in the latter part of the 19th century. L.J. Briggs of the Bureau of Plant Industry in the USDA conducted many transpiration studies early in the 20th century. Briggs toured the Great Plains states in the fall of 1905 and arranged cooperative work at six stations in the area. In 1910, Briggs and Shantz initiated their classic studies at Akron, Colorado on relative water requirements of plants. In 1916, they summarized their 1912-1914 work and recognized that solar radiation was the primary cause of cyclic change of environmental factors. They corrected measured solar radiation for the area of the plants exposed to direct sunlight and probably were the first to recognize and measure the significance of advected energy in the balance of transpiration. They stated: *Even on bright days, therefore, other sources of energy, such as indirect radiation from the sky and from surrounding objects and heat energy received directly from the air, contribute materially to energy dissipated through transpiration*. The concepts of the substantial impact of effective area of vegetation in intercepting and absorbing solar radiation and impact of micro-scale advection of convected and radiated thermal energy, although recognized by Briggs and Shantz (1916) over a century ago, have been frequently missed by practitioners today, for example in the operation of lysimeters (Allen et al. 2011a). Briggs and Shantz also evaluated the hourly loss of water from atmometers and evaporation pans in comparison with hourly transpiration and developed prediction equations for hourly transpiration using the vertical component of solar radiation and temperature rise, and solar radiation and vapor saturation deficit. This important relationship laid the foundation for energy-based ET estimating methods that remained dormant for 30 years until Penman (1948) developed the combination equation.

From 1920 to 1940, much emphasis was placed on estimating evaporation and seasonal ET. Engineers began studying the CU of irrigation water relative to general climatic conditions. Several empirical equations were developed, many of which were used for various engineering and water rights purposes until the latter part of the 20th century. Mean air temperature was the primary climatic parameter used in these equations. The USBR began studying the temperature and CU relationships in 1920. Hedke (1924) submitted a proposed procedure to the ASCE Duty of Water Committee. His method was based on the assumption that heat (energy) consumed in ET was determined by the energy available. He assumed that the influences of wind, humidity, and vapor pressure on CU were small compared to the influence of heat based on air temperature. The general theory was sound except that radiant energy was not considered.

In the 1920s, Blaney measured ET by alfalfa in California using soil sampling methods. He developed procedures for estimating CU using mean air temperature, percent of annual daytime hours, and average humidity (Blaney and Morin 1942). This approach was later modified by Blaney and Criddle (1945, 1950). Lowry and Johnson with the USBR developed a procedure for estimating seasonal CU using maximum temperature above 0°C (32F) during the growing season based on inflow-outflow data from irrigation projects (Lowry and Johnson 1942). Both of these methods involved developing empirical relationships between measured ET and weather

parameters that were commonly measured such as air temperature or that were available from standard tables such as potential hours of sunshine. Unfortunately, exoatmospheric solar radiation data, which was available in tables, was not used by these authors rather than potential hours of sunshine. Later, Olivier in England developed an estimating method based on a radiation-latitude factor derived from cloudless day solar radiation for latitudes of 5 to 55° and wet bulb depression (Olivier 1961).

In 1939, Thornthwaite and Holzman (1939, 1942) applied aerodynamic and gradient transport theory to ET estimation. They proposed a method that required measuring wind speed and humidity at two heights above the surface. Although theoretically correct, the method was difficult to apply due to difficulty and expense in accurately making the measurements. Thornthwaite later correlated mean air temperature with ET as determined by water balance in valleys with adequate soil water so as not to limit ET (Thornthwaite 1948). He defined this latter empirical and widely applied equation as an estimate of potential evapotranspiration. The 1948 method of Thornthwaite has been shown to estimate best in humid climates and to substantially underestimate in drier climates (Jensen et al. 1990). Pelton et al. (1960) thoroughly evaluated temperature-based methods for estimating potential ET. Tanner and Pelton (1960) developed potential evapotranspiration estimates based on the energy balance method of Penman.

Jensen and Haise (1963) developed a simple equation based on solar radiation and mean air temperature for estimating ET for well-watered crops at full cover. Their intent was to acquaint engineers with the concept of applying energy balance to obtain ET estimates. At that time, the Penman equation was thought to be too complicated to use, given the status of computational tools, weather data commonly collected during this period, and the training of engineers.

Christiansen and Hargreaves, working in California and Utah, developed a string of regression-based equations for predicting monthly grass ET based on pan evaporation, air temperature and humidity data (Christiansen 1968; Christiansen and Hargreaves 1969). They later reduced weather data requirements to only air temperature including calculated exoatmospheric radiation to predict potential available energy and used the difference between maximum and minimum air temperatures to estimate the effect of relative humidity and cloudiness. A culmination of these efforts was the widely accepted 1985 Hargreaves equation for grass reference ET (Hargreaves et al. 1985; Hargreaves and Samani 1985).

Much of the early development in ET methods was hampered and biased by substantial errors or biases in electronic and mechanical measurements of weather parameters or in-field measurements of ET that were based on lysimeters that were often plagued by "non-one-dimensionality." In many applications, water consumption measured from the lysimeter did not concur, energy-balance wise, to ET from vegetation in a large agricultural field environment. This was due to differences in vegetation growth such as density and height, management practices, watering regime, inner-outer tank gap, and sparseness of vegetation surrounding the lysimeter (Allen et al. 1991a, 2011a). The science of using lysimeters for measuring ET was well documented by a series of 49 papers published in an ASCE proceedings by Allen et al. (1991b).

In Europe, engineers and scientists also developed empirical equations for estimating ET. Makkink (1957) published a formula in the Netherlands for estimating potential ET based on solar radiation and air temperature, and Turc (1961) developed a formula in France for potential ET also based on mean air temperature and solar radiation. Makkink's equation utilized the energy weighting term of the Penman equation, solar radiation, and a small negative constant, and its use is still popular in the Netherlands today.

Today's methods for estimating ET using standard weather measurements of air temperature, humidity, wind, and solar radiation are based on the Penman equation (Penman 1948, 1956b, 1963). The Penman equation was developed by Howard Penman during World War II in support of the war effort. His objective was to predict soil surface wetness in Western Europe to determine whether Allied tanks and trucks could advance without bogging down (Penman and Schofield 1951). Penman, a British physicist, deviated from the traditional American engineering approach to estimating ET that was largely based on empiricism and commonly available data. He began with physics and a theoretical combination of weather parameters in the form of the energy balance equation where the components of evaporation, sensible heat flux and soil heat flux sum to available net radiation energy. Penman also formulated evaporation in terms of an empirical aerodynamic expression that was supported by measurements of Rohwer (1931). He then used his intellect to combine the energy balance and aerodynamic expressions by using the Bowen ratio concept so that he could eliminate all terms that relate to measurements at the evaporating surface. The result was the Penman "combination" equation that required measurements of only air temperature, humidity and wind speed at some height above the surface, along with solar radiation that was estimated initially from observations of cloud cover. Penman's comprehensive understanding of the physical processes involved in ET and the influence of plants was clearly evident in the introductory paper he presented at the informal meeting on physics that was held in The Netherlands in September 1955 (Penman 1956a). He concluded his paper with the sentence: "*Though the physicist still has some problems he can solve by himself, much of his future contribution to understanding evaporation in agriculture must be in collaboration with the biologist and the soil scientist.*"

Application of the Penman equation for routine ET predictions did not become widespread in the U.S. until the 1970's and 1980's when two activities occurred: 1) computerized irrigation scheduling models were being developed (Jensen et al. 1970) that required more accurate estimates of ET on a daily time-step basis, and 2) advancements in silicon-based and miniaturized computers made battery-based electronic data loggers available at relatively low cost. These dataloggers made the collection of weather data required for the Penman equation automated and much less expensive.

Following the development of the Penman equation, another UK researcher, John Monteith, based partly on his research work in California, and in 1965 reformulated the combination equation using a more theoretical equation for the aerodynamic transport component of the Penman equation. This new combination equation, commonly termed the Penman-Monteith (PM) equation, included the new parameters of aerodynamic resistance and surface resistance. The resistance parameters provided flexibility to the PM equation for application to a wide range of surfaces and vegetation types. Monteith's efforts (Monteith 1965) were mirrored by the development of a similar resistance-based combination equation in the Netherlands by Rijtema (1965). The MORECS system that applied the PM equation to all of the British Isles (Thompson et al. 1981) was the first notable effort at widespread operational application of the PM method. Ambiguity in predicting roughness and stomatal parameters for these terms impeded widespread application of the method. In 1989, standardized procedures were developed for estimating aerodynamic and surface resistance parameters for reference crops of grass and alfalfa (Allen et al. 1989). This effort was part of the revision of the 1974 ASCE "Consumptive Use and Irrigation Requirements" report (Jensen 1974) that was published in 1990 as ASCE Manual 70 (Jensen et al. 1990).

Throughout recent history, the development of new technology has been influenced by the need for better ET estimates than existed at the time. The development of the current Standardized Reference ET equation (ASCE-EWRI 2005) was stimulated by the Irrigation Association's 1999 request to the ASCE's ET Committee to help establish a benchmark reference ET equation. The resulting standardized equation represents the current state-of-the-art in estimating ET.

1.3. Revised Edition

When the first edition was started in the 1960s, the main methods for estimating ET used by engineers were empirical equations in which daily mean air temperature was the primary variable. The edition, its objectives and organization, were prepared so as to provide practicing engineers with basic background on the physics and results of research conducted since the 1950s showing that the ET process was largely controlled by net radiation when soil water was not limiting and a full plant cover existed. Comparisons of numerous empirical equations developed since about 1940 and more recent energy-based methods were made. Example calculations using most of these methods were included.

The revised edition contains substantial material from the first edition, but has a more narrowed focus on the recent improvements and standardizations in estimating and measuring ET and their application. Many details of these developments can be found in other publications such as chapter 4 of the updated ASCE Hydrology Handbook (Allen et al. 1996), the updated FAO publication on crop water requirements (Allen et al. 1998), and the ASCE Standardized Reference Evapotranspiration Equation (ASCE-EWRI 2005). As with the first edition, the revised edition emphasizes the need for users of the various methodologies to fully understand the physical foundations that govern and support the methods. Foremost is the law of conservation of energy that essentially fixes an upper limit on the rate of ET from a large expanse of vegetation. This law serves as a universal guide for assessing the quality and accuracy of ET measurements and as an upper bound on ET at both the field and regional scales. A knowledge of the physics describing thermal (long-wave) radiation emission from both the surface and atmosphere, short-wave transmission through the atmosphere, and turbulent convection processes is paramount to understanding the behavior of methods and in discerning when adjustments to the method application or data handling are warranted. Allen et al. (2011a) summarized the physical processes associated with modern ET measurement and estimation processes and Allen et al. (2011b) recommended documentation of ET measurements and calculations to be reported with data and method applications.

In 2000, a task committee of the ASCE Committee on Evapotranspiration in Irrigation and Hydrology organized a special session focused on the development of a single equation for estimating reference crop ET. The session was part of the 4th Decennial National Irrigation Symposium (Evans et al. 2000). The standardized equation is a reduced form of the ASCE Penman-Monteith equation. The development of the standardization was partly due to requests by the Irrigation Association and landscape industry for a single procedure for estimating reference ET. The objective of the request was to help standardize the basis for the myriad of landscape (i.e., crop) coefficients that have been developed since the late 1980's across the United States. The reduced form equation has been standardized for both a tall reference crop like alfalfa and short reference crop like clipped grass to support usage in both agricultural and landscape industries. Sets of equations and coefficients were developed for estimating daily or

hourly reference ET for the short and tall references. The various forms and applications of the PM and Penman equations, as well as commonly used empirical equations, have been implemented in various software including REF-ET (Allen 2012) and spreadsheets (Snyder 2004).

This edition contains a detailed summary of a reduced form, standardized Penman-Monteith equation for estimating reference ET. Details of that equation and its development were presented in separate papers at the 2000 ASAE conference (Allen et al. 2000; Itenfisu et al. 2000), in Itenfisu et al. (2003) and in the task committee report "Standardization of Reference Evapotranspiration Calculation" (ASCE-EWRI 2005).

2

Evaporation and Evapotranspiration Processes

2.1. Introduction

Evaporation (E) in the natural environment is a basic component of the hydrologic cycle. Evaporation is the physical process by which liquid water is transferred to the gaseous state of water vapor. Sublimation is the physical process of conversion of ice or snow directly to water vapor. Transpiration is the physical process by which water within plant cells evaporates and is transferred as water vapor to the air through plant surfaces, primarily via stomata. Minor amounts of transpiration occur by gutation, a process where water, in small quantities, is expelled from the tips of leaves usually at night following complete rehydration. Evapotranspiration (ET) is the sum of vaporization by the combined processes of evaporation and transpiration.

Potential evaporation (E_p) is the rate of evaporation from a surface when all surface-atmosphere interfaces are wet or from a free water surface, so that there is no surface restriction on the rate. Potential evapotranspiration (ET_p) is the rate of ET that can occur when all soil and plant surfaces are wet, and therefore, its rate is dependent on atmospheric conditions and surface characteristics such as its albedo and roughness. Since all soil and plant surfaces do not remain wet for long periods of time, ET_p, a term once used to describe the maximum rate of ET, has limited applications. Potential crop ET, ET_{cp}, is a term generally used to represent the maximum value of ET from a specific crop type having specific properties under conditions of full soil water supply, but not necessarily having a saturated surface, as is the case for E_p and ET_p. Under the same weather conditions, ET_{cp} values can vary according to the wetness of the soil surface and associated evaporation component.

Reference crop ET, or reference evapotranspiration (ET_{ref}), is a concept suggested by Jensen (1968), Wright and Jensen (1972) and Doorenbos and Pruitt (1975, 1977) to address some of the ambiguities associated with definitions for potential ET and to serve as a consistent climatic index for ET. ET_{ref} is the rate at which soil water, if readily available, would be converted to water vapor for a specific type and characteristics of the reference surface under given atmospheric conditions. The leaf surfaces of the well-watered reference crop typically are not wet, so that there is some minimum surface resistance. The term ET_{ref} has become the standard that is used to characterize the climatic effects on the ET rate. When estimating ET, the effects of crop cover such as leaf area and stage of growth such as maturation are related to ET_{ref} by a factor that varies with crop development. This factor is typically referred to as the crop coefficient, or the crop coefficient curve.

2.2 The Water Budget

When accounting for water evaporated from the soil-plant system, the conservation of mass for a hydrologic unit is called the water budget, or the water balance. Major components of the water budget for a given period of time are:

$$P + I - E + Q_i - Q_o - \Delta S = 0 \tag{2.1}$$

where P is the precipitation volume, I is the irrigation volume (if irrigation is applied), E is the evaporation (or evapotranspiration, ET) volume, Q_i is inflow volume besides from P and I, including lateral inflow and upward flow from a water table, Q_o is the outflow volume besides E, including surface runoff, subsurface lateral outflow, and vertical drainage, and ΔS is the change in water storage volume within the unit. For some hydrologic units, the rate of E, or ET, can be determined by measuring the components P, Q_i, Q_o, and ΔS expressed on a unit area basis per unit time. When a large soil mass is isolated from its surrounding soil mass and weighed as in a lysimeter, the E or ET rate can be measured as the change in mass over short time periods. This is the procedure by which many estimating methods are verified or calibrated. For unit land areas, and for most engineering applications, it is not practical to measure E or ET, Q_i, Q_o and ΔS. Therefore, the rate of E or ET is usually estimated using climate data, and in some cases, assisted with remotely sensed data. In controlled research and special investigations, if Q_i and Q_o are negligible, then E or ET can be determined by measuring the change in soil water content, ΔS, along with P over a period of time such as 5 days or more.

2.3. The Energy Budget

The process of converting water to water vapor requires a large amount of energy—about 600 times that required to raise the temperature of an equal quantity of water by 1 degree Celsius (C). Therefore, the most common method for estimating E or ET is to estimate the energy that is available for E or ET. The energy consumed in evaporating water is represented by the latent heat flux density, λE, so called because the energy flux is 'hidden' in the water vapor. That energy becomes 'visible' later on, in the form of sensible heating of the atmosphere when the vapor re-condenses to liquid during cloud formation. The energy budget for a unit land area is comprised of a balance between net radiation, R_n, latent heat flux density, λE, soil heat flux density by conduction, G, and sensible heat flux density to or from air by convection, H. Net radiation is the net amount of radiant energy exchange at a land or water surface considering incoming and reflected solar (i.e., short-wave) radiation and incoming, reflected, and emitted long-wave radiation. Net radiation is the primary energy source for evaporation and evapotranspiration. The main component of net radiation is incoming short-wave solar radiation. Long-wave (i.e., terrestrial) radiation, however, is also an important component of net radiation. When estimating E or ET using the energy balance equation, minor components such energy used in metabolism or stored within the canopy are generally neglected. λE is converted to ET depth by dividing λE by $\lambda \rho_w$, where λ is the latent heat of vaporization and ρ_w is the density of water. Dividing by λ yields E (or ET) having units of kg m^{-2} $time^{-1}$, and further division by ρ_w in kg m^{-3} yields ET depth having units of m $time^{-1}$, which are commonly converted to mm $time^{-1}$.

In semiarid and arid areas, the temperature of well-watered plant leaves can be lower than air temperature during afternoon hours. When this occurs, sensible energy is transferred from the air to the plants and H becomes negative. As a result, daily latent heat flux can be greater than net radiation, as illustrated in fig. 2.1, where 24-hour λE from alfalfa in southern Idaho exceeded 24-hour R_n by 50% on many days, due to advection (i.e., transfer) of sensible heat. Procedures for estimating net radiation and other terms of the energy balance equation are provided in chapter 4.

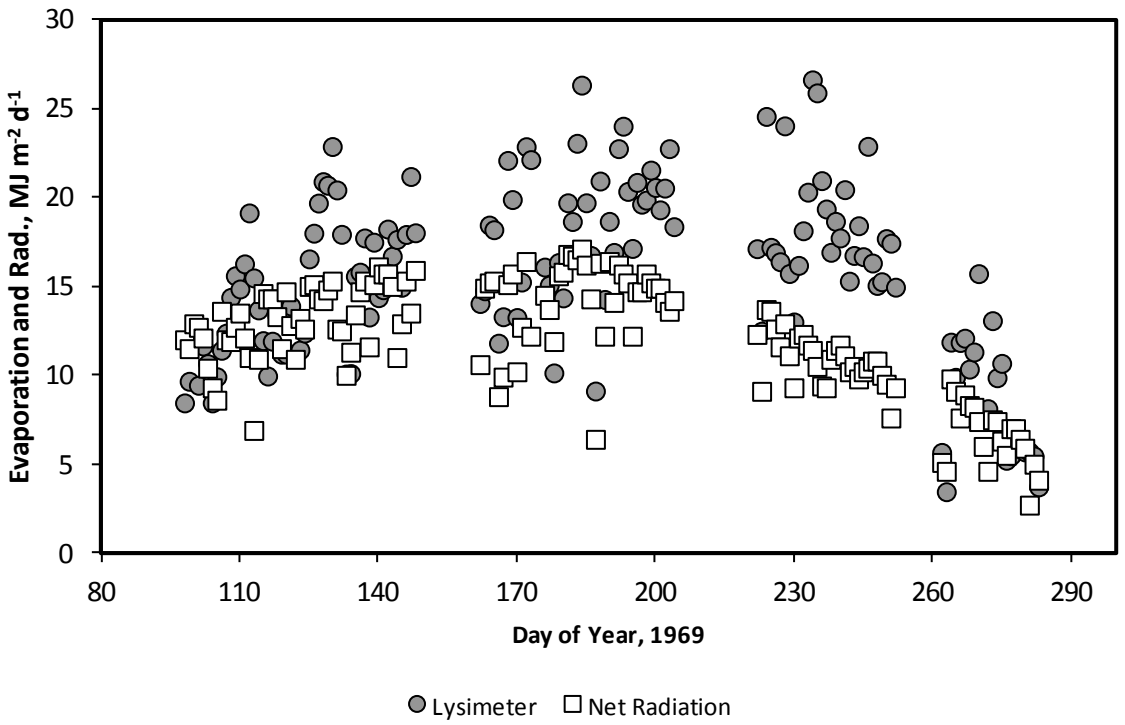

Fig. 2.1. Daily *ET* from full cover alfalfa (height > 0.3 m) collected during 1969 near Kimberly, ID by weighing lysimeter and expressed as λE in MJ m^{-2} d^{-1}, along with 24-hour R_n in MJ m^{-2} d^{-1}. Source: Data from Dr. J.L. Wright, USDA-ARS (ret.)).

2.4. Controlling Factors

Weather

The primary weather factor controlling E and ET is solar radiation. Solar radiation is the ultimate source of almost all of the energy required to vaporize water. Other important weather factors are humidity and wind speed. Air temperature also affects the E or ET rate, but it has a minor direct impact, although it is highly correlated with both solar radiation and ET. Since average daily temperatures of plant leaves, shallow water bodies, and soil surfaces are near air temperatures, water vapor pressure at the evaporating surface is generally exponentially related to mean air temperature. The saturation vapor pressure of water is the pressure exerted by its vapor when the liquid and vapor are in dynamic equilibrium at any given temperature. In meteorology, the term vapor pressure means the partial pressure of water vapor in the atmosphere. The water vapor gradient from the plant and soil surfaces to the air is dependent on surface vapor pressure and vapor pressure of the air, or air humidity. Drier air generally leads to a greater vapor pressure gradient. In addition to the vapor pressure gradient, wind speed affects the potential rate of vapor transfer from the evaporating surfaces to the air.

Vegetation

Agricultural Crops. Agricultural crops are the main vegetation for which estimates of ET are needed. For annual crops, the soil remains essentially bare after planting until new plants

emerge. The rate of ET from planting until about 10% plant cover is governed by the factors controlling the rate of evaporation from the soil. From about 10% plant cover until about 75% plant cover, or a leaf-area-index (LAI) of about 3.0, the rate of ET is influenced by increasing LAI. LAI is defined as the area of one side of plant leaves per land area including areas between plants and rows. The rate of ET increases in proportion to leaf-area development under given climatic conditions until the plant canopy reaches about 75%. After 75% cover, the relative ET rate (relative to ET_{ref}) remains essentially constant (Ritchie 1972; Tanner and Jury 1976; Wright 1982) until plants begin to mature, or senesce, after which the relative rate begins to decrease.

For well-watered perennial crops that are dormant during the winter period, the relative rate of ET begins to increase when plants green up in the spring. The increase in relative ET rate is similar to that for annual crops. The relative rate remains essentially constant at full cover until the crop is harvested, such as the cutting of a forage crop. For a short period after harvest, the relative rate of ET will be near that of bare soil if the forage is cut very short. The relative rate of ET increases during regrowth as the LAI again increases (Ritchie 1972; Tanner and Jury 1976; Wright 1982).

The maximum rate of ET for most common farm crops is nearly the same after the LAI exceeds about 3.0, or fraction of ground covered exceeds about 0.75 to 0.80, for given climatic conditions (Ritchie 1972; Tanner and Jury 1976; Wright 1982). The characteristics of the plants, such as aerodynamic roughness and stomatal resistance, also influence the maximum rate.

Natural Vegetation. As water supplies become limited, greater attention is given to water consumption by natural vegetation, both for water conservation and for sustaining important natural systems. During the growing season, these areas include wetland vegetation such as tulles and cattails that may be associated with leaking water conveyance systems. During the nongrowing season, estimates of evaporation from dormant vegetation and areas having varying amounts of organic residue are becoming more important in managing water supplies. Surface conditions such as bare soil and snow cover will be different from those of a reference crop and refined estimates of net radiation are required to account for surface conditions such as crop residue and snow (Allen and Robison 2007).

For deciduous plants that lose their leaves in the fall, the ratio of ET to reference ET increases rapidly as new leaves emerge in the spring. After reaching about 70% to 80% cover, the ratio of ET from well-watered natural vegetation to reference ET will generally remain nearly constant until leaves are shed in the fall. The maximum rate of ET is influenced by the height of the vegetation, which is generally greater for trees than for most agricultural crops, and the control of transpiration by leaf stomates. Trees and shrubs generally have more stomatal control than do agricultural crops. Typically, the stomatal control by evergreen trees is greater than that by deciduous trees.

Landscape Vegetation. Estimates of water requirements and ET for landscape vegetation are not as well established as they are for agricultural crops or large areas of uniform turf grass such as for golf courses. One of the problems associated with estimating landscape ET is that the areas involved are small, edge effects can be large, areas may be shaded part of the day by buildings, and parts of the grass areas and shrubs may be shaded by trees. Many landscape plantings are mixtures of groundcover, shrub and tree plants. Trees are often subjected to harsh environments such as within or surrounded by paved parking lots. Performance of landscape vegetation is usually based on appearance and function rather than optimal growth. Many species maintain

their esthetical and functional value when irrigated within a range of 20 to 80% of grass reference ET depending on the species and local conditions (Pittenger and Shaw 2004). Plant physiology research has shown that water use by some woody plants does not increase in proportion to reference ET throughout the day under harsh site conditions. Some species may actually use less water because their stomates close. Pittenger and Shaw (2004) recommend that for many landscape species with unknown water requirements, initial irrigation schedules should be set at 50% of grass reference ET. Plant performance must then be evaluated and irrigation increased or decreased incrementally as needed.

Field research on water requirements of non-turf landscape plants is limited to several commonly used groundcover, tree and shrub species (Pittenger and Shaw 2004). More information is available for turfgrass. For example, monthly crop coefficients for use with grass reference ET have been developed for cool-season and warm-season turfgrass in Californa (Pittenger and Shaw 2004). Cool-season species include tall fescue, ryegrass, bentgrass, and Kentucky bluegrass. Warm-season species include Bermuda grass, zoysia grass, and St. Augustine grass. Chapter 10 describes a method for estimating landscape coefficients that is traceable to Pittenger and Shaw (2004) and other research in California. Landscape coefficients for local areas having conditions different from those described in Chapter 10 can usually be found in publications such as that by Brown et al. (2001).

Soil Factors

The main soil factors that influence the rate of evaporation from bare soil include the soil's water content and its water characteristic curve, which describes the ability of a soil to hold water, and the soil's hydraulic and thermal conductivities. The hydraulic conductivity is largest at saturation and decreases as the soil water content decreases, and therefore influences the rate at which water moves to the surface. The hydraulic gradient toward the surface increases as the surface begins to dry, but the hydraulic conductivity decreases. An additional factor controlling both rate and amount of evaporation from soil is the influence of organic or man-made residue on the soil surface. Residue acts as both a reflective cover and as a thermal insulator, thereby reducing the amount of energy at the soil surface for evaporation. The main soil factor that may influence ET, depending on the frequency of irrigation or rainfall events, is the water holding capacity of the soil. A summary of soil water holding characteristics for various soil textures is given in chapter 3.

Water Bodies

Estimates of evaporation from water bodies can be obtained using a relationship between reference ET and pan evaporation, by estimating net radiation and the rate of change in energy storage for the water body and applying the Penman or Penman-Monteith equation, or by applying aerodynamically-based equations. The albedo for a water surface is much smaller than for a land area with a green crop, i.e. about 0.06 v. 0.20 – 0.25. Albedo is defined as the reflectance of incoming solar radiation from the surface, integrated across the entire solar radiation spectrum. Surface water temperatures are needed, but mean daily surface water temperatures may be relatively close to mean air temperatures for shallow water bodies. An important component in the energy available for evaporation is the advection of energy in the

inflow and outflow volumes to or from the water body, e.g., inflow and outflow such as occurs in reservoirs located within river systems.

When the temperatures are low enough that ice forms on the water body and remains over the winter period, estimates of net radiation for ice and snow-covered water becomes more complicated. Winter loss involves estimates of sublimation from ice and snow-covered ice.

Estimates of evaporation from deep-water bodies are more complex compared with shallow water bodies. During the increasing period of the annual cycle of solar radiation, for a relatively clear water profile, a significant portion of the net solar radiation penetrates below the surface where it is absorbed, warming the water body. Because evaporation is a surface phenomenon, there is a time lag before stored energy is transported to the surface where it contributes to evaporation or loss by sensible heat transfer to the atmosphere. During the energy storage period, a thermal profile extending to a depth of 20 m or more may develop in clear water and rate of evaporation will be less than the rate of E from shallow water bodies. During periods of decreasing daily solar radiation, transfer of the stored energy to the surface can increase the rate of evaporation to rates above that from a shallow water body. Part of the stored energy may be lost to the atmosphere by convection of sensible heat during cool periods, making deep, cold lakes and reservoirs relatively efficient storage devices as compared to shallow systems.

Management Factors

Available Soil Water. The major management factor affecting the ET rate for agricultural crops and landscapes is the level at which the soil water content is maintained. For high-value crops and those with adequate water supplies, managers endeavor to irrigate so as to maintain a consistently high soil water level so that plant growth and ET rate are not constrained. As competition for water increases and as supplies become limiting, irrigation of low-value crops such as forages may be reduced. Allowing the soil water to be depleted to lower levels reduces the rate of ET compared to that of a well-watered crop. For some crops like cotton, irrigation may be limited for a period during the vegetative growth period to limit plant size, encourage flowering, and enhance the production of fiber. Limiting irrigation during the vegetative stage may decrease seasonal ET somewhat with little or no loss in crop yield. Regulated deficit irrigation, irrigating less than that for maximum growth, is practiced with some types of orchard and vineyard production systems to reduce total seasonal ET.

Other Management Factors. Other factors that can affect the rate of crop ET include spacing of rows and plant population density, salinity level in the soil that is impacted by irrigation practices and water management, and the effects of plant pests and diseases. Crop yields are not a good indicator of ET unless soil water limits plant growth. For example, new plant cultivars and hybrids are more efficient in converting dry matter into marketable crop yields with similar ET as older cultivars. Yields of corn hybrids, for example have increased greatly over the past half-century. Jensen (1994) found that when hybrids were grown under similar nonirrigated or irrigated conditions, yields varied only with the date the hybrid was released. Side by side comparison of winter wheat varieties near Bushland, Texas made in the 1980s showed that the grain yield of the more recent cultivars was about twice that of the 1950s cultivars with no statistically significant difference in ET (Musick et al. 1984). Likewise, fertilizers may influence crop yields greatly when the soil is deficient in a plant nutrient. Such large increases in crop

yields are usually accompanied by small increases in seasonal ET rate due to more prolonged stomatal opening from healthier plants and generally greater leaf area (Howell 1990).

The type of irrigation system can affect the evaporation component of ET, especially in orchards and vineyards where plants are widely spaced. If the bare soil area is not wetted by the irrigation system, the overall ET rate for a mature vineyard, citrus grove, or a deciduous orchard will be less than for a comparable field having an irrigation system that wets the entire soil surface.

2.5. Estimating Concepts

Most current estimates of E and ET are based on some form of the energy balance equation, or a combination equation containing energy balance and aerodynamic components. Estimates of evaporation from shallow water bodies are often based on measured evaporation in evaporation pans. Estimates for deep water bodies may also be based on pan evaporation, but pan coefficients require adjustment for energy storage effects.

Evaporation from Water Surfaces

In the past, the evaporation pan was the most common method for estimating evaporation from small and shallow water bodies. The most commonly used pan in the USA and in many countries is the USA Class A pan. Numerous studies have been made relating pan evaporation to lake evaporation and evaluating pan evaporation as affected by type and size of pan and impact of the local pan environment. Examples of significant early papers are those of Rohwer (1931, 1934), Young (1947), Hounam (1958), Kohler et al. (1955), Pruitt (1960), and a review by Hounam (1973). The literature provides ample evidence of the extreme care that must be exercised in interpreting pan evaporation data, due to the substantial differences in energy balance between pans and many water bodies, to obtain reliable estimates of open water evaporation. Detailed procedures for estimating evaporation are presented in chapter 6.

Evaporation from Soils

Bare Soils. The evaporation rate from bare soil occurs in several stages. During the first stage, which may last for only one to three days in midsummer, the rate of evaporation is controlled by energy input, and can be greater than grass ET_{ref}. The duration of the first stage is influenced by the rate of evaporation, soil depth, and hydraulic properties of the soil (Gardner and Hillel 1962). The higher the rate of evaporation, the shorter the duration of the first stage (Bond and Willis 1970). The rate of first stage evaporation is also influenced by the amount of crop residue on the surface. The transition from the first to second stage of drying is variable and depends on climate and soil conditions. Visually, the transition begins when dry places appear on the soil surface. The transition can sometimes be identified by a measured change in albedo or color (Jackson et al. 1976).

During the second or falling stage, the surface has begun to dry and the source of water for evaporation is largely from below the soil surface. Water vapor from evaporation beneath the surface reaches the surface by molecular diffusion and mass flow that is influenced by fluctuating air pressure and vapor gradients. A dry surface soil greatly increases the effective surface resistance to evaporation. After the dry surface mulch has formed, the evaporation rate

from the soil, E_s, will be substantially less than ET_{ref}, and the rate is controlled mainly by soil characteristics, especially the hydraulic properties and the depth and extent of the original wetting of the soil profile. During the second stage the cumulative evaporation tends to increase with the square root of time for a given soil and relatively constant evaporation potential. Detailed estimating procedures are given in chapters 9 and 10.

Soils with Partial or Full Vegetative Cover. During the initial stages of annual crop development, the rate of ET is essentially the rate of evaporation until about 10% plant cover has been established. As leaf area develops, the fraction of total ET that is evaporation decreases and the transpiration fraction increases. As leaf area and light interception increase, the energy reaching the soil and resulting evaporation decrease. This principle is commonly used in models of soil evaporation (Boote and Loomis 1991; Villalobos and Fereres 1990; Bonachela et al. 1999). Procedures for estimating the proportions of E and transpiration (T) are provided in chapters 9-11.

Reference Evapotranspiration

The concept of reference ET was developed as a means to characterize weather effects on ET as independently as possible from specific crop and natural vegetation effects. This approach also enables comparing climate effects on ET rates in different regions and environments. Estimated reference ET is based on an assumed standard set of surface conditions including surface albedo, the type of well-watered uniform vegetation having a fixed surface resistance, and standardized coefficients for the aerodynamic component of a combination equation. The standardized surface, especially for grass and alfalfa reference ET, can be approximated using lysimeters and the rate of ET determined by measuring the change in weight of the lysimeter or by careful micrometeorologically-based (i.e., aerodynamic) measurements.

Crop Factors (Coefficients)

Crop factors, or crop coefficients, represent the rate of ET from various crops relative to a reference ET, and vary within growth stages. Current crop coefficients are based mainly on measurements of ET from sensitive weighing lysimeters or micrometeorological methods that have been related to calculated or measured reference ET. The objective of crop coefficients is to increase the transferability of costly ET measurements by normalizing them using reference ET. More detail on crop coefficients and application is provided in Chapter 10.

2.6. Measurement Methods

Conferences and workshops over the past 30 years have addressed various methods of measuring ET. One such workshop on ET from plant communities was held in Bunbury, Australia in May 1982 and included a series of papers on measurement of ET by various methods. A summary of this workshop was presented by Rose and Sharma (1984). Various methods of estimating ET were discussed at the 1993 ASCE National Conference on Irrigation and Drainage Engineering (Allen and Neale 1993), including a series of papers on calibration of the neutron probe used to measure changes in soil water and ET. Textbooks or monographs that describe measurement of ET via micrometeorology include Lee et al. (2004) and Hatfield et al.

(2005). Brief descriptions of the main methods for measuring ET are summarized in the following sections, with more detailed descriptions given in chapter 7.

Change in Soil Water

Determining ET under field conditions by measuring the change in soil water over a period of time is a method that has been used in the USA for nearly a century. Up until the early 1960s, the primary method was by soil sampling and gravimetric analyses to determine the soil water content. Beginning in the 1960s, the neutron soil water probe largely replaced the gravimetric procedure except for evaluating soil water content in the surface 0 to 0.2, or 0 to 0.3-m layer and for calibrating the neutron probe. Since the 1980's, new types of electromagnetic devices based on dielectric and capacitance properties have been used to measure soil water content. Some electromagnetic systems can have a small zone of influence and therefore may not be capable of sampling a large and representative volume of depleted water for determining ET.

Drainage from the zone sampled or the upward movement of water from a lower saturated zone into the zone sampled is a major potential source of error in ET determined by the soil water balance method. These errors are difficult to detect, but they can be minimized with proper precautions. The soil is usually sampled 2 to 4 days after irrigation and again 7 to 15 days later or just before the next irrigation. Since the change in soil water over the time interval is desired, most investigators fill the holes from which the soil cores were removed (gravimetric procedure) with soil, mark the site, and then take the next sample 0.3 to 0.4 m from the first core in order to minimize error due to soil variability.

With the neutron probe and some electromagnetic devices, access tubes are used and the water content at the same site is measured periodically. One of the problems encountered is damage to the plants around the access tube by technicians making the readings. Data obtained from sites with damaged plants will not be representative of field conditions. The average rate of ET in mm d^{-1} between sampling dates is then calculated as the change in total soil water plus effective rainfall minus any known drainage that may have occurred.

Determining reliable ET rates by soil sampling requires adequate precautions such as: 1) using at least 6 sampling sites representative of general field conditions, a minimum of 4 may be adequate when using neutron techniques. (Kamgar et al. 1993) described the number of neutron probe sites needed relative to plot size); 2) selecting sites where the depth to the water table is much greater than the root zone depth; 3) using only those sampling periods where rainfall is light since values for periods of high rainfall are questionable because runoff or drainage may occur; 4) drainage can be minimized by: a) applying a heavy preplant irrigation at least 10 days before planting, b) applying less water at each irrigation than the amount that can be retained in the root zone, c) waiting at least 2 days after a normal light irrigation before taking the first sample, and longer with heavier irrigations or when the ET rate is small, and d) using only the active root zone depth for ET computations. Detailed discussions of the problems encountered in determining ET by soil sampling have been presented by Robins et al. (1954), Jensen (1967), Jensen and Wright (1978) and Hignett and Evett (2002). General problems associated with soil sampling were discussed by Taylor (1955), Staple and Lehane (1962), Pratt et al. (1976) and Evett and Steiner (1995). More information is given in chapter 7.

Lysimetry

Weighing lysimeters (evapotranspirometers) are isolated blocks of soil or tanks filled with soil suspended on a weighing mechanism in which crops are grown. The amount of water lost by evaporation and transpiration is based on the change in weight of the lysimeter. This method provides a direct measurement of ET and is frequently used to study climatic effects on ET and to evaluate estimating procedures and to develop crop coefficients. However, lysimeter data may not be representative of field conditions. Soil conditions inside the lysimeters must be essentially the same as those outside. The lysimeter must be surrounded by the same crop that is growing in the lysimeter to insure one-dimensionality of the measurement (Allen et al. 1991a). Otherwise, errors as large as 200% can occur. Preferably, the lysimeter should be located within an open field of the same crop. Studies of advection at edges of fields suggest that the lysimeter should be located at least 100 m from the edge of the field.

Lysimeters surrounded by sidewalks or gravel will not provide reliable data, nor will lysimeters planted to a crop surrounded by shorter or taller vegetation. Differences in growth and maturity between the lysimeter plants and surrounding plants and resulting ET measured in the lysimeter relative to ET measured in the surrounding field can be significant (Pruitt and Lourence 1985). High crop coefficients reported in the literature may have been the result of such differences in plant growth between the lysimeter and the surrounding field. The lysimeter rim-area to lysimeter-area ratio should be less than 0.1 (Allen et al. 1991a). For example, with a 10-mm gap and 5-mm inner and outer walls of weighing lysimeter tanks, this ratio would be 0.08 for a lysimeter that has an inside dimension of 1 x 1 m [4(0.02)(1.02)/1.0].

Lysimeters can be grouped into three categories: 1) nonweighing, constant water-table type, which provides reliable data for weekly or longer time periods in areas where a high water table exists and where the water table level is maintained essentially at the same level inside as outside the lysimeter; 2) nonweighing, percolation type, in which changes in water stored in the soil are determined by sampling or neutron methods and the rainfall and irrigation percolate are measured (often used in areas of high precipitation); and 3) weighing types, in which changes in soil water are determined either by weighing the entire unit with a mechanical scale, counter-balanced scale and load cell, directly suspended by load cells, or by supporting the lysimeter hydraulically. Weighing lysimeters, if well managed, can provide the most accurate data for short time periods. However, mismanagement of the vegetation and vegetation area inside and outside the lysimeter can cause large error, regardless of the precision of the measurement (Allen et al. 1991a; 2011a). ET can be determined accurately over periods as short as 30 minutes with a mechanical scale, load cell system, or a floating lysimeter. Hydraulically weighed lysimeters generally are not accurate for periods less than 24 hours. A detailed summary of the use of lysimeters for ET can be found in publications by Harrold (1966), Aboukhaled et al. (1982), Howell et al. (1985), Marek et al. (1988), and Pruitt and Lourence (1985). The proceedings of an international symposium on lysimetry organized by ASCE provide many examples of poor lysimeter systems along with guidelines for the operation of lysimeters to assure high quality data for ET and related environmental purposes (Allen et al. 1991b).

Bowen Ratio Energy Balance (BREB)

The Bowen Ratio Energy Balance (BREB) method is a practical and relatively reliable micro-meteorological method. Use of the BREB concept (Bowen, 1926) has enabled solving the energy balance equation by measuring the ratio of sensible heat flux to water vapor flux over the land or water area being studied. Numerous special studies have been conducted over various

land surfaces using this methodology. The methodology enables measurement of latent heat flux for periods of an hour or less. The method works best when soil water is not limiting ET. As water becomes less readily available and the Bowen ratio (BR) increases, the relative error in λE increases due to errors as BR becomes larger (Angus and Watts 1984). Details and equations for the BREB method are given in section 7.4.

Todd et al. (1998) and Devitt et al. (1998) reviewed prior studies in which investigators used the Bowen ratio energy balance (BREB) methodology. They also compared measurements of alfalfa ET using BREB with ET measured with precision weighing lysimeters in the semiarid area of west Texas during a two-year period. The BREB overestimated ET when ET rates were greater than 6 mm d^{-1}. Overestimation occurred whether sensible heat flux was positive or negative. BREB error tended to be positive in the morning hours and negative in the afternoon. The accuracy of the BREB method is directly proportional to accuracy of the net radiation and soil heat flux measurements, which can be highly impacted by nonuniformity of vegetation and soil and by sensor calibration, placement and care. Details and equations for the BREB method are given in section 7.4.

Eddy Covariance

With the improvement in instrumentation technology, current technology has enabled direct measurement of water vapor flux using principles set forth a half century ago by Swinbank (1951). Early examples of eddy instrumentation were described by Tanner (1988) and Tanner et al. (1993). Since then, many advances in instrumentation have been made and more use of this method is now being made as illustrated by Baldocchi (2003) and Shaw and Snyder (2003). The eddy covariance method tends to suffer from what is referred to as lack of closure on the energy balance, where the sum of measured $\lambda E + H$ does not equal measured $R_n - G$ (Baldocchi et al. 1988; Twine et al. 2000; Wilson et al. 2002). Possible reasons for the lack of closure are storage of heat in canopies, horizontal advection, change in storage of heat in the developing boundary later below the instrumentation (causing flux divergence), frequency response of sensors relative to frequency spectrum of eddies, and regional scale heterogeneity of vegetation and ET that can cause large scale eddies that are effective in transport of λE and H, but are not readily sensed by eddy covariance systems that are usually placed within 20 m of the surface (Foken et al. 2008). Many users 'close' the energy balance by scaling $\underline{H}$ and λE in the same proportion (Twine et al. 2000) until the sum equals R_n - G. Details and equations for the eddy covariance method are given in section 7.5.

Water Balance

For integrated areas of land and water, the water balance, i.e., the inflow-outflow method has generally been used. Examples of ET by water balance are large areas such as valleys in which the inflow and outflow are determined from stream flow and precipitation measurements, and where the basin is confined to eliminate other significant sources of inflow or outflow. An early example of a water balance study that was used for determining the average ET for an area is that reported by Lowry and Johnson (1942). In that study, annual inflow-outflow data for irrigation projects were used to obtain an empirical relationship between the annual ET for an "equivalent valley area" of cropped, irrigated land and degree-days using maximum temperatures above 0 C. Such studies generally provide only gross seasonal estimates of the average water evaporated

and transpired from cropped and noncropped areas within a project. The results represent a combination of the crops grown and are generally applicable only to climatic, cropping and irrigation conditions similar to those existing in the study area. Thornthwaite (1948) correlated mean monthly air temperatures with ET as determined by water balance studies in the east central part of the U.S. Hydrological methods of estimating ET in catchments were described by Morton (1971) and Holmes (1984). An evaluation of large-scale models of an experimental catchment (watershed) and a river basin in Australia indicated satisfactory agreement in monthly values between the computed and measured ET. At the river basin level, acceptable estimates of ET were inferred on the basis of the monthly computed and measured runoff (Dunin and Aston 1984). A summary of water balance methodology is presented in section 2.2 of this chapter.

Remote Sensing-Energy Balance

New techniques using satellite imagery have been developed since about 1990 to determine E and ET from large areas using energy balance (Bastiaanssen et al. 1998a,b, 2005; Anderson et al. 1997, 2005; Kustas and Norman 1999; Kustas et al. 2003; Li et al. 2005; Norman et al. 2000, 2003; Allen et al. 2007a,b). The emerging technology of energy balance by satellite is showing substantial promise and has been used to quantify and illustrate the population variance in ET that can be associated with the same crop type and to refine crop coefficient curves (Tasumi et al. 2005a; Allen et al. 2007a,b; Singh and Irmak 2009). Remotely sensed energy balance techniques are also useful for identifying areas experiencing water stress and corresponding reductions in ET. Anderson et al. (2011, 2012) reviewed the use of thermal-imagery from satellite systems for estimating stress-limited ET as well as the ability to view the signatures of evaporation from wet soil. That review discussed the constraints caused by resolution of satellite imagery and derived ET images. Currently the Landsat system provides the highest resolution imagery (30 m pixel size) with repeatable coverage and thermal imager, having a 16 day return coverage required to follow the evolution of vegetation development and to follow increases or decreases in water stress. Satellite-based estimates of ET, and in particular, those based on Landsat imagery, will increasingly find their way into court proceedings, water transfers and hydrologic studies because of the high value of spatial coverage over an extended time period. For example, the thermal Landsat archive extends over a more than 30 year period beginning in 1982.

Chapter 3

Soil-Plant-Atmosphere System

3.1. Introduction

The purpose of this chapter is to provide a description of the soil-plant-atmosphere (SPA) system to support the development and calculation of ET methods presented in later chapters. The SPA system involves absorption and storage of energy in the soil, the storage of water in the soil, evaporation from the soil and plant surfaces, transpiration from leaves of plants, and transfer of water vapor, sensible heat and radiation from the soil and plants to the atmosphere. Liquid phase continuity exists in all actively growing plants from the water in the soil through the plant to the liquid-gas interface at evaporation sites in the leaves. The proliferation of roots in the soil provides an extensive absorbing surface across which passes most of the water and mineral nutrients utilized by plants.

Additional information about the SPA system can be found in various sources such as Slatyer (1967), Pierre et al. (1966), Kozlowski (1968a, 1968b,1972, 1976), Sharma (1984), Monteith and Unsworth (1990), Campbell and Norman (1998), Encyclopedia of Soils in the Environment, (2004), Encyclopedia of Hydrological Sciences (2002), and Stewart and Howell (2003). This chapter focuses on those items of concern to engineers in solving problems involving evaporation (E) and evapotranspiration (ET) from plant and soil communities, conducting research in E and ET, and managing water supplies and delivery systems. More detailed information is presented in chapters 4-7 dealing with estimates of E and ET.

3.2. Physical Properties of Water, Water Vapor, and Air

Liquid Water

Important physical properties of liquid water are summarized in table 3.1. All properties in table 3.1 change as temperature departs from 0°C. The maximum density of pure water is at 4°C.

Water Vapor

Vapor pressure is used as an indicator of the water vapor content of air and to describe mean humidity gradients in air that drive the evaporation process. Vapor pressure is the partial pressure in air caused by molecular-scale collisions by water molecules against a surface. At the water-air interface there is a continuous flow of molecules from the water surface to the air, and a return flow to the liquid surface. When equilibrium with pure water exists, the two flows are equal and the air is saturated with water vapor, e^o. The partial pressure exerted by the water vapor at this time is called the saturation vapor pressure. The vapor pressure at equilibrium depends on the liquid water pressure, temperature, and its chemical content (solutes). Typical values of saturation vapor pressure and density of water vapor over a plane surface of pure water at the same temperature and pressure are summarized in table 3.2. At the boiling point, e^o equals air pressure.

TABLE 3.1 Physical Properties of Liquid Water. Source: Data from Van Wijk and de Vries (1963)

Temperature (°C)	Density (kg m^{-3})	Surface tension (N m^{-1})	Dynamic viscosity (10^{-3} Pa s)	Latent heat of vapori-zation (MJ kg^{-1})	Specific heat (kJ kg^{-1} °C^{-1})	Thermal conductivity (J m^{-1} s^{-1} °C^{-1})
-10	997.94	--	--	2.525	4.271	--
-5	999.18	0.0764	--	--	--	--
0	999.87	.0756	1.792	2.501	4.218	0 .561
4	1000.00	.0750	--	2.492	4.205	0.596
5	999.99	.0748	1.519	2.489	4.202	0.574
10	999.73	.0742	1.308	2.477	4.192	0.586
15	999.13	.0734	1.140	2.466	4.186	0.595
20	998.23	.0727	1.005	2.453	4.182	0.603
25	997.08	.0719	0.894	2.442	4.180	0.611
30	995.68	.0711	0.801	2.430	4.178	0.620
35	994.06	.0703	0.723	2.418	4.178	0.628
40	992.25	.0695	0.656	2.406	4.178	0.632
45	990.24	.0687	0.599	2.394	4.179	0.641
50	988.07	.0679	0.549	2.382	4.181	0.645

TABLE 3.2 Physical Properties of Water Vapor. Source: Data from List (1984); ASTM (1976)

Temperature (°C)	Saturation vapor pressure over water (kPa)	Saturation vapor density over water (10^{-3} kg m^{-3})	Diffusion coefficient at P = 100 kPa (10^{-5} m^2 s^{-1})
0	0.61	4.85	2.26
5	0.87	6.80	--
10	1.23	9.40	2.41
15	1.70	12.83	--
20	2.34	17.30	2.57
25	3.17	23.05	--
30	4.24	30.38	2.73
35	5.62	39.63	--
40	7.38	51.19	2.89
45	9.59	65.50	--
50	12.34	83.06	--

1 kPa = 10 mb = 7.501 mm Hg
10^{-3} kg m^{-3} = 10^{-6} g cm^{-3}

Saturation vapor pressure in kPa can be calculated based on equations by Tetens (1930) and Murray (1967) for T in ^{o}C as:

$$e^{o} = 0.6108 \exp\left(\frac{17.27\,T}{T + 237.3}\right) \tag{3.1}$$

This expression provides values within 0.1% of those in the Smithsonian Meteorological Tables for temperatures in the range of 0 to 50°C (Allen et al. 1989). In some later chapters, e^{o} is expressed as $e^{o}(T)$ indicating that e^{o} is solved at temperature T. The slope of the saturation vapor pressure curve, Δ, kPa ^{o}C^{-1}, is obtained by differentiating eq. 3.1 (Allen et al. 1998):

$$\Delta = \frac{2503 \exp\left(\frac{17.27\,T}{T + 237.3}\right)}{(T + 237.3)^{2}} \tag{3.2}$$

Absolute humidity, ρ_v, is the water vapor density, i.e., the mass of water vapor per unit volume of air. It can be calculated from the ideal gas law:

$$\rho_v = \frac{1000\,e}{R_v T} \tag{3.3}$$

where ρ_v is the absolute humidity, kg m^{-3}, e is the vapor pressure, kPa (1 Pa = 1 N m^{-2}), R_v is the gas constant for water vapor (461.5 J kg^{-1} K^{-1}) and T is the absolute temperature in K. For e in kPa the density of water vapor in kg m^{-3} is:

$$\rho_v = \frac{2.167\,e}{T} \tag{3.4}$$

Specific humidity, q, is the relative density of water vapor, i.e., the mass of water vapor per unit mass of moist air:

$$q = \frac{\rho_v}{\rho_a} = \frac{m_v}{m_v + m_a} = \frac{0.622\,e}{P - 0.378\,e} \tag{3.5}$$

where q is the specific humidity, kg kg^{-1}, ρ_a is the density of moist air, m_v is the mass of water vapor, m_a is the mass of dry air, P is the total atmospheric pressure in kPa, e is the vapor pressure

in kPa, 0.622 is the ratio of the molecular mass of water (18.016) to the apparent molecular mass of dry air (28.966), and (1 – 0.622) = 0.378.

Vapor pressure deficit, *VPD*, of the air is a term used in the Penman and Penman-Monteith equations for ET:

$$VPD = e^o - e \tag{3.6}$$

Relative humidity, *RH*, is the dimensionless ratio of actual vapor pressure to saturation vapor pressure, usually expressed in percent. *RH* is defined as:

$$RH = 100 \frac{e}{e^o} \tag{3.7}$$

and *VPD* can be calculated as:

$$VPD = e^o \left[\frac{100 - RH}{100} \right] \tag{3.8}$$

Because of the very strong and nonlinear dependence of e^o on *T*, relative humidity by itself has limited utility in E and ET calculations unless air temperature or one of the vapor terms, which corresponds to the same time scale and interval as *RH*, is given.

Dew point temperature, T_d, is the temperature to which a parcel of air must be cooled at constant pressure and constant vapor content until saturation occurs, or the temperature at which saturation vapor pressure is equal to the actual vapor pressure of the contained vapor. At the dew point temperature, condensation will normally occur on a flat surface. Dew point temperature can be calculated from vapor pressure by inverting eq. 3.1:

$$T_d = \frac{116.91 + 237.3 \ln(e)}{16.78 - \ln(e)} \tag{3.9}$$

The thermodynamic wet bulb temperature is the temperature that is achieved in an adiabatic process when water is evaporated into the air until vapor pressure equals the saturation vapor pressure at the air-water interface. Energy for wet bulb evaporation comes from the air, so the air temperature drops as the vapor pressure increases. Wet bulb temperature, T_w, is the temperature that a moist evaporating surface may approach when the radiation energy balance is zero. In practice, the wet bulb temperature represents the equilibrium temperature of a thermometer covered with a cloth that has been wetted with pure water in air moving between 4 and 10 m s^{-1} (List 1984). The wet bulb thermometer cools as sensible heat transfers to the wet surface and vaporizes water, leading to water vapor flux from the surface and an increase in latent heat content of the contacted air. With sufficient ventilation (> 4 m s^{-1}) so that effects of radiation

transfer are small, the vapor pressure of the ambient air can be computed using the standard psychrometric constant, γ:

$$e = e_w^o - \gamma\left(T - T_w\right) \tag{3.10}$$

where e_w^o is saturation vapor pressure at T_w and T is ambient air temperature (i.e., dry bulb temperature). The pyschrometric constant, γ, is computed as:

$$\gamma = \frac{c_p P}{\lambda \varepsilon} \tag{3.11a}$$

where, P is atmospheric pressure, c_p is the specific heat of the air at constant pressure, λ is the latent heat of vaporization and ε is the ratio of the molecular mass of water to that of dry air (0.622). For P in kPa, λ in kJ kg^{-1}, γ has units of kPa $^oC^{-1}$. At sea level, P = 101.3 kPa = 1.0 Atm. A recommended value for c_p is 1.013 kJ kg^{-1} K^{-1} (Brutsaert 1982), representing air having relatively low humidity, (RH ~ 60% at T = 10°C, RH ~ 30% at T = 20°C, RH ~ 20% at T = 30°C, and RH ~ 10% at T = 40°C). Thus a good estimate of the pyschrometric constant, as used in the standardized calculation of the Penman-Monteith equation for ET_{ref}, assuming λ = 2450 kJ kg^{-1} is the simplification:

$$\gamma = 0.000665\ P \tag{3.11b}$$

where P is atmospheric pressure in kPa and γ has units of kPa $^oC^{-1}$.

The psychrometric constant used in eq. 3.10 to convert wet and dry bulb data from a psychrometer is commonly given by:

$$\gamma_{psy} = a_{psy} P \tag{3.12}$$

where a_{psy} is a coefficient depending on the type of ventilation of the wet bulb [°C^{-1}], and P is mean atmospheric pressure [kPa]. The coefficient a_{psy} depends primarily on the design of the psychrometer and on the rate of ventilation around the wet bulb and is essentially the same as the standard constant from eq. 3.11b under high ventilation conditions. When ventilation of the pyschrometer drops below 4 m s^{-1}, the wet bulb temperature can be influenced by the long-wave radiation balance of the pyschrometer. The following values are often used (ASCE-EWRI 2005):

a_{psy} = 0.000662 for ventilated (Asmann type) psychrometers, with air movement of approximately 5 m s^{-1},
= 0.000800 for naturally ventilated psychrometers with air movement of about 1 m s^{-1}, and
= 0.001200 for non-ventilated psychrometers installed in glass or plastic greenhouses (List 1984).

Using the above values, the values for γ in eq. 3.10 become about 1.2 times the standard pyschrometric constant for naturally ventilated psychrometers having air movement of about 1 m s^{-1}, and about 1.8 times the standard constant for non-ventilated psychrometers installed in glass or plastic greenhouses.

Air

Mean atmospheric air pressure, P, can be computed using the ideal gas law (List 1984; Burman et al. 1987) as:

$$P = P_o \left(\frac{T_o - \Gamma (z - z_o)}{T_o} \right)^{\frac{g}{\Gamma R}} \tag{3.13}$$

where P_o and T_o are standardized atmospheric pressure in kPa and absolute temperature in K at elevation z_o in m and z is the elevation of the location or instrument in m above mean sea level. The assumed constant adiabatic lapse rate, Γ, is normally taken as 0.0065 K m^{-1} for saturated air or 0.010 K m^{-1} for non-saturated air; g is gravitational acceleration, 9.807 m s^{-2} and R is the specific universal gas constant for dry air, 287.0 J kg^{-1} K^{-1}. Values for P_o, T_o, and z_o for the standard atmosphere (List 1984) are 101.3 kPa, 288K, and 0 m. The base value T_o is generally set to 293K (Smith et al. 1991; Allen et al. 1998) during calculation of ET_{ref} to better represent common field environments. Eq. 3.13 is relatively insensitive to the value of Γ for elevations up to 3,000 m. In the ASCE-EWRI report on standardization of ET_{ref} (ASCE-EWRI 2005), eq. 3.13 was simplified to:

$$P = 101.3 \left(\frac{293 - 0.0065 z}{293} \right)^{5.26} \tag{3.14}$$

where the base temperature is set at 293K. Air density, ρ_a, can be computed as

$$\rho_a = \frac{1000\ P}{T_v\ R} \tag{3.15}$$

where P is the barometric pressure in kPa, R is 287.0 J kg^{-1} K^{-1} and T_v is virtual temperature, in K. Barometric pressure is so called because barometers are used to measure it. It is the pressure exerted on the earth's surface by the weight of the air above the point that it is being measured. Virtual temperature is the temperature at which dry air possesses the same density as the moist air at the same pressure P and temperature T. T_v in eq. (3.15) enables the use of R for dry air. T_v can be computed as (Jensen et al. 1990):

$$T_v = \frac{T}{1 - 0.378\frac{e}{P}} \tag{3.16}$$

where T is air temperature, K, and e is mean vapor pressure of the air, kPa. Substitution of eq. (3.16) into (3.15) produces:

$$\rho_a = \frac{1000\ (P - 0.378e)}{T\ R} \tag{3.17}$$

where $(P - 0.378\ e)$ represents the partial pressure of dry air, and R is the universal gas constant for dry air.

Latent heat of vaporization, λ, in MJ kg^{-1} can be computed following Harrison (1963) as:

$$\lambda = 2.501 - 2.361\,x10^{-3}\ T \tag{3.18}$$

where T is mean air temperature in ^{o}C. If available, mean surface temperature or wet bulb temperature can be used to compute the value of λ which better represents conditions at the evaporating surface. λ has a value of 2.45 MJ kg^{-1} at 21.6°C, a value that was used during the standardization of the ET_{ref} calculation (ASCE-EWRI 2005).

Standard Atmosphere (Lower Atmosphere)

Characteristics of a standard atmosphere (average conditions for USA at latitude 40°N) are given in table 3.3 at a base temperature of 15°C. Characteristics of standard atmospheres at other latitudes are summarized by Burman et al. (1987). Characteristics of the lower atmosphere using a base temperature of 20°C are given in table 3.4.

TABLE 3.3 Standard Lower Atmosphere. Source: Data from List (1984)[1]

Altitude (m)	Temperature (°C)	Barometric Pressure (kPa)	(mb)	Density (kg m^{-3})
0	15.0	101.3	1013	1.226
500	11.75	95.5	955	1.168
1,000	8.50	89.9	899	1.112
1,500	5.25	84.6	846	1.058
2,000	2.00	79.5	795	1.007
3,000	-4.50	70.1	701	0.909

[1] Data from table 63, List (1984), and based on the assumption by List of dry air and an adiabatic lapse rate of 0.0065°C m^{-1}.

TABLE 3.4 Characteristics of the lower atmosphere using 20°C base temperature at sea level instead of 15ºC[1]

Altitude (m)	Temperature (°C)	Barometric pressure (kPa)	Density dry air (kg m^{-3})	Saturation vapor press. (kPa)	Virtual temp. at sat. (K)	Density saturated air (kg m^{-3})
0	20.00	101.3	1.204	2.34	295.7	1.193
500	16.75	95.5	1.148	1.91	292.1	1.139
1,000	13.50	90.0	1.094	1.55	288.5	1.087
1,500	10.25	84.8	1.042	1.25	285.0	1.037
2,000	7.00	79.8	0.992	1.00	281.5	0.988
3,000	0.50	70.5	0.898	0.63	274.6	0.895

[1] Calculated using eq. (3.13) – (3.15) and an adiabatic lapse rate of 0.0065°C m^{-1}.

3.3. Soil Properties

A unit volume of soil, V, contains solids, V_s, water, V_w, and air and water vapor, V_{av}, and can be expressed as:

$$V = V_s + V_w + V_{av} \tag{3.19}$$

The soil water content is commonly expressed on a volume basis as m^3 m^{-3}, θ:

$$\theta = \frac{V_w}{V} \tag{3.20}$$

or on a mass basis, kg kg^{-3}, θ_m:

$$\theta_m = \frac{m_w}{m_s} \tag{3.21}$$

where m_w and m_s are the masses of water and dry soil, respectively. In practice, the soil water content is determined by drying at 105°C.

Conversion of soil water content on a mass to a volumetric basis requires knowing the bulk density of the dry soil matrix, ρ_b, where $\rho_b = m_s/V$, from which

$$\theta = \frac{\rho_b}{\rho_w}\theta_m \tag{3.22}$$

where ρ_w is the density of liquid water, and units cancel.

The volumetric water content represents the equivalent depth of water per unit soil depth. Prior to the use of the neutron moisture probe and electromagnetic devices, which are calibrated to indicate θ, most field studies involved gravimetric determination of the water content per unit mass of dry soil, θ_m. To determine the volumes of water involved, eq. 3.22 was used and in most cases, ρ_b, once determined during a study, was considered to remain constant at a given depth throughout the season or study. This assumption is reasonable below the tillage depth, but can result in substantial measurement error in the total soil water in the tilled layer. The error is not great for determining changes in soil water content over 5- to 15-day periods. However, ρ_b should be adjusted for water content changes in swelling and cracking soils.

3.4. Soil-Water System

Energy State of Soil Water

Since the movement of water in soil is slow, its kinetic energy can be neglected. The major energy components that affect mass flow in soils are the gravitational and pressure potentials. These variables, when combined, are commonly expressed as hydraulic head, H, which is the sum of pressure and gravitational potentials.

$$H = \frac{P_w}{\rho_w \, g} + z = h + z \tag{3.23}$$

where P_w is the pressure of water (kPa or kJ m^{-3}), ρ_w is the density of liquid water (kg m^{-3}), g is the gravitational acceleration (m s^{-2}), h is the fluid pressure head (m), and z is the gravitational potential (m) or the vertical distance from the reference datum. The water pressure datum is normally taken as the free water surface or land surface under atmospheric conditions. A tensiometer can be used to directly measure h ranging from small positive values to about -0.8 m.

Most soils literature use the terms capillary potential, matric potential, and soil-water suction or tension when referring to the pressure potential of water in soils. Soil water energy terms and other commonly used units are presented in table 3.5. A pressure potential of -153 m water or a suction of 15 bars approximates the wilting point.

TABLE 3.5 Methods and Units of Soil-Water Energy

Soil-water suction or tension				Soil-water potential energy			
Head, H, of water (m)	(kPa)	(bar)	(MPa)	Per unit mass ($J\ kg^{-1}$)	Per unit volume (kPa)	(bar)	(MPa)
0.01	0.1	0.001	0.0001	-0.1	-0.1	-0.001	-0.0001
.10	1.0	0.010	0.0010	-1.0	-1.0	-0.010	-0.0010
1.02	10.0	0.100	0.0100	-10.0	-10.0	-0.100	-0.0100
152.952	1500.0	15.000	1.5000	-1500.0	-1500.0	-15.000	-1.5000

When considering the impact of total suction on water extraction by roots, soil scientists refer to the sum of the matric potential and osmotic potential caused by solutes in the soil water. Solutes may have little effect on mass flow, but become important in flow across membranes, including those in plant roots, in vapor diffusion and in measuring soil-water potential using vapor pressure techniques. Soil physics texts such as that by Jury et al. (1991) provide more information on the energy status of water in soils.

Soil-water Characteristic Curve

Soil water-holding characteristics are described by the soil-water characteristic curve. An example of such a curve is illustrated in fig. 3.1. When a parcel of soil is saturated, the fluid pressure may be positive or zero. As the water pressure decreases below atmospheric pressure, little change in water content occurs until the air-entry pressure is reached (the air entry region). Air entry pressure is the pressure at which the largest pore begins to empty. Decreasing the water pressure below the air-entry point results in a decrease in water content as illustrated fig. 3.1. The water content at a specific energy level is not unique. The curve shape depends on whether it was derived during a wetting or drying phase. The difference in curve shape due to wetting or drying is often referred to as hysteresis.

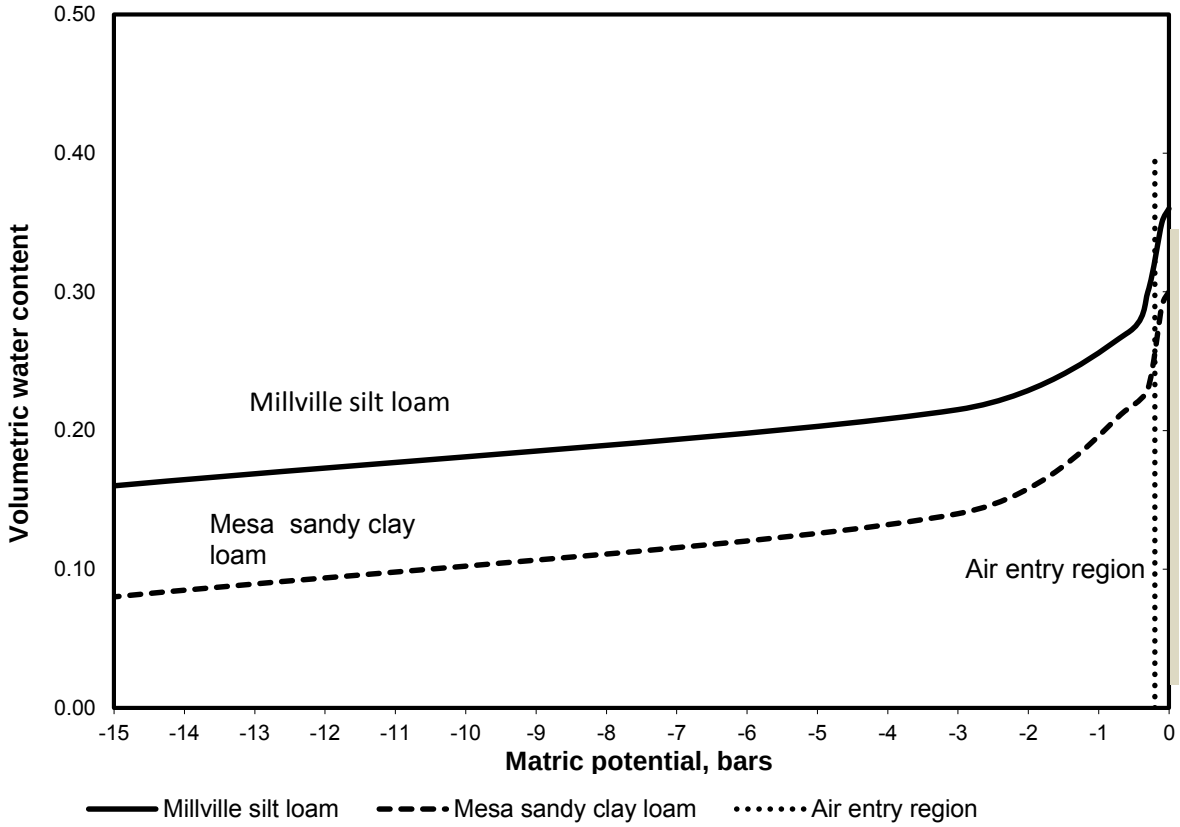

Figure 3.1 Water content related to matric potential for two soils. The volumetric water content at -15 bars is commonly considered the permanent wilting point (shown along the left vertical axis). Values shown are for Millville silt loam and Mesa sandy clay loam. Source: Data from James et al. 1982).

Flow of Water in Soils

The flow of water in soils is important in many applications such as when determining irrigation water requirements, determining average ET rates by measuring the change in soil water content over time, and in water balance studies. These flows are vertical unsaturated drainage from the root zone, upward flow from a shallow, saturated zone, and radial flow to plant roots. Darcy's law is often used to describe one-dimensional flow through soil.

$$v = -K\,\frac{\Delta H}{\Delta S} = -K\,\frac{\partial H}{\partial S} \tag{3.23}$$

where v is the bulk or average flow with units of discharge per unit cross-sectional area in the direction of increasing distance S, K is the hydraulic conductivity that varies with θ and H is the hydraulic head. Since $H = h + z$, vertical one dimensional flow can be expressed as:

$$v = -K\left[\frac{\partial h}{\partial z} + 1\right] \tag{3.24}$$

where z is positive upward and h is the water pressure head relative to atmospheric pressure (negative for unsaturated conditions). If v becomes negative, flow is downward, and always in the direction of decreasing H. For $v = 0$, or static conditions, $\partial h/\partial z$ must equal -1.0. When the water table is several meters below the effective root zone in irrigated fields, and excess water has been applied, it is not uncommon to find $\partial h/\partial z = 0$ and the downward hydraulic gradient is unity. Under these conditions, drainage occurs at a velocity $v = K$. The rate of drainage is normally not constant, but changes slowly with time. Therefore, θ and h may change only slightly along with a corresponding change in K.

For nonsteady flow, $\partial\theta/\partial t \neq 0$, Darcy's law and the continuity equation are combined and for the one-dimensional vertical case reduces to:

$$\frac{\partial \theta}{\partial t} = \frac{\partial}{\partial z}\left(K\frac{\partial H}{\partial z}\right) = \frac{\partial}{\partial z}\left(K\frac{\partial h}{\partial z}\right) + \frac{\partial K}{\partial z} \tag{3.25}$$

Eq. 3.25 is generally solved by numerical techniques using computers, for example, with the HYDRUS model (Šimunek et al. 2005). Challenges in applying eq. 3.25 for practical problems include obtaining accurate soils information (K vs. θ and h).

General Soil-Water Properties

Soils vary greatly in their ability to retain water. Estimates of the capacity of soils to retain irrigation water and precipitation and to release the water to plants are primary variables involved in scheduling irrigation depths and frequencies. Given adequate time, water at a point within a homogeneous soil profile will decrease, due to drainage caused by gravity, to a level on the characteristic curve which is at an energy level equivalent to the elevation of the point above the water table. For soils overlying deep water tables, drainage may continue for many days at a decreasing rate. The rate of decrease in water content in a given zone typically follows the function $d\theta/dt = a\ t^{-b}$ where a and b are constants for a given zone of soil, t is time in days after complete wetting and evaporation is prevented (Richards et al. 1956). As the water content of an initially saturated zone of soil depth decreases, it approaches a near equilibrium level called *field capacity* (Ratliff et al. 1983). This limit may not be reached until 2 to 12 days after a heavy irrigation or precipitation if ET rates are near zero. Field capacity has also been referred to as the "drained upper limit" (Ratliff et al. 1983), and is primarily a function of soil texture. Other factors also affect the shape of the characteristic curve. Generally, the water content at field capacity occurs at soil water potentials near -10 kPa (-0.1 bar) in coarse-textured soils and at potentials near -30 kPa (-0.3 bar) in medium to fine-textured soils. Average values and ranges of field capacities of general soil classes are presented in table 3.6. These values and ranges were summarized from similar data presented by McDole et al. (1974), Evans (1980) Ratliff et al. (1983) and Keller (1986).

TABLE 3.6 General Soil Water Classes for Agricultural Soils. Source: data from McDole et al. (1974); Evans (1980); Ratliff et al. (1983); and Keller (1986)

	WATER CONTENT, VOLUME BASIS (%)					
	Field Capacity		Permanent Wilting Point		Available water	
Texture class	Average (%)	Range (%)	Average (%)	Range (%)	Average (%)	Range (%)
			Coarse			
(Sand)	12	7 - 17	4	2 - 7	8	5 - 11
(Loamy sand)	14	11 - 19	6	3 - 10	8	6 - 12
			Moderately coarse			
(Sandy loam)	23	18 - 28	10	6 - 16	13	11 - 15
			Medium			
(Loam)	26	20 - 30	12	7 - 16	15	11 - 18
(Silt loam)	30	22 - 36	15	9 - 21	15	11 - 19
(Silt)	32	29 - 35	15	12 - 18	17	12 - 20
			Moderately fine			
(Silty clay loam)	34	30 - 37	19	17 - 24	15	12 - 18
			Fine			
(Silty clay)	36	29 - 42	21	14 - 29	15	11 - 19
(Clay)	36	32 - 39	21	19 - 24	15	10 - 20

As water is withdrawn from soil by root extraction or evaporation, it becomes increasingly difficult to withdraw additional water because the soil matric and osmotic potentials become more negative. In addition, as soil water content decreases, the hydraulic conductivity decreases, reducing the flow of water to roots. Because of the decrease in the "availability" of water to plant roots, a lower limit of available water is often set that has historically been termed the *permanent wilting point*. Water below this limit is considered to be unavailable to plants, with plants experiencing severe water stress with corresponding wilting and eventually plant death.

Other terms for permanent wilting point have included "lower limit of crop extractable water" and "lower limit of available water" (Ratliff et al. 1983). Traditionally, the permanent wilting point has been related to soil water at a matric potential of approximately -1500 kPa (-15 bars). However, the water potential equivalent to the permanent wilting point is a function of other factors in addition to the shape of the soil characteristic curve. These other factors include the ability of the plant to survive under stressed conditions, root densities and the magnitude of

evaporative demand. Typical values and ranges of the lower limit of extractable water of general soil textural classes are presented in table 3.6.

Available water is defined in this manual as the quantity of soil water between field capacity and permanent wilting point. It is the amount of stored soil water that can be extracted by plant roots. A portion of this amount is not "readily" available to the plant, i.e., the rate of uptake by the roots may be less than potential transpiration and plant growth may begin to decrease as water is extracted beyond a certain water content. Average values and ranges of available water are presented in table 3.6. In addition to the ultimate extraction of total available water, plants may extract some additional water temporarily stored at water contents above field capacity or the drained upper limit during the 2- to 5-day period required for soil water to approach field capacity after irrigation or heavy rain.

Soil-Plant Interactions

General Plant Rooting Depths. Root growth occurs as new cells are formed and expand. Many factors affect root growth (Taylor 1983). These include such variables as transpiration rate and water stress, aluminum content and salinity of soils, soil strength, aeration, temperature, nutrient supply, and soil water content. Root systems are generally of two main types, tap root and fibrous. Grass type plants have fibrous roots and dicotyledonous plants have a tap root and fibrous roots. Shoot and root growth are coordinated so that in water management, depth of rooting is often related to the development of shoots, or crop canopy.

Effective rooting depth is usually less than the maximum rooting depth of a mature plant due to decreased rooting density near the lower portions of the root zone. A general "rule of thumb" is that about 80 to 90 percent of a plant's feeder roots are contained in the upper 60 to 75 percent of the effective root zone (Hansen et al. 1979; Keller 1986). Typical maximum effective rooting depths for agricultural crops are presented in table 3.7. These represent rooting depths for healthy plants in soils under typical irrigated conditions with no soil or water-induced restrictions such as hard layers or nearly saturated profiles. Similar values for maximum effective rooting depth are contained in Appendix B based on the FAO-56 publication (Allen et al. 1998).

Annual crops typically attain maximum rooting depths shortly after developing a complete crop canopy. Borg and Grimes (1986) listed maximum rooting depths for a number of annual crops. They also described a sine-based function for estimating the increase in root depth, R_z, over time for annual crops in temperature climates having a nongrowing period:

$$R_z = R_{z\max}\left[0.5 + 0.5\sin\left(3.03\frac{D - D_p}{D_m - D_p} - 1.47\right)\right] \tag{3.26}$$

where $R_{z\,max}$ is the maximum effective rooting depth for a mature crop, D is the day of the year in the northern hemisphere, D_p is the planting date, and D_m is the date of crop maturity (near maximum root extent and based on local observation). D is constrained to $D_p \le D \le D_m$ and $R_z = R_{z\,max}$ when $D > D_m$. Parameters D, D_p, and D_m can be added to 180 in the southern hemisphere. Borg and Grimes (1986) showed good agreement between eq. 3.26 and field observations for soybean, cotton, wheat and oats. Martin et al. (1990) and Allen et al. (1998) described the growth in R_z as a linear function of time:

$$R_z = R_{z\,ini} + \frac{D - D_p}{D_x - D_p}\left(R_{z\max} - R_{z\,ini}\right) \quad for \;\; D < D_x \tag{3.27}$$

$$R_z = R_{z\max}, \;\; for \;\; D \geq D_x \tag{3.28}$$

where $R_{z\,ini}$ is the initial effective rooting depth at planting (or plant emergence) and D_x is the date of maximum effective root depth (often taken as the date of effective full cover for many annual crops). The value for $R_{z\,ini}$ is generally assumed to range from 0.05 to 0.15 m because of upward flow of soil water and rapid expansion of the root system following germination.

For annual crops, especially row crops, the increase in effective rooting depth and density is related to the increase in crop canopy. The basal crop coefficient (K_{cb}), which is defined in chapter 8, increases with the relative amount of actively transpiring crop canopy. Therefore, the increase in rooting depth for many annual crops before effective full cover can be estimated in proportion to the basal crop coefficient (Martin et al. 1990; Allen et al. 1998):

$$R_z = R_{z\,ini} + \frac{K_{cb} - K_{cb\,ini}}{K_{cb\,c} - K_{cb\,ini}}\left(R_{z\max} - R_{z\,ini}\right), \; for\, D < D_x \tag{3.29}$$

$$R_z = R_{z\max}, \;\; for \;\; D \geq D_x \tag{3.30}$$

where K_{cb} is the basal crop coefficient on the current day D, $K_{cb\,ini}$ is the initial basal crop coefficient (at planting or emergence), and $K_{cb\,c}$ is the basal crop coefficient at effective cover (on day D_x). Crop coefficients are described in chapter 10 and values for various crops are presented in the Appendices. Martin et al. (1990) presented a graphic comparison of the crop coefficient model, the linear model and the Borg-Grimes sine function model showing the general similarity of these models.

Soil-Water Depletion Levels. Only a portion of the available soil water between field capacity and the lower limit of extractable water is "readily" available to the plant. Because of decreases in hydraulic conductivity and soil water potential as soil water content decreases, the rate of extraction of soil water by plant roots may be less than the evaporative demand, and plant water stress begins to occur. The soil water content at which the supply to the roots is less than the evaporative demand is related to the magnitude of evaporative demand, the density of roots in the soil, the osmotic pressures in the soil, and the hydraulic properties of the soil. The concept of "management allowed depletion" or "management allowed deficiency" (Merriam and Keller 1978) is one approach that is used in scheduling irrigations to avoid plant water stress. The management allowed depletion (*MAD*) is defined as the management planned percentage of the available soil water (between field capacity and the lower limit of extractable water) that is depleted between irrigations. *MAD* contrasts to the yield threshold depletion, *YTD*, which is the fraction of available soil water that can be depleted before adversely affecting crop production. Another parameter, *p*, is the fraction of available water that can be depleted before sufficient stress is experienced to decrease transpiration (Doorenbos and Pruitt, 1977; Allen et al., 1998). Generally, *MAD* < *YTD*, however, *MAD* can exceed *YTD* in management systems where crop water stress is implemented to improve fruit quality or to optimize economics. The parameter

MAD is used in irrigation scheduling, whereas *p* is used to estimate reduction in ET caused by crop water stress.

Typical values for *MAD* for irrigated crops are included in table 3.7 and values for *p* are included in Appendix B. Values of *MAD* are typically about 25 to 40 percent for high-value, shallow or sparsely rooted crops, 50 percent for deep-rooted crops, and 60 to 65 percent for low value, deep-rooted crops. In addition to maintaining available soil water to meet the evaporative demand, adjustments in the value of *MAD* may be required to compensate for uncertainties in the estimated total available soil water, effective rooting depth and lateral distribution, soil water depletion, net irrigation depths and ET rates. Thus, the *MAD* also can provide a safety factor against plant water stress. Some crops require greater soil water depletions directly before harvest to enhance the quality of the fruit or grain. Greater depletion at harvest also enables storing a higher proportion of over-winter precipitation. The values for *MAD* in table 3.7 represent average conditions for ET rates of about 5 to 6 mm d^{-1}. Values may be decreased by 5 to 10 percent during periods with ET rates greater than 6 mm d^{-1} to maintain a higher soil hydraulic conductivity. The values for *MAD* and rooting depths listed in table 3.7 may need to be adjusted by the user to fit local conditions or varietal differences among crops.

The net maximum depth of soil water that should be depleted between irrigations to avoid significant plant water stress, and sometimes referred to as readily available water, *RAW*, can be estimated as:

$$RAW = \frac{p}{100} R_z \, AW \tag{3.31}$$

where *AW* is the average value of total available water (field capacity less the lower limit of extractable water) in the root zone of the soil profile. In many evaluations of impacts of water stress on ET, values for *p* are set equal to values for *MAD* as listed in table 3.7.

TABLE 3.7 General Maximum Effective Rooting Depths of Fully Grown Crops and Management Allowed Depletion Levels in percent of available water[1].

(a) Crop	Rooting Depth Range (m)	*MAD* (%)	Crop	Rooting Depth Range (m)	*MAD* (%)
Alfalfa	1.0 - 2.0	55	Maize, grain	1.0 - 1.7	60
Artichoke	0.6 - 0.9	45	Melons	1.0 - 1.5	35
Asparagus	1.2 - 1.8	45	Mint	0.4 - 0.8	40
Avocado	0.6 - 0.9	40	Olives	1.2 - 1.7	65
Banana	0.5 - 0.8	40	Onions	0.3 - 0.5	25
Barley	1.0 - 1.5	55	Palm trees	0.7 - 1.0	65
Beans (green)	0.5 - 0.7	45	Parsnip	0.6 - 0.9	40
Beans (dry)	0.6 - 0.9	45	Passion fruit	0.3 - 0.5	35
Beets	0.6 - 1.0	50	Peas	0.6 - 1.0	40
Berries	0.6 - 1.2	50	Peppers	0.5 - 1.0	25
Broccoli	0.6	40	Pineapple	0.3 - 0.6	50
Brussel sprout	0.6	40	Potatoes	0.4 - 0.6	35
Cabbage	0.4 - 0.5	45	Pumpkin	0.9 - 1.2	40
Cantaloupe	0.6 - 1.2	40	Radish	0.3	30
Carrots	0.5 - 1.0	35	Safflower	1.0 - 2.0	60
Celery	0.3 - 0.5	20	Sisal	0.5 - 1.0	80
Citrus	1.2 - 1.5	50	Sorghum	1.0 - 2.0	55
Clover	0.6 - 0.9	50	Soybeans	0.6 - 1.3	55
Cotton	0.8 - 1.7	60	Spinach	0.3 - 0.5	20
Cucumber	0.7 - 1.2	50	Squash	0.6 - 0.9	50
Dates	1.5 - 2.5	50	Strawberries	0.2 - 0.3	15
Deciduous Orch.	1.0 - 2.0	50	Sugarbeets	0.7 - 1.2	55
Egg plant	0.8	45	Sugarcane	0.8 - 1.8	65
Fig	0.9	50	Sunflower	0.8 - 1.5	45
Flax	1.0 - 1.5	50	Sweet potatoes	1.0 - 1.5	65
Grains, Small	0.9 - 1.5	60	Tobacco	0.5 - 1.0	55
Grains, Sm. Win.	1.5 - 2.0	60	Tomatoes	0.4 - 0.8	40
Grapes	1.0 - 2.0	35-45	Turnip (white)	0.5 - 0.8	40
Grass	0.5 - 1.5	50	Walnuts	1.7 - 2.4	50
Groundnuts	0.5 - 1.0	50	Watermelon	1.0 - 1.5	45
Hops	1.0 - 1.2	50	Wheat, spring	1.0 - 1.5	55
Lettuce	0.3 - 0.5	30	Wheat, winter	1.5 - 1.8	55

[1]Primary sources: Data from Doorenbos and Pruitt (1977) and Keller (1986). Additional values are given in Appendix B.

3.5. Vegetative (Crop) Properties

Foliage Factors

Leaf Area and Leaf-Area-Index (LAI). As emerging seedlings develop leaves and their roots systems permeate the soil, the plants increase in their effectiveness for transferring water from the soil to the atmosphere. The crop foliage factors that affect ET are the leaf-area-index, *LAI*, and the ground cover. *LAI* is defined as the area of one side of plant leaves per land area including areas between plants and rows. LAI is expressed as $m^2\ m^{-2.}$ Ground cover is the fraction of the total surface that is covered by foliage (i.e., shaded when the sun is directly overhead) and is expressed as a fraction or percentage. For many common agricultural crops, the rate of ET under given environmental conditions increases with *LAI* until the *LAI* reaches a value of about 2.7-3.0 or with ground cover up to 70 to 80%. Most of the energy available for evaporation is absorbed by a canopy with LAI = 3.0 so further leaf production does not usually increase energy absorption (Ritchie 1972, Wright 1982). The relationship between *LAI* and crop factors affecting ET rates is discussed in detail in chapter 10.

Stomatal Resistance (Conductance). Water moves in the liquid phase from the soil through the plants to the evaporation sites in cell walls. It then moves to the atmosphere in the vapor phase through the stomates. The stomates are openings in the plant leaves shielded by guard cells that enable plants to absorb carbon dioxide from the air. When plant leaves are turgid, the stomates are generally fully open in bright sunlight and the resistance to the flow of water vapor and carbon dioxide is at a minimum, or the conductance is at a maximum. As soil water begins to limit the rate at which water can be transferred to the atmosphere, the stomates begin to close increasing the stomatal resistance. The concept of resistance to vapor transfer at the leaf surface was introduced by Penman and Schofield (1951). Slatyer (1967) described the resistance to water vapor transfer for a whole leaf as

$$\frac{1}{r_l} = \frac{1}{r_{cu}} + \frac{1}{r_{st}} \tag{3.32}$$

where r_l is the total internal resistance of the whole leaf, and r_{cu} and r_{st} are the resistances in the cuticular and stomatal pathways in units of s m^{-1}.

Bulk Surface Resistance. Bulk surface (stomatal) resistance of plant leaves is a dynamic property that changes with sunlight, vapor pressure deficit, leaf temperature, and soil water potential, or available soil water. For a single-layer model of ET, such as the PM equation, the bulk surface resistance represents the integrated resistance of vapor flow through the stomates, vapor diffusion from the soil, and vapor transport within a dense plant canopy. Detailed discussion of bulk surface resistance, the factors affecting it and its magnitude are discussed in chapter 11.

Root Factors

Root Type and Density. The primary pattern of root system development depends on the plant species. Root system patterns are of three basic types: diffuse or fibrous characteristic of

most monocotyledonous crops and either tap rooted or modified tap root characteristic of most dicotyledonous plants. Root systems generally grow downward whereas individual roots can grow in any direction. Tap roots of dicotyledonous plants and the main seminal axes of cereal crops grow vertically downward while lateral roots grow perpendicular to the parent root, and may even grow upward. Stone et al. (2001) presented an example of measured changes in root density and root penetration over time for grain sorghum and sunflower based on soil core analyses. The soil was a silt loam with moderate permeability and high available water capacity. The root density results for grain sorghum, a fibrous root plant, shown in fig. 3.2 indicated that the downward growth of the root system was nearly linear with days after planting to a depth of 2 m. As depth of rooting increased the relative distribution of roots with depth also changed as illustrated in fig. 3.3. The downward growth of sunflower roots, a monocotyledon plant, was essentially linear for the first 80 days as it approached the maximum depth of 3 m. The root distribution for sunflower was similar to that of grain sorghum except for having a greater percentage of roots in the 0.15-m depth. A similar pattern of cotton root distribution was presented by Klepper (1990) and similar patterns of modeled maize root densities were presented by Jones et al. (1991).

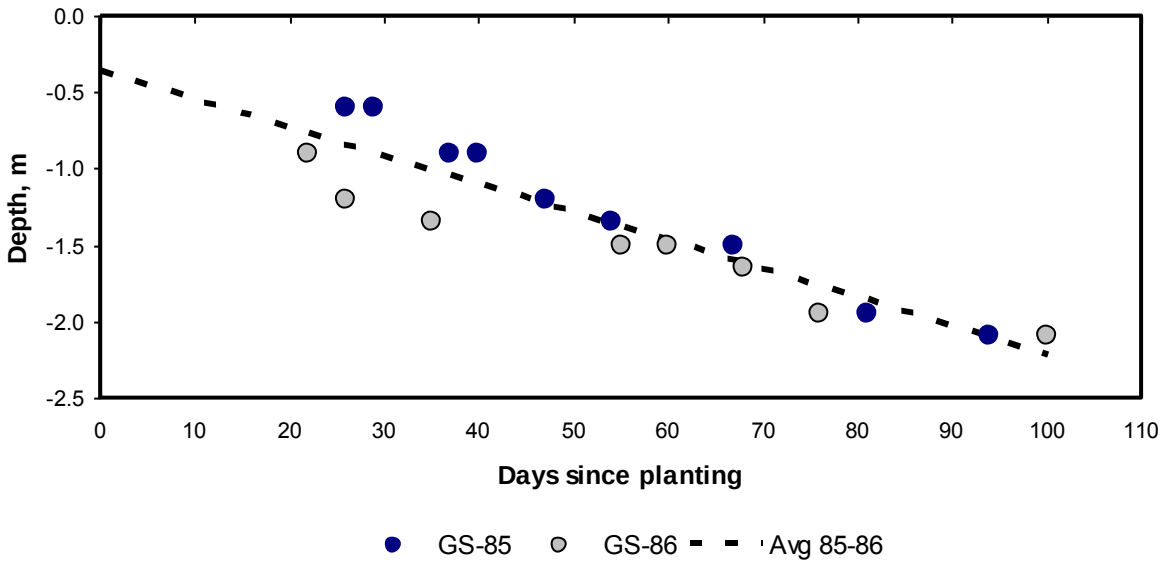

Fig. 3.2. Change in maximum depth of rooting by grain sorghum at Manhattan, KS with days after planting. (data from Stone et al. 2001).

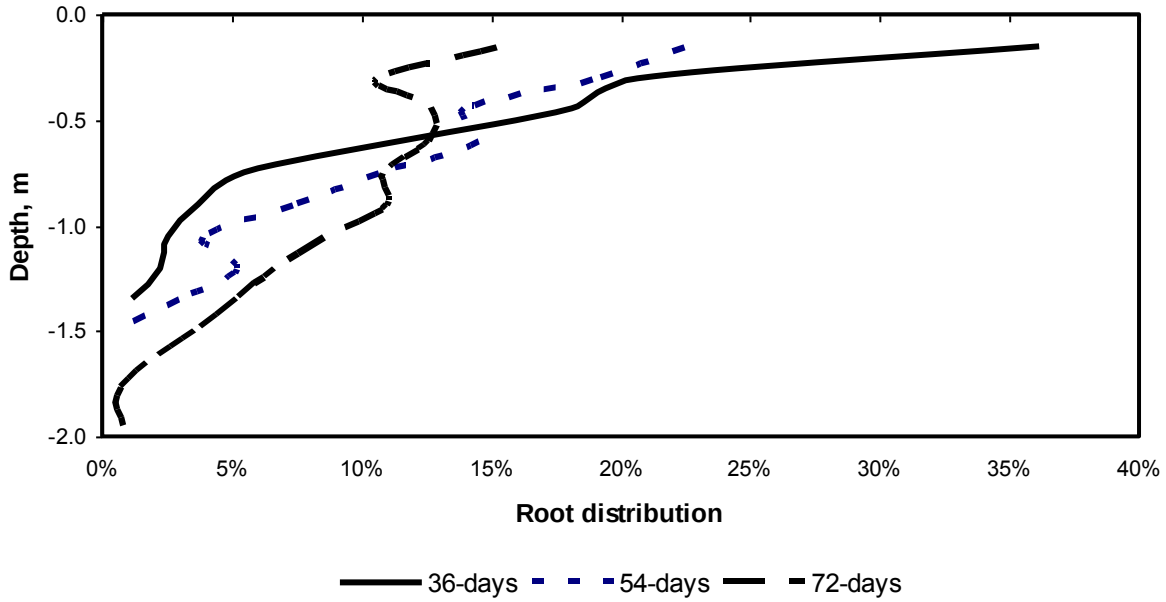

Fig. 3.3. Average percentage distribution of grain sorghum roots with depth at 36, 54 and 72 days after planting. Percentage values are approximate root lengths per 0.3 m (data from Stone et al. 2001).

Root-Soil Interactions. Many studies of plant root systems have been conducted since the 1960s and there is a vast amount of literature available on root growth and root-soil interactions. Two excellent sources of information with extensive bibliography are those by Taylor (1983) and Klepper (1990). Taylor presented an overview on soil environmental effects on root growth and function. Klepper presented a summary of the growth and water extraction by field crops including concepts for modeling water uptake by plant roots. She indicated that numerous soil and cultural factors influence root distributions in field soils. Environmental factors can also affect the ratio of leaf area to root length. Unfavorable soil conditions can reduce the rate of vertical and lateral root elongation. Details on modifying the root environment can found in a monograph by Arkin and Taylor (1981).

Roots grow as new cells are formed and then expand in volume. Elongation of both main roots and branches occurs as a result of cell enlargement immediately behind the root tip. Relative distinct characteristic development patterns exist between monocotyledonous and dicotyledonous species.

For high rates of cell elongation, roots need energy, which requires oxygen for oxidative phosphorylation. If oxygen levels fall below 3% in the soil atmosphere, which can occur in the presence of a shallow water table, root elongation will slow and eventually cease. Reduced oxygen also causes roots to be thicker. Large amounts of oxygen are required for biosynthesis of new cell materials such as membranes and wall materials. Another energy-requiring process is the active and selective accumulation of ions from the surrounding soil solution. To sustain rapid root elongation in soils, there must also be a rapid radial influx of water from the surrounding soil solution. Root growth is influenced greatly by soil factors including soil structure, strength, water content, temperature, porosity, gaseous diffusivity, pH, toxicity, and fertility. The requirement of space for new root material is often limited by traffic pans, plow pans, and other adverse subsoil conditions that limit pore space and cause excessive soil strength.

Large pores provide channels for easy root penetration and can affect the shape of the root system. Two factors that influence soil resistance to penetration are soil density and soil water content. Poor aeration is often a confounding factor when compaction decreases available pore space and when soil water content increases to a point where pore space is filled with water (Klepper 1990).

Root and shoot development are interdependent and limitations on one affect the other (Klepper 1990). In normal soils and with adequate soil water, roots develop to their full potential. Irrigation schedules are generally based on normal root-shoot development, weather, allowable plant water stress and the available water holding capacity of soils. When root development is impeded by physical or chemical soil conditions, adjustments in normal irrigation scheduling practices may be required.

BLANK PAGE

4

Energy Balance

4.1. Introduction

Historical and many recent studies of evaporation (E) and evapotranspiration (ET) clearly show that, where soil water is not limiting, the primary variable controlling the rate of E and ET is solar radiation impinging on the evaporating surfaces (irradiance). Part of the solar radiation is reflected back to the atmosphere and part of that which is absorbed at the surface changes to another energy state and may be reradiated back as long-wave radiation or convected to the air as sensible heat. Part of the loss of energy by the emitted long-wave radiation is compensated by the long-wave radiation emitted from the sky. The radiation balance determines the net radiant energy available at the evaporating surfaces. The most accurate methods of estimating E and ET require determining the radiation balance, or net radiation, for the surface. Many studies have shown that daily net radiation is closely related to the daily rate of E from shallow water bodies and ET when soil water is not limiting, especially in warm to hot subhumid and humid climates. During daytime, E or of ET are closely linked to changes in solar and net radiation, even over periods as short as five minutes. Examples that follow, however, reveal that the actual fraction of net radiation converted into E or ET can vary markedly depending upon air mass conditions above the surface and on the availability of water at the surface.

4.2. Energy Balance

The surface energy balance relates to the various ways in which net radiation, R_n, is balanced by the inputs or outputs of energy from non-radiative parameters. The vertical energy balance at the soil or water surface or at the "effective surface" of a crop is the sum of sensible heat flux to or from the air and soil (or water), latent heat, net radiation and other miscellaneous fluxes. The energy balance of land and water surfaces and the sign convention used in this manual is expressed as follows and illustrated in fig. 4.1:

$$R_n = \lambda E + H + G \tag{4.1}$$

where R_n is net radiation to the surface, λE is latent heat flux from the surface, H is sensible heat flux from the surface, and G is soil heat flux into the ground (Q_t is used in place of G for heat flux into water). The miscellaneous energy flux terms such as energy storage within the foliage, photosynthesis and respiration are generally less than a few percent and are neglected in eq. 4.1. The common energy units used in this manual are for cumulative fluxes over specific time periods such as MJ m^{-2} h^{-1} for hourly periods and MJ m^{-2} d^{-1} for daily values. Net radiation is defined as positive to the surface and values of the variables on the right side of eq. 4.1 are positive when the flux is away from the surface. By rearranging eq. 4.1, latent heat flux is computed as:

$$\lambda E = R_n - G - H \tag{4.2}$$

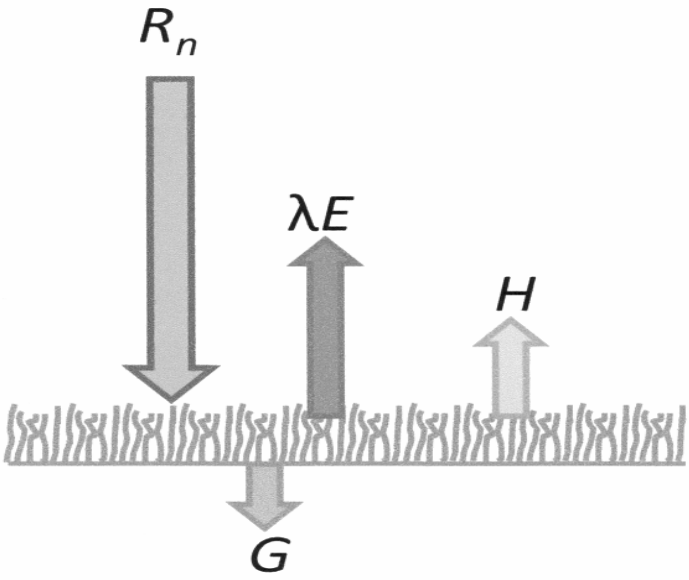

Fig. 4.1. Schematic showing the four primary components of the surface energy balance and directions of energy flow from the surface.

In cold, humid climates, or in cold winter months of temperate, semiarid zones, only 50 to 60 percent of the net radiation, R_n, may be converted to latent heat, even under high water availability. In hot, arid climates, latent heat may exceed net radiation by 10 to 50 percent, as shown in fig. 2.1, because sensible heat derived from the air is converted to latent heat via the process of sensible heat advection. Because of these variations, the surface energy balance approach to determining or estimating E and ET is recognized as a reliable and conservative method. A thorough understanding of the factors controlling the energy balance of a water body or land area enables making accurate estimates or predictions of E and ET. The purpose of this chapter is to provide sufficient material and understanding of underlying principles to enable users to estimate hourly and daily net radiation and soil heat flux as needed to solve E and ET problems.

4.3. Net Radiation

Net radiant energy absorbed by the land or water surface is the primary energy source for evaporation and evapotranspiration. The main component of net radiation is short-wave radiation, or solar radiation. Net radiation also involves a long-wave radiation component. These two components are described in the following sections along with methods for measuring or estimating their magnitudes.

Solar Radiation

The principal source of energy for E and ET and the major component of R_n is solar radiation, R_s. Although there are minor fluctuations in the intensity of solar radiation, they are

insignificant for practical purposes and the intensity of the source at the mean distance of the earth from the sun is commonly referred to as the *solar constant*. Measurements of solar radiation received on a surface normal to the incident radiation outside the earth's atmosphere indicate the constant to be 1367 J m^{-2} s^{-1}, or 1367 W m^{-2} (London and Frohlich 1982; Lean 1989). Total solar irradiance describes the radiant energy emitted by the sun over all wavelengths that falls each second on 1 square meter outside the earth's atmosphere. In this manual, solar irradiance is generally referred to as solar radiation, which has common usage. The total daily solar radiation in the absence of an atmosphere, termed exoatmospheric radiation or extraterrestrial radiation, R_a, varies with the solar angle, or elevation, that changes as the earth revolves about the sun and on the declination of the earth's axis. The annual variation in R_a for northern latitudes is shown in fig. 4.2.

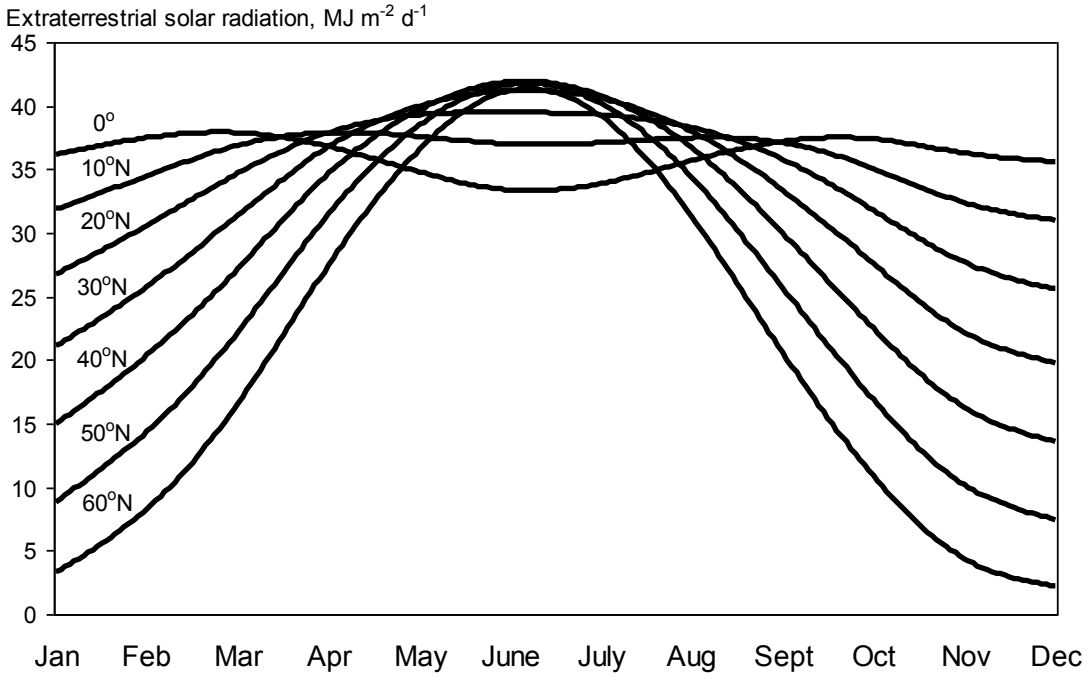

Fig. 4.2. Total daily undepleted (exoatmospheric) solar radiation for various latitudes in the northern hemisphere.

When measured at the earth's surface, R_s includes both direct and diffuse short-wave radiation and may be called "global radiation." The energy per unit area received at the Earth's surface is called "total global irradiance" or "irradiance" and is commonly expressed in the units W m^{-2} which is equivalent to J m^{-2} s^{-1}. The distribution of solar radiation energy by wavelength is illustrated in fig. 4.3. Solar radiation, or short-wave radiation, consists of radiation in wavelengths up to about 3 micrometers, μm. Diffuse radiation is due to absorption and forward and backward scattering of some of the direct (beam) radiation that occurs in the earth's atmosphere. Solar radiation can be measured directly with instruments ranging in complexity from bi-metallic sensors to complex sensors such as black sensor surfaces equipped with glass filters and thermopiles or solar radiation sensitive photovoltaic detectors, both of which are used with automated data-logging systems. The latter two systems of sensors are generally referred to as pyranometers.

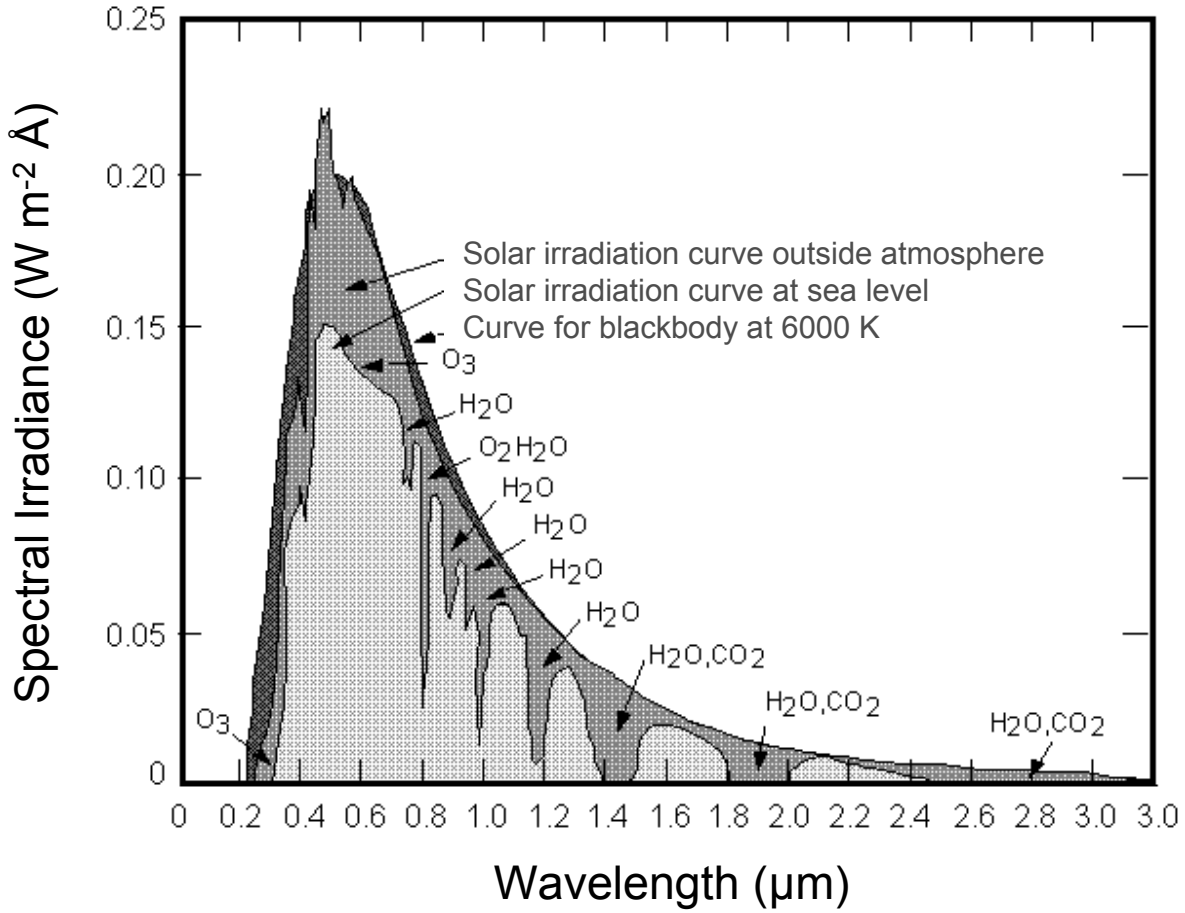

Fig. 4.3. Exoatmospheric solar radiation and solar radiation flux at the earth's surface compared with a 6000K black-body radiation curve. Arrows from O_3, H_2O and CO_2 point to regions of substantial absorption of radiation by those molecules. The Angstrom unit, Å, for the vertical axis is equivalent to 10^{-10} m. Source: Reprinted with permission from Center for Space Research Remote Sensing Group, Univ. Texas (http://www.csr.utexas.edu/projects/rs/hrs/pics/).

Cloudless Day Solar Radiation R_{so}. Radiation in the absence of the earth's atmosphere is called *extraterrestrial or exoatmospheric* radiation, R_a. On cloudless days, the atmosphere is relatively transparent to solar or short-wave radiation. About 70 to 80 percent of the exoatmospheric radiation reaches the earth's surface in semiarid areas as shown in fig. 4.3. The balance is reflected from dust particles or is absorbed by various gases in the atmosphere. Techniques for estimating atmospheric transmittance are presented by Idso (1981), Hatfield et al. (1983), Monteith and Unsworth (1990), Allen (1996b) and ASCE-EWRI (2005).

Estimates of daily cloudless day, or clear sky, solar radiation received at the earth's surface, R_{so}, can be made using the theoretical radiation received in the absence of the earth's atmosphere and atmospheric transmittance. The magnitude of R_{so} can be approximated under most conditions as

$$R_{so} = k_a R_a \tag{4.3}$$

where k_a is a clearness index that is largely a function of station elevation, sun angle (atmospheric thickness), atmospheric water content and atmospheric turbidity. For conditions of low turbidity, k_a can be approximated as a function of station elevation for locations less than 6,000 m using a relationship developed by Allen et al. (1994b):

$$k_a = 0.75 + 0.00002\,E \tag{4.4}$$

where E is elevation in m. Eq. 4.4 was derived by integrating eq. 3.15 (air density) with respect to elevation assuming constant turbidity with elevation and absorption and scattering of solar radiation in proportion to air density. Atmospheric pressure in eq. 3.15 was computed using eq. 3.14. Eq. 4.4 produces $k_a = 0.75$ at sea level, which agrees with eq. 4.24 for $n/N = 1$. For areas of high turbidity due to pollution or airborne dust, the k_a may need to be reduced as much as 10% depending on the relative amount of turbidity.

When needed, more accurate estimates of R_{so} can be obtained by considering the effects of sun angle and water vapor on absorption of short wave radiation and by separating the components of beam and diffuse radiation, so that:

$$R_{so} = (K_B + K_D)\,R_a \tag{4.5}$$

where K_B *is* the clearness index for direct beam radiation, K_D is the corresponding index for diffuse radiation, and R_{so} and R_a are in MJ m^{-2} d^{-1}, MJ m^{-2} h^{-1} or W m^{-2}.

The following equation for K_B, was extended from Majumdar et al. (1972) by Allen (1996b), and is applied here with coefficients improved by ASCE-EWRI (2005) over those recommended in Allen (1996b) and Allen et al. (1998):

$$K_B = 0.98 \exp\left[\frac{-0.00146\ P}{K_t \sin\beta} - 0.075\left(\frac{W}{\sin\beta}\right)^{0.4}\right] \tag{4.6}$$

where K_t is a clearness coefficient that is impacted by turbidity and haze ($0 < K_t \leq 1.0$. $K_t = 1.0$ for clean air and $K_t \approx 0.5$ for turbid, dusty or polluted air), P is atmospheric pressure in kPa, β is the angle of the sun above the horizon in radians, and W is the precipitable water in the atmosphere in mm. The improved coefficients are based on comparisons of R_{SO} from eq. 4.5 with observations measured at 42 locations across the U.S. as summarized by ASCE-EWRI (2005).

The value for K_t may vary with time of year and with cleansing of the atmosphere by precipitation. General values for K_t for a region can be determined using a pristine pyranometer that has a calibration traceable to the national or international solar standard. In general, for routine prediction of R_n and R_{so} envelopes, using $K_t = 1.0$ is sufficient, especially for agricultural areas where the air is generally relatively clean. An exception might be during the pre-monsoon season on the Indian subcontinent when substantial haze can exist. The ratio $P / K_t \sin\beta$ in eq. 4.6 represents the effective air mass along the solar beam. Aerosols and dust can substantially increase haziness of the atmosphere, especially when coupled with high humidity levels. Haze

reduces the beam component of solar radiation, but may increase the diffuse component through increased scattering of radiation. Under hazy conditions, a value $K_t = 0.5$ essentially doubles the effective thickness of the atmosphere and a value $K_t = 0.25$ quadruples the effective thickness.

Precipitable water is estimated from Garrison and Adler (1990) as:

$$W = 0.14\, e_a\, P + 2.1 \tag{4.7}$$

where W is the precipitable water in the atmosphere in mm, e_a is the actual vapor pressure of the air (at approximately a height of 2 m) in kPa, and P is mean atmospheric pressure in kPa. Tasumi et al. (2008) showed W from eq. 4.7 to agree well with W determined from profiling imagers onboard the MODIS satellite during tests in Idaho, New Mexico and Florida. The values for MODIS W were determined from atmospheric humidity profiles based on specific infrared soundings.

The diffuse radiation index is estimated from K_B (ASCE-EWRI 2005)

$$\begin{aligned} K_D &= 0.35 - 0.36\, K_B, \quad for\ K_B \geq 0.15 \\ K_D &= 0.18 + 0.82\, K_B, \quad for\ K_B < 0.15 \end{aligned} \tag{4.8}$$

The diffusive component increases as the direct beam component decreases when $K_B > 0.15$ due to the increased amount of scatter of the direct beam component. For clear sky conditions, K_B is always > 0.15 for daily data and is nearly always > 0.15 for hourly periods. Even for hours close to sunrise and sunset, generally K_D can be computed as $K_D = 0.35 - 0.36\, K_B$ for clear sky conditions, ignoring the second conditional.

For daily (24-hour) time periods, the mean daily sun angle, weighted according to R_a, can be approximated as (Allen 1996b):

$$\sin \beta_{24} = \sin\left[0.85 + 0.3\varphi \sin\left(\frac{2\pi}{365} J - 1.39 \right) - 0.42\varphi^2 \right] \tag{4.9}$$

where β_{24} is the average β during the daylight period, weighted according to R_a, in radians, φ is the latitude in radians, and J is the day in the year [1-366]. The '$\sin \beta_{24}$' variable is to be used in place of $\sin \beta$ in eq. 4.6 and represents the average sun angle during daylight hours. The value for β_{24} should be limited to positive values. Eq. 4.9 compares well to a theoretical, but more complicated solution for $\sin \beta_{24}$ by Allen et al. (2006b).

For hourly or shorter periods the sun angle β is calculated as:

$$\sin \beta = \sin \varphi \, \sin \delta + \cos \varphi \, \cos \delta \, \cos \omega \tag{4.10}$$

where φ is the latitude in radians, δ is the solar declination in radians, and ω is solar time angle at the midpoint of the hourly or shorter period in radians. The user is cautioned that eq. 4.3 – 4.8 produce only estimates for R_{so}, and that there may be reasons why measured R_s on cloud-free days may deviate from the theoretical R_{so} curve. These reasons include air turbidity and haziness caused by dust and aerosols that are not reflected by the equations, effects of nearly invisible clouds high overhead, and late afternoon clouding.

Estimates of R_{so} for a given area can also be developed from an envelope curve plotted through measured radiation data on cloudless days. Ordinarily, R_{so} should plot as an upper envelope of measured R_s as shown in fig. 4.4, where R_{so} values calculated using k_a from eq. 4.4 and the more complicated eq. 4.5-4.9 are plotted with measured R_s for daily timesteps. The inclusion of precipitable water in eq. 4.6 causes the R_{so} envelope to increase on dry days, which corresponds to increases in measured R_s on the same dry, cloud-free days. Reflection of solar radiation by adjacent clouds can occasionally increase measured R_s to levels that are above R_{so}. Meek (1997) described a detailed procedure for estimating R_{so} for specific locations using measured data and considering aerosol optical depth. The relationships $R_{so} = k_a R_a$ and/or $R_{so} = (K_B + K_D) R_a$ are useful for verifying correct operation of pyranometers.

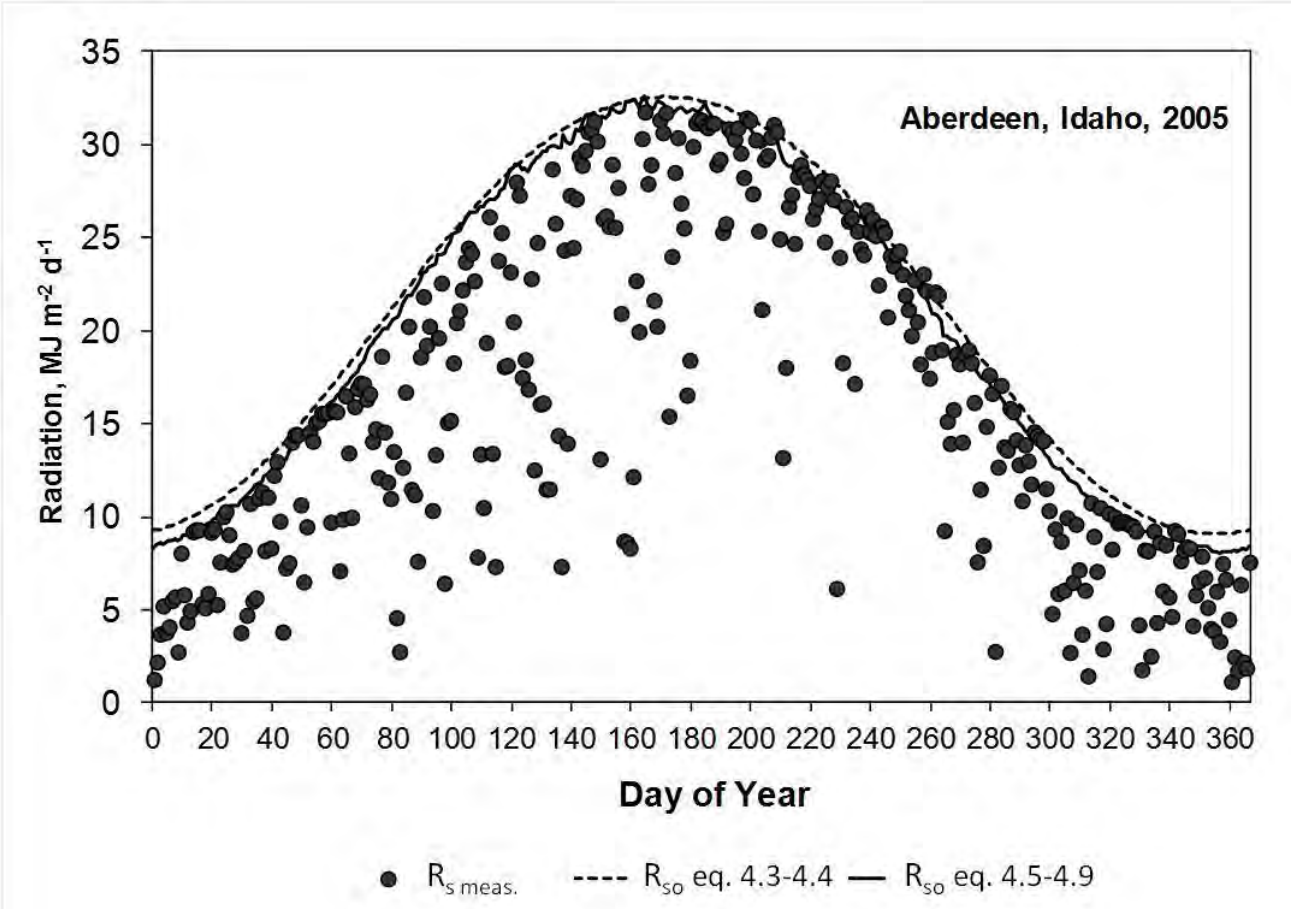

Fig. 4.4. Daily measured solar radiation and calculated cloudless day solar radiation eq. 4.3-4.4 (smooth curve) and eq. 4.5-4.9 for Aberdeen, Idaho during 2005. Source: Measured data are from the US Bureau of Reclamation Agrimet network.

Exoatmospheric Solar Radiation, R_a. Exoatmospheric radiation, R_a, can be computed for a location using integrated trigonometric relationships as a function of latitude and day of the year from Duffie and Beckman (1991) for 24-h time steps:

$$R_a = \frac{24}{\pi} G_{sc}\, d_r\, [\omega_s \sin(\phi)\sin(\delta) + \cos(\phi)\cos(\delta)\sin(\omega_s)] \quad (4.11a)$$

and for hourly or shorter time steps:

$$R_a = \frac{12}{\pi} G_{sc}\, d_r\, [(\omega_2 - \omega_1)\sin(\phi)\sin(\delta) + \cos(\phi)\cos(\delta)(\sin(\omega_2) - \sin(\omega_1))] \quad (4.11b)$$

where R_a is exoatmospheric radiation in MJ m^{-2} d^{-1} (eq. 4.11a) or MJ m^{-2} h^{-1} (eq. 4.11b), G_{sc} is the solar constant of 4.92 MJ m^{-2} h^{-1} [equivalent to 1367 W m^{-2}] as recommended by the International Association of Meteorology and Atmospheric Physics (London and Frohlich 1982), d_r is an eccentricity factor to account for the effect of the variation in the relative distance of the earth from the sun, ω_s is the sunset hour angle, ω_1 and ω_2 are sun hour angles at the beginning and end of an hourly period, all in radians, and ϕ is latitude of the station in radians (negative for southern latitudes). The declination, δ, in radians, can be estimated from Duffie and Beckman (1991) as:

$$\delta = 0.4093 \sin\left(2\pi \frac{(284 + J)}{365}\right) \quad (4.12)$$

where J is the day of the year (January 1st = 1). The term d_r is calculated as:

$$d_r = 1 + 0.033 \cos\left(\frac{2\pi J}{365}\right) \quad (4.13)$$

The sunset hour angle, ω_s, in radians can be calculated using eq. 4.14 or 4.15:

$$\omega_s = \arccos(-\tan(\phi)\tan(\delta)) \quad (4.14)$$

or if the arccos function is unavailable,

$$\omega_s = \frac{\pi}{2} - \arctan\left(\frac{-\tan(\phi)\tan(\delta)}{[1 - \tan^2(\phi)\tan^2(\delta)]^{1/2}}\right) \quad (4.15)$$

The argument in eq. 4.14 must be limited to less than or equal to 2.0 in extreme latitudes (> 55°) during winter months. If the argument is less than -1.0 in extreme latitudes (> 55°) during summer months, then the argument should be set equal to [tan(φ)tan(δ) - 2.0]. The maximum

value for ω_s is π radians, indicating no nighttime, and the minimum value is 0, indicating no daytime.

For hourly or shorter periods, the solar time angles at the beginning and end of each period are given by:

$$\omega_1 = \omega - \frac{\pi\ t_1}{24} \tag{4.16}$$

$$\omega_2 = \omega + \frac{\pi\ t_1}{24} \tag{4.17}$$

where ω is the solar time angle at the midpoint of the period in radians, and t_l is the length of the calculation period in hours (t_l is 1 for hourly periods and 0.5 for 30-minute periods). The solar time angle at the midpoint of an hourly or shorter period is:

$$\omega = \frac{\pi}{12}\left[(t + 0.06667(L_z - L_m) + S_c) - 12\right] \tag{4.18}$$

where t is <u>standard</u> clock time at the midpoint of the period [hour] (after correcting time for any daylight savings shift). For example for a period between 1400 and 1500 hours, t = 14.5 hours. Parameter L_z is the longitude of the center of the local time zone, expressed as positive degrees west of Greenwich, England. In the United States, L_z = 75, 90, 105 and 120° for the Eastern, Central, Rocky Mountain and Pacific time zones, respectively, and L_z = 0° for Greenwich, *345*° for Paris, France and *255*° for Bangkok, Thailand. Parameter L_m is the longitude of the solar radiation measurement site, expressed as positive degrees west of Greenwich, England, and S_c is seasonal correction for solar time in hours.

Because ω_s is the sunset hour angle and $-\omega_s$ is the sunrise hour angle (noon has $\omega = 0$), values of $\omega < -\omega_s$ or $\omega > \omega_s$ from eq. 4.18 indicate that the center of the solar disk is below the horizon, so that, by definition, R_a is zero and its calculation has no meaning. Therefore, when the values for ω_1 and ω_2 span or exceed the value for $-\omega_s$ or for ω_s, sunrise or sunset occurs within the hourly (or shorter) period and the integration limits in eq. 4.11b should be adjusted using the following conditionals:

$$\begin{aligned}
&\text{If } \omega_1 < -\omega_s \text{ then } \omega_1 = -\omega_s \\
&\text{If } \omega_2 < -\omega_s \text{ then } \omega_2 = -\omega_s \\
&\text{If } \omega_1 > \omega_s \text{ then } \omega_1 = \omega_s \\
&\text{If } \omega_2 > \omega_s \text{ then } \omega_2 = \omega_s \\
&\text{If } \omega_1 > \omega_2 \text{ then } \omega_1 = \omega_2
\end{aligned} \tag{4.19}$$

Equations 4.13, 4.14 and 4.18 are from Duffie and Beckman.

The above conditionals insure numerical stability of the application of eq. 4.11b for all timesteps. Eqs. 4.16-4.18 presume an extensive, flat ground surface and are based on a vector to the center

of the sun's disk. Where hills or mountains impede a view of the horizon, the hour angle when the sun first appears or disappears may increase for sunrise or decrease for sunset.

The seasonal correction for solar time from Duffie and Beckman (1991) is:

$$S_c = 0.1645 \sin(2\,b) - 0.1255 \cos(b) - 0.025 \sin(b) \tag{4.20}$$

$$b = \frac{2\pi(J-81)}{364} \tag{4.21}$$

where J is the number of the day in the year and b has units of radians.

Estimating Solar Radiation

Solar radiation, R_s, data are not always available and are frequently estimated. On a given day R_s is affected mainly by cloud cover. Therefore, if not measured, R_s can be estimated using R_{so} and either the degree of cloud cover or percent of sunshine. More reliable R_s estimates are obtained using recorded percent sunshine as compared to observed cloud cover data because observed cloud cover data are qualitative. The most accurate measurements of R_s are by pyranometers. Where cloud cover is not strongly influenced by local orographic features, measurement of daily R_s at a single station may be used for estimates over large areas (100-200 km in diameter) without significant error over 5 or 10 day periods. Constants developed for a linear equation for the USA are similar to those obtained in Canada and Australia (Fritz and MacDonald, 1949):

$$R_s = (0.35 + 0.61S)\,R_{so} \tag{4.22}$$

where S represents the ratio of actual to possible sunshine. Eq. 4.22 suggests that recording instruments tend to not measure a full record of sunshine on cloudless days, since 0.35 and 0.61 sum to 0.96.

Solar radiation also can be estimated from exoatmospheric radiation, R_a. Black et al. (1954) correlated exoatmospheric solar radiation and duration of sunshine as recorded by Marvin and Campbell-Stokes sunshine recorders. The resulting equation of Black et al. (1954), based on 32 stations, is:

$$R_s = (0.23 + 0.48\frac{n}{N})\,R_a \tag{4.23}$$

Doorenbos and Pruitt (1977) recommended a generalized form of the R_s equation:

$$R_s = \left(0.25 + \ 0.5 \ \frac{n}{N} \right) R_a \tag{4.24}$$

The quantity *n/N* was defined by Doorenbos and Pruitt (1977) as "the ratio between actual measured bright sunshine hours and maximum possible sunshine hours." In practice *n/N* and *S*/100 are usually assumed to be the same quantity. Doorenbos and Pruitt presented a table to convert cloudiness expressed in eights (octas) or in tenths to n/N values. Constants for eq. 4.24 were presented in an appendix table for a number of specific locations by Doorenbos and Pruitt (1977). *N* in eq. 4.24 can be calculated from the sunset hour angle as:

$$N = \omega_s \left(\frac{24}{\pi} \right) \tag{4.25}$$

where ω_s is sunset hour angle in radians, calculated using eq. 4.14 or 4.15.

Average R_s over 10-day to monthly periods can be approximated from the range in daily air temperature using an empirical equation derived by Hargreaves and Samani (1982):

$$R_s = K_{RS} \ (T_{\max} - T_{\min} \ )^{0.5} \ R_a \tag{4.26}$$

where T_{max} and T_{min} are maximum and minimum daily air temperature, °C. K_{RS} is an empirical coefficient equal to about 0.16 for interior regions (Hargreaves and Samani 1982) and about 0.19 for coastal regions[1]. R_s and R_a have the same units. Eq. 4.26 performs best using mean monthly data. When applied to daily data, eq. 4.26 tends to overestimate for cloudy days. R_s predicted by eq. 4.26 should be limited to $\leq R_{so}$. Allen (1997) demonstrated the application of eq. 4.26 with means to auto-calibrate K_{RS} using the R_{so} clear sky envelope for seven locations in the western U.S. Amatya et al. (2000) found the Allen auto-calibration technique to provide good estimates of daily solar radiation at three locations in North Carolina.

Bristow and Campbell (1984) developed an equation similar to eq. 4.26. However, their formulation requires regional calibration and is of similar accuracy to eq. 4.26 (Ball et al. 2004). Thornton and Running (1999) improved on the Bristow and Campbell equations and introduced a general calibration based on solar radiation data from across the U.S. Their method, rearranged and simplified, is:

$$R_s = R_{so} \left[1 - 0.9 \ \ \exp\left(- B \left(T_{\max} - T_{\min} \right)^{1.5} \right) \right] \tag{4.27}$$

[1] Hargreaves, G.H. 1994. Personal communication.

Where R_{so} is clear sky solar radiation having the same units as R_s and B is an empirical coefficient. T_{max} and T_{min} are maximum and minimum daily air temperature, °C. The equation for B by Thornton and Running for general application is:

$$B = 0.031 + 0.201 \ \exp\left(-0.185 \ \left(T_{\max} - T_{\min}\right)_{monthly}\right) \tag{4.28}$$

where $(T_{max} - T_{min})_{monthly}$ is the average difference between T_{max} and T_{min} over the one-month period of interest. Allen and Robison (2007) derived an equation for B based on data for two western U.S. stations (Portland and Eugene, OR) contained in Thornton and Running that produced more accurate estimates for R_s across southern Idaho:

$$B = 0.023 + 0.1 \ \exp\left(-0.2 \ \left(T_{\max} - T_{\min}\right)_{monthly}\right) \tag{4.29}$$

Eq. 4.27 has advantages over eq. 4.26 in that it is self-limiting to R_{so} as an upper bound and tends to estimate more representative ranges for R_s under cloudy conditions.

Solar Radiation Data Base, USA. The National Renewable Energy Laboratory has compiled a mean monthly solar radiation data base for hourly and daily data for a 30-year (1961-1990) record for 239 stations and for a fifteen-year record (1991-2005) for 1020 stations for the USA (NREL 1992). The data include measured and modeled solar radiation and meteorological data. They are available on digital media from the National Climate Data Center in Asheville, NC, and via the internet (http://rredc.nrel.gov/solar/old_data/nsrdb/).

Solar Radiation Estimated from GOES Satellite Images of Cloud Cover. Advancements have been made in estimating solar radiation from the Geostationary Operational Environmental Satellite (GOES) system, where nearly continuous observations of cloud cover can be translated into estimated solar radiation at the earth's surface. Applications for estimating R_s and, in some cases ET, have included Pinker and Lazlo (1992), Rossow and Garder (1993), Whitlock et al. (1995), Stewart et al. (1999), Garatuza-Payan et al. (2001a,b) and Jacobs et al. (2004). These satellite-based estimates provide spatial information on solar radiation that may be useful for developing solar radiation and ET maps.

Other sources of daily R_s and other weather data include gridded time series data by the U.S. National Weather Service's National Centers for Environmental Prediction (NCEP). NCEP runs a series of computer analyses and forecasts operationally, including the GLDAS (Global Land Data Assimilation System). Since 2001, the National Oceanic and Atmospheric Administration's GLDAS has been producing six-hourly climate parameter datasets for the globe at 1-degree spatial resolution that go back to about 1950. GLDAS data are complemented by NLDAS and NARR (North American Regional Reanalysis) gridded data sets that are based on similar modeling efforts. Information on these data can be found on the NCEP website[2]. Senay et al. (2008) have used the NCEP GLDAS data to calculate reference ET using the ASCE standardized Penman-Monteith equation for gridded areas and have made comparisons against reference ET

[2] http://ldas.gsfc.nasa.gov/gldas/ and http://www.emc.ncep.noaa.gov/mmb/rreanl/

obtained from California Irrigation Management Information System (CIMIS) stations. Caution is needed, however, in using air temperature and humidity from the NLDAS and NARR gridded data sets without verifying their conditioning to reflect evaporating environments associated with reference ET. More discussion on this need is given in the next section and in Chapters 8 and 11. Agricultural weather data from the CIMIS network have been interpolated into a 2 km gridded surface for the state of California (Hart et al. 2008). Readers are encouraged to consult the most recent literature on estimating solar radiation from satellite data and on gridded weather products, since these areas and products are evolving rapidly.

Long-wave Radiation

Net long-wave radiation is a component of net radiation. The atmosphere is less transparent to long-wave radiation as compared to short-wave radiation. Water vapor, carbon dioxide and ozone are good absorbers and emitters at some far infrared wavelengths as shown in fig. 4.5. Radiant energy absorbed by these various gases is emitted in all directions according to the radiation law.

$$R_L = \varepsilon_a \, \sigma \, T^4 \tag{4.30}$$

where ε_a is broad-band emissivity of the atmosphere, σ is the Stefan-Boltzmann constant, and T is the effective absolute temperature, K, (K = 273.15 + °C) of the atmosphere. Values of the Stefan-Boltzmann constant are:

$\sigma = 5.675 \times 10^{-8}$ J m^{-2} K^{-4} s^{-1} for R_L in W m^{-2},
$\sigma = 4.901 \times 10^{-9}$ MJ m^{-2} K^{-4} d^{-1} for R_L in MJ m^{-2} d^{-1}, and
$\sigma = 2.042 \times 10^{-10}$ MJ m^{-2} K^{-4} h^{-1} for R_L in MJ m^{-2} h^{-1}

Because of relatively high transparency of the atmosphere to the 8 to 13 μm wavelengths, there is a net loss of radiant energy to space within this range during cloudless and partly cloudy 24-hour periods. For practical purposes, only the long-wave radiation components are important between sunset and sunrise. A small amount of diffuse short-wave sky radiation is usually present just after sunset and prior to sunrise, respectively.

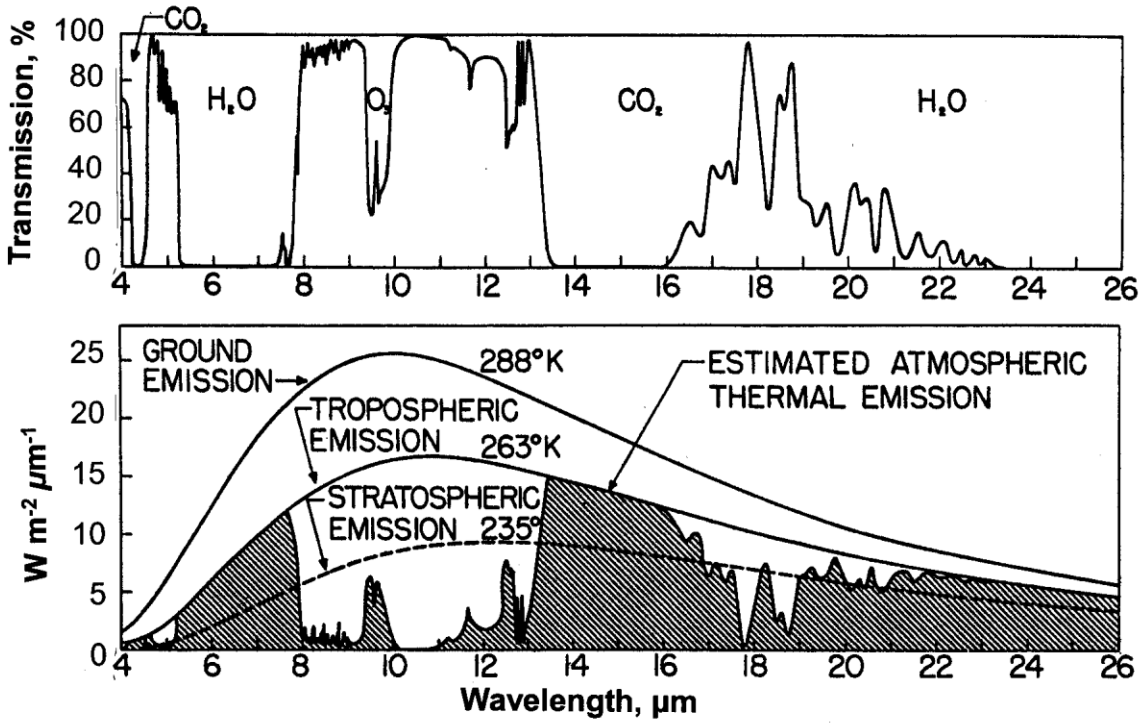

Fig. 4.5. Infrared (long-wave) transmission following absorption by atmospheric gases H_2O, CO_2, O_3 and O_2 (top) and the thermal emission from the ground (bottom) as a function of the wavelength. The cross-sectioned area is the estimated emission from the atmosphere at 263K. The area between the 288K curve and the cross-sectioned area represents the net loss of long wave radiation from the surface at 288K to a cloudless atmosphere having a uniform temperature at 263K. Source: Gates (1963). Figure reprinted with permission of Am. Scientist, magazine of Sigma Xi, the Scientific Research Society.

Measuring and Estimating Net Radiation

Net radiation flux can be measured directly using hemispherical net radiometers, or estimated from net short wave and net long wave components.

$$R_n = R_s \downarrow - \alpha R_s \uparrow + R_L \downarrow - R_L \uparrow = (1-\alpha) R_s - R_{nl} = R_{ns} - R_{nl} \tag{4.31}$$

where R_s is short wave radiation or solar radiation, R_L is long-wave radiation, R_{ns} is net solar radiation, and R_{nl} is net long-wave radiation. The arrows indicate direction, $(1 - \alpha)R_s$ represents the net short-wave radiation received by a water, soil or vegetated surface, and α is the short-wave broad-spectrum reflectance or albedo.

Rather than estimating net radiation for each vegetated surface, or for each crop and growth stage, net radiation, used in estimating ET_{ref}, is commonly measured or estimated for a well-watered reference crop like grass or alfalfa. Mean daily reflectance coefficients (albedo) for most green field crops with a full cover range from 0.20 to 0.25. A value of 0.23 for α is commonly used for vegetated surfaces with a full cover. This value (0.23) is used in the standardized

definitions for alfalfa and clipped grass reference ET (ASCE-EWRI 2005). Full cover generally exists when the leaf area index, which is the leaf area per unit land area, is 3 or greater (Ritchie 1972; Wright 1982).

Wright (1982) presented an equation for estimating net radiation received by alfalfa at Kimberly, Idaho in which the daily average albedo varies during the growing season (Jensen et al. 1990, eq. 6.67, p. 137). Dong et al. (1992) developed an equation for hourly albedo that varied with sun angle (i.e., time of day). Martin and Gilley (1993) integrated the Dong equation to obtain a daily albedo equation for grass. Brutsaert (1982) summarized albedo values as reported earlier by a number of researchers (table 4.1). The albedo values for inland water bodies range from 0.04 to 0.09. Bolsenga and Vanderploeg (1992) suggested a range from 0.07 - 0.15 depending upon water-surface conditions.

Long-wave radiation emitted by a surface can be estimated using eq. 4.32 if the surface temperature is known. The broad-band emissivity of a mixture of vegetation and soil surfaces, ε_{vs}, is about 0.98. Table 4.2 lists reported broad-band emissivity, ε_s, values for a number of surfaces. The emissivity of water surfaces is about 0.97. The MODIS UCSB Emissivity Library[3] contains ε_s for a wide range of soils, vegetation and metals. Data at the site show ε_s to vary widely with thermal wave length. Generally, the ε used in eq. 4.30 is the integrated broad-band emissivity covering the 8-13 μm band. The incoming long-wave radiation is more difficult to estimate since it must be an integrated value based on variations in water vapor and temperature with elevation above the ground surface, degree of cloud cover and temperature of the clouds. It can be directly measured during dark hours with a total hemispheric radiometer (upward facing), or indirectly computed during daylight hours by subtracting R_s from the radiometer readings. Dense clouds act as a black body and essentially block the long-wave window (8 to 13 μm) to outer space and they emit long-wave radiation to the ground. The temperature at the cloud base is required to accurately calculate this component of incoming thermal radiation.

Calculation of net thermal radiation is complex for partly cloudy conditions. A detailed analysis of the factors affecting net radiation involves both the atmospheric and surface emittances and cloud cover. Partly cloudy conditions have less effect under humid conditions because much of the long-wave radiation emitted from the surface is absorbed by water vapor in the near surface layer of the atmosphere (Anderson 1954). Calculation of R_n on sloping terrain is described by Allen et al. (2006b).

Kimball et al. (1982) derived a complex model involving the areas of cloud cover and cloud temperature and transmittance in the 8 to 13 μm wavelength window. For a more complete discussion, see Davies and Idso (1979) and Dong et al. (1992).

[3] http://www.icess.ucsb.edu/modis/EMIS/html/em.html

TABLE 4.1 Approximate Mean Albedo Values for Various Natural Surfaces. Source: Data from Brutsaert (1982)

Nature of Surface	Albedo
Deep Water	0.04-0.08
Moist dark soils; plowed fields	0.05-0.15
Gray soils; bare fields	0.15-0.25
Dry soils; desert	0.20-0.35
White sand; lime	0.30-0.40
Green grass and other short vegetation (e.g., alfalfa, potatoes, beets)	0.15-0.25
Dry grass; stubble	0.15-0.20
Dry prairie and savannah	0.20-0.30
Coniferous forest	0.10-0.15
Deciduous forest	0.15-0.25
Forest with melting snow	0.20-0.30
Old and dirty snow cover	0.35-0.65
Clean, stable snow cover	0.60-0.75
Fresh dry snow	0.80-0.90

TABLE 4.2 Values of the Broad-band Thermal Emissivities, ε, of Some Natural Surfaces

Nature of surface	Emissivity
Bare soil (mineral)	0.95-0.97
Bare soil (organic)	0.97-0.98
Grassy vegetation	0.97-0.98
Tree vegetation	0.96-0.97
Water	0.97
Snow (old)	0.97
Snow (fresh)	0.99

In theory, outgoing long-wave radiation integrated over the entire thermal spectrum is proportional to the fourth power of surface temperature:

$$R_L \uparrow = \varepsilon_{vs} \sigma T_s^4 \tag{4.32}$$

where ε_{vs} is vegetative and soil emittance and T_S is surface temperature in K. Incoming long-wave radiation is proportional to the fourth power of effective atmospheric temperature:

$$R_L \downarrow = \varepsilon_{sky} \sigma T_{sky}^4 \tag{4.33}$$

where ε_{sky} is the effective emissivity of the atmosphere and T_{sky} is the effective sky temperature, integrated over the hemisphere, K. Generally, T_{sky} is tens of degrees cooler than near surface air temperature (T) at 'screen height, i.e., 1 to 5 m above the surface. However, T_{sky} is generally closely coupled with T_s and T, due to the relatively large values for $R_L\uparrow$ and $R_L\downarrow$ that often average 300 to 400 W m^{-2} (25 to 40 MJ m^{-2} d^{-1}). These large values tend to keep surface and lower atmospheric temperature in a relatively close equilibrium.

It is absolutely essential to recognize that surface temperature can easily vary by 30°C between a wet, evaporating surface (including the reference condition for ET_{ref}) and a dry surface, such as hot, bare soil. Differences in $R_L\uparrow$ between the two surface conditions can therefore be as much as 200 W m^{-2}, which has enormous impact on the value for R_n and calculation of ET. For example, given common surface temperatures of 25°C for a wet surface and 45°C for a corresponding dry surface (20°C difference in temperature), $R_L\uparrow$ fluxes would be (assuming emissivity of 0.97 for both surfaces) 0.97 (5.675E-8) $(298.15)^4$ = 434 W m^{-2} and 0.97 (5.675E-8) $(318.15)^4$ = 563 W m^{-2}, for a difference of 129 W m^{-2} or 30% error in $R_L\uparrow$ for the reference condition. The impact of surface temperature on $R_L\uparrow$ and subsequently on R_n is one reason why practitioners are encouraged to estimate R_n using standard equations, when calculating reference ET, rather than attempting to measure R_n, because of the difficulty of maintaining a cooled, evaporating surface beneath the radiometer. As discussed in a later section, when under reference conditions where the surface is evaporating and transpiring at rates of ET_{ref}, air temperature at 2 m is often within a few degrees of surface temperature (Allen et al. 2006c), so that one can make relatively consistent and accurate estimates of R_n based on air temperature alone. This is not the case for nonreference conditions.

Because measurements of incoming long-wave radiation data or effective sky temperature are generally not available, incoming long-wave radiation is usually estimated based on near surface air temperature, T, and vapor pressure at near surface measurement height. The effects of cloud cover on long-wave atmospheric radiation and simple empirical equations to estimate net long-wave radiation are presented below.

The early work by Brunt (1932, 1952) related an 'apparent' clear-sky atmospheric emittance, ε_a, to vapor pressure at near surface humidity measurement height, e_a, which took the general form:

$$\varepsilon_a = a_b + b_b \sqrt{e_a} \tag{4.34}$$

where a_b and b_b were empirical coefficients. The value for ε_a does not represent true ε_{sky}, but is biased to work with near surface T:

$$R_L\downarrow = \varepsilon_a \sigma T^4 \tag{4.35}$$

For cloudy conditions, the net long-wave or thermal radiation loss, R_{nl}, is influenced by the degree of cloud cover, its elevation and temperature.

$$R_{nl} = R_L \uparrow - R_L \downarrow = R_{vs} - R_b = R_{vs} - (R_{bo} + R_c) \quad (4.36)$$

where R_{nl} is net long-wave radiation from the surface, R_{vs} is long-wave radiation emitted by the vegetation or soil surface, R_b is integrated long-wave radiation emitted by the sky (including clouds), R_{bo} is full spectrum long-wave radiation emitted by a cloudless sky, and R_c is additional long-wave radiation emitted by clouds and transmitted to the earth's surface, over the entire 8-13 μm wave band. In practice, because outgoing and incoming long-wave radiation terms in eq. 4.36 are usually calculated using only instrument height data, then:

$$R_{nl} = f_{cd} (\varepsilon_{vs} - \varepsilon_a) \sigma T^4 \quad (4.37)$$

where ε_a is apparent atmospheric emittance for clear sky, ε_{vs} is combined vegetation and soil emittance, T is near surface air temperature in K and f_{cd} is a factor to adjust for cloud cover. Eq. 4.37 assumes that the surface temperature and air temperature at instrument height are equal. This is a reasonable assumption for the reference ET surface (only), where the near surface temperature profile is nearly isothermal. This is a poor assumption when the surface is dry, with low relative ET flux.

The two emittances may be combined into a single term known as the net apparent emittance, ε', which represents the difference between the combined vegetation and soil emittance and apparent atmospheric emittance when a single temperature is used. Values for ε_{vs} for common, fully developed crops range from 0.94 to 0.995. A canopy value of 0.98 is recommended for most radiation balance calculations over vegetated surfaces. A value of 0.97 is recommended for water.

The Brunt expression for the net apparent emittance ε' is:

$$\varepsilon' = \varepsilon_{vs} - \varepsilon_a = a_1 + b_1 \sqrt{e_a} \quad (4.38)$$

where e_a is the actual vapor pressure, kPa, which equals the saturation vapor pressure at dew point temperature. When ε_{vs} and ε_a are combined, as in eq. 4.38, there is some loss in accuracy of the R_{nl} estimate because the cloud-cover factor, f_{cd}, is effectively multiplied by both the atmospheric and surface emissions, rather than by the atmospheric emission alone.

Combining eq. 4.37 and 4.38 results in a general equation for net outgoing long-wave radiation.

$$R_{nl} = f_{cd} \left(a_1 + b_1 \sqrt{e_a}\right) \sigma T^4 \quad (4.39)$$

For 24-hour or longer time steps, T^4 in eq. 4.39 should be replaced by $(T_{max}^4 + T_{min}^4)/2$ for greater accuracy, due to strong nonlinearity caused by the exponent on T, where T_{max} and T_{min} are daily maximum and minimum air temperatures in K at screen or shelter height. Experimental values of the coefficients for use in eq. 4.39 are presented in table 4.3. The Stefan-Boltzmann

constant, σ, is 4.901×10^{-9} MJ m^{-2} d^{-1} K^{-4} for daily calculations with R_{nl} in MJ m^{-2} d^{-1} and T_{max} and T_{min} in K. For hourly calculations, $\sigma = 2.042 \times 10^{-10}$ MJ m^2 h^{-1} K^{-4} and R_{nl} is in MJ m^{-2} h^{-1}and T is in K.

Wright and Jensen (1972) developed an expression for f_{cd} in eq. 4.39 that uses the ratio of observed solar radiation, R_s, to solar radiation under clear sky conditions, R_{so}, to represent the amount of cloudiness:

$$f_{cd} = a \frac{R_s}{R_{so}} + b \tag{4.40a}$$

where a and b are empirical coefficients. For hourly or shorter periods during nighttime, there is no R_s or R_{so} to utilize to estimate cloudiness effects. Therefore, for hourly or shorter time step calculations where the sun angle above the horizon, β, at the midpoint of the period is less than 0.3 radians (≈ 17º), a substitution is made so that:

$$f_{cd} = f_{cd\beta>0.3} \tag{4.40b}$$

where $f_{cd\beta>0.3}$ is the cloud cover function for the time period prior to when the sun angle β in the afternoon or evening falls below 0.3 radians (ASCE-EWRI 2005).

Since single level temperature measurements are used, eq. 4.38 represents ε' or the difference between the emittance for the reference crop surface and the effective, apparent emittance for the atmosphere under cloudless conditions. The dew point temperature does not change greatly during the day, and a single level dew point temperature observation during the day may be adequate for most daily estimates of R_{nl} for eventual calculation of E or ET. Where humidity measurements are not available, minimum air temperatures may be taken as the dew point temperature in subhumid and humid areas. In arid areas, the dew point temperature may be several degrees °C lower than the minimum air temperature. Simple calibration relationships can be developed to enable using minimum air temperature as a substitute for dew point temperature as discussed in Chapter 8.

The coefficients a and b are derived empirically and $a + b = 1.0$. Smith et al. (1991), Allen et al. (1994b, 1998) and ASCE-EWRI (2005) have recommended using a =1.35, b = - 0.35, a_1 = 0.34 and b_1 = - 0.14 at most locations for consistency in standardized reference ET calculations. Kjaersgaard et al. (2007) found eq. 4.40 to best fit a long time series of R_{nl} measurements in Denmark when a = 1.0 and b = 0. The a = 1.35 and b = 0.35 coefficients underestimated R_{nl}. The 1.0 and 0.0 coefficients consider the colder cloud temperatures and less downward thermal emission in Denmark (~55º north latitude), given the same R_s/R_{so} ratio. The a = 1.0 and b = 0 were also suggested by Jensen (1974) and Jensen et al. (1990) for use in humid regions.

TABLE 4.3 Experimental Coefficients for Net Long Wave Radiation eq. 4.39 and 4.40. Source: Data from Jensen et al. (1990)

Region	(a, b)	(a_1, b_1)
Davis, California	(1.35, -0.35)[1]	(0.35, -0.145)[2]
Southern Idaho	(1.22, -0.18)[3]	(0.325, -0.139)[3]
England	(not available)	(0.47, -0.206)[4]
England	(not available)	(0.44, -0.253)[5]
Australia	(not available)	(0.35, -0.133)[6]
Denmark	(1.0, 0.0)[7]	
General	(1.3, -0.3)[8]	(0.39, -0.158)[9]

For e in mb, divide b_1 values by $\sqrt{10}$.
[1] Pruitt, W.O. (1973, personal communication). [2] Goss and Brooks (1956).
[3] Wright and Jensen (1972). [4] Monteith and Szeicz (1962).
[5] Penman (1948). [6] Fitzpatrick and Stern (1965).
[7] Kjaersgaard et al. (2007) and Jensen (1974) and Jensen et al. (1990) for humid climates.
[8] Suggested for arid areas. [9] Budyko (1956).

Allen and DeBruin (2008) have demonstrated that net outgoing long-wave radiation, R_{nl}, can be estimated for well-watered, vegetated surfaces (e.g., for reference conditions) using a simple function of atmospheric transmissivity for short-wave radiation, τ_{sw}, represented, for clear sky conditions, by the sum of the indices K_B and K_D for beam and diffuse short-wave radiation as calculated for clear conditions using eq. 4.5 (i.e., $\tau_{sw} = K_B + K_D$):

$$R_{nl} = \left(170 - 33\sqrt{e_a}\right)\tau_{sw} \tag{4.41}$$

Where e_a is vapor pressure of the air, kPa, and units for R_{nl} are W m^{-2}. In the absence of data for vapor pressure, Allen and DeBruin recommended the simplification:

$$R_{nl} = 140\ \tau_{sw} \tag{4.42}$$

which represents e_a of about 0.83 kPa. In practice, τ_{sw} is equal to the ratio of R_s / R_a where R_s is the measured solar radiation which will be less than R_{so} under cloudy conditions and R_a is exoatmospheric solar radiation. Allen and DeBruin (2008) found eq. 4.41 and 4.42 to estimate well at locations in Germany, the Netherlands, Idaho and Oklahoma for hourly or shorter and for daily calculation timesteps. The use of τ_{sw} in the equations automatically accounts for impacts of cloud cover on incoming thermal radiation and thus R_{nl} and for impacts of sun angle on R_{nl}. For low sun angles and during nighttime, where the ratio R_s / R_a does not apply due to zero or near zero R_a , the following estimates for τ_{sw} are made:

$$
\begin{aligned}
&\text{if } \sin\beta \geq 0.09 \quad \text{then } \tau_{sw} = \frac{R_s}{R_a} \\
&\text{if } 0.09 > \sin\beta > -0.36 \quad \text{then } \tau_{sw} = min\left(\tau_{sw\,i-1},\, 0.6 - 0.2\left[\frac{\sin\beta - 0.09}{-0.36 - 0.09}\right]\right) \\
&\text{if } \sin\beta \leq -0.36 \quad \text{then } \tau_{sw} = min\left(\tau_{sw\,i-1},\, 0.4\right)
\end{aligned}
\tag{4.43}
$$

where $sin\ \beta$ is the sine of the angle of the sun above the horizon from eq. 4.10. Values 0.09 and –0.36 are in radians and correspond to angles of 5º and –20º. Variable $\tau_{sw_{i-1}}$ is the τ_{sw} from the previous timestep.

The relationships are valid for use in calculating ET_{ref}, only, particularly eq. 4.37, 4.39, 4.41 and 4.42. None of the relationships for R_n, R_{nl} and $R_L\uparrow$ given in this section apply for ambient conditions when ET from the surface is significantly less than ET_{ref}. Under those conditions, partitioning of net radiation into surface heating will cause an increase in $R_L\uparrow$, an increase in R_{nl}, and a decrease in R_n.

4.4 Soil Heat Flux Density

For daily or longer periods, soil heat flux density, *G,* can be ignored, although with large variation in R_n and/or air mass conditions from one day to the next, G over a 24-h period can be as large as 5% of R_n. For shorter periods, e.g. hourly, G must be taken into account. Some of the minor terms such as changes in energy storage in a canopy may also need to be considered, especially in forest canopies.

The magnitude of soil energy storage or release can be significant over a few hours, but is usually small from day to day because much of the energy stored early in the day as the soil warms is lost late in the day or at night as the soil cools. The rate of energy flux at any depth z can be expressed by:

$$G = K_{Ts}\frac{\partial T_{sl}}{\partial z} \tag{4.44}$$

where T_{sl} is the temperature of the soil and K_{Ts} is the thermal conductivity of the soil in J m^{-1} s^{-1} K^{-1}. Therefore G in eq. 4.44 has units of J m^{-2} s^{-1} (W m^{-2}) for T_{sl} in K and z in m. Typical values of K_{Ts} presented in table 3.1 are repeated in table 4.4. K_{Ts} varies widely with soil water content. Soil water provides thermal continuity between soil particles, thereby increasing bulk K_{Ts}. Brutsaert (1982, fig. 6.9) presented curves of thermal conductivity as a function of volumetric water content for four widely different soils. These values ranged from 0.1 to 2.5 J m^{-1} s^{-1} K^{-1}.

Soil heat flux density can also be estimated by monitoring the change in temperature of a soil or water profile over time:

$$G = C_s \int_0^{z_s} \frac{\partial T_{sl}}{\partial t} d z \tag{4.45}$$

where C_s is the heat capacity per unit volume of soil, MJ m^{-3} K^{-1}, t is time with the same units as used in G, and z_s is the depth of soil that responds to increased or decreased temperature change. C_s can be estimated from the following equation by de Vries (1963):

$$C_s = 1.93 V_m + 2.51 V_{om} + 4.19 \theta \tag{4.46}$$

where V_m, V_{om}, and θ represent the volume of minerals, organic matter and water per unit volume of soil, respectively. For example, if a soil has 50 percent solids and negligible organic matter, and a volumetric water content of 0.27, its estimated heat capacity will be 2.1 MJ m^{-3} K^{-1} and G from eq. 4.45, for z_s in m, will have units of MJ m^{-2} t^{-1}. Approximate values of thermal properties for soils and soil components are given in table 4.4. Eq. 4.45 is often used in combination with soil heat flux plates to estimate heat flux absorbed or contributed by the soil layer above a buried plate when calculating total soil heat flux at the soil surface as described in the following section.

Measuring Soil Heat Flux Density

For application to short-periods, e.g., when hourly data for G are required, it is customary to measure G, especially under research settings or when employing a surface energy balance, such as with the Bowen ratio ET measurement method. One method commonly used to measure G is to use heat flux plates installed near the soil surface, generally at 0.04 to 0.15 m depth with correction for heat storage above the plates using eq. 4.45. For full cover vegetation situations where temperature gradients near the surface are minor, heat flux plates can give reasonably accurate data for G. Strong temperature gradients exist near bare soil surfaces and differences in thermal conductivities of the plate and of the soil can produce large errors in estimating G if heat flux plates are placed too near the surface. Also, with the strong thermal gradients during day and night, condensation and evaporation near the upper or lower surface of the flux plate can be a significant problem. In addition, heat flux plates function as 'umbrellas' to infiltration of precipitation or irrigation water, so that more shallow placement depths impede water flow to greater degrees, causing a localized buildup of moisture above the plate and a dry area beneath the plate. These localized aberrations in moisture can seriously impact the thermal conductivity and heat storage near the plate, invalidating measurements. Soil heat flux plates should be placed below depths of evaporation in soil (generally 0.08 to 0.15 m) to avoid errors associated with H to λE conversion at depths below the plate. Ham (2001) recommended 0.12 m depth for plate installation to avoid energy balance errors associated with shallower placement. The measurement by the plate is corrected to the ground surface by measuring soil temperature at at least two depths in the soil layer above the plate and averaged over several locations to decrease impacts of spatial variation. The equation is:

$$G = G_{plate} + C_s \frac{T_{s2} - T_{s1}}{t_2 - t_1} z_{plate} \quad (4.47)$$

where G_{plate} is the measurement by the soil heat flux plat at depth z_{plate} beneath the soil surface, T_{s2} is average soil temperature of the surface to z_{plate} layer at time t_2, and T_{s1} is soil temperature at time t_1. Generally C_s is calculated using eq. 4.46, with soil water content θ measured to account for effects of variation in water content over time. For z_{plate} in m, G and G_{plate} will have units of MJ m^{-2} t^{-1}. Because of the strong thermal gradients near the soil surface during late morning and early evening, more than two temperature depths are generally recommended, with vertical depth increments of as small as 0.01 to 0.02 m near the surface. Zhao and Allen (2012) routinely placed heat flux plates at two depths (0.04 and 0.08 m) for rigorous energy balance study and generally obtained similar values for G between the two depth systems based on eq. 4.47. They used four depths for temperature measurement and explored the use of second and third degree polynomial equations to extrapolate the nonlinear temperature profiles to the surface to better account for large amounts of heat storage change within a few cm of the surface. The use of two depths for plate placement provided independent computation of G at the surface with different weighting of heat storage change and measured fluxes at depth. In applications where soil is saturated or is very dry, the user should check with the manufacturer to ascertain whether the standard plate calibration is applicable.

Estimating Soil Heat Flux Density

For Hourly or Shorter Periods. In situations where it is not possible to measure *s*oil heat flux density or where G is part of a standardized definition for ET, such as with the standardized reference ET conditions presented in chapter 8, G can be approximated for soil covered by vegetation using a universal relationship proposed by Choudhury et al. (1987) and Choudhury (1989) that is generally valid for daylight periods:

$$G = 0.4 \exp(-0.5\ LAI)\ R_n \quad (4.48)$$

where LAI is the leaf area index, and G has the same units as R_n. Eq. 4.48 estimates $G = 0.1\ R_n$ for an $LAI = 2.8$, which is a typical LAI for the clipped grass reference ET definition described in chapter 8. Eq. 4.48 estimates $G = 0.04\ R_n$ for an $LAI = 4.5$, which is typical for the alfalfa reference ET definition described in chapter 8. A very low value for G/R_n (0.036), was used by Verma et al. (1986) during daylight for a deciduous forest. For bare soil, where $LAI = 0$, eq. 4.48 estimates G/R_n as 0.4 which has been observed by Choudhury et al. (1987), and Kustas and Daughtry (1990). Tasumi (2003), using data from J.L. Wright of the USDA, Kimberly, ID, observed G/R_n for bare soils to range from about 0.45 when wind speed at 2 m was less than 1 m s^{-1} to 0.25 when wind speed exceeded 5 m s^{-1}. He also found the G/R_n ratio to increase with increased surface temperature. Some textbooks, for example Stull (1988) and Brutsaert (1982), have suggested estimating G as a function or ratio of sensible heat flux density, H, for

bare soil conditions. The principle behind a *G*:*H* relationship is that both are strong functions of surface temperature, with high correlation between them. Allen et al., (2011d) utilized the *G*:*H* concept in a surface energy balance-based *ET* method for processing thermal satellite data.

For nighttime conditions under grass forage, Allen et al. (1994b) observed $G = 0.5\ R_n$. At Davis, California, Pruitt[4] observed $G = 0.3\ R_n$ at night beneath clipped grass. In computerized evapotranspiration models where soil surface temperatures are calculated from surface heat exchange equations, *G* can be estimated using a "force-restore" method (Lin 1980). A thin surface layer is used to simulate surface temperature for use in estimating long-wave radiation and in "forcing" turbulent heat transfer to the air. A deeper second layer is used to "restore" the surface layer temperature.

For 24-h Periods. Under a crop canopy, daily soil heat flux is small due to cancellation of daytime and nighttime fluxes, and normally can be neglected for most practical estimates involving energy balance, in particular, for the reference surfaces of grass and alfalfa. The total value of *G* over a multi-day period however may be significant, especially for 30 days or longer where the soil profile is warming or cooling.

TABLE 4.4 Thermal Properties of Soil Constituents at 20°C and Standard Atmospheric Pressure. Source: Data from van Wijk and de Vries (1963)

Soil material	Density ρ (Mg m^{-3})	Specific heat [kJ kg^{-1} K^{-1}]	Volumetric heat capacity C_s [MJ m^{-3} K^{-1}]	Thermal conductivity λ [J m^{-1} s^{-1} K^{-1}]	Thermal diffusivity α [10^{-6} m^2 s^{-1}]
Quartz	2.65	0.733	1.93	8.37	4.3
Minerals*	2.65	0.733	1.93	2.93	1.5
Organic matter*	1.3	1.926	2.51	0.25	0.1
Water	1.00	4.187	4.19	0.59	0.142
Air	0.0012	1.005	0.0012	0.026	0.021

*Approximate average values
1000 kg m^{-3} = 1 g cm^{-3}
4186.8 J kg^{-1} K^{-1} = 1 cal g^{-1} C^{-1}
4.1868 MJ m^{-3} K^{-1} = 1 cal cm^{-3} C^{-1}
0.41 868 J m^{-1} s^{-1} K^{-1} = 0.41 868 W m^{-1} K^{-1} = l0^{-3} cal cm^{-1} s^{-1} C^{-1}
l0^{-6} m^2 s^{-1} = l0^{-2} cm^2 s^{-1}

For Monthly Periods. An approximation of the soil heat flux over long periods of time (≥ 30 days) can be obtained by assuming that the soil temperature to a depth of 2 m changes approximately with average air temperature, and that the average volumetric heat capacity for the soil is 2.1 MJ m^{-3} K^{-1},

[4] Pruitt, W.O. 1995. Personal communication.

$$G = -4.2\frac{T_{i-1} - T_{i+1}}{\Delta t} = 4.2\frac{T_{i+1} - T_{i-1}}{\Delta t} \quad (4.49a)$$

where G is the average daily soil heat flux in MJ m^{-2} d^{-1}, T equals the mean air temperature in °C or K for time period i, and Δt equals the time in days between the midpoints of the two periods. In real time predictions, where T_{i+1} is unknown, G for monthly or longer time periods can be estimated as:

$$G = 4.2\frac{T_i - T_{i-1}}{\Delta t} \quad (4.49b)$$

Additional information can be found in publications by van Wijk and de Vries (1963), de Vries (1963), and Brutsaert (1982).

5

Surface Energy andAir Mass Interactions and the Concept of Reference ET

5.1. Introduction

The conservation of energy at the evaporating surface controls the close linkage between solar or net radiation, the primary energy source, sensible heat flux (H) to and from the air and to and from the soil (G), and the resulting conversion of energy into latent heat flux (λE). An example of the partitioning of energy at the surface over a 24-hour period in a hot arid environment is illustrated in fig. 5.1from an early energy balance study by van Bavel and Ehrler (1968). The figure shows energy components from an irrigated grain sorghum crop with complete cover and a leaf-area-index of 4.2 on June 15 following irrigation on June 1 so that some soil water depletion had occurred. The figure shows that during the daytime hours, the interactions are very dynamic, while at night changes occur slowly. Fig. 5.1 shows negative values for H, indicating a downward flow of sensible heat from the air to the surface, thereby contributing additional energy to the ET process so that λE exceeded net radiation (R_n). Negative H can be common for well-watered surfaces in arid and semiarid climates where irrigated agriculture is surrounded by relatively dry lands that generate H that is then transferred to irrigated areas. This process is often referred to as advection. When estimating evapotranspiration (ET) the nighttime effects must be considered as well as daytime variables.

With annual crops, the soil-plant-atmosphere system changes as plants emerge and develop from bare soil at planting to full cover. With partial plant cover, the effect of a wet soil surface following a rain or irrigation is large, but the effect decreases as leaf area approaches full plant cover and most of the solar energy is absorbed by the plant canopy. An example of the daily dynamic changes that occur during the period from planting to maturity of cotton is illustrated in fig. 5.2 for a subhumid area of Texas. When plant cover was limited, the daily ratio of latent heat to net radiation, $\lambda E/R_n$, varied greatly as a function of rainfall events. The ratio generally increased to about 1.0 as leaf area developed and then decreased as the cotton crop began to mature. In contrast to the drier condition illustrated in fig. 5.1, little or no H was converted to latent heat, reflected by the ratio $\lambda E/R_n$ not exceeding about 1.1. The effects of G are not included in fig. 5.2. Just after planting cotton, when the bare soil surface was wet following rainfall, $\lambda E/R_n$ increased to nearly 1.0, but decreased rapidly as the soil dried. Typically, as soil dries, the soil water content decreases logarithmically with depth as illustrated in fig. 5.3. The dry soil near the surface greatly increases the resistance to vapor transfer to the atmosphere.

The factors illustrated in fig. 5.1-5.3 must be considered when estimating ET from annual crops. For deciduous tree crops and other perennial natural vegetation, there is a large change in canopy resistance as trees green up in the spring and as leaves mature during late summer and fall. For citrus groves that retain leaves all year, the area of leaves exposed to direct solar radiation increases as the elevation of the sun decreases during winter months.

Engineers and water managers routinely make estimates of ET for irrigation planning and scheduling, water balance computations, and various other purposes. In this chapter, the general interactions of the available surface energy and air-mass are described along with the common approaches that are used to obtain ET estimates.

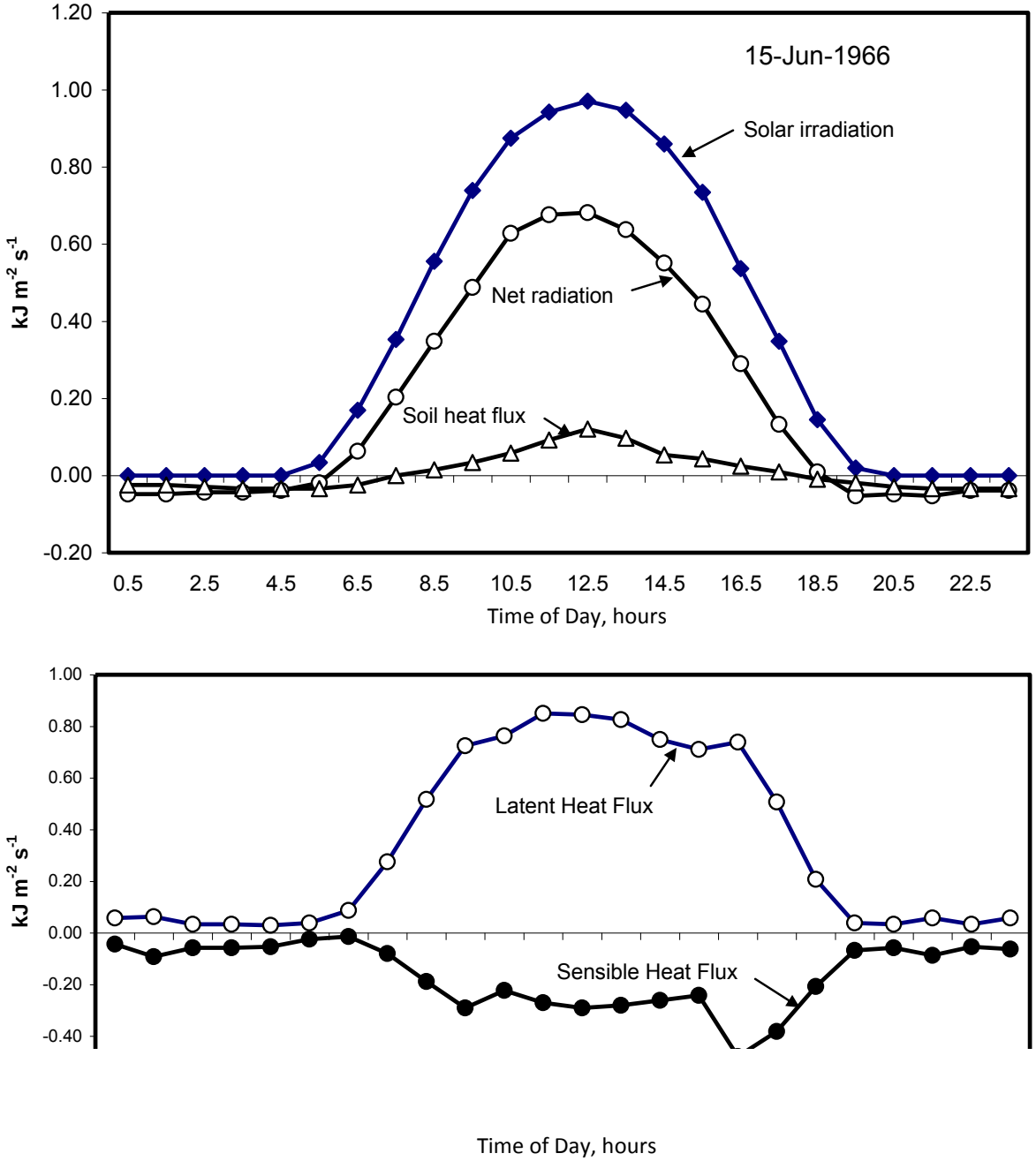

Fig. 5.1. Example energy balance components and resulting conversion of net radiation and advected (negative) sensible heat to latent heat and soil heat flux for a grain sorghum crop in central Arizona. Wind speed generally ranged from 1 m s^{-1} to 2.5 m s^{-1}. Grain sorghum leaf temperatures were consistently lower than air temperatures throughout the day. Source: Figure reproduced with permission from van Bavel and Ehrler (1968) (redrawn).

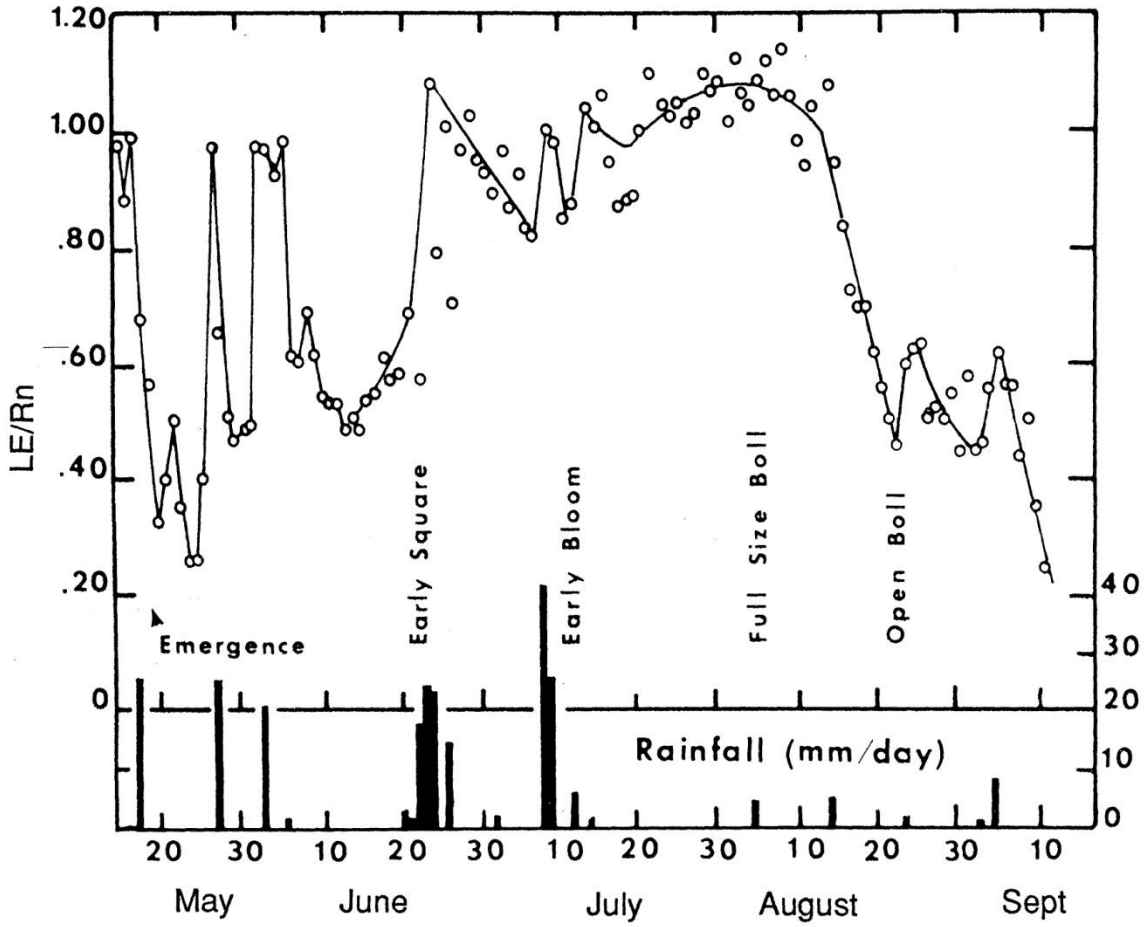

Fig. 5.2. Daily ratios of $\lambda E/R_n$ for a field of cotton in Texas. Rainfall is shown in the lower part of the graph. The solid line represents the averaged time-based trend in $\lambda E/R_n$ when the soil surface was dry and actual day-to-day changes in $\lambda E/R_n$ when the soil surface was wet or drying. Source: Figure reproduced with permission from Ritchie (1971).

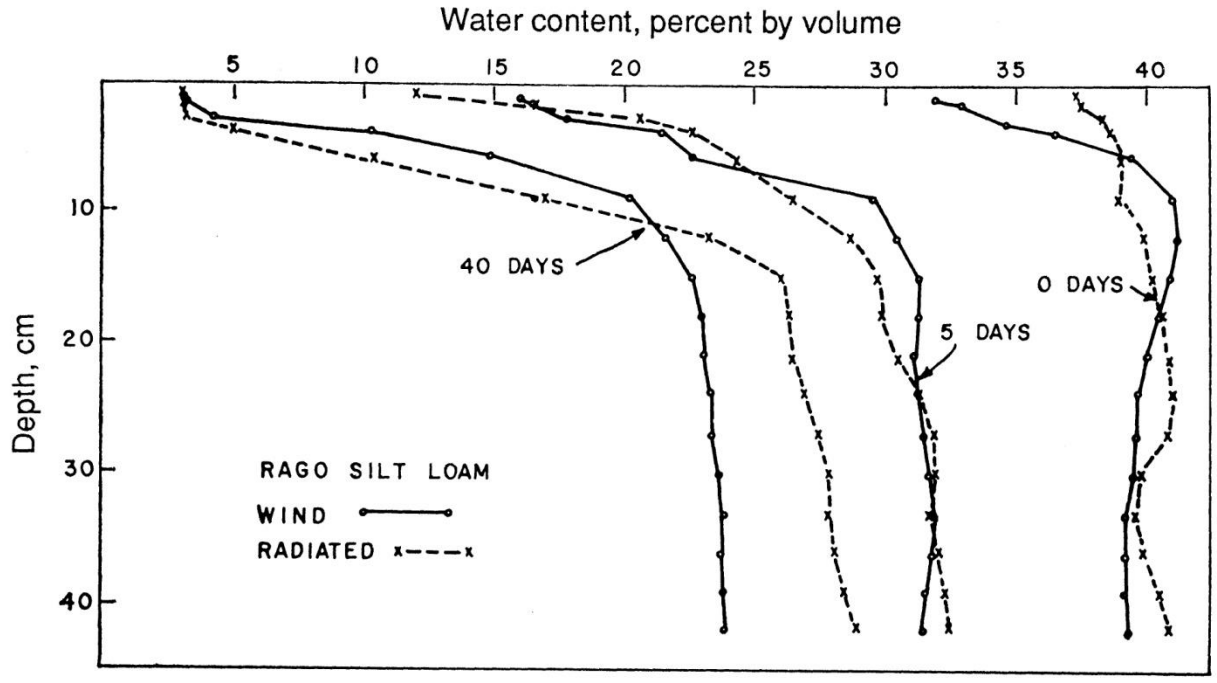

Fig. 5.3. Soil water profiles as a function of time and type of drying (energy supplied primarily by wind or radiation) for a silt loam soil. Source: Figure reproduced with permission from Hanks et al. (1967).

5.2. Weather and Surface Effects on Conversion of Energy to Latent Heat Flux

The combination energy balance-aerodynamic equations, such as those proposed by Penman (1948) or Slatyer and McIlroy (1961), are excellent models for illustrating how the various weather parameters interact to affect energy partitioning at evaporating surfaces. These models are based on empirically-determined aerodynamic wind functions while the more theoretically based Penman-Monteith (Monteith 1965) equation has a wind function term based on the log-law wind profile, and includes a canopy resistance term.

The PM equation will be used later in examples that describe the effects of air mass conditions and surface resistance on partitioning of net radiation at the surface into the various energy balance components. At this point, the simpler Slatyer-McIlroy equation is used to illustrate some aspects of weather-surface interactions and to introduce a widely-used method for estimating ET for non-advection conditions (Priestley and Taylor 1972):

$$\lambda E = \left[\frac{\Delta}{\Delta + \gamma} \right] (R_n - G) + h(D_z - D_s) \tag{5.1}$$

where λE is the latent heat flux density, γ is the psychrometric constant and Δ is the slope of the saturation vapor pressure vs. air temperature relationship calculated by Slatyer and McIlroy (1961) at the average of wet-bulb temperature of the air at the top of the canopy and the air temperature at height z. Units for λE, R_n and G are the same. D_z is the wet-bulb depression at

height z and D_s is the wet-bulb depression for air in equilibrium with the surface, ºC, and h is a wind-speed dependent heat-transfer coefficient that varies with canopy resistance, crop roughness, and stability conditions of the air mass above the surface. For units for λE, R_n and G in W m^{-2} or MJ m^{-2} t^{-1}, h will have units of W m^{-2} $^oC^{-1}$ or MJ m^{-2} t^{-1} $^oC^{-1}$. For a hypothetical effectively wet surface, D_s drops out of eq. 5.1 and, except for the empiricism of the wind-function term normally determined under non-wet surface conditions, eq. 5.1 becomes a predictor of potential evaporation, E_o, defined later.

Considering the effects of temperature alone on the energy balance, the term $\Delta/(\Delta + \gamma)$ in eq. 5.1 varies with temperature, e.g., at a barometric pressure of 101.3 kPa, it varies from 0.4 at 0ºC to 0.85 at 40ºC. Hence, under very humid conditions, where the second term of the equation has little significance, the equation indicates that the fraction of R_n converted to λE will be greater during warm fall months as compared to cooler spring months or greater in warm afternoon periods as compared to cold or cool morning periods. In more arid climates, warmer fall temperatures (or afternoon periods) will result in greater wet-bulb depressions, D_z, producing even higher fall or afternoon ratios of $\lambda E/R_n$. In locations well away from the equator, Pruitt (1964) showed that well-defined seasonal effects can be expected in the relationships of λE vs. R_n (or R_s) on an annual basis (fig. 5.4).

A case to consider and one that provides a realistic estimate of the lowest $\lambda E/R_n$ to be expected for potential evaporation cases is the use of the first term of eq. 5.1. This portion of the equation provides an estimate of so-called *equilibrium evaporation*, a condition described by Slatyer and McIlroy (1961) for cases where air in the lower meter is saturated, or nearly so. The modeled effects of wind become zero, (except as it affects temperature) and the ratio of $\lambda E/R_n$ is defined by $[\Delta/(\Delta + \gamma)]$, a function of only temperature for any given barometric pressure. Such conditions would seldom exist on a daily or longer period. On a diurnal basis however, in many climates, relative humidity (RH) is nearly 100% for the first hour or so of sunlight.

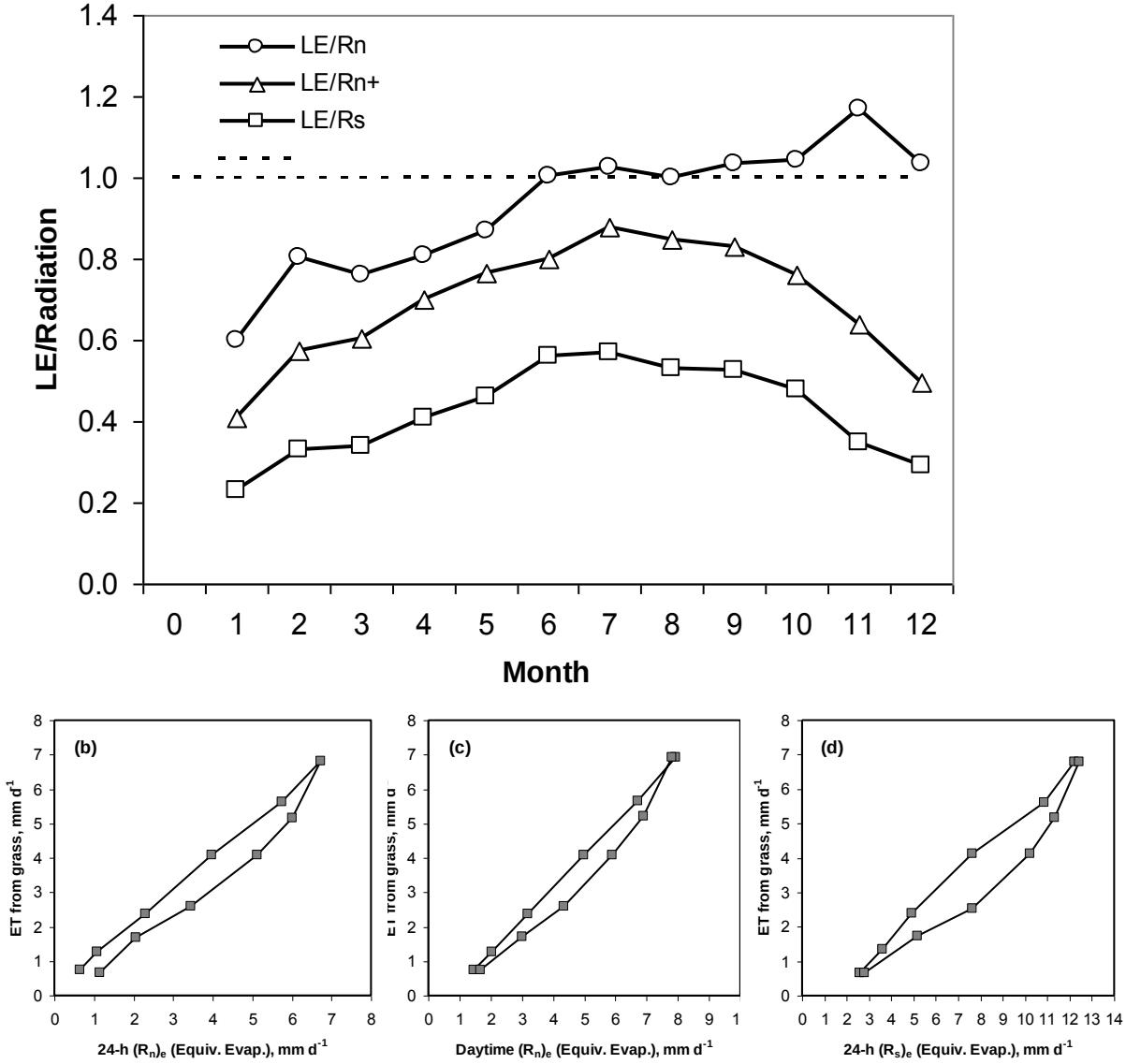

Fig. 5.4. (a) Mean monthly fractions of solar and net radiation used as λE (denoted at LE) by perennial ryegrass and (b – d), the seasonal, cyclic relationships of ET v. $(R_n)_e$, $(R_n+)_e$ and $(R_s)_e$,(equiv. mm evap.), Jan.–June 1960-63. Davis, CA. R_n+ indicates daytime net radiation. Source: Data from Pruitt and Angus (1960); Pruitt (1971).

The well-known Priestley-Taylor (1972) equation provides an estimate of *equilibrium evaporation* without the requirement of including the effects of aerodynamic transport shown in eq. 5.1. The Priestley-Taylor equation is expressed as:

$$\lambda E = \alpha \left(\frac{\Delta}{\Delta + \gamma}\right)(R_n - G) \tag{5.2}$$

where Δ is the slope of the saturation vapor pressure vs. air temperature relationship and α is a multiplier which essentially compensates for the lack of an aerodynamic term typical of combination aerodynamic-energy balance equations.

Priestley and Taylor analyzed data obtained in earlier studies conducted over both land and ocean surfaces and found that a value for α of 1.26 in eq. 5.2 provided estimates of ET for the land studies in good agreement with measured ET. However, this was the case only when data from land-based studies were restricted to include the first few days immediately following rainfall over an extensive upwind area and/or had sufficient long-term rainfall to supply potential ET and associated vegetation cover. Jensen et al. (1990) provided a comprehensive analysis of this and other methods using world-wide data. Steiner et al. (1991) reviewed values for α under arid environments.

It is important to recognize that the equilibrium evaporation estimated by eq. 5.2 can only occur when a large region (on the scale of 1000 km) is fully supplied with water to support the equilibrium evaporation rate and to humidify and cool the air mass to equilibrium conditions. This is an example of the strong negative feedback between evaporation rate and evaporation demand. The equilbirum condition rarely exists. Semiarid and arid climates occur because actual ET of a large region is less than the equilibrium rate and consequently air masses are drier and warmer than for the equilibrium condition. Advection of dry, warm air to smaller irrigated or riparian systems (smaller relative to the size of the region) can substantially increase the ET from those smaller systems to rates that substantially exceed the equilibrium rate. This is the basis of the complementary theory (Brutsaert 1982) and is why methods that include a humidity and aerodynamic term, such as the Penman and Penman-Monteith equations are essential to estimate ET from irrigated systems in dry climates.

5.3 Standardizing the Vegetative Cover

Potential Evaporation

Potential Evaporation. The Working Group on Water Requirements of the International Commission on Irrigation and Drainage defined potential evaporation as: "*the evaporation from a given surface when all surface-atmospheric interfaces are wet (saturated) so that there is no restriction due to either biological control or soil water content on the water vapor loss from the surface area*" (ICID 1985). The Working Group pointed out that the magnitude of evaporation will depend primarily on atmospheric conditions and surface albedo, but will also vary with geometric characteristics of the surface. In terms of hydrology, potential evaporation would apply only following precipitation, condensation (dew), fog interception, or a crop being irrigated by sprinkling. Allen (2005b) provided additional distinction between potential evaporation and reference evapotranspiration. Within this manual, potential evaporation is identified as E_o, and relates to the above definition.

Reference Evapotranspiration

Because of ambiguities in the definition of potential evaporation and difficulties in sustaining measurable rates of potential evaporation, the term reference crop evapotranspiration (ET_{ref}) is preferred for operational calculation of evaporative demand from vegetation. Two primary

'types' of reference crops have been and continue to be in use around the globe. These are clipped, cool season grass and tall, full-cover alfalfa (ASCE-EWRI 2005).

Grass and Alfalfa References. The magnitude of energy-balance and air-mass interactions can be more routinely quantified by eliminating, or minimizing, the effects of changes in plant characteristics and soil water content during the growing season. Penman (1956a) defined *potential transpiration* (evapotranspiration) as "*the amount of water transpired in unit time by a short green crop, completely shading the ground, of uniform height and never short of water*" with the intention of using potential transpiration as a climatic evaporative index. Others, such as Monteith (1981) defined potential transpiration or potential ET as evapotranspiration from vegetation having a saturated surface (surface resistance, r_s, = 0). This latter definition, although correct, has proven to be difficult to measure in the field and to apply, especially in the absence of weather data that are measured over a wet surface to preserve the requirement of equilibrium and feedback between surface and air, in this case reflecting a potential ET environment. Therefore, use of the term potential ET has been discouraged as a climatic index and for estimating ET from various surfaces. The term potential ET is, however, commonly used to represent the rate of ET expected from any vegetated surface when soil water content of the root zone is sufficient to support full transpiration so that the bulk canopy resistance of the vegetation is at a minimum, but nonzero value, for example, r_s = 30 s m^{-1} specified for the alfalfa reference described in the following paragraphs. In that usage, this condition can exist in the presence or absence of a wet soil surface and is in essence the rate of ET to expect under 'fully watered' or 'nonstressed' conditions for a specific crop. In that context, the potential ET can vary for each crop or vegetation type.

Jensen (1968) suggested that ET from a well watered crop of alfalfa (*Medigo sativa*) of a height of 0.3 to 0.5 m may approximate maximum ET (as constrained by available energy) for nonsaturated surface conditions. Jensen et al. (1971) and Wright and Jensen (1972) recommended the use of the term reference crop ET. Doorenbos and Pruitt (1975, 1977) described reference crop evapotranspiration (ET_o) as "*the rate of evapotranspiration from an extensive surface of 8-15 cm tall, green grass cover of uniform height, actively growing, completely shading the ground and not short of water*". Subsequently, this definition specified the grass cover as being that of one of the cool-season grasses with roughness, density, leaf area and canopy resistance characteristics similar to perennial ryegrass (*Lolium perenne*) or fescue (*Festuca arundinacea* Schreb. 'Alta'), since warm-season grass varieties, such as Bermuda (*Cynodon dactylon*), can exercise considerable control over transpiration.

Grass has served as a standard reference crop largely due to the preponderance of grass used in lysimeter studies around the world. Also, in much of the world, several species of cool-season grasses remain green throughout the year. With grass, it is possible to maintain a near-constant canopy with a leaf area index (LAI) of ~ 3, and with weekly or so mowing frequency, growth differences within and outside of a lysimeter, whether due to fertility or soil moisture differences, can be minimized.

There are disadvantages, however, in using cool-season, clipped grass as a reference. Because grass is short and aerodynamically quite smooth, the ET can be considerably lower than that which can occur with many other common crops and types of vegetation that have taller, aerodynamically rougher canopies, particularly in hot, dry and windy conditions. Also, cool-season grass varieties are not well adapted to warm tropical environments. Therefore, well-irrigated alfalfa, some 0.3 to 0.7 m in height, has been the other major crop used as a reference,

with the symbol ET_r (Jensen 1968; Jensen and Haise 1963; Jensen et al. 1990). Relatively few vegetative canopies have higher ET rates than 0.3 to 0.7-m tall alfalfa. Thus, in a two-step procedure (using ET_r and a crop coefficient K_c), there should be, for full-cover conditions, a narrower range in K_c values and a more predictable upper limit for K_c than when ET_o (grass) is used as a reference. This is especially the case when a wide range of climates and crops are involved.

There are some disadvantages when using measured ET from alfalfa as a reference if field validation is required. Cuttings remove most of the canopy and actual ET is drastically reduced for about a week following each cutting. Trampling of the crop in the vicinity of the ET measurement such as surrounding a neutron meter tube, or extension of the alfalfa canopy beyond the boundaries of a lysimeter, thereby increasing the ET measurement, can present much more of a problem than with a grass turf. Alfalfa can be difficult to grow in some tropical climates and at high altitudes. In addition, varieties of alfalfa may exhibit different amounts of erectness of stems and stomatal control. These variations may create differences in ET among varieties which are as large as 10% (Wright 1988). Similar variations in ET can occur between different varieties of cool-season grass.

The Working Group on Water Requirements of the International Commission on Irrigation and Drainage (ICID 1985) provided an updated terminology listing for evapotranspiration and water requirements. They defined Reference Crop Evapotranspiration as:

> "*The evapotranspiration from a given well-adapted crop selected for comparative purposes under given weather conditions and with adequate fetch (sufficient to make edge effects relatively unimportant) and for a standardized watering regime appropriate for this crop and the region concerned.*"

ASCE Standardized References. In 2000, a task committee (TC) of the Evapotranspiration in Irrigation and Hydrology Committee of the Environmental and Water Resources Institute of the American Society of Civil Engineers (abbreviated ASCE-ET) and the Irrigation Association (IA) Water Management Committee addressed the need for uniform reference crop ET methodology. The TC concluded that two ET_{ref} surfaces with *standardized* computational procedures were needed to support applications across agricultural, horticultural and landscape applications and to support current cultural practices (Walter et al. 2000; ASCE-EWRI 2005). The two adopted ET_{ref} surfaces were: (1) a standardized short crop (similar to clipped grass); and (2) a standardized tall crop (similar to full cover alfalfa). Additionally, the TC recognized that an equation capable of calculating both hourly and daily ET_{ref} was needed. The TC concluded that ET_{ref} from each of the two surfaces could be modeled using a single Standardized Reference Evapotranspiration (ET_{sz}) equation with appropriate constants and standardized computational procedures. The surfaces were defined as:

> *Standardized Reference Evapotranspiration for Short Reference ET_{os}:* Reference ET calculated for a *short* crop having height of *0.12* m (similar to grass), albedo of 0.23, surface resistance of 70 s m^{-1} for 24-h calculation timesteps, and 50 s m^{-1} for hourly or shorter periods during daytime and 200 s m^{-1} during nighttime with daytime G/R_n = 0.1 and nighttime G/R_n = 0.5.

Standardized Reference Evapotranspiration for Tall Reference ET_{rs}: Reference ET calculated for a *tall* crop having height of *0.50* m (similar to alfalfa) , albedo of 0.23, surface resistance of 45 s m^{-1} for 24-h calculation timesteps, and 30 s m^{-1} for hourly or shorter periods during daytime and 200 s m^{-1} during nighttime with daytime G/R_n = 0.04 and nighttime G/R_n = 0.2.

The ASCE-ETCommittee adopted the PM equation as parameterized by Allen et al. (1989) and Jensen et al. (1990) and simplified the terms to implement these definitions (ASCE-EWRI 2005). The two standardized surfaces are similar to known full-cover crops of grass and alfalfa that have received widespread use as ET_{ref} across the United States. Each reference has unique advantages for specific applications and times of the year. The short (ET_{os}) standardized reference is essentially the same as the ET_o of FAO-56 (Allen et al. 1998) for 24-h calculation timesteps. In addition, a recommendation by Allen et al. (2006c) to use the same 50 s m^{-1} surface resistance for hourly or shorter periods during daytime and 200 s m^{-1} during nighttime with the FAO-56 Penman-Monteith method has made the FAO ET_o and ET_{os} references equivalent for hourly timesteps as well as for 24-h periods. The form of the Penman-Monteith equation adopted to the above reference standardizations is introduced in Chapter 8. In chapter 7, data are presented and equations are used to illustrate some basic general interactions that occur between plants and the atmosphere.

Summary

Actual ET by crops can be significantly affected by air and surface interactions, by temperature and humidity levels, and by the degree of plant cover, stage of maturity and soil water status. The most accurate methods for estimating ET consider net radiation and the basic interactions between plants and the atmosphere that affect ET. This chapter illustrates the basic surface-energy basis for estimating ET and the premise for using reference ET concepts associated with standardized surfaces to promote consistency and reproduceability in estimating near maximum values for ET.

6

Evaporation from Water Surfaces

6.1 Introduction

Evaporation from water surfaces is a major component of the hydrologic cycle and must be considered in a wide variety of hydrologic and water resource studies. Because of its nature, evaporation from water surfaces is rarely measured directly, except over relatively small spatial and temporal scales (Jones 1992). Evaporation from a water surface is most commonly computed indirectly by one or more techniques. The techniques described here are applicable to many engineering and hydrologic studies. They include pan coefficients × measured pan evaporation, water balance, energy balance, mass transfer procedures, and combined techniques. The selection of the "best" technique to use for a particular computation is largely a function of the data availability, depth and turbidity of the water body, and the required accuracy of the computed evaporation.

Theories of evaporation from water surfaces go back to at least the 8th century B.C., but measurement and experimentation go back to the 17th and 18th centuries (Brutsaert 1982). Brutsaert credits Dalton's 1802 paper on aerodynamics of evaporation as a major event in the development of evaporation theory. One of the earliest detailed evaporation studies in the USA was that by Sleight (1917). Bowen (1926) developed what is now known as the Bowen ratio that has had a major impact on evaporation measurement technologies. McEwen (1930) described evaporation as a transformation of energy based on earlier work of Bowen (1926) and Cummings and Richardson (1927).

Many states have tabulated evaporation data measured with various types of evaporation pans. Some states have computed state-wide estimates of evaporation from shallow ponds and reservoirs (Borelli et al. 1998). Many early studies and reports have also addressed pan evaporation relative to large water bodies. More recently, studies have incorporated energy balance concepts. The purpose of this chapter is to describe some earlier and more recent USA research-oriented studies on estimating evaporation from water bodies. Particular emphasis will be on practical procedures and techniques that professionals can use to estimate evaporation from water surfaces using pan evaporation, available weather data, or new data collected specifically for estimating daily evaporation. A portion of material in this chapter was originally assembled by F.H. Quinn of the Great Lakes Environmental Research Laboratory of the National Oceanic and Atmospheric Administration, as part of Chapter 4 of the ASCE Handbook on Hydrology.

6.2 Methods for Estimating Evaporation from Water Surfaces

Pan Evaporation

Early USA Studies. One of the earliest studies of pan and lake evaporation was that by L.G. Carpenter at Fort Collins, Colorado (Carpenter 1898). He observed that water temperatures were higher in the shallow areas than in the deep areas, and that pan evaporation at night is almost the same as during the day. He reported 11 years of evaporation data measured in Colorado's 3 × 3

ft (0.91 × 0.91 m) sunken pan where the rim of the pan was within 5 cm of the ground surface. The Colorado pan was originally two feet deep and since 1889, three feet deep. That pan was considered to be a superior design relative to the elevated Class A Pan due to reduced heat transfer through the walls (Kohler et al. 1955). A significant observation was that during the day, the surface water warmed rapidly and the lower layers slowly. This thermal profile was caused by differential absorption of solar radiation with depth, which varies by solar wavelength, as illustrated in fig. 4.5 and 4.6. When cooling at night, the whole mass of water cooled as cooler, denser surface water settled.

During the early 1920s in the USA, a major concern of engineers was estimating the evaporation losses from the U.S. Bureau of Reclamation reservoirs. The principal method used was to estimate evaporation by multiplying a factor, or coefficient, by measured pan evaporation. No consensus existed on which of several pan designs would provide the best estimates. Houk (1926) presented a comprehensive summary of monthly pan evaporation, mean temperature and, when available, wind speed from 50 sites near Reclamation's projects in the western USA. Many of the discussants of his paper reported additional pan evaporation data and estimated reservoir evaporation. Houk, in his closing discussion, commented on each of the statements presented by the discussants.

In 1931, Rohwer (1931) published the results of a series of indoor studies of evaporation from water surfaces conducted from 1923 to 1925 and from ice in 1928 and 1929. Several outdoor studies were conducted in 1927-1928 that included evaluating elevation effects on evaporation. He reviewed several Dalton-type equations expressing evaporation as a function of wind speed and the vapor pressure deficit (VPD). The most notable outdoor study involved an 85-ft diameter (25.9 m) copper-lined reservoir 6.75 ft (2.06 m) deep along with several types of evaporation pans. Daily measurements reported for the periods of Oct.-Nov., 1926, Apr.-Nov., 1927, and Apr.-Nov., 1928 included surface water and air temperatures, VPD, wind speed, and evaporation. The other pans or tanks included the Geologic Survey floating tank, Colorado-type land tank, and the Weather Bureau (WB) Class A land tank. The floating tank was set in the middle of the reservoir. Rohwer contended that evaporation from a lake or reservoir is substantially the same as that from a circular tank 12 ft (3.66 m) in diameter and 3 ft (0.91 m) deep. The Class A pan is 0.254 m deep. He derived several evaporation formulas. Indoor controlled wind evaporation measurements were made using a 3 × 3 ft square tank 10 inches deep (0.91 × 0.91 × 0.25 m) from which he derived his formula 6 of $E = (0.44 + 0.118\ W)\ (e_s - e_d)$ where W is "water-surface" wind speed in mi/h and vapor pressures of the air and the water surface are in inches of mercury. Penman (1948) extrapolated Rohwer's evaporation equation made at 5,000 ft (1,524 m) elevation to sea level and to wind speed at a height of 2 m to obtain his eq. 3. He then showed in his fig. 4 that Rohwer's equation was similar to what he had derived in England, although Penman perceived that a power wind function [$E = (aW^b)\ (e_s - e_d)$] was more theoretical.

During a symposium addressing evaporation from water surfaces in 1933, two papers were added to the ASCE Final Report of the Special Committee on Irrigation Hydraulics by a subcommittee on the subject of evaporation. In this symposium Rohwer (1934) presented a detailed discussion of evaporation from different pans including a section by R. Follansbee who summarized national and international records of reservoir evaporation as related to pan evaporation. The papers were followed by nine discussions. A. Santos, Jr. from Brazil in his discussion stated that it was regrettable that not even passing mention was made by the authors of

work done by I.S. Bowen, N.W. Cummings, G.F. McEwen, B. Richardson and C. Montgomery who have succeeded in placing the physics of evaporation on a firm basis.

Hardy et al. (1939) summarized precipitation and evaporation data from locations throughout New Mexico as measured in 4-ft diameter standard pans and floating pans at two locations. Using suggested pan coefficients, they estimated annual evaporation from Elephant Butte reservoir to be about 72 in. (1830 mm). Meyer (1942) prepared a comprehensive document summarizing estimated evaporation from lakes and reservoirs based on fifty years of U.S. Weather Bureau records. Hickox (1946) conducted a study of evaporation from a pan 1 ft (0.305 m) in diameter and 6 in. (0.15 m) deep in still air under controlled conditions of 71.0ºF (21.7ºC) and 53.1% relative humidity. The pan was insulated with a 4-inch layer of hair felt. A detailed discussion of his results compared with others was presented. Based on his analysis, evaporation should vary with the 0.75 power of wind speed. This paper summarizes a dissertation submitted in July 1939 at the University of California. A list of 65 references on evaporation was included in the Appendix I of his paper. Lengthy discussions of this paper included those by C. Rohwer, C.W. Thornthwaite, H.F. Blaney, A.A. Young, A.A. Kalinske, A.F. Meyer, and M.L. Albertson, and a closing discussion by the author. Anyone planning an evaporation research study will find this paper of interest.

Young (1947) summarized pan records and coefficients in California. Pan coefficients for the WB Class A pan and a screened pan for Lake Elsinore were reported in his table 10. Lake Elsinore was a small lake near Los Angeles, CA with an area of about 2,220 ha and a maximum depth of about 6 m. The annual WB pan-to-lake ratio was 0.77 for Lake Elsinore. The screened pan was designed at Fullerton to approximate the evaporation from a 12-ft diameter ground pan. The screened ground pan was 2 ft (0.61 m) in diameter and 3 ft (0.91 m) deep and was covered with a quarter-inch mesh galvanized hardware screen midway between the rim and the water surface. The annual screened pan-to-lake ratio was 0.98 for Lake Elsinore. The coefficient averaged 0.89 for February-June and 1.11 for September-November due to energy storage early in the year and release later in the year. Monthly Class A pan coefficients for evaporation from Lake Elsinore, with evaporation showing the effects of energy storage and release, are shown in fig. 6.1. Also shown are pan coefficients for Lake Okeechobee, FL, a shallow lake in a warm humid climate with an average depth of about 3 m. The Young (1947) document was updated in 1959 with the addition of estimated evaporation for the San Francisco Bay and Sacramento-San Joaquin delta areas by Blaney and Muckel (1959).

Kohler (1954) used the results of the detailed U.S. Geologic Survey (USGS) Lake Hefner evaporation study combined with pan evaporation for estimating lake evaporation. One of his objectives was to derive a more reliable procedure for estimating lake evaporation from pan evaporation and related meteorological data normally collected by the Weather Bureau. A summary of pan coefficients that had been derived from previous studies was presented in a table. In some cases, evaporation from the 12-ft (3.66 m) sunken pan was assumed to be equivalent to lake evaporation. A summary of pan-to-pan ratios was also presented. The annual Class A pan coefficient derived for Lake Hefner was 0.69. Monthly coefficients varied because of the temperature lag in the lake due to differences in energy storage capacities of the two water bodies. Pan coefficients tended to be lower in spring months. Kohler concluded that annual lake evaporation could be estimated within 10-15% by applying the annual coefficient to pan evaporation. His analysis also substantiated the conclusions of Rohwer (1931) that the rate of evaporation is not influenced greatly by the area of the water surface in the range considered.

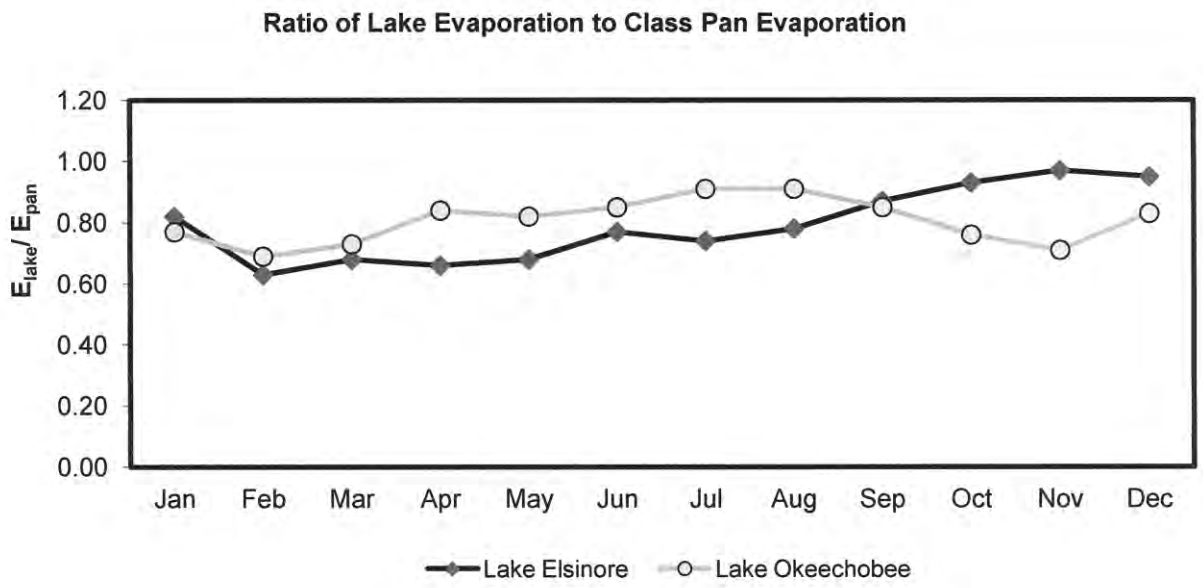

Fig. 6.1. Ratios of lake evaporation to Class A pan evaporation (Lake evap Epan^{-1}). Source: Lake Elsinore, CA data from Young (1947) and Lake Okeechobee, FL data from Kohler (1954).

Kohler et al. (1955, 1958) developed an empirical equation for estimating annual lake evaporation based on pan evaporation and weather data. Variables included: pan evaporation, atmospheric pressure, an advective factor related to pan wind movement, pan water temperature, and air temperature. They concluded that better results are obtained with monthly data than with annual data, and that further improvement might be expected if daily values were used.

Kohler et al. (1959) presented a series of maps of average Class A pan evaporation, and average annual lake evaporation in inches, average annual Class A pan coefficient in percent, and average annual May-October evaporation in percent of annual values. These maps still serve as a useful guide to expected annual evaporation in the USA although they have been replaced with free water surface evaporation estimates (Farnsworth et al. 1982).

These early studies of using pan evaporation to estimate evaporation from water bodies clearly showed that in deep water bodies, the rate of evaporation lags pan evaporation rates because of energy storage in the water body. The energy storage effects were illustrated by the parallel studies of evaporation from Pyramid Lake (a deep lake) and Lake Winnemucca (a shallow lake) (Harding 1962).

Traditional Pan Methods. Traditional methods for estimating evaporation from water bodies have been based on evaporation measured from a network of evaporation pans. The standard evaporation pan in the U.S. is the Class A Pan that is 1.21 m in diameter and 0.254 m deep placed 0.15 m above ground level on an open timber framework. Two other internationally used evaporation pans that have been rarely used in the USA are the Soviet GGI-3000 (0.3 m^2) pan and the GGI-20 m^2 tank, both placed in the soil with only 0.075 to 0.1 m of rim above the soil surface. Details can be found in World Meteorological Organization (1970). Daily evaporation is computed from the water balance of the pan, being the difference between the change in storage in the pan and inputs of precipitation and water added to maintain an adequate supply in the pan for evaporation. Due to differing thermal characteristics between the pan and large water bodies, evaporation from most surface pans exceeds the total amount of evaporation from large

water bodies and distort the seasonal distribution. For example, on a seasonal basis, pan evaporation usually peaks several months before the peak evaporation from deep lakes. Estimates based on pan evaporation are questionable during late fall and early winter periods when ice may form in the pan but not on large water bodies.

Annual lake evaporation estimates are often obtained by multiplying the annual pan data by an appropriate coefficient. Based on a US NWS Class A pan, these coefficients have been computed for a number of water bodies and tend to range in value from 0.65-0.85 (World Meteorological Organization 1973; U.S. Department of Commerce 1968). The coefficient is higher under humid conditions and lower under arid or dry conditions. A coefficient of 0.70 is applicable when water and air temperatures are approximately equal.

Early studies in the USA in semi-arid to arid climates revealed a very significant response in pan evaporation to pan size, but now it is clear that this was primarily the result of a decreasing effect of local advection with increasing size of the water surface area. Pruitt and Doorenbos (1977) reported almost no difference (4%) between evaporation from a 0.62-m diameter Soviet pan and a 5-m diameter Soviet pan when both were located in a 5-ha irrigated grass field. On the other hand, at a dry site in Nevada, evaporation from the smaller Soviet pan averaged some 1.6 times that of the larger pan, although when corrected for the net energy transfer from soil to the pans, a factor of 1.45 resulted (Hounam 1973).

Young (1947) discussed the problem of local pan environment in relation to estimating lake evaporation. Soon thereafter studies in India by Ramdas (1957) and studies at Prosser, Washington and in California (Pruitt 1960, 1966 and California, State of 1975) provided clear evidence that unless the local environment of the pan was taken into account, the estimation of lake evaporation was subject to errors of up to 35%. Fig. 6.2 presents some of the early results, which illustrate the problem (even for a given sized pan) associated with the environment just upwind of the pan. These results came from a study involving four Class A pans located within a large fallow field, with three of them placed within various-sized circular areas, flood irrigated frequently and planted to grass. The fifth pan located within a 5-ha irrigated grass field had a minimum upwind fetch of grass or irrigated pastureland of some 200 m. Data from the one pan in the fallow field, which had no surrounding grass, were plotted as if having a 0.3-m fetch of grass in order to use a log-linear plot. From this and other similar studies (e.g. Ramdas 1957, Pruitt 1960 and Stanhill 1962), Pruitt developed recommended pan coefficients (K_p) for estimating ET_o and in turn evaporation from shallow water bodies. Taken into account were the effects of upwind fetch (both dry and moist), mean relative humidity and total daily wind on K_p (Jensen 1974; Doorenbos and Pruitt 1975, 1977; Jensen et al. 1990)

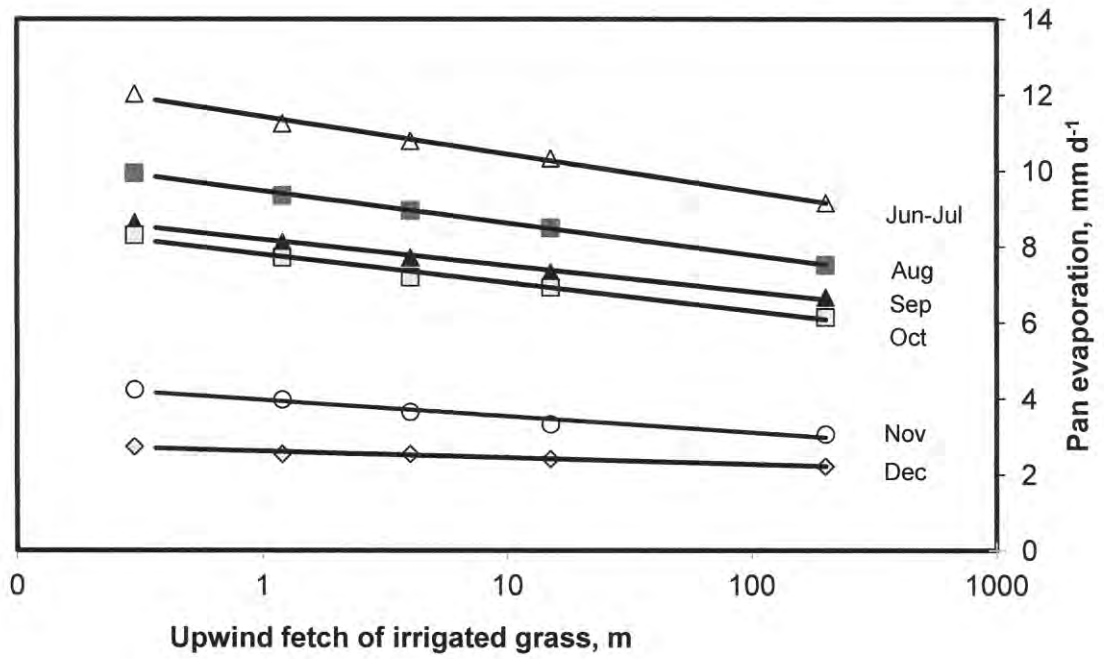

Fig. 6.2. Evaporation from NWS Class A Pans vs. upwind fetch of irrigated grass 0.07 to 0.15-m tall, Davis, California, 1959. The upwind fetch effect decreases from June to December. Source: Data from Pruitt (1966).

Mean monthly, seasonal, and annual Class A pan evaporation for individual stations throughout the United States have been tabulated by Farnsworth and Thompson (1982) and Farnsworth et al. (1982). The second reference *Evaporation Atlas for the Contiguous 48 States* contains maps with isolines of pan coefficients recommended for use with the evaporation maps in estimating so-called *free water surface evaporation* (FWS) from shallow water bodies. Fig. 6.3 presents a portion of the Annual FWS Evaporation map for the 48 States from that publication. Seasonal maps for the periods May-Oct and Nov-Apr are included in this NWS report. Farnsworth et al. (1982) defined FWS as evaporation from a thin film of water having no appreciable energy storage. They state that: "Only when the change in heat storage is negligibly small will FWS be a good estimation of the evaporation from the lake." Farnsworth did not address the problem of solar radiation that penetrates beneath the 'thin film.' Therefore, estimation of evaporation from lakes and reservoirs should not be based on the FWS data without adjustment. In nontropical climates in the spring, energy is stored in the water and actual lake evaporation can be much less than the computed FWS. During the fall, stored energy is released and the actual lake evaporation can be much greater than the FWS evaporation. The most reliable map in this publication is Map 2 covering the period May-October, the warmer period when pan evaporation data were available. A map for November-April, not published, was developed and the two seasonal maps were graphically added to obtain annual values (Map 3). In the northern part of the U.S. and especially in higher elevation western areas, a minimum value of 178 mm (7 inches) was estimated for the November through April FWS evaporation.

Many reservoirs are operated using estimated evaporation based on measured pan evaporation from the U.S. Weather Service Class A pan. The guidelines for siting and maintenance of evaporation pans, however, are not always followed closely. Some pans have

had screens placed on them to keep birds and animals from drinking the water. Even heating devices have been used to keep ice from forming on the pan in the spring and fall to facilitate observations, some pan sites have been moved to new locations that do not meet the criteria for a representative pan evaporation site for which original coefficients may have been developed, and some sites are not well-maintained. In the remainder of this chapter we will focus on estimating evaporation using potentially more accurate energy balance and aerodynamic approaches that have become feasible with the availability of daily and hourly weather data and the wide use of automated weather stations by various agencies and other entities.

Fig. 6.3. A portion (southcentral USA), of a map of estimated free water surface (FWS) Annual Evaporation for the 48 States showing relatively strong east-west gradients caused by decreasing humidity from east to west. Source: Figure from Farnsworth et al. (1982), U.S Gov. Web site http://www.weather.gov/oh/hdsc/studies/pmp.html

Behavior of Evaporation from Large Mid-Latitude Lakes. Estimation of evaporation from deep and/or clear water bodies from pan evaporation can be speculative due to potentially large differences in heat storage between water body and pan. Fig. 6.4 and 6.5 present data from Kondo (1994) and Croley et al. (1996) (NOAA Great Lakes Environmental Research Laboratory) that show the extreme lags possible between solar radiation and evaporation for large, cold lakes lying north of 40° latitude or south of -40° latitude. Evaporation can be low during summer when short wave radiative energy is absorbed by the cold water bodies and when vapor pressure gradients above the water are small due to high humidity of air caused by regional ET. Evaporation is high during winter as dry air from non-transpiring frozen regions is coupled with saturation vapor pressure at the water surface that may be much higher than the air. The

energy to evaporate the water during winter comes from stored energy. The pattern from Lake Towada of Japan, an 80-m deep lake, is similar to that of Lake Superior. The data from Kondo (1994) show that as mean depth of a water body decreases, the annual evaporation pattern approaches that of solar radiation. The trends of fig. 6.4 and 6.5 illustrate the inability to estimate evaporation from deep water bodies using pan evaporation records. The annual peaks and lows can be as much as 180 days out of synch due to the large changes in energy storage (Q_t) as discussed in a later section.

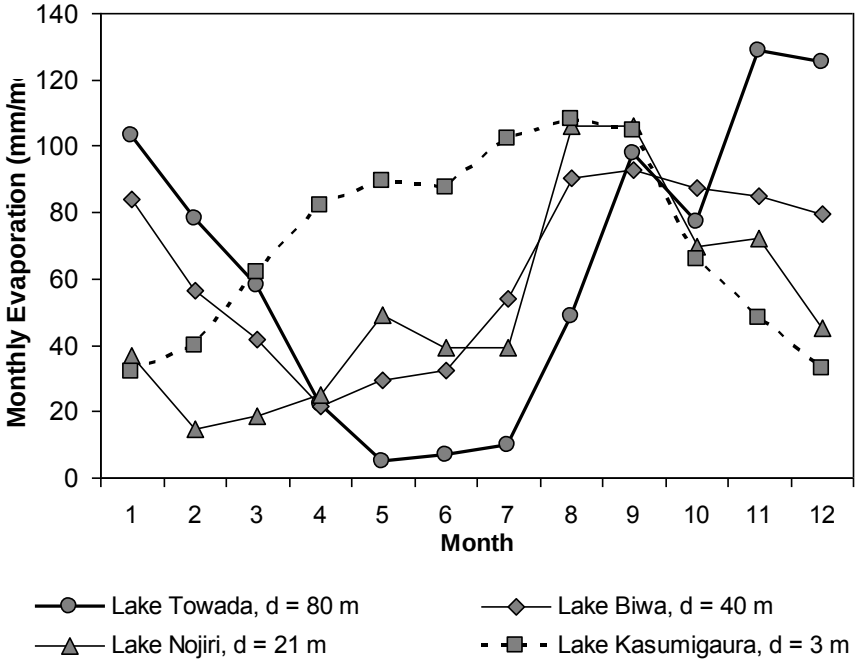

Fig. 6.4. Seasonal change of lake evaporation in Japan for water bodies of different depths. Source: Data from Kondo (1994).

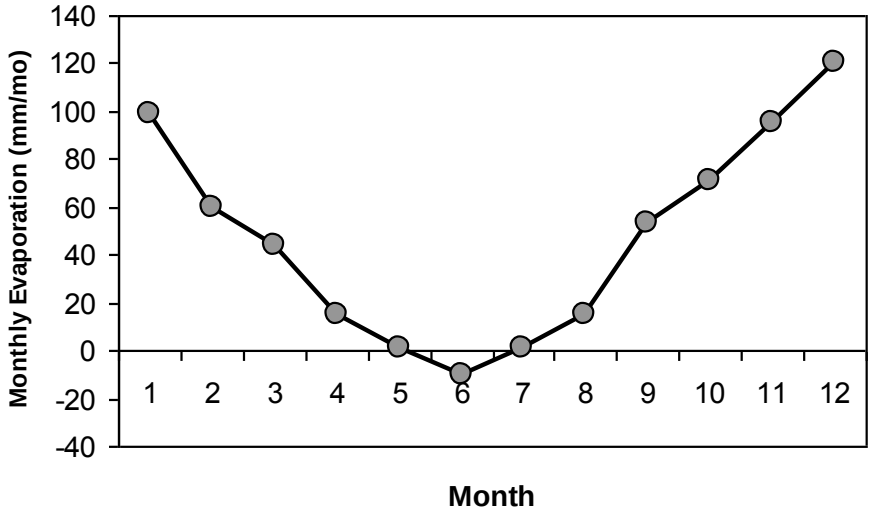

Fig. 6.5. Simulated values of evaporation for Lake Superior. Source: Data from Croley et al. (1996).

Water Budget Procedure

The water budget procedure is a simple method for computing evaporation for monthly, seasonal, or annual time periods. All of the terms in the water balance, except for evaporation, are either measured or estimated with the evaporation computed as a residual. The water balance procedure is based upon the hydrologic equation

$$Inflow = Outflow + \Delta Storage \tag{6.1}$$

Inflow terms consist of precipitation on the water surface, runoff from the land basin, major channel inflow from outside the immediate drainage basin, groundwater inflow and diversions from outside its basin into a free water body (lake, reservoir, pond, etc.). Outflow terms consist of evaporation from the water surface, major channel flow out of the water body, diversions out of the water body, and groundwater flow from the water body. The water balance equation can be expressed in terms of depth or volume of water evaporated from the surface per unit time as:

$$E = P_r + R + Q_i + G_{gw} + D_i - Q_o - D_o - \Delta S \tag{6.2}$$

Where E is the amount of water evaporated, P_r is the precipitation on the water surface, R is the runoff inflow from the drainage basin, Q_i and Q_o are major channel flows into and out of the water body, respectively, G_{gw} is the net groundwater flow into the water body, D_i and D_o are net diversions into and out of the water body respectively, and ΔS is the change in water body storage, where a positive value indicates an increase. Units for all parameters in eq. 6.2 are the same and can be expressed in terms of volume or in units of depth (i.e., in mm) over the water

body surface for a specified time interval. The computations are most accurate when the evaporation is of the same order of magnitude or larger than the other terms of the water balance. The groundwater component is usually the most difficult term to estimate due to its diffusive nature. For most lakes, the volume in storage and surface area is required to extrapolate volumes to depths.

Water balance data sources for the U.S. are the National Climatic Data Center, NOAA regional data centers, and state climatologists for precipitation data, the U.S. Geological Survey, State water agencies, and flood and conservation districts for runoff, major channel flows, and diversion data.

Aerodynamic Method (Mass Transfer)

Aerodynamic methods are among the most widely applied to determine evaporation from lakes and large reservoirs. The basic equations were tested on Lake Hefner in Oklahoma and Lake Mead in southern Nevada in the 1950's (U.S. Geological Survey 1954, 1958; Harbeck 1962). The basic Lake Hefner form of the mass transfer equation is

$$E = M\ \left(e_s - e_z\right) u_z \tag{6.3}$$

where E is the evaporation in mm t^{-1}, M is the mass transfer coefficient in mm s $(kPa\ m)^{-1}$ t^{-1} and includes conversion units for depth and time, e_s is the saturation vapor pressure in kPa at the surface water temperature, T_s, e_z is the vapor pressure of the air in kPa at level z in kPa, and u_z is the wind speed in m s^{-1} at level z. The vapor pressure of the air e_z is equivalent to the saturation vapor pressure of the air at the dew point temperature and can be computed by

$$e_z = 0.01\ RH\ \left(e_z^0\right) \tag{6.4}$$

where e_z^o is saturation vapor pressure in kPa at air temperature T_z at level z, and RH is the relative humidity in %. Saturation vapor pressure at the surface can be estimated using eq. 3.1 and water surface temperature when T_s has values close to T_z, which is typical. It is important that T_s represents the 'skin' temperature of the water body because of potentially strong thermal gradients within the first few cm of water during periods of strong solar radiation caused by absorption of infrared radiation near the surface and during night time during strong radiative cooling. Measurements made using thermal sensors such as thermocouples even one cm below the surface may be several degrees in error. This error can cause substantial error in the estimation of e_s and in emitted long-wave radiation. Generally, in modern systems, infrared transducer type sensors (IRTs) are used to measure skin temperature.

The mass transfer coefficient, M in eq. 6.3, is a function of the height of the meteorological measurements, the atmospheric stability and barometric pressure, roughness of the water surface, size of water body, and the density and viscosity of the air. For the Lake Hefner study (U.S. Geological Survey 1954), M was 0.097 for mean daily wind, temperature and humidity measurements at the 8-meter level, with vapor pressure expressed in kPa and E in mm d^{-1}. The basic mass transfer equation requires measurement of surface water temperature, air temperature, humidity or vapor pressure, and wind speed. A more complete and decomposed method is to use

a bulk transfer coefficient as in eq. 6.7, rather than a mass transfer coefficient, where the bulk transfer coefficient can be related to aerodynamic roughness. The wind speed can be adjusted from one level to another level over the same surface by the logarithmic law (Oke 1978; Allen et al. 1989; Jensen et al. 1990), provided that the effect of stability is negligible:

$$u_2 = u_1 \frac{\ln\left(\frac{z_2 - d}{z_{om}}\right)}{\ln\left(\frac{z_1 - d}{z_{om}}\right)} \tag{6.5}$$

where z_1 and z_2 are the measurement heights in m for level 1 and level 2, respectively, z_{om} is the roughness height in m for momentum transfer for water, and d is the zero-plane displacement in m. Literature values for z_{om} vary from 0.00001 to more than 0.001, depending on wind speed and wave type, with a value of 0.0001 m as a typical average. Brutsaert (1982) listed z_{om} of 0.0001 to 0.0006 m for large water bodies. d is generally 0 for water. The wind level adjustments over water are relatively insensitive to the value of z_{om}. The difference between using 0.0001 m and 0.001 m is approximately 5%, which is well within the application accuracy. Adjustment of wind speed to account for difference in roughness of the weather station measurement surface from the roughness of a water surface is done using eq. 11.60 of chapter 11. That equation can also be used to adjust for wind measurement height differences between the locations. Stull (1988) and Lofgren (2004) recommend the Charnock (1955) relation to describe z_{om} as a function of wind speed effects on wave height. The parameters suggested by Lofgren (2004) yield the equation

$$z_{om} = 4.5\ x10^{-7}\ u_{10}^{2.55} \tag{6.6}$$

where u_{10} is wind speed at 10 m height over water in m s^{-1}. A lower limit of 0.00005 m for the z_{om} estimate from eq. 6.6 is recommended, occurring at u_{10} of 6.5 m s^{-1}

Most mass transfer research over the past several decades has been directed towards the bulk aerodynamic equation. The bulk equations consider the impact of atmospheric stability as well as air mass characteristics on the evaporation rate. This equation can be written as

$$E = \frac{1000\ k_t\ C_E\ \rho_a\ (q_s - q_z)\ u_z}{\rho_w} \tag{6.7}$$

where E is the evaporation in mm t^{-1}, C_E is the bulk evaporation coefficient for level z (dimensionless), ρ_a is the density of air in kg m^{-3}, q_s is the saturation specific humidity at the water surface temperature in $kg_w\ kg_a^{-1}$ (subscripts 'w' and 'a' signify water and air), q_z is the specific humidity of the air at level z in $kg_w\ kg_a^{-1}$, u_z is the wind velocity at level z in m s^{-1}, ρ_w is the density of water in kg m^{-3}, 1000 converts from m to mm and k_t is a conversion for time (k_t =

86,400 for E in mm d^{-1} and $k_t = 3600$ for E in mm h^{-1}). The specific humidity is defined in eq. 3.5 where units of e and P are the same. In saline water bodies, salinity of the water will reduce the surface saturation vapor pressure and hence the surface specific humidity (List 1984). C_E is equivalent to the classical aerodynamic expression:

$$C_E = \frac{k^2}{\ln(z/z_{om})\ln(z/z_{ov})} = \frac{1}{u \cdot r_{av}} \tag{6.8}$$

for near neutral stability conditions where z_{om} and z_{ov} are roughness lengths for momentum and vapor transfer, k is the von Karman constant (0.41) and r_{av} is bulk aerodynamic resistance for vapor transfer between the surface and height z. The roughness height z_{ov} is generally considered to be similar in value to z_{om} or even exceeding the value for z_{om} when applied to water (Brutsaert 1982). For detailed, theoretical aspects of relationships between z_{ov} and z_{om} for water, the reader is referred to Brutsaert (1982).

Eq. 6.3 and 6.7 are nearly equivalent as shown by expressing eq. 6.7 in a form using vapor pressure:

$$E = k_t \ 1000 \ C_E \frac{\rho_a}{\rho_w} \frac{0.622}{P - 0.378\, e_z} \frac{e_s - K\, e_z}{} \ u_z \tag{6.9}$$

where E has units of mm t^{-1} and $K = (P - 0.378\ e_s)/(P - 0.378\ e_z)$. For typical values of P, e_z, and e_s, K over water tends to approach 1.0. The pressure correction term $0.378\ e_s$ in the denominator is generally small in relation to P and can be neglected with little error in E. The combined error of the two assumptions, on the order of 1 percent or less, is well within data precision. Thus, the mass transfer coefficient M can be expressed in terms of the bulk evaporation coefficient C_E as

$$M = 0.622\ (k_t\ 1000\ )\ \frac{\rho_a}{\rho_w}\ \frac{C_E}{P} \tag{6.10}$$

which shows a dependence of M on the air density, ρ_a, which varies with air temperature and barometric pressure, the barometric pressure, P, itself which varies with elevation, and on the bulk evaporation coefficient C_E.

The solution of eq. 6.3 and 6.10 is dependent upon the selection of the bulk evaporation coefficient, C_E, or the mass transfer coefficient M. Extensive research conducted during the International Field Year for the Great Lakes (IFYGL) (Aubert and Richards 1981) indicated an average value for C_E of 0.00125 for the 8 m level. The IFYGL Atmospheric Boundary Layer Panel (Aubert and Richards 1981) recommended $C_E = (1.5 \pm 0.3) \times 10^{-3}$ for the 3-m level, with all values in this range being equally possible. Kondo (1975) recommended $C_E = 0.0012$ for neutral conditions. Donelan et al. (1974), using a wind profile procedure, determined the following values of C_E at the 4-m level based on atmospheric stability: $C_E = 0.00131$ for neutral

conditions; C_E = 0.00159 for unstable conditions; and C_E = 0.00135 as the best overall estimate. Converting coefficients to the 8-m level yields values for C_E of 0.00115, 0.00140, and 0.00119 for neutral, unstable, and overall conditions, respectively. Parameters to which evaporation is most sensitive are wind speed, followed by the water surface and dew point temperatures and humidity.

For detailed studies on large lakes it may also be desirable to use ratios of over-lake to over-land wind speed and humidity and to consider atmospheric stability (Phillips and Irbe 1978). Quinn (1979) and Liu and Schwab (1987) discussed the estimation of C_E using wind speed and air-sea temperature differences. More discussion is provided later in the applications section.

Energy Balance Method

The energy balance procedure as applied to water bodies is based upon the principle of conservation of energy. As with the water balance procedure, the evaporation is computed as a residual. This procedure is the most data intensive of the standard evaporation procedures, but it has wide applicability to many differing water bodies for time periods of minutes to years. Evaporation determined by energy balance for a water body may be expressed as

$$E = \frac{1000}{\rho_w \lambda}\left[R_n - Q_t - H + Q_V - Q_w\right] \tag{6.11}$$

where E is the evaporation rate in mm t^{-1}, R_n is net radiative energy to the water body in MJ m^{-2} t^{-1}, Q_t is the change in energy stored in the water body in MJ m^{-2} t^{-1}, H is the energy convected from the water body as sensible heat in MJ m^{-2} t^{-1}, Q_V is the net energy advected into the water body by streamflow or ground-water in MJ m^{-2} t^{-1}, Q_W is the energy advected by the evaporated water in MJ m^{-2} t^{-1}, ρ_w is density of liquid water in kg m^{-3} and λ is the latent heat of vaporization in MJ kg^{-1}. The product $\lambda\rho_w E$ /1000 is the energy utilized by evaporation in MJ m^{-2} t^{-1}.

Net Radiation for Water. The net radiative energy flux at a surface was introduced in eq. 4.31. A more specific method for calculating R_n for water is:

$$R_n = (1 - \alpha) R_s \downarrow + (1 - \alpha_l) R_L \downarrow - \varepsilon\, \sigma (T_s)^4 \uparrow \tag{6.12}$$

for R_n, R_S and R_L in MJ m^{-2} t^{-1} where α is the solar albedo for water (0.04-0.15), dependent upon surface conditions (Brutsaert 1982; Bolsenga and Vanderploeg 1992), α_l is the long wave albedo, equivalent to (1 - ε) or approximately 0.03 (WMO 1970), σ is the Stefan-Boltzmann constant (4.901 $\times 10^{-9}$ MJ m^{-2} K^{-4} d^{-1} for daily time steps and 2.042 $\times$ 10^{-10} MJ m^{-2} K^{-4} h^{-1} for hourly time steps), ε is the long wave emissivity (0.92-0.97, with ε = 0.97 typically used (Anderson 1954) and T_S is the water surface temperature in K. It is important that estimation of emitted long wave radiation is based on T_S for the water surface, since water surface temperature can deviate substantially from air temperature, especially for small to medium-sized water bodies

surrounded by warmer or cooler land surfaces. In applying eq. 6.12, shortwave and long-wave radiation may be measured or can be estimated by a number of empirical equations (Croley 1989; Derecki 1976; Gray 1970; Sellers 1965).

Albedo varies with water turbidity, wave height and the ratio of diffuse to total solar radiation. Cogley (1979) presented a table of albedo for water surface as a function of latitude based on an accurate weighting for radiation received at different elevation angles. These were based on the Fresnel equation for a plane surface of pure water under direct radiation and modified by measurements made by Grishchenko (1959) for wave heights of 0.1 to 0.7 m and cloud cover of 0 to 25%. A summary of these values is presented in table 6.1.

Factors Governing Heat Storage, Q_t, of Water Bodies. An important distinction between R_n for a water body and R_n for vegetation or soil is that with soil and vegetation, essentially all of the R_n quantity is captured at the 'opaque' surface and is immediately available for conversion to λE or H or conduction into the surface as G. With water, however, much of the solar radiation, R_s, penetrates to some depth in the water body, depending on the turbidity of the water, where it is converted to Q_t. Therefore, with water bodies, R_n is the net radiation captured by the water body, but is not necessarily available at the surface for immediate conversion to λE or H. This is why the energy storage change, Q_t, is used in the energy balance for water rather than the ground energy flux density term, G, that is used for soil. The term G for soil is governed only by thermal conduction into the surface whereas Q_t for water is governed by both conduction and by penetration of solar radiation. The value for Q_t can be very large, as shown later in fig. 6.12 for American Falls Reservoir, Idaho.

Absorption of solar irradiance in pure water varies widely with the wavelength of spectral irradiance (fig. 6.6). The mean absorption depth is very shallow for wavelengths shorter than 0.4 μm, but it is relatively deep for wavelengths between 0.4 and 0.6 μm, which is primarily blue and green visible radiation. Most of the energy in solar irradiance occurs in the 0.2-1.0 μm wavelength band. Fig. 6.7 shows absorption of total solar radiation in pure (clear) water, indicating that most warming of clear water will occur at more than several m below the surface. However, there will always be some warming of the top 1 m of even clear water due to the ready absorption of the near and mid-infrared wavelengths. In addition, penetration of blue and green wavelengths is reduced with increasing turbidity of the water.

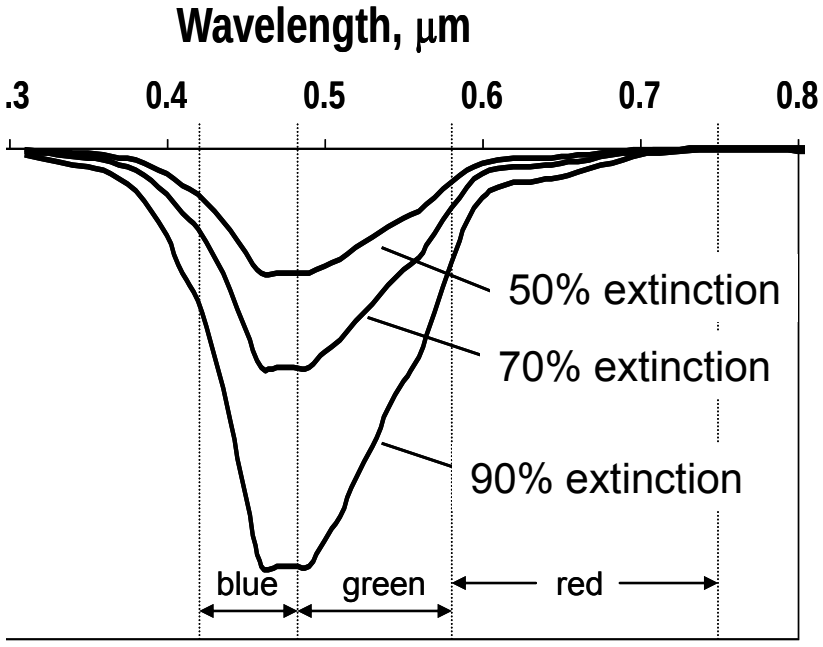

Fig. 6.6. Relative extinction depths for solar radiation in pure water as a function of wavelength.

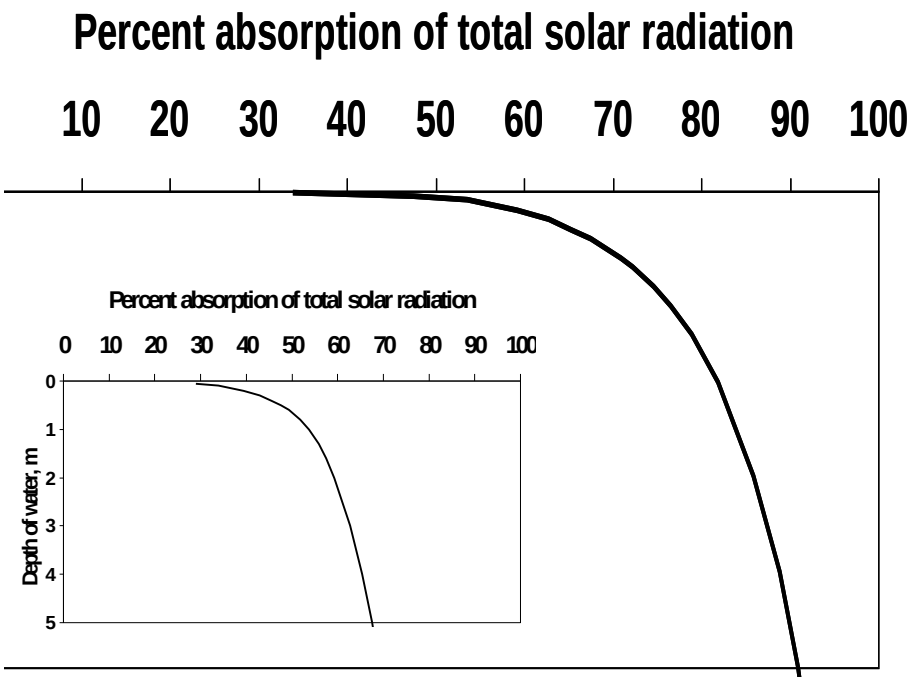

Fig. 6.7. Percent absorption of total solar radiation as a function of water depth for pure water. The inset provides detail over the first 5 m.

When inflow and outflow rates are significant, or when deep reservoirs are involved, estimating the change in energy storage over periods of time can become complex. The advection of energy must be considered as well as the energy stored as a thermal profile develops below the water surface of the reservoirs. Rosenberry et al. (1993) and Sturrock et al. (1992) reported measured energy storage in Williams Lake in north-central Minnesota. Measurements made over five seasons indicated that substitution of energy storage measured at one location in the lake from a raft placed in the center of the lake rather than at 16 locations distributed over the lake resulted in estimates within 2% of the best estimates. Williams Lake, a somewhat bowl-shaped basin, has an area of 36 ha and a maximum depth of about 10 m. Average annual evaporation was 670 mm. During May-June, solar energy storage input, Q_t, averaged 4-5 MJ m^{-2} d^{-1} or about 20% of R_n. Amayreh (1995) measured large values of Q_t of 9-10 MJ m^{-2} d^{-1} during June and July on Bear Lake in Idaho and Utah. Bear Lake is a clear, cold and deep high desert lake having a maximum depth of 60 m. A variety of other studies (Anderson 1954; Harbeck et al. 1958; Hughes 1967; Ficke 1972; and Keijman 1974) have applied a range of methods for measuring energy storage in water.

TABLE 6.1 Monthly mean Grishchenko (1959) albedo (percent) of open water for latitudes 0º to 70º N. Source: Data from Cogley (1979) table 5.

θ	Month												
(deg)	Jan	Feb	Mar	Apr	May	Jun	Jul	Aug	Sep	Oct	Nov	Dec	Year
70	30.1	33.8	22.9	14.8	11.6	11.2	11.4	13.4	20.2	31.3	30.1	- -	14.1
60	33.9	24.0	15.5	10.5	8.8	8.4	8.6	9.8	13.6	21.6	32.1	35.5	12.0
50	22.0	16.1	10.8	8.4	7.5	7.3	7.4	8.0	9.9	14.4	21.0	24.1	10.2
40	14.5	11.1	8.5	7.3	6.8	6.7	6.8	7.1	8.0	10.3	13.8	16.1	8.6
30	10.3	8.6	7.3	6.7	6.5	6.4	6.4	6.6	7.1	8.2	10.0	11.1	7.6
20	8.3	7.4	6.7	6.4	6.3	6.3	6.3	6.4	6.6	7.2	8.1	8.7	6.9
10	7.2	6.7	6.4	6.3	6.4	6.4	6.4	6.3	6.3	6.6	7.1	7.4	6.6
0	6.6	6.4	6.3	6.4	6.6	6.8	6.7	6.4	6.3	6.4	6.6	6.8	6.5

Energy Storage to Water Bodies from Thermal Profiles. One of the more difficult problems in applying the energy balance or the combination approach to estimating evaporation is that of estimating energy stored or released from the water body. The data shown in fig. 6.8 and 6.9 illustrate typical thermal profiles encountered as solar radiation is increasing during the year and after solar radiation begins to decrease. Fig. 6.8 shows the thermal profile that has developed as a result of solar radiation penetrating the water body and some conduction of energy downward. As shown in fig. 6.6, about 50% of total solar radiation penetrates to a depth of 1 m and 20% to a depth of 10 m in pure water. The thermal conductivity of water is not high and most of the increase in temperature is due to absorbed solar radiation that decreases exponentially with depth. At the end of October, as solar radiation has decreased and with the loss of energy due to evaporation, long-wave radiation emitted from the water surface and the transfer of sensible heat to the air, the surface of the water cools (fig. 6.9). Then, because of the increasing density of water near the surface as it cools, upper water layers settle until they reach the same temperature as water lower in the profile. The astute observation made in 1898 by Carpenter that the water in evaporation tanks is nearly uniform in the morning, while a thermal gradient exists during the day, illustrates this physical phenomenon of cooled water settling and mixing with deeper water in a container.

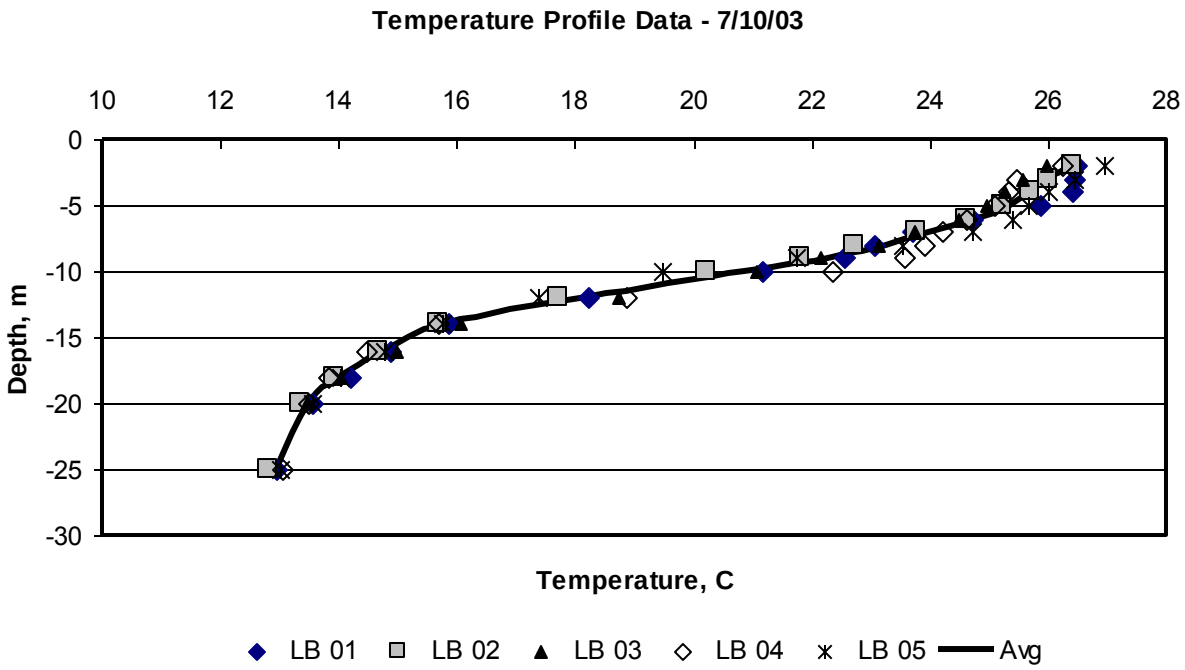

Fig. 6.8. Thermal profile data for Lake Berryessa, California on July 10, 2003. The various symbols refer to locations within the reservoir. Source: Figure from Jensen et al. (2005), © ASCE.

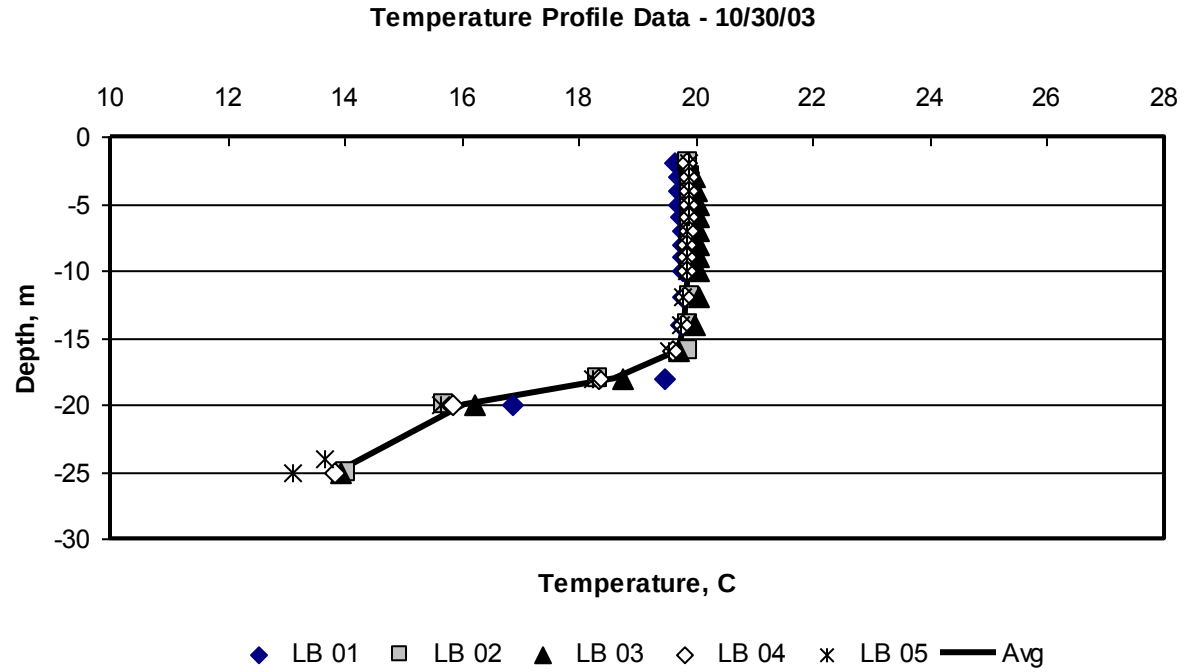

Fig. 6.9. Thermal profile data for Lake Berryessa, California on October 30, 2003. The various symbols refer to locations within the reservoir. Source: Figure from Jensen et al. (2005), © ASCE..

For shallow lakes and reservoirs of less than 3-5 m, measuring water temperature near the surface in the mornings will likely produce a good estimate of daily changes in energy storage. Daily measurements of near-surface temperature in the morning can enable calculating average rates of energy storage. The trend in average daily change in energy storage measured in Pretty Lake, Indiana and Williams Lake in Minnesota illustrates the magnitude of energy storage and release rates that can be expected for deep water bodies > 5-10 m (fig. 6.10). The values for Q_t shown in fig. 6.10, especially during early spring, late summer and fall are relatively large, averaging about ± 5 MJ m^{-2} d^{-1}, when R_n during these periods averaged only 5 to 20 MJ m^{-2} d^{-1}.

Energy storage in shallow to moderately deep water bodies (< 5-30 m depth) can use measurements of water temperature over various time periods and calculating the change in energy storage. Q_t is estimated by differencing water temperature profiles over time and multiplying by the specific heat of water, C_w:

$$Q_t = \rho_w C_w \frac{\left[\left(\int_{z_s}^{z_e} T(z)dz\right)_{t_2} - \left(\int_{z_s}^{z_e} T(z)dz\right)_{t_1}\right]}{t_2 - t_1} \tag{6.13}$$

where ρ_w is the density of liquid water in kg m^{-3}, C_w is the specific heat of water in MJ kg^{-1} K^{-1}, $T(z)$ is the temperature of water in K at depth z, evaluated at times t_1 and t_2. Depth z_s is generally at the water surface (z_s = 0) and z_e is a depth below the surface, m, where temperature change over time is small. Units for t in seconds will produce Q_t in MW m^{-2}, and t in h or d will produce MJ m^{-2} h^{-1} and MJ m^{-2} d^{-1}. Positive values for Q_t from eq. 6.13 indicate energy entering the water body system. For practical problems, the water density can be assumed to be 1000 kg m^{-3} and C_w = 4.1868 MJ m^{-3} K^{-1}. Because of the decrease in density with an increase in temperature, the average C_w over the range of 10 to 25°C is 4.18 MJ m^{-3} K^{-1}.

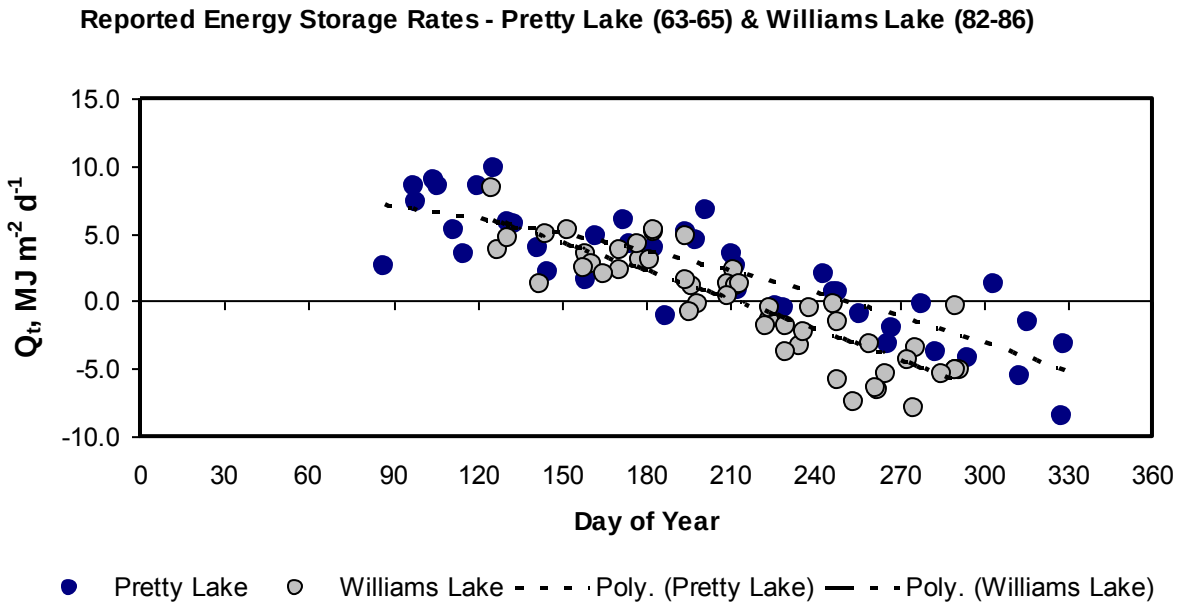

Fig. 6.10. Reported energy storage rates in Pretty Lake, Indiana, 1963-1965, and Williams Lake, Minnesota, 1982-1986. Source: Figure from Jensen et al. (2005), © ASCE.

Energy Storage to Water Bodies based on Meteorological Measurements. Estimates for Q_t can also be related to radiation received by a water body, since radiation is the primary source for heating water. Jensen et al. (2005) estimated daily energy storage in Pretty Lake, Indiana, Williams Lake, Minnesota, and Lake Berryessa, California, based on net short wave and long wave radiation:

$$Q_t = 0.5\,R_{sn} - 0.8\,R_{nl} \text{ , for Day of year <180} \quad (6.14a)$$

and

$$Q_t = 0.5\,R_{sn} - 1.3\,R_{nl} \text{ , for Day of year >180} \quad (6.14b)$$

where Q_t = average daily energy storage in the water body in MJ m^{-2} d^{-1}, R_{sn} = net solar radiation $(1 - \alpha)R_s$, and R_{nl} = net outgoing long-wave radiation [$R_{nl} = \varepsilon_l R_l\uparrow - (1 - \alpha_l)R_l\downarrow$]. Williams Lake is a small lake (36 ha) with a maximum depth of about 10 m. Pretty Lake has an area of about 75 ha, a maximum depth of about 25 m, and an average depth of about 8 m because of the large shallow areas. Lake Berryessa has an area of 8,320 ha when full, a maximum depth of 58 m near the dam, and an average depth of about 40 m. The r^2 for both equations combined was 0.63. A comparison of estimated Q_t from eq. 6.14 vs. reported or measured Q_t is shown in fig. 6.11.

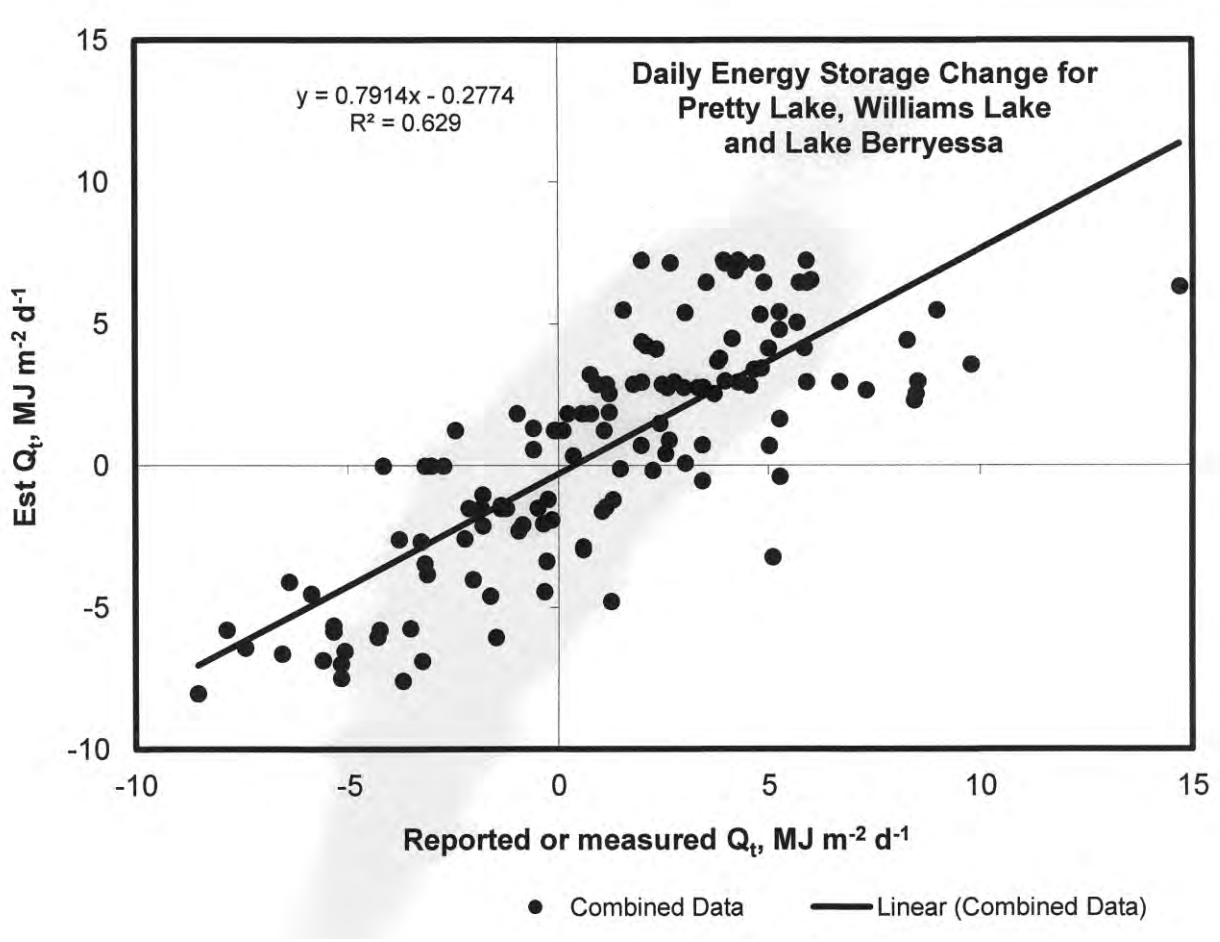

Fig. 6.11. Estimated daily Q_t from eq. 6.14 vs. reported or measured Q_t for Pretty Lake, Indiana (1963-1965), Williams Lake, Minnesota (1982-1986) and Lake Berryessa, California (2003-2004). Source: Data from Jensen (2006), pers. comm.

Data required to apply the energy balance method can be obtained from the National Climatic Data Center for radiation components, from satellite analysis for surface water temperature, and *in situ* measurements can be obtained from thermistor or thermocouple strings or water intakes for the changes in energy storage. A detailed energy budget for Lake Ontario is given by Aubert and Richards (1981). This includes an evaluation of all energy terms.

Q_t and Evaporation by indirect measurements. Fig. 6.12 shows average hourly patterns of R_n, λE, H and Q_t during two months of 2004 for American Falls Reservoir, Idaho, where mean water depth was 9 m (Allen and Tasumi 2005). The figures show the substantial addition of energy to the reservoir (positive Q_t) during daytime via the penetration of solar radiation. The rate of Q_t was lower in July due to the increased transfer of energy to the water surface and consequent higher rates of λE. Negative Q_t during nighttime supported the negative R_n from the surface as well as nighttime evaporation in July. Evaporation rates were relatively constant throughout the day and night due to close coupling between water surface temperature and air temperature.

Allen and Tasumi (2005) estimated Q_t as a residual of the energy balance by inverting eq. 6.11 and assuming that Q_v and Q_w terms were zero:

$$Q_t = R_n - H - \lambda E \tag{6.15}$$

and retaining λE in energy units. Evaporation and Q_t were using a combination of eddy covariance and Bowen ratio to determine λE and H, where the Bowen ratio (see also eq. 7.08) is expressed as

$$\beta = \frac{H}{\lambda E} = \gamma \frac{(T_s - T_z)}{(e_s^o - e_z)} = \gamma \frac{(T_1 - T_2)}{(e_1 - e_2)} \tag{6.16}$$

where β is the Bowen ratio, T_s is the water surface temperature and T_z is the air temperature at level z in °C, e_s^o is the saturation vapor pressure in kPa at T_s, e_z is the vapor pressure in kPa at level z, and γ is the pyschrometric constant kPa °C^{-1} (eq. 3.11a). Parameter β is dimensionless. The last set of terms in eq. 6.16 present an alternative means for measurement of β, where paired measurements of air temperature (T_1 and T_2) and vapor pressure (e_1 and e_2) are observed at two heights z_1 and z_2 above the water surface. Precision and bias correction or bias elimination is required in the measurement of the differences $T_1 - T_2$ and $e_1 - e_2$ due to their potentially small values under near neutral conditions or low evaporation rates.

The latent heat flux was computed in the Allen and Tasumi (2005) study using the measured Bowen ratio coupled with H measured by eddy covariance and inversion of the Bowen ratio relationship:

$$\lambda E = \frac{H_{EC}}{\beta} \qquad (6.17)$$

where H_{EC} is sensible heat flux determined by eddy covariance and β was determined by measuring humidity and temperature between two interchanging arms suspended over the water via eq. 6.16. Determination of λE from this approach cannot be used when the air temperature profile above the water surface is close to neutral, so that the determination of β via eq. 6.16 becomes close to zero. The minimum value for the absolute value for β for employment of eq. 6.17 should be about 0.05 to 0.10 to retain sufficient precision and management of residual measurement biases. Allen and Tasumi (2005) also estimated evaporation rates using aerodynamic transfer methods based on eq. 6.7 using the humidity and T measurements from the Bowen ratio arms and surface temperature measured using an infrared sensor. Those evaporation estimates were used as an independent check on λE derived from eq. 6.17.

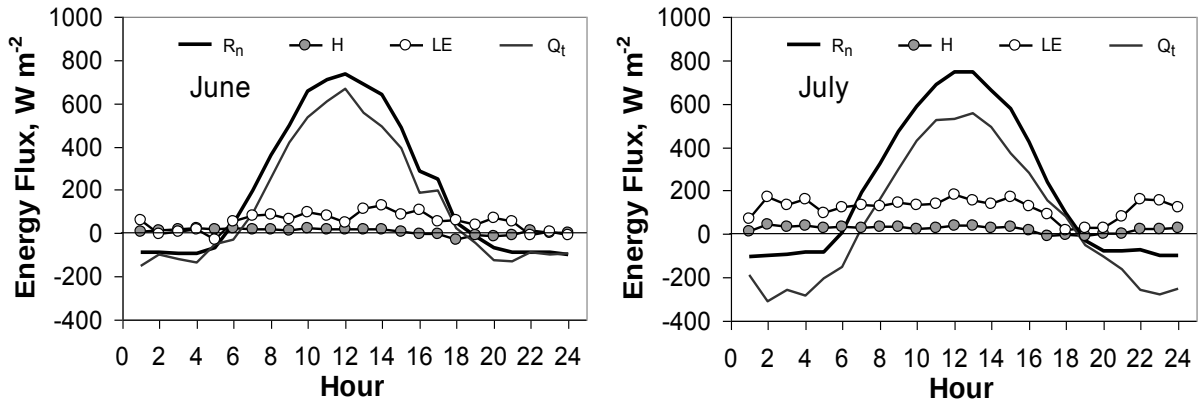

Fig. 6.12. Average hourly R_n, λE, sensible heat (H) and energy storage flux density (Q_t) during two months of 2004 for American Falls Reservoir, Idaho. Source: Data from Allen and Tasumi, (2005).

Other Components of the Energy Balance for Water. The energy advected by the evaporating water, Q_w, i.e. by the removal of water from the system, although typically less than 1% of λE, can be accounted for by:

$$Q_w = \rho_w C_w \frac{E}{1000}(T_s - T_b) \qquad (6.18)$$

where ρ_w is the density of liquid water in kg m^{-3}, C_w is the specific heat of water in MJ kg^{-1} K^{-1}, T_s is the temperature of the evaporated water in K (i.e. surface temperature) T_b is a base temperature, and E is the evaporation rate in mm t^{-1}. Eq. 6.18 accounts for the warming of water from the base temperature to the water surface evaporating temperature. Because the change in energy storage is used in calculating evaporation, the choice of base temperature is largerly immaterial (Harbeck et al. 1958). The base temperature can be set equal to the mean annual temperature of the water body, or, for convenience, to 0°C (273 K).

The net energy advected into a water body, Q_v, is composed of the energy transported into the water body by runoff, precipitation, and out of basin inflows. The energy advected out of a water body is composed of any outflows from the water body and the melting of solid precipitation at the lake surface. This quantity when expressed as energy per unit area per time step basis for a base operating temperature equal to 0°C in eq. 6.18 is:

$$Q_v = \left(V_r T_r + V_p T_p + V_i T_i - V_o T_o \right) \frac{\rho_w \ C_w}{A} - \frac{V_{sp} \ \rho_w \ \lambda_f}{A} \tag{6.19}$$

where V_r is the volume of diffuse runoff to the water body in $m^3\ t^{-1}$, T_r is the temperature of the runoff in °C, V_p is the volume of precipitation in $m^3\ t^{-1}$, T_p is the temperature of the precipitation in °C, V_i is the volume of basin inflow in $m^3\ t^{-1}$, T_i is the temperature of the inflow in °C, V_o is the volume of outflow in $m^3\ t^{-1}$, T_o is the temperature of the outflow in °C, A is the surface area of the water body in m^2, V_{sp} is the volume of solid precipitation in $m^3\ t^{-1}$, ρ_w is the water density in kg m^{-3}, and λ_f is the latent heat of fusion in MJ kg^{-1}. The energy advected into a lake is usually relatively small compared with other energy terms and may be neglected in many studies. The energy advected into or out of reservoirs, however, may be significant because outflow temperatures below dams are usually very cool and relatively stable because the depth of the normal outflow is near the bottom of the reservoir. The temperature of spills or overflows can be near the surface water temperature, depending on the geometry of the discharge structure. In reservoirs where water contents are warmed over time, T_o can exceed T_i. In some high elevation reservoirs, T_i is low due to melted snow being the primary water source.

Once estimates for all energy balance terms are collected, evaporation can be estimated from the relationship

$$E = 1000 \frac{R_n - Q_t + Q_v}{\rho_w \left[\left(1 + \beta \frac{1000}{\rho_w} \right) \lambda + C_w \ \left(T_s - T_b \right) \right]} \tag{6.20}$$

where E is the evaporation rate in mm t^{-1}, R_n is net radiation in MJ $m^{-2}\ t^{-1}$, Q_t is the rate of change in lake energy storage in MJ $m^{-2}\ t^{-1}$, Q_v is the net energy advected into the water body per unit area in MJ $m^{-2}\ t^{-1}$, ρ_w is the density of water in kg m^{-3} , λ is the latent heat of vaporization in MJ kg^{-1}, β is the Bowen ratio, and C_w is the specific heat of water in MJ kg^{-1} $°C^{-1}$. The latent heat of vaporization can be found in standard meteorological tables (List 1963, 1984) or computed by eq. 3.18. It should be noted that the computation of E via eq. 6.20 becomes unstable as the Bowen ratio approaches -1. Eq. 6.20 requires the measurement of β which involves measurement of air temperature and vapor pressure at two heights above the water surface or at one height with measurement of T_s via eq. 6.16, and it requires the measurement or estimation of Q_t, which can be large and uncertain.

Combination Methods

For many applications a combination of the aerodynamic and energy balance procedures is desirable. The first combined equation was derived by Penman (1948, 1956a) which in its general form is written as:

$$\lambda E = \frac{\Delta (R_n - Q_t) + \gamma E_a}{\Delta + \gamma} \tag{6.21}$$

where λE is the latent heat of evaporation in MJ m^{-2} t^{-1}, γ is the psychrometric constant in kPa $^oC^{-1}$, (eq. 3.11), Δ is the slope of the saturation vapor pressure curve at temperature T_a in kPa $^oC^{-1}$, (eq. 3.2), (R_n - Q_t) is the net radiation minus the change in energy storage in MJ m^{-2} t^{-1}, and E_a is a bulk aerodynamic expression in MJ m^{-2} t^{-1} containing an empirical wind function.

$$E_a = 6.43 \left(a_w + b_w u_z\right)\left(e_z^o - e_z\right) \tag{6.22}$$

where a_w and b_w are empirical wind function coefficients and u_z is wind speed at the z height, m s^{-1}. Variable e_z^o is the saturation vapor pressure and e_z is the actual vapor pressure at height z. The value 6.43 is for λE in MJ m^{-2} d^{-1}. For λE in MJ m^{-2} h^{-1}, the factor becomes 0.268. Various values for the empirical coefficients a_w and b_w have been proposed (Penman 1948; Cuenca and Nicholson 1982). Penman (1948) initially proposed a_w = 1.0, but later revised it to 0.5 for open water (Penman, 1956b, 1963), and b_w = 0.54 s m^{-1} for open water for z = 2 m and for e_z^o computed using mean daily air temperature.

An equation similar to eq. 6.21 results from application of the PM equation (introduced as eq. 8.2 in chapter 8 on Evapotranspiration from Land Surfaces: Reference Crop Methods) to water, where bulk surface resistance, r_s, in the PM equation is set equal to 0. Generally the z_{oh} roughness length parameter in the PM equation is similar in value to z_{om} or even exceeding the value for z_{om} when applied to water (Brutsaert 1982)

An important consideration in the use of combination equations (and others as well) is that the use of weather data collected over a typical weather station on land cannot be expected to give as reliable values as computations using data collected over the water surface. For one, the wind at a height z over aerodynamically smooth water may be significantly greater than wind at height z over a typical weather station site. Temperature and humidity may also be quite different over the two sites. Further discussion of effects of surfaces on weather data is included in chapter 11 on Evapotranspiration from Land Surfaces-Direct Penman-Monteith. That chapter includes suggestions for adjusting non-characteristic humidity, temperature and wind data according to the evaporating surface. Eq. 11.60 can be used to translate wind data measured over land to corresponding wind data representing conditions over water.

An important impediment to the use of combination equations is the estimation of Q_t that has been shown fig. 6.10-6.12 and 6.15 to be a potentially large component in the calculation of available energy in the combination equation (i.e., $R_n - G$). The estimation of Q_t can have large

uncertainties and should not be ignored in calculation of evaporation. This requirement has been ignored in a large number of previous evaporation studies and applications.

Simulation Studies

For many complex studies such as determining the impacts of potential climate change or variability on lake evaporation, it is necessary to combine the energy balance and mass transfer procedures (Croley 1989; Hostetler and Bartlein 1990). In this type of approach, the mass or bulk transfer equations are substituted for λE and H in the energy balance and solved for the water temperature T_s and the resulting energy stored in the lake, Q_t. The evaporation is determined using the computed T_s in the bulk transfer equation. Depending upon the accuracy desired and the overlying assumptions, many simplifications may be employed in the procedure. This type of technique has been applied in many water resource and climate-change studies (Henderson-Sellers 1986; Henderson-Sellers and Davis 1989).

Because of the complexity in accounting for changes in energy storage when there is significant inflow and outflow to the water body such as reservoirs within river systems, computer models for calculating the reservoir thermal structure may be used. One such model, CE-THERM, was developed by the U.S. Corps of Engineers (USACE 1995). Use of the CE-THERM model to evaluate the effects of large flow releases in 1995 on the physiological rates of organisms in the Blue Mesa Reservoir located in southwest Colorado was described by Johnson et al. (2004). The model was calibrated based on several daily time steps by adjusting radiation and mixing parameters during the calibration period. Turbidity, or Sechi[1] depths, and temperature profiles were measured biweekly during the 24-May to 16-Sep period in 1994. Temperature measurements at three stations showed only minor differences in the surface layer of the stratified water body in 1995. Temperature profile measurements in front of the dam and at a mid-lake location in 1995 were nearly indistinguishable. Data from 1987 were used to estimate total dissolved solids (TDS). Meteorological data from the Gunnison Airport, about 25 km upstream were used. Based on daily wind speed measurements at the airport and reservoir in 1996, wind speeds were increased by a factor of 1.7 to account for local topographic conditions.

6.3 Example Applications of Evaporation Estimation Methods and Measurements

Evaporation from a Shallow Lake

Using daily climate data for 1996, estimates of May-October evaporation from Home Lake near Alamosa, Colorado were made using the PM equation[2]. During that time, the depth of Home Lake varied from 0.3 to 3 m and averaged about 1.5 m. Twice daily temperature measurements were made at the 0.05-m, 0.3-m and 0.6-m depths at about 0800 and 1630 hours. The near-surface temperatures increased by 4 to 8ºC during the 8-hour daytime period because much of the solar radiation was absorbed near the surface. Some solar radiation likely penetrated to the bottom of the shallow lake. As surface water cooled at night due to evaporation and

[1] A Secci disk is a disk, divided into black and white quarters, used to gauge water clarity by measuring the depth at which it is no longer visible from the surface.

[2] Jensen, M.E. 2006. Personal communication. Based on data from L. Salazar as summarized in a memo from Jensen to Salazar, 21-Jan-99.

positive net outgoing long-wave radiation, the heavier cold water settled (Carpenter 1898), thereby mixing the water in the lake. Using a regression of the 0.3-m depth temperature and air temperature, the estimated daily average temperature at 0.3 m plus 3°C was used to represent daily average surface temperature and to estimate the change in daily energy storage. The lake surface was frozen by Oct. 29.

The estimated albedo varied from 0.06 to 0.08. Net long wave radiation was estimated using estimated surface water temperature and Brutsaert's eq. 6.18 (Brutsaert 1982). The variation in estimated daily energy storage change is shown in fig. 6.13 and was used to estimate (R_n - Q_t). These values for Q_t are substantially smaller than those shown in fig. 6.10 because of the shallowness of Home Lake and relatively rapid transfer of stored energy to the surface caused by thermally-induced mixing. The resulting estimated average monthly evaporation is shown in fig. 6.14. The estimated total evaporation from May through October 1996 was 890 mm (35 in.), essentially the same as in NWS-33 (Farnsworth et al. 1982). Estimated evaporation using FAO-56 ET_o x 1.05 for shallow water systems was about 5% lower than estimates based on the PM equation with specific (R_n - Q_t) for April-October with the majority of underestimation occurring during July-September.

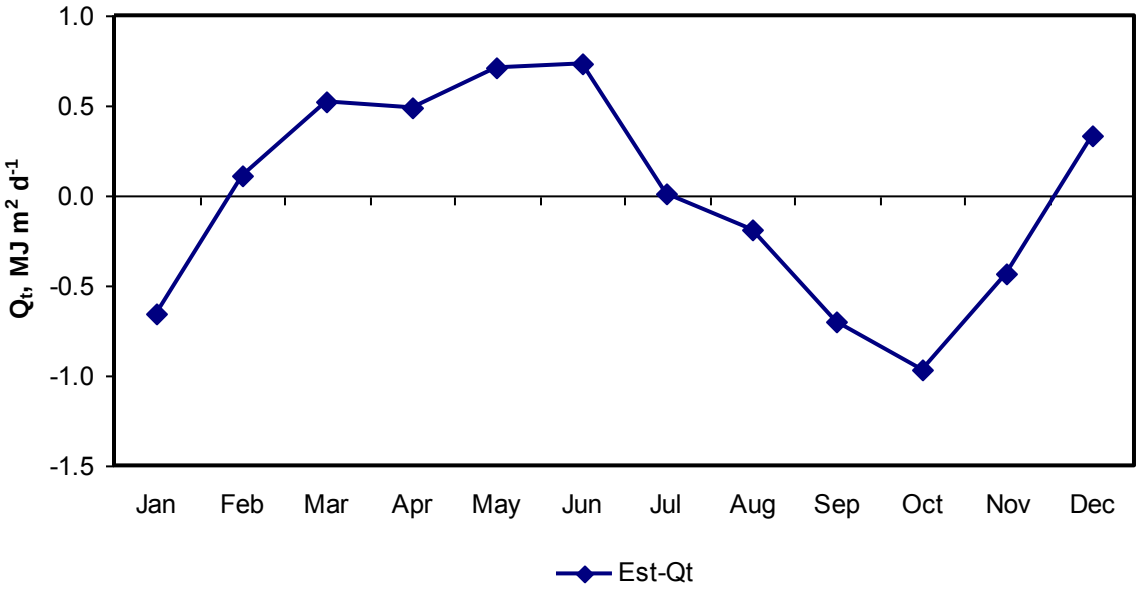

Fig. 6.13. Estimated energy storage rate for Home Lake assuming an average depth of 1.5 m. Source: Data from Jensen (2006), pers. Comm..

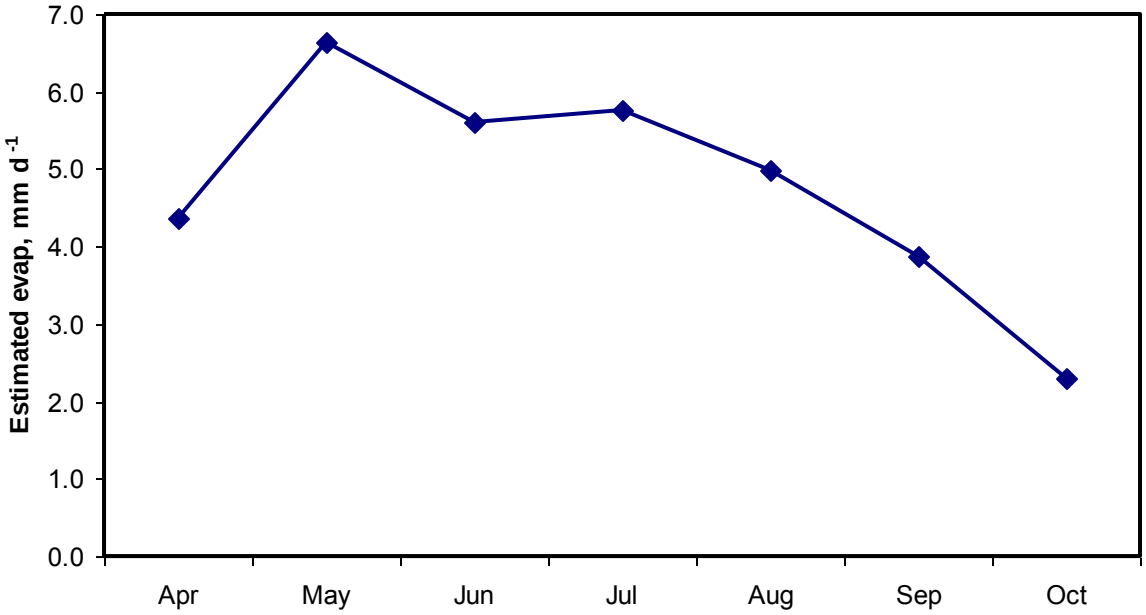

Fig. 6.14. Estimated evaporation from Home Lake near Alamosa, Colorado in 1996. Source: Data from Jensen (2006), pers. Comm.

Evaporation from shallow water bodies can be approximated by multiplying reference ET_o for short grass by a coefficient of 1.05 (Allen et al. 1998). Monthly multiplication coefficients based on ET_o from the PM equation increased linearly from 1.1 in May to 1.15 in October for the high elevation shallow lake example presented earlier in this chapter. For this example, the total May-Oct evaporation values by different methods were similar, indicating that any or a combination of methods would have provided reasonable values:

Estimating method	PM	Penman	NWS-33	ET_o x 1.05
Estimated evaporation, mm	894	906	889	852
Estimate, percentage of PM	100	101	99	95

Evaporation from Deep Lakes

A recent study estimated evaporation from Walker Lake, a relatively deep (23 m) terminal lake in western Nevada, using a Bowen ratio energy balance approach (Allander et al. 2009). Results of this study highlight the large amount of energy storage that can occur in deep water bodies. Fig. 6.15 summarizes the monthly average estimated energy storage (Q_t) and measured net radiation (R_n) from 2005 and 2006, where it is evident that 25 to over 40 percent of R_n was stored as energy during the spring and summer months due to penetrating solar radiation beneath the water surface. Fig. 6.16 shows the Bowen ratio energy balance-determined mean monthly lake evaporation by Allander et al. (2009), compared with the standardized ET_o computed using weather variables measured at the Bowen ratio station which was located on a floating platform at the center of Walker Lake. The effect of lake energy storage is evident in causing lake evaporation from the relatively deep lake to be significantly lower than the ASCE standardized grass reference ET (ET_o) during spring and early summer, and higher than the ET_o in fall and winter. The mean monthly ratio of E to ET_o varied from less than 0.5 in the spring to over 2.5 in

the late fall due to the impact of energy storage in reducing the available energy in spring and summer when Q_t was positive, and increasing available energy in the fall and winter when Q_t was negative (Huntington and Allen, 2010).

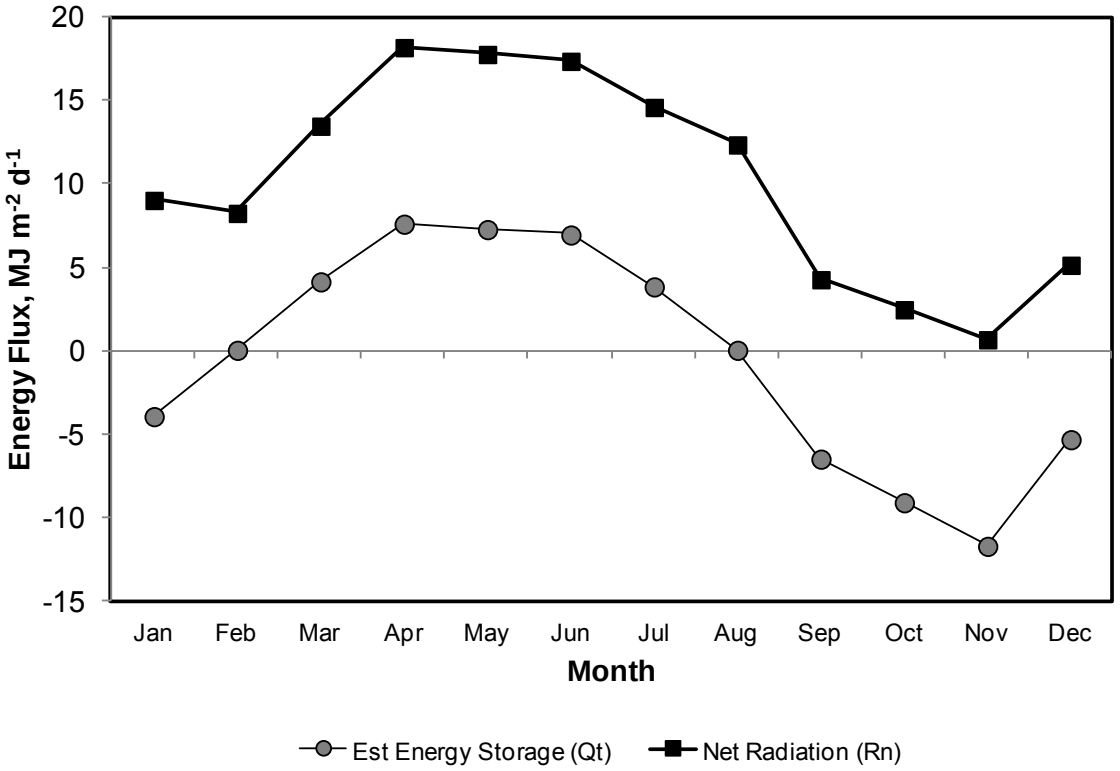

Fig. 6.15. Average monthly measured net radiation (R_n) and estimated energy storage (Q_t) for Walker Lake, Nevada during 2005 and 2006. Source: Data from Allander et al. (2009).

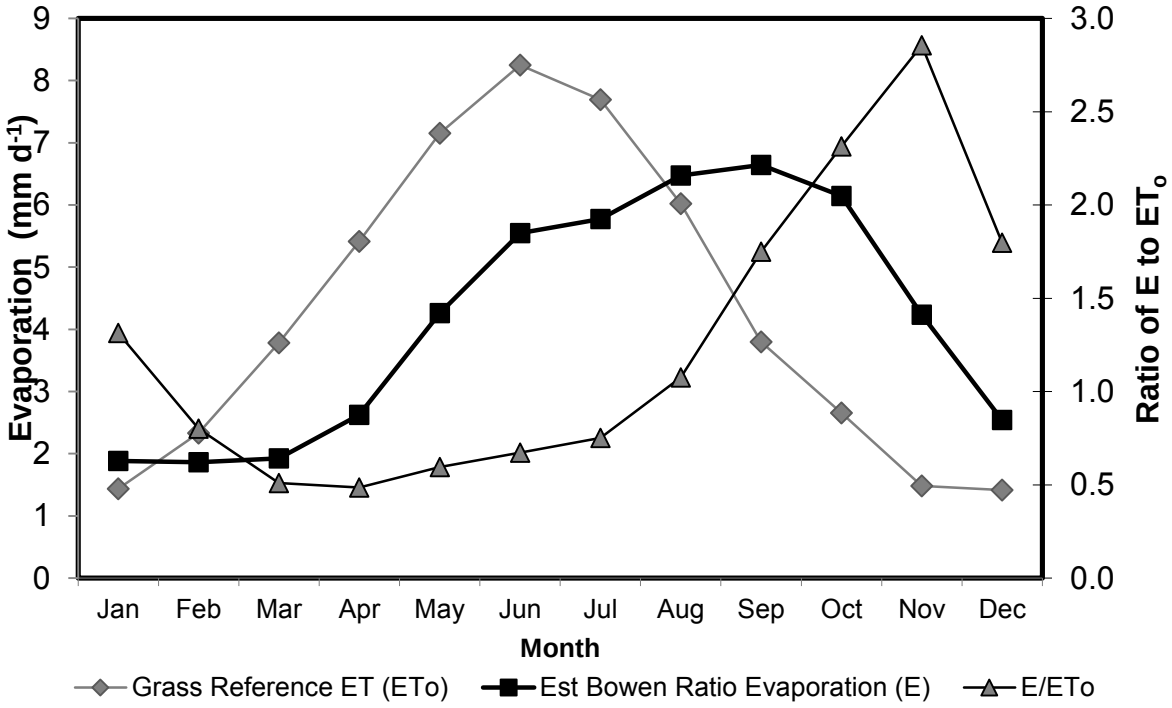

Fig. 6.16. Average monthly ET_o, estimated Bowen ratio energy balance evaporation (E), and the ratio of E to ET_o for Walker Lake, Nevada during 2005 and 2006. Source: Data from Allander et al. (2009) and Huntington and Allen (2010).

Trask (2007) recently applied three Dalton mass transfer formulations using measured air temperature, lake surface temperature, and regional atmospheric Mesoscale Model (MM5) simulated monthly dewpoint temperature and windspeed to estimate monthly evaporation from Lake Tahoe, California and Nevada over the period of 1968-2000. The three methods applied included the Harbeck, Ryan, and Adams methods (Harbeck, 1962; Ryan et al. 1974; Adams et al. 1990). Results indicate that energy storage in Lake Tahoe, which occurs primarily from penetrating solar radiation, significantly impacts the timing of evaporation such that the peak evaporation occurs during August through November (fig. 6.17), unlike pan evaporation measurements made in Tahoe City, which report peak rates occurring from June through August. Lake Tahoe is known for its clarity (ranging from 20 – 30 m) and its depth (maximum of 500 m). Even though Lake Tahoe is significantly deeper than Walker Lake, seasonal evaporation results for Lake Tahoe are similar to Walker Lake due thermal stratification that occurs in Lake Tahoe, where a strong thermocline has been documented to develop in June, and ranges from 21 m to 32 m deep from August to October, respectively (Coats et al. 2006).

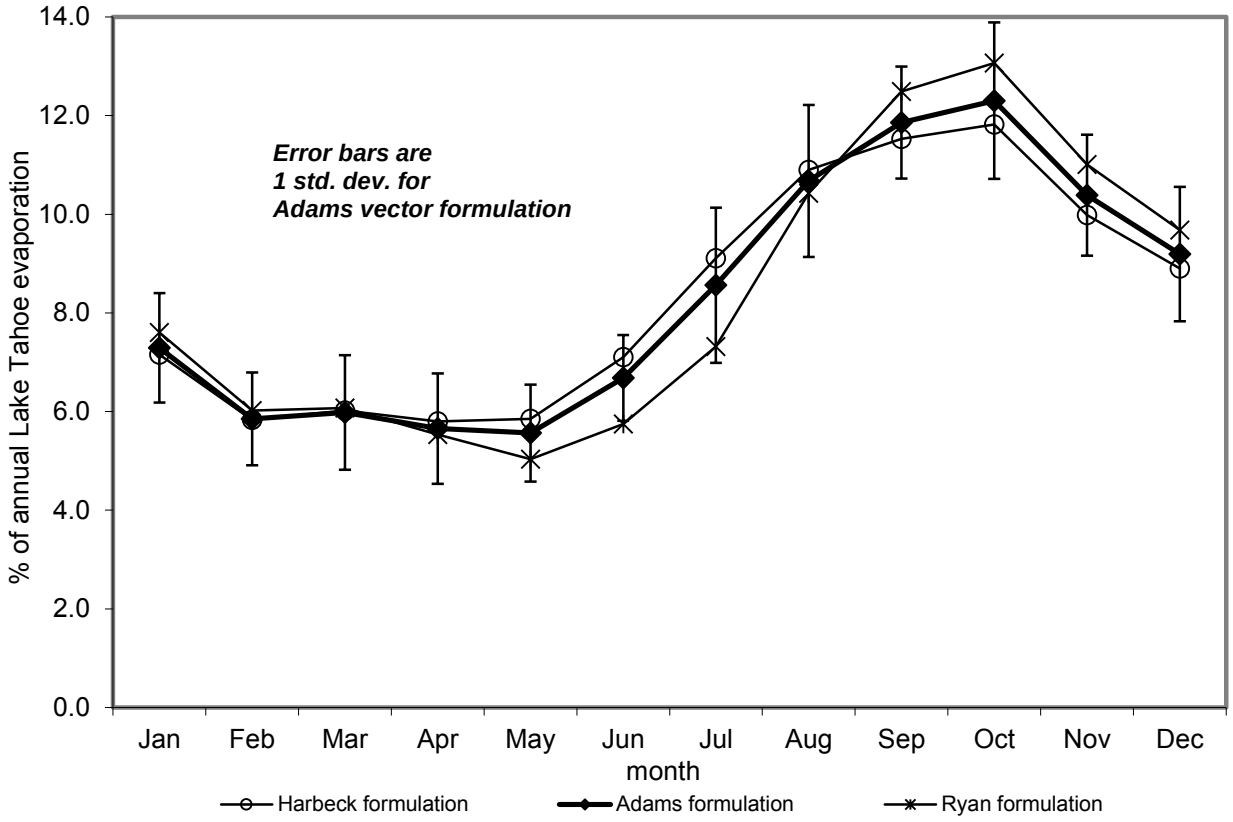

Fig. 6.17. Percent of average monthly annual evaporation from Lake Tahoe of 0.9 m, 0.97 m, and 1.24 m per year computed using three Dalton mass transfer formulations of Harbeck, Adams, and Ryan, respectively. See Trask (2007) for details on mass transfer applications and uncertainty estimates for Lake Tahoe. Source: Data from Trask (2007).

Evaporation from a River-Reservoir System

There are four sub-reaches of the Colorado River from Hoover Dam to Moreles Dam at the U.S.-Mexico border. The first is from Hoover Dam to Davis Dam, the second from Davis Dam to Parker Dam, the third from Parker Dam to Imperial Dam, and the fourth from Imperial Dam to Morelos Dam. Because of the immense size of Lake Mead, water is released from Hoover Dam at a nearly constant temperature of about 12-15°C. The average rates of flow vary greatly during the year from about 180 $m^3 s^{-1}$ in January and February to about 470 $m^3 s^{-1}$ in May. Water is exported to Arizona and Los Angeles from above Parker Dam and to the Imperial Valley from above Imperial Dam.

There are two reservoirs in this section of the river, Mohave Reservoir above Davis Dam and Lake Havasu above Parker Dam. Below Davis Dam the water temperature varies from about 11°C in January to about 19°C in July and August. Below Parker Dam the water temperature varies from about 11°C in December-January to about 25°C in August. Above Morelos Dam, the water temperature varies from about 13°C in December to about 31°C in August. The increases in water temperature in each sub-reach represent the net radiation absorbed by water surfaces and

is energy that is not immediately available for evaporation. The increase in water temperature leaving a sub-reach compared to inflow temperature represents the advection of energy out of each sub-reach.

In addition to estimating surface water temperature in a reservoir from limnology data, advected energy must be considered. The resulting estimated average depth of evaporation (calculated using several automated weather stations along the river and the PM equation) increased from the Davis-Parker sub-reach to the Imperial-Morelos sub-reach as shown in fig. 6.18. The average annual evaporation for 1999-2001 was estimated to be 1640, 1750 and 1920 mm (64.4, 69.0 and 75.4 inches) for the Davis-Parker, Parker-Imperial and Imperial-Morelos sub-reaches, respectively. Limited weather data were available for the Hoover-Davis sub-reach. Limnology studies show that a thermal profile exists in the reservoirs for much of the summer season even with the relatively large river flows. Mixing during the summer appears to occur only near the entry points to the reservoirs, as the cold higher density water inflows appear to plunge below the thermal layer. Complete mixing within the reservoirs does not occur until October-November. The changes in thermal profiles represent a significant component of the total change in energy storage in addition to very large changes due to horizontal advection because of the large flows. Therefore the value for Q_v for the reservoirs is negative.

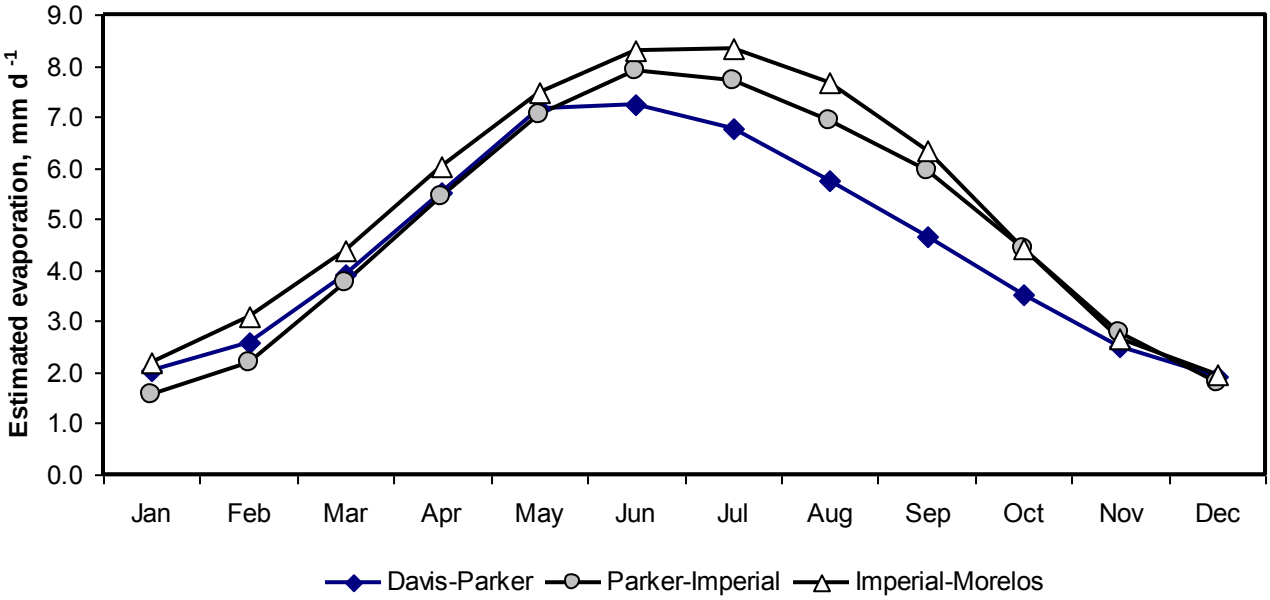

Fig. 6.18. Estimated evaporation from river and water surfaces of the Colorado River from Davis Dam to Morelos Dam for the period 1999-2001. Source: Data from Jensen (2003).

Evaporation from a Reservoir

$$Q_w = \rho_w C_w \frac{E}{1000}(T_s - T_b) \tag{6.18}$$

Estimates of evaporation from a reservoir or lake where advection of energy is relatively small require estimates of surface water temperature, the rate of energy flow into the body of water in the form of solar radiation, and the water temperature increase as illustrated in fig. 6.8 and 6.9. In an example application to Lake Berryessa Reservoir by Jensen et al. (2005), the change in daily energy storage was estimated using a slight modification of eq. 6.14a and 6.14b calibrated by measured changes in energy storage between several temperature profile determinations to a depth of 25 m and changes recorded by thermographs located near the dam with sensors at several depths. The equations for Q_t were $Q_t = 0.55\ R_{sn} - 1.20\ R_{nL}$ for day of year < 180 and $Q_t = 0.50\ R_{sn} - 1.50\ R_{nL}$ for day of year ≥ 180. These relationships differ somewhat from eq. 6.14a,b and are specific to Lake Berryessa. The reservoir surface area is 8,320 ha when full at an elevation of 137 m and 4,060 ha at an elevation of 110 m. Surface water temperature was estimated using measurements by a thermograph sensor at the 0.15-m depth. Those measurements were lower than skin temperature during daytime and higher during night. However, 24-hour averages were probably within 1°C. Surface temperature was used only to estimate R_{nl}. Inflow to the reservoir occurs during the November-February rainy period. Water release temperature at the dam was essentially constant at about 9°C all year resulting in a small advection of energy during the summer months (Jensen et al. 2005).

Estimated annual depth of evaporation in mm using the PM, Priestley-Taylor and Penman equations are compared below with estimates by reservoir operations using an evaporation pan and pan coefficients developed shortly after the reservoir was completed. The PM estimates were reduced by 5% because of the uncertainty associated with humidity and wind speed measurements made over land at a site adjacent to the reservoir and some shading of the water surface in several narrow segments of the reservoir. The results indicated that estimates based on pan evaporation data from an improper pan site and original pan coefficients were about 72% of those of PM. The same energy storage estimates were used for PM, P-T, and Penman equations.

Period	PM, mm	P-T, mm	Penman, mm	Pan evap × pan coeff, mm
Avg, 2003-20005	1,326	1,278	1,424	955

The main reason for the lower pan × coefficient-based estimates was from the use of pan evaporation measured by reservoir operators at a site in an area that was shaded part of the day by topography as well as surrounded by equipment and trees that obstructed wind movement. The measured pan evaporation was much lower than pan evaporation measured in a similar Class A pan located in an open area downwind from the reservoir. This outcome emphasizes the importance of evaporation pan location on providing consistent and standardized measurements. Penman equation estimates were higher than those of the PM mainly because the wind speed coefficient is the same as Penman (1956) derived for a rougher grass surface and not for a water surface.

Pan evaporation at the original pan site was about 70% of that at the new pan site downwind from the reservoir. Using pan evaporation at the new site and the recommended monthly pan coefficients for this site the average 2003-2005 estimated annual evaporation for the reservoir was 1,420 mm. The new recommended monthly pan coefficients were based on PM estimates of evaporation.

American Falls Reservoir, Idaho. The close coupling of surface temperature of many water bodies to the atmosphere provides the possibility for applying the direct aerodynamic method (eq. 6.7) using only measured air temperature. Fig. 6.19 shows fifteen-minute averages of water surface temperature and corresponding air temperature at 3 m for American Falls Reservoir during 2004. The two temperatures were closely coupled with regard to time and magnitude during the late May – early June period shown in the top of the figure when the water body was warming. Air temperature lagged T_s in both time and magnitude in early November when the water body was cooling. The close coupling is primarily caused by the strong relationship between outgoing and incoming thermal radiation terms. These two long-wave radiation components have magnitudes of 300 to 450 W m^{-2} (25 to 40 MJ m^{-2} d^{-1}) as compared to λE and H that averaged only about 20 to 100 W m^{-2} (2 to 10 MJ m^{-2} d^{-1}) over 24-h periods. Hence, the water surface and atmosphere become closely coupled via radiation exchange.

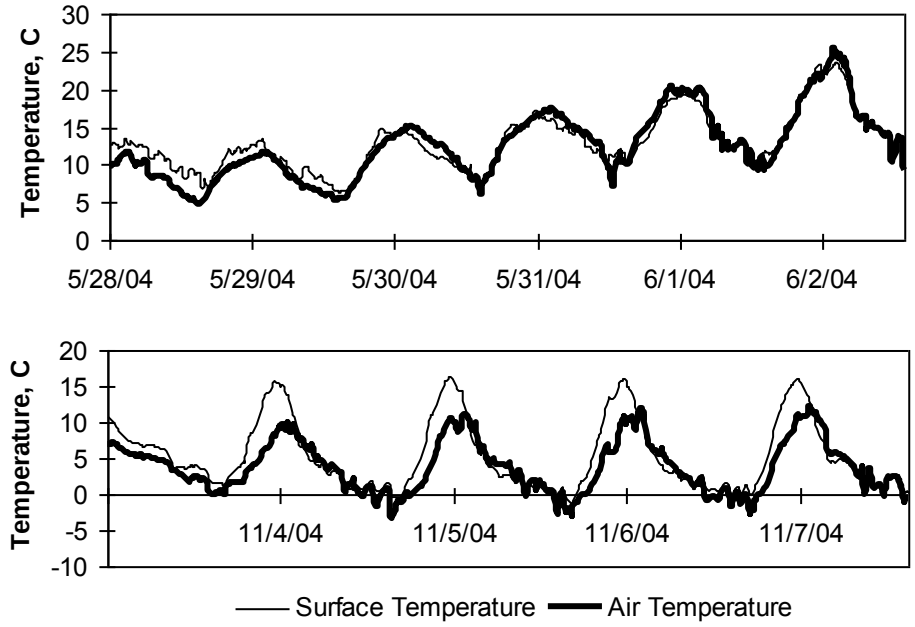

Fig. 6.19. Fifteen minute water surface temperature of American Falls Reservoir measured by infrared thermometer and air temperature at 3m during two periods in 2004. Source: Data from Allen and Tasumi (2005).

Fig. 6.20 shows daily mean surface and air temperature on the same water body. The close coupling permitted the estimation of daily mean T_s from T for application of the direct aerodynamic method (eq. 6.7) on a daily time step, where saturation specific humidity at the surface q_s, was estimated using estimated T_s, and specific humidity of the air at 3 m, q_z, was calculated from measured actual vapor pressure. The value for q_z was approximately $q_z = (RH/100)\ (q_s)$. The value for T_s was approximated as $T_s = T - b_t$ where b_t was an offset varied by month. Values for b_t varied from 0°C during spring and summer to 4°C during winter. A

value for $C_E = 0.0015$, equivalent to $z_{ov} \sim z_{om} = 0.00005$ m, was found to best fit evaporation measured by a combination of eddy covariance and Bowen ratio methods. Average monthly estimates for E are shown in fig. 6.21 where they are compared against the eddy covariance – Bowen ratio-based estimates described in an earlier section. Also shown in the figure is mean monthly reference evapotranspiration for the

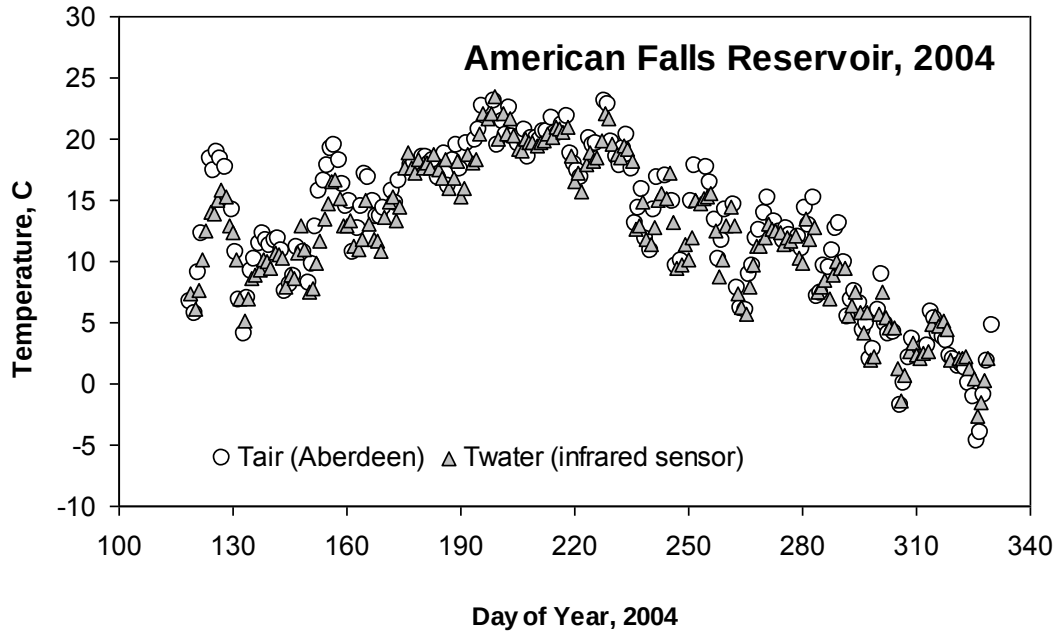

Fig. 6.20. Daily average water surface temperature of American Falls Reservoir measured by infrared thermometer and mean daily air temperature at 3m during 2004. Source: Data from Allen and Tasumi (2005).

standardized alfalfa reference method. The estimated evaporation from the approximately 9 m deep reservoir was substantially less than the alfalfa reference due to the large positive value for Q_t. The river temperature entering American Falls Reservoir (not measured) is relatively cold, especially during spring and early summer due to mountain snowmelt. The reservoir outflow is remarkably similar to surface temp and air temp all season long.

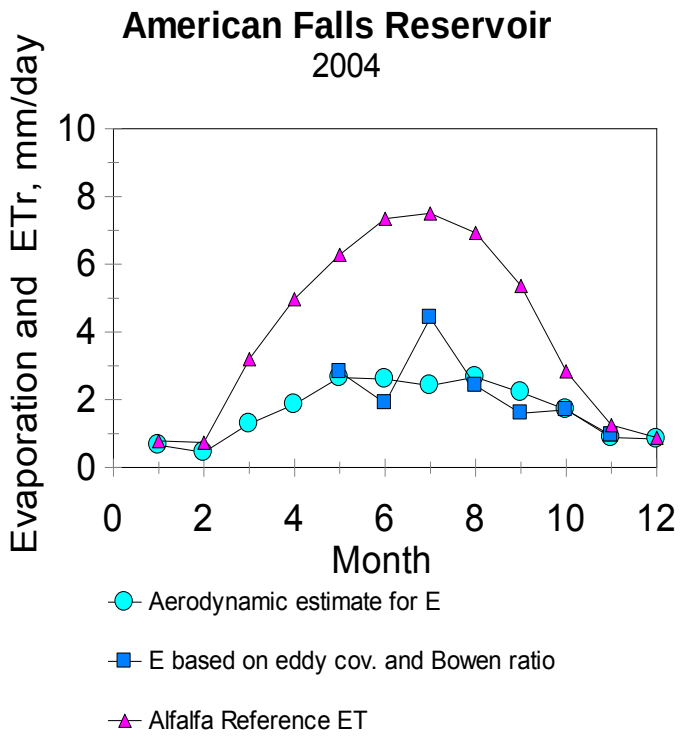

Fig. 6.21. Estimated monthly evaporation from American Falls Reservoir using the direct aerodynamic method (eq. 6.7) and an eddy covariance - Bowen ratio combination method by Allen and Tasumi (2005). Also plotted is alfalfa reference ET_r.

6.4 Summary—Methods for Estimating Evaporation from Water Bodies

Evaporation is rarely measured directly, even for small water bodies. It is usually estimated by association with measured evaporation from evaporation pans or calculated by water balance, energy balance, mass transfer or a combination of energy balance and aerodynamic techniques. The method selected depends on the depth of the water body and the availability of weather data or micrometeorological equipment.

Small Water Bodies

For small water bodies such as shallow lakes, the most widely used method is to multiply monthly coefficients by measured pan evaporation. The most commonly used pan in the USA is the Weather Service Class A pan. The accuracy of this method is related to the environment surrounding the pan as illustrated in fig. 6.2 and the pan coefficient. Monthly pan coefficients can be obtained from Map 4 for May-October in Farnsworth et al. (1982) or estimated using procedures outlined by Kohler et al. (1955). However, estimates based on Class A pan can be uncertain and biased. Evaporation estimates for some states may be available such as that by Borelli et al. (1998) for Texas. Local or regional calibration or verification of the coefficients used is recommended, and caution is needed to account for poor pan siting.

Evaporation from a shallow water body can be estimated using a combination method following procedures similar to those described for a shallow lake or the Penman equation

(Penman 1956, 1963) with wind speed coefficients of $a_w = 0.5$ and $b_w = 0.54$ for wind speed in m s^{-1} measured at about 2 m above the water surface and saturation vapor pressure based on mean air temperature. Attention must be given to the estimation of energy storage, Q_t, although heat storage is relatively smaller for shallow water bodies than for deep bodies.

Consideration should be given to employment of aerodynamic (mass transfer) methods, especially in situations where relationships between land-based air temperature and water surface temperature can be established.

Large Water Bodies

For water bodies greater than 2-3 m in depth, the increase in energy storage early in the season and release later in the season must be considered. If pan evaporation methodology is used, pan coefficients at latitudes of about 35° N can be expected to vary similarly to those for Lake Elsinore as shown in fig. 6.1. A check of estimated average rate of energy storage can be conducted using periodic temperature profile measurements made from the surface to bottom of the lake or reservoir or at least to a depth of about 30 m for relatively clear water. Several profile measurements, beginning when daily solar radiation begins to increase or when ice on frozen water bodies has melted, should be made at 2-3 week intervals near the center of the lake or reservoir to calculate the average daily change in energy storage. Commercial equipment can be obtained by simultaneously measuring depth and temperature. More measurements should be made at shallow depths where more rapid temperature change occurs. Profile measurements can cease when complete mixing occurs late in the season. Approximate average changes in heat storage can be made using eq. 6.17a and eq. 6.17b.

Other techniques such as a combination of eddy covariance and Bowen ratio methodology can be used to periodically measure changes in energy storage as illustrated in fig. 6.12 (Allen and Tasumi (2005). Periodic measurements of the rate of change in energy storage during the year can be used to estimate the average rates for a given lake or reservoir.

In some cases where inflow and outflow components can be measured and net advection is small, water budget procedures can be used to estimate mean monthly evaporation (eq. 6.2). For large water bodies, mass transfer procedures can be used (eq. 6.7 and 6.9). This usually requires measurement of wind speed and air humidity over the water as well as surface water temperature. Mean air temperature may act as a surrogate for surface water temperature.

For instream reservoirs, net advected energy must be considered when using an energy budget or combination method to estimate evaporation (eq. 6.21). Energy advected by evaporating water (eq. 6.18 and 6.19) is usually small and may generally be neglected. The net energy advected can be large if inflows to a reservoir are warm and the outflow temperatures are low which is common because release locations through the dam are usually near the bottom of the reservoir. The temperature of reservoir overflows or spills may be at the average water temperature near the surface.

7

Evapotranspiration from Land Surfaces: Water and Energy Balance Components for Measurement and Estimation

7.1 Introduction to Chapters 7 – 11.

Chapters 7 - 11 describe estimation and measurement methods that have been developed for vegetation and soil surfaces that are relatively uniform and, in the case of vegetation, have an adequate supply of soil-water. Extensions are made to natural vegetation and to vegetation that may be short of water. The methods are summarized and extended from FAO-24 (Doorenbos and Pruitt 1977), FAO-56 (Allen et al. 1998), the ASCE Hydrology Handbook (Wootton et al. 1996), the ASCE-EWRI report on standardization of reference ET calculation (ASCE-EWRI 2005) and from ASCE Manual 70 (Jensen et al. 1990). These chapters describe procedures for measuring ET and methods for estimating ET using aerodynamic and energy balance procedures, the combination equation, and association or inference methods. The combination equation is presented in chapters 8 and 11 and is applied both directly and as part of the reference ET-crop coefficient approach.

When estimating ET in areas where precipitation is greater than the potential ET rate for vegetative cover (ET_c), or where full irrigation is practiced, ET can be estimated using the reference ET concept and crop coefficients, or by direct application of the Penman-Monteith (PM) or some other resistance-based method using "well-watered" surface resistances (r_s). However, when precipitation is less than ET_c for extended time periods, actual evapotranspiration (ET_a) will usually fall below the potential ET for the particular surface and ET_c becomes more difficult to estimate accurately.

Incorporating soil water balance is usually required to estimate ET when precipitation and irrigation are less than ET_c. Two methods are discussed in chapters 8 and 11 that can be used to reduce the ET estimate according to available soil water. One method applies the $K_c \times ET_{ref}$ or crop coefficient approach. The other applies the direct application of the PM method or a combined set of energy balance and aerodynamic equations.

Other approaches to estimating ET from land surfaces during water shortage include making direct measurements of ET. This chapter describes various ET measurement approaches. The challenge with these approaches is in extrapolating point or localized measurements to large spatial scales and in extrapolating measurements to other time periods. ET measurement can be difficult and time consuming and is therefore generally used to develop and calibrate weather-based ET estimation methods that are then applied to larger scales and to different time periods. In addition to point measurements, methods employing energy balance based on satellite imagery can be applied successfully to estimate actual ET over large areas. This is a relatively new area of practice that is under substantial development.

7.2. Volumetric Measurements for Estimating ET

All ET estimating methods provide only estimates of the average actual ET from a field, watershed, or region under consideration. As might be expected, the larger and more diverse the area, the more uncertain the estimate.

Fortunately, the evaporation process is to a large extent controlled by solar radiation (or more directly, net radiation). Therefore, the variation of ET within areas of uniform vegetation and uniform access to water will be rather minor except for advective edge effects. Spatially uniform ET is normally the case for some time following extensive precipitation in an area having uniform vegetation or following irrigation of a farm field. Under limited water supply, as soil water becomes depleted in areas receiving less than the average water stored in a region, variability will increase. The uniformity of precipitation or water applied by irrigation is also a factor. The problem becomes difficult when the areas under consideration, e.g. watersheds or regions, involve a wide variety of vegetation species, vegetation heights, aerodynamic roughness, leaf development, rooting depth, soil type, and differing responses to soil water levels and weather conditions.

Soil Water Balance

The soil-plant-atmosphere (SPA) system was described in chapter 3. Soil water balance as applied to watersheds usually involves estimating water runoff where one of the components estimated independently is the ET. For small watersheds where inter-basin groundwater flow is highly restricted and runoff can be measured, ET can be determined from the hydrologic balance if watershed precipitation is known. In recent years this approach has been vital in developing water and salt balance data for large basins, especially in relation to irrigation projects. An example is the water balance evaluation of the large Imperial Valley in California (Oster et al. 1984; Allen et al. 2005c).

The basic soil water balance equation for a study volume (i.e., a defined area having depth z_s, thus constituting a volume) for a specific time period, Δt, can be written as:

$$\Delta\theta \; z_s = P - Q_r + I - ET_a - DP + GW \tag{7.1}$$

where, $\Delta\theta$ is the change in mean water content of the soil profile ($m^3\ m^{-3}$), z_s is the depth of the soil profile monitored (mm), P is total depth of precipitation plus any surface inflow from outside the study volume (mm), Q_r is the depth of surface runoff leaving the study area (mm), I is gross irrigation depth infiltrated over the area (mm), ET_a is actual evapotranspiration (mm), DP is the depth of percolation below depth z_s (mm), and GW is depth of ground water that has moved upward or a net depth that has entered horizontally into the profile (mm). Generally, the depth of soil profile of interest (z_s) is the plant root zone, which, by definition, is the upper portion of the soil where water extraction by plant roots occurs. In this case, *GW and DP* in eq. 7.1 are the sum of flux densities into and out of the bottom or sides of the root zone for the specific time period.

$\Delta\theta$ can be defined as:

$$\Delta\theta = -\frac{\int_0^{z_s} \theta_{1(z)}\, dz - \int_0^{z_s} \theta_{2(z)}\, dz}{z_s} \tag{7.2}$$

where $\theta_{1(z)}$ is volumetric water content at depth z ($m^3\ m^{-3}$) at time $t = 1$, $\theta_{2(z)}$ is volumetric water content at depth z ($m^3\ m^{-3}$) at time $t = 2$, z_s is the effective depth of the root zone (mm). Eq. 7.1 can be rearranged in terms of eq. 7.2 to estimate total soil water in the root zone or to greater depths, if of interest, as:

$$\int_0^{z_s} \theta_{2(z)}\, dz = \int_0^{z_s} \theta_{1(z)}\, dz + \Delta\theta\, z_s = \int_0^{z_s} \theta_{1(z)}\, dz + P - Q_r + I - ET_a - DP + GW \tag{7.3}$$

Reduction of ET_a below potential levels due to soil water deficiency is discussed later.

Generally, deep percolation flux density is estimated based on the field capacity (θ_{fc}) of the soil (also known as the drained upper limit). θ_{fc} represents the water content to which the soil will drain under a unit hydraulic gradient (gravity) 2 to 3 days after wetting. θ_{fc} represents the upper limit of the soil's ability to retain water after initial rapid drainage. Average values and ranges of θ_{fc} are given in table 3.6 for general soil texture classes along with values for the permanent wilting point (θ_{wp}) for the soil (also known as the lower limit of extractable water) and total retained water available for plant extraction (available water (AW)). Available water is calculated as $AW = \theta_{fc} - \theta_{wp}$. One item to note from the data in table 3.6 is that even though values for θ_{fc} and θ_{wp} vary widely with soil texture, values for available water vary less, especially for moderately coarse to fine textured soils. When possible, specific values for θ_{fc} and θ_{wp} should be determined from field studies (Ratliff et al. 1983).

When the calculation time step for eq. 7.3 is one day, DP is often assumed to occur if total θ of the root zone is greater than θ_{fc} on any day. In this case:

$$\begin{aligned} &If \int_0^{z_s} \theta_{2(z)}\, dz > \theta_{fc}\, z_s \\ &\quad then\ DP = \int_0^{z_s} \theta_{2(z)}\, dz - \theta_{fc}\, z_s \\ &\quad and\ \theta_{2(z)} = \theta_{fc}\ over\ 0\ to\ z_s \\ &\quad otherwise,\ DP = 0 \end{aligned} \tag{7.4}$$

One may wish to delay application of eq. 7.4 until 2 days after a major precipitation or irrigation event to account for some ET extracted from water above θ_{fc} during the first two days while the soil profile is draining to field capacity. In application of eq. 7.4 to layered soils having different water holding characteristics, the $\theta_{fc}\, z_s$ term can be replaced with an integral that integrates θ_{fc} over the 0 to z_s depth, where θ_{fc} may vary with z.

Generally, when solving the soil water balance equation for ET, one should sample θ to depths well below the root zone and attempt to schedule irrigation to avoid the occurrence of DP. If there is no change in soil water at lower depths between sampling dates, this does not assure that drainage is not occurring because drainage can be occurring under a unit hydraulic gradient

with no apparent change in soil water content. Generally, periods with little or no precipitation are selected for evaluation. Occasionally sharp changes in soil texture, such as a sand or gravel layer below the root zone, or the presence of bedrock, can reduce the rate of deep percolation and improve measurement accuracy.

One should avoid situations where saturated conditions (i.e., a water table) exist near the root zone. In the absence of a shallow water table ($GW = 0$) and with adequate sampling depth, a record of soil water change over a period of 7-10 days or more can yield reliable measurements of ET at the measurement site.

The careful use of a neutron moisture meter (also referred to as a neutron probe) can, in some cases, provide relatively accurate data. When calibrated with gravimetric sampling, it can provide data of adequate accuracy for ET studies or for irrigation scheduling programs. The difficulty with either of these procedures (neutron moisture meter and gravimetric sampling) is in estimating the water flux density (*DP* or *GW*) at the bottom of the measured profile. Often this difficulty limits the usefulness of applying the soil water balance equation to determine ET. Information on applying the neutron probe technique and relative error associated with the method is provided by Evett and Steiner (1995), Hignett and Evett (2002), and Evett et al. (2003, 2005). In addition, a suite of eight papers on accuracy of neutron probe operation and calibration is included in Allen and Neale (1993).

Usually soil water measurements are made at discrete depth increments, e.g., every 0.15 m. Total soil water in the profile can be estimated from discrete measurements as:

$$\int_0^{z_s} \theta_z \, dz \cong \sum_{i=1}^{n} d_i \, \theta_i \tag{7.5}$$

where θ_i is the volumetric soil water content representing layer i ($m^3\ m^{-3}$), d_i is the thickness of layer i (mm), and n is the total number of layers measured between 0 and z_s. Water content for the surface soil layer usually requires use of gravimetric or electronic measurement such as TDR due to problems of escaping neutrons from the surface when using the neutron probe method within 0.2 m or possibly 0.3 m of the surface (Evett and Steiner 1995). Using smaller depth increments for measurement within the top 0.15 to 0.20 m from the surface may provide more accurate estimation of total soil water content of the root zone due to the frequently rapidly changing θ_z with depth in that zone.

General practices to reduce the variability encountered with periodic soil water measurements for determining ET include:

1) Use a minimum time step of about 7 days for estimating ET with the soil water balance equation so that the magnitude of estimated ET is significantly greater than random errors associated with measurements of water content.
2) For gravimetric sampling, mark the site of the first samples taken after an irrigation or heavy rain and take the next set of samples within a 0.3 m radius so as to minimize variability caused by spatial differences in soil characteristics, root distribution and water infiltration.
3) It is essential to obtain soil samples or take sensor readings, and to install sensors or access tubes, without significantly altering the plant cover condition at the sampling site. ET from trampled plants can be drastically reduced as compared to ET by plants in a

pristine condition. Fig. 7.1 illustrates means to suspend the observer over vegetation while taking neutron probe readings to avoid any foot traffic within 1 m of the access tube. Besides damaging vegetation, foot traffic can alter density, aeration and infiltration characteristics of the surface soil, thereby affecting plant growth and ET.

4) Calculate ET for each set of measurements made for time periods spanning after an irrigation and prior to the next irrigation to screen for errors and to gain an understanding of measurement error and uncertainty.
5) Avoid periods following heavy rain, as deep percolation may continue to occur following the initial sampling date for the period. This can especially introduce error with shallow-rooted crops.

Example Gravimetric Data. Table 7.1 gives an example of results by Pruitt (1955) for a 6.5-day period when ET_a for a dense crop of ladino clover was estimated from a well-replicated (18 sites within a 0.2-ha plot) gravimetric soil sampling study. Even with near ideal soil and underlying conditions (sampling was from the surface to bedrock), the standard deviation (based on the 18 sampling sites) of estimated ET determined from each single measurement point was 13% of the mean ET determined by averaging depletions over all 18 sites over the 6.5 day period. In contrast, the standard error of the mean ET resulting from utilizing all 18 sites was only 3.1% of the mean ($13 / 18^{0.5} = 3.1\%$). This demonstrates the substantial value of multiple sample locations when estimating ET from soil water depletion measurements. The range in estimated ET between the high and low measurement sites was more than 50%. One might expect a lower standard deviation using a neutron probe at the same number of neutron access sites. However, at this particular site, the variation in the depth of this relatively shallow soil (0.99 -1.31 m), and the problem of interpreting both the uppermost and lowest-layer readings might have presented more of a problem with overall accuracy than that experienced in the gravimetric technique.

Other Soil Water Measurement Methods. Tensiometers, soil water electrical resistance blocks and heat dissipation electronic sensors can be valuable tools in computing a soil water balance. These devices measure matrix potential (or soil water tension) and, when soil water characteristic curves are available, can provide a means of following volumetric water content changes. In-depth discussion of some of these methods is provided by Campbell and Campbell (1982), Evett and Parkin (2005) and Evett et al. (2006). Bertuzzi et al. (1994) presented a detailed analysis of various sampling strategies for estimating ET.

Time domain reflectometry (TDR), time domain transmission (TDT) and capacitance-based sensors and probes are commonly used for measuring soil water content indirectly. Advantages of these electronic sensors are in-situ measurements with nearly continuous measurement. Disadvantages and challenges with capacitance-based sensors include the typically relatively small volumes of soil sampled (on the order of 1 cm extent from the sensor as compared to 10 cm for neutron probes) and the possibility of a need to calibrate sensors for soil type. The small volume of soil sampled makes the influence of air gaps around the sensor and lack of contact between sensor and soil problematic (Evett and Steiner 1995, Evett and Parkin (2005) and Evett et al. 2006).

Precipitation Measurement. Other biases in estimating ET from soil water balances stem from inaccuracies in measuring precipitation and irrigation additions or using data that are not representative for the sites. Precipitation gauges should be located within a few hundred meters

of the sampled area because precipitation can vary widely even over a few km distance. In addition to biases in spatial variation, precipitation amounts are often under-measured by gauges for both rain and snow amounts due to venturi effects, blow-out, splash-out and evaporation. Data should be corrected using wind functions such as those recommended by the World Meteorological Organization (Yang et al. 1998a). That publication recommends a correction to liquid precipitation catch by a standard US National Weather Service 8 inch (203 mm) gauge of:

$$P_{corrected} = P_{gauge}\left[exp\left(0.062\ u_g^{0.58}\right)\right] \tag{7.6}$$

where u_g is wind speed at gauge height, m s^{-1}, $P_{corrected}$ is the corrected precipitation and P_{gauge} is the original measurement, in the same units. The correction increases the estimated capture of P by 8% for wind speed of 2 m s^{-1} and by 13% when wind speed is 4 m s^{-1}. A stronger correction was recommended by Yang et al., (1998a) for snow. Yang et al., (1998b) and Yang et al., (1999) found needed corrections to U.S. National Weather Service (NWS) 203 mm standard gauges at 10 NWS climate stations in Alaska and to Hellmann gauge-measured precipitation at 12 stations in Greenland to range from 30 to 400 mm per year in Alaska and from 8 to 70 mm per year in Greenland for low rainfall areas. The German-style Hellmann gauge is similar to the NWS standard gauge. Of the biases, wind-induced undercatch was the source of greatest error, followed by gauge wetting loss and nonrecording of trace amounts of precipitation. Monthly correction factors differed by station and by type of precipitation (liquid vs. solid). The value for u_g in eq. 7.6 can be estimated from wind speed measured at a reference height above the surface using a logarithmic transformation, for example as given in eq. 6.5 or 11.60.

In addition to wind induced effects, all tipping bucket rain gauges can lose, on average, one-half tip equivalent of rain between wetting events through evaporation from the untipped bucket. Also, tipping gauges do not record precipitation received during part of the time interval in which the tip is occurring. This error is fairly insignificant except during high precipitation rates.

TABLE 7.1 An Example of a Gravimetric Soil Sampling Program to Determine ET. Washington State University Irrigation Experiment Station, Prosser, WA. Source: Data from Pruitt (1955).

Sampling Site	Sampling Depth, z_s (m)	June 4		June 10		Difference 6/4 - 6/10
		θ (%)	$\theta\ z_s$ (mm)	θ (%)	$\theta\, z_s$ (mm)	$\Delta\, \theta\, z_s$ (mm)
1	1.16	12.9	205	8.5	135	70
2	1.18	15.8	256	12.2	198	58
3	1.31	15.2	274	12.1	218	56
4	1.18	15.3	248	11.0	178	70
5	1.19	14.6	237	11.0	179	58
6	1.20	15.5	255	11.6	191	64
7	1.15	14.8	233	11.1	175	58
8	1.19	16.7	272	12.5	203	68
9	1.22	16.2	270	12.3	205	65
10	1.08	17.0	250	12.3	181	69
11	1.09	17.9	268	11.8	177	91
12	1.11	17.0	259	12.7	194	66
13	1.03	17.3	243	12.6	177	66
14	1.02	18.7	262	12.8	179	83
15	1.02	19.8	276	15.2	212	64
16	0.99	14.1	191	9.2	124	67
17	1.00	15.1	208	9.4	129	78
18	1.01	16.3	226	11.9	165	61
Avg.			246		179	67
				Std. Dev.		8.75
				100*(8.75)/67) =		13.0%

Typical problems associated with estimating ET by soil water sampling as well as advantages, disadvantages and requirements are summarized later in table 7.3.

Fig. 7.1.Taking a neutron-probe reading using a light, above-crop platform to avoid trampling of vegetation and compaction of soil near the access tube site. Photo from R.G. Allen (1992), personal communication.

7.3 Mass Balance Methods

Tanks and Lysimeters

Highly sensitive weighing or floating lysimeters are the best absolute method for accurately measuring water loss from soil and crop canopy surfaces. Therefore, the use of lysimeters has been very important in the development and testing of the more theoretical micro-meteorological methods for estimating ET. An example of a 2 m weighing lysimeter during installation is shown in fig. 7.2. The water evaporated even from very simple lysimeters may be accurately determined over 24-hour or longer periods. Weighing lysimeters have played an important role in providing accurate half-hourly or hourly ET data. Weighing lysimeter designs have included those by Ritchie and Burnett (1972), Wright (1982), Schneider and Howell (1991) and Allen and Fisher (1990). For detailed coverage of lysimeter types and designs, the following references are recommended reading: WMO (1966), Aboukhaled et al. (1982), Howell et al. (1985), Marek et al. (1988), Schneider and Howell (1991) and Allen et al. (1991a,b). The latter reference is the proceedings of an International Symposium on Lysimeters. It contains descriptions of many

lysimeter types in use around the world and results of research involving many of them, as well as cautionary information in lysimeter management and data interpretation.

Fig. 7.2.A 2 m weighing lysimeter system being installed near Kimberly, Idaho, USA. Photo courtesy of J.L. Wright (1990, USDA-ARS), personal communication.

Typical Problems

Advantages, disadvantages, problems and recommendations with lysimeters are summarized in table 7.3. Any lysimeter, no matter how precise a measuring system, provides a measure of ET from a very limited plant sample size. Therefore, one can only expect to obtain accurate estimates of actual field ET from lysimeters when plant density, height, and leaf area of vegetation inside the lysimeter are close to those of the surrounding field. When plant density or leaf area differs significantly, then even though the results may be valuable in plant physiology or other studies, the actual ET obtained will generally not represent actual field ET. Wind disturbance of mass readings can also produce significant errors for short time periods.

Differences between conditions inside the lysimeter and outside in the field (soil characteristics, water availability, fertility, soil temperature and rooting characteristics) can cause differences in crop growth, plant cover, leaf temperature and maturation, and thus produce differences in ET between the field and lysimeter. Differences in plant height in particular can produce erroneous data with the errors related significantly to the lysimeter area; the smaller the lysimeter size, the larger the possible error. Differences in maturation are typical in fairly shallow lysimeters unless irrigations are continued to near the season's end. An illustration of a well-managed weighing lysimeter system is shown in fig. 7.2 where vegetation inside the lysimeter has similar density and size as that immediately outside and no gaps in vegetation are visible at the lysimeter boundaries. One concern with the lysimeter management in fig. 7.2 is that the entire soil surface was wetted by irrigation inside the lysimeter, whereas only about 50% of the soil surface was wetted in the surrounding field. The increased surface wetting inside the lysimeter would cause the total ET measurement and estimation of evaporation from soil to be overstated, especially during periods of partial surface cover by vegetation.

Fig. 7.3. A sweet corn crop growing on a 2 m weighing lysimeter system near Kimberly, Idaho, USA. Photo courtesy of J.L. Wright (1999, USDA-ARS), personal communication.

Some of the very seriously-flawed lysimeter results have been produced by a so-called "bloom effect" where the area of exposed plant canopy has exceeded the assumed effective area of the lysimeter. Tanner (1967) provided an excellent discussion on lysimeters, and was probably one of the earliest to recognize how serious this problem can be. Coverage of this and other aspects of lysimetry was detailed by King et al. (1956), Pruitt and Lourence (1985), Meyer and Mateos (1990) and Allen et al. (1991b). Examples are frequent in the literature of reported crop or pan coefficients ranging from 1.3 to 1.8 or even higher. H.L. Penman's early comment may be a bit unrealistic (crop evaporation should never exceed evaporation from an open water surface); however any crop coefficient greater than 1.1 for use with the alfalfa reference ET or greater than 1.3 for use with the grass reference ET, should lead to a strong suspicion that the ET determinations (whether by lysimetry or meteorological techniques) are in error, or that they represent conditions other than continuous expanses of vegetative surfaces. This point is discussed further in chapter 10 on cover and crop coefficients.

Incorrect estimation of the effective evaporating area of a lysimeter is probably the most common error made in computing lysimeter ET. Equivalent, one-dimensional ET is computed from weighing lysimeters as the change in mass of the lysimeter divided by the evaporating area of lysimeter vegetation. Often, in practice, the dimension of the inside lysimeter tank is mistakenly used as the divisor, rather than using the true vegetative area, causing significant error. Because the area of net radiation absorption and aerodynamic exchange by lysimeter vegetation generally exceeds that of the inner lysimeter tank, measured ET will be overestimated if the inner tank area is used to represent the evaporative and vegetative area. This error seems subtle and insignificant at first glance. However, in reality, its effect can be quite significant.

For example, if a lysimeter is constructed with inside tank dimensions of 1 m square, and has an undesirable 10 cm gap between the inner tank and outer enclosure (including both inner and outer enclosure rims), the average vegetation and evaporating area should be approximated as having a dimension of 1.1 m x 1.1. This dimension is the average of the dimensions of the inner tank and of the outer enclosure, and is a reasonable approximation, assuming that vegetation from inside and outside the lysimeter reaches across the lysimeter rim and meet near the center. The ratio of effective vegetation area to inside area in this example is $1.1^2/1.0^2$ or 1.21. In other words, lysimeter measurements of ET will be overstated by 21 percent if the inner tank dimension is used to calculate the effective evaporating area. This type of bias in measuring ET is intolerable and greatly harms the compilation of representative and dependable ET measurement and associated crop coefficients. The effect is amplified if lysimeter vegetation is allowed to extend outside the lysimeter boundaries, replacing outside vegetation. The increased absorption of solar radiation and aerodynamic vapor exchange surface can be substantial. This problem frequently occurs when conditions immediately outside the lysimeter are impaired as described in the next paragraphs.

A serious problem with lysimeters relates to foot and farm machinery traffic in and around lysimeters as they are serviced. This can be especially serious with grain crops, alfalfa or other similar, closely-spaced tall crops. Similarly, compaction of soil surrounding lysimeters during construction or installation has disqualified (or should have disqualified) many lysimeter data sets due to subsequent stunted growth of crops outside of lysimeters and therefore opportunity for exhibition of the bloom effect and over-measurement of ET by the lysimeter systems.

Crop height differences inside and outside a lysimeter as produced by differing degrees of lodging, can be a problem. Again, the possible error in estimating actual field ET is greater with smaller lysimeters. Pruitt and Lourence (1985) provided an example which illustrates this problem, although in this case, with 29-m^2 lysimeters, errors of only 5 to 10% were noted for a barley crop in spite of extreme differences between lodging inside and outside the lysimeter. Another example of the impact of expanded lysimeter vegetative area described by Pruitt and Lourence (1985) and Allen et al. (1991b) was with beans grown on the 6.1-m diameter floating lysimeter at Davis, CA. In this case, the stand of beans inside and outside the lysimeter appeared, at first glance, to be uniform and of excellent quality (fig. 7.4a). However, upon inspection, it was discovered that a poor stand just to the north of the lysimeter's edge had resulted in excess bean vine growth from inside the lysimeter out into areas in the field as far as 0.9 m, taking up space where plants were sparse. When crowded back into the lysimeter and retained there by a short, wire fence (fig. 7.4b), average values of computed K_c dropped from 1.34 to 1.21 as shown in fig. 7.4. Even lower K_c's may have occurred if adequate plant material were in place in the partially bare areas outside the lysimeter.

A number of sensitive lysimeters capable of hourly determination of ET have been installed in forests (Fritschen et al. 1973; Reyenga et al. 1988; Dunin et al. 1985). In spite of the problems noted above, at least in some cases, the results with lysimeters about 10 m^2 in area have been shown to provide ET measurements for forest trees in good agreement with Bowen ratio ET determination (Dunin et al. 1985, 1991).

a)
b)

Fig. 7.4. Example of bean plant growth surrounding a lysimeter in the center of the picture (a) before a fence was installed to contain the plants within the lysimeter area and (b) closeup of a retaining fence surrounding the lysimeter to constrain inner vegetation. Source: Photo from Pruitt and Lourence (1985).

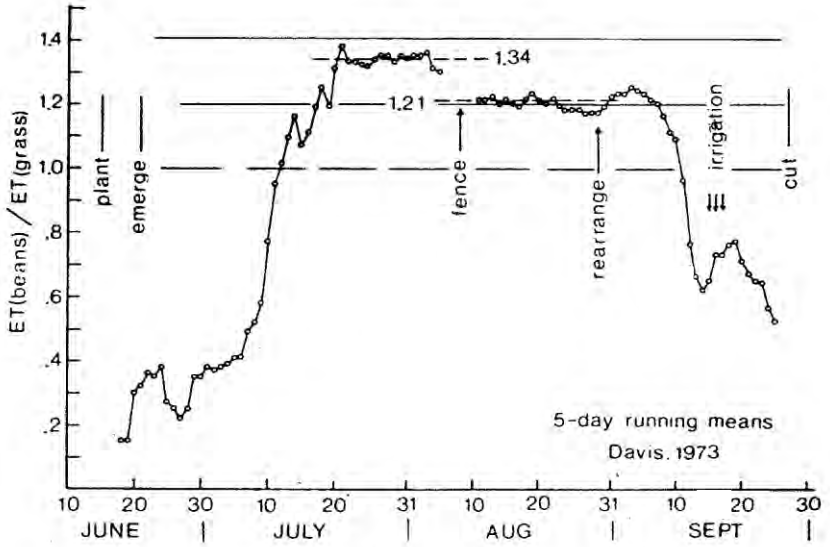

Fig. 7.5. Effect of constraining bean plant growth to the lysimeter area on measured ET before and after the fence was installed. Source: Figure reproduced with permission from Pruitt and Lourence (1985).

In general, weighing lysimeters are necessary to accurately determine ET. Nonweighing lysimeter types, where ET is determined by observing changes in the water table level are difficult to interpret, due to changes in soil water above the water table caused by water extraction by plant roots and changes in the capillary fringe above the water table with changing temperature (Hill and Allen 1991). Hydraulic weighing lysimeters have often been plagued by hysteresis of the hydraulic measurement systems and thermal problems (Kruse and Neale 1988), although such problems are likely insignificant for weekly or longer determinations.

With improvements in electronic load cells, low cost electronic weighing lysimeters which are suitable for daily measurements of ET have been developed for remote operation (McFarland et al. 1983; Kirkham et al. 1984; Allen and Fisher 1990). Some non-weighing lysimeters have been developed where the lysimeter acts merely as a hydraulic barrier to water movement into or out of the lysimeter and the change in soil water with time is measured by keeping records of all water added to the lysimeter (irrigation and precipitation), as well as any drainage or runoff. A few examples of the literally hundreds of such lysimeters around the world, are those described by Harrold and Dreibelbis (1958), Van Hylckama (1968), Niel and Zunino (1971), Sarraf and Bovée (1973), Boman (1991), and Evans et al. (1991).

Another difficulty with lysimeters is in applications with non-well-watered vegetation (e.g., in natural rainfall areas where precipitation is less than maximum ET for the vegetation). In these applications, differences in soil structure and soil profile (due to disruption during construction), fertility, salinity and thermal conditions inside lysimeters can make it difficult to control soil water conditions and consequently ET inside lysimeters to match conditions outside

the lysimeter. In most cases, undisturbed, natural monolith soil profiles are required in lysimeters in order to accurately measure natural ET in semiarid and arid regions (Armijo et al. 1972; Dugas et al. 1985; Marek et al. (1988); Schneider and Howell 1991). The latter two publications describe a useful tank 'pull-down' technique for obtaining an undisturbed, monolithic soil column inside the lysimeter.

Black et al. (1968) and Dugas and Bland (1991) cautioned against negative impacts of thermal conduction of heat along metal lysimeter container walls that significantly warms the lysimeter soil, especially over long time periods. This unnatural heat source can cause drying of the soil profile under bare soil conditions that exceeds that under natural conditions. It can also promote earlier and more extensive root growth and respiration within the lysimeter tank. Black et al. (1968) recommended insulation of the lysimeter soil tank.

In spite of all these important precautions and opportunities for error and bias, weighing lysimeters continue to be a valuable method for determining ET and crop coefficients (Wright 1982; Howell et al. 2004, 2006). Lysimeters provide the ability to inspect the vegetation and to test calibration of weighing mechanisms. The larger the surface area and the greater the depth, the more likely the attainment of a representative, one-dimensional ET sample.

7.4 Energy Balance Method – Bowen Ratio

The Bowen ratio energy balance (BREB) method rearranges the energy balance equation (eq. 4.1 and eq. 7.14 presented later) in order to cancel aerodynamic transport terms. This permits determination of λE by measuring air temperature and vapor pressure at two elevations above the surface in addition to R_n and G. Because the Bowen ratio β (Bowen 1926) represents the ratio of H to λE, the energy balance equation (for example eq. 7.14) can be rearranged to obtain the BREB equation for application to ET from vegetation:

$$\lambda E = \frac{R_n - G - S_{cb} - P_{syn}}{1 + \beta} \tag{7.7a}$$

where S_{cb} represents any change in energy storage in the canopy or boundary layer between the ground surface and height of the air temperature and vapor pressure measurement and P_{syn} is energy consumed by photosynthesis. S_{cb} and P_{syn} are generally assumed to be zero, but S_{cb} can be large in forests and during early morning when the boundary layer is warming and increasing. P_{syn} can consume a few percent of total energy for dense vegetation during daylight. The aerodynamic transport equations for λE were described in chapter 6 and equations for both H and λE can be found in Brutsaert (1982) and chapter 4 of the Hydrology Handbook (Allen et al. 1996). When S_{cb} and P_{syn} are assumed to be zero, the BREB equation for application to vegetation becomes:

$$\lambda E = \frac{R_n - G}{1 + \beta} \tag{7.7b}$$

Eq. 7.7b will overestimate λE if S_{cb} and P_{syn} are positive, but assumed zero.

Under most measurement conditions, the transport coefficients (inverse of aerodynamic resistances) for H and λE can be considered to be equivalent between the two measurement heights (Sellers 1965; Tanner 1968; Dyer 1974). However, for sparse vegetation, heat sources can be lower or higher in vegetation than vapor sources (see chapter 11), which may impact the transport coefficients differently. Given equivalent transport coefficients, the Bowen ratio β can be expressed in a finite difference form as:

$$\beta = \frac{H}{\lambda E} = \frac{c_p P}{\lambda \varepsilon} \frac{(\Delta T + \Gamma \Delta z)}{\Delta e} = \gamma \frac{[T_2 - T_1 + \Gamma(z_2 - z_1)]}{e_2 - e_1} \tag{7.8}$$

where T_2 and e_2 are air temperature and vapor pressure at height z_2 and T_1 and e_1 are air temperature and vapor pressure at height z_1. γ is the pyschrometric constant (eq. 3.13) and Γ is the adiabatic lapse rate, generally taken as 0.01°C m^{-1} for nonsaturated air. Units of c_p, P, and λ in eq. 7.8 should provide units for γ of kPa °C^{-1} so that, for T in °C and e in kPa, β is dimensionless.

Generally the z_1 height should be at least 0.3 m above the crop canopy for a smooth, dense canopy, and should be placed further above the canopy for tall, sparse crops where microscale turbulence among individual plants and differences between source locations for heat and evaporation can disturb exponentially shaped temperature and vapor profiles. Generally, the z_2 height is 1 to 2 m above z_1.

Bowen ratio systems are available commercially and are in widespread use for measuring λE above both agricultural and natural vegetation. An example of a commercial system is shown in fig. 7.6. Generally $T_2 - T_1$ is measured using differentially wired fine-wire thermocouples which may be naturally or artificially aspirated or using precision resistance thermometers that are shielded from the sun and that require artificial aspiration. Vapor pressure is generally measured at each height using aspirated wet and dry bulb psychrometers or electronic hygrometers, or by suctioning air samples from each height through a common chilled mirror hygrometer or a closed path gas analyzer. On some systems, the z_2 and z_1 sensors are automatically exchanged with one another each 10 minutes or so to remove instrumentation biases. Generally, λE is computed each 20 to 30 minutes and is summed over a daylight or 24-hour period to provide daily estimates of ET. Problems with naturally aspirated (exposed) thermocouples include contamination by dust and spider webs which increases radiation loading and thermal bias between T_1 and T_2 (Allen et al. 1994c). Other types of errors associated with BREB measurements were described by Sinclair et al. (1975), Ohmura (1982) and Payero et al. (2003).

Fig. 7.6. Systems, Inc. Bowen Ratio System at American Falls Reservoir (photo by R. Allen of a Radiation Energy Balance).

The net radiation measurement in the BREB calculation should be made from an elevation high enough to measure an average representative surface condition similar to that upwind of the T and e measurements. Because of the direct role that R_n plays in the λE measurement, multiple R_n sensors are recommended for improved spatial sampling and quality control. In heterogenous vegetation cover having variation in vegetation type, size or density on the scale of fives of meters or more, multiple net radiation systems should always be employed. Idso and Crooley (1971, 1972) and Idso (1974) provided guidance on net radiometer positioning and error analysis.

Soil heat flux density is generally measured at 0.08 to 0.15 m below the surface using soil heat flux plates (Campbell Scientific 2003; Ham 2001). The 0.08- to 0.15-m depth range is recommended to insure that the soil flux density is measured below the zone of soil water vaporization (Ham 2001) and to reduce the influence of the plate in impeding vertical conduction of heat and water flow near the soil heat flux plate. Heat flux plates tend to behave like umbrellas during vertical flow of water, for example after a wetting event, and can create dry areas below plates during infiltration and above plates during evaporation. Because thermal conductivity of soil near a plate is substantially influenced by water content, the spatial disruption of continuity in water content can cause substantial error in G and consequently the ET derived from BREB.

Sensible heat absorption and release above soil heat flux plates is estimated by measuring soil temperature change above the plate at multiple depths and at multiple locations. Generally, two or more installations of soil heat flux systems are recommended per BREB site to reduce effects of spatial heterogeneity and to improve representation for the area. The corrected soil heat flux density, G, is computed using eq. 4.47.

Important advantages of the BREB method are the ability to measure λE even from non-potential surfaces, the elimination of wind or turbulent transfer coefficients, and absence of surface measurements. The disadvantages are sophistication and fragility of sensors and data

logging equipment, the numerical instability of eq. 7.7 and 7.8 during periods of β near -1, and the substantial reliance on accurate and representative measurements of R_n and G. The requirement for adequate upwind fetch also places limits on the method.

Most evidence suggests that correction for air stability conditions in the use of the Bowen ratio-energy balance measurements is not needed, due to nearly equal impact on both λE and H, so that the usual assumption of the near-equality of transfer coefficients for heat and water vapor throughout a wide range of stability conditions is realistic (Cellier and Brunet 1992). However, the major source elevations for λE and H in the canopy should be similar for the transfer coefficients for the two processes to be nearly the same (Tanner 1967).

The Bowen ratio method is recognized as one of the most accurate ET measurement methods if R_n, G, and the gradients of temperature and humidity can be accurately measured, are spatially representative and β is small. For tree crops and forest canopies, accurate measurement of the gradients at a height far enough above the canopy to avoid effects of individual trees is difficult due to the very small gradients involved. Nevertheless, the Bowen ratio method has served and continues to serve as one of the major methods employed for forest research (McNaughton and Black 1973; Thom et al. 1975; McIlroy and Dunin 1982; Denmead and Bradley 1985; Fritschen and Simpson 1985; Dunin et al. 1985, 1991). Accuracies of well-designed and operated BREB systems have been estimated to be approximately 10% (Sinclair et al. 1975; Seguin et al. 1982). A disadvantage is the need to measure R_n and G, which can be problematic under some conditions such as with sparse or heterogeneous vegetation, and over water surfaces.

Typical Problems with Bowen Ratio Systems

Advantages, disadvantages and requirements of Bowen ratio systems are summarized in table 7.3. Because of the numerical instability of the BREB approach which develops as β approaches -1 (when sensible heat transport toward the surface is in near equilibrium with latent heat transport away from the surface), special procedures are required during such periods. Fortunately $\beta \rightarrow$ -1 generally occurs during periods of low R_n (at dawn and dusk) when ET is normally low. Angus and Watts (1984), in comprehensive analyses of sensor-produced errors, showed the potential for error in calculation of λE to increase rapidly as β drops below –0.2, with accuracy requirements for all sensors increasing. Ohmura (1982) and Payero et al. (2003) described relative errors associated with the BREB method as well as techniques for data quality analysis.

The problem with β close to –1 is illustrated in fig. 7.7. Part (a) shows the very excellent capabilities of the BREB method in estimating actual ET during most hours of the day. However the problem of $\beta \rightarrow -1$ is also clearly shown. Although errors are small in magnitude for the 1700 - 1800 h, it is obvious that 50 to 100 percent errors occur even prior to β reaching –0.5, a confirmation of the Angus and Watts (1984) paper. The data from eight days of an early micrometeorological study by Pruitt (1963) at Davis (March to October) are shown in fig. 7.7b, with twelve half-hour periods when $-1.5 < \beta < -0.5$ separated from the other 142 periods. The results also show the excellent response of the BREB method with these tests conducted under a wide range of conditions from cool and humid to hot and dry, and to a cold and dry day in March having strong-wind. There were periods of rather drastic errors in estimating ET when $\beta \rightarrow -1$.

Pruitt et al. (1987) utilized an hourly Penman equation to derive ET for periods affected by the problem when $\beta \rightarrow -1$. To obtain crop ET estimates for those problem periods, the ET_{ref}

from the Penman equation was multiplied by a reference ET fraction, ET_rF, determined during daylight periods prior to or following the periods of unstable BREB estimates by dividing measured ET by ET_{ref}. Tanner (1967) suggested, much earlier, that simple combination equations be substituted for BREB estimates during problem periods. This requires instrumentation for measuring wind speed. More details on BREB computations can be found in chapter 4 of the ASCE Hydrology Handbook (Allen et al. 1996) and in Allen et al. (2011a).

ET determined from BREB is often used to test or 'confirm' other energy balance-based models including the combination equation, for example, the PM equation. However, an often overlooked requirement for testing or confirming models is the requirement for independency between the tested method and the measured data. In comparisons of models against ET from the BREB, often, the same R_n measurements are used in both the combination equation and in the determination of ET from BREB. Because the R_n parameter can dominate both the combination equation and BREB-based ET, the ET estimated from the combination equation can not be confirmed using BREB-derived data, unless an independent measurement or estimation of R_n is used.

The Bowen Ratio (BREB) method is often superior to the direct use of turbulent transfer equations for estimating transfers of water vapor above a surface. This is primarily due to constraints on estimates made using the BREB method due to inclusion of the radiation balance in the method. Errors in estimating gradients of temperature or humidity are not directly related to the estimates of λE or H as is the case for strictly aerodynamic methods. There are situations, however, where net radiation or heat transfer below the surface is not readily measurable. For forests, brushlands, or orchards, accounting for changes in heat storage of the canopy can be important for periods shorter than 24 hours. For water bodies, accurate measurement of $R_n - Q_t$ is difficult. For these situations, consideration should be given to the use of aerodynamic methods, described later in this chapter, that avoid these problems.

Example Applications for Bowen Ratio Systems

Applications of the BREB system began in the 1960s (Tanner 1960; Fritschen 1965, 1966; Fritschen and Lourence 1966). A summary of numerous applications of the system over land surfaces was presented by Allen et al. (1996). The BREB approach is difficult to apply to evaporation measurements from water bodies due to the difficulty in measuring the energy (Q_t) absorbed into or liberated from the water, as described in Chapter 6. Applications of the BREB approach to water have been discussed by Andersen (1954), Keijman (1974), Hoy and Stephens (1979), Amayreh (1995), Allen and Tasumi (2005) and in Chapter 6.

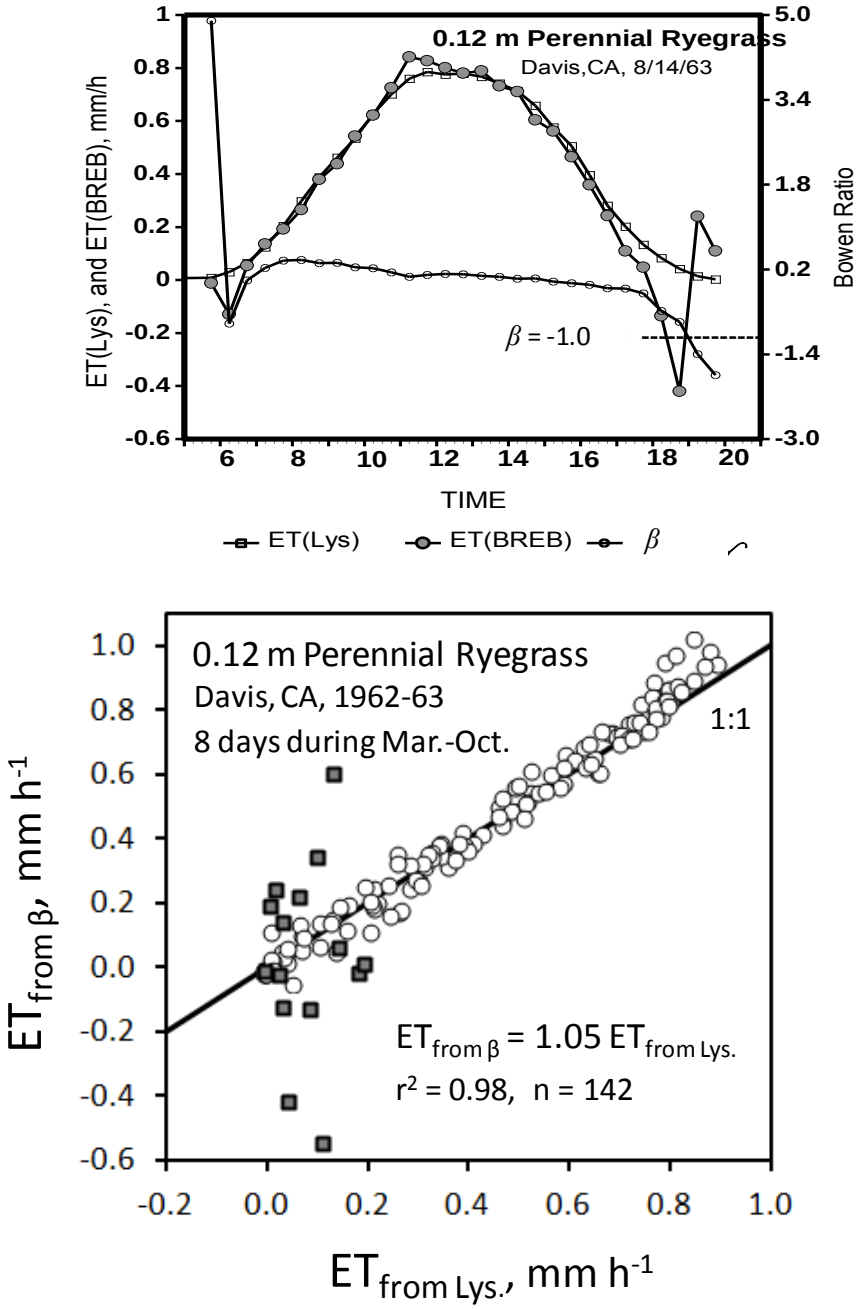

Fig. 7.7. Examples of early tests of the BREB method: (a) Comparison of ET from perennial ryegrass measured by lysimeter with BREB calculations for 14 August, 1963 at Davis, California including reference to ß. (b) Regression of ET from Bowen ratio against ET by precision-weighing lysimeter for half-hour time intervals spanning 8 days of data collected in 1962-63 at Davis. Twelve half-hour periods are plotted as square symbols when $-1.5 < \beta < -0.5$ and the estimation of ET became numerically unstable. The 12 periods were not included with the other 142 periods (round symbols) during regression. Source: Data from Pruitt (1963).

7.5 Mass Transfer Method using Eddy Covariance

ET can be measured directly using eddy covariance (EC) sampling of the boundary layer (Swinbank 1951) according to the relationship:

$$E = \rho_a \overline{w'q'} = \frac{0.622}{P} \rho_a \overline{w'e'} \tag{7.9}$$

where E is vapor flux in kg m^{-2} s^{-1}, equivalent to mm s^{-1}, q' is the instantaneous deviation of specific humidity from mean specific humidity (q), kg kg^{-1}, e' is the instantaneous deviation of vapor pressure from mean vapor pressure (e), kPa, w' is the instantaneous deviation of vertical wind velocity from mean vertical wind velocity (w), m s^{-1}, P is atmospheric pressure, kPa, and ρ_a is air density, kg m^{-3}, assumed to be constant. The overbar indicates means of the products of the instantaneous deviations over 15 to 30 minute periods.

Webb et al. (1980) recommended water vapor and air density corrections to the calculation of E (Fuehrer and Friehe 2002; Leuning 2007) that can be expressed as:

$$E = \rho_a \overline{w'q'} \left(1 + \frac{q}{1-q}\right) + \frac{q^2}{(1-q)} \frac{H}{c_p T} \tag{7.10}$$

where c_p is specific heat of moist air, J kg^{-1} K^{-1} and q and T are mean specific humidity and temperature over the averaging period in kg kg^{-1} and K. Units for H are W m^{-2}.

Residual λE can also be computed from the energy balance equation as $\lambda E = R_n - G - H$ (eq. 4.30), where sensible heat flux density is measured by eddy covariance as:

$$H = \rho_a c_p \overline{w'T'} \tag{7.11}$$

where T' is the instantaneous deviation of air temperature from mean temperature (T) in K and H has units of W m^{-2}.

The concept of eddy covariance (also referred to as eddy correlation) draws on the statistical covariance (correlation) between vertical fluxes of vapor or sensible heat within upward and downward legs of turbulent eddies. This requires high speed measurement of T, w, and e or q, usually at frequencies of 5 Hz (5 times per second) or faster using quick response sensors. Ten Hz is common. The vertical component of wind, w, is generally measured using a sonic anemometer and T is measured using ultra fine wire thermocouples (on the order of 13 µm diameter) or using sonically determined temperature corrected for humidity effects. Specific humidity is measured using quick response hygrometers such as Lyman-alpha, Krypton or other open path hygrometers or using closed path gas analyzers (Buck 1976; Campbell and Tanner 1985; Tanner 1988). All measurements must be made at nearly the same point in order to measure characteristics of the same eddy. Corrections are required for instrument separation, frequency response, coordinate rotation and to account for the type of hygrometer (Baldocchi et al. 1988; Tanner et al. 1993; Moncrieff et al. 1996; Villalobos 1997; Twine et al. 2000; Aubinet et

al. 2000, Paw U et al. 2000; Massman 2000; Sakai et al. 2001; Rannik 2001; Massman 2001; Wilson et al. 2002). Systems employing 3-D sonic anemometers allow coordinate (planar) rotation to be made to force mean vertical wind speed w toward zero (Baldocchi et al. 1988; Wilczak et al. 2001). Eddy covariance systems are commercially available. An example of an eddy covariance installation is shown in fig. 7.8 where two sonic anemometers were employed for data redundancy.

Fig. 7.8. Two three-dimensional sonic anemometers and an open path infrared water vapor and CO_2 sensor used to measure H, λE and CO_2 fluxes. The use of two sonic anenometers provided data redundancy, the ability for error checking and intercomparison, and the ability to assess error in λE and CO_2 fluxes caused by separation distances between anemometer and open-path infrared sensor. Photo courtesy of R.G. Allen.

A variety of software programs for correction of EC data have been produced, including ECPack from Wageningen University, TK2 software of the University of Bayreuth (Mauder and Foken 2004), EddySoft developed at the Max-Planck-Institute for Biogeochemistry in Jena (Kolle and Rebmann 2007), EdiRE software from the University of Edinburgh, APAK by Oregon State University (Vickers and Mahrt 1997, 2003) and Eddy-Pro by LI-COR, Inc. (2012). These software packages include mixtures of the corrections listed. In addition to these corrections are issues related to flux divergence in the equilibrium boundary layer, nonuniform vegetation or moisture conditions in the source area (i.e., footprint), improper averaging times and impacts of very large, episodic eddies and heat plumes that have large vertical components that are very efficient in heat and vapor transport, but are largely missed by the sonic sensor or covariance algorithm (Foken 2008a). Burba and Anderson (2008) give a good overview of corrections and precautions for eddy covariance.

Computing λE as a residual of the energy balance by measuring H as in eq. 7.11 has the advantage of eliminating the requirement for the quick response hygrometer which can be expensive or may require frequent maintenance. The disadvantage of this method is the need to measure R_n and G, which can be problematic under some conditions such as with sparse or heterogeneous vegetation, and over water surfaces. Eq. 7.11 can be used in an energy balance

closure check on eq. 7.10 using eq. 7.14. Allen and Tasumi (2005) combined H determined from eddy covariance with Bowen ratio from a BREB system to determine λE from open water as described in chapter 6.

Advantages, disadvantages and requirements of the eddy covariance method are summarized in table 7.3.Advantages of the eddy covariance method are the direct sampling of the turbulent boundary layer and measurement of ET over both potential and non-potential surfaces. Eddy covariance has disadvantages similar to other boundary layer sampling techniques, including complex instrumentation and fetch requirements. The sonic anemometer must be set parallel to the surface so that no component of wind speed parallel to the surface biases measurements. If not set parallel to the surface, coordinate rotation must be applied. When positioned over rough vegetation such as trees, the eddy covariance system must be far enough above individual limbs that impacts of limbs on air streamlines is minimized. Otherwise, the zero-plane of vertical velocities of streamlines past the anemometer will change with small changes in wind direction during the averaging period and will cause false flux readings that can not be corrected with coordinate rotation. In general, the eddy correlation method requires personnel who are well-trained in electronics, turbulent theory, and biophysics. Instrumentation is relatively fragile and expensive.

Lack of energy balance closure is common with eddy covariance measurements, where the sum of measured $\lambda E + H$ does not equal measured $R_n - G$ (Baldocchi et al. 1988; Twine et al. 2000; Wilson et al. 2002, Foken et al., 2006, Foken 2008a). Possible reasons for the lack of closure are storage of heat in canopies, horizontal advection, change in storage of heat in the developing boundary later below the instrumentation (causing flux divergence), frequency response of the sonic and water vapor sensors that does not span the entire spectrum of frequency of eddies, and regional scale heterogeneity of vegetation and ET fluxes that can cause large scale eddies that are effective in transport of λE and H, but are not readily sensed by eddy covariance systems that are typically placed within 20 m of the surface (Foken 2008a). Many users 'close' the energy balance by scaling $\underline{H}$ and λE in the same proportion (Twine et al. 2000) until the sum equals R_n - G. However, this places all source of lack of closure on H and λE and none on R_n - G. Allen (2008) suggested using multiple linear regression, where the most dependable component of R_n , G, H, and λE is set as the dependent variable and all others are set as independent variables for data collected during daytime conditions to indicate systematic biases in components. Allen (2008) gave illustrations where measurements of G were indicated by regression to be undermeasured by as much as 100 to 200%. The multiple regression approach does not explain why a component is biased and can only identify consistent, systematic biases in components. Additional detail on the eddy correlation method can be found in articles by Dyer (1961), Businger et al. (1967), McBean (1972), Brutsaert (1982), and Weaver et al. (1986), Kizer et al. (1990), Kizer and Elliot (1991), Twine et al. (2000), Wilson et al. (2002), Shaw and Snyder (2003) and Baldocchi (2003) and Foken (2008b).

7.6 Fetch Requirements for Boundary Layer Measurement

It has generally been suggested that upwind fetch for boundary layer instrumentation be on the order of 100 m for each meter z_2 is above the top of the zero plane displacement height of the surface (Brutsaert 1982) to insure establishment of an internal equilibrium boundary layer that is representative of the surface energy exchange being measured. Monteith and Unsworth (1990) recommended that a fetch of 50 to 1 is often adequate for micrometeorological measurement of

sensible and latent heat flux. Brutsaert (1982) has provided theoretical considerations of boundary layer development that can be used to estimate minimum fetch requirements as a function of surface roughness. If one assumes that the lower 10% of an internal boundary layer downwind of a surface discontinuity has reached full adjustment to a new equilibrium with the surface (Petersen 1969; Brutsaert 1982), then Brutsaert's eq. 7.39 can be expressed for minimum required fetch as:

$$x_f = \left(\frac{30(z - d)}{(z_{om})^{0.125}} \right)^{1.14} \tag{7.12}$$

where x_f is the minimum fetch distance required for complete boundary layer development, m, z is the maximum sensor height above the ground, m, d is zero plane displacement, m, and z_{om} is momentum roughness height of the surface, m. Eq. 7.12 estimates x_f for near neutral conditions (H near 0). The exponent (1.14) should be increased for situations of increasing stability and can be reduced somewhat for conditions of increasing instability (Brutsaert 1982). Eq. 7.12 indicates that as surface roughness increases, the fetch requirement (distance required for the new equilibrium to occur) decreases, as shown in table 7.2 where z_{om} and d for vegetation are estimated as 0.12 and 0.67 times canopy height, respectively. Eq. 7.12 estimates x_f for discontinuities between surfaces of similar roughness and may not predict well for large changes in vegetation height, such as transversing from forest to grass or vice versa.

TABLE 7.2 Minimum Recommended Upwind Fetch Distances, m, for Various Types of Surface Cover (from eq. 7.12) and Assumed Values for z_{om} and d.

	Height of the upper measurement above the ground			
Height and Type of Surface Cover	z = 1 m	z = 2 m	z = 3 m	z = 12 m
Water (d = 0, z_{om} = 0.0001 m)	180	400	630	3,000
0.12 m Grass (d = 0.08 m, z_{om} = 0.014 m)	80	190	300	1,500
0.5 m Alfalfa (d = 0.34 m, z_{om} = 0.06 m)	45	130	220	1,200
1.5 m Cattails (d = 1.0 m, z_{om} = 0.18 m)	n/a	60	140	950
10 m Dense Trees (d = 6 m, z_{om} = 1.2 m)	n/a	n/a	n/a	320

The values for minimum fetch in table 7.2, computed using eq. 7.12, indicate that eq. 7.12 follows the 100:1 rule for a relatively wide range of vegetation and equipment heights. According to the equation, the 100:1 rule represents most closely 0.12 m tall vegetation. Eq. 7.12 becomes sensitive to the lack of roughness as $z_{om} \rightarrow 0$ so that fetch requirements become large (e.g. for open water).

As an example of application, for a Bowen ratio installation with the z_2 height at 2 m above the ground surface having 0.1 m tall vegetation, the minimum fetch requirement under neutral conditions according to eq. 7.12 would be approximately 190 m. The 100:1 ratio (relative to equipment height above zero plane displacement) would suggest a fetch of 200 m. A fetch distance of 190 m in all directions would require a minimum vegetation stand size of 4 ha (10 acres) with the BREB system placed at the center. This requirement (which increases as vegetation height increases) makes it difficult to use the BREB or any other boundary layer sampling system to measure λE from small, isolated stands of vegetation. As a confirmation on the above estimates, Pruitt (1963) found no difference in BREB calculations of ET for 0.1 to 0.15 m-tall grass using z_1 and z_2 heights of 0.25 and 0.5 m respectively and z_1 and z_2 heights of 0.5 and 1.0 m, when upwind fetch of grass was 180-200 m. On the other hand, Dyer and Pruitt (1962), in tests on the same field with sensors of an eddy correlation system placed at 4.0 m height, reported the fetch of grass to be inadequate for sensors at that height. Eq. 7.12 suggests a fetch length of 430 m for $z_2 = 4$ m over a 0.1 m crop.

Additional guidelines on fetch requirements for BREB measurement were given by Heilman et al. (1989) and a number of publications describe a variety of models for estimating footprints for both scalar and flux measurement. The 'footprint' of a flux or scalar measurement represents the upwind surface area that is statistically responsible for the conditioning of the measurement (Hsieh et al. 2000). Schmid (2002) presented a good review of various models, their mechanics and limitations. An expression for estimating the fraction of λE sensed at a specific instrument height that is generated from a specific distance of upwind fetch was presented by Gash (1986), Schuepp et al. (1990), and Shuttleworth (1992):

$$F = \exp\left(\frac{-\left| (z-d)\left(1 - \ln\left(\frac{(z-d)}{z_{om}}\right)\right) - z_{om} \right| - \psi_{sm(z/L)}}{k^2 \, x_f \left(1 - \frac{z_{om}}{(z-d)}\right)} \right) \qquad (7.13)$$

where F is the fraction of vapor and sensible heat flux densities at the z height which is contributed by fetch having an upwind length of x_f m (i.e., F fraction of the flux is contributed by the surface lying along 0 to x_f), variable k (dimensionless) is the von Kármán constant (0.41) and $\psi_{sm(z/L)}$ (dimensionless) is the integrated stability correction function for momentum transfer, defined later in eq. 7.26. The subtraction of $\psi_{sm(z/L)}$ in the numerator of eq. 7.13 was added by Allen (2006) to account for effects of stability or instability of the equilibrium boundary layer. When $\psi_{sm(z/L)}$ is set equal to 0, eq. 7.13 represents F for conditions having neutral stability. Eq. 7.13 estimates lower F for stable conditions and greater F for unstable (buoyant) conditions.

Eq. 7.13 and the method of Hsieh et al. (2000) are useful for assessing quality of measurements by BREB and eddy correlation sensors, where F represents the fraction of λE or H measured which is generated by the fetch of vegetation or surface over which the sensors are located. Clearly, for measurements to be completely representative of the measurement surface F should be close to 1.0. Eq. 7.13 estimates $F \approx 0.8$ for values of x_f calculated using eq. 7.12, indicating that it recommends slightly greater fetch requirements than does eq. 7.12. When applied to BREB systems with $z = z_2$, eq. 7.13 estimates on the conservative side, since the lower BREB measurement would suggest a higher F if based on $z = z_1$. Eq. 7.13 estimates $F = 0.91$ and $F = 0.57$ for $z = 1$ m and $z = 4$ m, respectively, over 0.1 m grass for $x_f = 200$ m. These calculations agree with observations by Pruitt (1963) and Dyer and Pruitt (1962) described in the previous paragraph concerning adequacy of fetch.

Horst and Weil (1992), Hsieh et al. (1997), Leclerc et al. (1997), Schmid (2002) and Hsieh et al. (2000) applied Lagrangian stochastic and large eddy simulation (LES) strategies along with Gaussian or non-Gaussian diffusion assumptions to estimate three-dimensional distribution of point source or line source fluxes. These complex models were applied over a range of stability conditions to demonstrate sensitivities of flux and scalar measurements over a range of footprint conditions and discontinuities in fetch at several distances from the sensors.

Fetch Requirements for Weather Stations

Eq. 7.12 and 7.13 can be applied to assess the adequacy of green fetch around weather stations for use in estimating reference ET representing well-watered agriculture (Schmid 2002; Allen 2006). Allen (2006) applied results from Horst and Weil (1992) and Hsieh et al. (2000) to various fetch lengths of clipped grass and dry soil to demonstrate the impact that fetch at various lengths of distance has on air temperature and humidity measurements at weather stations. Allen showed the impact to increase more-or-less logarithmetically with distance upwind and to then decrease after some distance even further upwind. Results indicate that the 100:1 fetch distance:measurement height rule-of-thumb and eq. 7.13 appear to apply well to unstable conditions (positive Bowen ratio) for measurement of temperature and humidity at weather stations, and may underestimate the fetch requirement for neutral and stable conditions. Appendix H contains tables showing the relative influence of various distances of bare soil or well-watered grass on air temperature and humidity measurements, based on eq. 7.13. These tables are useful in judging the representativeness of weather station measurements of T and e_a to reference ET conditions (i.e., T and e_a occurring over a large expanse of well-watered, transpiring vegetation).

7.7 Advantages and Disadvantages of ET Measurement Methods

Table 7.3 contains a summary of advantages, disadvantages and requirements associated withestimating ET using soil-water balance, lysimetry, Bowen ratio and eddy covariance methods following Allen et al. (2011a). These four methods tend to be the primary methods in current practice. In addition, when ET measurements or crop coefficients are reported, a thorough description of measurement conditions and methods should be included with the measurements to help users of the data understand the context of the data: the condition, type and character of the vegetation measured, and a means to judge the likely accuracy of the data (Allen

et al. 2011b). It is highly recommended that multiple systems be employed as part of quality control and that the systems be co-located periodically for bias assessment and adjustment. Independent measurements using different types of methods or equipment from different vendors can be valuable for discovering measurement problems.

TABLE 7.3 Summary of advantages, disadvantages and requirements associated with estimating ET using soil-water balance, lysimetry, Bowen ratio and eddy covariance methods. Source: Data from Allen et al. (2011a).

Method	Characteristic
Soil Water Sampling and Balances	**Advantages** • Ability to obtain samples from multiple sites. • Can have low costs, depending on equipment and labor. • Direct measurement of depletions **Potential Problems** • horizontal and vertical variability of bulk density and water holding characteristics of the soil; • inaccuracies in measuring precipitation and irrigation additions or unrepresentative data; • possible deep percolation losses or gains by capillary rise; • the potential need for calibration of sensors for soil type; • for some vegetation types, it is difficult to obtain samples or take readings (or installing access tubes or sensors) without significantly altering the plant cover and soil surface conditions at the sampling site. ET from trampled plants can be drastically reduced as compared to ET by plants in a pristine condition. Fig. 7.1 illustrates the considerable effort one should consider to avoid this problem when taking neutron probe readings; • foot or equipment traffic may alter the density, aeration and infiltration characteristics of the surface soil. If water intake and/or aeration at and near the sampling site is quite different from general field areas, then plant growth is likely affected. This may reduce soil water extraction, leading to estimated ET unrepresentative of the field ET; • all irrigation systems apply water non-uniformly, and the degree and scale of non-uniformity varies with system management. Differential spatial wetting of soil due to spatial variation in irrigation applications, for example with drip or micro-sprinkler systems or even with some furrow systems. Accurately measuring changes in soil water content for fields irrigated with systems that distribute infiltration in radial patterns can be difficult and laborious; • differential spatial extraction of soil water due to spatial variation in root systems, for example with orchard and vine crops.
Lysimetry	**Advantages** • short-time scale • direct measurement of depletions • simple conceptually • calibration can be validated mechanically; • fetch requirement is smaller than for micrometeorological methods; • lysimeters can be fully automated; • the system is nearly fully visible for inspection. **Disadvantages** • lysimeter area often represents a small sample relative to a field area and therefore imperfections in vegetation or water management reduce measurement accuracy; • difficult to maintain or to reconstruct original soil profile characteristics, including density, layering and structure during and following construction; • difficult to reduce any edge effects in vegetation; • difficult to measure trees and plants having large spacing; • difficult to maintain exact field conditions for vegetation and soil water; • difficult to reproduce rooting characteristics of the surrounding field; • difficult to detect the presence of low levels of water stress due to subtle visual effects

	• difficult to accurately reproduce ET from non-potential (stressed) vegetation due to difficulty in matching soil water profile and thermal profile conditions to those of the surrounding field. **Potential Problems with the Lysimeter Environment** • two-dimensionality of lysimeter boundaries, • vegetation height and density differences between inside and outside, • different vegetation characteristics between immediate and local fetch around the lysimeter and around the weather station, • thermal conditions of the lysimeter soil block may differ from the surrounding soil profile, • thermal conditions and advective effects due to a high, exposed rim, • bulk density and lysimeter depth effects on root development, and effects of the specific moisture profile or water table within the lysimeter on evaporation and moisture extraction. **Requirements** • adequate fetch around the lysimeter, recommend a minimum of 50 m; • vegetation inside and immediately outside the lysimeter must be very similar in: o height o density and ground coverage o leaf area • vegetation inside and outside lysimeter should be carefully documented via photography and description; • effective area of the lysimeter vegetation must be accurately calculated; • water management of the lysimeter must be precise and similar to outside conditions; • salinity must be managed via drainage; • thermal characteristics of the lysimeter soil must be similar to that outside; • foot traffic should be minimized.
Bowen ratio	**Advantages** • nondestructive, direct sampling of the turbulent boundary layer; • no aerodynamic data are required; • simple measurement of air temperature and vapor pressure at two heights; • can measure ET over both potential and non-potential surfaces; • fluxes are averaged over a medium sized area (200 to 100,000 m^2); • automated. **Disadvantages** • requires accurate and representative R_n and G; • assumes that transfer coefficients K_h and K_v for H and λE are equal (therefore assumes that sources for heat and vapor are horizontally and vertically similar); • numerically unstable when H is near zero (however, this usually causes only minor problems); • measurements of T and e must be unbiased because ΔT and Δe can be small;; • requires medium to large fetch; • small stands of similar vegetation may be too small to use BREB, for example, narrow riparian systems, so that the Bowen ratio system samples T and e gradient artifacts created by areas upwind of the vegetation of interest (for example, from upwind areas of pasture, desert or agriculture) due to an underdeveloped equilibrium boundary layer. **Requirements** • uniform fetch of sufficient distance to establish an equilibrium boundary layer (EBL) deeper than the z_2 height (this is often violated) • sufficient sensor elevation above the canopy to avoid the roughness sublayer • accurate and representative measurement of R_n and G

- heterogeneous or sparse systems common to riparian vegetation generally require multiple net radiometers and soil heat flux stations

Recommendations for deployment of net radiometers

- mount sensors over representative vegetation away from any obstructions including:
  - o towers;
  - o other instruments below or above the radiometer, especially bright, white instruments;
  - o above or below solar panels that are dark and often hot;
- when over complex or sparse canopies, deploy a minimum of three radiometers in separate locations:
  - o mount to view the true proportion of sunlit vegetation, shaded vegetation, sunlit soil and shaded soil;
  - o multiple towers for R_n may be needed;
  - o consider deploying four-component radiometers for separate measurement of incoming and outgoing short-wave and long-wave components for improved quality assessment and control and for improved understanding of each component;
  - o deploy a minimum of six soil heat flux measurement systems under the same conditions;
- use some independent means for testing R_n measurements, for example, compare against remote sensing based Rn estimates, infrared thermometers, modeling R_n with standardized solar radiation-based algorithms, etc.

Eddy Covariance

Advantages

- nondestructive, continuous direct sampling of the turbulent boundary layer;
- can measure ET over both potential and non-potential surfaces;
- fluxes are averaged over medium sized (50 to 200 m) areas;
- systems are automated.

Disadvantages

- a number of "corrections" are needed – these are often not well defined and are often empirical;
- may miss transport by very small and very large eddies;
- energy balance closure error (R_n-G=λE+H) can be 10-30%;
- requires substantial fetch, generally 100 times the height of the instrument above the zero plane displacement height;
- narrow vegetation systems may cause the EC (or Bowen ratio) system to sample ET from areas upwind of the vegetation area (for example, with a narrow riparian system, from pasture, desert or agriculture that is beyond the riparian system);
- requires consistently nearly horizontal flowlines;
- change in vertical direction of flowlines during an averaging period causes large errors (portions of the streamline can be misinterpreted as w' (relative to mean vertical wind speed) so that $w'T'$ or $w'q'$ are overstated). This occurs when:
- sensors are too close to roughness elements such as tree limbs;
- the 'surface' of vegetation is irregular, for example, a convex shaped riparian system where the shape and vertical components of streamlines change with respect to wind direction;
- vertical components of streamlines can easily change with wind direction as wind direction changes;
- difficult to know impacts of wind direction changes on any change in vertical components of flow lines;
- problems in eddy formation if sensors are too close to the surface or are too close to individual roughness elements;
- results may be questionable when used for understory measurements because of a changing horizontal plane orientation during an averaging period;

- mounting of net radiometers and location of soil heat flux plates for energy balance closure assessment is difficult for representative sampling;
- mounting arm and other nearby equipment, including the hygrometer, can impede and distort flowlines and eddy shapes for some wind directions;
- tower or scaffolding may bend and distort flowlines;
- Instrumentation is relatively fragile and expensive;
- the method requires personnel who are well-trained in electronics, turbulent theory, and biophysics.

Requirements

- uniform fetch of sufficient distance to establish an equilibrium boundary layer (EBL) deeper than the instrument height (this is often violated);
- sufficient elevation of instruments above the canopy to reduce roughness sublayer impacts and to increase mean eddy size to match the sensor path length;
- a number of "corrections" are required to maximize accuracy;
- accurate, high frequency instrumentation and knowledge of physics of turbulence.

7.8 Combined Energy Balance and Mass Transfer Methods

This section describes the combined use of aerodynamic expressions for sensible heat transfer and energy balance methods to estimate ET as a residual of the surface energy balance. More details on direct use of aerodynamic expressions are found in Brutsaert (1982), Cellier and Brunet (1992), chapter 4 of the ASCE Hydrology Handbook (Allen et al. 1996), Hatfield et al. (2005), in chapter 6 for open water, and in chapter 11 where the AFIB method is described.

Mass Transfer with Direct Use of Aerodynamic Expressions

Calculating ET Using ($R_n - G - H$). For cases where λE exceeds H so that measurement or estimation errors of H are small relative to λE, the use of energy balance determination of λE, where H is calculated aerodynamically, avoids the measurement of humidity gradients or fluxes, still one of the more uncertain of micrometeorological measurements. If data for R_n and G are available (measured or calculated), the equation for ET for this approach can be expressed as:

$$ET = \frac{R_n - G - H - S_{cb} - P_{syn}}{\lambda\ \rho_w} \tag{7.14}$$

where ET is in mm s^{-1}, R_n, G, and H are in W m^{-2} (J m^{-2} s^{-1}), λ (eq. 3.17) is in KJ kg^{-1}, ρ_w is water density in kg m^{-3}, S_{cb} represents any changes in energy storage in the canopy or boundary layer between the ground surface and height of the H determination and P_{syn} is energy consumed by photosynthesis. S_{cb} and P_{syn} are generally assumed to be zero, but S_{cb} can be large in forests and during early morning when the boundary layer is warming and increasing in depth. P_{syn} can consume a few percent of total energy during daylight. Eq. 7.14 is commonly used in remote sensing applications using satellite imagery (Bastiannssen et al. 1998a,b; Allen et al. 2005, 2007; Tasumi et al. 2005a,b; Anderson et al. 2005, 2012).

Correction for Boundary Layer Stability. In calculating ET for short time periods (hourly or less) using aerodynamic approaches, the inclusion of stability-correction expressions in the log-law or other wind profile equations becomes vital as evidenced by Rossby and Montgomery (1935), Monin and Obukhov (1954), Swinbank (1955), Panofsky (1963), Businger (1966), Dyer (1967), Dyer and Hicks (1970), Webb (1970), Pruitt et al. (1973) and Oke (1978). Aerodynamic estimation of water vapor or sensible heat flux typically involves use of the Monin-Obukhov universal wind profile expression involving the modification of the log-law wind profile to provide applicability under non-adiabatic conditions. It can be expressed as:

$$\frac{\partial u}{\partial z} = \frac{u_*}{k\ (z - d\ )}\ \phi_M \tag{7.15}$$

where $\partial u/\partial z$ is the gradient of the horizontal component of wind speed at height z, u_* is the friction velocity in m s^{-1}, k is the von Karman constant (taken as 0.41), and d is the zero plane displacement of the wind profile by the canopy. The Monin-Obukhov (1954) ϕ_M is a gradiant function calculated at height z and is equal to 1.0 for neutral buoyancy conditions in the equilibrium boundary layer, less than 1.0 for unstable conditions, and greater than 1.0 for stable conditions. Monin and Obukhov related ϕ_M to their dimensionless height ratio, z/L, in a Taylor series expression. Only the first two terms have found wide usage, where

$$\phi_M = 1 + a_{mo}\ (z/L) \tag{7.16}$$

where z/L is a stability related function (Obukhov 1946) and α_{mo} was a constant determined experimentally by Monin-Obukhov (1954). The Obukhov scale length L in meters, as defined by Businger and Yaglom (1971) and Brutsaert (1982), is:

$$L = \frac{-\ u_*^3\ \rho_a}{k\ g\left(\dfrac{H}{T_a\ c_p} + 0.61\ ET\right)} \tag{7.17}$$

where u_* is in m s^{-1}, ρ_a is air density in kg m^{-3} (eq. 3.15), g is acceleration of gravity (9.807 m s^{-2}), H is the sensible heat flux density, W m^{-2}, (negative if to the surface), T_a is mean air temperature at the z height, K, and c_p is specific heat of moist air, J kg^{-1} K^{-1}. ET is evaporation flux density in kg m^{-2} s^{-1} (this is equivalent to mm s^{-1} when the ET flux is divided by the water density, ρ_w, in Mg m^{-3}). Generally, ρ_w = 1.0 Mg m^{-3}. Eq. 7.17 is often expressed without the 0.61 ET term, as the computation of L has only about 1/7 the sensitivity to λE as it does to H (both in W m^{-2}). The inclusion of ET in eq. 7.15 accounts for buoyancy caused by water vapor that has less density than dry air. ET in mm s^{-1} is obtained by dividing λE in W m^{-2} by λ in J kg^{-1}.

Generally, ϕ_M is not used in energy balance calculations because it is a gradient function and changes with elevation above the surface. Instead, an integration of ϕ_M (i.e., $\psi_{sm(z/L)}$) is used, as defined in the next section.

Sensible Heat from Temperature Differences

As indicated with the eddy correlation and aerodynamic methods, λE can be determined indirectly by solving the energy balance for λE, having computed H by other means. A promising typical method for determining H is the use of a near surface temperature gradient estimated using air temperature at some height z and surface temperature measured using an infrared thermometer. Hatfield et al. (1984) and Katul and Parlange (1992) are examples. Hatfield et al. (1984) provides results of testing the method at a number of USA locations and with several crops.

Sensible heat flux is commonly estimated by expressing the sensible heat equation in a difference form and by using an aerodynamic resistance term, r_a (s m^{-1}), leading to:

$$H = - \frac{\rho_a \, c_p}{r_a} \left(\theta_{T_z} - \theta_{T_o} \right) \tag{7.18}$$

where θ_{T_z} and θ_{T_o} are mean values for potential temperature at the z height and at the surface (K), calculated from T_z (air temperature at height z) and T_o (surface temperature) using eq. 7.19.

Potential temperature, θ_T for micrometeorological studies is defined as:

$$\theta_T = T + \Gamma \, z \tag{7.19}$$

where θ_T and T are in K. Γ is the lapse correction (°C m^{-1}) and z is the elevation of the T measurement relative to a specified datum. The potential temperature is the temperature that would result if air were brought adiabatically to the surface pressure level (Brutsaert 1982), and provides for inclusion of the effect of lapse rate in stability and H calculations. The use of θ_T in place of T has little effect on the calculation of sensible heat where sensors are within a few meters of one another. The aerodynamic resistance, r_a , between the surface and height z can be estimated by:

$$r_a = \frac{\left(\ln \left(\frac{z - d}{z_{om}} \right) - \psi_{sm(z/L)} \right) \left(\ln \left(\frac{z - d}{z_{oh}} \right) - \psi_{sh(z/L)} \right)}{k^2 \, u_z} \tag{7.20}$$

where d is the zero-plane displacement, z_{om} is the surface roughness length for momentum transfer (see chapter 8 for their estimation), z_{oh} is the surface roughness length for sensible heat

transfer (approximated for most vegetative surfaces as 1/10 of z_{om}), "ln" is the natural logarithmic function, and $\psi_{sm(z/L)}$ and $\psi_{sh(z/L)}$ are integrated stability functions for describing effects of buoyancy or stability between the surface and height z on sensible heat and momentum transfer. Massman (1999) and Su et al. (2001) describe more complicated approximations for z_{oh}. For water surfaces z_{oh} is characteristically 3 to 5 times the value of z_{om} based on relationships by Brutsaert (1982). A similar equation for r_a, but for where wind, temperature and humidity measurements are at different heights is presented as eq. 8.3 in the following chapter on Combination Methods.

Integrated Stability Functions

The bulk integrated stability-correction expressions $\psi_{sm_{(z/L)}}$ and $\psi_{sh_{(z/L)}}$ are recommended for all surface to air determinations of heat, vapor and momentum fluxes in place of the gradient ϕ functions. They are certain to be required for study over tall crops such as tree crops and forests and where strong stability (advection) or instability (low $\lambda E/R_n$ ratios) exists. As with the purely aerodynamic estimates of H or E, measurements of u and T should be based on 30-minute mean data or less. Stability corrections should not be applied with 24-hour means due to errors in averaging T_z and T_o over long periods and large change in $\psi_{sm(z/L)}$ and $\psi_{sh(z/L)}$ during the day. Another factor requiring attention in applying surface to air models for such applications is that the adiabatic lapse rate, Γ (approx. 0.01°C m^{-1}), must be taken into account, e.g. in the calculation of H, and use of virtual air temperature, T_v and potential virtual temperature θ_{T_v} may be important.

A comprehensive discussion on the subject of stability correction is given by Brutsaert (1982), where his formulas relate to the use of the Monin-Obukhov (1954) z/L stability parameter. The use of z/L requires an iterative solution to solve for several unknown parameters, with closure on the energy balance. Since most of the commonly used stability correction expressions were developed in relation to z/L, its use is recommended. A study by Katul and Parlange (1992) illustrated the use of iterative solution for z/L.

With some simplifying assumptions, the following presents the calculation of sensible heat flux H using integrated forms of stability correction for the aerodynamic method for exchange between the surface and some height or between two heights, along with the use of z/L.

Surface to Air Temperature Differences. When surface temperature is used, the profile expression involving sensible heat flux density, including correction for stability, is:

$$H = -a_h\, k\, u_*\, \rho_a\; c_p \frac{(\theta_{Tz} - \theta_{To})}{\left[\ln\left[\frac{z-d}{z_{oh}}\right] - \psi_{sh(z/L)}\right]} \tag{7.21}$$

where a_h, the ratio of k for heat to k for momentum, is generally assumed to be equal to or close to 1.0 and θ_{T_o} and θ_{T_z} are mean values for potential temperature at the surface and z heights, computed using eq. 7.19. Units for the z, d, and z_{oh} terms in eq. 7.21 must cancel and other terms must combine to provide H with units normally of J m^{-2} s^{-1} (i.e., W m^{-2}). The term $\psi_{sh(z/L)}$

(dimensionless) is the integrated stability function for heat transfer between the surface and z. Eq. 7.20 and 7.21 sometimes include a second $\psi_{sm(zom/L)}$ and/or $\psi_{sh(zoh/L)}$ term (Su et al. 2001). However, that term impacts the estimation of r_a or H by less than one percent for essentially all conditions except for very rough surfaces such as forest having low wind speed and large sensible heat fluxes, and can therefore generally be ignored.

With the assumptions that roughness lengths are normally much smaller than L, and that the Businger-Dyer expressions are valid, $\psi_{sh(z/L)}$ for unstable conditions ($z/L < 0$) can be expressed as (Paulson 1970):

$$\psi_{sh(z/L)} = 2 \ln\left[\frac{(1 + x^2)}{2}\right] \tag{7.22}$$

with

$$x = \left(1 - 16\frac{z-d}{L}\right)^{1/4} \tag{7.23}$$

Normally, $(z - d)/L$ is used in eq. 7.23 in place of z/L following Brutsaert (1982), where d is the zero-plane displacement length and L is the Monin-Obukhov stability length (eq. 7.17). In the case of surface to air differences, z in eq. 7.23 is the height of the air temperature and wind measurements.

The other unknown in eq. 7.21 is u_*, which can be obtained for surface to air applications from:

$$u_* = \frac{k\, u_z}{\ln\left[\frac{z - d}{z_{om}}\right] - \psi_{sm(z/L)}} \tag{7.24}$$

where $\psi_{sm(z/L)}$ (dimensionless) is the integrated stability correction function for momentum transfer, again, assuming that the roughness lengths are normally much smaller than L (Paulson 1970). The integral form of the expression for $\psi_{sm(z/L)}$ for unstable conditions for use with $T_o - T_z$ is:

$$\psi_{sm(z/L)} = 2 \ln[(1 + x)/2] + \ln[(1 + x^2)/2] - 2 \arctan(x) + \pi/2 \tag{7.25}$$

with x obtained from eq. 7.23 and where the arctan function is in radians.

For stable conditions, agreement as to appropriate stability functions is less certain. Fortunately, the method being considered, i.e. the estimation first of H using temperature differences and then solving for ET, allows for some uncertainty. Also, except for hot, arid or desert climates, stable conditions primarily relate to late afternoon to early morning periods when ET is small.

Assuming that the gradient stability functions for stable conditions ($z/L > 0$) are equal and acceptance of the functions of Webb (1970), the recommended relationships for integrated stability forms are:

$$\psi_{sm(z/L)} = \psi_{sh(z/L)} = -5.2\left(\frac{z-d}{L}\right) \tag{7.26}$$

for $0 < (z\text{-}d)/L < 1.0$ and where the Monin-Obukhov z/L parameter is computed as $(z - d)/L$. For $(z\text{-}d)/L > 1$, Brutsaert (1982) recommended limiting $\psi_{sm(z/L)}$ and $\psi_{sh(z/L)}$ to about > –5 or –6.

Calculation Steps. To calculate H and subsequently ET from the energy balance using the integrated stability functions and z/L, one should follow an iterative procedure, where one first uses eq. 7.21 and 7.24 to solve for H and eq. 7.14 to solve for ET, assuming neutral stability conditions ($\psi_{sh(z/L)}$ and $\psi_{sm(z/L)}$ are initially set equal to 0). Variable L is then calculated using eq. 7.17 using the initial estimates of H and ET. $\psi_{sh(z/L)}$ and $\psi_{sm(z/L)}$ are then solved using eq. 7.22, 7.25, or 7.26, depending on the sign of z/L, and eq. 7.24 and 7.21 are then resolved for u_* and H. ET for use in eq. 7.17 is recalculated using the energy balance equation, eq. 7.14, and the process is repeated until the values $(z\text{-}d)/L$, u_* and H become numerically stable. Generally only three to four iterations are required.

H from Air-to-Air Temperature Differences. When air temperature and wind are measured at two heights in the profile (rather than measuring T_o), the integrated forms of stability correction between z_1 and z_2 are employed, where the following variations on eq. 7.21 and 7.24 are used. The profile expression involved for sensible heat flux density, including correction for stability, is:

$$H = -a_h\, k\, u_*\, \rho_a\, c_p \frac{(\theta_{T_2} - \theta_{T_1})}{\left[\ln\left(\frac{z_2 - d}{z_1 - d}\right) - \psi_{sh(z2/L)} + \psi_{sh(z1/L)}\right]} \tag{7.27}$$

where θ_{T_2} and θ_{T_1} are potential temperatures at z_2 and z_1 heights, computed from T_2 and T_1 using eq. 7.19. Units for the z, d, and z_{oh} terms in eq. 7.27 must cancel and other terms must combine to provide H with units normally of W m^{-2}. The terms $\psi_{sh(z_2/L)}$ and $\psi_{sh(z_1/L)}$ (dimensionless) are integrated stability functions between the surface and z_2 and between the surface and z_1. Thus, the integrated stability adjustment for the distance between z_1 and z_2 is determined by differencing the two terms. The terms are calculated for sensible heat transfer using eq. 7.22 or 7.26, where $(z\text{-}d)/L$ is equal to $(z_2 - d)/L$ and $(z_1 - d)/L$ for $\psi_{sh(z_2/L)}$ and $\psi_{sh(z_1/L)}$, respectively.

Friction velocity, u_*, can be obtained from wind speed measurements at two heights as:

$$u_* = \frac{k(u_2 - u_1)}{\left[\ln\left(\frac{z_2 - d}{z_1 - d}\right) - \psi_{sm(z2/L)} + \psi_{sm(z1/L)}\right]} \tag{7.28}$$

where terms $\psi_{sm(z_2/L)}$ and $\psi_{sm(z_1/L)}$ (dimensionless) are integrated stability functions for momentum transfer and are calculated using eq. 7.25 or 7.26 with z/L equal to $(z_2 - d)/L$ and $(z_1 - d)/L$, respectively. Variables u_2 and u_1 are mean horizontal wind speed measurements at the z_2 and z_1 heights. Units for u_*, u_2, and u_1 are equivalent. In situations were T_1 and T_2 are measured at the z_1 and z_2 heights, but where only one measurement for u_z is made, then u_* can be calculated using eq. 7.24 using an estimation of surface roughness, z_{om}. This assumes constant u_* with height, which is a valid assumption because of conservation of momentum flux. The same iterative procedure for calculating H, u_* and z/L is followed as for surface to air measurements described previously.

Estimating ET from Air-to-Air Humidity Differences. As in the estimation of H from eq.7.27, ET can be estimated from humidity gradients:

$$ET = -a_v\, k\, u_*\, \rho_a \frac{(q_2 - q_1)}{\left[ln\left(\frac{z_2 - d}{z_1 - d}\right) - \psi_{sV(z2/L)} + \psi_{sV(z1/L)}\right]} \tag{7.29}$$

where a_v is the ratio of k for water vapor to k for momentum, commonly assumed to be 1.0. and the same steps used in solving for H in eq. 7.27 are used in solving for ET, assuming equality of the ψ_{sh} and ψ_{sv} functions. Parameters q_2 and q_1 are specific humidities at z_2 and z_1, kg kg^{-1}, defined in eq. 3.5. Units for ET will be kg m^{-2} s^{-1} which are equivalent to mm s^{-1} when the ET flux is divided by the water density, ρ_w, in Mg m^{-3}.

Chapter 11 describes an alternative application method for use when only air temperature, humidity and windspeed are measured at a single height, and iterative application of equations for H, λE, u^*, ψ_{sh} and ψ_{sm}, T_o, R_n, and G is made. The iteration is pursued until the estimate for T_o is numerically stable. As discussed in Chapter 11, the dependence of R_n, G, H, and λE on the estimate for T_o makes it important to determine T_o. That method can be more accurate than the Penman-Monteith method. Its application does require an estimate for bulk surface resistance, which can be uncertain.

Advantages, Disadvantages, and Precautions. The energy balance equation with H estimated using eq. 7.18, eq. 7.21 or eq. 7.27 has the advantage of ET estimation in areas where precipitation is less than ET and therefore where plant water stress occurs, since no knowledge of surface resistance (r_s) nor measurement of humidity profiles is required. The estimation of r_a or

use of surface temperature does require measurement of wind speed and perhaps surface roughness. Estimation of equivalent surface roughness, z_{om} and z_{oh}, along with measurement of a representative, average T_o in eq. 7.20 and 7.21 can be problematic in tall, sparse canopies such as found in forest and natural settings. Even in short agricultural crops, sensing the effective surface temperature can be a problem, where T_o at night may be influenced by leaf layers closest to the warm soil surface and where differences exist between radiometric T (as measured by an infrared thermometer) and aerodynamic temperature (the heat source temperature used in the aerodynamic equations for H) (Kustas et al. 1994; Qualls and Brutsaert 1996). For crops with sparse canopies, proper integration of soil and vegetation temperatures is especially difficult (Qualls and Brutsaert 1996).

An additional disadvantage of the energy balance approach is that T_1 and T_2 or T_o and T_z measurements need to be specific to the surface in question. Therefore, historic measurements of air temperature over standard weather surfaces are not useful with this method.

As with the Bowen ratio and eddy correlation methods and all boundary layer sampling techniques for that matter, it is critical that a large fetch of like vegetation occurs upwind of all sensors. This is necessary since the surface temperature-energy balance method, as with all boundary layer methods, assumes that equilibrium (one dimensional vapor, wind, and temperature profiles) has developed. Divergence from equilibrium energy exchange conditions may cause substantial estimation errors due to decoupling of the energy exchange surface from the boundary layer profile and resulting divergence of flux densities within the boundary layer. Fetch requirements for each sensor should be adhered to as discussed previously.

Estimating ET as $R_n - G - H$ generally requires the use of stability correction factors discussed previously, especially over dry surfaces. An example illustrating the seriousness of ignoring air profile stability conditions when using $ET = R_n - G - H$ is that reported by Pruitt and Lourence (1966) showing up to an order of magnitude of under-estimation of actual ET of grass during calm, mid-morning periods and an over-estimation of ET by a factor of 2 to 3 during late-afternoon stable periods with colder, heavier air near the surface. During periods with winds > 4 to 5 m s^{-1} stability correction was no longer needed over the transpiring crop due to the strong mechanical mixing and creation of turbulence, making the near-surface boundary layer nearly neutral.

Examples showing effects of stability correction on estimation of r_a using surface and air temperature measurements are given in fig. 7.9 for 0.23 m- and 0.12 m-high fescue grass at Logan, UT and at Davis, CA respectively. Both installations had full vegetation ground cover under fully watered conditions and with large fetch. Surface temperatures at both sites were made using IR thermometers. However, at Davis, T_o was based on averages of 5-cm and 10-cm leaf thermocouples for R_n less than 0 since the warm nighttime soil surface appeared to dominate the IR readings. At both locations surface temperature was lower than air temperature during nighttime and late afternoon periods, causing moderately strong stability of the boundary layer. Correction for this stability using eq. 7.24 with H calculated using eq. 7.21 (using an iterative solution for z/L) increased calculations of r_a dramatically, especially at Logan during nighttime periods where z/L became quite large due to low wind speeds ($u_2 < 1$ m s^{-1}). With the calm and cooler and more humid morning conditions during daytime between 0800 and 1400 hours at both sites which normally produce ratios of $\lambda E/(R_n - G) < 1.0$, T_o exceeded T_z and unstable conditions resulted. These unstable conditions lasted until mid-afternoon when z/L became

positive. The corrected values of r_a during some morning periods (made using eq. 7.20, 7.22, 7.25 and 7.28) ranged from 50 to 80 s m^{-1} lower than the uncorrected values for both locations.

The effects of stability and instability on estimation of r_a shown in fig. 7.9 appear to be quite significant. However, it is evident from fig. 7.10, where ET was estimated using the energy balance eq. 7.14 with H calculated using eq. 7.21, that only for the Davis study was there a large need for stability correction due to 15-20% over-estimation of ET, e.g., at mid-day, by the uncorrected log-law values. The corrections applied to calculate H for stability agreed very well for Davis with independent estimates of H made by subtracting lysimeter measurements of ET from $R_n - G$. Use of the calculated H in the energy balance resulted in under-estimation of ET (more negative values) at Davis during nighttime hours, although dewfall was occurring in this case. This underestimation may have been caused by errors in the measurements for R_n or G.

For the Logan results, only at night were there differences in corrected and non-corrected estimates of ET of more than a few percent, since the grass forage was transpiring during the day time at near maximum rates, so that little instability occurred and H was small. The magnitude of H at Davis was more than double that at Logan, no doubt due to cooler and more humid conditions of early May leading to greater instability at Davis. In applications over water - stressed natural vegetation, H may become large relative to λE and $T_o - T_z$ will increase. Such effects will increase the importance of applying stability corrections. The primary benefit of applying stability corrections at Logan was during the night time hours when the uncorrected H resulted in estimation of ET of about 0.05 mm h^{-1}, whereas, ET estimated using corrected H and ET measured by lysimeter indicated negative ET during this period. These errors are small, but would cause an error in the 24-hour sum for ET of almost 1 mm d^{-1} if the errors occurred over an an 8-hour night.

A second example of applying eq. 7.27 and 7.29 for H and ET using temperature and humidity gradients was by Allen and Tasumi (2005) over American Falls Reservoir, Idaho, as illustrated in fig. 6.16, where estimates for E by these equations (labeled 'aerodynamic estimate') were compared to E determined by a combination of eddy covariance and Bowen ratio.

Many satellite-based energy balance models for determining ET utilize eq. 7.14 with H from eq. 7.27. For example, the SEBAL (Bastiaanssen et al. 1998a, 2005) and METRIC (Allen et al., 2007a) remote sensing based models apply eq. 7.27, where the difference $\theta_{T_2} - \theta_{T_1}$ is estimated by indexing to surface temperature: $\theta_{T_2} - \theta_{T_1} = a + b\ T_s$, where a and b are empirical coefficients fitted specifically to each satellite image and T_s is surface temperature of each pixel in the satellite image. The relationship between $\theta_{T_2} - \theta_{T_1}$ and T_s is determined in SEBAL and METRIC by inverse calibration at extreme (wet and dry) conditions to reduce impacts of biases in estimates for net radiation, soil heat flux and other parameters (Allen et al., 2007a).

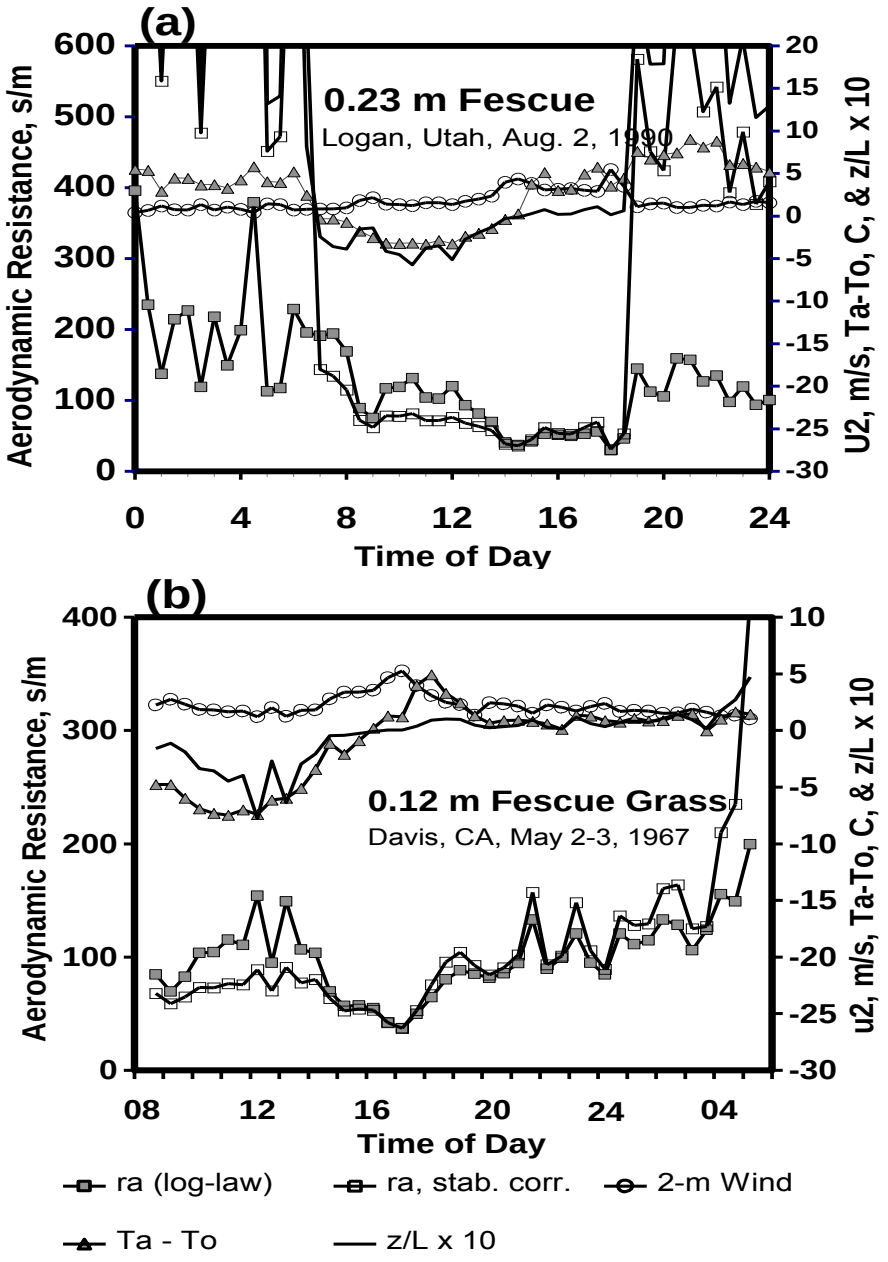

Fig. 7.9. Aerodynamic resistance (r_a) over grass computed with and without stability correction for studies at a) Logan, UT and b) Davis, CA. Included are measurements of T_z - T_o (expressed as $T_a - T_o$), 2-m wind speed, and z/L[1].

[1] From R. G. Allen (1994) personal communication and W. O. Pruitt (1994) personal communication for data from Morgan et al. (1971).

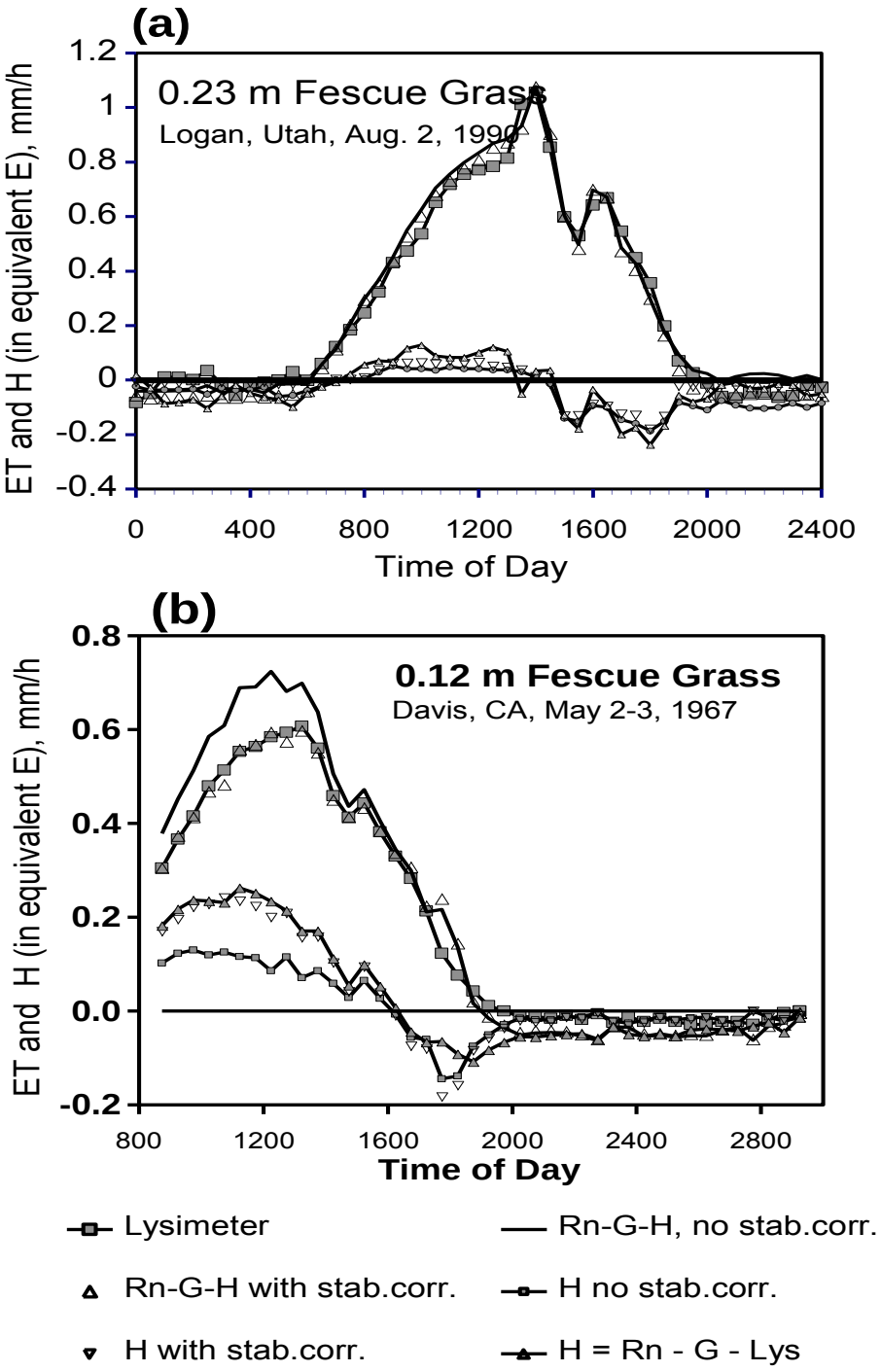

Fig. 7.10. Comparison of measured ET (lysimeter) with ET calculated from R_n - G - H with H calculated using the log-law and log-law corrected with integrated stability expressions at Logan, UT (a) and Davis, CA (b). Source: Data from Allen and Fisher (1990 and Pruitt (1994) personal communication with Davis data from Morgan et al. (1971).

8

Evapotranspiration from Land Surfaces: Reference Crop ET

8.1 Introduction

The combination of the sensible (eq. 7.18) and latent heat transfer equations (eq. 6.7) with the energy balance equation (eq. 7.14), following simplifying assumptions by Penman (1948, 1956b), 1963), results in the well known Penman equation, here expressed generically, to produce ET for a defined reference crop (generally clipped, cool season grass or full-cover alfalfa):

$$ET_{ref} = \frac{\Delta}{\Delta + \gamma} \frac{(R_n - G)}{\rho_w \lambda} + \frac{\gamma}{\Delta + \gamma} \frac{E_a}{\rho_w \lambda} \tag{8.1}$$

and

$$E_a = K_u (a_w + b_w u_2)(e_s - e_a) \tag{8.1a}$$

where R_n is net radiation and G is soil heat flux density into the ground in MJ m^{-2} t^{-1}, Δ is the slope of the saturation vapor pressure curve in kPa $°C^{-1}$, γ is the psychrometric constant in kPa $°C^{-1}$, E_a is the aerodynamic evaporation rate in MJ m^{-2} t^{-1}, K_u is a unit conversion factor typically in MJ m^{-2} t^{-1} kPa^{-1}, e_s is mean saturation vapor pressure at air temperature in kPa, e_a is actual vapor pressure of the air in kPa at height z, u_2 is wind speed in m s^{-1} at the 2 meter height, λ is the latent heat of vaporization in MJ kg^{-1}, ρ_w is density of water in Mg m^{-3} and a_w and b_w [s m^{-1}] are empirical wind function coefficients. These units produce ET_{ref} with units of mm t^{-1}. Penman's wind coefficients for grass were based on his original study and those for water were based on the Lake Hefner equation. Values for a_w and b_w are presented in chapter 6 for open water following eq. 6.18 and in appendix K for clipped grass and alfalfa references. Eq. 8.1 follows eq. 6.3 and 6.18.

8.2. The Penman-Monteith Equation

To better simulate the effects of behavior of vegetation with regard to energy balance, Monteith (1965) and Rijtema (1965) independently introduced a surface resistance parameter into the Penman equation and replaced the linear wind function term with an aerodynamic resistance parameter. The result is what is now commonly called the Penman-Monteith (PM) equation. Written in terms of evaporation or ET expressed as latent heat flux (λE):

$$\lambda E = \frac{\Delta(R_n - G) + \rho_a c_p (e_s - e_a)/r_a}{\Delta + \gamma\left(1 + \frac{r_s}{r_a}\right)} \tag{8.2}$$

where units of λE, R_n and G are in J m^{-2} s^{-1} (or W m^{-2}), ρ_a is air density, kg m^{-3}, computed using eq. 3.15, c_p is specific heat of dry air, J kg^{-1} ^{o}C^{-1}, generally taken as 1010 J kg^{-1} ^{o}C^{-1}, variables e_s and e_a are in kPa, r_a is aerodynamic resistance in s m^{-1}, r_s is the bulk surface resistance in s m^{-1}, and units for Δ and γ in eq. 8.2 are in kPa °C^{-1}. Equations for calculating e_s and e_a for use with 24-hour calculations in kPa °C^{-1} are given later in this chapter. For convenience, Δ is generally computed using eq. 3.2 at mean air temperature, which is a valid assumption when estimating λE for the reference crop which generally has near-neutral stability conditions. Aerodynamic resistance to vapor and heat transfer, r_a, in eq. 8.2 is computed using eq. 7.20 re-expressed as eq. 8.3. Bulk surface resistance, r_s, is defined in the following paragraphs. A derivation of the PM equation by combining aerodynamic and energy balance equations utilizing the Bowen ratio is included in Appendix J. λE from eq. 8.2 is converted to ET_{ref} (if the r_a and r_s parameters are defined for a reference crop) by dividing the numerator by λ (2.45 x 10^6 J kg^{-1}) and ρ_w (1000 kg m^{-3}) and multiplying by 1000 mm m^{-1}, so that λE in W m^{-2} and J m^{-2} s^{-1} yields ET_{ref} in mm s^{-1}. Further multiplication by 3600 s h^{-1} yields mm h^{-1} and multiplication by 86,400 s d^{-1} yields mm d^{-1}. Eq. 8.15 in this chapter is a simplified, standardized form of the PM equation with the conversion units to mm h^{-1} and mm d^{-1} embedded in the equation.

Aerodynamic resistance between the surface and height z for use in eq. 8.2 that uses the integrated stability correction forms is calculated as:

$$r_a = \frac{\left(\ln\left(\frac{z_u - d}{z_{om}}\right) - \Psi_m\right)\left(\ln\left(\frac{z_{T,e} - d}{z_{oh}}\right) - \Psi_h\right)}{k^2\, u_z} \tag{8.3}$$

where "ln" is the natural logarithm, k is the von Kármán constant (0.41), and measurement heights for wind speed, u_z, (at height z_u) and temperature and vapor pressure (at height $z_{T,e}$) may differ. The integrated stability functions in eq. 8.3 must be solved using $z/L = z_u/L$ (or $(z_u\text{-}d)/L$) for Ψ_m and $z/L = z_{T,e}/L$ (or $(z_{T,e}\text{-}d)/L$) for Ψ_h using procedures from chapter 7. These stability parameters can be set equal to zero for calculating λE for reference surfaces where near-neutral conditions typically exist (Allen et al. 2006c) and for calculation with 24-h time-steps. Variables z_{om} and z_{oh} are roughness parameters defined in eq. 8.7 and 8.8. Units for all z and d are in m.

For mean air temperature of T = 21.5 ^{o}C, λ has the value commonly used of 2.45 x 10^6 J kg^{-1}. When applied to 24-hour periods, R_n, G, r_a, and r_s in eq. 8.2 should represent 24-hour totals or averages for these parameters (Jensen et al. 1990; Allen et al. 1996, 1998; ASCE-EWRI 2005).

The combination equations that adhere to the form of eq. 8.1 (those by Penman (1948, 1963), Doorenbos and Pruitt (1977), Wright and Jensen (1972) and Wright (1982)) produce straight-line relationships for ET as a function of wind speed at given values of R_n - G. However, some findings have indicated that a curvilinear relationship might be more appropriate, e.g. Rijtema (1965), Pruitt and Doorenbos (1977, p 112-114) and Penman (1948, p.129). The Wright (1982) wind function coefficients, redefined in Jensen et al. (1990), have values for a_w and b_w that vary with time of year. With the inclusion of the surface resistance term in the PM equation, the equation projects a curvilinear wind function, where the rate of increase in ET decreases with increasing wind speed. The traditional Penman form with linear wind function may overestimate ET under moderate to strong winds if the winds continue through the night and RH_{max} remains low. However, in the PM method, aerodynamic resistance decreases with higher wind speeds,

resulting in an increase in $\gamma\ (1 + r_s/r_a)$ and, in turn, a decrease in $[\Delta/(\Delta + \gamma\ (1 + r_s/r_a))]\ (R_n - G)$. This has the effect of reducing the influence of the aerodynamic term of the PM equation on ET estimates for a given surface resistance, r_s. The PM method is thus less susceptible to over-estimation under high wind conditions than are the traditional Penman models. The PM equation has the further advantage of flexibility in assigning roughness and surface resistance values to fit various types and heights of vegetation. This extends its direct application to a wide variety of surfaces as well as soil moisture conditions. A disadvantage of the logarithmic function for r_a in the PM equation as opposed to the linear wind function of the Penman equation that has a constant offset, a_w, is the calculation of nearly infinite aerodynamic resistance as u_2 approaches 0. In reality, as u_2 approaches 0 under positive $R_n - G$, sensible heat flux caused by warming of the surface will create buoyancy forces and consequent instability that will cause r_a to be substantially lower than infinity. To account for this compensatory process, Allen et al. (1998) and ASCE-EWRI (2005) proposed limiting $u_2 \geq 0.5$ m s^{-1} during calculations.

The PM equation has been widely used to represent reference ET_o for use in irrigation management (Allen et al. 1989; Jensen et al. 1990; Martin et al. 1993; Allen et al. 1994ab, 1996, 1998, 2006c). When used with algorithms to increase surface resistance r_s (bulk stomatal resistance) under conditions of low soil water, the PM equation can be used to estimate actual ET, ET_a, for a wide variety of natural vegetation under non-potential soil water conditions, as addressed in Chapter 11.

Saturation vapor pressure, e_s, for hourly periods is calculated as:

$$e_s = e^o\left(T_{avg}\right) \tag{8.4a}$$

where T_{avg} is the average hourly temperature and $e^o()$ is the saturation vapor pressure function. For daily or longer calculation time-steps, e_s in the PM equation is computed using eq. 8.4b (Allen et al. 1989, 1996; ASCE-EWRI 2005):

$$e_s = \frac{e^o(T_{max}) + e^o(T_{min})}{2} \tag{8.4b}$$

where T_{max} and T_{min} are maximum and minimum daily air temperature for the 24-hour period at the z height, and e_s is the estimated average saturation vapor pressure during the period. Actual 24-hour vapor pressure of the air, e_z, or e_a, is generally computed as:

$$e_a = e^o(T_d) \tag{8.5}$$

where T_d is daily average or early morning dew point temperature. Parameter e_a can also be calculated as average e_a during the 24-hour period. ASCE-EWRI (2005) presented prioritized methods for estimating e_a from a variety of humidity parameters and summarized all calculation steps for the standardized ET_o and ET_r equations. This list is summarized in Appendix H (table H-4).

8.3 Aerodynamic and Surface Parameters for the PM Equation

When used to estimate ET from a dense grass or alfalfa reference, aerodynamic resistance in the PM equation can be calculated using the following parameter estimations (Allen et al. 1989, 1996; Jensen et al. 1990; Walter et al. 2000; ASCE-EWRI 2005):

$$d = 0.67\,h \tag{8.6}$$

$$z_{om} = 0.12\,h \tag{8.7}$$

$$z_{oh} = 0.1\,z_{om} \tag{8.8}$$

where d is the zero plane displacement height, z_{om} is roughness length impacting momentum transfer, and z_{oh} is roughness length impacting sensible heat and vapor transfer. z_{om}, z_{oh}, d, and mean plant height, h, are in m. Aerodynamic resistance, r_a, is computed using eq. 8.3. Additional equations for estimating z_{om} and d and general values for z_{om} for various types of vegetation are listed in chapter 11 on Evapotranspiration from Land Surfaces: Direct Penman-Monteith.

Surface resistance, r_s, for densely growing vegetation is generally computed as:

$$r_s = \frac{r_l}{LAI_{eff}} \tag{8.9}$$

where r_l is the bulk stomatal (or surface) resistance of the vegetation per unit LAI (s m^{-1}) and LAI_{eff} is the effective leaf area index contributing to ET and energy exchange. Parameter r_l is the inverse of g_l, the stomatal conductance per unit leaf area, which is also discussed in chapter 11. The value for r_l has been generally taken as 100 s m^{-1} for many well-watered agricultural crops (Monteith 1965; Szeicz and Long 1969; Allen et al. 1989, 1996; Jensen et al. 1990) when calculations are made on a 24-hour basis. When ET calculations are made on an hourly or shorter basis, r_l should be reduced to about 70 - 80 s m^{-1} for the well-watered and reference conditions. When deficient soil water reduces ET to less than maximum levels, r_l must be increased following procedures outlined in chapter 11.

A “minimum” or “unconstrained” surface resistance, $r_{s_{min}}$, is defined and listed in table 11.2 in chapter 11 as the surface resistance when all environmental parameters (notably R_s, T, VPD, and soil water) are at optimum levels. Under these conditions, values for a "minimum" r_l, $r_{l_{min}}$, may be about 40 s m^{-1} for many agricultural crops. However, values for $r_{l_{min}}$ should only be used in eq. 8.9 in combination with stomatal conductance reducing functions ($g(\ )$) (see chapter 11), since the environmental parameters are rarely all at optimum levels necessary to sustain the 40 s m^{-1} value (Allen et al. 1996; Allen et al. 2006c). For purposes of standardization of the definition and calculation of reference ET, the values for r_s in eq. 8.2 and consequently the value for r_l has been kept constant (ASCE-EWRI 2005).

Effective Leaf Area Index

A standardized LAI_{eff} has been established for grass and alfalfa reference crops (Allen et al. 1989, 1994b, 1996; Jensen et al. 1990) as:

$$LAI_{eff} = 0.5\,LAI \tag{8.10}$$

The 0.5 multiplier suggests that generally only the upper half of a dense canopy such as dense stands of grass and alfalfa is active in heat and vapor transport and is the zone of major net radiation absorption (Szeicz and Long 1969). The 0.5 multiplier has been supported by field research on wheat by Choudhury and Idso (1985).

Ben-Mehrez et al. (1992) presented an expression for LAI_{eff} that accounts for larger ratios of LAI_{eff}/LAI at small LAI and smaller ratios of LAI_{eff}/LAI when LAI is large:

$$LAI_{eff} = \frac{LAI}{0.3\,LAI + 1.2} \tag{8.11}$$

Eq. 8.11 was based on data from Shuttleworth (1991) and Rochette et al. (1991) for semidense agricultural crops and estimates $LAI_{eff} = 0.67\ LAI$ at $LAI = 1$ and $LAI_{eff} = 0.24\ LAI$ at $LAI = 10$. The equation estimates $LAI_{eff} = (0.4$ to $0.5)\ LAI$ at LAI's between 3 and 4, which are common for grass and alfalfa references, so that it is in general agreement with eq. 8.10 when used with standard reference vegetation heights. Eq. 8.11 is intuitively attractive for practical use, since it automatically reduces effective LAI as LAI becomes large and as shading of interior leaves increases and air exchange inside canopies decreases. The equation may not apply to sparse vegetation such as in forests.

The LAI for dense, clipped grass can be computed following Allen et al. (1989) as:

$$LAI = 24\,h \tag{8.12}$$

where LAI is defined as the total leaf area (one side) per unit land area, $m^2\ m^{-2}$, and h is mean crop height, m, limited in eq. 8.12 to ≤ 0.4 m. The LAI for an alfalfa reference crop was estimated by Allen et al. (1989) as:

$$LAI = 5.5 + 1.5 \ln(h) \tag{8.13}$$

where h is in m and $h > 0.03$ m. Additional relationships for estimating LAI are given in chapter 11.

Stability Correction

The combination energy balance-aerodynamic methods (combination equations), that are used to estimate surface to air transfers, are far less affected by stability conditions than are the purely aerodynamic equations (for example, eq. 7.29), especially for near-potential evaporation conditions and when estimating reference crop ET. However, for watersheds and other non-irrigated environments where inadequate precipitation reduces evaporation or transpiration to levels much lower than reference ET, it is recommended that hourly calculations with

combination equations include stability correction expressions. These sorts of applications are described in chapter 11. Under inadequate water conditions, reduction in surface conductance functions (increases in surface resistance) may be an even more important consideration. Under reference conditions, the surface and air temperatures are generally within a few degrees of one another because $\lambda E \rightarrow R_n - G$ so that $H \rightarrow 0$ and $T_s \rightarrow T_a$. Therefore, stability correction is usually small and is ignored during calculation of reference ET (Allen et al. 2006c).

Examples of applying the PM equation to grass cover are included in chapter 11. The first of these examples (shown in fig. 11.12), showing half-hourly calculations with and without stability correction at Logan, UT and Davis, CA for the same days as in fig. 7.5, indicates that correction for stability over the well-watered grass surfaces was not nearly as important and critical for the PM equation as it was in estimating ET as $\lambda E = R_n - G - H$. The presence of $1/r_a$ in both the numerator and denominator of the Penman-Monteith equation (PM) dampens the effect of aerodynamic stability or instability (and wind speed) on the ET estimate.

8.4 Reference ET_{ref} K_c Approach

The most common application of the Penman or PM equations to date for estimating evapotranspiration has involved a two step process. The two steps are 1) the determination of a reference ET_{ref}, which has generally been for either clipped grass (Doorenbos and Pruitt 1977; Allen et al. 1998; ASCE-EWRI 2005; Allen et al. 2006c) or alfalfa (Wright and Jensen 1972; Wright 1982; Allen et al. 1989, 1996; ASCE-EWRI 2005) and 2) multiplying ET_{ref} by a crop coefficient, K_c, to obtain an estimate of actual ET for a particular crop or surface condition, where:

$$ET_c = K_c \, ET_{ref} \tag{8.14}$$

The K_c used in eq. 8.14 must be the K_c associated with the specific reference type used (grass or alfalfa).

The two step K_c ET_{ref} approach has been successful and widely applied for several reasons. One reason is the ready "visualization" of the crop coefficient, K_c, which generally has fixed limits governed by potential energy availability. Another reason for the widespread use of the K_c ET_{ref} approach has been the standardization of the ET_{ref} estimate (Smith et al. 1991; Allen et al. 1998; ASCE-EWRI 2005) and the general consistency of K_c. Relating ET_{ref} to a specific reference and utilizing K_c's in a two step process that separates processes between energy/aerodynamics and crop has the additional major advantage of giving the individual making calculations a mental representation of the process. In addition, it is relatively straightforward to select consistent crop coefficients and to validate reference equations in new areas.

The alternative to using the K_c ET_{ref} approach is the direct application of the Penman-Monteith or other multi-layer combination equation to estimate actual ET directly (Monteith, 1965; Shuttleworth and Wallace 1985). This approach, having the potential for more accurate estimates through more direct and graphic description of surface characteristics, is generally more difficult to apply and usually includes uncertainty in the exact nature of surface parameters as well as uncertainties that occur when using weather data collected above a surface that differ

from than that for which ET is estimated (Allen et al. 2005a). Also difficult is the incorporation of evaporation from underlying soil that varies with time and fraction of ground covered by vegetation. As discussed in Chapter 11, accurate application of the PM method to partial cover vegetation or to stressed vegetation requires the iterative determination of surface temperature to accurately incorporate the impacts of surface temperature on the calculation of Δ, boundary layer stability, and emitted long-wave radiation from the surface. The impacts of surface temperature on all three terms can be substantial as shown in Chapter 11.

When surface temperature is iteratively determined for the PM by solving the aerodynamic expressions for H and λE, the need for the PM equation is eliminated. In fact, the PM equation, when the relations for H and for Δ as functions of surface temperature are inserted into the PM equation, reverts to the original energy balance equation that employs aerodynamic equations for H and λE. Therefore, one can conclude that the PM method is only applicable to, and should be reserved for, well-watered conditions only, such as those represented by the reference ET definition. In fact, a well-watered surface, where surface temperature and air temperature can be assumed to be nearly equal because H is small, was a basic tenet and requirement of the Penman (1948) paper, where Δ was computed using air temperature only.

Reference ET types and definitions

For grass reference ET, ET_o, it is generally accepted that the reference crop is a "cool-season", C-3 type of grass with roughness, density, leaf area and bulk surface resistance characteristics similar to clipped perennial ryegrass (*Lolium perenne* L.) or clipped tall fescue (*Festuca arundinacea*). Alfalfa reference ET, ET_r, was defined by Wright and Jensen (1972) as: "*...ET from well watered, actively growing alfalfa with 8 in. (20 cm) or more of growth...*" and by Wright (1982) as "*...when the alfalfa crop was well watered, actively growing, and at least 30 cm tall; so that measured ET was essentially at the maximum expected level for the existing climatic conditions.*" The height of alfalfa (*Medicago sativa* L. v. ranger) in the data set used to develop surface resistance algorithms for the ASCE PM application to ET_r (Jensen et al. 1990) ranged from about 0.15 to 0.80 m in height and averaged 0.47 m (Allen et al. 1989).

Generally, reference ET for a tall crop like alfalfa is about 1.1 to 1.4 times that of a short crop like grass, ET_o, during summer months due to the greater roughness, higher leaf area, lower G, and lower r_s of alfalfa. The higher value (1.4) represents the ratio of ET_r to ET_o under extremely arid and windy conditions (minimum daytime relative humidity (RH) < 20%, and wind speed > 5 m s^{-1} (11 mph)) and the lower value (1.1) represents the ratio of ET_r to ET_o under humid, calm conditions (Pereira et al. 1999; Wright et al. 2000). ET_r is sometimes preferred over ET_o because its larger roughness and leafiness cause it to better approximate the upper limit of ET expected from all types of vegetation (Pereira et al. 1999). However, alfalfa does not grow well under some tropical conditions and at elevations above about 2000 m and can be difficult to manage within reference conditions and therefore is not universally available to evaluate ET_r estimates. Cool season grasses can be cultivated over a wide range of climates, seasons and elevations, for example, at 4000 m in Bolivia (Garcia et al. 2004), with the primary exceptions being lower elevations in hot tropical environments.

Because of the challenges in growing and maintaining living reference vegetation, where the LAI and thus the value for r_s can vary between clippings for grass or cuttings for alfalfa by nearly a factor of two, a calibrated ET_{ref} equation is now generally used to represent the "hypothetical" and “fixed” reference. The Food and Agriculture Organization (FAO) of the United Nations

(Smith et al. 1991, 1996; Allen et al. 1998) has adopted the PM equation as a standardized definition for ET_o where values for r_s, surface albedo, and aerodynamic roughness are fixed (FAO-56). FAO Irrigation and Drainage Paper No. 56 defined ET_o in terms of the PM equation as the rate of evapotranspiration from "*a hypothetical reference crop with an assumed crop height of 0.12 m, a fixed surface resistance of 70 s* m^{-1} *and an albedo of 0.23*," and where the reference surface "*closely resembles an extensive surface of green grass of uniform height, actively growing, completely shading the ground and with adequate water*."

Penman-Monteith as a Definition for Reference ET

The PM equation was introduced in its full form as equation (8.2). The PM formulation of the combination equation incorporates aerodynamic and surface resistance terms that represent physical characteristics of the particular reference crop. Aerodynamic resistance in equation (8.2) is generally calculated using eq. 8.3. Normally Ψ_m and Ψ_h are assumed zero because the reference surface is well-watered so that boundary layer stability is close to neutral or only mildly unstable or stable and values for Ψ_m and Ψ_h are small (Allen et al. 2006c). This simplifies the calculation process and allows for the use of standard weather data of air temperature, vapor content, wind speed and solar radiation.

Reference ET Calculations

A range in height in the reference crop definitions (both for grass and alfalfa) has been necessary to allow the use of field ET measurements in calibrating and validating ET_{ref} equations. However, it is necessary to standardize reference crop heights when applying ET_o and ET_r equations such as the PM equation in order to specifically characterize the surface parameters (roughness and bulk stomatal resistance) and to produce standardized climatic references. Allen et al. (1989), Jensen et al. (1990), Smith et al. (1991) and Allen et al. (1994ab, 1996) have suggested adapting a fixed height of 0.12 m for the grass reference and 0.5 m for the alfalfa reference in the PM equation and associated fixed values for r_s.

Standardization of the PM Equation for ET_{ref}

Standardized parameterizations of eq. 8.2 and 8.3 have been proposed by the ASCE-EWRI (ASCE-EWRI 2005) for both a short crop, ET_o, and a tall crop, ET_r, following the format adopted by FAO-56 (Smith et al. 1991; Allen et al. 1998). When the supporting parameter equations for r_a, ρ_a and λ are reduced and combined into eq. 8.2, the FAO styled and reduced equation of ASCE-EWRI results:

$$ET_{ref} = \frac{0.408\Delta(R_n - G) + \gamma \dfrac{C_n}{T + 273} u_2 (e_s - e_a)}{\Delta + \gamma (1 + C_d u_2)} \tag{8.15}$$

where ET_{ref} applies to both clipped grass and alfalfa reference surfaces. ET_{ref} has units of mm

d^{-1} for 24-hour time-steps and mm h^{-1} for hourly time-steps, R_n and G are in MJ m^{-2} d^{-1} or MJ m^{-2} h^{-1}, T is mean daily or hourly air temperature (°C), u_2 is mean daily or hourly wind speed at 2-m height (m s^{-1}), e_s and e_a are in kPa, Δ and γ are in kPa $°C^{-1}$, and C_n and C_d are coefficients that change with calculation time-step, reference type (grass ET_o or alfalfa ET_r), and, in some cases, with time of day, as shown in table 8.1. Standardized terms for 24-hour and hourly versions are summarized in table 8.2. The values for hourly C_d for ET_o are based on the use of r_s = 50 s m^{-1} during daytime and r_s = 200 s m^{-1} during nighttime and the 24-hour time-step value for C_d is based on r_s = 70 s m^{-1}. ASCE-EWRI (2005) and Allen et al. (2006c) provide additional background on r_s for ET_o. For ET_r, the values for hourly C_d are based on the use of r_s = 30 s m^{-1} during daytime and r_s = 200 s m^{-1} during nighttime and the 24-hour time-step value for C_d is based on r_s = 45 s m^{-1}. The standardized definitions imply vegetation heights for the ET_o and ET_r surfaces of 0.12 and 0.5 m, respectively.

Parameter equations recommended for use with the ASCE-EWRI standardized ET_{ref} are listed in table 8.3 Wind measured at heights other than 2 m above the ground surface can be adjusted to 2 m using eq. 6.5 if the wind measurement is made over clipped grass and using eq. 11.60 for wind measurement made over a surface other than clipped grass. Net radiation, R_n, in eq. 8.15 can be measured, but is usually estimated due to challenges and expenses associated with accurate and unbiased measurement. When estimated, ASCE-EWRI (2005) recommended standardized estimation procedures that use a fixed albedo of 0.23.

TABLE 8.1. Values for C_n and C_d in Equation 8.15 and Ratios of G/R_n used to Estimate Soil Heat Flux Density. Source: Data from ASCE-EWRI (2005).

Calculation Time-Step	Short Reference, ET_o			Tall Reference, ET_r			Units for ET_o, ET_r	Units for R_n, G
	C_n	C_d	G/R_n	C_n	C_d	G/R_n		
Daily	900	0.34	0.00	1600	0.38	0.00	mm d^{-1}	MJ m^{-2} d^{-1}
Hourly during daytime	37	0.24	0.10	66	0.25	0.04	mm h^{-1}	MJ m^{-2} h^{-1}
Hourly during nighttime	37	0.96	0.50	66	1.7	0.20	mm h^{-1}	MJ m^{-2} h^{-1}

When eq. 8.15 is used with daily values for C_n and C_d of 900 and 0.34, respectively, it is equivalent to the FAO-56 PM equation (Allen et al. 1998). However, when applied hourly, the values for C_n, C_d, and G/R_n vary from Allen et al. (1998), although they are the same as a more recent recommendation on application of the FAO-56 equation on an hourly or shorter basis, where the coefficients of ASCE-EWRI (2005) were recommended (Allen et al. 2006c).

The use of the standardized definitions for ET_o and ET_r provide for a consistent index of evapotranspiration that is readily compared between climates, locations and time periods. The definition, although standardized, is tied to measurable surfaces, so that the full predictive equation (8.2) can be compared to local measurements when desired or necessary. When calculation of ET_o and ET_r follows that of ASCE-EWRI (2005), the products are referred to as for ET_{os} and ET_{rs} where the 's' subscript refers to 'standardization.'

The wind height for eq. 8.15 is fixed in the standardization at 2 m above the surface for consistency with prior usage (Pruitt and Doorenbos 1977, Wright 1982, Allen et al. 1998).

However, the ASCE-EWRI (2005) report on standardization encourages wind measurement at 3 to 4 m height, with subsequent adjustment to the 2 m standardized height using eq. 6.5 or eq. 11.60. The higher measurement height reduces impacts of tall agricultural crops, such as corn, and local obstacles, such as trees, buildings and fences, on the wind measurement. Field corn is often taller than 2 m and can substantially reduce wind speed measured by nearby anemometers placed at 2 m (ASCE-EWRI 2005). Wind speed measured over vegetation that is taller than about 0.3 m should be adjusted to that expected over clipped grass using eq. 11.60.

Preferred Time Steps for Reference ET Calculation

The ASCE-EWRI (2005) standardization supports both 24-h and hourly (or shorter) calculation time steps. The 24-h calculation time step has proven to be relatively consistent and accurate for estimating reference ET (Doorenbos and Pruitt, 1977; Jensen et al. 1990; ASCE-EWRI 2005) and many lysimeter based studies have used the 24-h time step as a basis for calibration or verification of reference ET methods. ASCE-EWRI (2005) used the ASCE-PM equation and associated component equations on a 24-h calculation time step as the basis for the development of standardization of reference ET calculation in the USA. (Itenfisu et al. 2003). The general consistency and accuracy of the PM method for 24-h time steps speaks to the combination equation's robustness in estimating evaporative behavior given a particular set of meteorological conditions.

ASCE-EWRI (2005) conducted a comprehensive comparison of major reference ET equations using weather data from 49 sites across the United States. The 16 states contributing data ranged from New York to California and from Florida toWashington, and represented diverse climates, ranging from humid to arid (Itenfisu et al. 2003). Site elevations ranged from 2 to 2895 m and mean annual precipitation ranged from 150 to 2030 mm. ASCE-EWRI (2005) showed the ASCE-PM, when applied hourly to the 49 locations and then summed daily, to closely match estimates made on 24-hour calculation time steps. The yearly ratio of summed hourly to daily estimates for the alfalfa reference averaged 0.98 and ranged from 0.90 to 1.07 over the 49 locations and the growing season ratios averaged 0.995 and ranged from 0.90 to 1.08. The yearly ratio of summed hourly to daily estimates for the grass reference (defined by the standardized ASCE-EWRI PM equation) averaged 1.01 over all locations and ranged from 0.94 to 1.08 with a standard deviation in ratios of 0.029 (ASCE-EWRI 2005; Allen et al. 2006c).

The standardized PM method applied daily is considered to be accurate and dependable during growing periods. It was, in fact, used during the ASCE-EWRI standardization work to confirm the selection of surface resistance values for hourly time step applications. The daily time step, however, may not accurately estimate reference ET during freezing winter and other nongrowing season periods, where conditions represented by the reference crop do not physically exist (surface resistance of 45 s m^{-1} for ET_{rs} and 70 s m^{-1} for ET_{os} over a 24 h period). The hourly calculation time step, because it keeps radiation and aerodynamic parameters synchronized in time, is considered to be more dependable and accurate in simulating the ET conditions represented by the standardized definitions, especially under conditions where wind speed, solar radiation and vapor pressure deficit are not in proximate time synchronization during the day. The use of hourly calculation time steps calculates the energy balance process more accurately than 24-h time steps during times of the year when daylength is relatively short. During these times, some of the compensating assumptions in the procedures for applying the combination method on a 24-h time step may break down.

Application of ET equations over only daytime periods (i.e., ignoring calculations during nighttime) is discouraged. This practice ignores any ET that may occur during nighttime and that can be as much as 15% of 24-h ET in arid and semiarid climates (Tolk et al. 2006). In addition, application of the combination or energy balance equation for a daytime period, only, requires estimation of soil heat flux, G, which cannot be assumed zero as it generally can for 24-h calculation time steps.

Values calculated for reference ET for nighttime hours occasionally take on negative values. The user may feel compelled to set negative values to zero before summing over the 24-hour period. However, in some situations, negative hourly computed ET_{os} or ET_{rs} may indicate some condensation of vapor during periods of early morning dew and should therefore be registered as negative during the summing of 24-hour ET. In other situations, negative hourly ET_{os} or ET_{rs} during nighttime reflect the uncertainties in some parameter estimates including R_n and assumptions implicit to the combination equation, and represent some of the random variation of ET estimates about a mean value that may be zero during some nighttime periods. These random, negative ET estimates should be retained in the 24-h sum to counterbalance random, positive ET estimates during the same nighttime period. In general, the impact of negative hourly values on ET summed over daily periods is usually less than a few percent.

TABLE 8.2 ASCE Penman-Monteith Terms Standardized for Application of the Standardized Reference Evapotranspiration Equation. Source: Parameters from ASCE-EWRI (2005).

Term	ET_{os}	ET_{rs}
Reference vegetation height, h	0.12 m	0.50 m
Height of air temperature and humidity measurements, z_h	1.5 – 2.5 m	1.5 – 2.5 m
Height corresponding to wind speed, z_w	2.0 m	2.0 m
Zero plane displacement height, d	0.08 m	0.08 m [a]
Latent heat of vaporization, λ	2.45 MJ kg^{-1}	2.45 MJ kg^{-1}
Surface resistance, r_s, daily	70 s m^{-1}	45 s m^{-1}
Surface resistance, r_s, daytime	50 s m^{-1}	30 s m^{-1}
Surface resistance, r_s, nighttime	200 s m^{-1}	200 s m^{-1}
Value of R_n for estimating daytime	> 0	> 0
Value of R_n for estimating nighttime	≤ 0	≤ 0

[a] The zero plane displacement height for ET_{rs} assumes that the wind speed measurement is over clipped grass, even though the reference type is tall. This is done to accommodate a majority of weather stations that are located over grass or other smooth surface. When wind speed is measured over a surface having a vegetation taller than about 0.3 m, it is recommended that the wind speed measurement be adjusted using eq. 11.60.

TABLE 8.3. Equation Numbers[1] for Recommended Parameter Estimation in the ASCE-EWRI (2005) Standardized Penman-Monteith ET_{os} and ET_{rs} Equations.

Parameter	Daily calculation timesteps		Hourly calculation timesteps	
	ET_{os}	ET_{rs}	ET_{os}	ET_{rs}
Δ	eq. 3.2			
γ	eq. 3.11b			
λ	2.45 MJ kg^{-1}			
P	eq. 3.14			
α	0.23			
R_n	eq. 4.31, 4.39 with $(T_{max}^4 + T_{min}^4)/2$, 4.40	eq. 4.31, 4.39 with $(T_{max}^4 + T_{min}^4)/2$, 4.40	eq. 4.31, 4.39, 4.40, 4.41	eq. 4.31, 4.39, 4.40, 4.41
G	0	0	0.1 R_n daytime 0.5 R_n nighttime	0.04 R_n daytime 0.2 R_n nighttime
R_{so}	eq. 4.3, 4.4			
u_2	eq. 6.5 or 11.60 with d = 0.08 m and z_{om} = 0.015 m			
e_s	eq. 8.4b	eq. 8.4b	eq. 8.4a	eq. 8.4a
r_a[2]	eq. 8.3 or App. J	eq. 8.3 or App. J	eq. 8.3 or App. J	eq. 8.3 or App. J

[1] Equation numbers in cells refer to equations in the main text and appendices.
[2] r_a is imbedded into the standardized PM form, with integrated stability terms set to zero.

1985 Hargreaves-Samani Equation

The Hargreaves-Samani equation (Hargreaves and Samani, 1982; Hargreaves and Samani 1985) is suggested as a means for estimating ET_o in situations where data are limited and contain only maximum and minimum air temperatures along with location latitude. The Hargreaves-Samani (H-S) equation is not recommended in regions with consistently windy conditions [daily mean $u_2 > \sim 3.0$ m s^{-1}] and/or low RH_{min} [$RH_{min} < \sim 20\%$] without calibration or confirmation using the ASCE-PM method. The equation may tend to overestimate in humid climates (Hargreaves and Allen 2004a) and should be verified using the ASCE-PM method. The form of the 1985 H-S equation is:

$$ET_o = 0.0023 (T_{max} - T_{min})^{0.5} (T_{mean} + 17.8) \left(\frac{R_a}{\lambda \rho_w} \right) \quad (8.16)$$

where T_{max} and T_{min} are maximum and minimum daily air temperature in °C, T_{mean} is mean daily air temperature ($(T_{max} + T_{min})/2$), and R_a is average daily extraterrestrial radiation (eq. 4.11) with units of MJ m^{-2} d^{-1}. ρ_w is the density of liquid water [1.0 Mg m^{-3}]. ET_o in eq. 8.16 has the same units as $R_a / (\lambda \rho_w)$, typically mm d^{-1}.

The 1985 H-S equation was the highest ranked temperature related method for calculating ET_o reported in the ASCE Manual 70 analysis (Jensen et al. 1990). Allen (1992) found eq. 8.16 to estimate well in a wide range of latitudes and climates for periods of 5 days or longer without significant error.

The principal feature of the Hargreaves equation is the inclusion of the difference between maximum and minimum daily air temperature. The temperature difference provides an indication of general humidity and cloudiness. This occurs due to the fact that when humidity levels are high, differences between T_{max} and T_{min} are relatively low and ET rates are relatively low. The lower temperature differences occur because higher dew point temperatures under conditions of high humidity hold T_{min} to relatively higher levels. When cloud cover occurs, maximum temperatures are less due to decreased solar radiation, and minimum temperatures are usually higher due to increased long wave emittance and reflection by nighttime cloud cover.

One advantage of an equation such as the 1985 H-S equation over more complex equations is the reduced data requirement. For the 1985 H-S equation, only maximum and minimum air temperatures are required in addition to extraterrestrial solar radiation which can be calculated for any latitude. This is advantageous in regions where solar radiation, humidity and wind data are unavailable or are of low quality. Generally, air temperature can be measured with less error and by less trained individuals than can the other three parameters required by combination equations. Eq. 8.16 can be calibrated against the PM equation (eq. 8.15) where data are available to produce a "regionally" calibrated temperature equation.

An alternative to using a temperature-based equation such as eq. 8.16 when data are lacking is to employ the PM equation using estimates for missing variables. Generally, applying eq. 8.15 on a daily or monthly basis with R_s estimated using eq. 4.26 or eq. 4.27 with eq. 4.28 or 4.29, $T_d = T_{min} - K_o$, where K_o varies from 0 for humid regions to as much as 5°C for arid regions (ASCE-EWRI 2005) and $u_2 = 2$ m s^{-1} estimates similarly to eq. 8.16 for agricultural weather sites (Droogers and Allen 2002; Hargreaves and Allen 2004; Allen and Robison 2006). Appendix E of ASCE-EWRI (2005) contains recommendations for estimating missing weather parameters. Selected material from appendix E is presented in the following section.

ET_o Software Programs

Software programs for computing ET_{ref} by various common and popular ET_{ref} equations have been made available by Allen (2004) and Snyder (2004). These personal computer-based programs are useful for calculating ET_{ref} and comparing estimates among various reference equations and for validating ET_{ref} computations.

8.5 Missing or Bad Weather Data

The calculation of reference ET with the standardized ASCE PM reference ET equation requires air temperature, vapor pressure, solar radiation, and wind speed data. The climate data should reflect the environment within the area for which an estimate of ET is required. If some of the required weather data are missing or do not accurately represent an irrigated site/region or are erroneous, then data may be estimated in order to apply the equation. The quality of calculated reference ET values depends on the quality and completeness of weather data. If the estimated data for missing periods are reasonably representative of a site within an irrigated area, then it is likely that the reference ET values from the standardized equation calculated with these data will be more reliable than reference ET estimates made using other more empirical ET methods. This section provides procedures for estimating solar radiation, vapor pressure, and wind speed data when they are missing or of questionable quality. Users should employ some type of “flagging” procedure to clearly identify data that have been estimated.

Minimum Data Requirements

Many of the suggested procedures for estimating missing data are based on measured maximum and minimum air temperatures. Daily maximum and minimum air temperature, or at the very least, daily mean air temperatures are considered to be the absolute minimum data requirements necessary to apply the standardized PM method. In situations where solar radiation, humidity and wind speed data are available, but air temperature data are missing, temperature may be estimated from a nearby weather station site using some form of regression or interpolation-extrapolation procedures. Estimated temperature data should not be used at a site if the temperature data are subsequently used to estimate humidity and solar radiation data, as the resulting ET_{ref} would essentially have been calculated using no local data.

Estimating Missing Humidity Data

Where daily humidity data are missing or are of questionable quality, vapor pressure, e_a, can be estimated for the reference environment by assuming that dew-point temperature (T_{dew}) is near the daily minimum air temperature (T_{min}):

$$T_{dew} = T_{\min} - K_o \tag{8.17}$$

whereK_o is approximately 2 to 5°C in dry (semiarid and arid) climates and K_o is approximately 0°C in humid to subhumid climates. Allen and Robison (2006) developed values for K_o that varied monthly for application thoughout Idaho. The values were based on observations of K_o at automated weather stations located in agricultural environments. Under extremely dry conditions, such as in the American southwest, where daytime *RH* can drop near 10% even under reference conditions, K_o may take on values of 5 to 10°C. An alternative to applying eq. 8.17 is to assume that relative humidity, *RH*, approaches 90 to 100% during early morning hours (before sunrise) over well-watered (i.e. reference) settings so that the assumption that $RH_{max} \sim 90\%$ or $RH_{max} \sim 100\%$ can be employed. Daily vapor pressure is then calculated using the estimated RH_{max} and measured T_{min}:

$$e_a = e^o(T_{min})\frac{RH_{max}}{100} \tag{8.18}$$

where e_a is estimated vapor pressure, kPa, $e^o(T_{min})$ is saturation vapor pressure at daily minimum temperature, kPa and RH_{max} is daily maximum relative humidity. However, use of $RH_{max} \sim 100\%$ is equivalent to using $K_o \sim 0$°C in eq. 8.17, which may overestimate T_{dew}.

When humidity data are available from a nearby station, for example within 100 km, the user can estimate T_{dew} for a site having no humidity data or having faulty data using eq. 8.19:

$$T_{dew} = T_{\min} - (T_{\min} - T_{dew})_{stn\,2} \tag{8.19}$$

where $(T_{min} - T_{dew})_{stn\,2}$ is the measured difference at the nearby weather station. This relationship presumes that differences between T_{dew} and T_{min} are similar between stations. Similar results and

estimates of humidity can be obtained by transferring *RH* measurements between locations and calculating e_a using the transferred *RH* data and local air temperature. The similarity in relationships between T_{dew} and T_{min} or in *RH* should be confirmed using temporary measurement of humidity or by analysis of data from adjacent stations having overlapping periods.

By definition, reference ET_{os}, or ET_{rs}, is ET from an extensive surface of well-watered vegetation. Therefore, when humidity data are available only from a site that is known to deviate substantially from a reference environment, then use of "adjusted" dew-point temperature in the standardized PM equation may produce more reliable and representative reference ET than those obtained using the original humidity data from the non-reference site. The user should "flag" any estimated humidity data and describe the procedures that were used.

Estimating Missing Solar Radiation Data

Solar Radiation Data Derived from Observed Sunshine Hours. If observed hours of sunshine are measured, solar radiation for 24-hour and longer time periods can be estimated using the Angstrom formula, which relates solar radiation to extraterrestrial radiation and relative sunshine duration (Doorenbos and Pruitt 1977):

$$R_s = \left(a_s + b_s \frac{n}{N} \right) R_a \tag{8.20}$$

where R_s is solar or shortwave radiation, MJ m^{-2} d^{-1}, n is actual duration of sunshine, hours, N is the maximum possible duration of sunshine or daylight hours, n/N is relative sunshine duration, dimensionless, R_a is extraterrestrial radiation, MJ m^{-2} day^{-1}, (chapter 4), a_s is a constant expressing the fraction of extraterrestrial radiation reaching the earth's surface on overcast days (when $n = 0$), b_s is a constant expressing the additional fraction of extraterrestrial radiation reaching the earth's surface on a clear day, $a_s + b_s$ = fraction of extraterrestrial radiation reaching the earth's surface on a clear day (when $n = N$).

R_s in eq. 8.20 is in MJ m^{-2} d^{-1} for R_a in MJ m^{-2} d^{-1}. Depending on atmospheric conditions (humidity, dust), solar declination (latitude and month) and typical cloud type and density, the Angstrom values a_s and b_s will vary. Where no actual solar radiation data are available and no calibration has been carried out for improved a_s and b_s parameters, the values $a_s = 0.25$ and $b_s = 0.50$ from FAO-24 and FAO-56 are recommended. Accuracy of eq. 8.20 and values for coefficients a_s and b_s should be assessed at a location in the region where measured R_s and n data are available.

The potential daylight hours, N, are given by:

$$N = \frac{24}{\pi} \omega_s \tag{8.21}$$

where ω_s is the sunset hour angle in radians and is calculated using eq. 4.14.

Solar Radiation Data from a Nearby Weather Station. For 24-hour and longer time periods, solar radiation can be relatively similar over large areas. Similarity in solar radiation depends on: (i) the size of the region; (ii) the air masses governing rainfall and cloudiness being similar

across the region; and (iii) the physiographic characteristics are similar. Differences in relief can strongly influence the movement of air masses and development of cloud systems, so that these should be small if radiation data are to be transferred between locations. Generally, calculations of daily reference ET using estimated radiation data are justified when utilized as a sum or as an average over a multiple-day period so that differences due to frontal activity or individual convective cloud systems tend to average out. This is the case for the computation of total ET demand between successive irrigations or when planning irrigation schedules. Under these conditions, the relative error for one day may be compensated by an error for another day within the time period.

Solar Radiation Data Derived from Air Temperature. Solar radiation can be estimated using an empirical equation derived using the difference between maximum and minimum air temperature and extraterrestrial solar radiation. The difference between the maximum and minimum air temperature is related to the degree of cloud cover at a location. Clear-sky conditions result in higher air temperatures during the day (i.e., T_{max}) than under cloudy conditions because the atmosphere is transparent to incoming solar radiation. Clear-sky conditions result in relatively lower air temperatures during nighttime (i.e., T_{min}) than under cloudy conditions because less outgoing long-wave radiation is absorbed and reemitted by the atmosphere. On the other hand, under overcast conditions, T_{max} is often lower than for clear days because a significant portion of the incoming solar radiation never reaches the earth's surface and is absorbed and reflected by the clouds. Similarly, T_{min} will be relatively higher because cloud cover acts as an absorbing and reemitting blanket and therefore decreases the net outgoing long-wave radiation. Therefore, the difference between the maximum and minimum air temperature (T_{max} - T_{min}) can be used as an indicator of the fraction of extraterrestrial radiation that reaches the earth's surface. This principle was used by Hargreaves and Samani (1982) to develop estimates of ET_o using only air temperature data. The Hargreaves-Samani style of radiation prediction formula (also introduced as eq. 4.26) has the form:

$$R_s = k_{Rs} \sqrt{(T_{\max} - T_{\min})}\, R_a \qquad (8.22)$$

where R_a is extraterrestrial radiation, MJ m^{-2} d^{-1}, T_{max} is maximum air temperature, °C, T_{min} is minimum air temperature, °C, and k_{Rs} is an adjustment coefficient (0.16 .. 0.19), °C$^{-0.5}$. The adjustment coefficient k_{Rs} is empirical and differs for 'interior' or 'coastal' regions[1]:

- for 'interior' locations, defined as where the local land mass dominates and air masses are not strongly influenced by a large water body, $k_{Rs} \cong 0.16$;
- for 'coastal' locations, situated on or adjacent to the coast of a large land mass and where air masses are influenced by a nearby water body, $k_{Rs} \cong 0.19$.

R_s estimated by eq. 8.22 should be limited to $\leq R_{so}$ which is the R_s for a cloud-free day. The temperature difference method is recommended for locations where it is not appropriate to import radiation data from a regional station, either because homogeneous climate conditions do not occur, or because data for the region are lacking. For island conditions, the methodology is not appropriate due to moderating effects of the surrounding water body. Bristow and Campbell (1984) developed an equation similar to eq. 8.22. However, their formulation is more complex

[1] The values presented here for k_{Rs} are from Allen et al. (1998).

to apply and is of similar accuracy (Ball et al. 2004). Allen (1997) demonstrated the application of eq. 8.22 with means to auto-calibrate K_{Rs} using the R_{so} clear sky envelope for seven locations in the western U.S. Amatya et al. (2000) found the Allen auto-calibration technique to provide good estimates of daily solar radiation at three locations in North Carolina. The Thornton and Running (1999) equation for estimating R_s from air temperature built on Bristow and Campbell (1984) and was introduced as eq. 4.27-4.28. The Thornton-Running method has advantages over eq. 8.22 in that it is self-limiting to R_{so} as an upper bound and tends to estimate more representative ranges in R_s under cloudy conditions, as illustrated by Allen and Robison (2006).

Missing Wind Speed Data

Wind Speed Data from a Nearby Weather Station. Extrapolating wind speed data from a nearby agricultural weather station, as for radiation data, relies on the assumption that the airflow is similar within the region. There can be large variation in wind speed through the course of a day, which can translate into substantial differences in concurrent measurements of wind speed at two locations. However, when averaged over time periods of one day or longer, differences between locations become smaller. Data from a weather station may be extrapolated to a nearby location where ET_{ref} is to be estimated if the governing air masses are of the same origin and where the same weather frontal systems govern the regional air flow. The surrounding relief of the two locations should be similar. In areas having large differences in relief, density-induced "drainage" of air and shielding and direction of air movement by relief can cause substantial differences in observed wind speed over relatively short distances. Where short periods of wind data are available for the location, ratios of wind speed between two locations can be established and used to estimate wind data for the data-short location.

Wind speed data from airports in the U.S. typically are measured at a height of 10 m. In arid and semiarid areas, the airport anemometer is often surrounded by non-irrigated, short grass. Wind speed from airports measured at 10 m height, when adjusted to 2 m height using the logarithmic wind profile, may exceed wind speed that is measured at 2 m height in an agricultural area during the growing season. This can occur because of larger vegetation roughness of agricultural crops as compared to airport environments, and more entrainment of higher velocity air from aloft over an airport because of increased air buoyancy caused by larger H.

When extrapolating wind speed data from another station, trends in other meteorological parameters and relief should be compared. Strong winds are often associated with low relative humidity and light winds are common with high relative humidity. Thus, trends in variation of daily maximum and minimum relative humidity should be similar in both locations. In mountainous areas, data should not be extrapolated from the nearest station but from nearby stations having similar elevation, similar vegetation surrounding the sensors, and exposure to the dominant winds. The pairing of stations may vary from one season to another, depending on the dominant winds.

Empirical Estimates of Monthly Wind Speed. The variation in average wind speed between monthly periods is often relatively small and fluctuates around average values. Therefore, in situations of no, or faulty, wind speed data, monthly values of wind speed may be estimated based on general information available for the regional climate, taking seasonal changes into account. Or, if regional information is unavailable, general values for wind speed suggested in table 8.4 can be employed with caution.

TABLE 8.4 General Classes of Wind Speed Data. Source: Data from FAO-56, Allen et al. (1998).

Description	mean wind speed at 2 m
light wind	≤ 1.0 m s^{-1}
light to moderate wind	1–3 m s^{-1}
moderate to strong wind	3–5 m s^{-1}
strong wind	≥ 5.0 m s^{-1}

A preliminary value of 2 m s^{-1} can be used as a first estimate of 2-m wind speed for an agricultural setting. This value is based on an average computed from over 2 000 weather stations around the globe (Allen et al. 1998). In general, estimated wind speed at 2 m should be limited to about $u_2 \geq 0.5$ m s^{-1} when used to calculate standardized reference ET. This lower limit accounts for the influence of boundary layer instability caused by buoyancy of air in promoting exchange of heat and vapor at the surface when air is calm. This effect occurs when the wind speed is small and buoyancy of warm air induces air exchange at the surface. As with humidity and solar radiation data, estimated wind speed data should be flagged in the data set and the user should describe procedures that were used to make the estimates.

A growing source of wind data is the use of 'gridded' weather data becoming more readily available from the North American Land Data Assimilation System (NLDAS) and Global Land Data Assimilation System (GLDAS). These data sets are described in a following section. The 'reanalysis' data sets provide some gridded data back to the 1950's are available via the internet. Certain precautions are needed in using these data sets for agricultural areas.

Missing Maximum or Minimum Air Temperature Data

Some weather data sets contain daily mean air temperature summaries, but do not contain values for maximum and minimum air temperature. Daily maximum and minimum air temperatures are used in the standardized reference ET procedure for calculating net radiation and the saturation vapor pressure. During the process of calculating daily ET_{ref} using data sets where T_{max} and T_{min} are not available, but where daily mean air temperature and solar radiation data are available, accuracy of calculations for net radiation and saturation vapor pressure can be improved by estimating values for T_{max} and/or T_{min} by inverting eq. 8.22 and solving for T_{max} - T_{min}:

$$(T_{max} - T_{min})_{est} = \left(\frac{R_s}{k_{Rs} R_a} \right)^2 \tag{8.23}$$

where R_s is measured solar radiation, MJ m^{-2} d^{-1}, R_a is extraterrestrial radiation, MJ m^{-2} d^{-1}, T_{max} is maximum air temperature, °C, T_{min} is minimum air temperature, °C, and k_{Rs} is an adjustment coefficient, defined previously, °C$^{-0.5}$.

Values for T_{max} and/or T_{min} can be estimated using $(T_{max} - T_{min})_{est}$ from eq. 8.23 as:

$$T_{max} = T_{mean} + \frac{(T_{max} - T_{min})_{\text{est}}}{2} \tag{8.24a}$$

$$T_{\min} = T_{mean} - \frac{(T_{\max} - T_{\min})_{\text{est}}}{2} \tag{8.24b}$$

The estimated values for T_{max} and T_{min} should be clearly identified in the data set as estimated values.

Gridded Weather Data from Climate and Land Process Models

Until recently, the modeling of reference ET has been solely based on important weather variables collected from weather stations that are generally located on selected agro-climatic locations. Since 2000, the North American Land Data Assimilation System (NLDAS) and Global Land Data Assimilation System (GLDAS) operated by the National Oceanic and Atmospheric Administration (NOAA), National Centers for Environmental Prediction (NCEP) and National Center for Atmospheric Research (NCAR) have produced climate parameter data sets each three and six hours that include the meteorological variables required to calculate daily reference ET. These data sets are produced for the whole globe at 1 degree spatial resolution and for North America at 12 and 32 km resolution. The data are produced by relatively complex land process models operated for weather forecasting and climate change modeling. The models are 'forced' using available weather measurements from selected sites around the globe. Results are generally available from NOAA and other web sites.

The USGS at the Center for Earth Resources Observation and Science (EROS) has been producing daily reference ET since 2000 (Senay and Verdin 2003) and the results have been used for a variety of models for drought and stream flow monitoring on an operational basis. Senay et al. (2005) and Senay et al. (2007) evaluated GLDAS-based reference ET estimates using data from the California Irrigation Management Information System (CIMIS). Daily CIMIS ET_o estimates from over 120 stations were compared with GLDAS-based ET_o at different spatial and temporal scales using 2004 data. Despite large differences in spatial scale (point measurements for CIMIS vs approximately 100 km gridded data for GLDAS), correlations between station-based ET and GLDAS-ET were high, exceeding 0.90 on a daily-basis to more than 0.98 on time scales of over 10 days (Senay et al. 2005).

A second gridded data set is the IWMI World Water and Climate Atlas[2] that includes monthly and annual summaries for weather data on a 10 minute arc (one-sixth of a degree) grid. The data include precipitation, air temperature, humidity, hours of sunshine, wind speed, total number of days with and without rainfall, days without frost and reference ET_o based on the FAO Penman-Monteith equation. The atlas grid was assembled from 30,000 weather stations

[2] http://www.iwmi.cgiar.org/WAtlas/

around the globe from the period 1961-1990. The Atlas data are intended to support irrigation and agricultural planning.

When used to calculate ET_{ref}, the GLDAS, NLDAS and other data sets should be reviewed to determine whether the gridded data contain substantial 'artifacts' of dryness of the original weather data used to drive the models and assumptions in the GLDAS models. These artifacts may produce weather data that are characteristic of regional weather systems, which in semiarid and arid climates, reflect general aridity of the region, and may not exhibit the conditioning effects of irrigation where air temperature is reduced and humidity content is increased by ET supplied by irrigation. Generally, the models creating the gridded data sets do not include irrigation in the daily soil water balances used to partition available energy into H and ET. The user can review daily RH_{max} or dewpoint and daily minimum air temperature data in the gridded data sets following recommendations by ASCE-EWRI (2005) to assess general aridity of the data sets. ET_o from the IWMI Climate Atlas were evaluated for aridity effects by Droogers and Allen (2002).

8.6 Reference ET by Analogy or Association

Evaporimeters and Atmometers

The use of evaporation pans to estimate evaporation from water bodies was introduced earlier along with some of the factors that can produce a wide range of results as related to the local environment, placement, size of pan, etc. Pans and atmometers have been used more widely in estimating crop water use than in lake evaporation estimation. Pruitt and Doorenbos (1977) listed fifteen references that involved some eight different countries where the pan evaporation method was used significantly in irrigation scheduling schemes. In terms of the percentage of irrigable land within a country, where evaporation pans have played an important part, the country of Israel probably leads the list. An early reference for Israel was that of Stanhill (1962) with summarization of ET/E_p relationships for many crops reported later by Shalhevet et al. (1981). A description of various types of evaporation pans is given in chapter 6.

Reference ET From Pan Evaporation. Pan evaporation data can be used to estimate ET_{ref} from the simple proportional relationship of:

$$ET_{ref} = k_p \, E_p \tag{8.25}$$

where ET_{ref} is reference crop ET, k_p is a pan coefficient that is dependent on the pan type involved and a number of other factors as discussed earlier, and E_p is measured pan evaporation. When the reference crop is short, well-watered grass, the reference ET is referred to as ET_o. Pruitt and Doorenbos (1977) gave the background of the development of the FAO-24 Pan Evaporation method that was first published in Jensen (1974) and subsequently by Doorenbos and Pruitt (1975,1977), Burman et al. (1980), Jensen et al. (1990), Shuttleworth (1992), ASCE Hydrology Handbook (Wootton et al. 1996), and Allen et al. (1998). The method was based primarily on studies on the effect of pan type, local environment and general weather conditions on k_p by Ramdas (1957), Pruitt (1960; 1966) and Stanhill (1962).

The FAO-24 Pan method provided tables of recommended k_p's for the Class A pan, upwind fetch of both dry- and wet-surface environments, mean relative humidity, and daily wind run. Table 8.5 reproduces the original tables for the Class A pan as developed by Pruitt in the FAO analysis, rounded off to the nearest 0.01 rather than to 0.05. Fig. 8.1 presents a sketch explaining an idealized situation for both dry (CASE A), and wet (CASE B) upwind fetches.

Many weather stations will not easily fit into the simplified classifications suggested in fig. 8.1. One exception is illustrated by a weather station planted to Bermuda grass which was dormant during several months of the year (CASE B) and was a green, growing crop during other months (CASE A). The CASE B classification might apply well for weather stations having bare soil environments during dry seasons of the year, but CASE A may be more appropriate during consistently rainy periods. Another complicated situation was envisioned by Doorenbos and Pruitt (1977), suggesting that when pans are placed in a small enclosure surrounded by tall crops, the coefficients for dry, windy climates should be increased by up to 30% to account for shielding of wind over the pan, but for calm, humid conditions, a 5 to 10% increase should be sufficient to compensate for wind shielding of the pan by the tall crop, since under humid conditions, evaporation is dominated by solar radiation.

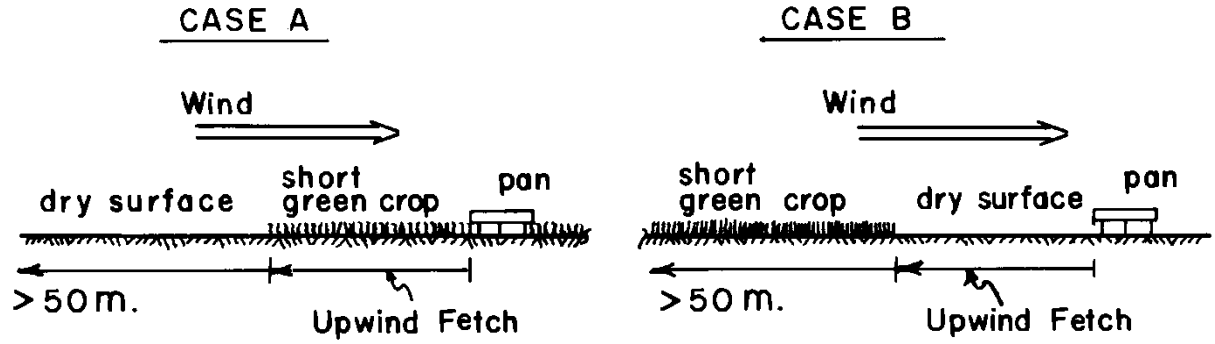

Fig. 8.1. Example environments of surroundings of evaporation pans for FAO-24 method. Source: Figure from Doorenbos and Pruitt (1975, 1977). Reproduced with permission.

In addition to the variation of k_p with wind and humidity, there is also an interaction with radiation intensity. Since smaller coefficients under drier and windier conditions are largely the result of greater response of pans to sensible heat advection as compared to crops (short, smooth crops) , the relative effect (and hence, coefficients) will be greater under the lower-radiation conditions of fall, winter, and spring than under the higher radiation of midsummer (Jensen et al. 1990).

Pan Coefficients

The coefficients in table 8.5 apply to National Weather Service (NWS) Class A pans mounted on a standard wooden platform such that the top of the pan is about 0.4 m above the surrounding ground level. For the CASE A siting, the grass should be irrigated during dry periods, frequently enough to insure low leaf resistances at all times and the extent of the grass surface should be 50 m in all directions. Also presumed is the maintenance of a water level within a zone ranging from 0.05 to 0.075 m below the top of the pan. If the pan is protected from birds, e.g. with 12.5-mm

(0.5-inch) mesh screen, coefficients should be increased 5 to 10% (Stanhill 1962). Pans made of monel metal, or older galvanized metal pans which have lost their original reflectance characteristics, may need a reduction of k_p of up to 5%. In general the water should be kept clean although turbidity differences appear to produce little difference in evaporation from Class A pans. The need to avoid contamination by oil-related products should be evident.

TABLE 8.5 Suggested Values of k_p for Relating Evaporation from a USA Class A Pan to ET from 0.08-0.15 m Tall, Well-watered Grass Turf (ET_o). Based on Original FAO Analysis Leading to FAO-24 Pan Method. Source: Data from Doorenbos and Pruitt (1975, 1977).

	CASE A: (Pan surrounded by Short, Green, Growing Crop, preferably grass, or a wet soil surface)				**CASE B**: (Pan surrounded by Dry, Bare Soil or Dry, Dormant Grass)			
		$(RH_{max} + RH_{min})/2$				$(RH_{max} + RH_{min})/2$		
2-m Wind km/day	Wet Upwind Fetch,m	Low <40%	Med 40-70%	High >70%	Dry Upwind Fetch,m	Low <40%	Med 40-70%	High >70%
Light	0	0.55	0.64	0.73	0	0.7	0.8	0.85
<175 km/d	10	0.66	0.75	0.82	10	0.6	0.7	0.8
(<2 m/s)	100	0.74	0.81	0.85	100	0.55	0.65	0.75
	1000	0.77	0.83	0.87	1000	0.5	0.6	0.7
Moderate	0	0.50	0.58	0.65	0	0.65	0.75	0.8
175-425 km/d	10	0.60	0.68	0.75	10	0.55	0.65	0.7
(2-5 m/s)	100	0.66	0.73	0.78	100	0.5	0.6	0.65
	1000	0.70	0.77	0.81	1000	0.45	0.55	0.6
Strong	0	0.45	0.52	0.59	0	0.6	0.65	0.7
425-700 km/d	10	0.52	0.60	0.67	10	0.5	0.55	0.65
(5-8 m/s)	100	0.58	0.66	0.71	100	0.45	0.5	0.6
	1000	0.62	0.70	0.75	1000	0.4	0.45	0.55
Very Strong	0	0.4 0	0.46	0.52	0	0.5	0.6	0.65
>700 km/d	10	0.45	0.53	0.61	10	0.45	0.5	0.55
(>8 m/s)	100	0.50	0.59	0.65	100	0.4	0.45	0.5
	1000	0.55	0.63	0.68	1000	0.35	0.4	0.45

For those using computer programs in estimating ET_o from the FAO Pan method, polynomial equations based on the data in table 8.5 were developed by Allen and Pruitt (1991) and published in Jensen et al. (1990), App. E and Allen et al. (1998). The equation for CASE A estimation of k_p is:

$$K_p = 0.108 - 0.0286u_2 + 0.0422\ln(Fetch) + 0.1434\ln(RHmean) - 0.000631[\ln(Fetch)]^2 \ln(RH_{mean}) \quad (8.26)$$

where u_2 is wind run at 2-m height in m s^{-1}, $Fetch$ is the upwind fetch in meters, and RH_{mean} is the average of daily maximum and daily minimum relative humidity in percent. For CASE B situations (dry fetch upwind), the suggested equation is:

$$K_p = 0.61 + 0.00341RH_{mean} - 0.000162u_2\,RH_{mean} - 0.00000959u_2\,Fetch + 0.00327u_2\ln(Fetch) - 0.00289u_2\ln(86.4u_2) - 0.0106\ln(86.4u_2)\ln(Fetch) + 0.00063[\ln(fetch)]^2\ln(86.4u_2) \quad (8.27)$$

Limits should be imposed on the above equations to avoid unreasonable estimates. They are: $30 \le RH_{mean} \le 84\%$; $1 \le u_2 \le 8$ m s^{-1} and $1 \le Fetch \le 1000$ m.

Thom et al. (1981) developed a "reasonably physically-based" approach to using Class A pan evaporation, although their paper did not deal specifically with upwind fetch conditions and distances, a factor of importance in semi-arid to arid conditions. Therefore, users must be cautious in applying this methodology.

More recently, Snyder et al. (2005) reviewed equations used to estimate grass reference ET from E_p and provided a simple method to convert pan evaporation to ET_o for conditions like those in California. The method accounts for fetch differences by first adjusting E_p rates to expected values for 100 m of grass fetch. Then, an empirical relationship between ET_o and adjusted E_p is used to determine ET_o values. The method eliminates the need for relative humidity and wind speed data which are often not available. The resulting equation was developed to estimate the fetch adjustment factor equivalent to 100 m of grass fetch (F_{100}) based on actual fetch distances:

$$F_{100} = -0.0035[\ln(Fetch)]^2 + 0.622[\ln(Fetch)] + 0.79 \quad (8.28)$$

where $Fetch$ is the actual amount of (well watered) green fetch in m. Then $E_{pa} = F_{100}$ x E_p provides an estimate of pan evaporation from a pan surrounded by 100 m of fetch, with the restriction that $E_{pa} \le 19.2$ mm d^{-1}. Then ET_o is estimated using the following equation:

$$ET_o = 10\,sin\left[\left(\frac{E_{pa}}{19.2}\right)\frac{\pi}{2}\right] \quad (8.29)$$

where ET_o and E_{pa} are in mm d^{-1}.

Atmometers

Atmometers are a class of small evaporimeters that generally consist of a wet, porous surface that is fed by a connected water reservoir. In some cases, the surface is covered with a fabric to simulate solar radiation characteristics of vegetation and to increase resistance to evaporation to mimic ET from vegetation. The water reservoir is filled with distilled water that evaporates out of the surface via a suction tube. Some atmometers have a special membrane to keep rain water from seeping into the porous surface. Atmometers are typically mounted on a post near or within

agricultural fields and are finding use in irrigation scheduling (Broner 1993; Irmak et al. 2005). Manually-read and electronically monitored atmometers are commercially available.

Phene et al. (1990) reviewed the use of several types of atmometers to estimate reference ET_o. Because of their low cost and ease of use, atmometers or evaporimeters have acceptance where weather station data or pan evaporation data are not available. Brutsaert (1982) described three types of atmometers that are in limited use today – the Piche evaporimeter developed in France, the Wild evaporimeter developed in Russia, and the Bellani-Livingston evaporimeter developed in Italy as a flat porous disk (Bellani) and now available commercially in the U.S.

The Piche atmometer is constructed with a transparent glass tube sealed at the top that is about 0.2 to 0.3 m long and 10 to 30 mm in diameter with a disk of moist blotting paper that is 800 to 1300 mm^2 exposed on the bottom. A small hole on the side of the tube serves as an air vent. The tube is filled with water, and as water evaporates from the paper, which is held in place with a steel wire spring, the water level will sink in the tube. The instrument is installed about 1.2 m above the ground in an instrument shelter. The evaporation from the Piche atmometer was related to the drying power of the atmosphere by Stanhill (1962) and Brochet and Gerbier (1972), and Thom et al. (1981) empirically inserted the Piche evaporation into the aerodynamic term of the Penman equation. Brochet and Gerbier developed procedures to estimate constants for the aerodynamic-Piche term for any latitude or time of year in France.

The Wild evaporimeter has a shallow cylindrical dish about 25 mm deep and 178 mm in diameter, filled with water and placed on a counter-balanced scale. The instrument is deployed similarly to the Piche atmometer at about 1.2 m above the ground in a shelter.

The Bellani-Livingston evaporimeter is a porous surface with a flat disk used for the Bellani type and a spherical surface used for the Livingston type (Livingston 1935). This instrument, unlike the Piche and Wild evaporimeters, can be directly exposed to the environment. Altenhofen (1985) modified the Bellani atmometer by placing various types and thicknesses of green canvas cover over the ceramic top to simulate the resistance and albedo of a green leaf. Evaporation from this instrument has been shown to correlate well with reference ET equations using meteorological data (Broner and Law 1991; Altenhofen, 1985; Irmak et al. 2004, 2005). An electronic readout version of the instrument is available for automatic recording or irrigation control (Parchomchuk et al. 1996) as well as canvas covers that simulate the surface resistances for either grass or alfalfa.

Precautions to be exercised with atmometers include the placement of the instruments and the dryness of the local environment. Similar to weather stations used to provide data for calculating reference ET, atmometers should be placed in local environments that are similar to those of the vegetation for which they are to provide ET indication, in terms of amount of relative wetness of the surrounding surface or vegetation. Manufacturers of the systems generally provide advice on standardized mounting heights for the instruments to produce desired aerodynamic exchange. However, the height of surrounding vegetation should be considered, especially with tall vegetation such as corn. Because of the 'artificial' surface of the atmometer system, the evaporation measurements should not be expected to reproduce calculated reference ET exactly. Because atmometers respond to the dryness of the surrounding environment, it might be possible to use atmometers to evaluate the impact of weather station dryness on the ET_{ref} calculation by locating one atmometer in the weather station environment and a second atmometer within a few km from the station, but in a more well-watered 'reference setting.' The ratio of evaporation from the two atmometers may give some indication of the 'aridity effect' of the weather station on calculated ET_{ref}. Research is needed on this application.

9

Evapotranspiration from Land Surfaces: Evaporation from Soil

9.1 Introduction

This chapter focuses mainly on evaporation from bare or nearly bare soils and includes procedures for adjusting estimated evaporation for partial plant cover. Estimates for evaporation from bare soil are important early and late in crop growing periods and during nongrowing periods, and for estimating effects of wet soil within vegetation on total ET. Evaporation losses from soil can comprise a substantial part of the total water balance under rainfed conditions in dry climates. A recent review of literature by Burt et al. (2005) describes some general models for estimating evaporation from soil and plant canopies as well as some experimental findings.

9.2 The Evaporation Process

When non-cracking soils dry, the soil water content initially decreases exponentially towards the surface as observations of soil water profiles have shown. For example, Rose (1968a) measured soil water profiles during drying and found that the soil water content in a sandy soil after four days was near air-dry at the surface and increased to near field capacity at a depth of 0.12 to 0.15 m. Hanks et al. (1967) measured soil water profiles in the laboratory when drying occurred under either wind or radiation conditions and reported similar profiles. Jackson (1973) conducted a comprehensive study of evaporation on a loam soil near Phoenix, AZ. He measured soil water profiles by 0.01 m increments to a depth of 0.09 m for 16 days after irrigation in July 1970 and for 37 days after irrigation during a relatively humid and cool period during March-April 1971 (fig. 9.1). The distribution of soil water for the first 10 days after irrigating showed an exponential distribution with depth similar to that reported by Rose (1968a). Profiles at 25 and 37 days tended to become less exponential in this upper layer.

Evaporation from bare soil has often been divided, time-wise, into two or three stages that characterize the form or nature of control on the evaporation process and rate. Stage 1 evaporation was defined by Ritchie (1972) and others as the rate of evaporation following wetting when the evaporation rate is limited only by energy availability. During stage 1, the soil is sufficiently wet so that water is transported to the surface at least at a rate equal to the evaporation potential. The duration of stage 1 and the amount evaporated are related to the hydraulic conductivity and water-holding capacity of the soil and evaporative conditions. In stage 2, the surface soil water content has decreased to where the hydraulic capacity of the soil is unable to supply the potential, energy-limited rate. The evaporation rate during stage 2 progressively decreases with time, often in proportion to the square root of time, as described later. Fig. 9.2 shows a typical evaporation trend line with stages 1 and 2. Occasionally, for example, with deep-cracking soils, a third evaporation stage is added, where a low, long-term evaporation rate is supplied by water exposed by deep cracks (Idso et al. 1974; Ritchie and Adams, 1974; Allen et al., 2005c, Burt et al. 2005).

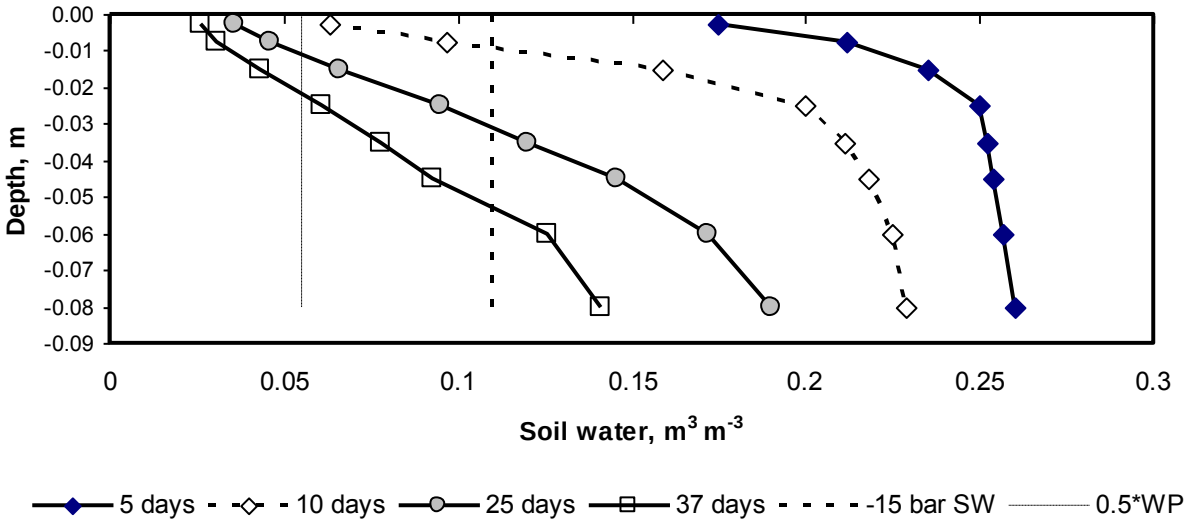

Fig. 9.1. Soil water distribution in a loam soil on day 5, 10, 25 and 37 after wetting near Phoenix, Arizona during March-April 1971. Source: Data from Jackson (1973).

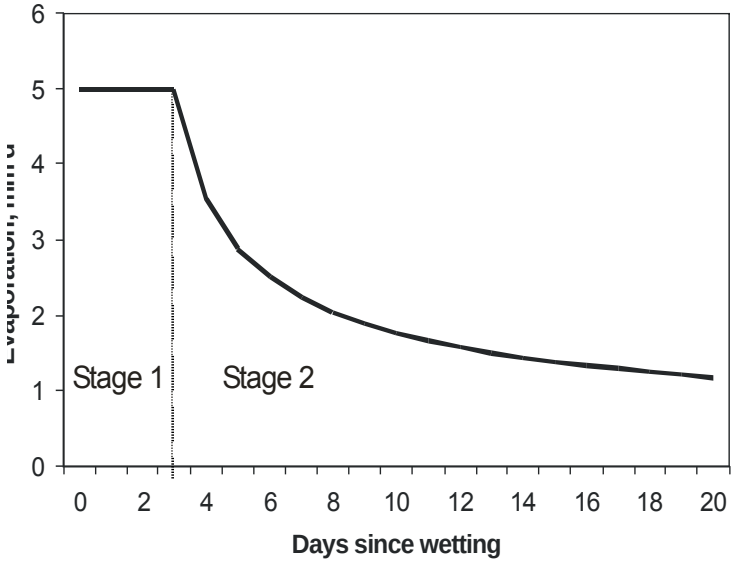

Fig. 9. 2. Idealized evaporation rate curve from bare soil showing sharp transition between stage 1 and stage 2 evaporation where the potential evaporation rate is 5 mm d^{-1}.

9.3 Diurnal Effects and Redistribution of Soil Water

Jackson made measurements of the 0–0.09 m surface layer at hourly intervals for 7 days in 1970 and at half hour intervals for 19 days in 1971. These data showed that large diurnal changes occur in the surface layer during the evaporation process similar to those shown by Rose (1968a). At the end of 7 days in July 1970, 69% of the total water evaporated came from the 0-

0.09 m depth. At the end of 16 days in March 1971, 66% of the total water evaporated came from the 0–0.09 m depth indicating an upward flux of about 1/3 of the evaporated water from below the top 0.09-m layer.

As the surface of the soil dries, the rate of evaporation decreases as the resistance to evaporation increases. In a field study on bare soil, van de Griend and Owe (1994) used an air circulation chamber to measure surface resistance to vapor diffusion in drying of the top soil in central Spain. Measurements were made on a fine sandy loam during a 13-day dry down period after wetting. Surface resistance began to increase at a water content of 15% by volume in the 0.01-m top layer, which was 50% of field capacity. The measurements showed a very pronounced diurnal pattern due to drying of the very top layer during the day and recovery of the soil water profile during nighttime hours similar to that reported by Rose (1968a) and Jackson (1973).

9.4 Stage 1 Evaporation

Stage 1 evaporation is defined as the rate of evaporation following wetting when the evaporation rate is limited only by energy availability. The evaporation rate during stage 1 drying is a function of evaporative drying power of the atmospheric boundary layer and is generally estimated as a coefficient $K_{e\ max}$ times reference ET_{ref}, as described in eq. 9.1 where ET_{ref} is reference ET for clipped grass, ET_o, or alfalfa, ET_r. The duration of stage 1 and the start of stage 2 may range from one to several days after rainfall or irrigation depending on the amount of water applied, the soil, and evaporative conditions.

The total depth of cumulative evaporation during stage 1, referred to as readily evaporable water (*REW*) in the FAO-56 procedure, varies with soil type. *REW* can be estimated using *REW* values from table 9.1 based on recommendations by Ritchie et al. (1989) or using eq. 9.23a-c presented later. Ritchie (1972) presented cumulative amounts of stage 1 evaporation for four soils ranging from 6 mm for sand to 12 mm for a clay loam. Stage 2 evaporation is often said to begin when the soil surface becomes visibly dry for most of the day. Local observation of *REW* is recommended. During stage 2, the evaporation rate (E_2) is governed by the flux of water through the upper layer of soil to or near the evaporation site and is limited by $K_{e\ max}\ ET_{ref}$.

The rate of E for stage 1 drying can be estimated using reference ET to represent potential evaporation energy as:

$$E_1 = K_{e\ max}\ ET_{ref} \tag{9.1}$$

where E_1 is the evaporation rate during stage 1, which can change daily, depending on the value for ET_{ref}. When the total E_1 summed over the stage 1 period, termed $\sum E_1$, exceeds REW, stage 1 is assumed to terminate and stage 2 begins. The parameter $K_{e\ max}$ generally ranges from 1.05 to 1.2 for use with ET_o and 0.8 to 1.0 for use with ET_r, depending on ambient temperature of the soil prior to wetting, where heat stored in hot, dry soil prior to wetting contributes to the evaporation rate. The parameter $K_{e\ max}$ is similar to parameter $K_{c\ max}$ described in eq. 10.3 of chapter 10, except that that no adjustment is made for height of vegetation, as is done for $K_{c\ max}$. Recommended 'standardized' values for $K_{e\ max}$ are 1.2 for use with ET_o and 1.0 for use with ET_r.

The duration of stage 1 evaporation beginning the day after irrigation or rain, designated t_1, is estimated as:

$$t_1 = \frac{REW}{\overline{E}_1} \tag{9.2}$$

where REW is in mm and E_1 is mean $\overline{E_1}$ in mm over the t_1 period in mm d^{-1}. An iterative solution or daily calculation of depletion from the evaporation layer, as presented in eq. 9.28, is required. Setting the calculation timestep to determine when $\sum E_1$ exceeds REW to less than one day in length makes it easier to identify the specific transition time. When using daily ET_{ref} one can, for example, divide the 24-hour period into tenths of a day and divide the daily ET_{ref} value by 10 to approximate shorter time steps. Alternatively, hourly ET_{ref} and calculation timesteps can be used. The duration of t_1 determined in this manner assumes that there is no redistribution of soil water during the following night similar to that observed by Rose (1968a), Jackson (1973) and van de Griend and Owe (1994). Redistribution of soil water can reinstate stage 1 evaporation the following morning for part of a day.

REW can be measured in the field or laboratory by conducting soil water balances and calculating the evaporation rate. When laboratory cores are used to determine REW, values can be much higher than field-determined values (Ritchie and Johnson (1990). By definition, the stage 1 ends when the measured E begins to decrease below $K_{e\,max}\,ET_{ref}$. REW equals the cumulative evaporation depth, $\sum E_1$, when this occurs. The soil must have been sufficiently wetted to at least a 0.3 m depth. Account can be made in eq. 9.2 for effects of slow drainage from the top 100 to 150 mm of soil that can hold water content of that layer above field capacity for some time duration and thereby increase the effective REW.

9.5 Stage 2 Evaporation

Estimating evaporation from the soil becomes more complex as the surface soil dries and stage 2 evaporation begins. Stage 2 evaporation begins following stage 1 when evaporation proceeds at less than potential rates due to hydraulic constraints. During stage 2, the evaporation rate is governed by the rate of water movement in the liquid phase and vapor phase to or near the surface when not limited by environmental conditions (Rose 1968a). Some soil water in the 'evaporation' layer may also be extracted by plant roots when plants are present. Villalobos and Fereres (1990) measured evaporation from soil using special small lysimeters of 0.3 m depth into which root growth was not restricted. Early in the morning, the roots were cut, the microlysimeters cleaned, sealed, weighed and replaced in their respective positions. The next day, they were weighed again to measure evaporation. Comparison of the soil water content in the microlysimeters with cotton was essentially the same as adjacent soil indicating little water extraction by cotton roots from the top 0.3-m layer at the time the roots were cut. With corn, the water content inside the microlysimeter was higher than adjacent soil indicating some extraction by corn roots from the top 0.3-m layer. Similar microlysimeter studies have been reported by Shawcroft and Gardner (1983), Klocke et al. (1985, 1996), Villalobos and Fereres (1990), Daamen et al. (1993), Evett et al. (1995), Jara et al. (1998) and Todd et al. (2000). Evett et al. (1995) described desirable characteristics in microlysimeter design.

The rate of stage 2 evaporation is governed by soil characteristics and the change in soil water content as described by the equation of Richards (1931). In terms of soil water pressure,

and with no water extraction by roots, the combined Darcy's law and continuity equation for one-dimensional vertical flow (Jensen and Hanks 1967) can be written as:

$$\frac{\partial \theta}{\partial t} = \frac{\partial}{\partial z}\left\{K(h)\frac{\partial H}{\partial z}\right\} \tag{9.3}$$

where θ is the volumetric soil water content, t is time, z is vertical distance, $K(h)$ is the hydraulic conductivity, H is the total hydraulic head ($H = P_w/\gamma_f + z = h + z$), z is the vertical coordinate, P_w is the pressure of the wetting fluid, h is the fluid pressure head, and γ_f is the weight of fluid per unit volume.

Entekhabi and Eagleson (1989) combined the diffusivity equation of Gardner (1959) and conservation of mass equations for porous media to describe the soil water desorption process as:

$$\frac{\partial \theta}{\partial t} = \frac{\partial}{\partial z}\left[D(\theta)\frac{\partial \theta}{\partial z}\right] + \frac{\partial K}{\partial z} \tag{9.4}$$

where $\partial K/\partial z$ is the rate of drainage due to gravity, and $D(\theta)$ is the soil water diffusivity defined as

$$D(\theta) = K(s)\frac{\partial \psi}{\partial \theta} \tag{9.5}$$

where $K(s)$ is the unsaturated hydraulic conductivity, s is relative saturation, and ψ is matric potential. The flow equation and boundary conditions without the gravity component were described by Black et al. (1969) as:

$$\frac{\partial \theta}{\partial t} = \frac{\partial}{\partial z}\left[D(\theta)\frac{\partial \theta}{\partial z}\right] \tag{9.6}$$
$$\theta = \theta_i, z \geq 0, t = 0$$
$$\theta = \theta_o, z = 0, t > 0$$

where θ_i is the initial water content for $t = 0$ and $z \geq 0$, θ_o is the water content at the boundary ($z = 0$), assumed constant for $t > 0$, and where z is defined as elevation above some depth in the soil profile where water content is considered to be constant.

Black et al. (1969) solved eq. 9.6 analytically (Crank 1956) for a semi-infinite slab with constant diffusivity, D, to yield flux at the surface, q, as

$$q = (\theta_i - \theta_o)(D/\pi t)^{1/2} \tag{9.7}$$

Integration of eq. 9.7 with respect to time gives the cumulative flux, E.

$$E = 2(\theta_i - \theta_o)(Dt/\pi)^{1/2} \tag{9.8}$$

When D can be expressed as a function of θ, D can be replaced by weighted-mean diffusivity $\overline{D}$. Crank (1956) gave expressions relating weighted-mean diffusivity to the true diffusivity. For the desorption process this relation is given by the integral:

$$\overline{D} = \frac{1.85}{(\theta_i - \theta_o)^{1.85}} \int_{\theta_o}^{\theta_i} D(\theta)(\theta_i - \theta)^{0.85}\, d\theta \tag{9.9}$$

For convenience a factor C was defined such that $E = C\, t^{1/2}$ so that

$$C = 2(\theta_i - \theta_o)(\overline{D}/\pi)^{1/2} \tag{9.10}$$

9.6 Evaporation Models

Square Root of Time (SRT) Model

Philip (1957) and Black et al. (1969) expressed the theoretical cumulative evaporation during stage 2 evaporation of an initially wet, deep soil as:

$$\sum E_2 = \alpha_r \sqrt{t}_2 \tag{9.11}$$

where $\sum E_2$ is the cumulative evaporation during stage 2, α_r is soil water desorptivity which is dependent on the hydraulic properties of the soil and t_2 is time in days since the start of stage 2 evaporation. Eq. 9.11 was developed by Philip (1957) and was used extensively in early evaporation and crop ET models (Ritchie 1972, 1974).

Ritchie (1972) presented values for α_r ranging from 3.34 mm $d^{-0.5}$ for sand to 5.08 mm $d^{-0.5}$ for a clay loam. Ritchie and Johnson (1990) reported several direct measurements of α_r in a diversity of soils resulting in values of about 3.5 mm $d^{-0.5}$. Ventura et al. (2001) reported values of α_r of about 4.0 mm $d^{-0.5}$ for a flood-irrigated field in the Imperial Valley of California.

Eq. 9.11 is differentiated to provide the evaporation rate at the end of day t_2 during stage 2 drying:

$$E_2 = \frac{\alpha_r}{2\sqrt{t_2}} \tag{9.12}$$

where E_2 is the evaporation rate during stage 2. Because Eq. 9.12 estimates the evaporation rate at the end of day t_2 of the stage 2 process, the evaporation rate averaged over day $t_2 > 1$ must be calculated as the difference between E_2 for t_2 and E_2 for $(t_2 - 1)$ based on eq. 9.11:

$$\begin{aligned} E_2 &= \alpha_r \left(\sqrt{t_2} - \sqrt{t_2 - 1}\right) \quad for\ t_2 > 1 \\ E_2 &= \alpha_r \quad for\ t_2 = 1 \end{aligned} \tag{9.13}$$

Estimating cumulative evaporation using eq. 9.8-9.11 requires knowledge of weighted-mean diffusivity $\overline{D}$ for the soil in question. Suleiman and Ritchie (2003) replaced the terms in eq. 9.8 to obtain an estimate of α_r:

$$\alpha_r = 2(\theta_{dul} - \theta_{ad})(\overline{D}/\pi)^{1/2} \tag{9.14}$$

where θ_{dul} is the drained upper limit (field capacity) and θ_{ad} is the air dry water content. They calculated the soil water diffusivity for each of 12 theoretical soils ranging in texture from sand to clay using the van Genuchten et al. (1991) soil water diffusivity function equations. Some properties were obtained from soil properties described by Rose (1968b). A comparison of calculated α_r vs. θ_{dul} indicated a linear relationship of the form:

$$\alpha_r = K_\alpha \ \theta_{dul} \tag{9.15}$$

where α_r is in mm $d^{-1/2}$, θ_{dul} is water content at the drained upper limit (field capacity) in $m^3\ m^{-3}$, and K_α is the slope of the relationship that they found to equal 13.9 mm $d^{-1/2}$ for the twelve theoretical soils. Entekhabi and Eagleson (1989) proposed a more complicated function for α_r that was based on the Brooks and Corey (1966) soil pore-size distribution index, porosity and saturated conductivity.

Since weighted-mean diffusivities values are not generally available for most soils, estimates of cumulative evaporation in mm can be obtained using the approximate relation between α_r and the θ_{dul} when α_r is not measured, as

$$\sum E_2 = 13.9\,\theta_{dul}\, t_2^{\,1/2} \tag{9.16}$$

where t_2 is the time in days since stage 2 evaporation began and $\sum E$ is the cumulative stage 2 evaporation in mm at the end of the time period in days. The rate of evaporation can be estimated using eq. 9.13.

The SRT evaporation estimates are based on the assumption that potential evaporation rate ($K_{e\,max}\ ET_{ref}$) is always greater than the estimated stage 2 evaporation rate. Furthermore, no provision is made for modifying evaporation estimates to account for intervening small amounts of rainfall or irrigation that may occur. The procedures for estimating stage 2 evaporation by Ritchie (1972) and Suleiman and Ritchie (2003) are intended for use in other models that require estimates of evaporation from the soil and that separately account for intervening small amounts of rainfall. Comparison of several methods for estimating evaporation during stage 2 are made later in this chapter.

The SRT function approaches, but never reaches a zero evaporation rate, due to its theoretical form. In practice, the hydraulic conduction of water toward the surface, and thus evaporation, may be disrupted by soil layering, incomplete wetting, plant root extraction, and tillage impacts, so that when applied to long time periods between wetting events, for example, longer than a month, a time limit should be considered, after which, E_2 is set to zero or to a very small value. In addition, the SRT model assumes that the soil begins the drying event with a fully wetted profile near field capacity. This assumption is required to support the continuous upward flow implicit to the method. Wetting events that do not fully rehydrate at least the upper 1 to 2 m of

the soil profile will have drying events that do not reach the evaporation rates estimated by the SRT model, especially after long periods of time.

When wetting events occur that do not fully rehydrate the surface evaporation layer of the soil, some means is needed to set back the 'clock' for the SRT method i.e., parameter t_2 in eq. 9.11. This can be done by inverting the equation to solve for an adjustment to t_2:

$$t_2 = \left(\frac{\left(\sum E_2\right)_j - \left(P_j - RO_j + I_j\right)}{\alpha_r} \right)^2 \tag{9.17}$$

where $(\sum E_2)_j$ is the cumulative stage 2 evaporation [mm] estimated for day j before any correction to t_2, and P_j and RO_j are precipitation and precipitation runoff from the soil surface on day j [mm] and I_j is the irrigation depth on day j that infiltrates the soil [mm]. The adjusted value for t_2 is used to replace the unadjusted value for the end of day (or timestep) j. If the sum of P_j - RO_j and I_j exceeds $(\sum E_2)_j$ then the evaporation process should be set back to stage 1 and eq. 9.17 is not utilized. Small depths of precipitation during stage 2 will wet the surface and may shift the stage back to stage 1 for a brief period of time depending on the precipitation amount, with a subsequent resumption of stage 2 drying. This is shown later for the FAO-56 model using the skin evaporation enhancement.

Crop Coefficient-based Evaporation Model

Various procedures have been proposed for adjusting or increasing the crop coefficient K_c, or calculating an evaporation coefficient, K_e, to account for evaporation following rainfall or irrigation.

Wright (1982) procedure. Wright (1982) suggested the following time-based expression for K_e applicable for limited times after rainfall or irrigation:

$$K_e = (K_{c\max} - K_s\, K_{cb}) \left(1 - \left(\frac{t}{t_d} \right)^{1/2} \right) f_w \tag{9.18}$$

where $K_{c\,max}$ is the maximum value for K_c normally occurring after rain or irrigation. $K_{c\,max}$ is generally 0.8 to 1.0 for an alfalfa-based K_c and 1.0 to 1.2 for a grass-based K_c. K_{cb} is the basal crop coefficient and K_s is the fraction of available soil water in the root zone. Variable t in eq. 9.18 represents the days after major rain or irrigation and t_d is the usual number of days required for the soil surface to visually appear dry. Variable f_w is the relative fraction of the soil surface wetted by rainfall or irrigation. Normally, for precipitation and sprinkler and surface irrigations that wet the entire soil surface, $f_w = 1.0$. For very small fractions of soil wetted, the effective area may be larger. Recent studies of evaporation from wet soil in drip-irrigated olive orchards indicate that the effective value of f_w for accurate estimation of evaporation may be greater than the actual fraction of area wetted due to micro-scale advection from surrounding dry soil (Bonachela et al. 2001).

Eq. 9.18 simulates the time-based reduction in evaporation as the soil dries. General values for t_d are 3 days for sandy soils, 5 days for silty soils, and 7 days for clayey soils (Wright 1982).

However the value for t_d will be longer during cool or humid periods and shorter for hot or dry periods. Variable t must be limited to $0 \le t \le t_d$. If soil wetting occurs in the morning, then t is generally set equal to 0 for that day. Most evaporation occurs in the first few days after the soil is wetted. Hill et al. (1983) and Martin and Gilley (1993) cautioned that t must be limited for each wetting event so that total evaporation estimated over the t_d period is constrained by the depth of precipitation or irrigation. Daily precipitation totals that are less than about 0.3 ET_o can be ignored.

General model for K_e. A general model for K_e for estimating the evaporation from the surface layer of soil after rain or irrigation was introduced in FAO-56 (Allen et al. 1998) for use with the basal crop coefficient:

$$K_e = K_r \, (K_{c\,max} - K_s K_{cb})$$
$$\textit{such that} \qquad (9.19)$$
$$K_e \le f_{ew} \; K_{c\,max}$$

where K_e is the soil evaporation coefficient, K_{cb} is the basal crop coefficient, $K_{c\,max}$ is the maximum value of K_c following rain or irrigation, K_s is a reduction coefficient to account for reduced transpiration under soil water shortage, K_r is a dimensionless evaporation reduction coefficient [0-1] and K_s is a dimensionless soil water stress factor [0-1]. K_r can be expressed as a function of time (i.e., eq. 9.18) or, in the FAO-56 dual K_c approach, as a function of the cumulative depth of water depleted by evaporation from the soil. Parameter f_{ew} is the fraction of soil surface from which most of the evaporation occurs and is generally taken as the fraction of soil surface that is both exposed to drying and is 'wetted' during the wetting event. The FAO-56 application of eq. 9.19 is intended to overcome problems that occur with eq. 9.18 regarding the value for t during small wetting events. Its use of cumulative depth of evaporation to estimate K_r tends to stretch out drying periods when ET_{ref} is low and shorten them when ET_{ref} is high. A daily water balance of the effective surface evaporation layer is required. In eq. 9.19, transpiration is given preference over evaporation from soil (i.e., $K_s \, K_{cb}$ is subtracted from $K_{c\,\max}$ before calculating K_e). In some ET models, such as that by Ritchie (1972), evaporation from soil has priority over transpiration. $K_s \, K_{cb}$ is set to 0 when eq. 9.19 is applied to completely bare soil.

In contrast to the SRT model where cumulative evaporation from bare soil is proportional to the increase in $\sqrt{t}$ after stage 2 evaporation begins (Philip 1957; Black et al. 1969; Ritchie 1971, 1972), the FAO-56 method uses a water balance of an effective evaporation layer to estimate the decreasing evaporation rate. The effective layer is typically the upper 0.1 to 0.15 m during the first three to four weeks of evaporation, potentially increasing to 0.20 to 0.25 m depth for longer time periods. For maximum accuracy, estimates of the upward flux of water into this layer from below may be required, especially for medium and fine-textured soils (Ventura et al. 2001). However, estimation of upward flux may require relatively complicated models and specific parameterization or soil hydraulic and thermal characteristics. Cahill and Parlange (1998, 2000) and Grifoll et al. (2005) applied sophisticated evaporation models that account for convective transport in both the gas and liquid water phases in addition to vapor dispersion and liquid sensible heat dispersion. Cahill and Parlange (2000) concluded that "the matter of describing coupled heat and moisture transport in soils remains unresolved." Therefore, for practical applications, a fixed potential depth of water depletion per drying event can be determined from

field observation for specific soils and the relatively simplified FAO-56 procedure used to determine the decreasing evaporation rate. In the absence of field data, the total evaporable water can be estimated using an effective depth of the evaporation layer as described in the next subsection. Comparisons against simulations by the HYDRUS finite element model shown in a later section tend to confirm this.

The FAO-56 Evaporation Model

The FAO-56 (Allen et al. 1998) evaporation procedure calculates a water balance for the effective evaporation layer of soil that tends to be approximately 0.1 to 0.15 m in depth. The method represents a compromise between complexity and general application by conducting a daily water balance of the upper soil layer where upward flux of water or vapor to the layer from below is considered to be negligible or is ignored, and the effective depth of the evaporating layer is specified as the depth of soil that dries, on average, to a threshold dryness point. In the case of the FAO procedure, the threshold point is taken as the mean soil water content half-way between air dry and wilting point. This is an arbitrary dry point, but one that is relatively straight forward for field application and one that is reproducible. The maximum depletion depth for the layer provides a consistent stopping point for the evaporation cycle to ensure conservation of mass and can be customized for each application to fit observations.

The FAO procedure assumes that evaporation takes place in two stages following Ritchie (1971): the energy limiting stage 1, and the falling rate stage 2. When the soil is wet (in stage 1), the evaporation reduction coefficient, K_r, in eq. 9.19 is assumed to be 1.0. When the water content in the effective evaporation layer begins to limit evaporation (in stage 2), K_r decreases to below 1.0. The value for K_r is set to zero when the total amount of water in the effective evaporation layer is depleted during the drying cycle. Assuming the soil is at field capacity (θ_{fc}) shortly after rainfall or irrigation and that it can dry to halfway between 0 and the wilting point (θ_{wp}), the total amount of water that can be depleted by evaporation (TEW) from the effective evaporation layer during a drying cycle is estimated as:

$$TEW = 1000\,(\theta_{fc} - 0.5\,\theta_{wp})\,z_e \qquad (9.20a)$$

where TEW is the 'total evaporable water' in mm, θ_{fc} and θ_{wp} are $m^3\ m^{-3}$ and z_e is the effective depth of the surface layer that is dried by evaporation in m. The value for θ_{fc} in eq. 9.20a may be set a few percentage points above normal values listed in table 3.6 to compensate for extra soil water retained in the evaporation layer above θ_{fc} for one or two days after wetting. The cumulative depth of evaporation, D_e, at the end of stage 1 is the readily evaporable water (REW) that normally ranges from 5 to 12 mm depending on soil texture (Ritchie 1972).

Downward adjustment of TEW was recommended by Allen et al. (1998, 2005c) during extended periods of low ET_{ref} (i.e., $ET_o < 5$ mm d^{-1}) commonly experienced during nongrowing periods. During cool conditions, for example during winter or other cool periods, less radiation energy is available for heating the soil surface layer and evaporate water, and total effective TEW representing a drying event will typically be smaller than during a warm period. Allen et al. (1998) suggested using ET_o as a surrogate for temperature and radiation conditions to reduce the value for TEW. When $ET_o < 5$ mm d^{-1}, TEW is estimated as:

$$TEW = 1000(\theta_{fc} - 0.5\theta_{wp})z_e\sqrt{\frac{ET_o}{5}} \quad (9.20b)$$

where ET_o is an average representing the general estimation period in mm d^{-1}. A monthly average for ET_o is recommended. Varying ET_o in eq. 9.20b on a daily basis is not recommended since it will cause *TEW* to vary daily, which can cause numerical inconsistencies.

During the falling rate stage, where $D_e > REW$, the evaporation rate is estimated in proportion to the amount of water remaining in the surface soil layer, and K_r of eq. 9.19 is calculated as:

$$K_r = F_{stage1} + (1 - F_{stage1})\, max\left(min\left[\frac{TEW - D_{e(i-1)}}{TEW - REW}, 1.0 \right], 0.0 \right) \quad (9.21)$$

where $D_{e(i-1)}$ is the cumulative depth of evaporation at the end of timestep $(i - 1)$, representing the previous timestep and $F_{stage\ 1}$ is the fraction of the time step (day or hour) that resides in stage 1 evaporation. 1- $F_{stage\ 1}$ of the timestep resides in stage 2. The use of $F_{stage\ 1}$ is an extension to the original FAO-56 model (Allen et al. 2012) to provide better definition of the transition from stage 1 to stage 2 drying during a timestep and provides a more accurate, averaged value for K_r during that transition timestep. The improved definition can be important when using daily calculation timesteps, especially for coarse soils having small *REW*. The 'max' function determines the greater of the two values in the parentheses that are separated by the comma and the 'min' function determines the lesser of the two values in the brackets that are separated by the comma. These functions effectively limit the value for K_r to $0 \le K_r \le 1.0$. Setting $F_{stage\ 1}$ to 0 causes eq. 9.21 to revert to the original FAO-56 form. Burt et al. (2005) found the linear proportionality of K_r to the depth of remaining evaporable water, as expressed by eq. 9.21, to follow experimental data by Chanzy and Bruckler (1993) well for three soil types spanning clay, silty clay loam and loam, as shown in fig. 9.3 for loam.

An example set of calculations was presented in FAO-56 (their Example 31) for applying the FAO-56 K_e method (Allen et al. 1998). Setting the effective depth of evaporation, z_e, can be subjective, since the entire z_e layer will not uniformly approach air-dry conditions during a drying period, and an upward flux to this layer from below is not considered. It is recommended that the selection of z_e be set to a value that causes the FAO-56 procedure to reproduce observed average total evaporation depth for the same or a similar soil after a long drying period, and therefore includes the effects of depletion of water from below the z_e layer (Allen et al. 2005c). Usually a value for z_e, of 0.1 or 0.15 m is used. For evaporation periods extending beyond three or four weeks, a transition in z_e to a depth of 0.2 to 0.25 m may be required to better represent the soil depth contributing to total evaporation (Raes et al. 2007).

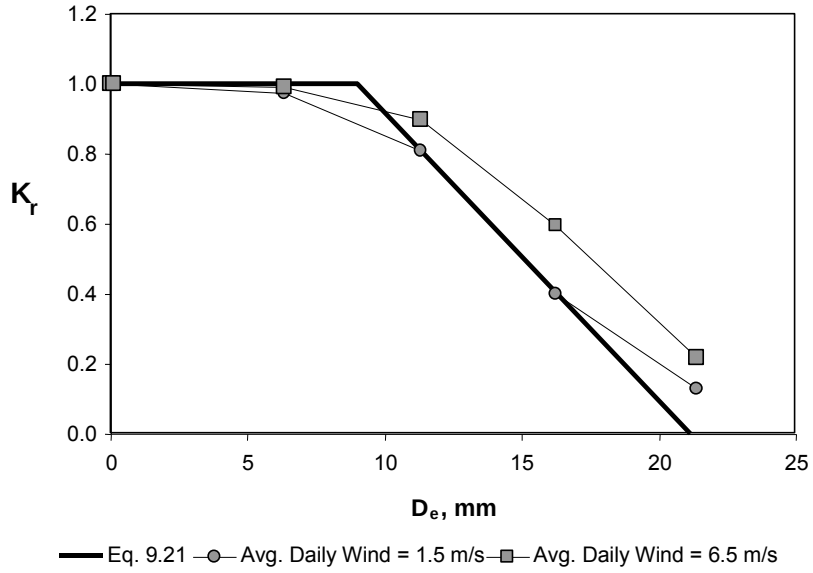

Fig. 9.3. Measured K_r reported by Chanzy and Bruckler (1993) for a loam soil near Avignon, France under two wind speed conditions and K_r modeled by Burt et al. (2005) using eq. 9.21 with REW = 9 mm and TEW = 21 mm based on z_e = 0.1 m, $F_{stage\ 1}$ = 0, and average θ_{fc} and θ_{wp} values for loam from table 3.6.

The fraction of calculation timestep i that resides in stage 1, $F_{stage\ 1}$, is approximated following Allen (2011) as:

$$F_{stage1} = \frac{REW - D_{REW_{i-1}}}{K_{e\,max}\, ET_{ref}} \quad , 0 \le F_{stage1} \le 1.0 \tag{9.22}$$

where timestep length can be one day, a tenth day or one hour, $D_{REW\ i\text{-}1}$ is the depletion of the upper "skin" soil surface layer that directly contributes to stage 1 drying, mm, at the end of timestep i-1, and $K_{e\ max}$ is the value for K_e expected during stage 1 drying. The value for $K_{e\ max}$ is tied to the reference ET type, where $K_{e\ max} \sim 1.0$ is recommended when using the alfalfa reference, ET_r, and $K_{e\ max} \sim 1.2$ is recommended when using the clipped grass reference, ET_o. Typically, $K_{e\ max}$ can be set equal to $K_{c\ max}$, defined earlier. $F_{stage\ 1}$ is limited to the range $0 \le F_{stage\ 1} \le 1.0$. The water balance equation for determining D_{REW} is given later as eq. 9.29. Fig. 9.4 illustrates the three depths describing contributing portions of the soil profile, referred to as the skin layer, the total evaporation layer, z_e, and the root zone depth, z_r, in the case of presence of plants. Each depth is contained within the domain of the next deeper depth in the FAO-56 model, which is different from most layered soil water models. In other words, each layer is a subset of the next deeper layer.

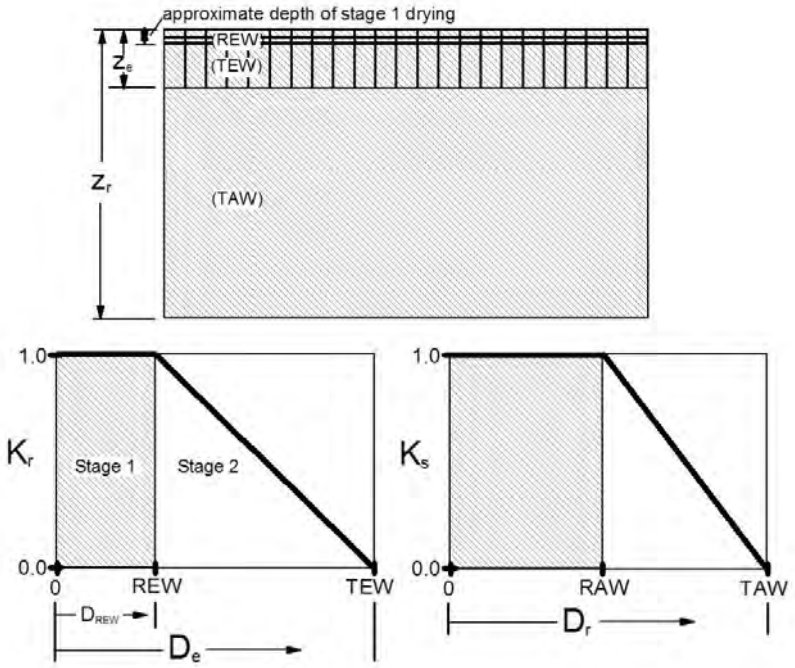

Fig. 9.4. Top: relative depths for the upper soil surface layer, referred to as the skin layer, contributing to stage 1 drying, the total evaporation layer, z_e, and the root zone depth, z_r, in the case of presence of plants; lower left: the shape of the K_r function vs. D_e and placement of *REW* and *TEW* defining stage 1 and stage 2 drying; lower right: the shape of the K_s function vs. D_r and placement of readily available water, *RAW,* and total available water, *TAW*.

Ritchie et al. (1989) suggested empirical equations to estimate potential values of *REW* based on soil texture:

$$REW = 20 - 0.15\ (Sa) \quad for \quad Sa > 80 \tag{9.23a}$$

$$REW = 11 - 0.06\ (Cl) \quad for \quad Cl > 50 \tag{9.23b}$$

$$REW = 8 + 0.08\ (Cl) \quad for \quad Sa < 80 \quad and \quad Cl < 50 \tag{9.23c}$$

where *Sa* and *Cl* are percentage fractions of sand and clay in the soil. Units for *REW* are mm. Typical values of *REW* suggested by FAO-56 are summarized in table 9.1. It is important to limit values for *REW* to less than *TEW*.

TABLE 9.1 Typical Values of *REW* by Soil Type. Source: Data from Allen et al. (1998).

Soil type (USA soil texture classification	Evaporation parameter (*REW*) mm
Sand	2 – 7
Loamy sand	4 - 8
Sandy loam	6 – 10
Loam	8 – 10
Silt loam	8 – 11
Silt	8 – 11
Silty clay loam	8 – 11
Silty clay	8 – 12
Clay	8 – 12

Experimental values for z_e, TEW and REW. Since the typical soil water distribution following evaporation follows an exponential relationship as illustrated in fig. 9.1, the surface 0-0.05 m layer can be expected to approach air-dry approximated as 0.5 θ_{wp}. Below 0.05 to 0.1 m, the soil likely will not dry to less than θ_{wp} between irrigation or rainfall events. After 37 days of evaporation from a loam soil near Phoenix, AZ the soil water content below 0.04 m had not decreased to air dry conditions and below 0.05 m was only approaching θ_{wp} (Jackson 1973). An alternate estimate of *TEW* would be to assume that only the 0-0.05 m layer would dry to 0.5 θ_{wp} and below this depth, the soil would dry only to θ_{wp}, or $TEW = 1000\ [(0.05 - 0)(\theta_{fc} - 0.5\ \theta_{wp}) + (z_e - 0.05)(\theta_{fc} - \theta_{wp})]$. However, this adjustment is typically implicitly incorporated into the establishment of the value for z_e and is generally not made.

The selection of the value of z_e to use in the calculation of *TEW* should be based on experimental data, when possible. Hunsaker et al. (2003) found good accuracy in application of the FAO-56 approach for K_r using $z_e = 0.125$ m in eq. 9.20 and $REW = 10$ mm for cotton on a clay loam soil in Arizona. Hunsaker et al. (2002) used $z_e = 0.15$ m, $TEW = 34$ mm and $REW = 10$ mm for a loam soil under alfalfa based on lysimeter observations. Tolk and Howell (2001) and Howell et al. (2004) used $z_e = 0.15$ m, $TEW = 33$-38 mm and $REW = 10$ mm for a clay loam soil and $z_e = 0.10$ m, $TEW = 20$ mm and $REW = 9$ mm for a fine sandy loam near Amarillo, Texas. Allen et al. (2005d) used $z_e = 0.10$ m, $TEW = 25$ mm and $REW = 10$ mm to fit lysimeter data on evaporation for a silt loam soil near Kimberly, Idaho. Allen et al. (2005c) found $z_e = 0.15$ m to fit observed evaporation data in Imperial Valley, California for silty clay and silty clay loam and $z_e = 0.35$ m for sand. The larger value for z_e for sand accounted for upward flow of water to the surface. Mutziger et al. (2005) used $z_e = 0.10$ m for a sandy clay loam and 0.15 m for a silt loam soils to fit experimental data using the two-stage FAO-56 model. They applied the extended three-stage model of Allen et al. (2005a,c) for three cracking soils to account for low level diffusive evaporation from crack faces over long time periods. Burt et al. (2005) used $z_e = 0.10$ m and mean values from table 3.6 for θ_{fc} and θ_{wp} in eq. 9.20a to model evaporation data reported by Chanzy and Bruckler (1993) for loam, silty clay loam and clay soils. The average absolute value of percent differences between measured and FAO-56 modeled cumulative evaporation was 5%. The $\theta_{fc} = 0.35$ and $\theta_{wp} = 0.13$ m^3 m^{-3} presented by Jackson (1973) for the loam soil near Phoenix in fig. 9.1 and a value of $z_e = 0.1$ m produces $TEW = 30$ mm. Jackson

(1973) observed maximum cumulative evaporation of 29 to 31 mm from the soil profile during his two test periods, which is in close agreement.

Stage 3 evaporation for cracking soils. Drying to depths as deep as 0.5 m or greater is possible for severely cracking soils containing large amounts of montmorillinite clay where cracks can extend as deep as 0.6 m (Ritchie and Adams 1974) and 1 m (Pettry and Switzer 1996). An extension to the FAO evaporation model (Allen et al. 2005c) created a stage 3 where evaporation progresses in soils that crack substantially upon drying, thereby exposing progressively deeper depths to the drying process. The progressive drying tends to continue at low rates over extended periods of time and prolongs the time for K_r to decrease to zero, thereby creating a prolonged 'base-line' evaporation rate.

In the extension for stage 3 drying, stage 2 is transitioned to stage 3 when K_r reduces to a threshold value labeled K_{r2}, as shown in fig. 9.5. For a 3-stage drying system with the skin evaporation extension, eq. 9.21 for K_r is replaced with eq. 9.24 for the second stage when $REW < D_{e\ i-1} < TEW_2$:

$$K_r = K_{r2} + (1 - K_{r2}) \left(F_{stage1} + (1 - F_{stage1})\ max\left(min\left[\frac{TEW_2 - D_{e,i-1}}{TEW_2 - REW},\ 1.0 \right],\ 0.0 \right) \right) \qquad (9.24)$$

and K_r during stage 3 when $TEW_2 \le D_{e,\ i-1} \le TEW_3$ is:

$$K_r = F_{stage\ 1} + (1 - F_{stage\ 1}) K_{r2}\ max\left(min\left[\frac{TEW_3 - D_{e,i-1}}{TEW_3 - TEW_2},\ 1.0 \right],\ 0.0 \right) \qquad 9.25)$$

where TEW_2 is the D_e when $K_r = K_{r2}$ (point at which evaporation transitions from stage 2 into stage 3 drying) [mm] and K_{r2} is the value for K_r at the junction of stage 2 and stage 3 drying. TEW_3 is maximum cumulative depth of evaporation (depletion) from the soil surface layer when the soil is dry and no further evaporation occurs ($K_r = 0$) [mm]. The value TEW_3 includes REW and TEW_2. K_r is 0 when $D_{e,\ i-1} \ge TEW_3$. In all cases, for eq. 9.24 and 9.25, K_r is limited to $0 \le K_r \le 1.0$. TEW_2 is typically set to TEW computed from eq. 9.20a,b using $z_e = 0.1$ or 0.15 m and TEW_3 is estimated from eq. 9.20a,b using a value for z_e greater than the z_e used to estimate TEW_2. Comparisons against observed data are recommended to determine best parameter values. Generally, the value for K_{r2} is some relatively low value between about 0.05 and 0.4, depending on the nature and degree of cracking as the soil dries. Allen et al. (1998, 2005c) recommended $K_{r2} \sim 0.2$ for cracking soils. Mutziger et al. (2001) found best fit values for K_{r2} for two cracking soils in Texas to be 0.3 and 0.2 when comparing against lysimeter measurements of evaporation for a black clay and clay loam. Stage 3 drying in the FAO-style model has been applied to cracking heavy clay soils in the Imperial Irrigation District of California (Allen et al. 2003, 2005c) and to two cracking or partially cracking soils in Texas (Mutziger et al. 2001). Values for the Imperial soils were $REW = 8$ mm, $TEW_2 = 50$ mm, $TEW_3 = 100$ mm and $K_{r2} = 0.2$. Best fit values to lysimeter evaporation measurements for the Houston black clay and Pullman clay loam soils of Mutziger et al. (2001) were $REW = 7$ mm; $TEW_2 = 30$ and 22 mm; and $TEW_3 = 50$ and 45 mm. The stage 3 option for the FAO-56 method can also be used to simulate effects

of upward flow from deeper soil layers for non-cracking soils as illustrated later in comparisons against the HYDRUS model.

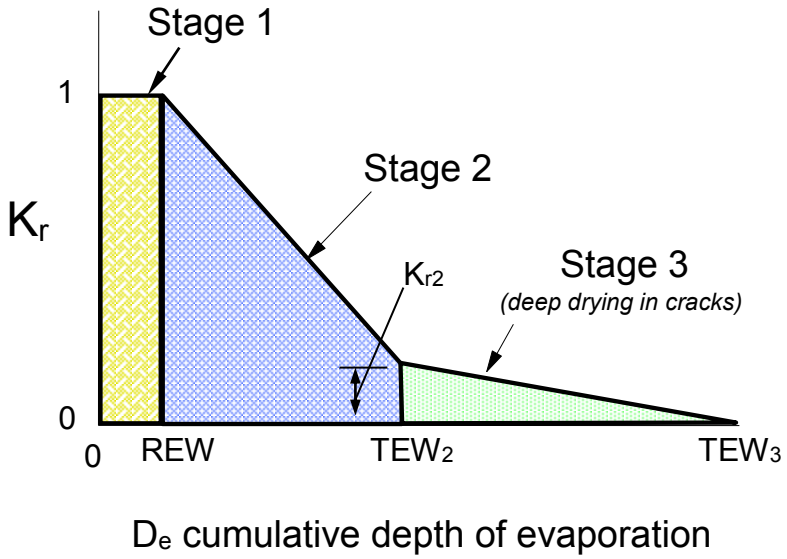

Fig. 9.5. General schematic showing the transition of the K_r function (eq. 9.24 and 9.25) for a cracking soil having 3-stage evaporation as a function of cumulative depth of evaporation depletion, D_e,. Source: Allen et al. (2005c), © ASCE.

Application within the dual K_c context. In the FAO-56 dual K_c model, described in chapter 10, f_w, the fraction of the surface wetted by irrigation and/or precipitation, is used to limit the potential spatial extent of evaporation. Common values for f_w are listed in table 9.2. When the soil surface is completely wetted, as by precipitation or sprinkler, the fraction of exposed wetted soil, f_{ew}, is set equal to $(1 - f_c)$, where f_c is the fraction of soil surface effectively covered by vegetation. For irrigation systems where only a fraction of the ground surface (f_w) is wetted, f_{ew} is limited to f_w:

$$f_{ew} = \min\left(1 - f_c\ ,\ f_w\right) \tag{9.26}$$

Both $(1 - f_c)$ and f_w, for numerical stability, have limits of [0.01 - 1]. In the case of drip irrigation, Allen et al. (1998) suggested that where the majority of soil wetted by irrigation may be beneath the crop canopy and is shaded, f_w be reduced to about one-half to one-third of that given in table 9.2. Their general recommendation for drip irrigation is to multiply f_w by [1- (2/3) f_c]. Pruitt et al. (1984) and Bonachela et al. (2001) have described evaporation patterns and extent under drip irrigation.

Using a three-dimensional crop energy balance model, Luquet et al. (2005) suggested that plant transpiration in a cotton canopy can increase by 10% when shifting from furrow irrigation to drip irrigation due to transfer of heat from dry soil to adjacent vegetation. This implies that the K_{cb} might increase by a small amount when irrigated by drip or other irrigation method

where only a small fraction of the surface is wetted. However, the increase is a function of the fraction of time that the soil surface is wet. Typically drip irrigation wets the surface more frequently than a surface irrigation method so that some of the reduced evaporation from smaller f_w and perhaps increased transpiration by heat transfer is compensated by more frequent wetting events as opposed to surface or sprinkle irrigation (Burt et al. 2005). A schematic illustrating common extent and location of f_w and $1 - f_c$ is shown in fig. 9.6.

TABLE 9.2 Common Values for the Fraction of Soil Surface Wetted by Irrigation or Precipitation. Source: Data from FAO-56, Allen et al. (1998).

Wetting event	f_w
Precipitation	1.0
Sprinkler irrigation, field crops	1.0
Sprinkler irrigation, orchards	0.7 … 1.0
Basin irrigation	1.0
Border irrigation	1.0
Furrow irrigation (every furrow), narrow bed	0.6 …1.0
Furrow irrigation (every furrow), wide bed	0.4 … 0.6
Furrow irrigation (alternate furrows)	0.3 … 0.5
Microspray irrigation, orchards	0.3 … 0.8
Trickle (drip) irrigation	0.3 … 0.4

The value for f_c is generally determined by visual observation. For purposes of estimating f_{ew}, f_c can be estimated using a general relationship between f_c and K_{cb} from FAO-56 as:

$$f_c = \left(\frac{K_{cb} - K_{c\,\min}}{K_{c\,\max} - K_{c\,\min}} \right)^{(1+0.5h)} \tag{9.27}$$

where $K_{c\,min}$ is the minimum (basal) K_c for dry bare soil with no ground cover and h is the height of the crop in m. The differences K_{cb} - $K_{c\,min}$ and $K_{c\,max}$ - $K_{c\,min}$ are limited to ≥ 0.01 for numerical stability. The value for f_c will change daily as K_{cb} changes. $K_{c\,min}$ ordinarily has the same value as the K_{cb} during the initial growth period for annual crops, $K_{cb\,ini}$, that represents nearly bare soil conditions (i.e., $K_{c\,min}$ ~ 0.10 to 0.15). However, $K_{c\,min}$ is set to 0 or nearly zero under conditions having large time periods between wetting events, for example in applications with natural vegetation in deserts. The value for f_c decreases during the late season period in proportion to K_{cb} to account for local transport of sensible heat from senescing leaves to the soil surface. K_{cb}, $K_{c\,min}$ and estimation of $K_{c\,max}$ are discussed in more detail in chapter 10. The FAO-56 dual K_c model can be applied using ET_o and ET_r references provided the K_{cb} values used in the procedure are associated with the specific reference.

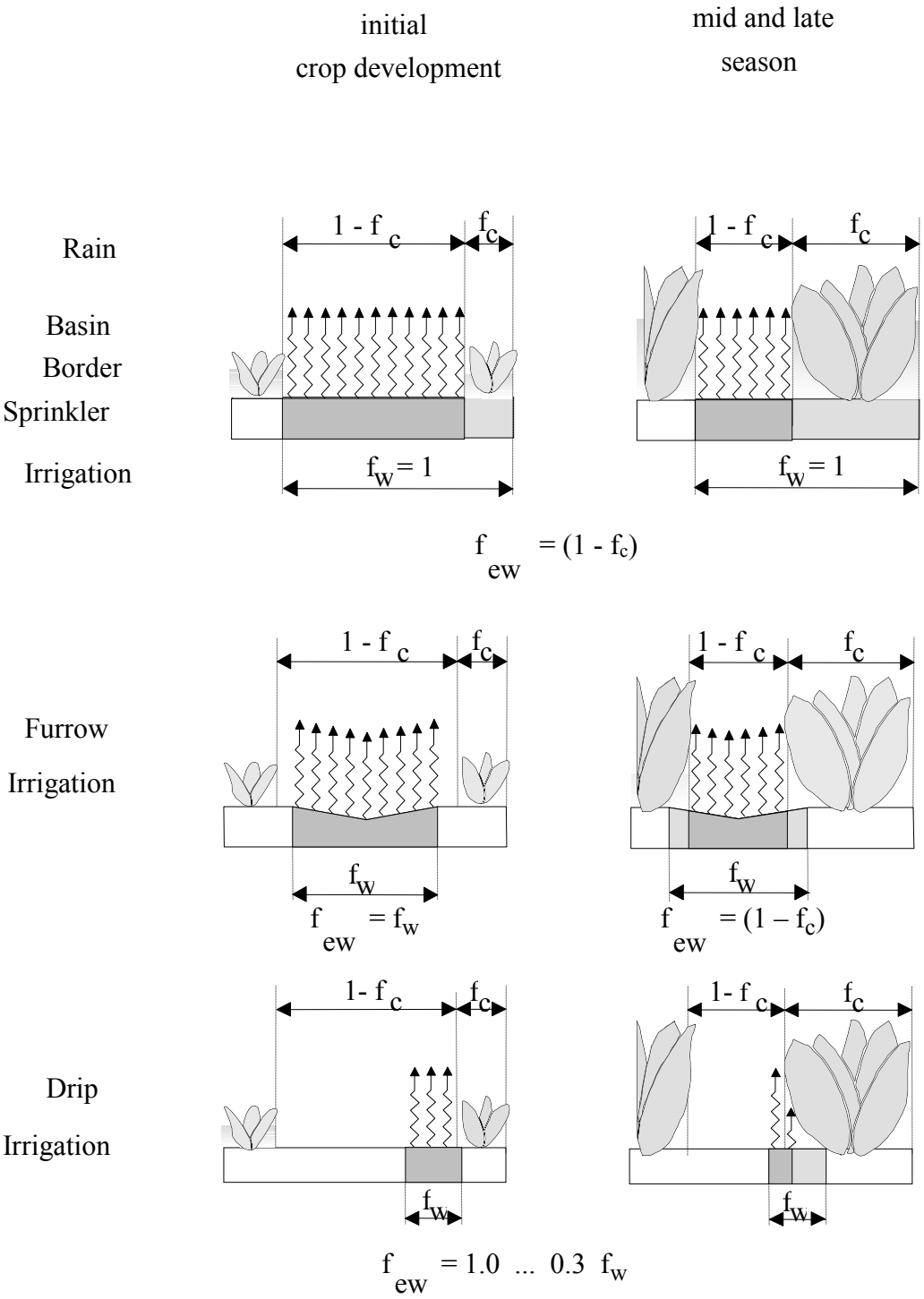

Figure 9.6. Determination of f_{ew} (greyed areas) as a function of the fraction of ground surface coverage (f_c) and the fraction of the surface wetted (f_w). Source: Figure from FAO-56, Allen et al. (1998). Reproduced with permission.

9.7 Relations Between Evaporation and Transpiration

For partial or full plant cover, the rate of stage 1 evaporation under a crop canopy relative to reference ET is strongly linked to the LAI, or plant cover, that affects net radiation at the soil surface. Allen et al. (1964) illustrated how crop canopies intercept radiation thus reducing energy for evaporation at the surface. Measurements of evaporation under corn, cotton and maize canopies in Spain by Villalobos and Fereres (1990) indicated that E/ET_o decreased as LAI increased (fig. 9.7) in a manner similar to the decrease in the ratio reported by Ritchie (1972). Ritchie and Burnett (1971) showed the ratio of net radiation at the soil surface (R_{ns}) to total net radiation above the canopy to decrease in a nearly identical proportion to the increase in LAI (fig. 9.7). These data indicate that variation in stage 1 evaporation for given weather conditions as LAI increases is largely due to the effect of LAI, or plant cover, reducing net radiation at the soil surface. In a similar manner, Villalobos and Fereres (1990) showed that the ratio of transpiration (T) to ET_o increased as LAI increased (fig. 9.8). The ratio T/ET_o at a given level of LAI varied depending on the wetness of the soil surface.

Villalobos and Fereres (1990) showed the interdependence of E and T processes. As evaporation from the soil decreased as the soil dried, there was an increase in transpiration at a given level of reference ET and LAI. They reported T/ET_o in cotton that was 1.1 at LAI = 3 when the soil surface was dry and E was low. When the soil was wetted by rain or irrigation, the calculated T/ET_o ratio dropped to 0.6 the first day after wetting. In the FAO-56 procedure, fraction of cover, f_c, is used as a surrogate for LAI, to proportion potential *T* and *E*.

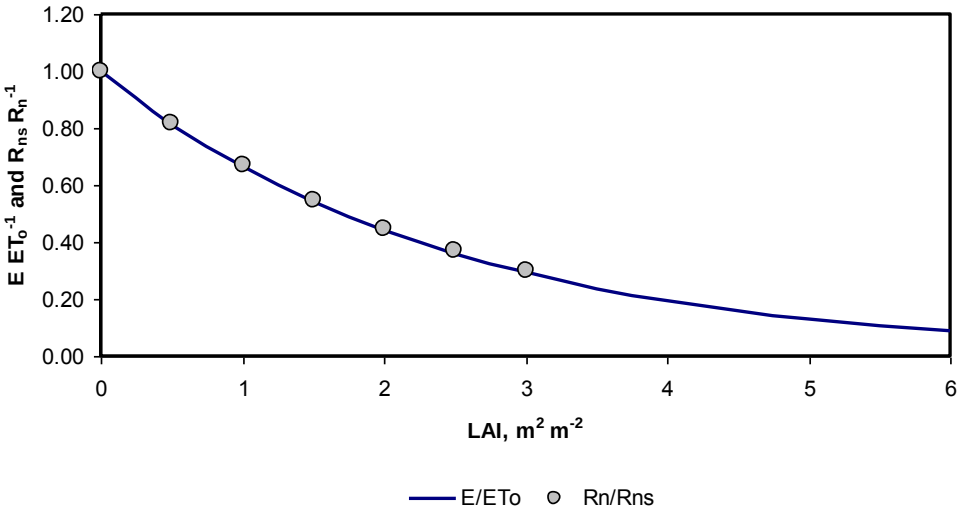

Fig. 9.7. Decrease in the ratios of E/ET_o during first stage evaporation in relation to LAI. Source: Data from Villalobos and Fereres (1990) and nearly identical to the calculated decrease in R_{ns}/R_n using the relationship presented by Ritchie and Burnett (1971) as LAI increases.

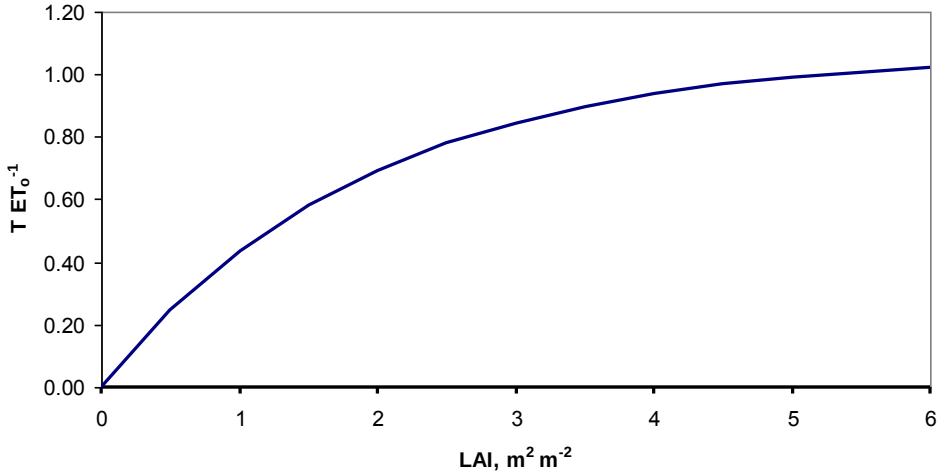

Fig. 9.8. Increase in the ratio of T /ET_o as LAI increases. Source: Data from Villalobos and Fereres (1990).

9.8 Water Balance of the Evaporation Layer

Estimation of K_e using the FAO evaporation model via eq. 9.17 and 9.19 requires a water balance conducted for the f_{ew} fraction of the surface soil layer on a daily or shorter timestep:

$$D_{e,i} = D_{e,i-1} - \left[(1-f_b)\left(P_i - RO_i + \frac{I_i}{f_w} \right) + f_b \left(P_{i+1} - RO_{i+1} + \frac{I_{i+1}}{f_w} \right) \right] + \frac{E_i}{f_{ew}} + T_{ei,i} \qquad (9.28)$$

where $D_{e,i-1}$ and $D_{e,i}$ are cumulative depletion depth at the ends of days *i-1* and *i* [mm], P_i and RO_i are precipitation and precipitation runoff from the soil surface on day *i* [mm], I_i is the irrigation depth on day *i* that infiltrates the soil [mm], E_i is evaporation on day i (i.e., $E_i = K_e$ ET_{ref}) [mm], $T_{ei,\,i}$ is the depth of transpiration from the exposed and wetted fraction of the soil surface layer on day *i* [mm], and f_b is the fraction of the precipitation and irrigation during a calculation time step (hour or day) that is assumed to contribute immediately to evaporation during that same timestep, with 1 - f_b of the precipitation and irrigation not contributing to evaporation until the following timestep, on average. If unknown, f_b can be set to 0.5. f_b has limits of 0 and 1.0. f_b effectively controls the immediacy of evaporation from a wetting event that may occur at an unknown time within the calculation timestep, for example, nighttime irrigations during a daily timestep. Eq. 9.28 is a form for $D_{e,i}$ proposed by Allen et al. (2012) to distribute *P* and *I* between adjacent timesteps in regard to their influence on the timing of the increase in *E* stemming from the wetting event. This may be important for daily timesteps, but generally is not important for hourly or shorter timesteps. Variables having subscripts '*i+1*' indicate values for the timestep following current timestep *i*. Assuming that the surface layer is at field capacity following heavy rain or irrigation, the minimum value for $D_{e,i}$ is zero. The deep percolation term of the original FAO-56 formulation for eq. 9.28 is omitted in the new equation forms for eq. 9.28 and 9.29, as it is not needed. Instead, $D_{e,i}$ and $D_{e,i-1}$ are constrained to limits of $0 \le D_{e,i} \le TEW$. Any *P* or *I* additions in excess of $D_{e,i}$ (and $D_{REW,i}$ in eq. 9.29) are assumed to infiltrate to depths in the soil below z_e (or below the skin in the case of $D_{REW,i}$).

The irrigation depth I_i is divided by f_w to approximate the infiltration depth to the f_w portion of the soil surface. Similarly, E_i is divided by f_{ew} because it is assumed that all E_i (other than residual evaporation implicit to the K_{cb} coefficient) is taken from the f_{ew} fraction of the surface layer. It is recognized that soil water content can exceed field capacity for a few days following a large wetting event and that some drainage in soil occurs at very small rates at water contents below field capacity. To some extent, impacts of these simplifying assumptions can be compensated for in setting the value for z_e or *TEW*.

The parameter $D_{REW\ i-1}$ in eq. 9.22 is the depletion of water from the *REW* layer, referred to as the skin layer, at the end of the prior *i-1* timestep. Eq. 9.22 estimates the $F_{stage\ 1}$ parameter used in eq. 9.19 and 9.21 to simulate any stage 1 evaporation that may occur from light wetting events or from heavy wetting events. Background is given in Allen (2011). For light wetting events, stage 1 evaporation may last for only part of a single timestep. The calculation of $D_{REW\ i}$ is designed, similar to eq. 9.28, to be forward looking with regard to the wetting event to consider soil surface wetting and corresponding evaporation from a wetting event occurring during the current timestep i:

$$D_{REW,i} = D_{REW,i-1} - \left[(1-f_b)\left(P_i - RO_i + \frac{I_i}{f_w} \right) + f_b \left(P_{i+1} - RO_{i+1} + \frac{I_{i+1}}{f_w} \right) \right] + \frac{E_i}{f_{ew}} \qquad (9.29)$$

where $D_{REW,i-1}$ and $D_{REW,i}$ are cumulative depletion depth at the ends of days *i-1* and *i* [mm] and all other terms are the same as for eq. 9.28. $D_{REW,i}$ and $D_{REW,i-1}$ are constrained to limits of $0 \le D_{REW,i} \le REW$.

The amount of transpiration extracted from the f_{ew} fraction of the evaporating soil layer is generally a small fraction of total transpiration. When the surface 0.01-m of soil dries, the resistance to evaporation increases greatly (van de Griend and Owe 1994; Aluwihare and Watanabe 2003). There are not likely to be healthy plant roots in the surface 0-0.05 m of soil that, depending on the rate of evaporation, may become air-dry within a few days following irrigation due solely to evaporation. Although there may be some roots and soil water extraction between 0.05 m and 0.10 m, under normal irrigation practices the decrease in soil water content of this layer due to transpiration will not significantly affect the evaporation rate that is controlled by the dry upper layer and the rate of water movement by liquid and vapor flow from lower depths. An exception to this is for shallow rooted crops like vegetables that may extract some water from this evaporation layer, which is hydrated more frequently.

For shallow-rooted annual crops having rooting depth less than about 0.5 m and where deep cultivation is not practiced, T_e may have significant effect on the water balance of the surface layer and therefore on estimation of the evaporation component during the development period. The following extension to FAO-56 from Allen et al. (2005a) estimates T_e from the f_{ew} fraction of the evaporation layer in proportion to the water content of that layer:

$$T_e = K_t\, K_s\, K_{cb}\, ET_{ref} \qquad (9.30)$$

where K_t, [0 – 1], is the proportion of basal ET (= $K_{cb}\, ET_{ref}$) extracted as transpiration from the f_{ew} fraction of the surface soil layer. K_s is the soil water stress factor computed for the root zone [0 – 1] (K_s is discussed in Chapter 10). K_t is determined by comparing relative water availability

in the z_e and root zone (z_r) layers (where the z_e layer is a subset of the z_r layer) along with the presumed rooting distribution. For the f_{ew} fraction:

$$K_t = \left(\frac{1 - \frac{D_e}{TEW}}{1 - \frac{D_r}{TAW}} \right) \left(\frac{z_e}{z_r} \right)^{0.6} \tag{9.31}$$

where the numerator and denominator of the first expression are limited to ≥ 0.001 and the value for K_t is limited to ≤ 1.0. z_e and z_r have the same units. D_r is depletion of the total effective rootzone, estimated from eq. 10.9 of chapter 10. In the simple water balance procedure of FAO-56, it is assumed that the soil water content is limited to ≤ θ_{fc} on the day of a complete wetting event. This is a reasonable assumption considering the shallowness of the surface layer.

9.9 Example Estimates of Evaporation

The following figures show example applications of the SRT model and various levels of the FAO-56 model for a bare silt loam soil near Kimberly, Idaho. Comparisons are made against evaporation measured by a large weighing lysimeter system. The first example compares evaporation measurements during stage 1 and stage 2 with estimates from the FAO-56 (Allen et al. 1998) method and with stage 2 evaporation estimates from the square root of time (SRT) model (eq. 9.1, 9.11) where α_r was estimated from the drained upper limit (field capacity) using eq. 9.15. Variable K_α for the SRT model was set = 13.9 mm d^{-1}, based on the weighted-mean diffusivity from θ_{dul} to θ_r (Suleiman and Ritchie 2003). Comparisons are shown for two drying series, one in mid August 1977 (Fig. 9.9) and one in early September 1977 (Fig. 9.10). In the first example, the 'original' form and application of the FAO-56 method is used where eq. 9.19, 9.20a and 9.21 were applied with the $F_{stage\ 1}$ parameter of Allen et al. (2012) set to 0. The second example applied the same equations and settings for z_e, *REW* and *TEW* as used for example 1, but with the water balance of the 0 to 0.15 m z_e evaporation layer experimentally modified to include an estimate of upward flux into the evaporation layer, based on the SRT model. This second example illustrates the relative sensitivity of the FAO-56 model to replacing the implicit assumption that deep upward flux to the z_e layer is reflected in the value for z_e with an explicit estimation of upward flux.

In the first two examples, the length of stage 1 evaporation and start of stage 2 evaporation for the SRT application was based on observing when the ratio of measured E to ET_o began to decay below 1.1 to 1.2. This occurred following the fourth day after irrigation for both time series. This type of observation is not typically available in practice, and the start of stage 2 evaporation generally needs to be estimated using a water balance of the skin evaporation layer, such as is done with eq. 9.29. In the experimental application of example 2, the upward flow into the evaporation layer during stage 2 was estimated as 0.2 of the stage 2 evaporation rate using the SRT(S-R) model, with day 1 occurring at the beginning of stage 2 evaporation. Impact of the inclusion of estimated upward flow was minor, as illustrated by comparing fig. 9.9 with fig. 9.11 and fig. 9.10 with fig. 9.12.

The lysimeter data were collected by Dr. J.L. Wright, USDA-ARS (ret), Kimberly, ID, in 1977 and were described in Mutziger et al. (2005). The Kimberly lysimeter system was a

precision weighing lysimeter 1.83 m on a side and 1.2 m deep and filled with Portneuf silt loam soil. Evaporation measurements were made hourly, but only 24-hour totals were commonly evaluated from the system (Wright 1982). Two time series of evaporation were available during August and September 1977 from a bare surface following harvest of a crop of peas. Irrigation of the lysimeter and surrounding field was by furrow. The relatively large irrigation doses to the lysimeter were spread over parts of a day to avoid overtopping the lysimeter during surface ponding. The irrigation amount for the August series was 103 mm on August 9. Irrigation amounts for the late August-early September series were 60, 19 and 34 mm on August 25, August 29 and September 1. The August 10-24 series represents an evaporation event following a single, large wetting event and the extended August 25 – September 24 series represents a series having multiple irrigations in succession at the beginning and a series of small precipitation events near the end. In examples 1 and 2, the starting date for the evaporation series was assumed to begin on September 2. For the third example, the full series with all three irrigation days and four precipitation events was evaluated. The large doses of irrigation on the Kimberly lysimeter and delayed drainage required delaying the transition out of stage 1 drying in examples 1 and 2 by delaying the final start of stage 1. This was done by setting D_e to 0 at the beginning of both 8/10 and 8/11 in eq. 9.21 in the first series and at the beginning of 9/2 and 9/3 for the second series. The need for the override was negated in example 3 by implementing a delay function for infiltration following the large irrigation doses. Parameter f_b in eq. 9.28 was set to 0 in all three examples.

For the first example, the *REW* for the FAO-56 model application was estimated to be 11 mm based on table 9.1. The *TEW* was estimated to be 39 mm based on z_e = 0.15 m and reported soil water values of θ_{fc} = 0.32, θ_{wp} = 0.12, and the assumption $\theta_{ad} = \theta_{wp}/2 = 0.06$ m^3 m^{-3}. The value for $K_{e\,max}$ was set to 1.2 for stage 1 evaporation estimates because grass reference ET_o was used. A summary of daily evaporation estimates for the first time series is presented in fig. 9.9 and estimates for the second drying series are presented in fig. 9.10. Use of $K_{e\,max}$ = 1.2 for September resulted in about 10% overestimation of evaporation during stage 1.

The estimated start of stage 2 evaporation for the two series in fig. 9.9 – 9.12 was August 14 (day 5 after irrigation) and September 6 (day 5 after irrigation). A summary of measured and estimated stage 2 evaporation values for August 14-24 and September 6-13 using the FAO-56 and SRT(S-R) models are:

		RMSD
August lysimeter measured stage 2 evaporation =	16.1 mm	
FAO-56 estimated stage 2 evaporation =	12.8 mm (80%)	0.42 mm d^{-1}
SRT(S-R) estimated stage 2 evaporation =	14.8 mm (92%)	0.50 mm d^{-1}
September lysimeter measured evaporation =	12.1 mm	
FAO-56 estimated stage 2 evaporation =	11.5 mm (95%)	0.18 mm d^{-1}
SRT(S-R) estimated stage 2 evaporation =	11.6 mm (96%)	0.75 mm d^{-1}

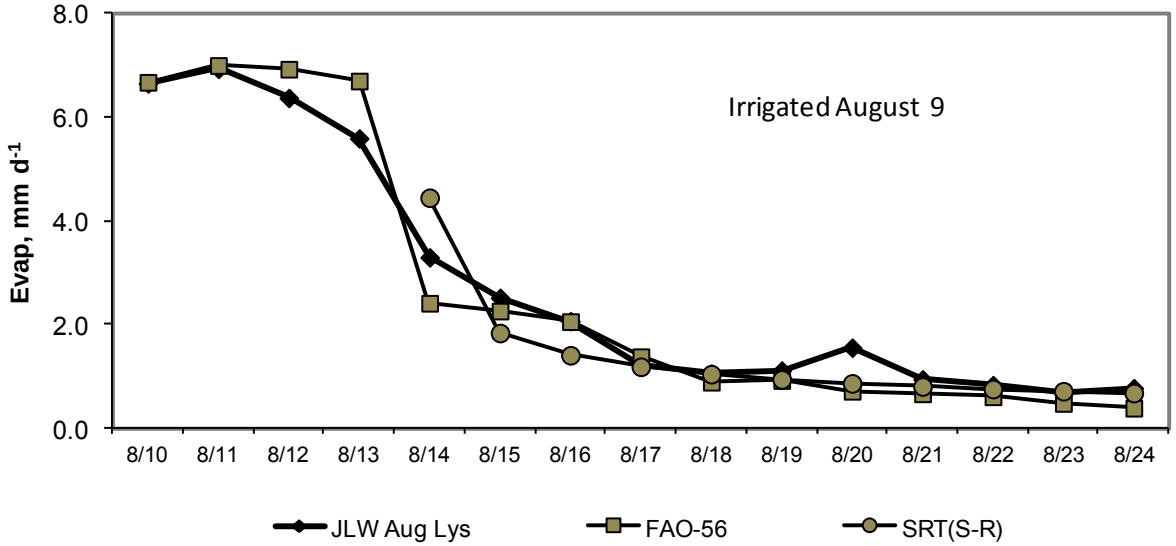

Fig. 9.9. Comparison of estimated evaporation with measured evaporation during August 10-24, 1977 near Kimberly, ID using the FAO-56 procedure (eq. 9.19, 9.20a and 9.21 with $F_{stage\ 1}$ set to 0) and using the square-root of time (SRT) model (eq. 9.11) with α_r estimated using eq. 9.15 with K_a = 13.9 mm d^{-1}. Source: Data from Dr. J.L. Wright, USDA-ARS (ret.).

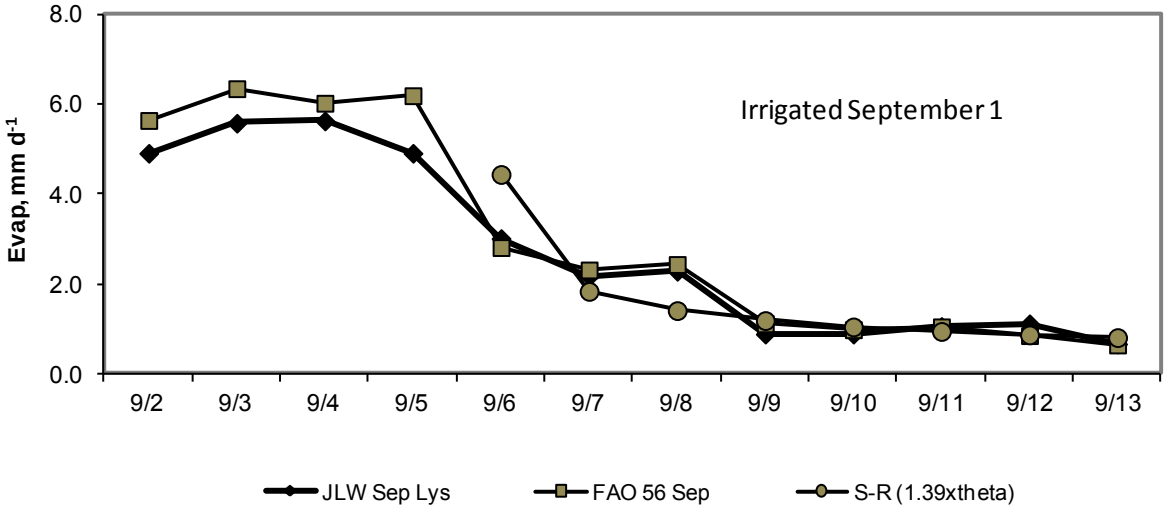

Fig. 9.10. Comparison of estimated evaporation with measured evaporation during September 2-13, 1977 near Kimberly, ID using the FAO-56 procedure (eq. 9.19, 9.20a and 9.21 with $F_{stage\ 1}$ set to 0) and using the square-root of time (SRT) model (eq. 9.11) with α_r estimated using eq. 9.15 with K_a = 13.9 mm d^{-1}. Source: Data from Dr. J.L. Wright, USDA-ARS (ret.).

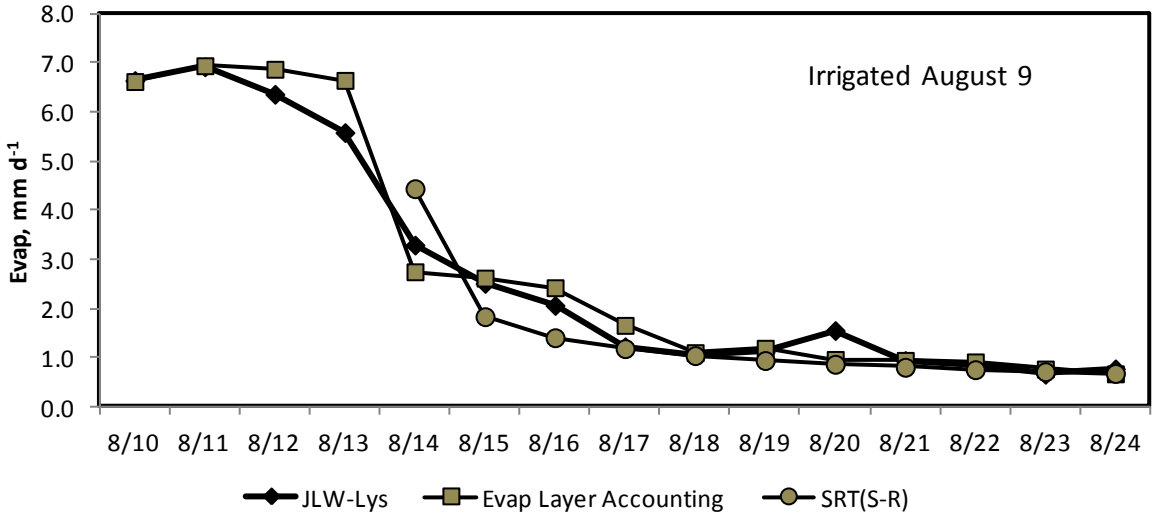

Fig. 9.11. Comparison of calculated evaporation with measured evaporation during August 10-24, 1977 near Kimberly, ID using the FAO-56 procedure (eq. 9.19, 9.20a and 9.21 with $F_{stage\ 1}$ set to 0) and using a water balance model that considers upward flux into the evaporation layer and using the square-root of time (SRT) model (eq. 9.11) with α_r estimated using eq. 9.15 with K_a = 13.9 mm d^{-1}. Source: Data from Dr. J.L. Wright, USDA-ARS (ret.).

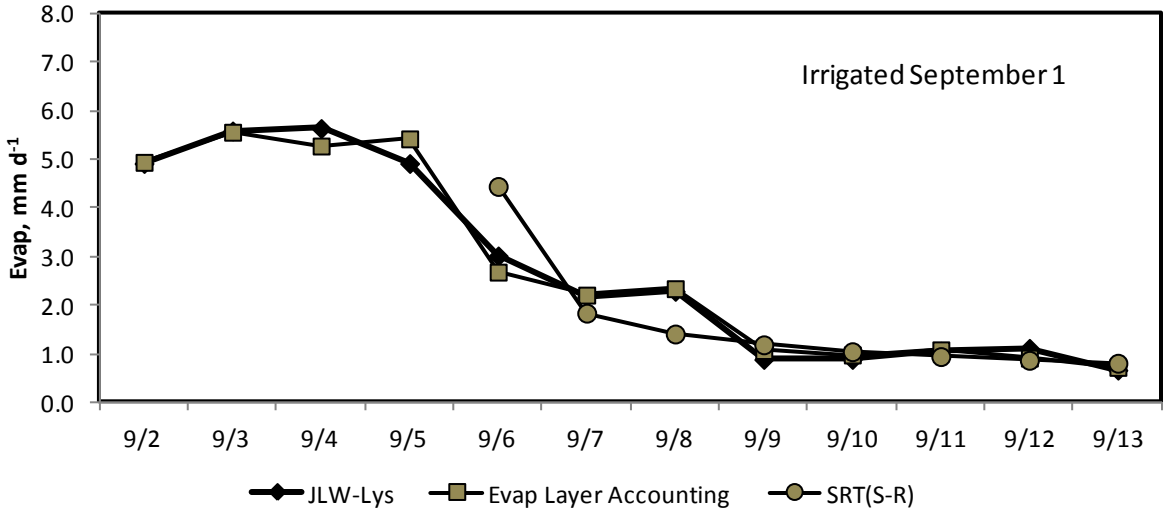

Fig. 9.12. Comparison of calculated evaporation with measured evaporation during September 2-13, 1977 near Kimberly, ID using the FAO-56 procedure (eq. 9.19, 9.20a and 9.21 with $F_{stage\ 1}$ set to 0) and using a water balance model that considers upward flux into the evaporation layer and using the square-root of time (SRT) model (eq. 9.11) with α_r estimated using eq. 9.15 with K_a = 13.9 mm d^{-1}. Source: Data from Dr. J.L. Wright, USDA-ARS (ret.).

A summary of measured and calculated stage 2 evaporation based on evaporation layer water balance for August 14-24 and September 6-13 using an experimental estimate of upward flux into the evaporation layer during stage 2 evaporation based on the SRT(S-R) model are shown below:

	RMSD	
August lysimeter measured stage 2 evaporation =	16.1 mm	
Water balance calculation of stage 2 evaporation =	15.6 mm (97%)	0.33 mm d^{-1}
September lysimeter measured evaporation =	12.1 mm	
Water balance calculation of stage 2 evaporation =	11.9 mm (98%)	0.18 mm d^{-1}

The FAO-56 method provided reasonable estimates with a root-mean square of the daily difference (RMSD) of 0.42 mm d^{-1} in August and 0.16 mm d^{-1} in September. The RMSD for the SRT(S-R) estimates were 0.50 and 0.71 mm d^{-1} for the August and September time series, respectively. When assuming that upward flux into the evaporation layer equaled one-half of the SRT(S-R) stage 2 evaporation, the RMSD of water balance calculated evaporation in August was reduced to 0.30 mm d^{-1}. For this example, day 1 of stage 2 for calculating the SRT(S-R) upward flux was August 10 and September 2. The estimated upward flux was about 25% of the calculated stage 2 evaporation. The upward flux resulted in higher calculated stage 2 evaporation closer to lysimeter measured evaporation in August than when upward flux was not considered. There was no reduction in the RMSD when considering upward flux for September.

A third example application for the FAO-56 model included eq. 9.19, 9.20a and 9.21 with the $F_{stage\ 1}$ parameter estimated using eq. 9.22 and eq. 9.29 to provide better definition of transition from stage 1 to stage 2 drying for 24-hour calculation timesteps and to improve estimation of evaporation following small wetting events. This example also illustrates the impact of using shorter 0.1 day calculation timesteps as compared to using 24-hour calculation timesteps. The example implemented a drainage rate of 75 mm d^{-1} from the z_e evaporation layer following irrigation at the beginning of the mid August series to account for delayed infiltration of surface ponded irrigation water when the large 103 mm dose was applied. The delayed infiltration in the lysimeter may have been caused by effects of entrapped air. The use of the drainage rate eliminated the need to reset depletion depth D_e to zero for one day following irrigation as was done with examples 1 and 2.

Results for the third example are shown in fig. 9.13 for the August 10-24 evaporation series and in fig. 9.14 for the August 25-September 24 series. K_e is presented in the form of E / ET_o. Delayed drainage (*Inf*) from the evaporation layer during the August 10-24 series, following the large irrigation dose, prolonged the length of stage 1 by about one day. The three irrigations over the first seven days of the second evaporation series (August 25-September 24) were close enough together, in time, to create an essentially single, extended stage 1 period having a length of 9 days and cumulative evaporation depth of over 40 mm before the start of stage 2 drying. The end of stage 1 was estimated as when $D_{e,j}$ exceeded the value for *REW*, which was 11 mm in all cases. The measured total cumulative evaporation during the two series was 43 and 87 mm. Both of these values were greater than the estimated *TEW* of 39 mm due to the extended lengths of stage 1 drying caused by delayed drainage in the first series and caused by multiple wetting events in the second series.

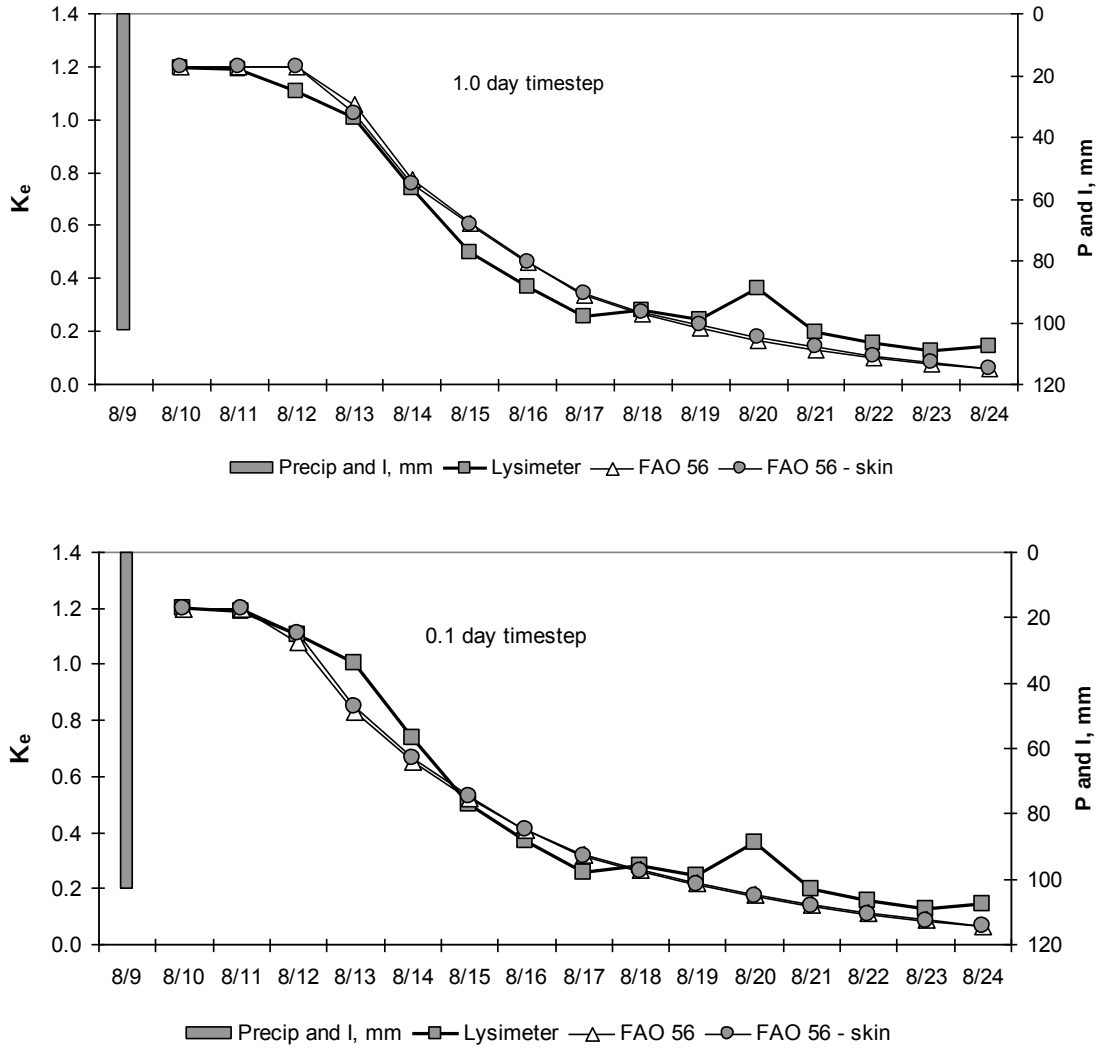

Fig. 9.13. Evaporation coefficient, K_e, during stage 1 and stage 2 drying for 12 days during August 10-24, 1977 near Kimberly, ID, using a 1 day calculation timestep (top) and 0.1 day calculation timestep (bottom) for the FAO-56 procedure (eq. 9.19, 9.20a and 9.21) with $F_{stage\ 1}$ set to 0 to represent the 'original' FAO-56 method (triangles) and with $F_{stage\ 1}$ calculated with eq. 9.22 and 9.29 to consider 'skin' evaporation (circles), compared against evaporation measured by weighing lysimeter. Irrigation of 103 mm occurred on day August 9, with infiltration of 28 mm delayed to August 10. Source: Data from Dr. J.L. Wright, USDA-ARS (ret.).

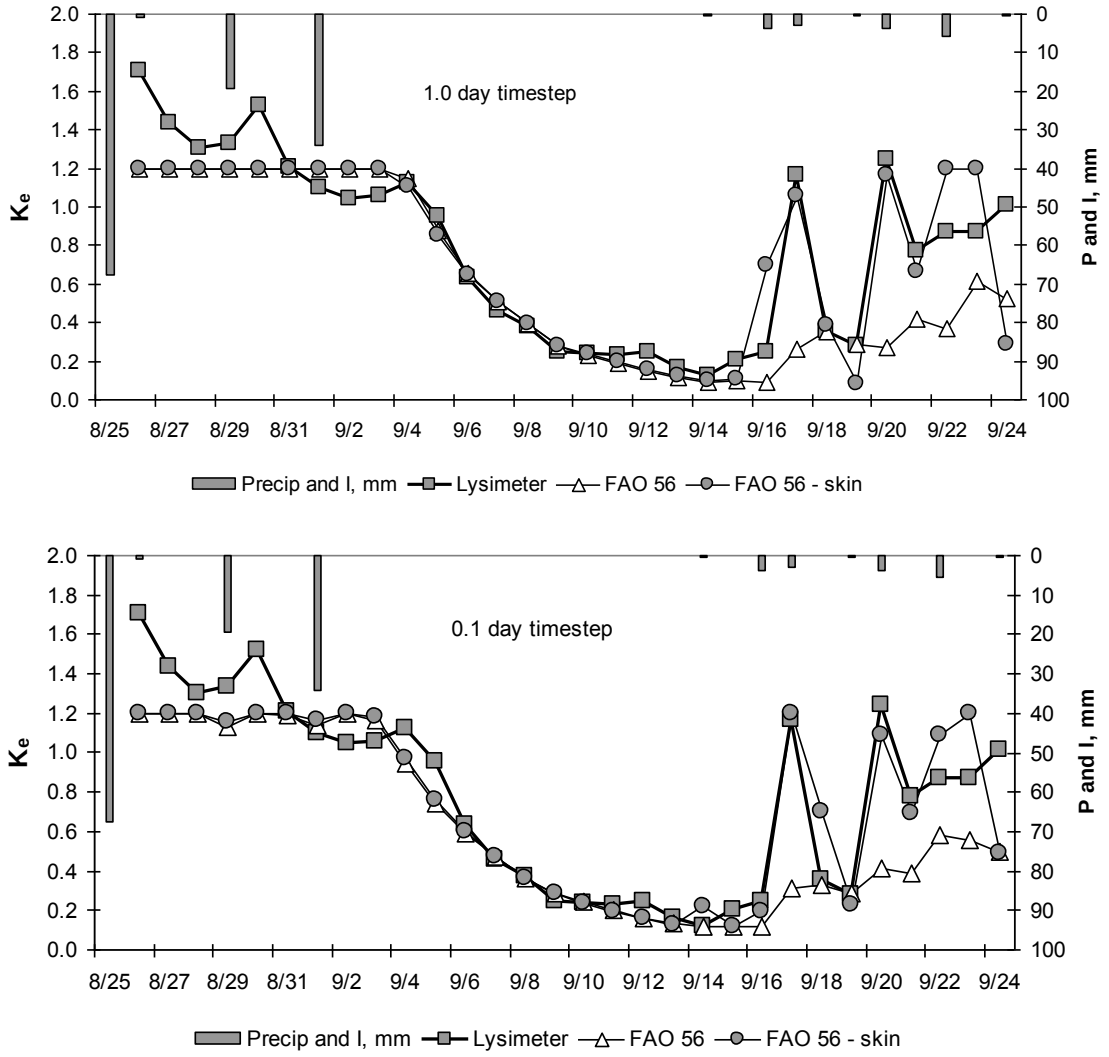

Fig. 9.14. Evaporation coefficient, K_e, during stage 1 and stage 2 drying for 30 days during August 25-September 24, 1977 near Kimberly, ID where three frequent irrigations occurred early in the period and four light precipitation events occurred late in the period, using a 1 day calculation timestep (top) and 0.1 day calculation timestep (bottom) for the FAO-56 procedure (eq. 9.19, 9.20a and 9.21) with $F_{stage\ 1}$ set to 0 to represent the 'original' FAO-56 method (triangles) and with $F_{stage\ 1}$ calculated with eq. 9.22 and 9.29 to consider 'skin' evaporation (circles), compared against evaporation measured by weighing lysimeter. Source: Data from Dr. J.L. Wright, USDA-ARS (ret).

The performance of the FAO-56 model was similar between the original application where skin evaporation was not considered and when using the skin evaporation for the first time series where there was only one large irrigation at the beginning of the period and no light events (Fig. 9.13). Differences did occur between the original formulation, where $F_{stage\ 1}$ was set to 0, and the newer formulation near the end of the second time series when small precipitation events of

less than 8 mm occurred. Under that situation, the original model mixed the small additions of water into the water balance for the z_e layer. The reduction in the value for D_e was not enough to transition the evaporation process, via K_r, into stage 1. The use of the $F_{stage\ 1}$ parameter via eq. 9.22 and 9.29 did transition the process into stage 1 until the new additions of water evaporated. That process simulated the 'flash' evaporation events by operating the separate water balance for the top '*REW*' layer. The 'skin' evaporation enhancement followed the measurements by the lysimeter relatively well during the light precipitation events, as shown in Fig. 9.14 for both calculation timesteps. The impact of calculation timestep length was not large for either time series. The 0.1 day timestep estimated an earlier transition from stage 1 to stage 2 than did the 1 day calculation timestep, but impacts were minor. The performance of the 'skin' evaporation enhancement was similar for the two timestep lengths.

Lysimeter measured K_e exceeded 1.3 for the first five days of the evaporation cycle, using the grass reference ET_o as the basis. These values exceed the maximum values for K_e expected and may have stemmed from stored heat in the soil from the dry period prior to the wetting event.

Cumulative evaporation during stage 1 and stage 2 drying is shown in Fig. 9.15 for the 30 day period from August 25-September 24, 1977 based on K_e calculations shown in Fig. 9.14. Results are for the 1 day calculation timestep and are similar to those from the 0.1 day calculation timestep. Fig. 9.15 also shows cumulative evaporation for the SRT model using the same settings as for examples 1 and 2. Stage 1 evaporation for the SRT application was estimated using the FAO-56 procedure (eq. 9.19). Therefore the cumulative evaporation is similar for FAO-56 and SRT model until stage 2. During stage 2, the SRT model estimated less evaporation than the FAO-56 model and as measured by the lysimeter. The long estimated time for stage 1 was caused by the multiple irrigation events which delayed the reduction in E by the SRT model for stage 2.

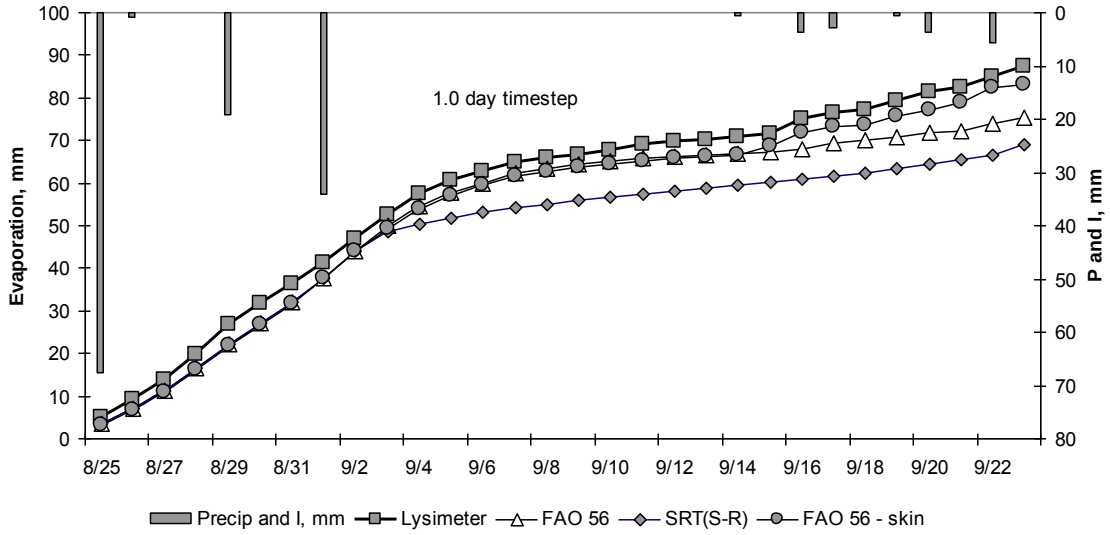

Fig. 9.15. Cumulative evaporation during stage 1 and stage 2 drying for the 30 day period from August 25-September 24, 1977 based on K_e calculations shown in Fig. 9.14 using a 1 day calculation timestep plus application of the SRT model using the same settings as for examples 1 and 2 with stage 1 evaporation estimated using the FAO-56 procedure. Source: Measured data from Dr. J.L. Wright, USDA-ARS (ret).

Comparison of the FAO-56 Model with HYDRUS 1D

HYDRUS 1D (Šimůnek et al., 1998, 2005) is a widely used, one-dimensional, gridded finite-difference model that employs the theoretical Richards equation for unsaturated flow (Richards 1931), including flow to the surface for evaporation. The evaporation rate in HYDRUS is governed by potential evaporative demand, soil water content and soil potential gradients near the surface, and hydraulic properties of the soil. A finite element numerical solution technique is used to solve gridded equations. Estimation of evaporation by HYDRUS is sensitive to the grid density near the surface, where a fine grid is required to cope with potentially large hydraulic gradients and finite changes in soil water content and hydraulic conductivity. The advantage of HYDRUS is its use of a hydraulic basis for evaporation and the ability to consider effects of soil water storage at various depths below the surface on the surface evaporation estimate. Disadvantages are the requirement for unsaturated hydraulic characteristics for the soil. However, standardized soil types residing within HYDRUS can be utilized (Šimůnek et al., 2005).

Fig. 9.16 and 9.17 illustrate the performance of the relatively simple FAO-56 model compared against the HYDRUS 1D model for a full calendar year of weather data collected near Kimberly, Idaho during 2002. The HYDRUS model was applied using standardized van Genuchten soil water potential and hydraulic conductivity parameters for the standard silt loam soil of HYDRUS (Šimůnek et al., 1999, 2005). The initial 2 m soil profile was assumed to be moist, with initial soil water potential set at -3 m, representing conditions near field capacity, to illustrate effects of upward flow from depth for a moist soil condition. The HYDRUS grid was designed using 5 mm soil layers to a depth of 2 m to provide high resolution in solutions for evaporation. The soil surface was assumed to be bare, with no transpiration extraction and using f_{ew} = 1.0 in the FAO-56 equations. The FAO-56 application was applied using typical values for

a silt loam soil, TEW = 25 mm and REW = 8 mm. These values are not the same values as used for the specific Portneuf silt loam soil in examples presented earlier. Weather data recorded at Kimberly, Idaho during a full year (2002) were used for the simulations, with ET_{ref} estimated using the tall ASCE standardized Penman-Moneith (alfalfa) reference method (ASCE 2005) and $K_{e\ max}$ set to 1.0 to reflect the tall reference. Potential evaporation in the HYDRUS application was estimated as $K_{e\ max}\ ET_{ref}$.

Fig. 9.16 shows daily comparisons of K_e (denoted as K_{er} to indicate the alfalfa reference basis) for the FAO-56 model where calculations were made on a 24-hour timestep a) without the skin evaporation enhancement ((eq. 9.19, 9.20a and 9.21 with $F_{stage\ 1}$ set to 0.0), b) with the skin evaporation enhancement ($F_{stage\ 1}$ calculated with eq. 9.22 and 9.29), and c) with the skin evaporation enhancement and with 3-stages of drying used (eq. 9.24 and 9.25). The HYDRUS 1D calculations for K_e were determined by dividing 24-hour E_s by 24-hour ET_{ref}, where 24-hour E_s was summed in HYDRUS 1D from internally determined timesteps that are dynamically varied in HYDRUS according to rates of change in state variables of potentials and water contents.

K_e estimated by the FAO-56 model compared well with that by HYDRUS 1D for all three variations of the FAO-56 model following substantial wetting events that rehydrated D_e of the z_e layer. For light wetting events, the FAO-56 model with the skin evaporation enhancement best estimated K_e, where short-lived K_e spikes extended toward $K_{e\ max} = 1.0$. The basic FAO-56 model without the skin evaporation enhancement underestimated the evaporation spikes because the 'slab' model assumes complete mixing of small additions of water into the z_e layer, thus only reducing the total depletion of the slab by a relatively small amount. In contrast, the Hydrus model tended to 'capture' small water additions near the soil surface and allowed them to evaporate relatively rapidly. The result was a larger spike in K_e, often reaching 1.0, and a short duration of decay. The use of the skin evaporation enhancement simulated the flash evaporation events relatively well and reduced the RMSD between the FAO-56 model and HYDRUS 1D runs for the 365 day period from 0.51 mm d^{-1} for the FAO-56 model with no skin evaporation enhancement to 0.27 mm d^{-1} with skin evaporation enhancement. The RMSD decreased further to 0.23 mm d^{-1} with both skin evaporation and 3-stage drying enhancements.

The differences in annual evaporation estimation were relatively small among applications, with total estimated annual evaporation of 159, 169 and 190 mm for the three applications of FAO-56 compared to 175 mm estimated by HYDRUS 1D and compared to 154 mm of precipitation. The annual evaporation estimates exceeded precipitation because of assumed water stored in the soil prior to January 1. The use of skin evaporation only increased the annual evaporation estimate by 10 mm, or less than 7%, due to the conservation of mass exercised by the FAO-56 model. Addition of stage 3 drying to simulate upward flow increased estimated evaporation by an additional 20 mm over the calendar year. Best agreement between low levels of K_e by the FAO-56 model and by HYDRUS over extended periods of drying during summer months were obtained with the 3 stage implementation using $TEW_3 = 60$ mm, with $TEW_2 = TEW = 25$ mm and with $K_{r2} = 0.05$. With the stage 3 drying option, the very low values for K_e during long drying periods ranged from 0.05 during May to near 0.0 in August. These values contrasted with the essentially 0.0 values estimated by the standard 2-stage FAO-56 model. The 0.05 values for K_e over the extended drying period tend to follow estimates by HYDRUS and were responsible for adding the addition 20 mm of evaporation to the annual total.

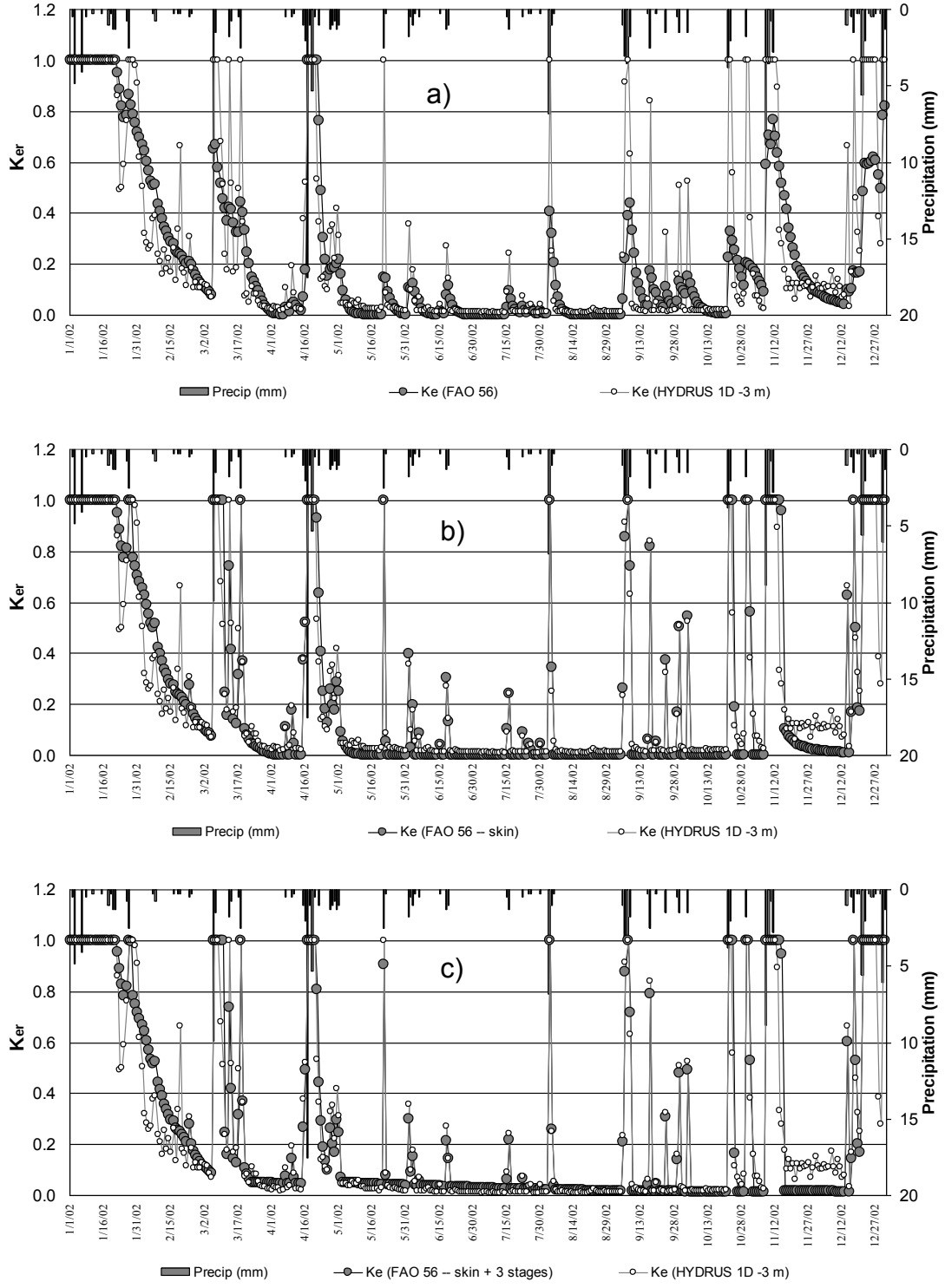

Fig. 9.16. Daily K_e (alfalfa reference basis) for FAO-56 calculations on a 24-hour timestep for a) the original FAO model without the skin evaporation enhancement ((eq. 9.19, 9.20a and 9.21

with $F_{stage\ 1}$ set to 0.0), b) with the skin evaporation enhancement ($F_{stage\ 1}$ calculated with eq. 9.22 and 9.29), and c) with the skin evaporation enhancement and with 3-stages of drying (eq. 9.24 and 9.25) compared against K_e from HYDRUS 1D (HYDRUS calculations by R. Dhungel and R.G. Allen, Univ. Idaho, Kimberly, personal communication).

Fig. 9.17 shows comparisons for the same data set and HYDRUS simulations, but where the FAO-56 model was operated using hourly calculation timesteps and hourly reference ET and precipitation data. The HYDRUS 1D model was populated with hourly potential evaporation and precipitation data. In both applications, hourly evaporation estimates were summed to daily timesteps prior to calculating K_e. The impact of using hourly timesteps as compared to daily timesteps was relatively minor, with results nearly indistinguishable from those with the daily calculation timestep. The RMSD between FAO-56 and HYDRUS 1D evaporation estimates was 0.39 and 0.38 mm d^{-1}, with and without the skin enhancement in the FAO model. The similarity of the two RMSD's was due to some overestimation by the skin evaporation option over some extended drying periods that was partly counterbalanced by underestimation of flash evaporation spikes by the original (non skin evaporation) model. For both applications (with and without the skin evaporation enhancement), total evaporation over the year was similar between the two FAO model runs (147 and 153 mm) and in comparison with the Hydrus run (169 mm). The RMSD was poorer for the FAO-56 model using the skin evaporation enhancement for the hourly timestep as compared with the 24-hour calculation timestep due to more variability in the transition from stage 1 to stage 2 evaporation with the hourly timestep as compared to HYDRUS.

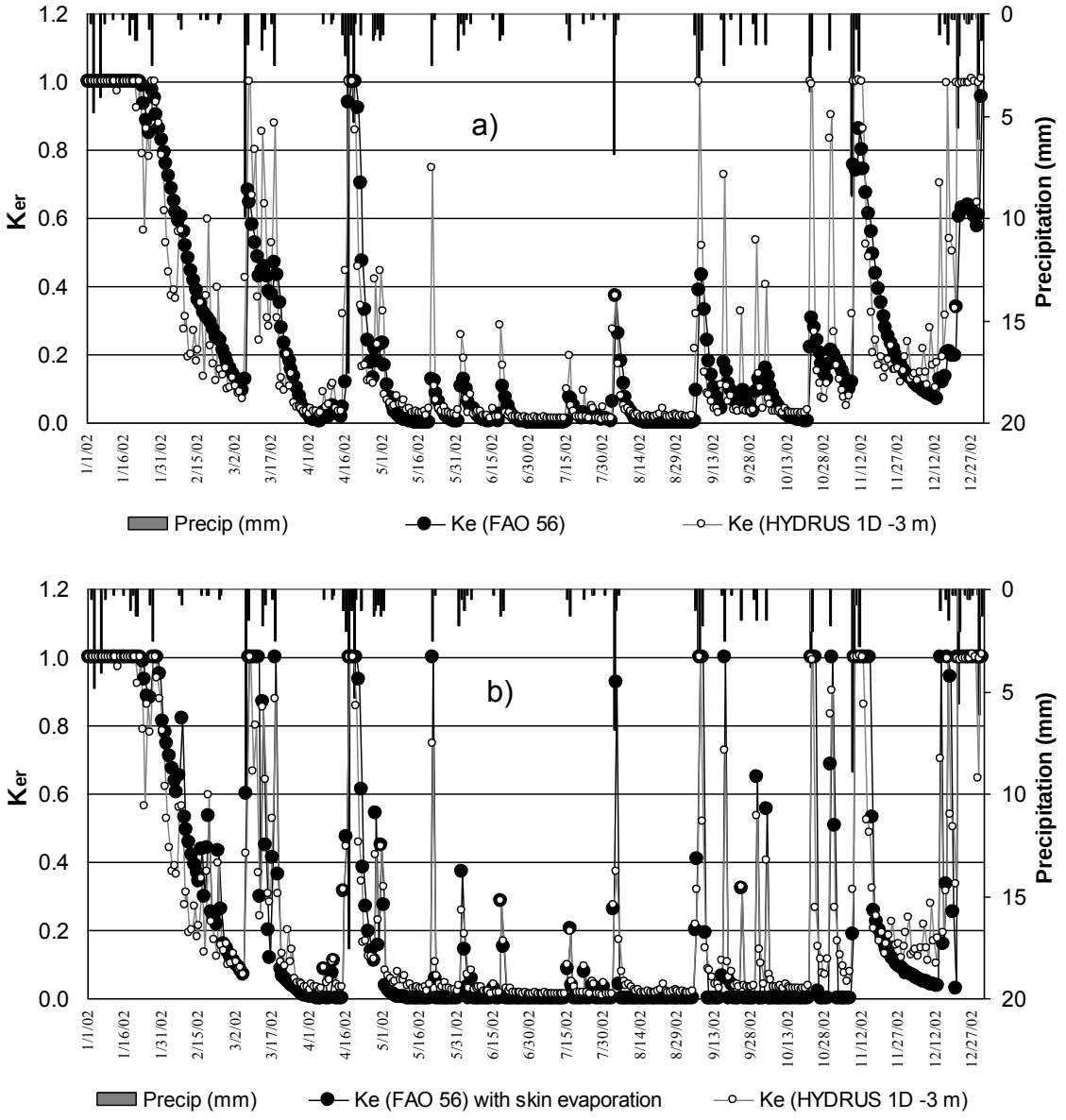

Fig. 9.17. Daily K_e (alfalfa reference basis) for FAO-56 calculations on an hourly timestep for a) the original FAO model without the skin evaporation enhancement ((eq. 9.19, 9.20a and 9.21 with $F_{stage\ 1}$ set to 0.0) and b) with the skin evaporation enhancement ($F_{stage\ 1}$ calculated with eq. 9.22 and 9.29) compared against K_e from HYDRUS 1D (HYDRUS calculations by R. Dhungel and R.G. Allen, Univ. Idaho, Kimberly, personal communication).

9.10 Summary

Estimating evaporation from soil is important when conducting soil water balances over extended periods. Evaporation can be a major component of ET for bare soil and for conditions of partial vegetation cover. The FAO-56 K_e model and Square Root of Time model (SRT) are both relatively simple models that adequately simulate evaporation from the soil surface when parameterized for the general soil type. The SRT model has the advantage of implicitly estimating upward flow from a wet soil profile, whereas the model has the disadvantages of overestimating upward flow when the lower soil profile is dry and requiring a separate water balance technique to estimate the start of stage 2 drying. Parameterization for some soil types may be uncertain. The FAO-56 model has the advantage of simplicity in calculation procedures and parameterization and disadvantages of not implicitly incorporating upward flow from below the slab layer. However, comparisons shown against lysimeter measurements and against HYDRUS 1D simulations indicate that the setting of the z_e depth can compensate for that simplification. The skin evaporation layer enhancement may be important for improving accuracy of the FAO-56 method when accuracy on a day to day basis is important. When evaporation estimates are aggregated over a period of one week or longer, the standard model without skin evaporation has similar accuracy as compared to use with the skin evaporation enhancement.

BLANK PAGE

Evapotranspiration from Land Surfaces: Crop Coefficient Method

10.1 Introduction

Chapter 8 describes the combination of equations for sensible and latent heat transfer, following simplifying assumptions, to produce the well-known Penman combination equation (Penman 1948). Monteith (1965) and Rijtema (1965) independently introduced a surface resistance parameter to the Penman equation and replaced the linear wind function term with an aerodynamic resistance parameter. That resulting combination equation, known as the Penman-Monteith (PM) equation, is now the most widely used basis for estimating evapotranspiration (ET) in engineering, agriculture and landscape applications, where the equation serves as the reference ET basis in the two-step crop coefficient (K_c) – reference ET (ET_{ref}) approach. The first step in the two-step approach is to estimate reference ET representing potential weather or climate impacts on the ET process. The calculation of ET_{ref} is described in chapter 8. The second step is to apply a crop or vegetation coefficient to estimate actual ET, ET_c, according to growth stage, plant type and cover, and wetness of the soil surface and soil profile. The same general two-step approach has also been applied in hydrologic studies. This chapter focuses on the use of the two-step approach for estimating ET for farm crops, landscapes and some natural vegetation. Applications to forests can be found in chapter 4 of the ASCE Hydrology Handbook (Allen et al. 1996).

10.2 The Crop Coefficient

The *crop coefficient* (K_c) having a basis of reference crop ET_{ref} was clarified in 1968 (Jensen 1968) and first used in a computerized irrigation scheduling program (Jensen 1969; Jensen et al. 1970; Jensen et al. 1971). The two-step procedures for estimating ET for well-watered agricultural crops can be applied to various types of natural vegetation and to crops under rainfed conditions as well as in general hydrologic studies. For these reasons, the K_c term might be more appropriately referred to as a "vegetation cover coefficient" rather than as a "crop" coefficient. Usage and application would be the same. However, to be consistent with past literature and applications, this manual adheres to the use of the term "crop coefficient" with the understanding that this term can be applied to nonagricultural vegetation as well as to bare soil.

Early K_c curves had non-reference bases, with values determined by measuring depletion of soil water between two or more sampling dates (Hargreaves 1948; Veihmeyer and Hendrickson 1955; Erie et al. 1965, 1982). Later, more refined curves were developed based on daily ET measured in lysimeters that were then related to a grass or alfalfa reference ET. Some curves were refined for conditions of dry surface soil, or when the soil visually appeared dry, and were called *basal crop* coefficients (Wright 1982). More accurate ET estimates could be obtained using basal coefficients and then adjusting for the wetness of the surface soil for several days following rains or irrigation using the 'dual' K_c approach (Wright 1982, Allen et al. 1998).

Numerous publications over the past decades have focused on measuring ET and calculating associated crop coefficients. Various ET measurement methods have been used, including eddy covariance, Bowen ratio, lysimeters and remote sensing. Many data sets have been based on

lysimeter data. Publications have included information on cereal crops, fiber crops such as cotton, forage crops, fruit tree crops like olives, apricots, peaches and pecans, grapes, cool and warm season grasses, turf grasses, legume crops like beans and peas, oil crops like safflower, root crops like potatoes, tropical fruits like banana, cassava, and coffee, and various vegetable crops. In addition, there have been coefficients for natural vegetation such as grasslands and wet vegetation such as cattails, grasses and reeds. Some of these publications have included models and systems for calculating the crop coefficient. Most of these publications have been from Australia, Brazil, China, India, Spain, England, Italy and the USA. A list of publications describing crop coefficients published since the mid-1990's is provided in Appendix G.

The primary factor causing an increase in the crop coefficient is an increase in plant cover or leaf-area per unit area (LAI) as the crop develops, resulting in a decrease in bulk surface resistance. Most publications on crop coefficient 'curves' have presented the K_c as a function of some form of absolute or scaled time-basis. However, some studies have related the rate of increase in LAI and therefore K_c for various crops as a function of daily weather such as cumulative degree-days.

Crop Coefficient Variables

By expressing ET_c and ET_{ref} in terms of the PM equation as shown in eq. 8.15, where the additional "*c*" subscripts represent characteristic values for the actual vegetation and the additional "*r*" subscripts represent the same for the reference crop, one can visualize that the value of K_c depends on the relative roughness, leaf area, and albedo (in the net radiation calculation) of the actual vegetative surface in relation to the same characteristics for the grass or alfalfa reference surface.

$$K_c = \frac{ET_c}{ET_{ref}} = \frac{\dfrac{\Delta (R_{nc} - G_c) + \rho c_p (e_z^o - e_z) / r_{ac}}{\Delta + \gamma (1 + r_{sc} / r_{ac})}}{\dfrac{\Delta (R_{nr} - G_r) + \rho c_p (e_z^o - e_z) / r_{ar}}{\Delta + \gamma (1 + r_{sr} / r_{ar})}} \tag{10.1}$$

The relative proportions of net radiation, wind, temperature and vapor pressure deficit all affect the value of K_c to some degree. Clearly, the more similar the vegetative cover is to the reference condition, especially at full cover, the closer the value of K_c will be to 1.0 and there will be less variation in the value of K_c with changing weather conditions. One precaution in applying eq. 10.1 is that the equation does not consider impacts of differences between ET_c and ET_{ref} on conditioning the near-surface equilibrium boundary layer above the vegetation. This conditioning can modify levels of T, e_z^o, e_z, Δ and wind speed to some degree, due to differences in partitioning available energy at the surface into H and λE when ET_c is different from ET_{ref}. These generally negative feedback effects can impact the value determined for K_c and are described in more detail in Chapter 11.

Field Scale Applications

When applying the standardized reference ET equation (eq. 8.15) under humid conditions, where a majority of energy for the ET process is from net radiation, the K_c for large expanses of similar vegetation does not exceed about 1.0 to 1.1 relative to the alfalfa reference and about 1.2 relative to the grass reference. In dry climates, where additional advection of warm dry air can occur to increase ET from irrigated surfaces, the K_c still does not exceed about 1.0 to 1.1 relative to the alfalfa reference but can reach maximum values of about 1.3 to 1.4 relative to the grass reference. The reason for the near constant 1.0 to 1.1 crop coefficients for the alfalfa reference is that the alfalfa reference crop has about the same albedo, leaf-area-index (*LAI*) and roughness as most agricultural crops at full cover and therefore converts similar amounts of radiant energy and sensible heat to vapor transfer. An expanse of reference crop (especially alfalfa) will approach the maximum conversion of available energy into λE, so that the ratio of λE for any other tall, leafy crop to alfalfa λE will be near 1.0. This observation is born out in viewing the maximum values for K_c reported by Wright (1982), reproduced for the standardized PM alfalfa reference in Appendices E and F, where none of Wright's K_c's, based on the alfalfa reference, exceed 1.03 when averaged over weekly or longer periods. In the case of the grass reference, where the vegetation is shorter and *LAI* may be less, values for K_c may approach 1.3 for tall, dense crops under arid and semiarid conditions (Doorenbos and Pruitt 1977; Allen et al. 1998).

Limiting K_c to approximately 1.0 for an alfalfa reference-base or to 1.3 for a grass reference-base applies to large expanses of vegetation (> 200 m diameter) and is significant and important when evaluating field measurements of ET. Higher values for K_c may very likely indicate problems with field measurements. Measurement problems include: 1) improper computation of vegetation area in lysimeter studies (Allen et al. 1991b, 2011a); 2) violation of necessary fetch requirements in boundary layer (energy balance) measurements; and 3) weather data collection difficulties and errors. The first two problems are discussed in chapter 7. All are discussed in detail in Allen et al. (2011a).

Small Expanses of Vegetation

When ET is measured from small expanses of vegetation, the internal boundary layer above the vegetation may not be in equilibrium with the new surface and may not have developed up to the height of instrumentation. In addition, small expanses of tall vegetation surrounded by shorter cover can result in a "clothesline effect" where the interchange between air and vegetation is much more efficient than with the logarithmic type of equilibrium boundary layer established over large fields. In these cases, ET from the isolated stands, on a per unit area basis, may be significantly greater than the corresponding ET_r or ET_o computed for an alfalfa or grass reference, assuming an infinitely large fetch of similar reference vegetation. An example of these situations would be ET from a single row of trees surrounded by short vegetation, ET from a narrow strip of cattails along a stream channel, or a vegetated lysimeter surrounded by shorter vegetation. Allen et al. (1994) reported K_c values for small (6-m wide) stands of cattails and bulrushes surrounded by grass pasture equal to 1.6 to 1.8 during midseason, relative to an alfalfa reference. These measurements indicated a strong clothesline effect. Coefficients were only 1.15 for a cattail wetland that was 200 m in diameter (Allen et al. 1994). In an extreme illustration, van Bavel et al. (1963) measured ET from 1-m tall sudangrass in Arizona following cutting of the grass around the lysimeter, so that the vegetation inside the lysimeter functioned as a clothesline. After cutting, 14.7 mm of ET during a 24-h period was measured compared with

9.8 mm three days earlier before the cutting—a 50% increase. The weather data were similar for both clear days. In a similar situation, Allen et al. (1991b) reported measured ET from 0.6 m fescue grass to increase by 1.6 times relative to the PM equation when the surrounding grass was clipped to 0.1 m, but the vegetation inside the lysimeter remained at 0.6 m. The ET rate from the lysimeter under the clothesline condition reached 16 mm d^{-1}, whereas the PM equation estimated 11 mm d^{-1} for 0.6 m grass having extensive fetch of other 0.6 m grass.

Pruitt (1976)[1] reported K_c values for a nearly isolated 4.2-m tall Monterey pine tree (*Pinus radiata*) varying from 1.4 in Feb-Mar to 2.0 during spring and summer and approaching 3.0 during late fall and dry, early-winter months relative to ET_o. The tree was growing on a 1.83-m by 2.44-m hydraulic-pillow lysimeter located within a one-ha dry, non-cropped field. It was near the middle of a 10-tree windrow oriented normal to prevailing winds near Davis, CA, thereby creating a clothesline effect.

The preceding discussion indicates the importance of knowing the type of setting for which ET estimates are needed and the conditions from which measurements are collected. If ET estimates are needed for small, isolated stands of vegetation, then the K_c may be allowed to exceed the 1.0 value for an alfalfa reference and the 1.3 value for a grass reference by up to 50%. However, if ET estimates are to represent large expanses of vegetation or small stands of vegetation surrounded by mixtures of other vegetation having similar roughness and soil water conditions, then K_c's will generally be less than or equal to 1.0 for alfalfa and 1.3 for grass references. Allen et al. (1998) proposed procedures for estimating K_c and ET for isolated stands of wetlands and tall wind breaks such as single rows of trees that are presented later in the section on natural vegetation. They cautioned that an upper limit on K_c exists for isolated vegetation that is governed by root uptake ability and stomatal behavior.

10.3 Crop (Vegetation Cover) Coefficients

Two families of K_c curves for agricultural crops have been developed for the two commonly used reference crops (tall and short). These are the grass-based curves by Pruitt (Doorenbos and Pruitt 1977; Jensen et al. 1990; Allen et al. 1998) and others and alfalfa-based K_c curves by Wright (1981, 1982) and others (Tolk and Howell 2001; Howell et al. 2004, 2006). The user must exercise caution in not mixing grass-reference-based K_c's with an alfalfa reference and vice-versa. Usually K_c's based on alfalfa reference can be "converted" for use with a grass reference during summer months by multiplying by a factor ranging from 1.1 to 1.3, depending on climate (1.1 for humid, calm conditions and 1.3 for arid moderately windy conditions). The conversion ratio can be estimated by ratioing ET_{rs} and ET_{os} from the standardized PM estimates from chapter 8. Grass-based K_c's are presented and discussed first in this manual (section 10.4) due to the large number of K_c's that have been presented in FAO-24, FAO-56, the ASABE publication Design and Operation of Farm Irrigation Systems (Allen et al. 2007c) and elsewhere (Snyder et al. 1989a,b) for agricultural crops. Alfalfa-based K_c's for eight irrigated crops in southern Idaho developed by Wright (1981, 1982) and presented in Manual 70, 1st edition (Jensen et al. 1990) have been updated in this edition of Manual 70 for use with standardized ET_{rs} and are presented in Appendix E.

[1] Personal communication.

Generalized crop coefficient curves for estimating crop ET_c for crops or other vegetation are shown in fig.10.1. The K_{cb} curve represents "basal" crop coefficients for conditions where the soil surface is visually dry, so that evaporation from soil is minimal, but where the availability of soil water does not limit plant growth or transpiration. This curve represents a minimum ET_c situation for adequate soil water. The "spikes" in fig. 10.1 indicate occurrences of precipitation or irrigation that wet the soil surface and temporarily increase total ET_c for one to five days. These spikes decay to the K_{cb} curve as the soil surface dries. The spikes generally approach a maximum value of 0.8 to 1.0 for an alfalfa ET_r base (Wright 1982) and 1.0 to 1.2 for a grass ET_o base (Allen et al. 1998). The K_{cm} curve in fig. 10.1 represents a so-called "mean" crop coefficient that includes averaged effects of wet soil (spikes) under specific rainfall or irrigation frequencies. Sometimes the K_{cm} is referred to as the "single" K_c. The final, "limited soil water" curve in the figure represents the decrease in ET_c when plant water uptake is limited by available soil water.

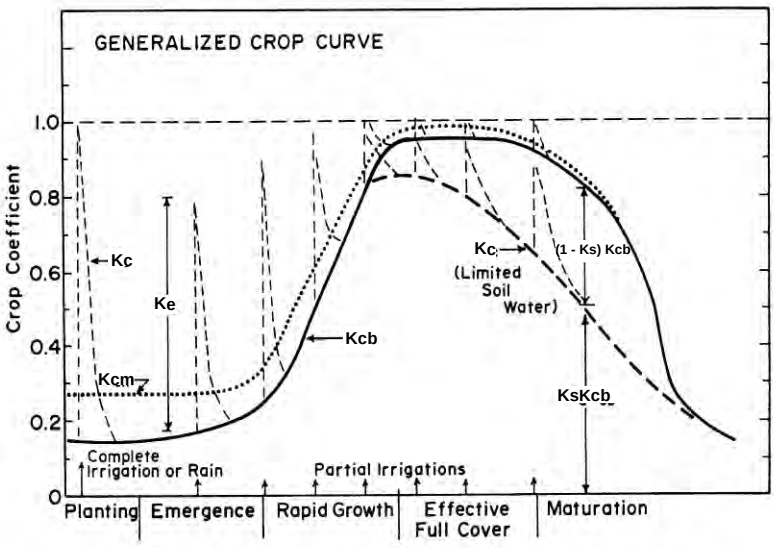

Fig. 10.1. Generalized cover coefficient curves showing the effects of growth stage, wet surface soil and limited available soil water. Source: Wright (1982); Jensen et al. (1990).

K_c and ET Terminology

Actual ET, denoted here as $ET_{c\ act}$ or ET_a, is the ET rate that occurs under actual field conditions. $ET_{c\ act}$ is often used interchangeably with the term crop ET, ET_c. The value for $ET_{c\ act}$ may be less than the value for potential ET_c, sometimes denoted as $ET_{c\ pot}$, when there is water stress in the vegetation. $ET_{c\ act}$ or ET_c are calculated using eq. 8.14 as $ET_{c\ act} = ET_c = K_c\ ET_{ref}$. Both $ET_{c\ act}$ and ET_c (and $ET_{c\ pot}$) terms can include varying degrees of direct evaporation from soil as represented by K_e.

In FAO and European literature, $ET_{c\ act}$ is often presented as "ET_{adj}" representing 'adjusted' ET, and is based on an 'adjusted' $K_{c\ adj}$ as determined from eq. 10.2 (Pereira et al. 1999a,b). That same literature generally reserves the use of the term 'crop ET,' denoted as ET_c, and the term K_c to represent only the potential, or upper limit on ET for a particular crop, in other words, representing a pristine, well-watered condition. In the European tradition, any reduction in K_c due to water stress or other factors such as reduced density, disease or salinity, are encapsulated into a second expression referred to as "actual" $K_{c\ act}$ or $K_{cb\ act}$ (Allen et al. 1998).

The traditional American usage of the terms ET_c and K_c have tended to be more 'relaxed' in their usage of the ET_c and K_c terms and allow these terms to represent both potential and actual conditions. The European usage is less ambiguous, but the American usage is more encompassing. The less formal American usage is defended by the fact that when using the mean K_{cm} of the following section, the value for K_{cm} changes substantially with wetting frequency and therefore is not a well defined, consistent coefficient. The differences between the two systems are largely semantic, but can cause confusion and some degree of frustration within the user community unless carefully defined. The American tradition is followed in this ASCE manual.

Basal Crop Coefficients

Basal crop coefficients represent primarily the transpiration component of ET and a small evaporation component from soil that is visually dry at the surface. Their use requires adjustment for wet soil effects after rain or irrigation. This results in more accurate estimates of ET_c on a daily basis for use in soil water modeling and irrigation scheduling than using mean coefficients in which the effects of local rainfall or irrigation frequencies are included. The total crop coefficient, K_c is computed from K_{cb} as:

$$K_c = K_s K_{cb} + K_e \tag{10.2}$$

where K_s is a dimensionless coefficient dependent on available soil water and K_e is a coefficient to adjust for increased evaporation from wet soil immediately after rain or irrigation. The value for K_s is 1 unless available soil water limits transpiration, in which case it has a value less than 1. Potential ET_c is estimated as $ET_c = K_c\ ET_{ref}$ when K_s in eq. 10.2 equals 1. Actual ET_a is estimated as $ET_a = K_c\ ET_{ref}$ when K_s in eq. 10.2 is less than 1. The values for K_e represent the "spikes" shown in fig. 10.1. Estimation of K_e for bare soil conditions is described in detail in chapter 9, where the square root of time (SRT) model and the FAO-56 K_e model (eq. 9.19-9.31) are presented and illustrated.

The value for $K_{c\ max}$. $K_{c\ max}$ is used in eq. 9.19 of chapter 9 to estimate the evaporation coefficient K_e, and represents the maximum value for K_c following rain or irrigation, under conditions of both bare soil or some degree of vegetation cover. The value for $K_{c\ max}$ is governed by the amount of energy available for evaporation of water, which is largely encapsulated by reference ET_{ref}. Because K_c is the ratio of ET to ET_{ref}, the value for $K_{c\ max}$ is not expected to exceed 1.0 to 1.3. Because of the lower value for the grass reference (ET_o) as compared to the alfalfa reference, $K_{c\ max}$ for use with ET_o ranges from about 1.05 to 1.3 and varies with general climate (Allen et al. 1998, 2005a):

$$K_{c\,max\,o} = max\left(\left\{1.2 + \left[0.04(u_2 - 2) - 0.004\,(RH_{min} - 45)\right]\left(\frac{h}{3}\right)^{0.3}\right\},\ \left\{K_{cb\,o} + 0.05\right\}\right) \qquad (10.3a)$$

where u_2 is average wind speed at 2 m during the growth stage or period, RH_{min} is average daily minimum relative humidity during the growth state or period and h is the mean plant height (m) during the period of calculation (initial, development, midseason, or late-season), and the max ( ) function indicates the selection of the maximum of values separated by the comma. $K_{c\,max\,o}$ denotes the use of $K_{c\,max}$ with ET_o and with K_{cb} based on ET_o, denoted as K_{cbo}. Parameters u_2 and RH_{min} are discussed later with eq. 10.15-10.17.

$K_{c\,max}$ for the tall reference ET_r, denoted as $K_{c\,max\,r}$, does not require adjustment for climate, due to the greater roughness of the reference basis:

$$K_{c\,max\,r} = \max\,(1.0,\ \{K_{cbr} + 0.05\}) \qquad (10.3b)$$

where K_{cbr} denotes a basal K_{cb} used with ET_r. Eq. 10.3a,b require that $K_{c\,max}$ is greater than or equal to the sum K_{cb} + 0.05, suggesting that wet soil increases the K_c value over K_{cb} by about 0.05 following complete wetting of the soil surface, even during periods of full ground cover. Eq. 10.3a and 10.3b, as well as the FAO-56 evaporation equations 9.19 – 9.31, can be applied with both the straight-line K_{cb} curve style of FAO and with the curvilinear K_{cb} curves such as by Wright (1982), as illustrated later in this section.

Adjusting for Water Stress

A number of linear and curvilinear functions have been proposed to adjust for the effects of decreasing available water on ET or for the K_s used in eq. 10.2. The simple linear model for estimating K_s as described in FAO-33 (Doorenbos and Kassam 1979) is commonly used:

$$K_s = \frac{\theta - \theta_{wp}}{\theta_t - \theta_{wp}} \qquad for\,\theta < \theta_t \qquad (10.4)$$

where θ is mean volumetric soil water in the root zone, $m^3\ m^{-3}$, and θ_t is the threshold θ below which transpiration is decreased linearly due to water stress. $K_s = 1.0$ for $\theta \geq \theta_t$. The wilting point, θ_{wp}, is the soil water at the lower limit of soil water extraction by plant roots, $m^3\ m^{-3}$. Typical values of θ_{wp} for various soil texture classes are listed in table 3.6. The threshold soil water, θ_t, can be estimated from the relationship:

$$\theta_t = (1 - p)(\theta_{fc} - \theta_{wp}) + \theta_{wp} \qquad (10.5)$$

where p is the average fraction of available soil water that can be depleted before water stress and ET reduction occur. Variable θ_{fc} is the soil water content at field capacity or the drained limit of the soil, $m^3\ m^{-3}$. Values for all θ parameters should represent averages over the effective root

zone. Values for θ_{fc} are listed in table 7.1 and values for p for agricultural crops are listed in Appendix B.

Parameter p normally ranges from 0.30 depletion of available soil water ($\theta_{fc} - \theta_{wp}$) for shallow rooted plants at high rates of ET_c (> 8 mm d^{-1}) to 0.70 for deep rooted plants at low rates of ET_c (< 3 mm d^{-1}) (Raes et al. (2009) and Appendix B). A value of 0.50 is commonly used for many agricultural crops. After computation of K_c, ET_c is computed using eq. 8.14.

An equivalent expression to eq. 10.4, but in terms of depletion, D_r, of available water in the root zone is, for $D_r > RAW$:

$$K_s = \frac{TAW - D_r}{TAW - RAW} = \frac{TAW - D_r}{(1-p)\,TAW} \qquad for\ D_r > RAW \tag{10.6}$$

where TAW is the total depth of available soil water in the root zone [mm], RAW is the depth of readily available water in the root zone [mm], and p is the fraction of TAW that a crop can extract from the root zone without suffering water stress. When $D_r \le RAW$, $K_s = 1.0$. The total available water in the root zone is estimated as the difference between the water content at field capacity and wilting point:

$$TAW = 1000\,(\theta_{fc} - \theta_{wp})\,z_r \tag{10.7}$$

where z_r is the effective rooting depth [m] and z_r contains z_e, the effective depth of the evaporation layer described in chapter 9 and illustrated in fig. 9.4. The 1000 factor converts from m to mm. RAW is estimated as:

$$RAW = p\,TAW \tag{10.8}$$

where RAW has the same units as TAW (mm). Appendix B contains typical maximum effective values for z_r.

The mean soil water balance for the root zone in terms of θ can be computed on a daily basis using eq. 7.3 and 7.4. Computations are made for the complete z_r root depth, including the evaporation layer.

The soil water balance for the root zone in terms of depletion is:

$$D_{r,i} = D_{r,i-1} - (P - RO)_i - I_i - CR_i + ET_{c\,act,i} + DP_i \tag{10.9}$$

where $D_{r,i}$ is root zone depletion at the end of day i [mm], $D_{r,i-1}$ is root zone depletion at the end of the previous day, i-1 [mm], P_i is precipitation on day i [mm], RO_i is runoff from the soil surface on day i [mm], I_i is net irrigation depth on day i that infiltrates the soil [mm], CR_i is capillary rise from the groundwater table on day i [mm], $ET_{c\,act,i}$ is actual crop evapotranspiration on day i [mm], and DP_i is water loss out of the root zone by deep percolation on day i [mm].

Although following heavy rain or irrigation, soil water content might temporally exceed field capacity, in the above equation, the total amount of water exceeding field capacity is assumed to be lost the same day via deep percolation, following any ET for that day. This does permit the extraction of one day's ET from this excess before percolation. That assumption can be modified

by delaying *DP* as in eq. 10.12b. The root zone depletion will gradually increase as a result of ET and percolation. In the absence of a wetting event, the root zone depletion will ultimately reach the value *TAW* that is defined from rooting depth, θ_{fc} and θ_{wp} from eq. 10.7. At that moment no water is left for ET, and K_s becomes zero, from eq. 10.6. Limits imposed on $D_{r,i}$ are consequently:

$$0 \le D_{r,i} \le TAW \tag{10.10}$$

The lower limit 0 can be relaxed if some delayed drainage from the root zone is allowed as discussed later with eq. 10.12b.

To initiate the water balance for the root zone, the initial depletion $D_{r,i-1}$ can be derived from measured soil water content by:

$$D_{r,i-1} = 1000\,(\theta_{fc} - \theta_{i-1})\,z_r \tag{10.11}$$

where θ_{i-1} is the average soil water content at the end of day *i-1* for the effective root zone. The 1000 factor converts from m to mm. Following heavy rain or irrigation, the user can assume that the root zone is near field capacity, i.e., $D_{r,i-1} \approx 0$. Daily precipitation in amounts less than about 0.2 ET_{ref} is normally entirely evaporated and can generally be ignored in depletion calculations (in both the computation of $D_{r,i}$ and computation of $ET_{c\,act}$). In the case of using the dual K_c method of eq. 10.2, light precipitation events will generally be evaporated using K_e and can be included in the *P* estimate. I_i is equivalent to the mean infiltrated irrigation depth expressed for the entire field surface. Runoff from the surface during precipitation can be estimated using standard procedures from hydrologic texts.

Capillary rise (CR). The amount of water transported upwards by capillary rise from the water table to the root zone or soil surface depends on the soil type, the depth of the water table and the wetness of the root zone. *CR* can normally be assumed to be zero when the water table is more than a few meters below the bottom of the root zone. Fig. 10.2 shows estimated flux of water from a shallow water table to a bare soil surface under dry conditions. Data in the figure were based on simulations by the UPFLOW model (Raes and deProost 2003, and Raes 2004). Similar figures for wet soil conditions and for flux into a 1-m root zone are presented in Appendix I along with regression equations that reproduce the figures. Appendix I also describes an analytical technique for estimating capillary rise by Brutsaert (1982). Medium textured soils tend to have higher upward fluxes than fine and coarse textured soils due to a favorable combination of capillarity and hydraulic conductivity.

Deep percolation from the root zone (DP). Following heavy rain or irrigation, the soil water content in the root zone may exceed field capacity. In application of eq. 10.9, *DP* is assumed to occur within the same day of a wetting event, so that the depletion $D_{r,i}$ becomes zero. Therefore,

$$DP_i = (P_i - RO_i) + I_i - ET_{c\,act,i} - D_{r,i-1} \tag{10.12a}$$

where DP_i is limited to $DP_i \ge 0$. As long as the soil water content in the root zone is below field capacity (i.e., $D_{r,i} > 0$), the soil is assumed to not drain and $DP_i = 0$. If drainage from the root

zone is expected to be delayed following a large infiltration event by a day or more, then daily DP_i in eq. 10.9 can be estimated as:

$$DP_i = max\left(min\left[\left(P_i - RO_i\right) + I_i - ET_{c\,act,i} - D_{r,i-1}\,,\, DR_i\right],\ 0\right) \qquad (10.12b)$$

where DR_i is an expected maximum rate of drainage from the root zone on day i, with units for DR_i the same as P and I. Limiting $DP_{r,i}$ to DR_i has the effect of causing $D_{r,i}$ in eq. 10.9 to be negative for one or more days. Values for DR_i can be estimated from hydraulic conductivity characteristics for the root zone soil layer.

Examples of application of the FAO-56 'dual' K_c procedure include Hunsaker (1999), Tolk and Howell (2001), de Medeiros (2001), Hunsaker et al. (2002, 2003, 2005), Howell et al. (2004), Mutziger et al. (2005) and Allen et al. (2005a).

Mean Crop Coefficients

In basin-wide water balance studies or irrigation system planning, use of mean, or 'single,' crop coefficients may be more useful and convenient than computing a daily K_c based on a combination of K_{cb}, K_s and K_e as used in the dual K_c method of eq. 10.2. The mean crop curve, K_{cm}, shown in fig. 10.1, lies above the basal curve by an amount that depends on the frequency of soil wetting. When a mean coefficient is used, usually no additional adjustment is made for the effects of surface soil wetness. Adjustments can be made for the effects of limited soil water as:

$$K_c = K_s K_{cm} \qquad (10.13)$$

where K_s is defined in eq. 10.4 and 10.6. Values for K_{cm} during partial crop cover are dependent on precipitation frequency and irrigation practices that wet all or part of the soil surface. K_{cm} curves can be generated from K_{cb} curves for known or simulated precipitation or irrigation frequencies using the dual K_{cb} approach.

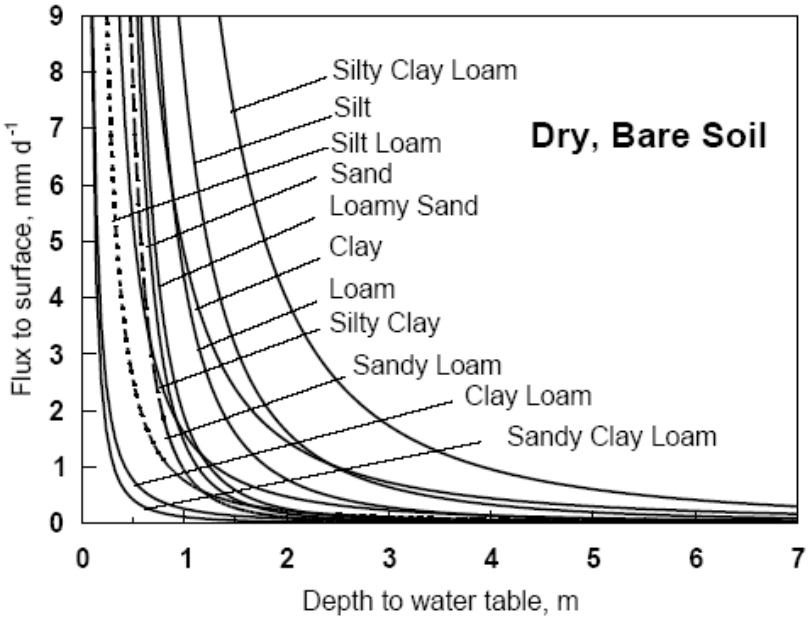

Fig. 10.2. Estimated flux of water to the ground surface for evaporation as a function of depth to the water table for a variety of soil textures, based on numerical simulations using the UPFLOW (Raes 2004) model.

10.4 FAO Grass-based Crop Coefficients

Although several crop coefficient models use a curvilinear curve shape, the linear segment model proposed by the FAO is widely used and easy to formulate (fig. 10.3). The procedure for constructing crop (cover) coefficients was presented in FAO-24 (Doorenbos and Pruitt 1977) and FAO-56 (Allen et al. 1998) publications. In the FAO procedure, a K_c curve such as that shown in fig. 10.3 is constructed by:

1. Dividing the growing season into four parts that describe crop phenology or growth stages:
   a. Initial period (1)
   b. Crop development period (2)
   c. Midseason period (3)
   d. Late season period (4)
2. Selecting three K_c values that represent
   a. Average K_c during the initial period ($K_{c\ ini}$)

end)
ı the

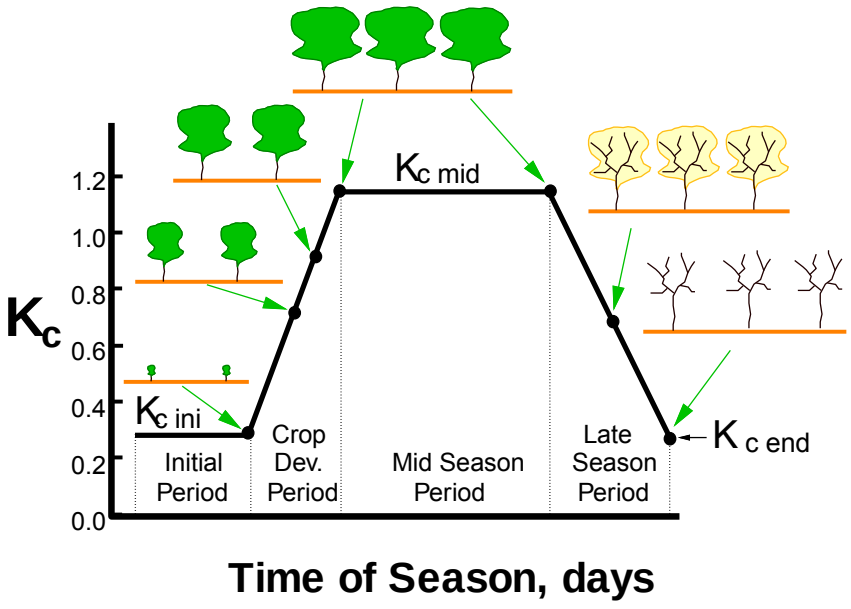

) ASCE.

Only three tabularized values for K_c are required to describe and construct the FAO-style K_c curve. $K_{c\ mid}$ represents the average value for K_c expected during the total midseason period, rather than the absolute peak daily K_c reached by the crop.

The four crop growth stages are generally characterized in terms of benchmark crop growth stages or cultivation practices. Definitions of these stages are given in table 10.1 and are closely tied to crop phenology.

Values for $K_{c\ ini}$, $K_{c\ mid}$ and $K_{c\ end}$ are listed in Appendix B for mean K_{cm} for various agricultural crops. Most information in Appendix B was taken from FAO-24 (Doorenbos and Pruitt 1977) and FAO-56 (Allen et al. 1998) with additional information from Wright (1982), Snyder et al. (1989a,b), Jensen et al. (1990), Allen and Pereira (2009) and Allen et al. (2011c). Lengths of growth stages common to crops are listed in Appendix C. Values for K_{cb} are listed in Appendix D. Lengths of growth stages are strongly influenced by air temperature, time of year and crop variety. Therefore the values for lengths in Appendix C are useful for general estimates, only, and should be verified or varied using local information and observation, including remote sensing (Bausch and Neale 1987; Neale et al. 1989; Tasumi et al. 2005; Singh and Irmak 2009).

TABLE 10.1 General Benchmark Growth Stages for Defining FAO Crop Stages.

Period	Growth stages
Initial:	*planting to 10 percent ground cover* (Length is strongly dependent on crop and time of year)
Crop development:	*10 percent ground cover to effective cover* (effective cover = initiation of flowering for many crops)
Midseason:	*effective cover to start of maturity* (start of maturity is often indicated by the beginning of aging, yellowing or senescence of leaves, browning of fruit, etc).
Late season:	*start of maturity to harvest*

Adjusting K_c for Climate

The ratio of ET_c to grass reference ET_o for many crops increases as wind speed increases and as minimum daily relative humidity, RH_{min}, decreases (Doorenbos and Pruitt 1977). This is due primarily to differences in roughness between tall agricultural crops and the clipped grass reference. The result is a high K_c value caused by increased roughness and perhaps leaf area for a tall crop, making the aerodynamic aspects of vapor transport more important and significant. The adjustment to K_c is generally required only for coefficients based on the grass ET_o reference. No adjustment for climate is necessary for coefficients based on the alfalfa ET_r reference because of the greater height, roughness and leaf area of alfalfa (Wright 1982, Pereira et al. 1999). The FAO procedure for adjusting the ET_o-based K_c values uses mean RH_{min} and wind speed, where $K_{c\ mid}$ and $K_{cb\ mid}$ values are adjusted for climates having RH_{min} greater than or less than 45% or having mean wind speed at 2 m (u_2) that are greater than or less than 2.0 m s^{-1}, as:

$$K_{c\,mid} = K_{c\,mid\,(table)} + \left[0.04\left(u_2 - 2\right) - 0.004\left(RH_{\min} - 45\right)\right]\left(\frac{h}{3}\right)^{0.3} \quad (10.14)$$

where $K_{c\,mid(table)}$ is the value for $K_{c\,mid}$ or $K_{cb\,mid}$ taken from Appendix B or D and h is the mean maximum plant height, m, during the midseason period, or full cover period. Eq. 10.14 is valid for h to 20 m. Mean values for h are listed in Appendix B for the crops and vegetation listed. For local applications, h should be based on field observations. Eq. 10.14 will increase $K_{cb\,mid}$ by about 0.1 for mean wind speed of 5 m s^{-1} or RH_{min} of 15% when crop height is about 1-2 m.

The $K_{c\,end}$ or $K_{cb\,end}$ at the time of termination of the growing period is adjusted for climate with RH_{min} less than or greater than 45% or with wind speed at 2 m (u_2) less than or greater than 2 m s^{-1} as:

$$K_{c\,end} = K_{c\,end\,(table)} + \left[\left(0.04\,u_2 - 2\right) - \left(0.004\,RH_{\min} - 45\right)\right]\left(\frac{h}{3}\right)^{0.3}, \text{ for } K_{c\,end(table)} \geq 0.4 \quad (10.15a)$$

$$K_{c\,end} = K_{c\,end\,(table)} + 0.001\,(RH_{\min} - 45), \quad \text{for } K_{c\,end(table)} < 0.4, \quad (10.15b)$$

where $K_{c\,end(table)}$ is the value taken from Appendix B or D.

Minimum daily relative humidity, RH_{min}, is defined as the average daily minimum relative humidity during a growth stage. It can be calculated as:

$$RH_{min} = \frac{e^o(T_d)}{e^o(T_{max})} \quad (10.16)$$

When dewpoint temperature or other hygrometric data are not available, then RH_{min} can be estimated by substituting T_{min} for T_d. Then:

$$RH_{\min} \cong \frac{e^o(T_{\min} - K_o)}{e^o(T_{\max})} \quad (10.17)$$

where K_o is a dewpoint offset coefficient introduced with eq. 8.17 and has values of approximately 2 to 5°C in semiarid and arid climates and approximately 0°C in humid to subhumid climates. The values for u_2 and RH_{min} in eq. 10.14 and 10.15 need only be approximate, averaged values representing the midseason or late season periods. Application of these equations can be made on a daily basis, but it may not improve accuracy over using averaged values.

Estimating Initial $K_{c\,ini}$ with the FAO Mean K_c Procedure

Values for mean $K_{c\,ini}$ in Appendix B represent mean soil wetting conditions expected for each type of crop during the initial period. These $K_{c\,ini}$'s can be used for making approximate estimates of ET during planning studies. More accurate estimates of $K_{c\,ini}$ consider local

characteristics including the frequency that the soil surface is wetted and soil type, as this significantly affects the ET rate during the initial and development periods, when ET is predominately comprised of evaporation. Values for $K_{c\ mid}$ and $K_{c\ end}$ are less affected by wetting frequency since vegetation during these periods is generally near full ground cover so that effects of surface evaporation are generally relatively small.

When the ground surface is bare or nearly bare, then $K_{c\ ini}$ is dominated by the evaporation from bare soil, denoted here for time-averaged periods as K_{soil}. Fig. 10.4a – 10.4c from FAO-56 present K_{soil} as a function of ET_o, soil type, and wetting frequency. Fig. 10.4a is used for all soil types when wetting events (precipitation and irrigation) are light (i.e., infiltrated depths average about 10 mm per wetting event), fig. 9.14b is used for "heavy" wetting events, where infiltrated depths are greater than 30 - 40 mm, on coarse-textured soils and fig. 10.4c is used for heavy wetting events on fine and medium-textured soils. In general, the mean time interval is estimated by counting all rainfall and irrigation events occurring during the initial period that are greater than a few mm. Wetting events occurring on adjacent days are typically counted as one event. When average infiltration depths are between 10 and 40 mm, the value for K_{soil} can be interpolated between fig. 10.4a and fig. 10.4b or fig. 10.4c. Besides the use of K_{soil} for $K_{c\ ini}$ when the ground is nearly bare during the initial period (so that $K_{c\ ini} = K_{soil}$), estimates for K_{soil} are used later in eq. 10.25c to estimate the impact of soil evaporation on the value for K_{cm} estimated from fraction of ground covered by vegetation. K_{soil} is also used to estimate landscape water use in eq. 10.33b.

In equation form, K_{soil} following Allen et al. (1998, 2005d) is:

$$K_{soil} = \frac{TEW \ - \ (TEW - REW)\ e^{\left(\frac{-(t_w\ E_{so} - REW)}{TEW - REW}\right)}}{t_w\ ET_{ref}} \qquad for\ t_w > t_1 \tag{10.18}$$

where TEW is total evaporable water, REW is readily evaporable water and t_w is the average time interval between wetting events in days and E_{so} is the potential evaporation rate during stage 1 drying in mm d^{-1}. The symbol 'e' in eq. 10.18 is the base of the natural logarithm. Eq. 10.18 is valid when $t_w > t_1$ where t_1 is the length of stage 1 evaporation in days. The length of stage 1, t_1, is calculated as

$$t_1 = \frac{REW}{E_{so}} \tag{10.19}$$

and parameter E_{so} is potential evaporation calculated as

$$E_{so} = \left(K_{c\max} - K_{cb}\right) ET_{ref} \tag{10.20}$$

where, during the initial period, when K_{cb} mostly represents residual, basal evaporation, K_{cb} can be set equal to 0.0 in eq. 10.20 to combine all evaporation, so that $E_{so} = K_{cmax}\ ET_{ref}$. Under frequent wetting, where $t_w \leq t_1$, the entire evaporation process resides within stage 1 and K_{soil} is calculated as:

$$K_{soil} = \frac{E_{so}}{ET_{ref}} = \frac{\left(K_{c\,max} - K_{cb}\right)}{ET_{ref}} \tag{10.21}$$

Fig. 10.4a-10.4c are reproduced from eq. 10.18 and 10.21 using the values for *TEW* and *REW* summarized in table 10.2. The max() and min() functions in table 10.2 indicate the selection of the maximum or minimum value of parameters separated by the comma. K_{soil} values from fig. 10.4 are for use with the grass reference ET_o. For use with the alfalfa reference ET_r, the K_{soil} from fig. 10.4 can be divided by 1.2. Eq. 10.13 – 10.21 can be applied directly with alfalfa reference ET_r using K_{cmax} = 1.0.

TABLE 10.2 Values for *TEW* and *REW* in mm to recreate fig. 10.4a-c in Allen et al. (2005c) where ET_o is grass reference ET in mm d^{-1}.

Figure	Parameter in eq. 10.18, 10.19
Fig. 10.4a	*TEW* = 10 mm *REW* = max(2.5, 6 / $(ET_o)^{0.5}$)
Fig. 10.4b	*TEW* = min(15, 7 $(ET_o)^{0.5}$) *REW* = min(6, *TEW* – 0.01)
Fig. 10.4c	*TEW* = min(28, 13 $(ET_o)^{0.5}$) *REW* = min(9, *TEW* – 0.01)

Allen et al. (1998, 2005c) described the calculation of t_w from precipitation and irrigation information. Allen et al. (2005c) provided calculation of a weighted f_w used in eq. 9.26 when f_w for irrigation is less than the f_w = 1 for precipitation.

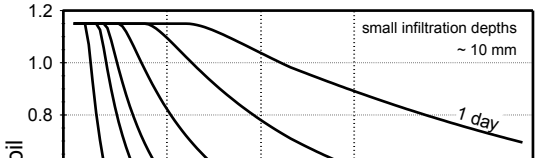

m)

new

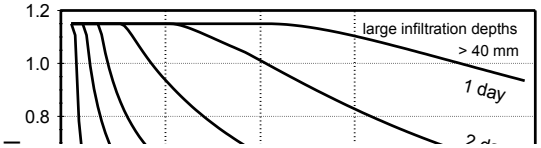

new

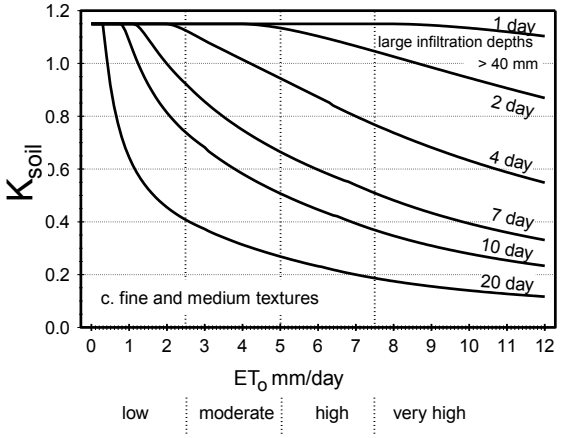

Fig. 1 lated to the level of grass
refere t rain during the initial
perio mm per event); (b) coarse-
textur nd (c) medium and fine-
textur K_{soil} is equivalent to $K_{c\ ini}$
when , Allen et al. (1998).

A second and more accurate procedure for estimating mean $K_{c\ ini}$ is to apply the dual $K_{cb} + K_e$ approach using actual sequences of precipitation and irrigation during the initial period for one or more years, assuming that the basal K_{cb} is 0.10 to 0.15 when the initial condition is nearly bare soil. A time-averaged value for $K_{cb} + K_e$ can then be determined.

Lengths of Growth Stages

The FAO-24 and FAO-56 publications provided general lengths for growth (development) stages for various types of climates and locations. This information has been summarized in Appendix C. The rate of vegetative development and attainment of effective full cover is affected by weather conditions, especially by mean daily air temperature (Ritchie and NeSmith 1991). Therefore, the length in time between planting or plant emergence and effective full cover for various crops or other vegetation will vary with climate, latitude, elevation and planting date (if cultivated) and with species and cultivar (variety). Generally, once effective full cover for a plant canopy has been reached, the rate of phenological development (flowering, seed development, ripening, and senescence (dying of leaf tissue)) often proceeds at a rate that is dependant on plant genotype and is less dependent on weather (Wright 1982). In some situations, the emergence of vegetation, greenup, and attainment of effective full cover can be estimated using cumulative degree-based regression equations or plant growth models (Sinclair 1984; Sammis 1985; Snyder 1985; Flesch and Dale 1987; Ritchie and NeSmith 1991; Ritchie 1991; Slack et al. 1996; Snyder et al. 1999; Cesaraccio et al. 2001; Spano et al. 2002; Sammis et al. 2004; Allen and Robison 2007). The use of cumulative growing degree days provides a quantitative stretching or shrinkage of the generated K_c curves for years or growing seasons that run cooler or warmer than average. K_c curves traceable to those of Wright (1981, 1982) for Kimberly, Idaho, converted to a cumulative growing degree day basis, are provided in Appendix F.

Local observations of plant stage development should be used when possible, with values in Appendix C used as a guide and for comparison. Local information can be obtained from farmers, ranchers, agricultural extension agents, local researchers or from remote sensing. When determining stage dates from local observations, the following guidelines may be helpful.

Effective full cover for row crops such as beans, sugar beets, potatoes, and corn is generally considered to occur when leaves of plants in adjacent rows intermingle so that soil shading becomes nearly complete near solar noon, or when plants reach nearly full size, if no intermingling occurs and plant cover >75% (Wright 1982). If, for some reason, shading of the soil does not become complete for crops that generally do nearly completely shade the soil, then the value for $K_{c\ mid}$ should be scaled down accordingly (perhaps 0.5% decrease in the standardized $K_{c\ mid}$ for each 1% of unshaded soil (Allen et al. 1998). Incomplete ground cover may occur from reduction in plant growth due to disease, grazing, pests, soil water stress, or with cultural practices calling for vegetation-free strips between crop rows.

Because it is difficult to visually determine when densely sown vegetation such as winter and spring cereals and grasses reach effective full cover, the more easily detectable stage of heading has been used (Wright 1982). For dense grasses, effective full cover will occur at about 0.10 - 0.15 m height. For thin stands of grass (dry rangeland), grass height may approach 0.3 to 0.5 m before effective full cover is reached. Densely planted forage such as alfalfa and clover reach effective full cover at about 0.3 to 0.4 m height.

For many agricultural plants, effective full cover is considered to occur when the leaf area index, *LAI*, approaches 3.0 (Ritchie 1972; Wright 1982; Ritchie and NeSmith 1991). Similar results have been reported by Kang et al. (2003) and Duchemin et al. (2006). *LAI* is defined as the average total area of leaves (one side) per unit area of ground surface.

The length of the initial and development periods may be relatively short for deciduous trees and shrubs that develop leaves in spring at relatively fast rates. Under some conditions, the initial period may include the time period from flowering until leaf bloom. The $K_{c\ ini}$ selected for trees and shrubs should reflect the ground condition prior to leaf bloom ($K_{c\ ini}$ is affected by the amount of grass or weed cover, wetness, mulch density, etc.). For example, the $K_{c\ ini}$ for a deciduous orchard having grass ground cover may be as high as 0.8 to 0.9 prior to and during leaf initiation in frost-free climates, whereas the $K_{c\ ini}$ for a deciduous orchard having a bare soil surface may be as low as 0.3 to 0.4 prior to leaf initiation if there is infrequent wetting of the soil by irrigation or by precipitation.

The end of the midseason and beginning of the late season is usually marked by senescence (browning or dying) of leaves, often beginning with the lower leaves of plants. This, along with less efficient stomates in aging leaf surfaces, causes the reduction in K_c. The length of the late season may be relatively short (on the order of 5 to 10 days) for vegetation killed by frost or for agricultural crops that are harvested fresh. The value of $K_{c\ end}$ used after the termination of plant growth or following harvest should reflect the condition of soil (surface soil water, mulch cover) and condition of the vegetation following plant death or harvest. Often times K_c after harvest can be estimated using $K_{c\ soil}$ from eq. 10.18 or fig. 10.4.

An FAO K_c Example

An example for constructing an FAO K_c curve under mean soil wetness conditions is presented in fig. 10.5 for spring barley planted at Logan, Utah (latitude of about 42°). The initial, development, midseason and late season stages were taken from Appendix C to have lengths equal to 20, 25, 60 and 30 days for March/April planting at a high latitude site (35-45°). Values for $K_{c\ ini}$, $K_{c\ mid}$ and $K_{c\ end}$ were selected from Appendix B as 0.3, 1.15, and 0.25. Mean wind speed at Logan during the mid and late seasons is about 2 m s^{-1} and average RH_{min} is about 30%. Therefore, $K_{c\ mid}$ is adjusted using eq. 10.14 as $K_{c\ mid} = 1.15 + [0.04(2 - 2) – 0.004(30 - 45)](1/3)^{0.3} = 1.19$. $K_{c\ end}$ was adjusted using eq. 10.15b as $K_{c\ end} = 0.25 + 0.001\ (30 – 45) = 0.23$. $K_{c\ end}$ is slightly lower than the value in Appendix B (which is for $RH_{min} = 45\%$), since the adjustment considers that the soil surface and crop during the late season would be slightly drier under the more arid conditions (Doorenbos and Pruitt 1977).

ET_o during the initial and development periods (April) averaged 4 mm d^{-1}, and the irrigation and precipitation wetting interval during April was about 12 days. Therefore, from fig. 10.4c, $K_{c\ soil}$ is approximately 0.5. This is an improved estimate for $K_{c\ ini}$ for Logan over that listed in Appendix B (0.3). An FAO mean K_c curve can now be constructed based on the three K_{cm} values of 0.5, 1.19, and 0.23 and the four lengths of growth stages (20, 25, 60 and 30 days) as shown in fig. 10.5.

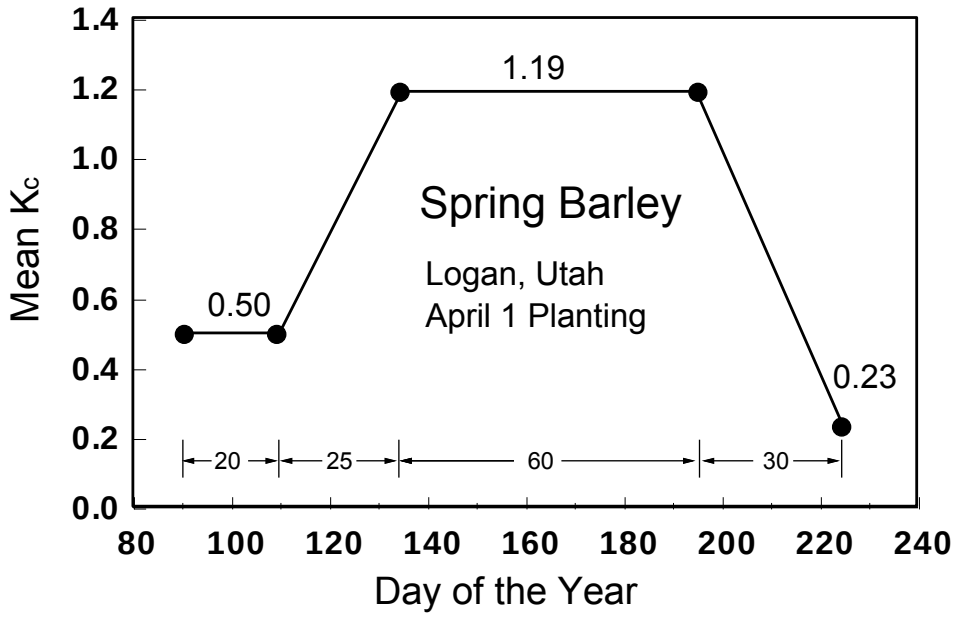

Fig. 10.5. Example construction of an FAO-24 crop coefficient curve.

Crops that are harvested several times during the growing season, such as forage crops, are typically modeled as a series of individually constructed curves, one for each growing cycle, as shown in Fig. 10.6. Lengths of growth stages may vary from cycle to cycle as weather conditions change.

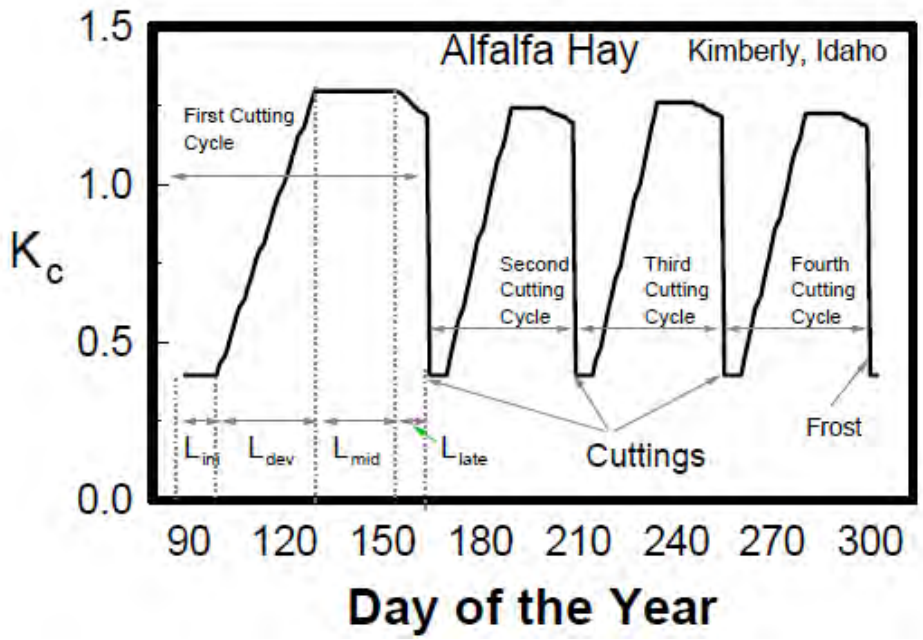

Fig. 10.6. Example mean K_c curve constructed for four growing cycles of alfalfa hay near Kimberly, Idaho using K_c values from Appendix B for grass reference ET_o following adjustment for climate using eq. 10.14-10.15.

Using the FAO Basal Crop Coefficient Procedure in Calculations

Estimates of K_c and ET_c made using the basal K_{cb} approach with calculations of soil evaporation made on daily time steps can be up to 10 to 20% more accurate than mean K_c estimates that are based on values in Appendices B and E, especially for the first few days following soil wetting. This is especially true during the initial and development periods.

The FAO crop coefficients can be used in basal calculations by selecting $K_{cb\ mid}$ and $K_{cb\ end}$ from Appendix D and by setting $K_{cb\ ini} = K_{c\ min}$ during the initial period to represent conditions having a nearly bare soil surface. Appropriate adjustment to $K_{cb\ mid}$ and $K_{cb\ end}$ for the ET_o basis is made using eq. 10.14 and 10.15 to reflect general humidity and wind speed conditions. The *basal* curve is then drawn using the values for $K_{cb\ ini}$, $K_{cb\ mid}$, and $K_{cb\ end}$ following the same procedures described previously for the general FAO K_c curve. $K_{c\ min}$ represents residual evaporation from relatively dry bare soil. A typical value for $K_{c\ min}$ for a nearly dry, bare agricultural soil is generally taken as 0.10 to 0.15, recognizing that periodic tillage, precipitation and irrigation tend to support this residual rate. Over extended fallow periods having no tillage, irrigation or precipitation, the value for $K_{c\ min}$ tends toward zero. For grasses, brush and trees, the $K_{c\ min}$ at the start of "green up" or leaf development may be on the order of 0.3.

The first step in applying the FAO K_c in basal computations is to construct the basal K_{cb} curve using $K_{cb\ ini}$, $K_{cb\ mid}$ and $K_{cb\ end}$ as described above. Eq. 10.2, repeated here,

$$K_c = K_s K_{cb} + K_e \tag{10.22}$$

is used to calculate K_c using the K_{cb} curve, where K_e and K_s are calculated on a daily time step using eq. 9.19 and 10.4 or 10.6. $K_{c\ max}$ in eq. 9.19 and 10.21 ranges from 1.2 to 1.25 for use with the grass-based FAO coefficients (eq. 10.3a) and generally equals 1.0 when used with alfalfa-based basal coefficients (eq. 10.3b).

An example of applying the FAO K_c procedure in a basal fashion is shown in fig. 10.7 for a sweet corn crop that was harvested as dry seed. The data in the figure were measured using a precision lysimeter system near Kimberly, Idaho (J.L. Wright 1990[2]). The 24-hour K_c measurements (symbols) were calculated by dividing daily measured ET_c by daily calculated ET_o. The agreement between the estimated daily K_c's from eq. 10.2 (shown as a thin, continuous line) and measured K_c's is relatively good. Measured and calculated K_c's increased following wetting by rainfall or irrigation. The measured K_c tended to be well above the K_{cb} line between days 230 and 250 due to effects of soil wetting on evaporation and thus total *ET*. This was reflected in the estimated K_c as well. A small amount of moisture stress may have occurred around day 220, where measured K_c fell below the K_{cb} curve, that was not picked up by the K_c simulation. Some of the day-to-day variation in measured K_c's shown in fig. 10.7 was due to measurement variation in the lysimeter (about 0 to 5%). However, much of the variation is likely caused by random error in the ET_o estimate caused by time-scale effects in the daily ET_o

[2] Personal communication.

equation and fixed aerodynamic, reflectance and surface conductance characteristics implicit to the ET_o definition that vary from the day-to-day characteristics of the sweet corn vegetation, and by error in weather measurements. Other error is caused by error in the K_e estimation and by the assumption of a relatively constant ratio of ET_c to ET_o (constant K_{cb}) from day to day. Total root mean square error (RMSE) calculated on a daily basis over the time period shown in fig. 10.7 is 0.17 on a K_c basis and 0.83 mm d^{-1} on an ET basis. The measured K_{cb} from the lysimeter for the silt loam soil averaged about 0.15 during the period from day 140 to 155 prior to growth of vegetation. That low, background rate was supplied by slow, diffusive evaporation from the wet subsoil. Even though the K_{cb} during late season was well below measured K_c, the addition of estimated K_e from irrigation and precipitation events caused the summed K_{cb} and K_e to approximate measured K_c relatively well.

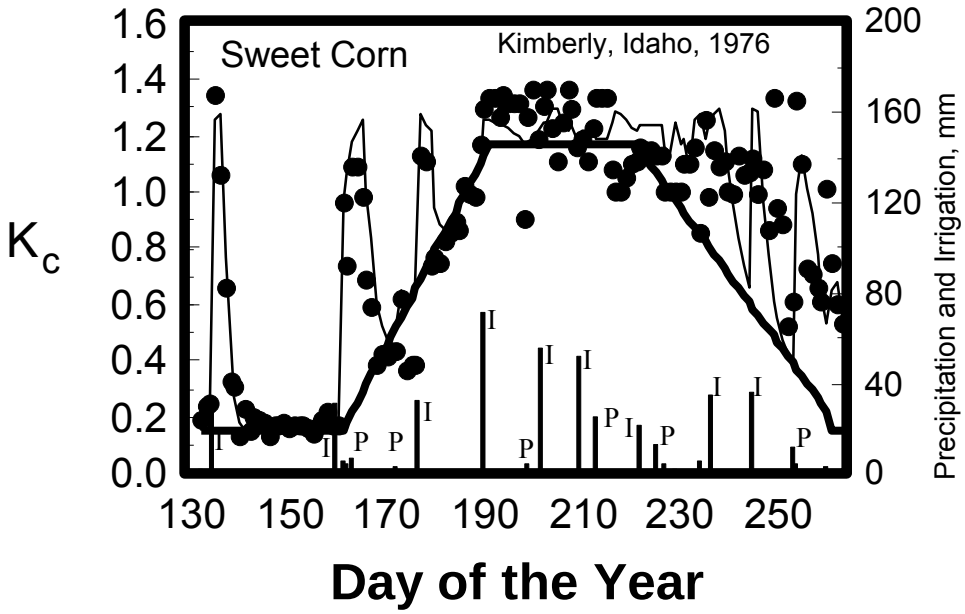

Fig. 10.7. Measured and estimated daily crop coefficients for a sweet corn crop near Kimberly, Idaho for grass reference ET_o. The basal crop curve (K_{cb}) was derived setting $K_{cb\ ini} = K_{c\ min} =$ 0.15 and using data from J.L. Wright 1990[3].

Application of the FAO-56 K_{cb} procedure involving eq. 9.19-9.31 and 10.2 was made by Hunsaker et al. (2002) over a growing season of alfalfa containing eight cutting cycles at a field site in Phoenix, Arizona. Estimated ET_c was compared against measurements by three weighing lysimeters with good results as shown in fig. 10.8. The RMSE for the Hunsaker et al. comparisons was 0.44 mm d^{-1}. Custom K_{cb} values for constructing local climate–adjusted FAO–56 style K_{cb} curves were determined as 0.30, 1.22, and 1.05 for the initial, mid–season, and end

[3] Personal communication from J.L. Wright to R.G. Allen.

of late season, respectively. Lengths of growth stages were varied for each cycle and lysimeter according to visual observation.

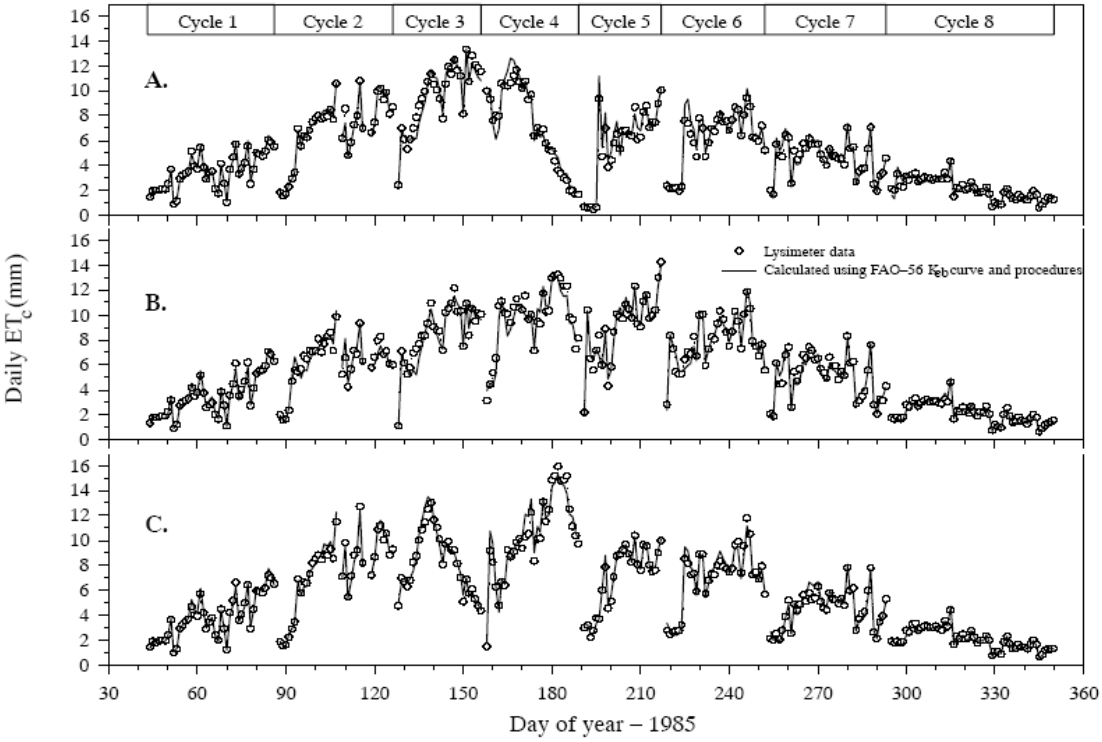

Fig. 10.8. Measured and estimated daily crop evapotranspiration over an entire growing season of alfalfa containing eight cutting cycles at a field site in Phoenix, Arizona. Measurements are shown for three lysimeter systems (A, B, C). Source: Figure from Hunsaker et al. (2002) with permission.

10.5 Alfalfa-based Crop Coefficients

Introduction

The primary set of alfalfa-based crop coefficients developed in the U.S. is traceable to data from Wright (1981, 1982) in southern Idaho. These have recently been supplemented by coefficients developed by Howell et al. (2006) from measurements in northern Texas. The Wright K_c curves are curvilinear, rather than linearly segmented like the FAO-style K_c curves, and attempt to more closely follow the expected progression of K_c with crop development. K_c curves were developed by Wright for eight crops common to the intermountain west of the USA. Wright's crop coefficients have been widely used in the USA and many engineers and agronomists are familiar with adjusting the time scale to match local crop conditions. The mean and basal alfalfa-based crop coefficients of Wright (1981, 1982), converted for use with the ASCE Standardized Reference ET Equation, are presented in Appendix E. Those same K_c's are converted to a cumulative growing-season time basis in Appendix F.

Procedure

Many of the principles and procedures described for using the FAO grass-based crop coefficients are applicable when using alfalfa-based crop coefficients. The main exception is that the alfalfa-based K_c's do not need to be adjusted for climate (eq. 10.14 and 10.15), since most agricultural crops at full cover have roughness and leaf areas similar to alfalfa. Therefore, alfalfa-based crop coefficients for many agricultural crops have a maximum K_c near 1.0. The proximity of measured maximum K_c near 1.0 under full cover conditions serves as a useful 'reality' check for field data and helps users visualize the development and shape of the crop coefficient curve for annual crops and forage crops that are cut periodically. Another advantage of alfalfa-based crop coefficients is that they are more convenient for use with satellite imagery-based energy balance methods for estimating ET over large areas, since maximum ET_c of many crops corresponds to the alfalfa based ET_r. For example, the Landsat satellite imagery program for Mapping Evapotranspiration at high Resolution (METRIC) described by Allen et al. (2007a) uses alfalfa based ET_r for calibration and produces crop coefficients that are alfalfa-based. The alfalfa-based K_{cb} values from Appendices E and F can be applied in eq. 10.2 with K_e derived from eq. 9.18 from Wright (1982) or the alfalfa-based K_{cb} values can be applied with the FAO-56 K_e procedure (eq. 9.19-9.31 and 10.2), with the $K_{c\ max}$ term in eq. 9.19 estimated using eq. 10.3b.

In the Wright K_c time-based procedure, the time base for K_c is scaled based on the relative time from planting to effective full cover and, following the time of effective full cover, on days after effective full cover. Effective (full) cover was defined by Wright (1982) as the time when leaves between row crops begin to interlock, at heading of grain, and flowering of peas. The shape of the K_c curve from planting or greenup to effective full cover is described by expressing values for K_c for each 10% of the total time length (Appendix E) and values for K_c for time after effective full cover are expressed for each 10 days following attainment of effective full cover. The K_c curves are constructed from the 'decadal' data (Appendix E) using linear or curvilinear interpolation between adjacent data columns or by fitting regression equations to the first half (planting to effective full cover) and to the second half (days after effective full cover) for each curve. Appendix E summarizes strategic dates of crop development recorded by Wright (1982).

The K_{cb} curves of Wright (1982) have been re-expressed in Appendix F as functions of cumulative growing degree days (CGDD) to provide automated flexure of the curve basis for varying weather conditions. Wright (1998) and Allen and Wright (2006) converted the Wright (1982) K_{cb} curves into CGDD-based curves where the K_{cb} values for the growing season were expressed as a ratio of the CGDD required for the crop to develop from the date of planting or greenup until effective full cover. The winter wheat curve of Allen and Wright (2006) was applied by Allen and Robison (2007) during the Idaho winter by beginning the curve in October, with reductions in CGDD applied when T_{min} fell below threshold values during cold winter periods.

An Alfalfa-based Example

Fig. 10.9 is an example comparing K_c estimated using basal alfalfa-based crop coefficients from Appendix F and the FAO-56 K_e procedure (eq. 9.19-9.31 and 10.2-10.3) with daily ET measured with a precision lysimeter for a sweet corn crop near Kimberly, Idaho (data by J.L.

Wright 1990[4] are the same as shown in fig. 10.7). The lysimeter data are the same data used by Wright (1982) to develop the K_{cb} curve, so that the K_{cb} estimates are not statistically independent of the measurements. The maximum K_{cb} for the sweet corn crop is about 0.9 for the alfalfa reference. The FAO-56 style method for estimating K_e performed relatively well with the curvilinear K_{cb} curve. The RMSE calculated on a daily basis over the time period shown in fig. 10.9 is 0.13 on a K_c basis and 0.75 mm d^{-1} on an ET basis. This compares with the RMSE of 0.17 on a K_c basis and 0.83 mm d^{-1} on an ET basis for the linear FAO-56 calculations of fig. 10.7. The magnitude of RMSE is impacted by how the K_{cb} curves were originally constructed and measurement data interpreted. In this case, the K_{cb} estimates are not statistically independent of the lysimeter measurements, although the K_e estimates are independent.

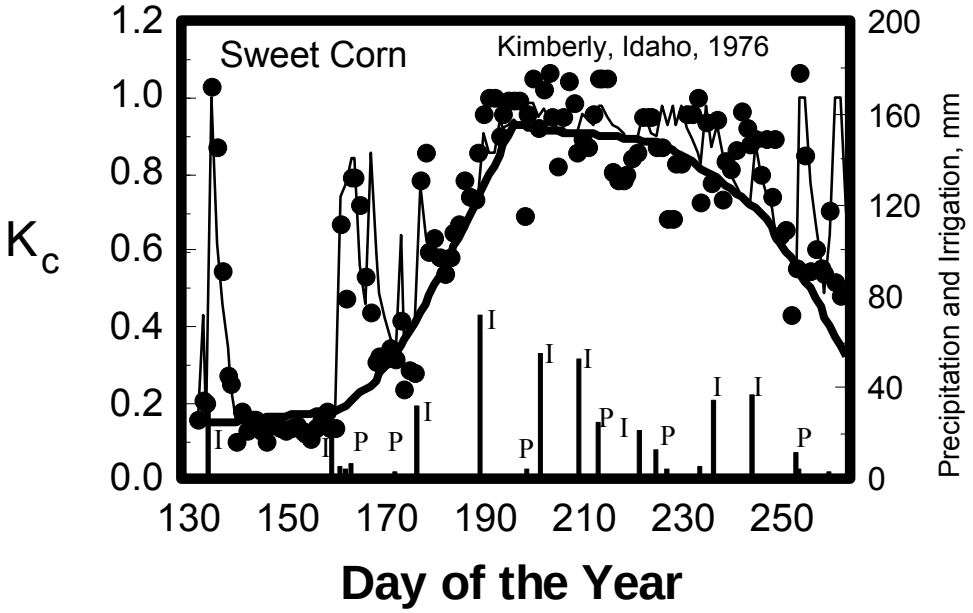

Fig. 10.9. Measured and estimated daily crop coefficients for a sweet corn crop near Kimberly, Idaho based on alfalfa reference ET_r. The basal (K_{cb}) crop curve is based on Wright (1982) curvilinear K_{cb} from Appendix F and K_e is based on the FAO-56 procedure (eq. 9.19-9.30 and 10.1-10.12). Source: Data from J.L. Wright (1990)[5].

Expression of K_c Curves and the Time Basis

Because of uncertainty in day-to-day values for K_c or K_{cb} due to random error in weather data and ET_{ref} estimates and in determination of K_c from field or research measurements, the straight-line K_c curve method of FAO method is generally appropriate for most applications. Hunsaker (1999) developed and compared K_{cb} curves for a cotton crop in Arizona using the straight-line method of FAO and curvilinear curves based on days after planting and based on

[4] Personal communication to R.G. Allen.
[5] Personal communication from J.L. Wright to R.G. Allen.

cumulative growing degree days (fig. 10.10). Hunsaker concluded that any of the three K_{cb} curve construction methods should result in good estimates of daily ET_c for the early-maturity cotton measured, when grown under climatic conditions similar to those of the study.

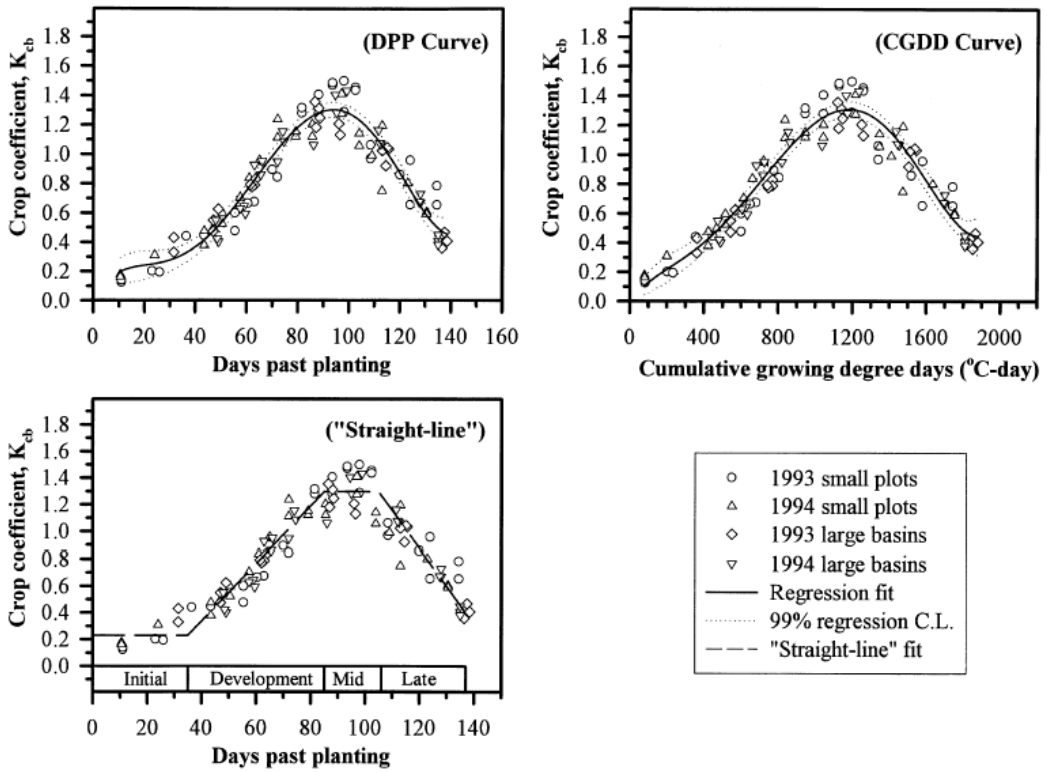

Fig. 10.10. Basal crop coefficient (K_{cb}) curves derived as functions of days past planting (DPP), cumulative growing degree days (CGDD), and using the FAO "straight-line" method for an early maturing cotton crop in Arizona with comparison to measurements (symbols). Source: Figure from Hunsaker, (1999) with permission.

10.6 Estimating K_c Curves for Natural and Agricultural Vegetation

The two-step K_cET_{ref} approach provides a simple, convenient way to estimate ET_c from natural vegetation, where K_c, if unknown, can be estimated according to the fraction of ground covered by vegetation. The developed cover (crop) coefficient curves represent the ratios of ET_c to ET_{ref} during various growth stages. Estimation of lengths of growth stages was described in a previous section. Often, for unknown K_c curves, the K_c during the peak growth period ($K_{c\ mid}$) can be estimated according to the amount of ground shaded by vegetation, the density and height of plants, and the amount of stomatal regulation under moist soil conditions. The value for K_c for conditions of low soil water availability is generally determined using eq. 10.4 or 10.6.

The K_c development process should adhere to upper limits for K_c of 1.1 for an alfalfa reference and about 1.25 for a grass reference for stands of vegetation larger than 500 to 2000 m^2. ET from these stands is governed by energy exchange principles within established equilibrium boundary layers and by the principle of conservation of energy as discussed in the

previous sections on Field Scale Applications and Small Expanses of Vegetation. K_c's for small stands (< 500 m^2) should also adhere to these limits when the vegetation height and leaf area is less than or equal to that of surrounding vegetation and soil water availability is similar. Only under conditions of "clothesline effects" (where vegetation height is greater than surroundings) or "oasis effects" (where vegetation has higher soil water availability than surroundings) will peak K_c's exceed the limits stated above. The user should exercise caution when extrapolating ET measurements from small vegetation stands or plots to large stands or regions, as overestimation of regional ET may occur.

Derived K_c values for natural vegetation based on vegetation amount represent the potential K_c when soil water is available for full *ET*. Often, however, soil water levels for natural plant communities fall below adequate supplies due to drought or, for riparian vegetation, due to declining water tables. Therefore, the frequency distribution of ET can be broad for a population of vegetation, as shown in fig. 10.11 where a frequency distribution of June and annual ET for cottonwood and salt cedar along the Middle Rio Grande valley is shown as derived from satellite-based energy balance (Allen et al. 2007b). ET from salt cedar (e.g. Tamarisk) showed larger variance due to its tendency to grow across a broad range of water availability (water table depth), soil types and salinity conditions, whereas cottonwoods, which exhibited a smaller variance in the population of ET, are typically found close to stream channels and consistent water supply. Wide variation was also noted for tree population density, which added to variance in the populations of ET.

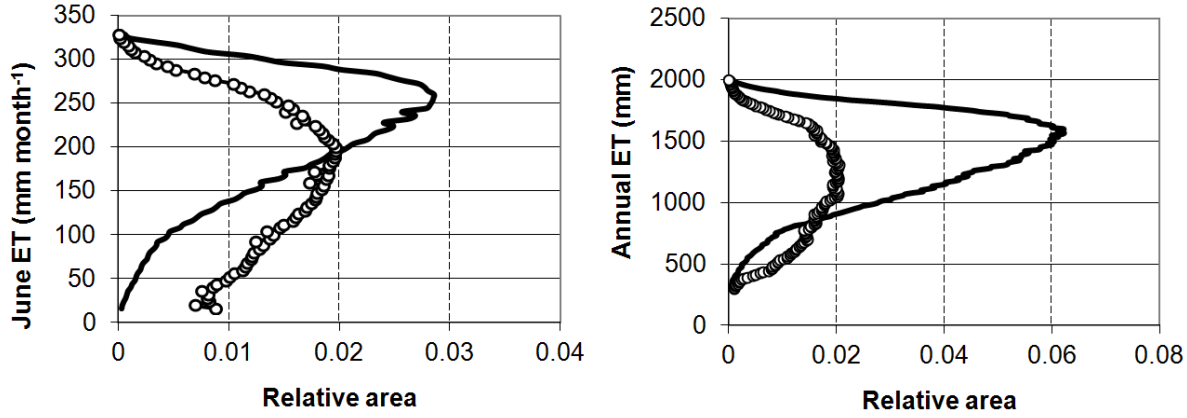

Fig. 10.11. Frequency distributions of ET from 6,000 ha of cottonwood and salt cedar (Tamarisk) along the Middle Rio Grande in New Mexico during June and all of 2002. Source: Allen et al. (2007), © ASCE.

Allen et al. (1998) proposed estimating K_c and ET for isolated, narrow stands of wetlands and tall wind breaks such as single rows of trees using a description of stand height and width and with dampening for vegetation that has a high degree of stomatal control:

$$K_c = \min\left(K_{c\,\max} + \frac{F_r\, h_{canopy}}{Width},\ 2.5 \right) \tag{10.23}$$

where $K_{c\ max}$, the maximum K_c expected for large fields, is 1.2 for use with ET_o and 1.0 for use with ET_r, F_r is a stomatal resistance correction factor, h_{canopy} is the mean vertical height of the canopy area in m, and *Width* is the horizontal thickness of the windbreak or patch of wetland vegetation normal to the general wind direction in m. For vegetation such as some desert vegetation and trees having leaf resistance significantly greater than that of most agricultural crops where r_l is commonly about 100 s m^{-1}, F_r can be approximated based on the FAO form of the PM equation:

$$F_r = \frac{\Delta + \gamma\left(1 + 0.34u_2\right)}{\Delta + \gamma\left(1 + 0.34u_2\,\frac{r_l}{100}\right)} \tag{10.24}$$

where r_l is the mean leaf resistance for the vegetation in question in s m^{-1}. The mean leaf resistance, r_l is 100 s m^{-1} for the ET_o and ET_r references and for many agricultural crops. Values for r_l for many agricultural and non-agricultural plants can be found in table 11.2 and Körner et al. (1979).

As discussed earlier, the value for $K_{c\ mid}$ for natural vegetation reduces when plant density or leaf area fall below full ground cover ($LAI < 3$). Because the K_c tends to increase in proportion to the amount of vegetation, the K_c at midseason, $K_{c\ mid}$, can be expressed as a function of a density coefficient, K_d, (Allen and Pereira 2009) where:

$$K_{cb\,mid} = K_{c\,min} + K_d\left(K_{cb\,full} - K_{c\,min}\right) \tag{10.25a}$$

where $K_{cb\ mid}$ is the approximation for K_{cb} during the midseason period, $K_{cb\ full}$ is the estimated basal K_c during peak plant growth for conditions of nearly full ground cover (or $LAI > 3$), and $K_{c\ min}$ is the minimum basal K_c for bare soil ($K_{cb\ min} \sim 0.15$ under typical agricultural conditions and $K_{cb\ min} \sim 0.0$ to 0.15 for native vegetation, depending on rainfall frequency). The density coefficient K_d can be estimated as a function of measured or estimated leaf area index *LAI* or as a function of fraction of ground covered by vegetation. For tree crops having grass or other ground cover, eq. 10.25a can take the form:

$$K_{\mathrm{cb\,mid}} = K_{\mathrm{cb}\,cover} + K_{\mathrm{d}}\left(max\left[K_{\mathrm{cb\,full}} - K_{\mathrm{cb}\,cover}\,,\ \frac{K_{\mathrm{cb\,full}} - K_{\mathrm{cb}\,cover}}{2}\right]\right) \tag{10.25b}$$

where $K_{cb\ cover}$ is the K_{cb} of the ground cover in the absence of tree foliage. The second term of the *max* function reduces the estimate for $K_{cb\ mid}$ by half the difference between $K_{cb\ full}$ and $K_{cb\ cover}$ when this difference is negative. This accounts for impacts of shading of the surface by vegetation having K_{cb} lower than that of the surface cover, due to differences in stomatal conductance. Eq. 10.25 can be applied to estimate K_{cb} during other periods besides the midseason by estimating K_d using eq. 10.27 and 10.28 with LAI or $f_{c\ eff}$ for that period.

Eq. 10.25 can be similarly applied to estimate a mean K_{cm} for any period having less than full vegetative cover by accounting for the effect of evaporation from predominately exposed areas of soil among the vegetation, much the same as is done in the dual $K_{cb} + K_e$ approach:

$$K_{\mathrm{cm}} = K_{soil} + K_{\mathrm{d}}\left(max\left[K_{\mathrm{cb\,full}} - K_{soil}, \frac{K_{\mathrm{cb\,full}} - K_{soil}}{2} \right] \right) \tag{10.26}$$

where K_{soil} is obtained from fig. 10.4 or eq. 10.18, and represents the average K_c from the non-vegetated (exposed) portion of the surface. The value for K_{soil} reflects the impact of wetting frequency, soil type and relative ET rate (i.e., ET_{ref}) during the same period as K_d and $K_{cb\,full}$. The K_{cm} represents an average K_c value that considers the mean impact of evaporation from soil. K_{cm} can be used to represent the midseason or other period as defined by K_d, K_{cm} and $K_{cb\,full}$.

For large stand size (> about 500 m^2), $K_{cb\,full}$ for use with $\mathrm{ET_o}$ can be approximated for crops not listed in Appendix D as a function of mean plant height and adjusted for climate similar to the $K_{\mathrm{cb\,mid}}$ parameter and following Allen et al. (1998):

$$(for\,ET_o)\ \ldots\ldots\ K_{\mathrm{cb\,full}} = \min\left(1.0 + 0.1h,\ 1.20\right) + \left[0.04(u_2 - 2) - 0.004(\mathrm{RH_{min}} - 45)\right]\left(\frac{h}{3}\right)^{0.3} \tag{10.27a}$$

For use with alfalfa reference $\mathrm{ET_r}$, $K_{cb\,full}$ can be approximated for crops not listed in Appendix F as:

$$(for\,ET_r)\ \ldots\ldots\ K_{\mathrm{cb\,full}} = \min\left(0.8 + 0.1h,\ 1.0\right) \tag{10.27b}$$

where h is mean maximum plant height in m, u_2 is the mean value for wind speed at 2 m height during the mid-season in m s^{-1}, and RH_{min} is the mean value for minimum daily relative humidity during the mid-season in %. The climatic correction is not required for $K_{\mathrm{cb\,full}}$ when used to derive the K_{cb} for $\mathrm{ET_r}$ because of the aerodynamic and canopy characteristics of the alfalfa reference crop.

The value $K_{c\,full}$ represents a general upper limit on $K_{cb\,mid}$ for tall vegetation having full ground cover and LAI > 3 under full water supply. The "min" function in eq. 10.27b selects the minimum expression in the parentheses. Eq. 10.27a and 10.27b produce general approximations for the increase in $K_{cb\,full}$ with plant height and climate. The estimate from eq. 10.27 may need adjustment downward if the vegetation exhibits more stomatal control on transpiration than is typical for agricultural crops, for example, for some types of trees or natural vegetation.

Where LAI can be measured or approximated, K_d can be approximated under normal conditions (Allen et al. 1998) as:

$$K_d = \left(1 - e^{[-0.7\,LAI]}\right) \tag{10.28}$$

LAI is defined as the area of leaves per area of ground surface averaged over a large area with units of m^2 m^{-2}. Only one side of 'green,' healthy leaves that are active in vapor transfer is considered. The relationship in eq. 10.28 is similar to one used by Ritchie (1974).

Where estimates of the fraction of ground surface covered by vegetation are available, the K_d can be estimated as (Allen and Pereira 2009):

$$K_d = min\left(1, M_L\, f_{c\,eff}, f_{c\,eff}^{\left(\frac{1}{1+h}\right)}\right) \tag{10.29}$$

where M_L is a multiplier on $f_{c\ eff}$ describing the effect of canopy density and conductance on maximum relative ET per fraction of ground shaded [1.5 – 2.0], and where $f_{c\ eff}$ is the effective fraction of ground covered or shaded by vegetation [0.01 - 1] near solar noon and h is the mean height of the vegetation in m. For canopies such as trees or randomly (nonrow) planted vegetation, $f_{c\ eff}$ can be estimated from Allen et al. (1998) as:

$$f_{c\ eff} = \frac{f_c}{\sin(\beta)} \qquad \le 1 \tag{10.30}$$

where β is the mean angle of the sun above the horizon during the period of maximum ET (generally between 11.00 and 15.00). Generally, $f_{c\ eff}$ can be assigned to solar noon (12.00), so that β can be calculated as:

$$\beta = \arcsin\left[\sin(\varphi)\sin(\delta) + \cos(\varphi)\cos(\delta)\right] \tag{10.31}$$

where parameters φ and δ are defined in chapter 4 (see eq. 4.10 for example). Fig. 10.12 is a schematic illustrating f_c, $f_{c\ eff}$ and β.

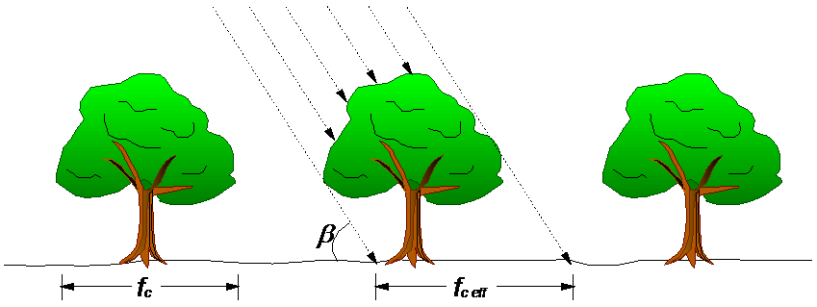

Fig. 10.12. Schematic showing extent of f_c, $f_{c\ eff}$ and β for tree vegetation where f_c is the fraction of surface covered by vegetation as measured from directly overhead.

The M_L multiplier on $f_{c\ eff}$ in eq. 10.29 imposes an upper limit on the relative magnitude of transpiration per unit of ground area as represented by $f_{c\ eff}$ (Allen et al. 1998) and is expected to range from 1.5 to 2.0, depending on the canopy density, thickness and maximum conductance. Parameter M_L is an attempt to simulate the physical limits imposed on water flux through the plant root, stem and leaf systems (Allen and Pereira, 2009). The value for M_L can be modified to

fit the specific vegetation. Values for M_L used to calculate values for K_{cb} for orchard crops in Appendix D and that served as the basis for K_{cm} for orchard crops in Appendix B are listed in table D.2 of Appendix D. Fig. 10.13 shows values for K_d over a range of $f_{c\ eff}$ and a range of h for M_L = 1.5 and for M_L = 2 when h = 5 m. The estimates by eq. 10.29 agree with those previously suggested by Fereres (1981) and Hernandez and Suarez (1988) for specific types of vegetation.

When the mean stomatal control by the vegetation is greater than for agricultural vegetation, then FAO-56 suggested that the estimate by eq. 10.29 be reduced by about 10 or 20 percent for each doubling of r_l above 100 s m^{-1}.

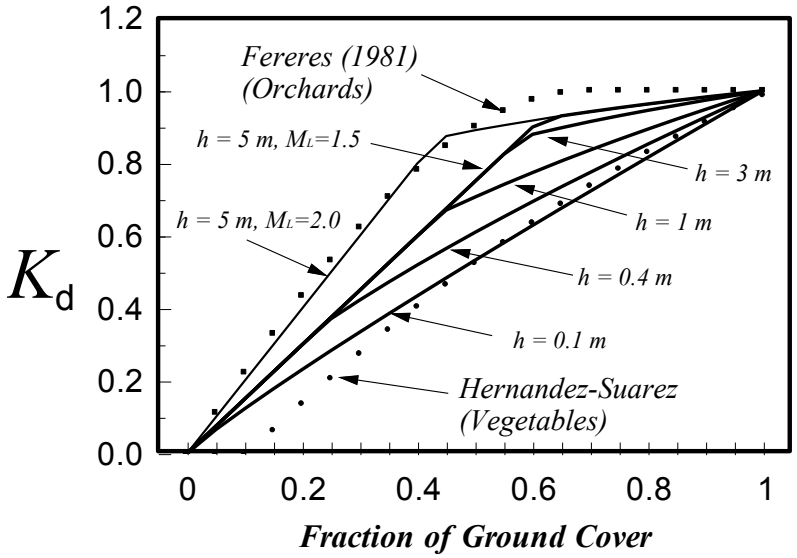

Fig. 10.13. Density coefficient, K_d, estimated from eq. 10.29 with M_L = 1.5 over a range of fraction of ground cover and various plant heights, and compared with estimates by Fereres (1981) for orchards and Hernandez-Suarez (1988) for vegetables. Source: Comparative data from Fereres (1981) and Hernandez-Suarez (1998).

The value for $K_{cb\ mid}$ estimated by eq. 10.25 is applied as a basal coefficient using the dual $K_{cb} + K_e$ method, where the actual K_c may increase to 1.0 for ET_r or 1.2 for ET_o following precipitation even if the estimated $K_{cb\ mid}$ is small, due to surface evaporation from among sparse vegetation. In addition, K_c should be reduced via eq. 10.2 or 10.22 using K_s from eq. 10.4 or 10.6 when soil water is low.

Eq. 10.29 suggests that as h increases, total leaf area and resulting net radiation capture will increase, thereby increasing K_c. In addition, as h increases, more opportunity for microadvection of heat from soil to canopy occurs and turbulent exchange within the canopy increases for the same amount of ground coverage. Both of these conditions increase the relative magnitude of $K_{cb\ mid}$. Values for $K_{cb\ end}$ can be scaled from $K_{cb\ mid}$ in proportion to the health and leaf condition of the vegetation at termination and the length of the late season period (i.e., whether leaves senesce slowly or are killed by frost). The f_c parameter and h are probably the simplest indices to estimate in the field.

Ringersma and Sikking (2001) applied eq. 10.25, 10.27a and 10.29 to estimate ET from Sahelian vegetation barriers. They found eq. 10.27a to overestimate $K_{cb\,full}$, even with adjustment using F_r, but found eq. 10.29 to produce representative estimates. Ringersma and Sikking suggested distinction between C3 and C4 photosynthetic behavior for LAI and f_c based estimation, since C4 vegetation can have limited stomatal control. Descheemaeker et al. (2007) applied eq. 10.25-10.26 and 10.29 to savannah vegetation in Ethiopia and found good agreement between estimated ET and ET measured gravimetrically. Vegetation types ranged from sparse, grazed grasses to full forest canopy.

10.7 Landscape Coefficients

Water requirements and consumption by residential and urban landscapes have become increasingly important due to both the quantity and value of water consumed. Procedures similar to those from agriculture have been adapted to estimate *ET* from landscapes. However, two distinctions are made between agriculture and landscapes: landscape systems are often comprised of mixtures of types and species of vegetation, thereby complicating the estimation of *ET*, and, typically, the objective of landscape irrigation is to promote appearance rather than biomass production, whereas biomass production is generally maximized in agriculture. Therefore, target *ET* for landscapes may include intentional water stress in the baseline estimate for ET_c, because landscape plants are watered less than they would be if they were irrigated like a crop. Landscape vegetation should generally be watered sufficiently for acceptable appearance and to survive, but the plants can often be stressed to some degree and will not be at maximum productivity. This adjustment can produce significant water conservation. The magnitude of the stress factor depends on physiological and morphological requirements of the plants; the goal is to sustain health and appearance with minimal irrigation. For example, water conservation studies on turfgrass have demonstrated water savings of 30% for cool-season turfgrasses and 40% for warm-season turfgrasses without significant loss of quality (Meyer and Gibeault 1986, Pittenger and Shaw 2001). Some shrubs and groundcovers can be managed for even more stress-induced reduction in *ET* (Kjelgren et al. 2000). A third departure of landscape *ET* from agricultural *ET* is that few landscape sites meet the "extensive surface" requirement needed to insure the equilibrium between the lower boundary layer of the atmosphere and the vegetation that is implied in the Penman-Monteith equation. Therefore, compensating adjustments are necessary to the landscape coefficient in the form of a microclimate factor to account for effects of local surroundings.

Because of the frequent inclusion of water stress in target *ET* values for landscape design and management, distinction must be made between these target *ET* values and actual *ET* values. Actual *ET* values may exceed target *ET* values if the landscape receives more water than required by the target that includes intentional stress. Under these conditions, landscape vegetation may exploit the additional available water, subject to some limit constrained by environmental energy available for evaporation and leaf area. The upper environmental energy limit, which follows behavior and principles used for agricultural crops, may exceed the targeted *ET* rate for the particular landscape cover. Conversely, actual *ET* may be less than targeted *ET* values if actual stress levels to the landscape are more excessive than targeted. Therefore, two *ET* values for landscape are distinguished here. The first is the *target landscape ET*, referred to as ET_L, that is based on minimum *ET* levels, relative to climate, necessary to sustain a healthy, attractive landscape. The second *ET* value is the *actual landscape ET*, $ET_{L\,act}$, that is based on landscape

type and on actual water availability. Traditionally, landscape *ET* estimation is based on the grass reference ET_o rather than on alfalfa reference ET_r. The target *ET* for a landscape is calculated as

$$ET_L = K_L\, ET_o \tag{10.32}$$

where ET_L is the target landscape *ET* (in mm d^{-1}, mm $month^{-1}$, or mm $year^{-1}$), and ET_o is the grass reference *ET* in the same units. K_L is the target landscape coefficient, similar to the crop coefficient used in agricultural applications.

There has been relatively limited experimental research on quantifying water needs of the vast and diverse array of landscape plant types (Pittenger and Henry 2005). Some of the leading work on landscape *ET* from groundcovers and shrubs has been done in California, where water applied to landscapes in southern California is estimated to be 25 to 30% of all water used in the region (Pittenger and Shaw 2001). St. Hilaire et al. (2008) produced a table of K_L values for 35 landscape groundcovers and shrubs that are targeted to provide acceptable landscape performance after initial establishment, and that induce a managed amount of moisture stress via limited water application. Costello et al. (2000) and IA (2003) described a recent procedure from California termed WUCOLS (water use classification of landscape species), where the K_L was decoupled into reproducible and visually apparent components representing the effects of three or four factors that control the value for K_L. The decoupling was done to facilitate application to the wide diversity of vegetation types and environments of landscape systems. Snyder and Eching (2004, 2005) proposed a similar decoupled procedure for estimating a formulated K_L that uses different ranges for the components:

$$K_L = K_v\, K_d\, K_{sm}\, K_{mc} \tag{10.33a}$$

where K_v is a vegetation species factor, K_d is a vegetation density factor, K_{mc} is a microclimate factor, and K_{sm} is a managed stress factor. K_v can be considered to be the ratio of ET_v to ET_o for a specific single or mixture of plant species *under full or nearly full ground cover* and *full soil water supply*, where ET_v is the vegetation *ET* assuming no water deficits and greater than 70 to 80% ground cover. Factors K_d, K_{mc} and K_{sm} modify K_v for less than effective full ground-cover (K_d), for impacts of shading or for exposure to advective or reflective sources (K_{mc}), and for intentional water stress (K_{sm}). Each of these factors can be estimated separately from the other based on visual observation of the landscape (for K_d and K_{mc}) and based on grower experience (for K_{sm}). Following the estimation of the individual factors, K_L is calculated using eq. 10.33 and represents a relatively accurate and reproducible estimate of relative landscape *ET*. The procedure of Snyder and Eching (2004, 2005), used in the University of California-Davis 'LIMP' software, differs from that of WUCOLS (Costello et al. 2000; IA 2003) in the ranges used to define K_d. The Snyder-Eching definition and range for K_d are congruent with estimates for K_d from eq. 10.29, where K_d ranges from 0 to 1.

An alternative form of eq. 10.33a conforms to the procedure used to derive the agricultural K_c as a function of vegetation density where separate account is made for evaporation from exposed bare soil among the vegetation. (see eq. 10.25a,b):

$$K_L = \left(K_{soil} + K_{vsd}\; K_d\, K_{sm}\right) K_{mc} \tag{10.33b}$$

where K_{vsd} is a coefficient describing the difference in ET, per unit of surface, between K_v and K_{soil}:

$$K_{vsd} = max\left[K_v - K_{soil}, \frac{K_v - K_{soil}}{2}\right] \quad (10.34)$$

and K_{soil} is the evaporation coefficient representing the evaporation (relative to ET_o) from bare soil caused by wetting by precipitation or irrigation. K_{soil} is included in eq. 10.33b to consider the impact of evaporation occurring from between plants and its inclusion becomes more significant with lower plant density (K_d) and with frequency of soil wetting. K_{soil} is estimated as a function of soil wetting frequency and magnitude of ET_o from fig. 10.4 or using eq. 10.18-10.21. As in eq. 10.25b and 10.26, the second term of the *max* function in eq. 10.34 reduces the estimate for K_L by about half the difference between K_v and K_{soil} when this difference is negative. This accounts for impacts of shading of the soil surface by vegetation having K_v lower than that of the evaporating soil, due to high stomatal resistance. As an alternative to eq. 10.33b, a daily dual $K_{cb} + K_e$ procedure, described previously, can be applied where K_{cb} is set equal to K_L from eq. 10.33b, using $K_{soil} = 0.15$, and K_e is estimated daily in accordance with wetting frequency. Eq. 10.33b reverts to eq. 10.33a when $K_{soil} = 0$. Eq. 10.33b is useful to assess the impact of irrigation frequency on total ET of turf having less than full ground cover. Impacts of evaporation of water intercepted by vegetation following irrigation or precipitation are estimated later using eq. 10.37.

The Vegetation Coefficient

The K_v for landscape vegetation represents the near maximum ratio of ET_v to $ET_{o\,mc}$ that occurs when there is generally 70% or more cover (shading) of the ground and with full soil water supply. $ET_{o\,mc}$ is the ET_o for the microclimate where the vegetation is grown. $ET_{o\,mc}$ can deviate from the standard ET_o, where ET_o is a regional estimate of reference evapotranspiration based on measured weather data, whereas $ET_{o\,mc}$ is a local ET_o corrected for microclimate differences. The microclimate coefficient, $K_{mc} = ET_{o\,mc}/ET_o$, is estimated or determined experimentally and is described in the following section. K_v establishes the maximum ratio $K_L = ET_v/ET_{o\,mc}$ for the vegetation under ideal conditions. Based on the definition for K_v, where K_v is the fraction of $ET_{o\,mc}$ when the foliage is at near maximum density ($K_d = 1$) and has full water availability ($K_{sm} = 1$), many types of landscape vegetation tend to exhibit similar values for K_v due to similarities in total leaf area, stomatal response, and energy absorption. Therefore, condensed tables of typical values for general species types can be used to provide general estimates for K_v, where K_v ranges from about 0.8 to 1.2. Because landscape vegetation is usually taller and rougher than grass, the upper limit for K_v can exceed 1.0 for well-watered landscapes. Table 10.3 contains general values for K_v for general types of landscape vegetation. Primary sources for values in Table 10.3 are listed in the table footnote.

TABLE 10.3 General Vegetation (species) Factors, K_v, for General Plant types for High Density Cover of the Ground and Full Water Supply. Source: Data from Irrigation Association (2011)

Vegetation Category[1]	K_v
Trees	1.15
Shrubs	
-- desert species	0.7
-- nondesert	0.8
Groundcover	1.0
Annuals (flowers)	0.9
Mixture of trees, shrubs, and groundcover[2]	1.2
Cool season turfgrass[3]	0.9
Warm season turfgrass[4]	0.9

[1] The tree, shrub, and groundcover categories listed are for landscapes that are composed solely or predominantly of one of these vegetation types with relatively dense coverage (shading) of the ground.

[2] Mixed plantings are composed of two or three vegetation types (i.e., where a single vegetation type does not dominate).

[3] Cool season grasses include Kentucky blue grass, fescues, and perennial ryegrass

[4] Warm season grasses include Bermuda grass, St. Augustine grass, buffalo grass, and blue grama

Primary sources:
Cool season turfgrass – Aronson et al. (1987); Brown et al. (2001)
Warm season turfgrass – Brown et al. (2001), Jia et al. (2009)
Other vegetation: Irrigation Association (2011)

The typical K_v values in table 10.3 represent full effective ground cover (f_c > ~0.7 – 0.8) and no water stress. The values are general and, under most conditions, these values are not met due to the density factor being less than 1.0 and due to intentional moisture stress (Brown et al. 2001; Jia et al. 2009). The K_v value for warm season grass is equal to that for cool season grass in table 10.3 because both of these grass types tend to have similar $ET_v/ET_{o\ mc}$ under conditions of no water stress. Typically, however, warm season grasses tolerate higher levels of moisture stress than cool season grasses; so that a lower managed stress factor can be applied to warm season grasses with less visual effect, as is illustrated later in table 10.5. The K_v values for both cool season and warm season grasses are less than 1.0 in table 10.3 due to the tendency for their mean height to be less than that of the standardized 0.12 m grass reference. Comparison of K_L for warm season grasses from eq. 10.33a and Tables 10.3-10.5 and measurements for a Florida application are presented later as Fig. 10.14.

K_v values for groundcover and annuals or flowers are assumed to be nearly or equal to 1.0, reflecting the likely K_v when the vegetation completely covers the ground (K_d =1.0) and when there is no stress (K_{sm} = 1.0). Because of the hundreds, if not thousands, of species of flowers and ground-cover types, it is difficult to estimate or establish K_v values for each of these species. Rather, the upper limit for K_v is established, which can be reduced when specific information on a species is determined. The K_v for mixed systems of trees, shrubs and/or groundcover is discussed in the next section.

Carrow (2004) suggested common target values for K_L for cool-season grasses to range from about 0.70 to 0.95 in the SE United States as compared to K_L for warm-season turfgrasses of 0.65 to 0.85 when the irrigation regime is 3 to 7+ days between events, which allows mild moisture stress during hot periods. At these K_L values, turf generally maintains acceptable quality and growth. As K_L values are decreased below these general ranges using a similar irrigation

schedule but with smaller doses per irrigation, turf performance and appearance may rapidly decline. Carrow (1995) reported turfgrass ET_c to be 40 to 60 % less in a humid environment compared to the same cultivar in an arid environment, but with similar K_L values for both environments.

Density Factor

Landscapes can vary considerably in vegetation density, due to wide variation in plant spacing and maturity. The plant density factor, K_d, can be estimated using eq. 10.29. Vegetation density refers to the collective leaf area of all plants in the unit landscape area. More densely growing vegetation will have a higher K_d and will transpire and require more water. Immature and sparsely planted landscapes have less total leaf area per unit landscape area than mature landscapes and have a lower value for K_d. Often, landscapes have two and three tiers (horizontal levels) of vegetation including turf or groundcover, shrubs, and trees. Overlapping tiers are capable of more radiative and other energy exchange and tend to increase *ET*, as shown by the K_v value of 1.20 in Table 10.3 for the "Mixture" class. When two substantial tiers of vegetation are present, for example trees shading grass or flowers, the value for height, *h,* can be approximated in proportion to the f_c for each tier. The important factor is the fraction of the sunlight intercepted by the plants and the fraction that reaches the ground. By observation at different times of the day, one can estimate the fraction of direct sunlight reaching the ground. The plant light interception is usually slightly more than the percentage of ground cover, so that the observed light interception can be used to estimate the K_d factor. If more than 80% of the sunlight onto the landscape is intercepted by the plants over the day, then one should expect the K_d factor to be close to 1.0.

Microclimate Factor

The microclimate factor, K_{mc}, accounts for impacts on *ET* by sun, shading, protected areas, hot and cool areas, reflected and emitted radiation from structures, wind, and transfer of heat energy from low *ET* surroundings. Structures and paved areas typical of urban landscapes can have pronounced effect on the local energy balance due the transfer of energy for evaporation from these surfaces to local vegetation. The environmental conditions of a landscape can vary significantly across the landscape, for example, areas on the south side of a building vs. areas on the north side. Vegetation plantings adjacent to paved, open areas may have 50% higher *ET* demand than similar plantings among other vegetation due to the transfer of energy to the vegetation from the nonevaporating areas. Conversely, plantings in areas shaded from sun and wind may have *ET* rates that are only one-half as high as those for open settings. Another important factor is wind blockage by buildings and vegetation. Reference evapotranspiration weather stations are typically placed in well exposed areas with wind speeds that represent the region. If the landscape is exposed to less wind due to shielding by buildings or vegetation, then the $ET_{o\,mc}$ (see earlier definition) may be less than ET_o. The LIMP program from Snyder and Eching (2004, 2005) provides a methodology to address these microclimate factors.

Values for K_{mc} are listed in table 10.4 for general classes of vegetation. The "high" category ($K_{mc} > 1$) in table 10.4 reflects harsh microclimate conditions such as planting in direct sunlight near paved or other non-vegetated surfaces, planting near reflective or heat-absorbing surfaces such as windows or buildings, or in exposed, windy conditions. The "low" category ($K_{mc} < 1$) represents environments where the plantings are located in shade, are shielded from wind, and

are away from dry, hot surfaces. The average or medium category (K_{mc} = 1) represents reference conditions similar to open settings, such as in parks, where conditions caused by buildings, pavement, shade, and reflection do not influence the *ET* by the landscape. The values given for K_{mc} are only approximate and local measurements can confirm or be used to derive local values. Values for K_{mc} can be interpolated between the high, average and low classes and should be selected for each sector of a landscape.

TABLE 10.4 Microclimate factor, K_{mc}, for landscape plant types. Source: Data from Irrigation Association (2003), (2011).

Vegetation	High (hostile environment)	Average (reference condition)	Low (protected or shaded environment)
Trees	1.4	1.0	0.5
Shrubs	1.3	1.0	0.5
Groundcover, flowers	1.2	1.0	0.5
Mixture of trees, shrubs, and groundcover	1.4	1.0	0.5
Turfgrass	1.2	1.0	0.8

Managed Stress Factor

Typically, the objective of landscape irrigation is to promote appearance rather than biomass production, as opposed to agriculture where biomass is generally maximized. Therefore, target *ET* for landscapes can include an intentional and managed "stress" factor in the baseline value for ET_L, where landscape plants are watered less than they would be if they were irrigated like a crop. This management is done by adjusting irrigation water schedules to apply less water than the vegetation will potentially transpire. The magnitude of the stress factor depends on physiological and morphological requirements of the plant**s.**

The managed stress factor, K_{sm}, represents the fraction of full *ET* rate targeted to obtain the functional and visual characteristics of the landscape vegetation. Parameter K_{sm} has a range of 0 to 1.0 where 1.0 represents conditions of no moisture stress and 0 represents complete lapse of plant transpiration and probable plant death or dormancy. High values for K_{sm} will sustain relatively lush, high leaf-area vegetation stands that tend to maximize *ET*. Low values for K_{sm} represent substantial managed plant water stress and reduction in *ET*, generally at the cost of biomass accumulation and potentially loss of pleasant visual effects (Richie and Pittenger 2000). Typical values for K_{sm} are presented in table 10.5. Those values, when inserted into eq. 10.33a with values for K_v from Table 10.3, produce values for K_L that are similar to those reported by Meyer and Gibeault (1986), Smeal et al. (2001), Carrow (2004) and Pittenger and Shaw (2004).

Many landscape species exercise significant stomatal control and can be 'forced' to relatively low levels of *ET*. For instance, the low range for K_{sm} for groundcover is 0.2, which is appropriate for a select group of drought-tolerant groundcover species. This value may not be appropriate for some ornamental groundcovers that require more water (and less water stress) to maintain health and appearance. One should consult local or regional sources to determine appropriate values for K_{sm}. Pittenger and Shaw (2001) suggested K_L for more than 30 groundcovers and shrubs grown in southern California that contain low K_{sm} components and thus provide good water conservation. Many of the vegetation types listed by Pettinger and Shaw are native desert vegetation types that tolerate water stress. Other sources of K_L information for specific species

include the WUCOLS publication by Costello and Jones (1999) where the K_L includes an implied $K_{sm} < 1$.

TABLE 10.5 Managed stress factors, K_{sm}, for general landscape plant types and the depletion fraction for no stress. Source: Data from Irrigation Association (2011).

Vegetation Category	High stress	Average managed stress	Low stress	Depletion fraction, p, for no stress
Trees	0.4	0.6	0.8	0.6
Shrubs				
-- desert species	0.3	0.4	0.6	0.6
-- nondesert	0.4	0.6	0.8	0.6
Groundcover	0.3	0.5	0.8	0.5
Annuals (flowers)	0.5	0.7	0.8	0.4
Mixture of trees, shrubs, and groundcover[1]	0.4	0.6	0.8	0.6
Cool season turfgrass	0.7	0.8	0.9	0.4
Warm season turfgrass	0.6	0.7	0.8	0.5

[1]Mixed plantings are composed of two or three vegetation types and where a single vegetation type does not predominate.

Management of landscape vegetation to implement a particular value for K_{sm} requires selection of a target depletion fraction prior to irrigation that produces the K_{sm}, on average. Typically the high stress category for trees, shrubs and groundcover does not require irrigation, but relies on natural rainfall. In situations where irrigation is practiced, the irrigation interval must be sufficiently long to produce increasingly greater stress as soil water is depleted so that the stress averaged over the entire interval equals the desired value for K_{sm}. The stress factor K_s equals 1.0, for no stress, for a period following irrigation (assuming that the irrigation depth was substantial) until the soil water depletion from the root zone exceeds *RAW*. Following that point in time, K_s will progressively decrease until the next irrigation. The K_s prior to the next irrigation will be less than the K_{sm}, since K_{sm} represents the average K_s over the entire interval. Table 10.6 lists target values for management allowed depletion fraction, *MAD*, at the time of irrigation to produce the desired average managed stress factor K_{sm} to be used in eq. 10.33. The target values for *MAD* (at the initiation of irrigation) are a function of the depletion fraction, p, when the particular vegetation begins to experience stress. The values for p in table 10.6 should be modified for specific vegetation types or species when information is available. The values for *MAD* in the table exceed the values for p that produce stress.

As an example, for $p = 0.4$, the *MAD* should be 0.76 prior to irrigation to produce a K_{sm} of 0.8. This means that 76% of the total available water (*TAW*) is depleted prior to irrigation. To produce a K_{sm} of 0.6, *MAD* must be 0.90, and the amount of depletion prior to irrigation is 0.9 x *TAW*. The values for *MAD* in table 10.6 were derived by integrating eq. 10.6 over a range in depletion, D_r, from 0 to *MAD* that produced an average value for K_s equal to K_{sm}.

TABLE 10.6a Management allowed depletion fraction, *MAD*, to produce the stated managed stress factor (K_{sm}), given the depletion fraction for no stress, (p) and assuming complete refilling of the root zone each irrigation. *MAD* is expressed as a decimal. Source: Data from Irrigation Association (2003, 2011).

Managed stress factor, K_{sm}	Depletion fraction, p, for no stress				
	0.3	0.4	0.5	0.6	0.7
1.00	0.30	0.40	0.50	0.60	0.70
0.95	0.47	0.57	0.66	0.75	0.86
0.90	0.55	0.65	0.73	0.81	0.88
0.85	0.62	0.71	0.79	0.86	--
0.80	0.68	0.76	0.83	0.89	--
0.75	0.74	0.80	0.87	--	--
0.70	0.78	0.84	0.89	--	--
0.65	0.82	0.88	--	--	--
0.60	0.86	0.90	--	--	--
0.55	0.90	--	--	--	--
0.50	--[1]	--	--	--	--

[1] "—" indicates that the value for *MAD* approaches or exceeds 1 so that the soil water content approaches or exceeds the permanent wilting point and the vegetation is, by definition, in danger of death or dormancy.

The values for *MAD* in table 10.6a assume that irrigation, when it occurs, completely replenishes soil water to field capacity so that depletion of the root zone, D_r, = 0 and the equivalent depth of water added equals *MAD* x *TAW*. It is important to note that for a typical p of 0.5, drying the soil 90% of the way to wilting point will only reduce the K_{sm} to 0.7 for an irrigation cycle comprised of large irrigations spaced relatively far apart. The reduced ET will still average 70% during the total period. This is due to the complete recharging of the root zone to field capacity after large irrigation events and a substantial period having no stress.

An alternative strategy to implementing soil water stress is to add less than *MAD* x *TAW* depth at a higher frequency, where irrigation additions are low enough to create some degree of moisture stress over a greater portion of the irrigation interval. This strategy can provide for less stress at the time of the more frequent, but reduced depth, irrigations and thus reduce the risk of plant death or dormancy. This can be done in an automated, soil moisture sensor-based irrigation system by applying relatively frequent, small doses of water but with the trigger soil moisture level setting at a 'dry' level. The percentage of water lost from evaporation from the soil surface increases as the irrigation frequency increases, especially when the irrigation doses are small. Evaporation of water from the soil surface is not nearly as effective in sustaining vegetation health and appearance as is transpiration through the plant system.

Table 10.6b lists *MAD* values required to produce the managed K_{sm} values listed, given the p value for the vegetation, and given that soil water depletion will be managed in the interval of *MAD* – 0.1 to *MAD* + 0.1. For example, given p = 0.4 for a specific plant variety and a target K_{sm} of 0.8, soil water depletion would be maintained between 0.41 and 0.61. In other words, the soil would be watered when 61% of available water is depleted, and enough water would be added by irrigation to reduce the depletion to 41% depletion of available water. Therefore, 20% of the water between field capacity and wilting point would be added back to the soil each

irrigation. This second strategy generally requires an automated and potentially a soil moisture sensor-based irrigation system that can apply relatively frequent, small doses of water but with the trigger soil moisture level setting at a 'dry' level. The percentage of water lost from evaporation from the soil surface increases as the irrigation frequency increases, especially when the irrigation doses are small. Evaporation of water from the soil surface is not nearly as effective in sustaining vegetation health and appearance as is transpiration through the plant system.

TABLE 10.6b Average management allowed depletion fraction, *MAD*, to produce the stated managed stress factor (K_{sm}), given the depletion fraction for no stress, (p) and assuming only partial refilling of the root zone each irrigation, where the depletion between wetting events is managed to range from *MAD* – 0.1 to *MAD* + 0.1. *MAD* is expressed as a decimal.

Managed stress factor, K_{sm}	Depletion fraction, p, for no stress				
	0.3	0.4	0.5	0.6	0.7
1.00	0.20	0.30	0.40	0.50	0.60
0.95	0.30	0.39	0.48	0.57	0.66
0.90	0.35	0.44	0.53	0.61	0.69
0.85	0.39	0.47	0.56	0.64	0.72
0.80	0.43	0.51	0.58	0.66	0.74
0.75	0.46	0.54	0.61	0.68	0.76
0.70	0.50	0.57	0.64	0.70	--
0.65	0.53	0.59	0.66	0.72	--
0.60	0.57	0.62	0.68	0.74	--
0.55	0.60	0.66	0.71	0.76	--
0.50	0.64	0.68	0.73	--	--
0.45	0.67	0.71	0.76	--	--
0.40	0.70	0.74	--	--	--
0.35	0.74	--	--	--	--

[1] "—" indicates that the value for *MAD* approaches or exceeds 1 so that the soil water content approaches or exceeds the permanent wilting point and the vegetation is, by definition, in danger of death or dormancy.

The values for *MAD* in table 10.6a were derived by integrating eq. 10.6 over a range in depletion, D_r, from 0 to *MAD* that produced an average value for K_s equal to K_{sm}. Values in table 10.6b were derived by integrating eq. 10.6 over a range of *MAD* – 0.1 to *MAD* + 0.1 that produced an average value for K_s equal to K_{sm}. As an example of using table 10.6a, for p = 0.4, the *MAD* should be 0.76 prior to irrigation to produce a K_{sm} of 0.8. This means that 76% of the total available water (*TAW*) is depleted prior to irrigation. To produce a K_{sm} of 0.6, *MAD* must be 0.90, and the amount of depletion prior to irrigation is 0.9 x *TAW*. Depleting soil water to 0.9 of available water is risky, in that, by definition, a depletion of 1.0 will result in 'permanent' wilting and generally plant death or dormancy. Following the second strategy of table 10.6b, where smaller doses of water maintain stress at a more level value would suggest recharging the root zone to *MAD* = 0.41 following irrigation and allowing the root zone to dry to *MAD* = 0.61 prior to irrigation, so that *MAD* averages 0.51 over the irrigation and drying cyle. That management strategy will produce a K_{sm} = 0.8. For more reduction in K_{sm}, managing for *MAD* ranging from

0.52 to 0.72 and averaging 0.62 will produce an average $K_{sm} = 0.6$. This latter range in *MAD* is less risky and likely easier to manage than the value of 0.9 required by the strategy of table 10.6a.

Actual *ET* from Landscapes

The vegetation coefficient K_v described in the previous sections represents the landscape K_c under a water supply that is sufficient to support full *ET* from relatively dense vegetation having near maximum ground cover and open environmental exposure. However, the K_L coefficient may contain an implicit amount of managed stress for purposes of water conservation. The degree of implied managed stress is quantified in eq. 10.33 by the K_{sm} term. As a result, the K_L derived from eq. 10.33a or 10.33b using a targeted K_{sm} term may not represent actual conditions where actual stress may be higher or lower than the target managed stress. Under these conditions, for purposes of water balance and determination of consumptive use from landscaped or larger areas, the 'managed stress' coefficient in eq. 10.33a,b is replaced by an 'actual' stress coefficient, K_s, where K_s is computed using eq. 10.4 or 10.6 based on soil water depletion determined from a daily balance of root-zone soil water. Eq. 10.33a therefore takes the form:

$$K_{L\,act} = K_v\, K_d\, K_s\, K_{mc} \tag{10.35a}$$

where K_{sm} in eq. 10.33a is replaced by an actual stress coefficient K_s and where $K_{L\,act}$ is the actual *ET* anticipated from the landscape under actual water availability. Eq. 10.33b becomes:

$$K_{L\,act} = \left(K_{soil} + K_{vsd}\, K_d\, K_s\right) K_{mc} \tag{10.35b}$$

where K_{vsd} is a coefficient describing the difference between K_v and K_{soil}, defined in eq. 10.34. Actual *ET* from the landscape under actual watering conditions is:

$$ET_{L\,act} = K_{L\,act}\, ET_o \tag{10.36}$$

When K_s is estimated from eq. 10.4 or 10.6, the depletion fraction '*p*' parameter, used to estimate *RAW*, should be set to specific values determined for the species if these are available. The effective depth of the root zone used to estimate *TAW* can be species or variety specific and therefore obtaining information specific to the variety is important.

Impact of Canopy Wetting and Irrigation Frequency on K_L

Wetting of landscape vegetation by irrigation or rainfall can substantially increase the potential ET from the landscape due to the combined influence of evaporation from exposed, wet soil and evaporation from water intercepted by vegetation during the wetting event, if by rainfall or sprinkler. The more frequent the wetting events, the greater the potential ET rate. Often, landscape irrigation is accomplished with automatic controllers that are easily set to irrigate frequently, even daily. The water intercepted and retained on the vegetation surfaces is freely evaporated during and following a wetting event, even if the underlying vegetation is experiencing some level of water stress and the soil is dry. Evaporation of intercepted water can occur even with nighttime irrigation where the primary evaporation may occur the following day.

The impact of evaporation from exposed soil among vegetation when the density coefficient, K_d, is less than 1 is accounted for using eq. 10.33b, coupled with estimates for K_{soil} from fig. 10.4 or eq. 10.18-10.21. The process of evaporation of intercepted water from vegetation is described in the form of the direct Penman-Monteith ET method in Chapter 11. Here, a simpler general method is used to estimate the impact of evaporation of intercepted water stored on the vegetation canopy on the value for K_L *for vegetation having full cover*, as:

$$K_L = K_{Lo} + \frac{S}{t_w\, ET_o}\left(1 - \frac{K_{Lo}}{K_{c\max}}\right) \tag{10.37}$$

where:

$$K_{Lo} = K_v K_d K_{sm}\, K_{mc} \tag{10.38}$$

and K_{Lo} represents the K_L estimated by eq. 10.33a under conditions where any exposed soil surface (when K_d is less than 1.0) is assumed to be dry. The value for K_{Lo} is the same as that produced by eq. 10.33a when effects of intercepted rain or wet exposed soil are not considered. Parameter S is the depth of intercepted water on vegetation leaves from precipitation or irrigation, mm, and t_w is the time between wetting events, days. K_{cmax} is the maximum limit on K_L, estimated from eq. 10.3a. ET_o has units of mm d^{-1}. Values for S are typically about 1 mm for trees (Table 11.5) and about 0.5 to 1 mm for turf (Hoffman et al. 1992; Breuer et al. 2003). The derivation of eq. 10.37 assumes that evaporation of intercepted water on leaves dominates the ET process until the vegetation surface is dry, so that transpiration is depressed by the energy consumed by E. This observation was noted by Tolk et al. (1995). In the application of eq. 10.37, the limits $K_{Lo} = K_v K_d K_{mc} K_{sm} \le K_{c\ max}$ and $K_L \le K_{c\ max}$ are applied.

Eq. 10.37 applies to vegetation having full ground-cover such as turf or solid cover by trees. For applications *where ground-cover is less than full* ($K_d < 1$), eq. 10.37 can be combined with a form of eq. 10.34b to yield:

$$K_L = K_{Lo} + (1 - K_d)(K_{soil} - K_{c\min}) + \frac{S}{t_w\, ET_o}\max\left(K_d - \frac{K_{Lo}}{K_{c\max}}, 0\right) \tag{10.39}$$

where K_{Lo} is calculated in eq. 10.38 and K_{soil} is taken from fig. 10.4 or eq. 10.18-10.21 and is a function of wetting frequency and ET_o rate. $K_{c\ min}$ is the minimum basal K_c for a 'dry' bare soil. Under typical landscape conditions, $K_{cb\ min} \sim 0.10$ to 0.15. The effect of eq. 10.39 is to increase the value for K_L over that estimated by eq. 10.33a or 10.33b alone.

The effect on K_L by evaporation of intercepted water from vegetation is illustrated in table 10.7 where eq. 10.37 is applied to a range of $K_{Lo} = K_v K_d K_{sm} K_{mc}$ under three levels of ET_o and for three irrigation intervals (1, 2 and 7 days). Interception depth, S, was assumed to be 1 mm and $K_{c\ max} = 1.2$. The impact of evaporation of intercepted water on K_L is most pronounced for daily watering intervals and at lower values for K_{Lo}. For turfgrass under typical conditions where when $ET_o = 4$ mm d^{-1}, K_d , $K_{mc} = 1$ and $K_{sm} = 0.9$ (mild imposed stress), $K_{Lo} = K_v K_d K_{mc} K_{sm} \sim 0.8$, and daily watering is estimated to increase K_L to 0.88 as compared to $K_L = 0.81$ for weekly watering. The K_L under daily watering increases to only 0.84 under $ET_o = 8$ mm d^{-1} since the

amount of interception (1 mm) becomes relatively small compared to the higher total daily ET rate.

TABLE 10.7 K_L estimated from eq. 10.37 for various levels of $K_v K_d K_{mc} K_{sm}$ and ET_o and for irrigation intervals, t_w, of 1, 2 and 7 days for conditions of a *surface fully covered by vegetation*[1].

	ET_o = 4 mm d^{-1}			ET_o = 6 mm d^{-1}			ET_o = 8 mm d^{-1}		
K_{Lo} =	t_w = 1	t_w = 2	t_w = 7	t_w = 1	t_w = 2	t_w = 7	t_w = 1	t_w = 2	t_w = 7
$K_v K_d K_{sm} K_{mc}$	K_L	K_L	K_L	K_L	K_L	K_L	K_L	K_L	K_L
1.2	1.20	1.20	1.20	1.20	1.20	1.20	1.20	1.20	1.20
1	1.04	1.02	1.01	1.03	1.01	1.00	1.02	1.01	1.00
0.8	0.88	0.84	0.81	0.86	0.83	0.81	0.84	0.82	0.81
0.6	0.73	0.66	0.62	0.68	0.64	0.61	0.66	0.63	0.61
0.4	0.57	0.48	0.42	0.51	0.46	0.42	0.48	0.44	0.41

[1] for interception depth S = 1 mm and $K_{c\ max}$ = 1.2. Units of t_w are in days.

Application of eq. 10.39, where evaporation of intercepted water on vegetation from sprinklers and evaporation from wet soil in between plants are both considered, is illustrated in table 10.8 over a range of K_{Lo} under two levels of ET_o and for irrigation intervals of 1, 2, 3 and 7 days. Two entries are shown for $K_{Lo} = K_v K_d K_{sm} K_{mc} = 0.8$, where K_d = 1.0 and 0.8. These two values for K_d represent a) full surface cover, as for turf grass, and b) a landscape having approximately 20% exposed soil, for dense ornamentals, for example. The impact of wet soil among vegetation that does not have complete ground-cover is pronounced. The K_L under daily watering approaches 1.0 under moderate ET_o = 4 mm d^{-1}, even when the 'dry' K_{Lo}, based on eq. 10.38 is only 0.4 to 0.6. This increase is caused by the contribution of evaporation from exposed soil among plants. The effect of daily watering is lower under high ET_o conditions because the water intercepted by vegetation surfaces evaporates quickly and evaporation becomes a smaller component of total ET.

The example values in table 10.8 give strong support for increasing intervals between watering events to conserve water. However, one needs to recognize constraints on long time intervals between watering events imposed by maximum water dosage rates to limit surface runoff on low intake soils and by water availability to shallow rooted vegetation on coarse soils.

In the case of cool season turf having mild imposed stress (K_{sm} = 0.9) so that $K_{Lo} = K_v K_d K_{sm} K_{mc} \sim 0.8$, under ET_o = 4 mm d^{-1}, increasing the watering interval from daily to 7 days could potentially reduce water consumption by (0.88 – 0.81)/0.88 = 8%. In the case of ornamentals where there is some exposed soil among plants so that K_d = 0.8, the reduction in water consumption for the same $K_{Lo} \sim 0.8$ would be (1.02-0.86)/1.02 = 16%. At an ET_o of 4 mm d^{-1}, about 5 mm out of a total irrigation dose of 23 mm would be conserved per irrigation.

TABLE 10.8 K_L Estimated from eq. 10.39 for Various Levels of $K_{Lo} = K_v K_d K_{sm} K_{mc}$ and Density Factor, Two Levels of ET_o and for Irrigation Intervals, t_w, of 1, 2, 3 and 7 Days[1].

		ET_o = 4 mm d^{-1}				ET_o = 8 mm d^{-1}			
		t_w = 1	t_w = 2	t_w = 3	t_w = 7	t_w = 1	t_w = 2	t_w = 3	t_w = 7
K_{Lo} = $K_v K_d K_{sm} K_{mc}$	K_{soil}: K_d	1.1 K_L	0.9 K_L	0.7 K_L	0.45 K_L	0.85 K_L	0.7 K_L	0.55 K_L	0.3 K_L
1.2	1.00	1.20	1.20	1.20	1.20	1.20	1.20	1.20	1.20
1	1.00	1.04	1.02	1.01	1.01	1.02	1.01	1.01	1.00
0.8	1.00	0.88	0.84	0.83	0.81	0.84	0.82	0.81	0.81
	0.80	1.02	0.97	0.92	0.86	0.96	0.92	0.89	0.83
0.6	0.60	1.01	0.91	0.83	0.72	0.89	0.83	0.76	0.66
0.4	0.50	0.92	0.80	0.69	0.56	0.77	0.69	0.61	0.48

[1] for interception depth S = 1 mm and $K_{c\ max}$ = 1.2. K_{soil} was selected from fig. 10.4 using ET_o and t_w and interpolation among charts. t_w has units of days.

Comparisons against Recent Measurements of K_L

Brown et al. (2001) reported K_L for Tiffany bermudagrass, a warm-season grass, in Tucson, AZ with daily watering ranging from 0.78 during high ET_o periods (June and July) to 0.83 during low ET_o periods (September). Using a K_v = 0.9 for warm-season grass from table 10.3, K_d = 1 and K_{mc} = 1 and mild stress K_{sm} = 0.9, the estimated K_{Lo}=$K_v K_d K_{sm} K_{mc}$ is ~ 0.8. From eq. 10.39 or table 10.8, the K_L associated with these values is 0.84 during high ET_o periods (ET_o = 8 mm d^{-1}) and 0.88 under low ET_o periods (ET_o = 4 mm d^{-1}). These values are about 10% higher than reported by Brown et al. The twice-weekly mowing height reported by Brown et al. (2001) was 2.2 to 2.5 cm, which is relatively short, and may explain the differences between K_L estimated by eq. 10.39 and reported K_L. If no moisture stress is assumed in the Brown study due to the daily watering, then K_{sm} = 1.0 and $K_{Lo} = K_v K_d K_{sm} K_{mc}$ ~ 0.9, and, from eq. 10.39 or table 10.8 (interpolated), K_L = 0.96 under ET_o = 4 mm d^{-1}and K_L = 0.93 under ET_o = 8 mm d^{-1}. These values are about 15% higher than reported by Brown et al. (2001), and again may be due to the short and frequent cutting heights in the study. Brown et al. (2001) reported K_L values for bermudagrass from the literature ranging from 0.57 to 0.83. These values included some amount of managed water stress.

Brown et al. (2001) reported K_L for Froghair intermediate ryegrass, a cool-season grass, overseeded into bermudagrass in Tucson, AZ with daily watering ranging from 0.85 to 0.90 during high ET_o periods (May and June) to 0.78 to 0.82 during low ET_o periods having relatively short day lengths (December to February). Using a K_v = 0.9 for cool-season grass from table 10.3, K_d = 1 and K_{mc} = 1 and mild stress K_{sm} = 0.9, the estimated K_{Lo} is ~ 0.8. From eq. 10.30 or table 10.8, the K_L associated with these values is estimated to be 0.84 during high ET_o periods (ET_o = 8 mm d^{-1}) and 0.88 under low ET_o periods (ET_o = 4 mm d^{-1}). These values are about 5% lower than reported by Brown et al for the high ET_o periods and about 10% higher than by

Brown et al. for the low ET_o periods. Brown et al. (2001) reported K_L values for cool-season turf grasses from the literature ranging from 0.60 to 1.04.

Fig. 10.14 and 10.15 show comparisons of monthly K_L for warm season grasses and cool season grasses derived using eq. 10.33b and Tables 10.3-10.5 made with measurements by eddy covariance from Florida (Jia et al. 2007) and by time domain reflectometry in Georgia (Carrow 1995). The K_L values reported for the warm season bahia grass measured by Jia included some moisture-stressed time periods, as did those by Carrow, where both wet and stressed periods were included in the two year data sets. The K_L from eq. 10.33b used $K_V = 0.9$ for both warm and cool season grasses during the growing season, $K_d = 1.0$, $K_{mc} = 1.0$, and $K_{sm} = 0.8$ for warm season and $K_{sm} = 0.9$ for cool season curves. The latter two values reflect influences of low amounts of stress, on average. A value of $K_{soil} = 0.2$ was used during the offseason to reflect background evaporation from dormat turf. It was assumed that no overseeding of cool season grass occurred during winter.

The K_L curve measured for bahiagrass in central Florida is higher than the straight line 'target' curve during April and May when the climate was generally wet and then relatively steadily followed the target curve during June – September when some stress occurred due to longer times between wetting events (Jia et al. 2007). The data of Carrow (1995) fell below the target curve during June-August when substantial stress occurred and rose above the target curve during the wetter period of September. The trends observed by Carrow (1995) for cool season tall fescue grasses were similar for the same reasons. On average, the observed data followed the steady target K_L values within uncertainties common to water measurement and management.

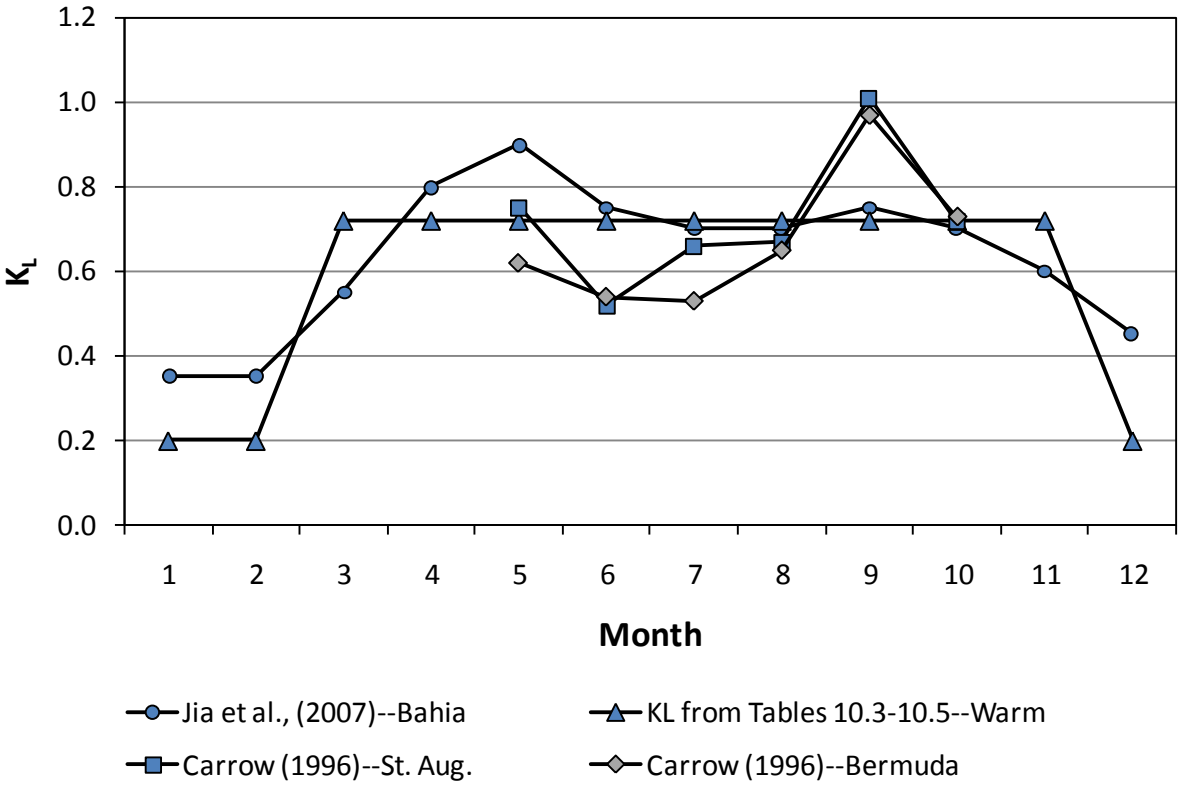

Fig. 10.14. Measured monthly K_L for Bahia grass in Florida by Jia et al. (2009) and for St. Augustine and Bermuda grasses in Georgia by Carrow (1995) compared to a steady, target

K_L from eq. 10.33b and Tables 10.3-5 for a warm season grass. Source: Data from Jia et al. (2009) and Carrow (1995).

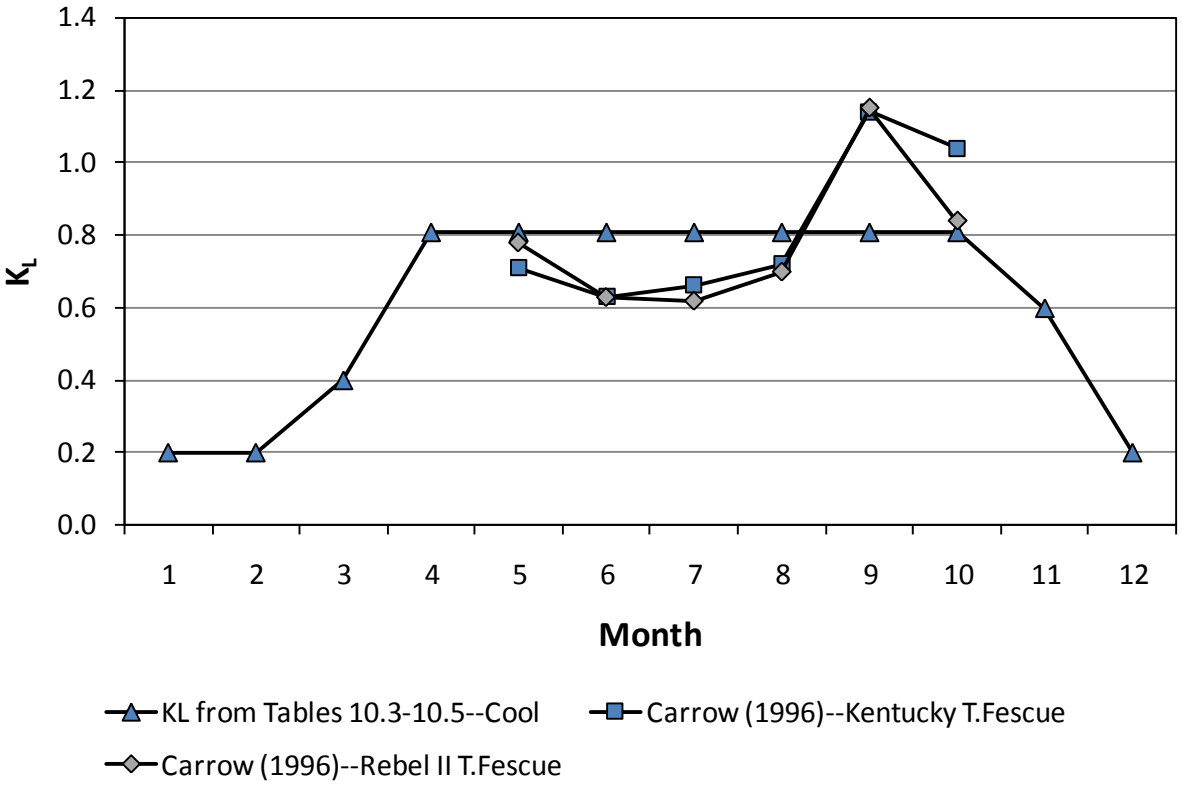

Fig. 10.15. Measured monthly K_L for two types of tall fescue grass in Georgia by Carrow (1995) compared to a steady, target K_L from eq. 10.33b and Tables 10.3-5 for a cool season grass. Source: Data from Carrow (1995).

10.8 Estimating K_c during Wintertime and Nongrowing Seasons

Non-growing periods are defined as periods during which no agricultural crop has been planted. In temperate climates, non-growing periods may include periods of frost and continuously frozen conditions. Estimation of ET during these periods can be important for annual water balances used in hydrologic studies and for estimation of accruals to soil water from precipitation during nongrowing seasons.

Types of Surface Conditions

The type and condition of the ground surface during non-growing periods dictates the range for ET_c. When the surface is bare soil, then K_c will be similar to the K_{soil} estimated earlier by eq. 10.18. When the surface is covered by dead or dormant vegetation or some type of organic mulch or crop residue, then K_c will be similar to that for agriculture having a surface mulch. When the surface is covered by weed growth or by 'volunteer' plants, then K_c will vary according to the leaf area or fraction of ground covered by the vegetation, as estimated by eq.

10.25 using K_d from eq. 10.28 or 10.29 and by the availability of soil water. When the surface is snow covered or frozen, then K_c is difficult to estimate and a low, constant value for ET_c may have to be assumed.

Bare soil. Where the ground is mostly bare following harvest or other removal of vegetation, then the K_c will be strongly influenced by the frequency and amount of precipitation. K_{cm} for bare soil can be calculated as $K_{cm} = K_{soil}$ where K_{soil} is estimated using eq. 10.18 or figure 10.4, and varies with frequency of wetting events and magnitude of reference ET. This approach was recommended by Martin and Gilley (1993) and Allen et al. (1998), and a similar approach was used by Snyder and Eching (2005) in the LIMP software to estimate a K_{cm} during winter that was then melded with a K_{cm} curve for the growing season. Where a daily soil water balance can be applied, the user may elect to apply the dual or basal K_{cb} approach (eq. 10.2). During long dormant periods, the topsoil layer may dry to very low water contents during periods having little or no precipitation. Under these conditions, the value for K_{cb} in eq. 10.2 and the value for $K_{c\ min}$ in other equations should be set to nearly zero. This provides the opportunity for $ET_c = 0$ during long periods having no rainfall and may be necessary to preserve the water balance of the evaporation layer and of the root zone in total.

Surface covered with dead vegetation. Stubbles and mulches reduce soil evaporation by providing a mechanical barrier to aerodynamic forces and they shield the soil surface from solar radiation. Mulches also reduce the connection between liquid or vapor in the soil and the air above (Burt et al. 2005). Burt et al. (2005) described a range of studies of evaporation experiments from organically mulched soil covers and reported a 20% reduction in E from a no-till standing wheat stubble as compared to conventional tillage in North Dakota, 40% reduction in E from standing wheat stubble in cotton in Texas, and nearly 50% reduction in E from soil covered with spread straw relative to bare soil in Nebraska. They noted that soil surface mulches were less effective at reducing soil evaporation under dryland conditions where longer periods for drying exist between wetting events as compared to conditions under irrigation.

When the ground surface has a plant residue or other dead organic mulch cover, or where part of the unharvested crop remains suspended above the surface in a dead or senesced condition, then the surface will respond similarly to a surface covered by mulch. In this case, K_c can be set equal to K_{soil} as estimated from fig. 10.4 or eq. 10.18, with the value for K_{soil} reduced by about 5% for each 10% of soil surface that is effectively covered by organic mulch (Allen et al. 1998). In applications using eq. 10.2 and eq. 9.19-9.31, evaporation from dead, wet vegetation can be substantial for a few days following a precipitation event. Therefore, in the FAO K_{cb} approach, the value for f_c during dormant periods should be set equal to zero to reflect the lack of green cover and f_w should be set equal to 1.0 to reflect the wetting of both soil and mulch cover by precipitation. The dead mulch or vegetation will dry more quickly than would the underlying soil if it were exposed. In addition, the soil will be protected somewhat from evaporation by the dead mulch or vegetation cover and total evaporation losses will be less than the *TEW* estimated from eq. 9.20. This can be accounted for by reducing the value for *TEW* by about 5% for each 10% of soil surface that is effectively covered by organic mulch (Allen et al. 1998). The value for REW may need to be reduced to account for quicker drying of the mulch fraction. The value for *REW* should be limited to less than or equal to that for *TEW*.

Surface covered with live vegetation. During frost-free periods following harvest, weeds may germinate and grow. This vegetation extracts water from storage within the soil profile and from any rainfall. In addition, crop seed lost during harvest may germinate following rainfall events and add to the ground cover. The amount of ground surface covered by vegetation will depend on the severity of weed infestation; the density of the volunteer crop; the frequency and extent of soil tillage; the availability of soil water or rain, and any damage by frost. The value for K_{cb} during the non-growing period can be estimated over time according to the amount of vegetation covering the surface using eq. 10.25 - 10.29 or from remote sensing images by way of a vegetation index. In the K_{cm} approach, the value for K_{cb} determined using eq. 10.25, 10.27 – 10.29 can be converted into an equivalent K_{cm} by adding 0.05 to 0.15 according to the frequency of rainfall and surface wetting or using eq. 10.26.

It is important that the K_c for vegetation during the non-growing period be limited by the amount of soil water available to supply evapotranspiration to satisfy the law of conservation of mass. Under all conditions, the integration of $K_c\ ET_{ref}$ over the course of the non-growing period cannot exceed the sum of precipitation occurring during the period plus any residual soil water in the root zone following harvest that can be subsequently depleted by the vegetation plus any upward flow from a shallow saturated system. The root zone in this case is the root zone for the weeds or volunteer crop. A daily soil water balance may provide for the best estimate of soil water induced stress and associated reduction in K_c and ET_c.

If using the dual crop coefficient approach (eq. 10.2), K_{cb} can be estimated according to the amount of surface that is covered by vegetation using eq. 10.25, 10.27 – 10.29. A daily soil water balance of the topsoil together with a full daily soil water balance of the root zone can be employed including estimation of K_s to account for any stress. The soil water balance will automatically adhere to the law of conservation of mass, so that total ET_c from the weed or volunteer vegetation will not be overestimated. Because the topsoil layer may dry to below wilting point under conditions of sparse rainfall, the values for K_{cb} and $K_{c\ min}$ for bare soil conditions should be set equal to zero or nearly zero for these conditions (Allen et al. 2005a).

Tasumi et al. (2005) and Allen et al. (2007b) sampled populations of K_c in south central Idaho for major crop types using a Landsat satellite-based surface energy balance. Fig. 10.16 shows distributions of the K_c populations for winter wheat crops on twelve satellite overpass dates between March 15 and October 20. The large variances in distributions of K_c during March and April reflect large variation in development of winter wheat fields coming out of winter. Values for K_c following harvest of the wheat crops averaged about 0.20 based on an alfalfa reference and varied according to amount of vegetation present in the form of weeds, nursed alfalfa, or volunteer wheat, as well as variation in irrigation of fields following harvest, coupled with cultivation. Variances of distributions of K_c during the period of peak K_c were relatively small since nearly all fields were at or near effective full cover so that K_c values clustered closely about 1.0.

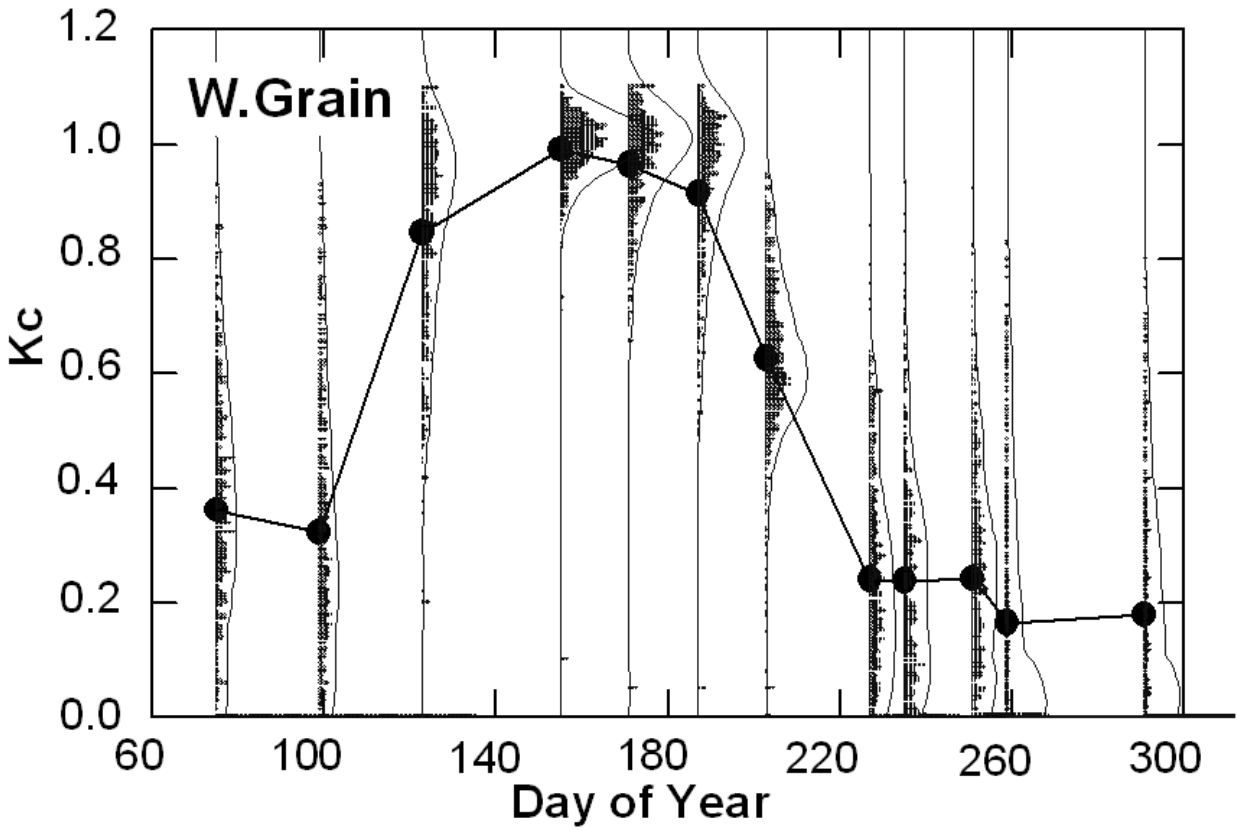

Fig. 10.16. Populations of K_c in south central Idaho for winter wheat fields using a Landsat satellite-based surface energy balance on twelve satellite overpass dates (vertical lines) between March 15 and October 20, 2000, where small symbols represent samples from individual fields and the large symbols are averages over all fields. Source: Data from Tasumi et al. (2005); and Allen et al. (2007b).

Frozen or snow covered surfaces. When the ground surface is snow covered or frozen, any vegetation will be largely non-responsive and will not contribute directly to ET_c. In these situations ET_c will be closely related to the availability of free water at the surface and to the albedo of the surface. The albedo of snow covered surfaces can range from 0.40 for old, dirty snow cover to 0.90 for fresh, dry snow as described in table 4.1. Therefore, the ET_c for snow cover will be less than ET_{ref}, as 25-85% less shortwave energy is available. In addition, some energy must be used to melt the snow before evaporation, besides energy consumed in melting snow that seeps into the snowpack. Under conditions of snow cover where the surface of the snow does not have a liquid film, the saturation vapor pressure at air temperature used in the vapor pressure deficit calculation in the Penman-Monteith reference equation should be computed over ice rather than water. Eq. 3.1 in chapter 3 for saturation vapor pressure over ice becomes (Murray 1967):

$$e^o_{ice} = 0.6108\ exp\left(\frac{21.87\,T}{T + 265.5}\right) \tag{3.1b}$$

for T in °C and e^o in kPa.

The use of ET_{ref} under such conditions is of limited value, as the assumption of conditions sustaining a green grass or alfalfa cover is violated. It is even possible to obtain negative values for ET_{ref} on some winter days where the longwave radiation from the surface is large and the vapor pressure deficit is small. It is under these conditions that net condensation of water from the atmosphere is possible, which corresponds to negative evaporation. Some negative values for ET_{ref} during winter occur from normal error in the ET_{ref} estimates and weather data. Given the limited utility for using ET_{ref} under snow covered or frozen conditions, use of a single, average value may be justified to estimate ET_c. Wright (1993) measured ET_c averaging 1 mm d^{-1} over nongrowing season periods at Kimberly, Idaho that were six months long (1 October to 30 March). The latitude of Kimberly is 42°N and the elevation is about 1 200 m. Over the six-year study period, the ground was at least 50% covered by snow for 25% of the time from 1 October to 30 March. The ground, when exposed, was frozen about 50% of the time. The K_c averaged 0.25 during periods when the soil was not frozen but where frosts were occurring (October and early November). When the ground had 50% or greater snow cover, ET_c averaged only 0.4 mm d^{-1}. Wright found that over the six-month non-growing period, total cumulative ET_c exceeded precipitation by about 50 mm, indicating a drying soil.

Fig. 10.17 shows averaged measurements of ET_c by Wright (1993) during 1985-1991winter periods. The measurements have high correspondence to the total shortwave radiation energy available on a clear day, R_{so}, estimated as 0.75 R_a. There is some lag between ET_c and R_{so} and R_s caused by cooler temperatures in January – March as compared to the October – December period. The ET_c/R_{so} ratio averaged only 0.17 over the six-month period, and averaged 0.11 from 1 December – 10 March. The ET_c/R_s ratio averaged 0.23 over the six-month period, and averaged 0.15 from 1 December – 10 March. The K_{cm} measured by Wright (1993), and converted to the standardized Penman-Monteith ET_r basis, averaged about 0.45 during the October-December period over years 1985-1991 for dormant fescue grass cover (fig. 10.18) and for nongrass covers including tilled soil (fig. 10.19). Even though these values for K_{cm} are relatively high due to relative wetness of the surface during the nongrowing periods, the total ET rates were relatively low due to low values for ET_r during these periods.

A similar study conducted in Logan, Utah (latitude 41.6°N, elevation 1 350 m) (Allen 1996) showed ET_c to vary widely with soil surface wetness and air temperature during winter months. The 'average' K_c from November to March was 0.5 for days having no snow cover. For days with snow cover, ET_c ranged from 0 to 1.5 mm d^{-1}.

A daily soil water balance using the dual crop coefficient approach may improve accuracy in estimating ET_c under freezing and snow covered conditions. In the dual crop coefficient method, a daily water balance is conducted for the topsoil and the estimate for K_c can be reduced according to available water. However, in addition to the limited validity of the concept of ET_{ref} under frozen or snow covered conditions, the evaporation coefficient, K_e, may have low values when the ground surface is frozen, as the water in a frozen state is less available.

Relatively complex models for estimating ET_c under non-growing season conditions, snow cover, and freezing, are available in the literature and should be consulted and perhaps applied when precise estimates for ET_c are required, for example Flerchinger (1991), Flerchinger et al. (1996) and Saxton and Willey (2005).

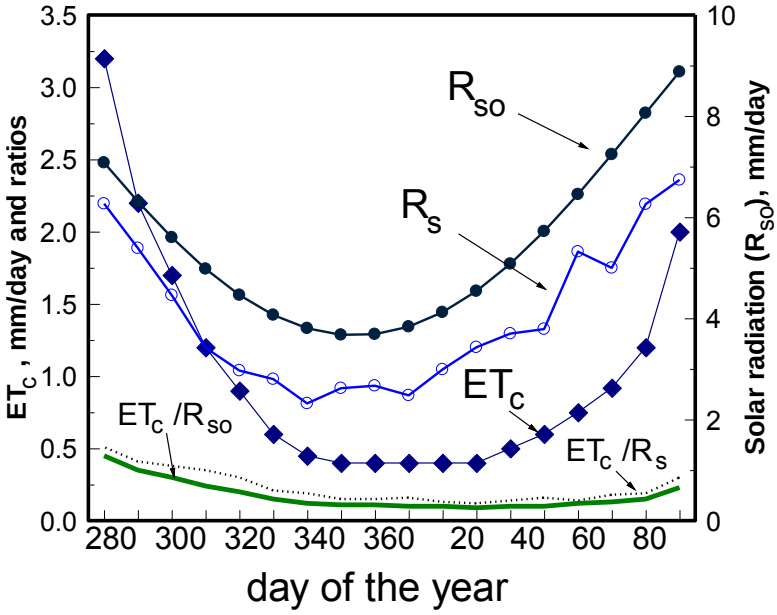

Fig. 10.17. Mean evapotranspiration measured during non-growing, winter periods at Kimberly, Idaho by Wright (1993). Source: Data from Allen et al. (1998).

The basis for the mean K_c values in fig. 10.18 and 10.19 is the ASCE standardized Penman-Monteith method. The ASCE PM alfalfa reference ET_r standard represents 0.5 m tall green alfalfa, even during winter, where the crop is a hypothetical potential reference. Therefore, under even wet conditions, the K_c during winter time is not expected to reach 1.0 since much vegetation may be frozen, cold-stressed or dormant. Mean K_c (K_{cm}) did approach or exceed 0.8 during Dec. 1988 - Mar. 1989 for the disked soil, a period having a nearly continuous distribution of precipitation and wet surface condition.

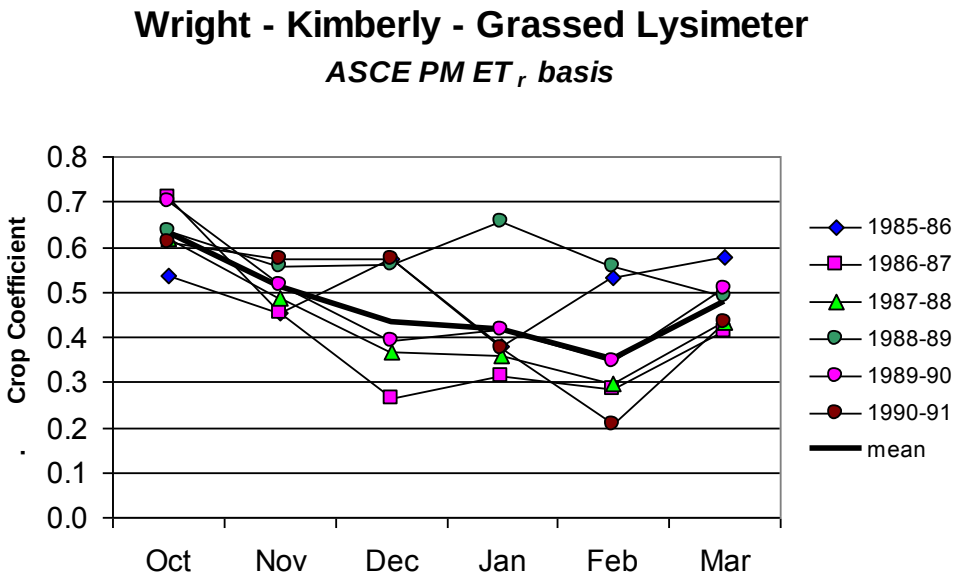

Fig. 10.18. Mean monthly K_c measured by Wright (1993) from dormant grass using a weighing lysimeter during nongrowing periods at Kimberly, Idaho, based on the ASCE PM alfalfa reference ET_r equation. Source: Data from Allen and Robison (2007).

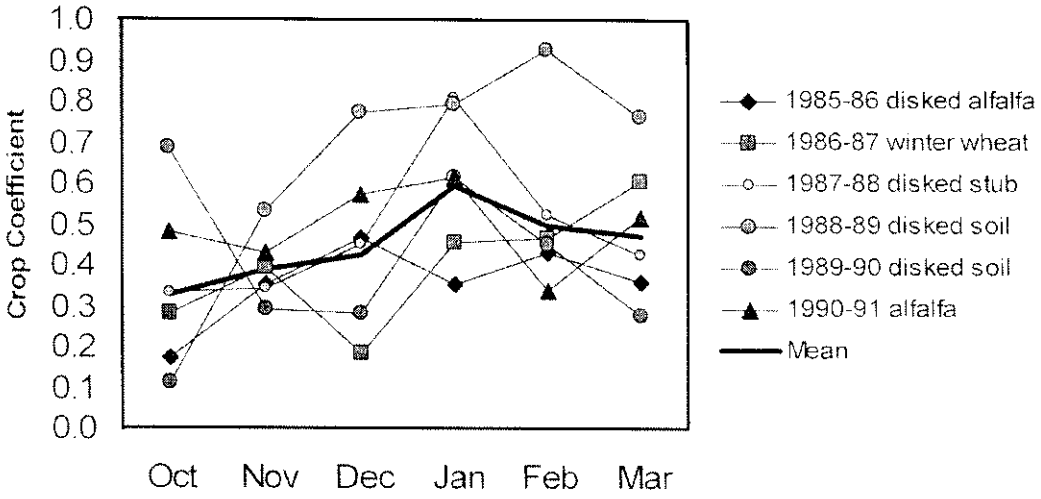

Fig. 10.19. Mean monthly K_c measured by Wright (1993) during nongrowing periods at Kimberly, Idaho using a weighing lysimeter for various types of nongrass cover, based on the ASCE PM alfalfa reference ET_r equation. Source: Data from Allen and Robison (2007).

Estimated Wintertime Evaporation

Allen and Robison (2007) estimated wintertime evaporation across the state of Idaho using daily calculation of eq. 10.2 (dual K_c approach) requiring a daily soil water balance. The wintertime calculations were combined with calculations for growing periods to produce daily ET estimates for entire annual periods. The nongrowing season (winter) period was defined by

Allen and Robison (2007) as the period beginning when a K_{cb} curve representing the growing cycle for a specific crop terminated or when a killing frost occurred, and ending at greenup or planting of the same crop the following year (or Oct. 1 in the case of winter wheat). A basal K_{cb} = 0.1 was used for bare soil conditions during nongrowing season periods, for surfaces covered with some amount of mulch, and for dormant turf/sod systems. The K_{cb} represented conditions when these surfaces had a dry soil surface, but had sufficient moisture at depth to supply some diffusive evaporation. The evaporation (K_e) component was estimated separately in the daily soil water balance, where $K_{c\ max}$ during the nongrowing period was 0.9 for bare soil, 0.85 for mulched surfaces and 0.8 for dormant grass cover. The lower value for grass accounted for insulative effects of the grass and its higher albedo. The use of a low value for K_{cb} permitted the K_e function in the daily calculations to increase the value for total K_c according to wetting frequencies by rain and snow. An effective 'rooting zone' of 0.10 m was used during the nongrowing season for the fraction of surface under the cover. For all surfaces, a daily soil water balance was conducted and a stress coefficient based on eq. 10.6 was applied when soil water content of the upper 0.10 m dropped below a critical value. This caused actual K_c to reduce below K_{cb} when both the ground surface and subsurface soil were dry. All land use types, including agricultural, landscape, horticultural and natural vegetation, were assigned one of the three winter cover conditions (dormant grass, bare soil or mulch classes) for estimating evaporation losses during winter. Functions for estimating sublimation from snow are described in Allen and Robison (2007).

Typical K_{cb} and K_c curves for spring wheat and potato crops for a full calendar year are shown for a location near Ashton, Idaho during 2004 in fig. 10.20. Simulated irrigation events, necessary to estimate evaporation from soil following unknown irrigation events, are shown as vertical bars. The K_c curves resulting from application of eq. 10.2 (dual K_c procedure using alfalfa ET_r) include the evaporation (K_e component) that appear as 'spikes' above the K_{cb} curves following precipitation and irrigation events. Actual K_c fell below K_{cb} curves during fall for the wheat and potato crops whenever the water content of the soil evaporation layer fell below levels required to support the K_{cb} = 0.10 values assumed for harvested surfaces that were mostly bare. Although values for K_c during winter time were relatively high due to wet soil surfaces and frequent snow cover (January – March 2004, for example), the total ET_c rates during wintertime were relatively low due to low values for ET_r during the Idaho winters. This is illustrated in the bottom figure of fig. 10.20 that shows daily actual ET_c for the spring grain.

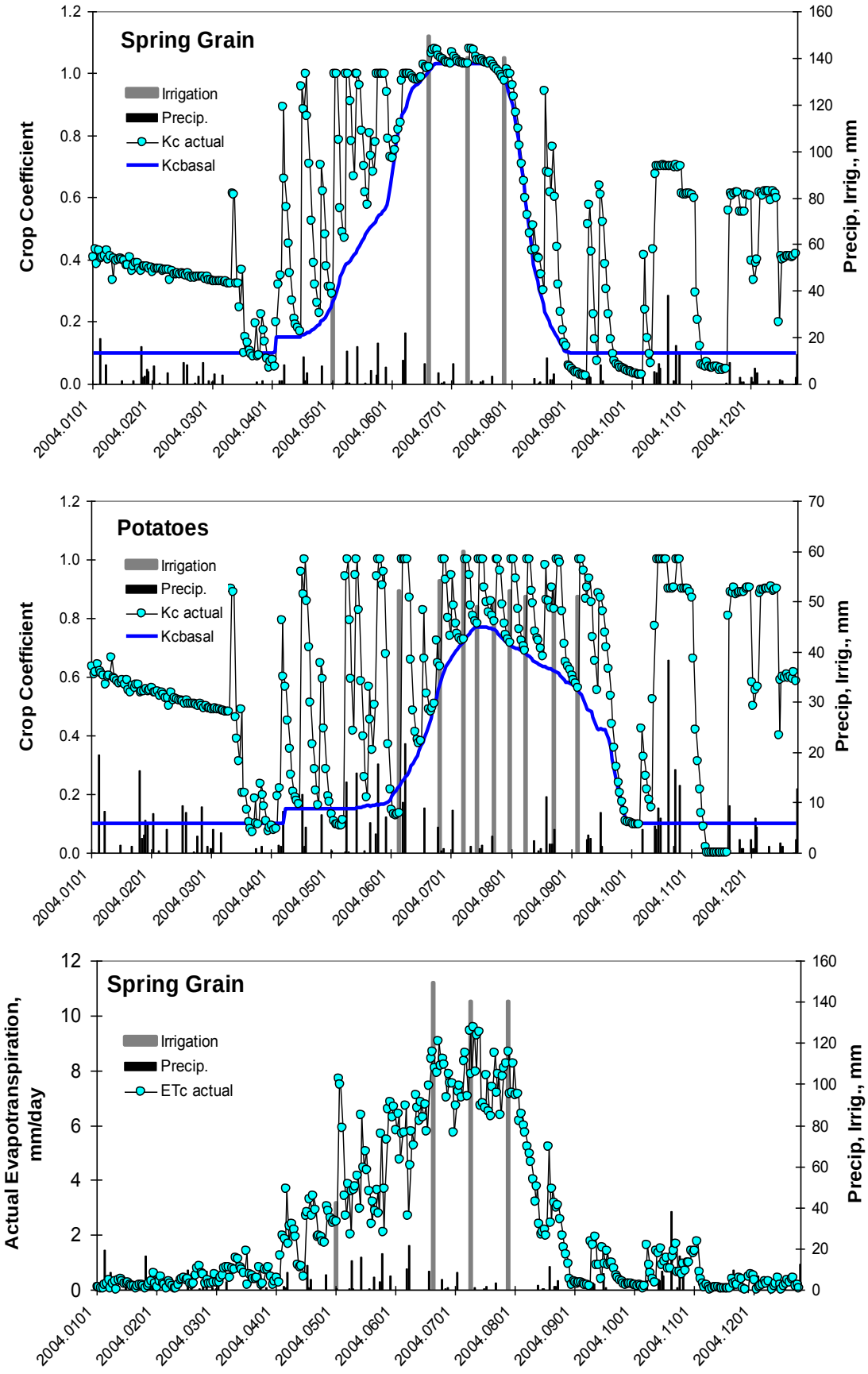

Fig. 10.20. Example K_{cb} ('K_{cbasal}') and resulting K_c ('$K_{c\ actual}$') curves for spring wheat and potato crops near Ashton, Idaho during 2004. Simulated irrigation events are shown as vertical bars. The $K_{c\ actual}$ traces include the evaporation (K_e components) that appear as 'spikes' above the K_{cb} curves following precipitation and irrigation events. Also shown in the bottom figure is daily actual ET_c for the spring grain.

10.9 Summary

In summary, the $K_c\, ET_{ref}$ approach is a convenient and robust method for estimating actual and potential ET from agricultural crops, landscapes and natural vegetation. The method adheres to energy conservation principles and implicitly incorporates environmental, boundary layer, and physiological factors affecting the ET_c from the particular vegetation. Many of these factors must be explicitly estimated when using a direct estimation equation such as the Penman-Monteith equation discussed in the next chapter. The dual K_c method provides means to estimate effects of wetting frequency on total water consumption and to estimate ET year round. Crop coefficients can be estimated for new or under-studied vegetation types via visual description of the vegetation density and general vegetation type. Publications will continue to present or update crop coefficients for new crops and for local areas. Some agencies and private entities post crop coefficients for their respective areas on the Internet.

Evapotranspiration from Land Surfaces: Direct Penman-Monteith and Aerodynamic-Energy Balance Equations

11.1 Introduction

Application of the Penman-Monteith (PM) and other resistance-based methods enables the user to adjust the physically-based parameters of surface roughness and bulk surface resistance to represent characteristics of the surface or vegetation type in question. This provides the means to produce estimates of ET without the need for empirical multipliers, as in the case of the two-stage crop coefficient x reference ET method. The flexibility and power in producing direct estimates does come at the cost of more complexity in determining and applying functions to estimate resistance-based parameters and in applying the technique to sparse canopies containing mixtures of vegetation and exposed soil. Typically, the user objectively characterizes a surface based on visual observations and measurements, remote sensing, or photography, and then estimates the corresponding roughness and bulk surface resistance parameters using approaches discussed in subsequent sections.

Advantages

The main advantage of the PM equation and other combination equations over direct aerodynamic approaches is that air temperature and humidity measurements are required at only one reference height, rather than measurement of air and humidity gradients or measurement of temperature and humidity at the surface. The PM equation is less sensitive to omission of stability correction adjustments as compared to gradient methods because the available energy component reduces weighting on the aerodynamic component, plus the aerodynamic resistance appears in both the numerator and denominator. The PM equation can be used to estimate ET on hourly, daily and even monthly calculation time steps (Allen et al. 1994b, 1996). The PM and direct aerodynamic approaches have advantage over the crop coefficient – reference ET (K_c ET_{ref}) method in that surface parameters impacting evaporation and transpiration, such as bulk surface resistance, aerodynamic roughness and water content of the surface soil layer impacting evaporation, can be specified for the specific surface and temporal conditions. However, specifying these parameters over time, especially for sparse vegetation cover, can be challenging, as described in the following section.

Disadvantages and Challenges

For applications in hydrology, and depending on equations being compared, a disadvantage of the PM equation includes the problem of characterizing average relationships between leaf stomatal resistance and solar radiation for sparse or multi-layered vegetation such as forests in semi-arid regions (Stewart 1983; and Denmead 1984) and developing crops. In these situations, mean heights and locations of sinks for momentum and radiation are different from mean heights and locations of sources of λE and H. These variations create differences in eddy diffusivities

(aerodynamic resistances) within and directly above canopies and also create problems in characterizing average relationships between leaf stomatal resistance and solar radiation.

Other challenges with the PM and other combination equations include difficulties in quantifying bulk surface resistance for complex canopies, especially when soil water is limiting. In addition, significant errors may be introduced when weather data used in the PM equation are measured above surfaces that may be significantly different from air properties occurring over a complex canopy. For example, applications may require using weather measurements taken over clipped grass to estimate ET from forest vegetation where conditioning of the air (temperature, vapor content, wind speed) is different. Because of nonlinear interactions between weather parameters, ET flux rates and buoyancy effects, direct Penman-Monteith and aerodynamic-energy balance equations are best applied using hourly or shorter time-period data. For many engineering applications, weather data from one or more existing weather stations may be the only data that are available for use. However, gridded weather data sets from land surface models associated with the National Center for Atmospheric Research (NCAR) Weather Research and Forecasting Model (WRF) are becoming widely available and many of these reflect the influence of underlying surface and vegetation conditions on the temperature, vapor and wind profiles. Many of the land surface models used with WRF employ some form of the Penman-Monteith equation for estimating the ET components of the surface energy balance and they also assimilate measured weather data as a correction mechanism. In many cases, however, especially in semiarid to arid environments, the WRF simulations do not consider impacts of irrigation in supplying water for ET and consequent conditioning of the local and regional air masses. Therefore, these data sets may require post-conditioning.

Furthermore, and as described in more detail in a later section, the PM works best under well-watered conditions of nearly full vegetation cover. It is under these conditions that surface temperature, T_s, is closest to air temperature, T_a, so that the assumptions explicit in Δ and emitted long wave radiation, that commonly assume that $T_s = T_a$, and that may neglect buoyancy corrections, are not large. Other challenges include the need for parallel modeling of evaporation from exposed soil that is impacted by frequency and amounts of wetting events and amount of vegetation cover. These issues and requirements also effect the $K_c\ ET_{ref}$ method, however, that method has more consistent and standardized procedures for estimating evaporation as outlined in Chapters 9 and 10.

11.2 Common Forms of Resistance-based Equations

Many land surfaces have vegetation canopies that do not completely cover the ground surface or understory. These surfaces include forests, cultivated row crops, orchards, vineyards and natural systems. Sensible heat and vapor fluxes from exposed soil fractions and from canopy can be quite different due to variations in water availability at these surfaces and aerodynamic characteristics. These fluxes can also interact between the two surfaces, with microadvection and radiative emission of heat, for example, from a dry soil surface into the adjacent canopy, or with the humidification of the boundary layer over a soil surface due to evaporation from an adjacent canopy. A variety of resistance-based networks and methods have been proposed over the past fifty years to describe fluxes of sensible heat and latent heat within both uniform and sparse canopies. Often these resistance networks have been incorporated into a Penman-Monteith type of combination equation to reduce the weather data requirements to only those measured at some reference height above the vegetation, thereby negating the need for

surface temperature measurements. As described later, however, knowledge of or iteration for surface temperature may be required for acceptable accuracy.

This section describes three resistance based methods for estimating ET from sparse canopies. These methods are the standard Penman-Monteith method, also known as the single layer model, the multi-layer method, also referred to as the interactive resistance model (Daamen and McNaughton 2000), and the two-source method, also referred to as the patch model. The interactive model is the most complex model and the Penman-Monteith the least complex. Following the introduction of these models, their strengths and weaknesses will be discussed. In addition, the PM is reverted back into its original energy balance and aerodynamic components to show the merits and advantages of using the original components to iteratively determine surface temperature. That method is known as the 'AFIB" method (aerodynamic fluxes using an iterative energy balance).

The general resistance networks used in the three models are illustrated in fig. 11.1 in terms of direct LE expressions and in fig. 11.2 in terms of direct sensible heat flux, H, expressions. The resistance diagrams for H may be implicitly built in to PM models or into multi-layer or multi-source models. Specific resistance terms in fig. 11.1 and 11.2 are defined in later equations for various model types. Two resistance networks are expressed for the single layer model in fig. 11.1 and subfigure a and b. The two source (patch) model is represented in both fig. 11.1 and 11.2, as subfigure c, and the two-layer (interactive) model is represented by subfigure d. Figure 11.1a shows how the soil surface can be partitioned into four conditions in regard to available energy (sunlight) and relative wetness of the soil surface. The partitioning of relative wetness can be important when simulating irrigated systems where only part of the ground surface is wetted. The combination of the four surface resistances representing these four soil surface conditions into a single equivalent r_{ss} is described in a later section, including its incorporation into a bulk surface resistance to be used in a single-layer model.

A highly recommended reading on these three resistance model types is Daamen and McNaughton (2000) who described and contrasted common formulations of the three model types and compared their estimated ET rates under a range of surface conditions. Much of the following material and contrasts follow from Daamen and McNaughton (2000).

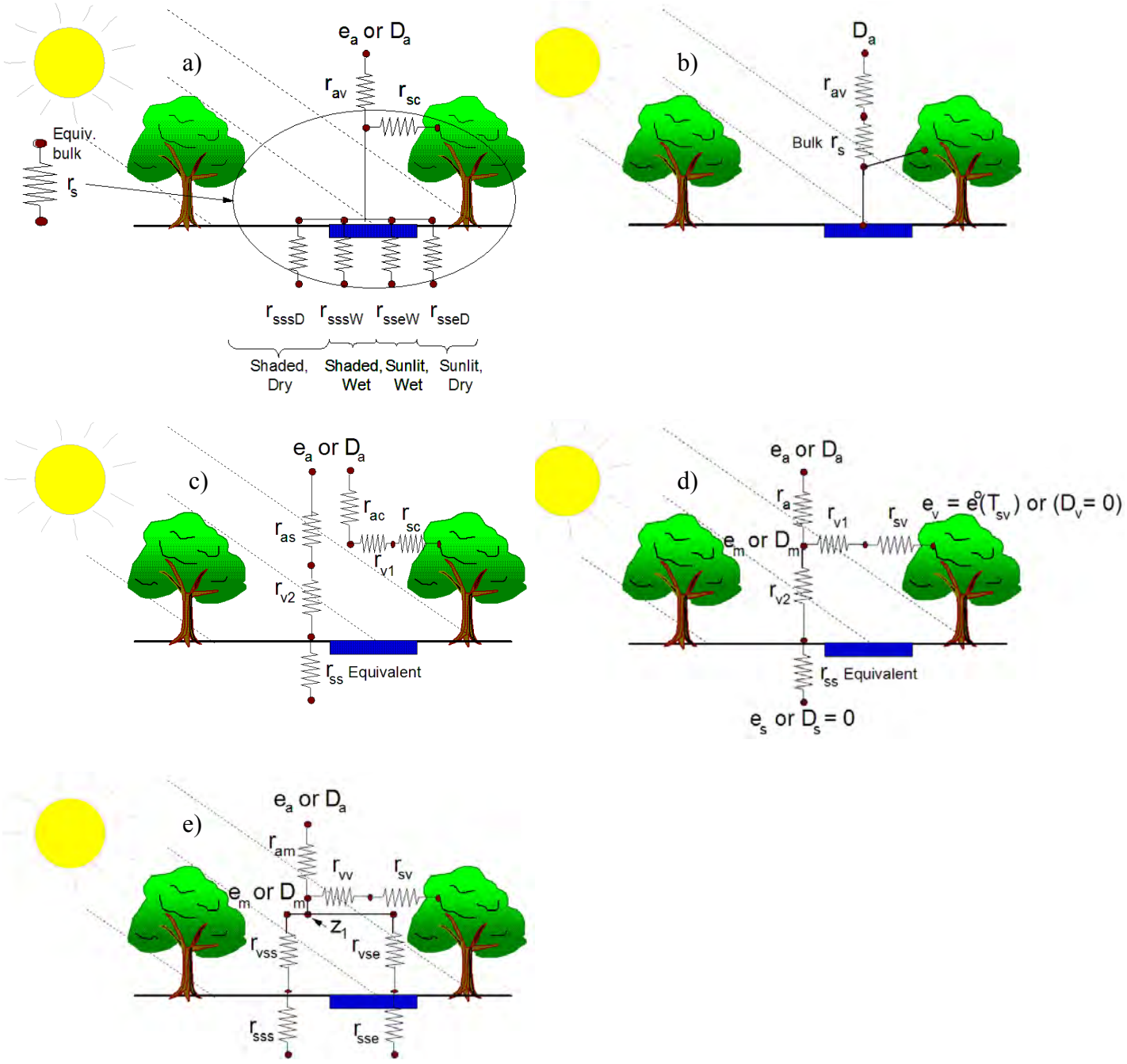

Fig. 11.1. Example general resistance networks used in three resistance-based ET models: a) single layer model represented by integrating a complex of parallel surface resistors, b) a bulk surface resistance expression for the single layer model, c) a two source (patch) model, d) a two-layer (interactive) model, and e) a two-layer (interactive) / three-source model.

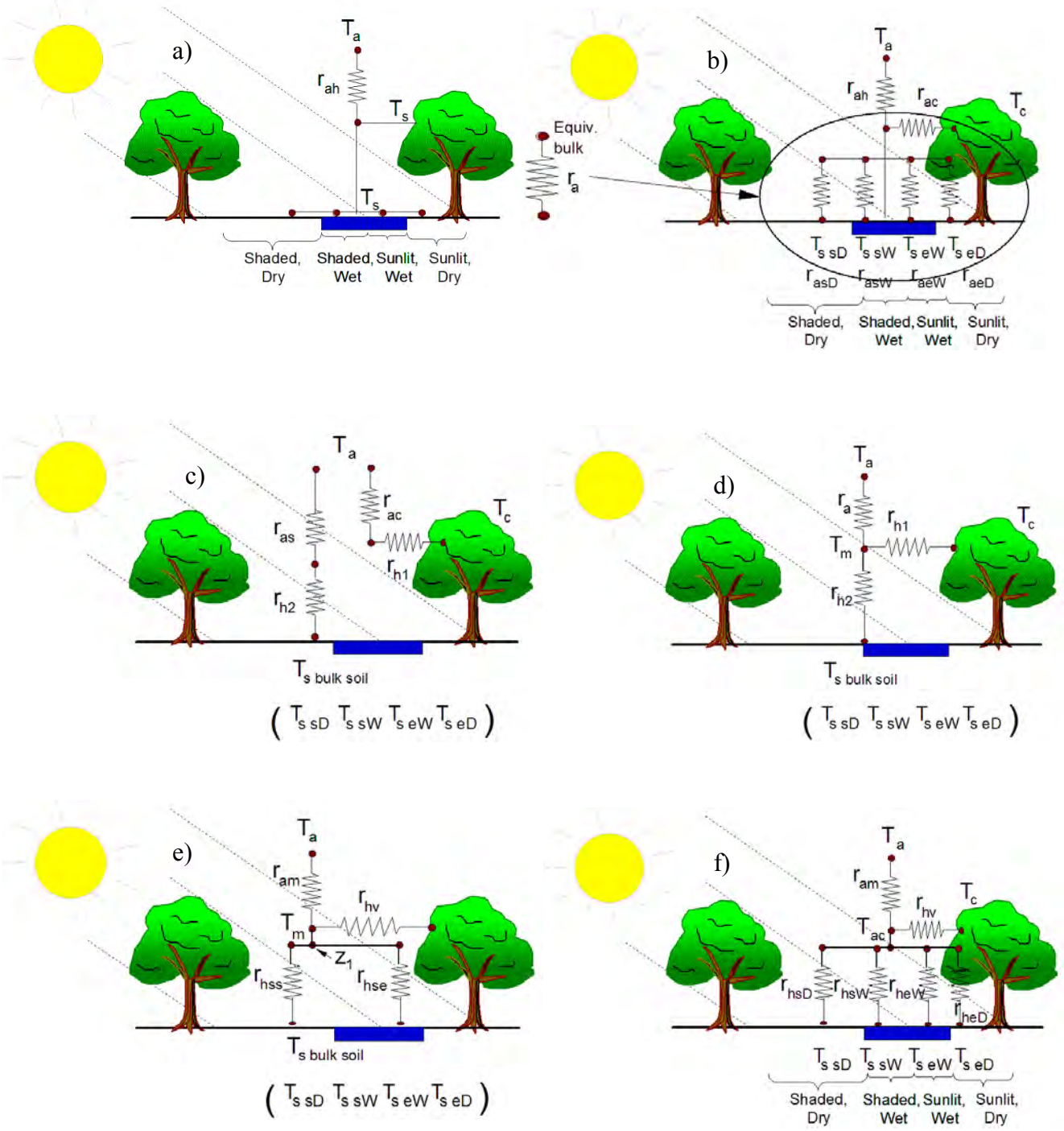

Fig. 11.2. Example general resistance networks used in three resistance-based models for sensible heat flux as counterparts of some ET models: a) single layer model, b) single layer model represented by integrating a complex of parallel aerodynamic resistors, c) a two source (patch) model, d) a two-layer (interactive) model, e) a two-layer (interactive) / three-source model and f) a two layer (interactive) / five-source model.

The Single-Layer Penman-Monteith Equation

Appendix J describes the derivation of the Penman-Monteith equation, which is similar to the derivation of the Penman equation except that the wind function of the Penman equation is replaced by an aerodynamic resistance term, and a bulk surface resistance term is explicitly placed between the inner leaf, where air is assumed saturated, and the midlevel of the crop canopy, where the mean source area for both heat and vapor is assumed to exist, and where aerodynamic resistance is assumed to begin. The 'breakthrough' of the combination (Penman and PM) equations was that by combining the radiation and aerodynamic terms and using Δ defined using air temperature only, the need for surface temperature is eliminated from the 'combined energy balance' and only more readily measured air parameters T, e and wind speed are required, in addition to net radiation. This simplified data set has made the single layer combination equation very successful, especially when applied as a reference method. The PM equation was introduced as eq. 8.2, and is repeated here:

$$\lambda E = \frac{\Delta(R_n - G) + \rho_a c_p (e_s - e_a) / r_{ah}}{\left(\Delta + \gamma\left(1 + \frac{r_s}{r_{ah}}\right)\right)} \tag{11.1}$$

where units of λE, R_n and G are in J m^{-2} s^{-1} (or W m^{-2}), ρ_a is air density, kg m^{-3}, c_p is specific heat of dry air, J kg^{-1} ^{o}C^{-1}, generally taken as 1010 J kg^{-1} ^{o}C^{-1}, and variables e_s and e_a are saturation vapor pressure at air temperature and actual vapor pressure of the air, in kPa. Parameter r_{ah} is bulk aerodynamic resistance to sensible heat transfer and is calculated using a combination of effective roughness for momentum, z_{om}, and effective roughness for sensible heat transfer, z_{oh}. Variable r_{ah} is essentially the equivalent of a combination of r_{am} and r_h introduced later with the multi-layer models. Parameter r_s is a bulk surface resistance that incorporates impacts of relative water availability and conductance from both vegetation and soil surfaces.

The PM equation was initially developed to describe the energy fluxes from a fully vegetated land surface and can have difficulty describing the combined fluxes from a sparsely vegetated surface where the point(s) where bulk surface resistance, describing resistance to vapor flow from both soil and vegetation, ends and where the bulk aerodynamic resistance, again, describing heat and vapor transfer from both soil and vegetation), begins. The single-layer PM model blends any variations of microclimate within the vegetation and assumes that each leaf surface that contributes to energy exchange is at the same temperature and sees the same saturation deficit at its surface. In the PM method, all surface resistance values for both leaf and soil subareas must contribute to the value for bulk r_s, as can be seen by studying fig. 11.1 and 11.2 where more sophisticated and complete resistance expressions shown in fig. 11.1c-e are simplified into the single layer, bulk expressions of fig. 11.1 b or fig. 11.2 a that are used in the PM equation.

An often overlooked requirement with application of the combination equation (Penman or Penman-Monteith) is the requirement that surface temperature is sufficiently similar to air temperature for the calculation of Δ to be based on air temperature, only. Dry surfaces tend to have substantially higher temperature than air temperature and, under these conditions, Δ should be calculated using eq. 11.3 with T_s solved by iterative application of equations for λE, H, G, and

R_n via energy balance. As illustrated in the following, the PM formulation is only completely accurate, in the commonly used form of eq. 11.1, where Δ is solved using T_a, only, when bulk surface temperature, T_s, has nearly the same value as T_a. It is under this condition where three important assumptions to the PM method, as generally practiced, hold. These three assumptions are that 1) Δ can be estimated using air temperature, only; 2) that stability correction to r_{ah} is not required; and 3) that long wave radiation emitted from the surface can be estimated using T_a, only. As shown later in table 11.5, under conditions of relatively low λE and relatively high H, as experienced under low vegetation cover or under conditions of water shortage, T_s, by physical requirement, exceeds T_a. Under extreme conditions, R_n can reduce by as much as 100 W m^{-2} with increasing T_s as compared to the 'reference condition' due to increased thermal radiative emission from the surface. In addition, buoyancy-driven mixing of the boundary layer with increased T_s compared to T_a caused by increasing H can require stability correction to reduce r_{ah} and provide correct estimation of λE.

Therefore, when vegetation cover is low or the water supply limits ET, i.e., the system is in a 'nonreference crop condition," T_s must be iteratively solved, for example using the following AFIB procedure. Ironically, when T_s is iteratively solved for or measured, the reason for the existence for the PM and other combination equations essentially evaporates, since substitution of a T_s and T_a based computation for Δ in the equation causes it to decompose back to the original component equations for H and λE. Effects of employing iteratively determined T_s for calculating Δ, $R_{l\,out}$, G, and stability correction are illustrated later in table 11.5.

The required suite of equations and inversion of the sensible heat equation to replace the PM equation includes the following and can be termed the 'AFIB' approach (aerodynamic fluxes via iterative solution of the energy balance):

$$R_n = (1-\alpha)R_s + R_{L-in}(1-\varepsilon) - \varepsilon\sigma T_s^4 \tag{11.2a}$$

$$G = \left[0.05 + K_G\, exp(-0.5\,LAI)\right](R_n + H) \tag{11.2b}$$

$$\lambda E = \frac{\rho_a\, c_p}{\gamma}\,\frac{\left(e^0(T_s) - e^0(T_a)\right)}{r_{av} + r_s} \tag{11.2c}$$

$$T_s = \frac{(R_n - G - \lambda E)\, r_{ah}}{\rho_a\, c_p} + T_a \tag{11.2d}$$

$$H = \rho_a\, c_p\,\frac{(T_s - T_a)}{r_{ah}} \tag{11.2e}$$

$$r_{ah} = r_{av} = \frac{\left[ln\left(\frac{z_u - d}{z_{om}}\right) - \Psi_m\left(\frac{z_u}{L(H)}\right)\right]\left[ln\left(\frac{z_T - d}{z_{oh}}\right) - \Psi_h\left(\frac{z_T}{L(H)}\right)\right]}{k^2\, u_z} \qquad (11.2f \text{ and } 7.20)$$

where z_u is the height above the ground surface for the wind speed measurement, d is the zero plane displacement of the logarithmic wind profile, z_{om} is a roughness length governing the transfer of momentum from the surface, ψ_m is the correction factor for momentum transfer to account for instability or stability of the boundary layer, z_T is the height of the air temperature measurement above the ground surface, z_{oh} is an assumed roughness length governing the transfer of sensible heat from the surface, ψ_h is a correction factor for sensible heat transfer to account for instability or stability of the boundary layer, k is the von Karman constant [0.41], and u_z is the wind speed measured at the z_u height. Equations for estimating ψ_m and ψ_h are given in chapter 7. Eq. 11.2b is from Allen et al. (2013) and represents the likelihood for G to be influenced by H due to their co-dependence on temperature gradients that share a common T_s. K_G is a fitting coefficient that is impacted by relative thermal conductivity of soil. A value of K_G = 0.2 is recommended for tilled soils and K_G = 0.10 to 0.15 is recommended for soils in a natural state having less bulk particle to particle contact. When H is low, and most R_n is converted into λE , G becomes a function of R_n, which is a traditional means for estimation (Choudhury et al. 1987). The $L(H)$ in eq. 11.2f indicates that the Monin L is a function of H and thus T_s. Equation 11.11.2f is also presented as eq. 7.20 in chapter 7 and eq. 8.3 in chapter 8 and the stability functions ψ are described in chapter 7. Eq. 11.2a–f are iteratively solved until the estimate for T_s is known. At that point, λE will be known from eq. 11.2c.

Once T_s is known, Δ can be estimated from eq. 11.3 for use in the PM equation, however, the calculation of λE from the PM equation using Δ, R_n, G, and r_{ah} from eq. 11.2a–f will be within a few percent of, or even identical to, λE solved using eq. 11.2c. In other words, the PM equation ceases to provide any new usefulness as compared to the AFIB method.

$$\Delta = \frac{e^0(T_s) - e^0(T_a)}{(T_s - T_a)} \qquad (11.3)$$

The solution of eq. 11.2a–f does not create computational challenges with modern computing systems, and once coded, tends to provide consistent estimates. The iteration can progress through any ordering of the equations, and can be initiated with the assumption that H = 0. Numerical stability in the solution can be insured by dampening calculations by averaging new values for T_s and, if needed, the Monin L with their values from the previous iteration step.

One is cautioned to not 'improve' the estimate for Δ without also improving all factors that impact both the estimate for T_s and the estimation by the PM itself. These factors include the inclusion of buoyancy correction and the net thermal radiation component of R_n, as described by eq. 11.2a–f above.

When the values for r_s, z_{om} and z_{oh} in eq. 11.2c and 11.2f are set to those for the standardized reference definitions, for example, r_s = 30 s m^{-1}, z_{om} = 0.062 m and z_{oh}= 0.0062 m, the AFIB process of eq. 11.2a–f will produce estimates for λE that are close to those from the standardized ASCE PM for the alfalfa reference, eq. 8.2, 8.15 or 11.1. This is because, under the 'reference conditions' which define a well-watered vegetation condition so that r_s = 30 s m^{-1}, T_s becomes similar to T_a and all simplifications and assumptions in eq. 8.15 are fulfilled (computing Δ and R_n using T_a only and ignoring buoyancy-induced boundary layer stability correction.).

One can make the following conclusions regarding the AFIB approach: i) the AFIB method of eq. 11.2a-f is, in essence, a decomposition of the PM equation into its original component equations; ii) the AFIB method of eq. 11.2a–f tends to reproduce estimates by the standardized reference equation for reference conditions using the standard reference crop settings; and iii) estimates from eq. 11.2a–f show the need to incorporate knowledge of T_s into the R_n, Δ, and r_{ah} terms of the PM equation under nonreference conditions. One can additionally conclude that the PM equation, or any combination equation, is only useful, and can only provide correct estimates that are T_a-based, only, under reference or nearly reference conditions. Under all other conditions where $\lambda E < \lambda ET_{ref}$, the AFIB method of eq. 11.2a–f is recommended. One limitation with both the direct Penman-Monteith and AFIB method are that each is best applied using hourly or shorter time-period data when actual ET rates are sufficiently less then reference ET rates to induce sensible heat flux rates that are more than 20 to 40% of available energy ($R_n - G$). This limitation is caused by the relatively strong nonlinearity in buoyancy or stability corrections that can vary hourly with ratios of H to R_n - G. Stability corrections applied using 24-h data will typically understate the power of buoyancy effects on surface energy exchange.

The Multi-Layer (Interactive) Resistance based Model

The saturation vapor deficit, D, is a principal term in the PM equation, and is defined as D = $e^o(T) - e_{air}$, or $e_s - e_a$, where $e^o(T)$ is saturation vapor pressure at temperature T and e_{air} is actual vapor pressure of the air or surface. In reality, in sparsely vegetated systems, not all parts of the vegetation surfaces and soil surfaces see the same surface saturation vapor deficit, D_s, but rather see a range of saturation deficits, depending on their position within the canopy structure and their relative water supply. In many multi-layer models, a single value for D, D_m, where the 'm' subscript represents 'mixed,' is assumed to exist at some point within the mixed canopy air space, as illustrated in fig. 11.1d and e. This D_m will be smaller than the D_a of the general air stream that exists at some reference height above the canopy. With the assumption of a common D_m within the canopy air space, a network of resistances are established in multi-layer or multi-source models that describe internal surface and boundary layer transfer of heat and vapor, as shown in fig. 11.1d, and these resistances can be used to tie applications of the PM-style equation together for the various layers. Were et al. (2008) assumed the mean height of common D_m within the canopy air space to occur at height $d + z_{om}$, which is typically at about 0.8 of canopy height, h_c.

Some interactive models use the PM model once to describe the flux between the canopy (overstory) surface and the in-canopy air space, and a second time for the flux from the understory surface to the in-canopy air space. In addition, the estimates for within canopy

aerodynamic resistances r_{vs} and r_{vv} (see fig. 11.1e, for example) are implicitly made for completely bare and completely vegetated conditions, and then averaged, based on an explicitly applied scheme. Differences in D at the component surfaces are maintained by boundary layer resistances r_{vi} as shown in fig. 11.1d. Fluxes from one component surface interact with fluxes from other component surfaces by influencing the in-canopy environment (T_m, e_m and thus D_m = f(T_m, e_m)), where T_m and e_m are temperature and vapor pressures in the mixed in-canopy air space.

Early derivations of multi-layer models included Shuttleworth and Wallace (1985), Shuttleworth and Gurney (1990), and Dolman (1993). These models have been widely tested and parameterized in research applications, but have not been widely used operationally due to the difficulty in establishing parameterizations for some of the internal resistances, which can change markedly with vegetation type and density and due to errors associated with impacts of unknown or unresolved T_s on Δ, $R_{L\text{-}out}$ and within and above canopy ψ as described previously for the PM model.

The following form of a multi-layer / multi-source model was suggested by Brenner and Incoll (1997) and Were et al. (2008) and is presented as an illustration of how a multiple-PM model can be formulated and how primary parameters and resistances are estimated. The Brenner-Incoll-Were model is a two-layer / three-source model having vegetation canopy (labeled i=1 or 'v'), shaded soil (labeled i=2 or 'ss') and exposed soil (labeled i=3 or 'se') sources. Typically, component within-canopy aerodynamic resistances, labeled r_v for vapor transport and r_h for heat transport, are assumed equal, and the r_h label is often assigned in the PM equation. Part of this assignment stems from the derivation of the PM equation, where a mixture of r_v for vapor transport and r_h is used (see Appendix J). The PM equation for each source area can be written as:

$$\lambda E_i = \frac{\Delta\left(R_n - G\right) + \dfrac{\rho_a c_p \; D_a}{r_{h_i} + r_{am}} - \Delta_i \left(R_{n\,i} - G_i\right)\dfrac{r_{h_i}}{r_{h_i} + r_{am}}}{\left(\Delta + \gamma\left(1 + \dfrac{r_{s_i}}{r_{h_i} + r_{am}}\right)\right)} \tag{11.4a}$$

where λE_i is the latent heat flux associated with each cover type i, D_a is the averaged, mixed vapor pressure deficit at some reference height above the canopy-surface system (fig. 11-1 d). The subscript i in Eq. 11.2a-c signifies the parameter assigned to each specific component surface (vegetation, understory, wet or dry exposed or shaded soil, etc). In the case of R_n and G, $R_n - G$ is the total bulk surface net radiation and soil heat flux density averaged over the entire surface, whereas R_{ni} and G_i represent values for the ith surface, where both parameters are influenced by the temperature of the ith surface.. Parameter $r_{h\,i}$ is the boundary layer resistance to the flow of heat and vapor from surface i to the place of the in-canopy air having deficit D_m, and $r_{s\,i}$ is the resistance to water vapor flow from inside surface i to immediately outside the surface. Resistance $r_{h\,i}$ is assumed equal to resistance $r_{v\,i}$ shown in fig. 11-1 d. Parameter Δ_i is best calculated as the slope of the saturation vapor pressure cuve using temperature of the specific i^{th} surface and air temperature at the reference height. Resistance r_{am} is the aerodynamic

resistance between the in-canopy location of D_m and the above canopy reference D_a. The formulation of eq. 11.4a allows for the omission of D_m. Because there is no express contact with a surface between these two locations, the formulation for r_{am}, as seen later, is for momentum transfer only, and its calculation does not include the parameter z_{oh}.

Were et al. (2008) expressed eq. 11.2a in a different form (an omitted term is corrected), but where Δ_i is assumed to be equal to the general, bulk Δ:

$$\lambda E_i = \frac{\Delta(R_n - G) r_{am} + \rho_a c_p D_a + \Delta\left((R_n - G) - \left(R_{n\,i} - G_i\right)\right) r_{h_i}}{\left((\Delta + \gamma)\left(r_{h_i} + r_{am}\right) + \gamma\, r_{s_i}\right)} \tag{11.4b}$$

The equation can be expressed in an even different form, if again, Δ_i is assumed to be equal to the general, bulk Δ:

$$\lambda E_i = \frac{\Delta(R_n - G) + \rho_a c_p D_a / r_{am} + \Delta\left((R_n - G) - \left(R_{n\,i} - G_i\right)\right) r_{h_i} / r_{am}}{\left(\Delta\left(1 + \frac{r_{h_i}}{r_{am}}\right) + \gamma\left(1 + \frac{r_{h_i}}{r_{am}} + \frac{r_{s_i}}{r_{am}}\right)\right)} \tag{11.4c}$$

The assumption that Δ_i equals the value for the general, bulk Δ that is computed from bulk surface temperature and bulk air temperature via eq. 11.3 may cause biases in model estimates. In the same way, the long-wave component for $R_{n\,i}$ should be based on an estimate of surface temperature of surface *i*. However, knowledge of T_s for surface i would require iterative solution using a system of equations similar to the AFIB equations 11.2a-f and is generally not done. The reader can note that if surface *i* is assumed to be directly 'coupled' to the above-canopy air stream, via r_{am}, so that within canopy aerodynamic resistance r_{hi} is 0, then Eq. 11.4a and 11.4c reduce to exactly the original PM equation (11.1), but where the typical r_{ah} is used in place of r_{am}.

Total ET from the complex surface is summed, in the multilayer, interactive model over the two or more types of surfaces:

$$\lambda E = \sum_i p_i C_i \lambda E_i \tag{11.5}$$

where p_i represents the fractional surface represented by cover *i* and C_i is a coefficient derived by combining resistances involved among the various sources, for example, *v*, *ss*, and *se,* representing the vegetation canopy, shaded soil or understory and exposed soil or understory. In a multi-source model such as the Were model, the sum of p_i over all surfaces, *i*, can total > 1.0, for example, in the case of understory vegetation or understory soil that can take up the same horizontal area as the overlying canopy. The C_i in eq. 11.5 are expressed in the Were et al. (2007, 2008) model as:

$$C_v = \frac{R_{ss}R_{se}(R_v + R_a)}{R_v R_{ss}R_{se} + f R_{ss}R_{se}R_a + f R_v R_{se}R_a + (1-f)R_v R_{ss}R_a} \tag{11.6a}$$

$$C_{ss} = \frac{R_v R_{se}(R_{ss} + R_a)}{R_v R_{ss}R_{se} + f R_{ss}R_{se}R_a + f R_v R_{se}R_a + (1-f)R_v R_{ss}R_a} \tag{11.6b}$$

$$C_{se} = \frac{R_v R_{ss}(R_{se} + R_a)}{R_v R_{ss}R_{se} + f R_{ss}R_{se}R_a + f R_v R_{se}R_a + (1-f)R_v R_{ss}R_a} \tag{11.6c}$$

where variables R_v, R_{ss} and R_{se} are defined as:

$$R_i = (\Delta + \gamma) r_{h_i} + \gamma r_{s_i} \tag{11.7}$$

where subscript *i* is replaced by subscripts '*v*', '*ss*' and '*se*' in Eq. 11.6a-c (see fig. 11.1d-e where r_{hi} is replaced by r_{vi}, and fig. 11.2d-e), and:

$$R_a = (\Delta + \gamma) r_{am} \tag{11.8}$$

Parameters *f* and (1-*f*) correspond to the fractional covers of vegetation and bare soil (or understory), respectively. Eq. 11.6a-c follow Brenner and Incoll (1997) and correct for an error in eq. 3-5 of Were et al. (2008).

One of the serious challenges in applying the multi-layer or patch models to sparse vegetation systems is in the parameterization of r_h, which is the aerodynamic resistance within and across the canopy or near surface boundary layers, and in the validity of applying the PM equation over this region. The traditional equations for aerodynamic resistances across *T* and *e* gradients assume that the *T*, *e* and *u* profiles follow semi-logarithmic shaped vertical profiles, the shapes of which are governed by surface roughness and density-induced buoyancies. However, within vegetation canopies, turbulent diffusion theory (K theory) has been shown to be inadequate to describe convective transfer where even counter gradient fluxes can exist (Raupach 1989, Van den Hurk and McNaughton 1995, McNaughton and van den Hurk 1995, Daamen and McNaughton 2000). Therefore, empirical formulations have to be applied. Examples of these are by Choudhury and Monteith (1988) and Zhao et al. (2006), where, for r_{hs}:

$$r_{hs} = \frac{h_c \, exp(n) \, ln\left(\frac{z_a - d}{z_o}\right)}{n k^2 u_a (h_c - d)} \left[exp\left(\frac{-n \, z_{os}}{h_c}\right) - exp(-0.76\, n) \right] \tag{11.9}$$

and by Shuttleworth and Wallace (1985) and Brisson et al. 1998):

$$r_{hs} = \frac{ln\left(\frac{z_a - d}{z_o}\right)}{k^2 u_a} \frac{h_c}{n(h_c - d)} \left[exp(n) - exp\left(n\left(1 - \frac{d + z_o}{h_c}\right)\right)\right] \tag{11.10}$$

where h_c is mean height of the vegetation canopy, z_a is the measurement height for wind speed and air temperature, *T,* and humidity, *d* is zero plane displacement height and z_o is the aerodynamic roughness length for the complete surface, u_a is wind speed at height z_a, z_{os} is aerodynamic roughness length for the underlying soil or understory, and n is an empirical eddy diffusion decay constant. $n = 2.5$ when $h_c < 1$ m, $n = 2.31 + 0.194\ h_c$ for $1 < h_c < 10$ m, and $n = 4.25$ for $h_c > 10$ m. Daamen and McNaughton (2000) used $n = 2.0$. It is important to note that r_{hs} is applied for both shaded soil, some of which may be beneath a dense vegetation canopy, and for exposed soil that may have substantial exposure to the boundary layer, especially with sparse vegetation. The former situation will have a high value for r_{hs} and the latter a lower value. In addition, r_{hs} for soil exposed to the sun can have substantial buoyancy boost to convection, lowering the value for r_{hs} from that estimated from eq. 11.9 and 11.10. Under those conditions, a buoyancy term can be added to those equations by replacing the $\ln((z_a\text{-}d)/z_o)$ term with $[\ln((z_a\text{-}d)/z_o) - \psi_m]$, where ψ_m is an integrated stability correction calculated from z_0 to z_a.

For the bulk boundary layer resistance between vegetation and in-canopy location z_m, Brisson et al. (1998) proposed treating all single leaf boundary layers as if in parallel:

$$r_{hv} = \frac{\sigma_b\, r_b}{LAI} \tag{11.11}$$

where σ_b is a shielding factor taken as 0.5 and with the single leaf boundary resistance based on an extinction function from Shuttleworth and Gurney (1990):

$$r_b = \frac{100}{n\left(1 - exp\left(\frac{-n}{2}\right)\right)}\left(\frac{w}{u_h}\right)^{0.5} \tag{11.12}$$

where w is the characteristic leaf width, mm, u_h is the wind speed at the top of the canopy, m s^{-1}, and n is the eddy diffusivity decay constant. Units of all resistances are s m^{-1}.

The aerodynamic resistance, r_{am}, between the in-canopy air space and reference height where the mean wind speed measurement is made is assumed to be well mixed and representative of the entire land surface structure. The formulation for r_{am} is similar to that formulated by Shuttleworth and Wallace (1985) where z_{oh} is omitted because the resistance does not include boundary layer effects, but where some decay of eddy diffusivity is assumed:

$$r_{am} = \frac{ln\left(\frac{z_a - d}{z_o}\right)\left[ln\left(\frac{z_a - d}{h_c - d}\right) + \frac{h_c}{n(h_c - d)}\left[exp\left(n\left(1 - \frac{d + z_o}{h_c}\right)\right) - 1\right]\right]}{k^2\, u_a} \tag{11.13}$$

Eq. 11.9-11.13 do not include corrections for density-induced buoyancy impacts on convective transport, which can be large over dry, warm surfaces. The equation for r_{am} was modified by Shuttleworth and Gurney (1990) to include buoyancy effects as:

$$r_{am} = \frac{ln\left(\frac{z_a - d}{z_o}\right)\left[ln\left(\frac{z_a - d}{h_c - d}\right)(1+\delta)^{\varepsilon} + \frac{h_c}{n(h_c - d)}\left[exp\left(n\left(1 - \frac{d + z_o}{h_c}\right)\right) - 1\right]\right]}{k^2 u_a} \tag{11.14}$$

Parameter $(1 + \delta)^{\varepsilon}$ is a stability correction factor based on the bulk Richardson number (Shuttleworth and Gurney 1990; Choudhoury and Monteith 1988) where:

$$\delta = \frac{5\, g\, (z_a - d)(T_o - T_a)}{T_a\, u_a} \tag{11.15}$$

where T_o is air temperature, K, at the intermediate height of D_m, and T_a is air temperature at reference height z_a. Parameter ε has a value of -2 for $\delta < 0$ and a value of -0.75 for $\delta > 0$ (Choudhoury and Monteith 1988). However, the use of $(1 + \delta)^{\varepsilon}$ only provides stability correction to the temperature profile in eq. 11.14 and not to the wind profile as represented by the first logarithmic term. In addition, stability correction formulations built on the Richardson number are not as robust at those based on Monin-Obukhov similarity theory (Brutsaert 1982; Allen et al. 1996). The $h_c - d$ expression in eq. 11.13-11.14 represents the beginning height, z, for the start of r_{am}. This is point z_1 in fig. 11.1e. Height z_a represents the endpoint for r_{am}.

An improved equation for r_{am} using stability correction based on Monin-Obhukov is:

$$r_{am} = \frac{\left[ln\left(\frac{z_a - d}{z_o}\right) - \Psi_{m\ z_a}\right]\left[\left[ln\left(\frac{z_a - d}{h_c - d}\right) - \left(\Psi_{h\ z_a} - \Psi_{h\ h_c}\right)\right] + \frac{h_c}{n(h_c - d)}\left[exp\left(n\left(1 - \frac{d + z_o}{h_c}\right)\right) - 1\right]\right]}{k^2 u_a} \tag{11.16}$$

where $\Psi_{m\ z_a}$ and $\Psi_{h\ z_a}$ are integrated stability correction parameters based on Monin-Obhukov formulations for momentum and heat fluxes, respectively, where the integration is along the vertical between momentum roughness height z_o and $z_a - d$ for momentum correction and along the vertical between $z_1 = h_c - d$ and $z_2 = z_a - d$ for heat flux profile correction (necessitating the subtraction of $\Psi_{h\ h_c}$ from $\Psi_{h\ z_a}$). Equations for the Monin-Obhukov formulations are presented in Chapter 7. Similar buoyancy corrections are needed for the r_h terms in both the multi-layer and patch models, especially when one of the surfaces is dry and sensible heat flux is relatively large. However, the nature and structure of buoyancy correction within a sparse canopy is uncertain, even though it can constitute a very effective mechanism for transport of sensible heat

and vapor upward within tall canopies such as trees, where mechanical mixing from wind is low due to sheltering. This increases uncertainty in applying multisource and multilayer models as formulated here.

Formulations for other parameters are available from the literature. Formulations for aerodynamic roughness and surface resistance are described in following sections. Lagos (2008) and Lagos et al. (2009, 2012) described application of an interactive model to partial cover vegetation having substantial surface residue.

Large differences in surface resistances of soil and vegetation components or soil and soil components can cause large differences in temperatures and vapor densities at the component surfaces. The resulting gradients between the surfaces may be enough to drive significant fluxes between surfaces. A common example occurs when a sparse overstory canopy well-supplied with water has an underlying dry soil surface. In this case a net sensible heat transfer (micro-advection) from the understory, having a relatively high surface temperature, to the overstory occurs. In contrast, when both the overstory and understory are water stressed, there is likely to be a positive sensible heat flux away from both surfaces and the interaction of fluxes is less important (Daamen and McNaughton 2000). In some situations, it may be more effective to use a patch type of model such as shown in fig. 11.c, and apply aerodynamic and energy balance equations directly, similar to the AFIB procedure of eq. 11.2a-f, rather than applying the Penman-Monteith method, but using formulations for r_a from eq. 11.9-11.16. Both approaches may require an iterative solution for surface temperature to adequately calculate emitted long wave radiation, soil heat flux and, in the case of the PM method, Δ, from the various surfaces.

The Two-Source (Patch) Resistance based Model

The ‘patch’ model is intermediate in complexity as compared to the more simple single-layer Penman-Monteith and AFIB models and the more complicated interactive layered models. The two-source model applies the PM equation or a full suite of aerodynamic AFIB-style equations for H and λE separately to two different component surfaces, assuming no interaction between the surfaces. Evaporation from the soil and ‘transpiration’ from vegetation is calculated separately for assumed homogeneous patches and the areal average is weighted according to the fractional cover of each patch type. The patch model essentially uses two non-interacting PM or AFIB models side-by-side and is justified at the scale where a boundary layer is fully developed over each patch so that separate temperature and vapor gradients wind speed profiles can be assumed to extend to some blended reference height close to each surface so that ‘K-theory’ can be assumed to apply, and where edge effects between patches are insignificant. As the size of patches decreases, the model becomes less valid. In some applications, a common r_{am} is used from a blending point above the two references up to the reference height where T, e and u are measured. This is done to account for blending effects of smaller patch size on the air stream near the canopy. Daamen and McNaughton (2000) suggested that patch size should be 10 times vegetation height or larger to satisfy the boundary layer requirements.

Examples of patch models have been the ENWATBAL model (Evett and Lascano 1993; Lascano 2000), a three-patch model by Brenner and Incoll (1997), and, using explicit equations for LE and H fluxes, the ‘TSEB” model of Kustas (1990), Kustas and Norman (1999) that is applied in a surface energy balance mode using thermal imagery. The patch model has been developed for simplicity. However, because direct interchange between surface types is ignored, it is often challenging to define appropriate resistance values. When patches are extensive in size

so that the microclimate of one does not affect the microclimate of the other, then the aerodynamics and resistances of different surface types can be characterized by different roughness lengths, and with quite different r_{am} values (Daamen and McNaughton, 2000). Conversely, when patch sizes are small (< 10 times vegetation height), each surface type (i.e., vegetation and bare soil) will tend to impact the aerodynamics of the other to some degree.

When written in the form of the PM equation, the patch model will have the form:

$$\lambda E_i = p_i \frac{\Delta\left(R_{n\,i} - G_i\right) + \rho_a c_p \left(D_a\right) / \left(r_{a\,i} + r_{h\,i}\right)}{\left(\Delta + \gamma\left(1 + \frac{r_{s_i}}{r_{a\,i} + r_{h\,i}}\right)\right)} \tag{11.17}$$

and

$$\lambda E = \sum_i p_i \, \lambda E_i \tag{11.18}$$

where p_i represents the fractional surface represented by cover *i*.

Often, the effective fraction of surface or fraction of net radiation absorbed by the overstory, f, is expressed as a function of leaf area index:

$$f = 1 - exp\left(-a\,LAI\right) \tag{11.19}$$

where *a* is an empirical constant that has been found to range from 0.5 for short grass steppe to 2.0 for sparse row crops to 3 for a sheltered kiwifruit orchard (Daamen and Mcnaughton 2000). Alternately, *f* can be estimated from remotely sensed vegetation indices such as the NDVI or SAVI indices (Carlson and Ripley, 1997).

11.3 Challenges with Types of Resistance-based Models

Complexity in models can bring complexity in parameterization of the models. This can definitely be the case with multi-layer and patch models where the characterization of heat and vapor transport within a canopy have, as a necessity, a degree of speculation and empiricism. If not formulated properly, these characterizations can induce more inaccuracy than accuracy (Were et al. 2008), especially if key factors such as buoyancy correction or penetration of air into the canopy by random eddy movement are not accounted for. For example, the required form and structure of formulations for internal resistances, r_h, may change with plant density, leaf area, patch size, wind speed and buoyancy. K theory, which establishes nearly logarithmic wind speed, *T* and *e* profiles above some zero plane displacement height, is not strictly applicable within canopies and along patch boundaries. Also difficult to accurately account for is the horizontal transfer of sensible heat (and vapor deficit) from understory into canopy and vice versa.

In addition to uncertainties in estimates for resistances, uncertainties exist in estimating the net radiation, $R_{n\,i}$, associated with specific component surfaces. A dry, warm soil surface exposed to the sun can emit up to 100 W m^{-2} more thermal radiation than a cool adjacent canopy. This reduces the available energy at the soil surface and substantially impacts the energy balance and boundary layer stability estimation. The calculation of $R_{n\,i}$ for soil is further complicated by whether the soil is shaded or exposed and by the estimation of downwelling thermal radiation,

which is a mixture of relatively lower rate from exposed sky and relatively higher rate from the relatively warmer canopy that is in view of the soil. A variety of canopy model formulations have dealt with the estimation of net thermal and net shortwave radiation as described later.

Estimation of soil heat flux densities can be uncertain under complex canopies, as thermal gradients and associated heat fluxes into soil change with solar angle and with surface temperature and water contents, which can be highly variable in a complex canopy. Even accurate measurement of G, required to parameterize a model, is extremely demanding in complex canopies and can require tens of locations within the canopy structure to adequately sample all combinations of shading, rainfall capture, plant root extraction, aerodynamic exposure, surface mulching, wetting by irrigation, and plant architecture.

As described for the single layer PM equation, an often overlooked requirement for any application, including multilayer applications, is error caused by assuming that surface temperature is sufficiently similar to air temperature for the calculation of Δ, or that all surfaces have similar T_s when calculating Δ , emitted long-wave radiation, and near-surface air buoyancy. Often, dry surfaces have substantially higher temperatures than air temperature and Δ should be solved by iterative application of AFIB types of equations such as eq. 11.2a-f. T_s for a specific surface is estimated using energy balance and aerodynamic theory:

$$T_{s\,i} = \frac{\left(R_{n\,i} - G_i - \lambda E_i\right) r_{a\,i}}{\rho c_p} + T_{a\,i} \tag{11.20}$$

where the i subscript denotes the ith component surface. $T_{s\,i}$ is surface temperature and $T_{a\,i}$ is air temperature at some height, with $r_{a\,i}$ the aerodynamic resistance over the vertical distance between $T_{s\,i}$ and $T_{a\,i}$. Depending on the placement of $T_{a\,i}$, $r_{a\,i}$ will include r_h and r_{am}. Once $T_{s\,i}$ is known, Δ can be estimated for use in the PM or PM_i equation with calculation made using $T_{s\,i}$ and $T_{a\,i}$. The estimate for $T_{s\,i}$ can be used to improve the estimation of thermal radiation emitted from the surface and in estimating buoyancy effects.

As noted earlier, one of the drawbacks of the single layer PM equation, especially for use in sparse canopies, is the implicit assumption that the mean horizontal plane of momentum sink within the canopy is at the same height ($d + z_{om}$) as that for sensible heat (source or sink) and for latent heat (source) so that common expressions for r_a can be used for H and LE components and the Bowen ratio can be used to derive the combined Penman form (see Appendix J). Similarity of source heights for H and LE is not generally true for sparse canopies or for dense canopies having intermittent gaps with exposed lower story vegetation or bare soil. Under these conditions, a significant amount of solar radiation can penetrate to levels below $d + z_{om}$ resulting in the generation of sensible heat at lower levels with only the possible conversion to latent heat. The combination of bulk stomatal resistance with soil resistance into a single surface resistance, r_s, as is done for the PM equation or AFIB method implies that the soil and canopy surfaces are at nearly the same vertical level. This is generally not the case and consequently the assumption ignores the aerodynamic resistance between the soil surface and the mean height of heat and vapor exchange in the canopy.

The errors induced by the assumption of a single exchange plane in the PM and AFIB methods are sometimes partially accounted for by varying the "apparent" z_{om} / h ratio, "effective" leaf area, single leaf resistance, or radiation extinction coefficient, K_r, during analysis of research data (Daamen and McNaughton 2000). However, because the transport resistances within the

canopy are dynamically linked to wind speed, canopy structure, radiation levels and soil water, fitted parameters may not transfer well to other growth stages or locations. Wind speed and movement within canopies was discussed and estimated by Ben-Mehrez et al. (1992), Rapauch (1989) and Rapauch et al. (1996).

11.4 Parameterizing the Penman-Monteith for Equivalency with More Complicated models

Often, operational models that are applied routinely over large types of vegetation and conditions are necessarily reduced in complexity to accommodate reliable parameterization and available data and observations. Many operational systems, including some land simulation (LSM) systems such as those used in the Weather Research and Forecasting (WRF) model have, in the past, been based on a single layer Penman-Monteith model (Mahrt and Ek, 1994, Chen and Dudhia, 2001), whereas more recent models use patch types of resistance-based models similar to the AFIB process where surface temperatures for vegetation and soil are estimated separately (Oleson et al. 2004, Niu et al. 2011). Resistance parameters in these models are typically formulated by combining and reducing resistances developed for the multi-layer and multi-source models.

Often, the uppermost aerodynamic resistors in the patch model, i.e., r_{as} and r_{ac}, are aligned in a network in the form of parallel resistors. In that situation, the equivalent total resistance of those resistors is equivalent to r_{am} as used in the multi-layer model, and the in-series combination of r_h and r_{am} are equivalent to the bulk r_{ah} as used in the single-layer PM model or AFIB models. The resistance values are calculated in simplified models as r_{as} / f_s and r_{ac} / f_c where f_c is the fraction of ground covered by vegetation and f_s is the fraction of exposed soil, where $f_s + f_c = 1.0$. This formulation effectively divides the air space from the canopy to the reference height between the two component surfaces (Daamen and McNaughton 2000).

Were et al. (2008) formulated effective surface and aerodynamic resistances for the single-layer PM model by aggregating various soil and plant resistances as used in a more complicated multilayer-multi source model. They solved for surface temperature using iteration. They compared estimates of ET with flux measurements and concluded that the use of effective surface resistances aggregated in parallel with effective aerodynamic resistances aggregated in series in a single-layer PM model produced similar accuracy as a multi-layer model for natural brush vegetation in SE Spain. In some cases they found the single-layer model to outperform the multi-layer model in terms of accuracy.

Net radiation

As described earlier, both total surface net radiation and net radiation of individual surface components, $R_{\mathrm{n\,i}}$, should include surface-specific estimation of emitted long wave radiation using eq. 4.32, especially for dry surfaces, where emitted long wave can be as much as 100 W m^{-2} greater, and thus $R_{n\,i}$ 100 W m^{-2} less, than that for the well-watered reference surface represented by eq. 4.37, where surface temperature is usually within a few degrees of near surface air temperature. When estimating $R_{n\,i}$ for bare, dry soil exposed to the sun, one should avoid estimating $R_{n\,i}$ as an exponential function of leaf area index multiplied by the total bulk surface net radiation as is sometimes done in many applications of multilayer models (Shuttleworth and Wallace 1985; Kelliher et al. 1995; Zhao et al. 2006), because of the potential

differences in surface temperature between bulk surface and soil. In addition, soil albedo can be substantially greater than the typical vegetation albedo of 0.2 to 0.25, when soils are dry and organic content is low, ranging as high as 0.4 to 0.5. Conversely, high organic, wet soil can have albedos as low as 0.1 to 0.15 (Fritschen 1967).

11.5 Comparative Model Performance

Daamen and McNaughton (2000) compared ET estimates by three evaporation models represented by combinations of eq. 11.4-11.16 for six different sparsely-vegetated land surfaces and a range of conditions of water supply. Vegetation types ranged from short-grass steppe to sparse rangeland to sparse cotton and millet to kiwi and lemon orchards. The three evaporation models (single layer, multi-layer and patch) based on the PM formulation were parameterized to measurements from the six locations and were then operated over ranges of water availability and combinations of relative resistance.

Estimates by the single-layer PM model application closely resembled those from the iterative (multi-layer) model when applied to shortgrass steppe over a broad range of surface and relative aerodynamic resistances due to the relatively dense structure of the grass. The exception was when the surface resistance from soil was set to 0, representing a saturated surface. Differences among models were greater for more sparsely vegetated surfaces, where ratios of r_{am} to r_h (fig. 11.1) were relatively small due to greater roughness.

Daamen and McNaughton (2000) showed the patch and interactive models to have best agreement as canopy sparcity and patch size increased, for example with the lemon orchard, and agreement decreased with plant density and increasing ratios of r_{am} to r_h. They found higher evaporation estimated by the interactive model than patch model under some conditions due to interactions of fluxes between the component surfaces. As expected, the flux interactions were largest when the surface resistances for the soil and vegetation components were most different (for example, dry soil surface and well-watered canopy) and when r_{am} was larger than r_{hv} and fractions of exposed soil and canopy were similar. When flux interactions were largest, differences between the single-layer and interactive (multi-layer) models were the smallest. This suggests that a land surface as a whole can be well approximated by a single homogeneous surface with appropriately averaged properties when there is a large interaction (mixing of fluxes and 'micro-scale advection') between the component surfaces.

Daamen and McNaughton (2000) suggested that the ratio of r_{am} to r_h in fig. 11.2e,f can be a good indicator of the best choice in type of simplified model (patch or single-layer). As r_{am} to r_h becomes small, the difference between the in-canopy vapor pressure deficit, D_m, and vapor pressure deficit of the air stream above the canopy becomes small in the interactive model, and the patch and interactive models approach each other. When the r_{am} to r_h ratio is large, D_m is closer to the vapor pressure deficits at the component surfaces and the single layer model can serve as a good approximation. A relatively small ratio r_{am} to r_h can occur under high wind speed or with relatively large vegetation roughness and a relatively large ratio can occur under lower wind speeds or with relatively small aerodynamic roughness.

Under dry conditions, differences among all three models became less significant. When surface resistances exceeded 300 s m^{-1}, the patch and single layer PM models estimated energy fluxes to within 50 W m^{-2} of the interactive model for the grass-steppe and millet land surfaces (Daamen and McNaughton 2000). At these higher surface resistances, evaporation is largely

controlled by surface resistance and interactions among fluxes become less important. However, under conditions of low available water, accuracy of ET estimates becomes sensitive to the value estimated for the surface resistances for both vegetation and soil surfaces.

Often, the total soil evaporation estimate is not overly sensitive to the parameterization of resistances when precipitation events are separated by periods of five days or more. This is due to the impact of conservation of water in the top soil layer on values assigned to surface resistance that are updated each calculation time step. Provided that the resistance and evaporation models implement upper limits on total evaporation, and provided a majority of evaporable water is depleted between events, evaporation rates from soil can be over or underestimated, but the final total evaporation estimate will not be greatly impacted. The partitioning between E and T is affected, however, and the partitioning between sunlit and shaded and wetted and shielded areas of soil remains important. Various functions for estimating soil surface resistances are described in section 11.8.

11.6 Roughness Length and Zero Plane Displacement

General Parameters

The direct application of the PM equation uses the basic PM combination equation (eq. 8.2) and the aerodynamic resistance, r_a or r_{ah}, computed using eq. 7.20, 8.3 or 11.2f. Bulk stomatal resistance is generally estimated as a function of leaf area index (*LAI*), and an average stomatal resistance. Alternatively, a minimum stomatal resistance ($r_{l_{min}}$) for well ventilated, sunlit leaves with no soil water limitation can be divided by multiplicative stomatal conductance reducing functions, $g(\ )$, which are based on environmental variables (Stewart 1989) as discussed in section 11.7.

Roughness length for momentum transfer, z_{om}, and zero plane displacement, d, required in eq. 7.20, 8.3 and 11.2f and can be estimated for relatively dense vegetation canopies ($LAI > 2$) using eq. 11.21 and 11.22 (Brutsaert 1975; Monteith 1981; Allen et al. 1989; Jensen et al. 1990).

$$d = 0.67\,h \tag{11.21}$$

$$z_{om} = 0.12\,h \tag{11.22}$$

where h is the mean maximum height of the plant canopy. Units for z_{om}, d, and h are the same. It is important to appreciate that both z_{om} and d are essentially 'synthetic' parameters that describe a mean, smoothed idealized wind profile as it dissipates to zero within the canopy. By definition, the idealized wind profile dissipates to zero at $d + z_{om}$. Both values can be determined by measuring wind at two or more heights above the roughness sublayer (Cellier and Brunet 1992 and Raupach et al. 1991) and fitting to an assumed smoothed and continuous profile, as described later in eq. 11.33 and 11.35. Alternatively z_{om} can be determined from friction velocity data obtained by 3-D sonic anemometers. The profile measurement and fitting is generally done under near-neutral conditions, although Zhao et al. (2008) described a procedure for estimating the parameters using data collected under unstable conditions. Generally the value for d decreases as density of vegetation decreases as shown later in eq. 11.29.

For tall vegetation or sparse vegetation, more complex and elaborate equations may be required to estimate z_{om} (Tanner 1968; Lettau 1969; Plate 1971; Brutsaert 1975; and Monteith 1981); for example, eq. 11.23 by Lettau (1969):

$$z_{om} = 0.5 h^* \frac{s}{S} \tag{11.23}$$

where h^* is the effective obstacle height of the vegetation in m, s is the silhouette area (area "seen" by wind), m^2, and S is the horizontal plane area (total ground area divided by the number of roughness elements), m^2.

Thom (1971) and Garratt and Hicks (1973) proposed the following equation for estimating z_{om} for forest canopies:

$$z_{om} = \sigma (h - d) \tag{11.24}$$

or alternatively

$$\frac{z_{om}}{h} = \sigma \left(1 - \frac{d}{h}\right) \tag{11.25}$$

where σ was suggested to be equal to 0.36, which is equivalent to the relationship suggested by Brutsaert (1982) for dense, uniform plant stands:

$$z_{om} = \frac{1}{e}(h - d) \tag{11.26}$$

where e is the natural number (2.718). When d is estimated as 0.67 h, then eq. 11.24 with σ = 0.36 and eq. 11.26 both reduce to $z_{om} = 0.12\ h$, which is equivalent to eq. 11.22.

Measurements of z_{om}/h and d/h by Leuning and Attiwill (1978) for 27-m eucalyptus trees having projected areas of 80% of the ground surface, measurements by Jarvis et al. (1976) for thirteen coniferous forest regions having mean tree heights of 10 to 28 m, and measurements by de Bruin and Moore (1985) for 18 m tall Scots pine (*Pinus sylvestris* L.) indicate a value of σ = 0.22. Canopy densities in these studies were not specified. Moore (1974) determined a value of $\sigma = 0.27 \pm 0.07$ for 105 published estimates of d, z_{om} and h for vegetation types ranging from smooth grass to forest. Zhao et al. (2006) varied the coefficient in eq. 11.22 in proportion to height, with the multiplier (and z_{om} / h ratio) reducing with increasing h:

$$\begin{aligned} z_{om} &= 0.13 h, && h \le 1 m \\ z_{om} &= 0.139 h - 0.009 h^2, && 1 < h < 10 m \\ z_{om} &= 0.05 h, && h \ge 10 m \end{aligned} \tag{11.27}$$

The 0.05 multiplier for tall vegetation is in line with the de Bruin and Moore (1985) value for σ = 0.22, which is equivalent to a direct multiplier on h of 0.07 for $d \sim 2/3\ h$.

The utility of eq. 11.24 is that it is applicable to canopies where zero plane displacement varies with plant density and height. Seginer (1974) discussed the variation in z_{om}/h and d/h with increasing canopy density from a theoretical point of view. It is logical that z_{om}/h varies

with stand density, since as stand density increases; more roughness elements are present to affect momentum transfer to the surface. However, as density increases beyond a particular limit, the logarithmic wind profile begins to become displaced upward in the canopy (d increases) so that length of roughness elements become less effective in momentum transfer and z_{om}/h begins to decrease.

Following this logic, Perrier (1982) proposed relationships to estimate z_{om}/h and d/h as a function of LAI for well-defined canopies:

$$\frac{z_{om}}{h} = \left(1 - e^{\frac{-a\,LAI}{2}}\right) e^{\frac{-a\,LAI}{2}} \tag{11.28}$$

$$\frac{d}{h} = 1 - \left(1 - \left[e^{\frac{-a\,LAI}{2}}\right]\right)\left(\frac{2}{a\,LAI}\right) \tag{11.29}$$

where LAI is total leaf area index ($m^2\ m^{-2}$) and a is an adjustment factor for LAI distribution within the canopy. Parameter $a = (2f)$ for $f \geq 0.5$ and $a = 1\ (2\ (1 - f))^{-1}$ for $f < 0.5$, where f is the proportion of LAI lying above $h/2$. Estimates by eq. 11.28 and 11.29 are shown in fig. 11.3 for $f = 0.5$ (uniform canopy structure), $f = 0.7$ (top heavy canopy), and $f = 0.3$ (sparsely topped canopy). Also included in fig 11.3 are z_{om}/h and d/h reported by Jarvis (1976) for coniferous forests and z_{om}/h estimated by eq. 11.25 using $\sigma = 0.27$ and d estimated by eq. 11.29 with f set equal to 0.7 to resemble structures of pine trees. The agreement in fig. 11.3 between eq. 11.28, 11.29 and measured values by Jarvis for coniferous forests is poor for $LAI < 3$, where d was underestimated and z_{om} was overestimated.

It is difficult to recommend which z_{om}/h relations will best predict z_{om} for sparse or tall canopies. Equations 11.28 and 11.29 may adequately predict z_{om}/h and d/h for dense forests and for sparse vegetation where LAI and h are large. The Perrier functions are intuitively sound, as they predict small d for low LAI and a peak in z_{om} as stand density thickens with $d/h < 0.5$. However, the ratio z_{om}/h estimated for $LAI > 5$ may become too low for $f > 0.3$. This can be corrected by establishing a lower limit on z_{om}/h in eq. 11.28 (for example, $z_{om}/h = 0.10$) for $LAI > 5$. The use of eq. 11.24 or 11.27 in conjunction with d estimated using eq. 11.29 may be a useful approach, with σ in the range of 0.20 to 0.40. This equation combination does estimate large z_{om}/h for small values of LAI (< 0.5), which may be unreasonable. However, at values of $LAI < 0.5$, r_s predicted for use in the PM equation should be relatively high, thereby keeping ET estimates low. Rapauch (1989) and Rapauch et al. (1996) reported similar approaches for estimating z_{om}.

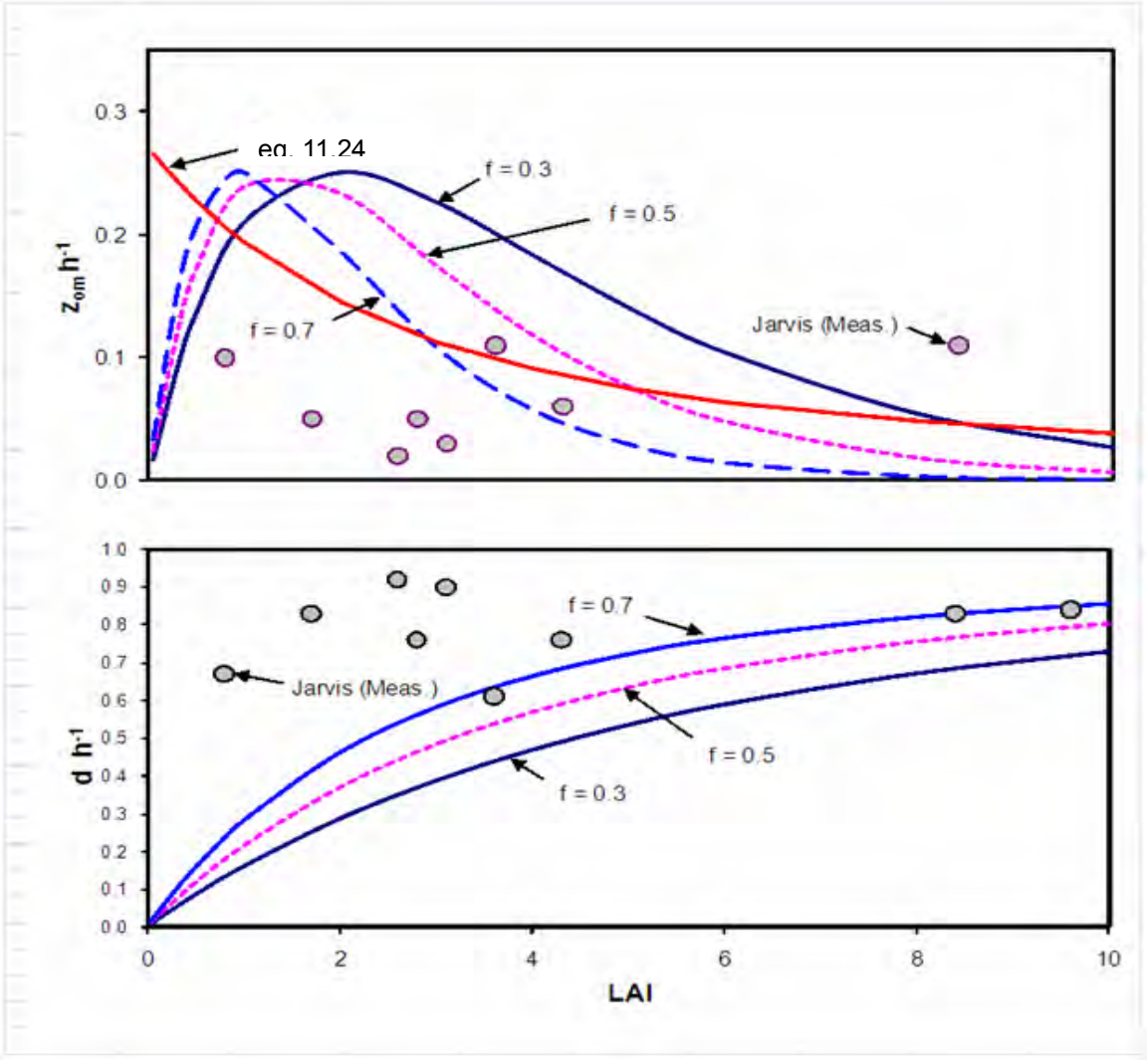

Fig. 11.3 Ratios of z_{om} /h and d/h computed using eq. 11.28 and 11.29 by Perrier (1982), and z_{om} /h estimated using eq. 11.24 with $\sigma = 0.27$ and with d estimated using eq. 11.29 with $f = 0.7$. Symbols represent measurements by Jarvis (1976) for coniferous forests. Source: Data from Jarvis (1996).

As an example of application of eq. 11.23, Lettau (1969) estimated s and S for 0.1-m clipped fescue grass cover as 4 cm^2 and 16 cm^2, so that eq. 11.23 estimated $z_{om} = 0.013$ m. Eq. 11.21 estimates $z_{om} = 0.012$ m for 0.1-m grass cover, which is equivalent. For dense, full cover alfalfa, where $h^* = 0.3$ m, silhouette area, s, of the upper portion of a stem may be 60 cm^2 and ground area per stem, S, may be 100 cm^2, z_{om} is estimated by eq. 11.23 to be 0.09 m. This indicates that eq. 11.23 may apply best to sparse vegetation (Lettau 1969).

Example values for z_{om} and ratios of z_{om}/h and d/h reported in the literature from various sources are listed in table 11.1. These are general values and are typical for various types of vegetation.

Research has shown that for many crops, d and z_{om} can vary considerably with wind speed. Szeicz et al. (1973) found z_{om} to range from under 0.01 m at 1.5 m s^{-1} to 0.07 m at 5 m s^{-1} for a crop of sorghum. The zero-plane displacement, d, of flexible crops is particularly susceptible to

varying wind speeds. In the PM method the estimate of aerodynamic resistance, r_a, is less sensitive to d when wind, T, and e measurements are taken at elevations that are greater than twice the crop height.

TABLE 11.1 Examples of Roughness Lengths for Various Surfaces and Associated Ratios of z_{om} /h (primary source is Brutsaert 1982)

Surface Description	z_{om}, m	z_{om} / h	d/h
Mud flats, ice	0.00001		
Smooth airport runway	0.00002		
Large water surface	0.0001 - 0.0006		
Grass lawn (h = 0.01m)	0.01	0.1	
Grass at airport	0.0045		
Prairie grass	0.00665		
0.075 m artificial grass	0.01	0.13	
0.1 m, thick grass	0.023	0.23	
0.12 m reference grass standard[0]	0.015	0.12	
0.5 m, thin grass	0.05	0.1	
0.18 m wheat stubble	0.024	0.14	
grass, scattered bushes	0.04		
1-2 m vegetation, Cape Canaveral	0.2	0.13	
10-15 m trees, Cape Canaveral	0.4 - 0.7	0.04	
Deciduous Trees[1]	0.015, 0.2, 1.0		
Orchards[1]	0.015, 0.2, 0.3		
Scotts Pine *Pinus sylvestris* (h = 18 m)[2]		0.069	0.69
Lodgepole Pine *Pinus Contorta* (h = 15 m, 4 m tree spacing)[3]	1.0	0.067	
Coniferous forests, general (h = 10 - 28 m)[4]		0.02 – 0.16 (mean = 0.07)	0.67 – 0.68
27 m eucalyptus[5]	1.9 - 4.1	0.07 - 0.15	
Savannah scrub (25% trees, 65% dry grass, 10% burnt grass, sand)	0.4		
Wyoming big sagebrush *Artemisia Tridentata* (h = 0.8 m)[3]	0.05 m	0.06	
Cotton (0.4 - 1.2 m)[6]	0.03 - 0.13	0.10	
Snap Beans (0.1 - 0.6 m)[7]	0.05 - 0.2	0.08 - 0.5 (mean = 0.13)	
Maize (0.2 - 2 m)[8]	0.01-0.14	0.065	
Impervious Urban[9]	1.0		
Bare Rock, Bare Soil[9]	0.005		

[0] FAO-56; [1] MORECS values by Thompson et al. (1981) for defoliated trees, trees at leaf emergence, and trees at full leaf, respectively; [2] de Bruin and Moore (1985); [3] Zhao, W. and R.Allen, 2013, Univ. Idaho, via sonic anemometer; [4] Jarvis et al. (1976); [5] Leuning and Attiwill (1978); [6] Pieri and Fuchs (1990); [7] Allen et al. (1995); [8] Jacobs et al. (1989); and [9] MORECS value by Thompson et al. (1981). All others are from Brutsaert (1982).

Lengths of Scalars. In the single-layer Penman-Monteith application, the 'bulk' aerodynamic resistance, r_{ah}, represents the total resistance between the heat and vapor exchange surfaces and a reference height, z, some vertical distance above the surface. The integration of r_{ah} begins at the roughness lengths for sensible heat and vapor transfer, z_{oh} or z_{ov}. In multilayer resistance-based applications (fig. 11.1 and 11.2), additional in-canopy boundary layer resistances are employed that use eddy diffusion decay techniques without the need for z_{oh} or z_{ov}. Generally, z_{oh} and z_{ov} used in calculating r_{ah} have values less than z_{om} due to effects of bluff body transfer (pressure effects) on momentum transfer that impact the value of z_{om} but do not significantly impact values for z_{oh} and z_{ov}, for example eq. 11.9 – 11.16. Brutsaert (1982) suggested that z_{oh} and z_{ov} can range from values slightly greater than z_{om} for aerodynamically smooth surfaces, e.g., smooth soil or water, to z_{oh}/z_{om} and z_{ov}/z_{om} ratios of 1/7 to 1/12 for permeable-rough surfaces, a category into which most vegetated surfaces fall. In this manual, we suggest using:

$$z_{oh} = z_{ov} = 0.1 z_{om} \tag{11.30}$$

in bulk r_{ah} calculations for agricultural surfaces having relatively dense vegetation. The ratios z_{oh}/z_{om} and z_{ov}/z_{om} are affected to some degree by the shape of the surface roughness elements and Reynold's number (Garratt and Hicks 1973). Thom (1972), Garratt and Hicks (1973), Brutsaert (1982), and Verma (1989) discuss in-depth the relationship between z_{oh}, z_{ov} and z_{om}, where the sublayer Stanton number B^{-1} is used to represent the differences among the roughness lengths. Basically, the ratio z_{oh}/z_{om} decreases to very small values with increasing wind speed and roughness for nonpermeable rough surfaces such as plowed soil and rigid vegetation with large leaves such as beets, cabbage, or vineyards (Brutsaert 1982; Verma 1989), where momentum is transferred to the surface much more efficiently than heat and vapor due to pressure forces, whereas, z_{oh}/z_{om} is relatively constant for surfaces or vegetation having more porous or fibrous roughness elements, such as for grass, corn, and forests (Brutsaert 1982). For vegetation having sparse canopy, the ratio z_{oh}/z_{om} is highly impacted by the mean source heights of heat and vapor in the canopy and the mean sink height for momentum (Qualls and Brutsaert 1996).

According to data summarized by Garratt and Hicks (1973), the following mean values can be used for general estimates of z_{oh}/z_{om} under conditions of neutral stability: short grass and agricultural crops: z_{oh}/z_{om} = 0.08 to 0.14 (mean = 0.10); pine forests: z_{oh}/z_{om} = 0.35; lake evaporation: z_{oh}/z_{om} = 1. Other observations have included heterogeneous forests with 1-m tall grass understory where z_{oh}/z_{om} = 0.08 (Garratt 1978b). Ratios of z_{ov}/z_{om} can be expected to be similar.

Additional work on z_{oh}/z_{om} ratios has been conducted by Zhao et al. (2008) and simulation of z_{oh}/z_{om} ratios was done by Lhomme et al. (1997). The NCAR Weather Research and Forecasting (WRF) Model's Noah land process submodel uses a formulation for z_{oh}/z_{om} that considers the Reynold's number as well as fractional density of vegetation (Zeng and Wang 2007):

$$z_{oh} / z_{om} = \exp\left(0.2 \left(1 - f\right)^2 R_e^{0.5}\right) \tag{11.31}$$

where f is fraction of green vegetation cover, and the Reynold's number is dimensionless:

$$R_e = \frac{(u^*)z_{om}}{\upsilon} \tag{11.32}$$

where $u*$ is friction velocity, m s^{-1} (eq. 7.23), and υ is kinematic viscosity, (m^2 s^{-1}).

Determinations from Wind Profile Measurements

Roughness Lengths. Roughness length for momentum transfer, z_{om}, can generally be determined for unfamiliar surfaces from wind profile measurements. For most measurements, a recommended minimum of four anemometers are placed above the vegetation canopy with increased spacing between instruments with height in order to better sample the wind profile. Although two anemometers are sufficient to determine z_{om} using the following equation 11.33, measurements with four anemometers are recommended to confirm adherence of the wind profile to a logarithmic relationship during neutral periods and to verify integrity of the anemometers used to solve for z_{om} (Monteith and Unsworth 1990). Eq. 7.21 of Chapter 7 expresses $u*$ from wind speed measured at z height, u_z, z_{om}, d and integrated stability correction function $\psi_{sm(z/L)}$ for momentum transfer:

$$u* = \frac{k\,u_z}{\ln\left[\frac{z - d}{z_{om}}\right] - \psi_{sm(z/L)}} \tag{7.24}$$

where k is the von Karman constant. By conservation of momentum, u* can be assumed to be constant with z, so that Eq. 7.24 can be expressed as:

$$u* = \frac{k\ u_{z1}}{ln\ \frac{z_1 - d}{z_{om}} - \psi_{sm(z_1/L)}} = \frac{k\ u_{z2}}{ln\ \frac{z_2 - d}{z_{om}} - \psi_{sm(z_2/L)}} \tag{7.24b}$$

If application of eq. 7.24b is limited to nearly neutral conditions so that $\psi_{sm(z/L)}$ can be assumed to be zero, the equation can be solved for z_{om}:

$$z_{om} = exp\left(\frac{u_2\,ln(z_1 - d) - u_1\,ln(z_2 - d)}{u_2 - u_1}\right) \tag{11.33}$$

where u_2 and u_1 are wind speeds at z_2 and z_1 elevations above the ground surface and d is the zero plane displacement height. z_{om} in eq. 11.33 has the same units as z, and d, which is normally m.

Generally, z_{om} is determined from wind speed profile data for neutral conditions, only, as stability or instability of the boundary layer profile will influence the wind profile shape. Neutral conditions can be verified by computing a discrete Richardson number, Ri, between the two sensor elevations as:

$$Ri = \frac{g\left[T_2 - T_1 + \Gamma(z_2 - z_1)\right](z_2 - z_1)}{0.5(T_2 + T_1)(u_2 - u_1)^2} \tag{11.34}$$

where g is in m s^{-2} , T_1 and T_2 are absolute air temperatures, K, at heights z_1 and z_2 (m) above the surface, and Γ is the dry adiabatic lapse rate (0.01 K m^{-1}). Values of T and u should be based on mean profile data, preferably involving periods of 30 minutes or less. Γ is usually ignored for investigations near the surface where (z_2 - z_1) is only a distance of a meter or two.

Generally, a range of $-0.01 < Ri < 0.01$ is used to indicate neutral buoyancy (Monteith and Unsworth 1990). In other words, the temperature profile should be nearly constant with z so that H and buoyancy are nearly zero. An alternative to using Ri is to calculate the Monin-Obukhov stability length, L, given in Eq. 7.15. Near-neutrality can be assumed to exist when $-0.2 < z_2/L < 0.2$. Measurements of u and T for profile analyses are normally averaged over periods of 30 minutes or less.

Values for z_{om} can also be computed by inverting eq. 7.24 for friction velocity, u_*, where measurements for u_* are derived from high frequency measurements by 3-dimensional sonic anemometers. These systems are becoming relatively commonplace and relatively low cost. The integrated stability correction function $\psi_{sm(z/L)}$ for momentum transfer can be solved using equations in chapter 7.

Garrett (1980) and Cellier and Brunet (1992) presented conclusive evidence that suggests that wind profile measurements must be made at elevations that are at least 2 to 3 times the canopy height or 3 times individual plant or tree spacing, whichever is greater, to obtain valid results from eq. 11.33. Jacobs et al. (1989) recommended placing instruments above the $d + 10$ z_{om} elevation. At elevations below those recommended, wind, temperature and vapor density profiles deviate from the classic Monin-Obukhov profile shapes and application of eq. 11.33 may underestimate the value for z_{om}. The minimum elevation applies to the lowest anemometer setting, so that sensor masts placed over tall vegetation must be quite high. The thickness of the "roughness sublayer" in which this problem occurs is greater for sparse canopies such as rangeland, arid land forests and sparsely planted orchards so that the potential for having wind profile measurements within the roughness sublayer increases with decreased vegetation density. For more detailed information concerning this precaution, the reader can consult Cellier and Brunet (1992), Thom et al. (1975), Raupach (1979, 1994), Garratt (1980, 1992), Cellier (1986), van de Griend and van Boxel (1989), and Raupach et al. (1991, 1996).

Zero-Plane Displacement. When three or more measurements of wind speed are available, zero plane displacement, d, can be obtained under neutral stability conditions by combining eq. 11.33 at two pairs of heights following Monteith and Unsworth (1990):

$$ln(z_{om}) = \frac{u_2\, ln(z_1 - d) - u_1\, ln(z_2 - d)}{u_2 - u_1} = \frac{u_3\, ln(z_1 - d) - u_1\, ln(z_3 - d)}{u_3 - u_1} \tag{11.33b}$$

so that:

$$\frac{(u_2 - u_1)}{(u_3 - u_1)} = \frac{u_2\, ln(z_1 - d) - u_1\, ln(z_2 - d)}{u_3\, ln(z_1 - d) - u_1\, ln(z_3 - d)} \tag{11.35}$$

where u_1, u_2, and u_3 are wind speeds at z_1, z_2, and z_3 heights and z and d have the same units. Eq. 11.35 is solved implicitly using a Newton-secant or other solution method. Zhao et al (2008) described an iterative method to solve for both z_{om} and d. Again, the same precautions in minimum height of anemometer placement must be exercised for determination of d as are followed for z_{om}.

11.7 Bulk Surface (Stomatal) Resistance

Resistance and Leaf Area

Factors Affecting Resistance. Stomatal resistance of leaves is a dynamic parameter which changes with sunlight illumination, vapor pressure deficit, leaf temperature, and soil water potential (Jarvis 1976; Stewart 1989; Price and Black 1989; Stewart and Verma 1992, Kelliher et al. 1995). For a single-layer model as the PM equation, the bulk surface resistance, r_s, represents the integration of resistance to vapor movement through leaf stomates, vapor diffusion from soil, and vapor transport within the canopy. For sparse crops, an integrated value for r_s is computed by considering resistances for exposed soil and vegetation in parallel, as is discussed in a later section. The single-layer PM equation should be considered as only an approximate estimate for *ET* from sparse vegetation or from crops during early development when the leaf area index is less than 1.0 due to complexities in energy exchange between the soil and canopy. In these situations, the user should consider using multi-layered equations (described earlier in sections 11.2-11.5) or even the simpler, but potentially more robust K_c ET_{ref} approach of chapter 10.

For vegetation where $LAI > 1$, the effect of soil evaporation is generally low relative to transpiration and r_s is dominated by the vegetation. Under these conditions, r_s can usually be estimated using eq. 8.9 with effective leaf area, LAI_{eff}, estimated from eq. 8.10 or eq. 8.11. For dense canopies, LAI_{eff} is the upper sunlit portion of the canopy where most heat and vapor transport activity occurs. Eq. 8.10 has been used by Szeicz and Long (1969) and Allen et al. (1989, 1998) to estimate LAI_{eff} for dense pine forest canopies, for wheat, and for grass and alfalfa reference surfaces. Eq. 8.11 may serve as a more universal estimate of LAI_{eff} for *LAI* ranging from sparse to very dense (Ben-Mehrez et al. 1992).

Parameter r_l in eq. 8.9 is average stomatal resistance for a single LAI layer ($LAI = 1$) characteristic to ambient soil water and other environmental factors such as R_s, *VPD*, and *T*. Monteith (1965, 1981) and Sharma (1985) suggested a value of $r_l = 100$ s m^{-1} for many agricultural crops under mean daytime conditions. Allen et al. (1989) and Jensen et al. (1990) found $r_l = 100$ s m^{-1} to approximate well for cool-season grass and alfalfa references for 24-hour calculation time steps. Valle et al. (1985) measured average values of $r_l = 120$ s m^{-1} for soybeans under ambient conditions. ASCE-EWRI (2005) and Allen et al. (2005) suggested $r_l = 70$ s m^{-1} for hourly and shorter periods for well watered grass and alfalfa references.

When stomatal conductance reducing functions, *g(env.)*, introduced in a later section, are employed, then r_l can be estimated as $r_l = r_{l_{min}} / g(env.)$, where $r_{l_{min}}$ is a minimum or unconstrained r_l when all environmental parameters are at optimum levels ($g(env.) = 1$), and where *g(env.)* is the composite conductance reducing factor for various environmental parameters, introduced in a later section. For most vegetation, r_l is about 1.5 to 3 times the value for $r_{l_{min}}$ since R_s, *VPD* and *T* are often at lower or higher levels than optimum for full stomatal opening (Kelliher et al. 1995).

Values for r_l for natural (nonagricultural) vegetation are likely to be substantially higher than those for agricultural crops due to selective breeding of the latter to maximize photosynthesis and biomass production. Some values for r_l in the literature are greater than the 100 s m^{-1} recommended here for agricultural crops because the value for r_l used here is intended to be congruent with the use of effective LAI_{eff} as described in Eq. 8.9. Leaf resistance is generally greater for trees than for agricultural crops. In conifers, stomatal pores are usually located at the bottom of an indentation in the leaf epidermis which is filled with wax tubes, resulting in higher r_l relative to nonconifers. The larger r_l for conifers enables trees to avoid rapid dehydration due to generally large LAI and small aerodynamic resistance r_a. Jarvis et al. (1976) summarized reported measurements of r_l for various types of conifers. Minimum values of r_l ranged from 120 to 300 s m^{-1} for new needles of most conifer types to 1100 to 1400 s m^{-1} for 3 and 4 year old needles (table 11.2). Jarvis et al. (1976) calculated general ratios of r_s/r_a between 20 to 40 for Sitka spruce and 20 to 70 for Scotts pine. Stewart (1988) reported similar values. These ratios contrast with ratios of r_s/r_a for field crops which are much lower, often between 1 and 2 (Monteith 1965).

Irmak et al. (2008b) scaled measured and simulated r_l to bulk r_s using photon flux densities on individual leaves in a maize canopy with relatively good comparison with r_s retrieved by inverting the PM equation using ET measured by Bowen Ratio. Stability correction was not utilized in the calculation of aerodynamic resistance so some bias in retrieved r_l likely existed. That study did document that effectiveness of total leaf area of a dense canopy changes with leaf area and with sunlight intensity.

TABLE 11.2 Typical Values for the Stomatal Resistance per Unit Leaf Area, r_l, and Bulk Stomatal Resistance, r_s, for Various Canopy Types. Parameters $r_{l_{min}}$ and $r_{s_{min}}$ are minimum daytime values[a] with $g(env.) = 1$. Source: Data from Garratt (1992) and other sources.

Canopy Type	r_l s m^{-1}	$r_{l_{min}}$ s m^{-1}	r_s s m^{-1}	$r_{s_{min}}$ s m^{-1}	Reference
Forest					
Tropical			125-150		Shuttleworth (1984)
			80		Shuttleworth (1989)
				50	Dorman and Sellers (1989)
Ficus Benjamin		45			Bailey et al. (1993)
Deciduous:			100-160	60 (LAI = 5)	Verma et al. (1986)
			70-100		Shuttleworth (1989)
				50	Dorman and Sellers (1989)
			100-150		Perrier (1982)
		150			Choudhury and Monteith (1986)
Amazon broadleaf			120	90	Dai et al. (2004)
Aspen	400				Sikka (1993)
Boreal Aspen-hazel nut			65		Blanken and Black (2004)
			100		
Aspen overstory			200		
Hazel nut understory					
Eucalyptus	200-400				Körner et al. (1979)
Maple	400-700	250			Körner et al. (1979)
Poplar	100	60			Bernacchi et al. (2003)
Coniferous:					
Pinus resinosa (Pine)					Waggoner and Turner (1971), as cited by Jarvis et al. (1976)
current year needles[b]		310			
1 year old		430			
2 year old		860			
3 year old		890			
4 year old		1,100			
Picea sitchansis (Sitka Spruce)					Ludlow and Jarvis (1971) and Neilson et al. (1972) as cited by Jarvis et al. (1976)
current year needles[b]		120			
1 year old		480			
2 year old		650			

3 year old		1,400			Milne (1979)
Mean		300	80	40 (LAI = 12)	
Pseudotsuga menziesii (Douglas Fir)		120-300			Jarvis et al. (1976)
			35		Humphreys et al. (2002)
	200	160		70	Dekker et al. (2000)
General conifers			90-150		Jarvis et al. (1976)
			70-100	56	Shuttleworth (1989)
				43	Noilhan and Planton (1989)
				60	Dorman and Sellers (1989)
				30-60	Kelliher et al. (1993)
			200-300		Perrier (1982)
			100	30	Shuttleworth (1989)
Other					
Savanah			100		Garratt (1978b)
Shrubs		240			Sikka (1993)
Sagebrush (*Artemisia tridentata*)	1000				Körner et al. (1979)
Mesophytes[c]	100-200				Gates (1980)
		150-500			Cowan and Milthorpe (1968)
Xerophytes[d]		800-2000			Cowan and Milthorpe (1968)
Grassland				40	Dorman and Sellers (1989)
		30-50		40-50 (LAI=1.3)	Kelliher et al. (1993)
Kansas Prairie				40 (LAI = 3)	Stewart and Verma (1992)
big bluestem (*Andropogon geradii*)					Stewart and Gay (1989)
Indian grass (*Sorghastrum nutrans*)				65 (LAI = 1.3)	
Purple false brome (*Brachypodium distachyon*)			90		Ryu et al. (2008)
Smooth cat's ear (*Hypochaeris glabra*)					
Clover, lesser Hop Trefoil (*Trifolium dubium*)					
temperate			100		Perrier (1982)
subtropical			200		
Crops, General	50-320				Slatyer (1967)
			40-130		Perrier (1982)

				20-75	Sellers and Dorman (1987)
				20-150	Noilhan and Planton (1989)
			30-35	30	Dorman and Sellers (1989)
	100				Monteith (1965), Sharma (1985)
Grain Sorghum	200	150	100-140 (LAI=2)		Szeicz et al (1973)
		150			Choudhury and Monteith (1986)
Snapbeans (*Phaseolus vulgaris*)		130			Choudhury and Monteith (1986)
Soybeans	120				Valle et al. (1985)
				50 (LAI=3.4)	Grant and Baldocchi (1992)
Maize		70	80	40	McGinn and King (1990)
		70		25 (LAI=3.5)	Jacobs et al. (1989)
		70			Rochette et al. (1991)
	160				Körner et al. (1979)
Barley	150-250 (young to old)		45	40	Szeicz and Long (1969)
			70		Perrier (1982)
Wheat			50	30	Hatfield (1985)
			60		Perrier (1982)
		50			Choudhury and Idso (1985)
Alfalfa	80	50			Cowan and Milthorpe (1968)
			40		Perrier (1982)
			30 (day-time)	20	McGinn and King (1990)
			30 (daytime)		Allen et al. (1989); ASCE-EWRI (2005)
Cotton		20			Stanhill (1976)
Sugar Beets		50			Cowan and Milthorpe (1968)
	100				Körner et al. (1979)
Citrus			250		Perrier (1982)
0.15 m Clipped grass	100-150		80-120	70	Szeicz and Long (1969)
0.10 to 0.12 Irrig., Clipped Grass	75	40	40 - 60	25 – 30	Pruitt (1994, Personal Communication)
			50		Allen et al. (2005); ASCE-EWRI (2005)

[a] $r_{l_{min}}$ and $r_{s_{min}}$ represent minimum daytime values of r_l and r_s which occur when all environmental variables are optimum. For example, full levels of irradiance, low vapor pressure

deficit, optimum leaf temperature, etc. These levels will occur in dense canopies only for sunlit leaves and only when all other variables are optimum. $r_{l_{min}}$ and $r_{s_{min}}$ should only be used in conjunction with the g() functions.

[b] Current year, 1, 2, 3 and 4 year refer to the age of needles measured.

[c] Mesophytes are tropical and temperate plants needing plentiful water for survival.

[d] Xerophytes are plants structurally adapted for life and growth with a limited water supply.

Estimating Leaf Area. Leaf area indices can often be estimated for various vegetation types as a function of mean plant height, shape and stand density. Due to the wide diversity in canopy structures and leaf design, *LAI* vs. *h* relationships are unique to specific vegetation types. Allen et al. (1989) and ASCE-EWRI (2005) have suggested eq. 8.12 for dense stands of clipped grass and eq. 8.13 for alfalfa. The equation for clipped grass indicates a proportional increase in leaf area with increasing height of grass due to uniform vertical leaf extension with height. This would probably not be the case with nonclipped range or pasture grass where much of the mature plant height may be due to stem and seed head extension rather than leaf extension. Eq. 8.13 for alfalfa suggests an exponentially decreasing rate of increase in *LAI* with increase in *h* as stem extension with less leaf development occurs in maturing plants. Alfalfa is generally grown in densely planted stands so that for *h* greater than approximately 0.2 m, leaf and stem development is essentially one-dimensional (vertical).

For row crops where plants are relatively round and extend similarly in width and height, a quadratic relationship can be employed, such as $LAI = 10\ h^2$ as suggested by Allen et al. (1996) for snap beans (*Phaseolus vulgaris*) planted in 0.6-m rows. Height was limited to $h \leq 0.75$ m.

The following relationships can be derived for maize, cotton, and grass prairie based on data presented by Jacobs et al. (1989), Pieri and Fuchs (1990), and Verma et al. (1992), respectively: for tall maize, $LAI = 1.6\ h$; for cotton, $LAI = 2.5\ h$ for $h \leq 0.4$ m and $LAI = 3.4 + 2.4 \ln(h)$ for $0.4 < h < 1.2$ m; for rainfed grass prairie in Kansas, $LAI = 5\ h$ before leaf senescence. The utility of basing *LAI* on *h* is that *h* is a relatively easy parameter to observe or to collect, and is required for estimating z_{om}. In rangeland and other situations having sparse plant density, plant density may need to be added to *LAI* - *h* relationships as discussed in the following paragraph. Tasumi (2003), using LAI and *h* data from J.L. Wright (USDA-ARS, Kimberly), established a relatively universal, linear relationship between LAI and *h* for potatoes, snap beans, sugar beets, peas, wheat and alfalfa as: $LAI = 6.7\ h$. Field corn had less LAI for the same *h* as other Idaho crops where $LAI = 3\ h$. Estimated LAI was limited to ≤ 6 in all cases for agricultural crops.

Leaf area indices for rangelands, brushlands and forests vary widely depending on grass, shrub or tree density, maturity and type. Rauner (1976) reported total *LAI* for deciduous forests ranging from 4 to about 7. Jarvis et al. (1976) listed *LAI* for ten conifer species based on projected canopy area at midday. The *LAI* per projected tree area (LAI_{pa}) ranged from 2.5 to 4.5 for many pine species and ranged from 8 to 10 for *Picea abies* and *Picea sitchensis* species of spruce. An areal average *LAI* was calculated by Jarvis et al. (1976) as:

$$LAI = LAI_{pa}\ A_s\ S_d \tag{11.36}$$

where LAI_{pa} is the projected area *LAI* (*LAI* based on the shaded ground area during midday), A_s is the midday shaded area per plant (m^2 $plant^{-1}$), and S_d is stand density (plants m^{-2}).

For annual types of vegetation, the increase in *LAI* during the growing season can often be expressed as a function of time or as a function of thermal units, similar to the approach used for

crop coefficients. When *LAI* or *h* functions are expressed in terms of LAI/LAI_{max} and h/h_{max}, respectively, where LAI_{max} is the maximum *LAI* of green leaves during the season and h_{max} is the maximum obtained plant height, the developed functions are more able to transfer to other cultivar types having different values for LAI_{max} and h_{max}.

General Bulk Surface Resistance Values

General Daytime Values. Transpiration increases with increasing *LAI* until nearly complete closure of the canopy. For agricultural crops, maximum transpiration is often attained after *LAI* = 3 (Ritchie 1972; Tanner and Jury 1976; Wright 1982; Sharma 1985). Increases in *LAI* above 3 generally increase *ET* little, depending on canopy structure, as most available energy (radiation and sensible heat) has been converted into λE within the canopy when $LAI > 3$. This provides the rationale behind using eq. 8.10 or eq. 8.11 for estimating LAI_{eff}. In general, the PM equation estimates show little increase in *ET* for $LAI > 3$.

Typical values for r_s and r_l reported in the literature are listed in table 11.2. Additional values for r_s that have been used by the British Meteorological Office rainfall and evaporation calculation system (MORECS) are listed in table 11.3 and mean "green" *LAI* values are listed in table 11.4 (Thompson et al. 1981). Values for r_l in column 1 and r_s in column 3 of table 11.2 represent constrained surface resistance for a unit *LAI* and complete canopies, respectively, and are intended for use in hourly, daily or monthly *ET* calculations where $g(\ )$ functions are not employed. Values for $r_{l_{min}}$ and $r_{s_{min}}$ in table 11.2 represent minimum r_l and r_s where all environmental variables (namely R_s, T, *VPD*, and θ) are at optimum levels and should only be used in conjunction with the $g(\ )$ functions.

The MORECS r_s values in table 11.3 were developed to support direct application of the PM equation across Great Britain on a 6 km grid. Parallel resistance calculations were used to integrate effects of soil evaporation and plant transpiration as discussed in a following section. Calculations in MORECS were made on daily time steps for daylight periods, so that values of r_s in table 11.3 represent general daytime values of r_s. Mean monthly values of r_s listed for grass and riparian vegetation are low during spring months with leaf development and increase late in the growing season as leaves senesce (die off) or go dormant. Additional values for r_l, which were summarized from a wide range of literature sources, can be found in Körner et al. (1979) in addition to table 11.2. Because values for r_l and r_s are typically solved by inversion of ET or AFIB models, values in tables 11.2 and 11.3 can be biased toward the procedure used to determine them.

For hourly or shorter calculation time steps, it may be useful to adjust r_l for levels of R_s, *VPD*, T, and θ as described in a following section. For hydrologic water balance studies, where water balances and *ET* are estimated on daily or longer calculation time steps, mean 24-hour or daytime values for r_s can be used where r_s is estimated as the quotient of mean values for r_l and effective leaf area, with additional adjustment for limited soil water and incidence of wet soil among foliage following rain or irrigation events.

TABLE 11.3 Generalized Daytime Values of Bulk Surface Resistance for Dense Green Cover in Great Britain Having Adequate Soil Water. Source: Data from Thompson et al. (1981).

Type of Cover	r_s, s m^{-1}
Grass and Riparian vegetation	80, 80, 60, 50, 40, 60, 60, 70, 70, 70, 80, 80 (Jan-Dec)
Cereals	40
Potatoes and Sugar Beets	40
Deciduous trees	80
Conifers	70[1]
Upland vegetation	120 Jan-Mar, 100 Apr-Sept, 120 Oct-Dec
Bare soil	100
Water	0

[1] At zero vapor pressure deficit and 20°C and assumed independent of soil surface resistance.

TABLE 11.4 Maximum Leaf Area Indices for Dense Green Cover in Great Britain as used in MORECS. Source: Data from Thompson et al. (1981).

Type of Cover	Green leaf area index
Grass and Riparian vegetation	2.0, 2.0, 3.0, 4.0, 5.0, 5.0 5.0, 5.0, 4.0, 3.0, 2.5, 2.0 (Jan-Dec)
Cereals	5.0
Potatoes	4.0
Sugar beets	4.0
Deciduous trees	6.0
Conifers	6.0

Hourly or Shorter Periods Values. For most vegetation, leaf resistance decreases with increasing irradiance (solar radiation) and may increase with increasing vapor pressure deficit. In addition, leaf resistance increases with decreasing soil water due to partial stomatal closure. Jarvis (1976), Stewart (1988, 1989), Price and Black (1989), Stewart and Verma (1992) and others (Daamen et al. 1998, Ortega-Farias et al. 2005, 2010) have proposed computing bulk surface resistance for short time periods in terms of meteorological variables and soil water deficit. Generally computations are expressed in terms of bulk surface conductance, g_s, which is the reciprocal of r_s ($g_s = 1/ r_s$). Monteith (1995) and Mott and Parkhurst (1991) have suggested that stomata and g_s may respond (decrease) primarily with the transpiration rate itself, rather than vapor pressure deficit. This suggests that plant systems may control maximum water fluxes through the root-stem-leaf systems. However, because potential transpiration is highly controlled by solar radiation, temperature and vapor pressure deficit, a strong correlation is observed between g_s and these parameters and behavior of g_s may be better explained by them.

A widely used surface conductance model proposed by Jarvis (1976) uses a multiplicative means for incorporating the effects of specific environmental factors and is commonly used with

both the single-layer and multi-layer Penman-Monteith models (Zhao et al. 2006). Stewart (1989) expressed the Jarvis function as:

$$g_s = g_{\max}\, g(env.) = g_{\max}\left[g(LAI)\; g(R_s)\; g(VPD)\; g(T)\; g(\theta)\right] \tag{11.37}$$

where g_{max} is the maximum bulk surface conductance when all other functions are not limiting. Functions $g(LAI)$, $g(R_s)$, $g(VPD)$, $g(T)$ and $g(\theta)$ represent reducing functions for leaf area, solar radiation, vapor pressure deficit, air temperature, and soil water, respectively. Variable $g(env.)$ represents the multiplicative effect of the individual functions. All reducing functions in eq. 11.37 are limited by $0 \le g(\,) \le 1$, including the cumulative $g(env.)$. The form of eq. 11.37 assumes that each environmental parameter will independently reduce g_s (increase r_s), with the reduction accelerated by changes in other parameters.

Price and Black (1989) presented an alternative equation to eq. 11.37, where they found better agreement with measured data when the reduction in g_s was based on only the most limiting environmental parameter. The equation suggested by Price and Black is:

$$g_s = g_{\max}\, g(env.) = g_{\max}\left[minimum\big(g(LAI)\; g(R_s)\; g(VPD)\; g(T)\; g(\theta)\big)\right] \tag{11.38}$$

where the $g(\,)$ functions are the same as those defined for eq. 11.37 and are limited to $0 \le g(\,) \le 1$. In the examples provided near the end of this chapter, the form of eq. 11.37 is employed.

When g_{max} is not measured, g_{max} can be estimated as $g\,(LAI_{max\ eff})$, where $LAI_{max\ eff}$ is maximum effective leaf area, estimated using eq. 8.10 or 8.11 and g_l is the maximum stomatal conductance per unit leaf area in the same units as g_{max}. Estimates of g_l can be made from table 11.2, where $g_l = 1/r_{l_{min}}$. In addition, g_{max} can be estimated from tables 11.2 and 11.3 where $g_{max} = 1/r_{s_{min}}$. Values for g_l and g_{max} decrease with leaf age (senescence), as noted in table 11.2 for conifer needles over a multi-year period. Conductances of leaves of annual plants may decrease with time through the growing season (Burrows and Milthorpe 1976), especially if damage from insects, environmental stress (soil water and air temperature), and disease or air pollution occurs.

Forms of reducing functions which have been suggested for use in eq. 11.37 and 11.38 include the following series of equations. For example, for $g(LAI)$ Stewart (1989) proposed:

$$g(LAI) = \frac{LAI_{\,eff}}{LAI_{\max eff}} \tag{11.39}$$

where $LAI_{max\ eff}$ is the maximum value of LAI during the year. The values for LAI_{eff} and $LAI_{max\ eff}$ in eq. 11.39 are "effective" LAI, as defined in eq. 8.10 or 8.11, to account for effects of shading on r_a and r_l within tall, dense canopies and the potential for nonlinearity of LAI_{max} relative to total LAI (eq. 8.11).

For a surface conduction based on solar radiation, $g(R_s)$, Stewart (1988, 1989) proposed:

$$g(R_s) = \frac{R_s\,(1000 + K_R)}{1000(R_s + K_R)} \tag{11.40}$$

where R_s is global short wave radiation, W m^{-2}, and K_R is an empirical factor ranging from 40 to 100 W m^{-2} for Scotts pine (*Pinus Sylvestris*) (Stewart 1988). Zhao et al. (2006) used K_R = 400 W m^{-2} for agricultural crops. The estimate for $g(R_S)$ reaches 0.8 at R_S = 130, 270, and 530 W m^{-2} for values of K_R = 40, 100 and 400 W m^{-2}. Therefore, a higher value for K_R indicates increasingly higher levels of R_S required to fully open stomates.

Price and Black (1989) proposed:

$$g(R_s) = 1 - e^{-0.003 R_s} \tag{11.41}$$

for a 22 year old stand of Douglas fir (*Pseudotsuga Menziesii*) where R_s is in W m^{-2}.

Stewart (1988, 1989) proposed a function for predicting effects of specific humidity deficit on $g(\,)$, which in terms of vapor pressure deficit is expressed as:

$$g(VPD) = 1 - K_{VPD} VPD \qquad \text{for } 0 < VPD < VPD_c \tag{11.42}$$

$$g(VPD) = 1 - K_{VPD} VPD_c \qquad \text{for VPD} \geq \text{VPD}_c \tag{11.43}$$

with K_{VPD} = 0.50 kPa^{-1} and VPD_c, a threshold vapor pressure deficit, = 1.5 kPa for Scotts Pine. Stewart and Gay (1989) found K_{VPD} = 0.12 to 0.19 kPa^{-1} for rainfed grass prairie in Kansas. Zhao et al. (2006) used K_{VPD} = 0.41 for 'short' vegetation and K_{VPD} = 0.24 kPa^{-1} for 'tall' vegetation in applications to the Mekong River basin. Price and Black (1989) proposed:

$$g(VPD) = 2.24\, e^{(-1.6 VPD^{0.45})} \tag{11.44}$$

for Douglas fir, where $g(VPD) \leq 1$. Kelliher et al. (1993) proposed a means for computing *VPD* at the leaf surface, which eliminates effects of r_a on the decoupling of the $g(VPD)$ vs. *VPD* relationships which are based on *VPD* computed above the canopy. These adjustments can improve the consistency and transferability of the above *VPD* relationships (Blanken and Black 2004).

For air temperature Stewart (1988, 1989) proposed a relationship after Jarvis (1976):

$$g(T) = \frac{(T - T_L)(T_H - T)^a}{(K_T - T_L)(T_H - K_T)^a} \tag{11.45}$$

where

$$a = \frac{(T_H - K_T)}{(K_T - T_L)} \tag{11.46}$$

and T is air temperature, °C, T_L and T_H represent lower and upper limits of stomatal activity, where T_L was taken as 0°C and T_H as 40°C by Stewart (1988) for a Scotts pine forest, and K_T is an empirical "optimum" conductance temperature fitted from field data. K_T ranged from 17 to 19 °C for Scotts pine. Articles by Ritchie and NeSmith (1991) and Norman and Arkebauer (1991) suggest values of T_L, K_T, and T_H equal to about 0, 25, and 40°C for wheat, 12, 35, and 48°C for corn and 5, 28, and 46°C for soybeans. Information in McArthur et al. (1975) suggests values of

16, 27, and 35°C for cotton. Noilhan and Planton (1989) published alternative formulations for $g(R_s)$, $g(VPD)$, $g(T)$ and $g(\theta)$.

Conductance functions ($g_s = 1/r_s$) based on soil water, θ, are generally used in hydrologic studies as surrogates for more direct and perhaps accurate functions based on leaf water potential or soil water potential. The surrogate $g(\theta)$ functions are used since estimates of θ are easily made available from soil water balance calculations, whereas, leaf water and soil water potentials must be measured or inferred from soil characteristic curves and plant models. For operational *ET* estimates, $g(\theta)$ are adequate for predicting the reduction in *ET* with reduction in soil water availability.

For the effect of decreasing soil water, three primary functions are recommended. The first is a function similar to that used by Stewart (1988), which is of the form:

$$g(\theta) = 1 - e^{-K_\theta \theta_e} \tag{11.47}$$

where K_θ is an empirical factor equal to about 6.7 for Scotts Pine. A second form of the function is by Stewart and Verma (1992):

$$g(\theta) = \frac{1 - e^{-K_\theta \theta_e}}{1 - e^{-K_\theta}} \tag{11.48}$$

where K_θ ranged from 0.25 to 0.12 for grass prairie. Variable θ_e in eq. 11.47 and 11.48 represents the effective fraction of available soil water, calculated as:

$$\theta_e = \frac{\theta - \theta_{wp}}{\theta_{fc} - \theta_{wp}} \tag{11.49}$$

where θ is the mean volumetric soil water in the root zone, $m^3\ m^{-3}$, θ_{wp} is the mean volumetric soil water at wilting point or the lower limit of soil water extraction by plant roots, $m^3\ m^{-3}$ (table 7.1), and θ_{fc} is the mean volumetric soil water at field capacity or the drained upper limit, $m^3\ m^{-3}$ (table 7.1).

The third $g(\theta)$ function is a sinusoidal relationship (Allen et al.1996, ;Hatfield and Allen 1996):

$$g(\theta) = K_{sf}\,\theta_e - \frac{\sin(2\pi\theta_e)}{2\pi} \tag{11.50}$$

where $g(\theta) \leq 1$, and θ_e is defined as in eq. 11.49. K_{sf} is an empirical "tenacity" factor ($K_{sf} \geq 1$) which describes the ability of plants to extract soil water before any reduction in $g(\theta)$. K_{sf} ranges from 1 for sensitive plants to 1.5 for moderately sensitive plants to 3 for insensitive (tenacious) plants. The value for $g(\theta)$ from eq. 11.50 must be limited to less than or equal to 1 during computations.

Eq. 11.50 predicts values for $g(\theta)$ which reduce slowly from 1 at high levels of θ_e, reaching maximum rates of reduction near $\theta_e = 0.5$, and which approach 0 when θ_e is approximately 0.2

(fig. 11.4). This type of response is realistic, as most plants leave stomates nearly wide open at high levels of θ_e (all other environmental factors at optimum) to maximize transpiration and photosynthesis, but close stomates almost completely before θ_e approaches θ_{wp}, and then "hold on" for sometimes long periods of low θ_e, transpiring at low subsistence rates controlled by diffusion through nearly closed stomates and through the leaf epiderm (Turner 1979; Jones 1979; Burrows and Milthorpe 1976). In some situations, the user may wish to reduce the value for K_{sf} towards 1.0 during periods having high ET rates to reflect difficulty of low soil hydraulic conductivity in supplying high ET rates. Sene (1996) used a direct exponential equation for soil surface resistance as $r_{sse} = 20\ (\theta/\ \theta_s)^{-2.3}$, s m^{-1}, for bare soil under a sparse grape canopy in Spain, where θ and θ_s are water content and saturation water content of the upper few cm of soil. Calvet et al. (1998) and Ortega-Farias et al. (2010) set $g(\theta) = \theta_e$.

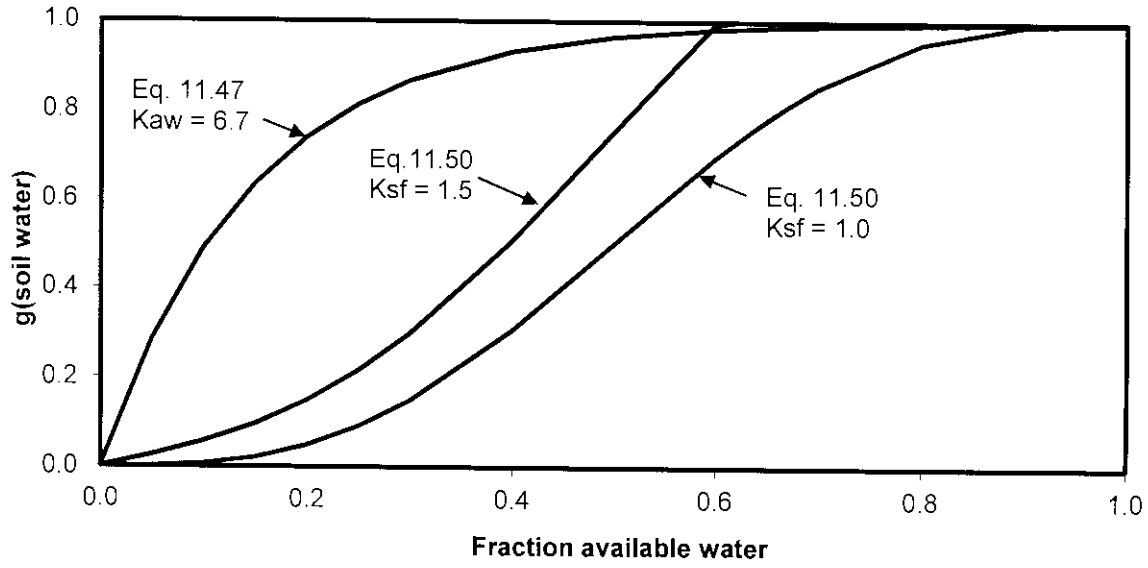

Fig. 11.4. Surface conduction functions for available soil water based on eq. 11.47 and 11.50 (K_{aw} is the same as K_θ).

The characteristics of eqs. 11.47 to 11.50 do not conform to that for the K_s function used in the crop coefficient approach (eq. 10.4 and 10.6), since g_s can reduce (and r_s increase) by nearly 40% in many agricultural situations before significant reductions in λE, as estimated by the PM equation occur. Effects of applying eq. 11.47 to 11.50 in a daily soil water balance are illustrated in a following section.

Applications of both approaches for reducing ET (g_s vs. θ and K_s vs. θ) are conservative, in that they are both based on a soil water balance. Therefore, errors in over or underestimating g_s or K_s will generally cause smaller relative error in estimated ET_a over long periods in low rainfall areas, where generally all precipitation is evaporated during the growing season. Therefore, in an arid or semiarid situation, error in g_s or K_s may affect the estimated timing in ET reduction, but may not significantly affect the total estimate of cumulative ET. This may not be the case in subhumid regions, where soil water deficits occur over short time periods, so that errors in the nature of the $g(\theta)$ and $K_r(\theta)$ functions are more critical.

A final environmental characteristic that can affect the value for g_s is the concentration of carbon dioxide. Some studies have concluded that as global concentrations of CO_2 increase, values for g_s may decrease in partial response to the increasing CO_2 levels (de Bruin and Jacobs 1993; Bernacchi et al. 2007). However, the decreases determined for g_s have generally been small and variable among experiments. Bernacchi et al. (2003) provided a good review of experimental literature on g_s vs CO_2 studies. Jacobs and De Bruin (1997) introduced methods based on plant physiology, where a correlation relationship between the leaf stomatal conductance and the net photosynthetic rate at leaf scale is used to up-scale conductance from a leaf to canopy. The latter method is able to incorporate impacts of CO_2 concentrations on stomatal conductance and thus transpiration, as well as direct effects of photo-synthetically active radiation (PAR) on primary productivity rate, leaf surface temperature and vapor pressure deficit.

Minimum Stomatal Conductance. Utilization of some of the $g(\ )$ functions described in this section can result in $g(\ ) = 0$, notably for eq. 11.39 (for $LAI = 0$), eq. 11.40 and 11.41 (for $R_s = 0$), and eq. 11.45 (for $T \leq T_L$ or $T \geq T_H$). However, $g(\ ) = 0$ implies that total surface conductance, g_s, = 0 so that r_s is infinity. This never occurs in nature (except perhaps in the desert), since all vegetation will have some cuticular conductance (about 0.0003 m s^{-1} per unit *LAI* (Rochette et al. 1991). In addition, a minimum residual g_s (or maximum residual r_s) must be retained to account for evaporation from soil beneath vegetation, for example, by making use of eq. 11.51 presented in the next section. As indicated in a later section, r_s is about 50 s m^{-1} for moist bare soil and exceeds 2000 s m^{-1} for dry soil. Therefore, depending on the soil surface soil water conditions and the amount of transfer of sensible heat and radiation through the vegetation cover to the soil, some residual g_s should be specified even for dense vegetation. In analyzing *ET* data from Davis for grass irrigated six days earlier, Pruitt (1994)[1] found nighttime values for r_s averaging almost 200 s m^{-1}. This was during a 2-h period around midnight, (R_s and $g(R_s) = 0$), and yet with a 5-m s^{-1} wind at 2 m, 20 °C air temperature, a *RH* of 60%, and a *VPD* of 0.95 kPa, *ET* was averaging 0.08 mm h^{-1}. A value of $r_s = 200$ s m^{-1} is also recommended in the ASCE-EWRI (2005) standardization for reference ET during nighttime and is equivalent to a minimum g_s of 0.005 m s^{-1}. That value was used by Pruitt (1994) during nighttime periods whenever the value of g_{max} $g(env.)$ fell below this value. When soil surface water is measured or can be predicted by a simulation model (using a soil surface layer balance or time since wetting), then the minimum value for g_s can be varied to fit the actual soil water conditions.

Applications. Other surface conductance or surface resistance functions have been proposed such as those by Szeicz and Long (1969), Szeicz et al. (1973), Hatfield (1985), and Choudhury (1983, 1989). In general, unique "*K*" coefficients should be determined for *g( )* functions for specific vegetation types. Stewart (1988) demonstrated difficulty in applying some $g(\ )$ coefficients among different years for the same type of vegetation.

Improvements in application of the $g(T)$ and $g(VPD)$ functions can be made when surface temperature and *VPD* at the leaf surface are used rather than *T* and *VPD* at some reference height (Collatz et al. 1991; Dickinson et al. 1991; Blanken and Black 2004), since the leaf responds most directly to environmental conditions at the leaf surface rather than to conditions in the boundary layer above. However, this increases the difficulty and computational complexity

[1] Personal communication.

involved in applying the PM equation, since one must conjunctively and iteratively utilize the energy balance equation (eq. 4.1) along with the PM equation to solve for H and then T_o and $g(T_o)$.

Dickinson et al. (1991) described three regional ET models that employed various forms of the $g(\ )$ functions described in this section. These models were used as components of general circulation models (GCM) to assess effects of climate change. Mission et al. (2004) provided additional testing for pine forests. The Jarvis algorithm (eq. 11.37) has been shown to perform well across many different forest types (Massman and Kaufmann 1991, Bosveld and Bouten 2001), including drought-stressed ecosystems (Running 1994). Reviews of mechanics and processes of stomatal conductance and environmental interactions were given by Allaway and Milthorpe (1976) and Burrows and Milthorpe (1976).

It is recommended that all $g(\ )$ functions that impact the value of g_s be utilized in estimating $g(env.)$, since the absence of any one of the parameters may bias estimates of g_s upward and may result in overestimation of ET. Note that in table 11.2, values for r_l (that represent average $g(env.)$ conditions) are generally 2 to 3 times the values given for $r_{l_{min}}$ for the same type of vegetation. Therefore, one should expect, under normal conditions, that g_s calculated from g_{max} when averaged over all daylight periods (preferably weighted according to ET flux density), to be only about one-half the value of g_{max}, especially in semiarid regions. This should occur when all relevant $g(\ )$ functions are included in the g_s calculation.

An example of use of $g(\ )$ functions is shown in fig. 11.5, where $g(\ )$ functions for R_s, T, and VPD are plotted during a typical summer day in Logan, UT and a spring day in Davis, CA, where ET was near maximum levels and soil water was high. These are the same days and locations used in ET calculations shown in fig. 7.5. Only data past 0800 hours were available for Davis on the 2nd of May.

The $g(R_s)$ function (eq. 11.40) with $K_R = 100$ W m^{-2} estimated $g(R_s)$ near 1 during most daylight periods at both locations, indicating sufficient sunlight to open stomates. Eq. 11.40 was relatively insensitive to the value used for K_R. Air temperature was also at near optimum levels ($g(T) = 1$) during daylight hours except at Logan during midafternoon when temperatures exceeded optimum levels and $g(T)$ decreased to about 0.7 (fig. 11.5a). Values for T_L, K_T and T_H in eq. 11.45 were set at 0, 20, and 40°C for the grass cover at both sites. Low values for $g(T)$ during early morning hours at Logan occurred when T was less than K_T.

The primary reducing function at both Logan and Davis during the days shown in fig. 11.5 was $g(VPD)$ (using eq. 11.42), which reached a minimum level (about 0.55) during afternoon periods at Logan and approached this minimum level during afternoon periods at Davis. Coefficients used in the $g(VPD)$ equation were $K_{VPD} = 0.3$ kPa^{-1} and $VPD_c = 1.5$ kPa. The $K_{VPD} = 0.3$ kPa^{-1} best fit g_s values calculated as residuals from the lysimeter data at both locations and is about half-way between the $K_{VPD} = 0.5$ kPa^{-1} used by Stewart (1988) for Scotts Pine and the $K_{VPD} = 0.12$ to 0.19 kPa^{-1} used by Stewart and Gay (1989) for natural prairie. The VPD_c value was the same as that used by Stewart (1988) for Scotts Pine. The net effect of the conductance reducing functions was to estimate $g(env.)$, using eq. 11.37 with $g(LAI)$ and $g(\theta) = 1$, equal to about 0.4 to 0.7 during daylight periods at Logan (fig. 11.5a) and $g(env.)$ equal to about 0.55 to 0.7 during daylight periods at Davis (fig. 11.5b). The g_{max} at both locations ($g_{max} = 0.07$ m s^{-1} for 0.23 m grass at Logan and $g_{max} = 0.036$ m s^{-1} for 0.12 m grass at Davis) was calculated as g_l LAI_{eff} where $LAI_{eff} = 0.5$ LAI (eq. 8.10). The value for g_l was set equal to the maximum g_l computed as $1/r_{l_{min}}$ where $r_{l_{min}}$ equaled 40 s m^{-1} (table 11.2, last row). This value for $r_{l_{min}}$ compares to a value of $r_l = 75$ s m^{-1} that best fit hourly lysimeter measurements of ET for cool

season grass at five lysimeter sites in the U.S. and Spain when no $g(\ )$ functions were employed (Allen et al. 2005). A minimum value for g_s was set equal to 0.002 m s^{-1} to account for evaporation from moist soil. Calculations of *ET* using the PM equation with r_s computed with and without $g(\ )$ functions are presented for these same two days and locations near the end of this chapter.

Values for g_{max} fitted from *ET* measurements have ranged from 0.018 to 0.024 m s^{-1} for Scotts Pine (Stewart 1988), equivalent to $r_{s_{min}}$ = 40 to 55 s m^{-1}. Price and Black (1989) estimated g_{max} for the Douglas fir forest as 0.022 m s^{-1}, which is equivalent to $r_{s_{min}}$ = 45 s m^{-1}. The *LAI* of the Douglas fir was about 3, while the understory had an *LAI* of about 2. Eq. 8.9 with $r_{l_{min}}$ = 120 s m^{-1} (table 11.2) would estimate $r_{s_{min}}$ = 48 s m^{-1} for LAI_{eff} = 0.5 *LAI* (eq. 8.10), which is in agreement with the measured values.

In application to big bluestem (*Andropogon geradii*) and Indian grass (*Sorghastrum nutrans*) prairie in Kansas, Stewart and Gay (1989) used g_{max} = 0.016 m s^{-1} which is equivalent to $r_{s_{min}}$ = 63 s m^{-1}. Coefficients used by Stewart and Gay in eq. 11.40 ranged from K_R = 190 for *LAI* = 0.5 to K_R = 500 for *LAI* = 1.3.

Constant vs. Variable Resistance. For 24-hour or longer calculation time steps, use of a constant value for r_s in the PM equation is generally adequate, with adjustments made only for low soil water. In some situations, increases in daily values for r_s can be made to account for stomatal closure during periods of low or very high air temperature during early spring, late fall, and midsummer (using eq. 11.45 or similar equation). The value used for r_s for 24-hour calculations should represent mean effects of $g(R_s)$ and $g(VPD)$ during the day. Perrier (1982) concluded that high values of r_s that occurred during the beginning and end of a day did not substantially affect the cumulative *ET* estimates for the whole day due to low energy availability (R_n) and low *VPD* during early and late day periods and due to the occurrence of dew during morning hours in some locations.

Use of a constant value for r_s in the PM equation for calculation time steps of less than 24 hours is often acceptable if the calculations are to be summed over daily or longer periods so that errors in specific hourly estimates are not relevant. Allen et al. (2005) and ASCE-EWRI (2005) suggested r_s = 50 s m^{-1} for the clipped cool season grass reference for hourly and shorter timesteps, and ASCE-EWRI (2005) suggested r_s = 30 s m^{-1} for the tall alfalfa reference for hourly and shorter timesteps. These values compare to r_s = 70 and 45 s m^{-1} for the standardized clipped grass and tall alfalfa references for 24-hour timesteps. Where coefficients for eq. 11.39 - 11.50 are available or can be fitted to field measurements, then the stomatal conductance functions described in eqs. 11.39 - 11.50 can be employed along with $r_{s_{min}}$ for hourly (or shorter) calculation time steps. The impact of using constant r_s without $g(\ )$ functions vs. r_s computed using $g(\ )$ for half-hourly data is demonstrated in the application examples in a following section.

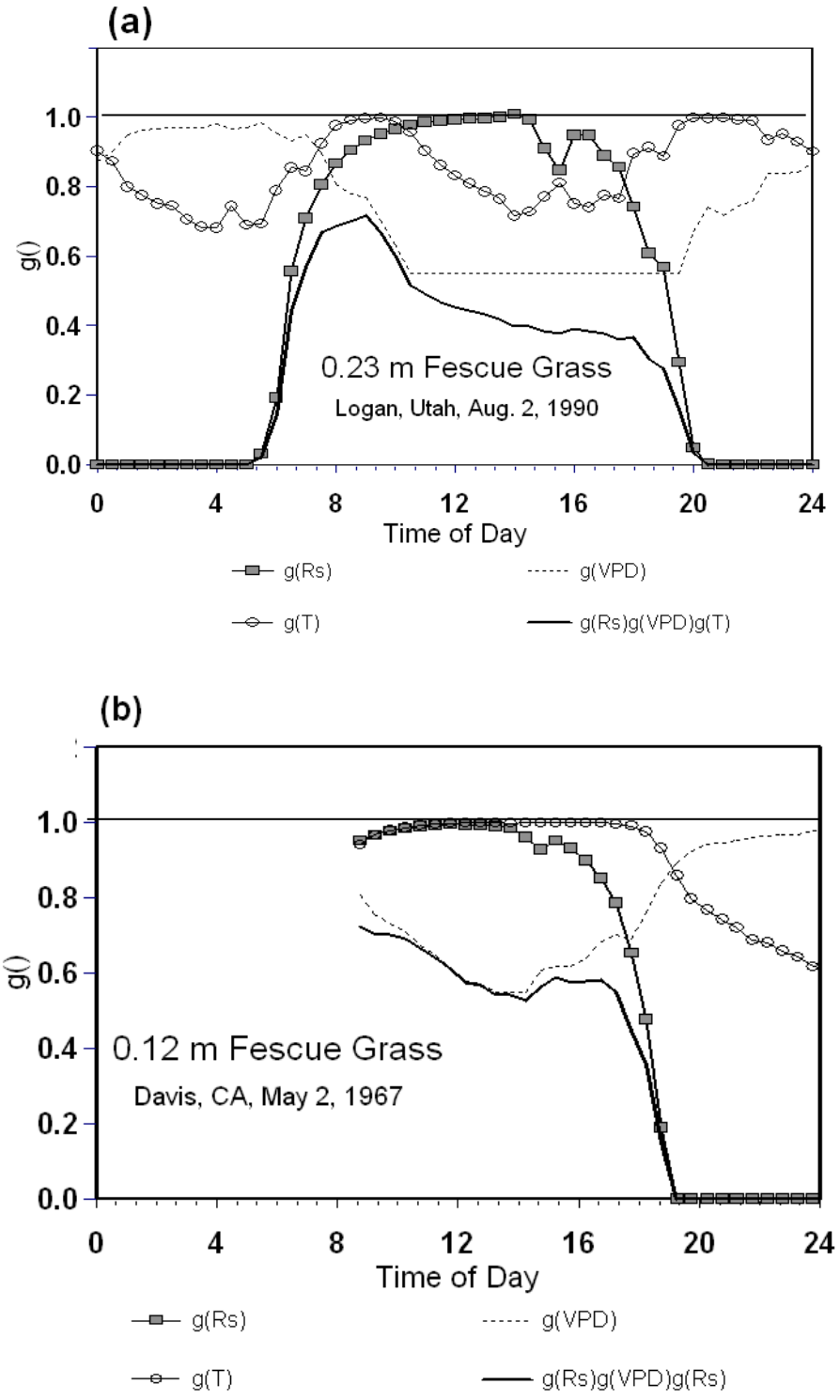

Fig. 11.5 Stomatal conductance functions for a) August 2, 1990 at Logan, UT (R.G. Allen, pers. comm.) and b) for May 2, 1967 at Davis, CA (W.O. Pruitt, pers. comm.) computed using eq. 11.37 - 11.46.

Example of applying the Penman-Monteith to a dry surface

Calculations summarized in table 11.5 illustrate the application of the PM method using weather measurements collected over a dry, rangeland surface where iterative solution of surface temperature, T_s, is used to calculate various parameters used in the PM equation in successive progression. The location of data collection was 4 km west of Balanced Rock, Idaho over dry grass rangeland having an estimated LAI of about 0.5. Standard weather parameters T_a, e_a, u_z and R_s were measured at hourly timesteps in addition to measurement of all four components of R_n (eq. 11.2a) using a four-component radiometer. Surface temperature was retrieved from measured $R_{l\,out}$ for comparison with T_s estimated by inverting eq. 4.32. The AFIB process of eq. 11.2a-f was applied to the standard measurements over a seven day period from Aug. 22 – 28, 2008 for the hourly period spanning 1 pm to 2 pm. Antecedent rainfall to the area was less than 15 mm over the prior two months, so a relatively high value for r_s = 1500 s m^{-1} was assigned. Aerodynamic roughness was assumed to be 0.005 m for the nearly bare soil condition and z_{oh} = 0.0005 m. A value for K_G = 0.15 was used in eq. 11.2b for G during the AFIB solution.

Table 11.5a lists weather measurements as well as R_n, G, T_s, and H calculated using iterative solution of eq. 11.2a-f (the AFIB method). The iteratively determined values for T_s averaged within 1.5ºC of measured T_s indicating reasonable settings of LAI, G, r_s, and z_{om} parameters. Iteratively determined T_s exceeded measured T_a by an average 14ºC, illustrating the large temperature gradients existing between surface and air temperature.

Table 11.5b lists λE based on aerodynamic eq. 11.2c and using T_s from iterative application of eq. 11.2a-f as well as a progression of solutions of the PM equation (eq. 11.1). The first PM solution applied 11.1 following the standardized reference crop application (see footnote of table 11.5b) using Δ, R_n and G calculated using T_a, only, ignoring stability correction. The exception was use of aerodynamic roughness characteristic of the sparse range-grass. The estimate for λE exceeded the λE calculated by the AFIB method by an average of 20%. The second column summarizes application of the PM with replacement of G with an estimate from eq. 11.2b, which is considered to be more realistic for the warm, dry surface than using the $G = 0.1\ R_n$ used in the hourly ET_o method. The replacement G averaged about 60 Wm^{-2} greater than the previous value. Deviation of λE from λE from eq. 11.2c reduced to 10%.

The third column for PM application represents the calculation of λE where T_s is solved iteratively by combining λE from eq. 11.1 with equations for H, G and R_n, and then using T_s to calculate Δ based on both T_a and T_s using eq. 11.3, but where the impact of T_s on G, R_{lout} and $\psi(z/L)$ is ignored. The impact of this approach is to create the greatest error in estimated λE, where λE is overestimated by an average of 34%, ranging from 18 to 51% over the seven day period, as compared to λE from eq. 11.2c. These results indicate that using an estimate for T_s in the calculation for Δ, only, is not sufficient and actually can induce greater error than using strictly T_a only, due to other compensating factors.

The fourth column for PM application represents the calculation of λE with the addition of $\psi(z/L)$ from eq. 7.22-7.26 as well as Δ from T_a and T_s. The addition of $\psi(z/L)$ to r_{ah} reduced the overestimation of λE from 34% to 18%. The fifth column for PM application includes the addition of calculating R_n from eq. 11.2a using R_{lout} based on T_s, along with G calculated from

eq. 11.2b using T_s, and Δ from T_a and T_s, but with $\psi(z/L) = 0$. The use of T_s to calculate $R_{l\ out}$ reduced the estimate for R_n by an average of 120 W m^{-2}, which is a substantial change caused by the increased thermal emission from the warm surface that averaged 14 °C warmer than measured air temperature. The use of the more correct estimate for R_n reduced the difference in λE from the PM equation from λE from eq. 11.2b to about 6%.

Finally, the sixth column in table 11.5b applies the PM equation (eq. 11.1) using all parameters based on iteratively determined T_s. These included R_{lout} (and R_n), G, calculated from T_s, $\psi(z/L)$, and Δ. The complete use of T_s for PM parameters reduced the difference in λE from the PM equation to about 5% lower than λE determined by eq. 11.2b and the AFIB method. The 5% difference is relatively small and stems from the linearization of the calculation for Δ.

In summary, the example calculations in table 11.5 provide illustration and support for why iterative solution using the AFIB method (eq. 11.2a-f) is preferred when a surface is sufficiently drier than the 'reference' condition so that departure of T_s from T_a creates the need to utilize T_s in the estimation of R_{lout}, G, Δ, and $\psi(z/L)$. When these latter parameters are calculated using T_s, especially Δ, the need for the PM combination equation is essentially eliminated. The PM can still be applied, however, if with iteratively determined R_{lout}, G, Δ, and $\psi(z/L)$ parameters, with little departure from λE estimated using eq. 11.2c. The example illustrates that all four parameters R_{lout}, G, Δ, and $\psi(z/L)$ are tied to measured or iteratively determined T_s, and that lack of a T_s basis for any one of them can introduce error.

Table 11.5a Calculations from 2 pm hourly weather measurements collected over dry rangeland near Balanced Rock, Idaho from August 22-28, 2008: R_n (col. 1), G (col. 2), T_s solved by iteration, (col. 5), H (col. 7), and Δ calculated using T_a, only (col. 10) and Δ calculated using T_a and iteratively determined T_s (col. 11). R_n, G, and H were calculated using T_s solved by iterative solution of eq. 11.2a-f (AFIB method). Also shown are measured T_a measured T_s (col. 6), and u_z at 3 m.

DoY	*Est.* $R_{n\ act}$ Wm^{-2}	*Est.* G_{act}, Wm^{-2}	$R_{n\ ref}$ Wm^{-2}	T_a, ^oC	iterative T_s, ^oC	measured T_s, ^oC	u_z, $m\ s^{-1}$	e_a, kPa	H, Wm^{-2}	Δ from T_a, kPa $^oC^{-1}$	Δ from T_a, T_s, kPa $^oC^{-1}$
	(1)	(2)	(3)	(4)	(5)	(6)	(7)	(8)	(9)	(10)	(11)
235	444	117	566	24.0	42.1	45.0	3.0	0.55	239	0.179	0.291
236	433	113	582	29.1	48.6	42.8	2.3	0.54	196	0.233	0.383
237	393	102	541	34.5	50.9	50.6	2.7	0.71	153	0.303	0.454
238	411	105	582	34.5	48.6	50.5	3.6	0.69	183	0.303	0.429
239	326	87	388	19.6	28.9	32.7	5.8	0.51	198	0.142	0.183
240	440	116	555	27.0	38.0	43.0	6.3	0.47	252	0.209	0.278
241	433	114	552	27.4	39.0	41.7	5.7	0.61	245	0.213	0.288
ave	411	108	538	28	42	44	4.2	0.58	209	0.226	0.329

Table 11.5b Calculations for λE for 2 pm hourly weather measurements collected over dry rangeland near Balanced Rock, Idaho from August 22-28, 2008 using the Penman-Monteith equation with progressively more parameters calculated using iteratively determined T_s, and percent differences from λE determined using aerodynamic equation 11.2c. Descriptions of each progression are given in the table footnotes.

		Penman-Monteith λE						% difference of Penman-Monteith λE from aerodynamic (AFIB) λE					
DoY	aero-dynamic λE, Wm^{-2}	with T_a, only Wm^{-2}	with T_a, G_{act}, Wm^{-2}	with Δ from T_a and T_s, G_{act}, Wm^{-2}	with Δ from T_a and T_s, $\psi(z/L)$, G_{act}, Wm^{-2}	with Δ from T_a and T_s, $R_{l\ out}$ from T_s, G_{act}, Wm^{-2}	with Δ from T_a and T_s, $R_{l\ out}$ from T_s, $\psi(z/L)$, G_{act}, Wm^{-2}	with T_a, only %	with T_a, G_{act}, %	with Δ from T_a and T_s, G_{act}, %	with Δ from T_a and T_s, $\psi(z/L)$, G_{act}, %	with Δ from T_a and T_s, $R_{l\ out}$ from T_s, G_{act}, %	with Δ from T_a and T_s, $R_{l\ out}$ from T_s, $\psi(z/L)$, G_{act}, %
	(0)	(1)	(2)	(3)	(4)	(5)	(6)	(1a)	(2a)	(3a)	(4a)	(5a)	(6a)
235	88	108	98	131	107	101	85	23	11	49	22	15	-4
236	124	157	143	188	148	137	111	27	16	51	20	10	-10
237	138	168	155	187	158	138	120	22	12	36	15	0	-13
238	123	151	140	165	148	126	115	23	14	34	20	2	-7
239	40	46	42	48	46	42	40	14	4	18	13	4	0
240	72	83	76	88	84	74	71	15	7	23	17	4	-1
241	74	87	80	93	88	77	73	17	8	26	19	4	-1
ave.	94	114	105	129	111	99	94	20	10	34	18	6	-5

col. (0): λE using aerodynamic eq. 11.2c using T_s from iterative application of eq. 11.2a-f (AFIB equations).

col. (1): λE from the PM equation (eq. 11.1) using T_{air} only: R_n and G calculated for the reference definition using eq. 4.31, 4.39, 4.40, 4.41 and G calculated as $0.1R_n$ and with $\psi(z/L) = 0$, and Δ from T_a.

col. (2): λE from the PM equation (eq. 11.1) using R_n calculated for the reference definition using eq. 4.31, 4.39, 4.40, 4.41 but G calculated from eq. 11.2b using T_s, and with $\psi(z/L) = 0$, and Δ from T_a.

col. (3): λE from the PM equation (eq. 11.1) using R_n calculated for the reference definition using eq. 4.31, 4.39, 4.40, 4.41 but G calculated from eq. 11.2b using T_s, and with $\psi(z/L) = 0$, and Δ from T_a and T_s.

col. (4): λE from the PM equation (eq. 11.1) using R_n calculated for the reference definition using eq. 4.31, 4.39, 4.40, 4.41 but G calculated from eq. 11.2b using T_s, and with $\psi(z/L)$ from eq. 7.22-7.26, and Δ from T_a and T_s.

col. (5): λE from the PM equation (eq. 11.1) using R_n calculated from eq. 11.2a using R_{lout} based on T_s, G calculated from eq. 11.2b using T_s, and with $\psi(z/L) = 0$, and Δ from T_a and T_s.

col. (6): λE from the PM equation (eq. 11.1) using R_n calculated from eq. 11.2a using R_{lout} based on T_s, G calculated from eq. 11.2b using T_s, and with $\psi(z/L)$ from eq. 7.22-7.26, and Δ from T_a and T_s.

11.8 Evaporation from Soil and Surface Resistance

Evaporation from soil generally dominates the computation of ET and r_s for low amounts of leaf area and should be considered in ET estimates when LAI is less than 2 to 3 or when a multilayer or multi-source application of the PM equation is applied. Complex models for simulating the flow of heat into and out of soil and evaporation of water from bare and partially vegetated soils have been introduced, including Horton and Wierenga (1983), Novak (1989), Horton and Chung (1991), Simunek et al. (1999, 2005), Saito et al. (2006), in addition to the multilayer models described earlier in this chapter. Many of these models are generally complex and may be too data intensive for routine application. Often, for purposes of estimating ET on a daily basis, soil water evaporation can be determined by varying surface resistance with cumulative evaporation.

For a single-layer PM model application, Grant (1975) proposed calculating an integrated surface resistance, r_s, for uniform vegetation cover which considers vegetative surface resistance and soil resistance in parallel. His equation is of the form:

$$\frac{1}{r_s} = \frac{1 - K_r^{LAI}}{r_{sn}} + \frac{K_r^{LAI}}{r_{ss}} \tag{11.51}$$

where r_{sn} = bulk stomatal (surface) resistance for a fully developed vegetative canopy, s m^{-1} and r_{ss} = effective soil resistance to evaporation, s m^{-1}. K_r is a "radiation extinction" coefficient, which helps to characterize the net exposure of vegetation and soil. Values for K_r equal to 0.85 and 0.70 were suggested by Monteith and Unsworth (1990) for beans and wheat, respectively. Eq. 11.51 is conservative in that it incorporates the bulk surface resistance for a fully developed canopy. The radiation extinction constant is used in eq. 11.51 to simulate the close coupling between radiation absorption within a canopy and the energy available for evaporation beneath the canopy. K_r also serves as a surrogate for ease of heat and vapor transport to and from 'deep' leaf layers in the canopy to the canopy surface.

Perrier (1982) suggested a relationship similar to eq. 11.51 for nonuniform vegetation cover of the form:

$$\frac{1}{r_s} = f_c \frac{LAI_{eff}}{r_l} + (1 - f_c)\frac{1}{r_{ss}} \tag{11.52}$$

where f_c is the fraction of soil covered and/or shaded by vegetation, and r_l is stomatal resistance, s m^{-1}, per unit LAI.

Soil resistance to evaporation, r_{ss}, varies significantly with soil water. Minimum values occur when the soil surface is nearly saturated. Values increase nearly exponentially as the

surface 1-cm layer dries due to evaporation (van de Griend and Owe 1994). The thickness of the total soil layer that dries by evaporation is a function of soil hydraulic and thermal properties as well as evaporative demand.

Early in a drying cycle, when bare soil near the surface is moist, water is transported toward the surface by liquid transport according to hydraulic properties of the soil. During this period, evaporation occurs at rates close to potential. This stage is often referred to as the "first stage of evaporation." After the soil surface has dried to the extent that hydraulic transport to the surface lags evaporative demand, then "second stage" drying begins. As the hydraulic conductivity near the soil surface decreases, evaporation occurs at lower rates and is limited by conduction of sensible heat (soil heat flux density) downward into the soil and by diffusion of vapor and liquid water from below the surface to the surface. Because the hydraulic conductivity and thermal conductivity of soil decrease with decreasing soil water, the rate of evaporation decreases with drying until it reaches a very low rate. At this point, r_{ss} assumes a maximum value. More description of stage 1 and 2 drying is given in Chapters 9 and 10.

Van de Griend and Owe (1994) proposed estimating r_{ss} from the water content of the top 1 cm of soil:

$$r_{ss} = 10 \exp\left(a_\theta \left(\theta_1 - \theta\right)\right) \tag{11.53}$$

where θ_1 is the volumetric water content, percent, at the end of stage 1 drying for the top 1 cm and θ is water content of the top 1 cm soil layer in percent and a_θ is an empirical coefficient, set to 0.356 by van de Griend and Owe (1994). Eq. 11.53 suggests r_{ss} = 10 s m^{-1} during stage 1 drying until the beginning of stage 2. Van de Griend and Owe (1994) estimated θ_1 as $\theta_{fc}/2$, where θ_{fc} is volumetric water content at field capacity. In contrast to the use of a shallow 10 mm soil depth to estimate r_{ss}, Ortega-Farias et al. (2010) used water content of the top 200 mm of soil in a vineyard, where $r_{ss} = 19\ (\theta / \theta_s)^{-3.5}$ and θ_s is water content at saturation. A time based water balance of the upper soil layer is needed to estimate θ for each timestep of a model. Farahani and Ahuja (1996), Lagos (2008) and Lagos et al. (2012) described functions to estimate resistance for soil having organic residue cover.

For many soils, r_{ss} can be expressed as a function of the amount of water evaporated from the soil relative to the maximum amount of water that can be evaporated:

$$r_{ss} = r_{ssn} + (r_{ssx} - r_{ssn}) \left(\frac{\Sigma E_s}{(\Sigma E_s)_x} \right)^{K_{rs}} \tag{11.54}$$

where r_{ssn} is minimum soil resistance, s m^{-1}, when the soil surface is wet from rainfall or irrigation and r_{ssx} is maximum soil resistance, s m^{-1}, when the upper soil layer has been depleted of all evaporable water. ΣE_s is the cumulative depth of water evaporated from the soil surface, mm, and $(\Sigma E_s)_x$ is the maximum cumulative depth of evaporable water, mm. The exponent K_{rs} in eq. 11.54 ($K_{rs} > 1$) simulates the length of first stage drying where r_{ss} remains close to r_{ssn} for 1 to 3 days while the soil supplies water for evaporation at nearly the potential rate and then begins a rapid increase in r_{ss} as the water in the soil surface nears depletion. Illustrative values for r_{ssn}, r_{ssx}, and K_{rs} are 50 s m^{-1}, 2000 s m^{-1} and 10, respectively, for a bare Portneuf silt loam soil in

Idaho (Allen et al. 1996, data from Wright (1991)[2]). $(\Sigma E_s)_x$ is best determined from empirical studies based on soil water depletion measured under bare soil conditions. Alternatively, $(\Sigma E_s)_x$, is made equivalent to the TEW term representing total evaporable water defined in chapter 9, and is estimated using eq. 9.20 based on estimated field capacity, wilting point and effective evaporation depth. The following eq. 11.55 is similar to eq. 9.20.

$$\left(\sum E_s\right)_x = 1000\left(\theta_{fc} - \frac{(\theta_{wp} + \theta_{od})}{2}\right) z_e \qquad (11.55)$$

where Z_e is the total estimated depth of soil, m, contributing to evaporation and water contents have dimensionless units of $m^3\ m^{-3}$.

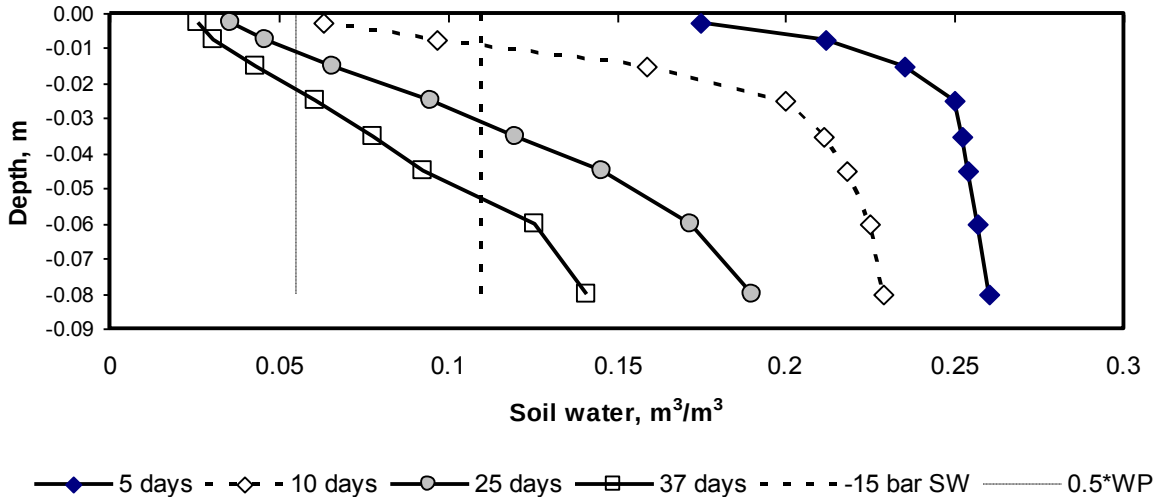

Fig. 11.6. Soil water distribution on day 5, 10, 25 and 37 after wetting. Source: Data from Jackson (1973).

For example, if a silt loam soil with $\theta_{fc} = 0.31\ m^3\ m^{-3}$, $\theta_{wp} = 0.14\ m^3\ m^{-3}$ and oven dry soil water content of less than $0.005\ m^3\ m^{-3}$ were dried by evaporation to a depth of 0.12 m, the total surface evaporable water, $(\Sigma Es)_x$, would be approximately:

$$\left(\sum E_s\right)_x = 1000\left(0.31 - \frac{(0.14 + 0.005)}{2}\right) 0.12 = 29\ mm$$

The value of $(\Sigma E_s)_x$ varies with soil texture, structure and organic cover and period of time. Approximate values for $(\Sigma E_s)_x$ are about 10 to 20 mm for a bare, sandy soil, 30 mm for a bare, silt loam, and 40 mm for a bare, clay-textured soil. $(\Sigma E_s)_x = 30$ mm for a bare Portneuf silt loam soil, based on data from Wright (1991)[2]. Soil covered with organic mulch or other insulative cover tends to reduce the peak evaporation rate and often the total depth of evaporation $(\Sigma E_s)_x$, as discussed in chapters 9 and10. Denmead (1984) suggested that evaporation from a forest floor

[2] Personal communication.

covered with litter might be only one-half of what is expected from a bare exposed soil. Gonzalez-Sosa et al. (1999) measured similar reductions for a corn field covered with organic mulch in France. Allen et al. (1998, 2005b) proposed similar reductions in TEW for organic and plastic covers. Li et al. (2003) reported field measured evaporation from plastic-covered soil that ranged from 11 to 70% of rates from an exposed bare soil.

ΣE_s can be estimated using a daily calculation time step basis using a soil water balance of the upper 0.10 to 0.20-m soil layer for normal drying cycles. A general equation for ΣE_s for the f_{ev} fraction of soil that is exposed to drying is:

$$\sum E_{s_i} = \sum E_{s_{i-1}} - P_i - I_i + \frac{ET_a - ET_b}{f_{ev}} \tag{11.56}$$

where $\Sigma E_{s\,i}$ is cumulative soil evaporation on day i, $\Sigma E_{s\,i-1}$ is cumulative soil evaporation on day i-1, P_i and RO_i are precipitation and precipitation runoff from the soil surface on day i, I_i is mean irrigation depth on day i, and ET_a is actual ET on day i computed using the PM equation where r_s includes the effects of r_{ss}. ET_b is a "basal" ET rate which reflects a visually dry soil surface and is computed using the PM equation where r_s is calculated using $r_{ss} = r_{ssx}$ for a dry soil surface. The difference $ET_a - ET_b$ represents the soil evaporation component and f_{ev} is the effective fraction of the total soil surface contributing to evaporation. The presence of f_{ev} in eq. 11.56 is intended to 'concentrate' the extraction of evaporation into the f_{ev} fraction of the ground surface, similar to that done in eq. 9.27 for the dual K_c procedure. The value of f_{ev} may be less than 1 when part of the soil is shaded by dense vegetation; $f_{ev} < 1$ causes $\Sigma E_{s\,i}$ to approach $(\Sigma E_s)_x$ more quickly. $\Sigma E_{s\,i}$ in eq. 11.56 has limits of 0 and $(\Sigma E_s)_x$.

Fig. 11.7 shows an example of estimating surface resistance using resistance data for maize reported by Jacobs et al. (1989). K_r in eq. 11.51 was estimated as 0.7. Surface resistance of the canopy at maximum LAI, r_{sn}, was estimated as 60 s m^{-1} based on r_l = 100 s m^{-1} and LAI_{eff} from eq. 8.11 for LAI = 3.8. Calculations were relatively insensitive to the value of K_r between 0.6 and 0.8. Eq. 11.52 was applied assuming r_l = 100 s m^{-1} and r_{ss} = 200 s m^{-1}, and f_c was assumed to range from 0.05 at LAI = 0.5 to 0.95 when LAI = 4. Jacobs et al. (1989) presented no information concerning occurrences of soil wetting. Therefore, r_{ss} = 200 s m^{-1} was used as an approximation for the entire period.

Eq. 11.51 and eq. 11.52 both replicated measured r_s relatively well, using the assigned estimates for r_{ss} and LAI_{eff}. Eq. 11.51 agreed more closely with observed measurements of r_s during periods of significant soil water evaporation (LAI < 1) than did the eq. 11.52 indicating the importance of the radiation extinction term. If the occurrences of soil wetting had been known, then eq. 11.55 could have been applied, where ΣE_s would have been computed on daily time steps using eq. 11.56.

The effect of ignoring soil evaporation in computing r_s (e.g., using eq. 8.9 with eq. 8.10 or 8.11, only) is significant at LAI < 1 as shown in fig. 11.7. The effect of ignoring soil evaporation was less when LAI > 1.5.

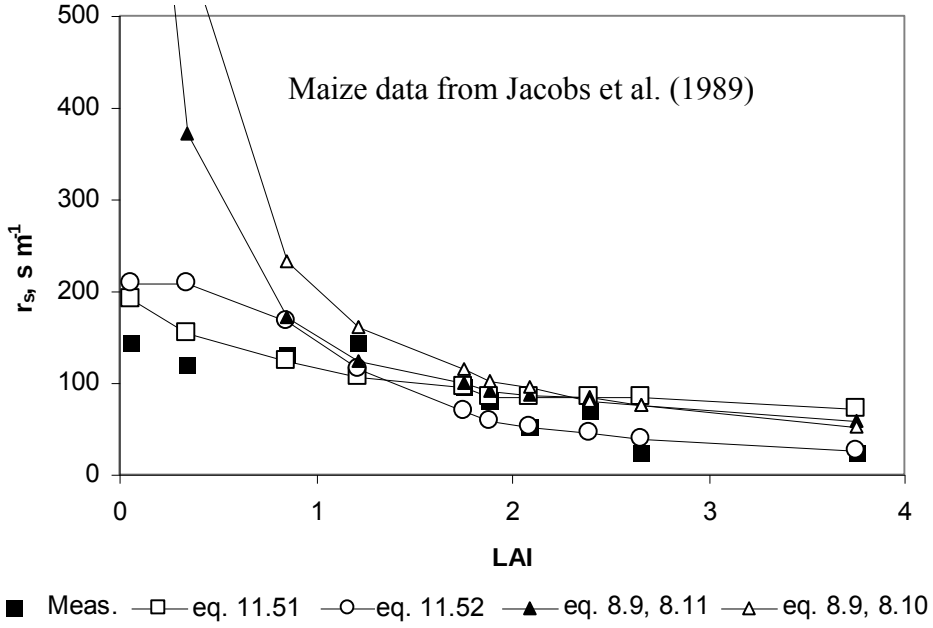

Fig. 11.7. Examples of calculations for total surface resistance using eqs. 8.9, 11.51 and 11.52 with application to data from Jacobs et al. (1989). Source: Data from Jacobs et al. (1989).

Grant's approach in Eq. 11.51 can be extended for sparse or immature crops or vegetation having exposed bare soil between plants or rows to apply to a mixture of shaded and nonshaded soil surface and, for incomplete wetting of the soil surface during irrigation, additionally for a mixture of wetted and nonwetted parts of the surface. This is done through combination of surface resistances, r_{sc} and r_{ss}, acting in parallel as expressed by Allen et al. (1996) according to the fractions of surface represented by each parallel resistance component:

$$\frac{1}{r_s} = \frac{f_c \left(1 - K_r^{LAI/f_c}\right)}{r_{sc}} + K_r^{LAI/f_c} \left(\frac{f_{csW}}{r_{sssW}} + \frac{f_{csD}}{r_{sssD}}\right) + \frac{f_{eW}}{r_{sseW}} + \frac{f_{eD}}{r_{sseD}} \qquad (11.57)$$

where f_c is the effective fraction of ground shaded by vegetation, and is computed as a function of sun angle, row height and width, leaf density, and row orientation. Fractions $f_{c\,sW}$, $f_{c\,sD}$, f_{eW} and f_{eW} are the fractions of the soil surface that are a) shaded and wet, b) shaded and dry, c) sunlit and wet, and d) sunlit and dry, as illustrated in fig. 11.1a and 11.8. By definition, $f_{c\,sW} + f_{c\,sD} + f_{eW} + f_{eD} = 1$ and $f_{c\,sW} + f_{c\,sD} = f_c$. Resistance r_{sc} is the surface resistance of the canopy, r_{sssW} is the surface resistance of soil shaded by the canopy that is wetted by irrigation or precipitation, r_{sssD} is the surface resistance of soil shaded by the canopy that is not wetted by irrigation or precipitation, r_{sseW} is the surface resistance of soil exposed to sunlight (not shaded by the canopy) and that is wetted by irrigation or precipitation, and r_{sseD} is the surface resistance of soil exposed to sunlight that is not wetted by irrigation or precipitation. The application of Eq. 11.57 requires a soil water balance for each of the f_{cs} and f_e fractions of the surface. Generally, r_{sssD} and r_{sseD}

can be assumed to equal maximum r_{ssx}, if those fractions of the soil surface are dry. Thompson et al. (1981) estimated f_c as LAI/4.

The use of the PM equation using r_s from eq. 11.57, even though r_s is well parameterized, uses a single aerodynamic resistance, r_a, thus assuming that all evaporation and heat transfer originates from a single plane. Thus PM is often referred to as the 'big-leaf' model (Monteith 1965). In situations where the vegetation canopy has substantial height, such as for trees, or where vegetation is relatively sparse, a multi-layer ET model, discussed in an earlier section, may produce better estimates. Also, differences in emitted long wave radiation between dry, sunlit soil and canopy can be as large as 100 Wm^{-2}, as illustrated in table 11.5. This can reduce the accuracy or consistency of applications of single layer PM equations comprised of blended resistances. Leuning et al. (1994) and Brisson (1998) applied separate Penman-Monteith equations for evaporation and transpiration and then recoupled them, similar to procedures

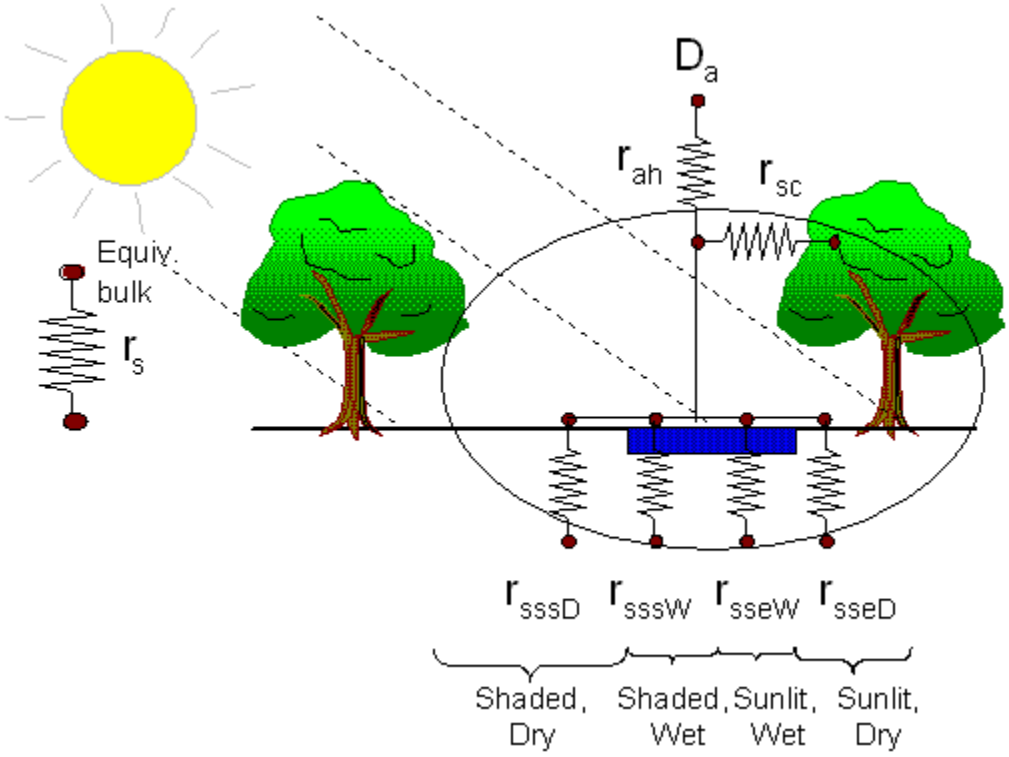

commonly used for multi-layer ET models.

Fig. 11.8. Schematic of soil resistances for evaporation for incomplete vegetation cover and spatially variable wetting of the soil surface.

For sun angles other than directly overhead, f_c can be estimated for a row crop following Allen et al. (1998) as:

$$f_c = \frac{W + h\left|\sin(\eta + \beta)\right| \tan\theta_z}{S} \tag{11.58}$$

where h is mean plant height, θ_z is the solar zenith angle (0 = nadir (overhead)), η is the sun azimuth angle (0 = north), and β is the row orientation relative to north (β = 0 for north-south orientation, $\beta = 90^o$ for east-west row orientation), W is row width and S is row spacing having the same units as h. Eq. (11.58) presumes a nearly rectangular continuous row shape of height h and width W and has an upper limit of $f_c = 1$. In some situations, W may not be measured or available, but an estimate of LAI may be available. In this case, f_c may be approximated during incomplete row closure as

$$f_c = \frac{LAI}{LAI_c} + \frac{h}{S} \left|sin(\eta + \beta)\right| \tan \theta_z \qquad (11.59)$$

where LAI_C is the LAI at complete row closure and shading of the ground. Variations on eq. 11.58 and 11.59 can be made to fit the particular row architecture, for example when there are spacings between tree canopies. Campbell and Norman (1998) suggested a simple model to estimate effects of tree canopies that do not extend to the ground. The value for f_c and, subsequently, for r_s changes with time of day and interacts with R_n, G, wind speed and temperature.

For 24-hour computation time steps, an average daily value for f_c is determined for computing soil moisture balances for shaded and unshaded soil. An average daily value for f_c for east-west rows can be determined by weighting Eq. 11.59 for sunlight intensity and integrating between the limits of sunrise and sunset or by standardizing on solar noon time. For north-south row orientation, all soil is sunlit and shaded at various times of the day, so one may set f_c = W..

An example of applying the direct PM equation using r_s from eq. 11.57 is shown in Fig. 11.9 for a growing season for snap beans near Kimberly, Idaho in 1974. The daily estimates were divided by alfalfa reference ET_r to normalize. The dry-soil curve represents estimates from the direct PM using r_{ssx} for a dry surface. The ratio of the dry-soil estimates to reference ET_r, varied from day to day due to differences between the direct PM, which used net radiation measured over the bean crop, and the standardized PM, which used standardized calculated net radiation. In this example $r_{sc\ min}$ was set at 25 s m^{-1}. Agreement between the direct PM and measurement data was relatively good. The RMSE was 1.1 mm d^{-1} (n = 86). The method overestimated peak ET on days having wet soil and partial vegetation cover early in the growing period, where $f_{c\,sW} + f_{eW} = 0.5$ was assumed.

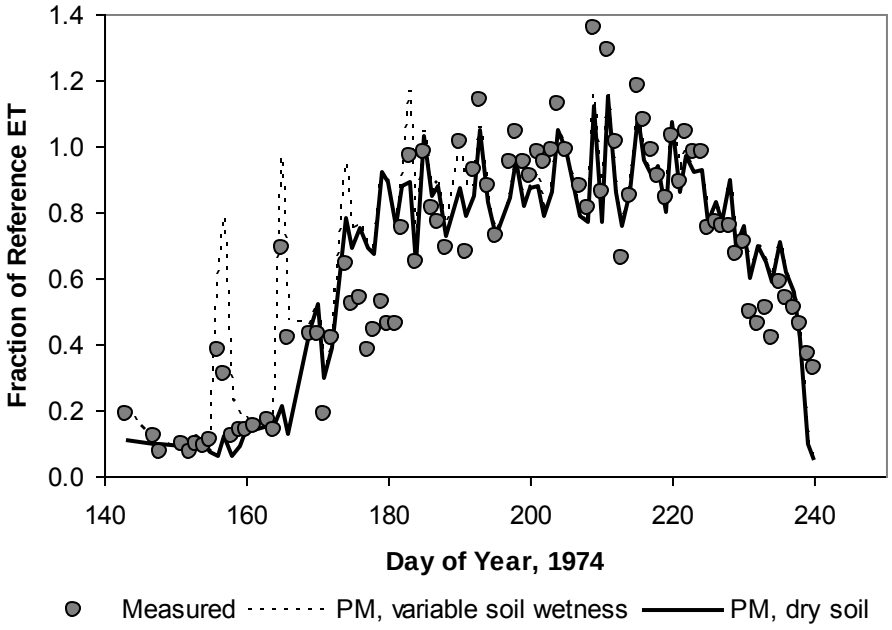

Fig. 11.9. Daily ET for a bean crop near Kimberly, Idaho calculated using the direct PM equation using r_s from eq. 11.57 where, for the dry soil condition, r_{ss} was set equal to r_{ssx}, and where ET is expressed as a fraction of daily alfalfa reference ET_r calculated using the ASCE standardized PM equation. Calculations are from Allen et al. (2000), lysimeter data compliments of Dr. J.L. Wright, USDA-ARS (ret.)). Source: Allen et al. (2000); Dr. J.L. Wright, USDA-ARS (ret,).

11.9 Weather Measurements for Direct Application of the Penman-Monteith and AFIB Methods and Reference ET Calculation

Basic Measurements

When applying the PM or other boundary layer equations, wind, humidity and temperature should be measured over the surface in question. This is important, as the rates of λE and H from a vegetative surface affect the shapes and magnitudes of vapor and air temperature profiles. In the same manner, the roughness of an evaporating surface affects the shape and magnitude of wind velocities above the surface. Vapor and air temperature profiles established above a surface function as feedback mechanisms to λE and H and play important roles in dampening differences in r_s and r_a among vegetation types.

As the value of r_s decreases (higher bulk stomatal conductance), λE increases and consequently H (if positive) decreases. The result is relatively higher vapor concentration in the equilibrium boundary layer above the surface and cooler temperatures. These two changes work together in reducing the vapor pressure deficit of the boundary layer, thereby dampening the increase in λE demand (negative feedback). An increase in the value of r_s works in the opposite direction. With an increase in r_s, the VPD of the boundary layer is increased due to reduced vapor concentration and increased air temperature, resulting in higher λE demand on the

vegetation (positive feedback). The higher λE demand of the boundary layer partially dampens decreases in λE caused by increases in surface resistance.

The functioning of boundary layer feedback processes and 'conditioning' of the near surface air stream are important and may present problems when *RH* and *T* data are measured over surfaces that have aerodynamic and surface characteristics and soil water availability that are different from the surface in question. This is an especially common problem in semiarid climates where irrigated agriculture can create 'oases' of relatively wet surfaces that have near surface boundary layers that can be quite different from those of the ambient, regional surroundings. Errors introduced to ET calculations based on using weather data reflecting the region or a locally dry condition can be substantial. Errors can also occur in the case of estimating evaporation of intercepted precipitation from tall, aerodynamically rough forest canopies using weather data from adjacent grassed weather sites. In this situation, the smoother aerodynamics and lower λE of the grassed site result in higher wind speeds, higher temperatures and lower vapor pressures. When transposed over a tall-vegetated surface with low r_s, overestimation of ET occurs. In addition to conditioning of the equilibrium boundary layer, the generally cooler surface temperature associated with an evaporating surface increases R_n by reducing $R_{l\,out}$. The cooler surface also often reduces *G* due to reduced thermal gradients. Both of these impacts increase available energy and ET that may counter some of the effects of the conditioning of the air stream.

In situations where ET is estimated for natural rainfed vegetation using a direct equation application such as with the PM equation, then humidity, air temperature and wind measurements should be made over the same type of vegetation or directly or iteratively adjusted to reflect the conditioning by that surface. In situations where the $K_c\ ET_{ref}$ approach is utilized, then humidity, temperature, and wind measurements should be made over a well-watered, agricultural surface, preferably clipped grass, since that is what the calibrations of the reference ET equations are 'expecting.' Most ET_{ref} equations have been calibrated against weather data gathered over well watered clipped grass (Doorenbos and Pruitt 1977; Wright 1982; and Jensen et al. 1990; ASCE-EWRI 2005) and K_c's are usually computed using this standardized ET_{ref}.

It is generally difficult to obtain humidity, temperature, and wind measurements over unique types of vegetative canopies, especially when estimating ET for historical periods. Often, such data are available only from grassed or even barren weather sites. Often weather measurement sites are located in nonagricultural, nongrassland, or nonforested sites such as in cities or near airport runways and buildings. Under these circumstances the user should make allowances for the uncharacteristic nature of the humidity, temperature and wind data and perhaps assign some type of uncertainty level to the ET estimates.

All weather station equipment used in estimating ET should conform to accepted standards and specifications regarding equipment type, placement, maintenance, calibration, and reporting frequency. Ley and Elliot (1993) reported on proposed standards for agricultural weather stations and discuss recommended standards and specifications. These standards are now available as the ASABE standard EP505 (ASABE 2004, revised 2009) Measurement and Reporting Practices for Automatic Agricultural Weather Stations.

Measurements of meteorological data should be screened for integrity and accuracy before use as recommended in Allen et al. (1998 and 2011b). Calibration and maintenance of sensors should be confirmed and documented. Air temperature and humidity data should be evaluated using procedures discussed in the next section. Daily and hourly solar radiation data should be plotted against clear sky solar radiation (R_{so}) to assess whether maximum measurements of R_s

follow the R_{so} "envelope." Occasionally, R_s can exceed R_{so} when clouds are present outside of the view angle of the sun, and reflect additional radiation toward the sensor. R_{so} can be estimated from extraterrestrial radiation (R_a) using eq. 4.3. Jensen et al. (1990), Allen et al. (1994b), Allen et al. (2005), and appendix H describe methods for computing R_a and R_{so} for hourly periods. Monthly values for R_s can be compared against R_s estimated using eqs. 4.24 and 4.26 to assess general data integrity.

Adjustments of Non-Characteristic Weather Data

Air Temperature and Humidity. When air temperature and humidity data are required for use in an ET_o calculation or in a direct application of a single or multi-layer PM equation, they may need to be adjusted to account for dryness of the weather station environment. Allen et al. (1983) and Allen and Pruitt (1986) developed empirical procedures for adjusting air temperature measurements from weather stations located in environments where ET was less than maximum rates due to limited soil water or green vegetation. The objective of the adjustments was to create air temperature data sets reflective of well-watered environments over clipped grass for use in an ET_{ref} equation. An aridity rating procedure was used to characterize effects of dryness of the local station environment as well as the region on required air temperature adjustments. In the application to weather stations in Idaho, daily maximum and minimum air temperatures were adjusted downward by as much as 4.5°C for stations having nonirrigated, nontranspiring surfaces surrounded by similar conditions. The magnitude of adjustments by Allen and Pruitt (1986) were based on paired observations of air temperatures by Allen et al. (1983).

Ley and Allen (1994) applied more complex methods for adjusting air temperature and humidity data from nonreference stations using energy balance and water balance relationships. These methods required measurement of R_s, T, humidity, wind, and precipitation on a daily basis. Allen (2012) applied surface energy balance and blending height theory to establish expected T, e and u profiles to a 200 m blending height above a weather surface and to then extrapolate back

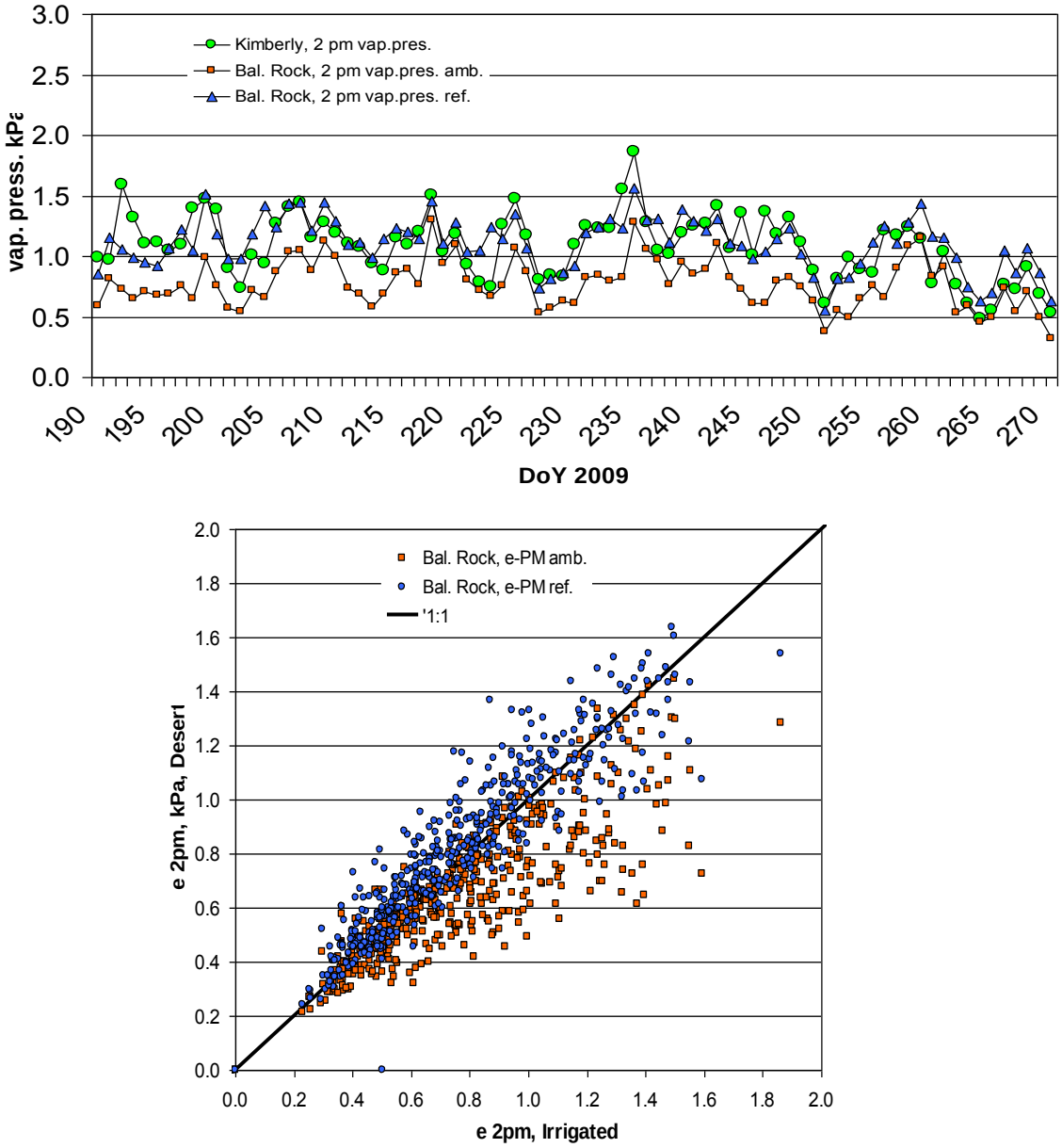

Fig. 11.10. a) Daily mid-afternoon vapor pressure measured over a dry desert location in southern Idaho near Balanced Rock, Castleford ("Bal. Rock, 2 pm vap. pres. amb.") and the same vapor pressure adjusted (i.e., conditioned using blending height and flux profile theory) to reflect vapor pressure expected over a 'reference ET' surface ("Bal. Rock, 2 pm vap. pres. ref.") compared with measured mid-afternoon vapor pressure at an irrigated site 60 km to the east "Kimberly, 2 pm vap. pres."; and b) the same data from Balanced Rock plotted against measured vapor pressure at the irrigated Kimberly location before ("Bal. Rock, e-PM amb.") and after ("Bal. Rock, e-PM ref.") adjustment by conditioning. Source: Data from Allen (2012).

to the surface using ET and energy balance estimated for a well-watered reference surface. The iterative procedure produces near surface T, e and u (at 2 m height) that reflect the conditioning

of a well watered, reference surface and that can be used to produce more accurate and representative reference ET calculations. In an application to weather data from an Idaho desert setting (annual P = 200 mm), Allen (2012) showed that conditioning of the desert air mass by localized or regional irrigation (or establishment of a 'reference ET' surface) nearly doubled humidity content at 2 m. This is shown in fig. 11.10. The blending height-flux profile procedure can be applied over other types of surfaces where a direct PM application is made to make iterative adjustments to T, e and u profiles that incorporate feedback effects from the surface.

Humidity measurements over arid, nonirrigated surfaces are in general lower than those made over well-watered grassed surfaces or over other well-watered vegetation. If humidity data are to be used to estimate ET_{ref}, which by definition is ET from a well-watered surface, then humidity measurements should be made in a well-watered environment. In an environment having healthy vegetation and adequate soil water, minimum daily air temperature, T_{min}, usually approaches dew point temperature, T_d, especially if the wind dies down by early morning. Air temperatures decrease during nighttime hours due to surface cooling caused by long-wave radiation and evaporation caused by a positive VPD until the dew point is reached, provided that wind speed is relatively calm so that large amounts of warm, dry air (in an arid region) are not transported to the surface. When near-surface air temperature nears T_d, T is prevented from decreasing below T_d by condensation of vapor from the air and the corresponding heating effect of released latent heat. Under these conditions, the relationship $T_{min} = T_d$ generally holds and can be used to assess the relative impact of non-representative station environment on humidity and air temperature on ET_{ref} calculations.

When soil water or vegetation cover limits ET to less than ET_{ref}, T_{min} may remain above T_d. This occurs due to two factors. The first factor is the large reservoir of sensible heat in the atmosphere which is transferred toward the surface during the night, reducing the effect of cooling by long wave emission. The large reservoir of heat is created during the daytime due to large flux densities of sensible heat, H, resulting from low ET. The second factor is the effect of lower soil water availability on limiting evaporative cooling during nighttime hours.

Under most evaporative conditions, T_d is higher during daytime hours than during nighttime hours due to humidification of the boundary layer by ET. Consequently, daytime measurements of absolute humidity may exceed nighttime values by 5 to 20 percent. Therefore, the relationship between T_{min} and T_d may not be strictly one-to-one when T_d is based on 24-hour or daylight averages. In these cases, especially during winter months, T_{min} measurements can be expected to go a few degrees below 24-hour average T_d measurements.

An example of the effect of dryness of weather station environment on proximity of T_{min} to T_d is shown in fig. 11.11 where mean monthly differences between T_{min} and T_d are plotted against ratios of mean monthly precipitation and ET_o for two data sets (26 Weather Service locations across the U.S.A (b); and two stations in southern Idaho (c)). The ratios of P to ET_o indicate the relative wetness of the station during a particular month and the likelihood of healthy, transpiring natural vegetation. Figs. 11.11a and b indicate that $T_d \approx T_{min}$ where vegetation of the weather sites is in a reference (well-watered) condition (monthly $P/ET_o > 1$). This would represent conditions within most large irrigation projects. The average absolute difference between T_{min} and T_d is about 2°C when $P/ET_o > 1$. When measured in a dry environment (monthly P/ET_o near zero), T_d can be as much as 20°C less than T_{min}. Daily differences between T_{min} and T_d are similar to the monthly averages shown.

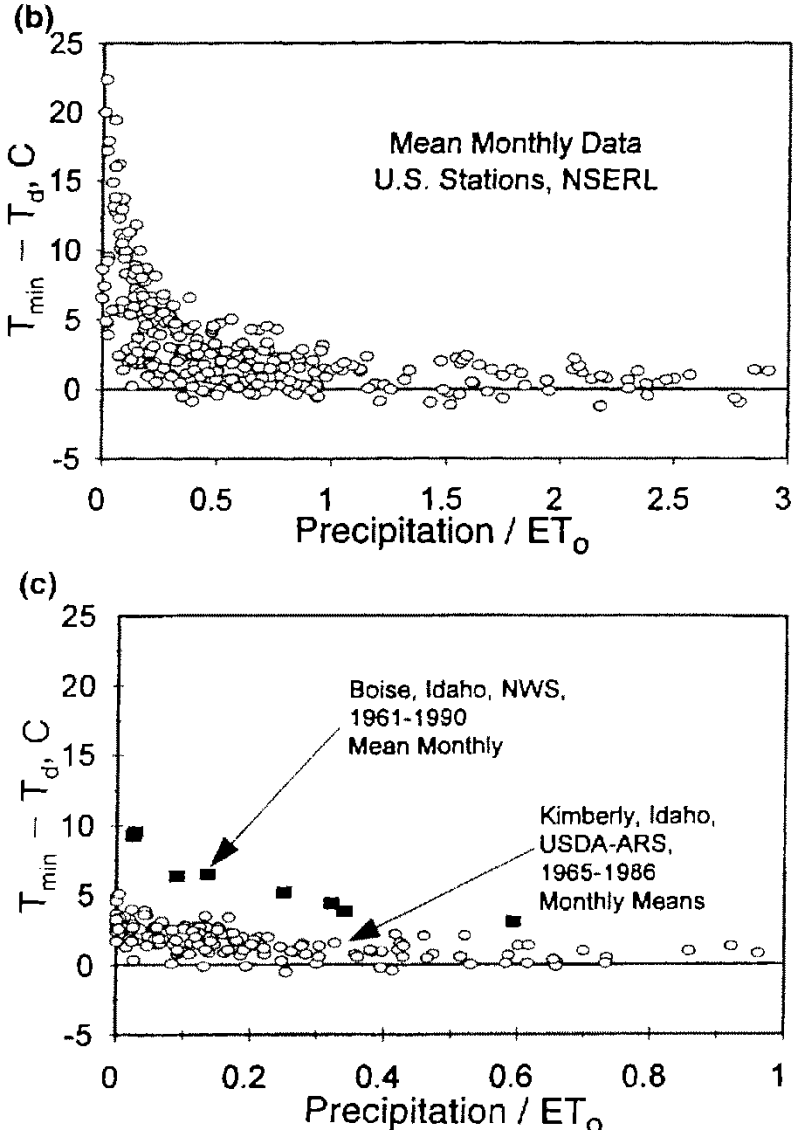

Fig. 11.11. Monthly mean T_{min} - monthly mean T_d for: a) 26 US Weather Service stations across the U.S.; and b) Two Weather Stations in Southern Idaho; Boise represents a dry, airport environment and Kimberly represents an irrigated environment.

The effect of irrigation on $T_{min} - T_d$ is shown in fig. 11.11b, where data from Kimberly and Boise, Idaho are measurements from a semiarid climate (annual rainfall < 250 mm per year), but where the Kimberly location is over irrigated grass surrounded by over 150,000 ha of patchwork irrigated land in which fields of crops are at various stages of growth. The Boise location is the Boise airport which is surrounded by predominately nonirrigated rangeland for a 10 km distance. Irrigated land lies beyond the nonirrigated rangeland in the predominate upwind direction. The effect of surrounding the weather station with well-watered vegetation is obvious. Values for $T_{min} - T_d$ would increase for both of these locations if they had been surrounded by large expanses of only rangeland.

Graphical comparisons of T_{min} vs. T_d can be used as a check on data integrity and how well the data represent well-watered conditions. When data are to represent a well-watered reference setting, then the relationship $T_d \approx T_{min} - K_o$ can be used as a comparative reference where K_o is an offset, generally equal to 0 to 2 K in subhumid and humid climates and 2 to 7 K in semiarid to arid climates during spring, summer and fall. During wintertime, K_o can be negative when comparing mean daily T_d to T_{min} since daytime evaporation and warming of air can increase humidity levels to those above saturation at nighttime T_{min} (Allen and Robison, 2007).

When measured T_{min} substantially exceeds T_d due to station dryness, and data representing a reference setting are desired, then one method to empirically adjust T_{max}, T_{min} and T_d is by subtracting 0.5 ΔT from T_{max} and T_{min} and by adding 0.5 ΔT to T_d, where $\Delta T = T_{min} - T_d - K_o$ (Allen et al. 1998). However, when applying the PM equation directly over dry vegetation, no adjustment of temperature and humidity data should be made. Additional suggestions for adjusting noncharacteristic humidity and temperature data are presented in the ASCE Hydrology Handbook (Allen et al. 1996), ASCE-EWRI (2005) appendices D and E and Appendix H of this text. One can also employ a more physically based boundary layer conditioning method (Allen 2012).

Wind Speed. Aerodynamic resistance computed by eq. 8.3 assumes that the wind speed at some reference height is measured above the surface in question and is therefore governed by exponentially shaped profiles for height above the zero plane displacement that are characteristic of the surface roughness. When wind measurements are made over 0.12 m grass, for instance, wind speed measured at 2 m will generally be significantly higher than that measured at 2 m above tall vegetation, for example, an adjacent forest of 10-m trees.

Rutter et al. (1975) found wind speeds measured at 2 m above the top of a 20-m tall pine forest to be 0.45 of wind speeds measured at 2 m above a nearby-grassed area. Allen and Wright (1997) found wind speeds at 1.3 m above the top of 0.7 m tall snap beans (2 m above ground surface) to be 0.7 of speeds measured at 2 m height over 0.12 m grass 0.8 km away. Wind speeds at 1 m above the top of 1-m tall winter and spring wheat (2 m above ground surface) were 0.6 times speed measured at 2 m height over 0.12 m grass. Ley et al. (2013) reported similar reduction in wind speed over alfalfa as compared to over clipped grass for the same measurement height relative to the ground surface. These differences were found to significantly affect estimates of ET made with aerodynamic methods. In addition, wind speeds measured over dry, warm surfaces are usually stronger than those measured over wetter, cooler surfaces due to impacts of instability (buoyancy-induced turbulence) on mixing of higher velocity air from aloft to the warmer surface. Adjustments for this effect can be made using the blending height – flux profile method of Allen (2012), however, assumptions of large fetches of both types of surfaces must be made.

Rutter et al. (1975) proposed adjusting wind measurements for differences in surface roughness and zero plane displacement by extrapolating upward from the measurement surface to some height of a "regional" internal boundary layer, z_{IBL_R}, where the mean horizontal wind velocity of the equilibrium boundary layer is an integration of regional effects and is presumed to be generally independent of underlying surface roughness of a specific location. The wind velocity at the z_{IBL_R} height was then extrapolated downward from the z_{IBL_R} height to some

elevation above the surface in question using aerodynamic parameters characteristic of the new surface.

Allen and Wright (1997) improved this procedure by combining equations for adjusting wind velocities for both roughness and wind sensor elevation differences into one equation, which considers the relative heights of internal boundary layers developed over both the weather station surface and the surface in question. The equation is of the form:

$$u_2 = u_{2w} = u_{zw} \frac{\ln\left(\frac{z_{IBLw} - d_w}{z_{om\ w}}\right)\ln\left(\frac{z_{IBL\ v} - d_R}{z_{om\,R}}\right)\ln\left(\frac{z_v - d_v}{z_{om\ v}}\right)}{\ln\left(\frac{z_w - d_w}{z_{om\ w}}\right)\ln\left(\frac{z_{IBL\ w} - d_R}{z_{om\ R}}\right)\ln\left(\frac{z_{IBL\ v} - d_v}{z_{om\ v}}\right)} \qquad (11.60)$$

where u_{z_v} is the wind speed adjusted to represent conditions at the z_v height over vegetation or water surface "*v*" and u_{z_w} is the original wind speed measurement at the z_w height over the weather station surface "*w*." Variable z_{IBL_w} is the height of the internal boundary layer developed over surface "*w*" which is in equilibrium with surface "*w*." Variable z_{IBL_v} is the height of the internal boundary layer developed over surface "*v*" which is in equilibrium with surface "*v*." These parameters are estimated using eq. 11.61. Variables z_{om_w} , z_{om_v} , and z_{om_R} are roughness lengths for momentum transfer characterizing the weather surface, the vegetation "*v*", and the integrated "region." Variables d_w, d_v and d_R are zero plane displacement heights for the weather surface, vegetation (or water surface) "*v*" and the region. Units of all *z* and *d* variables are the same (m) and units for *u* are in m s^{-1}. The z_{om} and *d* parameters can be estimated using eq. 11.21 - 11.29.

Values for z_{IBL_w} and z_{IBL_v} may range from only 1 to 2 meters for small fields of 1 ha size to more than 100 m for very large stands of homogeneous vegetation. On a regional scale, the height of a regional internal boundary layer, z_{IBL_R} , may vary from 10's of meters to perhaps 2000 m and may average about 100 to 400 m (Brutsaert 1982). Brutsaert (1982) presented an equation to predict boundary layer growth downwind of a discontinuity between two surfaces of similar but unequal roughness:

$$z_{IBL} = d + 0.33\, z_{om}^{\ 0.125}\, x_f^{\ 0.875} \qquad (11.61)$$

where z_{IBL} is the height of the perturbed IBL above a surface of new roughness (z_{om}) and zero plane displacement (*d*). Variable x_f in eq. 11.61 is the horizontal distance downwind of the surface discontinuity (horizontal fetch). Variables z_{IBL}, *d*, z_{om} and x_f in eq. 11.61 have units of m. Eq. 11.61 can be applied to estimate both z_{IBL_w} and z_{IBL_v} . Eq. 11.61 is a rearrangement of eq. 7.12, except that the difference ($z - d$) in eq. 7.12 is first multiplied by a factor of 10 to approximate the height of the full z_{IBL} which is generally 10 times that of the fully mixed internal sublayer, where flux densities of *H* and λE are in equilibrium with the new surface (Brutsaert 1982).

Limitations in the application of eq. 11.60 are that $z_w < z_{IBL_w}$ and $z_v < z_{IBL_v}$. If these conditions do not exist, then one should use alternate equations presented in Allen and Wright (1997). Other limitations in eq. 11.60 are that all *d*'s must be less than the corresponding

elevations (z) to prevent negative values and extrapolation of wind speed to below zero plane displacement heights and the assumption of near neutrality of the boundary layers. Ley et al. (2013) demonstrated the application of eq. 11.60 to adjust wind speed measured at 2 and 3 m over alfalfa in Colorado to an equivalent wind speed measured over clipped grass with good results.

In summary, in application of eqs. 11.60 and 11.61, u_{z_v} is wind speed predicted to have occurred at the z_v elevation if the ground cover was vegetation of type "v" rather than type "w". The postulation of eq. 11.60 is that wind speeds measured over surfaces can be extrapolated upward from z_w using a logarithmic relationship (assuming near neutral conditions) to some z_{IBL_w} height using aerodynamic roughness properties characteristic of the weather measurement surface, and then extrapolated further upward or downward using aerodynamic properties of the region, and then extrapolated back downward to near the surface using a logarithmic shape characteristic of roughness properties of the vegetation in question. This approach suggests that wind speeds above z_{IBL_w} and z_{IBL_v} are driven by the general speed of an air mass, but that logarithmic profiles in equilibrium with the underlying surfaces tie the regional or local air mass and momentum sink to the ground. This is a simplification of actuality, especially during periods of boundary layer thermal instability and due to the fact that wind profiles above intermixed vegetation stands do not remain completely separate of each other. However, the approach does provide an approximate adjustment mechanism, which has some application value. Eq. 11.60 can be modified to incorporate impacts of boundary layer instability by adding integrated stability corrections based on the Monin-Obhukov formulations (chapter 7). However, this requires knowledge or estimation of relative magnitudes of sensible heat fluxes from the various surfaces.

11.10 Example Applications of the Single Layer Penman-Monteith

The following section summarizes several example applications of using the single-layer PM method for estimating ET directly, without the use of crop coefficients. The first example was calculated using a half-hour data sets at Davis, CA and Logan, UT for grassed surfaces. The second example is for grass forage at Logan, Utah under soil water-stress conditions with calculations made on a daily (24-hour) basis.

Half-Hourly Calculations

The PM method with resistance algorithms for grass (eqs. 8.3, 8.6 - 8.10 and 8.12) was applied using half-hourly measurements of micrometeorological data at both Logan, Utah and Davis, California, with calculations compared to lysimeter measurements. The details of the data sets are the same as those described for the energy-balance method applications shown in fig. 7.5, with aerodynamic resistances computed using the same integrated stability corrections (eq. 7.22 - 7.26) based on infrared measurements of surface temperature. The micrometeorological data in this example were collected over the grass crops. Results of the application are shown in fig. 11.12a for the day of August 2, 1990 at Logan, UT and in fig. 11.12b for the days of May 2-3, 1967 at Davis, CA.

The grass at Logan was primarily fescue and was grown as forage. The grass height on Aug. 2 was 0.23 m. The *LAI* at Logan was estimated from eq. 8.12 as 5.5. The grass at Davis was alta fescue and was clipped as turf. The grass height on May 2-3 was 0.12 m and the *LAI* measured

on May 2 was 2.94. Bulk surface resistance, r_s, at both locations was calculated using eq. 8.9 with LAI_{eff} calculated using eq. 8.10. Net radiation was calculated at Logan from measured R_s using the standard procedures described in chapter 4, since the grass approximated a well-watered surface and would have similar surface temperature. Net radiation at Davis was an average of measurements by three net radiometers.

Two procedures were used to approximate r_l. In the first procedure, a constant value of r_l = 75 s m^{-1} was used during all time periods to represent a mean daily value for r_l for use with half-hourly calculations with stability correction (see last entry of table 11.2). Calculations of r_a were made with and without stability correction. Resulting calculations by the PM equation (eq. 8.2, 11.1) with these resistances are labeled "P-M, no stab.corr." and "P-M, Int.stab.corr." In the second procedure, a value of $r_{l_{min}}$ = 40 s m^{-1} was used in conjunction with the stomatal conductance reducing functions ($g(\ )$) to provide a variable r_l during the calculation periods. Calculations for r_a were made using integrated stability correction functions. Resulting calculations by the PM equation are labeled "P-M, Int.stab.corr.,g()" in fig. 11.12.

In the first procedure, (θ) was set equal to 1.0 to reflect high soil water conditions at each site. Data in fig. 11.5 show products of $g(R_s)$ $g(VPD)$ $g(T)$ calculated for Aug. 2, 1990 at Logan and May 2, 1967 at Davis reached highs of about 0.75 during midmorning hours and then decreased to about 0.4 to 0.6 during afternoon hours when both VPD and T increased. In the first procedure with constant r_l, the resulting values for r_s were 27 s m^{-1} at Logan and 50 s m^{-1} at Davis, the differences being due to differences in LAI.

In the second procedure, $r_{s_{min}}$ equaled 14 s m^{-1} for g_{max} = 0.07 m s^{-1} at Logan and $r_{s_{min}}$ equaled 27 s m^{-1} for g_{max} = 0.037 m s^{-1} at Davis. The inclusion of the $g(\ )$ functions increased the values for r_s in the second procedure from 14 s m^{-1} to 35 s m^{-1} during afternoon hours at Logan and from 27 s m^{-1} to about 50 s m^{-1} at Davis. Surface resistance during nighttime hour ($R_n < 0$) was set equal to 200 s m^{-1} to approximate r_s for moist soil beneath the grass canopies (see discussions in the section on Soil Evaporation and r_s).

The PM calculations fit lysimeter measured ET well using both procedures for estimating r_s (constant r_l = 75 s m^{-1} throughout the calculation periods and $r_l = r_{l_{min}}$ of 40 s m^{-1} divided by $g(R_s)g(T)g(VPD)$). Calculations were influenced little by inclusion of stability corrections at either location, where values for the Monin-Obukhov z/L numbers ranged from -0.5 to over 2 at Logan and -0.7 to 0.1 at Davis. This is in contrast to the $ET = R_n - G - H$ calculations presented in fig. 7.6 which were significantly influenced by stability corrections, especially at Davis. The seemingly lack of influence of stability correction on the PM estimates stems from the presence of $1/r_a$ in both the numerator and in the denominator of the PM equation, so that a major amount of change in $1/r_a$ due to stability correction is self-cancelling, depending on the relative magnitudes of $R_n - G$, $e_z^o - e_z$ and r_s. This was not the case with the energy balance calculations, which were shown in fig. 7.6. Under strong conditions of instability brought on by water stress, effects of stability correction on PM estimates would become noticeably stronger.

There was slight underestimation during the highest half-hour period at Davis at about 1300 hours and there was a slight "lag" in estimates relative to lysimeter measurements during morning hours at Logan. The PM equation predicted slight, net condensation of moisture (dew) during portions of nighttime periods at both locations, especially when corrected for stability. The gain in weight due to condensation was also indicated by most of the nighttime lysimeter records, especially at Davis. Under these conditions, r_s should technically be set to 0. However, without the use of a highly sensitive lysimeter or a leaf wetness sensor, it is often difficult to predict when condensation is occurring. In the examples shown in fig. 11.12a and 11.12b, use of

$r_s = 0$ rather than $r_s = 200$ s m^{-1} made very little difference in the ET predictions at night since aerodynamic resistances were high due to very light wind and stable conditions, along with very small *VPD*'s. The "dips" in calculated and measured ET during midafternoon periods at both locations were due to cloud fronts, which passed overhead, reducing net radiation and air temperatures. Overall, agreement between the PM equation and measurements was very good, with the equation showing very similar sensitivity to changes in solar radiation (overhead clouds) and wind speed as the lysimeter measurements.

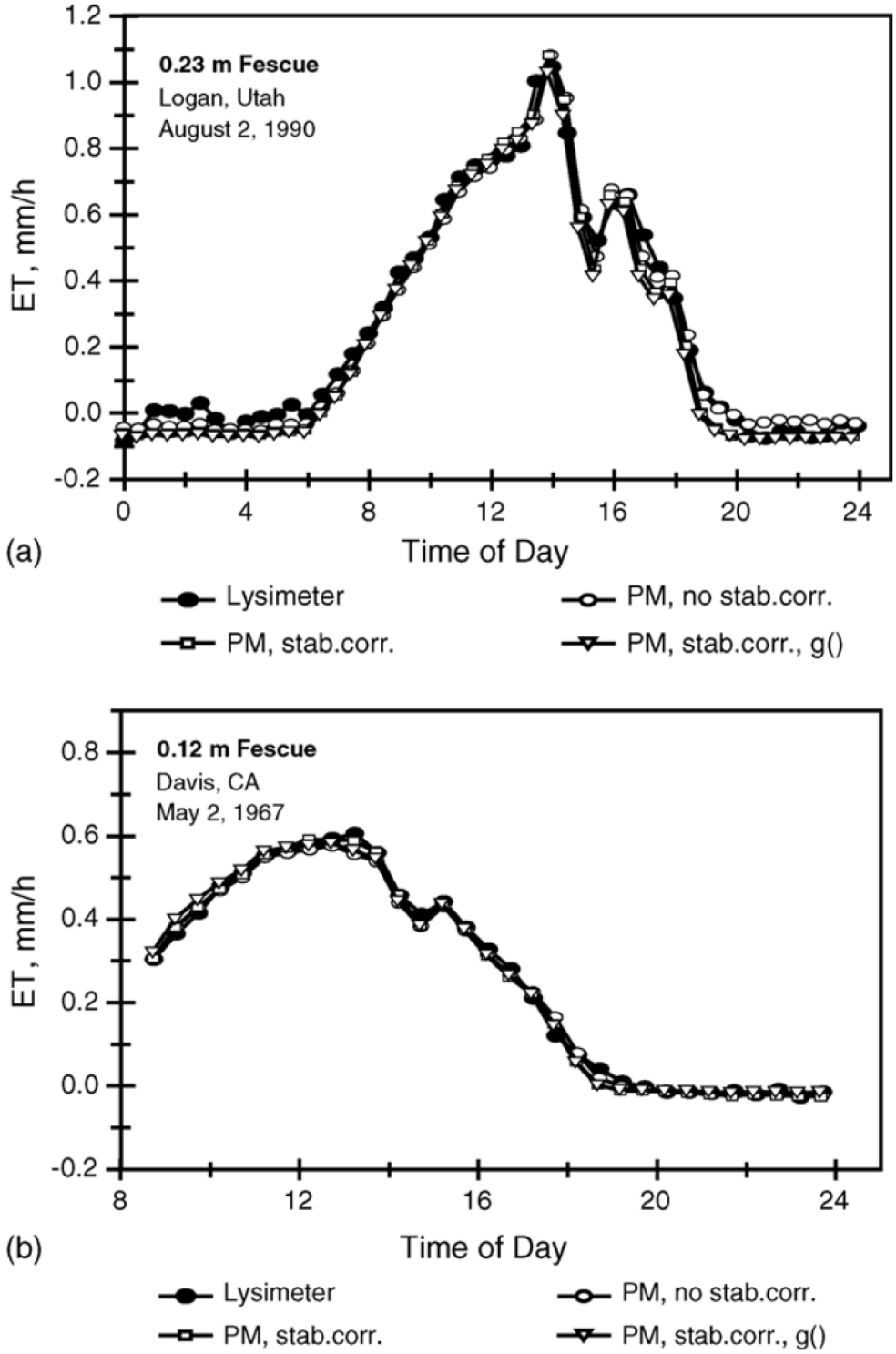

Fig. 11.12. Comparisons of measured ET and ET estimated using the PM equation (eq. 8.2, 11.1) with and without integrated stability correction with $r_l = 75$ s m^{-1}, and with integrated stability correction and $r_l = r_{l_{min}}$ of 40 s m^{-1} divided by $g(R_s)g(T)g(VPD)$ for: a) 0.23 m Fescue Grass at Logan, Utah, data from Allen and Fisher (1990); and b) 0.12 m Fescue Grass at Davis, CA (W.O.

Pruitt 1994[3], with data from Morgan et al. (1971)). Source: Data from Allen and Fisher, Morgan et al. (1971).

Daily Calculations under Conditions of Soil Water Stress

The PM equation was applied to a three-month data set of micrometeorological and lysimeter data from Logan, Utah which were collected during a March 20 - June 30, 1992 study. The grass cover was tall fescue grown for forage. All irrigation of the lysimeter and surrounding 40-ha field was withheld during 1992 so that the grass crop experienced progressively increasing water stress caused by progressively decreasing soil water. Fig. 11.13 exhibits daily (24-hour) calculations of ET made using the PM equation (eq. 8.2, 11.1), where the P-M (no stress) calculations were made using r_s calculated using eq. 8.9 with $r_l = 100$ s m^{-1}. This curve represents the upper limit of ET under conditions of limited water stress. The other curves in the figure represent calculations by the PM equation where r_s was reduced by dividing r_s by the product $g(T)g(\theta)$. The $g(\theta)$ function was calculated using the three methods described in the section on stomatal conductance functions (eqs. 11.47, 11.48, and 11.50). Because the computation time steps were 24-hour, the $g(R_s)$ and $g(VPD)$ functions, which apply to instantaneous values of R_s and VPD, were set equal to 1.0. However, because the first part of the season (late March and April) was cool, the $g(T)$ function was applied to the daily time steps to adjust for low stomatal conductance caused by low daytime temperatures. Parameters used in eq. 11.45 were $T_L = 0$°C, $K_T = 20$°C and $T_H = 40$°C. Because calculations were made on a 24-hour basis, a mean value of daytime air temperature for use in eq. 11.45 was approximated for each 24-hour period as $T = (2\ T_{max} + T_{min})/3$. In addition, no corrections for boundary layer instability were made since calculations were made on 24-hour time steps.

The grass height for the Logan data set ranged from 0.01 m on March 20 to 0.60 m in June. Leaf area index for the tall fescue was estimated as $LAI = 0.20\ h$, where h is mean plant height in m, based on a set of LAI measurements made at $h = 0.4$ m. LAI was linearly reduced after June 1 to account for leaf senescence and firing of leaves near the bottoms of plants caused by effects of the drought conditions. Total LAI was reduced by 1.5 after April 25 due to a hard frost (-5°C) on that date. Because of the tall height of the forage and large LAI, LAI_{eff} in eq. 8.9 was computed using eq. 8.11 by Ben-Mehrez et al. (1992).

Parameters applied in the $g(\theta)$ functions were $K_\theta = 1.2$ in eq. 11.47, $K_\theta = 0.25$ in eq. 11.48, and $K_{sf} = 1.2$ in eq. 11.50. A value of $K_\theta = 1.2$ was required in eq. 11.46 rather than the $K_\theta = 6.7$ suggested by Stewart (1988) for Scotts pine, in order to better follow measured data. The value $K_\theta = 0.25$ in eq. 11.48 which was suggested by Stewart and Verma (1992) for Kansas prairie worked well for the fescue at Logan. The values for θ_{DU} and θ_{LL} for the clay loam soil were 320 and 140 mm m^{-1}. The rooting depth for the fescue grass was taken as 1 m.

The $ET = K_c\ ET_o$ approach was also applied to this data set, with K_c estimated using eq. 10.2 ($K_c = K_s K_{cb} + K_e$). The K_{cb} curve was constructed using $K_{c1} = 0.4$ and $K_{c2} = K_{c3} = 1.1$. The K_s values were calculated using eq. 10.4 and K_e was calculated using eqs. 9.19, 9.21 and 9.22 where θ_{fc} and θ_{wp} had the same values as for the $g(\theta)$ functions and p in eq. 10.5 was set equal to 0.4. ET_o was calculated using eq. 8.15.

All three $g(\theta)$ functions performed relatively well in reducing the estimated ET according to soil water availability. Eq. 11.48 followed lysimeter ET most closely, with eq. 11.47 overestimating lysimeter measurements during June when soil water was low and with eq. 11.50

[3] Personal communication.

estimating well during April and May, but underestimating measurements during June by about 30%. The K_cET_o procedure overestimated lysimeter ET by about 20% during late April and early May since no reduction in K_c occurred until 40% of available soil water was depleted. The procedure underestimated lysimeter measurements during June by about 30%. In general, all four water-stress procedures or functions evaluated show usefulness in estimating effects of decreasing soil water.

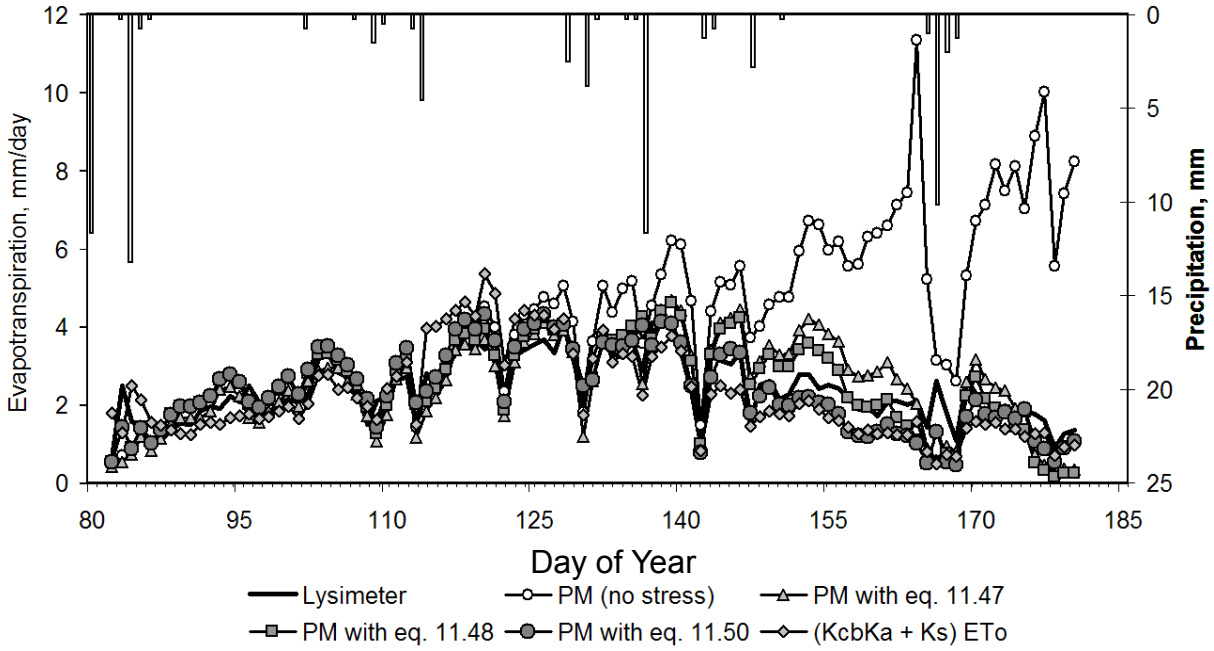

Fig. 11.13. Comparison between measured ET and ET estimated using the PM equation (eq. 8.2, 11.1) for Fescue Grass Forage at Logan, Utah, March - June, 1992 under conditions of low soil water using 24-hour calculation time steps for three $g(\theta)$ functions plus the dual crop coefficient method. Source: Data from R.G. Allen (1994)[4].

Other Applications of the Single-Layer Penman-Monteith Model

Kustas (1990) applied single- and two-layer PM resistance models to a furrowed cotton field having 20 percent cover and a dry soil surface in an arid environment. Results were compared with eddy correlation and remotely sensed energy balance methods. The single-layer model generally performed better than the two-layer model, but only when using a bluff-body correction to the aerodynamic resistance made by incorporating heat and water vapor transfer by molecular diffusion into Kolmogorov-scale eddies. However, the empirical adjustment to the surface resistance with the one-layer approach was not applicable over a wide range of conditions. For the two-layer model, large changes in parameters for computing soil evaporation had a relatively small impact on computed fluxes while a significant change in estimated leaf area appeared to amplify deviations between measured and modeled ET values.

[4] Personal communication.

Farahani and Bausch (1995) evaluated performance of single-layer PM and S-W ET models over a growing season by comparing against Bowen ratio-based measurements over irrigated maize near Fort Collins, Colorado. When LAI was < 2, the PM model, as parameterized for canopy resistance, only, did not perform well. When LAI exceeded 2, performance improved. The S-W model performed satisfactorily over the entire range of canopy cover, underestimating ET by 4% over the season. Farahani and Bausch found evaporation from soil estimated by the S-W model to comprise 29% of total ET. This figure was larger than expected for furrow-irrigated maize. Soil evaporation was only about 15% of total ET when LAI was greater than 3. Their study concluded that a generalized and straight forward functional relationship describing soil and canopy resistance is needed and that bulk stomatal resistance should be estimated using a dynamic calculation for effective LAI.

Schaap and Bouten (1996) compared evaporation from a forest floor beneath a dense Douglas fir stand with weighing lysimeter measurements during 44 days in early spring and summer. The single layer PM was used to model the evaporation rates. Values of resistance parameters were changed slightly when the Penman–Monteith model was optimized for measured evaporation rates rather than to reproduce measured temperature differences between air and surface. With appropriate parameter sets, the model estimated measured hourly forest floor evaporation rates and surface temperature dynamics relatively well. They showed that in a forest understory, the PM aerodynamic term dominates over the available energy term. As a result, the evaporation flux was matched by an almost equal, downward sensible heat flux to the surface from the canopy above. Forest floor water content dynamics exhibited a strong control on evaporation flux. Spatial variability in forest floor water contents caused the forest floor evaporation to range from 0.19 mm d^{-1} in a dry part of the forest to 0.3 mm d^{-1} in a wet part.

Daamen et al. (1998) conducted an interesting study of fluxes from trees and orchard floor in a sheltered lemon orchard where the canopy of the lemon trees covered 39% of the orchard floor and bare understory. Lemon tree transpiration was measured using the stem heat balance method with branch measurements scaled up to canopy level. Those measurements compared well with Penman–Monteith-based transpiration estimates. For the understory, the sum of latent and sensible heat fluxes measured by eddy correlation equaled available energy. Eddy correlation and Bowen ratio methods of flux measurement compared well in the understory.

Ortega-Farias et al. (2005) applied the single layer PM model to a furrow-irrigated tomato crop having LAI ranging from 1.3 to 3 under different soil water and atmospheric conditions. They used variable surface canopy resistance model where resistance was computed as a function of environmental variables air temperature, vapor pressure deficit, net radiation and soil heat flux and normalized soil water availability. Comparisons against ET from a Bowen ratio system indicated errors of 3.6% and 3.9% for 20-minute and daily periods. ET based on the FAO-56 K_c ET_o method underestimated daily ET with an error of 5.2%.

Were et al. (2008) combined internal boundary layer and surface resistances of a multi-layer / multi-source PM model similar to that described in fig. 11.1e for sparse brush vegetation to create bulk r_{ah} and r_s resistances to use in the single layer PM method. They found the best combination for r_s to be:

$$\frac{1}{r_s} = \frac{f_c}{r_{sv} + r_{sss}} + \frac{1 - f_c}{r_{sse}} \tag{11.62}$$

where f_c is the effective fraction of ground shaded by vegetation and r_{sv}, r_{sss} and r_{sse} are surface resistances for vegetation, shaded and exposed soil described in fig. 11.1e. The formulation of eq. 11.62 follows that of eq. 11.57 for combination of resistors in parallel. Were et al. (2008) found best agreement between the single layer PM and multilayer model when the bulk aerodynamic resistance, r_{ah}, in the single layer model was formulated from the multilayer resistances as:

$$r_{ah} = f_c\left(r_{hv} + r_{hss}\right) + \left(1 - f_c\right) r_{hse} + r_{am} \tag{11.63}$$

where the boundary layer resistances are defined in fig. 11.2e. Eq. 11.63 performed better than using the classical function for combining the boundary layer resistances in parallel with aerodynamic resistance in series.

Zhang et al. (2008) compared the single layer, multi-layer and patch models with Bowen ratio measurements of ET for a vineyard in the arid desert region of northwest China. Generally, the variation in estimated ET from all three models was similar to that of measured ET. They found the single layer model, as parameterized, to overestimate ET significantly, with the multilayer and patch models to agree better with measurements. Following a frost, the patch model significantly overestimated ET because the canopy resistance of the vines was substantially reduced.

Irmak and Mutiibwa (2009) applied the single layer PM to maize over a growing season in Nebraska with comparisons to Bowen ratio derived ET. They found a seasonal average minimum bulk canopy resistance of 56 s m^{-1} inversely computed from the BREBS data that was relatively consistent day to day. They also investigated the impact of source of meteorological data to the PM method, including using weather data from a 'near-reference' grassed weather station and using meteorological data from the BREBS system itself, measured over the maize canopy. There was good agreement (RMSD = 0.11 mm h^{-1}) between the PM estimates using grassed weather data and ET from BREBS with 9% overestimation. When applied using weather data measured over the maize crop, including measured R_n and G, the performance of the PM improved with estimations within 2% of the ET from BREBS and RMSD = 0.08 mm h^{-1}. A significant amount of this improvement was due to using common R_n and G in both the BREB and PM calculations, which compromised the independence of the two methods, as well as in the inverse solution of mean values for r_s. In general, the use of grassed weather station data did not substantially impact the application accuracy of the PM for the maize crop.

Zhao et al. (2010) applied the single layer PM model to a maize field in an arid region of Northwest China and estimated bulk canopy resistance using a Jarvis type of approach (eq. 11.37) with parameterization by Noilhan and Planton (1989) (N-P) and Jacobs and De Bruin (1997) (J-D) approach based on plant physiology, where a correlation relationship between the leaf stomatal conductance and the net photosynthetic rate at leaf scale is used to up-scale conductance from a leaf to the canopy. The latter method is able to incorporate impacts of CO_2 concentrations on stomatal conductance and thus transpiration as well as impacts of leaf temperature, radiation levels and vapor pressure deficit. ET estimates were compared with half-hourly measurements from an eddy covariance system. Results indicated that the N-P approach slightly underestimated bulk canopy resistance, while the J-D approach, as parameterized, overestimated. ET estimates using the N-P approach were more consistent than those with the J-D approach during the full growing season. The PM model with J-D bulk canopy resistance

slightly underestimated ET throughout the maize growing season, but overestimated ET during a period of dry soil surface. The relatively good fit of ET from the P-M model with N-P bulk canopy resistance on a half-hourly time step was concluded to be partially due to the relatively high homogeneity and lack of water stress in the maize field.

Examples of applications multi-layer Penman-Monteith models

Brenner and Incoll (1996) investigated the importance of clumping of vegetation for modeling evaporation from soil and shrubs in SE Spain using single layer, multilayer and patch models. Stomatal conductances of shrubs were found to decline linearly with increasing in-canopy water vapor saturation deficit (D_c). Soil surface resistances were found to increase quadratically with time after wetting of the soil surface. A patch model that included clumping was compared with single- and two-source models. The multilayer model included feedbacks between plant resistances, in-canopy vapor pressure saturation deficits, and total evaporation from the surface. The single-layer and two-source patch models overestimated transpiration by 1% and 8%, respectively, whereas the clumped model underestimated transpiration by 5%. They concluded that overestimation of transpiration by the conventional two-source model resulted primarily from over-estimation of radiation absorbed by the canopy. The underestimation by the clumping model may have resulted from underestimation of the long-wave radiation emitted from the soil and absorbed by the canopy.

Sene (1996) applied the two-layer Shuttleworth-Wallace (S-W) model to a sparse vineyard in Spain. The bulk canopy resistance was found to be generally proportional to single leaf resistance divided by total LAI. Diurnal variations in r_l exhibited a daily minimum value for r_l of about 200 s m^{-1}, increasing to about 700 s m^{-1} near dawn and dusk. The diurnal trend was similar from day to day suggesting that it was primarily linked to variations in solar radiation. A fixed diurnal pattern scaled on the midday value was used with the midday value determined as a function of leaf area index. Sene used a parameterization for soil heat flux of exposed soil as $G = G_{dry} [1 - 3(\theta / \theta_s)^2]$ where θ is the volumetric water content of the shallow surface soil layer, θ_s is the saturation water content, and G_{dry} is soil heat flux of a dry soil, $G_{dry} = 0.29 R_n - 23$, W m^{-2}. Undercanopy G was estimated as 0.7 of G for exposed soil.

Daamen (1997) applied a two-layer PM style model to sparse millet in Niger where the model was patterned after the S-W model and Choudhury and Monteith (1988). The exception was the use of a heat and mass transfer model for soil heat and vapor fluxes rather than parameterization of a soil surface resistance term. Simulated and measured values of daily evaporation from soil were not significantly different and simulated soil water content was generally within one standard deviation of the mean measured value. Using their model, they were able to test several parameterizations of the soil surface resistance term for the S-W model and found that a simple linear resistance model where soil resistance increased with time after rainfall may be adequate in a two source model when leaf area index is 2 or higher, but it is inadequate for lower leaf area indices. Daamen (1997) also simulated micro-scale transfer of heat from dry soil to the vegetation canopy and found the greatest increase of transpiration above the incident net radiation partitioned to the canopy occurred at LAI between 1.0 and 1.5.

Iritz et al. (1999) tested a modified version of the two-layer S-W model for a mixed 50–100 year old boreal forest in central Sweden and compared estimates against eddy correlation flux measurements. Their model had modified terms for bulk canopy resistance and aerodynamic

resistance. A soil moisture sub-model was used to estimate soil-water induced regulation on canopy resistance. That sub-model performed well in estimating ET over a growing season. Their model assumed that canopy stomata and boundary-layer resistances acted in parallel at some hypothetical level in the canopy.

Domingo et al. (1999) applied a two-source patch model to *Retama sphaerocarpa* shrubs in eastern Spain and tested model parameters for their importance in controlling evaporation. ET estimates were compared with measurements by a Bowen Ratio Energy Balance system (BREB) and transpiration estimates were compared against measurements by sap flow of shrub stems. Modifications were made to the original two source clumped model to significantly improve agreement between estimated and measured ET rates. Modifications included improved parameterization of soil surface conductance, a more detailed description of the radiation balance, and improved parameterization of the soil aerodynamic conductance terms. Improvements in the soil surface conductance estimates made the most significant improvement in model estimates, with the other two modifications showing less significant improvement in estimation of evapotranspiration. A sensitivity analysis indicated that relatively large variations of leaf area index or albedo caused little variation in ET, whereas variation in soil water content caused large change in estimated ET. Transpiration rates of shrubs (measured and modeled) were largely independent of surface soil moisture (0–25 cm) indicating that the shrubs accessed reserves of water deep in the soil.

Gardiol et al. (2002) compared a simplified patch model with the single layer PM and Shuttleworth–Wallace (S-W) models and against ET measurements from a corn crop obtained by soil water balance at Balcarce, Argentina. The single-layer model, as parameterized, underestimated ET. The S-W model, with improved simulation of soil evaporation estimated total ET relatively accurately for LAI < 4 (sparse canopy condition) but overestimated total ET when LAI > 4.

Fisher et al. (2004) applied a single layer PM and a two-layer S-W model to a ponderosa pine forest ecosystem at an Ameriflux site in Northern California. The S-W method performed better than did the Penman-Monteith (1965) model, although a simple Priestley-Taylor model with a defined α value performed best compared to the other models. This suggests difficulty in adequately describing surface and aerodynamic parameters in the more complex models or uncertainties in the eddy covariance measurements. A constant canopy resistance was used in the S-W and PM models. ET estimates increased by as much as 26% when canopy resistance was set to a minimum value and decreased by as much as 20 % when canopy resistance was set to a maximum value.

Mo and Bevan (2004) applied two and three-source multi-layer models to a wheat crop and showed that parameter sensitivities were different between the model types, with the three-source model having more constrained uncertainty bounds. They found net radiation on shaded leaves to be about 20% of that on sunlit leaves, whereas latent heat flux around noon from shaded leaves was 50% of that from sunlit leaves. They concluded that shaded leaves acted as sinks for sensible heat, reducing predicted temperature differences between the two groups of leaves.

Villagarcia et al. (2007) compared two methods for obtaining soil boundary-layer resistance (r_{hs} in fig. 11.2) in multi-layer models, with one method based on turbulent diffusion theory (TD) (i.e., eq. 11.9-11.12) and another based on inverse calculation of boundary-layer resistance using an energy balance between heated and unheated sources/sensors placed in the canopy (EB). They studied how estimates from each method were affected by canopy structure parameters for typical sparse vegetation. They found the EB-based boundary-layer resistances,

unlike those from TD, to implicitly consider peculiarities of plant architecture and structure, as well as the presence or absence of substrate under canopies. In contrast, when applying the TD method, quantitative descriptions for vegetation (average vegetation height, leaf area index, fractional vegetative cover, drag coefficient, and the eddy diffusivity decay constant, *n*) are all necessary, which is not only difficult to obtain in most applications, but also tended to be insufficient in explaining the development of the soil boundary layer in sparse semiarid vegetation. The advantages of using the EB method are both practical and theoretical, although in-situ measurements are required. Positioning of required heaters and sensors was relatively straightforward and did not require knowledge of the aerodynamic attributes of the vegetated area. Villagarcia et al. (2010) in a following study showed that soil surface resistance, r_{ss}, was best estimated using shallow simulation or measurements of soil surface water content, preferably at 1 cm depth.

Ortega-Farias et al. (2007) applied the two-layer S-W model to a drip-irrigated Cabernet Sauvignon vineyard in Chile and compared against half-hourly ET from eddy covariance with relatively good results. RMSE was 29 W m^{-2}. The largest disagreement occurred under dry atmospheric conditions. They found the S-W model formulation to be sensitive to error in leaf area index and mean stomatal resistance where change in ET was as high as ±20 and ±18% when these parameters were varied by ±30%. ET estimates were not substantially affected by error in estimation of aerodynamic resistance.

Poblete and Ortega-Farias (2009) expanded their application of multi-layer models on vines to a three-source clumped (patch) model with application to a drip-irrigated Merlot vineyard trained on a vertical shoot positioned system under semi-arid conditions in Chile. The vineyard had an average fractional cover of 30% and the model was partitioned among canopy transpiration, evaporation from soil under the vine canopy, and evaporation from soil between rows, with weighting according to fractional covers following a formulation by Brenner and Incoll (1997). Most parameterizations of resistances followed those of Shuttleworth and Wallace (1985) or Shuttleworth and Guerney (1990). Results were compared against two years of ET from an eddy covariance system. Accuracy of the clumped model, as parameterized, was good, with RMSE of 0.33 mm d^{-1} and RMSE for daytime LE of 36 W m^{-2}. They found major underestimation on clear days following rainfall or foggy days and during high evaporation demand periods when λE exceeded 300 W m^{-2}. Maximum values for both measured and simulated ET occurred about 2 h after the peak values of R_n due to lags in temperature and vapor pressure deficit. They concluded that application of a clumped model requires a good characterization of the vineyard architecture.

Ortega-Farias et al. (2010) employed variable canopy resistance functions in a two-layer S-W model over a drip-irrigated Merlot vineyard with RMSE = 34 W m^{-2}. Canopy resistance followed the Jarvis style of conductance functions (eq. 11.37) with parameterization for photosynthetically active radiation, vapor pressure deficit, air temperature and soil water stress.

Zhongmin et al. (2009) applied the two layer S-W model to partition ET into evaporation and transpiration (T) for four grassland ecosystems in China. Estimates were compared against ET from the eddy covariance technique. Monte Carlo simulations were used to estimate key parameters in the model and to evaluate the accuracy in model partitioning (i.e. E/ET). Results showed good agreement with measurements at both hourly and seasonal timescales. The model tended to underestimate ET by 3–11% on rainy days, probably due to the lack of model representation of rainfall interception. In general, E accounted for a large proportion of ET from the grasslands, with E/ET ranging from 12% to 56% during the peak growing season and annual

E/ET ranging from 50% to 67% across the four ecosystems. Canopy stomatal conductance controlled E/ET at the diurnal timescale, and the variations and magnitude of leaf area index (LAI) explained most of the seasonal, annual, and site-to-site variations in E/ET. A simple linear relationship between growing season LAI and E/ET explained 80% of the variation observed over the 10 modeled site-years. Daily E/ET decreased to a minimum value of 10% for values of LAI greater than 3 in a grass system having a dense canopy. The sensitivities of E/ET to changes in LAI increased with the decline in water and vegetation conditions at both the seasonal and the annual time scales.

11.11 Applications of Evapotranspiration Models using Remote Sensing Inputs.

The advantage of the PM and other models is that they can be applied with relatively routine weather data on hourly or daily timesteps. The continuous applications have the strong advantages of incorporating effects of precipitation and changing weather conditions on total aggregated ET. They also have the strong advantage of being coupled with soil water balances to provide feedback on relative water supply to support the ET process. A disadvantage of soil and weather-based process models is in the parameterization of these models over large areas having wide variation in vegetation and water availability. In these situations, the applications can be substantially assisted, or even made possible, by the use of vegetation information and thermal information provided by remote sensing. Generally the remotely sensed information is via satellite due to the large extents of coverage.

Satellite coverage at moderate resolution (< 50 m pixel sizes) is generally only available from polar-orbiting satellites such as Landsat, SPOT, ICONOS, Quickbird, etc., so that imagery for a particular location is relatively infrequent. For example, Landsat revisit time is each 16 days. The infrequent coverage is insufficient for estimating a time-integrated ET in and of itself (Allen et al. 2007a). However, when coupled with an hourly or daily ET process model, the use of the infrequent satellite imagery to improve estimates of surface albedo, surface temperature, surface roughness, and the partitioning of surface energy between latent and sensible heat fluxes can greatly improve the accuracy of the process-based estimates.

Moran et al. (1996) used remotely-sensed measurements of surface reflectance and temperature to apply the PM equation to partially-vegetated fields with improved estimates of percent vegetation cover and canopy resistance. The Penman-Monteith equation was combined with the energy balance equation to estimate the surface temperature (T_s) associated with four states: surfaces characterized by full-cover vegetation and bare soil with evaporation rates at potential and zero. T_s values from satellite data were linearly interpolated between full-cover and bare soil conditions to provide information for intermediate states. Maps of surface air temperature and wind speed were combined with maps of surface temperature and spectral vegetation index to produce regional estimates of evaporation rates for a grassland biome.

Kustas (1990), Kustas et al. (2004), Anderson et al. (2005), Li et al. (2005), Kustas and Anderson (2009) have led the development of the two-source patch model TSEB that utilizes radiometric surface temperature inputs from satellites, surface reflectance and vegetation indices to estimate ET from sparse canopies.

The METRIC model (Mapping Evapotranspiration at High resolution using Internalized Calibration) (Allen et al. 2007a) applies a full surface energy balance to Landsat, MODIS and other thermally equipped satellite image products to develop images of the fraction of alfalfa-reference ET, ET_rF, that are then interpolated using a spline function and multiplied by daily ET_r

to produce time series of daily and monthly ET. Satellite-based mapping of ET provides valuable spatial information on within-field and field-to-field variation in ET and will become increasingly used in water rights management, water transfers and streamflow depletion studies.

11.12 Measurement and Estimation of ET on Sloping Lands

Many studies of hydrologic processes under natural conditions involve sloping land surfaces. On sloping surfaces, the potential amount of solar energy converted into ET will increase for southward facing slopes (in the northern hemisphere) and will decrease for northward facing slopes. The increase or decrease will be related to the change in the angle between the slope and the angle of the sun (Swift 1976; Perez et al. 1986). Under most conditions of small slope (< about 15°), ET calculations can be made on a horizontal basis with little error. However, the user must bear in mind that the ET flux density calculated horizontally (for example expressed in mm or $m^3\ m^{-2}$) is based on a per unit horizontal land area. To convert to a unit area basis parallel to the land slope, a trigonometric adjustment should be made.

When calculations are made on an along-slope basis, then net radiation measurements or calculations should be made parallel to the slope, or calculations of R_n must be adjusted for the effect of slope. With slopes greater than about 15%, horizontally measured R_n adjusted for slope angle can deviate from R_n measured parallel to the slope, since the upper surface of a horizontally-placed radiometer may "see" some long-wave and reflected short-wave radiation from the ground or vegetation surface uphill (Nie and Kanemasu 1989; Fritschen and Qian 1990). When measurements of R_n are made parallel to slopes, the interpretation of measurements is more straightforward than if the radiometer is placed horizontally. When parallel to the slope, the upper surface(s) of the radiometer see an unobstructed view of sky (except for obstruction by cross-valley terrain) and the bottom surface(s) see ground and vegetation only. In mountainous areas, R_n on a slope can be impacted by long-wave emissions from cross valley slopes. In the case of a south facing slope, the cross valley emission will be smaller than in the case of a north facing slope that views a warmer south-facing slope. In all cases, the thermal emission of the cross-valley slope will be greater than that from the atmosphere and should be accounted for. Allen et al. (2006a) developed integrated equations for estimating daily net radiation on slopes assuming infinite slope lengths. Flint and Childs (1987) presented a more complex model for solar radiation on slopes that uses terrain models to aacount for surrounding ridges and tall trees that may block both direct beam and diffuse sky short wave radiation.

On slopes, wind speeds used in ET equations that are applied on an along-slope basis should represent wind movement parallel to the slope, and "z" heights used in resistance calculations are expressed as perpendicular to the slope. Examples of applications of ET equations for sloped areas include Dozier and Frew (1990) and Neale et al. (1995).

Other problems in calculating or measuring ET in areas having variable land slope include convergence or divergence of wind streamlines, especially downwind of abrupt changes in slope. This can cause severe errors in eddy correlation and Bowen ratio measurements. In addition, density-induced drainage of air in down-slope directions during periods of low solar radiation and in up-slope directions during periods of high solar radiation, can substantially affect local wind speeds, air temperatures and vapor gradients, especially during calm periods. In application of ET equations over areas having large changes in elevation, air temperatures can be

adjusted during extrapolation over areas with changing elevation using lapse correction (about 0.01°C m^{-1} for nonsaturated air).

11.13 Evaporation of Intercepted Rainfall

When leaves are wet from rain, r_l effectively becomes zero and evapotranspiration occurs at substantially higher rates than from dry leaves, all other micrometeorological factors being equal. Evaporation of intercepted rainfall can be a significant portion of the water balance, especially in forests with large total leaf area and where single leaf stomatal resistances are large.

Interception is usually measured as a difference between gross precipitation and that reaching the soil. In forests, the annual interception may be 10-40% of total precipitation (Zinke 1967; Sharma 1985), depending on canopy storage and rainfall amount, intensity and frequency. Rutter (1975) and Rutter et al. (1975) estimated canopy storage during individual rainfall events to vary from 0.8 to 1.5 mm for established forests, with no distinct difference between storage capacity of forests and herbaceous species. Dickinson (1984) approximated maximum canopy storage, S as:

$$S = 0.2\,LAI \tag{11.64}$$

where S is in mm and LAI is total leaf area index.

The potential increase in total ET due to evaporation of intercepted rainfall can be inferred from the PM equation (eq. 11.1), if one ignores feedback effects of evaporation on conditioning of the air boundary layer, as:

$$\frac{E_i}{ET_c} = \frac{\Delta + \gamma\,(1 + \frac{r_s}{r_a})}{\Delta + \gamma} \tag{11.65}$$

where E_i is potential evaporation (or ET) during evaporation of intercepted rainfall and ET_c is total ET during a similar period having a dry canopy, but with the same T, RH, and wind measurements. Because r_a of forests is generally small and r_s of forests is generally large relative to agricultural crops, the ratio of r_s / r_a is large for forests, characteristically ranging between 10 and 70 or more (Jarvis et al. 1976). This is in contrast to agricultural crops, which commonly have ratios close to 1. Therefore, the ratio E_i / ET_c can be as high as 5/1 for forests as compared to ratios of perhaps 1.6/1 for agricultural crops. These ratios assume that the canopies are exposed to the same weather conditions under wet and dry scenarios. However, this is seldom the case, where the large evaporative flux density from a wet forest canopy will invariably humidify and cool the equilibrium boundary layer above the canopy, thereby reducing the vapor deficit gradient and consequently the ratio of E_i / ET_c. The modification of the weather of the boundary layer was discussed previously in the section on weather measurement. It should also be understood that the period of E_i may be quite short, depending on the storage capacity of the canopy.

Rutter et al. (1975) proposed a generalized method for predicting evaporation of rainfall interception in forests. A variation of his proposed method is included here. If variable S is defined as the surface storage capacity of a canopy (maximum retained interception), expressed as mm depth over the land surface, then when the amount of water on a canopy, C, equals or exceeds S, evaporation of intercepted precipitation, E_c, is set equal to E_i as computed using the

PM equation (eq. 11.1) with $r_s = 0$. When $C < S$, then E_c is reduced in proportion to the ratio of C to S as:

$$E_c = E_i \frac{C}{S} \tag{11.66}$$

When $C \geq S$, it is assumed that transpiration during interception, T_i, is zero, and that all evaporative energy is consumed by evaporation of intercepted water. When $C < S$, T_i is estimated as:

$$T_i = \left(1 - \frac{C}{S}\right) ET_c \tag{11.67}$$

where ET_c is the ET rate from dry foliage, computed using eq. 11.1 with $r_s > 0$. Total evapotranspiration from the canopy, ET_i, at any time is computed as:

$$ET_i = E_c + T_i \tag{11.68}$$

When $C \geq S$, $ET_i = E_c = E_i$ and $T_i = 0$. When $C < S$, $ET_i < E_i$ and $T_i \leq ET_c$. When $C = 0$, $ET_i = T_i = ET_c$ and $E_c = 0$. This approach essentially assumes that evaporation from the forest floor during the interception event is zero and that all evaporation occurs within the wetted canopy. If this assumption is not true, for example in sparse canopies, then the soil evaporation component of the evapotranspiration flux should be included using procedures detailed in the preceding section on soil evaporation.

In the Rutter model, it is assumed that $(1 - p)\,P$ rainfall is added to the canopy (C term) during each computation time step, where p is the fraction of rain which falls between gaps in the canopy and P is rainfall depth during the time step. The drainage rate from the canopy, D, during a time step is computed as:

$$D = e^{(a + bC)} \tag{11.69}$$

where D has units of P and a and b are empirical coefficients. Rutter et al. (1975) suggested a value for $b = 3.7$ for most canopies for C in mm. Coefficient a is computed by noting canopy drainage rate when $C = S$. Rutter et al. (1975) determined D for a Corsican pine stand equal to 0.002 mm min^{-1} when $C = S$ and suggested estimating D for other canopies as 0.0019 S for S in mm. Table 11.6 lists typical values of p and S for forest stands evaluated by Rutter et al. (1975).

Due to the dynamic nature of the Rutter model in accounting for storage of water on the vegetative canopy with new additions of P and losses of D with time, it is important to use short measurement time steps for P and short computation time steps in the model. Rutter et al. (1975) suggested using hourly measurement and computation time steps, with time steps longer than 3 hours providing poor results.

TABLE 11.6 Values of Fraction of Rain Falling between Gaps in the Canopy, p, and Canopy Storage Capacity, S, per m^2 of Land Surface. Source: Data from Rutter et al. (1975).

Stand Type	mean tree height m	p	S mm
Corsican pine	20	0.25	1.05
Douglas fir	24	0.09	1.2
Norway spruce	10	0.25	1.5
Hornbeam, leafy	17	0.35	1.0
Hornbeam, leafless	17	0.55	0.65
Oak, leafy	15	0.45	0.88
Oak, leafless	15	0.80	0.28
Oak, defoliated	15	0.85	0.18

Generally, when computing ET on daily time steps, the increase in total ET due to evaporation of intercepted precipitation, E_{it}, can be approximated by the following:

$$E_{it} = (ET_i - ET_c)\, t_p + S \tag{11.70}$$

where ET_i is the potential rate of ET when leaves are wet, estimated using eq. 11.1 with $r_s = 0$, and ET_c is the ET rate when leaves are dry ($r_s > 0$). ET_i and ET_c should be computed using wind, humidity and air temperature measured during or surrounding the precipitation event. Parameter t_p is the duration of the precipitation event and S is canopy storage capacity. If E_{it} and S have units of mm and ET_i and ET_c have units of mm h^{-1} then t_p must have units of h. If the time of day of the precipitation event is unknown, then 24-hour averages of ET_i and ET_c can be used as a general approximation. The total evaporation of intercepted precipitation, E_{it}, converted to mm h^{-1} units, can be added to ET_c for the period encompassing the precipitation event to obtain total ET for the period. It is important to note that both ET_i and ET_c are almost always less during a rainfall event as compared to periods with no rainfall due to reduced net radiation, R_n, and generally increased humidity and decreased temperature during rainfall.

12

Evapotranspiration from Land Surfaces: Regional Estimates

12.1 Introduction

Estimates of regional evapotranspiration (ET) are necessary inputs to world climate models, to regional water use and supply planning and assessment, to estimating potential food production capacities and supplies, and for hydrologic studies. Methods for determining ET at specific locations cited in chapter 11 and listed in this chapter are valid for regional ET estimates when applied with gridded or spatially representative data. The major problem in estimating regional ET has been in extending information from point sources to larger areas. One approach is to aggregate water balance and weather data from watershed studies to produce watershed-averaged estimates. Remote sensing is becoming progressively used to produce spatial information regarding water consumption. Current applications typically involve remote sensing combined with surface energy balance models.

Agricultural cultivars have been selectively developed over the years for maximum agronomic production. Consequently, stomatal resistances of crop cultivars are generally low (unless developed specifically for drought tolerance) and cultivated plants transpire at near potential rates when water is not limiting. In contrast, natural vegetation in semiarid and arid areas has evolved over time to exercise stomatal control for survival under stressed conditions. Thus, its stomatal (or surface) resistances may be an order of magnitude greater than for cultivated vegetation and its root systems may be more aggressive. For regional ET computations, a logical division is to separate land uses into cultivated and natural vegetation. Regions can also be divided using primary precipitation gradients or into humid and arid climate zones.

For cultivated vegetation in semihumid to humid areas, regional ET is generally limited by the available energy ($R_n - G$) at the surface unless under drought. Therefore, a simple measurement or estimation of net radiation in humid areas can yield first order approximations of ET from cultivated vegetation. Regional ET may be somewhat less than R_n for natural vegetation in humid areas, ranging from 0.4 of R_n during cold periods of the year having daytime average temperature of about 0°C and approaching 1.0 x R_n during hot summer and fall months. In zones well away from the equator, a well defined cyclic relationship between λE, the latent heat of E and ET, and R_n can be expected, with higher ratios in fall than in spring. Regional ET is typically both water and energy limited in semiarid and arid areas. Therefore, a simple measurement or estimation of both net radiation and precipitation in arid areas can yield first order approximations of ET from nonirrigated cultivated vegetation.

12.2 Theory

Of the methods presented in previous chapters, the most readily applied for regional application are the water balance method, lysimeters, energy balance methods, and mass transfer or modeling methods. Application of these methods to regional studies is discussed here.

The Bowen Ratio Energy Balance method (BREB) is a combination of transport and energy balance equations measured locally. This method was presented in eq. 7.7 and 7.8 and operational procedures were discussed in chapter 7, Evapotranspiration from Land Surfaces: General Methods. The main assumptions in the Bowen ratio method, as described in chapter 7, are: 1) the transport of H and λE is one-dimensional (vertical); 2) the surface is homogeneous, dense and shallow (i.e., heat, water and momentum sources and sinks are indistinguishable); and 3) steady-state conditions exist. These assumptions are less demanding for BREB than for other meteorological techniques because the gradient measurements for the BREB are usually made close to the surface and wind speed measurements are not required. Recommendations on minimum fetch requirements are also discussed in chapter 11.

The other common method for measuring local fluxes is the eddy covariance method described in chapter 7. That method is relatively routine to set up, however, equipment maintenance and 'correction' of turbulent flux products can require substantial education and training in the physical sciences. Various precautions and recommendations are given in chapter 7 for both Bowen ratio and eddy covariance approaches.

Challenges with the BREB, eddy covariance, and other 'local' measurements of ET are in extrapolation over the region, where vegetation and water availability can be spatially variable. The BREB and eddy covariance methods can be used to calibrate or verify methods such as the Penman-Monteith method that can then be used with gridded weather and vegetation data and satellite-based energy balance and satellite-based vegetation-based methods.

For large areas of relatively wet surfaces having minimal advection, evaporation may approach an equilibrium condition. Priestley and Taylor (1972) developed an empirical relationship for equilibrium conditions:

$$\lambda E_{eq} = \alpha \frac{\Delta (R_n - G)}{\Delta + \gamma} \tag{12.1}$$

where λE_{eq} is equilibrium evaporation or evapotranspiration for a large wet area, R_n is net radiation, G is soil heat flux, γ is the psychrometric constant and Δ is the slope of the curve of saturation specific humidity versus temperature. Priestley and Taylor derived a value of $\alpha = 1.26$ for semihumid to humid areas when the region was wet following general rains. Stewart and Rouse (1977) reproduced the value of 1.26 for a saturated sedge meadow at 58° N latitude during the month of July, and for a 2-m deep lake at 46 °N latitude between June and September. The value of $\Delta/(\Delta + \gamma)$ at 25° C is approximately 0.74. Therefore, under these conditions, from eq. 12.1, $\lambda E = 1.26(0.74)\ (R_n - G) = 0.93\ (R_n - G)$ or equilibrium latent heat flux is approximately equal to net radiation.

Caution is needed in using eq. 12.1 during late-fall to late-winter months in zones well away from the equator where the long nights of negative R_n can negate to some extent the response of λET to solar radiation, R_s, and daytime positive R_n (see Nakayama et al. 1983; and Pruitt and Doorenbos 1977). They found the use of 24-h R_n to result in experimentally determined values of α close to 2.0 in winter months at Davis, California even under low or non-advection conditions. For higher latitude locations, e.g. Copenhagen, Denmark, the equation breaks down completely during winter periods when 24-h R_n becomes negative over extended periods even though some ET is produced by daytime positive net radiation. Under arid or semiarid

conditions with advection of heat in air masses, eq. 12.1 can significantly underestimate ET (Jury and Tanner 1975; Jensen et al. 1990; Jones and Kiniry 1986; Steiner et al. 1991). The recommended alternative is to estimate short crop reference ET for dry climates instead of using only R_n.

When the water supply is limited, ET will tend to be less than λE_{eq}. The Penman-Monteith (PM) type of resistance-based combination equation (eq. 8.2, 11.1) is recommended under these conditions. Values for the bulk surface resistance, r_s, for different canopies are summarized in table 11.2. Typical values are 100 s m^{-1} for forests, 40 s m^{-1} for grassland, and 30 to 50 s m^{-1} for crops. These are minimum values assuming that sufficient soil water is available. The value of r_s will increase with decreasing soil water, increasing vapor pressure deficit and decreasing R_s or R_n. Procedures for increasing r_s to reflect effects of decreasing soil water when applying the PM equation are described in chapter 11.

The value for the aerodynamic resistance term, r_a, of the PM equation is relatively large for smooth surfaces and relatively small for rough surfaces such as forests. Consequently the effect of r_s has the strongest effect over forests. For r_s = 40 s m^{-1}, $ET_c/ET_i \approx 0.9$ for grassland and ≈ 0.5 forest, where ET_c is the PM estimate for the particular cover under "well-watered" conditions (r_s = 40 s m^{-1}), and ET_i is the PM estimate with the same r_a value but with $r_s = 0$ (representing evaporation immediately following rain). The increased sensitivity of evaporation from forests to r_s was discussed in chapter 11 in the section on Evaporation of Intercepted Rainfall.

12.3 Applications

Complimentary Approach to Estimating ET

Whenever available soil water limits ET, it decreases below the maximum rate for the particular surface, and the component of sensible heat flux density to the air (H) increases, following eq. 4.1. This increases the heating of the boundary layer of air above the surface which is manifested in two ways: 1) air temperatures increase and 2) vapor pressure deficits increase. These two increases in turn increase the potential "evaporative demand" by the environment on the vegetation and form a type of feedback process, which further increases water stress in the vegetation. The total increased evaporative demand can be estimated by inserting the elevated temperatures and reduced vapor pressures measured over water-stressed vegetation into a Penman-type equation. This estimate, termed ET_{ps}, for ET potential over water-stressed vegetation, can be compared with an ET estimate which represents ET under conditions of unlimited soil water under regionally potential conditions, such as represented by the Priestley-Taylor equation (E_{eq}). Then the difference $ET_{ps} - E_{eq}$ can be used to represent the decrease in ET due to deficit soil moisture. In this case, actual ET from the water short vegetation, ET_a can be estimated as:

$$ET_a = E_{eq} - \left(ET_{ps} - E_{eq}\right) = 2\,E_{eq} - ET_{ps} \qquad (12.2)$$

Eq. 12.2 is known as the complementary approach and was first introduced by Bouchet (1963) and further developed by Brutsaert and Stricker (1979) and Morton (1983). A difficulty with the complementary method is in estimating E_{eq}, especially in semiarid areas where E_{eq} as estimated

with the Priestley-Taylor equation is less than the equilibrium, well-watered ET rate approached in semiarid regions even under moist soil conditions over long periods of time. Huntington et al. (2011) recommended estimating E_{eq} using net radiation, R_n, that represents conditions expected under well-watered conditions, which means a relatively cool surface. Discussions in chapter 11 describe how R_n can be 100 W m^{-2} greater for cool, evaporating surfaces as compared to hot, dry surfaces. Thilini et al. (2013) described applying the complementary relationship using gridded weather data from the NOAA Noah land surface model and North American regional reanalysis (NARR) data system. Szilagyi (2007) and Venturini et al. (2012) described combining complementary theory with thermal imagery from the MODIS satellite to estimate ET at the 1 km scale. For further information on the complementary method, the reader is referred to the articles by Brutsaert and Stricker (1979), Morton (1983), Szilagyi (2007), Huntington et al. (2011), and Venturini et al. (2012).

Application of Energy Balance Models to Forests and Grasslands

A number of models have been developed for estimating ET from large catchment areas. These models generally integrate various resistances affecting vapor and heat transfer within complex canopies and may consider the development of multistoried canopies over time. Early models include a forest ET–CO_2 uptake and water balance model by Running and Coughlan (1988), a forest transpiration–photosynthesis–CO_2 uptake model by Price and Black (1989), and a rangeland–snow melt–ET–heat and water flow model by Flerchinger and Pierson (1991). Some components of the Price and Black model were discussed in the previous chapter on surface conductance functions. Energy–balance–crop growth models have been developed for agricultural crops and include the CERES–Maize model (Jones and Kiniry 1986), CERES–Wheat (Ritchie and Otter 1985), ENWATBAL (Lascano et al. 1987), and SOYGRO (Jones et al. 1987). Various crop models for estimating climate risk and optimizing agronomic practices in response to climate risk were discussed at an international symposium in Brisbane, Australia in 1990 (Muchow and Bellamy 1991). Multi-layer or patch models described in chapter 11 that can be applied regionally include those by Brenner and Incoll (1997), Daamen and McNaughton (2000), Gardiol et al. (2002), Mo and Bevan (2004), Villagarcia et al. (2007), Were et al. (2008), and Lagos et al. (2009, 2012).

Sikka (1993) and Sikka et al. (1993) modified and applied the Running–Coughlan model to a 210 km^2 catchment area in northern Utah and utilized a fuzzy clustering algorithm along with LandSat thematic mapper (TM) data and digital elevation data to predict the variation in leaf-area-index (LAI) and vegetation types for hydrologic units within the watershed. Vegetation was comprised of a mixture of conifer, aspen, shrubs and sagebrush, with average LAI's for hydrologic units ranging from 0.6 to 2.5. Sikka et al. (1993) found the modified Running–Coughlan model to provide acceptable results provided computerized calibrations were made on the specific watershed using historical weather and streamflow data.

Mao et al. (2002) estimated ET for three wetland environments in Florida. Input data were based on measurements of climate data, ET and pan evaporation during 1996-1999. The results suggested that mean monthly ET for open water, cattails, and young and mature sawgrass calculated by the PM, Priestley-Taylor, reference ET and pan evaporation were all relatively close in the humid climate when monthly-varying coefficients were used. The PM method

required reliable values for canopy resistance. Seasonal and annual canopy resistance values for cattails and sawgrass for the region were presented in their tables 3 and 4.

In general, ET–vegetation development–energy balance models require rather extensive data describing the phenological development of vegetative canopy cover, photosynthetic–stomate interactions, and penetration of light within canopies. Therefore, these models are usually applied in specialized studies where accurate fluxes are needed during short time periods or in studies examining sensitivity of ET and other fluxes to changes in vegetation, climate or hydrology. Complex models will become increasingly applied with gridded weather data from the weather forecasting models coupled with land surface models.

Application of Energy Balance Models to Regional Cultivated Lands

Recently, combining satellite imagery with surface climate measurements has been used for estimating ET from large-scale cultivated lands and the productivity of water in these areas. Moran (2000) described the use of remote sensing for monitoring evaporation over managed watersheds. Bastianssen et al. (1998b, 2005) described a surface energy balance model (SEBAL) and Allen et al. (2005, 2007) and Kilic et al. (2012) described a similar model (METRIC) that takes into account slope and aspect, and measured weather data. Kite and Droogers (2000) compared estimates of ET for a basin in western Turkey using remote sensing, hydrologic models and field data. They concluded that no single method is ideal. Each has its advantages and disadvantages. A combination of methods may be better than a single method alone. They combined models at three scales, the field scale, irrigation-scheme scale, and the basin scale in the Turkey study. The three linked models enabled assessing water productivity at three scales and the impacts that changing water availability, management practices, and climate might have on the productivity of irrigation and other water uses within the basin (Droogers and Kite 1999). Kite (2000) described a basin-scale model used to estimate crop transpiration and evaporation from soil. Allen et al. (2002a,b, 2007b) described the use of satellite imagery for estimating ET for the southern part of the State of Idaho. Scott et al. (2003) evaluated the use of remotely sensed data for mapping root zone soil water on a river basin scale in Pakistan. Tasumi et al. (2005b) discussed operational aspects of satellite energy-based models for irrigated crops in the semiarid United States.

Singh et al. (2008) assessed the operational characteristics and performance of the surface energy balance algorithm for land (SEBAL) for estimating crop ET and other energy balance components, and mapping spatial distribution and seasonal variation of ET_c on a large scale in south-central Nebraska. Cloud free Landsat Thematic Mapper (TM)/Enhanced Thematic Mapper (ETM) satellite images from May to October were processed to generate ET_c maps and to estimate surface energy fluxes. Instantaneous and daily predictions from SEBAL were compared with the Bowen ratio energy balance system (BREBS)-measured fluxes over an irrigated corn field. The ET_c maps showed a progression of ET_c during the growing season. Overall, a good correlation was found between the BREBS-measured and SEBAL-estimated ET_c with a root-mean-square difference of 1.0 mm d^{-1}. Estimated ET_c was within 5% of BREBS-measured values. The model overestimated albedo by 25%, with the greatest difference early in the season before full canopy cover. The model underestimated soil heat flux and most of the underestimation occurred late in the late growing season. Local calibration improved the agreement between measured and estimated values. Anderson et al., (2011) provided an overview of estimating regional ET using thermally-based surface energy balance methods.

Cammalleri et al. (2013) explored the fusion of thermal and reflected imagery from the Landsat satellite having spatial resolution of 30 - 100 m with imagery from the MODIS satellite having spatial resolution of 500 – 1000 m to produce time series of ET in central Iowa having field-scale spatial resolution of 30 m and temporal resolution of approximately 8 days.

Approximating Monthly Streamflow for Ungaged Watersheds

The water balance technique, also referred to as the inflow-outflow or mass balance method, can be applied over large, integrated areas of land and water to develop watershed scale estimates of ET. These types of estimates are useful for calibration or validation of watershed and remote-sensing based models. Examples of ET by water balance are applications to large areas such as valleys where the inflow and outflow are determined from stream flow and precipitation measurements, and where the basin is confined to eliminate other significant sources of inflow or outflow such as groundwater underflow (Lowry and Johnson, 1942; Chow et al., 1988; McCabe and Markstrom, 2007; Gao et al., 2007; Dingman, 2008). Such studies generally provide only gross seasonal estimates of the average water evaporated and transpired from agricultural and nonagricultural areas within a watershed or project. The results represent ET from a combination of vegetation types and are generally applicable only to climatic, vegetation and water availability conditions similar to those existing in the study area. An evaluation of large-scale models of an experimental catchment (watershed) and a river basin in Australia indicated satisfactory agreement in monthly values between the computed and measured ET (Dunin and Aston, 1984). Wilson et al. (2001) found good agreement between ET derived from an inflow-outflow analysis of a 98 ha forested watershed and eddy covariance methods in Tennessee.

Mass balances require precipitation as the primary input and consequently the ET estimate can only be as accurate as the precipitation estimate. Fine resolution grids of precipitation on the scale of a km or less may be required in areas having substantial precipitation from convective storms and areas having substantial relief with orographic influence on precipitation amounts. As with soil water balance applications, precipitation data from standard gauges should be corrected for undercatch. Accurate measurement of basin or irrigation project outflow is necessary as is locating the measurement area boundaries to minimize ground water inflows and outflows.

Oftentimes, ET information is needed to estimate mean streamflow from ungaged watersheds. In locations where streamflows are not gaged, approximate estimates for monthly stream discharges can sometimes be made by employing a general, basic hydrologic balance:

$$Q = P - ET - GW - \Delta Storage \tag{12.3}$$

where Q is the monthly stream discharge from a watershed, having the same units as P, ET, and GW, GW is ground-water discharge from the basin and $\Delta Storage$ is the net change in soil water or ground-water storage in the watershed, with the same units as Q. In simple applications of eq. 12.3 to watersheds where ground-water flow discharge from the watershed is small, the last two terms of eq. 12.3 can be ignored, so that Q can be estimated as the difference between P and ET. Hargreaves (1993, 1995) found good agreement between monthly Q estimated as $Q = P - ET_o$ and measured Q for several watersheds in Central America and in the U.S.A, where ET_o was

calculated grass reference ET. ET_o provided a general approximation of ET throughout the watershed areas under the assumption that ET will approach ET_o when $P > ET_o$ during any month.

Data Sources in Cultivated Areas

An accurate and online database is required to fully utilize regional ET estimation methods. Since the 1970's, there has been a rapid expansion of nonfederal automated weather stations (AWS) across the United States and Canada. Many states have some sort of network of AWS: these include Alabama, California, Colorado, Florida, Georgia, Idaho, Louisiana, Minnesota, Nebraska, Nevada, New Mexico, New York, North Carolina, Ohio, Oklahoma, Oregon, South Dakota, Utah, Texas, Washington, and Wisconsin. Meyer and Hubbard (1992) reviewed early agricultural networks. Hubbard et al., (2005). Regional systems operated by the US Bureau of Reclamation include the Agrimet system. Most of the AWSs are part of a national network of Regional Climate Centers or part of agricultural weather networks such as those housed at the Agricultural Water Conservation Clearinghouse (http://agwaterconservation.colostate.edu/ET_Network_Information.aspx). Six Regional Climate Centers exist and are located in Nevada, Nebraska, Illinois, Louisiana, North Carolina, and New York.[1] Data and calculations from most of the AWS are available in real time and for low cost or free. Hubbard et al. (2005) reviewed some data quality control techniques for weather station networks and ASCE-EWRI (2005) described algorithms for supporting visual data quality assessments. The ASCE algorithms are summarized in Appendix H.

Data Sources in Natural Vegetation

In addition to the AWS systems, which can be expected to provide the most representative weather data for agricultural settings and for use in estimating ET from agricultural crops, other national networks typically located over natural vegetation include the Department of Energy Atmospheric Radiation Measurement program that contains the Cloud and Radiation Testbed (CART) (Xuebao et al. (2005), which measure evaporative flux by the energy balance Bowen ratio (BREB) and eddy covariance techniques. Other evaporative and energy balance flux collection programs include the Long Term Ecological Research (LTER) Program, Fluxnet, Ameriflux, ParkNet, National Atmospheric Deposition Program/National Trends Network, and Multistate Atmospheric Power Production Pollution Study. Weather data systems in wildland settings include the RAWS (remote automated weather system) systems operated by the US Forest Service and Bureau of Land Management. These data are generally available through the Regional Climate Centers.

Gridded Weather data

Gridded weather data sets are becoming increasingly common and more and more complete both nationally and globally. Data sets for the continental US include the PRISM set (Daily et al. 2008, Daley and Bryant 2013), Daymet (Maurer et al. 2002), NARR (North American Regional Reanalysis), NLDAS (North American Land Data Assimilation System) (Mitchell et al. 2004)

[1] http://www.ncdc.noaa.gov/oa/climate/regionalclimatecenters.html

and GridMet (Abatzoglou 2013). Global data sets include GLDAS (Global Land Data Assimilation System). These data sets utilize a wide range of techniques for assimilating measured weather data and making spatial and temporal assimilation. Grid sizes vary and wind speed and precipitation data have the least certain spatial accuracy (Luo et al. 2003). Precipitation data may originate from NEXRAD (Next-Generation Radar) sources or interpolation from point data. Because assimilated data originate from a variety of weather locations, many of which may not be in well-watered settings, for example, at regional airports, gridded weather data may have a pronounced aridity, with air temperature higher than and vapor pressure lower than expected over a well-watered vegetated surface. These data may benefit from conditioning prior to use to estimate reference ET.

The 30+ year (1979-present) NLDAS retrospective forcings have 1/8 degree resolution (~ 12km x 12 km). NLDAS phase 2 retrospective forcings (NDAS-2) contain daily precipitation, solar radiation, and 2m reference height temperature and humidity, and 10m reference height windspeed (http://www.emc.ncep.noaa.gov/mmb/nldas/). Model based NLDAS forcings of temperature, humidity, and windspeed are derived from spatially and temporally interpolated NCEP North American Regional Reanalysis (NARR) data.

Several NLDAS validation studies have been conducted with focus in Oklahoma (Luo et al. 2003; Robock et al. 2003), where NLDAS solar radiation, based on GOES satellite, was compared to ground-based observations. While Luo et al. (2003) showed fairly good correlation (correlation coefficient ~ 0.92) of simulated to measured hourly R_s, there was often bias caused by overprediction by NLDAS.

Agricultural data sets have also been organized into gridded systems, for example, in California, CIMIS weather data have been gridded by Hart et al. (2009). These gridded systems generally cover nonmountainous systems and better represent well-watered conditions.

13

Selecting an Appropriate Estimating Method

13.1 Introduction

All methods for calculating evaporation (E) and evapotranspiration (ET) that are based on climatological data produce only estimates of ET. The accuracy of estimates depends substantially on the quality of data and on the completeness and physical basis of the method. The best method to select for a particular application depends on the available timeframe for completing the task, the required accuracy, the area of coverage, the length of the calculation timestep, the availability of existing climate data or whether specific new climate data measurements can be made. The intended end use of the ET estimate is also a factor, for example, whether for use in project and system planning, design, operation, management practices, hydrologic studies, water rights management, water transfers, environment mitigation, or litigation. The method selected and its accuracy in application depends on the resources available to the user, including the capabilities of trained personnel to assess input data quality, apply models that combine remotely-sensed data and surface weather data, and calculation of parameters. The computing capacity available to the user should also be considered.

13.2 Timeframe and Required Accuracy

Considerations in both method selection and resource allocation include the time required to collect and screen climate data for quality and to process the climate data. Also to be considered is the time required to obtain associated relevant data such as soil type, crops being grown or landscape vegetation, and characteristics of the weather station sites used. Soils data bases for the United States include the STATSGO and SSURGO data bases (http://soils.usda.gov/survey/geography/ssurgo/).

The required accuracy of ET estimates depends on their intended use. The highest accuracy may require measured field data for development, calibration or verification. For moderate accuracy, the use of available crop and landscape vegetation coefficients along with calculated reference ET may be adequate. Generally, the longer the time interval for which ET estimates are produced, the higher the accuracy, for example, hourly vs. daily vs. 10-day vs. monthly, vs. growing season time intervals. The increase in accuracy occurs due to the tendency for random errors or bias in weather data or ET parameter settings to cancel over time. The cancelling mostly occurs when ET calculated for short time intervals is summed over longer time intervals. Most estimates of E and ET made using the equations and guidelines described in this manual can be considered to be useful for routine water planning and management purposes.

13.3 Input Data Collection, Screening and Processing

Some archived climate data provided by various service groups may have already been subjected to quality control, with bad or questionable data flagged. Even so, it is always prudent to review the available archived climate data for obvious data errors, and to independently

identify data that may be suspect due to bad sensors, gradual changes in calibration coefficients, or units errors. Likewise, current or real time data that are available via the Internet should be screened. The major weather variables that need to be reviewed are solar radiation, temperature, humidity and wind speed. Graphics-based procedures for screening weather data are described in ASCE-EWRI (2005) and in Appendix H.

Solar Radiation

The primary source of energy for E and ET is solar radiation. The best measured or estimated data should be used. Hourly and daily solar radiation data (R_s) should be screened by comparison with calculated cloudless day values (R_{so}) using eq. 4.11-4.15 or the detailed procedures outlined for the ASCE-EWRI standardized reference ET equation (ASCE-EWRI 2005). Measured R_s should approach the R_{so} values on cloudless days. Occasionally, daily or hourly values may slightly exceed R_{so} due to reflection from nearby clouds.

Humidity and Air Temperature

Humidity and air temperature data, whether collected specifically for a study, or when using data from an agency or private source, should be screened to identify possible erroneous or non representative values. The user should have a general knowledge of what values are reasonable or unreasonable. Maximum relative humidity (RH) more than about five percentage points above 100% in a natural environment may indicate a problem with the humidity sensor such as a faulty or drifting calibration coefficient. Values greater than 100% should be set to 100% prior to use in calculations. Maximum daily RH should generally approach 100% in humid and subhumid climates, but may be less in arid climates during warm summer periods. Minimum RH should not be less than about 30% in subhumid regions or less than about 10% in arid regions when collected over extensive, well-watered surfaces. Collection over extensive, well-watered surfaces conditions the humidity and temperature data to reflect the well-watered surface and is 'anticipated' by the reference ET methods.

Another check of humidity data is to calculate daily average dew-point temperature from RH data and compare it with daily minimum air temperature (T_{min}). Daily average dew point temperature can be calculated by first calculating average daily vapor pressure using RH_{max} and RH_{min} as follows:

$$e_a = \left[e^o(T_{\min}) \frac{RH_{\max}}{100} + e^o(T_{\max}) \frac{RH_{\min}}{100} \right] / 2 \qquad (13.1)$$

where e_a = actual average vapor pressure, kPa, and e^o = saturation vapor pressure calculated using eq. 3.1 for T_{min} and T_{max}. Dew-point is then calculated using eq. 3.9 and the average vapor pressure. Average calculated daily dew-point values should approach T_{min} most days in humid regions. In arid areas, daily dew-point values may be 2-5°C lower than T_{min} even when measurements are made at a site that meets reference crop requirements. Daily dew point temperatures that are much below (T_{min} – 5)°C indicate that the weather station site likely does not meet reference crop conditions, and some adjustment of humidity data may be required. Additional discussion of humidity data problems is presented in Appendix D of the ASCE-EWRI publication (ASCE-EWRI 2005) and in Appendix H.

Air temperature is the simplest and most consistent weather parameter that is commonly measured, especially when measured in a reference-type environment. Extreme air temperature data should be compared with historical record extremes for the site or region. Temperatures that routinely exceed recorded extremes indicate possible problems with the sensor or the radiation shield. Additional discussion of temperature data problems and the impacts of non-reference weather station site on humidity and temperature are presented in Appendix D of the ASCE-EWRI publication (ASCE-EWRI 2005) and in Appendix H.

Windspeed

For reference ET calculations, wind speed should be measured in open, field-like areas away from buildings and trees and over a grass-like surface. Accuracy of wind speed measurements is difficult to assess unless duplicate instrumentation is used. A comparison of reported wind speed data with historic means or those of nearby stations may indicate a malfunctioning anemometer, or temporary failure due to ice when temperatures are below 0°C. Consistently low readings may indicate worn out or dirty anemometer bearings or a failed anemometer. An assessment of the gust factor, calculated as the ratio of maximum hourly wind speed to average daily wind speed or as the ratio of a one- to five-minute wind speed to hourly wind speed, is another method for evaluating wind speed data. Consistently high gust factors indicate a failing anemometer that becomes sluggish during low wind speeds and creates nonlinearity in the anemometer response. However, one should recognize that wind speed during nighttime is often a factor of 2 to 3 times lower than wind speed during daytime. Wind speed data can be compared among local weather sites to note common behavior and trends, as illustrated in Appendix H.

13.4 Crop Coefficient method vs. Direct Methods

In general, the crop coefficient – reference crop coefficient method has proven to be accurate, robust, consistent, and relatively straightforward to apply. The reference crop ET method has been standardized through the FAO-56 and ASCE-EWRI (2005) definitions, which has facilitated establishing standardized sets of crop coefficients that should transfer across a wide range of climates. The crop coefficient method has a long legacy in irrigation water management, scheduling and in water rights proceedings.

The direct ET methods described in Chapter 11 have the potential for more precise measurements, but generally require more detailed parameterization and crop specific information. Weather data sets may not be available to drive some of these methods, especially those that expect that weather measurements are taken over the surfaces being estimated. This is especially important when estimating ET for irrigated fields in arid and semiarid climates. Direct ET methods may be useful for extrapolating ET measurements, for example, from eddy covariance and Bowen ratio systems, where the direct methods are parameterized or calibrated using the measurement data. Those fitted models can then be applied over larger areas and under different weather conditions.

Satellite-based mapping of ET is becoming increasingly used, with the advent of very low cost or even free satellite imagery beginning around 2000 and development of operational algorithms. Because of the wide variation in vegetation and land-form characteristics, satellite-based ET systems should utilize the best physically-based methods as possible, given time and resources constraints and the intended use of the ET products. When possible, satellite-based

approaches should be compared against measurements by ground-based systems and using independent models such as the crop coefficient and/or direct ET methods. Measurements by ground-based systems need to be subjected to quality assessment and control.

13.5 Evaporation and Evapotranspiration Calculations

In studies of effects of environmental stresses or climate change, energy balance methods using surface temperature measurements and/or the Penman-Monteith (PM) method with hourly or shorter time steps and iterative computation of surface temperature may be the most appropriate. In studies where effects of changes in vegetation type, density, height, or water availability are evaluated, the PM equation, AFIB (eq.11.2a-f), or more complex multi-layered energy balance equations should be used, since changes in vegetation characteristics can be more directly and readily incorporated into the calculations for aerodynamic and surface resistances. Where specific documentation of ET is required for small areas, direct measurements must usually be made using micrometeorological methods including the Bowen ratio and eddy covariance methods or using soil water balance methods including lysimeters and measured changes in soil profile water content between two dates. Various precautions that must be exercised when measuring ET by the soil water profile method are discussed in chapter 7.

Generally, when changing from a coefficient-reference ET approach (either the $K_{co}\ ET_o$ or $K_{cr}ET_r$) to a direct ET approach, the amount of data required increases, the required calculation time step decreases, and the requirement for accuracy of input data increases. It is difficult to apply the direct PM equation or AFIB method using historical data from standard weather stations, since the historical weather data generally reflect ET flux densities of the weather measurement surface. When applied to some other vegetation type, the direct methods may over or under predict, since the effect of feedback mechanisms between ET and vapor content and temperature of the boundary layer are not reflected in the data.

Energy balance methods, including the combination equations (Penman, eq. 8.1 and PM eq. 8.2), and energy balance equation (eq. 4.1, 11.2a-f), are generally more dependabl1e and consistent in estimating ET as compared to direct aerodynamic methods since the inclusion of energy availability in the former equations places an upper limit on ET estimates. In addition, instrumentation requirements are often less rigorous and demanding.

The $K_{co}\ ET_o$ or $K_{cr}\ ET_r$ procedure may be the best overall approach to estimating ET since the use of ET_o or ET_r provides a measure of general energy available for ET. The K_{co} or K_{cr} coefficient, where the subscript "*o*" or "*r*" identifies the coefficient to be used with either ET_o or ET_r, can incorporate a wide assortment of physiological and environmental factors affecting ET rate, including plant density, soil evaporation, and effects of sparse plant densities. The implicit incorporation makes the $K_c\ ET_o$ or $K_{cr}ET_r$ approach robust in application and fairly transferrable to other climates, regions and time periods. Physiological and environmental factors need to be explicitly identified and incorporated during direct application of the PM and other directly applied boundary layer equations, making these approaches usually more data intensive. However, application of the direct PM equation or AFIB method can often serve as a valuable check on validity of K_c values and can in some instances be used to develop K_c's for new types or variations of vegetation.

Usually, calculations made using the PM equation on a 24-hour basis are sufficient for hydrologic studies. Under most conditions, 24-hour estimates of ET_o or ET_r calculated using the PM equation using 24-hour time steps provide estimates of total 24-hour ET_o or ET_r which are

within 5 to 10% of 24-hour sums made using hourly timesteps for any given day, with differences varying randomly, depending on the general proportions of daytime to nighttime wind speeds and daylengths (Allen et al. 1994b, 2006b). Results are similar for calculations made using the direct PM equation and AFIB method. The exception is for situations where the stomatal conductance functions ($g(\ )$) or stability corrections are to be applied. In these situations, calculations should be made on an hourly or shorter basis. Energy balance methods using hourly or shorter time steps usually involve measurements or estimates of surface temperature, which are highly correlated with solar radiation, and corrections for stability are generally employed, especially under conditions of water stress.

Calculations of ET_o or ET_r on a monthly basis are generally equivalent to those made on a 24-hour basis and summed over the month (Jensen et al. 1990; Allen et al. 1994b). Alternative approaches to reviewing data and calculating E and ET are presented in FAO-56 (Allen et al. 1998). During the non-growing season, when actively growing vegetation does not exist and when daytime hours are less than nighttime hours, calculated ET_o and ET_r may serve as an index, but not a realistic estimate of reference ET conditions, since active vegetation is not present. Irmak et al. (2008) evaluated the ratios of calculated ET_r to ET_o (K_r) using different equations during the growing season (May-September) and non-growing season at locations in California, Florida, Missouri, Nebraska and Texas. The variability of K_r values among locations was large. Some of methods calculated unrealistically high values during the non-growing season since hypothetical reference conditions are usually not met during this period in many locations. Of the five locations, only Nebraska had long cold winters. The empirical equation for estimating ET_o using extraterrestrial solar radiation and mean air temperature by Hargreaves and Samani (1985) and Hargreaves et al. (1985) may also provide a non-growing season index.

As more experience is gained using various methods of calculating ET, refinements in the methods can be expected. Users should review publications summarizing the results of new studies before selecting a method for a particular study or application.

13.5 Summary

The method used to calculate or estimate evapotranspiration (ET) will depend on the type of application and the amount and accuracy of data available. For large-scale applications including basin-scale water balances, application of a crop coefficient-reference ET ($K_{co}\ ET_o$ or $K_{cr}\ ET_r$) approach with monthly calculation time steps may be appropriate. ET_o for monthly timesteps can generally be calculated using the Hargreaves air temperature method (eq. 8.16) or using the PM equation with estimated R_s, T_d and wind (see section 8.5) when these variables are not measured. For applications to smaller areas, especially those having relatively homogeneous surface cover, the $K_c\ ET_o$ or ET_r and direct PM approaches may be equally appropriate. Calculations using the PM method are commonly made on an hourly or 24-hour basis.

BLANK PAGE

14

Estimating Irrigation Water Requirements and Streamflow Depletion

14.1 Introduction

The irrigation water requirement includes several components, with the major component being the replacement of soil water depleted by evaporation (E) and crop or landscape evapotranspiration (ET). This component is water that is consumed via conversion from liquid to vapor during the ET process. Other components provide water for leaching, or controlling the soil salinity level, and provide water for various miscellaneous purposes such as assuring germination of seeds, controlling soil crusting, frost control, and conditioning the soil to enable harvesting root crops. Only part of the water for these other components is consumed by E or ET. The part not consumed remains somewhere in the water resources system, but may be degraded in quality.

14.2 Evaporation and Evapotranspiration – a review

Evapotranspiration

The use of reference crop ET methodology was described in chapter 8. Its use with basal and mean crop coefficients was described in chapter 10. Tabular values of mean FAO-56 crop coefficients for use with clipped grass (short reference crop) by growth stage are presented in Appendix B and lengths of growth stages are described in chapter 10, with tabular growth stage values presented in Appendix C. Basal coefficients are presented in Appendix D. Use of FAO-56 basal crop coefficients in the dual Kc procedure are described in chapter 10. In general, the dual Kc method is recommended, when possible, to fully account for the impact of wetting frequency by precipitation and irrigation. That method can be applied to produce estimates of evaporation and soil water accumulation during nongrowing periods (Allen and Robison 2007). Mean crop coefficient values are presented in Appendix E for alfalfa reference ET, which is the tall reference crop. Values for basal crop coefficients for use with alfalfa reference ET are presented in Appendix F.

Evaporation

Evaporation from soil is an important component of ET to estimate because it is the component that is most impacted by the wetting frequency of precipitation and irrigation. One needs to bear in mind the positive feedback between irrigation and evaporation from bare soil. As irrigation increases, especially in frequency, *E* increases. As *E* increases, more water may be called for from irrigation, especially if the evaporation makes less soil water available for transpiration, as may be the case with a shallow root zone. This is another reason to utilize an ET process such as the dual Kc approach that can separate the evaporation and transpiration components, so that the irrigation amounts can be tailored to replace soil water depletions stemming from transpiration, only.

General procedures for estimating evaporation from the water surfaces such as holding ponds and regulating reservoirs were described in chapter 6. For estimating evaporation from soils, general soil water-holding parameters for various soil textures were provided in table 7.1. General ET estimating methods are described in chapter 7. Use of crop coefficients for estimating evaporation from bare soil and as plant cover developed was described in chapter 9. The use of reference crop ET methodology was described in chapter 8 and the use of crop coefficients was described in chapter 10. Tabular values of crop coefficients by growth stage are presented in Appendices B-F. FAO-56 procedures for estimating the coefficient for the initial stage of crop development were described in chapter 10.

14.3 Net Irrigation Water Requirement and Effective Precipitation

The net irrigation water requirement, *NIWR*, can be referred to as a precipitation deficit, P_{def}, where P_{def} is the amount of soil water that must be made up to complete the potential ET requirement, ET_{pot}, and avoid undesirable water stress. P_{def} is generally calculated as $ET_{pot} - P_{rz}$ where P_{rz} is the precipitation infiltrating into and residing in the root zone. P_{def} represents the amount of additional water that the soil and crop would evaporate or transpire beyond P_{rz} if that water were made available at the right time during the growing or nongrowing season to fulfill the necessary *ET* requirement.

P_{def}, can have a negative value when calculated over a short period of time if the depth of precipitation during a period, for example, 3-, 7-, 15- or 30-days, is greater than the value of ET_{pot}. This is likely to occur during winter and periods having substantial rain. A negative value indicates precipitation in 'excess' of ET and a net recharge to soil water. When comparing P_{def} for a nonirrigated condition with P_{def} for the same crop that is irrigated, the P_{def} calculated for the nonirrigated condition is often lower than that for the irrigated condition. This is an artifact of the calculation of ET_{pot} using a dual Kc method where *E* for the rainfed crop does not contain *E* from soil following irrigation events. When determining the *IWR*, one should use the P_{def} for the irrigated condition to reflect the increased *E* for the irrigated condition, which, in essence, 'burns off' part of the added irrigation water.

It is useful to define precipitation that enters the soil in two different ways, in terms of its ultimate disposition into *E* or into transpiration, *T*. The ***Precipitation residing in the root zone*** ***(P_{rz})*** is the depth of gross reported precipitation infiltrating the soil (i.e., less any surface runoff) that remains in the root zone and is available for later consumption by *E* or *T*. P_{rz} is computed as $P - Runoff - DPerc$ where *P* is gross reported precipitation, *Runoff* is estimated surface runoff and *DPerc* is deep percolation of any precipitation below the maximum rootzone for the crop or land-use condition. The difference between P_{rz} and ET_{act} during extended periods of no irrigation, including the nongrowing season (where ET_{act} includes evaporation following precipitation events), represents the amount of 'recharge' to the root zone. During the nongrowing season, the difference $P_{rz} - ET_{act}$ represents an increase in soil water storage that is available at the start of the growing season to fulfill later plant water requirements. The ratio of $(P_{rz} - ET_{act})/P$ represents the 'efficiency' or effectiveness of gross precipitation, including snow, in building soil water for use during the growing season.

A second useful term and category for *P* that enters the root zone is the ***Precipitation residing in the root zone that is available for transpiration*** *(rather than for evaporation),* P_{efT}. P_{efT} is the amount of gross reported precipitation that infiltrates into the soil (i.e., less any surface runoff) and that remains in the root zone and is ultimately used to supply *T* by the crop or land use cover. P_{efT} does not include the amount of infiltrated precipitation that evaporates from the surface evaporation layer (for example the upper 100 mm of soil). One reason to separate the contributions of *P* into *E* and *T* is that, in many cases, only the *T* component of *P* and/or irrigation, *I*, is considered to be economically or 'beneficially' used. Conservation programs may promote means to reduce the evaporation components and maximize the transpiration components of both *P* and *I*.

The P_{efT} parameter is useful for estimating the amount of *P* during the nongrowing season that is stored and later made available for *T* requirements during the subsequent growing season. P_{efT} is also useful to calculate during the growing season to determine how 'efficient' or effective precipitation is in fulfilling the *T* requirement of a crop, as opposed to simply 'burning off' as *E* from the soil surface. P_{efT} is calculated as $P_{efT} = P_{rz} - E = P - Runoff - DPerc - E$, where P_{rz} is precipitation infiltrating and residing in the maximum root zone for the crop.

Typically, the effectiveness of *P* in satisfying *T* requirements is low if *P* occurs in frequent, small doses. In that situation, most *P* is converted into *E* and does not appreciably reduce the *NIWR*. In calculating the effectiveness, it is important to use an ET estimating method that has the ability to increase the estimate for *E* with increased frequency of *P*.

The *NIWR* is estimated similarly to P_{def}, where*:*

$$\begin{aligned} NIWR &= ET_{pot} - (P - Runoff - DPerc) \\ &= E + T_{pot} - (P - Runoff - DPerc) \\ &= E + T_{pot} - P_{rz} \\ &= T_{pot} - P_{efT} \end{aligned} \tag{14.1}$$

The alternative component expressions in eq. 14.1 illustrate the importance of including accurate estimation of *E* in the estimation of ET if the depth for *P* used in the same equation contains the portion of ET that becomes *E*. Otherwise, the *NIWR* may be underestimated and effectiveness of *P* overestimated.

Effective rainfall during historical periods is best estimated by applying a daily soil moisture balance, including estimated surface runoff, soil evaporation, unsaturated drainage and soil water - ET relationships. It is relatively straightforward to construct computer software or spreadsheets that make the necessary calculations. Water balance equations are introduced in chapters 9 and 10 for estimating or incorporating *E* and ET using the dual Kc approach, and examples of calculations using daily time-steps are shown.

The depth of effective rainfall stored in the soil during a period is dependent upon the frequency of occurrence and characteristics (amount, duration and intensity) of the precipitation, the soil surface condition, and the soil water storage capacity available at the time of rainfall. The amount lost to surface runoff is that portion of the rainfall in excess of the intake capacity of the soil and leaf interception unless the excess is ponded until intake occurs.

As described later, effective rainfall can also supply leaching requirements. Precipitation lost by runoff from the soil surface and by drainage through the soil is not considered effective in reducing ET water requirements, but the leaching requirement may be reduced by rainfall induced drainage. Precipitation that only redistributes salt concentrations through the soil within the root zone may not decrease the leaching requirement.

The soil water storage capacity available when rainfall occurs varies with the depth and characteristics of the soil within the root zone, the elapsed time since irrigation or rainfall, which impacts the infiltration rate, the depletion allowed before irrigation, and the rate of depletion by ET. Generally, rainfall effectiveness increases with higher *T* rates, greater allowed depletions between irrigations, and larger soil water storage capacities.

In the absence of a daily water balance simulation, effective rainfall stored in the soil can be estimated using a very general relationship presented by the USDA-SCS (USDA 1970), but with reduced accuracy. In the USDA-SCS procedure, average monthly effective rainfall, R_e, is estimated according to mean monthly rainfall, R_t, average monthly ET for the crop, and the normal depth of depletion prior to irrigation, *D,* mm:

$$R_e = f(D)[1.25\,R_t^{\,0.824} - 2.93][10^{0.000955\,ET}] \tag{14.2}$$

where units for rainfall and ET parameters are mm per month and *f(D)* is a factor to adjust for depletion depths other than 75 mm, described by the equation:

$$f(D) = 0.53 + 0.0116\,D - 8.94\,x10^{-5}\,D^2 + 2.32\,x10^{-7}\,D^3 \tag{14.3}$$

Depletion depth, *D,* accounts for impacts of soil water holding characteristics and rooting or soil depth and is similar to the term RAW estimated with eq. 10.7 and 10.8 of chapter 10. The value of R_e should be limited to the lesser of the values of R_t, ET or the equation estimate. The SCS relationships are based on a calculated daily accounting of soil water storage, rainfall, and evapotranspiration for a 50-year period at 22 weather stations in the United States representing climates from humid to arid, and for combinations of crops and soils common to irrigated areas. Irrigation was assumed to occur when soil water storage was depleted to a predetermined level. Daily rainfall in excess of available soil water storage was assumed lost to surface runoff or deep percolation.

Eq. 14.2 may be used to estimate effectiveness of fall and winter precipitation by substituting the remaining available soil water storage capacity at the beginning of each monthly or seasonal period for the normal depth of depletion, *D*, and setting ET to a low value. This relationship will not adequately predict effectiveness of winter precipitation if significant surface runoff occurs due to frozen soil conditions, if snow is removed by wind action, or if wetting events are frequent and light, with large fractions of *P* lost as increased *E*. As illustrated in the previous section, P_{efT} represents the most appropriate definition and expression of the effectiveness of *P* in supporting transpiration requirements of vegetation. Other empirical methods for estimating effective rainfall and reviews of the SCS method have been presented by Dastane (1974) and Kopec et al. (1984).

14.4 Leaching Requirement

All irrigation waters contain some dissolved salts. ET removes pure water from the soil, thereby concentrating the salts in the remaining soil water solution. Salts in the soil solution decrease the osmotic potential (greater negative pressure) as compared to pure water. Lower osmotic potential decreases the potential gradient of soil water to plant roots. Concentration of salts can result in conditions unsuitable for crop growth unless controlled. The practical method for controlling concentration of salts in the soil solution is by leaching. Leaching is considered a necessary and beneficial use of water and must be included in determining irrigation water requirements. Leaching is accomplished by having a portion of the infiltrated water percolate through the root zone. The portion that actually passes through the root zone is called the *leaching fraction* (Tanji 1990) calculated as:

$$LF = \frac{Q_{dp}}{Q_{iw} + Q_{ep}} \tag{14.4}$$

where *LF is the leaching fraction*, dimensionless, Q_{dp} is the volume of water that percolates through the root zone commonly expressed as volume per unit area (i.e., depth), Q_{iw} is the infiltrated irrigation water also expressed as depth, and Q_{ep} is effective precipitation expressed as depth. The leaching fraction can also be expressed in terms of soil salinity as:

$$LF = \frac{C_a}{C_d} \tag{14.5}$$

where C_a is the salt content of infiltrated water (irrigation plus precipitation) and C_d is the salt content of water draining through the root zone (Hoffman 1990). The salt content of water and the soil solution is commonly expressed in terms of electrical conductivity (EC) in units of deci-siemans per m (dS m^{-1}), where 1 dS m^{-1} = 1 mmho cm^{-1}. The latter unit was commonly used in the past. When expressed in terms of volume of water infiltrated ($V_{inf\,w}$) and drained (V_{dw}) per unit area and the EC of the waters, the *LF* becomes:

$$LF = \frac{V_{dw}}{V_{\inf\,w}} = \frac{EC_{iw}}{EC_{dw}} \tag{14.6}$$

where EC_{iw} is the salinity of the infiltrated water and EC_{dw} is the salinity of the drained water, dS m^{-1}.

The *leaching requirement* (*LR*) is the amount of leaching required to maintain a viable irrigated agriculture. It depends on the salt content of the irrigation water, the type of soil, the salt tolerance of the crop grown, the climate, and the irrigation management practices. The *LR* was originally defined in USDA Handbook 60 (U.S. Salinity Laboratory Staff 1954) as the lowest value of the *LF* that can be allowed without EC_{dw} becoming excessive for optimum plant growth. The required amount of water to be infiltrated ($V_{r\,inf}$) to replace soil water depleted by ET and the *LR* is:

$$V_{r\,\inf} = \frac{V_{ET}}{(1 - LR)} \tag{14.7}$$

where V_{ET} is the volume of soil water depleted by ET that is to be replaced per unit area and LR is the estimated leaching requirement. Rhoades (1974) introduced a procedure for estimating the LR based on the average soil EC calculated as the average of the saturated paste at the top and bottom of the root zone and an approximate ratio of the water content of the saturated paste and the water content at field capacity taken as 2. The EC of the saturated paste is about one-half of the EC of soil water content at field capacity. The resulting equation is:

$$LR_t = \frac{EC^*_{\inf w}}{(5\,EC^*_e - EC_{inf\,w})} \tag{14.8}$$

where LR_t is the traditional estimate of the LR, $EC^*_{inf\,w}$ is the EC of the infiltrated water and EC^*_e is the average EC of the saturated-paste extracts appropriate for a given crop allowing a tolerable yield depression (usually 10%) or so-called threshold level of salt tolerance (Maas 1990). The LR_t model has been used extensively (Ayers and Westcot 1985).

For soil salinity exceeding the threshold level for a given crop, the resulting relative yield (Y_r) is estimated as:

$$Y_r = 100 - b\,(EC_e - a) \tag{14.9}$$

where a is the salinity threshold level expressed in dS m^{-1}, b is the slope expressed as % per dS m^{-1}, and EC_e is the mean electrical conductivity of a saturated-soil extract taken from the root zone. Salt tolerance values for various crops expressed as the threshold level and slope per dS m^{-1} were presented by Maas (1990), tables 13.1 and 13.2, and in FAO-56, table 23 (Allen et al. 1998). Salt tolerance for selected common crops are summarized in this chapter in table 14.1.

Because of the complex chemical reactions that occur in soil solutions and the dynamics of the leaching process, transient-state solute transport models have been developed for estimating time-varying salinity within the crop root zone and the resulting LR. One model that requires limited input is WATSUIT (Rhoades and Merrill 1976). TETRANS is a simplified transient model which predicts changes in solute and soil water in irrigated crop root zones (Corwin et al. 1990). More details on the use of saline waters for irrigation can be found in several FAO publications (Rhoades et al. 1992; Rhoades et al. 1999). A recent detailed discussion on controlling salinity and salinity impacts on design and management of irrigation systems was presented by Hoffman and Shannon (2007). ASCE Manual 71 on Agricultural Salinity Assessment and Management, updated in 2011 (Wallender and Tanji 2011), contains substantial information on managing salinity and salt-effected soils and land application of wastes.

TABLE 14.1. Salt Tolerance of Selected Crops. Source: Tables 13.1, 13.2 of Maas (1990).

Crop		Electrical conductivity of saturated soil extract		
Common name	Botanical name	Threshold, dS m^{-1}	Slope, % per dS m^{-1}	Rating[a]
Cereals:				
Barley	*Hordeum vulgare*	8.0	5.0	T
Maize	*Zea mays*	1.7	12.0	MS
Maize (Sw corn)	*Zea mays*	1.7	12.0	MS
Millet, foxtail	*Setaria italica*			MS
Rice, paddy	*Oryza sativa*	3.0	12.0	S
Sorghum	*Sorghum bicolor*	6.8	16.0	MT
Wheat	*Triticum aestivum*	6.0	7.1	MT
Wheat, semi-dwarf	*Triticum aestivum*	8.6	3.0	T
Wheat, durum	*Triticum turgidum*	5.9	3.8	T
Forages:				
Alfalfa	*Medicago sativa*	2.0	7.3	MS
Bermuda	*Cynodyn Dactylon*	6.9	6.4	T
Clover, red	*Trifolium pratense*	1.2	12.0	MS
Fescue, tall	*Festica elatior*	3.9	5.3	MT
Rye-grass, perennial	*Lolium perenne*	5.6	7.6	MT
Sudangrass	*Sorghum sudanense*	2.8	4.3	MT
Wheatgrass, standard	*Agropyron sibiricum*	3.5	4.0	MT
Legumes:				
Bean	*Phaseolus vulgaris*	1.0	19.0	S
Cowpea	*Vigna unguiculata*	4.9	12.0	MT
Groundnut (peanut)	*Arachis hypogaea*	3.2	29.0	MS
Pea	*Pisum sativium*			S
Soybean	*Glycine max*	5.0	20.0	MT
Miscellaneous:				
Apples	*Malus sylvestris*			S
Citrus (Orange)	*Citrus sinensis*	1.7	16.0	S
Cotton	*Gossypium hirsutum*	7.7	5.2	T
Grapes	*Vitis sp.*	1.5	9.6	MS
Olives	*Olea europaea*			MT
Sugar beet	*Beta vulgaris*	7.0	5.9	T
Sugar cane	*Sachcharium officinarum*	1.7	5.9	MS
Sunflower	*Helianthus annuus*			MS
Vegetables:				
Broccoli	*Brassica oleracea botrytis*	2.8	9.2	MS
Cabbage	*Brassica oleracea capitata*	1.8	9.7	MS
Carrots	*Daucus carota*	1.0	14.0	S
Cauliflower	*Brassica oleracea botrytis*			MS

Celery	*Apium graveolens*	1.8	6.2	MS
Lettuce	*Lactuca sativa*	1.3	13.0	MS
Melons				
Onions	*Allium Cepa*	1.2	16.0	S
Pepper	*Capsicum annum*	1.5	14.0	MS
Potato	*Solanum tuberosum*	1.7	12.0	MS
Tomato	*Lycopersicon lycopersicum L.*	2.5	9.9	MS
Watermelon	*Citrullus lanatus*			MS

[a] Estimates: tolerant (T), moderately tolerant (MT), moderately sensitive (MS), and sensitive (S)

14.5 Miscellaneous Water Requirements

Several minor, but important water requirements must be considered for some crops. These requirements are often based on local practices and needs of specialty crops. Some of these are described below.

Germination

Many small-seeded crops such as lettuce, carrots, etc., cannot be established unless the surface soil water content is maintained near field capacity for several days after planting to insure germination and emergence of the seedlings. During midsummer, surface soil temperatures may reach levels fatal to the young plants unless cooled by frequent wetting during the high solar radiation periods. Sprinkler systems usually are more efficient for this purpose since several small intermittent applications per day may be required to maintain the desired soil water and temperature conditions. In the Imperial Valley of California, it has long been common practice to set up a sprinkler system to establish the crop, and then to furrow irrigate during the balance of the season, a practice based on research conducted by Robinson (1969).

Frost Protection

Application of water, usually by sprinkler irrigation, can be used to prevent or minimize frost damage to crops by utilizing the specific heat of water released in cooling to 0°C, and in the latent heat of fusion released as water changes from a liquid to a solid state. The water required for frost control is generally much in excess of daily ET requirements. It varies with the heat lost through convection, radiation, and evaporation. Wolfe et al. (1972) indicated that sprinklers operated for frost protection when air temperatures range from -4°C to -7°C must apply 2.5 to 4 mm h^{-1}. Leaf temperatures will not fall below 0°C in this range of air temperature if a film of unfrozen water is maintained on the ice-coated leaf. One limit to the continuous buildup of ice is the ability of the plant to support the weight of ice without damage to the plant. Water application must continue as long as the wet bulb temperature of the air is near or below the critical temperature. When the ambient air temperature rises above 0°C, the ice will begin to melt. Heat absorbed in evaporating water from the surface of the ice may lower the temperature of the ice below the danger level unless sprinkling continues. The system capacity must be large enough to permit simultaneous application of water to the entire cropped area to be protected. A

web-based publication on frost protection was made available by Snyder and Melo-Abreu (2000).

Blossom Delay

Water application from over tree sprinklers in fruit trees has been used to cool the developing buds on warm days in the early spring. This evaporative cooling can cause a delay in a blossoming of up to 21 days (Griffin et al. 1976) which increases the probability of avoiding the last spring frost. The resultant maturity delay has also been used by growers to schedule harvesting dates. Griffin et al. (1976) recommended that the Christiansen uniformity coefficient be at least 80%, and that the system be designed to provide 3.8 mm h^{-1} during high temperature periods. Pulsing of the system may be used to reduce the total volume of water as long as the desired cooling is attained.

Wind Erosion Protection

When establishing crops in high wind areas, especially those with sandy soils, sprinkler irrigation has been used to control wind erosion and reduce damage to seedlings. Applications of 10 to 15 mm per day during high wind periods following planting may be required to protect the soil from eroding. In this case, however, sprinklers are usually operated at night when the wind speeds are low to achieve a more uniform application of water.

Plant Cooling

Some plant components, such as flowers or seed heads, have a small number of stomata per unit area. With low wind speed, these plant components that are exposed to direct sunlight may reach temperatures that are 10ºC to 15ºC above the ambient temperature due to a lack of evaporative cooling. Periodic misting at 1 to 1.5 mm h^{-1} has been used to wet these plant parts, thereby reducing their temperatures substantially below that of air temperature, but not below the wet bulb temperature (Kohl and Wright 1974). The duration of the cooling depends on the amount of water retained on these plant parts. Similarly, there may be economic benefits from periodic misting of some fruit crops and lettuce provided increased disease incidence does not offset gains from plant cooling.

14.6 System Losses

Net Irrigation Water Requirements

The net irrigation requirement per unit area is the water that must be supplied by irrigation to satisfy ET, leaching, and miscellaneous water requirements that are not provided by water stored in the soil or by precipitation that enters the soil.

$$W_r = (W_{ET} - R_e + \Delta W_s) + W_L + W_m \tag{14.10}$$

where W_r is the unit irrigation water requirement for the period being considered, W_L is the water required for leaching, W_m is the miscellaneous requirement, R_e is the effective rainfall, W_{ET} is the

total water used in ET, and ΔW_s is the increase in soil water. Units are volume per unit area or depth. A negative value for the quantity or depth of ΔW_s represents a decrease in soil water during the period that can be utilized to fulfill W_r. R_e is set equal to P_{efT} if the W_{ET} does not include increased E stemming from wetting from P. R_e is set equal to P_{rz} if the W_{ET} does include the increased E associated with the P events.

Allowances for Non-uniform Distribution

Water cannot be applied with perfect uniformity nor without some unavoidable losses with most surface irrigation systems. World-wide, surface irrigation is still the predominant irrigation method. In flat land areas, basin system is the most common method and non-uniform surface elevation is the main reason for non-uniform water distribution. On sloping lands, surface runoff is inherent with most surface irrigation methods. Surface runoff is often captured and used on lower lying fields, or captured in holding ponds and pumped for reuse on the same field or on another field, thereby reducing the fraction of loss as the area of focus increases. An illustration of typical flow and intake characteristics for a uniformly graded surface irrigation system is illustrated in fig. 14.1. Fields may be diked at the lower end to enhance infiltration thereby resulting in little or no runoff. This practice may also reduce deep percolation near the upper end.

If water is applied to furrows with no end dikes until an adequate amount is infiltrated at the lower end of the field, then water application efficiency may be only 65% or less. The surface storage and subsurface storage illustrated in fig. 14.1 are typical characteristics for an average furrow. Design of surface irrigation systems typically involves a water balance, i.e., accounting for water stored on the surface and that infiltrated. Several computer models are available for computing the complex dynamics of surface irrigation such as those by Clemmens et al. (1995) and Strelkof et al. (1990). Details on the design of surface irrigation systems, including reviews of earlier publications by USDA (1974, 1984), can be found in publications by Clemmens et al. (2007), Walker (1989), Walker and Skogerboe (1987), and Kay (1986).

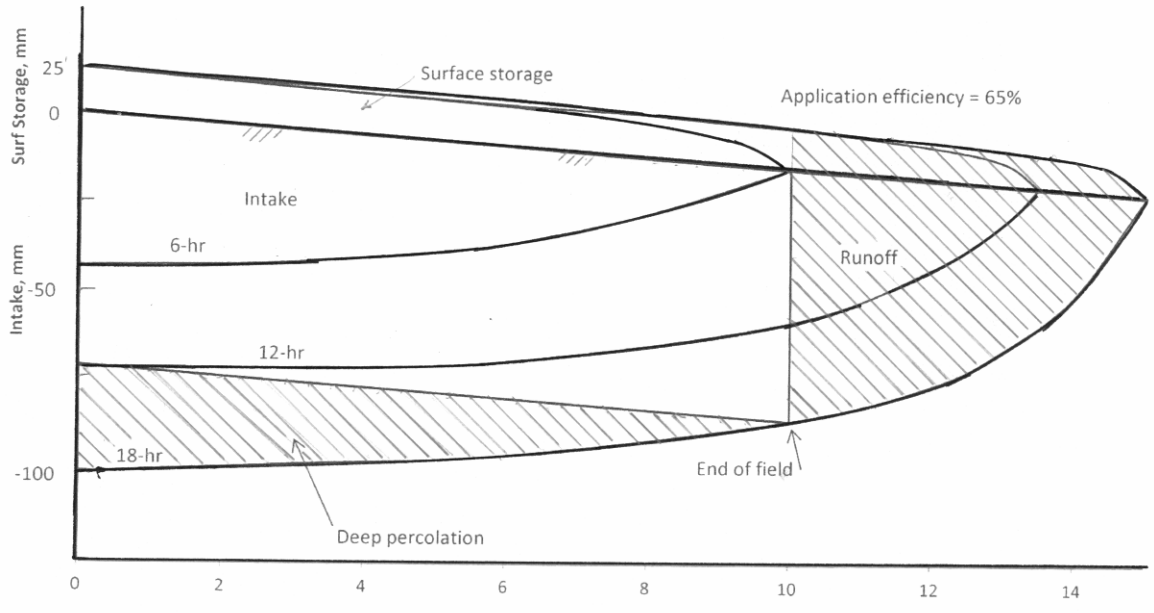

Fig. 14.1. Sketch of longitudinal water application profile along a furrow. Source: Jensen, personal communication.

The field application uniformity may be estimated as a modification from the average furrow by including the effects of soil variability along the furrow as well as intake differences between wheel rows and non-wheel rows and from variations in stream size, furrow shape and other miscellaneous losses. These variations can decrease the distribution uniformity for the field by 25 to 30% from the distribution uniformity calculated for a single furrow.

As with surface systems, sprinkler systems do not apply water with perfect uniformity under calm conditions and application uniformity is adversely affected as wind speed increases. Sprinkler application patterns typically follow a normal distribution of infiltration depths, i.e., there are some areas that receive more water than the average and other areas that receive less. With multiple irrigations under different wind speeds and directions there may be some compensation in the over- or under-irrigated areas. With sprinkler irrigation systems there is also some evaporation from the spray. Spray evaporation losses seldom exceed 5% except where wind causes spray drift which allows more time for evaporation to occur. Under some wind conditions evaporation losses from the sprinkler streams may be as high as 12-14%, however, much of that evaporation reduces ET demands of vegetation downwind of the evaporation through cooling and humidification of the near surface boundary layer. Therefore, on average, it is recommended that not more than 5% evaporation losses be used in estimating water depletion.

Sprinkler systems can have appreciable edge effects without mirrored overlap at field borders. They also may be subject to pressure differences due to elevation and friction head loss in the pipeline if pressure regulation is not part of the system. These differences can reduce the field distribution uniformity by 10 to 20%, depending on nozzle spacing and field size. There have been hundreds of papers written about sprinkler application uniformity and wind effects, spray losses, runoff, erosion, and crop yields since the 1950s. Examples of publications are those of Mateos et al. (1997), Jiusheng and Kawano (1996), Howell et al. (1995), Mantovani et al. (1995), Han et al. (1994), Seginer et al. (1991), Kranz and Eisenhauer (1990), Kohl and DeBoer (1984), Hathoot et al. (1994), and Yazar (1984). A recent publication on the design of sprinkler systems is that by Martin et al. (2007) and a center pivot design publication by Allen et al. (2000) contain procedures to estimate distribution uniformities and evaporation losses from these systems.

Use of drip or trickle irrigations systems, now called micro-irrigation systems, has expanded greatly since the 1960s. Typically, micro-irrigation systems are used mainly on high-value crops because of system costs. As with sprinkler systems, there have been numerous publications on emitters, tubing, filters and automatic controls. Design uniformities for micro-irrigation systems generally include the effects of pressure differences and the effects of plugging of emitters. A comprehensive review of the design and operation of micro-irrigation systems was presented by Nakayama and Bucks (1986). Edge effects are negligible. A recent publication on the design of micro-irrigation systems is by Evans et al. (2007).

Storage and Distribution System Losses

From a project viewpoint, a substantial portion of runoff from surface systems and canal or lateral leakage may be recovered for use within a project or for use on downstream projects,

depending on geology and topography. Estimates of evaporation from storage and regulating reservoirs may be required when estimating flow and storage capacities using procedures described in chapter 6. Leakage from canals, laterals and reservoirs may result in the growth of non-beneficial vegetation depending on local subsurface soil and geologic conditions. Estimates of these losses can be made using procedures described in chapters 9 and 10.

Expected Occurrences of ET

When using irrigation water requirements for irrigation or water resources systems planning and design, some level of probability is generally utilized to insure successful attainment of crop water demands for a specified number of years within a multi-year period. The probability level selected for design purposes should be based on an economic analysis considering both the reduction in crop yield and quality expected to occur should soil water availability be reduced below the desired minimum level during the averaging period, and the incremental increases in the farm irrigation distribution system cost to provide capacity for higher probability levels. The use of a 50% probability level would result in soil water availability less than the minimum level for full ET in one out of two years. The degree to which soil water is depleted below the minimum should also be considered. Usually a higher probability level (80 to 90 percent) is selected for high value, shallow-rooted crops than for common farm crops.

The expected reference ET on which to base the design capacity of farm or project irrigation systems will usually reduce with longer duration of the period, in days, being considered. The value will also vary with the desired probability level for the crop. A typical example of frequency distributions for reference ET is presented in fig. 14.2 where daily alfalfa reference ET_r estimated using the ASCE-EWRI standardized Penman-Monteith equation is shown for a 20-year period at Kimberly, Idaho. Comparing the top figure, where daily ET_r is plotted to the bottom figure, where 10-day running average ET_r is plotted, shows the substantial decrease in the range in reference ET values when they are averaged over several days. Overlain on the ET_r data are probability lines for various levels of nonexceedence, based on a normal probability distribution. *Nonexceedence* is defined as the value of ET that is not expected to be exceeded p% of the time, where p is the probability level.

A normal probability distribution presumes that the coefficient of skewness (CS) = 0, where CS is the ratio of skew to the population mean. Generally, with evapotranspiration, CS approaches 0, so that frequency estimates based on the normal distribution are generally valid (Allen and Wright, 1983; Allen et al. 1983). In the case of the normal distribution, an estimate for ET for a specific probability of nonexceedance is estimated as:

$$ET_{Pn} = ET_{mean} + K_{Pn}\ s \tag{14.11}$$

where ET_{Pn} is the ET rate expected to be exceeded only 100% – p% of the time, K_{Pn} is a probability factor, and ET_{mean} and s are the estimates for the mean and standard deviation of the underlying ET population. Generally, ET_{mean}, s, and ET_{Pn} are computed for a specific time period during the growing season, for example, for the peak 10- or 30-day period. Values for K_{Pn} are listed in Table 14.2 for the normal distribution.

Table 14.2. Probability factors (K_{Pn}) for a normal distribution.

Probability of non-exceedance, p (%)	2	5	10	25	50	75	80	90	95	98
Probability of exceedance (%)	98	95	90	75	50	25	20	10	5	2
Return period (years)	1.0	1.0	1.1	1.3	2	4	5	10	20	50
K_{Pn}	–2.054	–1.645	–1.28	–0.675	0.0	0.675	0.841	1.28	1.645	2.054

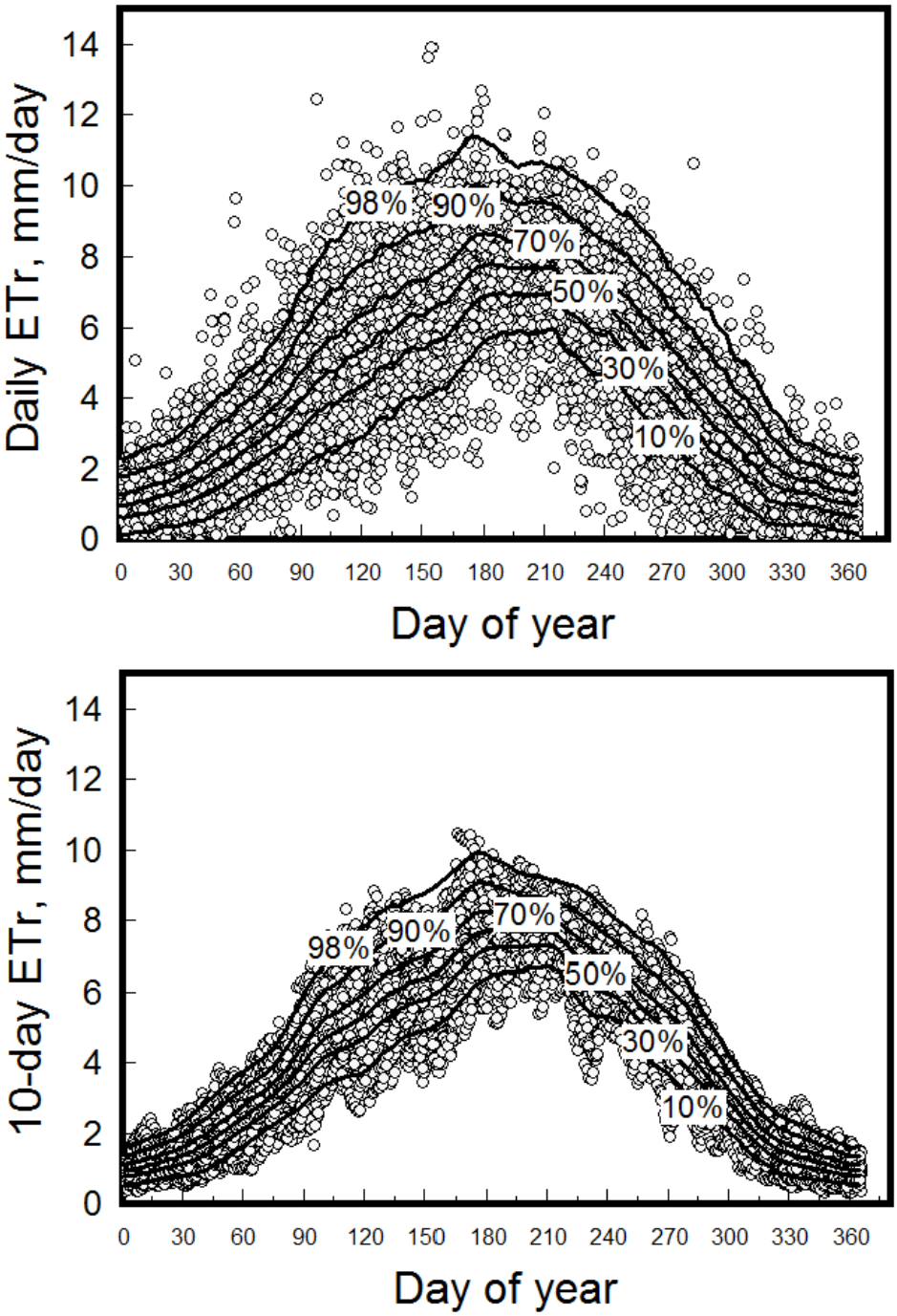

Fig. 14.2 Frequency distribution of alfalfa reference ET for Kimberly, ID vs time of year for daily timesteps (upper figure) and 10-day running averages (lower figure) over a 20-year period.

Available Water and Rainfall Effects

The peak period for ET may not last for more than three weeks for many annual crops. Therefore, the required capacity of the system may be impacted by the amount of soil water storage that is available for depletion during the peak use period. The minimum or net design capacity may be reduced if leaching can be delayed during the peak use period and water is applied for leaching off-season or when reference ET is not at its peak.

14.7 Improvements in Estimating Water Requirements

Impacts of Better Training

Approaches for estimating irrigation water requirements and procedures have changed greatly since the first edition of this manual. The training now received by most engineers includes some background in energy balance, meteorology, soil physics and plant science. Essentially every new engineer is computer literate and most have had some experience in solving multidisciplinary problems. Engineers associated with universities generally have immediate access to the latest worldwide literature in digital form. For others, the Internet can provide rapid access information on almost any subject. No longer must the recommended approach to solving a problem be "simple" as has generally been the practice in the past. However, the recommended approach to problem solving must still be rational and understandable by all engineers as well as by professionals in other disciplines who are involved in water supply and management issues.

Understanding Irrigation System and Water Consumption Interactions

For decades, policy makers and many engineers have misunderstood the meaning of the classic term *irrigation efficiency*. The frequent misinterpretation of reported low irrigation efficiencies was that if efficiency could be increased, less water would be consumed and there would be new water for other uses. Typically, the opposite is true because the classical efficiency term involves only the water diverted or applied to fields that is consumed. Both the consumed and non-consumed components of water extractions must be considered as part of a water balance, and the disposition of nonconsumed water must be determined during assessment of impacts of 'conservation' programs (Perry 2007; Perry et al. 2009; Fredericksen and Allen 2011). As an example of impacts of improving efficiency, Pfeiffer and Lin (2010) reported that when users in Kansas moved toward higher-efficiency water systems, water use tended to increase. With the better systems, farmers were able to meet crop water needs during mid-summer and, as a result, they tended to plant higher-water use and higher-return crops. As people moved to more and more efficient systems, less return flow to the groundwater occurred, that, in turn eventually entered river systems. Over the last decade, a region in Kansas has seen a shift away from the concept that increased water efficiency equals effective water conservation. They have found, in practice, that producers willingly adopt more efficient systems, but may use the same amount of water either for a higher-water-use crop or put more acres into production, depending on the maximum water extraction limits stipulated by state water law. Many state cost-share practices for upgrading irrigation systems have been reduced or eliminated (Pfeiffer and Lin, 2010).

Recent papers review the classic irrigation efficiency term and related terms. More recently the focus has been on the physical or economic productivity of water (Jensen 2007; Perry 2007; Perry et al. 2009; Molden 1997, 2007). Basically, irrigation water requirements involve mainly water consumption and "efficiency" is not directly involved. Overall, there is a better understanding of irrigation and its effect on water resources and crop production than existed when the first edition of this manual was published in 1990.

14.8 Estimating Depletions to the Water Resource

Often quantification of depletions to river discharge are required as part of multi-state compact management or for in-state water rights management, and depletions to ground-water systems are needed for managing long-term sustainability. Depletions to the water resource caused by irrigation are equivalent to the *NIWR* calculated in section 14.3 when the ET is at the potential value. This will occur when irrigation water is fully applied. Under water shortage or scarcity, however, crops may not receive a full water supply and some water stress may occur. In addition, irrigation of some crops may be managed to induce some stress during some stages of growth, even under full water supply, to impact market quality to maximize profits.

When $ET_{act} < ET_{pot}$, methods are needed to estimate the amount of reduction in ET_{act}. When water additions are known, a daily water balance can be made for irrigated fields, with a stress function, such as described in chapter 10, utilized. Often, however, field-scale water additions are not known on a multi-field basis. In those cases, a water balance can be conducted on an irrigation scheme or district basis, or watershed basis, with ET closed upon as a residual. Horizontal flows for groundwater and diffusive forms of returns of surface water to streams can make these calculations uncertain. Satellite-based surface energy balance is becoming more widely used to estimate ET_{act} for use in scheme or district scale water balance (Allen et al., 2007b, for example), where ET_{act} from hundreds or thousands of individual fields can be quantified, provided a moderate resolution satellite having thermal imaging capacity, such as Landsat, is available. A fourth means to estimate ET_{act} is through the employment of crop yield-ET relationships, where reductions in yield are associated with reductions in ET. These relationships generally need to be calibrated locally to account for lower yields caused by other than constrained water supply, such as disease, salinity or poor fertility.

On a field scale, the depletion to the water resource, D_{WR}, is estimated similar to *NIWR* (eq. 14.1), except that actual transpiration or actual ET is used rather than potential values:

$$\begin{aligned} D_{WR} &= ET_{act} - (P - Runoff - DPerc) \\ &= E + T_{act} - (P - Runoff - DPerc) \\ &= E + T_{act} - P_{rz} \\ &= T_{act} - P_{efT} \end{aligned} \tag{14.12}$$

The comments in section 14.7 apply to the quantification and characterization of D_{WR}, where returns of abstracted water back to streams or ground-water via surface runoff or percolation must be accurately measured or estimated and should not be considered to be part of D_{WR}, unless substantially impaired in quality, or lost directly to a saline sink such as the ocean (Fredericksen and Allen 2011, Molden 1997, 2007, Pfeiffer and Lin, 2010).

Appendix A

Conversion and Meteorological Tables

TABLE A1 Conversion Factors[1]

Length	
1 micrometer (:m) = 10^{-6} m	1 degree of latitude * (Elat.) = 111.14 km = 69.057 stat. mi.
1 millimeter (mm) = 10^{-1} cm = 10^{-3} m	1 inch (in.) = 25.4 mm = 2.54 cm = 0.0254 m
1 centimeter (cm) = 10^{-2} m	1 foot (ft) = 12 in. = 30.48 cm = 0.3048 m
1 meter (m) = 10^{2} cm = 3.2808 ft = 39.370 in.	1 statute mile (stat. mi.) = 5280 ft = 1609.3 m = 1.6093 km = 0.8684 nautical miles
1 kilometer (km) = 10^{5} cm = 10^{3} m = 3280.8 ft = 0.62137 stat. mi	
Area [b]	
1 square meter (m^2) = $10^{4}cm^2$ = 1550.0 $in.^2$ = 10.764 ft^2	1 acre = 43560 ft^2 = 4046.856 m^2 = 0.4047 ha
1 square foot (ft^2) = 144 $in.^2$ = 0.092903 m^2	1 hectare (ha) = 10^{4} m^2 = 2.471 acre

TABLE A1 *Continued*

Volume	
1 cubic meter (m^3) = 10^6 cm^3 = 35.315 ft^3 = 264.172 U.S. gal. = 219.97 Brit. gal. 1 liter (L) [see footnote a] (1 liter originally was defined as the volume occupied by 1 kilogram of water at its temperature of maximum density, but has been redefined) = 1000 cm^3 = 0.26417 U.S. gal.	1 cubic inch ($in.^3$) = 16.387 cm^3 1 cubic foot (ft^3) = 1728 $in.^3$ = 7.4805 U.S. gal. = 28.3168 L = 0.0283168 m^3 1 gallon, U.S. (U.S. gal.) = 231 $in.^3$ = 0.83267 Brit. Gal. = 3.78534 L = 3.78534 x 10^{-3} m^3 1 acre-foot = 1233.48 m^3
Time	
1 mean solar minute (min.) = 60 s 1 hour (h) = 3600 s = 60 min.	1 mean solar day (d) = 86400 s = 1440 min. = 24 h
Velocity (speed)	
1 meter per second (m s^{-1}) = 3.6000 km h^{-1} = 2.23694 mi. h^{-1} = 3.28084 ft s^{-1} 1 kilometer per hour (km h^{-1}) = 0.27778 m s^{-1} = 0.53959 knot = 0.62137 mi. h^{-1} 1 knot = 1 naut. mi. h^{-1} = 1.15155 mi. h^{-1} = 0.51479 m s^{-1} = 1.85325 km h^{-1}	1 mile per hour (mi. h^{-1}) = 0.86839 knot = 0.44704 m s^{-1} = 1.6093 km h^{-1} 1 foot per second (ft s^{-1}) = 0.68182 mi. h^{-1} = 0.3048 m s^{-1} = 1.0973 km h^{-1}

TABLE A1 *Continued*

Mass	
1 gram (g) = 0.0022046 lbm	1 pound avoirdupois (1 lb) = 453.59 g = 0.45359 kg
1 kilogram (kg) = 10^3 g = 2.2046 lbm	1 short ton = 2000 lbm = 0.089286 long ton = 0.90718 t
1 metric ton, tonne (t) = 10^3 kg = 2204.6 lbm	1 long ton = 2240 lbm = 1.12 short ton = 1.0160 t
Density of water (4 °C)	
1 g cm^{-3} = 62.428 lb ft^{-3} (Specific wt.) = 1 t m^{-3}	1 kg 10^{-3} m^{-3} = 10^{-3} kg cm^{-3} = 10^{-3} t 10^{-3} m^{-3} 1 Mg m^{-3} = 10^3 kg m^{-3} = 1 t m^{-3}
Force	
1 gram force = 980.665 dynes = 9.80665 x 10^{-3} N	1 newton (N) = 10^5 dynes = kg m s^{-2}
Energy, Work	
1 erg = 1 dyne-centimeter = 10^{-7} joule (J) = 2.3884 x 10^{-8} ITcal	1 kilowatt-hour (kW h) = 3.6 x 10^6 joules = 3.6 megajoules (MJ)
1 joule (J) = 10^7 ergs = 0.23884 ITcal = 1 N m	1 British thermal unit (Btu) (The Btu used here is defined by the relationship: 1 Btu EF^{-1} lb^{-1} = 1 ITcal EC^{-1} g^{-1} = 251.996 ITcal = 1055.07 joules
1 International Steam Tables calorie (ITcal) = 4.1868 joules	1 foot-pound (ft lb) = 1.35582 joules

TABLE A1 *Continued*

Pressure (1)	
1 dyne per square centimeter (dyne cm^{-2}) = 10^{-3} mb = 10^{-6} bar = 0.1 pascal (Pa)	1 standard inch of mercury (in. Hg (standard)) = 0.49115 lb $in.^{-2}$ = 33.864 mb = 25.4 mm Hg (standard) = 3.3864 kPa
1 millibar (mb) = 10^{3} dynes cm^{-2} = 0.750062 mm Hg (standard) = 0.029530 in. Hg (standard) = 100 pascal (Pa)	1 pound per sq. inch (1b $in.^{-2}$) = 2.0360 in. Hg (standard) = 68.9476 mb = 6.89476 kPa
1 bar (b) = 10^{6} dynes cm^{-2} = 10^{3} mb = 10^{5} N m^{-2} = 10^{5} pascal (Pa) = 10^{2} kPa	1 standard atmosphere = 1013.25 mb = 760 mm Hg (standard) = 29.921 in. Hg (standard) = 14.696 lb $in.^{-2}$ = 101.325 kPa
1 standard millimeter of mercury (mm Hg (standard)) = 1.333224 mb = 0.039370 in. Hg (standard) = 133.32 Pa	1 Pa = 1 N m^{-2}
Power	
1 watt (W) = 1 joule s^{-1}	1 kilowatt = 10^{3} J s^{-1} = 1 kJ s^{-1}
Energy per Unit Area	
1 langley (ly) = 1 cal_{15} cm^{-2} = 4.1855 joules cm^{-2}	1 Btu ft^{-2} = 11.357 kilojoules m^{-2}
1 joule cm^{-2} = 10 kilojoules m^{-2}	1 ITcal cm^{-2} = 4.1868 joule cm^{-2} = 41.868 kilojoules m^{-2}
Power per Unit Area	
1 cal cm^{-2} min^{-1} = 1 ly min^{-1} = 0.6978 kilowatts m^{-2}	1 Btu ft^{-2} min^{-1} = 0.18928 kilowatts m^{-2}

[1] Data from Table 1, List (1984); ASTM (1976), Wandmacher and Johnson (1995).
* Average value, 1/90 of meridian quadrant.
[2] The pressure units, one standard inch of mercury, one standard millimeter of mercury, and one standard atmosphere are defined in terms of the conventional standard value of gravitational acceleration of 980.665 cm s^{-2}, which was adopted by the International Committee on Weights and Measures. These units have been proposed for general meteorological use.
[a] The General Conference on Weights and Measures in 1964 redefined the liter to be exactly 1000 cm^3. Hence, the cubic decimeter, expressed as 10^{-3} m^3, dm^3, or 1000 cm^3 may be a preferred unit to avoid errors. However, for practical purposes the new and old liters are essentially the same.
[b] The unit of land area, hectare, is commonly used in the metric system, but its dimensions, 10^4 m^2, do not follow the SI guide of multiples of 10^3. The dunam = 10^3 m^2 is a more practical land unit, but it is not in common usage and its symbol may conflict with SI recommendations. The hectare with the symbol ha was derived from hecto, a multiple of 100 having the symbol h, and the "are" which is a unit of land area = 100 m^2 abbreviated "a".

TABLE A.2 Saturation Vapor Pressure Over Water[a]

°C	0 kPa	0.1 kPa	0.2 kPa	0.3 kPa	0.4 kPa	0.5 kPa	0.6 kPa	0.7 kPa	0.8 kPa	0.9 kPa
0	0.6108	0.6152	0.6197	0.6242	0.6288	0.6333	0.6379	0.6379	0.6472	0.6519
1	0.6566	0.6614	0.6661	0.6709	0.6758	0.6807	0.6856	0.6856	0.6955	0.7004
2	0.7055	0.7105	0.7156	0.7207	0.7259	0.7311	0.7363	0.7363	0.7469	0.7522
3	0.7575	0.7629	0.7683	0.7738	0.7793	0.7848	0.7904	0.7904	0.8016	0.8072
4	0.8129	0.8187	0.8245	0.8303	0.8361	0.8420	0.8479	0.8479	0.8598	0.8659
5	0.8719	0.8780	0.8842	0.8903	0.8966	0.9028	0.9091	0.9091	0.9218	0.9282
6	0.9346	0.9411	0.9477	0.9542	0.9608	0.9675	0.9742	0.9742	0.9877	0.9945
7	1.001	1.008	1.015	1.022	1.029	1.036	1.043	1.043	1.058	1.065
8	1.072	1.079	1.087	1.094	1.102	1.109	1.117	1.117	1.132	1.140
9	1.147	1.155	1.163	1.171	1.179	1.187	1.195	1.195	1.211	1.219
10	1.227	1.235	1.244	1.252	1.261	1.269	1.277	1.277	1.295	1.303
11	1.312	1.321	1.329	1.338	1.347	1.356	1.365	1.365	1.383	1.393
12	1.402	1.411	1.420	1.430	1.439	1.449	1.458	1.458	1.477	1.487
13	1.497	1.507	1.517	1.527	1.537	1.547	1.557	1.557	1.577	1.587
14	1.598	1.608	1.619	1.629	1.640	1.650	1.661	1.661	1.683	1.693
15	1.704	1.715	1.726	1.738	1.749	1.760	1.771	1.771	1.794	1.806
16	1.817	1.829	1.841	1.852	1.864	1.876	1.888	1.888	1.912	1.924
17	1.937	1.949	1.961	1.974	1.986	1.999	2.012	2.012	2.037	2.050
18	2.063	2.076	2.089	2.102	2.115	2.129	2.142	2.142	2.169	2.183
19	2.196	2.210	2.224	2.238	2.252	2.266	2.280	2.280	2.308	2.323
20	2.337	2.352	2.366	2.381	2.396	2.411	2.426	2.426	2.456	2.471
21	2.486	2.501	2.517	2.532	2.548	2.563	2.579	2.579	2.611	2.627
22	2.643	2.659	2.675	2.692	2.708	2.725	2.741	2.741	2.775	2.792
23	2.809	2.826	2.843	2.860	2.877	2.895	2.912	2.912	2.947	2.965
24	2.983	3.001	3.019	3.037	3.056	3.074	3.092	3.092	3.130	3.148
25	3.167	3.186	3.205	3.224	3.243	3.263	3.282	3.282	3.321	3.341
26	3.361	3.381	3.401	3.421	3.441	3.462	3.482	3.482	3.523	3.544
27	3.565	3.586	3.607	3.628	3.649	3.671	3.692	3.692	3.736	3.758
28	3.780	3.802	3.824	3.846	3.869	3.891	3.914	3.914	3.959	3.982
29	4.005	4.029	4.052	4.076	4.099	4.123	4.147	4.147	4.195	4.219
30	4.243	4.267	4.292	4.317	4.341	4.366	4.391	4.391	4.442	4.467
31	4.493	4.518	4.544	4.570	4.596	4.622	4.649	4.649	4.702	4.728
32	4.755	4.782	4.809	4.836	4.864	4.891	4.919	4.919	4.974	5.003
33	5.031	5.059	5.087	5.116	5.145	5.174	5.203	5.203	5.261	5.290
34	5.320	5.350	5.380	5.410	5.440	5.470	5.500	5.500	5.562	5.593
35	5.624	5.655	5.686	5.718	5.749	5.781	5.813	5.813	5.877	5.910
36	5.942	5.975	6.008	6.041	6.074	6.107	6.141	6.141	6.208	6.242
37	6.276	6.311	6.345	6.380	6.414	6.449	6.484	6.484	6.555	6.591
38	6.626	6.662	6.698	6.735	6.771	6.808	6.845	6.845	6.919	6.956
39	6.993	7.031	7.069	7.107	7.145	7.183	7.222	7.222	7.299	7.339
40	7.378	7.417	7.457	7.497	7.537	7.577	7.617	7.617	7.698	7.739
41	7.780	7.821	7.863	7.905	7.946	7.988	8.031	8.031	8.116	8.159
42	8.202	8.245	8.288	8.332	8.375	8.419	8.464	8.464	8.553	8.597
43	8.642	8.687	8.733	8.778	8.824	8.870	8.916	8.916	9.010	9.056
44	9.103	9.151	9.198	9.246	9.294	9.342	9.390	9.390	9.487	9.536
45	9.585	9.635	9.684	9.734	9.784	9.835	9.885	9.885	9.987	10.038
46	10.089	10.141	10.193	10.245	10.297	10.350	10.403	10.403	10.509	10.562
47	10.616	10.670	10.724	10.778	10.833	10.888	10.943	10.943	11.054	11.110
48	11.166	11.222	11.279	11.336	11.393	11.450	11.507	11.507	11.623	11.682
49	11.740	11.799	11.858	11.917	11.977	12.037	12.097	12.097	12.218	12.278
50	12.340	12.401	12.462	12.524	12.587	12.649	12.712	12.712	12.838	12.901

[a] Calculated using Goff-Gratch formulation (List, 1984, p.350). 1 mb = kPa × 10

TABLE A.3 Thermodynamic Constants[1]

Basic constants:

Apparent molecular weight of dry air, M_a

$M_a = 28.966$ g mol^{-1} or kg kmol^{-1}

Universal gas constant, $\boldsymbol{R}$

$\boldsymbol{R} = 8.3144$ joule mol^{-1} K^{-1} or kJ kmol^{-1} K^{-1}

$= 1.98583$ ITcal mol^{-1} K^{-1}

Specific gas constant for dry air, $R_a = \boldsymbol{R}/M_a$

$$R_a = \frac{8.3144 \text{ joule mol}^{-1} \text{ K}^{-1}}{28.966 \text{ g mol}^{-1}} = 0.28704 \text{ joule g}^{-1} \text{ K}^{-1}$$

$= 0.28704$ kJ kg^{-1} K^{-1}

$= 6.8557 \times 10^{-2}$ ITcal g^{-1} K^{-1}

Molecular weight of water vapor, M_v

$M_v = 18.0160$ g mol^{-1} or kg kmol^{-1}

Specific gas constant for water vapor, $R_v = R/M_v$

$$R_v = \frac{8.3144}{18.0160} = 0.46150 \text{ joule g}^{-1} \text{ K}^{-1}$$

$= 0.46150$ kJ kg^{-1} K^{-1}

$= 0.110226$ ITcal g^{-1} K^{-1}

Absolute temperature of the ice point, T_o

$T_o = 273.15$ K [2]

Specific heats:	**Recommended values**	**Range of actual values**
Dry air:		
constant pressure, c_p $7R_a/2$	= 0.240 ITcal g^{-1} K^{-1}	0.2394-0.2414
	= 1.0046 kJ kg^{-1} K^{-1}	1.0017-1.0101
constant volume, c_v $5R_a/2$	= 0.171 ITcal g^{-1} K^{-1}	0.171-0.172
	= 0.7176 kJ kg^{-1} K^{-1}	0.715-0.720
Water:		
liquid, c_w	1.000 ITcal g^{-1} K-1	0.999-1.3
	4.1868 kJ kg^{-1} K^{-1}	4.180-5.4
ice, c_i	0.5 ITcal g^{-1} K^{-1}	0.5-0.3
	2.0934 kJ kg^{-1} K^{-1}	2.092-1.26
Water vapor:		
constant pressure, c_{pv} $4R_v$	= 0.441 ITcal g^{-1} K^{-1}	0.44-0.46
	= 1.846 kJ kg^{-1} K^{-1}	1.84-1.92
constant volume, c_{vv} $3R_v$	= 0.331 ITcal g^{-1} K^{-1}	0.33-0.34
	= 1.3845 kJ kg^{-1} K^{-1}	1.381-1.42
Moist air:		
Brutsaert (1982)		
constant pressure, c_p	= $c_{pd}(1 + 0.84\, q)$	
where q = specific humidity	= 0.242 ITcal g^{-1} K^{-1}	
	= 1013 J kg^{-1} K^{-1}	

[1] Data from Table 70, List (1984).

[2] The International Temperature Scale of 1990 (ITS-90).

TABLE A.4 Density of Air[1]

The density of air in g cm^{-3} and kg m^{-3} is:

$$\rho = 10^{-3}\frac{P}{R_a / T_v} \text{ g cm}^{-3}, \text{ or } \rho = \frac{P}{R_a / T_v} \text{ kg m}^{-3}$$

where P = total barometric pressure, kPa; R_a = specific gas constant for dry air = 0.28704 kJ kg^{-1} K^{-1}; T_v = virtual temperature (the temperature dry air would have to be in order to have the same density as moist air at the same pressure).

$$T_v = T\frac{1 + r/0.622}{1 + r}$$

where r = the mixing ratio ($r = m_v/m_a \approx 0.622\ e/P$) and T = absolute temperature. For P in kPa, the density ρ is:

$$\Delta = 3.4838\ P/T_v \text{ kg m}^{-3} \text{ or } 0.0034838\ P/T_v \text{ g cm}^{-3}$$

Example: For P = 101.325 kPa and T_v = 273.15 K (0EC)

$$\Delta = 3.4838(101.325/273.15) = 1.292 \text{ kg m}^{-3}$$

$$\Delta = 0.0034838(101.325/273.15) = 0.001292 \text{ g cm}^{-3}$$

	Pressure (kPa)					
	110	**100**	**90**	**80**	**70**	**60**
T_v, (EC)	Density (kg m^{-3})					
0	1.4029	1.2754	1.1478	1.0203	0.8928	0.7652
5	1.3777	1.2525	1.1272	1.0020	.8767	.7515
10	1.3534	1.2303	1.1073	.9843	.8612	.7382
15	1.3299	1.2090	1.0881	.9672	.8463	.7254
20	1.3072	1.1884	1.0695	.9507	.8319	.7130
25	1.2853	1.1684	1.0516	.9348	.8179	.7011
30	1.2641	1.1492	1.0343	.9193	.8044	.6895
35	1.2436	1.1305	1.0175	.9044	.7914	.6783
40	1.2237	1.1125	1.0012	.8900	.7787	.6675
45	1.2045	1.0950	.9855	.8760	.7665	.6570
50	1.1859	1.0780	.9702	.8624	.7546	.6468

[1] Data from Table 71, List (1984).

TABLE A.5 Day of Year

In the many energy balance equations, the day of the year, *J*, is often required. A procedure for calculating *J* (ASCE-EWRI 2005) is:

$$J = D_M - 32 + \text{Int}\left(275\frac{M}{9} \right) + 2\ \text{Int}\left(\frac{3}{M+1} \right) + \text{Int}\left(\frac{M}{100} - \frac{\text{Mod}(Y,4)}{4} + 0.975 \right) \quad \text{(A5.1)}$$

where D_M is the day of the month (1-31), M is the number of the month (1-12), and Y is the number of the year (for example 1996 or 96). The "Int" function in eq. A5.1 finds the integer number of the argument in parentheses by rounding downward. The "Mod(Y,4)" function finds the modulus (remainder) of the quotient Y/4 and corrects for the effect of a leap year.

For monthly periods, the day of the year at the middle of the month (J_{month}) is approximately:

$$J_{month} = Int(30.4\ M - 15) \quad \text{(A5.2)}$$

The day of the year (*DofY*) for the 15th of each month is:

Month	*DofY*	Month	*DoY*
January	15	July	196
February	46	August	227
March	74	September	258
April	105	October	288
May	135	November	319
June	166	December	349

BLANK PAGE

Appendix B

Mean Crop Coefficients, K_c, for Well-managed Crops in Sub-Humid Climates[1] for use with clipped grass reference ET_o, Range of Maximum Effective Rooting Depth, and Soil Water Depletion Fraction for No Stress, p, based on FAO-56 (Allen et al. 1998)

Guidelines on applying K_c values in this appendix are given in Chapter 10.

Table B.1 Mean Crop Coefficients

Crop	$K_{c\ ini}$[2]	$K_{c\ mid}$	$K_{c\ end}$	*Max. Ht* *m*	*Max. Root depth*[3] *M*	p[4]
a. Small Vegetables	**0.7**	**1.05**	**0.95**			
Broccoli		1.05	0.95	0.3	0.4-0.6	0.45
Brussel Sprouts		1.05	0.95	0.4	0.4-0.6	0.45
Cabbage		1.05	0.95	0.4	0.5-0.8	0.45
Carrots		1.05	0.95	0.3	0.5-1.0	0.35
Cauliflower		1.05	0.95	0.4	0.4-0.7	0.45
Celery		1.05	1.00	0.6	0.3-0.5	0.20
Garlic		1.00	0.70	0.3	0.3-0.5	0.30
Lettuce		1.00	0.95	0.3	0.3-0.5	0.30
Onions - dry		1.05	0.75	0.4	0.3-0.6	0.30
- green		1.00	1.00	0.3	0.3-0.6	0.30
- seed		1.05	0.80	0.5	0.3-0.6	0.35
Spinach		1.00	0.95	0.3	0.3-0.5	0.20
Radish		0.90	0.85	0.3	0.3-0.5	0.30
b. Vegetables – Solanum Family (*Solanaceae*)	**0.6**	**1.15**	**0.80**			
Egg Plant		1.05	0.90	0.8	0.7-1.2	0.45
Sweet Peppers (bell)		1.05[5]	0.90	0.7	0.5-1.0	0.30
Tomato		1.15[5]	0.70-0.90	0.6	0.7-1.5	0.40
c. Vegetables – Cucumber Family (*Cucurbitaceae*)	**0.5**	**1.00**	**0.80**			
Cantaloupe	0.5	0.85	0.60	0.3	0.9-1.5	0.45
Cucumber – Fresh Market	0.6	1.00[5]	0.75	0.3	0.7-1.2	0.50
– Machine harvest	0.5	1.00	0.90	0.3	0.7-1.2	0.50
Pumpkin, Winter Squash		1.00	0.80	0.4	1.0-1.5	0.35
Squash, Zucchini		0.95	0.75	0.3	0.6-1.0	0.50
Sweet Melons		1.05	0.75	0.4	0.8-1.5	0.40
Watermelon	0.4	1.00	0.75	0.4	0.8-1.5	0.40
d. Roots and Tubers	**0.5**	**1.10**	**0.95**			
Beets, table		1.05	0.95	0.4	0.6-1.0	0.50
Cassava – year 1	0.3	0.80[6]	0.30	1.0	0.5-0.8	0.35
– year 2	0.3	1.10	0.50	1.5	0.7-1.0	0.40
Parsnip	0.5	1.05	0.95	0.4	0.5-1.0	0.40
Potato		1.15	0.75[7]	0.6	0.4-0.6	0.35
Sweet Potato		1.15	0.65	0.4	1.0-1.5	0.65
Turnip (and Rutabaga)		1.10	0.95	0.6	0.5-1.0	0.50
Sugar Beet	0.35	1.20	0.70[8]	0.5	0.7-1.2	0.55[9]

continued…

1 The values for $K_{c\ mid}$ and $K_{c\ end}$ are values expected in subhumid climates, where daily minimum relative humidity (RH_{min}) ~ 45% and daily mean wind speed at 2 m height (u_2) ~ 2 m s^{-1}. For different climatic conditions, the values given can be adjusted using eq. 10.14 and 10.15.

2 These are general values for $K_{c\ ini}$ under typical irrigation management and soil wetting. For frequent wettings such as with high frequency sprinkle irrigation or daily rainfall, these values may increase substantially and may approach 1.0 to 1.2. $K_{c\ ini}$ is a function of wetting interval and potential evaporation rate during the initial and development periods and is more accurately estimated using fig. 10.4, or using the dual $K_{cb\ ini} + K_e$.

3 The larger values for maximum root zone z_r are for soils having no significant layering or other characteristics that can restrict rooting depth. The smaller values for z_r may be used for irrigation scheduling and the larger values for modeling soil water stress or for rainfed conditions.

4 The values for p apply for $ET_c \approx 5$ mm/day. The value for p can be adjusted for different ET_c according to

$$p = p_{App\ B} + 0.04\ (5 - ET_c)$$

where p is expressed as a fraction and ET_c as mm/day.

5 Beans, peas, legumes, tomatoes, peppers and cucumbers are sometimes grown on stalks reaching 1.5 to 2 meters in height. In such cases, increased K_c values need to be taken. For green beans, peppers and cucumbers, 1.15 can be taken, and for tomatoes, dry beans and peas, 1.20. Under these conditions height h should be increased also.

6 The midseason values for cassava assume non-stressed conditions during or following the rainy season. The $K_{c\ end}$ and $K_{cb\ end}$ values account for dormancy during the dry season.

7 The $K_{c\ end}$ value for potatoes is about 0.40 and 0.35 for long season potatoes with vine kill.

8 This $K_{c\ end}$ value is for no irrigation during the last month of the growing season. The $K_{c\ end}$ value for sugar beets is higher, up to 1.0 and 0.9, when irrigation or significant rain occurs during the last month.

9 Sugar beets often experience late afternoon wilting in arid climates even at $p < 0.55$, with usually only minor impact on sugar yield.

Mean Crop Coefficient table continued

Crop	$K_{c\ ini}$[2]	$K_{c\ mid}$	$K_{c\ end}$	*Max. Ht* *m*	*Max. Root depth*[3] *m*	*p*[4]
e. Legumes (*Leguminosae*)	**0.4**	**1.15**	**0.55**			
Beans, green	0.5	1.05[5]	0.90	0.4	0.5-0.7	0.45
Beans, dry and Pulses	0.4	1.15[5]	0.35	0.4	0.6-0.9	0.45
Chick pea		1.00	0.35	0.4	0.8-1.2	0.45
Fababean (broad bean) – Fresh	0.5	1.15[5]	1.10	0.4	0.6-1.0	0.50
– Dry/Seed	0.5	1.15[5]	0.30	0.8	0.5-0.7	0.45
Grabanzo	0.4	1.15	0.35	0.8	0.5-0.7	0.45
Green Gram and Cowpeas		1.05	0.60-0.35[10]	0.8	0.6-1.0	0.45
Groundnut (Peanut)		1.15	0.60	0.4	0.6-1.0	0.45
Lentil		1.10	0.30	0.4	0.5-1.0	0.50
Peas – Fresh	0.5	1.15[5]	1.10	0.5	0.6-0.8	0.50
– Dry/Seed		1.15	0.30	0.5	0.6-1.0	0.35
Soybeans		1.15	0.50	0.5	0.6-1.0	0.40
f. Perennial Vegetables (with winter dormancy and initially bare or mulched)	**0.5**	1.00	0.80			
Artichokes	0.5	1.00	0.95	0.7	0.6-0.9	0.45
Asparagus	0.5	0.95[11]	0.30	0.2-0.8	1.2-1.8	0.45
Mint	0.60	1.15	1.10	0.6-0.8	0.4-0.8	0.40
Strawberries	0.40	0.85	0.75	0.2	0.2-0.3	0.20
g. Fiber Crops	**0.35**					
Cotton		1.15-1.20	0.70-0.50	1.2-1.5	1.0-1.7	0.50
Flax		1.10	0.25	1.2	1.0-1.5	0.50
Sisal[12]		0.4-0.7	0.4-0.7	1.5	0.5-1.0	0.80
h. Oil Crops	**0.35**	**1.15**	**0.35**			
Castorbean (*Ricinus*)		1.15	0.55	0.3	1.0-2.0	0.50
Rapeseed, Canola		1.0-1.15[13]	0.35	0.6	1.0-1.5	0.60
Safflower		1.0-1.15[13]	0.25	0.8	1.0-2.0	0.60
Sesame		1.10	0.25	1.0	1.0-1.5	0.60
Sunflower		1.0-1.15[13]	0.35	2.0	0.8-1.5	0.45
i. Cereals	**0.3**	**1.15**	**0.4**			
Barley		1.15	0.25	1	1.0-1.5	0.55
Oats		1.15	0.25	1	1.0-1.5	0.55
Spring Wheat		1.15	0.25-0.4[14]	1	1.0-1.5	0.55
Winter Wheat - with frozen soils	0.4	1.15	0.25-0.4[14]	1	1.5-1.8	0.55
- with non-frozen soils	0.7	1.15	0.25-0.4[14]			
Maize, Field (grain) *(field corn)*		1.20[15]	0.60,0.35[16]	2	1.0-1.7	0.55
Maize, Sweet *(sweet corn)*		1.15[15]	1.05[17]	1.5	0.8-1.2	0.50
Millet		1.00	0.30	1.5	1.0-2.0	0.55
Sorghum – grain		1.00-1.10	0.55	1-2	1.0-2.0	0.55
– sweet		1.20	1.05	2-4	1.0-2.0	0.50
Rice	1.05	1.05-1.20[18]	0.90-0.60	1	0.5-1.0	0.20[19]

continued…

[10] The first $K_{c\ end}$ is for harvested fresh. The second value is for harvested dry.

[11] The K_c for asparagus usually remains at $K_{c\ ini}$ during harvest of the spears, due to sparse ground cover. The $K_{c\ mid}$ value is for following regrowth of plant vegetation following termination of harvest of spears.

[12] K_c for sisal depends on the planting density and water management (e.g., intentional moisture stress).

[13] The lower values are for rainfed crops having less dense plant populations.

[14] The higher value is for hand-harvested crops.

[15] These $K_{c\ mid}$ values for maize are for robust, pristine crops having plant populations of 50,000 plants per ha or higher. For less dense populations or uniform growth, $K_{c\ mid}$ can be reduced by 0.10 to 0.2

[16] The first $K_{c\ end}$ value is for harvest at high grain moisture. The second $K_{c\ end}$ value is for harvest after complete field drying of the grain (to about 18% moisture, wet mass basis).

[17] If harvested fresh for human consumption. Use $K_{c\ end}$ for field maize if the sweet maize is allowed to mature and dry in the field.

[18] The lower value for rice is for dense, uniform stands having low aerodynamic roughness (smooth canopy surface) and low to moderate wind conditions (< 2 m s^{-1}). The higher value is for somewhat more sparse, but inundated (flooded) conditions having greater roughness and lower albedo caused by shadowing, due to the sparseness.

[19] The value for p for rice is 0.20 of saturation.

Mean Crop Coefficient table continued

Crop	$K_{c\ ini}$[1]	$K_{c\ mid}$	$K_{c\ end}$	*Max. Ht* *m*	*Max. Root depth*[2] *m*	p[3]
j. Forages						
Alfalfa Hay – averaged cutting effects	0.40	0.95[20]	0.90	0.7	1.0-2.0	0.55
– individual cutting periods	0.40[21]	1.20[21]	1.15[20]	0.7	1.0-2.0	0.55
– for seed	0.40	0.50	0.50	0.7	1.0-3.0	0.60
Bermuda hay – averaged cutting effects	0.55	1.00[20]	0.85	0.35	1.0-1.5	0.55
– Spring crop for seed	0.35	0.90	0.65	0.4	1.0-1.5	0.60
Clover hay, Berseem – averaged cutting effects	0.40	0.90[21]	0.85	0.6	0.6-0.9	0.50
– individ. cutting periods	0.40[21]	1.15[21]	1.10[21]	0.6	0.6-0.9	0.50
Rye Grass hay – averaged cutting effects	0.95	1.05	1.00	0.3	0.6-1.0	0.60
Sudan Grass hay (annual) – ave. cutting effects	0.50	0.90[21]	0.85	1.2	1.0-1.5	0.55
– individ. cutting periods	0.50[21]	1.15[21]	1.10[21]	1.2	1.0-1.5	0.55
Grazing Pasture - Rotated Grazing	0.40	0.85-1.05	0.85	0.15-0.30	0.5-1.5	0.60
- Extensive Grazing	0.30	0.75	0.75	0.10	0.5-1.5	0.60
Switchgrass[22]	0.20	1.05	0.20	1.0-2.0	1.5-2.0	0.60
Turf grass - cool season[23]	0.90	0.90	0.90	0.10	0.5-1.0	0.40
- warm season[23]	0.85	0.90	0.90	0.10	0.5-1.0	0.50
k. Sugar Cane	0.40	1.25	0.75	3	1.2-2.0	0.65
l. Tropical Fruits and Trees						
Banana – 1st year	0.50	1.10	1.00	3	0.5-0.9	0.35
– 2nd year	1.00	1.20	1.10	4	0.5-0.9	0.35
Cacao	1.00	1.05	1.05	3	0.7-1.0	0.30
Coffee – bare ground cover	0.90	0.95	0.95	2-3	0.9-1.5	0.40
– with weeds	1.05	1.10	1.10	2-3	0.9-1.5	0.40
Palms (including date palms) [24]				8	0.7-1.1 (1.5-2.5) [25]	0.65 (0.50) [25]
- no ground cover - high density (f_{ceff} = 0.7)[26]	0.90	0.95	0.95			
- no ground cover - med. density (f_{ceff} = 0.5)	0.80	0.80	0.80			
- no ground cover – low dens. / young (f_{ceff} = 0.25)	0.50	0.55	0.55			
- no ground cover - v. low dens./young (f_{ceff} = 0.1)	0.35	0.35	0.35			
- active ground cover[27] - high density (f_{ceff} = 0.7)	0.95	0.95	0.95			
- active ground cover - med. density (f_{ceff} = 0.5)	0.90	0.90	0.90			
- act. ground cover - low dens./young (f_{ceff} = 0.25)	0.85	0.85	0.85			
- act. ground cover - v. low dens./young (f_{ceff} = 0.1)	0.80	0.80	0.80			
Pineapple[28] – bare soil	0.50	0.30	0.30	0.6-1.2	0.3-0.6	0.50
– with grass cover	0.50	0.50	0.50	0.6-1.2	0.3-0.6	0.50
Rubber Trees	0.95	1.00	1.00	10	1.0-1.5	0.40
Tea – non-shaded	0.95	1.00	1.00	1.5	0.9-1.5	0.40
– shaded[29]	1.10	1.15	1.15	2	0.9-1.5	0.45
m. Grapes and Berries						
Berries (bushes)	0.30	1.05	0.50	1.5	0.6-1.2	0.50
Grapes – Table or Raisin[24]				2	1.0-2.0	0.35
- no ground cover - high density (f_{ceff} = 0.7) [30]	0.29	1.09	0.87[31]			
- no ground cover - med. density (f_{ceff} = 0.5)[26]	0.29	0.95	0.76[31]			
- no ground cover - low / young (f_{ceff} = 0.25)	0.27	0.58	0.48[31]			
Grapes – Wine				1.5-2	1.0-2.0	0.45
- no ground cover - high density (f_{ceff} = 0.7)	0.30	0.75[32]	0.60[31, 32]			
- no ground cover - med. density (f_{ceff} = 0.5)[26]	0.30	0.70[32]	0.55[31, 32]			

- no ground cover - low / young (f_{ceff} = 0.25)	0.30	0.45[32]	0.40[31, 32]			
Hops	0.3	1.05	0.85	5	1.0-1.2	0.50

continued…

[20] This $K_{c\ mid}$ coefficient for hay crops is an overall average $K_{c\ mid}$ coefficient that averages K_c for both before and following cuttings. It is applied to the period following the first development period until the beginning of the last late season period of the growing season.

[21] These K_c coefficients for hay crops represent immediately following cutting; at full cover; and immediately before cutting, respectively. The growing season is described as a series of individual cutting periods).

[22] These K_c values are based on measurements of ET from prairie in Kansas by Verma et al. (1989, 1992) comprised of switchgrass (*Panicum virgatum*), big bluestem (*Andropogon gerardii*) and indiangrass (*Sorghastrum nutans*). Values for height and rooting depth are from Elbersen et al. (2004).

[23] Cool season grass varieties include dense stands of bluegrass, ryegrass, and fescue. Warm season varieties include bermuda grass and St. Augustine grass. The values given here are for potential conditions representing a 0.06 to 0.08 m mowing height. Turf, especially warm season varieties, can be stressed at moderate levels and still maintain appearance (see section "Evapotranspiration Coefficients for Landscapes" in chapter 10). Generally a value for the stress coefficient K_s of 0.9 for cool season and 0.7 for warm season varieties can be employed where careful water management is practiced and rapid growth is not required. Incorporation of these values for K_s into an 'actual K_c' using potential values in this table will yield $K_{c\ act}$ values of about 0.8 for cool season turf and 0.65 for warm season turf.

[24] These values for $K_{c\ ini}$, $K_{c\ mid}$ and $K_{c\ end}$ were modeled using $K_{cb\ ini}$, $K_{cb\ mid}$ and $K_{cb\ end}$ modeled using eq. 10.25, 10.26a and 10.28 with parameters listed in Table D.3 of Appendix D, along with h from table D.2 for various $f_{c\ eff}$, where values listed in the last three columns of table D.3 were added to the values modeled for K_{cb}. to derive K_c that include average, expected amounts of evaporation from soil. $f_{c\ eff}$ is the effective fraction of ground covered or shaded by vegetation (0 to 1.0) near solar noon and h is the mean height of the vegetation, m.

[25] The values in parentheses apply to date palms.

[26] The values in this row are similar to the entry in FAO-56 (Allen et al., 1998).

[27] For non-active or only moderately active ground cover (active indicates green and growing ground cover with LAI > about 2), K_c should be weighted between K_c for no ground cover and K_c for active ground cover, with the weighting based on the "greenness" and approximate leaf area of the ground cover.

[28] The pineapple plant has very low transpiration because it closes its stomates during the day and opens them during the night. Therefore, the majority of ET_c from pineapple is evaporation from the soil. The $K_{c\ mid} < K_{c\ ini}$ since $K_{c\ mid}$ occurs during full ground cover so that soil evaporation is less. Values assume that 50% of the ground surface is covered by black plastic mulch and that irrigation is by sprinkler. For drip irrigation beneath the plastic mulch, K_c's given can be reduced by 0.10.

[29] Includes the water requirements of the shade trees.

[30] The values in this row are similar to those by Johnson et al. (2005).

[31] These $K_{c\ end}$ values represent K_c prior to leaf drop. After leaf drop, $K_{c\ end} \approx 0.20$ for bare, dry soil or dead ground cover and $K_{c\ end} \approx 0.50$ to 0.80 for actively growing ground cover.

[32] These $K_{c\ mid}$ and $K_{c\ end}$ values include an implicit K_s (stress) factor of about 0.7 (see eq. 10.13), which is common for wine production. In practice, a K_s model and estimate should be applied where K_s can range from 0.5 to 1.0. Under no stress, the $K_{c\ mid}$ and $K_{c\ end}$ for wine grapes may equal that for table grapes, depending on plant density, age, and pruning structure.

Mean Crop Coefficient table continued

Crop	K_c ini[1]	K_c mid	K_c end	Max. Ht m	Max. Root depth[2] m	p[3]
n. Fruit Trees						
Almonds, no ground cover[24]					1.0-2.0	0.40
- no ground cover - high density (f_{ceff} = 0.7)	0.40	1.00	0.70[31]	5		
- no ground cover - med. density (f_{ceff} = 0.5)[26]	0.40	0.85	0.60[31]	4		
- no ground cover – low dens. / young (f_{ceff} = 0.25)	0.35	0.50	0.40[31]	3		
- active ground cover[27] - high density (f_{ceff} = 0.7)	0.85	1.05	0.85[31]	5		
- active ground cover - med. density (f_{ceff} = 0.5)	0.85	1.00	0.85[31]	4		
- act. grnd cover – low dens. / young (f_{ceff} = 0.25)	0.85	0.95	0.85[31]	3		
Apples, Cherries, Pears[24]					1.0-2.0	0.50
- no ground cover – high density (f_{ceff} = 0.7)	0.50	1.15	0.80[31]	4		
- no ground cover – med. density (f_{ceff} = 0.5)[26]	0.45	1.05	0.75[31]	3		
- no ground cover – low dens./ young (f_{ceff} = 0.25)	0.40	0.70	0.55[31]	3		
- act. grnd cov.[27], killing frost – h.dens. (f_{ceff} = 0.7)	0.50	1.20	0.85[31]	4		
- act. grnd cov., killing frost – m.dens. (f_{ceff}=0.5)[26]	0.50	1.15	0.85[31]	3		
- act. grnd cov., killing frost – l.dens. (f_{ceff} = 0.25)	0.50	1.05	0.85[31]	3		
- act. grnd cov., no frosts – h. dens. (f_{ceff} = 0.7)	0.85	1.20	0.85[31]	4		
- act. grnd cov., no frosts – m. dens. (f_{ceff} = 0.5)[26]	0.85	1.15	0.85[31]	3		
- act. grnd cov., no frosts – l. dens. (f_{ceff} = 0.25)	0.85	1.05	0.85[31]	3		
Apricots, Peaches, Stone Fruit[24, 33]					1.0-2.0	0.50
- no ground cover - super density (f_{ceff} = 0.9)[30]	0.50	1.20	0.85[31]	3		
- no ground cover - high density (f_{ceff} = 0.7)[34]	0.50	1.15	0.80[31]	3		
- no ground cover – med. density (f_{ceff} = 0.5)[26]	0.45	1.0	0.70[31]	2.5		
- no ground cover – low dens./ young (f_{ceff} = 0.25)[35]	0.40	0.60	0.45[31]	3		
- act. grnd cov.[27], killing frost – s.dens. (f_{ceff} = 0.9)	0.50	1.25	0.85[31]	3		
- act. grnd cov., killing frost – h.dens. (f_{ceff} = 0.7)[26]	0.50	1.20	0.85[31]	2.5		
- act. grnd cov., killing frost – m.dens. (f_{ceff} = 0.5)	0.50	1.15	0.85[31]	3		
- act. grnd cov., killing frost – l.dens. (f_{ceff} = 0.25)	0.50	1.00	0.85[31]	3		
- act. grnd cov., no frosts – s. dens. (f_{ceff} = 0.9)	0.80	1.25	0.85[31]	2.5		
- act. grnd cov., no frosts – h. dens. (f_{ceff} = 0.7)[26]	0.80	1.20	0.85[31]	3		
- act. grnd cov., no frosts – m. dens. (f_{ceff} = 0.5)	0.80	1.15	0.85[31]	3		
- act. grnd cov., no frosts – l. dens. (f_{ceff} = 0.25)	0.80	1.00	0.85[31]	2.5		
Avocado[24]					0.5-1.0	0.70
- no ground cover - high density (f_{ceff} = 0.7)	0.50	1.00	0.90	4		
- no ground cover - med. density (f_{ceff} = 0.5)[26]	0.50	0.90	0.80	3		
- no ground cover – low dens. / young (f_{ceff} = 0.25)	0.40	0.65	0.60	3		
- active ground cover[27] - high density (f_{ceff} = 0.7)	0.85	1.05	0.95	4		
- active ground cover - med. density (f_{ceff} = 0.5)	0.85	1.00	0.95	3		
- act. grnd cover – low dens. / young (f_{ceff} = 0.25)	0.85	0.95	0.90	3		

continued…

Mean Crop Coefficient table continued

Crop	$K_{c\ ini}$[1]	$K_{c\ mid}$	$K_{c\ end}$	*Max. Ht* *m*	*Max. Root depth*[2] *m*	p[3]
Citrus[24]						
- no ground cover - high density (f_{ceff} = 0.7) [36]	0.95	0.90	0.90	3	1.2-1.5	0.50
- no ground cover - med. density (f_{ceff} = 0.5)	0.80	0.75	0.75	2.5	1.1-1.5	0.50
- no ground cover – low dens. / young (f_{ceff} = 0.25)	0.55	0.50	0.50	2	0.8-1.1	0.50
- active ground cover[27] - high density (f_{ceff} = 0.7)[37]	1.00	0.95	0.95	3		
- active ground cover - med. density (f_{ceff} = 0.5)	0.95	0.95	0.95	2.5	1.2-1.5	0.50
- act. grnd cover – low dens. / young (f_{ceff} = 0.25)	0.90	0.90	0.90	2	1.1-1.5	0.50
Conifer Trees[38]	1.00	1.00	1.00	10	1.0-1.5	0.70
Kiwi	0.40	1.05	1.05	3	0.7-1.3	0.35
Mango[24]				5-15	1.5	0.50
- no ground cover - high density (f_{ceff} = 0.7)[39]	0.35	0.90	0.75	5		
- no ground cover - med. density (f_{ceff} = 0.5)	0.35	0.75	0.60	4		
- no ground cover – low dens. / young (f_{ceff} = 0.25)	0.30	0.45	0.40	4		
Olives[24]				3-5	1.2-1.7	0.65
- no ground cover - high density (f_{ceff} = 0.7)[26, 40]	0.65	0.70	0.60	4		
- no ground cover - med. density (f_{ceff} = 0.5)[41]	0.60	0.60	0.55	4		
- no grnd cov. – low dens. / young (f_{ceff} = 0.25)[41, 42]	0.40	0.40	0.35	3		
- no grnd cov. - v. low dens./young (f_{ceff} = 0.05)[42]	0.30	0.25	0.25	2		
- active ground cover[27] - high density (f_{ceff} = 0.7)	0.80	0.75	0.75	4		
- active ground cover - med. density (f_{ceff} = 0.5)	0.80	0.75	0.75	4		
- act. grnd cover - low dens./young (f_{ceff} = 0.25)	0.80	0.75	0.75	3		
- act. grnd cover - v. low dens./young (f_{ceff} = 0.05)	0.80	0.75	0.75	2		
Pistachios[24]	0.80	0.75	0.75	3-5	1.0-1.5	0.40
- no ground cover - high density (f_{ceff} = 0.7)	0.40	1.00	0.70	3		
- no ground cover - med. density (f_{ceff} = 0.5)	0.35	0.85	0.60	2.5		
- no ground cover – low dens. / young (f_{ceff} = 0.25)	0.30	0.50	0.40	2		
- active ground cover[27] - high density (f_{ceff} = 0.7)	0.80	1.00	0.75	3		
- active ground cover - med. density (f_{ceff} = 0.5)	0.80	1.00	0.75	2.5		
- act. grnd cover – low dens. / young (f_{ceff} = 0.25)	0.80	0.85	0.75	2		
Walnut Orchard[24]					1.7-2.4	0.50
- no ground cover - high density (f_{ceff} = 0.7)[22]	0.50	1.10	0.65[31]	5		
- no ground cover - med. density (f_{ceff} = 0.5)	0.45	0.90	0.60[31]	4		
- no ground cover – low dens. / young (f_{ceff} = 0.25)	0.35	0.55	0.40[31]	4		
- active ground cover[27] - high density (f_{ceff} = 0.7)	0.85	1.15	0.85[31]	5		
- active ground cover - med. density (f_{ceff} = 0.5)	0.85	1.10	0.85[31]	4		
- act. grnd cover – low dens. / young (f_{ceff} = 0.25)	0.85	0.95	0.85[31]	4		

continued…

[33] Stone fruit category applies to peaches, apricots, pears, plums and pecans.
[34] The values in this row are derived from Girona et al. (2005) and Ayars et al. (2003) with f_{ceff} = 0.7 and and M_L = 1.5.
[35] The values in this row are similar to those by Paço et al. (2006) and Ayars et al. (2003) with f_{ceff} = 0.25 and and M_L = 1.5.
[36] The values for citrus are about 20% higher than those reported in FAO-56.
[37] The values in this row are similar to those by Rogers et al. (1983) for citrus in Florida having Bahia grass cover.
[38] Conifers exhibit substantial stomatal control due to soil water deficit. The K_c can easily reduce below the values presented, which represent well-watered conditions for large forests.

Mean Crop Coefficient table continued

Crop	$K_{c\ ini}$[1]	$K_{c\ mid}$	$K_{c\ end}$
o. Wetlands – temperate climate			
Cattails, Bulrushes, killing frost	0.30	1.20	0.30
Cattails, Bulrushes, no frost	0.60	1.20	0.60
Short Veg., no frost	1.05	1.10	1.10
Reed Swamp, standing water	1.00	1.20	1.00
Reed Swamp, moist soil	0.90	1.20	0.70
p. Special			
Open Water, < 2 m depth or in subhumid climates or tropics		1.05	1.05
Open Water, > 5 m depth, clear of turbidity, temperate climate		0.50 – 0.70[43]	0.80 – 1.30[43]

39 The values in this row are derived from de Azevedo et al. (2003).

40 Pastor and Orgaz (1994) found monthly K_c for olive orchards having f_c ~ 60% similar to the values shown, except that $K_{c\ mid}$ = 0.45, with stage lengths = 30, 90, 60 and 90 days, respectively for initial, development, midseason and late season periods (see Appendix C), and using K_c during the winter ("off season") in December to February = 0.50.

41 The values in this row are similar to those by Villalobos et al. (2000) when $f_{c\ eff}$ of ~ 0.3 to 0.4 are applied.

42 The values in this row are derived from Testi et al. (2004).

43 These K_c's are for deep water in temperate latitudes where large temperature changes in the water body occur during the year, and initial and peak period evaporation is low as radiation energy is absorbed into the deep water body. During fall and winter periods ($K_{c\ end}$), heat is released from the water body that increases the evaporation above that for grass. Therefore, $K_{c\ mid}$ corresponds to the period when the water body is gaining thermal energy and $K_{c\ end}$ when releasing thermal energy. The higher values for $K_{c\ end}$ represent climates having freezing winter conditions and where ET_o is low and therefore $K_{c\ end}$ is high. These K_c's should be used with caution.

*Primary source: FAO-56 (Allen et al, 1998), with information from Doorenbos and Kassam (1979), Doorenbos and Pruitt (1977); Pruitt (1986); Wright (1981, 1982), Snyder et al. (1989a,b) and Allen, Howell and Snyder (2011c).

BLANK PAGE

Appendix C

Lengths of Crop Development Stages[1] in days for Various Planting Periods and Climatic Regions based on FAO-24 (Doorenbos and Pruitt 1977) and FAO-56 (Allen et al. 1998)

Crop	Init. (L_{ini})	Dev. (L_{dev})	Mid (L_{mid})	Late (L_{late})	Total	Plant Date	Region
a. Small Vegetables							
Broccoli	35	45	40	15	135	Sept	Calif. Desert, USA
Cabbage	40	60	50	15	165	Sept	Calif. Desert, USA
Carrots	20	30	50/30	20	100	Oct/Jan	Arid climate
	30	40	60	20	150	Feb/Mar	Mediterranean
	30	50	90	30	200	Oct	Calif. Desert, USA
Cauliflower	35	50	40	15	140	Sept	Calif. Desert, USA
Celery	25	40	95	20	180	Oct	(Semi)Arid
	25	40	45	15	125	April	Mediterranean
	30	55	105	20	210	Jan	(Semi)Arid
Crucifers[2]	20	30	20	10	80	April	Mediterranean
	25	35	25	10	95	February	Mediterranean
	30	35	90	40	195	Oct/Nov	Mediterranean
Lettuce	20	30	15	10	75	April	Mediterranean
	30	40	25	10	105	Nov/Jan	Mediterranean
	25	35	30	10	100	Oct/Nov	Arid Region
	35	50	45	10	140	Feb	Mediterranean
Onion (dry)	15	25	70	40	150	April	Mediterranean
	20	35	110	45	210	Oct; Jan.	Arid Region; Calif.
Onion (green)	25	30	10	5	70	April/May	Mediterranean
	20	45	20	10	95	October	Arid Region
	30	55	55	40	180	March	Calif., USA
Onion (seed)	20	45	165	45	275	Sept	Calif. Desert, USA
Spinach	20	20	15/25	5	60/70	Apr; Sep/Oct	Mediterranean
	20	30	40	10	100	November	Arid Region
Radish	5	10	15	5	35	Mar/Apr	Medit.; Europe
	10	10	15	5	40	Winter	Arid Region
b. Vegetables – Solanum Family *(Solanaceae)*							
Egg plant	30	40	40	20	130	October	Arid Region
	30	45	40	25	140	May/June	Mediterranean
Sweet peppers	25/30	35	40	20	125	April/June	Europe and Medit.
(bell)	30	40	110	30	210	October	Arid Region
Tomato	30	40	40	25	135	January	Arid Region
	35	40	50	30	155	Apr/May	Calif., USA
	25	40	60	30	155	Jan	Calif. Desert, USA
	35	45	70	30	180	Oct/Nov	Arid Region
	30	40	45	30	145	April/May	Mediterranean
c. Vegetables - Cucumber Family *(Cucurbitaceae)*							
Cantaloupe	30	45	35	10	120	Jan	Calif., USA
	10	60	25	25	120	Aug	Calif., USA
Cucumber	20	30	40	15	105	June/Aug	Arid Region
	25	35	50	20	130	Nov; Feb	Arid Region
Pumpkin,	20	30	30	20	100	Mar, Aug	Mediterranean
Winter squash	25	35	35	25	120	June	Europe
Squash,	25	35	25	15	100	Apr; Dec.	Medit.; Arid Reg.
Zucchini	20	30	25	15	90	May/June	Medit.; Europe

continued…

[1] Lengths of crop development stages provided in this table are indicative of general conditions, but may vary substantially from region to region, with climate and cropping conditions, and with crop variety. The user is strongly encouraged to obtain appropriate local information.

[2] Crucifers include cabbage, cauliflower, broccoli, and Brussels' sprouts. The wide range in lengths of seasons is due to varietal and species differences.

Lengths of Crop Development Stages, continued

Crop	Init. (L_{ini})	Dev. (L_{dev})	Mid (L_{mid})	Late (L_{late})	Total	Plant Date	Region
Sweet melons	25	35	40	20	120	May	Mediterranean
	30	30	50	30	140	March	Calif., USA
	15	40	65	15	135	Aug	Calif. Desert, USA
	30	45	65	20	160	Dec/Jan	Arid Region
Water melons	20	30	30	30	110	April	Italy
	10	20	20	30	80	Mat/Aug	Near East (desert)
d. Roots and Tubers							
Beets, table	15	25	20	10	70	Apr/May	Mediterranean
	25	30	25	10	90	Feb/Mar	Mediterranean & Arid
Cassava: year 1	20	40	90	60	210	Rainy season	Tropical regions
year 2	150	40	110	60	360		
Potato	25	30	30/45	30	115/130	Jan/Nov	(Semi)Arid Climate
	25	30	45	30	130	May	Continental Climate
	30	35	50	30	145	April	Europe
	45	30	70	20	165	Apr/May	Idaho, USA
	30	35	50	25	140	Dec	Calif. Desert, USA
Sweet potato	20	30	60	40	150	April	Mediterranean
	15	30	50	30	125	Rainy seas.	Tropical regions
Sugarbeet	30	45	90	15	180	March	Calif., USA
	25	30	90	10	155	June	Calif., USA
	25	65	100	65	255	Sept	Calif. Desert, USA
	50	40	50	40	180	April	Idaho, USA
	25	35	50	50	160	May	Mediterranean
	45	75	80	30	230	November	Mediterranean
	35	60	70	40	205	November	Arid Regions
e. Legumes (*Leguminosae*)							
Beans (green)	20	30	30	10	90	Feb/Mar	Calif., Mediterranean
	15	25	25	10	75	Aug/Sep	Calif., Egypt, Lebanon
Beans (dry)	20	30	40	20	110	May/June	Continental Climates
	15	25	35	20	95	June	Pakistan, Calif.
	25	25	30	20	100	June	Idaho, USA
Faba bean,	15	25	35	15	90	May	Europe
broad bean	20	30	35	15	100	Mar/Apr	Mediterranean
dry bean	90	45	40	60	235	Nov	Europe
green bean	90	45	40	0	175	Nov	Europe
Green gram, cowpeas	20	30	30	20	110	March	Mediterranean
Groundnut	25	35	45	25	130	Dry season	West Africa
	35	35	35	35	140	May	High Latitudes
	35	45	35	25	140	May/June	Mediterranean
Lentil	20	30	60	40	150	April	Europe
	25	35	70	40	170	Oct/Nov	Arid Region
Peas	15	25	35	15	90	May	Europe
	20	30	35	15	100	Mar/Apr	Mediterranean
	35	25	30	20	110	April	Idaho, USA
Soybeans	15	15	40	15	85	Dec	Tropics
	20	30/35	60	25	140	May	Central USA
	20	25	75	30	150	June	Japan

continued…

Lengths of Crop Development Stages, continued

Crop	Init. (L_{ini})	Dev. (L_{dev})	Mid (L_{mid})	Late (L_{late})	Total	Plant Date	Region
f. Perennial Vegetables (with winter dormancy and initially bare or mulched soil)							
Artichoke	40	40	250	30	360	Apr (1st yr)	California
	20	25	250	30	325	May (2nd yr)	(cut in May)
Asparagus	50	30	100	50	230	Feb	Warm Winter
	90	30	200	45	365	Feb	Mediterranean
g. Fiber Crops							
Cotton	30	50	60	55	195	Mar-May	Egypt; Pakistan; Calif.
	45	60	45-75	45	195-225	Mar	Calif. Desert, USA
	30	50	60	55	195	Sept	Yemen
	30	50	55	45	180	April	Texas
Flax	25	35	50	40	150	April	Europe
	30	40	100	50	220	October	Arizona
h. Oil Crops							
Castor beans	25	40	65	50	180	March	(Semi)Arid Climates
	20	40	50	25	135	Nov.	Indonesia
Safflower	20	35	45	25	125	April	California, USA
	25	35	55	30	145	Mar	High Latitudes
	35	55	60	40	190	Oct/Nov	Arid Region
Sesame	20	30	40	20	100	June	China
Sunflower	25	35	45	25	130	April/May	Medit.; California
i. Cereals							
Barley/Oats/	15	25	50	30	120	November	Central India
Wheat	20	25	60	30	135	March/Apr	35-45 °L
	15	30	65	40	150	July	East Africa
	40	30	40	20	130	Apr	
	40	60	60	40	200	Nov	
	20	50	60	30	160	Dec	Calif. Desert, USA
Winter Wheat	20[3]	60[3]	70	30	180	December	Calif., USA
	30	140	40	30	240	November	Mediterranean
	160	75	75	25	335	October	Idaho, USA
Grains (small)	20	30	60	40	150	April	Mediterranean
	25	35	65	40	165	Oct/Nov	Pakistan; Arid Reg.
Maize (grain)	30	50	60	40	180	April	East Africa (alt.)
	25	40	45	30	140	Dec/Jan	Arid Climate
	20	35	40	30	125	June	Nigeria (humid)
	20	35	40	30	125	October	India (dry, cool)
	30	40	50	30	150	April	Spain (spr, sum.); Calif.
	30	40	50	50	170	April	Idaho, USA
Maize (sweet)	20	20	30	10	80	March	Philippines
	20	25	25	10	80	May/June	Mediterranean
	20	30	50/30	10	90	Oct/Dec	Arid Climate
	30	30	30	10[4]	110	April	Idaho, USA
	20	40	70	10	140	Jan	Calif. Desert, USA
Millet	15	25	40	25	105	June	Pakistan
	20	30	55	35	140	April	Central USA

continued…

[3] These periods for winter wheat will lengthen in frozen climates according to days having zero growth potential and wheat dormancy. Under general conditions and in the absence of local data, fall planting of winter wheat can be presumed to occur in northern temperate climates when the 30-day running average of mean daily air temperature decreases to 11°C or December 1, whichever comes first. Allen and Robison (2007a,b) reduced canopy development of winter wheat (and amount of K_c above $K_{c\ ini}$) whenever T_{min} was < -25°C and no snow cover was present. They further reduced development by a lesser amount whenever T_{min} was < -10°C as a retardation penalty after a cold freeze. Planting of spring wheat can be assumed to occur when the 30-day running average of mean daily air temperature ending on the planting date increases to 4°C. Spring planting of maize-grain can be assumed to occur when the 30-day running average of mean daily air temperature increases to 10°C.

[4] The late season for sweet maize will be about 35 days if the grain is allowed to mature and dry.

Lengths of Crop Development Stages, continued

Crop	Init. (Lini)	Dev. (Ldev)	Mid (Lmid)	Late (Llate)	Total	Plant Date	Region
Sorghum	20	35	40	30	130	May/June	USA, Pakis., Med.
	20	35	45	30	140	Mar/April	Arid Region
Rice	30	30	60	30	150	Dec; May	Tropics; Mediterranean
	30	30	80	40	180	May	Tropics
j. Forages							
Alfalfa, total Season[5]	10	30	var.	var.	var.		
Alfalfa[5]	10	20	20	10	60	Jan	Calif., USA.
1st cutting cycle	10	30	25	10	75	Apr (last -4° C)	Idaho, USA.
Alfalfa[5], other	5	10	10	5	30	Mar	Calif., USA.
cutting cycles	5	20	10	10	45	Jun	Idaho, USA.
Bermuda for seed	10	25	35	35	105	March	Calif. Desert, USA
Bermuda for hay (several cuttings)	10	15	75	35	135	---	Calif. Desert, USA
Grass Pasture[5]	10	20	--	--	--		
Sudan, 1st cutting cycle	25	25	15	10	75	Apr	Calif. Desert, USA
Sudan, other cutting cycles	3	15	12	7	37	June	Calif. Desert, USA
Switchgrass[6]	20	45	40	60	165	Apr	Kansas
k. Sugar Cane							
Sugarcane, virgin	35	60	190	120	405		Low Latitudes
	50	70	220	140	480		Tropics
	75	105	330	210	720		Hawaii, USA
Sugarcane, ratoon	25	70	135	50	280		Low Latitudes
	30	50	180	60	320		Tropics
	35	105	210	70	420		Hawaii, USA
l. Tropical Fruits and Trees							
Banana, 1st yr	120	90	120	60	390	Mar	Mediterranean
Banana, 2nd yr	120	60	180	5	365	Feb	Mediterranean
Pineapple	60	120	600	10	790		Hawaii, USA
m. Grapes and Berries							
Grapes	20	100	90	30	240	April	Low Latitudes
	20	100	90	30	240	Mar	Calif., USA
	20	90	50	20	180	May	High Latitudes
	20	90	80	20	210	April	Mid Latitudes (wine)
Hops	25	40	80	10	155	April	Idaho, USA
n. Fruit Trees							
Citrus	90	30	150	95	365	Jan	Mediterranean
Deciduous Orchard	10	10	160-190	30	210	March	High Latitudes
- light pruning	10	10	190	60	270	March	Low Latitudes
	10	10		30	240	March	Calif., USA
Deciduous Orchard	10	80	90	30	210	March	High Latitudes
-heavy pruning	10	80	120	60	270	March	Low Latitudes
	10	60	140	30	240	March	Calif., USA

continued…

[5] In climates having killing frosts, growing seasons can be estimated using specific temperature or cumulative growing degree days or running average air temperature to begin and killing frosts to terminate. For example for alfalfa and grass: *alfalfa*: last –4°C in spring until first –4°C in fall (Everson *et al.,* 1978) or accumulation of 240 degree-days since January 1 using 0° base for green up and first occurrence of -7°C frost in fall (Allen and Robison, 2007a,b). *grass:* 7 days before last –4°C in spring and 7 days after last –4°C in fall (Kruse and Haise, 1974) or 30 day running average mean air temperature for period ending on day of green up = 4°C and first occurrence of -5°C frost in fall (Allen and Robison, 2007a,b)

[6] Based on measurements of ET from prairie in Kansas by Verma et al. (1989, 1992) comprised of switchgrass (*Panicum virgatum*), big bluestem (*Andropogon gerardii*) and indiangrass (*Sorghastrum nutans*).

Lengths of Crop Development Stages, continued

Crop	Init. (L_{ini})	Dev. (L_{dev})	Mid (L_{mid})	Late (L_{late})	Total	Plant Date	Region
Mango	20	40	50	50	160	July	Brazil
Olives	10	20	150	90	270[7]	March	Mediterranean
Pistachios	10	20	80	40	150	Feb	Mediterranean
Walnuts	10	10	140	30	190	April	Utah, USA
o. Wetlands - Temperate Climate							
Wetlands	10	30	80	20	140	May	Utah, USA; killing frost
(Cattails, Bulrush)	180	60	90	35	365	November	Florida, USA
Wetlands (short veg.)	180	60	90	35	365	November	frost-free climate

[7] Olive trees gain new leaves in March and often have transpiration during winter, where the K_c continues outside of the "growing period" and total season length may be set to 365 days.

Values in this appendix are primarily from FAO-56 (Allen et al. 1998) with modification to period lengths for some tree crops.

Appendix D

Basal Crop Coefficients, K_{cb}, for Well-managed Crops in Sub-Humid Climates[1] for use with clipped grass reference ET_o, based on FAO-56 (Allen et al. 1998)

Guidelines on applying K_c values in this appendix are given in Chapter 10.

Table D.1 Basal Crop Coefficients

Crop	$K_{cb\ ini}$[2]	$K_{cb\ mid}$	$K_{cb\ end}$
a. Small Vegetables	**0.15**	**0.95**	**0.85**
Broccoli		0.95	0.85
Brussel Sprouts		0.95	0.85
Cabbage		0.95	0.85
Carrots		0.95	0.85
Cauliflower		0.95	0.85
Celery		0.95	0.90
Garlic		0.90	0.60
Lettuce		0.90	0.90
Onions - dry		0.95	0.65
- green		0.90	0.90
- seed		1.05	0.70
Spinach		0.90	0.85
Radish		0.85	0.75
b. Vegetables – Solanum Family (*Solanaceae*)	**0.15**	**1.10**	**0.70**
Egg Plant		1.00	0.80
Sweet Peppers (bell)		1.00[3]	0.80
Tomato		1.10[3]	0.60-0.80
c. Vegetables – Cucumber Family (*Cucurbitaceae*)	**0.15**	**0.95**	**0.70**
Cantaloupe		0.75	0.50
Cucumber – Fresh Market		0.95[3]	0.70
– Machine harvest		0.95	0.80
Pumpkin, Winter Squash		0.95	0.70
Squash, Zucchini		0.90	0.70
Sweet Melons		1.00	0.70
Watermelon		0.95	0.70
d. Roots and Tubers	**0.15**	**1.00**	**0.85**
Beets, table		0.95	0.85
Cassava – year 1		0.70[4]	0.20
– year 2		1.00	0.45
Parsnip		0.95	0.85
Potato		1.10	0.65[5]
Sweet Potato		1.10	0.55
Turnip (and Rutabaga)		1.00	0.85
Sugar Beet		1.15	0.50[6]

continued…

[1] The values for $K_{cb\ mid}$ and $K_{cb\ end}$ are values expected in semiarid climates, where daily minimum relative humidity (RH_{min}) ~ 45% and daily mean wind speed at 2 m height (u_2) ~ 2 m s^{-1}. For different climatic conditions, the values given can be adjusted using eq. 10.13 and 10.14.

[2] The values for $K_{cb\ ini}$ (and $K_{cb\ mid}$ and $K_{cb\ end}$) represent conditions having a dry soil surface. These values must be adjusted using the dual $K_{cb} + K_e$ procedure described in chapter 10.

[3] Beans, Peas, Legumes, Tomatoes, Peppers and Cucumbers are sometimes grown on stalks reaching 1.5 to 2 meters in height. In such cases, increased K_c values need to be taken. For green beans, peppers and cucumbers, 1.15 can be taken, and for tomatoes, dry beans and peas, 1.20. Under these conditions height h should be increased also.

[4] The midseason values for cassava assume non-stressed conditions during or following the rainy season. The $K_{c\ end}$ and $K_{cb\ end}$ values account for dormancy during the dry season.

[5] The $K_{cb\ end}$ values for potatoes are about 0.40 and 0.35 for long season potatoes with vine kill.

[6] This $K_{cb\ end}$ value is for no irrigation during the last month of the growing season. The $K_{cb\ end}$ value for sugar beets is higher, up to 1.0 and 0.9, when irrigation or significant rain occurs during the last month.

Basal Crop Coefficient table continued

Crop	$K_{cb\ ini}$[2]	$K_{cb\ mid}$	$K_{cb\ end}$
e. Legumes (*Leguminosae*)	**0.15**	**1.10**	**0.50**
Beans, green		1.00[3]	0.80
Beans, dry and Pulses		1.10[3]	0.25
Chick pea		0.95	0.25
Fababean (broad bean) – Fresh		1.10[3]	1.05
– Dry/Seed		1.10[3]	0.20
Grabanzo		1.05	0.25
Green Gram and Cowpeas		1.00	0.55-0.25[7]
Groundnut (Peanut)		1.10	0.50
Lentil		1.05	0.20
Peas – Fresh		1.10[2]	1.05
– Dry/Seed		1.10	0.20
Soybeans		1.10	0.30
f. Perennial Vegetables (with winter dormancy and initially bare or mulched)			
Artichokes	0.15	0.95	0.90
Asparagus	0.15	0.90[8]	0.20
Mint	0.40	1.10	1.05
Strawberries	0.30	0.80	0.70
g. Fiber Crops	**0.15**		
Cotton		1.10-1.15	0.50-0.40
Flax		1.05	0.20
Sisal[9]		0.4-0.7	0.4-0.7
h. Oil Crops	**0.15**	**1.10**	**0.25**
Castorbean (*Ricinus*)		1.10	0.45
Rapeseed, Canola		0.95-1.10[10]	0.25
Safflower		0.95-1.10[10]	0.20
Sesame		1.05	0.20
Sunflower		0.95-1.10[10]	0.25
i. Cereals	**0.15**	**1.10**	**0.25**
Barley		1.10	0.15
Oats		1.10	0.15
Spring Wheat		1.10	0.15-0.3[11]
Winter Wheat - with frozen soils	0.15-	1.10	0.15-0.3[11]
- with non-frozen soils	0.5[12]		
Maize, Field (grain) *(field corn)*	0.15	1.15[13]	0.50,0.15[14]
Maize, Sweet *(sweet corn)*		1.10[13]	1.00[15]
Millet		0.95	0.20
Sorghum – grain		0.95-1.05	0.35
– sweet		1.15	1.00
Rice	1.00	1.00-1.15[16]	0.70-0.45

continued…

7 The first $K_{cb\ end}$ is for harvested fresh. The second value is for harvested dry.

8 The K_{cb} for asparagus usually remains at $K_{cb\ ini}$ during harvest of the spears, due to sparse ground cover. The $K_{cb\ mid}$ value is for following regrowth of plant vegetation following termination of harvest of spears.

9 K_c for sisal depends on the planting density and water management (e.g., intentional moisture stress).

10 The lower values are for rainfed crops having less dense plant populations.

11 The higher value is for hand-harvested crops.

12 The two $K_{cb\ ini}$ values for winter wheat are a) for less than 10% ground cover and b) for during the dormant, winter period, if the vegetation fully covers the ground, and conditions are nonfrozen.

13 These $K_{cb\ mid}$ values for maize are for robust, pristine crops having plant populations of 50,000 plants per ha or higher. For less dense populations or uniform growth, $K_{cb\ mid}$ can be reduced by 0.10 to 0.2.

[14] The first $K_{cb\ end}$ value is for harvest at high grain moisture. The second $K_{cb\ end}$ value is for harvest after complete field drying of the grain (to about 18% moisture, wet mass basis).

[15] If harvested fresh for human consumption. Use $K_{cb\ end}$ for field maize if the sweet maize is allowed to mature and dry in the field.

[16] The lower value for rice is for dense, uniform stands having low aerodynamic roughness (smooth canopy surface) and low to moderate wind conditions (< 2 m s^{-1}). The higher value is for somewhat sparser, but inundated (flooded) conditions having greater roughness and lower albedo caused by shadowing, due to the sparseness.

Basal Crop Coefficient table continued

Crop	$K_{cb\ ini}$[2]	$K_{cb\ mid}$	$K_{cb\ end}$
j. Forages			
Alfalfa Hay – individual cutting effects	0.30[17]	1.15[17]	1.10[17]
– for seed	0.30	0.45	0.45
Bermuda hay – averaged cutting effects	0.50	0.95[18]	0.80
– Spring crop for seed	0.15	0.85	0.60
Clover hay, Berseem – averaged cutting effects			
– individ. cutting periods	0.30[17]	1.10[17]	1.05[17]
Rye Grass hay – averaged cutting effects	0.85	1.00[18]	0.95
Sudan Grass hay (annual) – ave. cutting effects			
– individ. cutting periods	0.30[17]	1.10[17]	1.05[17]
Grazing Pasture - Rotated Grazing	0.30	0.80-1.00	0.80
- Extensive Grazing	0.30	0.70	0.70
Switchgrass[19]	0.15	1.00	0.10
Turf grass - cool season[20]	0.80	0.85	0.85
- warm season[20]	0.75	0.80	0.80
k. Sugar Cane	0.15	1.20	0.70
l. Tropical Fruits and Trees			
Banana – 1st year	0.15	1.05	0.90
– 2nd year	0.60	1.10	1.05
Cacao	0.90	1.00	1.00
Coffee – bare ground cover	0.80	0.90	0.90
– with weeds	1.00	1.05	1.05
Palms (including date palms) [21]			
- no ground cover - high density (f_{ceff} = 0.7)[22]	0.80	0.85	0.85
- no ground cover - med. density (f_{ceff} = 0.5)	0.70	0.70	0.70
- no ground cover – low dens. / young (f_{ceff} = 0.25)	0.40	0.45	0.45
- no ground cover - v. low dens./young (f_{ceff} = 0.1)	0.25	0.25	0.25
- active ground cover[23] - high density (f_{ceff} = 0.7)	0.85	0.90	0.90
- active ground cover - med. density (f_{ceff} = 0.5)	0.80	0.85	0.85
- act. ground cover - low dens./young (f_{ceff} = 0.25)	0.75	0.80	0.80
- act. ground cover - v. low dens./young (f_{ceff} = 0.1)	0.70	0.75	0.75
Pineapple[24] – bare soil	0.15	0.25	0.25
– with unirrigated grass cover	0.30	0.45	0.45
Rubber Trees	0.85	0.90	0.90
Tea – non-shaded	0.90	0.95	0.90
– shaded[25]	1.00	1.10	1.05
m. Grapes and Berries			
Berries (bushes)	0.20	1.00	0.40
Grapes – Table or Raisin[21]	0.15	0.80	0.40
- no ground cover - high density (f_{ceff} = 0.7) [26]	0.19	1.04	0.82[27]
- no ground cover - med. density (f_{ceff} = 0.5)[22]	0.19	0.90	0.71[27]
- no ground cover - low / young (f_{ceff} = 0.25)	0.17	0.53	0.43[27]
Grapes – Wine	0.15	0.65	0.40
- no ground cover - high density (f_{ceff} = 0.7)	0.20	0.70[28]	0.55[27, 28]
- no ground cover - med. density (f_{ceff} = 0.5)[22]	0.20	0.65[28]	0.50[27, 28]
- no ground cover - low / young (f_{ceff} = 0.25)	0.25	0.40[28]	0.30[27, 28]
Hops	0.15	1.00	0.80

continued…

[17] These K_{cb} coefficients for hay crops represent immediately following cutting; at full cover; and immediately before cutting, respectively. The growing season is described as a series of individual cutting periods).

[18] This $K_{cb\ mid}$ coefficient for Bermuda and ryegrass hay crops is an overall average $K_{cb\ mid}$ coefficient that averages K_{cb} for both before and following cuttings. It is applied to the period following the first development period until the beginning of the last late season period of the growing season.

[19] These K_c values are based on measurements of ET from prairie in Kansas by Verma et al. (1989, 1992) comprised of switchgrass (*Panicum virgatum*), big bluestem (*Andropogon gerardii*) and indiangrass (*Sorghastrum nutans*).

[20] Cool season grass varieties include dense stands of bluegrass, ryegrass, and fescue. Warm season varieties include bermuda grass and St. Augustine grass. The values given here are for potential conditions representing a 0.06 to 0.08 m mowing height. Turf, especially warm season varieties, can be stressed at moderate levels and still maintain appearance (see section "Evapotranspiration Coefficients for Landscapes" in chapter 10). Generally a value for the stress coefficient K_s of 0.9 for cool season and 0.7 for warm season varieties can be employed where careful water management is practiced and rapid growth is not required. Incorporation of these values for K_s into an 'actual K_c' using potential values in this table will yield $K_{cb\ act}$ values of about 0.75 for cool season turf and 0.55 for warm season turf.

[21] These values for $K_{cb\ ini}$, $K_{cb\ mid}$ and $K_{cb\ end}$ were modeled using eq. 10.25a, 10.27a, and 10.29 with parameters listed in table D.3 of Appendix D, along with h from table D.2 for various $f_{c\ eff}$, where $f_{c\ eff}$ is the effective fraction of ground covered or shaded by vegetation (0 to 1.0) near solar noon and h is the mean height of the vegetation, m.

[22] The values in this row are similar to the entry in FAO-56 (Allen et al. 1998).

[23] For non-active or only moderately active ground cover (active indicates green and growing ground cover with LAI > about 2) , K_c should be weighted between K_c for no ground cover and K_c for active ground cover, with the weighting based on the "greenness" and approximate leaf area of the ground cover.

[24] The pineapple plant has low transpiration because it closes its stomates during the day and opens them during the night. Therefore, the majority of ET_c from pineapple is evaporation from the soil.

[25] Includes the water requirements of the shade trees.

[26] The values in this row are similar to those by Johnson et al. (2005).

[27] These $K_{cb\ end}$ values represent K_{cb} prior to leaf drop. After leaf drop, $K_{cb\ end} \approx 0.10$ to 0.20 for bare, dry soil or dead ground cover and $K_{cb\ end} \approx 0.50$ to 0.80 for actively growing ground cover.

[28] These $K_{cb\ mid}$ and $K_{cb\ end}$ values include an implicit K_s (stress) factor of about 0.7 (see eq. 10.2), which is common for wine production. In practice, a K_s model and estimate should be applied where K_s can range from 0.5 to 1.0. Under no stress, the $K_{cb\ mid}$ and $K_{cb\ end}$ for wine grapes may equal that for table grapes, depending on plant density, age, and pruning structure.

Basal Crop Coefficient table continued

Crop	$K_{cb\ ini}$[2]	$K_{cb\ mid}$	$K_{cb\ end}$
n. Fruit Trees			
Almonds, no ground cover			
- no ground cover - high density (f_{ceff} = 0.7)	0.20	0.95	0.65[27]
- no ground cover - med. density (f_{ceff} = 0.5)[22]	0.20	0.80	0.55[27]
- no ground cover – low dens. / young (f_{ceff} = 0.25)	0.15	0.45	0.35[27]
- active ground cover[23] - high density (f_{ceff} = 0.7)	0.75	1.00	0.80[27]
- active ground cover - med. density (f_{ceff} = 0.5)	0.75	0.95	0.80[27]
- act. grnd cover – low dens. / young (f_{ceff} = 0.25)	0.75	0.90	0.80[27]
Apples, Cherries, Pears[21]			
- no ground cover - high density (f_{ceff} = 0.7)	0.30	1.10	0.75[27]
- no ground cover - med. density (f_{ceff} = 0.5)[22]	0.30	1.00[29]	0.70[27]
- no ground cover - low dens./ young (f_{ceff} = 0.25)	0.25	0.65	0.50[27]
- act. grnd cov.[23], killing frost – h.dens. (f_{ceff} = 0.7)	0.40	1.15	0.80[27]
- act. grnd cov., killing frost – m.dens. (f_{ceff}=0.5)[22]	0.40	1.10	0.80[27]
- act. grnd cov., killing frost – l.dens. (f_{ceff} = 0.25)	0.40	1.00	0.80[27]
- act. grnd cov., no frosts – h. dens. (f_{ceff} = 0.7)	0.75	1.15	0.80[27]
- act. grnd cov., no frosts – m. dens. (f_{ceff} = 0.5)[22]	0.75	1.10	0.80[27]
- act. grnd cov., no frosts – l. dens. (f_{ceff} = 0.25)	0.75	1.00	0.80[27]
Apricots, Peaches, Stone Fruit[21, 30]			
- no ground cover - super density (f_{ceff} = 0.9)[26]	0.30	1.15	0.80[27]
- no ground cover - high density (f_{ceff} = 0.7)[31]	0.30	1.10	0.75[27]
- no ground cover – med. density (f_{ceff} = 0.5)[22]	0.25	0.95	0.65[27]
- no ground cover – low dens./ young (f_{ceff} = 0.25)[32]	0.20	0.55	0.40[27]
- act. grnd cov.[23], killing frost – s.dens. (f_{ceff} = 0.9)	0.40	1.20	0.80[27]
- act. grnd cov., killing frost – h.dens. (f_{ceff} = 0.7)[22]	0.40	1.15	0.80[27]
- act. grnd cov., killing frost – m.dens. (f_{ceff} = 0.5)	0.40	1.10	0.80[27]
- act. grnd cov., killing frost – l.dens. (f_{ceff} = 0.25)	0.40	0.95	0.80[27]
- act. grnd cov., no frosts – s. dens. (f_{ceff} = 0.9)	0.70	1.20	0.80[27]
- act. grnd cov., no frosts – h. dens. (f_{ceff} = 0.7)[22]	0.70	1.15	0.80[27]
- act. grnd cov., no frosts – m. dens. (f_{ceff} = 0.5)	0.70	1.10	0.80[27]
- act. grnd cov., no frosts – l. dens. (f_{ceff} = 0.25)	0.70	0.95	0.80[27]
Avocado[21]			
- no ground cover - high density (f_{ceff} = 0.7)	0.30	0.95	0.85
- no ground cover - med. density (f_{ceff} = 0.5)[22]	0.30	0.85	0.80
- no ground cover – low dens. / young (f_{ceff} = 0.25)	0.25	0.60	0.50
- active ground cover[23] - high density (f_{ceff} = 0.7)	0.75	1.00	0.90
- active ground cover - med. density (f_{ceff} = 0.5)	0.75	0.95	0.90
- act. grnd cover – low dens. / young (f_{ceff} = 0.25)	0.75	0.90	0.85
Citrus[21]			
- no ground cover - high density (f_{ceff} = 0.7) [33]	0.85	0.85	0.85
- no ground cover - med. density (f_{ceff} = 0.5)	0.70	0.70	0.70
- no ground cover – low dens. / young (f_{ceff} = 0.25)	0.45	0.45	0.45
- active ground cover[23] - high density (f_{ceff} = 0.7)[34]	0.90	0.90	0.90
- active ground cover - med. density (f_{ceff} = 0.5)	0.85	0.90	0.90
- act. grnd cover – low dens. / young (f_{ceff} = 0.25)	0.80	0.85	0.85

Conifer Trees[35]	0.95	0.95	0.95
Kiwi	0.20	1.00	1.00
Mango[21]			
- no ground cover - high density (f_{ceff} = 0.7)[36]	0.25	0.85	0.70
- no ground cover - med. density (f_{ceff} = 0.5)	0.25	0.70	0.55
- no ground cover – low dens. / young (f_{ceff} = 0.25)	0.20	0.40	0.35
Olives[21]			
- no ground cover - high density (f_{ceff} = 0.7)[22, 37]	0.55	0.65	0.55
- no ground cover - med. density (f_{ceff} = 0.5)[38]	0.50	0.55	0.50
- no grnd cov. – low dens. / young (f_{ceff} = 0.25)[38, 39]	0.30	0.35	0.30
- no grnd cov. - v. low dens./young (f_{ceff} = 0.05)[39]	0.20	0.20	0.20
- active ground cover[23] - high density (f_{ceff} = 0.7)	0.70	0.70	0.70
- active ground cover - med. density (f_{ceff} = 0.5)	0.70	0.70	0.70
- act. grnd cover - low dens./young (f_{ceff} = 0.25)	0.70	0.70	0.70
- act. grnd cover - v. low dens./young (f_{ceff} = 0.05)	0.70	0.70	0.70
Pistachios[21]	0.20	1.05	0.40
- no ground cover - high density (f_{ceff} = 0.7)	0.30	0.95	0.65
- no ground cover - med. density (f_{ceff} = 0.5)	0.25	0.80	0.55
- no ground cover – low dens. / young (f_{ceff} = 0.25)	0.20	0.45	0.35
- active ground cover[23] - high density (f_{ceff} = 0.7)	0.70	0.95	0.70
- active ground cover - med. density (f_{ceff} = 0.5)	0.70	0.95	0.70
- act. grnd cover – low dens. / young (f_{ceff} = 0.25)	0.70	0.80	0.70
Walnut Orchard[21]	0.40	1.05	0.60[20]
- no ground cover - high density (f_{ceff} = 0.7)[22]	0.40	1.05	0.60[27]
- no ground cover - med. density (f_{ceff} = 0.5)	0.35	0.85	0.55[27]
- no ground cover – low dens. / young (f_{ceff} = 0.25)	0.25	0.50	0.35[27]
- active ground cover[23] - high density (f_{ceff} = 0.7)	0.75	1.10	0.80[27]
- active ground cover - med. density (f_{ceff} = 0.5)	0.75	1.05	0.80[27]
- act. grnd cover – low dens. / young (f_{ceff} = 0.25)	0.75	0.90	0.80[27]

[29] For pears having f_{ceff} = 0.5, Girona et al. (2003) measured $K_{cb\ mid}$ = 0.85, which is estimated using eq. 10.24, 10.25a and 10.29 using $K_{cb\ full}$ = 1.1 and M_L = 1.5.

[30] Stone fruit category applies to peaches, apricots, pears, plums and pecans.

[31] The values in this row are derived from Girona et al. (2005) and Ayars et al. (2003) with f_{ceff} = 0.7 and and M_L = 1.5.

[32] The values in this row are similar to those by Paço et al. (2006) and Ayars et al. (2003) with f_{ceff} = 0.25 and and M_L = 1.5.

[33] The values for citrus are about 20% higher than those reported in FAO-56.

[34] The values in this row are similar to those by Rogers et al. (1983) for citrus in Florida having Bahia grass cover.

[35] Conifers exhibit substantial stomatal control due to soil water deficit. The K_c can easily reduce below the values presented, which represent well-watered conditions for large forests.

[36] The values in this row are derived from de Azevedo et al. (2003).

[37] Pastor and Orgaz (1994) found monthly K_c for olive orchards having f_c ~ 60% similar to the values shown, except that $K_{c\ mid}$ = 0.45, with stage lengths = 30, 90, 60 and 90 days, respectively for initial, development, midseason and late season periods (see Table 5.6), and using K_c during the winter ("off season") in December to February = 0.50.

[38] The values in this row are similar to those by Villalobos et al. (2000) when $f_{c\ eff}$ of ~ 0.3 to 0.4 are applied.

[39] The values in this row are derived from Testi et al. (2004).

*Primary source: FAO-56 (Allen et al, 1998), with information from Doorenbos and Kassam (1979), Doorenbos and Pruitt (1977); Pruitt (1986); Wright (1981, 1982), Snyder et al. (1989a,b) and Allen, Howell and Snyder (2011c).

Table D.2. Mean plant height, *h*, m, used in eq. 10.27a,b and 10.29 for estimating $K_{cb\ ini}$, $K_{cb\ mid}$ and $K_{cb\ end}$ in table D.1 and parameter M_L used in eq. 10.29.

Category	$f_{c\ eff}$ = 0.05-0.1	$f_{c\ eff}$ = 0.25	$f_{c\ eff}$ = 0.5	$f_{c\ eff}$ = 0.7	$f_{c\ eff}$ = 0.9	M_L
Almonds		3	4	5		1.5
Apples, Cherries, Pears		3	3	4		2.0
Apricots, Peaches, Stone Fruit		2.5	3	3	3	1.5
Avocado		3	3	4		2.0
Citrus		2	2.5	3		1.5
Mango		4	4	5		1.5
Olives	2	3	4	4		1.5
Pistachios		2	2.5	3		1.5
Walnut		4	4	5		1.5
Palms	8	8	8	8		1.5
Grapes - Table or Raison		2	2	2		1.5
Grapes - Wine		1.5	1.5	1.5		1.5

Table D.3. Parameters used in eq. 10.25a,b and 10.26 for estimating $K_{cb\ ini}$, $K_{cb\ mid}$ and $K_{cb\ end}$ in table D.1 and using $f_{c\ eff}$ in table D.2.

Category	$K_{cb\ full}$ -initial	$K_{cb\ full}$ -mid	$K_{cb\ full}$ -end	$K_{c\ min}$	$K_{cb\ cover}$ -initial[1]	$K_{cb\ cover}$ -mid, end[1]	Add[2] to $K_{cb\ ini}$ for $K_{c\ ini}$	Add[2] to $K_{cb\ mid}$ for $K_{c\ mid}$	Add[2] to $K_{cb\ end}$ for $K_{c\ end}$
Almonds - no grnd cover	0.20	1.00	0.70[2]	0.15	--	--	0.20	0.05	0.05
- ground cover	0.20	1.00	0.70[2]	0.15	0.75	0.80	0.10	0.05	0.05
Apples, cherries, pears - killing frost	0.30	1.15	0.80[2]	0.15	0.40	0.80	0.20	0.05	0.05
- no killing frost	0.30	1.15	0.80[2]	0.15	0.75	0.80	0.10	0.05	0.05
Apricots, peaches, pears, plums, pecans - killing frost	0.30	1.20	0.80[2]	0.15	0.40	0.80	0.20	0.05	0.05
- no killing frost	0.30	1.20	0.80[2]	0.15	0.70	0.80	0.10	0.05	0.05
Avocado - no grnd cover	0.30	1.00	0.90	0.15	--	--	0.20	0.05	0.05
- ground cover	0.30	1.00	0.90	0.15	0.75	0.80	0.10	0.05	0.05
Citrus	0.90	0.90	0.90	0.15	0.75	0.80	0.10	0.05	0.05
Mango - no ground cover	0.25	0.85	0.70	0.15			0.10	0.05	0.05
Olives	0.60	0.70	0.60	0.15	0.70	0.70	0.10	0.05	0.05
Pistachios	0.30	1.00	0.70	0.15	0.70	0.70	0.10	0.05	0.05
Walnut	0.40	1.10	0.65[2]	0.15	0.75	0.80	0.10	0.05	0.05
Palms - no ground cover	0.85	0.90	0.90	0.15			0.10	0.10	0.10
- ground cover	0.85	0.90	0.90	0.15	0.70	0.70	0.10	0.05	0.05
Grapes - Table or Raison	0.20	1.15	0.90[3]	0.15			0.10	0.05	0.05
Grapes – Wine	0.20	0.80	0.60	0.15			0.10	0.05	0.05

[1] The $K_{cb\ cover}$*–initial* and $K_{cb\ cover}$*–mid, end* values were used in eq. 10.25b to represent K_{cb} for ground cover during the initial and for the midseason and late season periods during estimation of $K_{cb\ ini}$, $K_{cb\ mid}$ and $K_{cb\ end}$ in table D.1 for tree crops having typical ground cover vegetation between or under trees. For non-active or only moderately active ground cover (active indicates green and growing ground cover with LAI > about 2) , $K_{cb\ cover}$ can be weighted between K_{cb} for no ground cover and $K_{cb\ cover}$ for active ground cover, with the weighting based on the "greenness" and approximate leaf area of the ground cover.
[2] The last three columns are values added to K_{cb} values estimated for the initial, midseason and late season periods during application of eq. 10.25a,b, 10.26 and 10.27a to obtain mean K_c values.
[3] These $K_{c\ full}$ values for end of season represent K_c for full cover conditions prior to leaf drop. After leaf drop, $K_{c\ end} \approx 0.20$ for bare, dry soil or dead ground cover and $K_{c\ end} \approx 0.50$ to 0.80 for actively growing ground cover.

Appendix E

Mean and Basal Crop Coefficients, K_c and K_{cb}, for Crops Common to Temperate and Continental Climates for use with Alfalfa Reference ET_r as Computed by the *ASCE Standardized Penman-Monteith Reference Method*

The crop coefficient curves developed by Wright (1981) and Wright (1982) for nine crops common to southern Idaho have been widely accepted in the western US for use in irrigation water management, irrigation water rights, irrigation water transfers and related legal applications. This section describes the conversion of the mean and basal crop coefficients of Wright (1981) and Wright (1982), as reported in Jensen et al. (1990), for application with the ASCE Standardized Reference Evapotranspiration equation (ASCE-EWRI, 2005) for the alfalfa reference (ET_{rs}). The Wright coefficients were originally derived for use with the 1982 Kimberly Penman equation, and small differences exist between the two reference calculations. The K_c and K_{cb} curves are traceable to time based curves based on weighing lysimeter measurements at Kimberly, Idaho.

The ASCE Standardized Penman-Monteith ET_r method, which is standardized for a 0.5 m tall vegetation reference for all times of the year, tends to estimate higher than the 1982 Kimberly Penman equation during early spring and fall months (Wright et al., 2000) and to estimate slightly below the 1982 Kimberly Penman method during the peak summer period. Conversion of the Wright (1981, 1982) coefficients to the standardized ET_r basis provides for equivalent calculation of crop ET_c for a southern Idaho type of climate using the ASCE standardized Penman-Monteith method.

The conversion was performed by Allen and Wright (2006, 2007) and used weather data sets collected at Kimberly (latitude = 42.5 ^{o}N, longitude = 114.4 ^{o}W, elevation = 1195 m) for the same year as was used for the original coefficient determination. The specific years are summarized later in Table E.4. The same original weather data sets were used so that target ET_c values produced from smoothed K_c curves of Wright (1981, 1982) are identical to those produced originally by Wright. The converted K_c curves for use with ET_{rs} reproduce cumulative ET_c vs. time series for the Kimberly crops that is the same as obtained using the original coefficients and the 1982 Kimberly Penman method. This procedure retains all decision-making and original curve shaping decisions made by Wright (1981, 1982). It is expected that the converted K_c curves will produce applicable and representative ET_c for other temperate and continental climates similar to Kimberly, Idaho that have cold winters with defined dormant periods.

During the conversion work, standardized ET_r, denoted as ET_{rs}, was computed daily using Kimberly weather data for air temperature, humidity and wind speed collected by the National Weather Service at the USDA-ARS Center at Kimberly, and using solar radiation data collected by the USDA-ARS at Kimberly. The weather data were quality checked and controlled using procedures from ASCE (2005) Standardized Report Appendix D, including comparison of measured solar radiation data with a theoretical clear sky curves and comparison

of daily dewpoint temperature with daily minimum air temperature. Solar radiation for portions of some years required adjustment.

The same crop coefficient tabular format as used by Wright (1982) was used to summarize the converted crop coefficient curves:

- K_c from planting to effective full cover expressed as a function of percent time from planting to effective full cover, in multiples of 10%, and
- K_c after effective full cover expressed as a function of days after full cover in multiples of 10 days.

For the conversion, target crop ET_c was computed daily as $ET_{c\ KP} = K_{c\ Wright}$ x $ET_{r\ KP}$ where $ET_{c\ KP}$ represented ET_c based on the original crop coefficient data set ($K_{c\ Wright}$) of Wright (1981) and Wright (1982), as reported in Jensen et al., (1990), Tables 6.6 and 6.9, and where some adjustment had been made by Wright (1995). $ET_{r\ KP}$ represented alfalfa reference ET calculated using the 1982 Kimberly Penman equation and associated equations (Wright, 1982). ET_c for the Standardized Penman-Monteith was computed as $ET_{c\ s} = K_{c\ s}$ x ET_{rs} where $ET_{c\ s}$ represents crop ET computed with the standardized ASCE procedure, and $K_{c\ s}$ represents the crop coefficients converted for use with ET_{rs}.

During the conversion work, tabularized values for $K_{c\ s}$ were adjusted so that cumulative $ET_{c\ s}$ vs. time was identical to cumulative $ET_{c\ KP}$ vs. time. The adjustments forced the two cumulative ET_c curves to graphically coincide, and the use of cumulative ET_c curves created a relatively smooth and continuous evolution in K_c vs. time, and minimized the total RMSD for the standardized mean K_c, denoted as $K_{cm\ s}$, or the standardized basal K_c, denoted as $K_{cb\ s}$. Results of the conversion are listed in Table E.1 for mean crop coefficients and in Table E.2 for basal crop coefficients. The planting, effective full cover and harvest dates reported by Wright (1981 and 1982) are summarized in Table E.3. Root mean square error (RMSD) between cumulative ET_c by the original and converted curves were generally less than 1 mm per decadal period, as summarized in Table E.4. This translates into less than about 0.2 mm d^{-1} RMSD in most cases. Graphical illustrations of the cumulative ET_c were given by Allen and Wright (2004).

The K_c curves for winter wheat were generated from the date of planting in fall until estimated dormancy in early winter and then again from greenup in spring until harvest following Wright (1982). Alfalfa K_c curves were converted for each of the four growth cycles as done by Wright (1981, 1982). In addition, a growing-season-long curve that smoothes the impacts of reduced K_c following cuttings was converted for use with ET_{rs}. Three years of weather and lysimeter data from 1969, 1970, 1971 had been used by Wright to construct the alfalfa curves. Therefore, a combined daily series for ET_r was created by averaging the daily ET_r from these three years. Similarly, two years, 1973 and 1974, were averaged to construct the daily ET_r curve for the snap bean crop, where those two years were used in defining the original K_c curves (Wright, 1982).

The second and third growth cycles for alfalfa at Kimberly use the same K_c and K_{cb} curves in Tables E.1 and E.2. That middle growth cycle curve was converted so that each of the two growth cycles shared any "error" created by the curve conversion. The clipped ryegrass crop was not reported by Wright (1981) nor Wright (1982), but was included in Jensen et al., (1990) and

traces to the Kimberly lysimeters operated by Wright, and was therefore converted and reported by Allen and Wright (2007). That crop was grown at Kimberly during years 1983 and 1984, so that the ET_r for those two years was averaged to produce a single daily time series.

Table E.1. Mean Crop Coefficients, K_C, for Crops Common to Temperate and Continental Climates for use with Alfalfa Reference ET_r Computed by the *ASCE Standardized Penman-Monteith Reference Method* *

	Mean ET Crop Coefficients, K_c										
	Pct, time from planting to effective cover										
Crop	**0**	**10**	**20**	**30**	**40**	**50**	**60**	**70**	**80**	**90**	**100**
Spring grain[1]	0.20[2]	0.20	0.20	0.25	0.37	0.50	0.63	0.76	1.00	1.03	1.03
Peas	0.15	0.17	0.19	0.21	0.32	0.42	0.52	0.63	0.73	0.83	0.93
Sugar Beets	0.26	0.26	0.26	0.26	0.26	0.28	0.30	0.38	0.55	0.74	1.03
Potatoes	0.20	0.20	0.20	0.22	0.30	0.41	0.53	0.67	0.73	0.77	0.80
Corn	0.20	0.20	0.20	0.20	0.24	0.34	0.44	0.58	0.72	0.90	1.00
Beans	0.20	0.20	0.22	0.26	0.35	0.45	0.55	0.68	0.83	0.95	0.97
Winter Wheat	0.25	0.25	0.27	0.38	0.60	0.80	0.90	0.96	1.00	1.03	1.03
	DT, days after effective cover										
Crop	**0**	**10**	**20**	**30**	**40**	**50**	**60**	**70**	**80**	**90**	**100**
Spring grain[1]	1.03	1.03	1.03	1.03	0.94	0.50	0.30	0.15	0.10		
Peas	0.93	0.93	0.70	0.54	0.38	0.22	0.12	0.10			
Sugar Beets	1.03	1.03	1.03	1.00	0.97	0.92	0.82	0.74	0.65	0.61	0.56
Potatoes	0.80	0.80	0.76	0.72	0.68	0.63	0.58	0.50	0.38	0.20	0.15
Field Corn	1.00	0.99	0.98	0.95	0.88	0.80	0.72	0.63	0.35	0.18	
Sweet Corn	1.00	0.97	0.94	0.90	0.84	0.70	0.55	0.35	0.20	0.10	
Beans	0.97	0.97	0.94	0.64	0.32	0.15	0.10	0.05			
Winter Wheat	1.03	1.03	1.03	1.03	1.00	0.55	0.25	0.15	0.10		
	Time from new growth or harvest to harvest (%)										
Crop	**0**	**10**	**20**	**30**	**40**	**50**	**60**	**70**	**80**	**90**	**100**
Alfalfa (1st cycle)[3]	0.50	0.62	0.73	0.83	0.88	0.94	1.00	1.00	1.00	0.98	0.95
(Intermediate cycles)	0.30	0.40	0.55	0.80	0.94	0.97	1.00	1.00	1.00	0.97	0.94
(Last cycle)	0.30	0.35	0.45	0.53	0.58	0.58	0.54	0.48	0.46	0.44	0.44
	Total season (days from beginning of spring growth)										
Crop	**0**	**20**	**40**	**60**	**80**	**100**	**120**	**140**	**160**	**180**	**200**
Alfalfa	0.45	0.69	0.87	0.88	0.7	0.75	0.88	0.81	0.88	0.71	0.65
(seasonal)	0.44	0.77	0.82	0.86	0.9	0.88	0.85	0.82	0.78	0.66	0.5
(seasonal mean)						**0.85**					
Perennial rye grass (8-15 cm)	0.55	0.66	0.77	0.80	0.80	0.80	0.78	0.76	0.72	0.68	0.55

* Converted from original crop coefficients of Wright (1981); Manual 70 Table 6.6; and updates by Wright (1995) and Allen and Wright (2007).

[1] Spring grain includes wheat and barley.

[2] The values 0.15 - 0.26 for all crops are appropriate for relatively dry surface soil conditions from planting until significant crop development. For moderately wet surface soil, as with preemergence irrigation(s) or some precipitation, use 0.35, and for very wet conditions use 0.50 for the first part of the growing season until that value is exceeded by a table value.

[3] 1st denotes first harvest, intermediate harvests may be one or more depending on length of season. The last harvest is when crop becomes dormant in cool weather. Cultivar used was Ranger.

Table E.2. Basal Crop Coefficients, K_{cb}, for Crops Common to Temperate and Continental Climates for use with Alfalfa Reference ET_r as Computed by the *ASCE Standardized Penman-Monteith Reference Method* *

	Basal ET Crop Coefficients, K_{cb}										
	Pct, time from planting to effective cover										
Crop	**0**	**10**	**20**	**30**	**40**	**50**	**60**	**70**	**80**	**90**	**100**
Spring grain[1]	0.15	0.15	0.15	0.19	0.24	0.36	0.48	0.62	0.92	0.98	1.03
Peas	0.12	0.13	0.14	0.15	0.18	0.27	0.36	0.50	0.65	0.78	0.92
Sugar Beets	0.15	0.15	0.15	0.15	0.15	0.16	0.17	0.21	0.40	0.66	1.03
Potatoes	0.15	0.15	0.15	0.15	0.15	0.20	0.34	0.49	0.64	0.72	0.77
Corn	0.15	0.15	0.15	0.16	0.17	0.20	0.27	0.41	0.55	0.80	0.96
Beans	0.15	0.15	0.17	0.19	0.23	0.35	0.46	0.6	0.78	0.93	0.95
Winter Wheat	0.12	0.12	0.14	0.22	0.45	0.70	0.84	0.96	1.00	1.03	1.03
	DT, days after effective cover										
Crop	**0**	**10**	**20**	**30**	**40**	**50**	**60**	**70**	**80**	**90**	**100**
Spring grain[1]	1.03	1.03	1.03	1.03	0.94	0.40	0.15	0.07	0.05		
Peas	0.92	0.92	0.72	0.52	0.32	0.16	0.07	0.05			
Sugar Beets	1.03	1.03	1.02	0.98	0.93	0.86	0.78	0.72	0.66	0.60	0.54
Potatoes	0.77	0.77	0.73	0.68	0.64	0.59	0.54	0.47	0.20	0.08	0.08
Field Corn	0.96	0.96	0.96	0.92	0.85	0.79	0.72	0.62	0.28	0.16	0.12
Sweet Corn	0.96	0.95	0.93	0.88	0.80	0.65	0.47	0.23	0.12		
Beans	0.95	0.95	0.88	0.64	0.30	0.09	0.05				
Winter Wheat	1.03	1.03	1.03	1.03	1.00	0.50	0.20	0.10	0.05		
	Time from new growth or harvest to harvest (%)										
Crop	**0**	**10**	**20**	**30**	**40**	**50**	**60**	**70**	**80**	**90**	**100**
Alfalfa (1st cycle)[2]	0.35	0.45	0.56	0.72	0.82	0.9	1.00	1.00	1.00	0.98	0.96
(Intermediate cycles)	0.25	0.30	0.42	0.72	0.90	0.95	1.00	1.00	0.98	0.96	0.94
(Last cycle)	0.25	0.27	0.36	0.42	0.50	0.45	0.35	0.3	0.25	0.22	0.22
	Total season (days from beginning of spring growth)										
Crop	**0**	**20**	**40**	**60**	**80**	**100**	**120**	**140**	**160**	**180**	**200**
Alfalfa	0.45	0.69	0.87	0.88	0.70	0.75	0.88	0.81	0.88	0.71	0.65
(seasonal)	0.50	0.74	0.82	0.86	0.88	0.88	0.86	0.84	0.78	0.70	0.50
(seasonal mean)						**0.85**					
Perennial rye grass (8-15 cm)	0.60	0.68	0.76	0.78	0.80	0.80	0.79	0.76	0.73	0.68	0.60

* Converted from original crop coefficients of Wright (1982); Manual 70 Table 6.6; and updates by Wright (1995) and Allen and Wright (2007).
[1] Spring grain includes wheat and barley.
[2] 1st denotes first harvest, intermediate harvests may be one or more depending on length of season. The last harvest is when crop becomes dormant in cool weather. Cultivar used was Ranger.

TABLE E.3. Dates of Various Crop Growth Stages for Crops Studied at Kimberly, Idaho 1968-1979 (after Wright, 1982, and Table 6.7 of Jensen et al. 1990)

	Date of Occurrence (Month/Day)							Days	
Crop	Planting	Emer-gence	Rapid Growth	Full Cover	Heading or Bloom	Ripening	Harvest	Planting to Full Cover	Full Cover to Harvest
(1)	(2)	(3)	(4)	(5)	(6)	(7)	(8)	(9)	(10)
Spring grain[1]	04/01	04/15	05/10	06/10	06/10	07/20	08/10	70	61
Peas	04/05	04/25	05/10	06/05	06/15	07/05	07/25	61	50
Sugar Beets	04/15	05/10	06/01	07/10			10/15	86	97
Potatoes	04/25	05/25	06/10	07/10	07/01	09/20	10/10	76	92
Field Corn	05/05	05/25	06/10	07/15	07/30	09/10	09/20	71	67
Sweet Corn	05/05	05/25	06/10	07/15	07/20		08/15	71	31
Beans	05/22	06/05	06/15	07/15	07/05	08/15	08/30	54	46
Winter Wheat[2]	(2/15)	(3/1)	03/20	06/05	06/05	07/15	08/10	(110)	66
Alfalfa (1st)[3]	04/01		04/20				06/15		
Alfalfa (2nd)[3]	06/15		06/25				07/31		
Alfalfa (3rd)[3]	07/31		08/10				09/15		
Alfalfa (4th)[3]	09/15		10/01				10/30		

[1]Spring grain includes barley and wheat.
[2]Effective dates are in parentheses. Crop was planted on 10/10 and emerged 10/25 the previous season.
[3]Effective planting date for established alfalfa is the date growth begins in spring or harvest of preceding crop. Dates for cuttings are indicated. Final harvest is the date crop became dormant.
Minor changes from Wright (1982) reflect additional data for some crops (Wright, 1984, personal communication).

Table E.4. Years of original lysimeter and weather data collection reported by Wright (1981) and Wright (1982) and RMSD for crop coefficient conversion.

Crop	Year of data	RMSD of ET_c produced during the conversion of K_{cm} from the Kimberly Penman basis to the ASCE Standardize Penman-Monteith Reference ET basis, mm per decadal[1] period
Spring grain (*Triticum aestivum*)	1979	1.1
Peas (*Pisum sativum*)	1977	1.0
Sugar Beets (*Beta Vulgaris*)	1975	0.9
Potatoes (*Solanum tuberosum*)	1972	0.7
Field Corn (*Zea mays*)	1976	0.9
Sweet Corn (*Zea mays* convar. *saccharata*)	1976	0.9
Snap Beans (*Phaseolus vulgaris*, cv. Slimgreen)	1973, 1974 (ave)	0.3
Winter Wheat (*Triticum aestivum*)	1977-78	1.4
Alfalfa (*Medigaco Sativa*, cv. Ranger)	1969, 1970, 1971 (ave)	0.7 (season) 0.4, 1.3, 1.3, 0.4 for cuttings 1, 2, 3, 4
Ryegrass (*Lolium perenne*)	1983, 1984	0.7

[1] A decadal period represents 10% of the planting to effective full cover period or each 10 days following effective full cover until harvest.

Appendix F

Basal Crop Coefficients, K_{cb}, for Crops Common to Temperate and Continental Climates for use with Alfalfa Reference ET_r as Computed by the *ASCE Standardized Penman-Monteith Reference Method* using a Growing-Degree-Day Basis

F.1 Introduction

The K_{cb} curves of Wright (1982) are traceable to weighing lysimeter measurements of ET at Kimberly, Idaho for nine crops common to southern Idaho. These K_{cb}'s have been widely accepted in the western US for use in irrigation water management, irrigation water rights, irrigation water transfers and related legal applications. The K_{cb} curves of Wright (1982) presented in Appendix E for the original time-basis are reformulated in this appendix as functions of cumulative growing degree days (CGDD). The use of CGDD provides automated flexure, expansion or compression of the K_c curve basis under varying weather conditions and eliminates the need to specify the time of effective full cover. Wright (1998) originally made the conversion of Wright (1982) K_{cb} curves to CGDD that was repeated by Allen and Wright (2006) following the conversion to the ASCE Standardized Reference Evapotranspiration equation (ASCE-EWRI, 2005) as an alfalfa reference (ET_{rs}) basis, as outlined in Appendix E. The conversion and basis for applying CGDD is described here. Description of state-wide application of the estimation procesures by Allen and Robison (2007) and Huntington and Allen (2010) are given for Idaho and Nevada.

F.2 Growing Degree Basis for K_c

Plant functions of evapotranspiration, photosynthesis, water and nutrient absorption and transport, enzyme activity, and other biological and chemical activities are regulated by temperature. For this reason, the development of the crop is generally closely related to the amount of heat the crop is exposed to, as opposed to using straight calendar days. In many applications, the emergence of vegetation, greenup, and attainment of effective full cover have been estimated using cumulative degree-based regression equations or plant growth models (Sinclair 1984; Sammis 1985; Ritchie and NeSmith 1991; Slack et al. 1996; Snyder et al. 1999; Cesaraccio et al. 2001; Ojeda-Bustamante et al., 2004; Allen and Robison 2007; Martínez-Cob, 2008; Ceglar et al., 2011; Ghamarnia et al., 2013; Payero and Irmak, 2013). The use of cumulative growing degree days provides a quantitative stretching or shrinkage of the generated K_c curves for years or growing seasons that run cooler or warmer than average, and reduces the need for manual estimation of these dates and intervention to the K_c estimation process. This approach is required for prospective studies of climate change impacts on crop water and irrigation requirements, for example by Saadi et al. (2014) and as a means to facilitate transfer of crop coefficients among regions.

Cumulative growing degree days (CGDD) since planting have commonly been used as a basis for crop coefficient development, as a means for automatically adjusting lengths of development and growth periods to account for variation in temperature among years (Sammis et al., 1985,

Slack et al. 1996, Howell et al. 1997, Mitchell 1997, Snyder et al. 1999, Wright, 2001, deTar, 2004, Marek et al., 2006, and Nebraska-HPCC, 2006). A range of computation methods for growing degree days (GDD) have been utilized. These include the standard method that has long been used for corn (Van den Brink et al. 1971):

$$GDD_{corn} = \frac{max(min(T_{max},30),10) + max(min(T_{min},30),10)}{2} - 10 \qquad \text{(F.1)}$$

where T_{max} is daily maximum air temperture, ^{o}C and T_{min} is daily minimum air temperature, ^{o}C. The standard corn equation is often referred to as a heat unit equation and is also known as the '86/50' method, referring to the maximum threshold of 30°C and minimum threshold of 10°C, which are 86 and 50 ^{o}F. The GDD equation for corn limits GDD accumulation above 30 ^{o}C, which assumes no growth at air temperatures above 30°C. The method also assumes no retardation or negative 'penalty' to growth rate if the minimum temperature goes below 10°C.

A common, basic formula for computing daily growing degree days (GDD) for crops other than corn is to average daily maximum and daily minimum air temperatures for each day and to subtract a minimum average daily temperature (base temperature) required for growth to proceed (Mitchell 1997 and Wright 2001). There is no penalty applied when T_{max} exceeds a threshold, as is done with corn, and no 'numerical boost' is given to T_{min} when it is lower than the minimum threshold, as is the case for corn. The basic equation for the general GDD is:

$$GDD = max\left(\frac{T_{max} + T_{min}}{2} - T_{base}, 0\right) \qquad \text{(F.2)}$$

where T_{base} is a base temperature representing when daily average air temperature is sufficient for plant growth to proceed. When T_{min} is far enough below T_{base} to cause the average daily temperature (T_{max} + T_{min})/2) to dip below T_{base}, then GDD is set to 0 ^{o}C-days. Days having high T_{max}, but with T_{min} below T_{base} are estimated by Eq. F.2 to have lower growth rates than by Eq. F.1, where T_{min} is 'boosted.' Wright (2001) suggested that Eq. F.2 is realistic for most crops grown in semiarid climates such as Idaho, where cold nighttime temperatures can retard growth during daytime even when mid day temperatures are high.

F.3. Conversion of Wright (1982) Kcb curves to the CGDD basis

The conversion of the K_{cb} curves of Wright (1982) from a time base to a normalized GDD base was produced by Allen and Wright (2006) and followed that originally developed by Wright (2001), but where the standardized ASCE-PM ET_r method was utilized as the basis. Weather data for the specific year of curve development was used to compute CGDD as

described in Appendix E. T_{base} values used for crops were based on selections by Wright (2001) and ranged from 0°C for early spring crops such as spring grain to 5°C for crops such as potatoes and dry beans as shown in Table 3.1. All crops used Eq. F.2 for GDD with the exception of corn, where the standard corn GDD method was used (T_{base} = 10 °C and Tupper threshold = 30 °C) for consistency with standardized usage within the U.S.
The approach of Wright (2001) was followed for conversion of the function basis, where the CGDD basis was normalized in terms of the quantity of CGDD required to advance from planting or green-up to effective full cover. This normalized CGDD (termed NCGDD) ranges from 0 to 1.0 over the period from planting or green-up until effective full cover. Normalization of CGDD provides the means to change only one number (the value for NCGDD at full cover) when fitting curves to a new variety or region. NCGDD ranges from 1.0 to typically more than 2.0 for the period from effective full cover to harvest or die-down. NCGDD was computed each day by dividing by the CGDD for that day by the CGDD at effective full cover:

$$NCGDD_i = \frac{CGDD_i}{CGDD_{planting\,to\,EFC}} \tag{F.1}$$

where $CGDD_i$ is cumulative growing degrees up to day *i*, and $CGDD_{planting\ to\ EFC}$ is CGDD from the date of planting or green up until the attainment of effective full cover of the crop. Effective full cover dates were taken from Table E.3, following Wright (1982).

The process for translation of K_{cb} curves to the ASCE-PM ET_r basis was similar to that for the time-based conversion of the K_{cb} curves described in Appendix E, where cumulative ET was computed vs. time using the 1982 Kimberly Penman ET_r applied using the weather data for the specific year of lysimeter measurement and multiplied by the crop coefficient curve of Wright (1982). The crop coefficient curve of Wright (1982) was constructed using the dates for planting, effective full cover and harvest given in that paper as well as the crop coefficients reported there or updated by Wright (1995) and listed in Table E.2. The result was a 'reconstructed' lysimeter ET data set that reflected the smoothing of the K_c curves and filtering and decision-making by Wright (1981, 1982, 1996). The cumulative ET vs. time curves were then paired against equivalent normalized CGDD calculated for the same year and weather data set, and the value for CGDD at the time of reported effective full cover was determined. NCGDD was computed each day by dividing by the CGDD for that day by the CGDD at effective full cover. Finally, percentile values for K_{cb} were selected from the plots, numerically in increments of 10% for NCGDD.

The snap bean crop, which also represents dry, edible beans, was grown at Kimberly in 1973 and 1974. The NCGDD curves for the beans were developed using data from 1973. For alfalfa hay, K_c v. NCGDD curves were established for individual cuttings using data from Wright (1981, 1982) and lysimeter records for the 1969-1971 period at Kimberly. Unique K_c vs. NCGDD were developed for the first growth period, for intermediate growth periods, and for the final growth period prior to frost. The unique K_c v. NCGDD shapes were established to account for differences in regrowth rates for the three periods. The NCGDD values for the first growing

cycle are accumulated beginning at greenup of the crop in spring, assuming a dormant or near-dorman period during winter. NCGDD for the other growth cycles are accumulated from the time of cutting. Green up was estimated for alfalfa using CGDD since January 1 and a temperature base of 0°C. The month of January in Idaho usually represents a period of no significant CGDD accumulation, and where the alfalfa crop is dormant. Therefore, this is a good starting point to begin the CGDD accumulation for alfalfa. A CGDD of 240 °C-days from Jan. 1 was used to signal greenup, based on Kimberly data and observations across southern Idaho. No penalties were applied to CGDD of alfalfa during winter or early spring as was the case for winter wheat, when subfreezing temperatures occurred. Huntington and Allen (2010) used CGDD of 300 °C-days from Jan. 1 to signal greenup in southern Nevada, a region having relatively warmer winters.

During the conversion, the K_c v. NCGDD curve for winter wheat was begun Oct. 1 and run through the winter, which deviates from Wright (2001) where his NCGDD curve began at an 'artificial' greenup date located in late winter or early spring. The Oct. 1 date is a typical planting date in many parts of Idaho and agrees with the Oct. 10 date reported by Wright (1982) for the winter wheat crop of 1977-78. The CGDD based K_{cb} curve for winter wheat that extends back to Oct. 1 and provides K_{cb} information during winter. The K_{cb} curve has a shape following the heading of the wheat crop that agrees closely with the Wright (1982) K_{cb} curve.

K_{cb} is expressed for potato crops for two classes of potatoes: long season, late-harvested varieties representing baking potatoes and other varieties that are harvested in September and October in southern Idaho and short season varieties representing processing potatoes that begin to be harvested as early as August. Planting and development dates for both varieties are generally similar and therefore a single curve is used for the period between planting and effective full cover. Separate curves are used for the period from effective full cover to harvest, both based on a normalized cumulative growing degree-day scale. The K_{cb} vs. NCGDD relationship for the long season class is that developed from Wright (1982) and listed in Table F.1 as curve no. 6. The K_{cb} vs. NCGDD relationship for the short season class (curve 7) was developed from that for the long season variety by shortening the relative time required for maturity and reducing values for K_{cb} beginning at about 1.75 times $NCGDD_{\text{Planting to Effective Cover}}$. The recommended CGDD at harvest for the long season variety is about 1800 °C-days and that for the short season variety is about 1600 °C-days.

The grass hay K_{cb} curve was constructed to follow the shape of the K_{cb} curve for first cycle alfalfa, but with peak K_{cb} of 0.95 rather than 1.0 and with 50% longer CGDD required until cutting (1300 °C-days at base 0°C). Following a first cutting (at NCGDD = 1.0), the K_{cb} is presumed to stay near 0.70 and then decline towards fall, when grazing may occur. The shape is similar to the K_{cb} curve developed and reported by the US Bureau of Reclamation Agrimet system (P.Palmer, USBR, 1999, pers. Comm.). The curve is terminated at killing frost.

Figure F.1 shows K_{cb} vs. NCGDD for the nine Kimberly crops plotted together. The NGCDD value at the attainment of effective full cover equals 1.0 in the figure. The shapes of the K_{cb} curves are similar to one another during the development period since all crops but alfalfa are annuals and because of the use of normalized CGDD as the basis for the K_{cb} vs. NCGDD curve. All of the K_{cb} curves run between 0.9 and 1.0 after effective full cover due to the

attainmnent of nearly full ground cover. The exception is the curve for potatoes, which peaked at about 0.80, due, perhaps to varietal effects for the Russet Burbank crop. Figure F.2 shows the first, intermediate and final K_{cb} vs. NCGDD curves derived for the Ranger variety alfalfa crop at Kimberly and Figure F.3 shows the K_{cb} vs. NCGDD curve developed for grass hay.

F.4. Application of K_{cb} curves with the CGDD basis

To apply the K_{cb} vs. NCGDD curves, one needs to determine the planting or greenup date to begin the season. No other information other than daily calculated CGDD is required. To construct the curve, CGDD from the estimated day of planting or greenup is accumulated using the Base temperature for the crop using Eq. F.2 for all crops except corn, where Eq. F.1 is used. The ratio NCGDD is calculated using Eq. F.1 by dividing CGDD accumulated since planting (or greenup of alfalfa) by the CGDD $_{\text{Planting to EFC}}$ value in Table F.1. For example, for spring wheat, the CGDD $_{\text{Planting to FC}}$ value is 935 ^{o}C-days. The ratio NCGDD is used as the entry point in column 1 of Table F.1 and the value for K_{cb} is selected by interpolation. This ratio is applied to the entire season or cutting cycle until either CGDD exceeds the value for CGDD $_{\text{Planting to Terminate}}$ that is in the table or when a killing frost occurs.

Adjustments in NCGDD-based K_{cb} Applications.

The Cumulative growing degree day values at the time of effective full cover (CGDD $_{\text{Planting to EFC}}$) values in Table F.1 are based on observed times of effective full-cover or timing of plateauing of the K_{cb} curve. Modern crop varieties may require the establishment of different values for CGDD $_{\text{Planting to EFC}}$ to account for more rapid or less rapid development rates for the same thermal conditions. For example, the following adjustments were made to the CGDD-based K_{cb} curves during application to 123 weather station locations in Idaho by Allen and Robison (2007). The adjustments were made to account for differences between Kimberly data derived from lysimeter measurements in the 1970's and 1980's and observations for more current crops and growing practices. Similar observations were made and adjustments applied in Nevada by Huntington and Allen (2010).

CGDD $_{\text{Planting to EFC}}$ values were increased by Allen and Robison (2007) for corn by 5% and CGDD $_{\text{Planting to Terminate}}$ was increased by about 20% relative to values that occurred during the specific year of lysimeter mesurements. This was done to produce seasonal curves that reflect behavior of current corn cultivars in Idaho. CGDD $_{\text{Planting to EFC}}$ values were reduced for potatoes by 5% relative to values that occurred during the specific year of lysimeter mesurements. This was done to produce seasonal curves that terminated naturally before killing frosts for more years accross major potato growing locations in southern Idaho. CGDD $_{\text{Planting to EFC}}$ values were reduced for spring grain by 10% and for winter grain by approximately 25% to shorten estimated season lengths to better match those currently observed across southern Idaho relative to that in the 1970's. The CGDD $_{\text{Planting to EFC}}$ value for sugar beets was increased from 710 to 970 ^{o}C-days to reflect current observation of growth rates for south-central Idaho. The CGDD $_{\text{Planting to Terminate}}$ value was increased from 1843 to 2600 ^{o}C-days.

K_{cb} vs. NCGDD curves for crops harvested fresh are derived from the full K_{cb} curves in Table F.1 by specifying a smaller value for NCGDD$_{\text{Planting to Termination}}$. For example, for fresh-

harvested peas, snap beans and sweet corn, Allen and Robison (2007) applied the K_{cb} curves for peas, dry beans and sween corn using $NCGDD_{Planting\ to\ Termination}$ values set to 1.6, 1.6 and 2.2, respectively. The K_{cb} value during post-harvest periods for fresh-harvested crops was set to 0.1 for bare, dry soil surface conditions or to a higher value if some residual green vegetation was present following harvest.

Additional adjustments were made to K_{cb} during fall periods for alfalfa, to account for effects of cold nighttime temperatures and occaisional light, but nonkilling frosts. The adjustments reduced the value for K_{cb} following the first occurrence of a -3°C in the fall by 0.005 each day following the -3°C temperature. This reduced the value for K_{cb}, for example, by 0.10 by the 20th day following the light frost. The killing frost temperature for alfalfa was set at -7°C by Allen and Robison (2007). Huntington and Allen (2010) found good performance by these parameter values in Nevada.

Adjustments during application of the winter wheat K_{cb} curve. The CGDD clock for winter wheat is assumed to begin on Oct. 1. When applying the winter wheat crop during winter, some periodic adjustments to the cumulative CGDD may be needed to account for impacts of extremely cold weather that tend to retard growth for several days or may even 'burn' the existing vegetation. These adjustments are based on observations of vegetation appearance during winter in southern Idaho and adhere to the following rules. In computing CGDD for fall, winter and early spring periods for winter wheat, the following adjustments can be made. These apply to winter wheat only:

- If T_{min} is < -4°C on a day, then GDD for that day is set to zero for that day, regardless of the value for T_{max} or T_{mean}. This is done as a delay penalty to the growth rate of winter wheat on the day of the cold temperature. The occurrence of little or no growth on days where T_{min} < -4°C is based on observations by Wright (2002, pers. comm.).
- Whenever T_{min} is < -10°C then the GDD for the following day, if greater than 0, is reduced by 5 GDD units. This reduction is enforced as a retardation penalty to the growth rate of winter wheat following a cold freeze. GDD on all days was limited to 0 or greater.
- Whenever T_{min} is < -25°C and there is no documented snow cover present, 10% of the current crop canopy is assumed to suffer from frost burn and no longer effective in facilitating growth or transpiration. This impact is enacted by reducing the CGDD that has been accumulated since Oct. 1 by 10% for the day following the occurrence of -25 °C.

Impact of weather station aridity. Chapter 8 discusses the impact of local and regional dryness on increasing measured values for T_{max} and T_{min} in the absence of irrigation. In applications to Idaho National Weather Service Coop stations, Allen and Robison (2007) reduced values for T_{max} and T_{min} for some stations according to perceived station aridity effects using aridity ratings described by Allen et al., (1983). This adjustment was done prior to calculating CGDD, since

the CGDD thresholds 'expect' to have input from weather stations having relatively well-watered surroundings. The adjusted T_{max} and T_{min} were not used in computation of ET_r, but only for calculation of NCGDD and K_{cb} values.

Table F.1. K_{cb} for use with the Standardized ASCE-EWRI Penman-Monteith based on Normalized Cumulative Growing Degree-Day from Planting to Effective Full Cover, traceable to Wright (1982) and the USDA-ARS Kimberly, Idaho lysimeter systems.

Curve no.:	1	2	3	4	5	6	7	8	9	10
Percent Normalized Cumulative GDD from Planting (or Greenup) to Effective Full Cover	**Spring wheat**	**Winter Wheat**	**Peas, seed**	**Peas, fresh**	**Sugar Beets**	**Late Harvest Potato**	**Early Harvest Potato**	**Grain Corn**	**Silage Corn**	**Sweet Corn**
0	0.15	0.12	0.12	0.12	0.15	0.15	0.15	0.15	0.15	0.15
10	0.15	0.12	0.14	0.14	0.15	0.15	0.15	0.15	0.15	0.15
20	0.20	0.15	0.15	0.15	0.16	0.15	0.15	0.15	0.15	0.15
30	0.28	0.20	0.16	0.16	0.17	0.17	0.17	0.17	0.17	0.17
40	0.40	0.27	0.20	0.20	0.18	0.23	0.23	0.19	0.19	0.19
50	0.50	0.40	0.32	0.32	0.21	0.35	0.35	0.28	0.28	0.28
60	0.59	0.72	0.46	0.46	0.40	0.48	0.48	0.42	0.42	0.42
70	0.82	0.93	0.63	0.63	0.57	0.62	0.62	0.54	0.54	0.54
80	0.95	0.99	0.77	0.77	0.73	0.69	0.69	0.73	0.73	0.73
90	0.99	1.03	0.85	0.85	0.88	0.74	0.74	0.86	0.86	0.86
(Eff. Full Cov.)100	1.03	1.03	0.92	0.92	1.03	0.77	0.77	0.96	0.96	0.96
110	1.03	1.03	0.92	0.92	1.03	0.77	0.77	0.96	0.96	0.96
120	1.03	1.03	0.92	0.92	1.03	0.77	0.76	0.96	0.96	0.95
130	1.03	1.03	0.91	0.91	1.03	0.75	0.72	0.96	0.96	0.94
140	1.03	1.02	0.84	0.84	1.02	0.72	0.70	0.96	0.96	0.93
150	1.03	1.00	0.78	0.78	1.01	0.70	0.68	0.94	0.94	0.90
160	1.03	0.72	0.71	0.71	0.99	0.68	0.65	0.90	0.90	0.86
170	1.01	0.43	0.65	0.65	0.97	0.66	0.63	0.86	0.86	0.82
180	0.97	0.25	0.58		0.95	0.64	0.59	0.82	0.82	0.78
190	0.88	0.15	0.52		0.91	0.61	0.54	0.78	0.78	0.73
200	0.64	0.10	0.45		0.87	0.58	0.40	0.73	0.73	0.65
210	0.41	0.05	0.38		0.82	0.54	0.10	0.65	0.65	0.20
220	0.28		0.31		0.77	0.48		0.44	0.20	0.10
230	0.16		0.27		0.73	0.16		0.22	0.10	0.10
240	0.10		0.22		0.69	0.10		0.13	0.10	
250	0.05		0.18		0.63					
260			0.14		0.57					
270			0.10		0.10					
280										
290										
300										
T_{base}, ^{o}C[a]	0	0	0	0	5	5	5	10-corn	10-corn	10-corn
$CGDD_{Planting\ to\ EFC}$[b]	935[e]	1350[e]	635	635	710[e]	780[e]	780	510[e]	510	510
$CGDD_{Planting\ to\ Terminate}$[c]	2160	2608	1616	1000	1843[f]	1850[f]	1600[f]	1200[f]	1000	800[f]

[a]The GDD Base, T_{base}, ^{o}C, is the base or minimum temperature threshold used when computing the growing degree day.

[b]The $CGDD_{Planting\ to\ EFC}$ is the cumulative growing degree days from planting (or greenup) until effective full cover. Effective full cover is set differently for each crop Wright (1982).

[c]The $CGDD_{Planting\ to\ Terminate}$ is the total cumulative growing degree days from planting (or greenup) until termination (harvest) of the crop. This parameter signals the end of the K_{cb} curve construction.

[e]The 935 value for spring wheat was changed to 840 during processing, the 1350 value for winter grain was changed to 1080 during processing, the 780 for baking potatoes was reduced to 700, the 710 for sugar beets was increased to 970 and the 510 value for corn was changed to 540 during processing by Allen and Robison (2007) to fit recent observations of crop development.

[f]The 1843 value for sugar beets was changed to 2600, the 1850 and 1600 for potatoes were changed to 1780 and 1550, and the 1200 value for field corn was changed to 1400 and the 800 value for sweet corn was changed to 1000 by Allen and Robison (2007) to fit recent observations.

Table F.1 continued. K_{cb} for use with the Standardized ASCE-EWRI Penman-Monteith based on Normalized Cumulative Growing Degree-Day from Planting to Effective Full Cover, traceable to Wright (1982) and the USDA-ARS Kimberly lysimeter systems, plus lentils, mint and grass hay.

Curve no.:	11	12	13	14	15	16
Percent PL-EC or PL-TM (type 1-2-4)	**Snap Beans-dry**	**Snap Beans-fresh**	**Alfalfa 1st cycle**	**Alfalfa Int cycle**	**Alfalfa Last cycle**	**Grass Hay**
0	0.15	0.15	0.25	0.25	0.25	0.20
10	0.16	0.16	0.51	0.33	0.29	0.46
20	0.19	0.19	0.73	0.45	0.38	0.68
30	0.23	0.23	0.84	0.80	0.56	0.79
40	0.38	0.38	0.90	0.93	0.79	0.85
50	0.49	0.49	0.98	0.99	0.91	0.93
60	0.60	0.60	1.00	1.00	0.96	0.95
70	0.74	0.74	1.00	0.99	1.00	0.95
80	0.86	0.86	0.99	0.97	0.99	0.94
90	0.94	0.94	0.97	0.96	0.96	0.92
(Eff. Full Cov.) 100	0.95	0.95	0.96	0.94	0.94	0.91
110	0.95	0.95				0.50
120	0.95	0.95				0.55
130	0.93	0.93				0.70
140	0.90	0.90				0.75
150	0.85	0.85				0.75
160	0.75	0.75				0.75
170	0.64					0.75
180	0.49					0.75
190	0.34					0.70
200	0.19					0.70
210	0.08					0.70
220						0.65
230						0.65
240						0.65
250						0.60
260						0.55
270						0.50
280						0.45
290						0.45
300						0.45
GDD Base, ^{o}C[a]	5	5	0	0	0	0
CGDD $_{\text{Planting to EFC}}$[b]	670	670	—	—	—	1300
CGDD $_{\text{Planting to Terminate}}$[c]	1350	950	850	1050[e]	1050[e]	4000
CGDD $_{\text{Planting to Terminate-alt}}$[d]			700	850[e]	850[e]	

[a]The GDD Base, ^{o}C is base or minimum threshold used when computing the growing degree day.

[b]The CGDD $_{\text{Planting to EFC}}$ is the cumulative growing degree days from planting (or greenup) until effective full cover. Effective full cover is set differently for each crop Wright (1982).

[c]The CGDD $_{\text{Planting to Terminate}}$ is the total cumulative growing degree days from planting (or greenup) until termination (harvest) of the crop. This parameter signals the end of the K_{cb} curve construction.

[d] For alfalfa hay, the 'alt' value of $CGDD_{\text{Planting to Terminate}}$ represents 'dairy hay' crops having relatively frequent cuttings.
[e]The value of 1050 (for 'beef style' alfalfa hay) was reduced to 900 during ET processing by Allen and Robison (2007) in Idaho and to 740 by Huntington and Allen (2010) in Nevada, and the 850 value (for 'dairy style' hay) was set to 650 by Allen and Robison (2007) for Idaho applications and to 880 by Huntington and Allen (2010) in Nevada to better match recent, local observations.

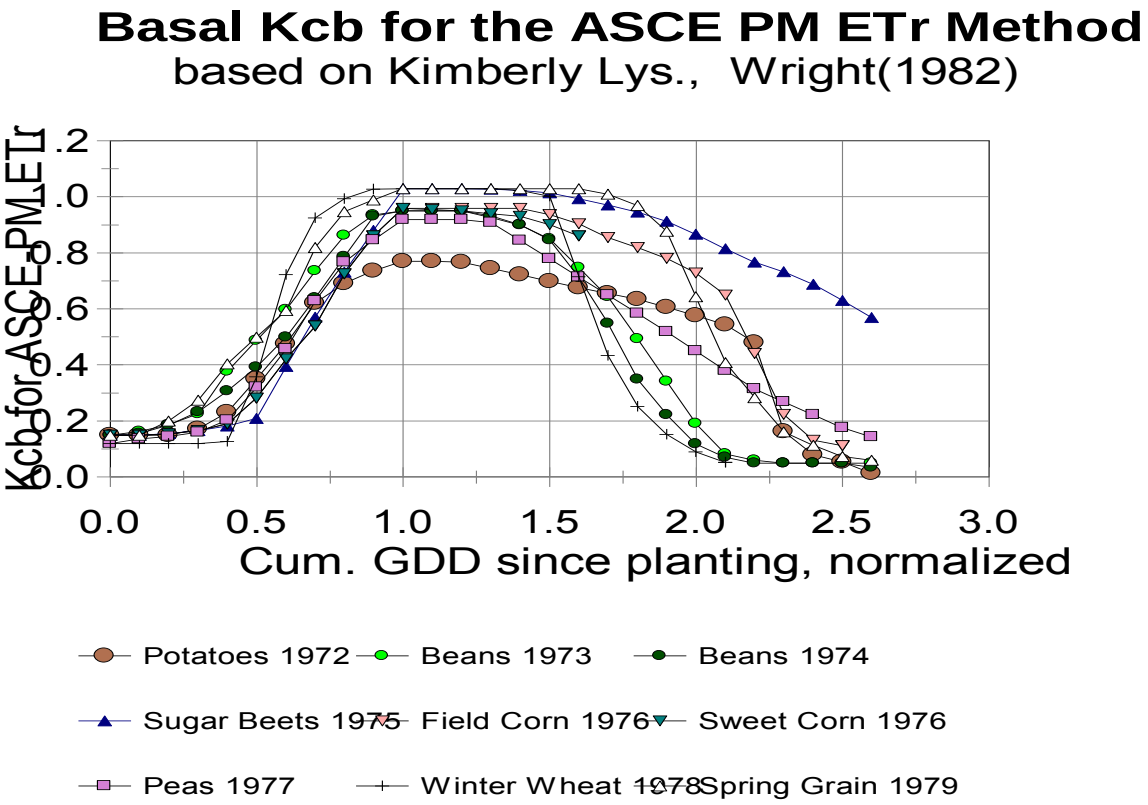

Figure F.1. K_{cb} vs. NCGDD for the crops grown on Kimberly lysimeters (data from Wright 1982 and pers. Commun.)

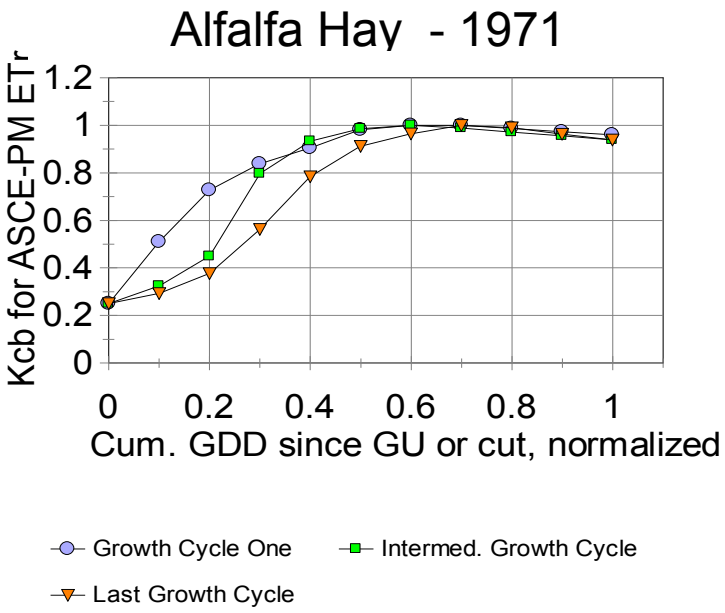

Figure F.2. K_{cb} vs. NCGDD for the Ranger variety alfalfa crop grown on Kimberly lysimeters (data from Wright 1982 and pers. Commun.)

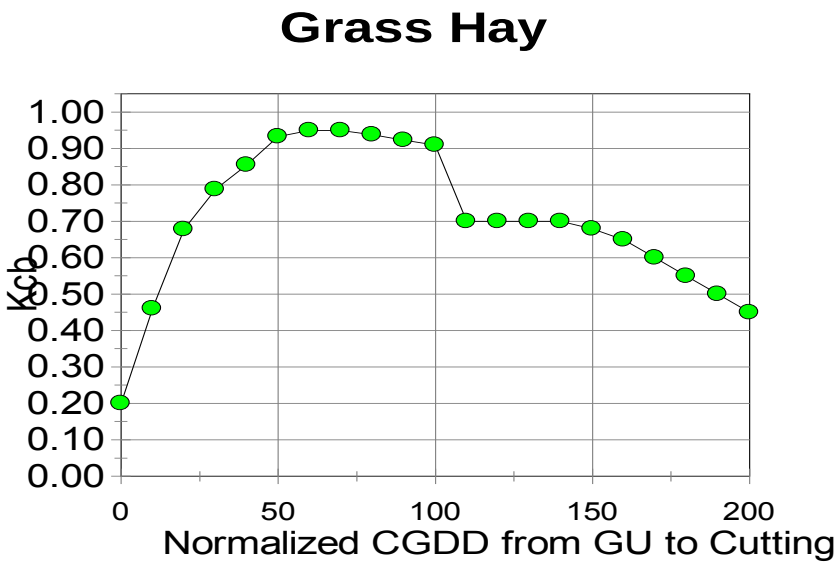

Figure F.3. K_{cb} vs. NCGDD for a grass hay crop grown in high elevation, mid latitude climates having a single mid-summer cutting and limited regrowth following the cutting.

F.5. Estimating Beginning and End of Growing Seasons

Automation of the estimation of planting dates and greenup dates for crops enables the K_c computation process to operate for multiple-year periods without manual intervention or specification of starting and ending dates for K_c curves. This is useful when estimating ET for extended time series such as for producing irrigation water requirement guidelines and in climate change impact studies. The greening (greenup) of perennial vegetation in spring can be strongly conditioned by short-term weather conditions, primarily by air temperature and to some degree by wetting events and general amounts of solar radiation. Strong correlation exists between air temperature, wetness and cloudiness. In general, air temperature can be used as a predictor of when perennial vegetation begins to greenup in spring. Planting of annual crops is strongly influenced by soil temperature at seed depth and relationships have been established for limited crops. However, soil temperature is not commonly measured at cooperative NWS weather stations and is generally available at regional stations only. Therefore, 30-day average mean daily air temperature is often used as a surrogate for soil temperature, based on correlation between soil temperature and air temperature over extended periods.

The use of a thirty-day running average mean air temperature (T_{30}) to estimate planting of annual crops was utilized by Allen and Robison (2007) and Huntington and Allen (2010) for state-wide estimation of ET_c for agricultural crops. Their development was based on lysimeter and cropping records at Kimberly, Idaho. The use of 30-day average temperature follows the SCS TR-21 (1967) where that publication listed typical mean monthly values for air temperature for planting and greenup of crops. However, some of those dates, for example, for alfalfa green up do not estimate well for Idaho (Allen and Robison 2007). In addition, SCS TR-21 T_{30} values are centered on the mid-point of the 30 day period, whereas the more logical method is to associate the T_{30} values with the date at the end of the 30 day period, since the T_{30} temperature during the previous 30 days is the temperature impacting the current soil temperature.

Figure F.4 shows variation in 30-day, 21-day, 15-day, and 10-day running average air temperature for year 1969 at Kimberly. The 30-day running averages are required to produce a generally monotonically increasing average temperature during the first half of the year in a temperate climate such as in southern Idaho. Temperature averages for shorter than 30 day periods that increase during warm periods, but then decrease after that during cold periods can produce unrealistically large swings in planting or greenup estimates. Figure F.5 shows running temperature averages at Kimberly for a long-term period for the same four averaging periods. The T_{30} exhibited better monotonicism than the 21-day average, with shorter periods having more episodic decreases in average temperature.

Table F.2 shows values for T_{30} at Kimberly that are equivalent to the planting dates noted by Wright (1982) for the Kimberly lysimeter crops. The values for T_{30} were selected from the year each crop was planted. These dates were used as a general basis for T_{30} dates used around the state for estimating startups for growing seasons. Some adjustments were made based on field observations by Allen and Robison (2007) across southern Idaho. These temperatures are for dates at the end of the 30 day periods.

In computing T_{30} for various NWS stations, local aridity of the station can elevate air temperature measurements above that expected within an agricultural field. Therefore, the

computed values for T_{30} at NWS stations were adjusted downward in cases where the weather station was considered to be 'arid' using aridity ratings and adjustments used by Allen and Brockway (1983) in a previous consumptive use study for Idaho. These aridity ratings are listed in Table 5.2 of Appendix 5. The amount of maximum adjustment by month is listed in Table 8.2.

During the estimation of planting or greenup dates for crops and natural vegetation, a "no earlier than" and "no later than" date can be used to constrain estimated planting or greenup dates to realistic ranges based on expected behavior of farmers or requirements of the vegetation itself. For many crops this may be +/- 40 days from the mean date based on a longterm average temperature (Allen and Robison 2007).

For alfalfa, better consistency in estimation of greenup in spring was found by Allen and Robison (2007) using cumulative growing degree days (CGDD) since January 1 rather than using T_{30}. This finding was based on observed greenup for lysimeter crops during 1969-1971 and on field observations by Allen and Robison (2007) between 1998 and 2005. CGDD = 240 ^{o}C-days using a 0°C GDD basis was selected by Allen and Robison (2007) to estimate greenup based on a CGDD analysis of daily ET and leaf area and height development data for alfalfa for years 1969-1971 by Wright at Kimberly. No penalty was applied for cold weather during the winter period. CGDD=240 ^{o}C-days estimates an average greenup date of March 30 for alfalfa at Kimberly, Idaho, on average, over the 1969-2005 period, with a standard deviation of 11 days. Huntington ar

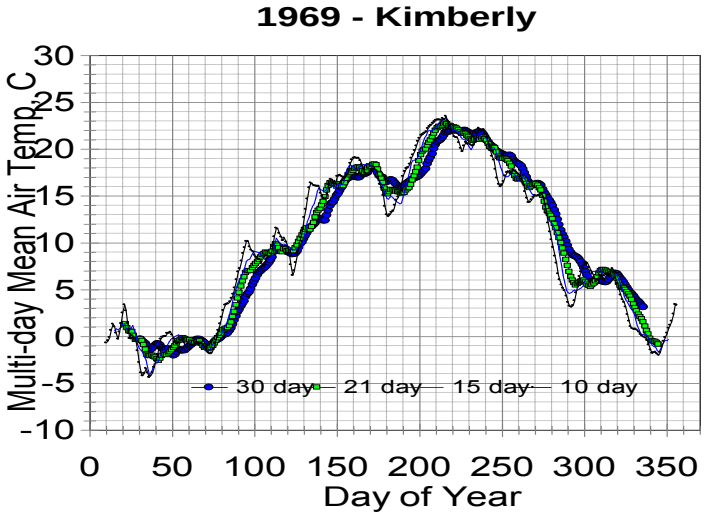

Figure F.4. 30, 21, 15 and 10-day running average air temperature at Kimberly, Idaho during 1969. The values are plotted on the last day within each average. 30-day running averge temperature is plotted as a thick blue line.

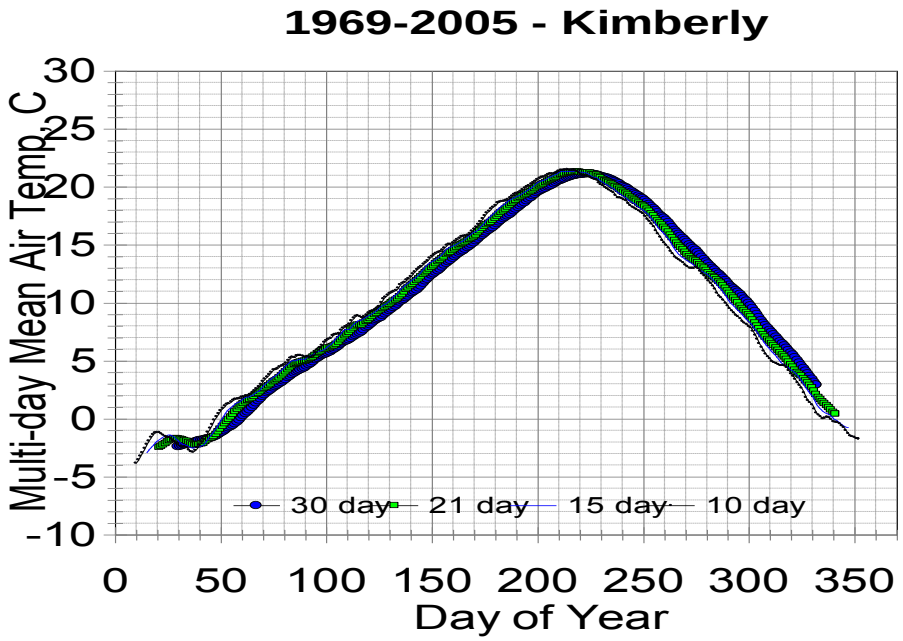

Figure F.5. 30, 21, 15 and 10-day running average air temperature at Kimberly, Idaho averaged over the 1969-2005 period. 30-day running averge temperature is plotted as a thick blue line.

Table F.2. 30-day mean air temperature for 30-day periods prior to the observed planting dates for Kimberly, Idaho crops associated with Wright (1982) dates for lysimeter crops and recommended T_{30} values based on the lysimeter data and field observations by Allen (pers. comm.) between 1999 and 2005.

Crop	Year	Planting Date	30-day T (C) ending on date	Recomm. T_{30} to use, ^oC
Barley or SpringWheat	1979	4/1/79	4.8	4.7
Peas	1977	4/10/77	4.4	5
Sugar Beets	1975	4/15/75	2.1	5 (8)**
Potatoes	1972	4/25/72	6.0	7
Corn	1976	5/5/76	7.9	8 (10)**
Beans	1973 1974	5/22	12.5 12.3	12 (14)**

** The value in parentheses was used in Allen and Robison (2007) calculations based on comparisons with satellite-based K_c determination using the METRIC energy balance model over the Kimberly, Idaho area and based on other local observations of planting dates across southern Idaho.

F.6. Estimation of Killing Frosts

Killing frosts can terminate growing seasons prematurely for crops that grow late into fall or for crops that are sensitive to even light frost. Temperatures for killing frosts can be assigned to crops based on literature and internet searches and personal field observation. The following list of killing frost temperatures was applied by Allen and Robison (2007) for a variety of crops and land-use types in Idaho:

-7 ^{o}C for alfalfa

–4 ^{o}C for field corn and silage corn and -5 ^{o}C for early sweet corn. No early frost death was estimated for late sweet corn, which was assumed to grow during a frost-free period until mechanical harvest as a fresh crop. The -4 and -5°C temperatures are lower than commonly used for some corn varieties, but account for differences between temperatures recorded inside radiation shelters at observation height at weather stations and that at the surface of a fully vegetated field of corn. They also may prevent unreasonably truncated growing seasons and to

-2 ^{o}C for wetland vegetation. Cattails commonly freeze at 0 or -1°C, however -2°C was used to account for differences between weather station

environments and wetland environments that benefit from heat transfer from water surfaces.

-4 °C for sugar beets
-2 °C for potatoes
-2 °C for melons
-3 °C for grapes
-3 °C for asparagus
-5 °C for turf and pasture
-5 °C for leaf fall on fruit trees and poplars,
-4 °C for cottonwoods and -6 °C for willows

F.7. Example of Lengths of Growing Seasons Estimated across Idaho

Figures F.6-F.9 show growing-season lengths averaged over multiple-year periods estimated by Allen and Robison (2007) for 123 weather station locations throughout Idaho. Estimates were based on the T_{30} method for all crops except alfalfa which used CGDD. Mean and mean plus/minus one standard deviation (over the period of record) are plotted vs. the elevation of the location. For alfalfa and field corn, season length has strong negative correlation with elevation due to the impact of elevation on reducing air temperature and crop growth rates. This affects both the start of the growing season and the duration. The growing season increased with elevation for dry beans, due to their relatively late planting date in late May and the longer duration required at higher elevation due to cooler air temperature. Season duration was relatively constant for spring wheat. The figures illustrate the outcome of basing growing season start and growing season duration on air temperature.

Figures F.6 – F.9. Growing season lengths estimated for alfalfa hay, dry beans, field corn and spring grain plotted against location elevation in feet above mean sea level using CGDD for alfalfa and T_{30} for the other crops for 123 locations in Idaho (after Allen and Robison 2007).

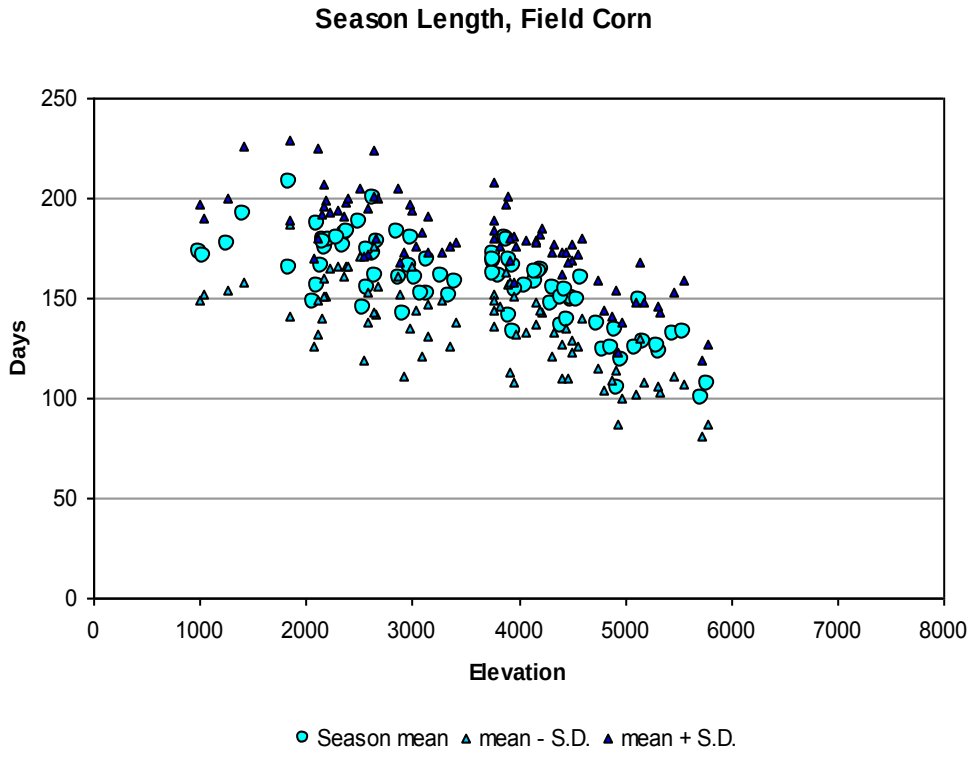
Season Length, Field Corn
250
200
150
100
50
0
Days
0
1000
2000
3000
4000
5000
6000
7000
8000
Elevation
Season mean
mean - S.D.
mean + S.D.

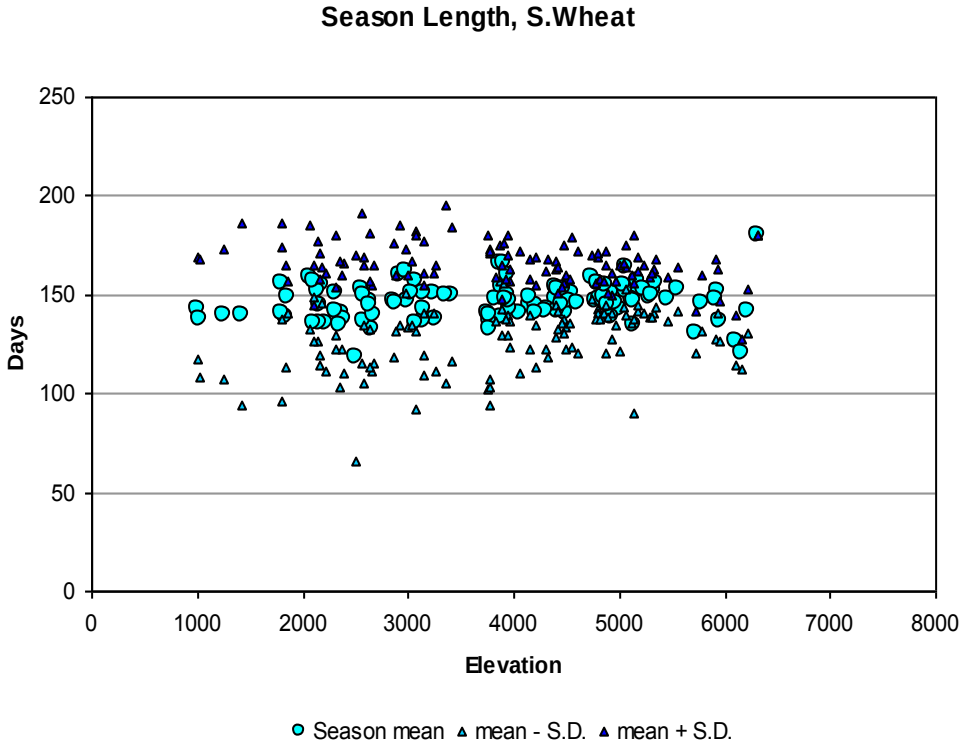
Season Length, S.Wheat
250
200
150
100
50
0
Days
0
1000
2000
3000
4000
5000
6000
7000
8000
Elevation
Season mean
mean - S.D.
mean + S.D.

Figures F.6 – F.9. Growing season lengths estimated for alfalfa hay, dry beans, field corn and spring grain plotted against location elevation in feet above mean sea level using CGDD for alfalfa and T_{30} for the other crops for 123 locations in Idaho (after Allen and Robison 2007).

Page 431 Rick will confirm this variety (Russet) with Jim Wright

Page 436, Fig, F.1 Rick will submit a redraw of this graphic to ASCE.

Page 446, Fig F.6-F.9 Rick will replot these using elevation in meters.

Appendix G

Documentation for Crop Coefficient and ET Data Reporting and Determination of ET from Remote Sensing and Sap Flow Measurement

G.1 Introduction

ET information is frequently used as a foundation for court determinations of injury among water users, for parameterization of important hydrologic and water resources planning and operations models, for operating weather and climate change forecasting models, and for water management and allocation in water-scarce regions, including the partitioning of water resources among states and nations. All too frequently the ET information used in these processes is deficient or uncertain, with too little descriptive information in the reporting to facilitate judgment of its quality.

Over the past decades there have been increasing numbers of publications reporting measured evapotranspiration (ET) and crop coefficients (K_c). Publications include information on cereal crops, fiber crops such as cotton, forage crops like alfalfa, fruit tree crops like olives, apricots, peaches and pecans, grapes, cool and warm season grasses, turf grasses, legume crops like beans, oil crops like sunflower, tropical fruit crops like banana, cassava, and coffee, and various vegetable crops. In addition, there have been coefficients for natural vegetation such as grasslands and wet vegetation such as cattails, grasses and reeds. Some of these publications have described the calibration of models and systems for calculating crop coefficients. Many publications include coefficients for multiple crops as a function of ground cover, for example Grattan et al. (1998), Parkes et al. (2005), Wang et al. (2007) and Allen and Pereira (2009).

The crop coefficient literature will continue to grow. Adherence to physics, careful measurement, quality control of data and reporting of details will be important. In general, future K_c values are not expected to change substantially, because ET relative to reference ET is strongly tied to vegetation amount. However, some variation in new K_c values is expected as a result of changes in crop varieties, agronomic practices, planting densities, and genetic modification to leaf structure to reduce vapor loss and ET.

ET data and ET models or model calibrations reported in the literature for even 'well-behaved' agricultural systems can contain serious biases caused by flaws in experimental design, measurement equipment, vegetation management, data reduction, model parameterization, and interpretation of results. Therefore, it is essential that reporting of ET measurements and related products such as crop coefficients or parameterized models contain sufficient description of the procedures used to measure and derive ET information so that readers can be aware of potential flaws or shortcomings in data measurement and can be alerted to the need to question representativeness of ET presentations.

Because of the wide range of complexities in making ET and associated weather measurements and the abundance of opportunities for biases to enter ET and weather data sets, users of ET literature need sufficient information reported in articles on ET to assess the likelihood for opportunities of bias or error to enter reported data as well as sufficient information to examine or recreate the reported data using some type of ET model. This is currently often not the case, and many journal articles do not contain sufficient information to enable readers to gauge accuracies and representativeness of information.

This appendix discusses upper limits to be expected for crop coefficients that supplements Chapter 10, contains a summary of precautions, recommendations and literature associated with sap flow and remote-sensing based determination of ET and K_c to supplement Chapter 7, and ends with a section listing detailed types of documentation that should accompany publication of ET and K_c data that are useful when applying or interpreting reported values.

G.2 Upper limits on ET and crop coefficients

Chapters 7 and 10 discuss maximum expected limits on ET and crop coefficients. This discussion is expanded here. Evaporation constitutes the conversion of liquid water to vapor and as a result requires substantial amounts of energy. The availability of energy incident to vegetation places a constraint on the potential evaporation rate and forces adherence to the law of conservation of energy. ET rates that exceed available radiation energy (R_n) at the surface less the energy conducted as sensible heat to the ground (G), i.e., R_n - G, must essentially extract that additional energy from the atmosphere via downward (negative) sensible heat flux (H) via convective transfer through the equilibrium boundary layer of air above the surface. Because increasingly negative H creates increasingly stronger density-induced stability to the equilibrium boundary layer, it becomes increasingly more difficult to transport the required H to the surface to support the conversion to ET, especially without strong mechanical mixing brought about by high wind speed (Brutsaert 1982; De Bruin et al. 2005). As a result there is an upper limit on ET, even under extreme advection, caused by limitations on aerodynamic transport and on equilibrium forces above a vegetation canopy. That upper limit on ET is relatively well represented by the tall (alfalfa) reference that has been defined by ASCE-EWRI (2005) using a parameterized Penman-Monteith equation (Allen et al. 1989, 2007c).

The upper limit on potential crop evapotranspiration (ET_c) is readily approximated by comparing against the widely used reference ET (ET_{ref}) through a crop coefficient (K_c). ET_{ref} may refer to two types of reference crops, clipped, cool-season grass or tall alfalfa (whose common symbols are ET_o and ET_r respectively), thus crop coefficients may be expressed in relation to clipped, cool-season grass as more often used (Allen et al. 1998, 2007c) or to alfalfa; for which the symbol K_{cr} is adopted (ASCE-EWRI 2005; Allen et al. 2007c). An alternative and synonymous expression for K_{cr} can be used, which is the term alfalfa reference ET fraction, ET_rF (ASCE-EWRI 2005; Allen et al. 2007a).

The terms K_c and ET_rF are defined as the ratio of ET for a specific surface, ET_c, to the ET of the standard reference surface, ET_{ref} and are discussed in detail in Chapter 10. An expression for K_c in terms of ratios of the Penman-Monteith equation (Monteith 1965) applied to the crop and to the reference crop is given as Eq. 10.1. That equation illustrates that the value for K_c (or ET_rF) depends on the relative roughness, leaf area, and albedo (impacting R_n) of the actual vegetative surface in relation to the same characteristics for the grass or alfalfa reference surface. Clearly, the more similar a vegetative cover is to the reference condition, especially at full cover, the closer the value of K_c (or ET_rF) will be to 1.0 and the less variation in the value of K_c (or ET_rF) with changing weather conditions (see discussions in Pereira et al. 1999 and ASCE-EWRI 2005).

Implicit to Eq. 10.1 is the consideration of impacts that differences between ET_c and ET_{ref} have on conditioning of the equilibrium boundary layer above the surfaces and on conditioning of the surfaces themselves. This conditioning modifies levels of e_z^o , e_z , Δ and wind speed

caused by differences in cooling and humidification brought about by rates of ET_c being different from ET_{ref}. This conditioning generally creates a negative feedback effect on the value for K_c (or ET_rF).

The tall (alfalfa) reference and its parameterizations in the PM equation tend to represent sufficiently low surface resistance and sufficiently high aerodynamic roughness to approximate near maximum rates of ET expected from large expanses of well-watered vegetation cover, even under conditions of strong regional advection (Allen et al. 1989; Pereira et al. 1999). Therefore, alfalfa reference-based crop coefficients tend toward a maximum of 1.0, and an expanse of tall, well-watered vegetation that fully covers the ground will approach the maximum conversion of available energy into latent heat flux (λE), and the maximum ratio of λE for any tall vegetation to alfalfa λE will be near 1.0. This observation is born out in viewing the maximum values for K_c reported by Wright (1982) for nine annual crops in southern Idaho, where none of Wright's K_c 's, when based on the standardized alfalfa reference (Allen and Wright 2006), exceeded 1.03. In the case of grass reference ET_o, values for K_c may approach 1.3 for tall, dense crops under windy arid and semiarid conditions because of the smoother roughness and small leaf area index of the grass reference as compared to the alfalfa reference.

In humid climates, ET is dominated more by net radiation availability and less by aerodynamics and vapor deficit. Because the grass and alfalfa reference crops have about the same albedo as many crops at full cover, their energy, heat and vapor transfer rates and thus ET and K_c rates are more similar in humid and semi-humid climates than under arid conditions. Based on total energy constraints, under humid conditions, where a majority of energy for the ET process is from net radiation and regional advection is relatively minor, the K_c generally can not exceed about 1.0 to 1.05 relative to the alfalfa reference for large expanses of similar vegetation and about 1.2 to 1.3 relative to the grass reference. In arid and semiarid climates, the constraint of $K_c \sim 1.0$ to 1.1 for the alfalfa reference holds because of the tendency toward similarity in aerodynamic exchange and leaf area between even tall vegetation and the alfalfa reference. In the case of the grass reference, however, differences in aerodynamic and surface conductances, coupled with potentially strong regional advection, may cause K_c based on the grass reference in arid and semi-arid climates to be as high as 1.2 to exceptionally high values of 1.4 for tall, well watered vegetation.

H.L. Penman's comment (Penman 1948) that crop evaporation should never exceed evaporation from an open water surface may be somewhat extreme; however the exceedance of measured or reported K_c above about 1.0 for alfalfa reference or 1.2 for grass reference in subhumid regions or above about 1.0 for alfalfa reference or about 1.2 to 1.4 for grass reference in arid regions should give cause for intense scrutiny of the ET measurements, the weather data used to calculate ET_{ref}, and the data processing procedure. Exceeding those values should also give cause for rejecting the data.

Limiting K_c to approximately 1.0 for an alfalfa reference-base or 1.2 for a grass reference-base in humid climates and to approximately 1.0 for an alfalfa reference-base or 1.2 to 1.4 for a grass reference-base in arid climates applies to large expanses of vegetation (> 200 m diameter) and is significant and important when evaluating field measurements of ET. Measuring ET from small expanses of vegetation should be avoided when the objective of the ET measurement is to represent general conditions of crop ET for medium to large (say > 200 m) fields or clusters of small fields. When ET is measured from small expanses of vegetation, the internal boundary layer above the vegetation may not be in equilibrium with the surface and may not have developed up to the height of any meteorological or flux instrumentation. In addition, small

expanses of tall vegetation surrounded by shorter cover cause a "clothesline effect" where the interchange between air and vegetation is much more efficient than with the logarithmic type of boundary layer established over large fields and that is assumed in essentially all aerodynamically based ET equations. In these cases, ET from the isolated stands, on a per unit area basis, may be significantly greater than the corresponding ET_{ref} computation and will not represent large expanses. These situations are discussed in more detail in Chapter 10.
When calculating reference ET, the global standardizations of ASCE and FAO are highly recommended for consistency and transferability of results and derived coefficients (Allen et al. 1998, 2006; ASCE-EWRI 2005).

G.3 More on ET measurement

In many agricultural systems, plant density, height, vigor and water availability are generally uniform, and the application of estimation algorithms and the measurement of ET can be relatively straightforward, although they are still not without substantial challenge. In the case of nonagricultural systems such as forest, desert and riparian systems, the heterogeneous nature of vegetation, terrain, soils and water availability make surface energy and aerodynamic processes highly variable and poorly defined. This is especially true, for example, for riparian systems such as cottonwood, tamarisk and Russian olive in semiarid regions that can have widely varying vegetation density, tree height, stand extent and availability of water. Most information and estimates of water consumption by forest and riparian systems come from in-place measurements that have a strong empirical and local character.

Chapter 7 includes describes requirements and considerations for technique, equipment, and data handling when determining ET or K_c from soil water balance, lysimeters, Bowen ratio, and eddy covariance methods. Besides those four common and important methods, other means to estimate Kc include use of sap flow methods and remote sensing. The following sections briefly describe the merits and challenges of those additional methods and complement the information in Chapter 7 and 10. Additional general information on sap flow systems and expected error is given in Shackel et al. (1992), Ewers and Oren (2000), Nadezhdina et al. (2002), Green et al. (2003), Steppe et al. (2010) and Allen et al. (2011a).

Sap flow methods

Sap flow methods generally introduce a source of low grade heat into the trunk or branch of a plant and measure the flow of water in the xylem by either the velocity of a heat pulse carried away from the heat source in the transpiration stream or by the dissipation of heat energy in the stem due to convection in the transpiration stream. These methods do not measure the direct evaporation component of ET, but only the plant transpiration component. This can be an advantage if the goal is to measure plant water use, but a disadvantage if the goal is to project total evaporation over a heterogeneous surface. Three main methods are employed: the heat pulse-sap velocity method (Green and Clothier 1988; Green et al. 2003); the Granier heat dissipation method (Granier 1985, 1987); and the tissue-heat balance method (Sakuratani 1981; Valancogne and Nasr 1989, 1993; Kjelgaard et al. 1997). Swanson (1994) suggested that no one set of theory and instrumentation is applicable to all sizes or species of trees. As outlined below, each method has important limitations that need to be considered when interpreting ET rates based on sap flow methods.

Sap flow methods may require scaling from branches or whole plants to stands of plants to provide wide area estimates of ET. Granier sensor studies typically use a stem census method for scaling, in which the cross sectional area of gauged trunks are related to the density and cross sectional area of trees in the area of interest (Hultine et al. 2010). Stem census methods can be difficult to apply to natural stands of plants, especially when the plants present a myriad of branches of different sizes (Hultine et al. 2010), as in the case of riparian systems such as tamarisk and deciduous forests. Tissue-heat-balance methods require a further scaling step, to scale from branches to whole plants and then to stands of plants. Leaves or leaf areas on gauged branches can be harvested and measured, and scaling can then be accomplished by measuring LAI in plant stands of interest (e.g., Nagler et al. 2009). However, optical methods for estimating LAI must be calibrated by leaf-harvesting, because many plant stands violate the geometric assumptions built into the optical measurement devices. For example, the commonly-used Licor LAI 2000 measurements are based on the amount of light transmitted through the canopy at five different angles as measured by a fish-eye type lens system. Assuming a uniform overhead canopy in thickness and leaf density, LAI can be calculated from Beers Law, by calculating a relative path length of light through the canopy at each view angle and combining the estimates to get a single estimate of LAI. Multiple view angles are needed to account for leaf and branch angle effects on LAI. Unfortunately, individual tree canopies, or irregular canopies with gaps between plants, seriously violate the assumption of a uniform canopy and there is no simple way to correct the instrument readings except by combining them with leaf harvest methods, a step which is often omitted. Nagler et al. (2004) found that Licor LAI 2000 measurements of LAI on individual cottonwood and willow canopies were low by a factor of three when compared to leaf harvesting methods.

Scaling ET from individual limbs to full plants and from full plants to large areas is uncertain due to differences among tree structure, radiation interception per tree, and water availability. Shaded limbs tend to have lower rates of transpiration than sunlit limbs, and limbs lower in a canopy tend to have less aerodynamic exchange of energy and vapor. Besides scaling of transpiration from specific species of trees, additional uncertainty in areal ET is caused by stands of multiple species, presence of understory vegetation, and evaporation from bare soil. Mackay et al. (2002) used a two-source evaporation model with sap flow data to produce total ET. Users should consider that large uncertainties can exist when determining transpiration using sap flow methods and determining accurate, quantitative ET estimates.

Remote sensing energy balance to determine crop coefficients

New techniques using satellite imagery have been developed since about 1990 to estimate E and ET from large areas using energy balance (Bastiaanssen et al. 1998a, b, 2005; Kustas and Norman 1999; Moran 2000; Kustas et al. 2003; Allen et al. 2007a, b; Irmak et al. 2011). The emerging technology of energy balance by satellite shows promise for application over large areas and over a wide range of vegetation types and water availability. The approach has been used to quantify and illustrate population variance in ET from the same vegetation type and to refine K_C or ET_rF curves (Tasumi et al. 2005a; Anderson et al. 1997, 2005; Kustas et al., 2003; Kustas and Norman 1999; Li et al. 2005; Norman et al. 1995, 2000, 2003; Allen et al. 2007a, b; Tasumi and Allen 2007; Singh and Irmak 2009). Remotely sensed energy balance techniques are useful for identifying areas experiencing water stress and corresponding reductions in ET and to populate hydrologic models (Irmak and Kamble 2009; Kamble and Irmak 2009). Users of this

information must bear in mind, however, that satellite-based ET data are simply retrievals and rely on best estimates of aerodynamic and radiative processes as viewed from space, and can not be considered to be "measurements." Estimation by remotely sensed energy balance should be expected to adhere to the same limitations and physics as other measurement methods. Nevertheless, remotely sensed energy balance is increasing in use to estimate K_c and ET over large areas.

Some 'operational' satellite-based energy balance models such as SEBAL (Bastiaanssen et al. 1998a, b, 2005) and METRIC (Allen et al. 2007a, b; Kilic et al. 2011) employ an internal calibration technique referred to as CIMEC ('calibration using inverse modeling at extreme conditions') (Allen et al. 2008). The CIMEC technique involves the inverse calibration of the energy balance process via the sensible heat flux, *H*, computed by specifying ET, and thus the energy balance equation, at two extreme conditions (dry and wet) in the satellite image. ET is estimated at the two conditions based on knowledge of available energy and surface conditions, usually with ties to ground-based weather data. The outcome of the CIMEC calibration is to imbed all systematic estimation biases in R_n, *G* and other intermediate components that are endemic to nearly all satellite-based calculations into the estimate and calibration of *H*. These biases are in turn removed when ET is computed for the millions of pixels in a typical image as $ET = \lambda E/(\lambda \rho_w) = (R_n - G - H)/(\lambda \rho_w)$, where the calculation of *H* is a function of surface temperature. Other more regional-scale models such as the ALEXI model (Anderson et al. 2005) use inversion based on radiosonde profilings over time to estimate large scale heat flux and evaporation. Ordinarily, surface energy balance models that do not apply endpoint calibration will be impacted by the various biases that can plague satellite-based component estimation.

Advantages of remote sensing-based energy balance (RSEB) models for determining Kc and ET:

- the energy balance yields actual ET that may be lower than potential ET due to water and other stresses;
- the process covers large areas, enabling sampling and integration over diverse areas;
- RSEB procedures are generally more economic than point measurements;
- RSEB procedures can be used to extend or extrapolate high intensity point measurements of ET to large areas;
- products can have high spatial resolution (30 m for satellite, 2 to 5 m for aerial);
- RSEB procedures are valuable for determining spatial variation in ET for highly variable systems such as riparian or forest.

Disadvantages of remote sensing-based energy balance models:

- time gaps exist between estimates of ET for many satellite systems, especially those having high spatial resolution, where images are obtained only periodically for a specific location, for example, every 16 days for a Landsat satellite; therefore, effects of evaporation from precipitation events occurring in between satellite overpasses may be missed, or processing of 'wet' images from recent precipitation events may bias seasonal estimates (Allen et al. 2007a);
- data collection using aerial platforms including unmanned aerial vehicles can be expensive;
- satellite pixels over narrow vegetation systems such as riparian systems and small agricultural fields may overlay broad mixtures of vegetation types and densities so that surface temperature signals are mixed and the ET retrievals are difficult to interpret;

- uncertainty in estimating aerodynamic components and surface temperature retrievals may require 'inversion' techniques to calibrate;
- most remote-sensing energy balance processes assume 1-D aerodynamics:
    - this may not hold true for narrow, tall systems such as riparian:
        - aerodynamic exchanges in narrow vegetation systems may be three-dimensional and therefore flowlines are poorly behaved;
        - Klaassen et al. (2002) found that horizontal penetration of flowlines and heat transfer into the leading edge of a forest canopy increased available energy by 15% over the first 400 m of canopy;
        - Klaassen and Sogachev (2006) concluded that flux measurements over riparian systems should be corrected for impacts of horizontal variations in turbulence downwind of the edge;
        - The problem of narrowness of stands and edge effects impacts nearly all measurement systems that use aerodynamics or energy balance (EC, scintillometry, remote sensing based EB), even sap flow due to change in transpiration with distance into the system;
- satellite view angles can impact reflectance (albedo) and surface temperature estimates:
    - the Landsat satellites have a view angle that is nearly nadir (directly overhead);
    - the MODIS satellites have a large scan angle, with the view angle varying from -55 to +55 degrees; this viewing angle variation impacts reflectance measurements and requires correction;
    - the satellite (and aerial) measurement of reflectance is 'bidirectional' whereas - the reflectance needed in energy balance (for R_n) is directional-hemispherical;
    - bidirectional reflectance may be lower than directional-hemispherical reflectance for tall canopies containing shadows, especially at lower sun angles and for nadir looking satellites;
    - potential bias in nadir-derived albedo and surface temperature for tall canopies may cause overstatement of ET by 5 to 10% (this impact needs further investigation);
- potential biases exist in retrieved albedo and surface temperature (T_S) from satellite and airborne systems, making CIMEC or other bias-correcting calibration methods necessary.

Satellite-based ET using vegetation indices

Satellite-based or ground-based energy balance methods generally require extensive time investment and require learned skill sets. The energy balance products can be used, however, to calibrate more simple methods that utilize general vegetation indices (VI) to estimate crop coefficients (i.e, K_c or ET_rF) (Tasumi et al. 2005a; Tasumi and Allen 2007; Singh and Irmak 2009). The estimate of K_c from VI is possible because of the generally close correspondence between vegetation amount and transpiration, where, as vegetation cover increases, leaf area increases, and transpiration increases (reviewed in Glenn et al. 2007). Challenges with VI based methods are estimating evaporation from bare soil following precipitation events and estimating reduced ET associated with soil-water shortage, because these processes are not adequately reflected in the VI.

A common VI is the Normalized Difference Vegetation Index (NDVI) that is estimated from two shortwave bands typically measured by satellites: the red band (~0.6–0.7 μm) and the near infrared band (~0.7–1.3 μm). A linear relationship between the NDVI and the crop coefficient K_C was introduced by Heilman et al. (1982) and theoretically established by Choudhury (1994). The resulting equation is:

$$K_{co} = 1.25\, NDVI + 0.2 \quad \text{(G.1)}$$

where K_{co} represents the grass based crop coefficient. Tasumi et al. (2005b) and Tasumi and Allen (2007) found a similar relationship for eight major irrigated crops in Idaho, as did Singh and Irmak (2009) for irrigated corn and soybeans in Nebraska, which, when expressed for the alfalfa reference is approximately:

$$K_{cr} = ET_r F = 1.25\, NDVI \quad \text{(G.2)}$$

Generally, NDVI values from different satellites show close correlation (Calera-Belmonte et al., 2005). However, some differences occur due to differences in band widths. The degree and type of atmospheric correction of the image can also have an impact.

It is important to establish, with K_c vs. NDVI or other VI relationships, whether the relationships are to represent the average ET that includes averaged amounts of evaporation from the soil surface caused by precipitation and irrigation or are to represent a 'basal' K_{cb} condition where the VI-based relationship is established to represent conditions where the soil surface is dry enough to reduce evaporation from the soil surface to relatively low levels, when compared to transpiration, but transpiration still occurs (Allen et al. 2005a). The basal K_{cb} *vs*. NDVI relationship is more consistent because transpiration has a much closer association with vegetation amount than does evaporation from soil. When K_{cb} vs. NDVI relationship is used, then estimates for soil evaporation are determined separately and added to produce total evaporation (Burnett et al. 2008). Allen et al. (2011b) showed that NDVI was a better basis for the K_c vs. VI relationship than was the Soil Adjusted Vegetation Index (SAVI) because NDVI tends to reach a maximum value (e.g. 'saturate') at about the same time as does K_c, which is at about LAI of 3.0, whereas SAVI tends to continue to increase with increasing LAI beyond 3.0

Advantages of VI-based crop coefficient (K_c and K_{cb}) estimation are:

- quick analyses can be made by mid-level technicians;
- large areas can be covered;
- relationships can be calibrated using satellite-based energy balance;
- spatial resolution can be high, especially if aerial imagery is used.

Disadvantages of VI-based K_c and K_{cb} estimation are:

- relationships may vary with type of vegetation;
    - stomatal control, and thus K_c or K_{cb} vs. VI relationships, can vary among types of vegetation. Therefore, single K_c and K_{cb} vs. VI or ET vs. greenness indices can vary;
    - trees, when short of water can exhibit more stomatal control than agricultural crops and therefore cause a shift in the K_c vs VI relationship;
- relationships tend to overestimate ET during conditions of acute water shortage because of time lag in adjustment in vegetation amount (NDVI) following reduced stomatal conductance and water use.
- estimation of the evaporation (from soil) component is less certain than the transpiration component because of the lack of a direct relationship with vegetation amount;

- quality estimates of reference ET are required to transform K_c into ET where the reference ET calculation requires quality weather data;
- VI's may not identify or quantify multi-storied canopies and their effects on total ET, especially for more dense vegetation.

Nagler et al. (2009) found a reasonable correspondence between saltcedar ET estimated by sap flow sensors and satellite estimates based on a VI at the Cibola National Wildlife Refuge on the lower Colorado River. However, at any given measurement station, ground measurements showed high variability of ET due in part to differences in stomatal conductance due to stress effects, which were not captured in the remote sensing estimates.

G.4 Crop Coefficient and ET Data Reporting

ET information available in the literature is often deficient in regard to documentation necessary to judge its quality and representativeness. Allen et al. (2011b) described desired documentation of published evapotranspiration (ET) information, including description of field procedures, instrumentation, data filtering, model parameterization, and site review. This information is important to readers to assist with discerning the accuracy and representativeness of reported data and ET parameters, including derived crop coefficients. Documentation should include a description of the vegetation, its aerodynamic fetch, water management and background soil moisture, types of equipment and calibration checks, photographs of the measured vegetation / equipment combinations, and independent assessments of measured ET using models or other means. Documentation and assessment should include a description of, or reference to, all weather recording equipment and parameters, including the vegetation and water management environment of the weather station. Suggestions are given for documentation describing the primary types of ET measuring systems including recommended independent testing.

In addition to documentation on ET measurements and associated weather data that may be used in models, documentation should describe the nature of the vegetation measured, including type, variety, density, age, health, water availability, timing of development and senescence, height, fraction of ground cover or leaf area index, type of irrigation, if practiced, and other features useful to users of the data or users of derived crop coefficients and other ET parameters. Sufficient description of canopy architecture is needed to assist modelers in setting model parameters and, more simply, to compare against findings from similar studies. In the case of crop coefficients, the documentation should describe whether the reported crop coefficient(s) represent potential (i. e., well-watered and nonstressed) conditions and whether they are intended to represent the basal (ET from vegetation having a mostly dry soil surface condition) or an average crop coefficient condition (Allen et al. 1998, 2005, 2007).

Authors of ET data and model results are encouraged to apply careful study and critique of the measurement method and application procedures prior to publication, and to compare ET data or derived Kc's against ET estimates derived from more-or-less standard models and/or prior published Kc's. Dependable models, when parameterized based on description of the vegetation, weather and soil and water conditions, can be expected to reproduce general magnitudes of calibrated data within some error tolerance, for example, ± 20%, and preferably even closer, on average. The model estimates should include estimation of both soil evaporation and vegetation transpiration and should consider all weather parameters impacting evaporation (air temperature, humidity, solar radiation and wind speed).

Recommended documentation

Tables G.1 and G.2 list descriptive items that are recommended when reporting studies and measurements of ET. These items provide reviewers and users of data means by which to scrutinize integrity of data as well as with means to place reported results in their environmental and physiological contexts. The lists illustrate the types of information that can be asked by potential users of the data prior to the data usage.

Table G.1 lists general documentation and information that is useful to accompany ET data sets or the findings that are based on a data set. Table G.2 describes additional documentation or tests that are useful to accompany data collected from eddy covariance, Bowen ratio, lysimeter, soil water differencing and sap flow systems to improve descriptions of the implementation of these systems and the handling of data. Those systems are described Chapter 7 and in this appendix. The left hand columns of Tables 1 and 2 list what considered to be essential information to supply and the right hand columns list desirable, but less essential, information that can assist in data assessment for integrity, bias, accuracy and representativeness.

In many cases, prior publications containing descriptive information can be cited, especially when measurement procedures are relatively standard. In the case of lysimeters, for example, the lysimeter system installation may have been previously described and can be cited. Cited material should be readily assessable to the public via journals or maintained web pages. Journals that publish articles that report findings or models based on ET data should encourage this type of information in submitted and accepted manuscripts.

TABLE G.1. Recommendations on Essential and Desired Information Reporting with Measured Evapotranspiration and Water Consumption Data, Crop Coefficients or Resistance-based ET methods (Data from Allen et al. 2011b).

Essential	Desired

All Systems
Vegetation:
• Vegetation variety(s)
• Dates of crop stages or phenological stages
  • planting or green-up
  • full cover or effective cover or maximum cover
  • flowering
  • start of senescence
  • harvest, or maturation or end of season
• Plant density
• Plant spacing along row (if agricultural)
• Spacing between plant rows
• Measured or estimated vegetation height vs. time
• Measured or estimated fraction of ground cover vs. time
• Size of field (or stand of trees) containing the measurement system
• Location of measurement system relative to the field, system or expanse of vegetation measured
• Size of general agricultural area (or other vegetation system) surrounding the measurement field
• Mulch type, density and coverage (if present)
 	
If an orchard, tree crop or forest, additional information includes:
• Age of trees
• Size of trees, height and crown diameter
• Tree spacing along row and between rows
• Ground covered by mulch:
  • type of mulch,
  • density
  • coverage,
• Ground covered by active substory vegetation
  • understory vegetation height
  • density
  • tillage and ground cover management
  • soil moisture management
	• Leaf area index (LAI) vs. time and measurement method
	• Crop yield
	• Photographs of crop and of the ET measurement system (photographs can be placed with metadata)
	• Relative adequacy of soil water in fields (or vegetation systems) surrounding the field (or vegetation system) being measured
	• Error analysis for the measurement system
	• Fitting of measured ET data to a Penman-Monteith-type equation and indication of required surface resistances for the fitting (including statistics)
	• Any calibration of a model to the ET data with reporting of:
	  • statistical evaluation of model fit
	  • model calibration methods
	  • method to estimate roughness height and values in model
	  • method to estimate evaporation from soil
	
	If a tree crop or forest, additional information:
	• Photos of :
	  • individual trees
	  • community of trees (can be placed with metadata)
	• Pruning
	• Description of uniformity of trees
	• Dates for treatments that may change ground cover by the trees
	  • leaf out
	  • leaf fall

Supporting Meteorological Data: • Reference ET method, if used, and procedures for calculation (can be a citation of published work) • Description of supporting meteorological data for calculating ET, including solar radiation, net radiation, soil heat flux, air temperature, surface temperature, soil temperature, vapor pressure, wind speed • Summary of primary weather data relative to the experimental period • Location(s) of meteorological system/sensors • Size of weather station area and vegetation type and maintenance of station • Soil moisture management of the weather station • Degree and type of QA/QC applied, including calibration adjustment and procedures for filling missing data.	• Description of other weather or micrometeorological equipment • Description of local climate for a period of several years • Description of weather data source (and url if from or on a public web site)

Soil and Irrigation Description
• Soil type and layering or NRCS soil taxonomy (USDA 1999)
• Irrigation type (method and system)
• Irrigation frequency and duration
• Irrigation application depth per irrigation and total
• Irrigation treatments (if applied) with description of
  • non-stressed treatments
  • stressed treatments in relation to non-stressed
  • relative adequacy of soil water in stressed or non-stressed treatments
• Whether incidental water stress occurred
• Method for measuring irrigation input (depth)
• Fraction of surface wetted by irrigation
• Description of treatment of rain events (measurement of rain, inclusion of the rainy day)
• Method for soil water measurement
• Drainage management
• Tillage system type
• Salinity levels and management (if impacting ET)
	• Soil information (by layer)
	  • textural characteristics
	  • Field capacity and wilting point
	  • Soil bulk density
	  • Soil permeability (or NRCS soil taxonomy (USDA 1999))
	• Irrigation
	  • equipment
	  • factors affecting performance
	  • application uniformity
	  • system for delivery of water to the fields
	• Fertility
	  • what fertilizers were applied
	  • rates and timing of applications
	  • how fertilizer rates were determined
	• Any pesticides or growth regulation chemicals (dates of application, application method, rate of active ingredient)

Crop Coefficient Information
• If K_c is reported, provide basal and/or averaged K_c's based on the standardized reference ET
• If K_c is reported, indicate whether it should represent well-watered conditions,
• Refer to reported K_c as $K_{c\ adj}$ when some type of environmental stress had reduced the reported value
• Comparison of derived K_c to literature values with comments on:
  • if grass-reference based, the agreement or lack of agreement for K_c for full cover conditions to the expected range of 1.1 - 1.3
  • if alfalfa-reference based, the agreement or lack of agreement for K_c for nearly full cover conditions to the expected range of 0.95 - 1.0
  • specific explanations of values exceeding the above ranges, especially if K_c values are to represent agricultural field settings
• If grass-reference based, co-reporting of midseason K_c values based on the standard FAO climate of RH_{min} = 45% and wind speed at 2 m height = 2 m s^{-1}. (see Allen et al., 1998, eq. 62, Allen et al., 2005a, eq. 5 or Allen et al., 2007c, eq. 8.59)
  • Average daily minimum relative humidity and average wind speed during the four growth stages
	• Provide basal and/or averaged K_c's based on a second reference (optional)
	• Type of filtering or moving average used on the ET and/or K_c data
	•

TABLE G.2. Recommended Essential and Desired Descriptive Information for ET Measurement systems Eddy Covariance, Bowen Ratio, Lysimeters, Soil Water Differencing and Sap Flow (Data from Allen et al. 2011b).

Essential	Desired

Eddy Covariance
• Measurement frequency
• Averaging period
• Height of sonic anemometer and hygrometer relative to a) ground, b) mean vegetation height, c) maximum vegetation height or limb height
• Anemometer and Hygrometer instrument separation distances and orientation. A photo is desireable.
• Types of corrections to the flux measurements and specific software used for corrections
• Type of coordinate rotation employed
• Fetch length in predominate wind directions and direction thresholds for data filtering
• Description of measurement of R_n and G for energy balance (EB) closure assessment
• Description of a) closure error amount and b) method of closure
• Brands and maintenance procedures for R_n and G sensors, sonic anemometer, and hygrometer, including purchase and last rebuild dates
• Description on numbers of and placement of R_n and G sensors relative to vegetation and individual plants
• Height of R_n sensor to a) ground, b) mean vegetation height, c) maximum vegetation height (or limb)
• For G, method for measuring soil water content and soil temperature
• For vegetation, a description of:
  • distribution of height
  • fraction of ground cover by vegetation
  • LAI (measured or estimated)
• Description of vegetation type, extent and soil water status upwind of the vegetation being monitored.
	• Description of multiple R_n and G sensors, especially when the fraction of ground cover is < 0.8 or when mean vegetation height is > 2 m.
	• Footprint analysis
	• Indication of adequacy of soil water supply to support transpiration
	• Description of soil water content monitoring in the vegetation root zone
	• Soil type, field capacity, wilting point (and how these values were determined)
	• Estimated rooting depth
	• Summary of QC analysis on R_n measurements using measured R_S and estimated or measured albedo and net long-wave radiation (if there is no R_S measured, use calculated R_{SO} for comparing on clear days)
	• Collocation with a Bowen Ratio system to confirm values for ratios of H/LE and to provide independent 'looks' at LE from EC and BR methods as well as aerodynamic estimates of H and LE based on $T_1 - T_2$ and $e_1 - e_2$.
	• Ages of all sensors and loggers and information on annual maintenance and storage
	• Datalogger type and model

Bowen Ratio	

• Brands and maintenance procedures for vapor and temperature sensors, R_n and G sensors, including purchase and last rebuild dates
• Procedures to determine the instrument psychrometric constant
• Description on numbers of and placement of R_n and G sensors relative to plants
• For G, method for measuring soil water content and soil temperature
• Separation of the T and e sensors and placement relative to a) ground and b) vegetation
• Timing of exchange of sensors, if applicable
• If sensors are not exchanged, indication of system for bias reduction between T and e measurements at the two elevations
• Values of typical dT and de measured
• For vegetation, a description of:
  • distribution of height
  • fraction of ground cover by vegetation
  • LAI (measured or estimated)
• Fetch length in predominate wind directions and direction thresholds
• Description of vegetation type, extent and soil water status upwind of the vegetation being monitored.
	• Description of multiple R_n and G sensors, especially when the fraction of ground cover is < 0.8 or when mean vegetation height is > 2 m.
	• Footprint analysis
	• Indication of adequacy of soil water supply to support transpiration
	• Description of soil water content monitoring in the vegetation root zone
	• Soil type, field capacity, wilting point (and how these values were determined) or NRCS taxonomy (USDA 1999)
	• Estimated rooting depth
	• Summary of QC analysis on R_n measurements using measured R_S and estimated or measured albedo and net long-wave radiation (if there is no R_S measured, use calculated R_{SO} for comparison on clear sky days)
	• Collocation with an eddy covariance system to confirm values for ratios of H/LE and to provide independent 'looks' at LE from EC and BR methods as well as to provide wind speed or friction velocity, u*, estimates for aerodynamic estimation of H and LE based on $T_1 - T_2$ and $e_1 - e_2$.
	• Datalogger type and model

Lysimeter[1]
• Dimensions (width, length and depth):
  • a. inner tank
  • b. outer tank
• Tank material and thickness
• Insulation of inner tank walls
• Gap between inner and outer tank
• Photos of lysimeter without vegetation
• Photos of lysimeter with vegetation including immediate area outside lysimeter
• Crop yields for the lysimeter and from the field
• Photo of landscape surrounding the lysimeter
	• Report on two or more lysimeters with the same vegetation and water treatments with error analysis between/among them
	• Salinity measurements of lysimeter drainage water
	• Confirmation of adequacy of soil water supply to support transpiration
	• Soil water content monitoring in the vegetation root zone
	• Soil type, field capacity, wilting point (and how these values were determined)

[1] Some of the details listed for lysimeter specifications can be referenced to previously published information on the specific lysimeter installation, provided the reference material is accessible via the internet or journal articles.

• How the representative effective areas of the lysimeter are calculated for evaporation and transpiration determination
• Scale type and specifications
• No. scans of load cell(s) per reporting period
• Calibration checks and estimated precision and accuracy
• Method of lysimeter soil construction (monolithic vs. reconstructed)
• Comments and notes on any differences between lysimeter vegetation and that of surrounding field or expanse including relative vegetation amount, fraction of ground cover, height, LAI, soil water availability
  • plant density of field or expanse and that inside lysimeter
  • fraction of soil visible inside and outside lysimeter
  • plant height inside and outside lysimeter
• Drainage process for lysimeter
• Soil layering inside and outside of the lysimeter
• If lysimeter area is not an integer multiplier of average area per plant, including space between plant rows (if applicable), describe how evaporation from nonsampled areas is estimated
• Description of supporting vegetation data including height (vs. time), LAI
	• Estimated rooting depth

Soil Water Differencing • Soil water holding properties by layer to depths greater than the rooting depth • Description of equipment • Maximum depth of measurement • No. of locations measured • Locations of measurement sites • No. of depths observed and respective intervals • Time intervals for measurements • Comments on monitoring locations vs. areas wetted by irrigation, shadows cast by trees, etc. • Special treatment of surface layer • Estimation procedure for drainage and upward flow, including evidence that fluxes were small or negligible • Treatment of rainfall and irrigation events in the water balance	• Errors in observations • Validation of pedo-transfer functions when used to characterize soil water holding capacity • Description of the model when one is used, with particular attention to procedures for estimation of deep percolation and groundwater contribution • Procedures used when the crop season includes winter-time with frozen soil

• Sampling procedures when observations are performed for tree and vine crops • Procedures used when there is mulch • Procedures used when there is active ground cover • Procedures for estimation of soil evaporation	
Sap flow • Clear reference to the method used • Information about sampling, concerning the number of plants equipped with sap flow sensors and the selection criteria for different dimensions/species in a stand • Description of scaling-up method to the stand level • Number of sensors per plant and sensor technical characteristics (ex.: probe length, number of measurement points in a probe) • Data treatment procedures, including corrections • Information about calibration procedures, if performed	• Sensor orientation • Height of sensor installation • Description of insulation method

G.5. Summary

Substantial measurement biases or incorrect data extrapolations can easily occur in ET data sets, many of which may not be recognized or identified and rectified prior to refereed publication. Precautions need to be exercised to produce accurate and defensible ET data and to recognize quality data. Data collection systems need to be combined with rigorous quality assessment and quality control procedures. For example, sap flow systems need to include sufficient numbers of trees to reduce statistical error and to sample a representative population of trees. While remote sensing systems do not 'measure' ET, but rather deduce it via energy balance or vegetation indices, these methods are quite powerful in spatial coverage and quantification of spatial variation in ET, especially those based on thermally driven energy balance. However, they benefit from testing against ground-truth data and comparison against independent data sets. Accuracy of ET measurement requires well calibrated and well-maintained systems, and, in many cases, a foundational knowledge of the underlying physics of turbulence and heat and radiation transfer that govern the particular measurement. Knowledge of underlying physics is necessary to reduce the impacts of oversight of important biasing factors. In addition, an attitude of thoughtful approach to measurement and critical assessment of data are essential.

Recommendations are provided on the types of documentation that should accompany ET data sets and associated products when published and that should be referred to from journal publications. This documentation describes data measurement and handling by the data collectors and can provide insight to readers of articles and users of data as to data representativeness, context and quality.

Appendix H

Weather Data Integrity

H.1. Introduction

Accurate estimation of evapotranspiration (ET) requires accurate and representative weather data. Combination equations such as the Penman-Monteith (PM) equation are relatively sensitive to error in weather data. The degree of sensitivity changes with time of year and climate. During summer, solar radiation can dominate the ET estimate. Therefore, especially in humid and subhumid climates, where the relative power of the vapor pressure deficit / wind term of the PM is small relative to the radiation term, error in solar radiation can be the most impacting on the ET estimate. During wintertime, if solar radiation is low, wind speed and vapor pressure deficit can be strong drivers of the ET calculation. Error in wind speed and vapor pressure deficit can also dominate in arid and semiarid climates. Gong et al. (2006) evaluated a 41-year record of daily weather data at 150 national meteorological observatory stations in China. Reference ET (ET_{ref}) estimated by the FAO-56 Penman-Monteith method was most sensitive to relative humidity, followed by shortwave radiation, air temperature and wind speed. The rank of the four climatic variables varied with season and region. Values for sensitivity coefficients were impacted by regional wind-speed patterns. Ley et al. (1994a) analyzed sensitivity of the 1982 Kimberly Penman model at 20 weather stations in central Washington State where 24-hour estimates were most sensitive to combined error in daily maximum and minimum air temperatures, followed by error in daily maximum air temperature, solar radiation, dew point temperature, wind speed, and daily minimum air temperature , when the weather parameters were varied up to an amount equal to the standard deviation of the measured values for specific time periods of the growing season . Ley et al (1994b) showed that when realistic levels of weather measurement variability (estimated either as the manufacturer's specification of sensor accuracy, or as actual measurement variability) are analyzed, 24-hour estimates of ET_{ref} are most sensitive to solar radiation measurement error, followed by dewpoint temperature, maximum temperature, and wind speed measurement errors, respectively, for the central Washington climate. In general, sensitivity coefficients for ET_{ref}, defined as the percentage change in ET_{ref} per percentage change in the variable, were less than 1.0 (Ley et al. 1994a), which suggests that ET_{ref} estimates are somewhat robust to error in weather data. However, the relative sensitivity of any one variable is impacted by the strength of the other weather variables, for example, in the case of the essentially multiplicative influences of vapor pressure deficit and wind speed in the PM aerodynamic term.

One note made here is that it is often awkward or irrational to express error in some weather parameters in terms of percent error, for example, with air temperature, which, when using a Celsius basis, a 1 ^{o}C error at a temperature of 1°C constitutes a 100% error, whereas, if expressed on the basis of absolute scale (K), the 1°C error constitutes less than 0.4% error, which is at the other extreme. Because of the impact of the basis for expression of percent error, some recent sensitivity analyses have expressed sensitivity of ET_{ref} in terms of mm of error in ET_{ref} per unit error in temperature, wind speed, radiation or vapor pressure, expressed as ^{o}C, m s^{-1}, W m^{-2} or kPa (Irmak et al. 2006). All analyses demonstrate the need to exercise care in measuring and handling weather data.

Weather data should be screened before use in an ET_{ref} equation to ensure that the data are of good quality and are representative of well-watered conditions. This is especially important with electronically collected data, since human oversight and maintenance may be limited. When weather measurements are determined to be faulty, they can be adjusted or corrected using a justifiable and defensible procedure, or the user may elect to replace perceived faulty data with estimates. This Appendix reviews some general procedures that may prove useful when assessing the integrity and representativeness of weather data used for ET_{ref} calculation. Procedures are provided for estimating data in situations where data are shown to be of poor quality or are missing.

H.2. Importance of the Weather Station Location

Most modern automated weather stations (AWS) measure the primary variables affecting ET: solar radiation, air temperature, wind speed and humidity, and therefore provide relatively complete data for estimating ET as compared to the older manually-operated weather stations that measured only air temperature and that were routinely used in the past. An AWS should measure temperature, humidity and wind speed within the dynamic boundary overlying the ground surface. Properties of this boundary layer characterize the energy balance at the surface and are used to estimate the ET rate. As studies in southern Idaho by Burman et al. (1975) and modern blending height/profile theory models (Chen and Dudhia, 2001) have shown, the humidity, temperature and wind speed levels in the lower level of the atmosphere change when going from desert to a patchwork of irrigated and non-irrigated fields. When making calculations of ET_{ref}, weather measurements should reflect the environment that is defined by the reference surface. This is important because most reference ET equations were developed for use with meteorological data collected primarily over and downwind of dense, fully transpiring grass or similar vegetation exhibiting behavior similar to the definition of the reference surface condition. Feedback exists between the boundary layer above the surface and the surface, so that the energy balance and evaporation at the surface impacts temperature, humidity and wind speed of the air layer above.

Ideally, weather stations should be centered within large, nearly level expanses of uniform vegetation that are supplied with sufficient water through precipitation and/or irrigation to support ET near maximum levels. The preferred vegetation for the site is clipped grass. However, alfalfa or a grass-legume pasture maintained at a height of less than about 0.5 m may also serve as effective vegetation for the site. Vegetation height should be shorter than about 0.5 m to not impact the wind speed measurement. Meteorological measurements made over other short, green, actively transpiring crops will approach reference measurements, provided canopy cover exceeds approximately 70%. A station may be located on the periphery of a vegetated field, but over a surface having low vegetation cover, provided that the station is downwind of the vegetated field during daytime hours so that the sampled air stream is conditioned to reflect a reference environment. In an ideal setting, the well-watered vegetation extends at least 100 m in all directions from the weather station. However, it is recognized that frequently such a weather station site is not available, and that often some nonvegetated areas or roadways will be present near the station. Allen (2006) summarized a source-area footprint approach to estimate the impact on weather measurements of a local area of dryness in the immediate vicinity of a weather station having transpiring vegetation further upwind, and vice-versa. That approach can be used to assess whether the size of a patch of bare or dry ground surrounding a weather station,

for example, in the corner of a center pivot irrigated field, is large enough to impact the temperature and humidity measurements by more than some fixed percent. It can also be used to indicate whether a small patch of well-watered vegetation surrounding a weather station is sufficiently large to condition the near surface boundary layer measured by the weather station so that it represents 'reference' conditions. Some guidelines based on the method are presented in the next section.

Meteorological data sets obtained from true reference settings are generally difficult to come by. Often, weather stations are located over or adjacent to: 1) annual row crops that proceed through a distinct annual growth (and cover) cycle, or 2) range and/or pasture land that is subject to seasonal deficits in soil moisture or is within the vicinity of small buildings and roadways. Many urban weather stations fail both the underlying surface requirement and the recommended separation distance from obstacles. Failure of a weather station site to meet the definition of a reference condition described above does not preclude use of the data for estimation of ET_{ref}. However, data from such a station should be examined carefully before use, and may, in some cases, require adjustment to make the data more representative of reference conditions. New weather stations installed for the express purpose of estimating ET_{ref} should be located in sites that closely approximate the reference conditions outlined above.

It is the intent of this Appendix to encourage the use of weather data and to locate weather stations that adhere to the preferred guidelines. When weather data are not from an agricultural or reference environment and are shown to be substantially impacted by the lack of local ET, the user should be willing to adjust the data using procedures of this Appendix and other publications, for example, ASCE-EWRI (2005), or to abandon the use of the data.

Weather stations should be isolated from nearby obstacles and obstructions that can impede airflow and/or shade the site. The recommended horizontal separation distance from such obstacles should exceed 10 times the height of the obstacle (ASAE 2004). Fences used to protect the station from unwanted intrusions by animals should be made of a porous fencing material (e.g., woven wire or chain link); fence height should not extend above the height of the anemometer.

H.3. Estimating the Impact of Local Environment on Temperature and Humidity Measurements

The contribution of surface conditions at various distances upwind of temperature (T) and humidity (e) measurements and associated vapor and sensible heat flux measurements has been extensively studied by the micrometeorological and air quality modeling communities (Horst and Weil, 1992; Hsieh et al. 2000; Schmid 2002). The total spatial area that influences the value of a scalar (T and e) or flux (H and LE) is known as the source area 'footprint'. Models developed from footprint studies are useful for assessing the influence of fetch of evaporating cover upwind of an agricultural weather station on conditioning of T and e measurements and consequently estimates of ET_{ref}. The models can also be used to estimate impacts of nonevaporating surfaces in the vicinity of a weather station, for example, a station sited in the bare corner of a field or near a road, on negative conditioning of the T and e measurement.

The following tables are summarized from Allen (2006) to show the relative influence of local ground surface condition, evaporation wise, on T and e measurements. The tables were computed using a footprint model by Hsieh et al. (2000), which was applied over a range of fetch distances for two surface conditions common to weather stations: well-watered grassed fetch that

is recommended for the ideal weather station setting and a nearly dry, bare soil fetch that represents a nonideal weather station setting. The information in the tables can be used to recommend minimum distances of grassed or other vegetation required to promote measurement of *T* and *e* representing well-watered conditions at a weather site and the negative impact of dry surfaces in the immediate vicinity of a weather station.

During model application, the well watered grass fetch condition was assumed to be of 0.12 m height in the analyses, and net radiation loading was set at 500 W m^{-2} for each surface. *LE* was set at 350 W m^{-2} for the grass and 50 W m^{-2} for the dry soil. A residual amount of *LE* is specified for the bare soil surface to represent residual evaporation common to bare soil in an agricultural area. The results were not very sensitive to *LE* = 50 W m^{-2} vs. *LE* = 0. The resulting values for soil heat flux, *G*, and *H* were 47 and 103 W m^{-2} for the grass and 250 and 200 W m^{-2} for the dry, bare soil. The station elevation was set at 500 m, but results were insensitive to elevation. The Bowen ratios (*H*/*LE*) for the grassed and bare soil conditions were 0.5 and 5. The values for R_n , *LE* and *H* are typical of midsummer during midday, and when buoyancy effects are large. The values for *LE* are approximately equivalent to daily ET rates of 7 and 1 mm d^{-1}, depending on the day length.

The data presented in Table H.1 suggest the influence of a weather station surface having x_f dimension of one of the vegetation conditions (grassed or bare) in the upwind direction on the measurement of *T* or *e* at 2 m height. The influences are expressed as a fraction (*F*) of total influence (0 to 1.0) for a range of upwind fetch lengths (x_f) of 5 to 200 m and over a range of wind speeds of 0.5 to 5 m s^{-1}. The influences, in essence, represent the fraction of the *T* and *e* "concentrations" (i.e., measurements) that are traceable to the x_f distance of fetch. One way that the table can be used is to indicate, for example, that a weather station that is placed over bare, dry soil with 20 m to the edge, and having well-watered vegetation beyond that, will 'feel' the influence of the bare soil in the form of only a 14% impact on the *T* and *e* measurements if the wind speed is a typical 2 m s^{-1}. The *T* and *e* measurements will therefore be 86% similar to that measured by an equivalent weather station placed over and surrounded completely by transpiring vegetation and only 14% like *T* and *e* measured over a very large expanse of dry surface. In contrast, for very calm wind conditions of 0.5 m s^{-1}, the influence of the underlying dry soil surface, although only 20 m in length in an upwind direction, is 52% on the *T* and *e* measurement. This occurs due to the relative strength of the buoyancy mechanism of the heated air at the dry surface in transporting warm, dry air parcels upward toward the *T* and *e* sensors, when horizontal wind movement and mechanical turbulence is low. As wind speed increases, the heated parcels, in essence, move past and below the sensors to a greater degree. Table H.2. shows similar values for *F* as for Table H.1, but for a sensor height of 1.5 m that is typical of many weather stations. Differences between the two tables are greatest for smaller values of fetch length, as expected.

The presence of bare soil or other dry surface beneath or nearby a weather station can be cause for concern for reference weather stations due to the perception of aridity impacts and negative conditioning of the air stream by the dry vicinity. However, Tables H.1 and H.2 suggest that dry fetch of up to 20 m has relatively small impact on *T* and *e* measurements for wind speeds greater than 2 m s^{-1}. Impact of local dry fetch increases, however, with calm wind speed. Table H.2 suggests that 38% of the sensor signal at 1.5 m height will be conditioned by a 10 m fetch of bare soil. Given typical average wind speed at 2 m of about 2 m s^{-1}, dry fetch distances of 20 m or less upwind of a weather station are probably tolerable for production of

reference weather data sets, provided surfaces beyond 20 m exhibit well-watered characteristics for some extended distance.

Table H.1 is also useful to gauge the adequacy of the relative size of a 'patch' of transpiring vegetation in influencing the *T* and *e* measurements. For a patch of grass that is 40 m in diameter so that 20 m of transpiring grass extends upwind of a weather station having *T* and *e* sensors at 2 m height, with a dry surface beyond, the grass has only 7% influence on the *T* and *e* measurements when wind speed is 2 m s^{-1}, and 93% of the *T* and *e* signals will stem from the energy partitioning conditions over the dry soil further upwind. Therefore, the weather data can be expected to exhibit aridity of the region if the region is dry, even though the weather station is 'technically' located over irrigated, clipped grass.

This example suggests that operators of 'agricultural' weather stations should not be lulled into assuming that *T* and *e* measurements collected over small patches of grass fulfill needed environmental conditions for a 'reference' weather station and will produce weather data that exhibit the conditioning that is anticipated by an ET_{ref} method that has been calibrated to 'reference' weather data.

TABLE H.1. The fraction (0 to 1.0) of total contribution by a weather station surface, having x_f dimension in the upwind direction, on the temperature and vapor "concentrations" (i.e., measurement) taken at a 2 m height, as influenced by wind speed at 2 m (Data from Allen 2006).

Distance to upwind boundary, m (x_f)	Clipped grass				Bare, dry soil			
	Wind Speed at 2 m, m/s				Wind Speed at 2 m, m/s			
	0.5	1	2	5	0.5	1	2	5
5	0.03	0.00	0.00	0.00	0.07	0.01	0.00	0.00
10	0.18	0.05	0.00	0.00	0.27	0.11	0.02	0.00
20	0.42	0.23	0.07	0.00	0.52	0.33	0.14	0.01
50	0.71	0.56	0.34	0.06	0.77	0.65	0.45	0.13
100	0.84	0.75	0.58	0.24	0.88	0.80	0.67	0.37
200	0.92	0.86	0.76	0.49	0.94	0.90	0.82	0.61

Table H.1 shows *F* to increase somewhat log arithmetically with fetch distance for both surface conditions and show *F* to decrease somewhat exponentially with increasing wind speed. Influences of both fetch distance and wind speed were large for both conditions. The impact of larger instability of the near surface boundary layer over the dry soil did not substantially influence the value for *F*, as compared to transpiring grass, for any particular fetch length. However, the table may underestimate the impact of a hot dry surface because wind speed is held constant. Wind speed may accelerate significantly over hot, dry surfaces due to more efficient entrainment and transfer of higher velocity air from high above the surface toward the surface.

TABLE H.2. The fraction (0 to 1.0) of total contribution by a weather station surface, having x_f dimension in the upwind direction, on the temperature and vapor "concentrations" (i.e., measurement) taken at a 1.5 m height, as influenced by wind speed at 2 m (Data from Allen 2006).

Distance to upwind boundary, m (x_f)	Clipped grass				Bare, dry soil			
	Wind Speed at 2 m, m/s				Wind Speed at 2 m, m/s			
	0.5	1	2	5	0.5	1	2	5
5	0.08	0.01	0.00	0.00	0.14	0.04	0.00	0.00
10	0.28	0.11	0.02	0.00	0.38	0.19	0.05	0.00
20	0.53	0.34	0.13	0.00	0.61	0.43	0.22	0.02
50	0.77	0.65	0.44	0.11	0.82	0.72	0.54	0.21
100	0.88	0.80	0.66	0.34	0.91	0.85	0.74	0.46
200	0.94	0.90	0.82	0.58	0.95	0.92	0.86	0.68

Tables H.1 and H.2 illustrate the influence of surface dryness and subsequent partitioning of surface energy into sensible heat and latent heat fluxes on the *T* and *e* measurements. One other important influence of surface temperature on the *T* measurement at some sensor height is not expressed in the tables, however. That influence is the thermal radiation emitted from a warm surface close to the sensor or sensor enclosure on the sensor reading. A dry surface under full sun conditions can be 30 ^{o}C warmer than an evaporating or transpiring surface that is cooled by the evaporation. Because thermal emission is proportional to absolute temperature to the fourth power, the thermal emission from a dry surface can be as much as 100 W m^{-2} greater than from an evaporating surface. Consequently, the 'radiation loading' of a temperature sensor enclosure can increase substantially, especially under low wind speed, where convective cooling of the enclosure is low. The effect is much like the 'heat' felt by a human when approaching a large fire. That sensation is caused by the thermal radiation from the hot fire. This additional warming factor may tend to cause values in Tables H.1 and H.2 to underestimate the impact of the dry surface. The total amount of impact is unknown and is influenced by the sensor enclosure design (i.e., the design of the radiation shield, use of aspirated vs. nonaspirated air flow, etc.).

Even though the data in Tables H.1 and H.2 show the fallacy of locating a weather station over a small area of grass or other vegetation (of 10 or 20 m diameter), but surrounded by dry, poorly vegetated further upwind, positive effects of a small area of grass that are not expressed by the tables would be the cooling effect caued by the lower thermal radiation emission by the grass as compared to dry soil and the consequent reduced radiation loading of sensor shields. This benefit may be small relative to impacts of lack of upwind fetch.

Impacts of Fetch Length for Short Vegetation

The results in Tables H.1 and H.2 suggest that a 100:1 fetch to height ratio for instruments placed over well-watered grassed or other vegetated surface will produce *T* and *e* measurements that are within 75% of 'reference' or 'conditioned' values (as would occur if downwind of a very large expanse of well-watered vegetation having dimensions of km) when wind speed is 2 m s^{-1} or less. The other '25%' of the *T* and *e* measurement will have characteristics of the ground surface beyond x_f. If this 'beyond' surface is also well-watered or semi-well-watered, then the *T*

and *e* values measured at the weather site will be expected to exhibit 'representative' values for *T* and *e* under all wind speeds. The contribution of surfaces upwind of x_f increase beyond the 25% value expected for the 100:1 ratio when wind speed exceeds 2 m s^{-1} due to the increased horizontal air movement relative to the buoyancy influenced movement.

Leclerc and Thurtell (1990) applied a Lagrangian particle trajectory model and found that the 100:1 fetch to height 'rule of thumb' underestimated fetch requirements for flux measurements over smooth surfaces under stable conditions. This finding was also evidenced in Hsieh et al. (2000) who found fetch:height ratios of 100:1 for unstable, 250:1 for neutral and 300:1 for stable conditions needed to condition fluxes over a surface having roughness of 0.04 m.

Location of Maximum Influence

Hsieh et al. (2000) differentiated the equation for x_f to solve for the location, *x*, of the distance upwind of sensors having largest influence on a flux measurement. Allen (2006) added an approximate adjustment for scaling differences between flux and scalar footprints based on findings of Schmid (1994). Estimates of locations of maximum influence on *T* and *e* measurements are shown in Table H.3 for 1.5 and 2 m measurement heights for the same conditions used to create Tables H.1 and H.2. The value for *x* has a relatively low value at low wind speeds and increases substantially with wind speed. Distance *x* is relatively close to the sensor location under nearly all conditions, even though the fraction of impact at the distance may be relatively low. This phenomenon is due partially to the fan shape of the footprint source area, where a narrowing horizontal dimension of the function in the direction of the sensor results in a smaller horizontal area contributing to the sensor location. This narrowing causes locations further from the sensors to have relatively larger impact. The centroid of the *F* area is at significantly greater distance than *x*.

TABLE H.3. Locations of the distance having the most relative influence on *T* and *e* measurements (m) at *z* height (Data from Allen 2006).

Height of measurement, *z* (m)	Clipped grass				Bare, dry soil			
	Wind Speed at 2 m, m/s				Wind Speed at 2 m, m/s			
	0.5	1	2	5	0.5	1	2	5
1.5	8	13	25	65	6	10	18	47
2	10	17	32	85	8	13	24	60

Variation of fetch influences over time

Wind speed and direction vary naturally during the course of a day, month and season. The impact estimates from Tables H.1 or H.2 can be applied to a series of wind speed and direction data to derive a frequency distribution of *F* for a range of wind directions, provided a two-dimensional map of fetch for the weather station is available. Such a distribution can be used to rate a site in terms of fetch impact and to make estimates on the impact of local conditioning by fetch on sensor measurements. Conditioning of *T* or *e* by fetch can be estimated as $T_{meas} = F\ T_{fetch} + (1\text{-}F)\ T_{beyond}$ and $e_{meas} = F\ e_{fetch} + (1\text{-}F)\ e_{beyond}$ where T_{meas} is the expected value for

the temperature measurement given value F, T_{fetch} is the temperature measured over an extensive area having the same surface as the fetch and T_{beyond} is the temperature measured over an extensive area having the same surface as that beyond the fetch distance.

Tables H.1 and H.2 may serve as a first approximation of the amount of impact that upwind fetch of distance x_f has on conditioning or negatively influencing measured air temperature or humidity at height z above the surface. This information is useful for judging adequacy of green fetch upwind of a weather station and for judging the amount of impact that a dry surface in the vicinity of a weather station has on the T and e measurements.

H.4. Weather Data Quality Assessment and Quality Qontrol

Meteorological data acquired for the purposes of estimating ET_{ref} should be subjected to a number of quality control checks prior to use. The first and most important quality control check involves gathering information describing the origin of the weather data and conditions impacting measurements. These data should include:

1. Local siting of the weather station including the 'greeness' of vegetation in the vicinity of the station and beyond.
2. Type and exposure of meteorological sensors employed at the station.
3. Procedures used to maintain and calibrate sensors.
4. Quality control procedures performed and/or data adjustments already performed on the data.
5. Availability of shorter interval data sets (e.g., hourly) to aid the overall QC process.
6. The station operator's experience and/or recommendations pertaining to use of the data for ET_{ref} assessment.

Recommendations pertaining to station siting were discussed in the opening section of this appendix. Where precise location of the station is known, internet tools such as Google Earth provide excellent opportunities to visually note the nature and extent of vegetation and wetness conditions for the station. The types of sensors employed and their exposure (e.g., height of installation or type of radiation shelter) provide insight into expected error levels for specific measurements, and may identify measurements requiring some form of adjustment (e.g., height adjustment for wind speed).

Procedures used to maintain and calibrate meteorological sensors are of extreme importance. Maintenance can be divided into non-technical and technical categories. Non-technical maintenance activities include site maintenance (e.g., mowing, irrigation, and fence repair); cleaning sensors; and leveling radiation sensors and rain gauges. Technical maintenance involves repair and replacement of sensors and equipment, and represents an important component of the overall calibration process. Technical maintenance should be based on the concept of preventive maintenance; that is, replacement of sensors and equipment before their performance degrades. On-site calibration can be performed at regular intervals by comparing sensors with calibrated sensors that are taken to the site for inter-comparison purposes. The operator of the station should provide both the technical and non-technical maintenance protocols and schedule logs either on a request basis or on a public web site. This information should be reported with ET estimates following recommendations, for example, by Allen et al. (2011b) on relevant information to include in publications on crop coefficients and ET estimates

and measurements. The ASAE Engineering Practice 505: "Measurement and Reporting Practices for Automatic Agricultural Weather Stations" (ASAE, 2004) provides specifications for sensor accuracy, resolution, placement and monitoring, as well as intervals and procedures for sensor maintenance and calibration.

Data from weather stations operated as part of a weather network are generally subjected to some form of QA/QC (e.g., Snyder et al. 1985; Stanhill1992; Meek and Hatfield, 1994; Snyder et al. 1996; Shafer et al. 2000). It is useful to investigate the rule structure and guidelines used in the various quality control (QC) routines employed to determine if they are sufficient to provide complete adjustment needed to data. Common quality assessments include comparing incoming parameters against relevant physical extremes (e.g., relative humidity >100%); using statistical techniques to identify extreme or anomalous values; and comparing data with neighboring stations. Some networks flag questionable data while other networks may replace questionable data with estimated values. The user should be aware, however, that QA procedures of some networks contain rather broad or coarse data range assessments, so that application of a QA procedure does not necessarily provide valid data. Furthermore, the QA system may only identify and flag questionable data. Adjustment to the data via a subsequent QC process may or may not incorporate complete or reliable procedures. Seeking the advice of the data facilitator regarding the fitness of a given meteorological data set for ET_{ref} assessment is advisable. The facilitator may have insight into whether station sites approach reference conditions, and if not, suggestions on how to correct or adjust either the raw meteorological data or the final ET_{ref} values.

Subsequent sections of this appendix describe procedures recommended by ASCE-EWRI (2005) for assessing the integrity of meteorological data sets used in the computation of ET_{ref}. Procedures are described to adjust data to better represent reference conditions. While these procedures are applicable in many circumstances, they are by no means a universal solution to all potential problems with meteorological data. Users of the standardized ASCE Penman-Monteith reference ET equation are encouraged to seek local input regarding the subject of assessment and correction of meteorological data for use in computation of ET_{ref}.

Solar Radiation

Solar radiation data can be screened by plotting measurements against clear sky R_{so} envelopes for hourly or daily timesteps. Generally, the best estimates for R_{so} should be used, which may require applying equations that include the influence of sun angle, turbidity, atmospheric thickness, and precipitable water, for example, eq. 4.5 – 4.10 presented in chapter 4. For daily data sets, one can plot measured R_s and computed R_{so} against the day of the year (see fig. H-1 following). For hourly data, one can plot measured R_s and computed R_{so} against time of day, one day at a time, for perhaps five to ten selected "clear sky" days (fig. H-3).

The overlays of plotted R_s and R_{so} allows one to observe whether measured R_s "bumps" up against the clear sky envelope some of the time (i.e., on cloud-free days for daily data or during cloud-free hours for hourly data). R_s will fall below the clear sky curve on cloudy or hazy days and during times when the atmosphere is more turbid than under conditions of clean air. Conditions of relatively clean air occur following cleansing rain or snow showers and routinely in many areas of the western US. The transmissivity of the atmosphere and R_{so} can shift by

several percent from day to day due to changes in water vapor, particulate matter and aerosols, which are all net absorbers and scatterers of solar radiation. If the "upper" values of measured R_S lie routinely above or below the computed R_{SO} curve by more than 3 to 5%, then the user should scrutinize the maintenance and calibration of the R_S sensor. Improper calibration, leveling errors, the presence of contaminants on the sensor (e.g., dust, salt, or bird droppings), or electrical problems can cause R_S to deviate from R_{SO} on clear days. "Abrupt" changes in the clear-day relationship between R_S and R_{SO} generally indicate: 1) accumulation or removal of contaminants from the sensor; 2) change in sensor level; 3) change in sensor calibration; 4) sensor replacement; 5) problem with wiring or data-acquisition system; or 6) improper programming. Pyranometer maintenance records, if available, may help explain changes in the relationship between R_S and R_{SO} and aid decisions related to data adjustment. Occasionally, R_S during hourly periods may exceed R_{SO} due to reflection of sunlight from nearby clouds.

Values for R_S that are consistently above or below R_{SO} on clear days can be adjusted by dividing R_S by the average value of R_S/R_{SO} on clear days. This adjustment should be used with appropriate caution as the procedure assumes: 1) computed values for R_{SO} are correct; 2) clear days can be effectively identified (for example, during midseason at Greeley in fig. H.2, there is a substantial period having no completely cloud-free days); and 3) the factor causing R_S to deviate from R_{SO} is static over time. The R_{SO} curves computed by eq. 4.5 – 4.10 or by the simpler eq. 4.3 – 4.4 are not "perfect." They assume clean air and common relationships between the diffuse and beam components of short wave radiation along with typical spectral densities within the short wave band. Identification of clear days can be difficult in cloud prone areas, especially if hourly R_S data are not available to aid in the assessment process. Finally, many of the factors causing R_S to deviate from R_{SO}, including leveling errors and contaminant accumulation (see Stanhill, 1992), may not be static over time.

Daily measured R_S is plotted in fig. H.1 for a full year at two CIMIS weather stations in the Imperial Valley of California. R_{SO} has been calculated using both methods of chapter 4: eq. 4.3 – 4.4 and eq. 4.5 – 4.10. Eq. 4.3 – 4.4 is a simplified procedure, where R_{SO} is computed as a constant fraction of R_a, with the constant estimated from site elevation. In the case of Imperial Valley, which is at or below sea level, the coefficient in Eq. 4.3 is about 0.75 for both stations. Comparison of the R_{SO} curves with measured R_S from Calipatria, California in fig. H.1a indicates that the pyranometer was measuring about 12% low on clear-sky days through about day 200. At around day 200, the sensor was replaced, and readings for clear-sky days increased to about 5 to 10% higher than the R_{SO} curves. R_S data from the nearby Seeley weather station (about 40 km to the SW) during the same year did not exhibit this shift in data. Therefore, for the Calipatria data for year 1999, the data user would be encouraged to contact the data collector and provider for information concerning pyranometer calibration and the user may wish to pursue options for applying some sort of correction to the data, for example, by multiplying R_S by about 1.12 for days prior to day 200 and by about 0.95 for days following day 200. The user could also consider substituting data from the nearby Seeley station. The more theoretical R_{SO} estimation by eq. 4.5 – 4.10 exceeded the simpler R_{SO} curve from eq. 4.3 – 4.4 by a few percent during mid summer at Seeley and Calipatria, and fit the measured R_S on clear-sky days more closely at

Seeley during mid-summer (fig. H.1b). R_s measured at Seeley on some of the clear-sky days during spring and fall routinely plotted a few percent above the R_{so} curves. This indicates that the pyranometer calibration may have been a few percent high or that the theoretical R_{so} curve is a few percent low for this location due to the very dry atmosphere and potential overestimation of absorption by atmospheric water vapor. The data user may wish to investigate the pyranometer calibration at this site and perhaps conduct an independent assessment of clear-sky R_s using an accurate pyranometer having calibration traceable to the National Standard housed with the Solar Radiation Research Laboratory (http://srrl.nrel.gov/bms/) located in the National Renewable Energy Laboratory (NREL) at Golden, CO (http://www.NREL.GOV/). However, agreement between measured R_s and R_{so} at Seeley appears to be close enough (within 3 – 5%) for application for estimating reference ET without any adjustment or correction.

A few unreasonably low values of R_s are shown in figures H-1a and b, where measured R_s was reported as less than 0.1 R_a. Generally, the lower bound for 24-hour R_s is about 0.2 R_a. The very low values probably occurred due to sensor or datalogger malfunction or missing data occurring during site maintenance. Users can investigate whether a precipitation event, especially snow, may have blocked light transmission or that very dense stratus cloud decks occurred, for example, during winter. Missing or faulty data can be substituted by data from surrounding stations.

Fig. H.2 is a plot of daily measured R_s for a full year at Greeley, Colorado, where both R_{so} curves (eq. 4.3 – 4.4 and 4.5 – 4.10) follow the upper bound of measured R_s quite well. Agreement is good throughout the year, except for the late spring – early summer period, when there were no days having completely clear conditions. The relatively long 120 day period with $R_s < R_{so}$ could be interpreted as a period during which time the pyranometer was dirty, out of level, partially blocked from the sun or sky, or where a calibration error or program error (saturation of the analog signal) occurred, rather than due to a lack of completely cloud-free days. However, the lack of completely cloud-free days was confirmed by plotting records of hourly R_s against R_{so}, for example, as a series of plots similar to fig. H-3, which showed that essentially all days at Greeley during late spring – early summer were subject to afternoon clouding during year 2000. Therefore, no correction to the R_s data was made to this period. This example is included to caution the data user that sometimes deviation of measured R_s from the R_{so} curve for extended periods may be real and valid. The good agreement between measured R_s for cloud-free days and the computed R_{so} curve for winter, early spring and fall periods supports using the solar radiation data from this weather station for the year shown. The R_{so} curve computed using eq. 4.5 – 4.10 dropped a small amount below the R_{so} curve from Eq. 4.3 – 4.4 during summer (day 180 on) due to increased absorption by relatively higher humidity levels of the atmosphere during this period.

Fig. H.3 illustrates a comparison of hourly measured solar radiation with R_{so} computed using the simple method of eq. 4.3 – 4.4 and using the more complicated method of eq. 4.5 – 4.10. The data are from the agricultural weather station near Greeley, Colorado, and data from only two days in August are shown. August 5 had a brief period of cloudiness at around 0800 and then some cloudiness during the afternoon. August 6 was essentially a cloud-free day. The R_s data from August 6 compared well with both R_{so} methods throughout the day. The measured

data plotted slightly higher than the simpler R_{so} estimate from Eq. 47 during the morning hours and slightly below the R_{so} estimate during the afternoon. This may hint of a slight error in the level of the instrument or an incorrect time setting for the data-logger clock. In general, the solar radiation data appear to be of excellent quality and calibration.

Plotting hourly measured R_s against the theoretical R_{so} can be helpful in detecting errors or shifts in the reported times associated with the data set (i.e., errors in datalogger time clocks). Plotting of data can also provide an indication of a lack of level of the instrument. Shifts in time and lack of instrument level can both cause measured R_s to plot out of phase with the theoretical R_{so} curve.

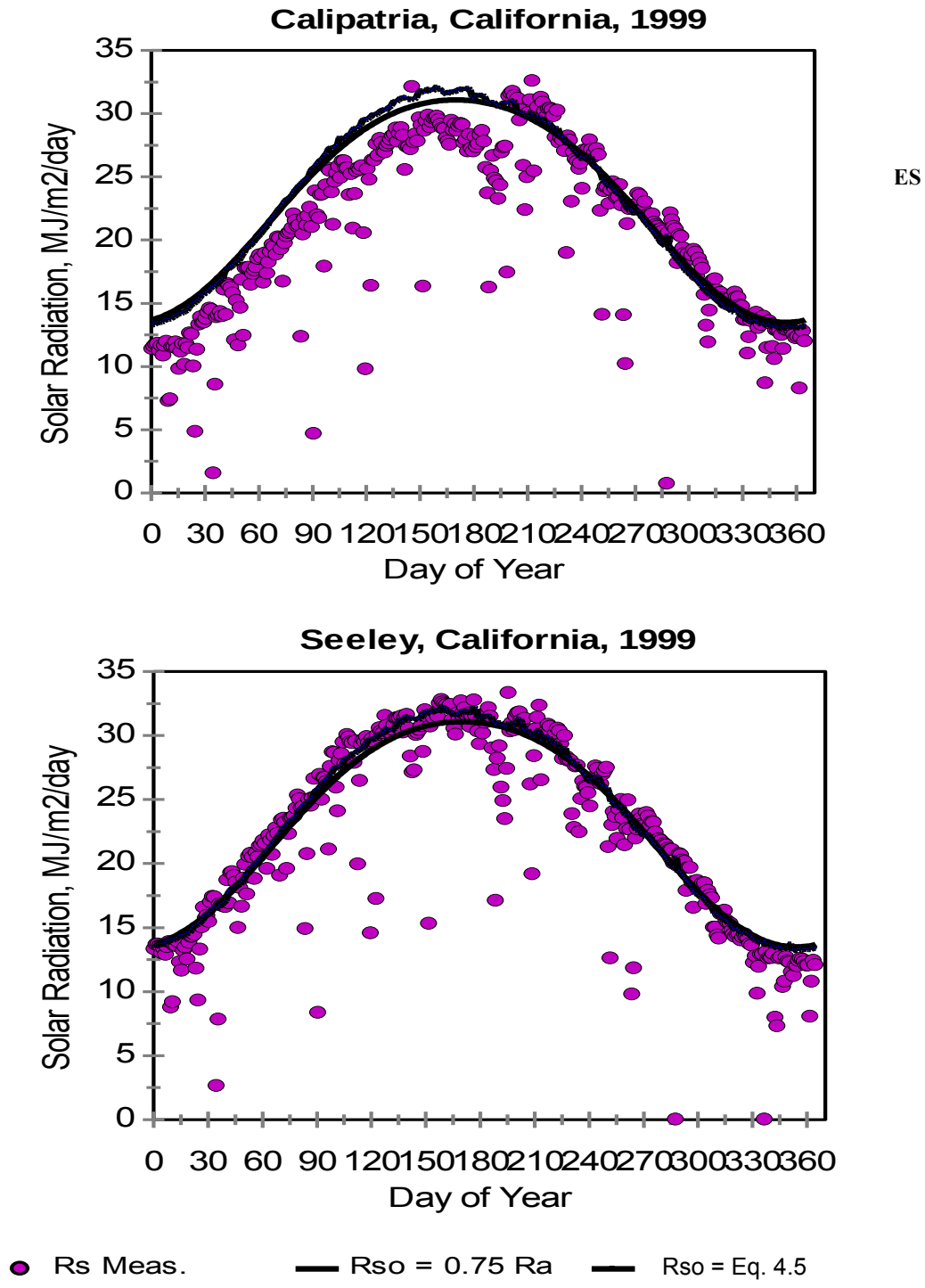

ES

Figure H-1. Daily Measured R_s and Calculated R_{so} using eq. 4.3

Fig. H.1 Daily Measured R_s and Calculated R_{so} using eq. 4.3 – 4.4 (resulting in R_{so} = 0.75 R_a) and using eq. 4.5 – 4.10 for Calipatria (top) and Seeley Fig. H.1 Daily Measured R_s and Calculated R_{so} using eq. 4.3 – 4.4 (resulting in (bottom), California CIMIS stations in the Imperial Valley during 1999.

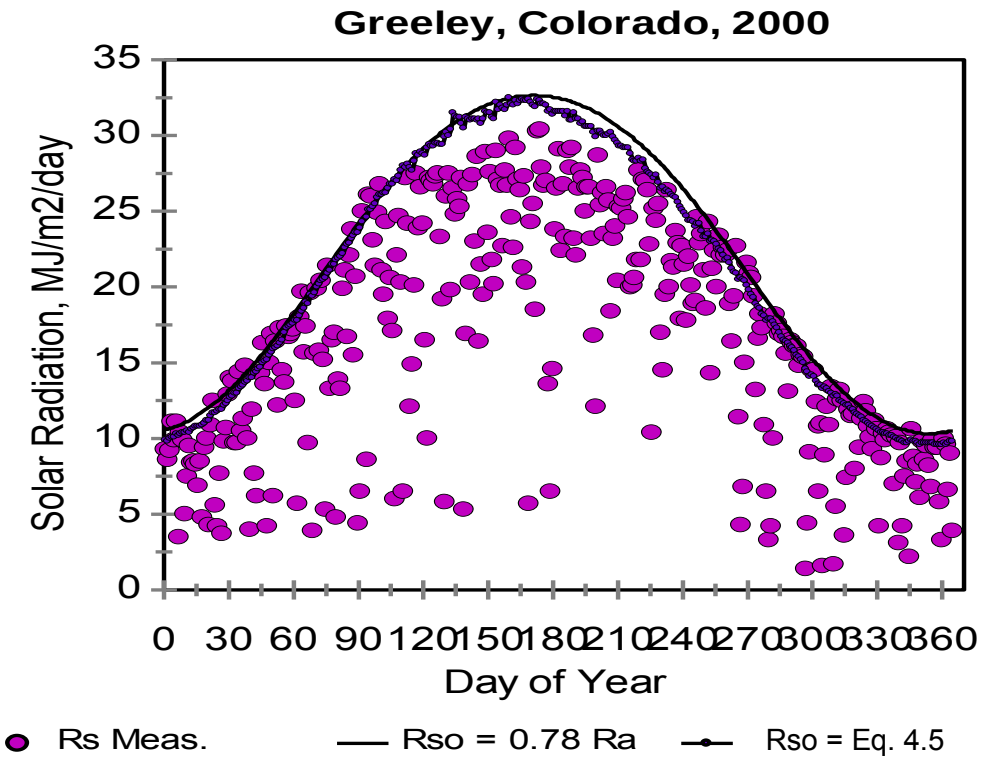

Fig. H.2. Daily measured R_s and calculated R_{so} using eq. 4.3 – 4.4 (resulting in R_{so} = 0.78 R_a) and using eq. Eq. 4.5 – 4.10 for Greeley, Colorado.

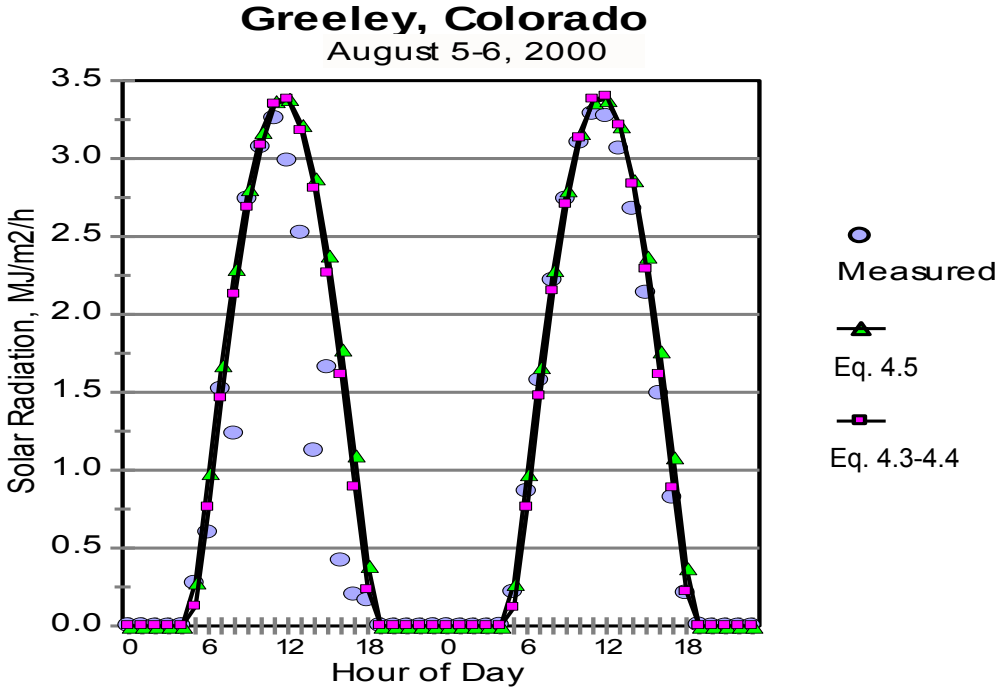

Fig. H.3. Hourly measured solar radiation and clear-sky envelopes for two days in August, 2000 near Greeley, Colorado.

Net Radiation

Where net radiation data are measured, values can be compared with R_n estimated from equations that use solar radiation as an input as a means of integrity assessment, for example, using the equations 4.31 – 4.44 from chapter 4. One should not expect measured R_n to exactly agree with estimated R_n. However, significant variation between the two should be cause for a closer investigation of the measured data. Some net radiometers do not accurately measure the long wave component of net radiation, and in general, net radiometers are more sensitive to dust and salt stains on the sensor surface than are pyranometers. In addition, net radiometers include the additional input of radiation reflected and emitted from the vegetation surface below. Therefore the total measurement has less certainty and more opportunity for error. For use in estimating reference ET, the R_n measurement must be made over a well-watered surface of clipped grass or full-cover alfalfa so that albedo is similar to that defined for ET_{sz}, and, as, or even more importantly, so that the emitted long-wave radiation from the surface, which is proportional to surface temperature to the fourth power, represents that from a surface that is cooled by active transpiring vegetation. As noted previously and discussed in detail in chapter 11, a hot, dry surface can emit 100 W m^{-2} more thermal radiation than cool, transpiring vegetation. This difference can lower the R_n measurement by the 100 W m^{-2}, which is substantial.

A shift in the relationship between measured and estimated R_n may reflect a change in the quality or condition of the surface at the measurement site. Other measurement related factors that can shift the relationship between measured and estimated R_n include scratched or dirty radiometer domes, an off-level sensor, or condensation of moisture inside domes of the R_n sensor. When financially possible, and where, for research or other reasons, it is desirable to measure R_n rather than to calculate it, it is recommended that the user utilize a four-component net radiometer system that has separate sensors and signals for the four major components of incoming and outgoing short-wave and long-wave radiation, as described in eq. 4.31. Using four-component systems has several important advantages: one, it is possible to test and verify the functioning and accuracy and level of each component using independent sensors such as pyranometers and infrared transducers or using theoretical means such as R_{so} for incoming short-wave; secondly, one can use the separate data to test or improve upon components of the radiation balance, for example, R_{nl} and $R_L\downarrow$. All R_n sensors, whether single, two- or four-component systems, should be verified for accuracy before deployment. It is much too common for even expensive sensors costing more than $5000 to suffer from calibration error or manufacturing quality (Allen et al. 2011a,b). Zhao and Allen (2014 (submitted)) described extensive side-by-side intercomparisons of four-component radiometers, means to discern calibration error of new instruments, and means for correcting them.

Fig. H.4 shows hourly measured net radiation and net radiation calculated using the standardized net radiation procedure for one day at Kimberly, Idaho. Agreement between measured and calculated R_n is judged to be very good, even during nighttime periods, suggesting that good accuracy from both measured R_n and from calculated R_n can be obtained when quality of sensors and quality of operation and placement is high and when conditions factored into equations are fulfilled, for example, placement over vegetation having albedo near 0.23 and

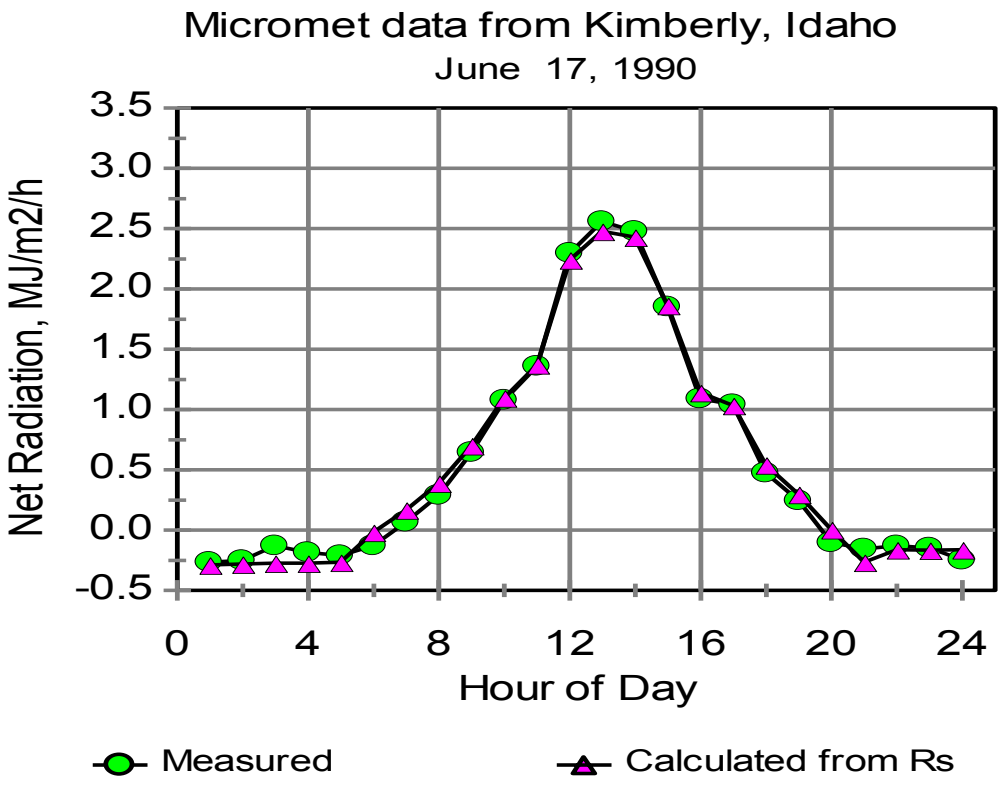

Figure H.4. Measured and calculated hourly net radiation for one day at Kimberly, Idaho over clipped grass (R_n was calculated using eq. 36-40). Data courtesy of Dr. J.L. Wright, USDA-ARS, Kimberly (ret.).

Humidity and Air Temperature

*Relative Humidity***.** Humidity and air temperature data should be screened to identify questionable or erroneous data. A portion of the screening process requires the user to have a sense of what are reasonable and unreasonable values. For example, relative humidity (*RH*) values chronically lower than 5 to 10% in arid regions and lower than 30% in subhumid regions are uncommon and may indicate problems with the sensor. Similarly, *RH* values in excess of 100% do not occur in the natural environment and may indicate that the sensor is out of calibration. The accuracy of most modern-day electronic *RH* sensors is generally within +/- 5% *RH* (ASAE, 2004); thus, recorded *RH* values in excess of 105% may suggest that the sensor is out of calibration. One should use *RH* data sets containing values in excess of 100% with caution. Furthermore, *RH* values in excess of 100%, if not accompanied by a QC flag, may indicate that the data set has not been subjected to rigorous QC. All RH values in excess of 100% should be set equal to 100% prior to use in the ET_{SZ} computation process. Use of this simple adjustment procedure, however, does not mitigate sensor calibration errors for recorded *RH* data that lie below 100%. Some type of proportional adjustment to all data may be warranted.

If hourly data are available, it is useful to examine the diurnal variation of *RH* over a series of days to ensure that *RH* approaches maximum and minimum levels during the coolest and warmest portions of the day, respectively. Hourly time series of *RH* should be examined for the presence of spikes and spurious values of *RH* that may indicate sensor malfunction. Finally, one should check *RH* data on several days having heavy and/or sustained precipitation events or when dew or fog events are known to have occurred. Relative humidity should approach 90-100% during a sustained precipitation, fog, or dew event, and should approach 100% in the evening hours following a heavy rain event. In the case of dew formation, some allowance should be made for the likelihood of higher temperature at a 1.5 or 2 m measurement height as compared to the surface where dew is formed, plus any residual heat storage of the temperature enclosure. Both of these factors may keep *RH* at reference height from reaching 100% during radiatively-caused dew formation.

Dew Point Temperature. Dew point temperature (T_d), as calculated from *RH*, may be reported in lieu of *RH* in some data sets. T_d is the temperature at which air becomes saturated with water vapor, and therefore, $e^o(T_d) = e_a$. T_d is a useful and singular representation of the vapor content of the air at the measurement height. Any error in *RH* will cause error in e_a, since $e_a = RH*e^o(T)/100$) and thus the computed T_d. Values for daily average or early morning T_d should be compared to daily minimum temperatures (T_{min}). In humid regions, the T_d measurement will approach T_{min} on many days. Exceptions occur on days that feature a change in air mass (e.g., frontal passage), or that have high winds and/or cloudiness at night. Average daily T_d may exceed T_{min} in humid and subhumid climates and during winter in nearly all cold climates because of reduction of near surface vapor content during dew formation near the time of T_{min} and subsequent evaporation of the dew and increase in vapor content after sunrise. In addition, evaporation during daytime will generally increase the 24-hour average for T_d over that occurring during the time of T_{min} in humid climates and during winter in nearly all climates by a few degrees C. T_d may approach T_{min} in arid and semiarid environments if nighttime winds are

light and measurements are made over a surface exhibiting behavior similar to the reference definition (i.e., sufficient evaporation to cause evaporative cooling). It is not uncommon in arid and semiarid regions to have T_d 2 to 5 ºC lower than T_{min} under reference conditions (see discussion below) but well below T_{min} if the measurement site is subjected to local aridity. If daily average T_d routinely exceeds T_{min} by a substantial amount (for example, more than 3 or 4 ºC), then the humidity sensor may be out of calibration. Such data should be examined closely and possibly adjusted prior to use. When it is not observed, T_d can be computed from e_a using eq. 3.9.

Fig. H.5 illustrates the use of comparisons between T_{min} and T_d and use of plots of daily RH_{max} and RH_{min} to detect errors in hygrometer data from an AWS in SE Colorado. The large shifts in mean daily T_d relative to T_{min} at days 15 and 200 are obvious. Following day 200, the data began to follow an expected pattern and relationship with T_{min}, with T_d in close proximity to T_{min}. Similar obvious shifts in RH_{max} and RH_{min} are apparent also (bottom plot of fig. H.5). During the last half of the year, values for RH_{max} exceeded 100% by a small amount. However, these errors in *RH* are considered to be small relative to those occurring during the first part of the year, where the T_d data required substantial correction. Daily RH_{min} after day 200 regularly fell below 10%, which is considered to be a very low reading for a reference site. This reflects a relatively "harsh" evaporative environment. The proximity of T_d to T_{min} during the same period indicated the general presence of an evaporative surface.

Fig. H.6 shows T_d and T_{min} for the same station and year as in fig. H.5, but following correction of T_d using the relationship of eq. 8.19 in chapter 8 where data from a second station are used following adjustment for local air temperature. The use of eq. 8.19 preserved the difference observed between T_{min} and T_d observed at the second station, and therefore the relative dryness of the air mass, but adjusted for differences in minimum daily air temperature between the two sites. The resulting plots of T_{min} and T_d in fig. H.6 illustrate good continuity of the relationship between T_{min} and T_d for the corrected period (days 15 – 200) and original observations following day 200. The occasionally low values for T_d during days 15 – 200 were present in the data set for station 2.

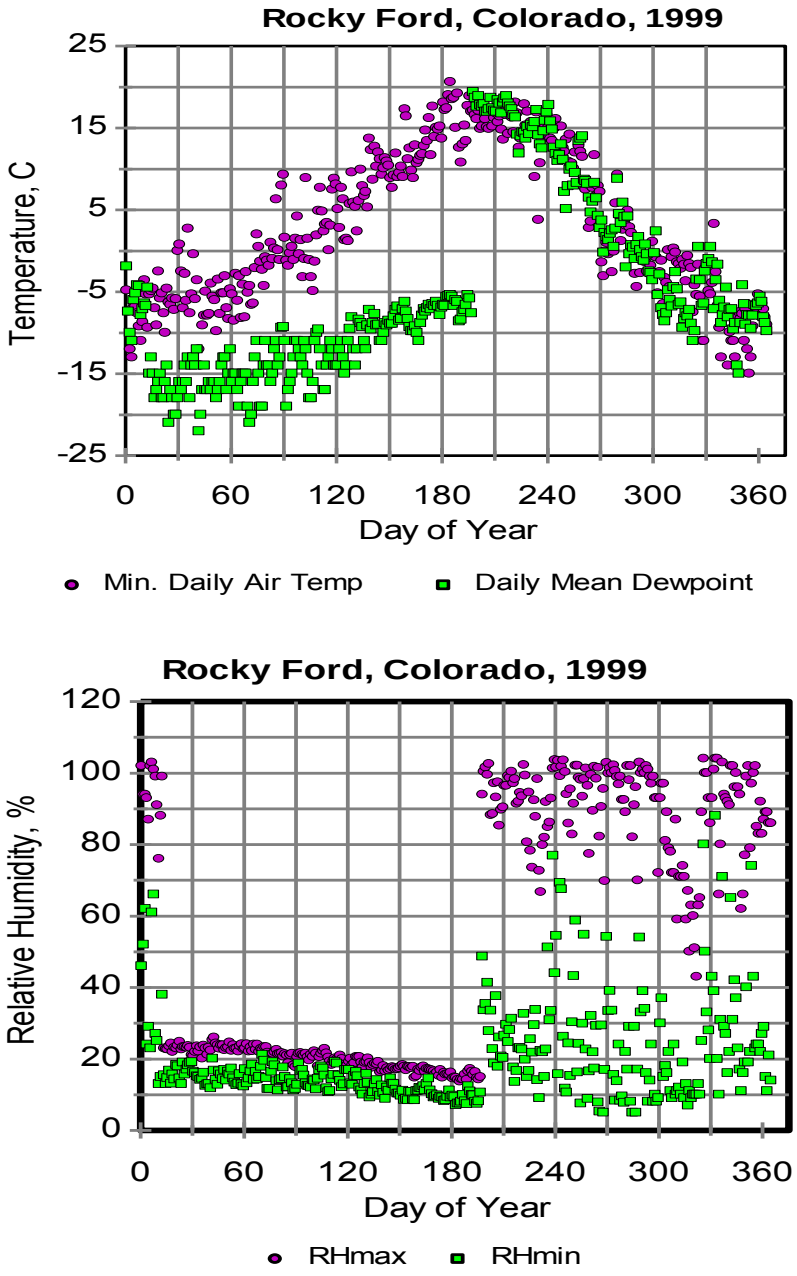

Fig. H.5. Measured daily minimum air temperature and mean daily dew point temperature (top) and daily maximum and minimum relative humidity (bottom) recorded for Rocky Ford, Colorado during 1999.

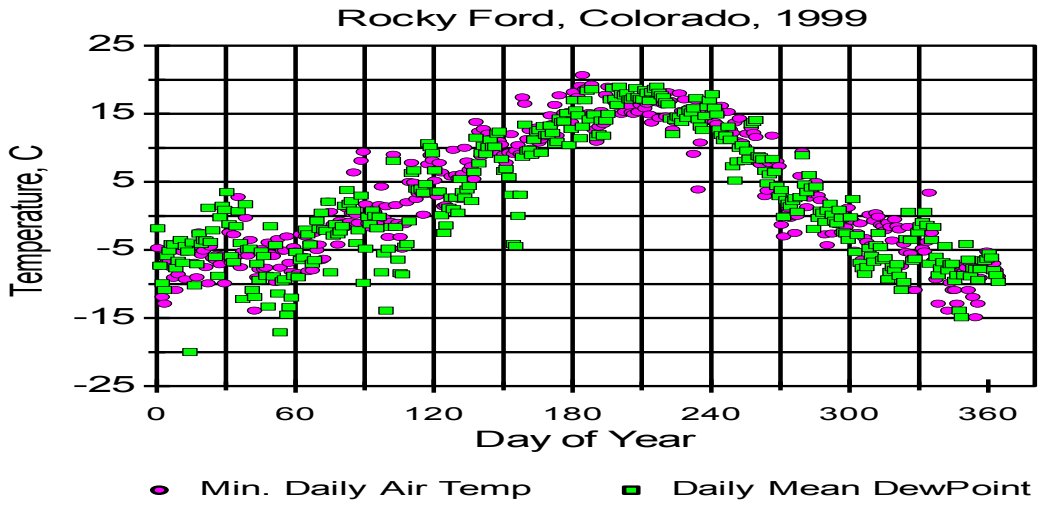

Figure H.6. Measured daily minimum air temperature and mean daily dew point temperature for Rocky Ford, Colorado during 1999, where T_d for days 15 to 200 was replaced by estimates using eq. H-1.

Plots of hourly or shorter period T_d data may assist in identifying problems in T_d data. Dew point and vapor pressure are relatively conservative parameters and often exhibit little change over a day, especially in humid regions. Often, T_d will increase somewhat during midmorning due to evaporation of water and increased capacity for the air to contain vapor (see for example, fig. H-7 and H-10). Dew point will then stabilize or decline slightly during the mid-day hours as the vapor near the surface gets mixed into a progressively deeper boundary layer. Hourly variation in T_d is greater in semiarid and arid settings, especially in areas prone to strong regional advection, where T_d can drop substantially during afternoon as warm, dry air from outside an irrigated area "breaks into" the boundary layer established over the irrigated area. However, large changes in T_d during the day, except under circumstances such as a change in air mass (e.g., frontal activity or sea/land breeze) or large change in wind direction, could signal an error or bias in the T_d measurement. It is common in the western Great Plains of the U.S. to have distinct drylines, which extend either N-S or NE-SW. A dryline, which is an atmospheric transition zone having large gradients in vapor content, may move during the day, with larger T_d values in front of the dryline (typically the eastern side) and with substantially smaller T_d values behind the dryline (typically the western side). Allen (1996) provided illustrative plots of hourly T_d data and expected trends over time. Comparison of hourly T_d to T over a 24-hour period is illustrated in Figure H.7.

ASCE-EWRI (2005) presented prioritized methods for estimating e_a from a variety of humidity parameters and summarized all calculation steps for the standardized ET_o and ET_r equations. These are listed in Table H-4. The recommendations are based on the likelihood that the data will have integrity and that estimates for e_a will be representative. The availability and quality of local data, as well as site conditions, may justify a different order of preference.

TABLE H.4. Recommended method by ASCE-EWRI (2005) for calculating e_a for use in calculating daily ET_{sz}

Method No.	Method	Preference Ranking	Equation(s)
1	e_a averaged over the daily period (based on hourly or more frequent measurements of humidity)[a,b]	1	---
2	Measured or computed dew point temperature (based on hourly or more frequent) averaged over the daily period	1	---
3	Wet-bulb and dry-bulb temperature averaged over the daily period	2	3.10
4	Measured or computed dew point or measured wet-bulb and dry-bulb temperature at 7 or 8 am	2	3.10
5	Daily maximum and minimum relative humidity	2	H-1
6	Daily maximum relative humidity	3	H-2, 8.18
7	Daily minimum relative humidity	3	H-3
8	Daily minimum air temperature	4	8.17, 8.19
9	Daily mean relative humidity	4	H-4

[a] In many data sets, e_a may be expressed in terms of an equivalent dew point temperature.

[b] Some data logging systems may measure *RH* and *T*, but calculate e_a or T_d internally for output as averaged values over some time interval. See ASAE (2004) for further detail.

When using *RH* data, it is essential that the *RH* and air temperature data are "paired," i.e., that they represent the same time of day or time period and that they are taken at the weather measurement site. For daily data, daily maximum relative humidity (RH_{max}) can be paired with T_{min}, which will both occur, generally, during early morning. Daily minimum relative humidity (RH_{min}) is paired with T_{max}.

Depending on the availability of the *RH* data, the following equations apply, with preference of method listed in table H-4:

- Daily e_a from RH_{max} and RH_{min}.

$$e_a = \frac{e^o(T_{min})\frac{RH_{max}}{100} + e^o(T_{max})\frac{RH_{min}}{100}}{2} \quad \text{(H.1)}$$

where:

e_a = actual vapor pressure [kPa],
$e°(T_{min})$ = saturation vapor pressure at daily minimum temperature [kPa],
$e°(T_{max})$ = saturation vapor pressure at daily maximum temperature [kPa],
RH_{max} = daily maximum relative humidity [%], and
RH_{min} = daily minimum relative humidity [%].

- Daily e_a from RH_{max}

Older styles of electronic relative humidity sensors, for example those manufactured before about 1990, often experienced difficulty in accurately measuring *RH* when at low levels. When using equipment where errors in estimating RH_{min} may be large, or when integrity of the *RH* data is doubtful, the actual vapor pressure can be computed from RH_{max}:

$$e_a = e^o(T_{min})\frac{RH_{max}}{100} \quad \text{(H.2)}$$

When accuracy of *RH* data is in doubt, error in RH_{max} causes smaller error in e_a than error in RH_{min}, due to the smaller value for the multiplier $e^o(T_{min})$ as compared to $e^o(T_{max})$. In addition, RH_{max} data are generally easier to assess for accuracy than is RH_{min}. The value of RH_{max} generally exceeds 90% and approaches 100% in well-watered settings such as within irrigation projects and in sub-humid and humid climates. This proximity to 100% serves as a first check on reasonableness, representativeness, and integrity of the data. Exceptions to this trend are where substantial advection of dry or warm air from dry regions outside the area occurs during nighttime, including, but not limited to some desert areas of New Mexico, Arizona and California.

- Daily e_a from RH_{min}

Sometimes, only high quality estimates of daily RH_{min} are available and must be used to predict e_a:

$$e_a = e^o(T_{max})\frac{RH_{min}}{100} \quad \text{(H.3)}$$

However, estimates using eq. H-3 may be less desirable than estimates using eq. H-1 or H-2, due to greater impact of error in RH_{min} on e_a, as discussed previously. In addition, it is more difficult to assess the integrity of RH_{min} data.

- Daily e_a from RH_{mean}

In the absence of RH_{max} and RH_{min} data, but where daily RH_{mean} data are available, the actual vapor pressure may be estimated as:

$$e_a = \frac{RH_{mean}}{100} e^o(T_{mean}) \quad (H.4)$$

where RH_{mean} is the mean daily relative humidity, generally defined as the average between RH_{max} and RH_{min} and T_{mean} is mean daily air temperature, generally estimated by averaging T_{max} and T_{min}. Eq. H-4 is less desirable than eqs. H-2 or H-3 because the $e^o(T)$ relationship is nonlinear. Eq. H-4 produces estimates of e_a that are closer to those by Eq. H-1 and to daily average e_a computed from hourly values than is the use of alternative forms of eq. H.4, such as $e_a = RH_{mean}/100\ [e^o(T_{max})+e^o(T_{min})]/2$ as described in Allen et al. (1998) or as $e_a = RH_{mean}/100\ [1/(50/e^o(T_{max}) + 50/e^o(T_{min}))]$ as described in Smith et al. (1991). These latter two methods are not recommended in the standardized procedure. In the case of hourly or shorter time periods, ASCE-EWRI (2005) recommended the preference ranking shown in table H-5 for calculating actual vapor pressure.

TABLE H.5. Recommended method by ASCE-EWRI (2005) for calculating e_a for use in calculating ET_{sz} for hourly or shorter time periods.

Method No.	Method	Preference Ranking	Equation(s)
1	e_a averaged over period[a,b]	1	--
2	Measured or calculated dew point temperature averaged over period	1	--
3	Average *RH* and *T* for the hour	1	H-5
4	Wet-bulb and dry-bulb temperature	2	3.10
5	Daily minimum air temperature (see chapter 8)	3	8.17, 8.19

[a] In many data sets, e_a may be expressed in terms of an equivalent dew point temperature.
[b] Some data logging systems may measure *RH* and *T*, but calculate e_a or T_d internally for output as averaged values over some time interval.

The actual vapor pressure of air for hourly periods can be calculated from relative humidity (*RH*) and saturation vapor pressure at the corresponding air temperature ($e^o(T)$ from eq. 3.1):

$$e_a = \frac{RH}{100} e^o(T) \quad (H.5)$$

where:
RH = mean relative humidity for the hourly period, %, and
T = mean air temperature for the hourly period, °C.

Air Temperature. In general, air temperature is the simplest and most consistent weather parameter to measure and the parameter most likely to be of highest quality, provided it is

measured in a reference-type of environment. Air temperature extremes in a data set should be compared to historical record extremes, if such data are available for locations near the site. Temperatures that routinely exceed the recorded extremes for a region indicate a problem with either the sensor or with the radiation shield used to house the sensor. Sensors mounted in non-aspirated radiation shields may produce erroneously high temperatures on days having light winds due to solar heating of the shield (Gill 1983; Tanner et al. 1996). Consistently hot temperatures from a sensor mounted in an aspirated radiation shield may indicate problems with the ventilation system. An effective check for spuriously high or low temperature extremes is to compare the average of the daily extremes (T_{max} and T_{min}) with the mean daily temperature as averaged by the data logger for the day. Many automated weather stations now generate a recorded average temperature for the 24-hr period that can be used in this comparison. Differences between the average computed from the daily temperature extremes and the recorded 24-hr average for the day will generally run within 2 °C. Data should be subjected to closer scrutiny on days when the two averages deviate by more than 3 °C. Precipitation events, air mass changes, and unusual wind conditions can cause deviations in excess of 3 °C.

When hourly temperature data are available, it is advisable to plot the trend of temperature during the day for selected dates to confirm that temperatures attain maximum and minimum values at the appropriate times of the day. For most locations, minimum temperatures occur shortly before sunrise, and maximum temperatures occur in mid-afternoon (1400-1600). It is also important to examine hourly time series of temperature for spikes or spurious temperatures that could indicate a malfunctioning sensor. Comparison of mean 24-hour air temperature calculated from T_{max} and T_{min} against the mean computed by averaging hourly (or shorter) temperature is a straightforward way to indicate the potential occurrence of spikes or missing values in the hourly set or some type of problem with the T_{max} and T_{min}.

Fig. H.7 illustrates hourly measurements of both air temperature and dew point temperature

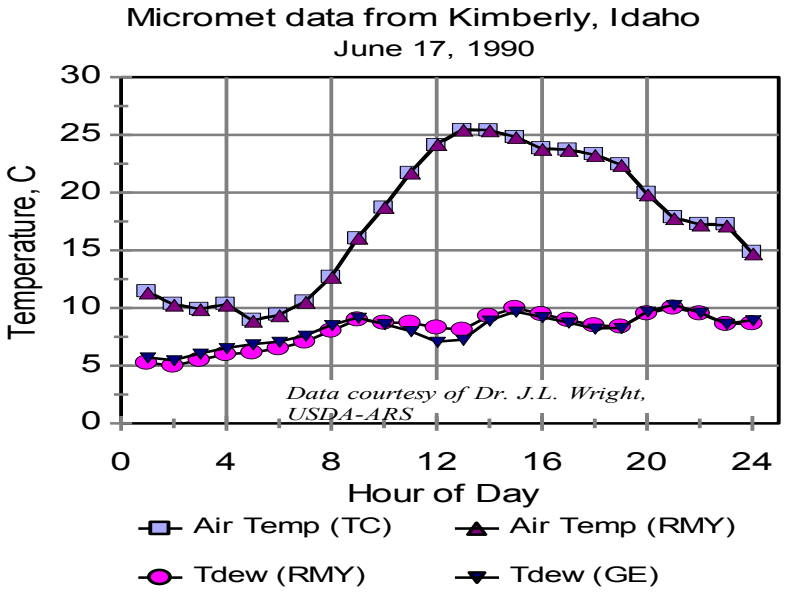

Fig. H.7. Hourly air temperature and measured dew point temperature from dual sensor systems near Kimberly, Idaho, July 17, 1990. Data courtesy of Dr. J.L. Wright, USDA-ARS, Kimberly, Idaho.

during a single day over a grassed surface near Kimberly, Idaho, which has a semiarid climate. Measurements were made using electronic instrumentation and dual measurements using independent systems from different manufacturers were used for purposes of data back-up and redundancy. The two air temperature sensors (TC = thermocouple and RMY = RM Young chilled mirror system) tracked each other consistently throughout the 24-hour period. The two dew point temperature measurements (RMY = RM Young chilled mirror system and GE = General Eastern chilled mirror system) tracked each other closely throughout the period. The closeness of the data measurements from two independent, colocated systems is useful in confirming the accuracy of the data and the proper functioning of both instrument systems. In addition to validation of the air temperature and measured dew point temperatures, the data in fig. H-7 show that minimum daily air temperature, recorded as 9.0 ^{o}C at about 5 am was about 3 ^{o}C above the dew point temperature (6.2 ^{o}C) measured at the same time. This difference is in line with that expected from a well-watered reference environment as discussed previously and in the following section.

Impact of Non-Reference Weather Station Site on Temperature and Humidity

Temperature and humidity data that pass QA/QC checks still may not be advisable for use in estimating ET_{ref}. The moisture status of the underlying surface impacts both temperature and humidity due to the energy balance and impacts of evaporative cooling. Therefore, data collected away from well-watered vegetation (e.g., at airports or over dry, paved, and fallow surfaces) can be negatively influenced by the local aridity, especially in arid and semiarid climates. Data from dry or urban settings may cause overestimation in ET_{os} or ET_{rs} because of air temperature measurements that are too high and humidity measurements that are too low, relative to the reference condition. Under these "arid" measurement conditions, the ET_{os} and ET_{rs} calculations may reflect ET demand of the "ambient," "non-reference" environment, for instance where average net rainfall plus irrigation is substantially less than ET_o or ET_r, so that air temperature is elevated. These estimates of ET_{os} and ET_{rs} tend to over-estimate the ET_{os} and ET_{rs} that would occur for a well-watered setting. An extreme example of the impact of local aridity on ET_{os} was observed in a study near Parker, AZ, (Brown 2001) where weather stations were installed in adjacent 15-ha fields containing irrigated alfalfa and fallow ground. Data from each station were used to estimate ET_{os} using the ET_{sz} equation. Monthly totals of ET_{os} computed using the fallow station data set exceeded similar ET_{os} totals computed using the alfalfa data set by 18-26% during months of June through September (Figure E-8).

Often, an assessment of RH, T_d, and e_a can indicate whether meteorological data were collected in a reference type of environment. Under reference conditions, daily RH_{max} generally exceeds 90% and may approach 100% during early morning hours, provided skies are clear and winds are light (Allen 1996). Minimum temperatures under these circumstances will approach T_d. One can therefore plot and then visually scan plots of RH_{max} or average (or early morning) T_d and T_{min} as a function of time to determine if humidity data reflect the reference condition.

For example, fig. H-9a shows daily T_{min} and T_d for the year 2000 for the agricultural weather station near Greeley, Colorado. Mean daily T_d (calculated from daily average measured vapor

pressure) follows T_{min} relatively closely throughout the year, and is generally within a few degrees Celsius of T_{min}. Fig. H-9b shows daily maximum and minimum *RH* for 2000 at Greeley. The RH_{max} tends toward 90 to 100% during many days. Minimum relative humidity (RH_{min}) runs a little below the expected 25 to 35% range for a reference setting in a semi-arid environment (Allen et al. 1983; Allen 1996; Allen et al. 1996). Overall, the humidity and air temperature data at Greeley during 2000 are judged to be relatively accurate and reflective of a "reference" condition.

If RH_{max} is consistently below 80% for a substantial portion of the growing season record, or if T_d tends to run more than 3–4 ºC lower than T_{min} for a substantial portion of the growing season record, then the humidity data should be subjected to further scrutiny. Among the factors to investigate are: 1) type, maintenance, and calibration of the *RH* or T_d equipment; 2) presence of cloudiness or wind flow at night, which tend to reduce RH_{max}; 3) that the site may not be representative of well-watered conditions; and 4) that the region has characteristically very dry air so that irrigated areas are subject to substantial advection of hot, dry air, for example in Imperial Valley, CA, and portions of Arizona and New Mexico. Historically, humidity has been among the most difficult routine meteorological parameters to accurately measure. The quality of *RH* measurements has improved in recent years due to improvements in sensor technology. Prior to 1990, many agricultural weather networks used polystyrene humidity sensors. These sensors degraded rather quickly in agricultural environments (Howell at al. 1984; Brown et al. 1988), and *RH* measurement errors in excess of 5% *RH* were common under the best of circumstances (Brown et al. 1988). Most networks now utilize thin-film capacitance *RH* sensors that are stable for periods in excess of one year and are generally accurate to within 2-3% *RH*.

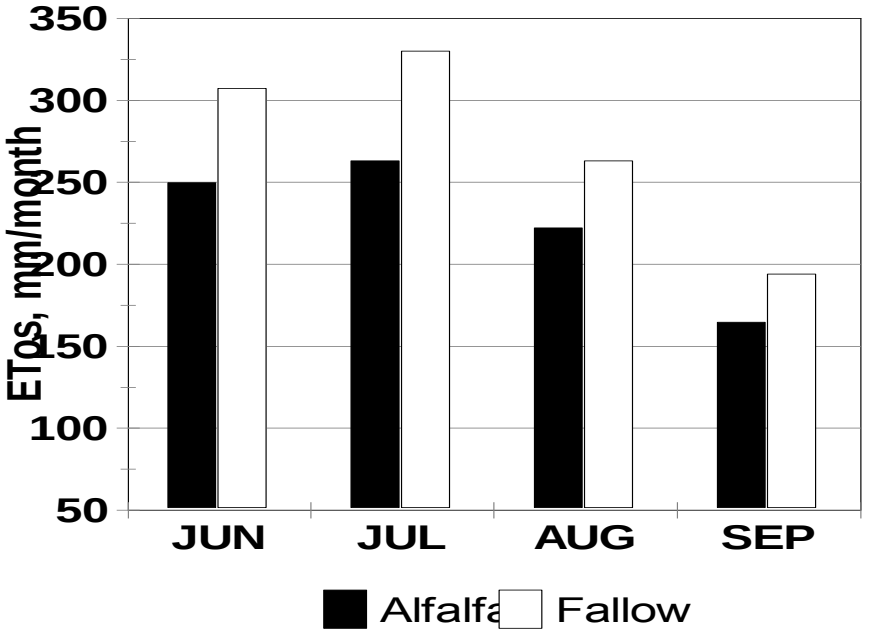

Fig. H.8. ET_{os} by month for the summer of 2000 at Parker, AZ computed using meteorological data collected under reference (alfalfa) and non-reference (fallow) conditions (from ASCE-EWRI (2005)).

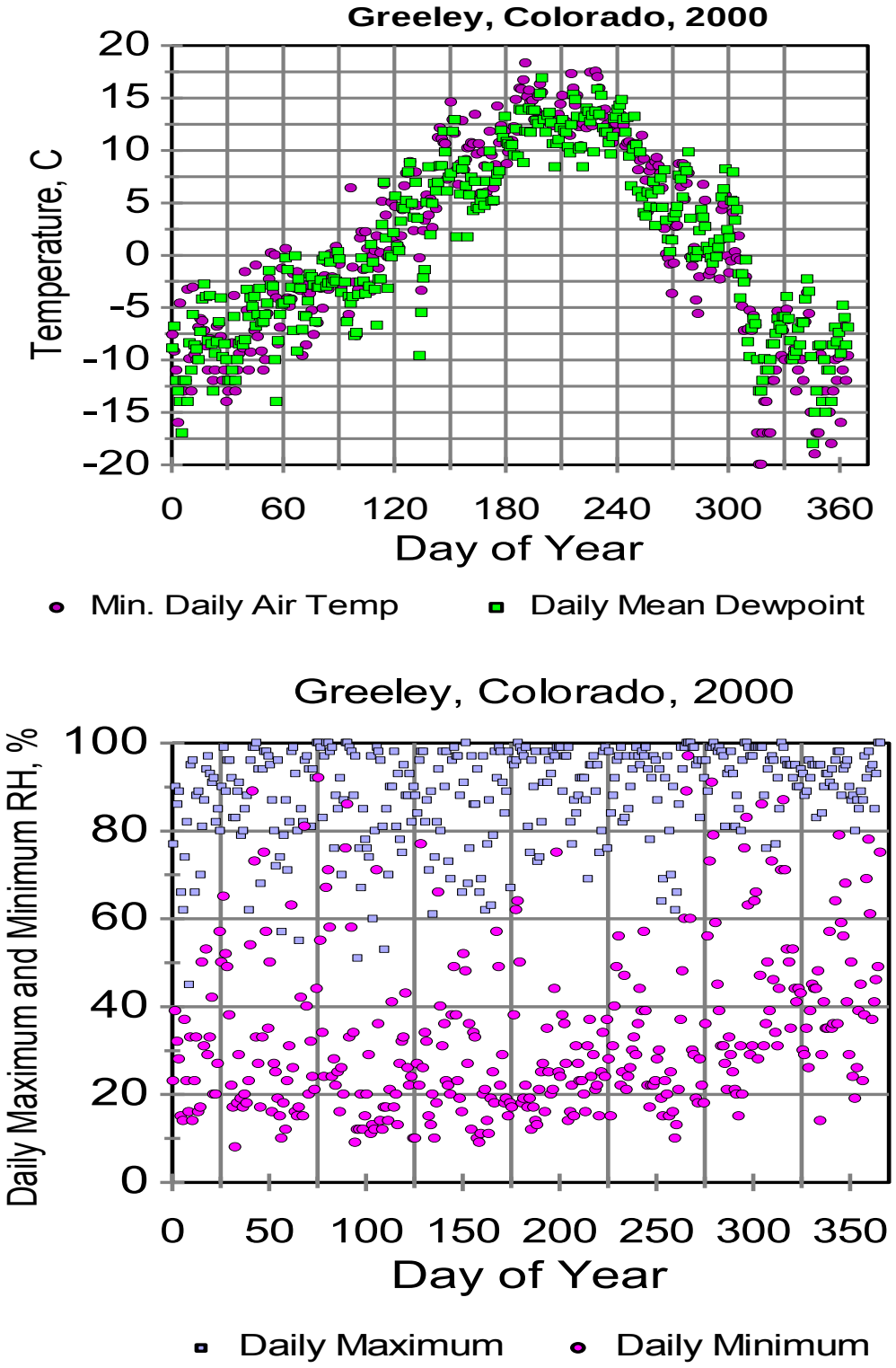

Fig. H.9. a) Daily minimum air temperature and daily mean dew point temperature vs. day of the year and b) daily maximum and daily minimum relative humidity vs. day of the year for Greeley, Colorado, during 2000.

Psychrometers, dewcells, and chilled mirror hygrometers can provide high quality humidity data, as shown in fig. H.7, provided the sensors receive proper maintenance and are operated within the design range. These sensors are not in widespread use for general climate monitoring in remote, automated weather stations due to cost and maintenance factors. The RH and T_d assessments described here may not be effective for identifying data representative of a suitable reference environment in regions prone to cloudiness and large nighttime winds. Cloudiness lowers net loss of long-wave radiation at night, which inhibits cooling and may prevent T_{min} from approaching T_d at night. High nighttime wind speed enhances the transfer of sensible heat and dry air to the surface, slowing the rate of cooling and preventing full humidification of the atmospheric boundary layer above well-watered surfaces.

Often, dew point temperature is consistent between locations having similar surface conditions. For example, Fig. H-10 shows hourly dew point temperatures for four Agrimet weather stations (data from U.S. Bureau of Reclamation) in southern Idaho that are up to 140 km apart. The recorded dew point temperatures and their trend during the day are largely consistent. The four stations (Rexburg, Monteview, Ashton, and Aberdeen) are situated in irrigated agricultural settings. Dew point data taken from a desert weather station operated by the Idaho Dept. Transportation (Flint Creek, Idaho, lat. 42.08º, long. 112.18º) is substantially lower, averaging 11 ºC below the average for the four Agrimet stations. Air temperature at Flint Creek averaged 4 ºC above the Agrimet stations over the 24-hour period. The impact of aridity on both dew point temperature and air temperature at Flint Creek is obvious and is manifested in erroneously high ET_{ref} estimates if applied without adjustment.

One final example of the impact of local and regional transpiration from irrigated crops on the conditioning of air temperature and humidity of air is shown in fig. H-11 – H-13 where temperature and humidity data from two locations in southern Idaho, Kimberly and Balanced Rock, are contrasted. The Kimberly site was irrigated alfalfa in the center of a nearly 200,000 ha irrigated region of desert. The Balanced Rock site is approximately 50 km west of Kimberly and is over sparse desert grass surrounded by desert, with mostly desert for more than 200 km in the typical upwind direction. Average annual rainfall is 200 mm.

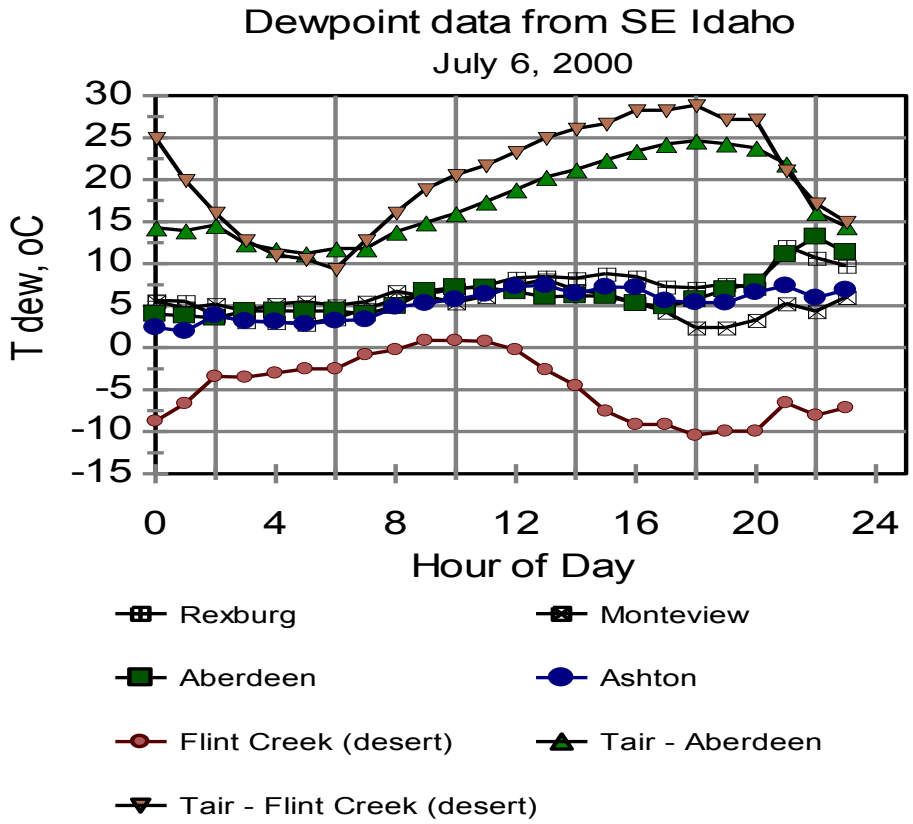

Fig. H.10. Hourly dew point from four irrigated regions of southeast Idaho and from a desert weather station (Flint Creek) on July 6, 2000. Also shown are air temperatures at Aberdeen and Flint Creek.

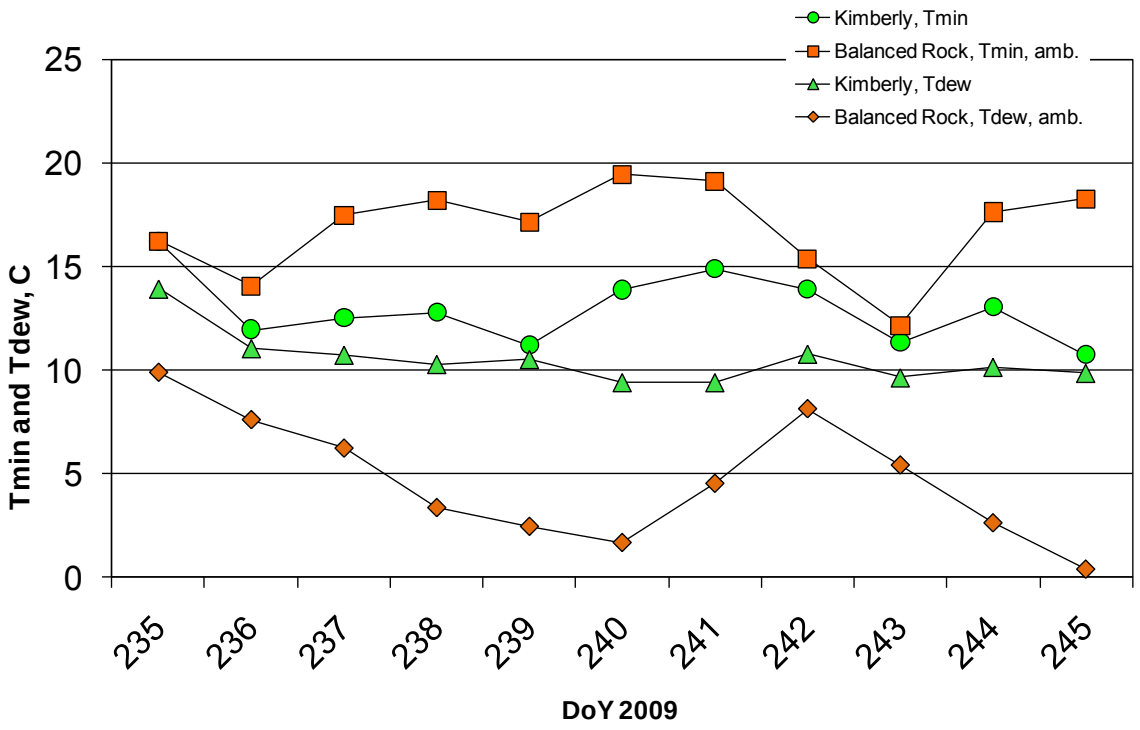

Fig. H.11. T_{min} and daily average T_d at an irrigated alfalfa site near Kimberly, Idaho and at a desert grass site near Balanced Rock, 50 km west of Kimberly for an eleven day period in August of 2009. The data from Balanced Rock are the unadjusted, or "ambient" data.

The daily T_{min} over the desert ran 5 to 6 °C higher than that over the irrigated site, and the dew point temperature over the desert ranged 3 to 7 °C lower than that over the irrigated site. These data illustrate the cooling and humidifying effect that irrigation had on desert air masses as they passed over the substantial irrigation region. The difference between T_{min} and T_d was reduced to a range of 1 to 5 °C at Kimberly by the conditioning effect of ET. As shown in fig. 11.10 of chapter 11, but for a longer period, the vapor content of the near surface boundary layer, expressed in terms of vapor pressure, nearly doubled at Kimberly due to ET from the irrigation. The "Bal. Rock Cond. 2pm vap.pres. ref." series is the vapor pressure measured at the desert site, but following the application of a 'conditioning' routine based on profile and flux theory as introduced in chapter 11. The conditioning routine adjusted the desert data so that values agreed more closely with the humidity measured over the irrigated site, which better approximates a reference environment for calculating reference ET.

The impact of using weather data collected from dry weather sites surrounded by dry conditions without any conditioning of the data is shown in fig. H-12 where the data from the Kimberly and Balance Rock sites were used to calculate the grass reference ET_o using the standardized ASCE-EWRI (2005) Penman-Monteith equation. The result of using the data from the Balanced Rock desert site was to increase calculated ET_o by up to 20 to 30%.

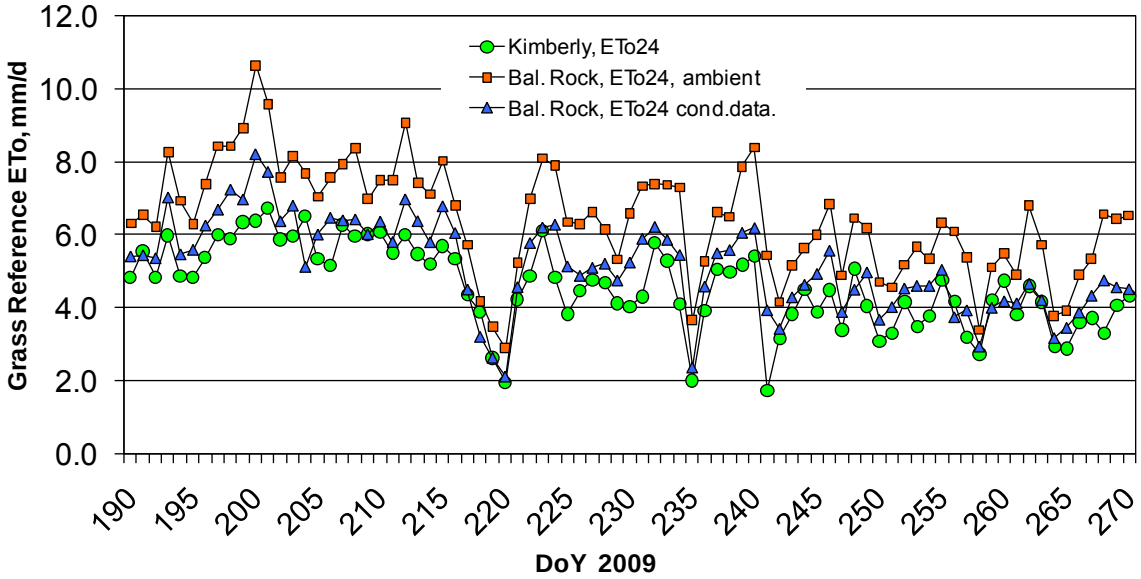

Fig. H.12. Grass reference ET_o from the standardized ASCE-EWRI (2005) Penman-Monteith equation using air temperature, vapor pressure, wind speed and radiation data collected over an irrigated alfalfa site near Kimberly, Idaho and over a desert grass site near Balanced Rock, 50 km west of Kimberly over an 80 day period in 2009. The "ambient" data from Balanced Rock used the unadjusted, or "ambient" data and the "cond." data used Balanced Rock ambient data following conditioning to simulate reference conditions (Allen 2013, manuscript in preparation).

Wind Speed

Accuracy of wind speed measurements is difficult to assess unless duplicate instruments are used. Nevertheless, one should visually inspect wind records for the presence of consistently low wind speed values that may indicate a malfunctioning or failed anemometer or the presence of ice if air temperatures are near or below 0 °C. Consistent and low wind speeds can indicate dirty anemometer bearings that will increase the anemometer wind speed threshold and might eventually seize and stop the anemometer altogether. Wind speeds from failed anemometers will usually appear as small, constant values (less than 0.5 m s^{-1} or the wind speed threshold for a new anemometer) if the anemometer is monitored with a data logger. With a failed anemometer, recorded maximum and mean wind speeds will often have the same values and be equal to any numerical offset in the calibration equation.

Maximum wind speed data, if available, can assist in the assessment of low wind speed data by caculating a gust factor, computed as the ratio of maximum wind speed (m s^{-1}) to mean daily wind speed (m s^{-1}). If a plot of gust factors over time indicates a period of excessively large values, then the anemometer may be malfunctioning. For example, fig. H-13a shows data from an anemometer that was malfunctioning between Day 109 to 117 due to bearing contamination. Gust factors often increase as contamination increases the friction in the bearings. The increasing bearing friction has a greater impact on cup rotation at small as opposed to large wind speeds and thus causes an increase in the ratio of maximum to mean wind speed. The gust factor will exhibit a sudden drop to 1.0 when the anemometer seizes or fails electronically. The

data analyst must be cautious, however, in interpretation of a gust factor, because some weather periods can have more gusty, turbulent air flow than others.

Any appreciable period having daily mean wind speeds of less than 1.0 m s^{-1} should be viewed with caution. Aside from exceptionally calm periods or anemometer problems, other possible reasons for daily wind speeds of less than 1.0 m s^{-1} would include excessive vegetation height at the station or the presence of blocking structures in the nearby landscape (e.g., solid fences or buildings).

Data from a nearby station may also assist in the assessment of wind speeds at a particular site. In some cases, winds at two nearby locations are related which indicates the ratio of the wind speeds at the two locations will remain nearly constant. By plotting this ratio over time, one can identify a problem anemometer. A sudden and consistent change in the ratio often indicates a failed anemometer; a gradual change in ratio may indicate growing contamination in the bearings (fig. H.13b).

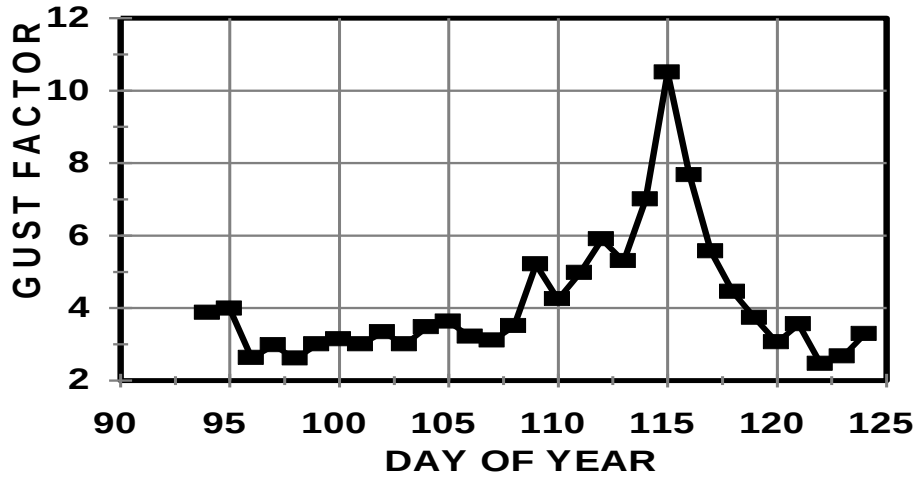

Figure H-13.a) Plot showing the increase in the gust factor at Eloy, AZ during a period when an anemometer was failing due to bearing contamination (from ASCE-EWRI 2005).

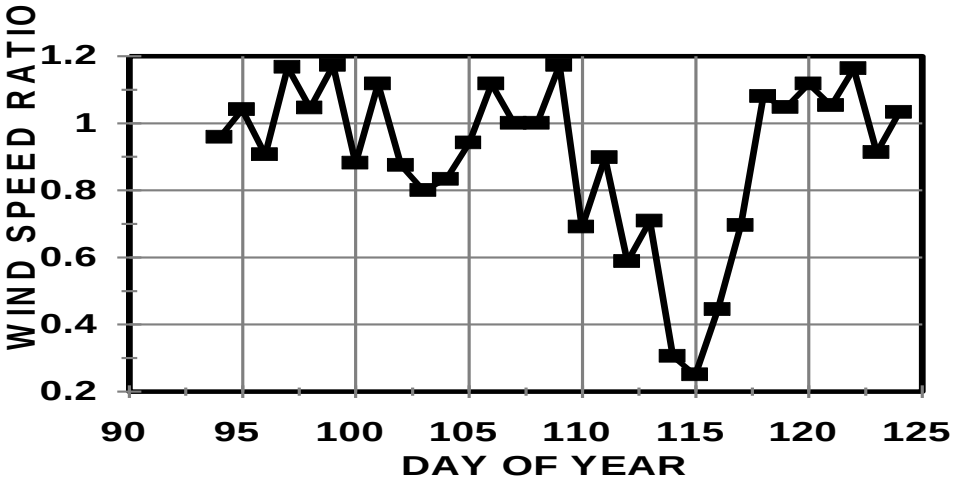

Fig. H.13b) Ratio of daily mean wind speeds at Eloy, AZ to those at Maricopa, AZ during the period of anemometer failure described in a) (from ASCE-EWRI 2005).

As an illustration of comparing wind speed data from two or more locations, daily wind speed data from three neighboring CoAgMet AWS stations located in the Arkansas River Valley of Colorado are plotted in fig. H-14a. The Vineland and Avondale stations are within 15 km (10 miles) of one another and the Rocky Ford station is about 60 km (40 miles) further east. All stations are located in agricultural environments and wind was measured at 2 m above the ground. The similarity in wind speed records is apparent. The Vineland station had some fields of corn planted near the weather station during 1995 (personal commun., Allen 2001) that impeded wind speed measurements during late summer. This is evident in viewing the daily wind plot in fig. H-14a, where daily wind speeds for Vineland fell below those at Avondale and Rocky Ford from day 190 through day 270. Ratios of wind speed for Vineland to wind speed at Rocky Ford show a similar pattern (fig. H-14b), with ratios routinely falling below 0.7 during the period from day 210 through day 270 when the corn crop was tallest. Ratios of wind speed for Avondale to Rocky Ford followed a consistent average of 1.0 all year, as is expected, with some inconsistencies during winter months. This example illustrates the use of data from neighboring stations to discern shifts or anomalies in a data set.

A good preventive maintenance program is required to keep anemometers functioning at peak performance levels. Weather station anemometers should be replaced with newly reconditioned (new bearings) and calibrated anemometers at regular intervals. An annual replacement in light to normal wind regions or semi-annual replacement in windy regions should be considered for anemometers located in agricultural settings. Some providers of weather data employ a standard practice of replacing anemometers on a regularly scheduled basis. The replacement schedule is typically based on local experience or recommendations of the manufacturer and may be as short as six months. ASAE (2004) provides detailed recommendations on periodic sensor maintenance. An alternative technique for evaluating anemometers involves redundancy in instrumentation and requires placement of a second anemometer[1] of the same design, but with fresh bearings, at the weather station for a three or four day period at least once each year, and comparing recorded values. Variations between recordings can signal a need to replace bearings, switches, or other parts. Two- and three-dimensional sonic anenometers use speed-of-sound-based measurements so that the systems have no moving parts. These systems are capable of measuring very low wind velocities.

Wind speeds over non-reference surfaces may exhibit a systematic upward bias relative to wind speeds measured over reference surfaces. Vegetation in excess of the recommended reference-surface height will impose a greater frictional drag on the near surface atmosphere and reduce wind speed relative to the reference condition. Smooth, dry surfaces will generate an opposite bias; wind speeds over these surfaces will generally be higher than those measured over reference surfaces. In addition, substantial sensible heat flux from surfaces having low ET due to dryness have greater amounts of buoyancy-induced mixing of the lower atmosphere and tend to entrain higher velocity air toward the surface, thereby increasing near surface wind speed. Allen and Wright (1997) have suggested procedures for adjusting non-reference wind speed data to better represent reference conditions; however, these procedures assumed neutral buoyancy

---

[1] If a second data logger is used to record the temporary anemometer, one should be careful to synchronize data logger clocks. Also, one should be careful that adjacent anemometers do not interfere with one another's wind stream.

conditions. Ley et al. (2013) have conducted recent tests of these procedures with good results over irrigated alfalfa in Colorado.

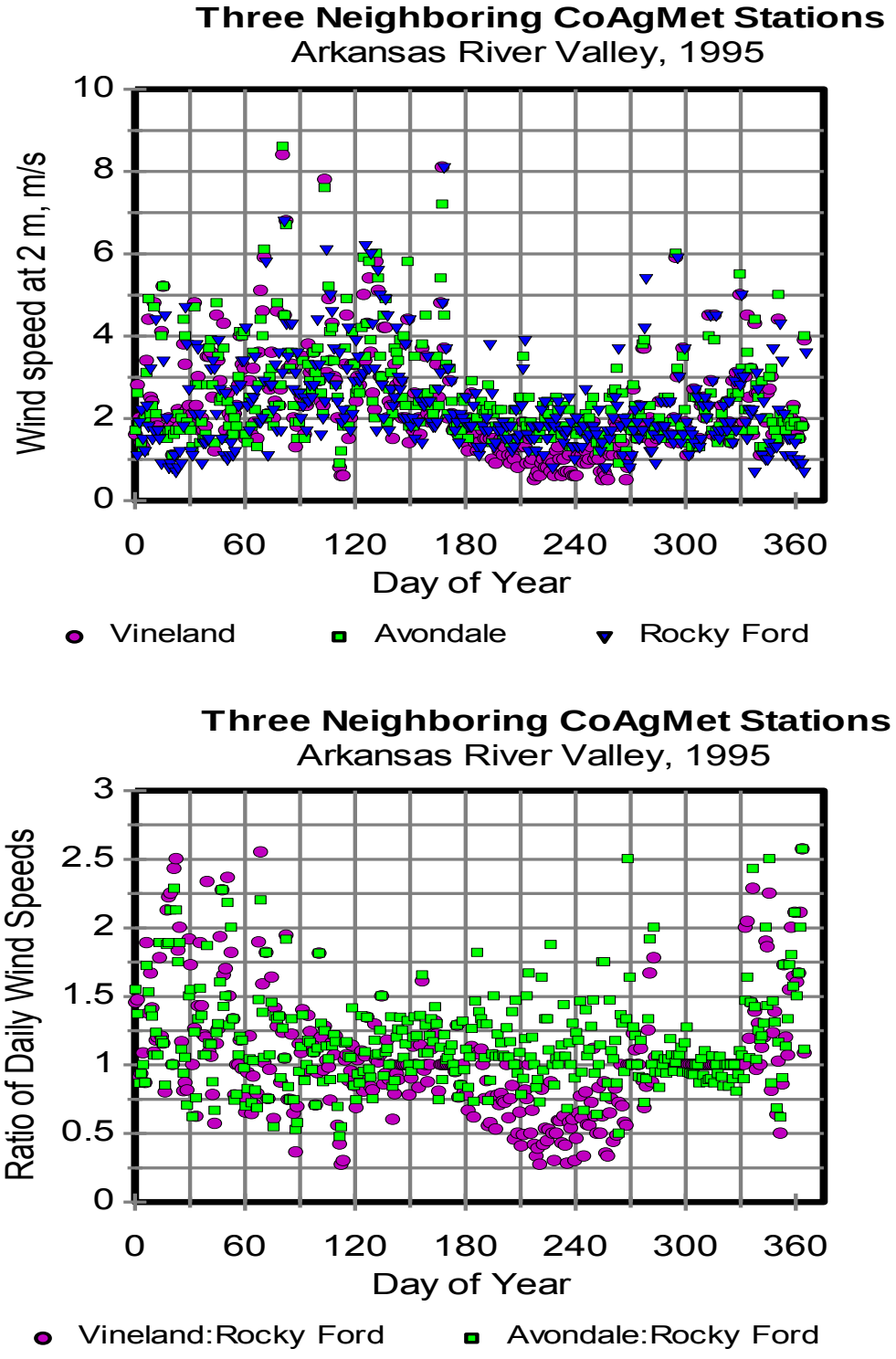

Fig. H.14 Daily mean wind speeds recorded at three neighboring AWS stations in SE Colorado during 1995 (a) and ratios of wind speeds to those at Rocky Ford for the same stations (b).

H.4 Adjustment of Weather Data

Adjustment of temperature and/or humidity data may be warranted when the weather station site is known to be in a local environment that substantially departs from a reference condition and assessment of humidity data indicates that the aridity is impacting the weather data. Allen and Pruitt (1986) and Allen (1996) suggested simple, empirical adjustment procedures to make "non-reference" weather data more representative of well-watered reference conditions by subtracting month-specific adjustments from the non-reference data in proportion to the 'aridity rating' of the particular station. An example of these adjustments is given in Table H.6. The adjustments will generally vary with climate and precipitation patterns. Annex 6 of FAO-56 includes procedures for evaluating and adjusting humidity and air temperature data for aridity of the weather station site. Allen and Gichuki (1989) and Ley et al. (1996) suggested more sophisticated, but still empirical approaches that adjusted both air temperature and humidity data. Allen and Robison (2008, 2009) and ASCE-EWRI (2005) recommended adjusting only humidity data, rather than air temperature data, or replacing arid humidity data completely by tying estimates for dew point temperature to minimum daily air temperature. The intended result was for both air temperature and dew point temperature to carry similarly signed biases that in turn tend to compensate during calculation of vapor pressure deficit in the Penman or Penman-Monteith equations. All of these methods have an empirical basis and require at least regional calibration or confirmation of adjustment coefficients. Allen (2013, manuscript in preparation) introduced a more theoretically-based boundary layer development – blending height approach to adjust air temperature, humidity and wind speed data for aridity effects. However, this approach requires a full complement of daily or hourly weather data (solar radiation, air temperature, humidity, wind speed and precipitation).

TABLE H.6. Average monthly observed departures (elevation) of daily maximum, minimum and mean air temperature for a desert location in southern Idaho during 1981 from that measured at an irrigated reference site (Allen et al. 1983, Allen and Pruitt 1986) and the smoothed standardized monthly departure used by Allen and Brockway (1983) for estimating reference ET in Idaho.

Month	T_{max}, °C	T_{min}, °C	T_{mean}, °C	Standard Departure, °C	30 year desert precipitation, mm
April	2.7	2.4	2.5	1	23
May	1.3	0.6	0.9	1.5	28
June	2.4	1.8	2.1	2	22
July	4.8	2.9	3.8	3.5	3
August	5.2	4.3	4.7	4.5	8
September	3.3	2.7	3	3	11
October	0.3	1.6	0.9	0	13

Estimating T_d using T_{min}

Often, substituting $T_d = T_{min} - K_o$ for measured T_d can improve estimates of daily ET_{os} and ET_{rs} when data are from a non-reference, arid setting. In arid and semiarid regions, it is best to check with the source of weather data to determine if K_o values have been developed for the area. For example, in Arizona the value of K_o was found to vary from 2 to 5 °C and even higher over the course of a year depending on the regional aridity (Brown 2001). When local information on K_o is not available, a K_o in the range of 2 to 4 °C is recommended for semiarid and arid regions (Allen 1996). In humid regions where T_d approaches T_{min} on most nights, K_o is set equal to 0 °C. Some irrigated areas in very dry, advective climates can have extended periods during which T_{min} is more than 5 °C above T_d. These areas include portions of SE California, southern Arizona and New Mexico. Caution should be exercised in the specification of K_o.

Using minimum air temperature measurements from a non-reference setting to estimate dew point temperature using K_o with eq. 8.17 may tend to overestimate the true T_d and e_a that would have occurred under reference conditions. This occurs because measured T_{min} is higher in the dry setting than in a reference setting and thus T_d based on $T_{min} - K_o$ where T_{min} is elevated due to aridity may be somewhat overestimated. However, because e_s in the Penman-Monteith equation will be estimated using the same T_{min} values used to estimate T_d, e_s and e_a will be essentially equally "inflated." Therefore, the $e_s - e_a$ difference in the standardized ET_{ref} equation in general will approximate the $e_s - e_a$ difference anticipated for the reference condition. As a consequence, a more accurate estimate for ET_{os} or ET_{rs} may result than if the actual measurement of T_d from the arid setting had been used. When humidity is adjusted using $T_d = T_{min} - K_o$, no further adjustment is generally needed to the air temperature data set to account for effects of aridity of the weather measurement site.

Use of the $T_d = T_{min} - K_o$ adjustment may produce a slight upward bias in computed net radiation (R_n). The adjustment when T_{min} is impacted by station aridity inflates e_a above levels expected for reference conditions. This error in e_a causes atmospheric long-wave radiation to be overestimated, which in turn causes a 1 to 3% overestimation in R_n. This impact is considered to be relatively minor.

Appendix I

Contribution of Capillary Flow from a Shallow Water Table to Evaporation and Evapotranspiration

The contribution of water to evaporation and evapotranspiration from shallow ground-water can be an important part of water balances and determination of irrigation water requirements. Quantification of capillary flow is also important for managing water logging and soil salinization. This appendix contains a description of an analytical procedure as well as employment of software simulations to estimate the contribution of water from a shallow water table to the ground surface for direct evaporation or into a root zone for extraction by plant roots. The analytical procedure follows Brutsaert (1982) and provides a relatively simple approximation of potential upward flux of water from a water table. In reality, the actual flow and evaporation process can be complicated by soil layering, soil disturbance, soil cracking, soil temperature and tillage. Therefore, the simplified analytical approach provides only an approximation of upward flow. Detailed field studies and modeling are recommended where high accuracy is needed. The software model, UPFLOW by Raes and deProost (2003) and Raes (2004) considers effects of soil layering, root density, soil moisture distribution and anaerobiosis effects on upward flux. This model was used here to develop general curves of upward flux vs. depth to ground-water and associated regression equations. Detailed studies of upward flow of water from shallow ground-water, especially under transient conditions, may warrant use of more sophisticated models than are considered here.

I.1 The Brutsaert-Gardner Analytical Procedure

A number of simplified methods and computer models have been developed for estimating upward flux from shallow ground-water systems. Analytical models include Milly (1988), Miyazaki (1993), Yuana and Zhiming (2005) and numerical models include SWAP (Kroes and van Dam 2003), HYDRUS (Simunek et al. 2005), and UPFLOW (Raes, 2004). Many of these methods use specific algorithms to describe the shapes of soil water potential-soil water content and soil water potential-hydraulic conductivity curves for unsaturated soil. A general method of Gardner (1958) and Brutsaert (1982) is presented here that employs traditional, general shape factors to describe hydraulic characteristics for the particular soil. Only saturated hydraulic conductivity and a single pair of hydraulic conductivity – soil water potential data, along with a general shape parameter are required.

The upward flux rate to the surface, termed capillary rise, *CR*, was derived by Brutsaert (1982), based on Gardner (1958) and Cisler (1969) as:

$$CR = a \left(\frac{\pi}{n \sin\left(\frac{\pi}{n}\right)} \right)^{n} d_w^{-n} \qquad \text{(I.1)}$$

where *CR* is the potential steady upward flux rate to the surface, m d^{-1}, given a depth, d_w, to the water table where *CR* is less than the evaporative demand of the atmosphere. Depth d_w is in m. Parameter *n* is a shape parameter describing the relationship between hydraulic conductivity, *k*, and soil water potential, and *a* is an empirical coefficient defined by Gardner (1958) that describes the hydraulic conductivity vs. soil water potential relationship:

$$k = \frac{a}{\left(\frac{-p_w}{\gamma_w}\right)^n + b} \qquad \text{(I.2)}$$

where *k* is hydraulic conductivity, m d^{-1}, *a* and *b* are constants where $a/b = k$ at saturation (i.e., a/b = saturated hydraulic conductivity, k_s), m d^{-1}, and p_w/γ_w is the soil water potential expressed in m of water (p_w/γ_w is negative above the water table). The value for *b* equals the value $(-p_w/\gamma_w)^n$ associated with *k* when $k = 0.5\ k_s$. This value is selected from a plot of *k* vs. p_w/γ_w . Typical values for *n* range from 2 for clayey soils to 4 or more for sandy soils (Gardner, 1958, Brutsaert, 1982). Other functions for describing *k* vs. p_w/γ_w can be converted into eq. I.2 by plotting the function, noting values for k_s and p_w/γ_w at 0.5 k_s, and iteratively testing values for *n* to obtain a fit between the functions.

CR represents a potential flux to the soil surface under evaporation demands that equal or exceed *CR*. When potential evaporation, as estimated from the Penman-Monteith method, for example, is less than *CR*, then the actual evaporation flux must be limited to the potential evaporation amount that is governed by weather demands.

Capillary rise into the root zone

In conditions having vegetation and active root systems, the depth to the water table, d_w, is expressed as the distance from the water table to a point in the root zone where sufficient roots are present to extract the upward flux of water. This point may be some distance above the z_r depth that represents the effective depth of the root zone, due to insufficient root density at z_r. A reasonable estimate for d_w, assuming the central extraction point to be 1/4 z_r distance from the bottom of the effective root zone, is: $d_w = z_w - 0.75\ z_r$ where z_w is the depth of the water table below the ground surface and z_r is the effective depth of the root zone. All depths are in m. The UPFLOW simulation model described in the following section employs root density functions to estimate the net sink depth for ground-water extraction by roots.

Under conditions where a water table is chronically near the effective root zone so that lower portions of the root zone are saturated or nearly saturated, hypoxia of roots may develop due to limited oxygen and the effective root depth may be less than potential depths. Adjustments should be made to z_r under these conditions. In addition, salinity of ground-water will reduce the rate of extraction by plant roots and adjustments are needed under those conditions. The UPFLOW and HYDRUS models employ functions to make these adjustments.

Example of application of eq. I.1

An example of applying eq. I.1 and I.2 is shown here for the example k vs. p_w/γ_w data of Brutsaert (1982), expressed in his figure 11.5, which was in turn, based on data by Gardner and Fireman (1958) for a Chino clay. The equation for k vs. p_w/γ_w for the Chino clay according to Brutsaert (1982) is: $k = 0.00108 / [(-p_w/\gamma_w)^2+0.05541]$ where k has units of m d^{-1}, and p_w/γ_w has units of m of water. The plot of this function is given in fig. I.1.

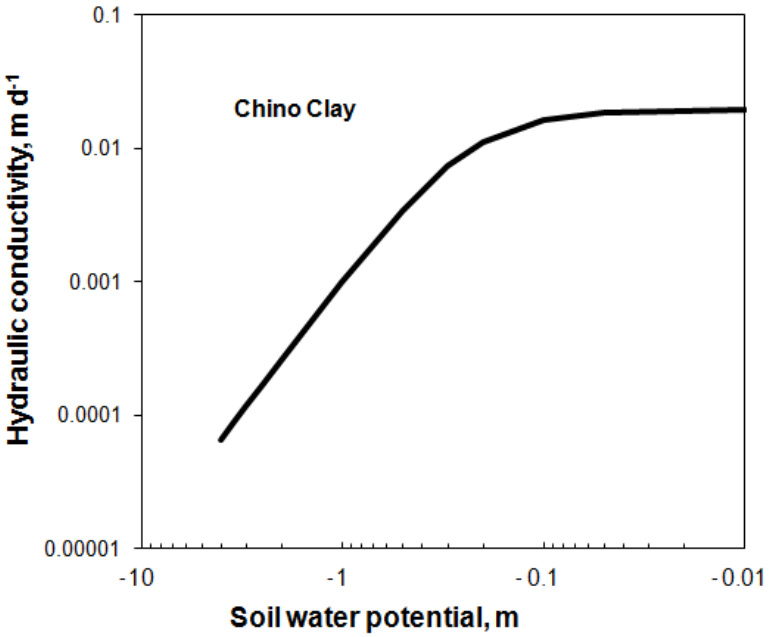

Fig. I.1. Plot of hydraulic conductivity vs. soil water potential for the Chino clay data of Brutsaert (1982).

Using the values $a = 0.00108$ m d^{-1} m^n, $b = 0.05541$ m d^{-1} m^n and $n = 2$, the solution of eq. I.2 provides estimates for CR shown in fig. I.2, which reproduce Brutsaert's Figure 11.5. The estimates by eq. I.1 and I.2 in fig. I.2 are accompanied by estimates of CR by the UPFLOW model described in the next section. Estimates by UPFLOW for the general clay and silty clay textures in UPFLOW for wet and dry conditions tend to bracket the estimates by the Brutsaert-Gardner functions for the Chino clay. The estimates by UPFLOW for a wet clay soil follow the Brutsaert-Gardner function closely.

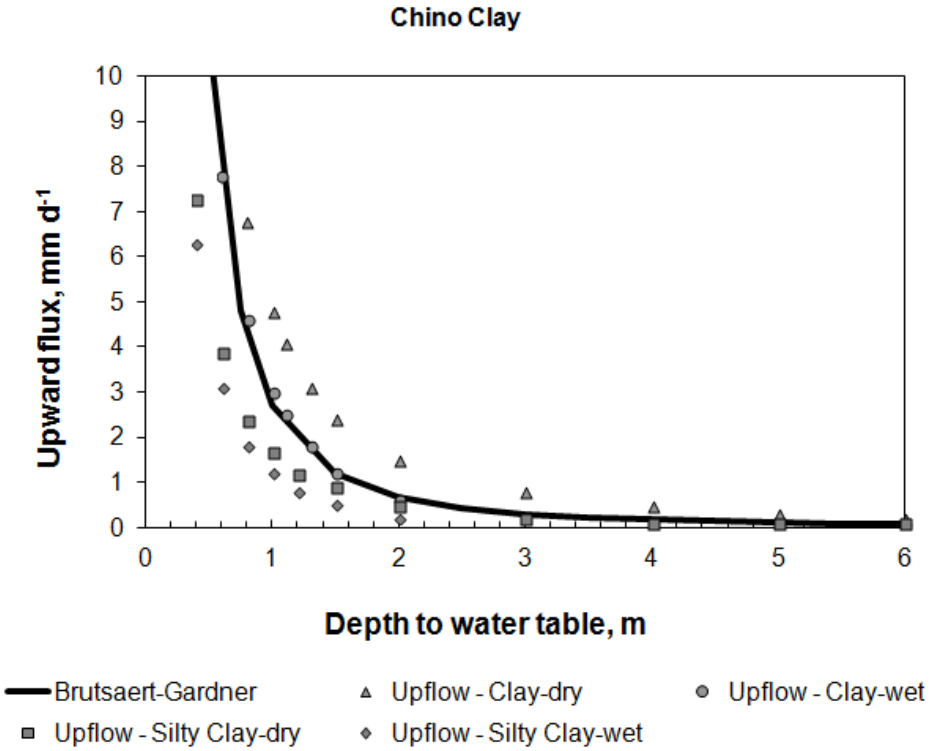

Fig. I.2. Estimated capillary rise for a bare soil surface condition vs. depth to water table (m) based on the Brutsaert-Gardner function (eq. I.1 and I.2) and based on simulations by the UPFLOW model of Raes (2004) for general clay and silty clay soil textures having dry and wet conditions.

I.2 The UPFLOW Simulation Model

UPFLOW (Raes and deProost, 2003 and Raes 2004) is a software tool that estimates upward water movement from a shallow water table to the root zone during a specific period (typically 10-day) under specific environmental conditions. The one-dimensional, steady-state program is designed to work with limited data and contains various sets of soil water retention curves described by Schaap et al. (1999) using van Genuchten et al. (1991) functions or specific soil curves defined in terms of discrete values. The general soil textures in UPFLOW represent a broad range of typical soil types. UPFLOW considers the influence of evaporative or evapotranspirative demand, the relative soil wetness in the upper soil profile, the depth to ground water, the water extraction pattern of the plant roots, the thickness and characteristics of successive soil layers and salinity of the water table. Hydraulic flow computations are made using an integrated Darcy equation. The software estimates aeration conditions in the root zone when the water table is close to the soil surface and the associated effect on reduced root extraction and crop evapotranspiration. Field measurements from loamy sand and sandy loam soils in Belgium were used to confirm UPFLOW simulations (Raes 2004). UPFLOW is public domain software and an installation disk and manual can be downloaded from the web.

UPFLOW simulations for the clay and silty clay soil textures and default parameters are compared against results from eq. I.1 and I.2 in fig. I.2 and agreed relatively well. UPFLOW was applied to a range of soil textures and default Schaap et al. (1999) van Genuchten parameters for bare soil and cropped conditions to create general figures for *CR* and to develop some simple regression functions as shown in fig. I.3 through I.6 and summarized in tables I.1 and I.2. The UPFLOW software was run for the two surface conditions of bare soil and a cereal (small grain) crop having a 1 m root zone. Two soil water contents in the upper soil profile were established, where a 'wet' condition represented conditions similar to field capacity and a 'dry' condition represented about 60% depletion of available soil water content. The two soil water content conditions bracket conditions expected under irrigated agriculture. Simulations were run for a series of depths to ground water and estimated rates of capillary rise under steady state conditions were noted. Collected pairs of depths to water table, d_w, and *CR* were processed using a regression analysis where a simple power relationship was used to describe the relationship between *CR* and d_w:

$$CR = a_f \, d_w^{b_f} \tag{I.3}$$

Where, in eq. I.3, d_w is depth of water table below the surface (m) for the bare soil condition and depth below the bottom of the effective root zone for the vegetated condition, *CR* is capillary rise in mm d^{-1}, and a_f and b_f are regression coefficients.

Fig. I.3 through I.6 show the relationships estimated using the regression functions derived from UPFLOW results for the two surface conditions and two soil water content conditions for the collection of soil textures evaluated. Tables I.1 and I.2 summarize the regression coefficients for each condition and soil texture, the r^2, and assumed saturated hydraulic conductivity, k_s, and volumetric water contents for the wet and dry conditions.

The agreement between the simple power function and simulated data was very high for the bare soil conditions, but agreement was poorer for cropped conditions, especially for a wet upper soil profile. A more complex function than eq. I.3 may be needed to characterize simulated data points when a crop is present.

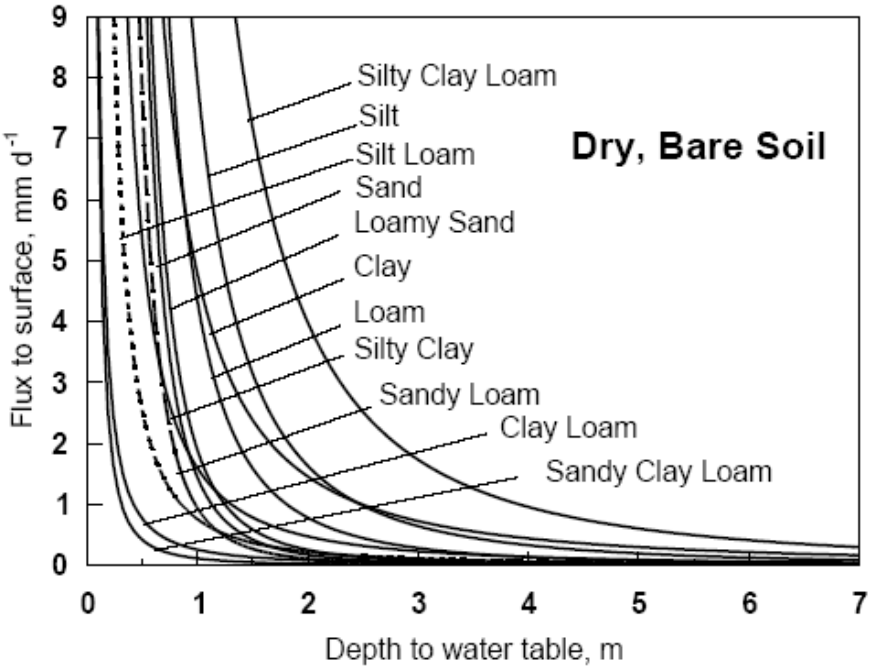

Fig. I.3. Estimated flux of water to the ground surface for evaporation as a function of depth to the water table for a variety of soil textures for a dry, bare soil condition, based on numerical simulations by the UPFLOW (Raes 2004) model.

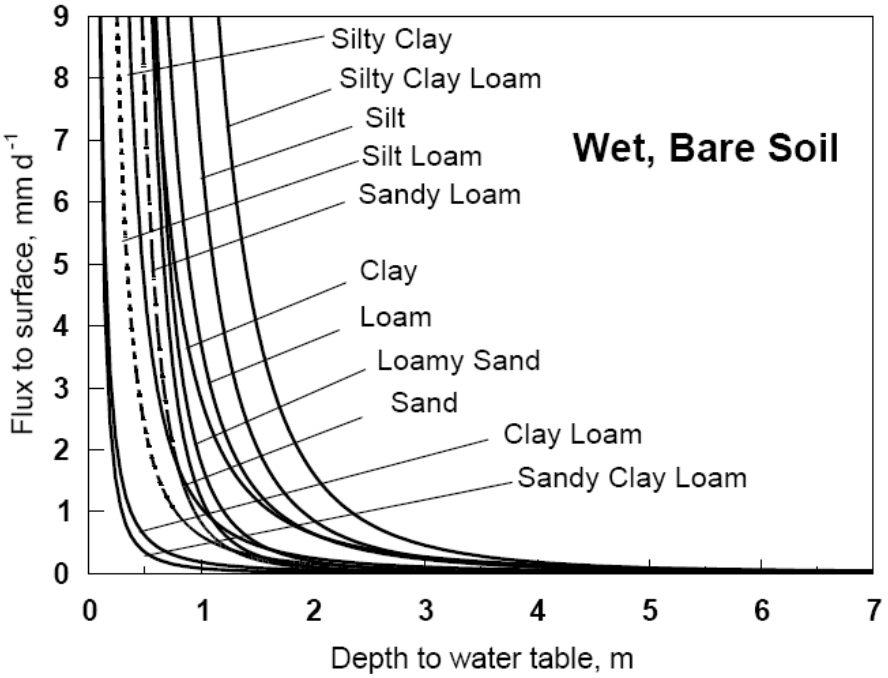

Fig. I.4. Estimated flux of water to the ground surface for evaporation as a function of depth to the water table for a variety of soil textures for a wet, bare soil condition, based on numerical simulations by the UPFLOW (Raes 2004) model.

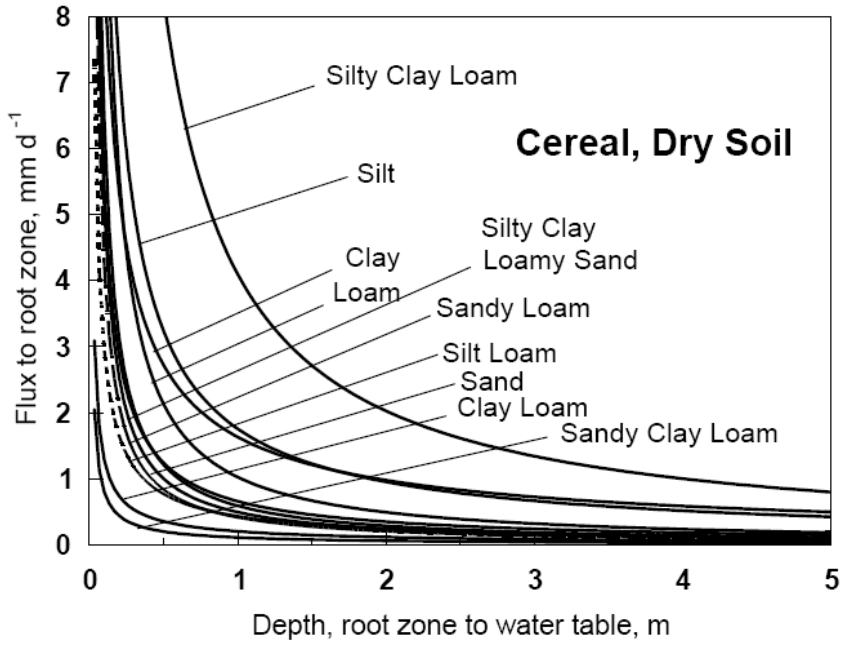

Fig. I.5. Estimated flux of water into the root zone as a function of depth from bottom of the root zone to the water table for a variety of soil textures for a cereal crop having relatively dry soil condition, based on numerical simulations by the UPFLOW (Raes 2004) model..

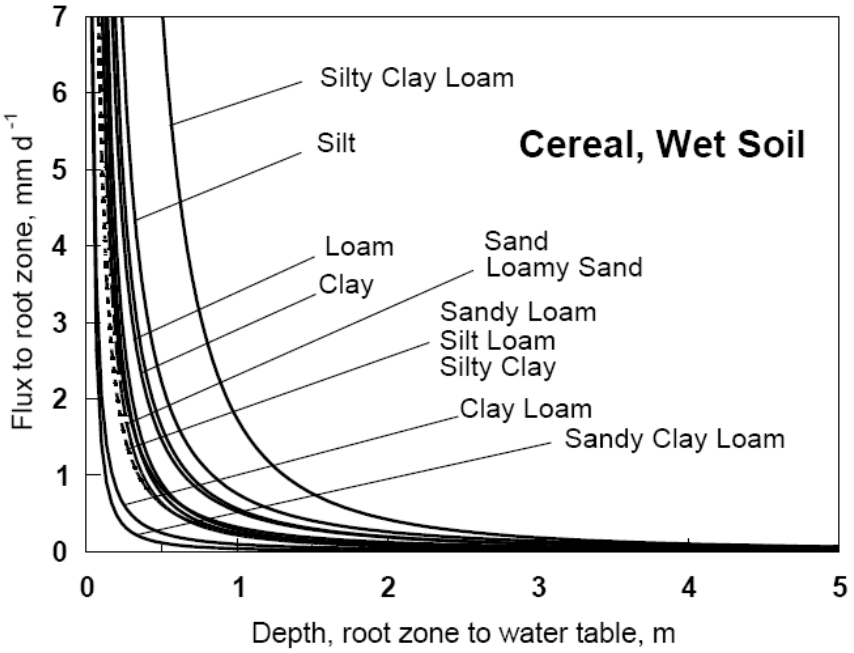

Fig. I.6. Estimated flux of water into the root zone as a function of depth from bottom of the root zone to the water table for a variety of soil textures for a cereal crop having relatively wet soil condition, based on numerical simulations by the UPFLOW (Raes 2004) model.

Table I.1 Regression parameters for the soil textures simulated in UPFLOW for a bare soil surface for dry and wet conditions along with assumed saturated hydraulic conductivities and soil water contents of the upper soil profile.

		Dry, bare soil				Wet, bare soil			
	k_s, m d^{-1}	θ_v	a_f	b_f	r^2	θ_v	a_f	b_f	r^2
Clay	0.05	44	4.77	-1.70	1.00	54	2.82	-2.13	1.00
Silty Clay	0.10	37	1.60	-1.73	0.99	49	1.07	-2.08	0.99
Clay Loam	0.08	28	0.27	-1.54	0.99	40	0.19	-1.70	0.99
Silty Clay Loam	0.11	30	16.50	-2.05	1.00	44	14.20	-3.12	0.98
Sandy Clay Loam	0.13	24	0.12	-1.81	0.99	33	0.09	-1.99	0.99
Silt	0.44	17	7.92	-2.27	0.99	32	6.80	-2.97	0.96
Silt Loam	0.18	19	0.76	-1.73	0.99	32	0.61	-1.94	0.97
Loam	0.25	20	4.32	-2.45	0.99	31	3.69	-2.52	0.99
Sandy Loam	0.38	14	0.94	-3.02	0.99	22	0.83	-3.19	0.99
Loamy Sand	1.05	10	1.89	-2.85	0.99	16	1.79	-3.16	1.00
Sand	1.20	8	1.44	-2.98	1.00	13	1.22	-3.48	1.00

Table I.2 Regression parameters for the soil textures simulated in UPFLOW for a cereal crop having 1 m root zone for dry and wet conditions along with assumed saturated hydraulic conductivities and soil water contents of the upper soil profile.

		Dry soil				Wet soil			
	k_s, m d^{-1}	θ_v	a_f	b_f	r^2	θ_v	a_f	b_f	r^2
Clay	0.05	44	1.63	-0.74	0.89	54	0.53	-1.47	0.68
Silty Clay	0.10	37	0.66	-0.91	0.88	49	0.32	-1.38	0.73
Clay Loam	0.08	28	0.21	-0.80	0.92	40	0.10	-1.32	0.79
Silty Clay Loam	0.11	30	4.10	-1.02	0.95	44	1.75	-2.04	0.75
Sandy Clay Loam	0.13	24	0.11	-0.86	0.90	33	0.04	-1.55	0.69
Silt	0.44	17	1.76	-0.88	0.85	32	0.76	-1.54	0.64
Silt Loam	0.18	19	0.43	-0.84	0.89	32	0.24	-1.33	0.75
Loam	0.25	20	1.03	-1.06	0.86	31	0.57	-1.53	0.70
Sandy Loam	0.38	14	0.42	-1.01	0.84	22	0.22	-1.55	0.74
Loamy Sand	1.05	10	0.59	-1.04	0.89	16	0.29	-1.63	0.72
Sand	1.20	8	0.50	-1.02	0.84	13	0.25	-1.62	0.75

Appendix J

Derivation of the Penman-Monteith equation

J.1 Introduction

It is useful to review the derivation of the PM equation to understand how it functions and some of the assumptions made in its development. There are two fundamental approaches to estimate evaporation (E) and evapotranspiration (ET). These are the surface energy balance equation and the aerodynamic equation. Each equation uses a different approach and each has difficulties for solution when using general weather data comprised of solar radiation, air temperature, vapor pressure, and wind speed. Penman (1948) combined these two approaches into the so-called combination or Penman equation that can be solved using standard weather data only. Monteith (1965) later improved on the Penman (1948) equation by including a surface resistance term and a more rigorous term for aerodynamic transfer. It is useful to review the combination of the two approaches.

J.2. Surface Energy Balance

The surface energy balance equation relates to the various ways in which net radiation energy from the sun and atmosphere is balanced at the surface by inputs or outputs of energy from non-radiative parameters. The vertical energy balance at the surface is the sum of sensible heat flux to or from the air and to or from the soil, along with latent heat flux, net radiation and other miscellaneous fluxes. The major components of the vertical energy balance are expressed as

$$R_n = G + \lambda E + H \tag{J.1}$$

where λE is the latent heat flux (positive during evaporation), G is conductive heat transfer into the soil (positive when heat is transferred downward in the soil), and H is the sensible heat exchange from the surface to air (positive if the air is warming). In (J.1), E (or ET) is expressed in terms of the energy required to convert the amount of liquid evaporated into vapor by multiplying by λ. The miscellaneous terms involved in the surface energy balance, such as heat storage within foliage, photosynthesis and respiration are generally insignificant relative to magnitudes of R_n, λE, H and G, and are commonly neglected. Under some conditions, change in heat storage in a canopy may need attention, especially in forest canopies. If R_n and sensible heat flux densities H and G can be measured or estimated reliably, then the latent heat flux density, λE, can be computed from (J.1) as follows

$$\lambda E = R_n - G - H \tag{J.2}$$

Eq. (J.2) is listed as Eq. (4.2) in Chapter 4. The challenge to the solution of (J.2) using standard weather data is in solving for H using commonly available weather data. The traditional aerodynamic expression for H is given as

$$H = \frac{\rho_a c_p (T_o - T_a)}{r_{ah}} \tag{J.3}$$

where T_o is surface temperature, T_a is air temperature and r_{ah} is the aerodynamic resistance to heat transfer between some mean height within the surface to some height a few m above the surface. Eq. (J.3) is listed as eq. 7.16 in chapter 7.

Eq. J.3 is analogous to Ohm's law for electrical current flow, where T_o and T_a are equivalent to voltages or potentials, r_{ah} is equivalent to an electrical resistor, and H is analogous to current. Thus, eq. J.3 behaves as a linear electrical circuit, so that if the difference between T_o and T_a is doubled, H will double. If resistance r_{ah} is halved (through a doubling of wind speed), then H will double.

The challenge of eq. J.3 and thus eq. J.2 is in the parameter T_o which is surface temperature. T_o can be measured using infrared thermometers if surface emissivity is known or it can be measured using a fine-thermocouple or other temperature sensor placed just beneath the surface skin. However, these measurements are not common due to the high operational and maintenance requirements of the instruments and difficulty in transfer of measured values to other locations and surface conditions, even those nearby.

The traditional equation for r_{ah} (reported earlier as eq. 7.20 in chapter 7 and eq. 8.3 in chapter 8) is given as

$$r_{ah} = \frac{\left(\ln\left(\frac{z_u - d}{z_{om}}\right) - \psi_m\right)\left(\ln\left(\frac{z_T - d}{z_{oh}}\right) - \psi_h\right)}{k^2 u_z} \tag{J.4}$$

where z_u is the height above the ground surface for the wind speed measurement, d is the zero plane displacement of the logarithmic wind profile, z_{om} is a roughness length governing the transfer of momentum from the surface, ψ_m is a correction factor for momentum transfer to account for instability or stability of the boundary layer, z_T is the height of the air temperature measurement above the ground surface, z_{oh} is an assumed roughness length governing the transfer of sensible heat from the surface, ψ_h is a correction factor for sensible heat transfer to account for instability or stability of the boundary layer, k is the von Karman constant [0.41], and u_z is the wind speed measured at the z_u height. Equations for estimating ψ_m and ψ_h are given in chapter 7. Eq. J.4 is sometimes criticized for it use of z_{oh}, commonly expressed as some fraction of z_{om}, whereas in reality the ratio of z_{oh}/z_{om} can vary substantially, especially for dry, sparse vegetation (Qualls and Brutsaert 1996). Other forms of eq. J.4 can be written that rely on differences in T_a at two different heights above the surface. These forms eliminate the need for z_{oh}, however, measurement of T_a at two heights is not common and it is challenging to produce an unbiased pair of measurements.

The aerodynamic-based expression for λE based on the surface to air vapor pressure gradient is given as

$$\lambda E = \frac{\lambda \rho_a \varepsilon (e_o - e_a)}{P(r_{av} + r_s)} = \frac{\rho_a c_p (e_o - e_a)}{\gamma (r_{av} + r_s)} \tag{J.5}$$

where ε is the mole ratio of water vapor to air [0.622], P is barometric pressure, e_o is vapor pressure "inside" the surface, for example inside a leaf stomatal cavity or beneath the soil skin, e_a is vapor pressure of the air at some z height above the ground surface, γ is the pyschrometric constant [eq. 3.11a], r_{av} is aerodynamic resistance to turbulent vapor transfer from the surface to some z height above the surface, and r_s represents any surface resistance to flow of vapor. Aerodynamic resistance r_{av} is computed exactly as for r_{ah}, i.e, using eq. J.4, except that z_T becomes z_v (height of vapor pressure measurement above the ground), z_{oh} becomes z_{ov}, which is an assumed roughness length governing the transfer of vapor from the surface, and ψ_h becomes ψ_v, a correction factor to account for effect of instability or stability of the boundary layer on vapor flow. Generally, $z_T = z_v$ (air temperature and humidity sensors are typically collocated at the same height), and z_{ov} is assumed equal to z_{oh} and ψ_v is assumed equal to ψ_h, so that r_{av} can be assumed equal to r_{ah}. As discussed in chapter 7, stability parameters ψ_v, ψ_h and ψ_m can generally be assumed to be close to zero when estimating ET from well-watered (moist) surfaces such as the grass and alfalfa covered reference surfaces.

As with eq. J.3, the aerodynamic vapor transfer equation is analogous to Ohm's law, where e_o and e_a are equivalent to voltages or potentials, r_{av} and r_s are equivalent to electrical resistors in series, and λE (vapor flux) is analogous to electrical current. Fig. J.1 is a schematic showing the relative locations of resistances r_a (or r_{ah} and r_{av}) and r_s, where r_s represents the internal resistance of the soil (if no vegetation) or of the soil, leaves and canopy in parallel.

Vapor pressure of air can be determined from coincident measurements of relative humidity and air temperature, which are commonly available, or from measurement of dewpoint temperature, also commonly available. Vapor pressure inside the soil or plant surface, on the other hand, is rarely measured, however, so that as with eq. J.2, eq. J.5 is challenging to apply in routine practice. Hence the need for the Penman or Penman-Monteith combination equation.

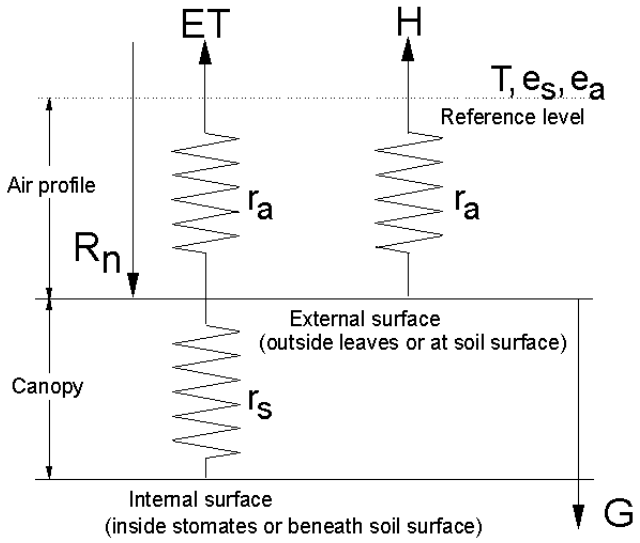

Fig. J.1. Schematic showing linkage between resistance terms in the PM equation relative to the surface and elevation of temperature and humidity measurements. One common shortcoming of this physical analogy is that the sources of heat and vapor must be at $d + z_{oh}$ (or $d + z_{ov}$), which might be explicitly invalid, particularly with taller vegetation like forests. A multiple-layer PM approach can be written (Choudhury and Monteith 1988), but the single layer PM may still be more functional (Raupach and Finnigan 1988).

To create the PM equation, one utilizes the Bowen ratio, which is simply the ratio between H and λE. Expanded into the equations for H and λE and written for transfer from inside the surface to the air above, one obtains

$$\beta = \frac{H}{\lambda E} = \frac{\rho_a c_p (T_o - T_a) \gamma (r_{av} + r_s)}{\rho_a c_p (e_o - e_a)(r_{ah})} \tag{J.6}$$

By cancelling similar terms and defining γ as in eq. 3.11a, one obtains

$$\beta = \frac{H}{\lambda E} = \gamma \frac{(T_o - T_a)\ (r_{av} + r_s)}{(e_o - e_a)\,(r_{ah})} \tag{J.7}$$

The energy balance equation can be written as

$$\lambda E = \frac{R_n - G}{1 + \beta} = \frac{R_n - G}{1 + \gamma \dfrac{(T_o - T_a)\ (r_{av} + r_s)}{(e_o - e_a)\,(r_{ah})}} \tag{J.8}$$

The next step in the derivation of the PM equation is to define the term Δ, which is defined as the slope of the saturation vapor pressure vs. temperature relation. The $e^o(T_a)$ function is based on T_a and describes the ability of air to hold more vapor as temperature increases. The slope Δ

of the $e^o(T_a)$ vs. T_a psychrometric curve that can be expressed as a linear approximation for a segment of the saturation curve between two temperatures T_o and T_a:

$$\Delta = \frac{e_o - e_s}{T_o - T_a} \tag{J.9}$$

where e_o, e_s, T_o and T_a were defined previously. Vapor pressure inside the surface, e_o, is assumed to be saturated and is therefore equivalent to $e^o(T_o)$. The e_s term is the saturation vapor pressure associated with T_a, so that $e_s = e^o(T_a)$. Using the relationship from eq. J.9 to define $(e_o - e_s) / \Delta = T_o - T_a$ and parsing $(e_o - e_s)$ into an equivalent expression of $(e_o - e_s) = (e_o - e_a) - (e_s - e_a)$ so that $T_o - T_a = [(e_o - e_a) - (e_s - e_a)] / \Delta$, this expression is substituted into eq. J.8 so that one obtains

$$\lambda E = \frac{R_n - G}{1 + \beta} = \frac{R_n - G}{1 + \frac{\gamma}{\Delta}\frac{\left[(e_o - e_a) - (e_s - e_a)\right]\,(r_{av} + r_s)}{(e_o - e_a)\,(r_{ah})}} = \frac{R_n - G}{1 + \frac{\gamma}{\Delta}\left[1 - \frac{(e_s - e_a)}{(e_o - e_a)}\right]\,\frac{(r_{av} + r_s)}{r_{ah}}} \tag{J.10}$$

We define one more temporary term, λE_a, following Penman (1948) as

$$\lambda Ea = \frac{\rho_a\, c_p\, (e_s - e_a)}{\gamma\, r_{ah}} \tag{J.11}$$

where λE_a is similar to eq. J.5, the aerodynamic expression for λE, except that r_s is omitted and $(e_o - e_a)$ is replaced with $(e_s - e_a)$. Term $(e_s - e_a)$ is known as the vapor pressure deficit (*VPD*) of the air, because it represents the difference between the saturation vapor pressure at air temperature $[e_s = e^o(T_a)]$ and actual vapor pressure of the air (e_a). Both e_s and e_a can be determined from commonly available humidity and air temperature data measured at some height above the surface, generally 1.5 to 2 m. It is important to note that λE_a is not a <u>real</u> vapor flux, but only a convenient temporary parameter. Dividing eq. J.11 by eq. J.5, and rearranging, one obtains

$$\frac{e_s - e_a}{e_o - e_a} = \frac{\lambda E_a}{\lambda E}\,\frac{r_{ah}}{r_{av} + r_s} \tag{J.12}$$

Eq. J.10 then becomes the following upon substitution of eq. J.12

$$\lambda E = \frac{R_n - G}{1 + \frac{\gamma}{\Delta}\left[1 - \frac{\lambda E_a}{\lambda E}\,\frac{r_{ah}}{r_{av} + r_s}\right]\,\frac{r_{av} + r_s}{r_{ah}}} \tag{J.13}$$

Rearranging eq. J.13 and setting $r_{av} = r_{ah}$, one obtains the resulting Penman-Monteith equation expressed as

$$\lambda E = \frac{\Delta\left(R_n - G\right) + \gamma\, \lambda E_a}{\Delta + \gamma\left(1 + \frac{r_s}{r_{ah}}\right)} \tag{J.14}$$

or, in its common form containing the vapor pressure deficit term as

$$\lambda E = \frac{\Delta(R_n - G) + \rho_a\, c_p\, (e_s - e_a)/r_{ah}}{\Delta + \gamma\left(1 + \frac{r_s}{r_{ah}}\right)} \tag{J.15}$$

The evaporation (E in mm s^{-1}) or evapotranspiration (ET in mm s^{-1}) rate is given as

$$E \text{ or } ET = \frac{\lambda E}{(\lambda\, \rho_w)} \text{ or } \frac{\lambda ET}{(\lambda\, \rho_w)} \tag{J.16}$$

where ρ_w is the water density [1.0 Mg m^{-3}], and λ is the latent heat of vaporization [~2.45 x 10^6 J kg^{-1} at 20°C] and where λE or λET are expressed in W m^{-2}.

The PM equation has the valuable advantage of requiring only commonly available weather data, namely solar radiation (used to calculate R_n), air temperature (used to calculate ρ_a, e_s and Δ), humidity data (used to calculate e_a and assist with R_n), and wind speed (for r_{ah}). G is generally estimated as a function of R_n. The surface resistance r_s is generally estimated as a function of amount of vegetation or amount of surface wetness, if the soil is wet. The PM equation (and historically the Penman equation where r_s is assumed zero and $1/r_{ah}$ is replaced by a simpler empirical "wind function") is widely used around the world as a standard means to estimate evaporation and evapotranspiration.

In practice, Δ is often calculated as the slope of $e^0(T)$ vs. T $\{\partial[e^o(T)]/\partial T\}$ at T_a only, since T_o is usually not known. This is generally acceptable for applying the PM equation to reference vegetation, since T_o is typically within a few degrees of T_a and thus little computational error occurs. However, in applications of the PM equation to sparse or water-stressed vegetation, T_o can exceed T_a by more than 10°C and therefore should be included in the computation for Δ. This can be accomplished using T_a only by iteratively (Budyko 1956) estimating λE using eq. J.15 (the PM equation) using $T_o = T_a$ for Δ the first iteration, but then estimating H from eq. (J.1) and T_o from an inversion of eq. J.3. Parameter Δ and λE are then recomputed using eq. (J.9) and J.15 and the process is repeated until estimates for T_o, Δ and λE are stable. This type of iterative process (using eq. J.15 or alternatively using eq. J.5 for λE) was described by Brown and Rosenberg (1971) and Paw U and Gao (1987). However, as illustrated in chapter 11, under conditions where values for T_o and T_a are substantially different, the user should also apply stability correction as described in chapter 7 and calculate outgoing long-wave radiation using T_o. With modern computing systems, the 'AFIB' method of eq. 11.2a-f can, in principle, replaces the need for iteration using the PM when values for T_o and T_a are substantially different. Other parameters in the PM equation are described in the main text.

Appendix K

Regional Estimating Methods and Methods Not Commonly Used in the USA

K.1 Introduction

Several methods for estimating evapotranspiration (ET) that have been used in the past were discussed in the first edition, but are not covered in detail in the second edition because they are no longer commonly used. However, because some studies and litigations may involve historical ET data calculated with methods not commonly used, the methods are briefly summarized in this appendix to preserve this information and to point to general references. Other methods, such as the 1982 Kimberly Penman method (Wright 1982) and CIMIS Penman method, have been used in specific regions of the USA.

K.2 Combination Methods

The classical form of the Penman equation (Penman, 1948, 1956, 1963) is:

$$ET = \left(\frac{\Delta}{\Delta+\gamma}(R_n - G) + K_u \frac{\gamma}{\Delta+\gamma}(a_w + b_w u_2)(e_s - e_a) \right) / (\lambda \rho_w) \qquad \text{(K.1)}$$

where R_n is net radiation and G is soil heat flux density into the ground in MJ m^{-2} t^{-1}, Δ is the slope of the curve relating saturation vapor pressure to temperature in kPa $°C^{-1}$, γ is the psychrometric constant in kPa $°C^{-1}$, K_u is a unit conversion factor typically in MJ m^{-2} t^{-1} kPa^{-1}, a_w and b_w are wind function coefficients, u_2 is wind speed in m s^{-1} at the 2 meter height, e_s is mean saturation vapor pressure at air temperature in kPa, e_a is actual vapor pressure of the air in kPa at height z, λ is the latent heat of vaporization in MJ kg^{-1}, and ρ_w is density of water in Mg m^{-3} (taken as 1.0 Mg m^{-3}). These units produce ET_{ref} with units of mm t^{-1}. Eq. K.1 can be applied to 24-hour data or to hourly (or shorter) data. Parameter K_u = 6.43 for ET in mm d^{-1} and K_u = 0.268 for ET in mm $hour^{-1}$. The a_w and b_w terms are empirical wind coefficients that have often received local or regional calibration and apply to a specific reference type of crop or surface.

1963 Penman Method

The values for a_w and b_w for the original Penman equation, first applied by Penman (1948) to open water and implicitly to grass, and later by Penman (1963) to clipped grass were a_w = 1.0 and b_w = 0.537, respectively, for wind speed in m s^{-1}, e_s - e_a in kPa and grass ET_o in mm d^{-1}. The equations were intended for use with daily computations. In application of the 1963 Penman, saturation vapor pressure is traditionally based on mean daily air temperature rather than on T_{max} and T_{min}.

Penman FAO-24

The FAO-24 publication by Doorenbos and Pruitt (1975, 1977) presented a modified Penman equation for estimating reference ET for grass, ET_o. The major modifications involved a more sensitive wind function than that used by Penman, and an adjustment factor "*c*" that is based on local climatic conditions. The assumption that G = 0 for daily periods was the same as Penman used. The vapor pressure deficit is calculated using saturated vapor pressure at mean air temperature minus saturation vapor pressure at dew point temperature when dew point temperature data are available or otherwise using saturation vapor pressure at mean air temperature times one minus mean relative humidity in percent [$e_a = e^o(T_{mean})(1 - RH_{mean})/100$].

The main differences between the original Penman equation and the 1977 FAO-24 combination method is that the FAO-24 Penman equation is multiplied by a factor, *c*, to adjust for the effect of differences in day and night weather conditions. In the format used in the FAO-24 manual, the FAO-24 equation is:

$$ET_o = c\left[\frac{\Delta}{\Delta+\gamma}(R_n - G) + \frac{\gamma}{\Delta+\gamma}2.7W_f\,(e^o{}_z - e_z)\right] \qquad \text{(K.2)}$$

in which the wind function W_f was defined as $W_f = (1 + 0.01\ u_2)$ for wind run in km d^{-1} and vapor pressure in kPa. In eq. K.2, R_n and G are in mm d^{-1} and ($e^o{}_z$ - e_z) in kPa is based on mean air and dew point temperatures. The factor *c* is based on daytime/nighttime wind ratio, U_d/U_n, maximum relative humidity, RH_{max}, solar radiation, R_s, and daytime wind speed (FAO-24, Table 16).

Frevert et al. (1983) expressed the adjustment factor (*c*) in FAO-24 Table 16 as a polynomial. Later, Cuenca (1987)[1] rounded the coefficients and terms while maintaining comparable accuracy.

$$c = 0.68 + 0.0028\,RH_{\max} + 0.018\,R_s - 0.068\,U_d + 0.013\,(U_d/U_n) + 0.0097\,U_d\,(U_d/U_n) \qquad \text{(K.3)}$$

where RH_{max} is in percent, R_s is in mm d^{-1} and U_d and U_n are in m s^{-1}. The term (U_d/U_n) is the day/night wind ratio defined as the mean ratio of daytime (7am – 7 pm) to nighttime (7 pm – 7 am) wind speed.

Evaluations of the FAO Penman method have indicated a tendency to over-estimate grass reference ET in semiarid and arid areas. Doorenbos and Pruitt (1977, p. 117) indicated a 15 to 20 percent over-estimation at Davis, California. Batchelor (1984) also indicated that the method may over-estimate ET in semiarid and arid areas. Pruitt (1984) and Pruitt et al. (1987a) indicated a need to adjust the ET_o estimates downward for most regions of California except in the hot, low-desert region.

1982 Kimberly Penman Method

The 1982 Kimberly Penman equation was developed from intensive studies of evapotranspiration at Kimberly, Idaho using measurements of full-cover alfalfa ET from precision weighing lysimeters (Wright and Jensen 1972; Wright 1981; Wright 1982; Wright

[1] Personal communication.

1988). The 1982 version of the method uses eq. K.1 with wind coefficients that vary with time of year. In addition, the coefficients used for computation of net radiation and the method to estimate 24-hour soil heat flux are unique to the Kimberly method.

The Kimberly Penman and associated wind functions are intended for application with 24-hour time steps ($K_u = 6.43$). The form and all units and definitions are the same as those in eq. K.1. The Kimberly wind function coefficients a_w and b_w for alfalfa vary with time of year and are computed for ET_r as (Wright 1987, pers. comm. and Jensen et al. 1990):

$$a_w = 0.4 + 1.4 \exp\left(-\left[\left(\frac{J - 173}{58}\right)^2\right]\right) \quad \text{(K.4)}$$

$$b_w = 0.605 + 0.345 \exp\left(-\left[\left(\frac{J - 243}{80}\right)^2\right]\right) \quad \text{(K.5)}$$

where J is the day of the year. For latitudes south of the equator, one should use J' in place of J, where J' = (J - 182) for J ≥ 182 and J' = (J + 182) for J < 182. The (e_s - e_a) term in the 1982 and 1996 Kimberly Penman equations is computed the same as for the standardized Penman-Monteith equation (e_s is computed at both daily maximum and daily minimum temperatures and averaged).

In the 1982 Kimberly Penman equation, net long wave radiation is estimated using eq. 4.39 and 4.40, which is similar to the ASCE-EWRI (2005) standardization, except that coefficients a_1, a and b are calculated using the following equations. Parameter a_1 for alfalfa at Kimberly (42 ^{o} N) was defined by Wright (1982) as:

$$a_1 = 0.26 + 0.1 \exp\left(-[0.0154\ (J - 180)]^2\right) \quad \text{(K.6)}$$

where J is the day of the year, and where J for the southern hemisphere is replaced with J' as described for eq. K.4 and K.5. Parameter $b_1 = -0.139$ in Wright (1982). Wright (1982) estimated a and b in eq. 4.40 as:

$$\begin{aligned} a &= 1.126 \quad and \quad b = -0.07 \quad for \quad R_s / R_{so} > 0.7 \\ a &= 1.017 \quad and \quad b = -0.06 \quad for \quad R_s / R_{so} \le 0.7 \end{aligned} \quad \text{(K.7)}$$

Wright (1982) estimated albedo as:

$$\alpha = 0.29 + 0.06 \sin\left[(J + 96) / 57.3\right] \quad \text{(K.8)}$$

where J is the day of the year, and where J for the southern hemisphere is replaced with J' as described for eq. K.4 and K.5.

Soil heat flux for 24-hour periods is estimated for the alfalfa reference of Wright (1982) using the difference between mean air temperature of the current day and the mean air temperature of the previous three days:

$$G_{24} = 0.38\left(T_{mean} - \sum_{i=1}^{3} T_{mean\ i} / 3\right) \quad \text{(K.9)}$$

where G_{24} is 24-hour soil heat flux in MJ m^{-2} d^{-1}, T_{mean} is mean air temperature on the current day and $T_{mean\ i}$ is the mean air temperatures of the previous three days. Equation K.9 may not estimate well under all conditions. In a study on 24-hour heat flux at Kimberly and Logan, Utah, Allen and Wright (unpublished research, 1996) found that using G=0 for 24-hour periods under alfalfa and grass produced less error relative to measured G than using Eq. K.9.

The CIMIS Penman Method.

Pruitt (Pruitt and Doorenbos 1977a) developed a_w and b_w for estimating grass ET_o for hourly periods for a clipped grass reference. These coefficients were adopted for standard ET_o estimation in the California Irrigation Management Information Service (CIMIS) by Snyder and Pruitt (1985) and Snyder and Pruitt (1992). The result is the "CIMIS" Penman ET_o equation where $a_w = 0.29$ and $b_w = 0.53$ for $R_n > 0$ and $a_w = 1.14$ and $b_w = 0.40$ for $R_n \leq 0$. These coefficients are applied hourly using eq. K.1 where ET_o = mm $hour^{-1}$, R_n = MJ m^{-2} $hour^{-1}$, and $K_u = 0.268$. The net radiation calculation as applied by CIMIS is similar to that by Dong et al.(1992) and is different than that of the standardized Penman-Monteith method described in chapter 4. Standard CIMIS calculations assume G = 0, even for hourly applications.

K.3 Radiation Methods

Turc Method

Turc (1961) simplified earlier versions of an equation for potential evapotranspiration (assumed to be ET_o) for 10-day periods under general climatic conditions of Western Europe. When expressed on a daily basis in mm d^{-1}, the equations are:

For RH > 50%

$$ET_o = 0.013\frac{T}{T+15}(R_s + 50) \quad \text{(K.10)}$$

For RH < 50%

$$\lambda ET_o = 0.013\frac{T}{T+15}(R_s + 50)\left(1 + \frac{(50 - RH)}{70}\right) \quad \text{(K.11)}$$

where T is the average temperature in °C, RH is daily mean relative humidity, %, and R_s is in cal cm^{-2} d^{-1}.

Makkink Method

The Makkink (1957) method is similar to the Turc method and is commonly used in Western Europe:

$$ET_o = 0.61 \frac{\Delta}{\Delta + \gamma} \frac{R_s}{2.45} - 0.12 \quad \text{(K.12)}$$

where ET_o is in mm d^{-1}, R_s is in MJ m^{-2} d^{-1}, and Δ and γ are as defined for the Penman equations [kPa °C^{-1}]. Constant 2.45 is latent heat of vaporization at approximately 20 °C.

The FAO-24 publication of Doorenbos and Pruitt (1977) included a radiation-based method similar to the Makkink equation:

$$ET_o = c \frac{\Delta}{\Delta + \gamma} \frac{R_s}{2.45} - 0.3 \quad \text{(K.13)}$$

where ET_o is in mm d^{-1}, R_s is in MJ m^{-2} d^{-1}, and Δ and γ are as defined for the Penman equations [kPa °C^{-1}]. Constant c was a calibration factor that was a function of mean daily relative humidity (RH_{mean}) and daytime wind speed (u_d). Doorenbos and Pruitt (1977) presented values for c in the form of tables. Allen and Pruitt (1991) developed a regression equation for c having the form:

$$c = 1.066 - 0.00128\ RH_{mean} + 0.045\ u_d - 0.0002\ RH_{mean} u_d - 0.0000315\ (RH_{mean})^2 - 0.001103\ (u_d)^2 \quad \text{(K.14)}$$

where RH_{mean} has limits $0 \le RH_{mean} \le 100\%$ and u_d has limits $0 \le u_d \le 10$ m s^{-1}.

Jensen-Haise Alfalfa-Reference Radiation Method

Jensen and Haise (1963) evaluated 3,000 observations of ET as determined by soil sampling procedures over a 35-year period. From about 100 values for well-watered crops with full cover in the Western USA, a linear relationship of a solar radiation coefficient and mean air temperature was apparent. From these data, the constants for the following linear equation were $C_T = 0.014$ and $T_x = 26.4$ for temperature in °F, and 0.025 and -3 for temperature in °C. R_s has the same units as λET_r.

$$\lambda ET_r = C_r (T - T_x) R_s \quad \text{(K.15)}$$

where ET_r is alfalfa reference ET as defined, C_r is a temperature coefficient and T_x is the intercept of the temperature axis. These coefficients were considered to be constants for a given area. Jensen (1966b) later defined C_r as:

$$C_r = \frac{1}{C_1 + C_2 C_H} \quad \text{(K.16)}$$

$$C_H = \frac{5.0}{(e_2 - e_1)} \quad \text{(K.17)}$$

where e_2 and e_1 are the saturation vapor pressures in kPa at the mean daily maximum and mean daily minimum temperatures, respectively, for the average warmest month of the year in an area, and C_1 and C_2 are constants (C_2 = 13 °F or 7.3 °C). Jensen et al. (1970) defined the coefficients in eq. K.16 and K.17 as follows for temperature in °C, elevation in m, vapor pressure in kPa, and C_2 =7.3 °C.

$$C_1 = 38 - (2\,Elev/305) \tag{K.18}$$

$$T_x = -2.5 - 1.4(e_2 - e_1) - Elev/550 \tag{K.19}$$

The long-term air temperatures for July, generally the warmest month, are used to determine the constants T_x , C_H , C_1 , and C_T (Burman et al. 1983).

Priestley-Taylor Method

Priestley and Taylor (1972) proposed a simplified version of the combination equation for use when surface areas generally are wet, which is a condition required for potential evaporation, E_p. The aerodynamic component was deleted and the energy component was multiplied by a coefficient, α = 1.26, when the general surrounding areas were wet or under humid conditions. The Priestley-Taylor equation provides estimates for no or low advective conditions. Therefore, if used without calibration (α = 1.26), the resulting estimates would be low for wet surfaces under arid conditions where the advection component of energy balance is significant. Basically, this equation is not valid without calibration in semiarid and arid areas. However, the method is still used for approximate comparisons under wet surface conditions and estimates of evaporation from water surfaces.

$$\lambda E = 1.26\,\frac{\Delta}{\Delta + \gamma}(R_n - G) \tag{K.20}$$

The Priestley-Taylor method is described in more detail in chapter 5 (eq. 5.2) and chapter 12 on regional ET estimation (eq. 12.1). Steiner et al. (1991) reviewed values for α under arid environments.

K.4 Temperature Methods

SCS Blaney-Criddle Method

The Blaney-Criddle procedure for estimating ET is well known in the western United States and has been used extensively throughout the world. The basic procedures were based on measurements of ET in the 1920s and 1930s, using primarily soil sampling techniques. Blaney and Morin (1942) first developed an empirical relationship between ET and mean air temperature, average relative humidity, and mean percentage of daytime hours. This relationship was later modified by Blaney and Criddle (1945, 1950, 1962) and Blaney et al. (1952) by excluding the humidity term. The original relationship was developed and intended for seasonal estimates. The basic assumption was that ET varies directly with the sum of the products of

mean monthly air temperature and monthly percentage of annual daytime hours for an actively growing crop with adequate soil moisture.

$$U = KF = \sum kf \tag{K.21}$$

As originally defined, U = estimated evapotranspiration (consumptive use) in inches for the growing period or season; K is an empirical consumptive use coefficient (irrigation season or growing period); F is the sum of monthly consumptive use factors, f, for the season or growing period ($f = tp/100$ where t = mean monthly air temperature in ^{o}F, and p = mean monthly percentage of annual daytime hours); and k = monthly consumptive use coefficient. The monthly percentages of daytime hours by latitudes as used by the USDA Soil Conservation Service was updated Martin and Gilley (1993) (table 2.18) for daily percent of annual daytime hours, and in their table 2A-1 for monthly percent of annual daytime hours for northern latitudes.

The monthly crop coefficients originally proposed for the Blaney-Criddle equation apparently represent both meteorological and crop effects. For Ladino clover, which would be similar to alfalfa, Pruitt (1960) determined that for conditions near Prosser, Washington, short period estimates could be improved by using $k = 0.04 + 5.52\ (tp/100)$ where p = daily percent of annual daytime hours and t is in ^{o}F.

The Soil Conservation Service (USDA, 1970) proposed a composite climatic and crop coefficient, $k = k_t k_c$ where $k_t = 0.0173t - 0.314$. However, k_c is not constant for a crop like alfalfa in midsummer, indicating that these modified k_c values also are not independent of climate (Pelton et al. 1960). For example, in a discussion of a paper by Quackenbush and Phelan (1965), Jensen (1966a) showed that after introducing the temperature coefficient, k_t, ($u = k_t k_c f = k_t k_c tp/100$) and separating the temperature and crop components ($k_t t/10$ and $k_c p/10$), the product $k_c p/10$ decreased from a maximum ratio in proportion to $R_s/R_{s(max)}$. This decrease was substantially greater than could be accounted for by the percent of daytime hours, p. Since in this case the crop coefficient represented grass, it indicated that the SCS k_c values still contained a meteorological component and that day length did not adequately compensate for radiation changes. The relative change in monthly $p/100$ at mid latitudes is not as great as the relative change in monthly potential solar radiation during spring and fall months.

FAO Blaney-Criddle Method

Doorenbos and Pruitt (1977) presented the most fundamental revision of the Blaney-Criddle method since its introduction. The FAO-24 Blaney-Criddle method requires the intermediate step of estimating a grass-related reference crop evapotranspiration, ET_o, prior to applying grass-related crop coefficients, $K_c(grass)$, to obtain crop ET. Earlier versions of the Blaney-Criddle method were not related to the use of reference crop ET.

After calculating ET_o, grass-related crop coefficients from FAO-24 or another source should be used to estimate crop ET. The FAO-24 Blaney-Criddle method is based on the general linear relationship found between measured reference ET and the Blaney-Criddle "f" factor for many world-wide sites that were investigated. By placing the data from these sites in various classifications based on ranges of daytime wind speed, minimum RH, and sunshine expressed as n/N, an expression for a was developed and a table of values for b was presented for use as follows:

$$ET_o = a + bf \tag{K.22}$$

$$f = p(0.46T + 8.13) \quad \text{(K.23)}$$

$$a = 0.0043\,RH_{\min} - n/N - 1.41 \quad \text{(K.24)}$$

where ET_o = grass reference ET in mm d $^{-1}$, p = mean daily percent of annual daytime hours, T = daily mean air temperature in ^{o}C, n/N is the ratio of possible to actual sunshine hours, RH_{min} is the minimum daily relative humidity in percent, and U_d is daytime wind at 2-m height (m s^{-1}). (Note: FAO-24, pages 3 and 110, gives $f = p(0.46\ T + 8)$, but the computer program listed uses $f = p(0.46\ T + 8.13)$ which is a more exact conversion from inches to mm. Doorenbos and Pruitt (1977) provided tables for b. Frevert et al. (1983), Allen and Pruitt (1991), Jensen et al. (1990) and Allen et al. (1998) provided an equation for calculating b as a function of RH_{min}, n/N and U_d, where U_d is the mean daytime (7 am to 7 pm) wind speed at 2 m height.

K.5 Pan Evaporation Methods

Pan evaporation data can be used to estimate reference ET using the following simple proportional relationship.

$$ET_o = k_p E_{pan} \quad \text{(K.25)}$$

where k_p is dependent on the type of pan involved and other factors. Several special methods described in the first edition of this manual such as that of Christiansen (1968) and Christiansen and Hargreaves (1969) are no longer commonly used. Pan evaporation data are still used to estimate evaporation from shallow lakes and some reservoirs, as described in Chapter 6. Use of E_{pan} as a reference is described in Chapter 8.

K.6 Other Methods of Estimating ET

Many methods for estimating ET were compared in Chapter 7 of the first edition of this Manual. Comparisons of several of the better known methods of estimating ET are presented in Appendix L. Appendix I includes tables summarizing the statistics and ranking for monthly estimates of ET at arid and humid locations for the methods compared.

K.7 References

Batchelor, J.F. (1984). "The accuracy of evapotranspiration estimated with the modified Penman equation. *Irrig. Sci.*, 5:223-233.

Blaney, H.F., and Criddle, W.D. (1945). "Consumptive use of water in the irrigated areas of the upper Colorado River Basin." (processed), 17 pp.

Blaney, H.F., and Criddle, W.D. (1950). "Determining water requirements in irrigated areas from climatological and irrigation data." *USDA Soil Conserv. Serv. SCS-TP 96*, (processed), 44 pp.

Blaney, H.F., and Criddle, W.D. (1962). "Determining consumptive use and irrigation water requirements." *USDA Tech. Bull 1275*, 59 pp.

Blaney, H.F., and Morin, K.V. (1942). Evaporation and consumptive use of water empirical formulas." *Am. Geophys. Union Trans.*, Aug. 76-83.

Blaney, H.F., Rich, L.R., Criddle, W.D., et al. (1952). "Consumptive use of water." *Trans. ASCE*, 117:948-967.

Burman, R.D., Cuenca, R.H., and Weiss, A. (1983). "Techniques for estimating irrigation requirements." pp. 335-394, *In*: Hillel, D. (ed), *Advances in Irrigation*, Vol. 2, Academic Press, New York.

Christiansen, J.E. (1968). "Pan evaporation and evapotranspiration from climatic data." *J. Irrig. and Drain. Div.*, 94:243-265.

Christiansen, J. E., and Hargreaves, G. H. (1969). "Irrigation requirements from evaporation." *Trans. Int. Comm. on Irrig. and Drain.*, Vol. III, 23.569-23.596.

Doorenbos, J. and Pruitt, W.O. (1975). "Crop water requirements." *FAO Irrigation and Drainage Paper No. 24*, Food and Agriculture Organization of the United Nations, Rome, Italy, l79 pp.

Doorenbos, J., and Pruitt, W.O. (1977). "Guidelines for predicting crop water requirements."*FAO Irrig. and Drain. Paper No. 24, 2nd ed.*, Food and Agriculture Organization of the United Nations, Rome, Italy, 156 pp.

Frevert, D.K., Hill, R.W., and Braaten, B.C. (1983). "Estimation of FAO evapotranspiration coefficients." *J. Irrig. and Drain.*, 109(IR2):265-270.

Jensen, M. E. (1966a). Discussion of "Irrigation water requirements of lawns." *J. Irrig. and Drain. Div.*, 92:95-100.

Jensen, M.E. (1966b). "Empirical methods of estimating or predicting evapotranspiration using solar radiation." pp. 57-61, *In*: *Proc. Conf. on Evapotranspiration*, Am. Soc. Agr. Eng. Chicago, Dec.

Jensen, M. E. and Haise, H. R. (1963). "Estimating evapotranspiration from solar radiation." *J. Irrig. and Drain. Div*., Am. Soc. Civ. Engr., 89:l5-41.

Jensen, M. E., Robb, D.C.N., and Franzoy, C.E. (1970). "Scheduling irrigations using climate-crop-soil data." *J. Irrig. and Drain. Div.*, 96:25-28.

Martin, D.L., and Gilley, J. (1993). "Irrigation Water Requirements." Chap. 2, Part 623, *National Engineering Handbook*, USDA, Soil Conservation Service, 284 pp.

Pelton, W. L., King, K. M., and Tanner, C. B. (1960). "An evaluation of the Thornthwaite and mean temperature methods for determining potential evapotranspiration." *Agron. J.*, 52:387-395.

Priestley, C.H.B. and Taylor, R.J. (1972). "On the assessment of surface heat flux and evaporation using large-scale parameters." *Monthly Weather Rev.* 100:81-92.

Pruitt, W.O. (1960). "Relation of consumptive use of water to climate." *Trans. of the ASAE*, 3(l):9-l3, l7.

Pruitt. W.O. (1984). "Procedures for development of ET_o maps for California." *Int'l. Comm. on Irrig. and Drain. Bull.*, 32(2):61-65.

Pruitt, W.O., Fereres, E., Kaita, K., and Snyder, R.L. (1987). "Reference evapotranspiration (ET_o) for California." *Agr. Exp. Sta. Bull. 1922*, Univ. of Calif, 16 pp. and 12 maps.

Quackenbush, T.H., and Phelan, J.T. (1965). "Irrigation requirements of lawns." *J. Irrig. and Drain. Div.*, 91:11-19.

Turc, L. (1961). "Evaluation des besoins en eau d'irrigation, evapotranspiration potentielle, formule climatique simplifice et mise a jour" (In French) English title: Estimation of irrigation water requirements, potential evapotranspiration: A simple climatic formula evolved up to date). *Ann. Agron.*, 12:13-49.

U.S. Dept. of Agric., Soil Conserv. Service. (1970). "*Irrigation water requirements.* Tech. Release No. 21, (Revised), 92 pp.

BLANK PAGE

Appendix L

Comparison and Ranking of Methods for Estimating ET

L.1 Methods Selected for Evaluation

Some of the methods for estimating ET not commonly used in the USA (Appendix K) that were compared and ranked in chapter 7 of the 1st edition may still be used when comparing estimates made with modern methods for special studies or when comparing estimates still being made for litigation purposes. Therefore, most of the methods compared in chapter 7 of the first edition are summarized in this appendix for documentation purposes (table L.1). Several methods that were compared have not been used extensively in the USA are not repeated in this appendix. These methods are: the FAO-PPP-17 Penman, the Businger-van Bavel, Thornthwaite, and the Christiansen pan evaporation methods.

All of the methods evaluated, with the exception of the SCS Blaney-Criddle, were defined by the originators to provide either an estimation of "potential evapotranspiration," which was not always defined, or ET for a specific well-watered reference crop whose leaf surfaces are typically not wet. A summary of the type of estimate intended by authors or originators of each method is presented in table L.2.

The length of period for which the methods are applicable was not always stated in the references. Applicable periods should be about the same as the data from which the various empirical coefficients in the methods were derived. Applications of the methods for shorter time periods may reduce their accuracy. A summary of applicable time periods recommended for each method is presented in table L.3. Those recommendations are based on the time periods used in deriving coefficients and the recommendations of the authors of this manual.

Methods that were evaluated and considered as typical were selected because they were in use at the time. Regression equations developed by Frevert et al. (1983) were used to estimate the adjustment factor "*c*" in the FAO-24 Corrected Penman method, "*b*" in the FAO-24 Radiation method, "*b*" in the FAO-24 Blaney-Criddle method, and k_p in the FAO-24 Pan method. Since completing these evaluations, Allen and Pruitt (1991) found the Frevert et al. (1983) regression equations to overestimate these coefficients by as much as 10-14 percent for some climatic conditions where maximum relative humidity is above 80 percent, solar radiation is above 10 mm d^{-1}, and U_d/U_n ratios are less than 2. The coefficient equations developed by Allen and Pruitt (1991) are recommended for computer calculations, or interpolations made from the FAO-24 tables and figures.

TABLE L.1 Classification of Estimating Methods and Principal References.

Classification	Method	References
Combination	Penman (1963)	Penman (1963), VPD-1 and VPD-3[1]
	1972 Kimberly-Penman	Wright and Jensen (1972)
	1982 Kimberly-Penman	Wright (1982)
	FAO-24 Penman (c = 1)	Doorenbos and Pruitt (1975, 1977)
	FAO-24 Corrected Penman	Doorenbos and Pruitt (1977)
	Penman-Monteith	Monteith (1965; Allen (1986); Allen et al. (1989)
Radiation	Jensen-Haise	Jensen and Haise (1963); Jensen et al. (1971)
	FAO-24 Radiation	Doorenbos and Pruitt (1977)
	Priestley-Taylor	Priestley and Taylor (1972)
	Turc	Turc (1961); Jensen (1966)
Temperature	SCS Blaney-Criddle	USDA (1970)
	FAO-24 Blaney-Criddle[2]	Doorenbos and Pruitt (1977); Allen and Pruitt (1986)
	Hargreaves-Samani	Hargreaves et al. (1985); Hargreaves and Samani (1985)
Evaporation Pan	FAO-24 Pan[2]	Doorenbos and Pruitt (1977)

[1] VPD-1 is based on saturation vapor pressure at mean air temperature minus saturation vapor pressure at dew point temperature. VPD-3 uses the mean saturation pressure at maximum and minimum air temperatures minus saturation pressure at mean dew point temperature determined early in the day.
[2] Regression equations by Frevert et al. (1983) were used to calculate the coefficients used in these equations.

TABLE L.2. Classification of Estimating Methods and Principal References.

Method	Type of estimate	Remarks
Combination:		
Penman (1963)	Potential ET	Short green crop completely shading the ground and never short of water.
1972 Kimberly-Penman	Alfalfa reference, ET_r	Full cover alfalfa at Kimberly, Idaho.
1982 Kimberly-Penman	Alfalfa reference, ET_r	Full cover alfalfa at Kimberly, Idaho.
FAO-24 Penman (c = 1)	Grass reference, ET_o	8-15 cm grass reference at various international locations.
FAO-24 Corrected Penman	Grass reference, ET_o	8-15 cm grass reference at (variable c) various international locations.
Penman-Monteith	Reference evaporation ET_r and ET_o	Reference type is dependent on surface roughness and canopy or bulk stomatal resistances used.
Radiation:		
Jensen-Haise	Alfalfa reference, ET_r	Reference crop is alfalfa (lucerne), well-watered, with 30-50 cm of growth. Coefficients derived from U.S.A. data.
FAO-24 Radiation	Grass reference, ET_o	8-15 cm grass reference at various international locations.
Priestley-Taylor	Large rainfed land areas following regional rains	Australia and USA.
Turc	Potential ET	Crop factor = 70, derived from western Europe data.
Temperature:		
Hargreaves-Samani	Grass reference, ET_o	8-15 cm clipped rye grass at Davis, CA.
SCS Blaney-Criddle	Evapotranspiration	Evaluated for alfalfa and from specific crop grass references using SCS crop coefficients and adjustment to negate effects of cuttings.
FAO-24 Blaney-Criddle	Grass reference, ET_o	8-15 cm grass reference from various international locations.
Pan:		
FAO-24 Pan	Grass reference, ET_o	8-15 cm grass reference from various international locations.

TABLE L.3 Recommended Minimum Time Periods for Various Estimating Methods.

Method	Recommended minimum time period	Remarks
Combination:		
Penman (1963)	Daily	
1972 Kimberly-Penman	Daily	
1982 Kimberly-Penman	Daily	
FAO-24 Penman (c = 1)	Daily	
FAO-24 Corrected Penman	Daily	
Penman-Monteith	Hourly or daily	Daily when using equations for approximate canopy resistance.
Radiation:		
Jensen-Haise	5 days	
FAO Radiation	5 days	
Priestley-Taylor	5 days	Regional evapotranspiration under wet surface conditions.
Turc	10 days	
Temperature:		
SCS Blaney-Criddle	Seasonal Monthly	Recommended by USDA-SCS. If locally calibrated.
FAO Blaney-Criddle	5 days	If only long term estimates of humidity, windspeed and sunshine data are available, the time period should be limited to monthly.
Hargreaves-Samani	10 days	
Pan:		
FAO Pan	5 days	

L.2 Locations and Data Selected for Evaluation

Data used to evaluate the various methods were selected from publications or obtained by personal communications with investigators working at locations where lysimeter data for well-watered grass or alfalfa were available along with adequate supporting climatic data. The evaluations were based on mean monthly and daily measured ET and all relevant climatic data. The sites selected ranged in elevation from 30 m below sea level to 2774 m above sea level. Latitudes ranged from 38°S at Aspendale, Australia to 56 °N at Copenhagen, Denmark and near the equator in Yangambi, Zaire. A description of the lysimeter sites, climates and locations is presented in table L.4. A description of the lysimeter vegetation types and general irrigation practices is presented in table L.5. The years of available data and principal references for each site are summarized in table L.6. In many cases it was necessary to estimate some climatic parameters or to obtain them from indirect sources such as the ESSA Climatological Atlas of the United States (U.S. Dept. Commerce,1968). The origin of data used in estimating ET for each site is summarized in table L. 7.

TABLE L.4 Climatic Description of Lysimeter Sites.

Site	Lat.	Elev., m	M[1]	T[2]	e[3]	R_s[4]	R_n[5]	Wind[6]
Aspendale	38° S	3	N	18	1.3	22.4	12.9	3.0
(Victoria, Australia)			J	23	1.7	28.6	18.5	3.0
			M	19	1.5	17.8	10.3	2.8
Brawley	34° N	-30	M	23	1.1	28.5	16.7*	1.7
(Imperial Valley, CA)			J	32	2.0	26.9	15.7*	1.5
			S	29	1.7	21.2	11.2	1.9
Copenhagen	56° N	28	M	11	0.9	17.6	8.9	4.2
(Denmark)			J	15	1.4	17.4	9.3	3.2
			S	14	1.2	10.8	3.7	3.9
Coshocton	40° N	360	M	17	1.3	16.2	9.7*	2.0
(Ohio)			J	22	2.0	17.7	11.2*	1.8
			S	19	1.7	13.6	7.7*	1.8
Davis	39° N	16	M	17	1.1	27.4	14.6	2.7
(California)			J	23	1.4	30.2	16.4	2.0
			S	20	1.2	21.1	9.8	2.2
Kimberly	42° N	1195	M	12	0.7	23.9	12.5*	3.2
(Idaho)			J	21	1.2	27.0	13.9*	2.2
			S	15	0.8	18.4	8.7	2.4
Lompoc	35° N	26	M	14	1.1	26.8	15.6*	2.0
(California)			J	16	1.3	28.4	17.0*	2.0
			S	17	1.3	21.7	11.9*	1.7
Scottsbluff	42° N	1280	M	- -	- -	- -	- -	- -
(Nebraska)			J	22	1.3	26.0	15.0*	2.3
			S	21	1.2	21.4	10.5*	1.9
Seabrook	39° N	37	M	17	1.2	20.2	9.5*	3.2
(New Jersey)			J	25	2.1	21.3	11.6*	3.2
			S	20	1.7	16.1	8.0*	3.6
South Park	39° N	2774	M	6	0.6	22.9	12.8*	2.7
(Colorado)			J	14	1.4	20.3	11.9*	1.6
			S	7	0.8	16.7	8.5*	1.9
Yangambi	0° N	474	N	25	2.3	17.3*	9.3*	1.0
(Zaire)			J	25	2.3	16.6*	8.0*	0.8
			M	26	2.4	17.8*	9.6*	0.9

* Estimated.

[1] Months represent May, July and September for N latitudes and November, January, and March for S latitudes.

[2] Mean air temperature, °C.

[3] Mean vapor pressure, kPa.

[4] Solar radiation, MJ m^{-2} d^{-1}.

[5] Net radiation, MJ m^{-2} d^{-1}.

[6] Extrapolated to a standard height of 2 m.

Evaporation pans at all sites were assumed to be Class A pans with at least 1000 m of green upwind fetch. Deviations from expected pan values were observed at several sites. The pan at Scottsbluff, Nebraska was located less than 4 m from adjacent fields of corn in the predominant wind direction during the period of measurement. This exposure likely reduced wind speed at the pan level and reduced evaporation from what would have occurred with an open setting recommended for common practice. The type of pan and exposure at Seabrook was unknown.

TABLE L.5 Lysimeter Vegetation and Management.

Site	Vegetative description	Irrigation
Aspendale	Clover and perennial rye grass maintained at 6 to 10 cm	Often daily
Brawley	Afalfa, harvested as hay. Weather measured over 12-cm grass	Normal commercial irrigation[2]
Copenhagen	Dense clover-grass maintained at 12 to 14 cm height	Watered on 30 mm soil water deficit
Coshocton	Grass-legume, harvested as hay Weather measured over 15 cm grass	Natural rainfall only[1, 2]
Davis	Perennial rye grass, 1959-63 Alta fescue grass, 1964-69 Mowed weekly to 10 cm	Watered on 50 percent depletion
Kimberly	Alfalfa, harvested as hay Weather measured over 12 cm grass	Normal commercial irrigation
Lompoc	Perennial rye grass, maintained at 6 to 15 cm	Weekly and sometimes longer
Scottsbluff	Alfalfa, harvested as hay	Normal commercial irrigation[2]
Seabrook	Clipped rye grass.	Daily by sprinkling
South Park	Native meadow, harvested as hay	Very shallow water table[1, 2]
Yangambi	*Brachiari Mutica* grass	Drainage lysimeter

[1] Periods of significant plant water stress were not used in developing the mean reference evapotranspiration curve for the site.

[2] Periods of regrowth after cutting were not used in developing the mean reference evapotranspiration curves for these sites.

TABLE L.6 Years of Data, Months per Year, and Principle Reference for Each Site.

Site	Years	Period	Mo/year	Principle reference
Aspendale	3	1959-61	12	McIlroy and Angus (1963, 1964)
Brawley	1	1971	8	LeMert (1972, 1973), and Pruitt (1986)
Copenhagen	11	1955-66	8	Jensen and Aslyng (1967)
Coshocton	3	1977-79	9	Harlukowicz (1984)
Davis	4	1959-63[1]	12	Pruitt (1971, personal communication)
	3	1967-69[2]		
Kimberly	3	1969-71	7	Wright (1985, personal communication); (1988)
Lompoc	4	-------	12	Nixon (1971, personal communication)
Scottsbluff	1	1977	4	Weiss (1981, personal communication)
Seabrook	10	1949-59	12	Yoshioka and Mather (1967)
South Park	1	1969	4	Kruse and Haise (1974)
Yangambi	1	1959	12	Bernard (1954), and Pruitt (1986, PC)

[1] Period of record used in monthly analysis.
[2] Period of record used in daily analysis.

TABLE L. 7 Origin of Data Used in Evaluating Estimating Methods.

Location	T	T_d[1]	u_z	R_a	R_{so}	R_s	R_n	G	d_a	n/N	L_d	P	El
Aspendale	P	P	P	E	C	P	E	E	E	P	E	P	P
Brawley	P	P	P	E	C	P	E	E	E	C	E	P	P
Copenhagen	P	P	P	E	C	P	P	P	P	P	E	P	P
Coshocton	P	P	P	E	C	P	E	E	E	P	E	P	P
Davis	P	P	P	E	P	P	P	E	E	P	E	P	P
Kimberly	P	P	P	E	P	P	E	E	E	C	E	P	P
Lompoc	P	P	P	E	C	P	E	E	E	C	E	P	P
Scottsbluff	P	P	P	E	E	P	E	E	E	E	E	C	C
Seabrook	C	C	C	E	C	C	E	E	E	C	E	P	P
South Park	P	P	P	E	C	P	E	E	E	C	E	P	P
Yangambi	P	P	P	E	E	P	E	E	E	E	E	-	P

P Indicates parameter found in principal publication for location;
E Indicates parameter estimated using procedures outlined in this chapter; and
C Indicates parameter taken from a climatological source such as the ESSA Climatological Atlas of the U.S. (ESSA, 1968).
[1] Dewpoint temperatures were often calculated from relative humidity data.

L.3 Calculating Climatic Parameters

Most methods of estimating evapotranspiration require the computation of parameters such as saturation vapor pressure, latent heat of vaporization, the psychrometric constant, etc. from climatic data. The methods used generally followed those described in chapters 3 and 4 and are not repeated here.

A summary of conversion factors for specific equations is presented in table L.8. No adjustments were made to equations for which no specific reference crop was specified in the literature (i.e., the Priestley-Taylor and Turc equations). Heights of lysimeter vegetation and heights for vegetation for weather station surfaces at each lysimeter site that were used in calculation of parameters for the Penman-Monteith equation are given in table L.9. These heights were based on ranges published with the original data or by personal communication, when available. Where no information concerning vegetation height was available, heights were estimated based on general cultural practices and climate in the area. The lysimeter locations where specific ranges of vegetation heights were unavailable and therefore required estimates were Scottsbluff, South Park and Yangambi. General ranges of heights and/or cutting dates were available for Brawley, Coshocton and Kimberly.

TABLE L.8 Coefficients used to Adjust Estimates of ET Obtained With Various Equations to Approximate the Reference Crop Grown in the Lysimeter[1].

Site	Alfalfa lysimeter	Grass lysimeter
Penman (1963) (original VPD method)	1.15	1.0
Penman (1963) (v. p. def. Meth. #3)	1.15	1.0
Kimberly Penman 1972	1.0	0.87
Kimberly Penman 1982	1.0	0.87
FAO-24 Penman	1.15	1.0
FAO-24 Corrected Penman	1.15	1.0
Penman-Monteith	1.0[2]	1.0[2]
Jensen-Haise	1.0	0.87
FAO-24 Radiation	1.15	1.0
Priestley-Taylor	1.0	1.0
Hargreaves-Samani	1.15	1.0
Turc	1.0	1.0
SCS Blaney-Criddle	1.22[3]	1.1[4]
FAO-24 Blaney-Criddle	1.15	1.0
FAO-24 Pan	1.15	1.0

[1] Values of 1.15 were used in the 1990 edition of Manual 70 to convert grass ET to alfalfa equivalent and 1/1.15 = 0.87 was used to convert alfalfa ET to grass equivalent. More recent study and analyses suggest that 1.2 to 1.3 is a more appropriate ratio of alfalfa ET to grass ET (Allen et al. 1989; ASCE-EWRI 2005).

[2] Vegetation heights and corresponding surface roughness and leaf area indices were set to specific values for each site (table L.9).

[3] Monthly values from the SCS Blaney-Criddle coefficient curve for alfalfa hay were multiplied by 1.22 to convert to an alfalfa reference.

[4] Monthly values from the SCS Blaney-Criddle coefficient curve for grass pasture were multiplied by 1.1 to convert to a grass reference (Doorenbos and Pruitt, 1977).

TABLE L.9 Vegetation Heights Used in Reference Estimates with the Penman-Monteith Method.

Location	Month	Lysimeter vegetation height, cm	Height of weather surface vegetation, cm
Aspendale	All	10	10
Brawley	4	25	12
	5	40	12
	6	45	12
	7	50	12
	8	50	12
	9	30	12
	10	25	12
	11	25	12
Copenhagen	All	12	12
Coshocton	3	7	7
	4	10	10
	5	25	15
	6	25	15
	7	25	15
	8	20	15
	9	20	15
	10	15	15
	11	10	10
Davis	All	12	7
Kimberly	4	25	12
	5	40	12
	6	60	12
	7	50	12
	8	40	12
	9	40	12
	10	20	12
Lompoc	All	9	9
Seabrook	All	12	12
Scottsbluff	6	50	50
	7	50	50
	8	45	45
	9	50	50
South Park	5	12	12
	6	35	35
	7	35	35
Yangambi	All	25	25

L.4 Alfalfa and Grass Reference ET Measurements and Estimates

Measurements of ET from both alfalfa and grass were commonly used to approximate the evaporative demand as represented by reference crop ET. Typically, ET from grass, ET_o, was expected to be only 80 to 87% of that from alfalfa, ET_r, under arid conditions. Grass is often adaptable to more diverse climates and locations than alfalfa, although there can be significant differences in grass ET due to differences in variety, season, and height. Hargreaves (1983) and Marsh et al. (1980) have noted differences in ET rates between warm and cool season grasses and between clipped and non-clipped surfaces. Wright (1988) noted differences in water use between alfalfa varieties at Kimberly, Idaho.

The lysimeter data sets included measurements of either grass or alfalfa ET. Therefore, the ET estimates provided by alfalfa reference equations needed to be adjusted to provide estimates for grass ET at the grass lysimeter sites, and ET estimates provided by grass reference equations needed to be adjusted to provide estimates for alfalfa at alfalfa sites to enable comparisons of all equations at all lysimeter sites. An approximate alfalfa to grass ET ratio of 1.15 was used to adjust ET_o estimates to ET_r values and vice versa at all lysimeter locations evaluated. This constant does not fully reflect differences in cultivars and crop heights or climatic parameters between locations, but the authors felt that the advantages of using this approximation outweighed the disadvantages.

A post-analysis of the same data sets by Allen et al. (1989) indicated that average ratios of ET_r to ET_o during the growing season months at the eleven lysimeter sites, computed with the Penman-Monteith equation with eq. 8.9 for r_s, ranged from 1.12 for humid, low wind conditions at Yangami, Zaire to 1.39 for windy conditions at Seabrook, New Jersey and averaged 1.32. The post-analysis indicates that an average ET_r/ET_o ratio of 1.2 to 1.25 may have been more representative of the eleven lysimeter sites evaluated. These adjustments have not been made in this second edition in order to preserve the original results from the first edition.

The SCS Blaney-Criddle method estimates were converted to an approximate, equivalent grass or alfalfa reference by multiplying the equation estimates by the appropriate SCS k_c value for either grass pasture or alfalfa hay (USDA, 1970). This product was then divided by a reference based coefficient to convert the pasture or hay ET value to the equivalent grass or alfalfa reference. In the case of a grass lysimeter reference, the SCS Blaney-Criddle grass pasture ET estimate was divided by the ratio of the FAO-24 coefficients for mean and peak pasture which is 0.91 (Table 23 of FAO-24, Doorenbos and Pruitt, 1977). In the case of an alfalfa lysimeter reference, the SCS Blaney-Criddle alfalfa hay ET estimate was divided by the mean alfalfa hay coefficient given in table 6.9 (1st edition) as 0.82. This coefficient is roughly equivalent to the ratios of FAO-24 coefficients for mean and peak alfalfa hay which are both 0.83 (Table 23 of FAO-24).

The SCS k_c curves for grass pasture and alfalfa hay were approximated using the following polynomials where J_r is a relative ratio of time within the calendar year, calculated for the Northern hemisphere as:

$$Jr = \frac{(M + D/30.5 - 1)}{12} \tag{L.1}$$

where M is the month of the year (1-12) and D is the day of the month (1-31). The polynomial equation used for the SCS k_c for alfalfa was:

$$k_c = 0.606 + 0.0552\ J_r + 10.29\ J_r^2 - 26.7\ J_r^3 + 24.0\ J_r^4 - 7.6\ J_r^5 \quad \text{(L.2)}$$

and the polynomial equation used for the SCS k_c for grass pasture was:

$$k_c = 0.472 + 0.273\ J_r + 8.53\ J_r^2 - 24.4\ J_r^3 + 24.3\ J_r^4 - 8.8\ J_r^5 \quad \text{(L.3)}$$

L.5 Comparative Analyses of Monthly and Seasonal ET Estimates

Comparisons of monthly ET estimates vs. lysimeter measured ET for all eleven lysimeter locations for each of the nineteen ET estimating methods and for measured pan evaporation were presented in fig. 7.56 through 7.75 of the first edition. The estimates were adjusted to represent the type of crop grown in the lysimeter (alfalfa or grass) using the factors listed in table L.8. Separate tables and statistics were presented for the peak months because the accuracy of these estimates is important in the design and operation of irrigation systems, in water rights determinations and regulation, and in allocating limited water supplies.

In this appendix, only ET estimates for each of the 16 methods expressed as percentages of the corresponding lysimeter-measured ET for peak ET months are presented (L.10) for each of the 11 lysimeter locations. The average relative values for peak ET months for arid locations and humid locations are presented near the bottom of table L.10 along with the overall average. A value of 100 indicates perfect agreement between the ET estimate and lysimeter ET, but one must bear in mind the impact of uncertainties in converting between the two reference types. The relative consistency of ET estimates by a method from location to location indicates the robustness of an estimating method in performance over a variety of climates.

The average of the peak ET estimates for the arid and humid locations in table L.10 indicates that most of the methods underestimated ET during peak months at the six arid locations and overestimated ET at the five humid locations.

Ratios of seasonal ET to seasonal lysimeter-measured expressed as percentages are presented in table L.11 for the 11 lysimeter locations and for the arid and humid locations. The average of the seasonal ET estimates for the arid and humid locations in table L.11 indicates that most of the methods also underestimated seasonal ET at the six arid locations and overestimated ET at the five humid locations.

L.6 Statistical Analyses of Monthly Estimates

Standard errors of estimate, *SEE*s, were calculated between ET estimates and lysimeter measurements according to the equation:

$$SEE = \left[\frac{\sum_{i=1}^{n} (Y_i - Y_{ei})^2}{n-1} \right]^{0.5} \quad \text{(L.4)}$$

where Y_i is the average *ith* month lysimeter ET, Y_{ei} is the corresponding ET estimate, and n is the total number of observations. The *SEE* is a measure of the differences between the measured

and estimated values and indicates how well each method estimated lysimeter ET measurements over all months of record at each location and over all locations. The *SEE*, as calculated with eq. L. 4 has units of mm d^{-1} and *n-1* degrees of freedom.

*SEE*s calculated for monthly ET estimates at each lysimeter location for all months and for peak months are presented in table L.12 (former table 7.14). These *SEE* values indicate the goodness of fit of ET estimates and lysimeter-measured ET without any adjustment or calibration. *SEE* values also indicate the performances to be expected by methods when used directly "off the shelf", i.e., directly from the principal publications listed in table L.1.

If the distribution of errors or differences between ET estimates and lysimeter measurements follow a normal distribution, then the *SEE* represents the maximum error in mm d^{-1} for 68 percent of all estimates by that method. Average *SEE*s for the various methods for all months over all locations ranged from 0.36 mm d^{-1} for the Penman-Monteith method to 1.34 mm day^{-1} for the pan evaporation method.

TABLE L.10 Average Peak[1] Monthly ET Estimates Expressed as Percentage of Lysimeter-measured ET

	Combination							Radiation				Temperature			Pan		
Location	Penman (1963)	Penman (1963) VPD3	1972 Kimberly Penman	1982 Kimberly Penman	FAO-24 Penman (c = 1)	FAO-24 Corrected Penman	Penman-Monteith	Jensen-Haise	FAO-24 Radiation	Priestley-Taylor	Turc	SCS Blaney Criddle	FAO-24 Blaney Criddle	Hargr. et al. (1985)	FAO-24 Pan	Pan evap	All methods[2]
Aspendale	93	98	98	103	105	122	82	71	98	81	74	75	82	82	89	111	92
Brawley	88	96	94	104	100	107	99	92	97	61	64	96	101	89	110	123	95
Copenhagen	123	126	127	129	149	158	100	61	143	104	116	139	160	133	92	115	123
Coshocton	107	111	104	112	116	127	107	79	107	102	93	126	109	117	118	141	111
Davis	99	110	106	116	110	130	97	105	114	87	88	86	115	102	101	124	106
Kimberly	88	95	93	101	100	111	98	95	109	64	67	93	104	90	101	110	95
Lompoc	130	134	124	131	133	160	103	79	146	133	118	89	116	100	137	165	125
Scottsbluff	83	87	88	92	94	96	98	73	98	57	59	79	94	66	64	74	81
Seabrook	99	104	106	111	118	126	93	74	103	81	83	121	116	98	61	76	98
South Park	89	96	90	98	98	106	102	101	96	86	71	84	82	119	105	125	97
Yangambi	93	97	86	79	97	106	90	99	105	95	100	132	87	132	86	100	99
Arid locations	89	96	95	102	101	111	96	87	102	70	69	86	97	88	94	109	93
Humid loc.	109	113	109	111	121	134	98	79	119	102	100	120	115	114	97	117	110
All locations	99	105	102	107	111	122	97	83	110	86	85	103	106	101	95	113	102

[1] Equation estimates have been adjusted for the reference crop of the lysimeter.

[2] Average of all equation estimates (excluding FAO-PPP-17, Businger-van Bavel, Thornthwaite, and Christiansen pan methods in former table 7.12).

TABLE L.11 Seasonal ET Estimates[1] Expressed as Percentage of Lysimeter-measured ET

	Combination							Radiation				Temperature			Pan		
Location	Penman (1963)	Penman (1963) VPD3	1972 Kimberly Penman	1982 Kimberly Penman	FAO-24 Penman (c = 1)	FAO-24 Corrected Penman	Penman-Monteith	Jensen-Haise	FAO-24 Radiation	Priestley-Taylor	Turc	SCS Blaney Criddle	FAO-24 Blaney Criddle	Hargr. et al. (1985)	FAO-24 Pan	Pan evap	All methods[2]
Aspendale	104	110	111	104	121	128	90	74	105	84	87	85	93	90	96	119	100
Brawley	96	104	102	100	108	112	100	95	99	66	65	98	102	90	118	129	99
Copenhagen	127	127	134	127	161	156	102	58	138	95	119	148	157	146	92	115	125
Coshocton	110	115	113	108	122	123	106	69	97	93	87	120	100	121	101	121	105
Davis	108	120	121	113	124	135	106	102	118	82	93	81	118	105	107	131	110
Kimberly	94	103	105	102	109	114	101	83	107	63	62	72	95	84	106	116	95
Lompoc	130	137	130	121	134	152	107	77	142	118	119	85	121	110	135	162	124
Scottsbluff	90	95	93	96	99	104	102	81	105	65	65	87	100	76	79	87	89
Seabrook	115	124	135	121	149	148	111	71	115	74	88	104	124	78	49	81	106
South Park	92	100	96	99	102	105	97	91	96	82	65	70	89	114	120	148	97
Yangambi	98	102	90	88	102	111	94	112	118	103	115	142	100	143	96	110	108
Arid locations	98	106	106	103	112	118	99	88	106	73	74	84	100	91	105	121	99
Humid loc.	114	120	118	110	129	135	104	82	122	97	105	117	116	125	95	114	113
All locations	106	113	112	107	121	127	101	85	114	85	90	101	108	108	100	118	105

[1] Equation estimates have been adjusted for the reference crop of the lysimeter.

[2] Average of all equation estimates (excluding FAO-PPP-17, Businger-van Bavel, Thornthwaite, and Christiansen pan methods in former table 7.13).

TABLE L.12 Standard Errors of Estimates[1] of seasonal ET vs. Lysimeter-measured ET[2] in mm d^{-1}

	Combination							Radiation				Temperature			Pan		
Location	Penman (1963)[3]	Penman (1963) VPD3	1972 Kimberly Penman	1982 Kimberly Penman	FAO-24 Penman (c = 1)	FAO-24 Corrected Penman	Penman-Monteith	Jensen-Haise	FAO-24 Radiation	Priestley-Taylor	Turc	SCS Blaney Criddle	FAO-24 Blaney Criddle	Hargr. et al. (1985)	FAO-24 Pan	Pan evap	All methods[4]
Aspendale	0.33	0.45	0.49	0.45	0.86	1.25	0.65	1.24	0.37	0.73	0.91	0.86	0.58	0.65	0.41	0.83	0.69
Brawley	0.97	0.94	1.11	0.57	1.14	1.47	0.44	0.72	0.97	3.23	3.29	1.96	0.64	1.08	1.65	2.62	1.43
Copenhagen	0.64	0.67	0.76	0.67	1.31	1.28	0.11	0.92	0.94	0.26	0.45	1.14	1.34	1.02	0.21	0.33	0.75
Coshocton	0.40	0.54	0.58	0.33	0.78	0.79	0.26	0.96	0.24	0.39	0.43	1.04	0.22	0.68	0.67	1.32	0.60
Davis	0.39	0.83	0.88	0.68	1.02	1.57	0.36	0.22	0.83	0.77	0.45	0.89	0.89	0.28	0.32	1.36	0.73
Kimberly	0.69	0.62	0.91	0.24	0.90	1.17	0.25	1.27	0.69	2.69	2.75	2.20	0.49	1.18	0.69	1.35	1.13
Lompoc	0.97	1.20	0.95	0.79	1.11	1.75	0.33	0.80	1.41	0.83	0.64	0.65	0.76	0.49	1.23	2.06	1.00
Scottsbluff	1.34	0.96	0.94	0.66	0.48	0.73	0.53	2.30	0.69	4.00	3.99	1.66	0.83	2.90	3.08	2.43	1.72
Seabrook	0.54	0.78	1.11	0.73	1.50	1.52	0.48	0.93	0.60	0.82	0.44	0.68	0.90	0.47	1.91	1.12	0.91
South Park	0.67	0.61	0.64	0.44	0.47	0.53	0.27	1.06	0.74	1.16	2.05	1.82	1.29	1.00	1.30	2.81	1.05
Yamgambi	0.24	0.23	0.41	0.52	0.24	0.44	0.32	0.52	0.67	0.26	0.60	1.79	0.33	1.54	0.34	0.45	0.56
Arid loc.	0.58	0.65	0.73	0.48	0.83	1.17	0.41	0.94	0.64	1.79	1.84	1.29	0.66	0.92	0.99	1.52	0.97
Humid loc.	0.57	0.71	0.75	0.59	0.99	1.17	0.31	0.76	0.81	0.55	0.49	1.05	0.71	0.86	0.88	1.17	0.77
All locations	0.57	0.57	0.67	0.49	0.65	0.65	0.36	0.71	0.59	1.02	1.07	1.15	0.64	0.88	0.88	0.87	1.01
Peak month arid	1.22	0.80	0.81	0.72	0.50	1.47	0.72	1.85	0.64	3.40	3.32	1.58	0.99	2.02	1.93	2.12	1.51
Peak month humid	0.84	0.96	0.83	1.09	1.34	2.02	0.37	1.27	1.33	0.99	0.75	1.35	1.26	1.02	1.60	1.98	1.19
Peak month all	0.95	0.77	0.72	0.79	0.84	1.53	0.52	1.44	0.88	2.34	2.26	1.31	0.98	1.47	1.58	1.82	1.26

[1] Values are standard errors of estimate for ET estimates that have not been adjusted by regression.

[2] Unless noted, all statistics are or monthly values over the entire season of record.

[3] Equation estimates have been adjusted for the reference type of lysimeter.

[4] Average of all equation estimates (excluding FAO-PPP-17, Businger-van Bavel, Thornthwaite, and Christiansen pan methods in former table 7.14).

L.7 Method Performance

Combination Methods

Estimates of ET using combination equation methods correlated well with lysimeter measurements at ten of the eleven sites. The exception was at South Park because of limited data. In general, the combination methods tended to overestimate reference ET. For the arid locations, the average percentage for seasonal estimates was 0.99 (table L.11). For the humid climates, the average percentage was 113 (table L.11). Much of this overestimation occurred during months of low ET since the average percentages for peak months were 93 and 110, respectively, for the arid and humid locations (table L.10).

All combination methods with the exception of the 1963 Penman method, which underestimated ET, and the FAO Corrected Penman, which overestimated ET, performed very well in estimating peak monthly ET in the arid locations. All combination methods with the exception of the Penman-Monteith equation generally overestimated ET during all months in the humid locations.

Methods Based Primarily Upon Solar Radiation

The Priestley-Taylor method is a simplification of the combination equation. It is the product of $\Delta/(\Delta + c)$, net radiation and a coefficient. The other radiation methods are based on the relationship between air temperature and ratio of ET/R_s. The radiation methods were nearly always in phase with the monthly measured ET. They produced reasonably good estimates of lysimeter ET in the humid locations with the exception of the Jensen-Haise method which tended to underestimate and the FAO-24 Radiation method which tended to overestimate ET. The Priestley-Taylor and Turc methods typically provided good estimates of both peak and seasonal ET in the humid climates. All radiation methods with the exception of the FAO-24 Radiation method substantially underestimated both peak and seasonal ET in the arid climates. The advection of sensible heat energy is taken into account by the aerodynamic term of the Penman equation, but is absent in the Priestley-Taylor and Turc equations.

Methods Using Primarily Air Temperature

Of the temperature methods, the SCS Blaney-Criddle method and Thornthwaite method (not included in the tables), were generally the poorest in estimating lysimeter ET of all methods evaluated. The SCS Blaney-Criddle typically underestimated reference ET in the arid climates and overestimated both peak and seasonal ET in humid climates.

The addition of other parameters to the FAO Blaney-Criddle temperature method improved its performance at the majority of locations. Both the Hargreaves-Samani and FAO Blaney-Criddle methods tended to overestimate ET by 15 to 25 percent in humid climates. The Hargreaves-Samani method tended to underestimate ET by about 10 percent in arid climates. The FAO Blaney-Criddle method provided good estimates of both peak and seasonal ET at the arid lysimeter locations. The temperature difference term, *TD*, in the Hargreaves-Samani method incorporates some additional effects of humidity and cloud cover. The Hargreaves-Samani method greatly overestimated ET in the humid, low radiation climate of Yangambi, Zaire.

Pan Evaporation Methods

The Christiansen (not included in the tables) and the FAO-24 pan evaporation methods were severely affected by apparently poor or non-representative measurements of pan evaporation. Some of the variation between pan evaporation ET estimates and lysimeter ET measurements is due to unavoidable differences in heat retention, surface roughness of the surrounding area, and variation in exposure of pans with time of season. It appears that poor performance of pan evaporation may have been due to problems in data collection and pan and site maintenance. For example, the evaporation pan at Scottsbluff, Nebraska was partially surrounded by tall field corn during much of the 1977 growing season. The tall crop would have reduced the wind speed over the pan and reduced the evaporation rate relative to the ET rate from alfalfa lysimeter. This is one of the disadvantages of the pan method, in that its performance is tightly controlled and affected by the consistency and care (or lack thereof) in pan operation and maintenance including site conditions.

L.8. Evapotranspiration Estimates by Location

Most of the empirical ET estimating methods evaluated were developed from data collected in temperate mid-latitudes and usually at relatively low elevations. Some of the methods behaved differently at the high elevation site of South Park, at the equatorial latitude of Yangambi, at the northern latitude of Copenhagen, and under the coastal climate found at Lompoc than they did in the low elevation, temperate sites in which they were developed. The consistency of any ET estimating method over a wide range of latitudes, elevations and humidity indicates the "robustness" of that method and its ability to represent the physical processes controlling ET.

A complicating factor when comparing methods at various sites is the effect of differences in data quality between locations. Data used in this study were not equally available for all locations and were not all of equal quality. Considerable effort was made to include only data sets from lysimeter and weather station locations for which information was available to indicate a high level of professional care and integrity in operation and maintenance of the site and in data reduction. The resulting data sets in the 1st edition of this manual were of improved quality as compared to data sets used in the original ASCE report (Jensen 1974).

Poor data quality tends to more heavily penalize the physically based methods, such as the Penman equation, which require more parameters (solar radiation, wind speed, air temperature and dewpoint temperature) as compared to single weather parameter methods, such as air temperature used in the Hargreaves-Samani method. Air temperature data tend to be of higher quality more of the time than the radiation or humidity data. Measuring mechanisms for air temperature are simpler and are standardized. Extra effort was made during the 1st edition study to include only those locations with good data integrity in all parameter measurements. However, the quality and accuracy of weather and lysimeter ET measurements are never known with complete confidence. As a result, some of the differences between locations in this comparison which appear to be associated with climate may actually be due to differences in data quality. Detailed discussion of estimates by location can be found in the first edition of this manual.

L.9. Ranking of ET Methods Using Monthly Estimates

Desirable characteristics sought in an evapotranspiration equation are accuracy in estimating peak ET requirements, accuracy in estimating seasonal ET requirements, and ability to accurately estimate ET in a variety of climates and locations. In addition, if methods overestimate or underestimate ET within a specific climate, then an additional attribute would be that the estimation errors be systematic and correctable using simple linear adjustments.

The standard error of estimate, *SEE*, as defined in eq. L. 4 was used to gage method accuracy and consistency in providing monthly reference ET estimates at the eleven lysimeter locations. Two *SEE* values were calculated; 1) the *SEE* of method estimates vs. lysimeter measurements; and 2) the *SEE* of method estimates adjusted using a coefficient based on a linear regression through the origin vs. lysimeter measurements, *ASEE*. The use of these two *SEE*s provided information on both accuracy of unadjusted ET estimates and ease with which the methods can be adjusted or "corrected" with a simple coefficient to fit location ET. The *SEE* values were calculated for all months, and for peak months.

Weighted *SEE*s were calculated by weighting seasonal values 70 percent and peak monthly values 30 percent. Within each of these two groupings, two-thirds (67 percent) weight was placed on the unadjusted *SEE* and one-third (33 percent) weight was placed on the *SEE* of regression-adjusted estimates. The resulting values of the weighted *SEE* indicate the ability of methods to accurately estimate ET during all months (47 percent weight), the ability to accurately estimate peak reference ET (20 percent weight) and the ability to be corrected using a linear multiplier (33 percent weight).

Summary statistics and ranking of ET methods over all eleven lysimeter locations are presented in table L.13. The Penman-Monteith equation with aerodynamic and canopy resistances estimated according to Allen (1986) and Allen et al. (1989) had the lowest *SEE* and highest correlation coefficients of all methods. Average standard errors of estimate for the Penman-Monteith method were 0.52 and 0.36 mm d^{-1} for peak months and all months, respectively over all eleven lysimeter locations.

The top five methods were forms of the combination equation, with the FAO-24 Radiation and FAO-24 Blaney-Criddle methods placing sixth and seventh. The 1982 Kimberly Penman (Wright 1982) was ranked second overall, with a standard error of estimate for peak months of 0.79 mm d^{-1} and standard error of estimate for all months of 0.53 mm d^{-1}. Use of the 1963 Penman equation with the vapor pressure deficit calculated as the average of deficits at maximum and minimum daily air temperatures (VPD #3) did not generally improve the performance of the original Penman equation and is therefore not recommended. The 1972 Kimberly Penman ranked fifth overall and produced relatively good estimates of peak monthly ET, but overestimated reference ET over all months by about 12 percent.

Weighted *SEE*s were similar for the third through seventh place methods, indicating fairly equal performances by these five methods in estimating both peak month and seasonal ET in all types of climates evaluated. The FAO-24 Radiation method was the best performing radiation method having a ranking of sixth place overall. This method overestimated ET by an average of 14 percent over all months, which reduced its ranking. The *SEE* by the FAO-24 Radiation method was much improved after adjustment by regression. The FAO-24 Blaney-Criddle method was the best performing temperature method over all locations, producing *SEE*s for peak months which were more than 30% lower than those for the Hargreaves-Samani method. It should be noted, however, that the FAO-24 Blaney-Criddle method required estimates of solar

radiation, wind speed and relative humidity, whereas, the Hargreaves-Samani equation required only measurements of minimum and maximum daily air temperature.

The correction term, *c*, in the FAO-24 Penman method tended to increase the overestimates with this method. The correction also increased the *SEE*s after adjustment by regression for peak months. About 3-5% of the overestimation would have been avoided by using the FAO-24 "*c*" table rather than the Frevert et al. (1983) equation. The FAO-24 Corrected Penman was ranked below the "uncorrected" FAO-24 Penman with *c* set equal to 1.0. The Jensen-Haise method, ranked ninth overall, had fairly high values of *SEE* for peak months, even after adjustment by regression (table L. 13). The Jensen-Haise method averaged about 15 percent low over all locations.

The SCS Blaney-Criddle method, adjusted to approximate a reference ET estimate produced *SEE*s which were 70 percent greater than those for the FAO-24 Blaney-Criddle method.

The two radiation methods (Turc and Priestley-Taylor) which ranked second and fourth when only humid locations were considered and ranked within the last two places when all locations were evaluated together. This result is due to the extreme underestimation by these two methods in areas with large daily vapor pressure deficits.

Table L.14 summarizes statistics and ranking of methods for daily estimates of ET at three locations having multi-year data sets of daily lysimeter and weather data. Rankings were similar to those for monthly calculation timesteps.

L.10 Summary

The comparisons that were made and reported in the 1st edition of Manual 70 were based on data available during the period of about 1959 through 1979. When considering the quality of lysimeter ET measurements and the associated climatic data, the analyses clearly showed that the better estimates of ET were made with methods that incorporated energy balance components. The best ET estimates were obtained when methods incorporated both energy balance and aerodynamic components (combination methods).

Since publication of the 1st edition in 1990, many studies have been made comparing methods of estimating ET. Those studies have provided more detail on the theoretical basis of the Penman-Monteith combination equation and its applications. Those studies also resulted in the development of a comprehensive publication prepared by an ASCE task committee entitled *The ASCE Standardized Reference Evapotranspiration Equation* (ASCE-IWR, 2005).

TABLE L.13 Summary of Statistics and Ranking of Methods for Monthly Estimates of ET at All Locations[1]

		All Months					Peak Month					Weighted
Rank	Method	%[2]	SEE[3]	b[4]	r[5]	ASEE[6]	%	SEE	b	r	ASEE	SEE[7]
(1)	(2)	(3)	(4)	(5)	(6)	(7)	(8)	(9)	(10)	(11)	(12)	(13)
1	Penman-Monteith	101	0.36	1.00	0.99	0.36	97	0.52	1.03	0.99	0.47	0.40
2	1982 Kimberly-Penman	107	0.53	0.95	0.98	0.49	107	0.79	0.96	0.98	0.73	0.59
3	Penman (1963)	106	0.57	0.99	0.97	0.57	99	0.95	1.07	0.96	0.81	0.67
4	Penman (1963), VPD #3	113	0.67	0.93	0.97	0.57	105	0.77	1.00	0.96	0.77	0.68
5	1972 Kimberly Penman	112	0.74	0.93	0.96	0.67	102	0.72	1.03	0.97	0.70	0.72
6	FAO Radiation	114	0.73	0.91	0.97	0.59	110	0.88	0.95	0.96	0.78	0.73
7	FAO-24 Blaney-Criddle	108	0.68	0.95	0.96	0.64	106	0.98	0.98	0.94	0.97	0.76
8	FAO-24 Penman (c = 1)	121	0.91	0.88	0.96	0.65	111	0.84	0.95	0.96	0.76	0.82
9	Jensen-Haise	85	0.84	1.11	0.95	0.71	83	1.44	1.15	0.92	1.06	0.95
10	Hargreaves et al. (1985)	108	0.88	1.00	0.93	0.88	101	1.47	1.07	0.87	1.39	1.05
11	FAO-24 Corrected Penman	127	1.16	0.82	0.96	0.65	122	1.53	0.86	0.93	1.00	1.10
12	FAO-24 Pan	100	0.92	0.94	0.92	0.88	95	1.58	1.03	0.82	1.57	1.11
13	SCS Blaney-Criddle	101	1.16	0.99	0.87	1.15	103	1.31	1.05	0.89	1.26	1.20
13	Pan Evaporation	118	1.34	0.82	0.92	0.87	113	1.82	0.88	0.83	1.56	1.35
14	Turc	90	1.30	1.20	0.89	1.07	85	2.26	1.31	0.84	1.49	1.46
15	Priestley-Taylor	85	1.29	1.22	0.90	1.02	86	2.34	1.28	0.78	1.72	1.48

[1] All equations were adjusted for the reference crop of the lysimeter (excluding FAO-PPP-17, Businger-van Bavel, Thornthwaite, and Christiansen pan methods in former table 7.20).

[2] Average percentage of lysimeter measurements.

[3] Standard error of the estimate or ET estimates in mm d^{-1} that have not been adjusted by regression.

[4] Regression coefficient (slope) for regression through the origin of lysimeter versus equation estimate.

[5] Correlation coefficient for regression through the origin of lysimeter versus equation estimate.

[6] Standard error of estimate for ET estimates in mm d^{-1} that have been adjusted by regression through the origin.

[7] Weighted standard error of estimated calculated as 0.7(Col. 4) + 0.33(Col. 7) + 0.3[0.67(Col. 9) + 0.33(Col. 12)].

TABLE L.14 Summary of Statistics and Ranking of Methods for Daily Estimates of ET at Kimberly, Idaho, Coshocton, Ohio, and Davis, California[1]

		All Months				Peak Month				Weighted
Rank	**Method**	**SEE[2]**	**b[3]**	**r[4]**	**ASEE[5]**	**SEE**	**b**	**r**	**ASEE**	**SEE[6]**
(1)	**(2)**	**(3)**	**(4)**	**(5)**	**(6)**	**(7)**	**(8)**	**(9)**	**(10)**	**(11)**
1	Penman-Monteith	0.77	0.98	0.92	0.75	0.70	1.04	0.80	0.66	0.74
2	1982 Kimberly-Penman	0.88	0.94	0.92	0.73	1.03	0.96	0.80	0.64	0.85
3	FAO-24 Blaney-Criddle	0.91	0.94	0.92	0.77	0.99	0.93	0.68	0.69	0.87
4	Penman (1963)	0.95	0.99	0.90	0.83	0.88	1.07	0.81	0.63	0.88
5	1972 Kimberly Penman	1.09	0.92	0.88	0.92	0.92	1.04	0.81	0.62	0.97
6	FAO-24 Penman (c = 1)	1.18	0.86	0.89	0.88	0.91	0.93	0.81	0.62	1.00
7	FAO- Radiation	1.10	0.89	0.89	0.89	1.23	0.91	0.70	0.77	1.05
8	FAO-24 Corrected Penman	1.22	0.84	0.91	0.79	1.34	0.87	0.80	0.65	1.09
9	Jensen-Haise	1.22	1.21	0.87	0.97	1.06	1.16	0.63	0.79	1.09
10	Hargreaves et al. (1985)	1.25	0.99	0.79	1.14	1.23	0.99	0.39	1.11	1.21
11	FAO- Pan	1.27	0.87	0.77	1.10	1.42	0.86	0.62	1.09	1.25
12	Priestley-Taylor	1.63	1.26	0.82	1.12	1.69	1.26	0.53	0.90	1.45

[1] All equations were adjusted for the reference crop of the lysimeter.
[2] Standard error of the estimate for ET estimates in mm d^{-1} that have not been adjusted by regression.
[3] Regression coefficient (slope) for regression through the origin of lysimeter versus equation estimates.
[4] Regression coefficient for regression through the origin of lysimeter versus equation estimates.
[5] Standard error of estimate for ET estimates in mm d^{-1} that have been adjusted by regression through the origin.
[6] Weighted standard error of estimated calculated as 0.7[0.67(Col. 3) + 0.33(Col. 6) + 0.3[0.67(Col. 7) + 0.33(Col. 10)].

L.11 References Excluded in the 2nd Edition

References cited in this appendix that are not in the main list of references are listed here. Many references cited in chapter 7 of the 1st edition were not included in the main list of references for this edition.

Allen, R.G. and Pruitt, W.O. (1986). "Rational use of the FAO Blaney-Criddle Formula." *J. Irrig. and Drain. Eng. Div.*, 112(IR2):139-155.

Bernard, E.A. and Frére, M. (1959). "L'etude evapotranspiration et climatologie du Congo Belgium." *L'institut national pour l'etude agonomique du Congo Belgium. Div. Climatologic*.

Environmental Science Service Administration, U.S. Dept. Com. (1968). *Climate atlas of the United States*. Environ. Serv. Adm., U.S. Dept. Com., U.S. Govt. Printing Office, Washington, D.C., 80 pp.

Frevert, D.K.; Hill, R.W. and Braaten, B.C. (1983). "Estimation of FAO evapotranspiration coefficients." *J. Irrig. and Drain. Eng.*, 109(IR2):265-270.

Hargreaves, G.H. (1983). "Discussion of `application of Penman wind function' by Cuenca, R.H. and Nicholson, M.J." *J. of Irrig. and Drain. Eng.*, 109(2):277-278.

Harlukowicz, T.J. (1984). "Weather and lysimeter data for Coshocton, Ohio." Personal Communication.

Jensen, S.E. and Aslyng, H.C. (1972). "Weather and lysimeter data for Copenhagen, Denmark." Personal Communication.

Kruse, E.G. and Haise, H.R. (1974). "Water use by native grasses in high altitude Colorado." *USDA ARS-W-6*. 59 pp.

LeMert, R.D. (1973). "Weather and lysimeter data for Brawley, California." Personal Communication.

Marsh, A.W., Strohman, R.A., Spaulding, S., Youngner, V., and Gibeault, V. (1980). "Turf grass irrigation research at the University of California: Warm and cool season grasses tested for water needs." *Irrig. J.*, July/August. pp. 20-21, 32-33.

McIlroy, I.C. and Angus, D.E. (1963). "The Aspendale multiple weighed lysimeter installation." *C.S.I.R.O. Div. Meteorol. Phys. Techn. Paper*, 14:27.

McIlroy, I.C. and Angus, D.E. (1964). "Grass, water and soil evaporation at Aspendale." *Agric. Meteorol.*, 1(3):201-224.

Nixon, P.R. (1971). "Weather and lysimeter data for Lompoc, California." Personal Communication.

Pruitt, W.O. (1986). Personal communication.

Turc, L. (1961). "Evaluation des besoins en eau d'irrigation, evapotranspiration potentielle, formule climatique simplifice et mise a jour" (in French). (English title: Estimation of irrigation water requirements, potential evapotranspiration: a simple climatic formula evolved up to date). *Ann. Agron.*, 12:13-49.

Weiss, A. (1981). "Weather and lysimeter data for Scottsbluff, Nebraska." Personal Communication.

Wright, J.L. (1986). "Variability in alfalfa growth, yield, and ET." Personal Communication.

Yoshioka, G.A. and Mather, J.R. (1967). "Influence of site and exposure evapotranspiration." *Factors of heat and water balance of different surfaces*, J.R. Mather (ed), Part I Analysis, Vol. 20(2), C.W. Thornthwaite and Assoc., Elmer, N.J, 253-266.

Appendix M

Glossary[1]

absolute humidity—Mass of water vapor per cubic meter.

adiabatic process—A reversible thermodynamic change of state of a system without the addition or removal of heat or mass.

advection—Horizontal transfer of heat energy by large-scale motions of the atmosphere.

aerodynamic—Refers to forces acting upon the soil or crop surface by moving air.

aerodynamically rough surface—A surface whose roughness elements are sufficiently large that the turbulent boundary layer reaches the surface.

aerodynamically smooth surface—A surface whose roughness elements are sufficiently small to be entirely embedded in the laminar sub-layer.

albedo—The ratio of electromagnetic radiation reflected from a soil and crop surface to the amount incident upon it. In practice, the value is applied primarily to solar radiation.

anemometer level—The height above ground at which an anemometer is exposed.

arid climate—Generally any extremely dry climate.

arithmetic mean— 1. (Also called mean, average, simple average.) Usually denoted by the symbol & is the sum of $x_1 + x_2 + .. + x_n$ divided by n. 2. Pertaining to a *random variable*, same as *expected value*.

bar—A unit of pressure equal to 10^6 dynes per cm^2, 100 kilopascals, 29.53 inches of mercury.

black body—A hypothetical "body" which absorbs all electromagnetic radiation striking it; a body which neither reflects nor transmits any of the incident radiation.

Bowen ratio—The ratio of energy flux upward as sensible heat to latent energy flux in the same direction (negative when the fluxes are in opposite directions).

BPI pan—A circular evaporation pan, 6 feet in diameter and 2 feet deep, made of unpainted galvanized iron. The pan is buried in the ground so that about 4 inches of the rim extend above the surrounding ground and the water surface is maintained at about ground level. (BPI stands for Bureau of Plant Industry, U.S.D.A., which introduced this instrument).

calorie—(Abbreviated cal) A unit of heat required to raise the temperature of 1 gram of water from 14.5 degrees Celsius to 15.5 degrees Celsius. The International Steam Table calorie equals 1.00032 cal (List 1984).

capillary fringe—A shallow zone of soil above a water table that is nearly saturated by capillary action in the smaller pore spaces.

Celsius—Same units as centigrade temperature scale.

class A pan—The U. S. Weather Bureau evaporation pan is a cylindrical container fabricated of galvanized iron or monel metal with a depth of ten inches and a diameter of forty-eight inches. The pan is placed on an open 2 x 4-inch wooden platform with the top of the pan about 41 cm (16 inches) above the soil surface. It is accurately leveled at a site which is nearly flat, well sodded, and free from obstructions. The pan is filled with water to a depth of eight inches, and periodic measurements are made of the changes of the water level with the aid of a hook gage set in the still well. When the water level drops to seven inches, the pan is refilled. Its average pan coefficient is about 0.7 for lake evaporation.

[1] The principle source for this glossary was the American Meteorological Society's Glossary of Meteorology (Huschke 1959). Additions were from various other sources.

consumed fraction—The fraction of water withdrawn from a surface or ground water source that is evaporated, transpired, incorporated into products or crops, consumed by humans or livestock, or otherwise removed from the immediate water environment.

consumptive use—That part of water withdrawn that is evaporated, transpired, incorporated into products or crops, consumed by humans or livestock, or otherwise removed from the immediate water environment (also referred to as water consumed). Water consumed may be defined as beneficial if there are economic or environmental benefits or non-beneficial if there are no direct economic or environmental benefits.

crop coefficient—The ratio of evapotranspiration occurring with a specific crop at a specific stage of growth to reference crop evapotranspiration at that time usually denoted by the symbol K_c (Not the same as K used in the Blaney-Criddle method).

Darcy's law—The law stating that the velocity of a fluid in permeable media is directly proportional to the hydraulic gradient.

crop water requirements—The depth of water needed to meet evapotranspiration of a disease-free crop, growing in large fields under nonrestricting soil conditions and achieving full production potential is a given growing environment.

day length—The length of day from sunrise to sunset expressed in hours.

deep percolation—The drainage of soil water by gravity below the maximum effective depth of the root zone.

depletion—Net rate of water use from a stream or groundwater aquifer for beneficial and non-beneficial uses. For irrigation or municipal uses, the depletion is the headgate or well-head diversion less return flow to the same stream or groundwater aquifer.

dew point—The temperature to which a given parcel of air must be cooled at constant pressure and at constant water vapor content until saturation occurs, or the temperature at which saturation vapor pressure of the parcel is equal to the actual vapor pressure of the contained water vapor.

diffusion—Turbulent diffusion results from atmospheric motions diffusing water vapor, heat and other gaseous components by exchanging parcels called eddies between regions in space in apparent random fashion.

duty of water—The total volume of irrigation water required to mature a particular type of crop. It includes consumptive use, evaporation and seepage from ditches and canals, and water eventually returned to streams by percolation and surface runoff (no longer in common use).

effective precipitation—Precipitation which remains on the foliage or in the soil that is available for evapotranspiration, and reduces the withdrawal of soil water by a like amount.

emissivity—The ratio of the emittance of a given surface at a specified wavelength and emitting temperature to the emittance of an ideal black body at the same wavelength and temperature. For energy balance computations under natural conditions, the emissivity is commonly taken as the ratio of the total emittance of a surface to the total emittance of an ideal black body.

enthalpy—In meteorology, enthalpy is sensible heat. In thermodynamics, it is the internal energy plus the product of pressure and volume.

evaporation—The physical process by which a liquid or solid is transformed to the gaseous state which in irrigation usually is restricted to the change of water from liquid to gas.

evapotranspiration—The combined processes by which water is transferred from the earth's surface to the atmosphere; evaporation of liquid or solid water plus transpiration from plants. (also see consumptive use).

extraterrestrial radiation—Solar radiation received "on top of" the earth's atmosphere (also known as exoatmospheric radiation).

Fahrenheit temperature scale—(Abbreviated F) A temperature scale with the ice point at 32° and the boiling point of water at 212°. Conversion of the temperature in Celsius (C) to temperature in °F = 1.8°C + 32.

fetch—(Also generating area) The length of fetch area, measured in the direction of the wind from the site in question.

flux density—The rate of flow of any quantity through a unit area of specified surface.

gas constant—The constant factor in the equation of state for perfect gases. The universal gas constant is **R** = 8.3144 joules mol^{-1} K^{-1}.

global radiation—The total of direct solar radiation and diffuse sky radiation received by a unit horizontal surface (essentially less than about 3 micrometers).

hydraulic conductivity - The proportionality factor in the Darcy flow law, which states that the effective flow velocity is proportional to the hydraulic gradient.

hydraulic head—The total of fluid pressure head and elevation with respect to a specified datum.

hydrostatic pressure—The pressure in a fluid in equilibrium which is due solely to the weight of fluid above.

insolation—(Contracted from incoming solar radiation). Solar radiation received at the earth's surface.

irrigation efficiency—The ratio of the volume of water required for a specific beneficial use as compared to the volume of water delivered for this purpose. It is commonly interpreted as the volume of water stored in the soil for evapotranspiration compared to the volume of water delivered for this purpose, but may be defined and used in different ways.

irrigation water requirements—The quantity of water exclusive of precipitation that is required for various beneficial uses, particularly evapotranspiration.

joule—The unit of energy or work done when the point of application of 1 newton is displaced a distance of 1 meter in the direction of force, 1 joule = 1 watt second.

laminar flow—A flow in which fluid moves smoothly in streamlines in parallel layers or sheets (non-turbulent flow).

langley—A unit of energy per unit area that was commonly used in radiation measurements which is equal to 1 gram calorie per square centimeter.

latent heat—The heat released or absorbed per unit mass of water in a reversible, isobaric-isothermal change of phase.

leaching requirement—The fraction of water entering the soil that must pass through the root zone in order to prevent soil salinity from exceeding a specific value.

leaf area index—The area of one side of leaves per unit area of soil surface, commonly abbreviated LAI.

logarithmic velocity profile—The variation of wind speed with height in the surface boundary layer. For rough surfaces the profile is: $u/u_* = 1/k \ln (z/z_o)^2$, $z \geq z_o$ where z_o is the constant related to the average height of the surface irregularities and is called the roughness length; u_* is the friction velocity; k is the von Kármán's constant and z is the elevation above the surface.

long-wave radiation—Electromagnetic radiation with a wave length greater than 0.8 micrometers. (For convenience, long-wave radiation is normally considered to include all wave lengths greater than solar radiation or essentially 3 micrometers).

micrometer—(Abbreviated μm) A unit of length equal to one-millionth of a meter, or one-thousandth of a millimeter.

millibar—(Abbreviated mb) A pressure unit of 0.1 kPa, and equal to one-thousandth of a bar. Atmospheric pressures are commonly reported in millibars, or in kilopascals.

mixing ratio—The ratio of the mass m_v of water vapor to the mass m_a of dry air with which the water is associated, $r = m_v/m_a$.

mole—A unit of mass numerically equal to the molecular weight of the substance.

net radiation—The difference of the downward and upward solar and long-wave radiation flux passing through a horizontal plane just above the ground surface.

neutral stability—The state of an unsaturated or saturated column of air in the atmosphere when its environmental lapse rate of temperature is equal to the dry-adiabatic lapse rate or the saturation adiabatic lapse rate respectively. Under such conditions, a parcel of air displaced vertically will experience no buoyant acceleration.

newton—The unit of force in the mkgs system of units; the force which gives to a mass of 1 kg an acceleration of 1 m/s^2.

non-consumptive use—That part of water withdrawn that is not evaporated, transpired, incorporated into products or crops, consumed by humans or livestock, or otherwise removed from the immediate water environment. Water withdrawn that is not consumed may be recoverable for further use or non-recoverable or lost to further use such as flows to saline sinks or flows to the sea.

pascal—The unit of pressure in the SI system; 1 pascal equals 1 newton per square meter.

potential evapotranspiration—The rate at which water if available would be removed from *wet* soil and plant surfaces expressed as the rate of latent heat transfer per unit area or an equivalent depth of water.

power-law profile—An alternative to the logarithmic velocity profile.

psychrometric chart—A nomograph for graphically obtaining relative humidity and dew point from wet and dry bulb thermometer readings.

pyranometer—A general name for actinometers which measure the combined intensity of incoming direct solar radiation and diffuse sky radiation.

radiation—The process by which electromagnetic energy is propagated through free space as distinguished from conduction and convection. (also see global, long-wave, net, short-wave, solar and thermal radiation).

random variable—A variable characterized by random behavior in assuming its different possible values. Mathematically it is described by its probability distribution which specifies the possible values of a random variable together with the probability associated with each value.

relative humidity—The dimensionless ratio of actual vapor pressure of the air to saturation vapor pressure, commonly expressed in percent.

Richardson number—A non-dimensional number associated with the shearing flows of a stratified fluid. $Ri = (g/T)(\partial T/\partial z)(\partial u/\partial z)^{-2}$.

saline soil—A non-alkali soil containing soluble salts in such quantities that they interfere with the growth of most plants.

saturated air—Moist air in a state of equilibrium with a plane surface of pure water or ice at the same temperature and pressure; i.e., air whose vapor pressure is the saturation vapor pressure and whose relative humidity is 100 %.

saturation deficit—(Also called vapor pressure deficit). The difference between the actual vapor pressure and the saturation vapor pressure at the existing temperature.

sensible heat—Same as enthalpy and is used in meteorology in contrast to latent heat.

short-wave radiation—A term used loosely to distinguish solar and diffuse sky radiation from long-wave radiation.

soil water—Water present in the soil pores (also called soil moisture which would include water vapor).

soil water tension—(Also called matric or capillary potential) The work that must be done per unit quantity of pure water to transport it from free water at the same elevation to soil water.

solar constant—The rate at which solar radiation is received outside the earth's atmosphere on a surface normal to the incident radiation. (0.0820 MJ m^{-2} per minute or 1.959 calories per cm^2 per minute, London and Frohlick, (1982); Science (1997), 277:1923-1924, 1367.5 W m^{-2} = 0.08205 MJ m^{-2} per min or 1.957 calories per cm^2 per minute; and Wilson (1997), 277:1963-1965.)

solar radiation—The total electromagnetic radiation emitted by the sun (see insolation).

specific heat—The heat capacity of a system per unit mass.

Stefan-Boltzmann law—One of the radiation laws which states that the amount of energy radiated per unit time from a unit surface area of an ideal black body is proportional to the 4th power of the absolute temperature of the black body $R = \sigma T^4$.

Stefan-Boltzmann constant, σ—$\sigma = 5.673 \times 10^{-8}$ J m^{-2} K^{-4} s^{-1}

$\sigma = 5.673 \times 10^{-8}$ W m^{-2} K^{-4}

$\sigma = 4.901 \times 10^{-9}$ MJ m^{-2} K^{-4} d^{-1}

stream depletion— see depletion.

surface tension—A phenomenon caused by a strong attraction towards the interior of the liquid action on liquid molecules in or near the surface in such a way to reduce the surface area. The tension that results is usually expressed in N per m.

thermal radiation—See long-wave radiation.

transpiration—The process by which water in plants is transferred as water vapor to the atmosphere.

triple point—The temperature and pressure at which a substance can exist in the liquid, solid and gaseous state.

triple point of water—The triple point of pure water is at 0.01 °C and 4.56 mm Hg (0.611 kPa) and is used to calibrate thermometers.

turbulence—A state of fluid flow in which instantaneous velocities exhibit irregular and apparently random fluctuations.

vapor pressure—The partial pressure of water vapor in the atmosphere.

water potential—The capability of soil water to do work compared with free water.

water storage changes—Changes in water storage include the effect of any flows of the same quality to or from ground-water aquifers or surface reservoirs.

water use—Water that is used for a specific purpose such as domestic use, irrigation, or industrial processing.

watt—Rate of doing work or expending power which gives rise to the production of energy at a rate of 1 joule per second.

wet bulb depression—The difference in degrees between the dry bulb temperature and the wet bulb temperature.

wet bulb temperature—The temperature an air parcel would have if cooled adiabatically to saturation at constant pressure by evaporation of water into it with all latent heat being supplied by the parcel.

withdrawal—Water abstracted from surface- or ground-water sources for any use.

zero plane displacement—An empirically determined constant introduced into the logarithmic velocity profile to extend its applicability to very rough surfaces or to take into account the displacement of a profile above a dense crop.

As of 05-September-2014

References

Note: in the final copy, repeated author names will be replaced with "——."

Abatzoglou, J.T. (2013). "Development of gridded surface meteorological data for ecological applications and modeling." *Int. J. Climatology* doi:10.1002/joc. 3413.

Aboukhaled, A., Alfaro, A., and Smith, H., (1982). "Lysimeters." *FAO Irrig. and Drain. Paper No. 39*, FAO, Rome, Italy, 68 pp.

Adams, E. E., Cosler, D. J., and Helfrich, K. R. (1990). "Evaporation from heated water bodies: Predicting combined forced plus free convection. *Water Res. Res.*, 5(3):425-435.

Allander, K.K., Smith, J.L., and Johnson, M.J. (2009). "Evapotranspiration in the Lower Walker River Basin, West-Central Nevada, Water Years 2005-07." *U.S. Geological Survey Sci. Inv. Rept 2009-5079*, 62 p.

Allaway, W.G., and Milthorpe, F.L. (1976). "Structure and functioning of stomata." pp. 57-102. *In*: Kozlowski, T.T. (ed). *Water Deficits and Plant Growth*, Academic Press, New York, Vol IV:57-102.

Allen, R.G. (1986). "A Penman for all seasons." *J. Irrig. and Drain. Eng.*, 112(4):348-368.

Allen, R.G. (1992). "*Evaluation of a temperature difference method for computing grass reference evapotranspiration*." Report submitted to Water Resources Development and Management Service Land and Water Development Division, UN-FAO, Rome, Italy. Revised January 8, 1993.

Allen, R.G., (1993b). "Error analysis of bulk density measurements for neutron moisture gauge calibration." pp1120-1127, *In:* Allen, R.G. (ed) *Management of Irrigation and Drainage Systems: Integrated Perspectives*. Proc., Nat'l Conf. on Drain. Eng., Park City, UT, July, 1223 pp.

Allen, R.G. (1996a). "Nongrowing Season Evaporation in Northern Utah." *Proc. N. Am. Water and Environ.Congr.*, ASCE, Annaheim, CA, 6 p.

Allen, R.G. (1996b). "Assessing the integrity of weather data for use in reference evapotranspiration." *J. Irrig. and Drain. Eng.*, 122(2):97-106.

Allen, R.G. (1997). "A self-calibrating method for estimating solar radiation from air temperature." *J. Hydrol. Engng*, ASCE 2(2):56-67.

Allen, R.G. (1998). "Predicting evapotranspiration demands for wetlands." ASCE Wetlands Engineering and River Restoration Conference Denver, Colorado March 20-29, 1998. 15 pp.

Allen, R. G. (2000). *REF-ET, Reference Evapotranspiration Calculator Version Windows 2.0*. Univ. of Idaho Res. and Ext. Center, Kimberly, ID, 82 pp.

Allen, R.G. (2004). "*Penman-Monteith Equation.*" Entry in the Encyclopedia of Soils in the Environment (manuscript no. 399). Elsevier Ltd., Oxford, U.K. © 2005 ISBN 0-12-348530-4, Vol. 3, p. 180-188.

Allen, R.G. (2005a). "*REF-ET, Reference Evapotranspiration Calculator, Version Windows 3.0*." Univ. of Idaho Res. and Ext. Ctr., Kimberly, ID. 93 pp.

Allen, R.G. (2005b). "Potential Evaporation." *Encyclopedia of Hydrological Science*. John Wiley and Sons Ltd, London. 6 p.

Allen, R.G. (2006). "Footprint Analysis to Assess the Conditioning of Temperature and Humidity Measurements by the Weather Station Vicinity." *Proc. ASCE-EWRI Water Resources Conference,* Omaha, NE, May 22-25. Published on CD-ROM, ASCE. 12 p.

Allen, R.G. (2008). "Quality assessment of weather data and micrometeorological flux - impacts on evapotranspiration calculation." *J. Agric. Meteorol.*, 64(4):191-204.

Allen, R.G. 2011. "Skin layer evaporation to account for small precipitation events—An enhancement to the FAO-56 evaporation model." *Agri. Water Mngmt*., 99(1):8-18.

Allen, R.G. (2012). "*REF-ET: Reference Evapotranspiration Calculation Software for FAO and ASCE Standardized Equations*." Users Manual. Univ. of Idaho. 86 p. http://extension.uidaho.edu/kimberly/files/2013/03/Ref-ET-V3.1-Users-Manual.pdf

Allen, R.G. (2013). "Algorithm to conditioning weather data collected in dry settings prior to calculation of reference crop evapotranspiration." *Ag. Water Man. (in prep.)*

Allen, R.G. and DeBruin, H.A.R. (2008). "Estimating net outgoing long-wave radiation from vegetation. in the Idaho RAPID study" Res. Rep., Univ. Idaho, Kimberly, Idaho. 27 p.

Allen, R.G., and Fisher, D.K. (1990). "Low-cost electronic weighing lysimeters." *Trans. of the ASAE*, 33(6):1823-1833.

Allen, R.G. and F.N. Gichuki. 1989. "*Effects of Projected CO2 - Induced Climatic Changes on Irrigation Water Requirements in the Great Plain States (Texas, Oklahoma, Kansas, and Nebraska). The potential effects of global climate change on the United States: Appendix C – Agriculture*," Vol.1, EPA-230-05-89-053, J.B. Smith and D.A. Tirpak, eds., U.S. Environ. Prot. Agency, Office of Policy, Planning and Evaluation, Washington, D.C., p 6/1-6/42.

Allen, R.G. and Neale, C.M.U. (eds). (1993). "*Management of Irrigation and Drainage Systems: Integrated Perspectives."* Proc., Nat. 1993 Conf. on Irrig. and Drain. Engrg., ASCE,Park City, UT, Jul. 21-23, 1223 pp.

Allen, R.G., and Pereira, L.S. (2009). "Estimating crop coefficients from fraction of ground cover and height." *Irrig. Sci.*, 28(1):17-34.

Allen, R.G., and Pruitt, W.O. (1986). "Rational use of the FAO Blaney-Criddle formula." *J. Irrig. and Drain. Engrg.*, 112(2):139-155.

Allen, R.G., and Pruitt, W.O. (1991). "FAO-24 reference evapotranspiration factors." *J. Irrig. and Drain. Engrg.*, 117(5):758-753.

Allen, R.G. and C.W. Robison. (2007). "Evapotranspiration and consumptive irrigation water requirements for Idaho." *Univ. of Idaho Rep.*, submitted to the Idaho Dept. Water Resources. 149 pp.

Allen, R.G. and M. Tasumi. (2004). "Evapotranspiration from Riparian Vegetation along the Middle Rio Grande Basin using METRIC™ ET Products." Rep. to Keller-Bliesner Engineering. Univ. of Idaho Kimberly Res. and Ext. Ctr. 18 p.

Allen, R.G. and Tasumi, M. (2005). "Evaporation from American Falls Reservoir in Idaho via a Combination of Bowen Ratio and Eddy Covariance." Proc. EWRI World Water Conference, Anchorage, AK (CD-ROM).

Allen, R.G. and J.L. Wright. (1997). "Translating wind measurements from weather stations to agricultural crops." *J. Hydrol. Engrg.*, 2(1): 26-35.

Allen, R.G., and Wright J.L. (2006). "Conversion of Wright (1981) and Wright (1982) alfalfa-based crop coefficients for use with the ASCE Standardized Penman-Monteith reference evapotranspiration equation." *Univ. of Idaho internal rept*, 38 p. (http://www.kimberly.uidaho.edu/water/asceewri/Conversion_of_Wright_Kcs_2c.pdf)

Allen, R.G., and Wright, J.L. (2007). "Conversion of Kimberly, Idaho crop coefficients to the ASCE standardized Penman-Monteith reference evapotranspiration basis." *In-house report, Univ. Idaho*, Kimberly, Idaho.

Allen, R.G., Bastiaanssen, W., Wright, J.L., Morse, A., Tasumi, M., and Trezza, R. (2002a). "Evapotranspiration from satellite images for water management and hydrological balances." *Q. 51, R. 2.10*, Int'l. Comm. on Irrig. and Drain., Montreal, July, 16 pp.

Allen, R.G., Brockway, C.E., and Wright, J.L. (1983). "Weather station siting and consumptive use estimates." *J. Water Resour. Plng. and Mgmt.,* 109(2):134-146.

Allen, R.G., Clemmens, A.J., Burt, C.M., Solomon, K., and O'Halloran, T. (2005c). "Prediction accuracy for project-wide evapotranspiration using crop coefficients and reference evapotranspiration." *J. Irrig. and Drain. Engrg,* ASCE 131(1):24-36.

Allen, R.G., Hill, R.W., and Vemulapali, S.. (1994c). "Evapotranspiration parameters for variably-sized wetlands." *Paper No. 942132*, presented at the 1994 Summer Meeting of the Am. Soc. of Agr. Engrs., 24 pp.

Allen, R.G., Howell, T.A., Pruitt, W.O., Walter, I.A., and Jensen, M.E. (eds). (1991b). "*Lysimeters for Evapotranspiration and Environmental Measurements*." Proc., Int'l. Symp. on Lysimetry, Am. Soc. Civ. Engrs., Honolulu, HI, July,

Allen, R.G., T.A. Howell and R.L. Snyder. (2011c). "*Irrigation Water Requirements."* Chp. 5, p. 93-172 in *Irrigation*, 6th ed., Stetson, L.E., and Mecham B.Q. (ed.), Irrig. Assoc., Falls Church, VA.

Allen, R.G., Irmak (Kilic), A., Trezza, R., Hendrickx, J.M. H., Bastiaanssen, W., Kjaersgaard, J. (2011). "Satellite-based ET estimation in agriculture using SEBAL and METRIC." Proc. 25(26):4011-4027.

Allen, R.G., Jensen, M.E., Wright, J.L, and Burman, R.D. (1989). "Operational estimates of evapotranspiration." *Agron. J.*, 81:650-662.

Allen, R.G., Kjaersgaard J., Garcia M., Tasumi M., Trezza R., 2008. "Fine-tuning components of inverse-calibrated, thermal-based remote sensing models for evapotranspiration." *Proc. 17th Pecora Conf. on the Future of Land Imaging*, Denver, Nov. 18-20, 11 p.

Allen, R.G., Morse, A., Tasumi, M., Trezza, R., Bastiaanssen, W., Wright, J.L., and Kramber, W. (2002b). "Evapotranspiration from a satellite-based surface energy balance for the Snake River plain aquifer in Idaho. pp. 167-178. *In*: *Burt, C.M., and Anderson, S.S. (eds)*, San Luis Obispo, CA, 9-12 July.

Allen, R.G., Pereira L.S., Howell T.A., Jensen M.E. (2011a). "Evapotranspiration information reporting: I Requirements for accuracy in measurement." Agric. Water Manage. 98(6): 899–920.

Allen, R.G., Pereira L.S., Howell T.A., Jensen M.E. (2011b). "Evapotranspiration information reporting: II Recommended Documentation." Agric. Water Manage. 98(6): 921–929

Allen, R.G., Pereira, L.S., Raes, D. and Smith M., (1994b). "An update for the calculation of reference evapotranspiration." *ICID Bulletin*, 43(2):35-92.

Allen, R.G., Pereira, L.S., Raes, D. and Smith M., (1998). "Crop evapotranspiration: Guidelines for computing crop water requirements." *Irrig. and Drain. Paper No. 56*, United Nations Food and Agriculture Organization, Rome, Italy, 300 pp.

Allen, R.G., Pereira, L.S., Smith , M., Raes, D. and Wright, J.L. (2005a). "FAO-56 dual crop coefficient method for estimating evaporation from soil and application extensions." *J. Irrig. and Drain. Engrg.,* ASCE 131(1):2-13.

Allen, R.G., Pruitt, W.O., Businger, J.A., Fritschen, L.J., Jensen, M.E., and Quinn, F.H. (1996). "Evaporation and Transpiration." Chap. 4, pp. 125-252 *In*: Wootton et al. (Task Com.), *ASCE Handbook of Hydrology, 2nd ed*" Am. Soc. Civ. Engrs., New York, NY., 784 pp.

Allen, R.G., Pruitt, W.O., and Jensen, M.E., (1991a). "Environmental requirements of lysimeters." pp. 170-181.3, *In*: R.G. Allen et al. (eds) *Lysimeters for Evapotranspiration and Environmental Measurements*, Am. Soc. Civ. Engrs., New York, 456 pp.

Allen, R.G., Pruitt, W.O., Raes, D., Smith, M. and Pereira, L.S. (2005d). "Estimating evaporation from bare soil and the crop coefficient for the initial period using common soils information." *J. Irrig. and Drain. Engrg.,* ASCE 131(1):14-23.

Allen, R.G., Pruitt, W.O., Wright, J.L., Howell, T.A., Ventura, F., Snyder, R., Itenfisu, D., Steduto, P., Berengena, J., Yrisarry, J.B., Smith, M., Pereira, L.S., Raes, D., Perrier, A., Alves, I., Walter, I., Elliott, R. (2006c). "A recommendation on standardized surface resistance for hourly calculation of reference ET_o by FAO56 Penman-Monteith method." *Agric. Water Manage.*, 81:1-22.

Allen, R.G., Smith, M., Perrier, A., and Pereira, L.S. (1994a). "An update for the definition of reference evapotranspiration." *ICID Bulletin.* 43(2):1-34.

Allen, R.G., Smith, M., Pereira, L.S., and Perrier, A. (1994b). "An update for the calculation of reference evapotranspiration." *ICID Bulletin*, 43(2):35-92.

Allen, R.G., Tasumi, M, and Trezza, R., (2005). "*METRIC Mapping Evapotranspiration at High Resolution*." Applic. Manual for Landsat Imagery, v. 2.0, Univ. of Idaho, 68 pp. + App. 1-12.

Allen, R.G., Trezza, R., and Tasumi, M. 2006a. "Analytical integrated functions for daily solar radiation on slopes." *Agric. and For. Meteorol.*, 139(1-2): 55-73.

Allen, R.G**.**, Trezza, R., and Tasumi, M. (2006b). "Analytical integrated functions for daily solar radiation on slopes for use in energy balance and evapotranspiration studies. *Agric. and For. Meteorol.*, 139:55-73.

Allen, R.G., Tasumi, M., and Trezza, R. (2007a). "Satellite-based energy balance for mapping evapotranspiration with internalized calibration (METRIC)—Model." *J. Irrig. and Drain. Engng.*, 133(4):380-394.

Allen, R.G., Tasumi, M., Morse, A., Trezza, R., Wright, J.L., Bastiaanssen, W., Kramber, W., Lorite, I., and Robison, C.W. (2007b). "Satellite-based energy balance for mapping evapotranspiration with internalized calibration (METRIC)—Applications." *J. Irrig. and Drain. Engng.*, 133(4):395-406.

Allen, R.G., Trezza, R., Tasumi, T. and Kjaersgaard, J. (2013). "METRIC^{tm} Mapping Evapotranspiration at High Resolution using Internalized Calibration Applications Manual for Landsat Satellite Imagery. *Ver. 2.0.8, Univ. Idaho, Kimberly, Idaho*, 250 p.

Allen, R.G., Vanderkimpen, P.J., and Wright, J.L. (1995). "Development of resistance parameters for operational application of the Penman-Monteith equation." Memo., Dept. Biol. and Irrig. Engrg., Utah State Univ., Logan, UT, 12 p.

Allen, R.G., I.A. Walter, R.L. Elliott, T.A. Howell, D. Itenfisu, M.E. Jensen, and R.L. Snyder.(eds), (2005a). *The ASCE Standardized Reference Evapotranspiration Equation*. Am. Soc. Civ. Engrs., 69 pp. +App. A-F and Index.

Allen, R.G., Walter, I.A., Elliott, R., Mecham, B., Jensen, M.E., Itenfisu, D., Howell, T.A., Snyder, R., Brown, P., Echings, S., Spofford, T., Hattendorf, M., Cuenca, R.H., Wright, J.L., Martin, D. (2000). "Issues, requirements and challenges in selecting and specifying a standardized ET equation." *Proc. 4th Nat'l. Irrig. Symp.*ASAE, Phoenix, AZ, Nov., 2000. 8 p.

Allen, R.G., Wright, J.L., Pruitt, W.O., Pereira, L.S. and Jensen, M.E. (2007c). "Water requirements." pp. 208-288, *In*: Hoffman, G.J., Evans, Evans, R.G., and Jensen, M.E. (eds), *Design and Operation of Farm Irrigation Systems*, Am. Soc. Agr. and Biol. Eng., St Joseph, MI.

Allen, L.H., Yocum, C.S., and Lemon, E.R. (1964). "Photosynthesis under field conditions. VII. Radiant energy exchanges within a corn crop canopy and implications in water use efficiency." *Agron. J/*, 56:253-259.

Altenhofen, J. (1985). "A modified atmometer for on-farm evapotranspiration determination." *In*: *Proc. Nat'l. Conf. Advances in Evapotranspiration*, Dec. 16-17, 1985, Chicago, Illinois. ASAE, St. Joseph, Michigan. pp.177-184.

Aluwihare, S., and Watanabe, K. (2003). "Measurement of evaporation on bare soil and estimating surface resistance." *J. Environ. Eng.*, 129(12):1157-1168.

Amatya, D.M., Skaggs, R.W., Cheschier, G.M. and Fernandez, G.P. (2000). "Solar and net radiation for estimating potential evaporation from three vegetation canopies." ASAE Proceedings Paper No: 002135, 20 p.

Amayreh, J.A. (1995). "*Lake Evaporation: A Model Study*." PhD Thesis, Irrig. Engrg., Utah St. Univ., 190 pp

Am. Soc. Agr. Engrs. (1985). "*Advances in Evapotranspiration."* Am. Soc. Agr. Engrs. Publ., 14-85, 462 pp.

Anderson, E.R. (1954). "Energy-budget studies." pp. 71-119, *In*: Water-Loss Investigations: Lake Hefner Studies, Tech. Rep., *Geological Survey Prof. Paper 269*, 170 pp.

Anderson, M.C., Allen, R.G., Morse, A. and Kustas, W.P. (2012) . "Use of Landsat thermal imagery in monitoring evapotranspiration and managing water resources." *Remote Sensing Environ.,* 122:50-65.

Anderson, M.C., Hain, C., Wardlow, B., Pimstein, A., Mecikalski, J.R. and Kustas, W.P. (2011). "Evaluation of drought indices based on thermal remote sensing of Evapotranspiration over the Continental United States." *J. Climate*, 24(8), 24(8):2025-2044.

Anderson, M.C., Norman, J.M., Diak, G.R., Kustas, W.P., and Mecikalski, J.R. (1997). "A time-integrated model for estimating surface fluxes using thermal infrared remote sensing." *Remote Sensing Environ*., 60: 195-216.

Anderson, M.C., Norman, J.M., Kustas, W.P., Li, F., Prueger, J.H., and Mecikalsi, J.R. (2005). "Effects of vegetation clumping on two-source model estimates of surface energy fluxes from an agricultural landscape during SMACEX." *J. Hydrometeorol.,* 6(12): 892-909.

Anderson, C.E., Johnson, H P., and Powers, W.L. (1978). "A water balance model for deep loess soils." *Trans. of the ASAE,* 21(2):314-320.

Angus, D.E. and Watts, P.J., (1984). "Evapotranspiration -- How good is the Bowen ratio method?" *Agr. Water Mgmt*., 8:133-150.

Anonymous, (1930). "Consumptive Use of Water in Irrigation." Prog. Rep., Duty of Water Comm., Irrig. Div., *Trans. of ASCE*, 94:1349-1399.

Anonymous, (1949). "Evaporation and transpiration." Chap. 4, *Hydrology Handbook*, Man. of Eng. Practice, No. 28, ASCE.

Anonymous. (1990). "Atmospheric radiation measurement program plan." *DOE/ER-0441*, U.S. Department of Energy, Washington, D.C.

Arkin, G.F., and Dugas, W. A. (1981). "Making weather and climate dependent crop management decisions." Computer Techniques and Meteorological Data Applied to Problems of Agriculture and Forestry: a Workshop, A. Weiss, (ed.), Dep. of Agric. Meteorol., Univ. of Nebr.-Lincoln, 223-237. [*Nat'l. Tech. Info. Serv., Accession No. PB82192436*, Springfield, VA.].

Arkin, G.F., and H.M. Taylor, eds., (1981). "*Modifying the Root Environment to Reduce Crop Stress*." Mono. No. 4, Am. Soc. Agr. Engrs., St. Joseph, MI, 419 pp.

Armijo, J.D., Twitchell, G.A., Burman, R.D., and Nunn, J.R. (1972). "A large undisturbed weighing lysimeter for grassland studies." *Trans. of the ASAE,* 5(5):827-830.

Aronson, L. J., Gold, A. J., & Hull, R. J. (1987). Cool-season turfgrass responses to drought stress. *Crop Science*, *27*(6), 1261-1266.

ASAE. (1985). "*Advances in Evapotranspiration*," Am. Soc. of Agr. Engr., Chicago, Dec. 16-17, 66 p.

ASAE, 1997. "Design and installation of surface irrigation runoff reuse systems." EP408.1 in *ASAE Standards 1997*.

ASABE (2004, R2009). "ASAE Engineering Practice 505: Measurement and Reporting Practices for Automatic Agricultural Weather Stations." Eng. Practice 505, St. Joseph, MI, 21 pp.

ASCE-EWRI. (2005). "*The ASCE Standardized Reference Evapotranspiration Equation*." Allen, R.G., Walter, I.A., Elliott, R.L., Howell, T.A., Itenfisu, D. Jensen, M.E., and Snyder, R.L.(eds), Am. Soc. Civ. Engrs., 69 pp. +App. A-F and Index.

ASTM, (1976). "*Standards for metric practice*." Am. Soc. for Testing Materials, ANSI/ASTM E #380-76, 37 pp.

Ashktorab, H., Pruitt, W.O., Paw, K.T. "Partitioning of evapotranspiration using lysimeter and micro-Bowen-ratio system*." J. Irrig. and Drain. Eng.*, 120(2):450-464.

Aubert, E.J., and T.L. Richards. (1981) "*IFYGLThe International Field Year for the Great Lakes*." Great Lakes Environmental Research Laboratory, Ann Arbor, MI, 410 pp.

Aubinet, M., Grelle, A., Ibrom, A., Rannik, U., Moncrie , J., Foken, T., Kowalski, A.S., Martin, P.H., Berbigier, P., Bernhofer, C., Clement, R., Elbers, J., Granier, A., Grunwald, T., Morgenstern, K., Pilegaard, K., Rebmann, C., Snijders, W., Valentini, R., and Vesala, T. (2000). "Estimates of the annual net carbon and water exchange of forests: The EUROFLUX methodology." *Adv. in Ecolog. Res.*, 30:113-175.

Ayers, R.S., and Wescot, D.W. (1985). "Water quality for agriculture." *Irrig. and Drain. Paper No. 29, rev. 1*," United Nations Food and Agric. Organ., Rome, Italy, 174 pp.

de Azevedo, P. V., da Silva, B. B., & da Silva, V. P. (2003). "Water requirements of irrigated mango orchards in northeast Brazil." *Agric. Water Manage.*, *58*(3), 241-254.

Bailey, B.J., Montero, J.I., Biel, C., Wilkinson, D.J., Anton, A., and Jolliet, O. (1993). "Transpiration of *Ficus benjamina*: comparison of measurements with predictions of the Penman-Monteith model and a simplified version." *Agr. and For. Meteorol.* 65:229-243.

Baldocchi, D.D., (2003). "Assessing the eddy covariance technique for evaluating carbon dioxide exchange rates of ecosystems: past, present and future." *Global Change Biol.*, 9:479-492.

Baldocchi, D.D., Hicks, B.B. and Meyers, T.P., 1988. "Measuring biosphere-atmosphere exchanges of biologically related gases with micrometeorological methods." Ecology, 69(5): 1331-1340.

Ball, R.A., Purcell, L.C. and Casey, S.K. (2004). "Evaluation of solar radiation prediction models in North America." *Agron. J.* 96:391-397.

Batchlelor, C.H. (1984). "The accuracy of evapotranspiration estimated with the FAO modified Penman equation." *Irrig. Sci.*, 5:223-233.

Bastiaanssen, W.G.M., Menenti, M., Feddes R.A., and Holtslag, A.A.M., (1998a). "The Surface Energy Balance Algorithm for Land (SEBAL): Part 1 formulation." *J. Hydrol*. 212-213: 198-212.

Bastiaanssen, W.G.M., Noordman, E.J.M., Pelgrum, H., Davids, G, Thoreson, B.P., and Allen, R.G., (2005). "SEBAL model with remotely sensed data to improve water resources management under actual field conditions." *J. Irrig. and Drain. Eng.*, 131(1):85-93.

Bastiaanssen, W.G.M., Pelgrum, H., Wang, J., Ma, Y., Moreno, J., Roerink, G.J., and van der Wal, T., (1998b). "The Surface Energy Balance Algorithm for Land (SEBAL): Part 2 validation." *J. Hydrol*. 212-213: 213-229.

Bausch, W.C., and Neale, C.M.U. (1987). "Crop coefficients derived from reflected canopy radiation: A concept." *Trans. ASABE*, 30(3):703-709.

Ben-Mehrez, M., Taconet, O., Vidal-Madjar, D., and Valencogne, C. (1992). "Estimation of stomatal resistance and canopy evaporation during the HAPEX-MOBILHY experiment." *Agr. and For. Meteorol.*. 58:285-313.

Bernacchi, C.J., Calfapietra, C., Davey, P.A., Wittig, V.E., Scarascia-Mugozza, G.E., Raines, C.A., and Long., S.P. (2003). "Photosynthesis and stomatal conductance responses of poplars to free-air CO_2 enrichment (POPFACE) during the first growth cycle and immediately following coppice." *New Phytologist*, 159(3):609-621.

Bernacchi, C.J., Kimball, B.A., Quarles, D.R., Long, S.P., and Ort, D.R. (2007). "Decreases in stomatal conductance of soybean under open-air elevation of [CO_2] are closely coupled with decreases in ecosystem evapotranspiration." *Plant Physiology*, 143(1):134-144.

Bernard, E. A. (1954). "Sur diverses consequences de la methode du bilan d'energie pour l'evapotranspiration des cultures ou des couvertures vegetales naturelles." *Ass. Int. d'Hydrologie Sei. Rome-Assembley*, *8*(161), 2.

Bertuzzi, P., Bruckler, L., Bay, D., and Chanzy, A.. (1994). "Sampling strategies for soil water content to estimate evapotranspiration." *Irrig. Sci.*, 14:105-115.

Black, J. N., Bonython, C. W., and Prescott, J. A. (1954). "Solar radiation and duration of sunshine." *Proc. Roy. Meteorol. Soc.*, 80:231-235.

Black, T.A., Gardner, W.R., and Thurtell, G.W. (1969). "The prediction of evaporation, drainage, and soil water storage for a bare soil." *Soil Sci. Soc. Am. Proc.,* 33:655-660.

Black, T.A., Thurtell, G.W. and Tanner, C.B. (1968). Hydraulic load cell lysimeter, construction, calibration and tests. *Soil Sci. Soc. Am. Proc.* 32:623-629.

Blaney et al. (1938). "Field methods of determining consumptive use of water." Nat'l. Cong. Cuban Engr. Proc. 4, 16 pp.

Blaney, H.F., and Criddle, W.D. (1945). "Determining water requirements in irrigated areas from climatological data." *Processed*, 17 p.

Blaney, H.F., and Criddle, W.D. (1950). "Determining Water Requirements in Irrigated Areas from Climatological and Irrigation Data." *USDA, SCS-TP-96*, 50 p.

Blaney, H.F., and Criddle, W.D. (1962). "*Determining Consumptive Use and Irrigation Water Requirements"*. USDA Tech. Bul. 1275, 59 pp.

Blaney, H.F., Ewing, P. E., Israelsen, O. W., and others, (1938). "*Regional planning, Part VI-Upper Rio Grande: Part III, Water Utilization*," Natl. Resour. Comm. pp. 293-428.

Blaney, H.F., and Morin, K.V. (1942). "Evaporation and consumptive use of water formulas." *Am. Geophys. Union Trans.*, pt.1:76-82.

Blaney, H.F., and Muckel, D.C. (1959). "Evaporation from water surfaces in California." *Calif. Dept. Water Resources Bull. 73*. 90 pp., plus map.

Blanken, P.D., and Black, T.A. (2004). "The canopy conductance of a boreal aspen forest, Prince Albert National Park, Canada." *Hydrologic Processes*, 18(9):1561-1578.

Boegha, E., Soegaarda, H., Thomsen, A., 2000. "Evaluating evapotranspiration rates and surface conditions using Landsat TM to estimate atmospheric resistance and surface resistance." *Remote Sens. of Environ.*, 79(2-3): 329-343

Bolsenga, S.J., and Vanderploeg, H.A. (1992). "Estimating photosynthetically available radiation into open and ice-covered freshwater lakes from surface characteristics; a high transmittance case study." *Hydrobiologia,* 1:243-244.

Boman, B.J. (1991). "Alfalfa ET measurements with drainage lysimeters." pp. 264-271 *In: Lysimeters for Evapotranspiration and Environmental Measurements*, R.G. Allen, T.A. Howell, W.O. Pruitt, I.A. Walter, and M.E. Jensen, (eds), Am. Soc. Civ. Engrs., New York, NY.

Bonachela, S., Orgaz, F., Villallobos, F.J,and Fereres, E. (1999). "Measurement and simulation of evaporation from soil in olive orchards." *Irrig. Sci.*, 18(4):205-211.

Bonachela, S, Orgaz, F., Villalobos, F.J., and Fereres, E. (2001). "Soil evaporation from drip-irrigated olive orchards." *Irrig. Sci.*, 20:65-71.

Bond, J.J. and Willis, W.O., (1970). "Soil water evaporation: First stage drying as influenced by surface residue and evaporation potential." *Soil Sci. Soc. Am. Proc.*, 34:924-928.

Boote, K.J. and Loomis, R.S. (ed.) (1991). "*Modeling Crop Photosynththesis—from Biochemistry to Canopy*." Proc. 1988 Symp. of Crop Sci. Soc. of Am. and Am. Soc. Agron. CSSA spec. publ. no. 19. 120 p.

Borrelli, J., Fedler, C.B., and Gregory, J.M. (1998). "*Mean Crop Consumptive Use and Free-Water Evaporation for Texas*." Dept. of Civ. Engng, Texas Tech Univ., 271 pp.

Borg, H. and Grimes D.W., (1986). "Depth development of roots with time: an empirical description." *Trans. of the ASAE* 29(1):194-197.

Bosveld, F.C., and Bouten, W. (2001). "Evaluation of transpiration models with observations over a douglas-fir forest." *Agr. and Forest Meteorol.*, 108(4):247-264.

Bouchet, R.J. (1963). "Evapotranspiration reele et potentielle, signification climatique." *Publ. 62*, pp. 134-142. General assembly Berkeley, *Int'l. Assoc. Sci. Hydrol.*, Gentbrugge, Belgium.

Bowen, I.S., (1926). "The ratio of heat losses by conduction and by evaporation from any water surface." *Physics Review*, 27:779-787.

Brenner, A.J., Incoll, L.D., 1996. "The effect of clumping and stomatal response on evaporation from sparsely vegetated shrublands." *Agric. and For. Meteorol.*, 84(3-4): 187-205.

Breuer, L.,Eckhardt, K., and Frede, H.G. (2003). Plant parameter values for models in temperate climates. *Ecological Modelling.* 169(2–3):237–293.

Briggs, L.J., and H.L. Shantz. 1916. "Hourly transpiration rate on clear days as determined by cyclic environmental factors." *J. Agr. Res.*, V(14):583-648.

Brisson, N. (1998). "An analytical solution for the estimation of the critical available soil water fraction for a single layer water balance model under growing crops." *Hydrology and Earth Sys. Sci.* 2(2-3):221-231.

Brisson, N., Itier, B., L'Hotel, J.C., and Lorendeau, J.V. (1998). "Parameterisation of the Shuttleworth-Wallace model to estimate daily maximum transpiration for use in crop models." *Ecological Modelling*, 107(2-3):159-169.

Bristow, K.L., and Campbell, G.S. (1984). "On the relationship between incoming solar radiation and daily maximum and minimum temperature." *Agr. and For. Meteorol.*, 31:159-166.

Brochet, P. and Gerbier, N. (1972). "Une méthode pratique de calcul de l'évaporatranspiration potentielle. " *Ann. Agron.* 23(1):31-49.

Broner, I. (1993). "Irrigation scheduling with atmometers. " *Colo. State Univ. Crop Series*, 4.706 (5 p.).

Broner, I. and Law, R.A.P. (1991). "Evaluation of a modified atmometer for estimating reference ET. " *Irrig. Sci*. 12(1):21-26.

Brooks, R.H., and Corey, A.T. (1966). "Properties of porous media affecting fluid flow." *J. Irrig. and Drain. Div.*, 92(IR2):61-88.

Brown, P.W. (2001). Personal communication.

Brown, P.W., Mancino, C.F., Young, M.H., Thompson, T.L., Wierenga, P.J., and Kopec, D.M. (2001). Penman Monteith crop coefficients for use with desert turf systems. *Crop Sci*., 41:1197-1206.

Brown, K. W., & Rosenberg, N. J. (1971). "Turbulent transport and energy balance as affected by a windbreak in an irrigated sugar beet (Beta vulgaris) field." Agron. J., 63(3), 351-355.

Brown, P.W., Kopec, D. and Mancino, C. (1988). "Estimating turfgrass water use with AZMET. Turfgrass and Ornamentals Research Summary." Ariz. Agr. Exp. Stn. P-75:25-33.

Brown, K. W., and Rosenberg, N. J.. 1971. "Turbulent transport and energy balance as affected by a windbreak in an irrigated sugar beet (*Beta vulgaris*) field." *Agron. J*. 63: 351-355.

Brunt, D. (1932). "Notes on radiation in the atmosphere: I." *Quart. J. Roy. Meteor. Soc.*, 58:389-420.

Brunt, D. (1952). *Physical and Dynamical Meteorology*. 2nd ed, Univ. Press, Cambridge, 428 pp.

Brutsaert, W. (1975). "The roughness length for water vapor, sensible heat and other scalars." *J. Atm. Sci.*, 32:2028-2031.

Brutsaert, W. (1982). "*Evaporation into the Atmosphere."* D. Reidel Publishing Co. Dordrecht, Holland. 300 pp.

Brutsaert, W., and Stricker, H. (1979). " An advection-aridity approach to estimate actual regional evapotranspiration." *Water Resources Res.,* 15(2):443-450.

Buck, A. (1976). "The variable path Lyman-alpha hygrometer and its operating characteristics." *Bull. Am. Meteorol. Soc.*, 51:1113-1118.

Budyko, M.I., (1948). "*Evaporation Under Natural Conditions*." (Translated from Russian). U.S. Dept. Com. Israel Program Sci. Transl. 751. 130 pp.

Budyko, M.I. (1956). "The heat balance of the earth's surface." (Translated by N. A. Stepanova, 1958). *U.S. Dept. Com. Weather Bur. PB 131692*. 259 pp.

Burba, G., Anderson, D. (2008). "Introduction to the eddy covariance method: general guidelines and conventional workflow." LiCor Corporation, Lincoln, NE. www.licor.com/env/PDF_Files/EddyCovariance_readonly.pdf last accessed Dec. 26, 2010. 141 p.

Burman, R.D., Wright, J.L., and Jensen, M.E. (1975). "Changes in climate and estimated evaporation across a large irrigated area in Idaho." *Trans. Am. Soc. Agric. Engirs.*, 18(6): 1089-1093.

Burman, R.D., Jensen, M.E., and Allen, R.G., (1987). "Thermodynamic factors in evapotranspiration." pp. 28-30. *In:* James, L. G. and English, M. J. (ed.). *Proc. Irrig. and Drain. Spec. Conf.*, ASCE, Portland, Oregon, July.

Burman, R.D., Nixon, P.R., Wright, J.L., and Pruitt, W.O. (1980). "Water requirements." pp 189-232 *In:* Jensen, M.E. (ed) *Design and operation of farm irrigation systems*. Am. Soc. Agr. Engrs., St. Joseph, MI, 840 pp.

Burnett, B., Allen R.G., Robison C.W., Tasumi M., Lorite I. (2008). "Estimating the soil surface evaporation and transpiration components from satellite images in the absence of a

thermal band." *Paper presented at the 2008 World and Environmental Resources Congress of ASCE and EWRI*, Honolulu, HI, May 12-16, 2008. Publ. on CD-ROM, ASCE. 18 p.

Burrows, F.J., and Milthorpe, F.L. (1976). "Stomatal conductance in the control of gas exchange." pp. 103-152. *In*: Kozlowski, T.T. (ed.). *Water Deficits and Plant Growth*, Academic Press, New York, Vol IV.

Burt, C.M., Mutziger, A.J., Howes, D.J., and Solomon, K.H. (2005). "*Evaporation from irrigated agricultural land in California*." Study funded by CAFED and Calif. Tate Univ./Agric. Initiative. (http://www.itrc.org/reports/reportsindex.html)

Burt, C.M., Solomon, K., and O'Halloran, T. (2005c). "Prediction accuracy for project-wide evapotranspiration using crop coefficients and reference evapotranspiration." *J. Irrig. and Drain. Engrg,* ASCE 131(1):24-36.

Businger, J. A., (1966). "Transfer of heat and momentum in the atmospheric boundary layer." *Proc. Arctic Heat Budget and Atmospheric Circulation*, Santa Monica, CA. RAND Corp. pp. 305-332.

Businger, J.A., and Yaglom, A.M. (1971). "Introduction to Obukhov's paper on 'Turbulence in an atmosphere with a non-uniform temperature'." *Boundary-Layer Meteorol* 2:3-6.

Businger, J.A., Miyake, M., Dyer, A.J., and Bradley, E.F. (1967). "On direct determination of turbulent heat flux near the ground." *J. Appl. Meteorol.* 6(6):1025-1032.

Bussière, F., 1996. In: *Actes de l'école chercheurs INRA en bioclimatologie- Le Croisic 3-7 avril 1995* 1 De la plante au couvert végétal.

Cahill, A.T. and Parlange, M.B. (1998). "On water vapor transport in field soils." *Water Resources Res.*, 34(4):731-739.

Cahill, A.T. and Parlange, M.B. (2000). "Reply to On water vapor transport in field soils." *Water Resources Res.*, 36(10):3107-3110.

Calera-Belmonte A., Jochum A.M., Cuesta-Garcia A., Montoro-Rodriguez A., Lopez-Fuster P. (2005). "Irrigation management from space: Towards user-friendly products." *Irrig. and Drain. Systems*, 19:337–353

Calif. Dept. of Public Works. (1948). "*Evaporation from Water Surfaces in California*." Bull. No. 54-A, 205 pp.

California, State of. (1967). "Vegetative water use." *Dept. Water Resour. Bull. No. 113-2*, 82 pp.

California, State of. (1975). "Vegetative water use in California, 1974." *Dept. of Water Resour. Bull. No. 113-3*, 104 pp.

California, State of. (1986). "Crop water use in California." *Dept. of Water Resour. Bull. No. 113-4*. 117 pp.

Calvet, J.C., Noilhan, J. and Besseoulin, P. (1998). "Retrieving the root zone soil moisture from surface soil moisture or temperature estimates: A feasibility study on field measurements." *J. Appl. Meteorol.* 37:371-386.

Cammalleri, M., Anderson, M.C., Gao, F., Hain, C.R. and Kustas, W.P. (2013). "A data fusion approach for mapping daily evapotranspiration at field scale." *Water Resour. Res.* 49:1-15.

Camp, C.R., Sadler, E.J., Yoder, R.E. (eds), (1996). "*Evapotranspiration and Irrigation Scheduling."* Am. Soc. of Agr. Engrs., San Antonio, Nov. 3-6, 1184 pp.

Campbell Scientific Inc. (2003). "HFT3 soil heat flux plate." *Instruction Manual*. Logan, UT, 12 p.

Campbell, G.S. and Campbell, M.D. (1982). "Irrigation scheduling using soil moisture." pp. 25-42 *In*: Hillel, Daniel (ed) *Advances in Irrigation*. Academic Press, New York, NY.

Campbell, G.S. and J.M. Norman. 1998. "*An introduction to environmental biophysics."* Springer-Verlag, NY, NY. 286 p.

Campbell, G.S. and Tanner, B.D. (1985). "A krypton hygrometer for measurement of atmospheric water vapor concentration." *Moisture and humidity*. ISA, Research Triangle Park, NC, pp. 609-612.

Carlson, T.N. and Ripley, D.A. 1997. "On the relation between NDVI, fractional vegetation cover, and leaf area index." *Remote Sensing of Environment,* 62(3): 241–252.

Carpenter, L.G. (1898). "The loss of water from reservoirs by seepage and evaporation." *Agr. Exp. Stn. Bull. No. 45*, 32 pp.

Carrow, .RN. (1995). "Drought resistance aspects of turfgrasses in the Southeast: evapotranspiration and crop coefficients." *Crop Sci*. 35, 1685-1690.

Carrow, R.N. (2004). "Can we maintain turf to 'customers' satisfaction with less water?" *Proc., 4th Intl. Crop Sci. Congr.*, 26 Sep – 1 Oct 2004, Brisbane, Australia. Publ. on CDROM. Web site www.cropscience.org.au. 12 p.

Cellier, P. (1986). "On the validity of flux-gradient relationships above very rough surfaces." *Boundary-Layer Meteorol.*, 36:417-419.

Cellier, P., and Brunet, Y. (1992). "Flux-gradient relationships above tall plant canopies." *Agr. and For. Meteorol.* 58:93-117.

Cesaraccio, C., Spano, D., Duce, P. and Snyder, R.L. (2001)." An improved model for degree-days from temperature data." *Int'l. J. Biometeorol.* 45(4): 161-169.

Changnon, S.A., Lamb, P.J., and Hubbard, K.G. (1990). "Regional climate centers: New institutions for climate services and climate-impact research." *Bull. Am. Meteorol. Soc.*, 71(4):527-537.

Chanzy, A., and Bruckler,L (1993). "Significance of soil surface moisture with respect to daily bare soil evaporation." *Water Resour. Res.*, 29:1113-1125.

Charnock, H. (1955). "Wind stress on a water surface," *Quart. J. Roy. Soc*. 81, 6

Chen, J. (1984). "Uncoupled multi-layer model for the transfer of sensible and latent heat flux densities from vegetation." *Boundary-Layer Meteorol*., 28:213-225.

Chen, F., and Dudhia, J., (2001). "Coupling an advanced land surface-hydrology model with the Penn State-NCARMM5Modeling System. Part I: Model implementation and sensitivity." *Monthly Weath. Rev.* 129, 569–585.

Choudhury, B.J. (1983). "Simulating the effects of weather variables and soil water potential on a corn canopy temperature." *Agr. Meteorol.*, 29:169-182.

Choudhury, B.J. (1989). "Estimating evaporation and carbon assimilation using infrared temperature data: vistas in modeling." pp. 628-690. *In*: Ghassem, A. (ed). *Theory and Applications of Optical Remote Sensing,* John Wiley & Sons. New York.

Choudhury, B.J., Ahmed N.U., Idaho S.B., Reginato R.J., Daughtry C.S.T. (1994). "Relations between evaporation coefficients and vegetation indices: studies by model simulation." *Remote Sensing of Environ.* 50:1-17.

Choudhury, B.J., and Idso, S.B. (1985). "Evaluating plant and canopy resistances of field-grown wheat from concurrent diurnal observations of leaf water potential, stomatal resistance, canopy temperature, and evapotranspiration flux." *Agr. and For. Meteorol.*, 34:67-76.

Choudhury, B.J., Idso, S.B., and Reginato, R.J. (1987). "Analysis of an empirical model for soil heat flux under a growing wheat crop for estimating evaporation by an infrared temperature based energy balance equation." *Agr. and For. Meteorol.*, 39:283-297.

Choudhury, B.J., and Monteith, J.L. (1986). "Implications of stomatal response to saturation deficit for the heat balance of vegetation." *Agr. and For. Meteorol.*, 36:215-225.

Choudhury, B.J., and Monteith, J.L. (1988). "A four-layer model for the heat budget of homogenous land surfaces." *Quart. J. Roy. Meteorol. Soc.*, 114:373-398.

Chow, V., Maidment D., Mays L. (1988). "*Applied Hydrology*." 2nd ed. McGraw-Hill. 572 p.

Christiansen, J.E. (1968). "Pan evaporation and evapotranspiration from climatic data." *J. Irrig. Drain. Div.,* ASCE 94:243-265.

Christiansen, J.E., and Hargreaves, G.H. (1969). "Irrigation requirements from evaporation. *Trans. Int. Comm. On Irrig. and Drain.*, Vol. III, 23:569-23.596.

Císler, J. (1969). "The solution for maximum velocity of isothermal steady flow of water upward from water table to soil surface." *Soil Science*, 108(2), 148.

Clemmens, A. J. (2000). "Level basin irrigation systems: adoption, practices, and the resulting performance." pp. 273-282. *In*: *4th Decennial Nat. Irrig. Symp.*, Nov. 14-16, Phoenix, AZ. Am.

Soc. Agr. Engrs., St Joseph, MI.
Clemmens, A.J., Dedrick, A.R. and Strand, R.J. (1995). "*BASIN: A Computer Program for the Design of Level-Basin Irrigation Systems*." WCL Report #19, U.S. Water Conservation Lab., USDA/ARS, Phoenix, AZ.
Clemmens, A.J., Walker, W.R., Fangmeier, D.D., and Hardy, L.A. (2007). "Design of surface systems." pp. 499-531, *In*: Hoffman, G.J., Evans, Evans, R.G., and Jensen, M.E. (eds), *Design and Operation of Farm Irrigation Systems*, Am. Soc. Agr. and Biol. Engrs., St Joseph, MI.
Coats, R.N., Perez-Losada, J., Schladow, G., Richards, R., and Goldman, C. (2006). "The warming of Lake Tahoe." *Climatic Chge.*, 76:121-148.
Cogley, J.G. 1979. "The albedo of water as a function of latitude." *Monthly Weather Rev.*, 107:775-781.
Collatz, C.J., Ball, J.T., Grivet, C. and Berry, J.A. (1991). "Physilogical and environmental regulation of stomatal conductance, photosynthesis and transpiration: a model that includes a laminar boundary layer." *Agr. and For. Meteorol*., 54:107-136.
Corwin, D.L., Waggoner, B.L., and Rhoades, J.D. (1990). "A functional model of solute transport that accounts for bypass." *J. Environ. Qual.*, 20:647-658.
Costello, L.R., Matheny, N.P., and Clark, J.R. (2000). "Estimating the irrigation water needs of landscape plantings in California: Part 1: The landscape coefficient method." *Univ. Calif. Coop. Ext. and Calif. Dept. Water Resources*. 23 p.
Costello, L.R., and Jones, K.S. (1999). "A guide to estimating irrigation water needs of landscape plantings in California." *Univ. of Calif. Ext.*, pp. 45-144.
Cowan, I.R., and Milthorpe, F.L. (1968). "Plant factors influencing the water status of plant tissues." pp. 137-193. *In*: Kozlowski, T.T. (ed.) *Water Deficits and Plant Growth*, Academic Press, New York, Vol I.
Crank, J. (1956). "*The Mathematics of Diffusion.*" Oxford Press, London.
Croley, T.E. II. (1989). "Verifiable evaporation modeling on Laurentian Great Lakes." *Water Resources Res.*, 25(5):781-792.
Croley, T.E., F.H. Quinn, K.E. Kunkel and Changnon, S.A. (1996). "Climate transposition effects on the Great Lakes Hydrologic Cycle." *NOAA Techn. Memo. ERlGLERL-89*. 107 pp.
Cuenca, R.H., and Nicholson, M.T. (1982). "Application of Penman equation wind function." *J. Irrig. & Drain. Div.*, ASCE, 108(IR1):13-24.
Cummings, N.W., and Richardson, B. (1927). "Evaporation from lakes." *Phys. Review*, 30:527-534.
Curry, R.B., Klink, J.C., Holman, J.R., Elwell, D.L., and Sciarini, M.J. (1988). "Current Ohio experience with an automated weather station network." *Appl. Eng. Agr.*, 4:150-155.
Daamen, C.C. 1997. "Two source model of surface fluxes for millet fields in Niger." *Agr. and For. Meteorol.* 83(3-4):205-230.
Daamen, C.C., Dugas, W. A., Prendergast, P. T., Judd, M. J. and McNaughton, K. G. 1998. "Energy flux measurements in a sheltered lemon orchard." *Agr. and For. Meteorol.*, 93(3):171-183.
Daamen, C.C and McNaughton K.G., 2000. "Modeling energy fluxes from sparse canopies and understorys." *Agron. J.,* 92:837–847
Daamen, C.C., Simmonds, L.P., Wallace, J.S., Laryea, K.B., and Sivakumar, M.V.K. (1993). "Use of lysimeters to measure evaporation from sandy soils." *Agr. And For. Meteorol.*, 65:159-173.
Dai, Y., Dickinson, R.E., Wang, Y-P. (2004). "A two-big-leaf model for canopy temperature, photosynthesis, and stomatal conductance." *J. Climate*, 17:2281-2299.

Daley, C. and Bryant, K. (2013). "The PRISM climate and weather system – an introduction." www.prism.oregonstate.edu/documents/PRISM_history_june2013.pdf, 5 p.
Dalton, J. (1802). "Experimental essays on the constitution of mixed gasses; on the force of steam or vapour from water and other liquids in different temperatures, both in Torricellian vacuum and in air; on evaporation; and on the expansion of gasses by heat." *Memoirs*, *Manchester Literary and Philosophical Society*. Series 1, Vol. 5, Part 2, pp. 535-602.

Daly, C., Halbleib, M., Smith, J.I., Gibson, W.P., Doggett, M.K., Taylor, G.H., Curtis, J., and Pasteris, P.P. (2008). "Physiographically sensitive mapping of climatological temperature and precipitation across the conterminous United States." *Int. J. Climatology.* 28(15):2031–2064.

Dastane, N.G. (1974). "Effective rainfall in irrigated agriculture." *Irrig. and Drain. Paper No. 25*, United Nations Food and Agriculture Organization, Rome, Italy, 62 pp.

Davies, J.A., and Idso, S.B. (1979). "Estimating surface radiation balance and its components." pp. 183-210. *In*: Barfield, B.J., and Gerbes, J.F. (ed.). *Modification of the Aerial Environment of Plants*., Am. Soc. Agr. Engrs. Mono No. 2. 544 pp.

de Azevedo, P. V., da Silva, B. B., and da Silva, V.P.R. 2003. "Water requirements of irrigated mango orchards in northeast Brazil." *Agric. Water Man.* 58: 241-254.

de Bruin, H.A.R. 1982. "Temperature and energy balance of a water reservoir determined from weather data of a land station." *J. Hydrology*, 59:261-274.

De Bruin, H.A.R., Hartogensis, O.K., Allen R.G., Kramer J.W.J.L. (2005). "Note on the regional advection perturbations in an irrigated desert (RAPID) experiment." *Theor. and Applied Climatology* 80, 143-152

de Bruin, H.A.R., and Jacobs, C.M.J. (1993). "Impact of CO_2 enrichment on the regional evapotranspiration of agro-ecosystems, a theoretical and numerical modeling study." *Vegetation*, 104-105(1):307-318.

de Bruin, H.A.R., and Moore, C.J. (1985). "Zero-plane displacement and roughness length for tall vegetation, derived from a simple mass conservation hypothesis." *Boundary- Layer Meteorol.*, 31:39-49.

Dekker, S.C., Bouten, W. and Verstraten, J.M. (2000). "Modeling forest transpiration from different perpectives." *Hydrol. Proc.* 14(2):251-260.

de Medeiros, G.A., Arruda, F.B., Sakai, E.,Fujiwara, M. (2001). "The influence of crop canopy on evapotranspiration and crop coefficient of beans (*Phaseolus vulgaris L.*)." *Agr. Water Manage.* 49(3): 211–224.

Denmead, O.T. (1984). "Plant physiological methods for studying evapotranspiration: problems of telling the forest from the trees." *Agr. Water Manag.* 8:167-189.

Denmead, O. T., and Bradley, E.F. (1985). "Flux-gradient relationships in a forest canopy." pp. 421-442, *In*: B.A. Hutchison and B.B. Hicks, (eds), D. Reidel Publishing Co.

Derecki, J.A. (1976). "Multiple estimates of Lake Erie evaporation." *J. Great Lakes Res.*, 2(1):124-149.

Derecki, J.A. (1981). "Operational estimates of Lake Superior Evaporation based on IFYGL findings." *Water Resources Res.*, 17(5):1453-1462.

Descheemaeker, K., Raes, D., Allen, R.G., Nyssen, J., Poesen, J., Muys, B.T., Haile, M., Deckers, J.. (2011). "Two rapid appraisals of FAO-56 crop coefficients for semiarid natural vegetation of the northern Ethiopian highlands." *J. Arid Environments*. 75:353-359.

Devitt, D.A., Sala, A., Smith, S.D., Cleverly, J., Shaulis, L.K., and Hammett, R. (1998). "Bowen ratio estimates of evapotranspiration for *Tamarix ramosissima* stands on the Virgin River in southern Nevada." *Water Resources. Res*. 34:2407-2414.

DeTar, W. R. (2004). "Using a subsurface drip irrigation system to measure crop water use." *Irrig. Sci.,* 23(3): 111-122.

de Vries, D.A. (1963). "Thermal properties of soils." pp. 210-235. *In*: van Wijk, W.R. (ed.). *Physics of Plant Environment*, North Holland Pub. Co., Amsterdam, 382 pp.

Dickinson, R.E. (1984). "Modeling evapotranspiration for three-dimensional global climate models." pp. 58-72. *In*: *Climate Processes and Climate Sensitivity*, Hansen, J.E. and Takahashi, T. (eds), AGU Geophysical Mongraph 29.

Dickinson, R.E., Henderson-Sellers, A., Rosenzweig, and Sellers, P.J. (1991). "Evapotranspiration models with canopy resistance for use in climate models, a review." *Agr. and For. Meteorol.*, 54(204):373-388.

Dingman, S.L. (2008). "*Physical Hydrology*." 2nd ed. Waveland Pr Inc. 575 p.

Dolman, A.J. (1993). "A multiple-source land surface energy balance model for use in general circulation models." *Agr. and For. Meteorol.*, 65(1-2):21-45.

Domingo, F.,*, Villagarci'a, L., Brenner, A.J., Puigdefa'bregas, J., 1999. "Evapotranspiration model for semi-arid shrub-lands tested against data from SE Spain." *Agr. and For. Meteorol.*, 95(2):67-84.

Donelan, M.R., Elder, F.C., and Hamblin, P.F. (1974). "Determination of the aerodynamic drag coefficient from wind set-up (IFYGL)." *Proc. Conf. Great Lakes Res.,pp.* 778-788.

Dong, A., Grattan, S.R., Carroll, J.J., and Prashar, C.R.K. (1992). "Estimation of net radiation over well-watered grass". *J. of Irrig. and Drain. Eng.*, 118 (3):466-479.

Doorenbos, J., and Kassam, A.H. (1979). "Yield response to water." *FAO Irrig. and Drain. Paper No. 33, 2nd ed*, Food and Agriculture Organization, United Nations, Rome, Italy. 202 pp.

Doorenbos, J. and Pruitt, W.O., (1975). "Guidelines for prediction of crop water requirements." *FAO Irrig. and Drain. Paper No. 24*, FAO, Rome, Italy. 179 pp.

Doorenbos, J., and Pruitt, W.O. (1977). "Guidelines for predicting crop water requirements." *FAO Irrig. and Drain. Paper No. 24, 2nd ed*, Food and Agriculture Organization, United Nations, Rome, Italy. 156 pp.

Dorman, J. L., and Sellers, P.J. (1989). "A global climatology of albedo, roughness length and stomatal resistance for atmospheric general circulation models as represented by the simple biosphere model (SIB)." *J. Appl. Meteor.*, 28:833-855.

Dozier, J., and Frew, J. (1990). "Rapid calculation of terrain parameters for radiation modeling from digital elevation data." *IEEE Trans. Geoscience and Remote Sens.*, 28:963-969.

Droogers, P. and R.G. Allen. 2002. "Estimating reference evapotranspiration under inaccurate data conditions." *Irrig. and Drain. Syst.*, (16):33-45.

Droogers, P., and Kite, G. (1999). "Water productivity from integrated basin modeling." *Irrig. and Drain. Syst.*, 13(3):249-273.

Duchemin, B., Hadria, R., Boulet, G., Maisongrande, P., Chehbouni, A., Escadafal, R., Ezzahar, J., Hoedjes, J.C.B., Kharrou, M.H., Khabba, S., Mougenot, B., Olioso, A., Rodriguez, J.C., and Simonneaux, V. (2006). "Monitoring wheat phenology and irrigation in Central Morrocco: On the use of relationships between Evapotranspiration, crop coefficients, leaf area index and remotely-sensed vegetation indices." *Agr. Water Mgmt.*, 79(1):1-27.

Duffie, J.A. and Beckman, W.A. (1991). *Solar Engineering of Thermal Processes*. John Wiley and Sons, New York. pp. 216 pp.

Dugas, W.A. and Bland, W.L. (1991). "Springtime soil temperatures in lysimeters in Central Texas." *Soil Sci* . 152(2):87-91

Dugas, W.A., Upchurch, D.R. and Ritchie, J.T. (1985). "A weighing lysimeter for evapotranspiraiton and root measurements." *Agron. J.*,77:821-825.

Dunin, F.X., and Aston, A.R. (1984). "The development and proving of models of large scale evapotranspiraton" An Australian study." *Agr. Water Mgmt.*, 8(1-3):305-323.

Dunin, F. X., McIlroy, I.C., and O'Loughlin, E.M. (1985). "A lysimeter characterization of evaporation by eucalypt forest and its representativeness for the local environment." pp. 271-291, *In*: B.A. Hutchison and B.B. Hicks, (eds). *The Forest Interaction*. Proc., Forest Environ. Measur. Conf., Oak Ridge Tennesee, 1983.

Dunin, F.X., Reyenga, W., and McIlroy, I.C. (1991). "Australian lysimeter studies of field evaporation." pp. 237-245, *In*: R.G. Allen, T.A. Howell, W.O. Pruitt, I.A. Walter, and M.E. Jensen, (eds). *Lysimeters for Evapotranspiration and Environmental Measurements*. Am. Soc. Civ. Engrs., New York, NY, 456 pp.

Duty of Water Committee. (1930). "Consumptive use of water in irrigation." Progr. Rept., Duty of Water Committee of the Irrig. Div., *Trans. Am. Soc. Civ. Engr.*, 94:1349-1399.

Dyer, A.J. (1961). "Measurements of evaporation and heat transfer in the lower atmosphere by an automatic eddy-convection technique." *Quart. J. Roy. Meteorol. Soc.,* 87:401-412.

Dyer, A. J. (1967). "The turbulent transport of heat and water vapour in an unstable atmosphere." *Quart. J. Roy. Meteorol. Soc*., 93:50l-508.

Dyer, A.J. (1974). "A review of flux-profile relationships." *Boundary-Layer Meterol.,* 7:363-372.

Dyer, A. J. and Hicks, B.B. (1970). "Flux-gradient relationships in the constant flux layer." *Quart. J. Roy. Meteorol., Soc*., 96:715-721.

Dyer, A. J., and Pruitt, W.O. (1962). "Eddy Flux measurements over a small irrigated area." *J. Applied Meteorol*., 1(4):471-473.

LI-COR, Inc. (2012). "EddyPro Eddy Covariance Software – User's Guid and Reference." Li-Cor, Inc., Lincoln, NE. 200 pp.

Edlinger, J.E., Duttweiler, D.W., and Geyer, J.C. 1968. "The response of water temeperatures to meteorological conditions." *Water Resources Res.*, 4(5):1137-1143.

Elbersen, H. W., Christian, D.G., El Bassam, N., Sauerbeck, G., Alexopoulou, E., Sharma, N. and Piscioneri, I. (2004). "A management guide for planting and production of switchgrass as a biomass crop in Europe." *2nd World Conference on Biomass for Energy, Industry and Climate Protection*, 10-14 May 2004, Rome, Italy. 3 p.

Encyclopedia of Soils in the Environment, (2004). "*Encyclopedia of Soils in the Environment*." Witamy W. International Publishing Service.

Encyclopedia of Hydrological Sciences, (2002). "*Encyclopedia of Hydrological Sciences*." John Wiley & Sons, Ltd.

Entekhabi, D., and Eagleson, P.S. (1989)."Land surface hydrology parameterization for atmospheric general circulation models including subgrid scale spatial variability." *J. Climate*, 2:816-831.

Erie, L.J., French, O.F. and Harris, K. (1965). "Consumptive use of water by crops in Arizona." Univ. of Ariz. Agri. Exp. Sta. Tech. Bull. 169.

Erie, L.J., French, O.F., Bucks, D.A. and Harris, K. (1982). "Consumptive Use of Water by Major Crops in the Southwestern United States. USDA, Conservation Res. Rep. No. 29, 42 pp.

Eshel, A,. and T. Beeckman, ed.(2013). "*Plant Roots: the Hidden Half*," 4th ed. CRC Press, 848 p.

U.S. Dept. of Commerce. (1968) "Climate Atlas of the United States." USDOC ESSA Env. Data Svc., 80 pp.

Evans, R.G. (1980). "*Irrigation Scheduling Guide*." No. 4.708, Colo. State Univ. Ext. Serv., 2 pp.

Evans, R.G., Benham, B.L., and Trooien, T.P. (eds). "*National Irrigation Symposium*," (2000). Proc., 4th Decennial Symp., Am. Soc. Agr. Engrs., St. Joseph, MI, 693 pp.

Evans, R.G., Kroeger, M.W., and Mahan, M.O. (1991). "Installation and operation of large drainage lysimeters on grapes." pp. 388-396, *In*: *Lysimeters for Evapotranspiration and Environmental Measurements*, Allen, R.G., Howell, T.A., Pruitt, W.O., Walter, I.A., and Jensen, M.E. (eds), Am. Soc. Civ. Engrs., New York, New York, 456 pp.

Evans, R.G., Wu, I-Pai, and Smajstrala, A.G. (2007) "Microirrigation systems." pp. 632-683 *In*: Hoffman, G.J., Evans, Evans, R.G., Martin, D.L., and Jensen, M.E. (eds), *Design and Operation of Farm Irrigation Systems*, Am. Soc. Agr. and Biol. Eng., St Joseph, MI.

Everson, D.O., Faubion, M., and Amos, D.E.. (1978). "Freezing temperatures and growing seasons in Idaho." *Univ. Idaho Agric. Exp. Sta. Bull. 494*.

Evett, S.R. and Lascano, R.J. (1993). "ENWATBAL.BAS: a mechanistic evapotranspiration model written in compiled basic." *Agron. J.*, 85(3):763-772.

Evett, S.R. and Parkin, G.W. (2005). "Advances in Soil Water Content Sensing," *Vadose Zone J.* 4(4): 986-991.

Evett, S. R. and Steiner, J. L. (1995). "Precision of neutron scattering and capacitance type soil water content gauges from field calibration. *Soil Sci. Soc. Am. J.* 59(4):961-968.

Evett, S.R., Howell, T.A., and Schneider, A.D. (1995). "Energy and water balances for surface and subsurface drip irrigated corn." pp. 135-140, *In*: *Proc., 5th Int. Microirrigation Congr.*, Am. Soc. Agric. Engrs., St. Joseph, MI.

Evett, S.R., Tolk, J.A., and Howell, T.A. (2003.). "A depth control stand for improved accuracy with the neutron probe." *Vadose Zone J.* 2:642-649.

Evett, S.R., Tolk, J.A., and Howell, T.A. (2005). "TDR laboratory calibration in travel time, bulk electrical conductivity, and effective frequency." *Vadose Zone J.* 4:1020-1029.

Evett S.R., Tolk, J.A . and Howell, T.A. (2006). "Soil Profile Water Content Determination." *Vadose Zone J.* 5(3):894-907.

Ewers, B.E., Oren R. (2000). "Analyses of assumptions and errors in the calculation of stomatal conductance from sap flux measurements." *Tree Physiology* 20, 579-589.

Farahani, H.J., and Ahuja, L.R. (1996). "Evapotranspiration modeling of partial canopy/residue covered fields." *Trans. of the ASAE* 39:2051-2064.

Farahani, H.J., and Bausch, W.C. 1995. "Performance of evapotranspiration models for maize-bare soil to closed canopy." *Trans. of the ASABE,* 38(4):1049-1059.

Farnsworth, R.K., Thompson, E.S. (1982). "Mean monthly, seasonal, and annual pan evaporation for the United States." *NOAA Techn. Rept. NWS 34*, 3 pp.

Farnsworth, R.K., Thompson, E.S., and Peck, E.L. (1982). "Evaporation atlas for the contiguous 48 United States." *NOAA Techn. Rept. NWS 33*, 27 pp.

Fereres, E. 1981. "Drip irrigation management." *Leaflet No. 21259*. Berkeley, Calif.: Cooperative Ext., Univ. California.

Ficke, J.F. (1972). "Comparison of evaporation computation methods, Pretty Lake, LaGrange County, Northeastern Indiana." *Geological Survey Prof. Paper*, 686-A, i-v, and A1-A49.

Finch, J.W. 2001. "A comparison between measured and modeled open water evaporation from a reservoir in south-east England. *Hydrological Proc.*, 15:2771-2778.

Finch, J.W., and Gash, J.H.C. 2002. "Application of a simple finite difference model for estimating evaporation from open water." *J. Hydrology*, 255:253-259.

Fisher, J. B., DeBiase, T. A., Qi, Y., Xu, M., Goldstein, A. H., 2004. "Evapotranspiration models compared on a Sierra Nevada forest ecosystem." *Environ. Modeling & Software*, 20(6):783-796.

Fitzpatrick, E.A., and Stern, W.R. (1965). "Components of the radiative balance of irrigated plots in a dry monsoonal environment." *J. Applied Meteorol.*, 4:649-660.

Flerchinger, G.N. (1991). "Sensitivity of soil freezing simulated by the SHAW Model." *Trans. of the ASAE*, 34(6):2381-2389.

Flerchinger, G.N., Hanson, C.L., Wight, J.R., (1996). "Modelling of evapotranspiration and surface energy budgets across a watershed." *Water Resour. Res*., 32(8):2539-2548.

Flerchinger, G.N. and Pierson, F.B. (1991). "Modeling plant canopy effects on variability of soil temperature and water." *Agr. and For., Meteorol.* 56:227-246.

Flesch, T.K. and Dale, R.F. (1987). "A leaf area index model for corn with moisture stress reductions." *Agron. J.*, 19:1008-1014.

Flint, A.L. and Childs, S.W. 1987. "Calculation of solar radiation in mountainous terrain." *Agr. and For. Meteorol.,* 40(3):233-249.

Foken, T. (2008a). "The energy balance closure problem: an overview." *Ecol. Appl*. 18(6):1351-1367.

Foken, T. (2008b). "*Micrometeorology*." Springer-Verlag. ISBN 978-3-540-74665-2. 307 p.

Foken, T., Wimmer, F., Mauder, M., Thomas, C., Liebethal, C. (2006). "Some aspects of the energy balance closure problem." *Atmos. Chem. Phys*., 6:4395-4402.

Fredericksen and Allen (2011). Cited in chp 14, p.

Fritschen, L.J. (1965). "Accuracy of evapotranspiration determinations by the Bowen ratio method." *Bull. Int'l. Soc. Sci. Hydrol.*, 2:38-48.

Fritschen, L.J. (1966). "Evapotranspiration rates of field crops determined by the Bowen ratio method." *Agron. J.*, 58:339-342.

Fritschen, L.J. (1967). Net and solar radiation relations over irrigated field crops. *Agric. Meteorol.*, 4(1):55–62.

Fritschen, L. J., and Lourence, F.J. (1966). p. 146, Chp 7.
Fritschen, L., and Qian, P. (1990). "Net radiation, sensible and latent heat flux densities on slopes computed by the energy balance method." *Boundary-Layer Meteorol.*, 53:163-171.
Fritschen, L. J., and Simpson, J.R. (1985). "Evapotranspiration from forests: Measurement and modeling." pp. 393-404, *In*: *Advances in Evapotranspiration*., Public. No. 74-85, Am. Soc. Agr. Engrs., St. Joseph, Michigan.
Fritschen, L. J., Cox, L., and Kinerson, R. (1973). "A 28- meter Douglas fir in a weighing lysimeter." *Forest Science*, 4:256-261.
Fritz, S., and MacDonald, J.H. (1949). "Average solar radiation in the United States." *Heating and Ventilating*, 46:61-64.
Fuehrer, P.L., Friehe, C.A. (2002). "Flux corrections revisited." *Bound.-Layer Meteor.* 102(3):415-458.
Gao, G., Chen D., Xu C., Simelton E. (2007). "Trend of estimated actual evapotranspiration over China during 1960–2002." *Journal Geophysical Research*, 112:D11120, doi:10.1029/2006JD008010.
Garatuza-Payan, J., Pinker, R.T. & Shuttleworth, W.J. (2001a). High resolution day-time cloud observations for northwestern Mexico from GOES-7 satellite data. *J. Atm. and Oceanic Techn.* 105(1): 39–56.
Garatuza-Payn, J., Pinker, R.T., Shuttleworth, W.J. & Watts, C. (2001b). Solar radiation and evapotranspiration in northern Mexico estimated from remotely sensed measurements of cloudiness. *J. Hydrol. Sci.*, 46(3): 465–478.
Garcia, M., Raes, D., Allen, R., Herbas, C. 2004. Dynamics of reference evapotranspiration in the Bolivian highlands (Altiplano). *Agric. and For. Meteorol.*, 125(1-2): 67-82.
Gardiol, J. M., Serio, L. A., Maggiora, A. I. D. 2002. "Modeling evapotranspiration of corn (Zea mays) under different plant densities." *J. of Hydrol.*, 271(1-4): 188-196
Gardner, W.R. (1958). "Some steady state solutions of the unsaturated moisture flow equation with application to evaporation from a water table." *Soil Sci.*, 85(4):228-232.
Gardner, W.R. (1959). "Solutions of the flow equation for the drying of soils and other porous media." *Proc. Soil Sci. Soc.Am.*, 23(2):__-__.
Gardner, W.R., and Fireman, M. (1958). "Laboratory studies of evaporation from soil columns in the presence of a water table." *Soil Sci.*, 85(4):244-249.
Gardner, W.R. and Hillel, D.I., (1962). "The relation of external evaporative conditions to the drying of soils." *J. Geophys. Res.*, 67:4319-4325.
Garratt, J.R. (1978a). "Flux profile relations above tall vegetation." *Quart. J. Roy. Meteorol. Soc.*, 104:199-211.
Garratt, J.R. (1978b). "Transfer characteristics for a heterogeneous surface of large aeroydynamic roughness." *Quart. J. Roy. Meteorol. Soc.*, 104:491-502.
Garratt, J.R. (1980). "Surface influence upon vertical profiles in the atmospheric near-surface layer." *Quart. J.Roy. Meteorol. Soc.*, 106:803-819.
Garratt, J.R. (1992). *The Atmospheric Boundary Layer.* Cambridge Univ. Press, 316 p.
Garrison, J.D. and Adler, G.. P. (1990). Estimation of precipitable water over the United States for application to the division of solar radiation into its direct and diffuse components. *Solar Energy,* 44(4), 225-241.
Garratt, J.R. and Hicks, B.B. (1973). "Momentum, heat and vapor transfer to and from natural and artificial surfaces." *Quart. J. Roy. Meteorol. Soc.*, 99:680-687.
Gash, J.H.C. (1986). "A note on estimating the effect of a limited fetch on micrometeorological evaporation measurements."*Boundary-Layer Meteorol. Soc.*, 35:409-413.
Gates, D.M. (1963). "The energy environment in which we live." *Am.* Scientist, 51:327-348..
Gates, D.M. (1980). "*Biophysical Ecology*." Springer-Verlag, New York. 611 pp.

Gill, G.C. (1983). “Comparison testing of selected naturally ventilated solar radiation shields.” NOAA Rep. Contract NA-82-0A-A-266, Stennis Space Center, MS, 15 pp

Gilman, E.F. (1990. “Tree root growth and development: I. form, spread, depth and periodicity.” *Environ. Hort.* 8(4):215-220.

Girona, J., Marsal, J., Mata, M., & Del Campo, J. (2003). “Pear crop coefficients obtained in a large weighing lysimeter.” In IV International Symposium on Irrigation of Horticultural Crops 664 (pp. 277-281).

Girona, J., Gelly, M., Mata, M., Arbones, A., Rufat, J., and Marsal, J. (2005). “Peach tree response to single and combined deficit irrigation regimes in deep soils.” *Agric. Water Manage.*, 72:97-108.

Glenn, E.P., Huete, A,, Nagler, P., Hirschoock, K., Brown, P. (2007). Integrating remote sensing and ground methods to estimate evapotranspiration.” *Critical Rev. in Plant Sci.* 26, 139-168.

Gong, L., Xu, C. Y., Chen, D., Halldin, S., & Chen, Y. D. (2006). Sensitivity of the Penman–Monteith reference evapotranspiration to key climatic variables in the Changjiang (Yangtze River) basin. *J. Hydrology*, 329(3), 620-629.

Gonzalez-Sosa, E. Braud,I., Thony, J.L., Vauclin, M., and Bessemoulin, P. (1999). “Modeling heat and water exchanges of fallow land covered with plant residue mulch.” *Agr. and Forest Meteorol.*, 97:151-169.

Goss, J.R., and Brooks, F.A. (1956). "Constants for empirical expressions for downcoming atmospheric radiation under cloudless skies." *J. Meteorol.*, 13:482-488.

Grable, A.R. and Siemer, E.G. 1968. Effects of bulk desnity, aggregate size and soil water suction on oxygen diffusion, redox potentials and elongation of corn roots. *Soil Sci. Soc. Am. J.* 32(2):180-186.

Grant. (1975). “Comparison of evaporation from barley with Penman estimates, *Agr. Meteorol.*, 15:49-60.

Grant, R.F. and Baldocchi, D.D. (1992). "Energy transfer over crop canopies: simulation and experimental verification." *Agr. and For. Meteorol.*, 61:129-149.

Grable, A.R., and Siemer, E.G. (1968). “Effects of bulk desnity, aggregate size and soil water suction on oxygen diffusion, redox potentials and elongation of corn roots.” *Soil Sci. Soc. Am. J.* 32(2):180-186.

Granier, A., (1985). “Une nouvelle méthode pour la mesure du flux de sève brute dans le tronc des arbres.” *Annales des Sciences Forestières*, 42, 193-200.

Granier, A. (1987). “Evaluation of transpiration in a Douglas-fir stand by means of sap flow measurements.” *Tree Physiol.* 3, 309-320.

Gray, D.M. (1970). “*Handbook on the principles of hydrology.*” Secriatariat Canada Nat’l. Com. For the Int’l. Hydrological Decade, Ottawa, Canada.

Green, S., Clothier B., ,Jardine B. (2003). “Theory and practical application of heat pulse to measure sap flow.” *Agron. J.*, 95:1371-1379.

Green, S.R., Clothier, B.E. (1988). “Water use of kiwifruit vines and apple trees.” *J. Exp. Botany*, 39, 115-123.

Griffin, R.E., et al. (1976). "Reducing fruit losses caused by low spring temperatures." *Final Rep. Proj. 562-366-084, Four Corners Reg. Comm.* Utah Agr. Exp. Stn., Utah State Univ., Logan, UT.

Grifoll, J., Gasto, J.M. and Cohen, Y. (2005). Non-isothermal soil water transport and evaporation. *Adv. in Water Resources* 28:1254-1266.

Grishchenko, D.L. 1959. “The dependence of albedo of the sea on the altitude of the sun and disturbance of the sea surface. *Tr. Glav. Geofis. Observ.*, 80:32-38. [OOENV TR359, Dept. Fisheries Environ., Ottawa, 1973].

Hahn, G. L. (1981). "Use of weather data in the rational selection of livestock management practices." Computer Techniques and Meteorological Data Applied to Problems of Agriculture and Forestry: a Workshop, A. Weiss, (ed.), Department of Agricultural Meteorology, University of Nebraska-Lincoln, 362-382.

Ham, J. M. (2001). "On the measurement of soil heat flux to improve estimates of energy balance closure." Am. Geophys. Union, Fall Meeting 2001, abstract B51A-0183 and poster, http://www.oznet.ksu.edu/envphys/Research/Poster%20PDFs/DPHP_and_Soil_Heat_Flux_AGU01.pdf (last accessed Nov. 24, 2006).

Han, S., Evans, R.G., and Kroeger, M.W. (1994). "Sprinkler distribution patters in windy conditions. *Trans. of the ASAE*., 37(5)1481-1490.

Hanks, R.J., Gardner, H.R., and Fairbourn, M.L. (1967). "Evaporation of water from soils as influenced by drying with wind or radiation." *Soil Sci. Soc. Am. Proc.*, 31:593-598.

Hansen, V.E., Israelsen, O.W. and Stringham, G.E. (1979). *Irrigation Principles and Practices*. John Wiley and Sons, Inc. New York. 417 pages.

Hansen, E.A., and Dickinson, R.E. (1979). "Water and mineral nutrient transfer between root systems of juvenile Populus", *For. Sci.*, 25(2):247-252.

Harbeck, G.E. Jr. (1962). "A practical field technique for measuring reservoir evaporation using mass transfer theory." pp. 101-105, *U.S. Geological Survey Prof. Paper 272-E*.

Harbeck, G.E., Kohler, M.A., Koberg, G.E. (1958). Water-Loss Investigations: Lake Mead Studies, *Geological Survey Prof. Paper 298*, 110 pp.

Harding, S.T. (1962). "Evaporation from Pyramid and Winnemucca Lakes, Nevada." *Proc. Am. Soc. Civ., Engrs. and Drain. Div.*, 88(IR1):1-13.

Hardy, E.L., Overpeck, J.C., and Wilson C.P. (1939). "Precipitation and evaporation in New Mexico." *New Mexico Agr. Exp. Stn. Bull. 269*, 68 pp.

Hargreaves, G. H. (1948). Irrigation Requirement Data for Central Valley Crops, US Bur. of Recl., Branch of Proj. Planning, Sacramento, California. 33 pp.

Hargreaves, G.H. (1983). "Discussion of `application of Penman wind function.'" Cuenca, R.H. and Nicholson, M.J. J. of Irrig. and Drain. Eng., 109(2):277-278.

Hargreaves, G.H. (1993). "Estimating runoff from precipitation and temperature." pp. *402-408*. *In*: Allen, R.G., and Neale, C.M. (eds) *Management of Irrigation and Drainage Systems*, Proc., 1993 National Conference on Irrigation and Drainage Engineering, ASCE.

Hargreaves, G.H. and.Allen, R.G. (2004). "History and evaluation of the Hargreaves evapotranspiration equation." *J. Irrig. and Drain. Engrg.*, 129(1):53-63.

Hargreaves, G.H., and Allen, R.G. (2004a). "Closure to 'History and evaluation of Hargreaves evapotranspiration equation'." *J. Irrig. and Drain. Engrg.*, 130(5):448-449.

Hargreaves, G.H. and Z.A. Samani. (1982). "Estimating potential evapotranspiration." Tech. Note, *J. Irrig. and Drain. Eng.*, 108(3):225-230.

Hargreaves, G.H., and Samani, Z.A. 1985. "Reference crop evapotranspiration from temperature." *Appl. Eng. in Agr*., 1(2):96-99.

Hargreaves, G.L., G.H. Hargreaves, and J.P. Riley. 1985. Agricultural benefits for Senegal River Basin, *J. Irrig. and Drain. Eng.,* 111(2):113-124.

Harlukowicz, T.J. (1984). "Weather and lysimeter data for Coshocton, Ohio." Personal Communication.

Harrison, L.P. (1963). "Fundamental concepts and definitions relating to humidity." *In*: Wexler, A. (ed). *Humidity and Moisture*, Vol 3, Reinhold Publishing Co., New York.

Harrold, L.L., (1966). "Measuring evapotranspiration by lysimetry." pp. 28-33. *Proc. Conf. on Evapotranspiration*, Am. Soc. Agr. Engrs., Chicago, IL. December.

Harrold, L.L. and Dreibelbis, F.R. (1958). "Evaluation of agricultural hydrology by monolith lysimeters." Tech. Bull. No. 1179, USDA, Washington, D.C., 166 pp.

Hart, O.J., Brugnach, M., Temesgen, B., Rueda, C., Ustin, S.L., Frame, K. (2009). "Daily reference evapotranspiration for California using satellite imagery and weather station

measurement interpolation." *Civil Engrg. and Envir. Sys.*, 26(1):1933. http://dx.doi.org/10.1080/10286600802003500.

Hatfield, J.L. (1985). "Wheat canopy resistance determined by energy balance Techniques." *Agron. J.,* 77:279-283.

Hatfield, J.L., and Allen, R.G. (1996). "Evapotranspiration estimates under deficient water supplies." *J. Irrig. Drain Eng.*, 122(5), 301–308.

Hatfield, J.L. (ed.) (2004). "*Micrometeorology in Agricultural Systems.*" Amer. Soc. Agron.

Hatfield, J.L., Baker, J.M., Viney, M.K.. 2005. *Micrometeorology in agricultural systems.* Agron. Mono. No.47. 584 pp. ISBN 0-89118-158-X.

Hatfield, J.L., Reginato, R.J., and Idso, S.B. (1983). "Comparison of longwave radiation calculation methods over the United States." *Water Resour. Res.*, 19:285-288.

Hatfield, J.L., Reginato, R.J., and Idso, S.B. (1984). "Evaluation of canopy temperature-evapotranspiration over various crops." *Agric. Meteorol.*, 32:41-53.

Hathoot, H.M., Abo-Ghobar, H.M., Al-Amoud, A.I., and Mohammad, F.S. (1994). "Analysis and design of sprinkler irrigation laterals. *J. Irrig. and Drain. Eng.*, 120(3):534-549.

Hedke, C.R. 1924. *Consumptive use of water by crops*. New Mexico State Engr. Office, July.

Heermann, D.F., Harrington, G.J., and Stahl, K.M. (1985). "Empirial estimation of clear sky solar radiation." *J. Climate and Applied Meteorol.*, 24(3):206-214.

Heilman, J.L., Brittin, C.L., Neale C.M.U. (1989). "Fetch requirements for Bowen ratio measurements of latent and sensible heat fluxes." *Agric. Forest Meteorol.*, 44: 261–273.

Heilman, J.L., Heilman W.E., Moore D.G. (1982). "Evaluating the crop coefficient using spectral reflectance." *Agric. J.*, 74:967-971

Henderson-Sellers, B. (1986). "Calculating the surface energy balance for a lake and reservoir modeling: A review." *Rev Geophys.*, 24:625-649.

Henderson-Sellers, B. and Davis, A.M. (1989). Thermal stratification modeling for oceans and lakes. pp. 86-156, *In*: Tien, C.L., and Chaula, T.H.(eds). *Annual Rev. of Num. Fluid Mech. and Heat* Transfer. Vol. II, Hemisphere, New York.

Hernandez-Suarez, M. (1988). Modeling irrigation scheduling and its components and optimization of water delivery scheduling with dynamic programming and stochastic ETo data. Ph.D. Diss. Davis, Calif.: Univ. California, Davis. 137 p.

Hickox, G.H. (1946). "Evaporation from a free water surface." *Am. Soc. Civ. Engrs. Trans.*, 111:1-66.

Hignett, C., and Evett, S.R. (2002). "Neutron thermalization." Section 3.1.3.10 *In* Dane, H.D., and Topp, G.C. (eds.) *Methods of Soil Analysis*. Part 4 - Physical Methods. pp. 501-521.

Hill, R.W., and Allen, L.N. (1991). "Water table lysimeter data interpretation." pp. 254-263, *In*: R.G. Allen, T.A. Howell, W.O. Pruitt, I.A. Walter, and M.E. Jensen, (eds), *Lysimeters for Evapotranspiration and Environmental Measurements*, Am. Soc. Civ. Engrs., New York, N Y, 456 pp.

Hill, R.W., Johns, E.L. and Frevert, D.K. (1983). Comparison of equations used for estimating agricultural crop evapotranspiration with field research. USDI, Bur. Recla., 242 pp.

Hoffman, G.J. (1990). "Leaching fraction and root zone salinity control. pp. 236-261, *In*: Tanji, K.K. (ed), Agricultural *Salinity Assessment and Management*. ASCE Manuals and Reports on Engineering Practice No. 71, Am. Soc. Civ. Engrs., New York, 630 pp.

Hoffman, O.F., Thiessen, K.M., Frank, M.L., and Blaylock, G.B. (1992). Quantification of the interception and initial retention of radioactive contaminants deposited on pasture grass by simulated rain. *Atmospheric Environment.* Part A. General Topics, 26(18), 3313-3321.

Hoffman, G.J., and Shannon, M.C. (2007). Chapter 4. Salinity. *Developments in Agri. Engrg*, 13, 131-160.

Holmes, J.W., (1984). "Measuring evapotranspiration by hydrological methods." *Agr. Water Mgmt.*, 8:29-40.

Hooghart, J.C. (ed.) (1987). *Evaporation and weather*. TNO Com. on Hydrol. Res., Proc. and Info. No. 39, 111 pp.

Horst, T.W. and Weil, J.C. (1992). Footprint estimation for scalar flux measurements in the atmospheric surface-layer. *Boundary-Layer Meteorol* 59:279-296.

Horton, R., and Chung, S.O. (1991). "Soil heat flow." Chap. 17, pp. 397-438. *In*: Hanks, R.J. and Ritchie, J.T. (eds). *Modeling Plant and Soil Systems*, Agronomy Series No. 31, Am. Soc. Agron., Madison, Wisc.

Horton, R., and Wierenga, P.J. (1983). "Estimating the soil heat flux from observations of soil temperature near the surface." *Soil Sci. Soc. Am. J.*, 47: 14-20.

Hostetler, S.W., and Bartlein, P.J. (1990). "Simulation of lake evaporation with application to modeling lake level variations of Harney-Malheur Lake, Oregon." *Water Resources Res.*, 26(10):2603-2612.

Houk, I.E. (1926). "Evaporation on United States Reclamation Projects." *Trans. Am. Soc. Civ. Engrs.*, 90:266-378.

Hounam, C.E., (1958). "Evaporation pan coefficients in Australia." pp. 52-60. *In:* Climatology and Microclimatology, UNESCO.

Hounam, C.E., (1973). "Comparison between pan and lake evaporation." *Rapport of Rapporteur on Lake Evaporation of the Commission for Hydrology*, World Meteorology Technical Note 126, WMO, Geneva Switzerland,

Howell, T.A., (1990). "Relationship between crop production and transpiration, evapo-transpiration, and irrigation." pp.391-434, *In:* Stewart, B.A, and Nielsen, D.R. (eds), *Irrigation of Agricultural Crops*, Agron. Series 30, Am. Soc. Agron., Madison, WI, 1245 pp.

Howell, T.A., Evett, S.R., Tolk, J.A. and Schneider, A.D. (2004). Evapotranspiration of Full-, Deficit-Irrigated, and Dryland Cotton on the Northern Texas High Plains. *J. Irrig. and Drain. Engrg.*, ASCE 130(4):277-285.

Howell, T.A., Dusek, D.A., Tolk, J.A., Copeland, K.S., Colaizzi, P.D., Evett, S.R. 2006. Crop Coefficients Developed at Bushland, Texas for Corn, Wheat, Sorghum, Soybean, Cotton, and Alfalfa. In proceedings of the 2006 World Environmental and Water Resources Congress, EWRI (on CD-ROM).

Howell, T.A., McCormick, R.L., and Phene, C.J., (1985). "Design and installation of large weighing lysimeters." *Trans. Am. Soc. Agr. Engrs.*, 28:106-112, 117.

Howell, T. A., Steiner, J. L., Schneider, A. D., Evett, S. R., and Tolk, J. A. (1997). "Seasonal and maximum daily evapotranspiration of irrigated winter wheat, sorghum, and corn-Southern High Plains." *Trans. of the ASAE*, 40(3), 623–634.

Howell, T.A., Yazar, A., Schneider, A.D., Dusek, D.A., and Copeland, K.S. (1995). "Yield and water use efficiency of corn in response to LEPA irrigation." *Trans. of the ASAE*, 38(6):1737-1747.

Howell, T.A., Meek, D.W., Phene, C.J., Davis, K.R., and McCormick, R.L. (1984). Automated weather data collection for research on irrigation scheduling. *Trans. of the ASAE*, 27(2):386-391.

Hoy, R.D., and Stephens, S.K. (1979). "Field study of lake evaporation: Analysis of data from phase 2 storages and summary of phase 1 and phase 2." *Tech. Paper No. 41*. Austria Water Resources Council, Dept. of National Devel., 177 pp.

Hsieh, C.I., G. Katul, and T. Chi. (2000). "An approximate analytical model for footprint estimation of scalar fluxes in thermally stratified atmospheric flows." *Adv. Water Resources* 23:765-772.

Hsieh, C.I., Katul, G.G., Schieldge, J., Sigmon, J.T. and Knoerr, K.K. (1997). "The Lagrangian stochastic model for fetch and latent heat flux estimation above uniform and non-uniform terrain." *Water Resources Res.* 22:427-438.

Hubbard, K. G., Goddard, S., Sorensen, W.D., Wells, S. N. , and Osugi, T. T. (2005) "Performance of Quality Assurance Procedures for an Applied Climate Information System." *J. Atmos. Oceanic Technol.*, **22**, 105–112.

Hughes, G.H. (1967). "Analysis of techniques used to measure evaporation from Salton Sea, California." pp. 151-176, *U.S. Geologic Survey Prof. Paper 272-H*.

Hultine, K.R., Nagler, P.L., Morino, K., Bush, S.E., Burtch, K.G., Dennison, P.E., Glenn, E.P., Ehleringer, J.R. (2010). "Sap flux-scaled transpiration by tamarisk (Tamarix spp.) before, during and after episodic defoliation by the saltcedar leaf beetle (Diorhabda carinulata)" *Agric. and For. Meteorol.,* 150(11):1467-1475.

Humphreys, E.R., Black, T.A., Ethier, G.J., Drewitt, G.B., Spittlehouse, D.L., Jork, E.M., Nesic, Z., and Livingston, N.J. (2002). "Annual and seasonal variability of sensible and latent heat fluxes above a coastal Douglas-fir forest, British Columbia, Canada." *Agr. and Forest Meteorol.*, 115(1-2):109-125.

Hunsaker, D.J. (1999). "Basal crop coefficients and water use for early maturity cotton." *Trans. of the ASAE* 42(4):927-936.

Hunsaker, D.J. Pinter, P.J., Cai, H. 2002. Alfalfa basal crop coefficients for FAO-56 procedures in the desert regions of the southwestern U.S., Trans. of the ASAE, 45(6):1799-1815

Hunsaker, D.J., Barnes, E.M., Clarke, T.R., Fitzgerald, G.J., Pinter Jr, P.J. (2005). "Cotton irrigation scheduling using remotely-sensed and FAO-56 basal crop coefficients." *Trans. of the ASAE*. 48(4):1395-1407.

Hunsaker, D.J. Pinter, P.J. Jr., Barnes, E.M. and Kimball, B.A. (2003). "Estimating cotton evapotranspiration crop coefficients with a multispectral vegetation index." *Irrig Sci* 22:95–104.

Hunsaker, D.J., Pinter, Jr., P.J. and Cai, H. (2002) Alfalfa basal crop coefficients for FAO–56 procedures in the desert regions of the southwestern U.S. *Trans ASAE*. 45(6):1799–1815.

Huntington, J.L. and Allen, R.G. (2010). "Evapotranspiration and net irrigation water requirements for Nevada. *State of Nevada, Div. of Water Resourc*. 260 p.

Huntington, J.L, Szilagyi, J., Tyler, S. and Pohll, G. (2011). "Evaluating the complementary relationship for estimating evapotranspiration from arid shrublands." *Water Resour. Res.* 47, W05533, doi:10.1029/2010WR009874.

Huntington, J.L., and Allen, R. (2010). "Evapotranspiration and Net Irrigation Water Requirements for Nevada." *Nev. State Eng. Office Publ.*, 266 pp.

Huschke, R.E. (ed). (1959). "*Glossary of meteorology*." Am. Meteorol. Soc., Boston, 638 pp.

Idso, S.B., (1974). "The Calibration and Use of Net Radiometers." *Adv. Agron.*, 26:261-275.

Idso, S.B. (1981). "A set of equations for full spectrum and 8-14 μm and 10.5-12.5 μm thermal radiation from cloudless skies." *Water Resourc. Res.*, 17:295-304.

Idso, S.B. and Cooley, K.R. (1971). "The vertical location of net radiometers I. The effects of the underlying air layer. *J. Meteorol. Soc. Jpn.,* 49(5):343-349.

Idso, S.B. and Cooley, K.R. (1972). "The vertical location of net radiometers II. The effects of the net radiometer's shadow." *J. Meteorol. Soc. Jpn*., 50(1):49-58.

Idso, S.B., Reginato, R.J., Jackson, R.D., Kimball, B.A., and Nakayama, F.S. (1974). The three stages of drying of a field soil. *Soil Sci. Soc. Am.,* 38(5):831-837.

Irrigation Association. (2003). "*Landscape Irrigation Scheduling and Water Management: Practices Guidelines*." Rept. by Water Manage. Com., McCabe, J., Ossa, J., Allen, R.G., Carleton, B., Carruthers, B., Corcos, C., Howell, T.A., Marlow, R., Mecham, B., and Spofford, T.L. (eds).

Irrigation Association. 2011. *Irrigation*, 6th ed., Irrig. Assoc., Falls Church, VA. 1114 p.

Int'l Comm. on Irrig. and Drain. (1985) "On updated evapotranspiration and crop water requirement terms for the ICID Multilingual Technical Dictionary on Irrigation and Drainage, 1967." *ICID Bulletin*, 34:1-5

Iritz, Z., Lindroth, A., Heikinheimo, M., Grelle, A. and Kellner, E., 1999. "Test of a modified Shuttleworth-Wallace estimate of boreal forest evaporation." *Agr. and For. Meteorol*., 98-99: 605-619.

Irmak (Kilic), A. and Kamble. B. (2009). "Evapotranspiration data assimilation with genetic algorithms and SWAP model for on-demand Irrigation." *Irrig. Sci.,* 28:101-112.

Irmak, S., Dukes, M.D. and Jacobs, J.M. (2005). "Using modified Bellani plate evaporation gauges to estimate short canopy reference evapotranspiration." *J. Irrig. and Drain. Eng.* 131(2):164-175.

Irmak, S., Irmak, A., Allen, R.G., and Jones, J.W. (2003). "Solar and net radiation-based equations to estimate reference evapotranspiration in humid climates." *J. Irrig. and Drain. Eng.*, 129(5):336-347.

Irmak, S., Irmak, A., Howell, T.A., Martin, D.L., Payero, J.O., and Copeland, K.S. (2008a). "Variability analysis of alfalfa-reference to grass-reference evapotranspiration ratios in growing and dormant seasons." *J. Irrig. and Drain. Engr.*, 134(2):147-159.

Irmak, S. and Mutiibwa, D. 2009. "On the dynamics of evaporative losses from Penman-Monteith with fixed and variable canopy resistance during partial and complete maize canopy." *Trans. of the ASABE*, 52(4):1139-1153.

Irmak, S, Mutiibwa, D.,A. Irmak (Kilic), T.J. Arkebauer, A. Weiss, D.L. Martin, D.L., and Eisenhauer, D.E. (2008b). "On the scaling up leaf stomatal resistance to canopy resistance using photosynthetic photon flux density." *Agr. and For. Meteorol*., 14 8:103 4–1044.

Irmak, S., Payero, J.O. and Martin, D.L. (2004). "Using modified atmometers (ETgage®) for irrigation management. *Univ. Nebr. NebGuide G1579*. Lincoln, NE. 4 p.

Irmak, S., Payero, J.O., Martin, D.L., Irmak A., and Howell, T.A. (2006). "Sensitivity analyses and sensitivity coefficients of standardized daily ASCE-Penman-Monteith equation." *J. Irrig. and Drainage Engineering*, ASCE, 132(6):564-578.

Irrigation Association. (2005). "*Landscape Irrigation Scheduling and Water Management: Practices Guidelines*." Rep. by Water Management Committee. McCabe, J., Ossa, J., Allen, R. G., Carleton, B., Carruthers, B., Corcos, C., Howell, T. A., Mar-low, R., Mecham, B., and Spofford, T. L. (eds). 51 p. http://www.irrigation.org/uploadedFiles/Resources/BMP_Revised_12-2010.pdflast.

Itenfisu, D., Elliott, R.L., Allen, R.G, and Walter, I.A. (2000). "Comparison of reference evapotranspiration calculations across a range of climates." pp. 217-227, *In*: Evans, R.G., Benham, B.L., and Trooien, T.P. (eds). *National Irrigation Symposium*, Proc., 4th Decennial Symp., Am. Soc. Agr. Engrs., St. Joseph, MI, 693 pp.

Itenfisu D., Elliott, R.L., Allen, R.G, and Walter, I.A. (2003). "Comparison of reference evapotranspiration calculations as part of ASCE standardization effort." *J. Irrig. and Drain. Engrg*. 129(6):440-448.

Jackson, R.D. (1973). "Diurnal changes in soil water content during drying." pp. 37-__. *In*: Bruce, R.R., Flach K.W., and Taylor, H.M. (eds). *Field Soil Water Regime*, SSSA Spec. Publ. No. 5, Soil Sci. Soc. Am., Madison, WI, 224 pp.

Jackson, R.D., Kimball, B.A., Reginato, R.J., and Nakayama, F.S. (1973). "Diurnal soil-water evaporation: Time-depth-flux patterns." *Soil Sci. Soc.Am. Proc.*, 37:505-509.

Jackson, R.D., Idso, S.B., and Reginato, R.J., (1976). "Calculation of evaporation rates during the transition from energy-limiting to soil-limiting phases using albedo data." *Water Resour. Res.*, 12:23-26.

Jacobs, J., Anderson, M.C., Freiss, L.C., and Diak, G.R. (2004). "Solar radiation, longwave radiation and emergent wetland satellite evapotranspiration estimates from Florida (USA)." *Hydrological Sci. J.* 49(3):461-476.

Jacobs, C. M. J. and De Bruin, H. A. R. 1997. "Predicting regional transpiration at elevated atmospheric CO2: influence of the PBL vegetation interaction." *J. Appl. Meteorol. Clim.*, 36:1663–1675.

Jacobs, A.F.G., Halbersma, J. and Przybyla, C. (1989). "Behaviour of the crop resistance of maize during a growing season." pp. 165-173. In: *Estimation of Areal Evapotranspiration*, Black, T.A., Spittlehouse, D.L., Novak, M.D., and Price, D.T. (ed)., IAHS Pub. No. 177.

Jagtap, S.S., and Jones, J.W. (1989a). "Evapotranspiration model for developing crops." *Trans. of the ASAE,* 32:1342-1350.

James, D.W., Hanks, R.J., Jurinak, J.J., (1982). *Modern Irrigated Soils*. John Wiley & Sons, New York, 245 pp.

Jara, J., Stockle, C.O., and Kjelgaard, J. (1998). "Measurement of evapotranspiration and its components in a corn (*Zea Mays L.*) field." *Agr. and For. Meteorol.*, 92:131-145.

Jarvis, P.G.. (1976). "The interpretation of the variations in leaf water potential and stomatal conductance found in canopies in the field." *Phil. Trans. Roy. Soc.*, London., B 273: 593-610.

Jarvis, P.G., James, G.B. and Landsberg, J.J. (1976). "Coniferous forest." pp. 171-240, *In*: Monteith, J.L. (ed.). *Vegetation and the Atmosphere*, 2. Academic Press, London.

Jensen, M.E. (ed.), (1966). *Evapotranspiration and its Role in Water Resources Management*. Proc. Conf. on Evapotr., Am. Soc. Agr. Engrs., Chicago, IL. December. 65 pp.

Jensen, M.E., (1967). "Evaluating irrigation efficiency." *J. Irrig. and Drain. Div.*, ASCE, 93(IR1):83-98.

Jensen, M.E., (1968). "Water consumption by agricultural plants." 1-22. *In*: Kozlowski, T. T. (ed). *Water Deficits and Plant Growth*, Vol. II, Academic Press, New York., 401 pp.

Jensen, M.E. (1969). "Scheduling irrigations with computers." *J. Soil and Water Conserv.*, 24(5):193-195.

Jensen, M.E. (2003). "Data from *Vegetative and Open Water Coefficients for the Lower Colorado River Accounting System*. Addendum to a 1998 Report submitted to the U.S. Bureau of Reclamation, Boulder City, NV, December 2003. 24 pp..

Jensen, M.E. (ed). (1974). *Consumptive Use of Water and Irrigation Water Requirements*." Rep. Tech. Com. on Irrig. Water Requirements, Irrig. and Drain. Div., ASCE, 227 pp.

Jensen, M.E. (2007). "Beyond irrigation efficiency." *Irrig. Sci.*, 25:233-245.

Jensen, M.E. and Allen, R.G., (2000). "Evolution of practical ET estimating methods." pp.52-65, *In:* Evans, R.G., Benham, B.L., and Trooien, T.P. (eds). *National Irrigation Symposium*, Proc., 4th Decennial Symp., Am. Soc. Agr. Engrs., St. Joseph, MI, 693 pp.

Jensen, Sv.E., and Aslyng, H.C. (1967). "Net radiation and long-wave radiation at Copenhagen 1962-1964. *Archiive für Meteorologie, Geophysik and Bioklimatologie*, Series B: Allegemeine und biologische Klimatologie, Band 15, Helt 1-2:127-140.

Jensen, M.E., Burman, R.D. and Allen, R.G. (1990). *Evapotranspiration and Irrigation Water Requirements*. ASCE Manuals and Reports on Engineering Practice No 70, 350 pp.

Jensen, M.E, Dotan, A. and Sanford, R. (2005). "Penman-Monteith estimates of reservoir evaporation." Paper presented at the 2005 ASCE Conference in Palmer, Alaska, May 19.

Jensen, M.E., and Erie, L.J. (1971). "Irrigation and water management." pp. 189-222. *In*: Johnson, R.T. et al. (eds.). *Advances in Sugarbeet Production*, Iowa State Univ. Press, Ames, IA.

Jensen, M. E. and Haise, H. R. (1963). "Estimating evapotranspiration from solar radiation." *J. Irrig. and Drain. Div*., Am. Soc. Civ. Engrs., 89:l5-41.

Jensen, M.E., and Hanks, R.J. (1967). "Nonsteady-state drainage from porous media." *J. Irrig and Drain. Div.*, 93(IR3):209-231.

Jensen, M. E., Robb, D.C.N., and Franzoy, C.E. (1970). "Scheduling irrigations using climate-crop-soil data." *J. Irrig. and Drain. Div.*, 96:25-28.

Jensen, M.E. and Wright, J.L., (1978). "The role of evapotranspiration models in irrigation scheduling." *Trans. of the ASAE*, 21(1):82-87.

Jensen, M.E., Wright, J.L., and Pratt, B.J. (1971). "Estimating soil moisture depletion from climate, crop and soil data." *Trans. of the ASAE*, 14:954-959.

Jensen, S., (1994). *Genetic Improvement of Maize for Drought Tolerance*. Paper presented at the NRC Water Sci. and Techn. Bd. Workshop on Future of Irrigation, Irvine, CA, 2-3 June.

Jia, X., Dukes, M.D. and Jacobs, J.M. (2007). Development of bahiagrass crop coefficient in a humid climate. *ASABE Paper No. 07-2151*.

Jiusheng, L., and Kawano, H. (1996). "The areal distribution of soil moisture under sprinkler irrigation." *Agr. Water Mgmt*., 32(1):29-36.

Johnson, M., Saito, L., Anderson, M.A., Weiss, P., Andre, M., and Fontaine, D.G. (2004). "Effects of climate and reservoir and dam operations on reservoir thermal structure." *J. Water Resources Planning and Management*, 130(2):112-122.

Johnson, R. S., L. E. Williams, J. E. Ayars and T. J. Trout. 2005. "Weighing lysimeters aid study of water relations in tree and vine crops." *Calif. Agric.* 59(2):133-136.

Jones, H.G.. (1979). "Stomatal behaviour and breeding for drought resistance." pp. 406-428. *In*: Mussell, H., and Staples, R.C. (eds). *Stress Physiology in Crop Plants*, John Wiley & Sons, New York, NY.

Jones, F.E. (1992). "*Evaporation of Water: with Emphasis on Applications and Measurement."* Lewis Publ., Inc., Chelsea, MI, 200 pp.

Jones, C.A. and Kiniry, J.R. (1986). (eds). "*CERES-Maize: A simulation model of maize growth and development.*" Texas A&M Univ. Press, College Station.

Jones, C.A., Bland, W.L., Ritchie, J.T., and Williams, J.R. (1991). "Simulation of root growth." pp.91-123. *In* Hanks, J.R., and Richie, J.T. (eds) *Modeling Plant and Soil Systems.* Agron. Series. 31, Am. Soc. of Agron, Madison, WI, 565 pp.

Jones, J.W., Boote, K.J., Jagtap, S.S., Wilkerson, G.G., Hoogenboom, G., and Mishoe, J.W. (1987). "*SOYGRO V5.4 Technical Documentation*." Agr. Eng. Dept. Res. Rept., Univ. of Florida, Gainesville, FL.

Jones, A.L., Fisher, P.D., and Croft, B.A. (1981). "Implementing pest management models using real time weather data." pp. 223-237. *In*: Weiss, A. (ed) *Computer Techniques and Meteorological Data Applied to Problems of Agriculture and Forestry: a Workshop*, Dept. of Agr. Meteorol., Univ. of Nebraska-Lincoln.

Jury, W.A., Gardner, W.R, and Gardner, W.H. (eds), (1991). *Soil Physics*. John Wiley & Sons, Inc., New York, 345 pp.

Jury, W.A., and Tanner, C.B. (1975). "Advection modification of the Priestley and Taylor evapotranspiration formula." *Agron. J.*, 67:569-572.

Kamble, B., Irmak A. (2009). "Combining remote sensing measurements and model estimates through hybrid data assimilation scheme to predict hydrological fluxes." *Proc. of the IEEE In'tl. Geosci. and Remote Sensing Symp.*. July 6-11, 2008. Boston, MA.

Kamgar, A., Hopmans, J.W., Wallender, W.W. and Wendroth, O. (1993). "Plotsize and sample number for neutron probe measurements in small field trials." *Soil Sci.*, 156(4):213-___.

Kang, S., Gu, B., Du, T., and Zhang, J.(2003). "Crop coefficient and ratio of transpiration to evapotranspiration of winter wheat and maize in a semi-humid region." *Agr. Water Mgmt.*, 59:239-254.

Katerji, N. and Perrier, A. (1985). "Determination de la resistance globale d'un couvert vegetal a la diffusion de vapeur d'eau et de ses differentes composantes." *Agr. and For. Meteorol*., 34:105-120.

Kato, T., Kimura, R., and Kamichika, M., 2003. "Estimation of evapotranspiration, transpiration ratio and water-use efficiency from a sparse canopy using a compartment model." *Agr. Water Manage.*, 65(3): 173-191.

Katul, G.G. and Parlange, M.B. (1992). "Estimation of bare soil evaporation using skin temperature measurements." *J. Hydrol*., 132:91-106.

Kay, M. (1986). "*Surface Irrigation Systems and Practice.*" Cranfield Press, Cranfield, UK, 152 pp.

Keijman, J.Q. (1974). "The estimation of the energy balance of a lake from simple weather data." *Boundary-Layer Meteorol.*, 7:399-407.

Kelliher, F.M., Leuning, R., Raupach, M.R., and Schulz, E.D. (1995). "Maximum conductances for evaporation from global vegetation types." *Agr. and Forest Meteorol.*, 73:1-16

Keller, J. (1986). *Sprinkler and trickle irrigation.* Dept. Agr. and Irrig.Eng., Utah State Univ., Logan, UT 84322-4105. 621 pp.

Kilic (Irmak), A., Allen, R.G., Kjaersgaard, J. Huntington, J. , Kamble, B. , Trezza, R. and Ratcliffe, I. (2012). "Operational remote sensing of ET and challenges." Chp. 21 in *Evapotranspiration – Remote Sensing and Modeling* (A. Irmak, editor), Publisher: InTech

Kilic (Irmak), A., Ratcliffe I., Ranade P., Hubbard K.G., Singh R.K., Kamble B., Allen R.G., Kjaersgaard J., (2011). "Estimation of land surface evapotranspiration: A satellite remote sensing procedure." *Great Plains Res.*.v21(1), Apr. 2011.

Kelliher, F.M., Leuning, R., and Schulze, E.D. (1993). "Evaporation and canopy characteristics of coniferous forests and grasslands." *Oecologia*, 95:153-163.

Kimball, B.A., Idso, S.B., and Aase, J.K. (1982). "A model of thermal radiation from partly cloudy and overcast skies." *Water Resour. Res.* 18(4):931-936.

King, K.M., Tanner, C.B. and Suomi, V.E. (1956). "A floating lysimeter and its evaporation recorder." *Trans. Am. Geophys. Union*, 37(6):738-742.

Kirkham, R.R., Gee, G.W. and Jones, T.L. (1984). Weighing lysimeters for long-term water balance investigations at remote sites. *Soil Sci. Soc. Am. J.*, 48:1203-1205.

Kite, G. (2000). "Using a basin-scale model to estimate crop transpiration and soil evaporation." *J. of Hydrol.*, 229(1-2):59-69.

Kite, G., and Droogers, P. (2000). "Comparing evapotranspiration estimates from satellites, hydrological models, and field data." *J. of Hydrol.*, 229(1-2):3-18.

Kizer, M. A. and R. L. Elliott. 1991. Eddy correlation systems for measuring evapotranspiration. *Trans. of the ASAE* 34(2):387-392.

Kizer, M. A., R. L. Elliott and J. F. Stone. 1990. "Hourly ET model calibration with eddy flux and energy balance data." *J. of Irrig. and Drain. Eng.*, 116(2):172-181.

Kjaersgaard, J.H., Cuenca, R.H., Plauborg, F.L., and Hansen, F.L. (2007). "Long-term comparisons of net radiation calculation schemes." *Boundary-Layer Meteorol.* 123:417–431.

Kjelgaard, J.F., Stockle C. O., Black R.A., Campbell G.S. (1997). "Measuring sap flow with the heat balance approach using constant and variable heat inputs." *Agric. and For. Meteorol.*, 85(3-4):239-250.

Kjelgren, R., Rupp, L., and Kilgren, R. (2000). "Water conservation in urban landscapes." *HortScience*, 35(6):1037-1040.

Klaassen, W., Sogachev A. (2006). "Flux footprint simulation downwind of a forest edge." *Boundary Layer Meteorol.* 121, 459-473.

Klaassen W., Van Breugel P.B., Moors E.J., Nieveen J.P. (2002). "Increased heat fluxes near a forest edge." *Theor Appl Climatol*, 72:231–243

Klepper, B., (1990). "Root growth and water uptake." pp. 281-322, *In:* Stewart B.A. and Nielsen, D.R. (co-editors), *Irrigation of Agricultural Crops*, Agron. Series 30, Am. Soc. Agron., Madison, WI, 1245 pp.

Klocke, N.L., Heermann, D.F., and Duke, H.R. (1985). "Measurement of evaporation and transpiration with lysimeters. *Trans. of the ASABE*, 28(1):183-189.

Klocke, N.L., Todd, R.W., and Schneekbth, J.P. (1996). "Soil water evaporation in irrigated corn." *Appl. Engr. In Agric.*, 12(3):301-306.

Kohl, R.A., and DeBoer, D.W. (1984). Drop size distributions for low pressure spray type agricultural sprinkler. *Trans. of the ASAE*, 27(6):1836-1840.

Kohl, R.A., and Wright, J.L. (1974). "Air temperature and vapor pressure changes caused by sprinkler irrigation." *Agron. J.*, 66(1), 85-88.

Kohler, M.A. (1954). "Lake and pan evaporation." pp. 127-148, *In*: Water-Loss Investigations: Lake Hefner Studies, Tech. Rep., *Geological Survey Prof. Paper 269*, 170 pp.

Kohler, M.A., Nordenson, T.J., and Fox, W.E., (1955). "*Evaporation from Pans and Lakes*." U.S. Dept. Com., Weather Bur. Res. Paper 38. 21 pp.

Kohler, M.A, Nordenson, T.J., and Fox, W.E. (1958). "Pan and lake evaporation." pp. 38-60, *In*: Harbeck, G.E. Jr., Kohler, M.A., Koberg G.E., and others. "Water Loss Investigations: Lake Mead Studies." *Geological Survey Prof. Paper 298*, 112 pp.

Kohler, M.A, Nordenson, T.J., and Fox, W.E. (1959). "Evaporation maps for the United States." *Technical Paper No. 37*, Weather Bureau, U.S. Dept. of Com., 15 pp plus five maps.

Kolle, O., Rebmann, C. (2007). "EddySoft - Documentation of a software package to aquire and process eddy covariance data." *Max-Planck-Institut f. Biogeochemie*, Jena, Tech. Rept. 10, 85 pp.

Kondo, J. (1975). Air-sea bulk transfer coefficients in diabatic conditions. *Boundary-Layer Meteorology* 9:91-112.

Kondo, J. (1994). *Meteorology of the Water Environment*. Asakura Shoten Press, Japan, 350pp., (in Japanese).

Kopec, A.R., Langley, M.N., and Bos, M.G. (1984). "Major variables which influence effective precipitation." *Int'l. Comm. on Irrig. and Drain. Bull.*, 33(2):65-70, 84.

Körner, C., Scheel, J.A., and Bauer, H. (1979). "Maximum leaf conductance in vascular plants." *Photosynthetica*, 13(1):45-82.

Kozlowski, T.T., (1964). "*Water Metabolism in Plants*." Harper & Row, New York. 227 pp.

Kozlowski, T.T. (ed), (1968a). "*Water Deficits and Plant Growth*." Vol. I, Development, Control and Measurement. Academic Press, New York, 401 pp.

Kozlowski, T.T. (ed), (1968b). "*Water Deficits and Plant Growth*." Vol. II, Plant Water Consumption and Response. Academic Press, New York, 345 pp.

Kozlowski, T.T. (ed), (1972). "*Water Deficits and Plant Growth*." Vol. III, Plant Responses and Control of Water Balance. Academic Press, New York, 382 pp.

Kozlowski, T.T. (ed), (1976). "*Water Deficits and Plant Growth*." Vol. IV, Soil Water Measurement, Plant Responses, and Breeding for Drought Resistance. Academic Press, New York, 397 pp.

Kranz, W.L., and Eisenhauer, D.E. (1990). "Sprinkler irrigation runoff and erosion control using interrow tillage techniques." *Appl. Eng. in Agr.*, 6(6):739-744.

Kroes, J.G., and van Dam, J.C. (2003) (eds). *Reference Manual SWAP version 3.0.3*.

Alterra, "*Green World Research.*"Wageningen, the Netherlands, Alterra-report 773. 211 pp.

Kruse, E.G., and Haise, H.R. (1974). "Water use by native grasses in high altitude Colorado meadows." *W. Reg. Rept. ARS-W-6-1974*. Washington, D.C.: USDA-ARS.

Kruse, E.G., and Neale, C.M.U. (1988). "Sources of error in hydraulic weighing lysimeter measurements." *Trans. of the ASAE,* 32(1):81-88,96.

Kustas, W. P., 1990. "Estimates of evapo-transpiration with a one and two layer model of heat transfer over partial canopy cover." *J. of Appl. Meteorol.*, 29(8): 704-715

Kustas, W., and Anderson, M. 2009. "Advances in thermal infrared remote sensing for land surface modeling." *Agr. and For. Meteorol.*, 149:2071–2081.

Kustas,W.P. and C.S.T.Daughtry, 1990. "Estimation of the soil heat flux/net radiation ratio from spectral data," *Agric. and For. Meteorol.*, 49:205-223.

Kustas, W. P., Moran, M. S., Humes, K. S., Stannard, D. I., Pinter, J., Hipps, L., and Goodrich, D. C. (1994). "Surface energy balance estimates at local and regional scales using optical remote sensing from an aircraft platform and atmospheric data collected over semiarid rangelands." *Water Resources Research*, 30(5), 1241-1259.

Kustas, W.P., and Norman, J.M. (1999). Evaluation of soil and vegetation heat flux predictions using a simple two-source model with radiometric temperatures for partial canopy cover. *Agric.and For. Meteorol*. 94:13-29.

Kustas, W.P., Norman, J. M., Anderson, M.C., and French, A. N. (2003). “Estimating subpixel surface temperatures and energy fluxes from the vegetation index-radiometric temperature relationship.” *Remote Sensing Environ.*, 85:429-440.

Kustas, W.P., Norman, J.M., Schmugge, T.J., Anderson, M.C., 2004. “Mapping surface energy fluxes with radiometric temperature.” *In*: Quattrochi, D.A., Luvall, J.C. (eds.), *Thermal Remote Sensing in Land Surface Processes*. CRC Press, Boca Raton, FL, pp. 205–253.

Lafleur, P.M., and Rouse, W.R. (1990). "Application of an energy combination model for evaporation from sparse canopies." *Agr. and For. Meteorol.*, 49:135-153.

Lagos LO (2008) “A modified surface energy balance to model evapotranspiration and surface canopy resistance.” *PhD Dissert. Univ. of Nebr.-Linc. Lincoln., Nebr.*. 208 p.

Lagos L.O. Martin D.L., Verma S. Suyker A. and Irmak S. (2009). “Surface energy balance model of transpiration from variable canopy cover and evaporation from residue covered or bare soil systems.” *Irrig. Sci.*. (28)1:51-64.

Lagos, L.O., Merino, G., Martin, D., Verma, S. and Suyker, A.. 2012. “Evapotranspiration of partially vegetated surfaces.” Chp. 13 IN *Evapotranspiration - Remote Sensing and Modeling, Edited by Ayse Irmak, ISBN 978-953-307-808-3, Hard cover, 514 pages.*

Lascano, R.J. (2000). “A general system to measure and calculate daily water use.” *Agron. J.*, 92(5):821-832.

Lascano, R.J., van Bavel, C.H.M., Hatfield, J.L., and Upchurch, D.R. (1987). "Energy and water balance of a sparse crop: simulated and measured soil and crop evaporation." *Soil Sci. Soc. Am. J.*, 51:1113-1121.

Lean, J. (1989). "Contribution of ultraviolet irradiance variations to changes in the sun's total irradiance." *Science*, 244:197-200.

Leclerc, M.Y., Shen, S.H. and Lamb, B. (1997). “Observations and large-eddy simulation modeling of footprints in the lower convective boundary layer.” *J. Geophy. Res. Atmos.* 102:9323-9334.

Leclerc, M.Y. and Thurtell, G.W. (1990). “Footprint prediction of scalar fluxes using a Markovian analysis. *Boundary-Layer Meteorol.*, 52:247-258.

Lee, X., Massman, W. and Law. B. (eds) (2004). “*Handbook of Micrometeorology : A Guide for Surface Flux Measurement and Analysis*.” Atmos. and Oceanographic Sci. Library, Kluwer.

LeMert, R.D. (1972). “Water use of alfalfa in the Imperial Valley.” *Imp. Agr. Briefs* (July)13:16.

LeMert, R.D. (1973). "Weather and lysimeter data for Brawley, California." Personal Communication.

Lettau, H.H. (1969). "Note on aerodynamic roughness-parameter estimation on the basis of roughness-element description." *J. Appl. Meteorol.*, 8:828-832.

Leuning, R. (2007). “The correct form of the Webb, Pearman and Leuning equation for eddy fluxes of trace gases in steady and non-steady state, horizontally homogeneous flows.” *Bound.-Layer Meteor.* 123(2):263-267.

Leuning, R., and Attiwill, P.M. (1978). "Mass, heat and momentum exchange between a mature Eucalyptus forest and the atmosphere." *Agr., Meteorol.*, 19:215-241.

Leuning, R., Condon, A.G., Dunin, F.X., Zegelin, S., and Denmead, O.T. (1994). “Rainfall interception and evaporation from below a wheat canopy.” *Agr. and For. Meteorol.*, 115(1-2):109-125.

Ley, T.W., and Allen, R.G. (1994). "Energy and soil water balance analyses of arid weather sites." 1994 Summer Meeting of the Am. Soc. Agr. Engrs., Kansas City, Mo., ASAE Paper No. 94-2078. 26 pp.

Ley, T.W., Allen, R.G., and Hill, R.W. (1996). “Weather station siting effects on reference Evapotranspiration.” *Proc. Int’l. Conf. on Evapotranspiration and Irrig. Scheduling*, Nov.3-6, San Antonio, TX, ASAE, St. Joseph, MI.

Ley, T.W, Allen, R.G., and Jensen, M.E. (2013). "Translating wind speed measuremed over alfalfa having varying height for use in the ASCE Standardized Reference ET Equation. *J. Irrig. and Drain. Engr.*, 139(6):463-465.

Ley, T.W., and Elliott, R.L. (1993). "Standards for automated agricultural weather stations." pp. 977-984. *In*: Allen, R.G., and Neale, C.M. (eds) *Management of Irrigation and Drainage Systems: An Integrated Approach*, Proceedings, National Conference on Irrigation and Drainage Engineering, ASCE, New York, NY.

Ley, T.W. and Evans, R.G. (1990). "Washington public agriculture weather system." pp. 261-269. *In*: *Visions of the Future*, Proc. Third Nat'l. Irrig. Symp., Am. Soc. Agr. Engrs., St. Joseph, MI.

Ley, T.W., and Kroeger, M.W. (1988). "Washington public agricultural weather system." Am. Soc. Agr. Engrs. *Paper #PNR88-106*. 12 pp.

Ley, T.W., Hill, R.W., Jensen, D.T. (1994a). "Errors in Penman-Wright alfalfa reference evapotranspiration estimates. I Model sensitivity analyses." *Trans. of the ASAE*, 37(6):1853-1861.

Ley, T.W., Hill, R.W., Jensen, D.T. (1994b). "Errors in Penman-Wright alfalfa reference evapotranspiration estimates. II Effects of weather sensory measurement variability." *Trans. of the ASAE*, 37(6):1863-1870.

Lhomme, J.P. (1988a). "Extension of Penman's formulae to multi-layer models." *Boundary-Layer Meteorol.*, 42:281-291.

Lhomme, J.P. (1988b). "A generalized combination equation derived from a multi-layer micrometeorological model." *Boundary-Layer Meteorol.*, 45:103-115.

Lhomme, J.P., D. Troufleau, B. Monteny, A. Chehbouni, S. Bauduin. 1997. "Sensible heat flux and radiometric surface temperature over sparse Sahelian vegetation II. A model for the kB -I parameter." *J. of Hydrology*, 188-189:839-854.

Li, F., Kustas, W.P., Prueger, J.H., Neale, C.M.U., Jackson, T.J. (2005). "Utility of remote sensing-based two-source energy balance model under low- and high-vegetation cover conditions." *J. Hydrometeorol.* 6(12), 878-891.

Li, Y., Shao, M., Wang, W., Wang, Q., and Horton, R. (2003). "Open-hole effects of perforated plastic mulches on soil water evaporation." *Soil Science,* 168(11):751-758.

Licor. (2012). "EddyPro users manual." http://www.licor.com/env/products/eddy_covariance/software.html?gclid=CIG-ktWrsboCFaY1QgodNU0AFw

Liu, P.C., and Schwab, D.J. (1987). "A comparison of methods for estimating u* and for given uz and air-sea temperature differences. J. Geophysical Res. 92(C6):6488-6494.

Lin, J.D., 1980. On the force-restore method for prediction of ground surface temperature. *J. Geophys Res.*, 85(C6), 3251-3254.

List, R.J. (1963). *Smithsonian Meteorological Tables*. Smithsonian Miscellaneous Collections Volume 114. Smithsonian Institution, Washington, DC.

List, R.J., (1984). *Smithsonian Meteorological Tables*, 6th rev. ed, Smithsonian Institution, Washington. 539 pp.

Liu, P.C., and Schwab, D.J. (1987). "A comparison of methods for estimating u* and for given uz and air-sea temperature differences. *J. Geophysical Res.* 92(C6):6488-6494.

Livingston, B.E. (1935). "Atmometers of porous porcelain and paper, their use in physiology ecology." *Ecology*, 16(3):438-472.

Livingston, G.J. (1908-9). "An annotated bibliography of evaporation." *Mo. Weather Rev.*, Vol. 36:181-186, 301-306, 375-371-375; 37:68-72, 103-109, 157-160, 193-199, 248-242.

Lofgren, B.M. (2004). "A model for simulation of the climate and hydrology of the Great Lakes basin." *J. Geophys. Res: Atmospheres (1984-2012)*, 109:D18108. doi:10.1029/2004JD004602.

London, J. and Fröhlich, C. (eds). (1982). *Extended Abstracts Presented at the Symposium on the Solar Constant and the Spectral Distribution of Solar Irradiance*. IAMAP Third Scientific Assembly, August 17-28, 1981, Hamburg, Federal Republic of Germany. 41 pp.

Lowry, R.L., and Johnson, A.F., (1942). "Consumptive use of water for agriculture." *ASCE Trans.*, 107:1243-1302.

Ludlow, M.M., and Jarvis, P.G. (1971). "Photosynthesis in Sitka Spruce (*Picea sitchensis*)(Bong.) Carr.). I. General Characteristics." *J. Appl. Ecol* 8:925-953.

Luo, L., et al. (2003), "Validation of the North American land data assimilation system (NLDAS) retrospective forcing over the southern Great Plains." *J. Geophys. Res.*, 108(D22), 8843, doi:10.0129/2002JD003646.

Luquet D., Vidal A., Smith M., Dauzat J. (2005). "More crop per drop': How to make it acceptable for farmers?" *Agric. Water Manage.*, 76(2):108-119.

Maas, E.V. (1990). "Crop salt tolerance." pp. 262-304, *In*: Tanji, K.K. (ed), Agricultural *Salinity Assessment and Management*. ASCE Manuals and Reports on Engrg. Practice No. 71, Am. Soc. Civ. Engrs., New York, 630 pp.

Mackay, D.S., Ahl, D.E., Ewers, B.E. Gower, S.T., Burrows, S.N., Samanta, S., Davis, K.J. (2002). "Effects of aggregated classifications of forest composition on estimates of evapotranspiration in a northern Wisconsin forest. *Global Change Biology*. 8(12):1253–1265.

Mahrt, L., and M. Ek (1984), "The influence of atmospheric stability on potential evaporation," *J. Clim. Appl. Meteorol*., 23:222–234.

Majumdar, N.C., Mathur, B.L., and Kaushik, S.B. (1972). "Prediction of direct solar radiation for low atmospheric turbidity." *Solar Energy* 13:383-394.

Makkink, G.F. (1957). "Testing the Penman formula by means of lysimeters." *J. Inst. Water Engng.,* 11(3):277-288.

Mantovani, E.C., Villalobos, F.J., Orgaz, F., and Fereres, E. (1995). "Modelling the effects of sprinkler irrigation uniformity on crop yield." *Agr. Water Mgmt.*, 27(3):243-257.

Mao, L.M., Bergman, M.J., and Tai, C.C. (2002). " Evapotranspiration measurement and estimation of three wetland environments in the upper St. Johns River Basin, Florida." *J. Am. Water Resour. Assoc.*, 38(5):1271-1285.

Marciano, J.J., and Harbeck, G.E.. 1954. "Mass transfer studies." pp. 46-70, *In*: "Water-Loss Investigations: Lake Hefner Studies." Technical Report, *Geol. Survey Prof. Paper 269*, 170 pp.

Marek, T., P. Colaizzi, T.A. Howell, D. Dusek, and D. Porter. (2006). "Estimating seasonal crop ET using calendar and heat unit based crop coefficients in the Texas High Plains Evapotranspiration Network." ASABE Pap. no: 062206, 2006 ASABE Ann. Int. Mtg, Portland, Oregon, 9 - 12 July 2006, 11 p.

Marek, T.H., Schmeider, A.D., Howell, T.A., and Ebeling, L.L., (1988). "Design and construction of large weighing monolithic lysimeters." *Trans. of the ASAE*, 31(2):477-484.

Marsh, A.W., Strohman, R.A., Spaulding, S., Youngner, V., and Gibeault, V. (1980). "Turf grass irrigation research at the University of California: Warm and cool season grasses tested for water needs." *Irrig. J.*, July/August. pp. 20-21, 32-33.

Martin, D.L. and Gilley, J. (1993). "Irrigation Water Requirements." Chap. 2, Part 623, *National Engineering Handbook*, USDA, Soil Conservation Service, 284 pp.

Martin, D.L., Kincaid, D.C., and Lyle, W.M. (2007). " Design of sprinkler systems." pp. 557-631, *In*: Hoffman, G.J., Evans, Evans, R.G., and Jensen, M.E. (eds), *Design and Operation of Farm Irrigation Systems*, Am. Soc. Agr. and Biol. Eng., St Joseph, MI.

Martin, D.L., Gilley, J.R., Carmack, W.J., and Hardy, L.A. (1993). "SCS methods for determining irrigation water requirements." pp. 1013-1038, *In*: Allen, R.G., and Neale, C.M.U. (eds). "*Management of Irrigation and Drainage Systems."* Proc., 1993 Nat. Conf. on Irrig. and Drain. Engrg, ASCE,Park City, UT, Jul. 21-23, 1223 pp.

Martin, D.L., Stegman, E.C., and Fereres, E.. (1990). “Irrigation scheduling principles.” Chp. 7, pp. 157-203, *In* Hoffman, G.,J. Howell, T.A., and Solomon, K.H. *Management of Farm Irrigation Systems*. ASAE Mono., St. Joseph, MI, 1055 pp.

Martin, E.C, Shayya, W.H., Bralts, V.F., Loudon, T.L., and Johnson, J.A., (1990). “Irrigation scheduling: a statewide program in Michigan.” pp. 700-706, *In: Visions of the Future*, Proc.3rd Nat’l. Irrig. Symp., Am. Soc. Agr. Engrs., St. Joseph, MI, 775 pp.

Martsolf, J.D. (1981). "Satellite frost forecasting system for Florida." pp. 223-237. *In*: Weiss, A. (ed). *Computer Techniques and Meteorological Data Applied to Problems of Agriculture and Forestry: a Workshop*. Dept. of Agr. Meteorol., Univ. of Nebr.-Lincoln.

Massman, W.J. (1999). “A model study of kB_u^{-1} for vegetated surfaces using ‘localized near-field’ Lagrangian theory. *J. Hydrol.*, 223:27-43.

Massman, W.J. (2000). “A simple method for estimating frequency response corrections for eddy covariance systems. *Agric. and For. Meteorol.*, 104:185-198.

Massman, W.J. (2001). “Reply to comment by Rannik on: A simple method for estimating frequency response corrections for eddy covariance systems." *Agric. and For. Meteorol.*, 107:247-251.

Massman, W.J., and Kaufmann, M.R. (1991). “Stomatal response to certain environmental factors: a comparison of models for subalpine trees in the Rocky Mountains.” *Agr. and For. Meteorol.*, 54(2-4):155-167.

Mateos,L., Mantovani, E.C., and Villalobos, F.J. (1997). “Cotton response to non-uniformity of conventional sprinkler irrigation.” *Irrig. Sci*., 17(2):47-52.

Mauder, M., and Foken, T., 2004. “Documentation and instruction manual of the eddy covariance software package TK2.” Universitaet Bayreuth, Abt. Mikrometeorologie, Print, ISSN 1614-8916, 20Arbeitsergebnisse 26, 44 pp.

Maurer, E.P., Wood, A.W., Adam, J.C., Lettenmaier, D.P., and Nijssen, B. (2002). “A Long-term hydrologically-based data set of land surface fluxes and states for the conterminous United States.” *J. of Climate* 15(22), 3237–3251.

McArthur, J.A., Hesketh, J.D., and Baker, D.N. (1975). "Cotton." pp. 297-325. *In*: Evans, L.T. (ed.) *Crop Physiology*, Cambridge Univ. , pp 297-325.

McBean, G.A. (1972). “Instrument requirements for eddy correlation measurements.” *J. Appl. Meteorol.*, 11:1078-1084.

McCabe, G.J., Markstrom, S.L., (2007). “A monthly water-balance model driven by a graphical user interface.” Open-File Report 2007–1088, U.S. Dept. of the Int., U.S. Geolog. Surv. http://wwwbrr.cr.usgs.gov/projects/SW_MoWS/software/thorn_s/thorn.shtml

McDole, R.E., McMaster, G.M., and Larson, D.C., (1974). "Available water-holding capacities of soils in southern Idaho." *Current Info. Ser. No. 236*, Univ. of Idaho, Moscow, ID. 4 pp.

McEwen, G.F. (1930). “Results of evaporation studies conducted at the Scripps Institute of Oceanography and the California Institute of Technology.” *Bull. of the Scripps Inst. of Oceanography, Techn. Series*, 2(11):401-415.

McFarland, M.J., Worthington, J.W., and Newman, J.S. (1983). "Design, installation and operation of a twin weighing lysimeter for fruit trees." *Trans. of the ASAE,* 26(6):1717-1721

McGinn, S.M., and King, K.M. (1990). "Simultaneous measurements of heat, water vapor and CO_2 fluxes above alfalfa and maize." *Agr. and For. Meteorol*., 49: 331-349.

McIlroy, I.C. and Angus, D.E. (1963). “The Aspendale multiple weighed lysimeter installation.” *C.S.I.R.O. Div. Meteorol. Phys. Techn. Paper*, 14:27.

McIlroy, I.C. and Angus, D.E. (1964). "Grass, water and soil evaporation at Aspendale." *Agric. Meteorol.*, 1(3):201-224.

McIlroy, I. C., and Dunin, F.X. (1982). "A forest evaporation technique comparison experiment." The First Nat’l. Symp. on For. Hydrol., Melbourne. The Inst. of Engrs., Australia, May.

McNaughton, K.G., and Black, T.A. (1973). "A study of evapotranspiration from a Douglas fir forest using the energy balance approach." *Water Resources Res*., 9:1579-1590.

McNaughton, K.G., and van den Hurk, B.J.J.M. (1995). "A 'Lagrangian'revision of the resistors in the two-layer model for calculating the energy budget of a plant canopy." *Boundary-Layer Meteorol.*,74:261–288.

Medeiros, G.A de, Arruda, F.B., Sakai, E. and Fujiwara, M. (2001). The influence of crop canopy on evapotranspiration and crop coefficient of beans (*phaseolus vulgaris* L.). *Ag. Water. Manage*. 49:211-224.

Meek, D.W. (1997). "Estimation of maximum possible daily global solar radiation." *Agr. and For. Meteorol.* 87:223-241.

Meek, D.W., and Hatfield, J.L. (1994). "Data quality checking for single station meteorological databases." *Agr. and Forest Meteorol*., 69:85-109.

Merriam, J.L. and Keller, J., (1978). "*Farm irrigation system evaluation: A guide for management*." Agr. and Irrig. Eng. Dept., Utah State Univ., Logan, UT. 171 pp.

Meyer, A.F. 1942. *Evaporation from lakes and reservoirs*. Minn. Resources Commission, St. Paul, 56 pp. plus 11 maps and numerous graphs.

Meyer, J.L. and Gibeault, V.A. (1986). "Turfgrass performance under reduced irrigation." *Calif. Agric.*, *40*(7), 8.

Meyer, S. J., and Hubbard, K.G. (1992). "Nonfederal Automated Weather Stations and Networks in the United States and Canada: A Preliminary Survey." *Bull. Am. Meteorol. Soc.* 73(4):449-457.

Meyer, S. J., Hubbard, K.G. and White, D.A. (1989). "Estimating potential evapotranspiration: The effect of random and systematic error." *Agr. Forest Meteorol.* 46:285-296.

Meyer, W.S. and Mateos, L. (1990). "Soil type effects on soybean crop water use in weighing lysimeters III. Effect of lysimeter canopy height discontinuity on evaporation." *Irrig. Sci*. 11:233-237.

Milly, P. C. D. (1988). "Advances in modeling of water in the unsaturated zone." *Transp. in Porous Media* 3(5): 491-514.

Milne, R. (1979). "Water loss and canopy resistance of a young sitka spruce plantation." *Bound.-Layer. Met.*, 16:67-81.

Misson, L., Panek, J.A., Goldstein, A.H., (2004). "A comparison of three approaches to modeling leaf gas exchange in annually drought stressed ponderosa pine forests." *Tree Physiol.* 24 (5), 529.

Mitchell, R.B., Moore, K.J., Moser, L.E., Fritz, J.O. and Redfearn, D.D. (1997). "Predicting developmental morphology in switchgrass and big bluestem." *Agron. and Hort. Faculty Publ.* Digitalcommons.unl.edu/agronomyfacpub/67.

Mitchell, K. E., et al. (2004). "The multi-institution North American Land Data Assimilation System (NLDAS): Utilizing multiple GCIP products and partners in a continental distributed hydrological modeling system." *J. Geophys. Res., 109, D07S90, doi:10.1029/2003JD003823*

Miyazaki, T. (1993). "*Water Flow in Soils*." Books in Soils, Plts. and the Environ., Marcel-Decker, Inc., New York. ISBN 0-8247-8982-2. 296 p.

Mo, X., and Beven, K. 2004. "Multi-objective parameter conditioning a three-source wheat canopy model." *Agri. and For. Meteorol.*, 122:39-63.

Molden, D. (1997). "Accounting for water use and productivity." IN *IWMI/SWIM Pap. No. 1*, Int'l. Water Mgmt. Inst., 25 pp.

Molden, D. (2007). "*Water for Food, Water for Life: A comprehensive Assessment of Water Management in* Agricultue."
Int'l. Water Mgmt. Inst., 645 pp.

Moncrieff, J.B., Malhi, Y. and Leuning, R. (1996). "The propagation of errors in long-term measurements of land-atmosphere fluxes of carbon and water." *Global Change Biology*, 2:231-240.

Monin, A.S., and Obukhov, A.M. (1954). "The basic laws of turbulent mixing in the surface layer of the atmosphere." *Akad. Nauk. SSSR Trud. Geofiz. Inst*., No. 24 (151):163-187.

Monteith, J.L. (1965). "Evaporation and the environment." pp. 205-234. *In*: *The state and movement of water in living organisms*, XIXth Symposium. Soc. for Exp. Biol., Swansea, Cambridge Univ. Press.

Monteith, J.L., (1973). "*Principles of Environmental Physics*." American Elsevier Publishing Company, New York, 241 pp.

Monteith, J.L. (1981). "Evaporation and surface temperature." *Quart. J. Roy. Meteorol. Soc.*, 107:1-27.

Monteith, J.L., (1987). "In memoriam Howard Latimer Penman (1909-1984)" *Irrig. Sci.*, 8:77-79.

Monteith, J.L. (1995). "Accommodation between transpiring vegetation and convective boundary layer." *J. of Hydrology*, 166(3-4):251-263.

Monteith, J. L., and Szeicz, G. (1962). "Radiative temperature in the heat balance of natural surfaces." *Quart. J. Roy Meteorol. Soc.*, 88:496-507.

Monteith, J.L., and Unsworth, M.H. (1990). "*Principles of Environmental Physics*, 2nd Ed." Edward Arnold, London, New York. 291 pp.

Moog, P.R., and Janiesch, P. (1990). "Root growth and morphology of *Carex* species as influenced by oxygen deficiency." *Functional Ecology* 4(2):201-208.

Moore, C.J. (1974). "A comparative study of forest and grassland micrometeorolgy." Ph.D. Thesis, The Flinders, Univ. of S. Australia. 237 pp.

Moore, C.J. (1986). "Frequency response corrections for eddy correlation systems." *Boundary-Layer Meteorol.*, 37, 17-35.

Moran, S. (2000). "Use of remote sensing for monitoring evaporation over managed watersheds." *ASCE CD ROM*, 13 pp.

Moran, M.S., Rahman, A.F., Washburne, J.C., Goodrich, D.C., Weltz, M.A., Kustas, W.P., (1996). "Combining the Penman-Monteith equation with measurements of surface temperature and reflectance to estimate evaporation rates of semiarid grassland." *Agr. and For. Meteorol.*, 80(2-4): 87-109.

Morgan, D.L., Pruitt, W.O., and Lourence, F.J. (1971). "Analyses of momentum, energy and mass transfers above vegetative surfaces." *Res. and Development Tech. Rep.*, ECOM 68-G10-F, Univ. of Calif., Davis, 142 pp.

Morton. F.I. (1971). "Catchment evaporation and potential evaporation – further development of a climatological relationships." *J. Hyrol.*, 12:81-99.

Morton, F.I. (1983). Operational estimates of areal evapotranspiration and their significance to the science and practice of hydrology. *J. Hydrol.*, 66:1-76.

Mott K.A. and Parkhurst D.F. (1991). "Stomatal responses to humidity in air and helox." *Plant, Cell and Environment* 14, 509-515.

Muchow, R.C., and Bellamy, J.A. (1991). "*Climate Risk in Crop Production: Models and Management for the Semiarid Tropics and Subtropics."* Proc., Int'l. Symp. on Climate Risk in Crop Production: Models and Management for the Semiarid Tropics and Subtropics., Brisbane, Australia, 2-6 Jul., 558 pp.

Murray, F.W., (1967). "On the computation of saturation vapor pressure." *J. Appl. Meteor.*, 6:203-204.

Musick, J.T., Dusek, D.A., and Mathews, A.C., (1984). "Irrigation water management of winter wheat." Paper 84-2094, Am. Soc. Agr. Engrs., St. Joseph, MI.

Mutziger, A.J., Burt, C.M., Howes, D.J. and Allen, (2001). "Comparison of measured and FAO-56 modeled evaporation. App. E , *ITRC Rept. R 02-001*, Calpoly,San Luis Obispo, Calif. (http://www.itrc.org/reports/EvaporationCA/EvaporationCA.html)

Mutziger, A.J., Burt, C.M., Howes, D.J. and Allen, R.G. 2005. Comparison of measured and FAO-56 modeled evaporation from bare soil. *J. Irrig. and Drain. Engrg*., 131(1):59-72.

Nadezhdina, N, Eermák J., Ceulemans R. (2002). "Radial patterns of sap flow in woody stems of dominant and understory species: scaling errors associated with positioning of sensors." *Tree Physiology*, 22:907–918

Nagler, P.L., Glenn, E.P., Thompson, T.L., Huete, A. (2004). "Leaf area index and normalized difference vegetation index as predictors of canopy characteristics and light interception by riparian species on the Lower Colorado River." *Agric. and For. Meteorol.* 125(1-2):1-17.

Nagler, P.L., Morino, K., Didan, K., Erker, J., Osterberg, J., Hultine, K.R., Glenn, E.P. (2009). "Wide-area estimates of saltcedar (Tamarix spp.) evapotranspiration on the lower Colorado River measured by heat balance and remote sensing methods." *Ecohydrol*. 2, 18–33.

Nakayama, F.S., and Bucks, D.A. (1986). *Trickle Irrigation for Crop Production: Design, Operation and Management*, Elsevier, Amsterdam, 393 pp.

Nakayyama, K., Pruitt, W.O., and Chandio, B. (1983). "Some aspects of the Priestley and Taylor model to estimate evapotranspiration." *The Tech. Bull. of the Fac. of Hort.,* Chiba Univ., No. 32:25-30.

National Energy Renewable Lab. (1992). "*Users Manual National Solar Radiation Data Base*." NSRDB Vol. 1, 100 pp. + App. A-D.

Neale, C.M.U., Artan, G.A., Tarboton, D.G., and Hanson, C.H. (1995). "A spatially distributed energy balance model: development, validation and application." *Proc. 25th Conf. Agr. and For. Meteorol.*, Am. Meteorol. Soc., Jan. 1995, Dallas, TX.

Neale, C.M.U., Bausch, W.C., and Heermann, D.F. (1989). "Development of reflectance-based crop coefficients for corn." *Trans. of the ASABE*, 32(6):1891-1899.

Nebraska High Plains Climate Center. (2006). "Crop Coefficients, Phenology, and Growing Degree Day Accumulation." http://www.hprcc.unl.edu/crop/

Niel, P., and Zunino, J.P. (1971). "Essais sur les besoins en eau des cultures au cours des années 1969 et 1970." *L'Irrigant. Revue de la Soc. du Canal de Provence No. 55* (Sept-Dec.).

Neilson, R.E., Ludlow, M.M., and Jarvis, P.G. (1972). "Photosynthesis in Sitka spruce (*Picea sitchensis* (Bong.) Carr.)," *J. Appl. Ecol.*, 9:721-745.

Nielsen, R.L. (2012). Heat unit concepts related to corn development. Purdue University Corny News Network Article. http://www.kingcorn.org/news/timeless/HeatUnits.html, accessed August 24, 2014.

Nie, D., and Kanemasu, E.T. (1989). "A comparison of net radiation on slopes." pp. 142-143. *In*: *Proc. 19th Conf. Agr. and For. Meteorol.*, Am. Meteorol. Soc., March 1989, Charleston, S. Carolina.

Niu, G.-Y., Yang, Z.-L., Mitchell, K.E., Chen, F., Ek, M.B., Barlage, M., Longuevergne, L., Kumar, A., Manning, K., Niyogi, D., Rosero, E., Tewari, M., and Xia, Y. (2011). "The community Noah land surface model with multiparameterization options (Noah-MP): 1. Model description and evaluation with local-scale measurements." J. Geophys. Res., doi:10.1029/2010JD015139,

Noilhan, J. and Planton, S. (1989). "A simple parameterization of land surface processes for meteorological models," *Monthly Weather Rev.* 117:536-549.

Norman, J. M., Anderson, M.C., Kustas, W.P., French, A.N., Mecikalski, J., Torn, R., Diak, G.R., Schmugge, T.J., and Tanner, B.C.W. (2003). "Remote sensing of surface energy fluxes at 10^1-m pixel resolutions." *Water Resources Res.*, 39(8):1221, doi:10.1029 / 2002WR001775.

Norman, J.M., and Arkebauer, T.J. (1991). "Predicting canopy light-use efficiency from leaf characteristics." Chp. 7, pp. 125-143. *In*: Hanks, R.J. and Ritchie, J.T. (eds). *Modeling Plant and Soil Systems*, Agronomy Series No. 31, Am. Soc. Agron., Madison, Wisc.

Norman, J.M., Kustas, W.P., and Humes, K.S. (1995). "A two-source approach for estimating soil and vegetation energy fluxes from observations of directional radiometric surface temperature." *Agr.and For. Meteorol.* 77: 263-293.

Norman, J. M., Kustas, W.P., Prueger, J.H., and Diak, G. R. (2000). "Surface flux estimation using radiometric temperature: A dual-temperature-difference method to minimize measurement errors." *Water Resources Res.,* 36(8):2263-2274.

Novak, M.D. (1989). "The use of analytical solutions to determine the evapotranspiration from bare and vegetated surfaces." pp. 133-152. *In*: Black, T.A., Spittlehouse, D.L., Novak M.D. and Price, D.T. (eds). *Estimation of Areal Evapotranspiration*, IAHS Pub. No. 177. .

NREL. (1992). *Interim Solar Radiation Data Manual*. Nat'l. Renewable Energy Lab., NREL/TP-463-5176, 80 pp.

Obukhov, A.M. (1946). "Turbulence in an atmosphere with non-uniform temperature," *Trudy Instit. Teoret. Geofiz*: AN-S.S.S.R., No. 1 (English Trans.: (1971), *Bound. Layer Meteorol.* 2:7-29.

Ohmura, A. (1982). "Objective criteria for rejecting data for Bowen ratio flux calculations." *J. Applied Meteorol.*, 21(4): 595-598.

Oke, T.R. (1978). "*Boundary Layer Climates*." John Wiley & Sons, New York, A Halsted Press Book, 342 pp.

Oleson, K.W., Dai, Y., Bonan, G., Bosilovich, et al. (2004). "Technical description of the Community Land Model (CLM), NCAR Tech. Note NCAR/TN 461+STR, 174 pp., Natl. Cent. for Atmos. Res., Boulder, Colo. (Available at www.cgd.ucar.edu/ tss/clm/distribution/clm3.0/index.html.)

Olivier, H. (1961). "*Irrigation and Climate*". Edward Arnold, Ltd, London, 250 pp.

Olioso, Y. Inoue, S., Ortega-FARIAS, J., Demarty, J.P., Wigneron, I., Braud, F., Jacob, P., Lecharpentier, C., OttlÉ and Calvet, J.-C. et al. 2005. "Future directions for advanced evapotranspiration modeling: Assimilation of remote sensing data into crop simulation models and SVAT models." *Irrig. and Drain. Syst.*, 19(3-4):377-412.

Ortega-Farias, S., Carrasco, M., Olioso, A., Acevedo, C. and Problete, C. (2007). "Latent heat flux over Cabernet Sauvignon vineyard using the Shuttleworth and Wallace model." *Irrig. Sci* 25(2): 161-170.

Ortega-Farias, S., Olioso, A., Antonioletti, R., Brisson, N. 2003. "Evaluation of the Penman-Monteith model for estimating soybean evapotranspiration." *Irrig. Sci.*, 23(1):1-9.

Ortega-Farias, S. O, Olioso, A., Fuentes, S., Valdes, H., 2005. "Latent heat flux over a furrow-irrigated tomato crop using Penman–Monteith equation with a variable surface canopy resistance." *Agr. Water Manage.,* 82(3):421-432.

Ortega-Farias et al. (2010). "Parameterization of a two-layer model for estimating vineyard evapotranspiration using meteorological measurements." *Agr. and For. Meteorol.* 150(2):276-286.

Oster, J. D., Meyer, J.L., Hermsmeier, L., and Kaddah, M.. (1984). "Imperial Valley: irrigation, drainage and runoff." *Soil and Water No. 60*, Fall 1984. Coop. Ext., Univ. of Calif., Oakland, CA 94608.

Paço, T. A., Ferreira, M.I., and Conceição, N. (2006). "Peach orchard evapotranspiration in a sandy soil: comparison between eddy covariance measurements and estimates by the FAO 56 approach." *Agr. Water Manage.* 85(3):305-313.

Panofsky, H. A. (1963). "Determination of stress from wind and temperature measurements." *Quart. J. Roy. Meteorol. Soc*., 89:85-94.

Pastor, M., and Orgaz, F. (1994). "Los programas de recorte de riego en olivar." *Agricultura* 746: 768-776.

Parchomchuk, P., Bernard, R.C., and Van der Gulik, T.W. (1996). "Automated irrigation scheduling using an electronic atmometer." pp 1099-1104, *In*: Camp, C.R., Sadler, E.J., and Yoder, R.E. (eds.), *Proc. Int'l. Conf. Evapotranspiration and Irrig. Scheduling*, Nov. 3-6, San Antonio, Texas. ASAE, St. Joseph, MI.

Paulson, C.A. (1970). "The mathematical representation of wind speed and temperature profiles in the unstable atmospheric surface layer." *J. Appl. Meteorol*. 9:857-861.

Paw U, K.T. and Gao, W. (1988). "Applications of solutions to non-linear energy budget equations." *Agr. and For. Meteorol*., 43:121-145.

Paw U., K.T., Baldocchi, D.D., Meyers, T.P. and Wilson, K.B. (2000). "Correction of eddy covariance measurements incorporating both advective effects and density fluxes." *Boundary-Layer Meteorol.*, 97:487-511.

Payero, J.O., Neale, C.M.U., Wright, J.L., and Allen, R.G. (2003). "Guidelines for validating Bowen ratio data." *Trans. of the ASAE*, 46(4):1051-1060.

Pelton, W.L., King, K.M., and Tanner, C.B. (1960). An evaluation of the Thorntwaite and mean temperature methods for determining potential evapotranspiration. *Agron. J.*,52:387-395.

Penman, H.L., (1948). "Natural evaporation from open water, bare soil and grass." *Proc. Roy. Soc. London*, A193:120-146.

Penman, H.L. (1956a). "Evaporation: An introductory survey." *Neth. J. Agr. Res.*, 4(1):9-29.

Penman, H.L. (1956b). Estimating evaporation. *Am. Geophys. Union Trans.*, 37:43-50.

Penman, H.L. (1963). "*Vegetation and Hydrology".* Tech. Comm. No. 53, Commonwealth Bureau of Soils, Harpenden, England, 125 pp.

Penman, H.L. and Schofield, R.K., (1951). "Some physical aspects of assimilation and transpiration." *Proc. Symp. nr. Soc. Exp. Biol.*, 115-129.

Pereira, A. R., Green, S., Nova, N. A. V. 2005. "Penman–Monteith reference evapotranspiration adapted to estimate irrigated tree transpiration." *Agr. Water Manage.*, 83(1-2):153-161.

Pereira, L.S., Perrier, A., Allen, R.G., and Alves, I. (1999). "Evapotranspiration: Concepts and future trends." *J. Irrig. and Drain. Engrg.*, 125(2):45-51.

Pereira, L.S., Smith, M., and Allen, R.G. (1999). "Crop water requirements." pp. 213-262, *In*: *CIGR* (*International Association of Agricultural Engineers) Handbook of agricultural engineering*. Vol. I, Sec. 1.5.1, Am. Soc. Agr. Engrs., St. Joseph, MI.

Pereira, L.S. (1995). "Crop-water-simulation models in practice: Selected papers of the 2nd Workshop on Crop-Water-Models." Proc. 15th Congr. Int'l. Comm. on Irrig. and Drain. (ICID), The Hague, The Netherlands in 1993. 339 p.

Perez, R.,Stewart, R., Arbogast, C., Seal, R., and Scott, J. (1986). "An isotropic hourly diffuse radiation model for sloping surfaces: descriotion, performance, validation, site dependency evaluation." *Solar Energy*, 36:481-497.

Perrier, A. (1982). "Land surface processes: vegetation." pp. 395-448 *In*: Eagleson, P. (ed.) *Land Surface Processes in Atmospheric General Circulation Models*. Cambridge Univ. Press.

Perrier, A. (ed.), (1985). *Crop Water Requirements*. Proc., Int. Conf., Institut National de la Recherche Agronomique, Paris, 947 pp.

Perrier, A., and Jensen, M.E. (Engl. Version), (1979). "Question 1 - terminology, and question 2 - measurement methods." pp. A-120-A-145. *Int. Round Table Conf. on Evapotranspiration*, Int. Comm. on Irrig. and Drain., Budapest, Hungary, May 26-28, 1977. Ann. Rep., New Delhi, India.

Perry, C. (2007). "Efficient irrigation; inefficient communication; flawed recommendations." *Irrig and Drain.*, 56(4):367-378.

Petersen, E.W. (1969). "On the relation between the shear stress and the velocity profile after a change in surface roughness." *J. Atmos. Sci*., 26:773-774.

Pettry,D.E., and Switzer, R.E.. (1996). "Sharkey soils in Mississippi." *Miss. Agric. and For. Exp. Sta. Bul. 1057*. (http://msucares.com/pubs/bulletins/b1057.htm) Accessed Oct. 2003.

Pfeiffer, L. and Lin, C. (2008). « The effect of irrigation technology on groundwater Use. «*Choices Magazine*. 25(3). 6 pp.

Phene, C.J., Reginato, R.L., Itier, B., and Tanner, B.R. (1990). "Sensing irrigation needs." pp 208-261. *In*: Hoffman, G.J., Howell, T.A., and Solomon, K.H. (eds.). *Management of Farm Irrigation Systems*, ASAE Mono., ASAE, St. Joseph, Michigan.

Philip, J.R. (1957). "Evaporation and moisture and heat fields in the soil." *J. Meteorol*., 14:354-366.

Phillips, W.D. and Irbe, J.G. (1978). "Land-to-lake comparison of wind temperature and humidity on Lake Ontario during the International Field Year for the Great Lakes (IFYGL)." Rep. CLI-2-77, *Atmos. Environ. Serv.,* Environ. Canada, Downsview, Ontario.

Pieri, P., and Fuchs, M. (1990). "Comparison of Bowen ratio and aerodynamic estimates of evapotranspiration." *Agr. and For. Meteorol.*, 49:243-356.

Pierre, W.H., Kirkham, D., Pesek, D., and Shaw, R. (1966). *Plant Environment and Efficient Water Use*. Am. Soc. of Agron., Madison, WI, ___ pp.

Pinker, R.T. and Lazlo, I. (1992). Modeling surface solar irradiance for satellite applications on a global scale. *J. Appl. Meteorol.*, 31(2): 194–211.

Pittenger, D.R., and D. Shaw. (2001). "Applications of recent research in landscape irrigation management." *In*: Proc. UCR Turfgrass and Landscape Management Field Day, 17-18. Riverside, Calif.: Univ. Calif

Pittenger, D.R., and Shaw, D. (2004). "What we know about landscape water requirements." *CO-Hort*, Coop. Ext., Univ. of Calif., Vol. 6.1, pp. 1-4.

Pittenger, D. and Henry, J.M. (2005). "Refinement of urban landscape water requirements." Univ. of Calif. Coop. Ext., Central Coast & South Region. 10 Mar. 2011. <http://groups.ucanr.org/CLUH/files/25773.pdf>.

Pittenger, D.R., Shaw, D.A., Hodel, D.R., and Holt, D.B. (2001) "Responses of landscape groundcovers to minimum irrigation." *J. Environ. Hort.*, 19(2):78-84.

Plate, E. J. (1971). "Aerodynamic characteristics of atmospheric boundary layers." *U.S. Atomic Energy Comm., Critical Review Series*, TID-25465.

Poblete-Escheverria, C. and Ortega-Farias, S. (2009). "Estimation of actual evapotranspiration for a drip-irrigated Merlot vineyard using a three-source model." *Irr. Sci*. 28(1):65-78.

Pratt, P.F., Warner, J.E., and Nash, P.A., (1976). "Sampling the unsaturated zone in irrigated field plots." *Soil Sci. Soc. Am. J.*, 40:277-279.

Price, D.T., and Black, T.A. (1989). "Estimation of forest transpiration and CO_2 uptake using the Penman-Monteith equation and a physiological photosynthesis model." pp. 213-227. *In*: Black, T. A., Spittlehouse, D. A., Novak, M. D., and Price, D. T. (eds) *Estimation of Areal Evapotranspiration*, IAHS Pub. No. 177.

Priestley, C. H. B., and Taylor, R. J. (1972). "On the assessment of surface heat flux and evaporation using large scale parameters." *Mon. Weath. Rev.*, 100:81-92.

Pruitt, W.O. (1955). "*1955 Annual Report*." Wash. Agr. Exp. Stn., Prosser, Wash. State Univ., Pullman, WA, pp. 50-66.

Pruitt, W.O., (1960). "Relation of consumptive use of water to climate." *Trans. of the ASAE*, 3(1):9-13, 17.

Pruitt, W.O. (1963). "Application of several energy balance and aerodynamic evaporation equations under a wide range of stability." *Final Report to USAEPG on Contract DA-36-039-SC-80334*, Univ. of Calif., Davis, pp. 107-124.

Pruitt, W. O. (1964). "Cyclic relations between evapotranspiration and radiation." *Trans. of the ASAE,* 7(3):271-275, 280.

Pruitt, W.O. (1966). "Empirical method of estimating evapotranspiration using primarily evaporation pans." *Proc. Conf. on Evapotranspiration and its Role in Water Resources Management*. Chicago. Dec. Am. Soc. Agr, Engrs., pp. 57-61.

Pruitt, W.O. (1971). "Factors affecting potential evapotranspiration." Pp. 82-102 *In*: Monke, E.J. (ed). *Biological Effects in he Hydrological Cycle*, Proc. 3rd Int'l. Seminar for Hydrology Professors. Purdue Univ., W. Lafayette, IN, July.

Pruitt. W.O. (1984). "Procedures for development of ET_o maps for California." *Int'l. Comm. on Irrig. and Drain. Bull.*, 33(2):61-64, 84.

Pruitt, W. O. 1986. "Traditional methods: Evapotranspiration research priorities for the next decade." ASAE Paper No. 86-2629. St. Joseph, Mich.: ASAE.

Pruitt W.O. and Angus, D. E. (1960). "Large weighing lysimeter for measuring evapotranspiration." *Trans. Am. Soc. Agr. Engrs.,* 3(2):13-15,18.

Pruitt, W.O. and Doorenbos, J. (1977). "Empirical calibration, a requisite for evapotranspiration formulae based on daily or longer mean climatic data?" *International Round Table Conference on Evapotranspiration*, Budapest, Hungary, Int'l. Comm. on Irrig. and Drain., 20 pp.

Pruitt, W.O., and Lourence, F.J. (1966)."Tests of aerodynamic, energy balance and other evaporation equations over a grass surface." In: *Investigations of Energy, Momentum, and Mass Transfers near the Ground.* Final Rept., USAEPG Contract. Univ. of Calif., Davis,pp 37-63.

Pruitt, W.O. and Lourence, F.J. (1985). "Experiences in lysimetry for ET and surface drag measurements." pp. 51-69. *In: Advances in Evapotranspiration*. Am. Soc. of Agr. Engrs. Public. No. 74-85.

Pruitt, W. O., Fereres, E., Martin, P. E, Singh, H., Henderson, D.W., Hagan, R. M., Tarantino, E., and Chandio, B. (1984). "Microclimate, evapotranspiration, and water-use efficiency for drip- and furrow-irrigated tomatoes." *Proc. 12th Congr., Int'l. Comm. on Irrig. and Drain.*, Ft. Collins, CO., p. 367-394.

Pruitt, W.O., Morgan, D.L., and Lourence, F.J. (1973). "Momentum and mass transfers in the surface boundary layer." *Quart. J. Roy. Meteorol. Soc.*, 99:370-386.

Pruitt, W.O., Swann, B.D., Held, A., Sutton, B., Matista, A., and Hsiao, T.C. (1987). "Bowen ratio and Penman: Australian-Californian tests." pp. 149-158, *In*: James, L.G., and English, M.J. (eds), *Irrigation Systems for the 21st Century*, Proc., ASCE Conf. Irrig. and Drain. Engrg., Portland, OR, 780 pp.

Qualls, R., and Brutsaert, W. (1996). "Effect of vegetation density on the parameterization of scalar roughness to estimate spatially distributed sensible heat fluxes." *Water Resources Res.*, 32(3), 645-652.

Quinn,F.H. (1979). "An improved aerodynamic evaporation technique for large lakes with application to the International Field Year for the Great Lakes." *Water Resources Res.*, 15(4):935-940.

Raes, D. (2004). *UPFLOW*. "Water movement in a soil profile from a shallow water table to the topsoil (capillary rise)." *Ref. Man. Vers. 2.2.* K.U.Leuven University, Fac. of Appl. Biosci. and Eng., Dep. Land Manage., Vital De Costerstraat 102, 3000 Leuven, Belgium. 18. p.

Raes, D. and deProost P. (2003). "Model to assess water movement from a shallow water table to the root zone." *Agric. Water Manage.*, 62(2):79-91.

Raes, D., Steduto, P., Hsiao, T.C., and Fereres, E. (2009). AquaCrop—The FAO crop model to simulate yield response to water: II. Main algorithms and software description. *Agron. J.,* 101(3):438-447.

Ramdas, L.A. (1957). "Evaporation and potential evapotranspiration over the Indian Sub-Continent." *Indian J. Agr. Sci*., 27(2):l37-l49.

Rannik, U. (2001). "A comment on the paper by W.J. Massman: A simple method for estimating frequency response corrections for eddy covariance systems." *Agr. and For. Meteorol.*, 107:241-245.

Ratliff, L.F., Ritchie, J.T., Cassel, D.K., (1983). "Field-measured limits of soil water availability as related to laboratory-measured properties." *Soil Sci. Soc. Am. J.*, 47:770-775.

Rauner, J.L. (1976). "Deciduous forests." pp. 241-264. *In*: Monteith, J.L. (ed.) *Vegetation and the Atmosphere*, 2. Academic Press, London.

Raupach, M. R. (1979). "Anomalies in flux-gradient relationships over forest." *Boundary Layer Meteorol.* 16:467-486.

Raupach, M. R. (1994). "Simplified expressions for vegetation roughness length and zero-plane displacement as functions of canopy height and area index." *Boundary-Layer Meteorology*, 71(1-2), 211-216.

Raupach, M.R. 1989. "A practical Lagrangian method for relating scalar concentrations to source distributions in vegetation canopies." *Q. J. R. Meteorol. Soc.*, 115: 609-632.

Raupach, M.R., Antonia, R.A., and Rajagopalan, S. (1991). "Rough-wall turbulent boundary layers." *Appl. Mech. Rev.*, 44:1-25.

Raupach, M.R., Finnigan, J.J. and Brunet, Y. (1996). "Coherent eddies and turbulence in vegetation canopies: the mixing-layer analogy." *Boundary-LayerMeteorology* 78: 351-382.

Rawson, H.M., and Clarke, J.M. (1988). "Nocturnal transpiration in wheat." *Aust. J. Plant Physiol*, 15:397-406.

Reich, P.B. (2002). "Root life span." Chpt. 12 *In:* Waisel, Y., Eshel, A. and Kafkafi, U., eds. "*Plant Roots: the Hidden Half*," 3rd ed. CRC Press. 1136 pp.

Reynolds, H.L. and D'Antonio, C.M. (1996). "The ecological significance of plasticity in root weight ratio in response to nitrogen: Opinion." *Plant and Soil* 185:75-97.

Richie, W.E., and Pittenger, D.R. (2000). "Mixed landscape irrigation research findings." *Proc. UCR Turfgrass and Landscape Management Research Conf.,* 12-13.

Rijtema, P.E. (1958). "Calculation methods of potential evapotranspiration." *Rept. on the Conf. on Supplemental Irrigation*, Comm. V1 Int•l. Soc. Soil Sci., Copenhagen, June 30-July 4.

Rijtema, P.E. (1965). "*Analysis of actual evapotanspiration.*" Agric. Res. Rep. 69, Centre for Agric. Publ. and Doc. Wageningen, 111 pp.

Reyenga, W., Dunin, F.X., Bautovich, B.C., Rath, C.R., and Hulse, L.B. (1988). "A weighing lysimeter in a regenerating eucalypt forest: design, construction, and performance." *Hydrol. Processes*, 2:301-314.

Reynolds, H.L,. and D'Antonio, C.M. (1996). "The ecological significance of plasticity in root weight ratio in response to nitrogen: Opinion." *Plant and Soil* 185:75-97.

Rhoades, J.D. (1974). "Drainage for salinity control." pp. 433-461, *In*: van Schilfgaarde, J. (ed), *Drainage forAgriculture*, Agron. Mono. 17, Madison, WI.

Rhoades, J.D., and Merrill, S.D. (1976). "Assessing the suitability of water for irrigation: theoretical and empirical approaches." pp. 69-109, *In*: Prognosis of salinity and alkalinity*, Soils Bulletin 31,* United Nations Food and Agriculture Organization,. Rome, Italy.

Rhoades, J.D., Chanduvi, F., and Lesch, S. (1999). "Soil salinity assessment: methods and interpretation of electrical conductivity measurements." *Irrig. and Drain. Paper No. 57*, United Nations Food and Agriculture Organization,. Rome, Italy, 150 pp.

Rhoades, J.D., Kandiah, A., and Mashali, A.M. (1992). "The use of saline waters for crop production." *Irrig. and Drain. Paper No. 48*, United Nations Food and Agriculture Organization,. Rome, Italy, 133 pp.

Richards, L.A. (1931). "Capillary conduction of liquids through porous media." *Physics*, 1:318-333.

Richards, L.A., Gardner, W.R., and Ogata, G., (1956). "Physical processes determining water loss from soil." *Soil Sci. Soc. Am. Proc.*, 20:310-314.

Richie, W.E., and Pittenger, D.R. (2000). "Mixed landscape irrigation research findings." *Proc. UCR Turfgrass and Landscape Management Research Conf.,* 12-13.

Rijtema, P. E. (1965). "Analysis of actual evapotranspiration." *Agr. Res. Rep. No. 69*, Centre for Agr. Publ. and Doc., Wageningen, lll pp.

Ringersma, J. and Sikking, A. F. S. (2001). "Determining transpiration coefficients of Sahelian vegetation barriers." *Agroforestry systems* 51:1-9.

Ritchie, J.T. (1971). "Dryland evaporative flux in a subhumid climate: I. Micrometeorological influences." *Agron. J.*, 63:51-55.

Ritchie, J.T., (1972). "Model for predicting evaporation from a row crop with incomplete cover." *Water Resour. Res.,* 8:1204-1213.

Ritchie, J. T. (1974). "Evaluating irrigation needs for southeastern U.S.A." pp. 262-273. *Proc., Irrig. and Drain. Spec. Conf.*, Am. Soc. Civ. Engrs.

Ritchie, J.T. (1991). "Wheat Phasic Development." 31-54. *In*: R.J. Hanks and J.T. Ritchie (eds), *Modeling Plant and Soil Systems*, Agron. Series No. 31, Am. Soc. Agron., Madison, WI.

Ritchie, J.T. and Adams, J.E. (1974). "Field measurement of evaporation from soil shrinkage cracks." *Soil Sci. Soc. Am. Proc.*, 38:131-134.

Ritchie, J.T. and Burnett, E. (1971). "Dryland evaporative flux in a subhumid climate: II. Plant influences." *Agron. J* ., 63:56-62.

Ritchie, J.T., Godwin, D.C., and Singh, U. (1989). "Soil and weather inputs for the IBSNAT crop models." pp. 31-45, *In*: *Proc., IBNAT Symp.: Decision Support System for Agrotechnology Transfer:Part 1*, IBSNAT, Dept. Agron. and Soil Sci., Coll. of Trop. Agric. and Human Resources, Univ. of Hawaii, Honolulu.

Ritchie, J.T., and Johnson, B.S. (1990). "Soil and plant factors affecting evaporation." pp.363-390, *In:* Stewart, B.A, and Nielsen, D.R. (eds), *Irrigation of Agricultural Crops*, Agron. Series 30, Am. Soc. Agron., Madison, WI, 1245 pp.

Ritchie, J.T., and NeSmith, D.S. (1991). "Temperature and crop development." pp. 5-29. *In*: Hanks, R.J., and Ritchie, J.T. (eds). *Modeling Plant and Soil Systems*, Agronomy Series No. 31, Am. Soc. Agron., Madison, Wisc.

Ritchie, J.T. and Otter, S. (1985). "Description and performance of CERES-Wheat: a user-oriented wheat yield model." pp. 159-175. *In*: *ARS Wheat Yield Project. ARS-38*. Nat'l. Tech. Info. Serv., Springfield, VA.

Robins, J. R., Pruitt, W.O., and Gardner, W.H., (1954). "Unsaturated flow of water in field soils and its effect on soil moisture investigations." *Soil Sci. Soc. Am. Proc.*, 18:344-347.

Robinson, F. E. (1969). "Stands for automation achieved by sprinkling." *J. Irrig. and Drain. Eng.*, 95(3):385-389.

Robinson, J.M., and Hubbard, K.G. (1990). "Soil water assessment model for several crops in the High Plains." *Agron. J.*, 82:1141-1148.

Robock, A., et al. (2003) "Evaluation of the North American Land Data Assimilation System over the southern Great Plains during the warm season." *J. Geophys. Res.,* 108(D22), 8846, doi:10.1029/2002JD003245.

Rochette, P., Pattey, E., Desjardins, R.LO., Dwyer, L.W. and Stewart, D.W. (1991). "Estimation of maize canopy conductance by scaling up leaf stomatal conductance". *Agr. For. Meteorol*., 54:241-261.

Rogers, J. S., Allen, L. H., and Calvert, D. J. (1983). "Evapotranspiration for humid regions: Developing citrus grove, grass cover." *Trans.of the ASAE* 26(6): 1778-83, 92.

Rohwer, C., (1931). "Evaporation from Free Water Surfaces." *USDA Tech. Bull. 271*. 96 pp.

Rohwer, C., (1934). "Evaporation from water surfaces." Symposium, Evaporation from Different Types of Pans, *Trans. ASCE.*, 99:673-703.

Rohwer, C. (1957). "Discussion of evaporation from free water surfaces at high altitudes." *J. Irrig. and Drain. Div.*, 83(1):15-16.

Rose, C.W. (1968a). "Evaporation from bare soil under high radiation conditions." *9th Int'l. Congr. of Soil Sci. Trans.*, Vol. I, pp. 57-66.

Rose, C.W. (1968b). "Water movement in porous materials III. Evaporation of water from soil." *Br. J. of Appl. Physics Ser. 2*, 1:1779-1791.

Rose, C.W. and Sharma, M.L., (1984). "Summary and recommendations of the workshop on evapotranspiration from plant communities." pp. 325-342, *In:* Sharma, M.E. (ed.), *Evapotranspiration from plant communities*. Dev. in Agr. and Managed For. Ecol., 13, Elsevier Science Publishers. B. V., New York, NY, 350 pp.

Rosenberg, N.J., Blad, B.L., and Verma, S.B. (1983). "*Microclimate: The Biological Environment*." 2nd Ed. John Wiley & Sons, Inc.

Rosenberry, D.O., Sturrock, A.M., and Winter, T.C. (1993). "Evaluation of the energy budget method of determining evaporation at Williams Lake, Minnesota, using alternative instrumentation and study approaches." *Water Resources Res.*, 29(8):2473-2483.

Rossby, C.G.., and Montgomery, R.B. (1935). "The layer of frictional influence in wind and ocean currents." *Papers Phys. Oceanogr. Meteor*., Vol. III, No. 3, Woods Hole Oceanographic Institution, M.I.T.

Rossow, W.B. and Garder, L.C. (1993). Cloud detection using satellite measurements of infrared and visible radiances for ISCCP. *J. Climate* 6: 2341–2369.

Running, S.W. (1994). “Testing forest-BGC ecosystem process simulations across a climatic gradient in Oregon.” *Ecolog. Appl.* 4(2):238-247.

Running, S.W., and Coughlan, J.C. (1988). "A general model of forest ecosystem processes for regional applications: I. Hydrologic balance, canopy gas exchange and primary production processes." *Ecological Modeling* 42:125-154.

Raupach, M.R., Antonia, R.A., and Rajagopalan, S. (1991). "Rough-wall turbulent boundary layers." *Appl. Mech. Rev.*, 44:1-25.

” UN-FAO, Rome, Italy, 54 p.

Rutter, A.J. (1975). “The hydrologic cycle in vegetation.” pp. 11-54 IN Monteith, J.L. (ed) *Vegetation and the Atmosphere*, Vol. 1, Academic Press, NY.

Rutter, A.J., Morton, A.J., and Robins, P.C. (1975). "A predictive model of rainfall interception in forests: II. Generalization of the model and comparison with observations in some coniferous and hardwood stands." *J. Appl. Ecol.*, 12: 367-380.

Ryan, P. J., Harleman, D.R.F., and Stolzenbach, K.D. (1974). “Surface heat loss from cooling ponds.” *Water. Resour. Res.*, 10:930-938.

Ryu, Y., Baldocchi, D.D., Ma, S. and Hehn, T. (2008). ”Interannual variability of evapotranspiration and energy exchanges over an annual grassland in California,” *J. Geophys. Res.,* 113 (D09104) (2008) http://dx.doi.org/10.1029/2007JD009263.

Sagar, R.M., Hubbard, K.G., Norman, J.M., and Holtzer, T.O. (1988). "Estimation of corn canopy temperature and water budget using automated weather station data." *CAMAC Progress Report* 88-4, Dept. of Agr. Meteorol., Univ. of Nebr.-Lincoln, 143 pp.

Saito, H., Simunek, J., and Mohanty, B.P. (2006). “Numerical analysis of coupled water, vapor, and heat transport in the vadose zone.” *Vadose Zone J.*, 5(2):784-800.

Sakai, R.K., Fitzjarrald, D.R. and Moore, K.E. (2001). “Importance of low-frequency contributions to eddy fluxes observed over rough surfaces.” *J. of Appl. Meteorol.*, 40: 2178-2192.

Sakuratani (1981). “A heat balance method for measuring water flux in the stem of intact plants.” *Jap. Agric. Meteorol.*, 37: 9-17.

Sammis, T.W. (1985). “Evapotranspiration crop coefficients predicted using growing-degree-days.” *Trans. of the ASAE*, 28(3):773-780.

Sammis, T.W., Mapel, C.L., Lugg, D.G., Lansford, R.R. and McGuckin, J.T. (1985). “Evaporation crop coefficients predicted using growing degree days. *Trans.of the ASAE*, 28:773-780.

Sammis, T.W., Mexal, J.G., and Miller, D. (2004). “Evapotranspiration of flood-irrigated pecans.” *Agric. Water Manage.*, 69:179–190.

Sarraf, S., and Bovée, A.C.J. (1973). "Evapotranspiration of bananas" *Magon Série Tech. No. 20*, IRA, Lebanon (in French). 18 pp.

Saxton, K.E., Johnson, H.P., and Shaw, R.H. (1974). "Modeling evapotranspiration and soil moisture." *Trans. of the ASAE*, 17(4):673-677.

Saxton, K.E. and Willey, P.H. (2005). “The SPAW Model for Agricultural Field and Pond Hydrologic Simulation.” Book Chapter in *Mathematical Modeling of Watershed Hydrology*, V. P. Singh and D. Frevert, Editors; CRC Press LLC.

Schaap, M.G. and Bouten, W. 1996. “Forest floor evaporation in a dense Douglas fir stand.” *J. of Hydrol.*, 193(1-4): 97-113.

Schaap, M.G., Leij, F.J. and Van Genuchten, F.J. (1999). “Estimation of the soil hydraulic properties.” pp. 501-509, *In*: Looney and Falt, (ed.) *Vadose Zone – Science and Technology Solutions*. Battelle Press,

Schmid, H.P. (1994). “Source areas for scalar and scalar fluxes.” *Boundary-Layer Meteorol.*, 67:293-318.

Schmid, H.P. (2002). “Footprint modeling for vegetation atmosphere exchange studies: a review and perspective.” *Agr. and For. Meteorol.*, 113:159-183.

Schmid, H.P., Grimmond, C.S.B., Cropley, F.D., Offerle, B., Su, H.B., (2000). "Measurements of CO2 and energy fluxes over a mixed hardwood forest in the midwestern United States." *Agr. and For. Meteorol.*, 103:355–373.

Schneider, A.D., and Howell, T.A. (1991). "Large, monolithic, weighing lysimeters." pp. 37-45, *In*: R.G. Allen, T.A. Howell, W.O. Pruitt, I.A. Walter, and M.E. Jensen, (eds), *Lysimeters for Evapotranspiration and Environmental Measurements*, Am. Soc. Civ. Engrs., New York, NY, 456 pp.

Schuepp, P.H., Leclerc, M.Y., MacPherson, J.I., and Desjardins, R.L. (1990). "Footprint prediction of scalar fluxes from analytical solutions of the diffusion equation." *Boundary-Layer Meteorol.* 50:355-373.

Scott, C.A., Bastiaanssen, W.G.M., and Ahmad,M. (2003). "Mapping root zone soil moisture using remotely sensed optical imagery." *J. Irrig. and Drain. Eng.*, 129(5):326-335.

Seginer, I. (1974). "Aerodynamic roughness of vegetated surfaces." *Boundary-Layer Meteorol.*, 5:383-393.

Seginer, I., Nir, D., and von Bernuth, R.D. (1991). "Simulation of wind-distorted sprinkler patterns."*J. Irrig. and Drain. Eng.*, 117(2):285-306.

Seguin, B., Brunet, Y., and Perrier, A. (1982). "Estimation of evaporation: a review of existing methods and recent developments." *In*: *European Geologic Society Symposium on Evaporation*. Leeds, U.K., August, 1982, 21 pp.

Sellers, W.D. (1965). "*Physical Climatology*." Univ. of Chicago Press, Chicago, 284 pp.

Sellers, P. J., and Dorman, J.L. (1987). "Testing the simple biosphere model (SIB) using point micrometeorological and biophysical data." *J. Clim. Appl. Meteor.*, 26:622-651.

Senay, G.B., Budde, M., Verdin, J.P., and Melesse, A.M. (2007). "A coupled remote sensing and simplified surface energy balance approach to estimate actual evapotranspiration from irrigated fields." *Sensors*, 7:979-1000.

Senay, G. and Verdin, J. (2003). "Characterization of yield reduction in Ethiopia using a GIS-based crop water balance model." *Remote Sensing* 29(6):687-692.

Senay, G., Verdin, J. and Lietzow, R. (2005). "Global daily reference ET modeling and evaluation." (2005). Meeting of the American Geophysical Union (abstract).

Senay, G.B., J.P. Verdin, R. Lietzow and A. M. Melesse (2008). "Global daily reference evapotranspiration modeling and validation." *J. Am. Water Resources Res.* 44(4):969-979.

Sene, K.J. 1996. "Meteorological estimates for the water balance of a sparse vine crop growing in semiarid conditions." *J. of Hydrol*., 179:259-280.

Shackel, K.A., Johnson, R.S., Medawar, C.K., Phene, C.J. (1992). "Substantial errors in estimates of sap flow using the heat balance technique on woody stems under field conditions." *J. Am. Soc. for Hort. Sci.*, 117(2):351-356.

Shafer, M.A., Fiebrich, C.A., Arndt, D.S., Fredrickson, S.E. and Hughes, T.W. (2000). "Quality assurance procedures in the Oklahoma Mesonet." *J. Atmos. Oceanic Technol*., 17, 474-494.

Shalhevet, J., Mantell, A., Bielorai, H., and Shimshi, D. (eds). (1981). "*Irrigation of field and orchard crops under semi-arid conditions*." Int'l. Irrig. Information Ctr., Bet Dagan, Israel. l32 pp.

Sharma, M.E. (ed.), (1984). *Evapotranspiration from plant communities*. Dev. in Agr. and Managed For. Ecol., 13, Elsevier Science Publishers. B. V., New York, NY, 350 pp.

Sharma, M.L. (1985). "Estimating Evapotranspiration." pp. 213-281. *In*: Hillel, D (ed.) *Advances in Irrigation, Volume 3*. Academic Press, Inc.

Shaw, D.A., and Pittenger, D.R. (2004) "Performance of landscape ornamentals given irrigation treatments based on reference evapotranspiration." Proc., 4th Int'l. Symp. on Irrig. of Hort. Crops, Sept. 1-6, 2003. *Acta Horticulturae*, 664:607-613.

Shaw, R., and Snyder, R.L. (2003). "Evaporation and eddy correlation." pp. 235-237, *In*: *Encyclopedia of Water Sci.*, Marcel Dekker, Inc., New York.

Shawcroft, R.W., and Gardner, H.R. (1983). "Direct evaporation from soil under a row crop canopy." *Agric. Meteorol.*, 28:229-238.

Shuttleworth, W. J. (1984). "Eddy correlation of energy partition for Amazonian forest." *Quart. J. Roy. Meteorol. Soc.*, 110:1143-1162.

Shuttleworth, W. J. (1989). "Micrometeorology of temperate and tropical forest." *Phil. Trans. Roy. Soc. London B*, 324:299-334.

Shuttleworth, W.J. (1991). "Evaporation models in hydrology." pp. 93-120. *In*: Schmugge, T.J. and André, J.C. (eds). *Land Surface Evaporation, Measurement and Parameterization*. Springer, New York.

Shuttleworth, W.J. (1992). "Evaporation." Chap. 4 *In*: D.R. Maidment (ed), *Handbook of Hydrology*. McGraw-Hill Inc., New York, NY

Shuttleworth, W.J., and Gurney, R.J. (1990**)**. "The theoretical relationship between foliage temperature and canopy resistance in sparse crops." *Qtr. J. Roy. Meteorol. Soc.*, 116:497-519.

Shuttleworth, W.J., and Wallace, J.S. (1985). "Evaporation from sparse crops - an energy combination theory." *Quart. J. Roy. Meteorol. Soc.*, 111:839-853.

Sikka, A.K. (1993). "Modeling the influence of climate change on evapotranspiration and water yield." *Unpublished Ph.D. dissertation*, Dept. Civ. Eng., Utah State Univ. 330 pp.

Sikka, A.K., Gunderson, R.W., Limaye, A.S., and Riley, J.P. (1993). "Application of distributed parameter watershed model for determining the effects of climate change on water resources." pp. 464- 471. *In*: Allen, R.G., and Neale, C.M. (eds). *Management of Irrigation and Drainage Systems: An Integrated Approach*, Proc., Nat'l. Conf. on Irrig. and Drain. Eng., ASCE, New York, NY .

Šimůnek, J., Šejna, M., and van Genuchten, M.Th . (1998). "*The HYDRUS-1D software package for simulating the one-dimensional movement of water, heat, and multiple solutes in variably-saturated media.* Vers. 2.0." IGWMC-TPS-70. Int. Grd. Water Mod. Ctr., Colo. Sch. of Mines, Golden.

Šimunek, J., van Genuchten, M.Th., and Sejna, M. (2005). "*The HYDRUS-1D Software Package for Simulating the One-Dimensional Movement of Water, Heat, and Multiple Solutes in Variably-Saturated Media*. Vers. 3." U.S. Salinity Lab., USDA-ARS, Riverside, Calif., 240 pp.

Šimůnek, J. Wendroth, O., and van Genuchten, M.T. (1999). "Estimating unsaturated soil properties from laboratory tension disc infiltrometer experiments." *Water Resources Res.*, 35(10):2965-2979.

Sinclair, T.R. (1984). "Leaf area development in field-grown soybeans." *Agron. J.*, 76:141-146.

Sinclair, T.R., Allen, L.H, and Lemon, E.R. (1975). "An analysis of errors in the calculation of energy flux densities above vegetation by a Bowen ratio profile method." *Boundary-Layer Meteorol.*, 8:129-139.

Singh, R.K., Irmak (Kilic), A., Irmak, S. and Martin, D.L. (2008). "Application of SEBAL for mapping evapotranspiration and est. surface energy fluxes in south central NE." *J. Irrig. and Drain. Eng.,* ASCE 134(3):273-285.

Singh, R. and Irmak (Kilic), A. (2009). "Estimation of Crop Coefficients Using Satellite Remote Sensing." *J. Irrig. Drain Eng.*, 135(5), 597–608.

Slack, D.C., Martin, E.C., Sheta, A.E., Fox Jr., F., Clark, L.J., and Ashley, R.O. (1996). "Crop coefficients normalized for climatic variability with growing-degree-days." Proc. Int'l. Conf. on Evapotranspiration and Irrigation Scheduling, San Antonio, TX, ASAE, St. Joseph, MI p.892-898.

Slatyer, R.O., (1967). "*Plant Water Relationships."* Academic Press, New York. 366 pp.

Slatyer, R.O., and McIlroy, I.C. (1961). "*Practical Climatology*." C.S.I.R.O., Melbourne, UNESCO, Paris. 340 pp.

Sleight, R.B. (1917). "Evaporation from surfaces of water and riverbed materials." *J. Agric. Res.*, 10(5):209-262.

Smeal, D., Owen, C.K., Arnold, R.N., Tomko, J.F., Gregory, E.J., (2001). "Thirty years of climatological data: 1969 to 1998." NMSU's Agr. Sci. Center at Farmington, New Mexico. Agr. Exp. Stn. Res. Rep. 744. New Mexico State University, Las Cruces, NM

Smith, M., Allen, R., Monteith, J., Perrier, A., Pereira, L. and Segeren, A. (1991). "*Report of the expert consultation on procedures for revision of FAO guidelines for prediction of crop water requirements*." UN-FAO, Rome, Italy, 54 p.

Smith, M., Allen, R.G., and Pereira, L. (1996). "Revised FAO methodology for crop water requiremens." pp. 116-123. *In*: C.R. Camp, E.J. Sadler, and R.E. Yoder (eds). *Evapotranspiration and Irrigation Scheduling*. Proc., Int'l. Conf., San Antonio, TX, Nov., 1184 pp.

Smith, M., Segeren, A., S. Pereira, L.,S., Perrier, A., and Allen, R. (1991). "*Report on the Expert Consultation on Procedures for Revision of FAO Guidelines for Prediction of Crop Water Requirements*. Rome, Italy, 28-31 May 1990. 45 p.

Snyder, R.L. 2004. "Hourly Reference Evapotranspiration (ETo) Calculator User's Guide for HRPM.EXE." Univ. California, Davis. http://biomet.ucdavis.edu/Evapotranspiration/HRPMexe/HRPM.htm

Snyder, R.L. (1985). "Hand calculating degree days." *Agr. and For. Meteorol.*, 35:353-358

Snyder, R.L., Brown, P.W., Hubbard K.G. and Meyer S.J. (1996). "A guide to automated weather station networks in North America." *In: Advances in Climatology* Vol. 4. G.Stanhill (Ed.) Springer Verlag, Berlin. p. 1-61

Snyder, R.L. and de Melo-Abreu, J.P. (2000). "Frost Protection: fundamentals, practice, and economics." *Environ. and Nat'l. Resources Series 10*, Food and Agriculture Organization, Vol. 1. http://www.fao.org/docrep/008/y7223e/y7223e00.HTM

Snyder, R.L, and Eching, S.O. (2004). "Landscape irrigation management program," *IS005 Quick Answers.*

Snyder, R.L, and Eching, S.O. (2005) "Urban landscape evapotranspiration. *Calif. Water Plan Update 2005."* 4:691-693.

Snyder, R. L., Bali, K., Ventura, F., and Gomez-MacPherson, H. (2000). "Estimating evaporation from bare or nearly bare soil." *J. Irrig. Drain. Engrg.*, 126(6), 399–403.

Snyder, R.L., Lanini, B.J., Shaw, D.A., and Pruitt, W.O. (1989a). "Using reference evapo-transpiration (ETo) and crop coefficients to estimate crop evapotranspiration (ETc) for agronomic crops, grasses, and vegetable crops." *Coop. Ext., Univ. of Calif., Berkeley, CA, Leaflet No. 21427*, 12 p.

Snyder, R.L., Lanini, B.J., Shaw, D.A., and Pruitt, W.O. (1989b). "Using reference evapo-transpiration (ETo) and crop coefficients to estimate crop evapotranspiration (ETc) for trees and vines." *Coop. Ext., Univ. Calif., Berkeley, CA, Leaflet No. 21428*, 8 p.

Snyder, R.L., Orang, M., Matyac, S., and Grismer, M.E. (2005). "Simplified estimation of reference evapotranspiration from pan evaporation data in California." *J. Irrig. and Drain. Eng.*, 131(3):249-253.

Snyder, RL, Spano, D., Cesaraccio, C. and Duce, P. (1999). "Determining degree-day. thresholds from field observations." *Int. J. Biomet*. 42:177-182.

Spano, D., Cesaraccio, C., Duce, P. and Snyder, R.L. (2002). "An improved model for estimating degree days." *ISHS Acta Horticulturae 584: VI International Symposium on Computer Modelling in Fruit Research and Orchard Management*.

St. Hilaire, R., Arnold, M.A., Wilkerson, D.C., Devitt, D.A., Hurd, B.H., Lesikar, B.J., Lohr, V.I., Martin, C.I., McDonald, G.V., Morris, R.L., Pittenger, D.R., Shaw, D.A., and Zoldoske, D.F. (2008). "Efficient Water Use in Residential Urban Landscapes." *HortScience.* 43:2081-2092.

Stanhill, G. 1962. «The use of the Piche evaporimeter in the calculation of evaporation. » *Quart. J. Roy. Meteorol. Soc*., 88:80-82.

Stanhill, G., (1962). "The control of field irrigation practice from measurements of evaporation." *Israel J. Agr. Res*., 12:51-62.

Stanhill, G. (1976). "Cotton." pp. 121-150. *In*: Monteith, J.L. (ed). *Vegetation and the Atmosphere*, 2. Academic Press, London.

Stanhill, G. (1992). Accuracy of global radiation measurements at unattended, automatic weather stations. *Agr. and For. Meteorol.*, 61(1), 151-156.

Staple, W.L., and Lehane, J.J., (1962). "Variability in soil moisture sampling." *Canadian J. Soil Sci.*, 42:157-164.

Steiner, J.L., Howell, T.A., and Schneider, A.D. (1991). "Lysimetric evaluation of daily potential evaporation models for grain sorghum." *Agron J.*, 83:240-247.

Steppe, K., De Pauw, D.J.W., Doody, T.M. Teskey, R.O. (2010). "A comparison of sap flux density using thermal dissipation, heat pulse velocity and heat field deformation methods." *Agr. and For. Meteorol.,* 150(7-8):1046-1056.

Stewart, J.B. (1983). "A discussion of the relationships between the principal forms of the combination equation for estimating crop evaporation." *Agr. Meteorol.*, 30:111-127.

Stewart, J.B. (1988). "Modelling surface conductance of pine forest." *Agr. For. Meteorol*., 43:19-35.

Stewart, J.B. (1989). "On the use of the Penman-Monteith equation for determining areal evapotranspiration." pp. 3-12. *In*: Black, T.A., Spittlehouse, D.L., Novak, M.D., and Price, D.T. (ed)., *Estimation of Areal Evapotranspiration*, IAHS Pub. No. 177.

Stewart, J.B., and Gay, L.W. (1989). "Preliminary modelling of transpiration from the FIFE site in Kansas." *Agr. and Forest Meteorol.*, 48:305-315.

Stewart, B.A., and Howell, T.A. (eds). (2003). "*Encyclopedia of Water Science.*" Marcel-Dekker, Inc., New York, New York, 1076 pp.

Stewart, R.B., and Rouse, W.R. (1977). "Substantiation pf the Priestley-Taylor parameter $\alpha = 1.26$ for potential evaporation at high latitudes." *J. Applied Meteorol.*, 16:649-650.

Stewart, J.B. and Verma, S.B. (1992). "Comparison of surface fluxes and conductances at two contrasting sites within the FIFE area." *J. Geophys. Res.*, 97(D17):18,623-18,628.

Stewart, J.B., Watts, C.J., Rodriguez, J.C., De Bruin, H.A.R., van den Berg A.R. and Garatuza-Payan, J. (1999). "Use of satellite data to estimate radiation and evaporation for northwest Mexico." *Agr. Water Manage.* 38: 181–193.

Stone, L.R., Goodrum, D.E., Jaafar, M.N., and Khan, A.H. (2001). "Rooting front and water depletion depths in grain sorhum and sunflower." *Agron. J.*, 93:1105-1110.

Strelkoff, T. (1990). "*SRFR: A Computer Program for Simulating Flow in Surface Irrigation Furrows-Basins-Borders*." WCL Report #17, U.S. Water Conservation Laboratory, USDA/ARS, Phoenix, AZ.

Stull, R.B. (1988). "*An introduction to boundary layer meteorology*." Kluwer, Doordrecht, the Netherlands. 680 p.

Sturrock, A.M., Winter, T.C., and Rosenbery, D.O. (1992). "Energy budget evaporation from Williams Lake: A closed lake in north central Minnesota." *Water Resources Res.*, 26(6):1605-1617.

Su, Z., Schugge, T., Kustas, W.P. and Massman, W.J. (2001). "An evaluation of two models for estimation of the roughness height for heat transfer between the land surface and the atmosphere." *J. Appl. Meteorol*., 40:1933-1951.

Suleiman, A.A., and Ritchie, J.T.. (2003). "Modeling soil water redistribution during second-stage evaporation." *Soil Sci. Soc. Am. J.*, 67:377-386.

Swanson, R.H. (1994). "Significant historical developments in thermal methods for measuring sap flow in trees." *Agric. and For. Meteorol.* 72(1-2):113-132.

Swift, L.W. (1976). "Algorithm for solar radiation on mountain slopes." *Water Resources Res*., 12:108-112.

Swinbank, W.C., (1951). "The measurement of vertical transfer of heat and water vapour by eddies in the lower atmosphere." *J. Meteorol.*, 8:135-145.

Swinbank, W. C. (1955). "An experimental study of eddy transports in the lower atmosphere." *Tech. Paper No. 2*, C.S.I.R.O. Div. of Meteorological Physics. Melbourne, Australia.

Szeicz, G. and Long, I.F. (1969). "Surface resistance of crop canopies." *Water Resources. Res*., 5:622-633.

Szeicz, G., Van Bavel, C., and Takami, S. (1973). "Stomatal factor in the water use and dry matter production by sorghum." *Agr. Meteorol*., 12:361-389.

Szilagyi, J. (2007). "On the inherent asymmetric nature of the complementary relationship of evaporation." *Geophys. Res. Letters* 34:L02405, ISSN 0094-8276.

Tanji, K.K. (1990). "Conceptual irrigation return flow hydrosalinity model. pp. 504-529, *In*: Tanji, K.K. (ed), Agricultural *Salinity Assessment and Management*. ASCE Manuals and Reports on Engineering Practice No. 71, Am. Soc. Civ. Engrs., New York, 630 pp.

Tanner, C.B. (1960). "Energy balance approach to evapotranspiration from crops." *Soil Sci. Soc. Am. Proc.*, 24:1-9.

Tanner, C.B. (1967). "Measurement of Evapotranspiration." pp. 534-574, *In*: R.M. Hagan, H.R. Haise, and T.W. Edminster, (eds). *Irrigation of Agricultural Lands*. ASA Mono. No. ll, Am. Soc. of Agron., Madison, WI.

Tanner C.B. (1968). "Evaporation of water from plants and soils." pp. 73-106. *In*: Kozlowski, T.T. (ed). *Water deficits and plant growth.* Vol. I, Academic Press, New York.

Tanner, B.D., (1988). "Use requirements for Bowen ratio and eddy correlation determinination of evapotranspiration." pp. 605-616, *In:* Hay, D.R. (ed), *Planning Now for Irrigation and Drainage in the 21st Century,* Proc., Irrig. and Drain. Div, Conf. Lincoln, NE, July, 795 pp.

Tanner, C.B., and Jury, W.A. (1976). "Estimating evaporation and transpiration from a crop during incomplete cover." *Agron. J.*, 68:239-242.

Tanner, C.B., and Pelton, W.L. (1960). "Potential evapotranspiration estimates by the approximate energy balance method of Penman." *J. Geophys. Res.*, 65(10):3391-3413.

Tanner, B.D., Swiatek, E., and Greene, J.P., (1993). "Density fluctuations and use of the krypton hygrometer in surface flux measurements." pp. 945-952, *In:* Allen, R.G. and Neale C.M.U. (eds). Management of irrigation and drainage systems: Integrated perspectives. *Proc., Nat'l Conf. on Drain. Eng.*, Park City, UT, July, 1223 pp.

Tanner, B., E. Swiatek and C. Maughn. 1996. "Field comparisons of naturally ventilated and aspirated radiation shields for weather station air temperature measurements." p. 227-230, 22nd Conf. on Agricultural and Forest Meteorology, Am. Meteorol. Soc., Session P1.16.

Tasumi, M. (2003). "Progress in operational estimation of regional evapotranspiration using satellite imagery." Ph.D. Dissertation, University of Idaho, Moscow, ID, 357p.

Tasumi, M., R.G. Allen. (2007). "Satellite-based ET mapping to assess variation in ET with timing of crop development." *Agric. Water Manage.* 88(1-3):54-62.

Tasumi, M., Allen, R.G., and Trezza, R. (2008). "At-surface reflectance and albedo from satellite for operational calculation of land surface energy balance." *J. Hydrol. Engrg.,* 13(2):51-63.

Tasumi, M., Allen, R., Trezza, R., and Wright, J. (2005a). "Satellite-based energy balance to assess within-population variance of crop coefficient curves." *J. Irrig. Drain Eng.*, 131(1), 94–109.

Tasumi, M., Trezza, R., Allen, R.G., and Wright, J.L. (2005b). "Operational aspects of satellite-based energy balance models for irrigated crops in the semi-arid U.S." *Irrig. and Drain.Syst.*, 19:355-376.

Taylor, H.M. 1983. "Managing root systems for efficient water use: An overview." pp.87-113, *In:* Taylor, H.M., Jordan, W.R., and Sinclair, T.R. (eds). *Limitations to Efficient Water Use in Crop Production*, Am. Soc. Agron., Madison, WI, 552, pp.

Taylor, S.A., (1955). "Field determination of soil moisture." *Agr. Eng.*, 36:645-659.

Testi, L., Villalobos, F. J., and Orgaza, F. (2004). "Evapotranspiration of a young irrigated olive orchard in southern Spain." *Agric. and For. Meteorol*. 121(1,2):1-18.

Tetens, O., (1930). "Uber einige meteorologische Begriffe." *Z. Geophys.*, 6:297-309.

Thilini, J., Shridhar, V. Huntington, J., and Khanal, M. (2013). “Evaluation of the complementary relationshiop using Noah Land Surface Model and North American Regional Reanalysis (NARR) data to estimate evapotranspiration in semiarid ecosystems.” *J. Hydrometeorology* 14:345-359.

Thom, A.S. (1971). "Momentum absorption by vegetation." *Quart. J. Roy. Meteorol. Soc.*, 97:414-428.

Thom, A.S. (1972). "Momentum, mass and heat exchange of vegetation." *Quart. J. Roy. Meteorol. Soc.*, 98:124-134.

Thom, A.S., Stewart, J.B., Olivier, H.R. and Gash, J.H.C. (1975). "Comparison of aerodynamic and energy budget estimates of fluxes over a pine forest." *Quart. J. Roy. Meteorol. Soc.*, 101:93-105.

Thom, A. S., Thony, J.L., and Vauclin, M. (1981). "On the proper employment of evaporation pans and atmometers in estimating potential transpiration." *Quart. J. Roy. Meteorol. Soc*., 107:711-736.

Thompson, N., Barrie, I.A., and Ayles, M. (1981). "The Meteorological Office rainfall and evaporation calculation system: MORECS." Great Britain Hydrological Memorandum No. 45. 67 pp.

Thornthwaite, C.W., (1948). "An approach toward a rational classification of climate." *Geograph. Rev.*, pp. 38, 55.

Thornthwaite, C.W., and Holzman, B. (1939). “The determination of evaporation from land and water surfaces.” *Monthly Rev.*, 67:4-11.

Thornthwaite, C.W., and Holzman, B. (1942). “Measurement of evaporation from land and water surfaces.” *USDA Tech. Bull.*, 817, 143 p.

Thornton, P.E. and Running, S.W. (1999). “An improved algorithm for estimating incident daily solar radiation from measurements of temperature, humidity and precipitation,” *Agric. and For. Meteorol.*, 93:211-228.

Todd, R.W., Evett, S.R., and Howell, T.A., (1998). “Latent heat flux of irrigated alfalfa measured by weighing lysimeter and Bowen ratio-energy balance.” *Paper 98-2119*, Am. Soc. Agr. Engrs., St. Joseph, MI.

Todd, R.W., Evett. S.R., Howell, T.A., Klocke, N.L. (2000). “Soil temperature and water evaporation of small steel and plastic lysimeters replaced daily.” *Soil Sci.* 165:890-895.

Tolk, J.A. and Howell, T.A. (2001). “Measured and simulated evapotranspiration of grain sorghum with full and limited irrigation in three High Plains soils.” *Trans. ASAE*, 44(6):1553–1558.

Tolk, J.A., Howell, T.A., Steiner, J.L., Krieg,D.R., and Schneider, A.D. (1995). “Role of transpiration suppression by evaporation of intercepted water in improving irrigation efficiency.” *Irrig. Sci.*, 16(2):89-95.

Tolk, J.A., Howell, T.A., and Evett, S.R. (2006). “Nighttime evapotranspiration from alfalfa and cotton in a semiarid climate.” *Agron J.*, 98:730-736.

Trask, J.C. (2007). “Resolving hydrologic water balances through novel error analysis with focus on inter-annual and long-term variability in the Tahoe Basin. Univ. of Calif., Davis, *Ph.D. Dissertation*. 378 p.

Turc, L. (1961). “Evaluation des besoins en eau d•irrigation, evapotranspiration potentialle, formule climatique simplifice et mise a jour. (English: Estimation of irrigation water requirements, potential evapotranspiration: A simple climatic formula evolved up todate).” *Ann. Agron.*, 12:13-49.

Turner, N.C. (1979). "Drought resistance and adaptation to water deficits in crop " pp. 343-372. *In*: Mussell, H., and Staples, R.C. (eds) *Stress Physiology in Crop Plants*, John Wiley & Sons, New York, NY.

Turner, N.C. (1991). "Measurement and influence of environmental and plant factors on stomatal conductance in the field." *Agr. and For. Meteorol.*, 54:137-154.

Twine, T.E., Kustas, W.P., Norman, J.M., et al. (2000). “Correcting eddy-covariance flux underestimates over a grassland.” *Agr. and For. Meteorol.*, 103:279-300.

U.S. Army Corps of Engineers. (1995). "CE-QUAL-R1: A numerical one-dimensional model of reservoir quality: User's manual." *Instruction Rep. No. E-82-1, Revised ed*, Waterways Exp. Stn., Vicksburg, MS.

U.S. Dept. of Agr. (1967). "*Irrigation water requirements*." Soil Conserv. Service. Tech. Rel. No. 21, 88 pp.

U.S. Dept. of Agr. (1970). "*Irrigation water requirements*." Soil Conserv. Service. Tech. Rel. No. 21, (Rev.), 92 pp.

U.S. Dept. of Agr. (1974). "*Border Irrigation."* National Engineering Handbook, Chapter 4, Sect. 15. Soil Conserv. Serv., USDA, Washington, D.C.

U.S. Dept. of Agr. (1984). "*Furrow Irrigation*." National Engineering Handbook, Chapter 5, Sect. 15. Soil Conserv. Serv., USDA, Washington, D.C.

U. S. Dept. of Agr. (1999). "*Soil Taxonomy: A Basic System of Soil Classification for Making and Interpreting Soil Surveys*." Nat'l Resources Conserv. Serv. 2nd ed.. 870 pages.

U.S. Dept. of Comm. (1968). "*Climatic Atlas of the United States*." Nat'l Clim. Data and Info. Center, Ashville, N.C.

U.S. Geological Survey. (1954). "Water-loss investigations: Vol. 1, Lake Hefner studies." Tech. Rep., U.S. *Geolog. Survey Circ. 229*, 170 pp.

U.S. Geological Survey. (1954). "Water-loss investigations: Lake Hefner studies." Tech. Rep., *U.S. Geolog. Survey Prof. 269*, 170 pp.

U.S. Geological Survey. (1958). "Water-loss investigations: Lake Mead studies." *U.S. Geolog. Survey Prof. Paper 298*, 109 pp.

U.S. Salinity Laboratory Staff. (1954). "*Diagnosis and Improvement of Saline and Alkali Soils.*" U.S. Dept. of Agr. Handbook 60, 160 pp.

Valancogne, C., Nasr, Z. (1989). "Une méthode de mesure du débit de sève brute dans de petits arbres par bilan de chaleur." *Agronomie*, 9:609-617.

Valancogne, C., Nasr, Z. (1993). "A heat balance method for measuring sap flow in small trees." *In:* Borghetti, M., Grace, J., Raschi, A. (ed.), *Water Transport in Plants Under Climatic Stress*, Cambr. Univ. Press, UK, p. 166-173.

Valle, R., Mishoe, J.W., Jones, J.W., and Allen, L.H. (1985). "Transpiration rate and water use efficiency of soybean leaves adapted to different CO_2 environments." *Crop Sci.*, 25:477-481.

van Bavel, C.H.M., and Ehrler, W.L. (1968). "Water loss from a sorghum field and stomatal control." *Agron. J.*, 60:84-86.

Van Bavel, C.H.M., Fritschen, L.J., and Reeves, W.E. (1963). "Transpiration by sudangrass as an externally controlled process." *Science* 141:269-270.

van de Griend, A.A., and Owe, M. (1994). "Bare soil surface resistance to evaporation by vapor diffusion under semiarid conditions." *Water Resources Res.*, 30(2):181-188.

van de Griend, A.A., and van Boxel, J.H. (1989). "Water and surface energy balance model with a multilayer canopy representation for remote sensing purposes." *Water Resources Res.*, 25:949-971.

Van den Brink, C., Strommen, N.D. and Kenworthy, A.L. (1971). "Growing degree days in Michigan." *Michigan State Univ. Agr. Exp. Sta. Res. Rep. no. 131*. East Lansing, MI, 50 p.

Van den Hurk, B.J.J.M., and McNaughton, K.G. (1995). "Implementation of near-field dispersion in a simple two-layer surface resistance model." *J. of Hydrology*, 166(3-4):293-311.

van Genuchten, M.Th., Leij, F.J., and Yates, S.R. (1991). "The RETC code for quantifying the hydraulic functions of unsaturated soils," Version 1.0. *EPA Report 600/2-91/065*, U.S. Salinity Laboratory, USDA, ARS, Riverside, California.

Van Hylckama, T.E.A. (1968). "Water level fluctuation in evapotranspirometers." *Water Resources Res.*, 4:761-768

van Wijk, W. R., and de Vries, D. A. (1963). "Periodic temperature variations in a homogeneous soil." pp. 102-143. *In*: van Wijk, W. R. (ed.). *Physics of the Plant Environment*. North-Holland Publishing Co., Amsterdam.

Veihmeyer, F.J., and Hendrickson, A.H. (1955). "Does transpiration decrease as the soil moisture decreases'?" *Trans. Amer. Geophy. Un*. 36:425-448.

Ventura, F., Faber, B.A., Bali, K.M., Snyder, R.L., Spano, D., Duce, P., and Schulbach, K.F. (2001). "Model for estimating evaporation and transpiration from row crops." *J. Irrig. and Drain. Engrg*., 127(6): 339-345.

Venturini, V. Krepper, C. and Rodriguez, L. (2012). "Evapotranspiration estimation based on the complementary relationships." Chp. 2 in *Evapotranspiration – Remote Sensing and Modeling*, Ayse Irmak (Kilic) (ed.), Intech. 23 p.

Verma, S.B. (1989). "Aerodynamic resistances to transfers of heat, mass and momentum." pp. 13-20. *In*: Black, T.A., Spittlehouse, D.L., Novak, M.D. and Price, D.T. (eds). *Estimation of Areal Evapotranspiration*, IAHS Pub. No. 177.

Verma, S.B., Baldocchi, D.D., Anderson, D.E., Matt, D.R., and Clement, R.J. (1986). "Eddy fluxes of CO_2, water vapour, and sensible heat over a deciduous forest." *Boundary Layer Meteorol.*, 36:71-91.

Verma, S. B., Kim, J., and Clement, R. J. (1989). "Carbon dioxide, water vapor and sensible heat fluxes over a tallgrass prairie." *Boundary-Layer Meteorology*, 46(1-2), 53-67.

Verma, S.B., Kim, J., and Clement, R.J. (1992). "Momentum, water vapor, and carbon dioxide exchange at a centrally located prairie site during FIFE." *J. Geophys. Res.*, 97(D17):18,629-18,639.

Vickers, D., Mahrt, L. (1997). "Quality control and flux sampling problems for tower and aircraft data." *J. Atmos. Oceanic Technol*., 14, 512–526.

Vickers, D., Mahrt, L. (2003). "The cospectral gap and turbulent flux calculations." *J. Atm. and Oceanic Tech.* 20, 660-672.

Villagarcı´a, L., Were, A., Domingo, F., Garcı´a, M., Alados-Arboledas, L. 2007. "Estimation of soil boundary-layer resistance in sparse semiarid stands for evapotranspiration modeling." *J. of Hydrol.*, 342(1-2): 173-183.

Villagarcía, L., Were, A., García, M., Domingo, F. 2010. "Sensitivity of a clumped model of evapotranspiration to surface resistance parameterisations: Application in a semi-arid environment." *Agr. and For. Meteorol.*, 150:1065–1078.

Villalobos, F.J. (1997). "Correction of eddy covariance water vapor flux using additional measurements of temperature." *Agric. For. Meteorol*., 88:77-83.

Villalobos, F.J., and Fereres, E. (1990). "Evaporation measurements beneath corn, cotton, and sunflower canopies." *Agron. J.*, 82:1153-1159.

Villalobos, F.J., Orgaz, F., Testi, L., and Fereres, E. (2000). "Measurement and modeling of evapotranspiration of olive orchards." *European J. Agron.* 13:155-163.

Waggoner, P.E., and Turner, N.C. (1971). "Transpiration and its control by stomata in a pine forest." *Bull. Conn. Agr. Exp. Station 726*.

Walker, W.R. (1989). "Guidelines for designing and evaluating surface irrigation systems." *FAO Irrig. and Drain. Paper 45*, FAO of the United Nations, Rome, Italy, 137 p.

Walker, W.R., and Skogerboe, G.V. (1987). "*Surface Irrigation: Theory and Practice*." Prentice-Hall, Inc., Englewood Cliffs, New Jersey, 386 p.

Wallace, J.S., Roberts, J.M., and Sivakuma, M.V.K. (1990). "The estimation of transpiration from sparse dryland millet using stomatal conductance and vegetation area indices." *Agr. and Forest Meteorol.*, 51:35-49.

Wallender, W.W. and Tanji, K.K. (ed). 2011. "*Agricultural Salinity Assessment and Management."*, ASCE Manual of Practice No. 71. ASCE, Reston, VA, 2nd edition. 1094 pp.

Walter, I.A., Allen, R.G., Elliott, R., Jensen, M.E., Itenfisu, D., Mecham, B., Howell, T.A., Snyder, R., Brown, P., Eching, S., Spofford, T., Hattendorf, M., Cuenca, R.H., Wright J.L., and Martin, D. (2000). "ASCE's Standardized Reference Evapotranspiration Equation." *Proc., 4th National Irrig. Symp.*, ASAE, Phoenix, AZ.

Wandmacher, C., and Johnson, A.I. (1995). "*Metric Units in Engineering: Going SI*." ASCE Press, New York, 331 pp.

Weaver, H.L., Weeks, E.P., Campbell, G.S., Stannard, D.I., and Tanner, B.D. (1986). "Phreatophtye water use estimated by eddy-correlation methods." pp. 847-854, *In*: *Proc., Water Forum '86*, Am. Soc. Civ. Engrs., New York, NY..

Webb, E. K. (1970). "Profile relationships: the log-linear range, and extension to strong stability." *Quart. J. Roy. Meteorol. Soc*., 96:67-90.

Webb, E. K., Pearman, G. I. and Leuning, R. (1980). "Correction of flux measurements for density effects due to heat and water vapour transfer." *Qtr. J .R. Meteorol. Soc*., 106:85-100.

Were, A., Villagarcia, L., Domingo, F., Alados-Arboledas, L., and Puigdefábregas, J. (2007). "Analysis of effective resistance calculation methods and their effect on modeling evapotranspiration in two different patches of vegetation in semi-arid SE Spain." *Hydology and Earth Sci. Disc. Discussions*, 4(1):243-286.

Were, A., Villagarcia, L., Domingo, F. Moro, M.J. (2008). "Aggregating spatial heterogenity in a bush vegetation patch in semi-arid SE Spain: A multi-layer model versus a single-layer model." *J. of Hydrology*, 349(1-2):156-167.

Wesseling, J. (1974). "Hydraulic conductivity of natural Pachappa soil columns." *Soil Sci*., 118:6-10.

Westenburg, C., DeMeo, G.A., and Tanko, D.J. (2006). "Evaporation from Lake Mead, Arizona and Nevada, 1997-1999". *USGS Sci. Investigations Rept*. 2006-5252, 24 pp.

Whitlock, C.H., Charlock, T.P., Staylor,W.F., Pinker, R.T., Laszlo, I., Ohmura, A., Gilgen, H., Konzelman, T., DiPasquale, R.C., Moats, C.D., LeCroy, S.R. and Ritchey, N.A. (1995). "First global WCRP shortwave surface radiation budget data set." *Bull. Am. Meteorol. Soc.* 76(6): 1–18.

Wilson, K.B., Goldstein, A.H., Falge, F., et al. (2002). "Energy balance closure at FLUXNET sites." *Agric. and For. Meteorol.*, 113:223-243.

Wilczak, J.M., Oncley, S.P. and Stage, S.A. (2001). "Sonic anemometer tilt correction algorithms." *Boundary-Layer Meteorol.*, 99:127-150.

Wolfe, J.W., Brooks, R.H., and Lombard, P.B. (1972). "Measurement of the frost protection capability of a sprinkler irrigation system in an orchard." *Ore. Agr. Exp. Stn. Spec. Rep. 346*, 45 pp.

Wootton, T.P., Cecilio, C.H., Fowler, L.C., and Hui, S.L. (Task Com.). (1996). "*ASCE Handbook of Hydrology, 2nd ed*" Am. Soc. Civ. Engrs., New York, NY., 784 pp.

World Meteorological Organization. (1966). "Measurement and estimation of evaporation and evapotranspiration." *Tech. Note No. 83*, Working Group on Evaporation Measurement, WMO, Geneva, Switzerland. 121p.

World Meteorological Organization. (1970)."Guide to Hydrometeorological Practices." *WMO No. 168.TP.82*. Geneva, Switzerland.

World Meteorological Organization. (1973). "Comparison Between Pan and Lake Evaporation." *Tech. Note No. 126*, *WMO Publication No. 354*. Geneva, Switzerland.

Wright, J.L. (1981). Crop coefficients for estimates of daily crop evapotranspiration. *Irrig. Sched. for Water and Energy Conserv. in the 80's*, Am. Soc. of Agr. Engrs., Dec. 18-26.

Wright, J.L. (1982). "New evapotranspiration crop coefficients." *J. Irrig. and Drain. Div.*, 108(2):57-74.

Wright, J.L. (1988). "Daily and seasonal evapotranspiration and yield of irrigated alfalfa in southern Idaho." *Agron. J.*, 80:662-669.

Wright, J.L. (1993). "Nongrowing Season ET from Irrigated Fields." *In:Management of Irrigation and Drainage Systems*." Proc. ASCE Spec. Conf. Park City, UT July 21-23. Pp 1005-1014.

Wright, J.L. (1995). "Calibrating an ET procedure and deriving ET crop coefficients." *In*: *Proc. of the 1995 Specialty Seminar.* Sponsored by the Water Res. Comm., Am. Consulting Engng. Council of Colo. and the Colo. State Engineers Office.

Wright, J.L. (2001). Growing degree day functions for use with evapotranspiration crop coefficients. CD-ROM. American Society of Agronomy. Agronomy Abstracts.

Wright, J.L., and Jensen, M.E., (1972). "Peak water requirements of crops in Southern Idaho." *J. Irrig. and Drain. Div.*, ASCE, 96(IR1):193-201.

Wright, J.L., Allen, R.G. and Howell, T.A. (2000). "Conversion between evapotranspiration references and methods." p. 251-259. *Proc., 4th Decennial Nat. Irrig. Symp.*, Phoenix, AZ, Am. Soc. Agr. Engrs., St. Joseph, MI.

XuebaoW., Li, J., Zhang, W., Wang, F. (2005). "Atmospheric profile retrieval with AIRS data and validation at the ARM CART site." *Adv. in Atm. Sciences* 22(5):647-654.

Xuebao, W., Jun, L., Wenjian, Z., and Fang, W. (2005). "Atmospheric profile retrieval with AIRS data and validation at the ARM CART site." *Adv. in Atm. Sciences*, 22(5): 647-654.

Yamamoto, G., and Kondo, J. (1968). "Evaporation from Lake Nojiri." *J. Meteorol. Soc. Japan.* 46:166-176.

Yang, D., Goodison, B.E., Metcalfe, J.R., Golubev, V.S., Bates, R., Pangburn, T., and Hanson, C.L. (1998a). "Accuracy of NWS 80 Standard nonrecording precipitation gauge: Results and application of WMO intercomparison." *J. Atmospheric and Oceanic Tech.* Amer. Met. Soc. 15:54-68.

Yang, D., Goodison, B.E., Ishida, B., and Benson, C.S. (1998b). "Adjustment of daily precipitation data at 10 climate stations in Alaska: Application of World Meteorological Organization intercomparison results." *Water Resources Res.*, 34(2):241–256.

Yang, D., Ishida, S., Goodison, B.E. and Gunther, T. (1999). "Bias correction of daily precipitation measurements for Greenland." *J. Geophysical Research: Atmospheres* 104(D6):6171–6181.

Yazar, A. (1984). "Evaporation and drift losses from sprinkler systems under operating conditions." *Agr. Water Mgmt.*, 8(4):439-449.

Yoshioka, G.A. and Mather, J.R. (1967). "*Influence of site and exposure evapotranspiration. Factors of heat and water balance of different surfaces."* J.R. Mather (ed), Part I Analysis, Vol. 20(2), C.W. Thornthwaite and Assoc., Elmer, N.J, 253-266.

Young, A.A. (1947). "Evaporation from water surfaces in California: A summary of pan records and coefficients 1881 to 1946." *State of Calif., Dept. of Public Works, Div. of Water Resources, Bull. No. 54*, 68 pp.

Young, A.A., (1947). *Evaporation from Water Surfaces in California*. Dept. of Public Works, Div. of Water Resources and U.S. Dept. of Agr. Soil Conserv. Serv. Bull No. 54., 68 pp.Zinke (1967). "Forest interception studies in the United States." pp. 137-161. *In*: Sopper, W.E., and Lull, H.W. (eds), *Forest Hydrology*. Pergamon, Oxford.

Yuana, F. and Zhiming, L. (2005). Analytical solutions for vertical flow in unsaturated, rooted soils with variable surface fluxes. *Vadose Zone J.*, 4:1210-1218.

Zeng, X., and Wang, A. 2007. "Consistent parameterization of roughness length and displacement height for sparse and dense canopies in land models." *J. of Hydrometeorol.*, 8:730-737 .

Zhang, B., Kang, S., Li, F., and Zhang, L. (2008). "Comparison of three evapotranspiration models to Bowen ratio-energy balance method for a vineyard in an arid desert region of northwest China." *Agr. and For. Meteorol.*, 148 (10): 1629-1640.

Zhao, W. and Allen, R.G. (2012). "Placing soil heat flux plates at two depths for ground heat flux integrity assessment." Univ. Idaho Res. Memorandum. Kimberly R&E Center. 13 p.

Zhao, W., Qualls, R.J. and Berliner, P.J. 2008. "A two-concentric-loop iterative method in estimation of displacement height and roughness length for momentum and sensible heat." *Int. J. Biometeorology,* 52(8):849-858.

Zhao, L., Li, Y., Xu, S., Zhaou, H., Gu, S., Yu, G. and Zhao, X. (2006). "Diurnal, seasonal and annual variation in net ecosystem CO_2 exchange of an alpine shrubland on Qinghai-Tibetan plateau." *Global Change Biology*, 12:1940–1953.

Zhao, W.Z., Ji, X.B., Kang, E.S., Zhang, Z.H., and Jin, B.W. (2010). "Evaluation of Penman-Monteith model applied to a maize field in the arid area of Northwest China." *Hydrol. Earth Syst. Sci. Discuss.*, 7:461-491.

Zemei, Z., Li, Z., Shenggong, L., (2009). "Partitioning of evapotranspiration and its controls in four grassland ecosystems: Application of a two-source model." *Agr. and For. Meteorol.*, 149(9): 1410-1420.

Zeng, X and Wang, A. (2007). "Consistent parameterization of roughness length and displacement height for sparse and dense canopies in land models." *J. of Hydrometeorol.*, 8:730-737 .

Zhongmin, H., Guirui, Y., Yanlian, Z., Xiaomin, S., Yingnian, L., Peili, S., Yanfen, W., Xia, S., Zemei, Z., Li, Z., Shenggong, L. (2009). "Partitioning of evapotranspiration and its controls in four grassland ecosystems: Application of a two-source model." *Agr. and For. Meteorol.*, 149(9):1410-1420.

Zinke, P.J. (1967). "Forest interception studies in the United States." Pp. 137-161, *In*: Sopper, W.E., and Lull, H.W. (eds), *Forest Hydrology*, Pergamon, Oxford.

---A—
Absolute humidity,
Air temperature,
Air density,
Alfalfa-reference,
    comparison with grass,
    crop coefficients,
Allowable soil-water depletion,
Aridity rating,
Atmospheric pressure,
Available water,

---B—
Basal crop coefficients,

--C—
Climate parameters,
Cloud cover,
Combination equations,
Computer models,
Consumptive use,
Crop canopy,
Crop coefficients,
    basal,
    mean,
Crop Evapotranspiration,

---D—
Daily evapotranspiartion,
    estimating,
Dewpoint temperature,

---E---
Eddy covariance,
Effective rainfall,
Energy balance,

Evaporation,
    estimating methods,
    from soil,
    from water,
Evapotranspiration,
    daily estimates,
    estimating,
    measuring,
    reference,

---F---

---G---
    Grass-reference ET,
        crop coefficients,
        estimating,

--H—
    Hargreaves-Samani equation,

---I---
    Irrigation,
        efficiency,
        scheduling,
        water requirements,
        historical background,

---J---
Jensen-Haise equation,

---K---
Kimberly Penman equation,

---L---
Latent heat of vaporization
Leaching,
Leaf-area index,
Long-wave radiation,
Lysimeters,

Index

p

---M---
Mass transfer,
Mean crop coefficients,
Meteorological data,
Mixing ratio,
Monthly Evapotranspiration,

---N---
Net radiation,

---O---
Osmotic pressure,

---P---
Pan evaporation,
Penman equation,
    Wright wind function,
Penman-Monteith equation,
Plants, water potential,
Priestley-Taylor equation,
Psychrometric constant,

---R---
Radiation equations,
    Hargreaves-Samani,
    Jensen-Haise,
    Turc,
Rainfall,
    effective,
Reference crop evapotranspiation,
    alfalfa,
    grass,
    estimating,
Relative humidity,
Rooting depth,

---S---
Salts,
Saturation vapor pressure deficit,
Scheduling equations,
SCS Blaney-Criddle equation,
Sesible heat,
Short-wave radiation,
Soil heat flux,
Soil properties,
Soil water,
    characteristic curve,
    depletion,
    storage capacity,
        available water,
Solar radiation,
Specific, humidity,
Standard atmosphere,
Surface runoff,

---T---
Temperature estimating methods,
Thermal radiation,
Turc estimating method,

---U---

---V---
Vapor pressure,
    deficit,
    saturation,
Vegetation heights,
    Standardization
Von Kármán constant,

---W---
Water, physical properties,
Water balance,
Water vapor,
    physical properties,
    relative density,
Weather data,
Wet bulb temperature,
Wilting point,
Wind speed,

---Y---